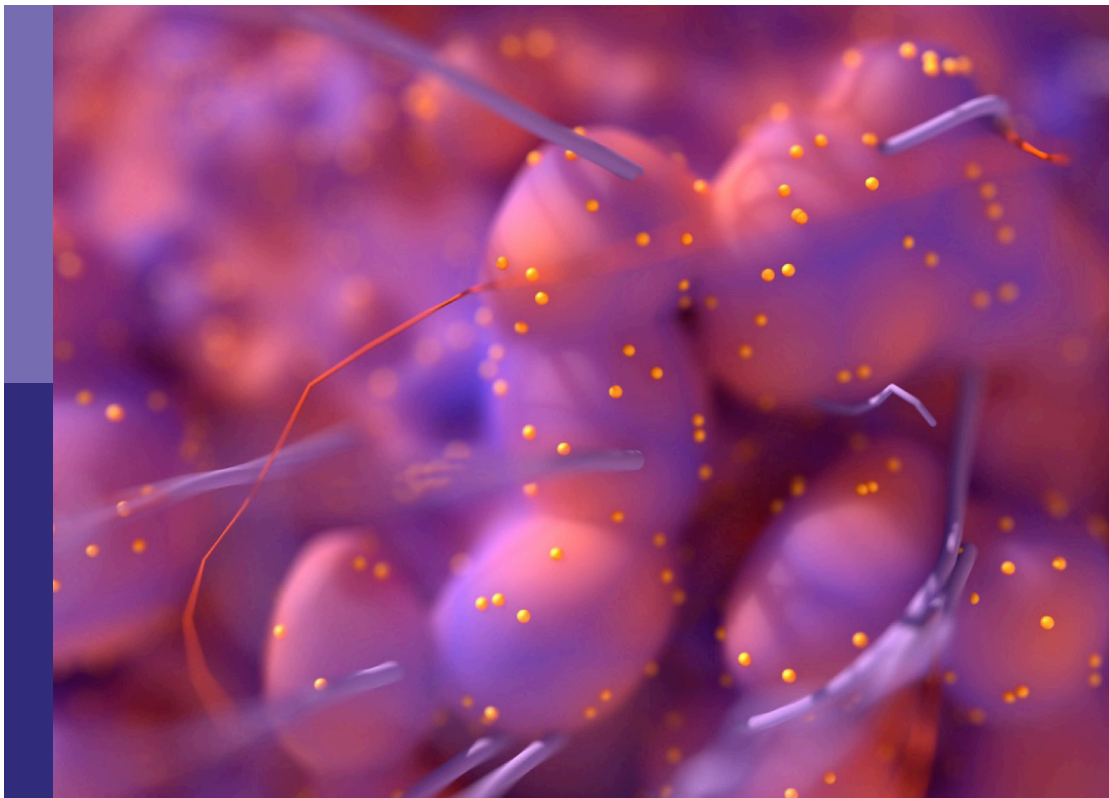
frontiers | Research Topics

Women in Gynecological oncology 2021

Edited by
Priya Ranjit Bhosale

Published in
Frontiers in Oncology



FRONTIERS EBOOK COPYRIGHT STATEMENT

The copyright in the text of individual articles in this ebook is the property of their respective authors or their respective institutions or funders. The copyright in graphics and images within each article may be subject to copyright of other parties. In both cases this is subject to a license granted to Frontiers.

The compilation of articles constituting this ebook is the property of Frontiers.

Each article within this ebook, and the ebook itself, are published under the most recent version of the Creative Commons CC-BY licence. The version current at the date of publication of this ebook is CC-BY 4.0. If the CC-BY licence is updated, the licence granted by Frontiers is automatically updated to the new version.

When exercising any right under the CC-BY licence, Frontiers must be attributed as the original publisher of the article or ebook, as applicable.

Authors have the responsibility of ensuring that any graphics or other materials which are the property of others may be included in the CC-BY licence, but this should be checked before relying on the CC-BY licence to reproduce those materials. Any copyright notices relating to those materials must be complied with.

Copyright and source acknowledgement notices may not be removed and must be displayed in any copy, derivative work or partial copy which includes the elements in question.

All copyright, and all rights therein, are protected by national and international copyright laws. The above represents a summary only. For further information please read Frontiers' Conditions for Website Use and Copyright Statement, and the applicable CC-BY licence.

ISSN 1664-8714
ISBN 978-2-8325-2648-4
DOI 10.3389/978-2-8325-2648-4

About Frontiers

Frontiers is more than just an open access publisher of scholarly articles: it is a pioneering approach to the world of academia, radically improving the way scholarly research is managed. The grand vision of Frontiers is a world where all people have an equal opportunity to seek, share and generate knowledge. Frontiers provides immediate and permanent online open access to all its publications, but this alone is not enough to realize our grand goals.

Frontiers journal series

The Frontiers journal series is a multi-tier and interdisciplinary set of open-access, online journals, promising a paradigm shift from the current review, selection and dissemination processes in academic publishing. All Frontiers journals are driven by researchers for researchers; therefore, they constitute a service to the scholarly community. At the same time, the *Frontiers journal series* operates on a revolutionary invention, the tiered publishing system, initially addressing specific communities of scholars, and gradually climbing up to broader public understanding, thus serving the interests of the lay society, too.

Dedication to quality

Each Frontiers article is a landmark of the highest quality, thanks to genuinely collaborative interactions between authors and review editors, who include some of the world's best academicians. Research must be certified by peers before entering a stream of knowledge that may eventually reach the public - and shape society; therefore, Frontiers only applies the most rigorous and unbiased reviews. Frontiers revolutionizes research publishing by freely delivering the most outstanding research, evaluated with no bias from both the academic and social point of view. By applying the most advanced information technologies, Frontiers is catapulting scholarly publishing into a new generation.

What are Frontiers Research Topics?

Frontiers Research Topics are very popular trademarks of the *Frontiers journals series*: they are collections of at least ten articles, all centered on a particular subject. With their unique mix of varied contributions from Original Research to Review Articles, Frontiers Research Topics unify the most influential researchers, the latest key findings and historical advances in a hot research area.

Find out more on how to host your own Frontiers Research Topic or contribute to one as an author by contacting the Frontiers editorial office: frontiersin.org/about/contact

Women in gynecological oncology: 2021

Topic editor

Priya Ranjit Bhosale — University of Texas MD Anderson Cancer Center, United States

Citation

Bhosale, P. R., ed. (2023). *Women in gynecological oncology: 2021*. Lausanne: Frontiers Media SA. doi: 10.3389/978-2-8325-2648-4

Table of contents

07 Editorial: Women in gynecological oncology 2021
Mayur Virarkar and Priya Ranjit Bhosale

10 Application of Single-Port Laparoscopic Surgery in Myomectomy
Lili Jiang, Deming Tong, Yan Li, Qifang Liu and Kuiran Liu

17 High-Risk HPV16 E6 Activates the cGMP/PKG Pathway Through Glycosyltransferase ST6GAL1 in Cervical Cancer Cells
Jun Wang, Gao Liu, Mei Liu, Qinzhen Cai, Cong Yao, Hao Chen, Neng Song, Chunhui Yuan, Decai Tan, Yuhai Hu, Yun Xiang and Tian Xiang

31 The Surgeon's Proficiency Affected Survival Outcomes of Minimally Invasive Surgery for Early-Stage Cervical Cancer: A Retrospective Study of 851 Patients
Ying Yang, Yue Huang and Zhengyu Li

39 An Assessment of Ovarian Cancer Histotypes Across the African Diaspora
Sophia H. L. George, Ayodele Omotoso, Andre Pinto, Aisha Mustapha, Alex P. Sanchez-Covarrubias, Usman Aliyu Umar, Ali Bala Umar, Timothy Abiola Oluwasola, Clement Abu Okolo, Umeh Uchenna Anthony, Francis Ikechukwu Ukekwe, Maisaratu A. Bakari, Aminu M. C. Dahiru, Habiba Ibrahim Abdullahi, Bawa Ahmed Abimiku, Aisha Abdurrahman, Asmau Usman, Saad Aliyu Ahmed, Hadiza Abdullahi Usman, Abba Kabir, George Uchenna Eleje, Michael Emeka Chiemeka, Emily Nzeribe, Ikechukwu Nweke, SaiduAbubakar Kadas, Dauda E. Suleiman, Etim Ekanem, Umemmuo Maureen Uche, Jibrin Paul, Uzoma Maryrose Agwu, Felix O. Edegbe, Rose I. Anorlu, Adekunbiola Banjo, Kayode Olusegun Ajenifuja, Adegboyega Adisa Fawole, Ibrahim O. O. Kazeem, Francis Magaji, Olugbenga Silas, Boma Precious Athanasius, Nyengidiki Kennedy Tamunomie, Emem Bassey, Kunle Abudu, Ibrahim G. Ango, Kabiru Abdullahi, Ishak Lawal, Suleiman Aliyu Kabir, Victor Ekanem, Michael Ezeanochie, Usman Rahman Yahaya, Melissa Nicole Castillo, Vishal Bahall, Vikash Chatrani, Ian Brambury, Saida Bowe, Darron Halliday, George Bruney, Raleigh Butler, Camille Ragin, Folakemi Odedina, Srikar Chamala, Matthew Schlumbrecht and Bala Audu

49 MRI Radiomic Features: A Potential Biomarker for Progression-Free Survival Prediction of Patients With Locally Advanced Cervical Cancer Undergoing Surgery
Mengting Cai, Fei Yao, Jie Ding, Ruru Zheng, Xiaowan Huang, Yunjun Yang, Feng Lin and Zhangyong Hu

60 Homologous Recombination Deficiency Associated With Response to Poly (ADP-ribose) Polymerase Inhibitors in Ovarian Cancer Patients: The First Real-World Evidence From China
Jing Ni, Wenwen Guo, Qian Zhao, Xianzhong Cheng, Xia Xu, Rui Zhou, Hongyuan Gu, Chen Chen and Xiaoxiang Chen

69 Prognostic Signatures Based on Ferroptosis- and Immune-Related Genes for Cervical Squamous Cell Carcinoma and Endocervical Adenocarcinoma
Chaoqun Xing, Huiming Yin, Zhi-Yong Yao and Xiao-Liang Xing

80 Comparison of Minimally Invasive Versus Abdominal Radical Hysterectomy for Early-Stage Cervical Cancer: An Updated Meta-Analysis
Mengting Zhang, Wei Dai, Yuexiu Si, Yetan Shi, Xiangyuan Li, Ke Jiang, Jingyi Shen and Liying Ying

92 MRVI1 and NTRK3 Are Potential Tumor Suppressor Genes Commonly Inactivated by DNA Methylation in Cervical Cancer
Huihui Ji, Kehan Li, Wenxiao Jiang, Jingwei Li, Jian-an Zhang and Xueqiong Zhu

105 Noninvasive Predictor for Premalignant and Cancerous Lesions in Endometrial Polyps Diagnosed by Ultrasound
Jianying Xu, Xuan Rao, Weiguo Lu, Xing Xie, Xinyu Wang and Xiao Li

114 PFKFB3 Regulates Chemoresistance, Metastasis and Stemness *via* IAP Proteins and the NF-κB Signaling Pathway in Ovarian Cancer
Yu-xin Jiang, Michelle K. Y. Siu, Jing-jing Wang, Thomas H. Y. Leung, David W. Chan, Annie N. Y. Cheung, Hextan Y. S. Ngan and Karen K. L. Chan

127 Assessing Post-Treatment Pathologic Tumor Response in Female Genital Tract Carcinomas: An Update
Frediano Inzani, Damiano Arciuolo, Giuseppe Angelico, Angela Santoro, Antonio Travaglino, Nicoletta D'Alessandris, Giulia Scaglione, Michele Valente, Federica Cianfrini, Antonio Raffone and Gian Franco Zannoni

137 DLC1 Is a Prognosis-Related Biomarker Correlated With Tumor Microenvironment Remodeling in Endometrial Carcinoma
Yalan Wu, Li-e Zheng, Shumin Chen, Chengyu Lv and Yuxiu Huang

150 Early Cervical Lesions Affecting Ovarian Reserve and Reproductive Outcomes of Females in Assisted Reproductive Cycles
Qiyu Yang, Juan Hu, Meng Wang, Zhou Li, Bo Huang, Lixia Zhu, Qingsong Xi and Lei Jin

158 Machine Learning-Assisted Ensemble Analysis for the Prediction of Response to Neoadjuvant Chemotherapy in Locally Advanced Cervical Cancer
Yibao Huang, Qingqing Zhu, Liru Xue, Xiaoran Zhu, Yingying Chen and Mingfu Wu

167 Risk Factor Assessment of Lymph Node Metastasis in Patients With FIGO Stage IB1 Cervical Cancer
Mu Xu, Xiaoyan Xie, Liangzhi Cai, Yongjin Xie, Qiao Gao and Pengming Sun

174 Association Between Endometriosis and Prognosis of Ovarian Cancer: An Updated Meta-Analysis
Peng Chen and Chi-Yuan Zhang

185 VEGF-D Serum Level as a Potential Predictor of Lymph Node Metastasis and Prognosis in Vulvar Squamous Cell Carcinoma Patients
Antonella Ravaggi, Angela Gambino, Federico Ferrari, Alessandro Olivari, Laura Zanotti, Chiara Romani, Laura Ardighieri, Paolo Antonelli, Giorgia Garganese, Daniela Gallo, Giovanni Scambia, Eliana Bignotti, Enrico Sartori, Stefano Calza and Franco Odicino

196 Current Prognostic and Predictive Biomarkers for Endometrial Cancer in Clinical Practice: Recommendations/ Proposal from the Italian Study Group
Gian Franco Zannoni, Emma Bragantini, Francesca Castiglione, Matteo Fassan, Giancarlo Troncone, Frediano Inzani, Anna Pesci, Angela Santoro and Filippo Fraggetta

216 Prognostic Effect of Primary Recurrence Patterns in Squamous Cervical Carcinoma After Radical Surgery
Zongkai Zhang, Long Jiang, Rui Bi, Xiaohua Wu, Guihao Ke and Jun Zhu

225 How Immunotherapy Modified the Therapeutic Scenario of Endometrial Cancer: A Systematic Review
Brigida Anna Maiorano, Mauro Francesco Pio Maiorano, Gennaro Cormio, Annamaria Maglione, Domenica Lorusso and Evaristo Maiello

240 Discussion on the Treatment Strategy for Stage IIA1 Cervical Cancer (FIGO 2018)
Xiaolin Chen, Wentong Liang, Hui Duan, Minling Wu, Xuemei Zhan, Encheng Dai, Qiubo Lv, Qinghuang Xie, Ruilei Liu, Yan Xu, Xiaonong Bin, Jinghe Lang, Ping Liu and Chunlin Chen

247 Hypermethylated *CDO1* and *ZNF454* in Cytological Specimens as Screening Biomarkers for Endometrial Cancer
Lei Wang, Lanlan Dong, Jun Xu, Lin Guo, Yiran Wang, Kangkang Wan, Wei Jing, Lanbo Zhao, Xue Feng, Kailu Zhang, Miao Guo, Yuliang Zou, Lianglu Zhang and Qiling Li

257 30-Year Experience With 22 Cases of Malignant Transformation Arising From Ovarian Mature Cystic Teratoma: A Rare Disease
Yan Li, Meng Qin, Ying Shan, Huan-wen Wu, Xiao-ding Liu, Jie Yin, Yu Gu, Wei Wang, Yong-xue Wang, Jia-yu Chen, Li Ma, Ying Jin and Ling-ya Pan

267 Real-World Efficacy of Bevacizumab in Patients With Recurrent Epithelial Ovarian Cancer
Jo-Ni Hung, Shih-Tien Hsu, Lou Sun, Sheau-Feng Hwang, Chih-Ku Liu, Yu-Hsiang Shih, Ming-Jer Chen, Jun-Sing Wang and Chien-Hsing Lu

275 Molecular Classification in Patients With Endometrial Cancer After Fertility-Preserving Treatment: Application of ProMisE Classifier and Combination of Prognostic Evidence
Xuting Ran, Tingwenyi Hu and Zhengyu Li

284 Efficacy and Safety of Placebo During the Maintenance Therapy of Ovarian Cancer in Randomized Controlled Trials: A Systematic Review and Meta-analysis
Jin-feng Wang, Lan-bo Zhao, Ya-di Bin, Kai-lu Zhang, Chao Sun, Yi-ran Wang, Xue Feng, Jing Ji, Li-song He, Fang-yao Chen and Qi-ling Li

298 Integration of scRNA-Seq and TCGA RNA-Seq to Analyze the Heterogeneity of HPV+ and HPV- Cervical Cancer Immune Cells and Establish Molecular Risk Models
Erdong Wei, Amin Reisinger, Jiahua Li, Lars E. French, Benjamin Clanner-Engelshofen and Markus Reinholz

309 Differences in the Impact of Heart Rate Variability on the Surgical Approach in Patients With Early Cervical Cancer: Laparoscopic versus Open Surgery
Jian Liu, Jingfeng Wang, Zhaoya Deng, Shiqi Liu, Guangqiao Li, Yilin Sun, Longfei Gao, Chenghui Li and Bo Shi

317 Nomograms of Combining MRI Multisequences Radiomics and Clinical Factors for Differentiating High-Grade From Low-Grade Serous Ovarian Carcinoma
Cuiping Li, Hongfei Wang, Yulan Chen, Chao Zhu, Yankun Gao, Xia Wang, Jiangning Dong and Xingwang Wu

326 *BRCA* Variants Do Not Increase the Risk of Adverse Reactions in Patients With Ovarian Cancer: A Single-Center Real-World Study
Kemin Li, Jing Zeng, Mengpei Zhang, Rutie Yin and Zhengyu Li

331 Exploring the Pharmacological Mechanism of the Effective Chinese Medicines Against Gynecological Cancer Based on Meta-Analysis Combined With Network Pharmacology Analysis
Ning Ren, Lulin Yu, Lihui Qian, Gewei Ye, Zhenzheng Zhu, Jieru Yu, Leitao Sun and Leyin Zhang

347 Cervical cancer screening in high-altitude areas in China: A large cross-section study of 25,173 women in northern Tibet
Qimin Wang, Yingying He, Fang Long, Chaoran Li, Zhuowei Shen, Dongxing Guo, Duoji Zhaxi, Lamu Bumu, Zhengyu Hua, Zhigang Sun, Nan Jiang, Xu Han, Jing Li, Keqing Yan, Siqi Bai, Muhan Tao, Xiaoguang Xu and Zhen Xiao

frontiers | Frontiers in Oncology

TYPE Editorial
PUBLISHED 24 May 2023
DOI 10.3389/fonc.2023.1220467

Check for updates

OPEN ACCESS

EDITED AND REVIEWED BY
Sophia George,
University of Miami, United States

*CORRESPONDENCE
Mayur Virarkar
mayur.virarkar@jax.ufl.edu
Priya Ranjit Bhosale
priya.bhosale@mdanderson.org

RECEIVED 10 May 2023
ACCEPTED 18 May 2023
PUBLISHED 24 May 2023

CITATION
Virarkar M and Bhosale PR (2023) Editorial: Women in gynecological oncology 2021. *Front. Oncol.* 13:1220467. doi: 10.3389/fonc.2023.1220467

COPYRIGHT
© 2023 Virarkar and Bhosale. This is an open-access article distributed under the terms of the Creative Commons Attribution License (CC BY). The use, distribution or reproduction in other forums is permitted, provided the original author(s) and the copyright owner(s) are credited and that the original publication in this journal is cited, in accordance with accepted academic practice. No use, distribution or reproduction is permitted which does not comply with these terms.

Editorial: Women in gynecological oncology 2021

Mayur Virarkar[1]* and Priya Ranjit Bhosale[2]*

[1]Department of Radiology, University of Florida, Jacksonville, FL, United States, [2]Department of Diagnostic Radiology, University of Texas MD Anderson Cancer Center, Houston, TX, United States

KEYWORDS

gynecological, oncology, original research, treatment, review

Editorial on the Research Topic
Women in gynecological oncology: 2021

Introductions

This editorial summarizes the contributions to the Frontiers Research Topic "*Women in gynecological oncology 2021*". The cohort comprises 33 articles with one clinical trial, 25 original research, 6 systemic analyses, and 1 review article. They were published from September 2021 through August 2022 period. As of May 2023, the article's impact analysis has over 61,000 views, with US and China leading viewers. The editorial has over 300 authors, and the article view ranges from 1000- 4000. These Research Topic aimed to explore recent developments in the area of gynecological oncology diagnosis, treatment, and the latest research.

Clinical trial

The only clinical trial (ChiCTR2000035061) in the editorial by Wang et al. comprised a screening program to investigate the prevalence of human papillomavirus (HPV) and HPV genotype distribution to reveal cervical cancer and its precursor, which led to morbidity among women in northern Tibet. They reported total HPV infection rate among women in Nagqu was 13.42%. In addition, they identified the five most common HPV genotypes, accounting for more than 60% of all HPV infections in Nagqu people, were HPV 16, 58, 31, 18, and 52.

Original articles

While summarising all the original research articles in the cohort will be beyond the scope of the editorial. We have discussed the four most viewed articles below.

Wei et al. analyzed the heterogeneity from transcriptional to immune infiltration between HPV+ and HPV- samples by Single-cell RNA sequencing (scRNA-seq) and bulk RNA sequencing. The study revealed heterogeneity from the transcriptional state to immune infiltration. They believe that single-cell transcriptomics is a powerful tool to explore the heterogeneity of HPV+ and HPV- tumors, which can facilitate assessing the impact of HPV infection on cancer biology by identifying gene markers for diagnosis, prognosis, and therapy.

The study by Ni et al. aimed to perform homologous recombination deficiency (HRD) testing of ovarian cancer in the real world in China and correlate HRD status and clinical characteristics with therapeutic outcomes. The results demonstrated that patients with high HRD scores tended to enrich in BRCA mutation and HRR mutation. The study is the first real-world study of Next-Generation Sequencing (NGS) -based HRD in Chinese ovarian and fallopian tube cancer patients.

The pilot study by George et al. evaluates population-level patterns of ovarian cancer in Black women globally and locally and describes the correlative patterns between age and histologic distribution in our Transatlantic Gynecologic Cancer Research Consortium. -member cohorts. The analysis revealed that the burden of ovarian cancer is increasing annually. By 2040, there is an expected 49.6-86.8% increase in ovarian cancer incidence in Africa, Latin America, and the Caribbean, which is much greater than the modest 9.6-25.9% increase expected among the predominantly White regions of Europe and North America.

`Xing et al. aimed to screen ferroptosis- and immune-related differentially expressed genes (FI-DEGs) to identify appropriate prognostic signatures for cervical squamous cell carcinoma patients endocervical adenocarcinoma (CESC). They found that Dual oxidase 1 (DUOX1) expression increased in CESC patients and suggested that DUOX1 may play different roles in different cancers, and the abnormal DUOX1 expression was only the result of CESC.

Review article

The only review article by Zannoni et al. focused on summarizing the histological features and immunohistochemical and molecular biomarkers useful to characterize endometrial cancer. The authors believe molecular classifiers should be combined with clinical risk groups and pathological parameters in an integrated histo-molecular approach to better discriminate outcomes for different patients.

Systemic review

The systemic analysis primarily focused on treatment, with one focusing on the association between endometriosis and ovarian cancer (Chen et al.).

Zhang et al. performed a meta-analysis to compare and evaluate medium- (3-year) and long-term (5-year) survival outcomes in patients with early-stage cervical cancer who underwent MIS (laparoscopic or robot-assisted radical hysterectomy) or Abdominal radical hysterectomy (ARH). The meta-analysis included 48 studies with 23346 patients and reported that early-stage cervical cancer undergoing MIS had a poorer prognosis than those undergoing ARH.

Inzani et al. reviewed the post-treatment pathological scoring systems for gynecological malignancies. According to current guidelines, the chemotherapy response score (CRS) system applied to the omental tissue is mandatory in pathological reports to evaluate the response of post-neoadjuvant high-grade serous carcinoma. Pressurized intraperitoneal aerosol chemotherapy (PIPAC) has emerged in recent years as a novel method of intraperitoneal drug administration to treat inoperable peritoneal metastasis from different origins. A 4-degree system called peritoneal regression grading score (PRGS) is used to monitor histological response on biopsies made during PIPAC procedures.

Maiorano et al. systematically reviewed the clinical trials regarding immune checkpoint inhibitors (ICIs) for the treatment of advanced Endometrium Cancer (EC). They reported that ICIs were an effective option for pretreated advanced EC patients with tolerable profiles and combining ICIs and Tyrosine kinase inhibitors (TKIs) are more effective in Microsatellite stable (MSS) women than monotherapy and pretreated advanced/recurrent EC.

Wang et al. meta-analysis evaluated the efficacy and safety of a placebo during the maintenance therapy of ovarian cancer (OC) patients in randomized controlled trials (RCTs). In total, 41 articles with 20,099 patients were included in this meta-analysis and reported that placebo did not improve or reduce the progression-free survival (PFS) and overall survival (OS) benefits of OC patients in RCTs but increased the incidences of common adverse effects (AEs).

Ren et al. performed a network pharmacology analysis to explore traditional Chinese medicine's potential pharmacological mechanisms and targets (TCM) in treating gynecological cancer (GC). The study, which included 11 RCTs of 863 GC patients, showed that TCM plus chemotherapy could provide more durable disease control and improve GC patients' Quality of life (QOL) without substantially increasing AEs compared with chemotherapy alone.

In the meta-analysis conducted by Chen et al. to uncover the differences in PFS and OS within endometriosis-associated ovarian cancer (EAOC) and non-EAOC patients. Twenty-one studies involving 38641 patients were included and reported that EAOC patients tended to have better OS and PFS than non-EAOC patients.

Conclusion

This Research Topic is very insightful and helpful in understanding the accurate research methodology and getting up to date with biomarkers in gynecological oncology. The authors hope to impact the reader's interest in respective Research Topic and will push them to pursue their future endeavors in gynecological oncology.

Author contributions

PB and MV contributed to the conception and design of the study. PB and MV wrote sections of the manuscript. All authors contributed to the manuscript revision, and read, and approved the submitted version.

Acknowledgments

We sincerely thank all the authors and reviewers participating in this Research Topic.

Conflict of interest

The authors declare that the research was conducted in the absence of any commercial or financial relationships that could be construed as a potential conflict of interest.

Publisher's note

All claims expressed in this article are solely those of the authors and do not necessarily represent those of their affiliated organizations, or those of the publisher, the editors and the reviewers. Any product that may be evaluated in this article, or claim that may be made by its manufacturer, is not guaranteed or endorsed by the publisher.

frontiers in Oncology

ORIGINAL RESEARCH
published: 24 September 2021
doi: 10.3389/fonc.2021.722084

Application of Single-Port Laparoscopic Surgery in Myomectomy

Lili Jiang[1], *Deming Tong*[2], *Yan Li*[1], *Qifang Liu*[1] *and Kuiran Liu*[1]*

[1] Department of Obstetrics and Gynecology, Shengjing Hospital of China Medical University, Shenyang, China, [2] Department of General Surgery, General Hospital of Northern Theater Command, Shenyang, China

Research Question: The use of a power morcellator in laparoscopic myomectomy is a controversial topic. The application of single-port laparoscopy solves this problem, but its safety, efficacy and prognosis are also challenges. The purpose of this study was to compare the clinical application of single-port laparoscopy and traditional three-port laparoscopy in myomectomy.

Design: This is a retrospective review of a total of 120 patients who underwent single-port laparoscopic myomectomy (n=60) or traditional three-port laparoscopic myomectomy (n=60), performed between January 2019 to December 2020. The operation time, intraoperative blood loss, specimen removal time, hemoglobin change after operation, postoperative ambulation time, first exhaust time after surgery, the length of hospital stay, pain score on the day, the first day after operation and the satisfaction of abdominal wall scar were evaluated for the surgical outcomes.

Results: Compared with the traditional three-port laparoscopic group, the specimen removal time, postoperative ambulation time, first exhaust time after surgery, the length of hospital stay were all shorter, the satisfaction of abdominal wall scar were higher in single-port laparoscopic group. The duration of surgery was longer in single-port laparoscopic group significantly. The differences were statistically significant ($P<0.05$). The intraoperative blood loss, hemoglobin change after operation, pain score on the day of operation and the first day after operation of the two groups had no differences ($P>0.05$).

Conclusions: The clinical effect of single-port laparoscopic myomectomy is satisfactory and can be popularized in clinic.

Keywords: myomectomy, single-port access (SPA) laparoscopic surgery, three-port laparoscopic surgery, uterine fibroids, gynecological surgery

OPEN ACCESS

Edited by:
Priya Ranjit Bhosale, University of Texas MD Anderson Cancer Center, United States

Reviewed by:
Michael Stark, New European Surgical Academy (NESA), Germany
Maurizio Rosati, Spirito Santo Hospital, Italy

***Correspondence:**
Kuiran Liu
liukr1585@163.com

Specialty section:
This article was submitted to Gynecological Oncology, a section of the journal Frontiers in Oncology

Received: *08 June 2021*
Accepted: *08 September 2021*
Published: *24 September 2021*

Citation:
Jiang L, Tong D, Li Y, Liu Q and Liu K (2021) Application of Single-Port Laparoscopic Surgery in Myomectomy. Front. Oncol. 11:722084. doi: 10.3389/fonc.2021.722084

INTRODUCTION

Uterine myoma is a common benign tumor of female reproductive organs, the overall incidence rate was 40% to 60% at the age of 35 years, 70% to 80% at 50 years of age (1). About 30% of the patients had abnormal uterine bleeding (increased menstruation, secondary anemia) and pelvic compression symptoms (abnormal urination, constipation and diarrhea) (2). A large number of clinical practice

shows that the main treatment is still surgery. In recent years, laparoscopic myomectomy has become the first choice because of its less invasive and better surgical outcome (3). Single-port laparoscopic technology has become a hot spot recently, the advantages of it can be maximized by reducing postoperative pain and improving aesthetics. However, the feasibility and safety of it has not been determined. This study aims to explore the feasibility of single-port laparoscopic myomectomy in the field of gynecology by studying the efficacy and recovery of patients with uterine fibroids undergoing single-port laparoscopic myomectomy and traditional three-port laparoscopic myomectomy.

METHODS

General Information

This study selected 120 patients with uterine fibroids who underwent laparoscopic myomectomy in the gynecologic department of Shengjing Hospital of China Medical University from January 2019 to December 2020. The medical information of each patient was reviewed retrospectively. The inclusion criteria: ①All patients were diagnosed as hysteromyoma by pelvic ultrasound and pelvic MR before operation. ②The patients had signed the informed consent. ③The umbilicus is normal. Exclusion criteria: ①Conversion to open surgery or other surgical methods (Massive bleeding occurred during laparoscopic surgery, and it was impossible to stop bleeding under the laparoscopy; It was found that the anatomical structure was unclear and the adhesion was serious during the operation, which made the laparoscopic surgery could not be carried out; Intraoperative frozen pathology showed malignant transformation of hysteromyoma,etc). ②Malignant transformation of uterine fibroids. ③Submucosal fibroids. ④Severe medical system diseases (heart, lung, brain, liver, kidney and other organ abnormalities). The patients were randomly divided into the observation group and the control group (60 cases in each group) according to the different operation methods. The patients in the observation group were treated with single-port laparoscopic surgery, and the patients in the control group were treated with traditional three-port laparoscopic surgery. Postoperative pathology was uterine leiomyoma. There were no significant differences in age, pregnancy, birth and other general conditions between the two groups. The study was approved by the China Medical University Research Ethics Committee. All of the operations were performed by surgeons experienced in laparoscopic surgery.

Surgical Procedure

All patients in the two groups received standardized preoperative nursing preparation and general anesthesia. Single-port laparoscopic surgery was performed using the following techniques. After partial eversion of the umbilicus, a 2-3cm longitudinal incision was made at the umbilicus. The umbilical incision was lifted, the skin and subcutaneous tissue were incised layer by layer, and the peritoneum was incised after confirming that there was no intestinal adhesion below the incision. The disposable incision protection sleeve (Lookmed, Jiangsu, China) was placed in the incision, the inner ring was placed in the abdominal cavity, and the outer ring was left to the abdominal wall to form a single-port laparoscopic approach platform (**Figure 1A**). A sterile glove was connected with the outer ring. The thumb of the glove was cut, and 10mm trocar (Dike, Guangzhou, China) was placed as the access of a scope and laparoscopic instruments. In order to prevent air leakage and loosening at the joint, No. 7 silk thread was used to fix and tie tightly, and the 5mm (Dike, Guangzhou, China) trocars were inserted into the other two fingers as the instrument port (**Figures 1B, C**). This is a self-made simple laparoscopic single-port (**Figures 1C, D**). The advantage is that it can save the cost for the patients without affecting the operation.

The remaining procedures were the same as those of multi-port laparoscopic surgery. Carbon dioxide was injected at a pressure of 13 mm Hg and a rigid 0° or 30° 5-mm laparoscope was inserted (Karl Storz, tutlingen, Germany). 30° laparoscope is a better choice because it provides a wide field of vision. The presence, location and size of leiomyomas were examined. In order to reduce the bleeding of leiomyoma, the uterus was injected with Pituitrin after dilution, and the blood pressure and heart rate were observed. The myomas were completely removed by longitudinal incision along the capsule of uterine myoma and hemostasis was performed by bipolar electrocoagulation. Uterine fibroids were removed from the umbilicus using endopouch specimen retrieval bag (Wellead, Guangzhou, China). 1-0 absorbable sutures were used for the uterine wound closure. Through the umbilicus, a drainage tube was left in place after surgery. The umbilicus was sutured in three layers. The operation pictures are shown as follows (**Figures 2A–F**).

Observation Index

①The duration of surgery, specimen removal time, intraoperative blood loss during surgery, Changes of hemoglobin after operation, first exhaust time after surgery, postoperative ambulation time and the duration of the postoperative hospital stay were observed and recorded. ②Visual analogue scale (VAS) was observed and recorded. Mild pain (1-3, slight pain can be tolerated), moderate pain (4-6, pain and affect sleep, can be tolerated), severe pain (7-10, gradually strong pain, unbearable, affect appetite and sleep). ③30 days after operation, the satisfaction of the two groups on abdominal scar was compared. The score was 1-5 according to the wound recovery basing the subjective evaluation of patients after operation. The higher the score, the higher the satisfaction.

Statistical Analysis

SPSS ver. 26.0 (SPSS Inc., Chicago, IL, USA) was used to perform the Statistical analysis. The p-values less than 0.05, as calculated using the chi-square test or Fisher's exact test, were considered to indicate statistical significance.

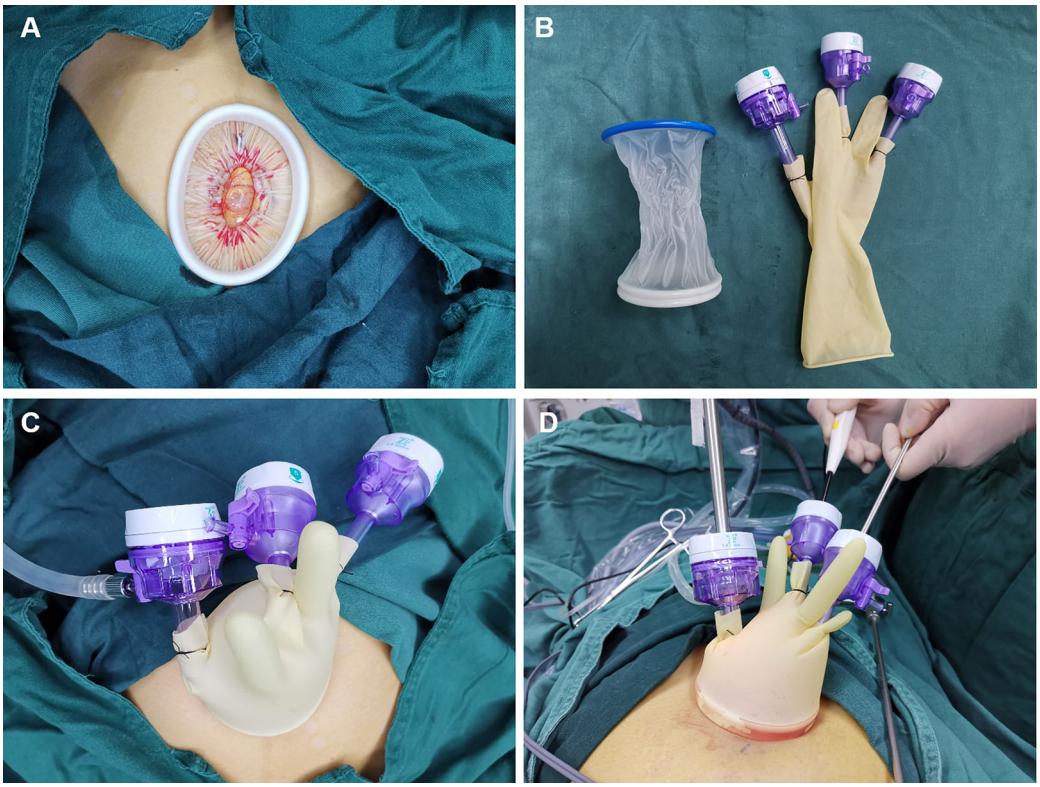


FIGURE 1 | **(A)** The disposable incision protection sleeve (Lookmed, Jiangsu, China) was placed in the incision. **(B)** Single-port laparoscopic approach connection instrument. **(C)** Self-made simple single-port laparoscopic access. **(D)** The instruments enter the abdominal cavity through single-port laparoscopic access.

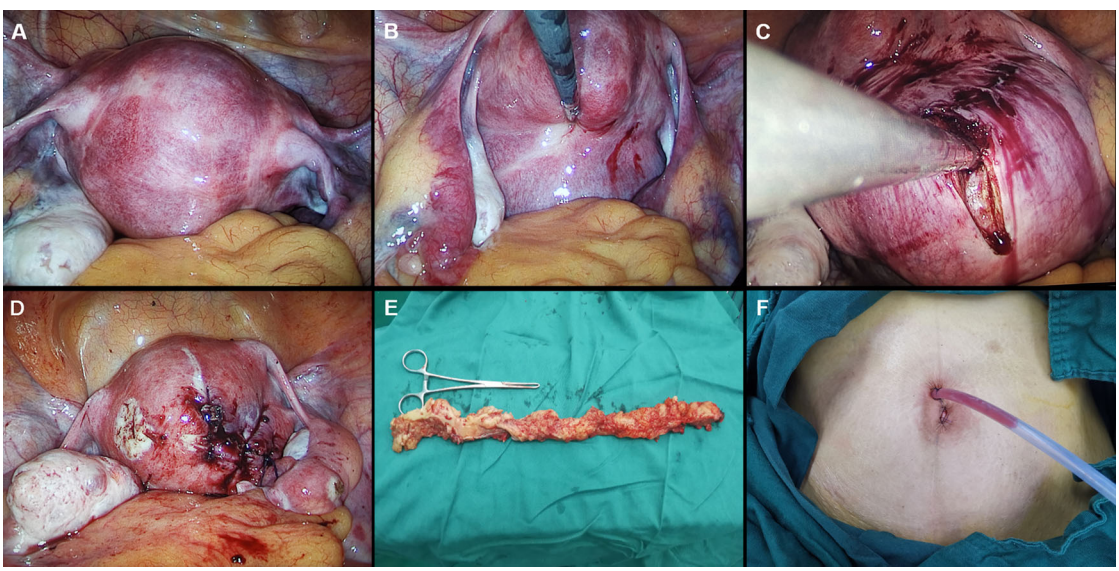


FIGURE 2 | **(A–F)** The operation pictures.

RESULTS

The mean age of the women who accepted single-port laparoscopic myomectomy was 38.1 years (range, 25–47 years). Their average number of gravidity and parity were 1.57 ± 1.33 and 0.83 ± 0.65. The number of previous abdominal operations was 0.70 ± 0.75. There was no significant difference between single-port laparoscopic group and traditional three-port laparoscopic group in age, pregnancy, labor and other general conditions (**Table 1**).

Surgical outcomes are shown in **Table 2**. During the surgery, the mean number of myomas resected by myomectomy and size of myomas in single-port laparoscopic group were 1.70 ± 1.02 and 7.85 ± 3.10cm which had no differences with the traditional three-port laparoscopic group. The surgical outcomes were not affected by the size and number of myomas. The operation time in single-port laparoscopic group was 80.67 ± 18.37 minutes, which was longer than the traditional laparoscopic group($P<0.05$). The specimen removal time was 1.70 ± 0.65 minutes, which was shorter than the traditional laparoscopic group($P<0.05$). After operation, the ambulation time and first exhaust time were 12.65 ± 4.32 hours and 27.70 ± 9.14 hours in single-port laparoscopic group. Calculated ($P<0.05$), indicating a statistically significant difference with the traditional laparoscopic group. There was no extension of the postoperative hospital stay in single-port laparoscopic group. On the contrary, the postoperative hospital stay was shortened ($P<0.05$). The intraoperative blood loss of single-port laparoscopic group was 57.00 ± 35.44 ml, which was not significantly different from that of the 54.67 ± 34.01 ml in traditional laparoscopic group ($P>0.05$). The hemoglobin change after operation was 19.00 ± 10.44g/L in the single-port laparoscopic group which was not significantly different between the two groups.

After operation, we evaluated the pain score of the two groups and the follow-up of scar satisfaction 30 days after operation to evaluate the operation effect. The data were shown in **Table 3**. Visual analogue scale (VAS) was observed and recorded to evaluate the pain score. Mild pain (1-3, slight pain can be tolerated), moderate pain (4-6, pain and affect sleep, can be tolerated), severe pain (7-10, gradually strong pain, unbearable, affect appetite and sleep). On the day of the operation, the VAS in the single-port laparoscopic group 4.13 ± 0.63. On the first day after operation, the VAS was 3.07 ± 0.89 in the single-port laparoscopic group. There were no statistical differences between the single-port laparoscopic group and traditional laparoscopic group($P>0.05$). 30 days after operation, the satisfaction of the two groups on abdominal scar was compared. The score was 1-5 according to the wound recovery basing the subjective evaluation of patients after operation. The higher the score, the higher the satisfaction. The score of the single-port laparoscopic group was 4.17 ± 0.46 which was higher than the traditional laparoscopic group($P<0.05$).

TABLE 1 | Clinical characteristics of the patients in single-port laparoscopic group and traditional three-port laparoscopic group.

Characteristics	Single-port laparoscopic group (n = 60)	Traditional three-port laparoscopic group (n = 60)	t/χ^2	P Value
Age	38.10 ± 6.47	37.17 ± 6.54	0.556	.580
Gravidity	1.57 ± 1.33	1.53 ± 1.48	0.092	.927
Parity	0.83 ± 0.65	0.63 ± 0.56	1.283	.205
No. of previous abdominal operations	0.70 ± 0.75	0.53 ± 0.57	0.968	.337

DISCUSSION

Uterine myoma is a very common disease of female reproductive system. The pathogenesis is related to many factors, such as race,

TABLE 2 | Surgical outcomes of the patients in single-port laparoscopic group and traditional three-port laparoscopic group.

	Single-port laparoscopic group (n = 60)	Traditional three-port laparoscopic group (n = 60)	t/χ^2	P Value
No. of myomas resected by myomectomy	1.70 ± 1.02	1.86 ± 1.55	-0.492	.624
Size of myomas (cm)	7.85 ± 3.10	7.40 ± 2.03	0.665	.509
Operation time (min)	80.67 ± 18.37	70.47 ± 17.11	2.225	.030
Blood loss (ml)	57.00 ± 35.44	54.67 ± 34.01	0.260	.796
Specimen removal time(min)	1.70 ± 0.65	3.27 ± 0.58	-9.815	.000
Hemoglobin change after operation(g/L)	19.00 ± 10.44	19.87 ± 10.18	-0.326	.746
Postoperative ambulation time(h)	12.65 ± 4.32	15.12 ± 4.83	-2.089	.041
First exhaust time after surgery(h)	27.70 ± 9.14	33.16 ± 5.31	-2.833	.006
Postop. hospital stay (days)	4.03 ± 0.99	4.67 ± 0.88	-2.600	.012

TABLE 3 | Comparison of VAS score and abdominal scar satisfaction score of each group.

	Single-port laparoscopic group (n = 60)	Traditional laparoscopic group (n = 60)	t/χ^2	P Value
VAS score on operation day	4.13 ± 0.63	4.03 ± 0.85	0.518	.606
VAS score on the first day after operation	3.07 ± 0.89	2.93 ± 0.58	0.698	.488
Abdominal scar satisfaction score	4.17 ± 0.46	3.47 ± 0.63	4.917	.000

age, menarche age, genetic factors and so on (4). Many myomas are asymptomatic, about 30-40% of cases can show different symptoms, depending on the location and size of myoma, which can lead to abnormal menstruation, dysuria, abortion, infertility and so on (5). In previous epidemiological studies, the prevalence of uterine myoma was underestimated as the majority of studies focused on symptomatic women (6) Menorrhagia can be secondary to anemia, and even life-threatening (7). In previous epidemiological studies, the prevalence of leiomyoma was underestimated because the majority of studies focused on symptomatic women (8). Myomectomy is a common surgical method for the treatment of uterine fibroids. The choice of treatment depends on the age of the patient and the desire to preserve fertility or avoid radical surgery (9). With the increase of marriage age and the increase of infertility associated with myomas, this kind of operation method has increased (10). In recent years, minimally invasive surgery has been widely used in the field of gynecology. A meta-analysis of 576 cases compared transabdominal myomectomy with laparoscopic myomectomy showed that laparoscopic myomectomy had faster recovery, less intraoperative blood loss, less postoperative pain, and lower overall complications, which was a better choice than open surgery (11). Laparoscopic myomectomy is considered more difficult by many gynecologists, but its advantages are real, and there is no difference in reproductive outcomes compared with traditional open surgery (2, 12). With the continuous development of minimally invasive concept, it is the pursuit of surgeons to minimize surgical trauma and achieve the best cosmetic effect. Single-port laparoscopic surgery has become a hot spot because it uses the natural pores of the navel to hide the surgical incision and has the characteristics of beautiful incision and fast postoperative recovery.

In our study, we compared the effect of single-port laparoscopy and traditional three-port laparoscopy in myomectomy. Compared with the control group, the specimen removal time, the first exhaust time after surgery, the postoperative ambulation time and the Postoperative hospital stay in the observation group were shorter, and the differences were statistically significant (P<0.05). It showed that single-port laparoscopy had the characteristics of less trauma and faster recovery. This was consistent with the research results of You et al (13) that compared with traditional laparoscopy, single-port laparoscopic surgery didn't lead to prolong suture time and hospital stay. As the incision at the belly button can reach 3cm after being opened, the specimen is easier to take out which makes the single-port laparoscope having more advantageous. Postoperative pain is an important indicator that affects the patient's recovery, not only affecting the patient's time to get out of bed after surgery, but also causing a serious psychological burden on the patient. In our study, the VAS score on operation day was 4.13 ± 0.63 and the VAS score on the first day after operation was 3.07 ± 0.89. The VAS scores of the single-port laparoscopic group had no difference with traditional laparoscopic group. It indicated that although the umbilical incision of single-port laparoscopic surgery was larger relatively, it did not increase the postoperative pain of the patients. In a follow-up study of patients' satisfaction with abdominal scars at 30 days after surgery, the score of the single-port laparoscopic group was higher than those of the traditional three-port laparoscopic group significantly. It showed that single-port laparoscopic surgery uses the skin folds naturally formed in the belly button as a channel, truly achieving "scar-free", the incision was more beautiful and patients' satisfaction improved.

In the study, there was no significant difference in intraoperative blood loss and postoperative hemoglobin changes between the observation group and the control group, suggesting that single-port laparoscopic myomectomy didn't increase the risk of bleeding, and there was no difference in surgical safety between the two groups. The results of this study also showed that the operation time of the observation group was longer than that of the control group (P<0.05). The possible reason was that the operation space of single port laparoscopic surgery was limited, the operation time was short, the operation technology was difficult and more clinical experience was needed. Through skilled operation, the operation time could be shortened (14).

In traditional three-port laparoscopic myomectomy, we used the laparoscopic uterine power morcellation to remove the fibroids. One of the main problems with power morcellation was that the removed tissue spreads to the surrounding area (15). The spread of benign lesions such as leiomyomas can lead to recurrence (16). Paul (17) et al. reported a case of recurrence in a short period of time after laparoscopic myomectomy in a young woman, which was considered to be caused by the residual tumor body during the first operation or the spread of tumor fragments caused by the laparoscopic uterine power morcellation. More worrying is the risk of the spread of malignant tumors, such as endometrial cancer, which may lead to a decline in overall survival rate (18). In 2014, the U.S. FDA issued a statement warning that in order to prevent the damage caused by the spread of unknown uterine fibroids to patients, it opposes the use of uterine power morcellation in laparoscopic hysterectomy or myomectomy (19). It is worthwhile to integrate that the single-port laparoscopic myomectomy procedure avoids the risk of tumor dissemination caused by the traditional three-port laparoscopic uterine power morcellation. During single-port laparoscopic myomectomy, the removed fibroids were placed in the specimen retrieval bag and lifted to the umbilical incision and removed by cold knife, which reduced the risk of fibroids dissemination. The endopouch specimen retrieval bag is an innovative single-use disposable device designed to be used as a receptacle for benign tissue mass during gynecological procedures such as laparoscopic myomectomy or laparoscopic hysterectomy. There is another new type of tissue morcellation bag which can be used in conjunction with the tissue morcellation system to safely contain and remove the shredded benign tissue mass. The device has unique features to allow for quick deployment, insufflation, morcellation and spill-proof withdrawal of the bag. Thereby reducing the patients' pain and surgical trauma caused by recurring diseases and even life threatening caused by medical dissemination.

Single-port laparoscopic surgery also has limitations in the treatment of uterine fibroids. Because the relevant instruments can only enter the abdominal cavity through the umbilical incision, the instruments are relatively concentrated and interfere with each other. It is difficult to form an operation triangle. The operation lacks a sense of space and three-dimensionality. The difficulty increases in operation and an experienced surgeon is required to perform the operation. The operation time of the single-port laparoscopic group in our study is higher than that of the traditional three-port laparoscopic group, which reminds that the surgeon needs to master skilled techniques and continuously accumulate experience in order to reduce the operation time. Moreover, the conditions of the operation should be comprehensively evaluated, the indications should be grasped and choose a more appropriate surgical method for patients with contraindications before the operation.

CONCLUSION

In summary, the use of single-port laparoscopic surgery to treat uterine fibroids can effectively reduce postoperative pain, accelerate postoperative recovery of patients, improve incision beauty and patients' satisfaction which can be applied to the treatment of uterine myoma and is worthy of promotion.

DATA AVAILABILITY STATEMENT

The original contributions presented in the study are included in the article/supplementary material. Further inquiries can be directed to the corresponding author.

ETHICS STATEMENT

The studies involving human participants were reviewed and approved by Medical Ethics Committee of Shengjing Hospital of China Medical University. The patients/participants provided their written informed consent to participate in this study. Written informed consent was obtained from the individual(s) for the publication of any potentially identifiable images or data included in this article.

AUTHOR CONTRIBUTIONS

LJ conducted main part of the study design and was the major contributor in writing the manuscript. DT was responsible for part of the literature search. YL collected specimens and took the images. QL was responsible for drawing and reviewing pictures. KL was responsible for checking the data, reviewing, and revising the article. All authors contributed to the article and approved the submitted version.

FUNDING

This research received the support from "Scientific research funding project of Liaoning Provincial Department of Science and Technology (No.2020JH2/10300050)".

ACKNOWLEDGMENTS

The authors thank the support of the funding "Scientific research funding project of Liaoning Provincial Department of Science and Technology (No.2020JH2/10300050)" to this article.

REFERENCES

1. Krimou Y, Erraghay S, Guennoun A, Mamouni N, Bouchikhi C, Banani A. Myoma Praevia and Pregnancy. *Pan Afr Med J* (2019) 33:216. doi: 10.11604/pamj.2019.33.216.14898
2. Donnez J, Donnez O, Dolmans MM. With the Advent of Selective Progesterone Receptor Modulators, What is the Place of Myoma Surgery in Current Practice? *Fertil Steril* (2014) 102(3):640–8. doi: 10.1016/j.fertnstert.2014.06.041
3. Rossetti A, Sizzi O, Soranna L, Cucinelli F, Mancuso S, Lanzone A. Long-Term Results of Laparoscopic Myomectomy: Recurrence Rate in Comparison With Abdominal Myomectomy. *Hum Reprod* (2001) 16(4):770–4. doi: 10.1093/humrep/16.4.770
4. Donnez J, Dolmans MM. Uterine Fibroid Management: From the Present to the Future. *Hum Reprod Update* (2016) 22(6):665–86. doi: 10.1093/humupd/dmw023
5. Sparić R. Uterine Myomas in Pregnancy, Childbirth and Puerperium. *Srp Arh Celok Lek* (2014) 142(1-2):118–24. doi: 10.2298/sarh1402118s
6. Wise LA, Laughlin-Tommaso SK. Uterine Leiomyomata. In: MB Goldman, R Troisi, KM Rexrode, editors. *Women and Health*. San Diego: Academic Press (2013). p. 285–306.
7. Nelson AL, Ritchie JJ. Severe Anemia From Heavy Menstrual Bleeding Requires Heightened Attention. *Am J Obstet Gynecol* (2015) 213(1):97.e1–6. doi: 10.1016/j.ajog.2015.04.023
8. Okolo S. Incidence, Aetiology and Epidemiology of Uterine Fibroids. *Best Pract Res Clin Obstet Gynaecol* (2008) 22(4):571–88. doi: 10.1016/j.bpobgyn.2008.04.002
9. De La Cruz MS, Buchanan EM. Uterine Fibroids: Diagnosis and Treatment. *Am Fam Physician* (2017) 95(2):100–7.
10. Alessandri F, Lijoi D, Mistrangelo E, Ferrero S, Ragni N. Randomized Study of Laparoscopic Versus Minilaparotomic Myomectomy for Uterine Myomas. *J Minim Invasive Gynecol* (2006) 13(2):92–7. doi: 10.1016/j.jmig.2005.11.008
11. Jin C, Hu Y, Chen XC, Zheng FY, Lin F, Zhou K, et al. Laparoscopic Versus Open Myomectomy–a Meta-Analysis of Randomized Controlled Trials. *Eur J Obstet Gynecol Reprod Biol* (2009) 145(1):14–21. doi: 10.1016/j.ejogrb.2009.03.009
12. Bhave Chittawar P, Franik S, Pouwer AW, Farquhar C. Minimally Invasive Surgical Techniques Versus Open Myomectomy for Uterine Fibroids. *Cochrane Database Syst Rev* (2014) 10):CD004638. doi: 10.1002/14651858.CD004638.pub3
13. You SH, Huang CY, Su H, Han CM, Lee CL, Yen CF. The Power Law of Learning in Transumbilical Single-Port Laparoscopic Subtotal Hysterectomy. *J Minim Invasive Gynecol* (2018) 25(6):994–1001. doi: 10.1016/j.jmig.2018.01.015
14. Chen X, Liu H, Sun D, Zhang JJ, Fan Q, Shi H, et al. Transvaginal Natural Orifice Transluminal Endoscopic Surgery for Tubal Pregnancy and a Device Innovation From Our Insitutionp. *J Minim Invas Gynecol* (2019) 26(1):169–74. doi: 10.1016/j.jmig.2018.05.013
15. Kho KA, Anderson TL, Nezhat CH. Intracorporeal Electromechanical Tissue Morcellation: A Critical Review and Recommendations for Clinical Practice. *Obstet Gynecol* (2014) 124(4):787–93. doi: 10.1097/AOG.0000000000000448
16. Leren V, Langebrekke A, Qvigstad E. Parasitic Leiomyomas After Laparoscopic Surgery With Morcellation. *Acta Obstet Gynecol Scand* (2012) 91:1233–6. doi: 10.1111/j.1600-0412.2012.01453.x
17. Paul PG, Koshy AK. Multiple Peritoneal Parasitic Myomas After Laparoscopic Myomectomy and Morcellation. *Fertil Steril* (2006) 85(2):492–3. doi: 10.1016/j.fertnstert.2005.10.017

18. Anupama R, Ahmad SZ, Kuriakose S, Vijaykumar DK, Pavithran K, Seethalekshmy NV. Disseminated Peritoneal Leiomyosarcomas After Laparoscopic "Myomectomy" and Morcellation. *J Minim Invasive Gynecol* (2011) 18:386–9. doi: 10.1016/j.jmig.2011.01.014
19. *Laparoscopic Uterine Power Morcellation in Hysterectomy and Myomectomy: FDA Safety Communication* (2014). Available at: http://www.fda.gov/MedicalDevices/Safety/AlertsandNotices/ucm393576.htm (Accessed July 2,2014).

Conflict of Interest: The authors declare that the research was conducted in the absence of any commercial or financial relationships that could be construed as a potential conflict of interest.

Publisher's Note: All claims expressed in this article are solely those of the authors and do not necessarily represent those of their affiliated organizations, or those of the publisher, the editors and the reviewers. Any product that may be evaluated in this article, or claim that may be made by its manufacturer, is not guaranteed or endorsed by the publisher.

Copyright © 2021 Jiang, Tong, Li, Liu and Liu. This is an open-access article distributed under the terms of the Creative Commons Attribution License (CC BY). The use, distribution or reproduction in other forums is permitted, provided the original author(s) and the copyright owner(s) are credited and that the original publication in this journal is cited, in accordance with accepted academic practice. No use, distribution or reproduction is permitted which does not comply with these terms.

frontiers in Oncology

ORIGINAL RESEARCH
published: 20 October 2021
doi: 10.3389/fonc.2021.716246

High-Risk HPV16 E6 Activates the cGMP/PKG Pathway Through Glycosyltransferase ST6GAL1 in Cervical Cancer Cells

Jun Wang[1†], Gao Liu[2†], Mei Liu[3†], Qinzhen Cai[1], Cong Yao[4], Hao Chen[5], Neng Song[6], Chunhui Yuan[1], Decai Tan[7], Yuhai Hu[3*], Yun Xiang[1*] and Tian Xiang[8*]*

[1] Department of Laboratory Medicine, Wuhan Children's Hospital (Wuhan Maternal and Child Healthcare Hospital), Tongji Medical College, Huazhong University of Science & Technology, Wuhan, China, [2] Department of Gastrointestinal Surgery, Central Hospital of Enshi Tujia and Miao Autonomous Prefecture, Enshi Clinical College, Medical School of Hubei Minzu University, Enshi, China, [3] Department of Laboratory Medicine, Wuhan Hankou Hospital, Wuhan, China, [4] Health Care Department, Wuhan Children's Hospital (Wuhan Maternal and Child Healthcare Hospital), Tongji Medical College, Huazhong University of Science & Technology, Wuhan, China, [5] Department of Pathology, Zhongnan Hospital of Wuhan University, Wuhan, China, [6] Department of Laboratory Medicine, Hubei Provincial Hospital of Integrated Chinese & Western Medicine, Wuhan, China, [7] Department of Science and Education, Central Hospital of Enshi Tujia and Miao Autonomous Prefecture, Enshi Clinical College, Medical School of Hubei Minzu University, Enshi, China, [8] Department of Laboratory Medicine, Central Hospital of Enshi Tujia and Miao Autonomous Prefecture, Enshi Clinical College, Medical School of Hubei Minzu University, Enshi, China

Alterations in glycosylation regulate fundamental molecular and cellular processes of cancer, serving as important biomarkers and therapeutic targets. However, the potential association and regulatory mechanisms of E6 oncoprotein on glycosylation of cervical cancer cells are still unclear. Here, we evaluated the glycomic changes *via* using Lectin microarray and determined the corresponding enzymes associated with endogenous high-risk HPV16 E6 expression in cervical cancer cells. α-2,6 sialic acids and the corresponding glycosyltransferase ST6GAL1 were significantly increased in E6 stable-expressing HPV$^-$ cervical cancer C33A cells. Clinical validation further showed that the expression of ST6GAL1 was significantly increased in patients infected with high-risk HPV subtypes and showed a positive association with E6 in cervical scraping samples. Interfering ST6GAL1 expression markedly blocked the oncogenic effects of E6 on colony formulation, proliferation, and metastasis. Importantly, ST6GAL1 overexpression enhanced tumorigenic activities of both E6-positive and E6-negative cells. Mechanistical investigations revealed that E6 depended on activating YAP1 to stimulate ST6GAL1 expression, as verteporfin (inhibitor of YAP1) significantly suppressed the E6-induced ST6GAL1 upregulation. E6/ST6GAL1 triggered the activation of downstream cGMP/PKG signaling pathway and ODQ (inhibitor of GMP production) simultaneously suppressed the

OPEN ACCESS

Edited by:
Jian-Jun Wei,
Northwestern University,
United States

Reviewed by:
Raffaella Ergasti,
Università Cattolica del Sacro Cuore,
Italy
Wenyi Gu,
The University of Queensland,
Australia

***Correspondence:**
Decai Tan
t700102@163.com
Yuhai Hu
2434377339@qq.com
Yun Xiang
xiangyun5272008@163.com
Tian Xiang
xiangt0504@whu.edu.cn

[†]These authors have contributed equally to this work

Specialty section:
This article was submitted to Gynecological Oncology, a section of the journal Frontiers in Oncology

Received: 28 May 2021
Accepted: 30 September 2021
Published: 20 October 2021

Citation:
Wang J, Liu G, Liu M, Cai Q, Yao C, Chen H, Song N, Yuan C, Tan D, Hu Y, Xiang Y and Xiang T (2021) High-Risk HPV16 E6 Activates the cGMP/PKG Pathway Through Glycosyltransferase ST6GAL1 in Cervical Cancer Cells. Front. Oncol. 11:716246. doi: 10.3389/fonc.2021.716246

oncogenic activities of both E6 and ST6GAL1 in cervical cancer cells. Taken together, these findings indicate that ST6GAL1 is an important mediator for oncogenic E6 protein to activate the downstream cGMP/PKG signaling pathway, which represents a novel molecular mechanism and potential therapeutic targets for cervical cancer.

Keywords: cervical cancer, E6 protein, YAP1, ST6GAL1, cGMP/PKG

INTRODUCTION

Cervical cancer remains the fourth most frequently diagnosed cancer and the fourth leading cause of cancer-related deaths among women worldwide (1). The major causative factor that leads to the development of cervical cancer has been identified as human papillomavirus (HPV) persistent infection (2). High-risk HPV16 is the most common carcinogenic HPV subtype and is responsible for more than half of cervical cancers (3–5). Due to the wide coverage of cancer screening and HPV vaccination programs, incidence and mortality rates of cervical cancer have progressively declined in well-developed countries (6), but an increasing incidence and mortality trend is observed in China, especially in young women (7). Furthermore, the vaccine ISA101, one of the most promising therapeutic vaccines that directly targeted the HPV16 E6 and E7 oncoproteins, has been shown to be ineffective for invasive cancer by itself alone (8).

In infected malignant cells, HPV16 genome frequently (>76%) integrated into the host cell DNA (9). The E6 oncoprotein is one major driver of oncogenesis in the normal cervical epithelium and plays important roles for controlling epithelial differentiation, cellular growth, and immune function (10, 11). Mechanistically, E6 forms a complex with host E3 ubiquitin ligases and mediates proteasomal degradation of a number of host targets, such as tumor suppression protein p53 (12), and also increases telomerase activity to prevent apoptosis and promote the immortalization of infected cells (13). Specifically, E6 protein of high-risk HPV16 and HPV18 can further bind and regulate a selection of PSD95/DLG/ZO-1 (PDZ) domain-containing proteins, like DLG1 and SCRIB, to increase oncogenic potential (14). However, HPV16 E6 preferentially binds SCRIB over DLG1 and *vice versa* for HPV18 E6. Furthermore, HPV16 E6 also promotes NHERF1 degradation to enhance the metastasis of cervical cancer cells, whereas NHERF1 is not targeted by HPV18 E6 (15). Recently, disruption of the direct interaction between E6 and host proteins or chimeric antigen receptor T cells (CAR-T cells) targeted to E6 have been shown to be effective for $HPV16^+$ cervical cancers (16, 17). Thus, a further detailed clarification of the oncogenic molecular mechanisms of high-risk HPV16 E6 would be beneficial for the development of therapeutic interventions directed against $HPV16^+$ malignancies.

Glycosylation alterations frequently occurred in tumor cells and participate in numerous fundamental biological processes, including cellular signaling, proliferation, adhesion, extracellular matrix interactions, proximal and distal communication, inflammation, and immune surveillance (18). For example, with the ability to enhance the biosynthesis of poly-N-acetyllactosamine chains and generation of the backbone components of dimeric sialyl Lewis A, B3GNT3/B3GNT2-mediated glycosylation of both PD-L1 and PD-1 enhances their interaction, and downregulation of these enzymes represents a potential strategy to enhance immune checkpoint therapy (19–21). Sialylation is another important abnormal glycan modification found in the vast majority of cancers, which leads to the hyperactivation of the receptor tyrosine kinases (RTKs), like epidermal growth factor receptor (EGFR), MET, and RON (22, 23). Increased expression of β-galactoside α2,6-sialyltransferase I (ST6GAL1), an enzyme generated α2,6-sialylated lactosamine, is often associated with invasive phenotype and poor prognosis in several cancers, including colon, stomach, and ovarian cancers (24). Moreover, ST6GAL1 endows resistance of cancer cells to gefitinib (EGFR inhibitor) and trastuzumab (anti-ErbB2 antibody) and also predicts the sensitivity of lenvatinib treatment to patients with hepatocellular carcinoma (25). Thus, targeting glycosylation alterations holds potent promise to augment the available strategies in both therapy and biomarker field of cancers.

Recently, increased sialylation, GlcNAcylation, and reduced fucosylation have been found to be upregulated in carcinomas of the cervix (26–28) and patients with metastatic cervical cancer (29). However, the glycosylation alterations of cervical cancer in response to high-risk HPV16 E6 stimulation, and the potential regulatory mechanisms remain largely unknown. In the present study, we confirmed that E6 increases level of α2-6 sialic acids in cervical cancer HPV^- C33A cells *via* using Lectin microarray, and ST6GAL1 is an important mediator for E6 to perform oncogenic activities. In details, E6 depends on activating YAP1 to stimulate ST6GAL1 expression and subsequently results in the activation of downstream cGMP/PKG pathway. Importantly, knockdown ST6GAL1 or blocking cGMP/PKG pathway with specific inhibitor ODQ suppressed the oncogenic activities of both E6-positive and E6-negative cervical cancer cells. Therefore, our findings provide novel insights into the molecular mechanisms involved in HPV16 E6-induced oncogenesis and suggest that targeting ST6GAL1 or cGMP–PKG signaling might be potential therapeutic strategies for cervical cancer.

MATERIALS AND METHODS

Cell Culture

The human embryonic kidney (HEK293T) cells, C33A (HPV^-) cells, were purchased from the cell bank of the Chinese Academy of Sciences (Shanghai, China) as we previously described (30). HEK293T cells and C33A and C33A-E6 cells were grown in

Dulbecco's modified Eagle's medium (DMEM)–low glucose (Gibco, USA) containing 10% fetal bovine serum (FBS) (Gibco, USA), 100 U/ml penicillin, and 100 μg/ml streptomycin (Beyotime, Shanghai, China) under a humidified atmosphere containing with 5% CO_2 at 37°C.

Collection of Cervical Specimens

Samples of all patients were collected with a clinically approved disposable cervical abscission cell sampler (158-0001, Kang Jian Medical, Jiangsu, China). The instructions for use of these cervical sampling brush were as follows: expose the cervix, wipe off the secretions with a cotton swab, carefully insert the brush head into the endocervical canal until the outer bristles touch the outer cervical neck, rotate clockwise five to eight times, and finally insert the brush head into the preservation solution bottle. Genomic DNA was first extracted from the collected samples using a DNA extraction kit (Chaozhou Hybribio Biochemical Co., Ltd., Chaozhou, China) according to the manufacturer's instructions. According to the clinical detection results of HPV typing as we presented in our previous study (31), 10 samples of five groups were collected respectively and stored at −80°C, and then, ST6GAL1 and E6 gene tests were performed. The five groups including (1) single HPV16-positive specimens, (2) mixed HPV16-positive specimens, (3) other high-risk HPV-positive specimens, (4) low-risk HPV-positive specimens, and (5) HPV-negative specimens. The overview of the clinical characteristics of patients are shown in **Supplementary Table S1**. The study was approved by the Institutional Review Board of the Wuhan Children's Hospital (Wuhan Maternal and Child Healthcare Hospital) (2020R079-E01).

Lentivirus Production and Transduction

HPV16 E6 stable-expressing C33A cells were constructed according to our previous study (32). In brief, HPV16 E6 (GenBank accession no. FJ415228.1) was cloned into the lentiviral backbone pLVX-mCMV-ZsGreen-IRES-Puro. Then, the plasmids, pCAG-HIVgp (RDB04394, Riken, Japan) and pCMV-VSV-G-RSV-Rev (RDB04393, Riken, Japan), were simultaneously transfected into HEK293T using Lipofectamine 2000 (Invitrogen, Shanghai, China). Lentiviral particles in the supernatant were harvested at 72 h after transfection. C33A cells were then infected with pLVX-E6 or control pLVX lentivirus [multiplicity of infection (MOI) = 50] in the presence of 8 μg/ml polybrene. The cells were treated with puromycin (5 μg/ml) for 2 weeks to select the stably transfected cells.

Lectin Microarray

A lectin microarray was produced using 95 lectins (Raybiotech Lectin Array 95 kit, Cat. No. GA-Lectin-95, RayBiotech, Inc.) with different binding preferences covering *N*- and *O*-linked glycans and analyzed as previously described (33, 34). Whole-cell lysates labeled with fluorescent dye Cy3 (GE Healthcare, UK) were applied to the lectin microarrays, which were then scanned with a Genepix 4000B confocal scanner (Axon Instruments, CA, USA). The acquired images were analyzed at 532 nm for Cy3 detection by Genepix 3.0 software (Axon Instruments, Inc.). Raw values of fluorescent intensities less than the average background were removed. The median of the valid data for each lectin was globally normalized to the sum of the medians of all valid data for 95 lectins. The relative change in protein glycosylation in response to HPV16 E6 stimulation was evaluated by comparison of the data from E6 stable-expressing versus control C33A cell lysates.

Transient Transfection

Short-hairpin RNA targeting human ST6GAL1 (pSilencer 1.0-U6-shST6GAL1) and negative control shRNA (pSilencer 1.0-U6-shNC) were designed and chemically synthesized by the TSINGKE Biological Technology (Wuhan, China). According to the targeting sequences, oligonucleotides coding for each short-hairpin RNA (shRNA) were designed and listed as follows: shRNA ST6GAL1, forward 5′-GGGAGTTACTATGATTCCTTTTTCAA GCTTAAAGGAATCATAGTAACTCCCTTTTT-3′; reverse, 5′-AATTAAAAAGGG AGTTACTATGATTCCTTTAA GCTTGAAAAAGGAATCATAGTAACTCCCGGCC -3′); shRNA-negative control (NC) (forward, 5′-TTCTCCGAAC GTGTCACGTTCAA GCTTCGTGACACGTTCGG AGAATTTTT-3′; reverse, 5′-AATTAAAAATTCTCC GAACGTGTCACGAAGCTTGAACGTGACACGT TCGGAGAAGGCC-3′). Messenger RNA (mRNA) of ST6GAL1 (GenBank accession no. NM_173216.2) was synthesized and inserted into the pcDNA3.1 vector (Invitrogen, Carlsbad, CA, USA); empty vector transfection was transfected as the control. C33A or C33A-E6 cells were grown to a density about 70–80% in 6-cm dishes and then transfected with indicated plasmids by Lipofectamine 2000 Transfection Kit (Invitrogen, Shanghai, China) following the manufacturers' instruction. Forty-eight hours posttransfection, the selective overexpression or silencing of ST6GAL1 was detected by Western blot.

mRNA Sequencing

Total RNA was extracted from C33A and C33A-E6 cells with Trizol reagent (Invitrogen, CA, USA). Then, the RNA was quantified using a NanoDrop ND-2000 (Thermo Scientific), and its integrity was assessed using the Agilent Bioanalyzer 2100 (Agilent Technologies, USA). Next, the mRNA molecules were purified from the total RNA using oligo (dT) magnetic beads and fragmented into small pieces and then subjected to transcriptome analysis (OEbiotech, Shanghai, China). The E6-dysregulated mRNAs were identified by the combination of the absolute value of the |log2 [fold change of reads per kilo base per million mapped reads (RPKM)]| ≥ 1 and $p < 0.05$. ST6GAL1-associated mRNAs were analyzed using R2: Genomics Analysis and Visualization Platform (http://r2.amc.nl) as we previously described (32); the cutoff correlation p-value was <0.01. Cluster Profiler R package was used for Kyoto Encyclopedia of Genes and Genomes (KEGG) pathway enrichment analysis. MEV software was used for hierarchical cluster analysis of mRNA expression according to the protocol provided by OEbiotech.

Quantitative Real-Time PCR

Total RNA extracted from indicated cervical cancer cells with Trizol reagent (Invitrogen, CA, USA). Subsequently, complementary DNA was generated from 1 μg total RNA

using Prime Script RT Master Mix (Takara Bio Inc., Kusatsu, Japan). Real-Time PCR (qRT-PCR) was conducted using 2× SYBR green PCR master mix (TaKaRa, Dalian, China) according to the manufacturer's protocol to detect mRNA levels of indicated genes. The ABI 7500 (Applied Biosystems, CA, USA) was used to perform the amplification reaction. Each experiment was performed in triplicate. Gene expression values were normalized relative to expression of the housekeeping gene glyceraldehyde 3-phosphate dehydrogenase (GAPDH) by the $2^{-\Delta\Delta Ct}$ method. The gene-specific primer sequences are listed in **Table 1**.

Western Blot

Cells were lysed on ice with radioimmunoprecipitation assay (RIPA) buffer (Beyotime, China) containing a protease inhibitor cocktail. The concentration of protein was detected by a BCA Protein Assay Kit (Beyotime). Protein samples (30 μg) were separated by 8–12% (v/v) sodium dodecyl sulfate polyacrylamide (SDS-PAGE) gel electrophoresis and transferred onto a polyvinylidene fluoride (PVDF) membrane (Millipore, MA, USA) for subsequent experiments. The membranes were blocked by 5% defatted milk for 2 h at room temperature and then incubated with primary antibodies against HPV16E6 (sc-460; 1:1,000; 16 kDa; Santa Cruz), ST6GAL1 (14355-1-AP; 1:1,000; 47 kDa; Proteintech), B3GNT2 (sc-134231; 1:1,000; 46 kDa; Santa Cruz), FUT2 (sc-100742, 1:1,000; 39 kDa; Santa Cruz), B4GALT1 (sc-515551, 1:1,000; 50 kDa; Santa Cruz), Bcl-2 (ab196495; 1:1,000; 26 kDa; Abcam), Bax (50599-2-lg; 1:10,000; 21 kDa; Proteintech), p53 (ab26; 1:1,000; 53 kDa; Abcam), YAP1 (ab56701; 1:1,000; 49 kDa; Abcam), p-YAP1^{S397} (#13619; 1:1,500; 75 kDa; CST), VASP (13472-1-AP; 1:1,000; 46 kDa; Proteintech), p-VASP^{Ser239} (ab194747; 1:1,000; 40 kDa; Abcam), Smad2 (ab119907; 1:1,000; 52 kDa; Abcam), p-Smad2^{S467} (ab53100; 1:1,000; 58 kDa; Abcam), E-cadherin (13-1700; 1:1,000; 110 kDa; Invitrogen), sGC (ab189176, 1:1,000; 71 kDa; Abcam), PKG1 (#3248, 1:1,000; 48 kDa; CST), PKG2 (55138-1-AP; 1:1,000; 87 kDa; Proteintech), PDE5A (ab28761, 1:1,000; 95 kDa; Abcam), and GAPDH (sc-47724; 1:1,000; 37 kDa; Santa Cruz) at 4°C overnight. Next, the membranes were incubated with horseradish peroxidase (HRP)-conjugated secondary antibodies and visualized by chemiluminescence (Pierce ECL Western Blotting Substrate).

Cell Counting Kit-8 Assay

Cells (1.5×10^3) were seeded into 96-well plates and incubated with 5% CO_2 at 37°C, after incubation for 24, 48, 72, and 96 h, 10 μl Cell Counting Kit-8 (CCK-8) reagent (Yeasen, Shanghai, China) was added into each well and incubated for another 4 h. Cell viability was assessed by detecting the absorbance of the dye solution at 450 nm in a microplate reader (Bio-Rad, CA, USA). All samples were prepared in triplicate and normalized to a blank control.

Colony Formation Assay

Cells (1×10^3) were plated in six-well plates for 24 h and then received indicated transfection or drug treatment. Cells were then cultured in fresh medium for another week. Colonies were fixed with methanol and stained with crystal violet (0.05%, w/v) for 30 min. Photographs were acquired, and colonies containing more than 50 cells were counted. All the experiments were performed in triplicate.

Cell Apoptosis Assay

For cell apoptosis analysis, cells were incubated with Annexin V-FITC and propidium iodide using an Annexin V-FITC Apoptosis Detection Kit (Biolegend) according to the manufacturer's protocol at 4°C in the dark for 30 min. The fluorescence of the stained cells was examined by flow cytometry (FACSCanto II, Becton-Dickinson, USA) and analyzed by FlowJo 10.5.4 software.

Wound-Healing Assay

A wound-healing assay was used to evaluate the migration of C33A and C33A-E6 cells. Briefly, cells (1×10^5) were seeded in 24-well plates for growth to 80–90% confluence. Then, the monolayers were wounded by scratching the surface as uniformly as possible with a pipette tip. The remaining cells were washed thrice in phosphate-buffered saline (PBS) to remove cellular debris and incubated at 37°C with serum-free medium. Migrating cells at the wound front were photographed under an Olympus IX73 microscope after 24 h. The area of the wound was measured with ImageJ software (NIH, USA).

TABLE 1 | Primer sequences for genes.

Gene	Forward primer (5′-3′)	Reversed primer (5′-3′)
HPV16 E6	ATGCACCAAAAAGGAACTGCAATGT	TTACAGCTGGGTTTCTCTACGTGTT
B3GALNT1	CTCCTGAGTTTCTTTGTGATGTGG	CATTACGTACTTGGCATTGGGG
B4GALNT1	GGAACCTGGCCGTGTCTCAAGTAAC	CCAGGAAGAAGTTAACCACGCCGTC
ST6GAL1	CTACCATTCGCCTGATGAACTCT	TCTGGGGCTTGAGGATGTAAAAG
ST6GAL2	CTGAATGGGAGGGTTATCTGCC	ACCTCAGGACTGCGTCATGATC
MAN2A1	TTAAGCCGCCAGTTCACCG	ACATTGAGAGCTGGCCCTGAG
B4GALT1	TGAGTTTAACATGCCTGTGGACCTG	AATGAGGTCCACGTCACTAAACAC
FUT1	ATTAGGTGACAAGCGGGCAGAGGC	TTCCGGTGCCAGGGCTTAGAG
FUT2	GTCACCGATGCTGGAAGGGTTT	GTCCCAGTGCCTTTGATGTTGAG
B3GNT3	TATGTGTCTGGAGCTTGAGG	AAGGATGTGTAGGAGTTCGC
B3GNT2	CTGCTCCCGGACAAGATATGA	GTACTGCCGGTTCAGCTTCT
GAPDH	GGGAGCCAAAAGGGTCAT	GAGTCCTTCCACGATACCAA

Transwell Assay

Transwell assay was used to investigate cells invasion in C33A and C33A-E6 cells as we described previously (30, 32). Briefly, 24-well Transwell plates (pore size, 8 μm; Corning, Inc.) with 100 μl Matrigel (BD Biosciences) in upper chamber were used for cell invasion assays. Cells (5×10^4) were resuspended in serum-free medium and placed into the upper chamber. Complete medium in the lower chamber was considered as a chemical attractant. After incubating for 24 h, the invaded cells attached to the lower surface were fixed with 4% formaldehyde for 15 min and then stained with 0.05% crystal violet for 30 min. The invasion cells were photographed under an Olympus IX73 microscope. Experiments were performed in three independent times and six random fields were scanned in each time.

Statistical Analysis

The data were presented as mean ± standard deviation of at least three independent experiments and analyzed by GraphPad Prism 8.0 Software (GraphPad Software Inc., La Jolla, CA, USA). Unpaired *t*-test or one-way ANOVA followed by Newman–Keuls *post-hoc* test was performed for data analysis. A $p < 0.05$ was considered as statistically significant ($^*p < 0.05$, $^{**}p < 0.01$, $^{***}p < 0.001$).

RESULTS

The High-Risk HPV16 E6 Protein Results in Altered Glycosylation in Cervical Cancer Cells

To examine the relationship between HPV16 E6 and altered glycosylation in cervical cancer, we constructed HPV16 E6-stable expressing HPV$^-$ C33A cervical cancer cells (C33A-E6) and detected the glycan repertoire of cellular glycoproteins *via* using 95-lectins microarray. In general, C33A-E6 cells showed higher levels of α-2,6 sialic acids (bound by lectin SNA-I), N-acetylgalactosamine (WFA, SHA), α-1,3- and α-1,6-linked mannose (HHA, NPL), β-galactosidase (GAL9), and lower levels of lactose/galactose (RCA120, RCA60, PHA-E), and α-1,2 fucose structures (UEA-I) than the corresponding control C33A cells (**Figures 1A, B**; **Table 2**). To gain insight into the biosynthetic underpinnings of these changes, we then focused on glycogenes (glycosyltransferases) known to be involved in the synthesis of glycan epitopes bound by these lectins. Consistent with our observed glycan changes, C33A-E6 cells displayed higher expression levels of N-acetylgalactosamine branching enzymes (B3GALNT1 and B4GALNT1), sialyltransferases (ST6GAL1 and ST6GAL2), and α-1,3- and α-1,6-linked

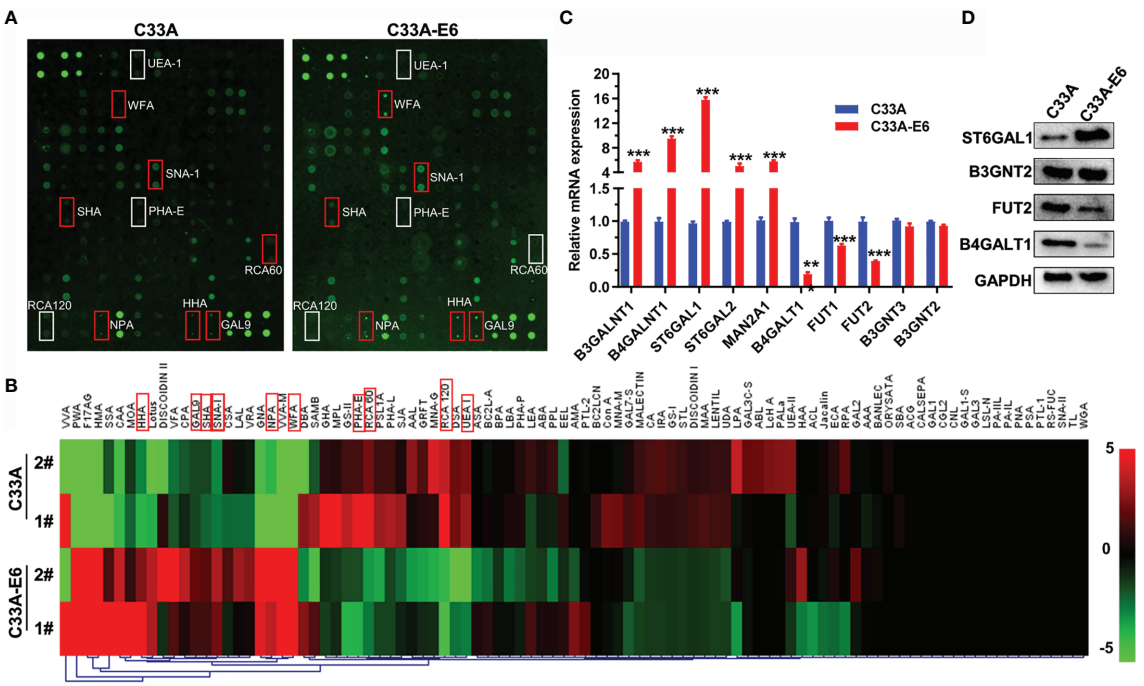


FIGURE 1 | The high-risk HPV16 E6 protein results in altered glycosylation in cervical cancer cells. **(A)** C33A cells were infected with pLVX-E6 or empty control pLVX lentivirus (MOI = 50) to select the stably transfected cells with the presence of puromycin (5 μg/ml). Then, glycosylation changes in whole-cell lysates of C33A and C33A-E6 cells (E6 stable expressing) were detected by lectin microarray (included 95 lectins). The slide with two replicates of the lectin array is shown. The lectin microarrays with high fluorescence intensities in C33A-E6 cells are marked with red frames, and low fluorescence intensities in C33A-E6 cells are marked with white frames. **(B)** Fluorescence intensities of samples from C33A and C33A-E6 cells were scanned and analyzed. Heat map and hierarchical clustering analysis of the 95 lectins with two biological replicates were presented. The significant different lectins were marked with red frames. **(C)** qRT-PCR was performed to detect the mRNA expression of lectin-corresponding glycotransferases of C33A and C33A-E6 cells. Data were presented as mean ± SD from the three independent replicates. **(D)** Protein expression of several glycotransferases were confirmed by Western blot. $^{**}p < 0.01$, $^{***}p < 0.001$.

TABLE 2 | Differences in glycan patterns between C33A and C33A-E6 cells by lectin microarray analysis.

Lectin	Abbreviation	Carbohydrate specificity	Glycosyltransferase	Fold change (C33A-E6 vs. C33A)	*p*
Sambucus nigra I	SNA-I	α-2,6 sialic acid	ST6GAL1, ST6GAL2	3.13	0.0099
Wisteria floribunda	WFA	GalNAc	B3GALNT1, B4GALNT1	2.62	0.022
Salivia horminum lectin	SHA	GalNAc	B3GALNT1, B4GALNT1	1.11	0.0106
Hippeastrum hybrid	HHA	α-1,3-Linked mannose	MAN2A1	1.95	0.0299
Narcissus pseudonarcissus	NPA	α-1,6-Linked mannose	MAN2A1	2.19	0.0179
Ulex europaeus I	UEA-I	α-1,2-Fucose structures	FUT1, FUT2	0.58	0.0364
Ricinus communis agglutinin I	RCA 120	Galactose, lactose	B4GALT1	0.17	0.005
Ricinus communis agglutinin II	RCA 60	Galactose, lactose	B4GALT1	0.46	0.0191
Phaseolus vulgaris erythroagglutinin	PHA-E	galactose	B4GALT1	0.64	0.0238

mannose extension enzymes (MAN2A1) than control C33A cells, and lower levels of lactose/galactose branching enzyme B4GALT1 and α-1,2 mannosidases (FUT1 and FUT2) (**Figures 1C, D**). In addition, poly-N-acetyllactosamine (DSA, WGA) and its corresponding enzymes (B3GNT2 and B3GNT3) showed no changes (**Figures 1A–D**). These results indicate that E6 results in altered glycosylation in cervical cancer cells. Given the strong evidence for a relationship between the glycosylation and cancer progression (18), we hypothesized that altered expression of these glycogenes and their corresponding changes in glycan epitopes may be involved in the oncogenic activities of HPV16 E6.

ST6GAL1 Is a Pivotal Oncogenic Mediator of the High-Risk HPV16 E6

Knockdown of ST6GAL1 suppresses subcutaneous tumor growth and increases cisplatin sensitivity of cervical cancer cells (35); we therefore presumed that ST6GAL1 may be a candidate oncogenic mediator of HPV16 E6 protein. To validate this speculation, we first detected ST6GAL1 expression in cervical scraping samples of patients with different subtypes of HPV infection. The expression of ST6GAL1 was significantly higher in patients infected with high-risk HPV subtypes, including $HPV16^+$, $HPV18^+$, or others (**Figure 2A**). Moreover, Ct value of ST6GAL1 showed a positive association with E6 in E6-detected cervical scraping samples (**Figure 2B**). Then, ST6GAL1 was silenced in both C33A and C33A-E6 cells *via* transient transfecting with short-hairpin RNA targeting ST6GAL1 (shST6GAL1) or a non-targeting control (shNTC) (**Figure 2C**). CCK-8 and clonogenic assays revealed that ST6GAL1 knockdown markedly attenuated the oncogenic effects of E6 on cellular proliferation (**Figure 2D**) and colony formulation (**Figures 2E, F**). Comparing to shNTC-transfected C33A-E6 cells, the apoptotic rate (**Figures 2G, H**) and expression of proapoptotic proteins, Bax and p53, were also significantly increased in cells transfected with shST6GAL1, and antiapoptotic factor Bcl-2 was significantly decreased (**Figure 2I**). Furthermore, ST6GAL1 knockdown significantly attenuated the metastatic potential of C33A-E6, including migration (**Figures 2J, K**) and invasion (**Figures 2L, M**) in wound-scratching and Transwell assays. Therefore, these data demonstrate that ST6GAL1 is a pivotal mediator for E6 to perform oncogenic activities in cervical cancer cells.

ST6GAL1 Promotes Oncogenic Activities in Both E6-Positive and E6-Negative Cervical Cancer Cells

Knockdown of ST6GAL1 suppresses the oncogenic activities of $HPV18^+$ Hela cells (35) and also HPV^- C33A cells (**Figure 2**). To further confirm the oncogenic potential of ST6GAL1 with or without the status of HPV infection, we then transiently overexpressed ST6GAL1 in both C33A and C33A-E6 cells (**Figure 3A**). Cellular proliferation (**Figure 3B**) and colony formulation (**Figures 3C, D**) of both C33A and C33A-E6 cells were significantly increased in response to ST6GAL1 overexpression. In addition, overexpression of ST6GAL1 also significantly decreased the apoptotic rates (**Figures 3E, F**) and the expression of proapoptotic proteins, Bax and p53 (**Figure 3G**) in both C33A and C33A-E6 cells. Antiapoptotic protein Bcl-2 was significantly increased in response to ST6GAL1 overexpression (**Figure 3G**). With regard to the metastatic potential, ST6GAL1 overexpression significantly increased migrating (**Figures 3H, I**) and invading (**Figures 3J, K**) abilities of both C33A and C33A-E6 cells as revealed in wound-scratching and Transwell assays. Taken together, these data demonstrate a crucial oncogenic role of ST6GAL1 in both E6-positive and E6-negative cervical cancer cells.

HPV16 E6 Promotes ST6GAL1 Expression by Activating YAP1

To identify the potent regulatory mechanism of HPV16 E6 on ST6GAL1, mRNA sequencing was performed on both C33A and C33A-E6 cells, and the results showed that E6-stable expression resulted in dysregulation of 658 mRNAs, including 439 upregulated and 219 downregulated mRNAs (**Figures 4A, B**). Importantly, 466 of 658 mRNAs were significantly associated with ST6GAL1 expression in TCGA cervical cancer dataset (**Figure 4C**). KEGG enrichment analysis revealed that these 466 mRNAs were mainly involved in glycan biosynthesis, pathways in cancer, and TGF-β, cGMP/PKG, and Hippo signaling pathways (**Figure 4D**). Next, selective enzyme inhibitors were used to examine which signaling pathway mediated the upregulation of ST6GAL1 in C33A-E6 cells. The mRNA expression of ST6GAL1 was significantly suppressed with the presence of verteporfin, an inhibitor of YAP1 in the Hippo signaling, whereas cGMP/PKG inhibitor ODQ and TGF-β inhibitor LY-364947 showed no obvious effects (**Figure 4E**). E6 stable expression in C33A cells significantly suppressed Ser397-

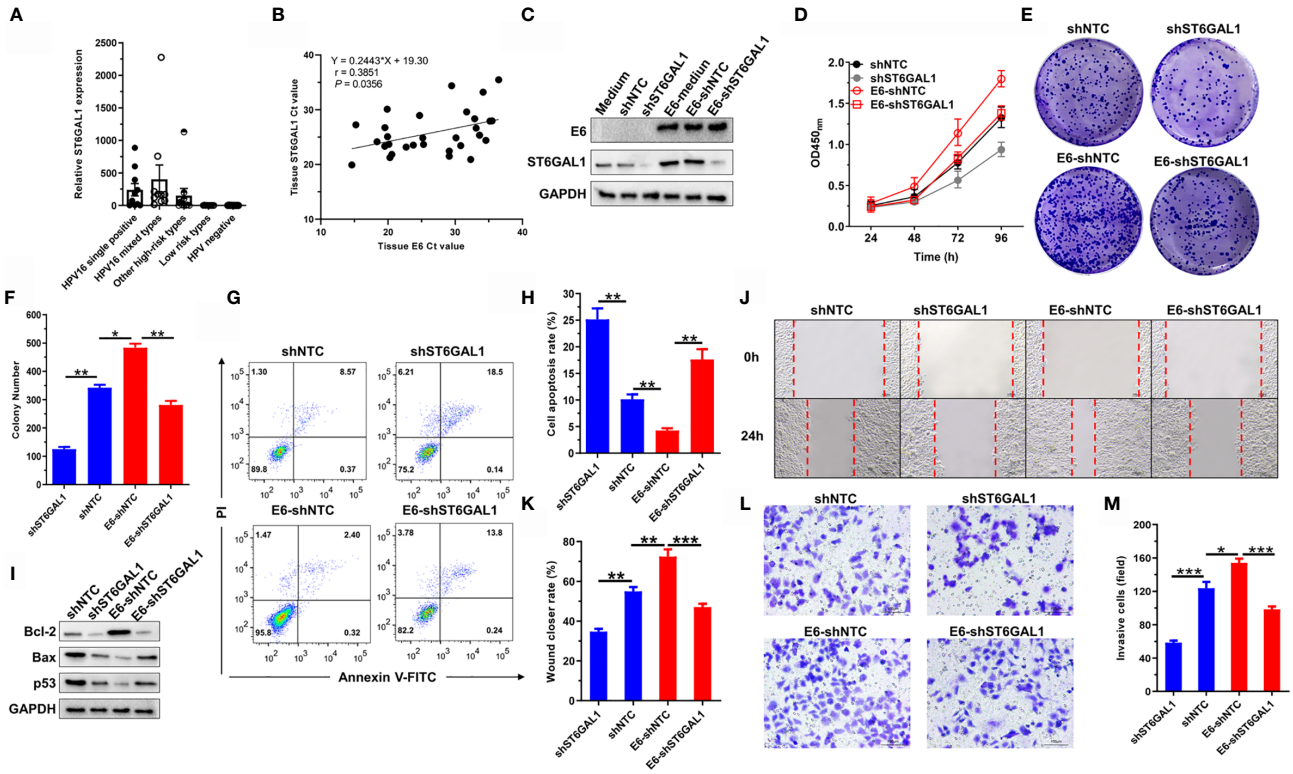


FIGURE 2 | ST6GAL1 is a pivotal oncogenic mediator of the high-risk HPV 16 E6. **(A)** Analysis of ST6GAL1 expression in cervical scraping samples of five patient groups (n = 10 in each group). HPV-negative samples were used as control group, and ST6GAL1 expression values were normalized relative to expression of the housekeeping gene GAPDH by the $2^{-\Delta\Delta Ct}$ method. **(B)** The association of ST6GAL1 to E6 in E6-detected samples was analyzed by Spearman analysis (n = 30). **(C)** C33A and C33A-E6 (E6 stable expressing) cells were transiently transfected with short hairpin RNA targeting ST6GAL1 (shST6GAL1) or a non-targeting control (shNTC). Then, protein expression of E6 and ST6GAL1 were detected by Western blot. **(D)** Proliferation of indicated cells were detected by CCK-8 assay. **(E)** The clones of indicated cells were visualized by crystal violet staining. **(F)** Statistical analysis of colony numbers in C33A and C33A-E6 cells. **(G, H)** Apoptosis of indicated cells were detected by flow cytometry, and then, apoptotic rates were statistically analyzed. **(I)** Western blot was used to detect the expression of apoptosis-related proteins. **(J, K)** Migrative abilities of indicated cells were detected by wound-healing assay and statistically analyzed. **(L, M)** Invasive abilities of indicated cells were detected by Transwell assay and statistically analyzed. Data were presented as mean ± SD from the three independent replicates. *$p < 0.05$; **$p < 0.01$; ***$p < 0.001$.

phosphorylated YAP (degradation status) and enhanced total YAP expression (**Figure 4F**). Consistent with mRNA results, only the addition of verteporfin significantly downregulated ST6GAL1 protein expression in both C33A and C33A-E6 cells (**Figure 4F**) but not ODQ (**Figure 4G**) and LY-364947 (**Figure 4H**). Thus, these findings provide compelling evidence that activation of YAP1 is critical to ST6GAL1 expression and is a major mediator of E6-induced ST6GAL1 upregulation.

ST6GAL1 Activates cGMP/PKG Signal Axis to Play Oncogenic Activities

We next examined the effects of ST6GAL1 on TGF-β, cGMP/PKG, and Hippo signaling pathways. The phosphorylation of VASP (a major effector indicates cGMP/PKG signaling activation) and Smad was significantly increased by ST6GAL1 overexpression and *vice versa* for ST6GAL1 knockdown (**Figure 5A**). The expression of E-cadherin was significantly reduced, and YAP1 expression showed no response to ST6GAL1 overexpression (**Figure 5A**). These results indicated that ST6GAL1 activates both cGMP/PKG and TGF-β signaling. Activation of cGMP/PKG promotes chemoresistance and maintenance of cancer stem cells in cervical, breast, ovarian, and gastric cancers (32, 36). Thus, we further investigated the therapeutic potential of cGMP/PKG inhibitor ODQ on ST6GAL1 overexpression. The ST6GAL1-enhanced cellular proliferation (**Figure 5B**) and colony formulation (**Figures 5C, D**) of C33A cells were significantly suppressed by ODQ treatment. In addition, ODQ also significantly promoted apoptosis (**Figures 5E, F**) and blocked the migration (**Figures 5G, H**) and invasion (**Figures 5I, J**) of ST6GAL1-overexpressing cells. Taken together, these results demonstrate that ST6GAL1 depends on activating cGMP/PKG signaling axis to play oncogenic activities in C33A cervical cancer cells.

HPV16 E6 Activates cGMP/PKG Signaling Pathway Through ST6GAL1

The activation of cGMP/PKG signaling plays oncogenic roles in both HPV16$^+$ Siha and HPV18$^+$ Hela cells (37). Thus, we further evaluated whether HPV16 E6 activates cGMP/PKG signaling and the role of ST6GAL1 in this process. As expected, the

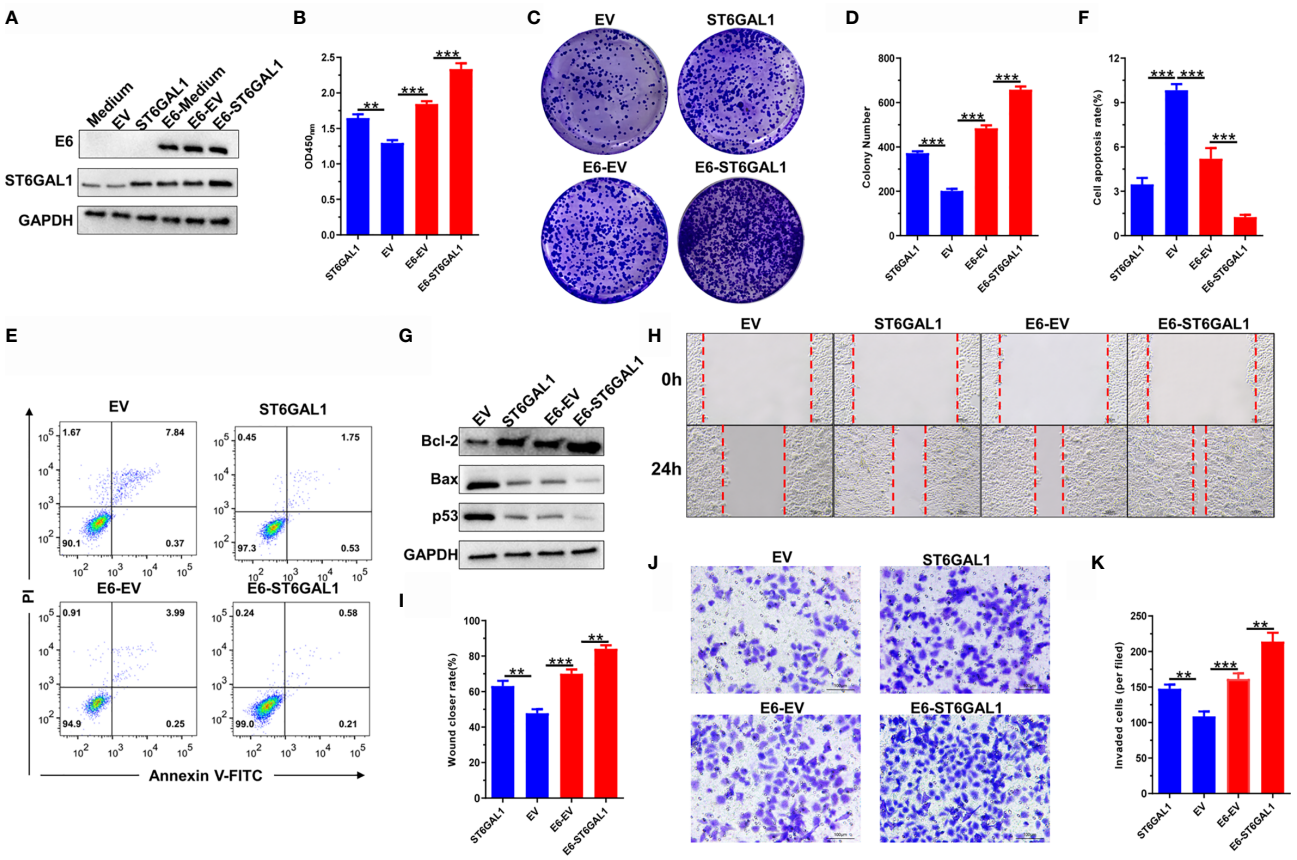


FIGURE 3 | ST6GAL1 promotes oncogenic activities in both E6-positive and E6-negative cervical cancer cells. **(A)** C33A and C33A-E6 (E6 stable expressing) cells were transiently transfected with pcDNA3.1-ST6GAL1 overexpressing plasmid (ST6GAL1) or empty vector (EV). Then, protein expression of E6 and ST6GAL1 were detected by Western blot. **(B)** Proliferation of indicated cells were detected by CCK-8 assay. **(C)** The clones of indicated cells were visualized by crystal violet staining. **(D)** Statistical analysis of colony numbers in C33A and C33A-E6 cells. **(E, F)** Apoptosis of indicated cells were detected by flow cytometry, and then, apoptotic rates were statistically analyzed. **(G)** Western blot was used to detect the expression of apoptosis-related proteins. **(H, I)** Migrative abilities of indicated cells were detected by wound-healing assay and statistically analyzed. **(J, K)** Invasive abilities of indicated cells were detected by Transwell assay and statistically analyzed. Data were presented as mean ± SD from the three independent replicates. $^{**}p < 0.01$; $^{***}p < 0.001$.

molecules indicate that cGMP/PKG signaling activation, including sGC, PKG1, PKG2, PDE5A, and p-VASP, was significantly upregulated by E6-stable expression in HPV$^-$ C33A cells (**Figure 6A**). ST6GAL1 knockdown markedly attenuated E6-induced activation of cGMP/PKG signaling, and its overexpression further elevated p-VASP levels in C33A-E6 cells (**Figure 6B**). These results indicate that HPV16 E6 activates cGMP/PKG signaling in cervical cancer cells, and ST6GAL1 is critical for this process. The effects of ODQ on E6-mediated oncogenic activities were next evaluated, and the results revealed that ODQ significantly suppressed cellular proliferation (**Figure 6C**) and colony formulation (**Figures 6D, E**) in both C33A and C33A-E6 cells. The apoptotic rates were also increased in response to ODQ treatment (**Figures 6F, G**). Furthermore, the migration (**Figures 6H, I**) and invasion (**Figures 6J, K**) of both C33A and C33A-E6 cells were significantly decreased with the presence of ODQ. Taken together, these data demonstrate a requirement for ST6GAL1-cGMP/PKG signaling axis in oncogenic properties of E6 and supports its inhibition as a viable therapeutic strategy against cervical cancer.

DISCUSSION

HPV16 E6 oncoprotein plays multifunctional roles on post-translational modifications (PTMs), including ubiquitination, acetylation, and phosphorylation, and thereby contributes to the viral life cycle and to the induction of malignancy (38–40). Serving as an important kind of PTMs, glycosylation can act as a key regulatory mechanism to control cancer progression and highlight its application in the clinical setting as appealing targets for personalized medicine (41). However, the glycosylation alterations that associated with HPV infection and their role in controlling the progression of cervical cancer remain largely unknown. In the present study, our results confirmed that HPV16 E6 oncoprotein induces significant glycosylation

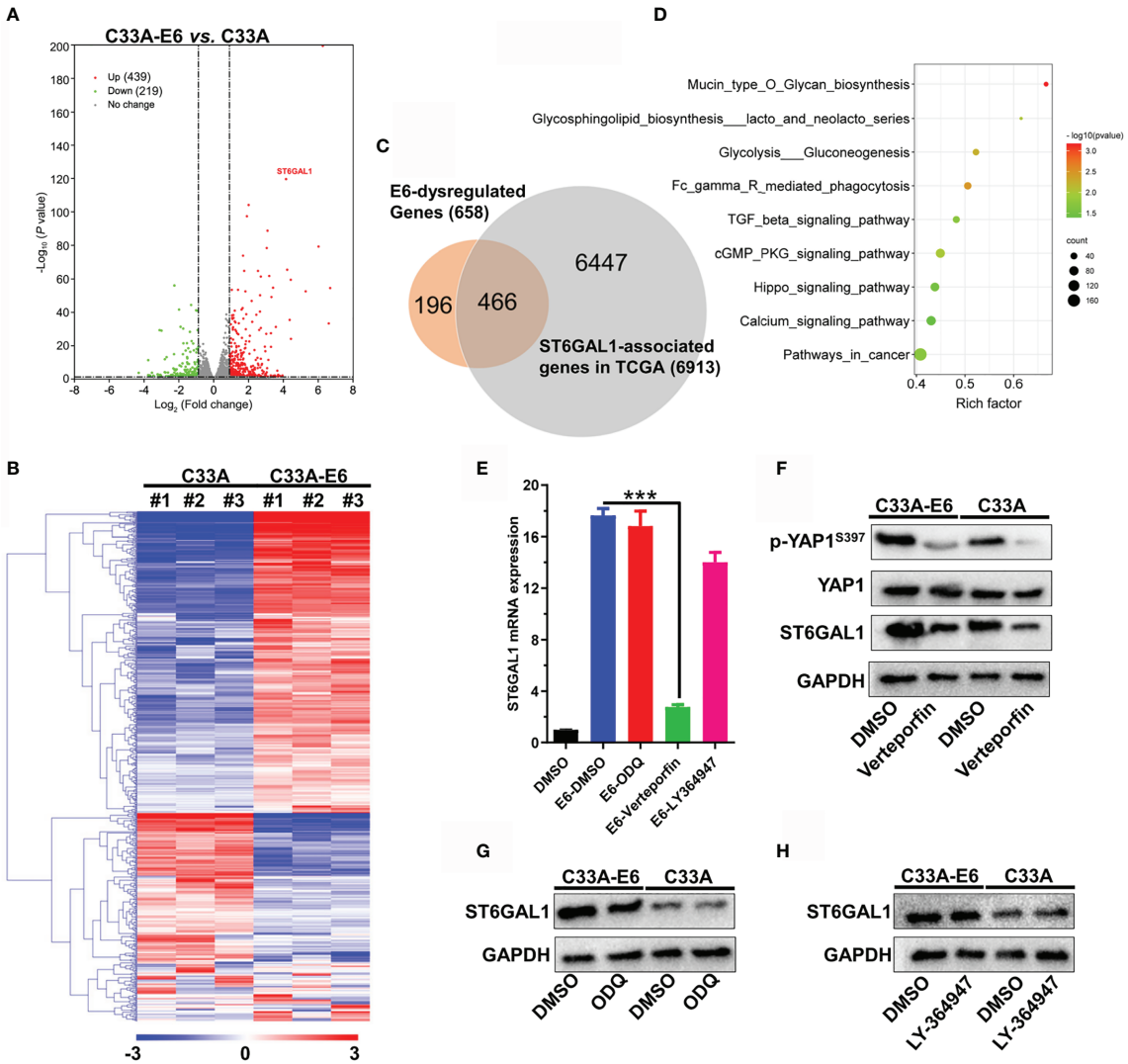


FIGURE 4 | HPV16 E6 promotes ST6GAL1 expression by activating Hippo signaling pathway. **(A)** Dysregulated mRNAs between C33A and C33A-E6 (E6 stable expressing) cells were detected by mRNA sequencing. **(B)** Heat map and hierarchical clustering analysis of 658 dysregulated mRNAs with three independent biological replicates were presented. **(C)** Venn diagram of 658 E6-dysregulated mRNAs and 6,913 ST6GAL1-asscociated mRNAs in TCGA dataset (N = 305). ST6GAL1-associated mRNAs were identified using R2: Genomics Analysis and Visualization Platform (http://r2.amc.nl). **(D)** KEGG enrichment analysis of 466 mRNAs that simultaneously associated with E6 and ST6GAL1. **(E)** C33A and C33A-E6 cells were treated with verteporfin (5 μM, Hippo signaling inhibitor), ODQ (10 μM, cGMP/PKG inhibitor), and LY-364947 (5 μM, TGF-β inhibitor) for 24 h, and then, qRT-PCR was used to detect ST6GAL1 mRNA expression. DMSO was used as solvent control. ST6GAL1 protein expression of C33A and C33A-E6 cells in response to **(F)** verteporfin, **(G)** ODQ, and **(H)** LY-364947 treatment was detected by Western blot. Data were presented as mean ± SD from the three independent replicates. ***$p < 0.001$.

alterations in HPV$^-$ C33A cells *via* using 95-lectins microarray, including increased expression of α-2,6 sialic acids (corresponding glycotransferases, ST6GAL1, ST6GAL2), α-1,3- and α-1,6-linked mannose (MAN2A1), and N-acetylgalactosamine (B3GALNT1, B4GALNT1), and decreased levels of lactose/galactose (B4GALT1) and α-1,2 fucose structures (FUT1, FUT2).

Remarkably, numerous studies have confirmed that these glycosylation alterations induced by E6 stable expression play important roles in modulating cancer signaling, tumor progression, metastasis, antitumor immunity, and responses of current cancer-targeted therapies (18). For example, FUT1 and FUT2 promote growth, adhesion, migration, and cancer stem cell (CSC) properties of breast cancer (42). Increased expression of B4GALNT1 promotes metastasis of lung adenocarcinoma and melanoma (43, 44). B4GALT1 upregulates glycosylation of CDK11^{p110} and therefore confers chemoresistance of pancreatic ductal adenocarcinomas (45). Although poly-N-acetyllactosamine and its corresponding glycotransferases (B3GNT2 and B3GNT3) that facilitate PD-L1/PD-1 stabilization and interaction (19–21) showed no changes in response to exogenous E6 expression, the enhanced MAN2A1 expression has been reported to result in the dysfunction of T cells in tumor microenvironment, and its

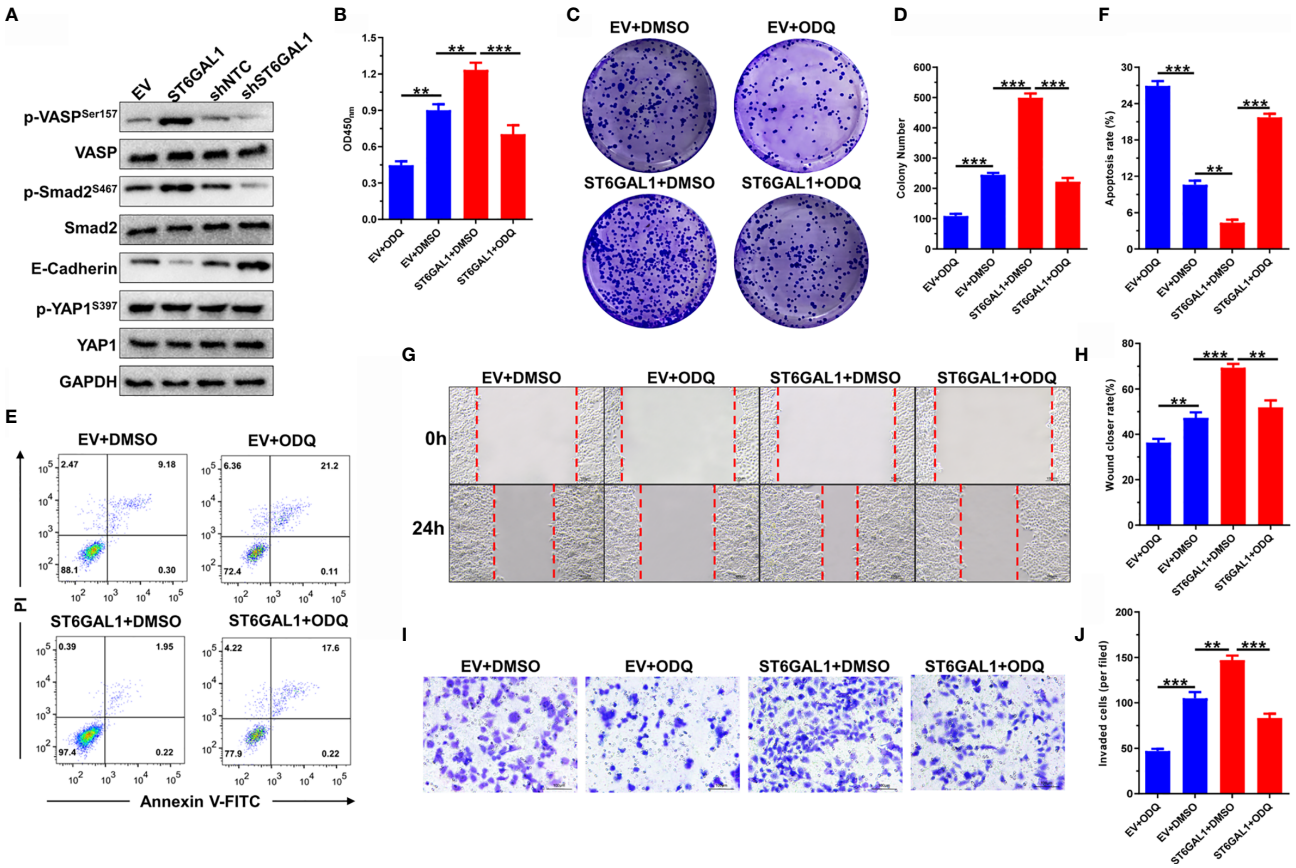


FIGURE 5 | ST6GAL1 activates cGMP/PKG signal axis to play oncogenic activities. **(A)** C33A cells were transiently transfected with pcDNA3.1-ST6GAL1 overexpressing plasmid (ST6GAL1), empty vector (EV), short hairpin RNA targeting ST6GAL1 (shST6GAL1), or a non-targeting control (shNTC). Forty-eight hours later, expression of classic proteins involved in TGF-β, cGMP/PKG, and Hippo signaling pathways were detected by Western blot. **(B)** Proliferation of indicated cells were detected by CCK-8 assay. **(C)** The clones of indicated cells were visualized by crystal violet staining. **(D)** Statistical analysis of colony numbers in C33A cells received indicated treatment. **(E, F)** Apoptosis of indicated cells were detected by flow cytometry, and then, apoptotic rates were statistically analyzed. **(G, H)** Migrative abilities of indicated cells were detected by wound-healing assay and statistically analyzed. **(I, J)** Invasive abilities of indicated cells were detected by Transwell assay and statistically analyzed. Data were presented as mean ± SD from the three independent replicates. $^{**}p < 0.01$; $^{***}p < 0.001$.

inhibition enhances the immune response to anti-PD-L1 in human tumors (46). More importantly, HPV16 or HPV18 E6 enhances c-MYC stability *via* promoting its *O*-GlcNAcylation on Thr58 (28). Knockdown of O-GlcNAc transferase (OGT) or ST6GAL1 suppresses tumorigenesis and metastasis of HPV18$^+$ cervical cancer Hela cells (28, 35). Hence, alteration of glycosylation is apparently a crucial step for the E6 to initiate and promote cervical cancer progression and urgently needs to be clarified in future.

ST6GAL1, responsible for the terminal α2,6-sialylation of *N*-glycans, can be upregulated by HPV16 E5 oncoprotein, and its inhibition increases cisplatin sensitivity of HPV18$^+$ cervical cancer cells (35, 47). In the present study, we found that ST6GAL1 expression in cervical scraping samples is significantly increased in patients infected with high-risk HPV subtypes (HPV16, HPV18, HPV52, etc.) compared to low-risk subtypes or HPV-negative samples. Because all the samples with various groups of patients (HPV positive and/or negative) were collected from Asian origin, this could represent a limitation. For further studies, possibly multicenter (e.g., American Indian or Alaska Native, Indian, Black or African American, and White ethnicity) and with a larger number of patients (especially in developing countries where cervical cancer is still widespread) will be enrolled. Furthermore, ST6GAL1 positively associates with E6 expression in cervical samples and serves as an important oncogenic mediator in both HPV16 E6-positive and E6-negative C33A cervical cancer cells. Due to having a type I PDZ binding motif (PBM) at the C-terminus, high-risk HPV E6 proteins interacts with many PDZ proteins, like PTPN3, LRCC1, and DLG1, and thus promotes the nuclear localization of transcriptional coactivator YAP1, the major effector of the Hippo pathway (48). Through mRNA sequencing and associated molecular analysis, we found that YAP1 is a pivotal mediator for E6 to induce ST6GAL1 expression. Taken together, we thus speculated that ST6GAL1 may have an important role in cervical cancer, especially in high-risk HPV-induced carcinogenesis.

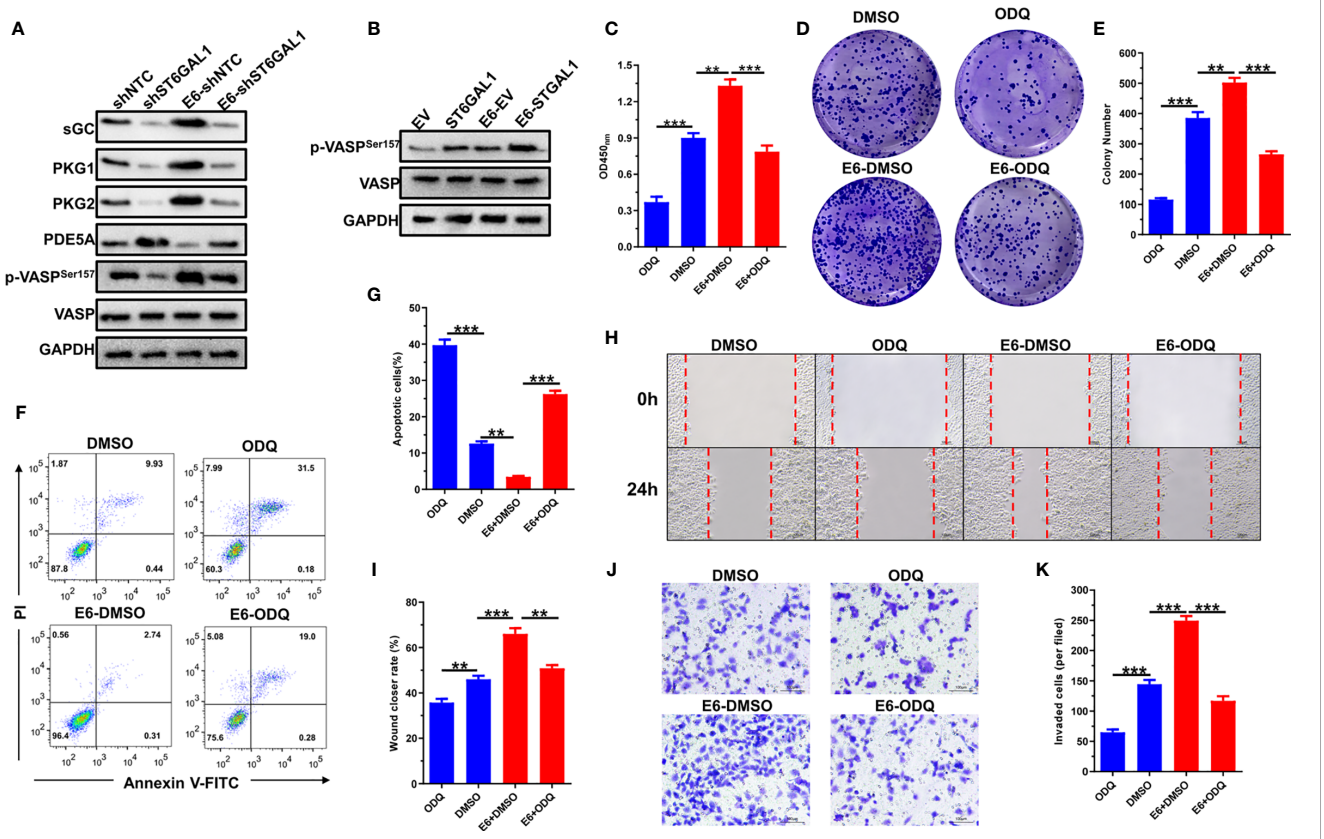


FIGURE 6 | HPV16 E6 activates cGMP/PKG signaling pathway through ST6GAL1. **(A)** C33A and C33A-E6 (E6 stable expressing) cells were transiently transfected with short hairpin RNA targeting ST6GAL1 (shST6GAL1) or a non-targeting control (shNTC). Forty-eight hours later, the expression of cGMP/PKG signaling pathway-related proteins were detected by Western blot. **(B)** C33A and C33A-E6 cells were transiently transfected with pcDNA3.1-ST6GAL1 overexpressing plasmid (ST6GAL1) or empty vector (EV). Forty-eight hours later, phosphorylated VASP expression in indicated cells were detected by Western blot. **(C)** Proliferation of indicated cells were detected by CCK-8 assay. **(D)** The clones of indicated cells were visualized by crystal violet staining. **(E)** Statistical analysis of colony numbers in indicated cells. **(F, G)** Apoptosis of indicated cells were detected by flow cytometry, and then, apoptotic rates were statistically analyzed. **(H, I)** Migrative abilities of indicated cells were detected by wound-healing assay and statistically analyzed. **(J, K)** Invasive abilities of indicated cells were detected by Transwell assay and statistically analyzed. Data were presented as mean ± SD from the three independent replicates. $^{**}p < 0.01$; $^{***}p < 0.001$.

Hippo/YAP signaling pathway plays a critical role in the progression of cervical cancer and can further interact with the ErbB2 and EGFR RTKs to form a positive feedback autocrine/paracrine loop (49). ST6GAL1 endows resistance of cancer cells to gefitinib (EGFR inhibitor) and trastuzumab (anti-ErbB2 antibody) (25) and also confers tumor cell resistance against hypoxia *via* enhancing hypoxia-inducible factor-1α (HIF-1α) expression (50). Recently, molecular analysis has confirmed that ST6GAL1 decreases the sensitization of cancer cells to trastuzumab-induced cytotoxicity through directly enhancing α2,6-sialylation of ErbB2, which results in the increased activation of both ErbB2 and EGFR RTKs (51). Thus, ST6GAL1 may serve as a linker that bridges Hippo/YAP signaling and RTKs activation. With the fact that hyperactivation of genes involved in Hippo/YAP signaling–RTKs-positive feedback loop occurring in most advanced/recurrent cervical cancer patients (>70%) (9, 49, 52) and directly targeting the HPV-16 E6 has been shown to be ineffective for invasive cancer by itself alone (8), target inhibition of ST6GAL1 may be a promising combinational therapeutic strategy for RTK inhibitors or E6-directed therapies in cervical cancer.

In the present study, since we did not perform in-depth mass spectrometry-based glycomic and glycoproteomic analysis, the exact target proteins of ST6GAL1 cannot be confirmed. However, we found that ST6GAL1 activates cGMP/PKG and TGF-β signaling according to the data obtained in mRNA sequencing and association analysis. Aberrant activation of cGMP/PKG signaling promotes chemoresistance, maintenance of cancer stem cells, and cell survival in various human cancers, including lung, cervical, breast, ovarian, and gastric cancers (32, 37). Moreover, we found that blocking cGMP/PKG signaling with ODQ eliminates the oncogenic activities of both E6 and ST6GAL1 in cervical cancer cells. The puzzled question is that activation of cGMP/PKG signaling induces MST/LATS kinases, resulting in the phosphorylation and cytosolic degradation of YAP1 in prostate cancer cells (53), while HPV16 E6 has been showed to have little or no effect on the LATS1/2 (49). Thus, E6

may play a sophisticated role in the progression of cervical cancer, and the detailed molecular targets of ST6GAL1 need to be further identified for unveiling its contribution in E6-induced carcinogenesis.

CONCLUSION

In this paper, we demonstrated that high-risk HPV16 E6 oncoprotein induced significant glycosylation alterations in cervical cancer cells. In-depth analyses further revealed that α2,6-sialyltransferase, ST6GAL1, was a novel E6-induced oncogenic protein and performed oncogenic activities in both E6-positive and E6-negative cervical cancer cells. E6 depended on YAP1 to stimulate ST6GAL1 expression and subsequently resulted in the activation of downstream cGMP/PKG pathway. Most importantly, knockdown ST6GAL1 or target inhibition of cGMP/PKG pathway suppressed colony formulation and metastasis of cervical cancer cells. Therefore, ST6GAL1 or cGMP/PKG signaling might be novel targets for the development of drugs against cervical cancer.

DATA AVAILABILITY STATEMENT

The datasets presented in this study can be found in online repositories. The names of the repository/repositories and accession number(s) can be found in https://portal.gdc.cancer.gov/.

ETHICS STATEMENT

The studies involving human participants were reviewed and approved by Institutional Review Board of the Wuhan Children's Hospital (Wuhan Maternal and Child Healthcare Hospital). Written informed consent for participation was not required for this study in accordance with the national legislation and the institutional requirements.

AUTHOR CONTRIBUTIONS

DT, YH, YX, and TX: study conception and design. JW, GL, ML, QC, CYao, and HC: data acquisition. CYuan and NS: analysis and data interpretation. JW and GL: drafting of the manuscript. All authors contributed to the article and approved the submitted version.

FUNDING

This study was supported by the National Natural Science Foundation of China (81760540 and 82060539), Natural Science Foundation of Wuhan Municipal Health Commission (grant no. WX18Q27), Natural Science Foundation of Hubei Municipal Health Commission (grant no. WJ2021M016), The Top Medical Young Talents of Hubei Province (2016), and The Open Research Fund Program of the State Key Laboratory of Virology of China (grant no. 2015KF010).

SUPPLEMENTARY MATERIAL

The Supplementary Material for this article can be found online at: https://www.frontiersin.org/articles/10.3389/fonc.2021.716246/full#supplementary-material

REFERENCES

1. Sung H, Ferlay J, Siegel RL, Laversanne M, Soerjomataram I, Jemal A, et al. Global Cancer Statistics 2020: GLOBOCAN Estimates of Incidence and Mortality Worldwide for 36 Cancers in 185 Countries. *CA Cancer J Clin* (2021) 71(3):209–49. doi: 10.3322/caac.21660
2. Olusola P, Banerjee HN, Philley JV, Dasgupta S. Human Papilloma Virus-Associated Cervical Cancer and Health Disparities. *Cells* (2019) 8(6):622. doi: 10.3390/cells8060622
3. National Institutes of Health. Virus Genome Variants. In *PapillomaVirus Episteme*. Bethesda, MA, USA: NIH. (2019). Available at: https://pave.niaid.nih.gov/#.
4. Bhatt KH, Neller MA, Srihari S, Crooks P, Lekieffre L, Aftab BT, et al. Profiling HPV-16-Specific T Cell Responses Reveals Broad Antigen Reactivities in Oropharyngeal Cancer Patients. *J Exp Med* (2020) 217(10): e20200389. doi: 10.1084/jem.20200389
5. Long W, Yang Z, Li X, Chen M, Liu J, Zhang Y, et al. HPV-16, HPV-58, and HPV-33 Are the Most Carcinogenic HPV Genotypes in Southwestern China and Their Viral Loads Are Associated With Severity of Premalignant Lesions in the Cervix. *Virol J* (2018) 15(1):94. doi: 10.1186/s12985-018-1003-x
6. Buskwofie A, David-West G, Clare CA. A Review of Cervical Cancer: Incidence and Disparities. *J Natl Med Assoc* (2020) 112(2):229–32. doi: 10.1016/j.jnma.2020.03.002
7. Chen W, Zheng R, Baade PD, Zhang S, Zeng H, Bray F, et al. Cancer Statistics in China, 2015. *CA Cancer J Clin* (2016) 66(2):115–32. doi: 10.3322/caac.21338
8. Massarelli E, William W, Johnson F, Kies M, Ferrarotto R, Guo M, et al. Combining Immune Checkpoint Blockade and Tumor-Specific Vaccine for Patients With Incurable Human Papillomavirus 16-Related Cancer: A Phase 2 Clinical Trial. *JAMA Oncol* (2019) 5(1):67–73. doi: 10.1001/jamaoncol.2018.4051
9. Burk RD, Chen Z, Saller C, Tarvin K, Carvalho AL, Scapulatempo-Neto C, et al. Integrated Genomic and Molecular Characterization of Cervical Cancer. *Nature* (2017) 543(7645):378–84. doi: 10.1038/nature21386
10. Kuguyo O, Tsikai N, Thomford NE, Magwali T, Madziyire MG, Nhachi CFB, et al. Genetic Susceptibility for Cervical Cancer in African Populations: What Are the Host Genetic Drivers? *OMICS* (2018) 22(7):468–83. doi: 10.1089/omi.2018.0075
11. Tewari KSS, M W, Long HJ. Improved Survival With Bevacizumab in Advanced Cervical Cancer. *N Engl J Med* (2017) 377(7):702. doi: 10.1056/NEJMx170002
12. Li S, Hong X, Wei Z, Xie M, Li W, Liu G, et al. Ubiquitination of the HPV Oncoprotein E6 Is Critical for E6/E6AP-Mediated P53 Degradation. *Front Microbiol* (2019) 10:2483. doi: 10.3389/fmicb.2019.02483
13. Katzenellenbogen R. Telomerase Induction in HPV Infection and Oncogenesis. *Viruses* (2017) 9(7):180. doi: 10.3390/v9070180
14. Thomas M, Myers MP, Massimi P, Guarnaccia C, Banks L. Analysis of Multiple HPV E6 PDZ Interactions Defines Type-Specific PDZ Fingerprints That Predict Oncogenic Potential. *PloS Pathog* (2016) 12(8):e1005766. doi: 10.1371/journal.ppat.1005766
15. Wang Q, Song R, Zhao C, Liu H, Yang Y, Gu S, et al. HPV16 E6 Promotes Cervical Cancer Cell Migration and Invasion by Downregulation of NHERF1. *Int J Cancer* (2019) 144(7):1619–32. doi: 10.1002/ijc.31876
16. Draper LM, Kwong ML, Gros A, Stevanović S, Tran E, Kerkar S, et al. Targeting of HPV-16+ Epithelial Cancer Cells by TCR Gene Engineered T

Cells Directed Against E6. *Clin Cancer Res* (2015) 21(19):4431–9. doi: 10.1158/1078-0432.ccr-14-3341
17. Celegato M, Messa L, Goracci L, Mercorelli B, Bertagnin C, Spyrakis F, et al. A Novel Small-Molecule Inhibitor of the Human Papillomavirus E6-P53 Interaction That Reactivates P53 Function and Blocks Cancer Cells Growth. *Cancer Lett* (2020) 470:115–25. doi: 10.1016/j.canlet.2019.10.046
18. Mereiter S, Balmaña M, Campos D, Gomes J, Reis CA. Glycosylation in the Era of Cancer-Targeted Therapy: Where Are We Heading? *Cancer Cell* (2019) 36(1):6–16. doi: 10.1016/j.ccell.2019.06.006
19. Lee HH, Wang YN, Xia W, Chen CH, Rau KM, Ye L, et al. Removal of N-Linked Glycosylation Enhances PD-L1 Detection and Predicts Anti-PD-1/PD-L1 Therapeutic Efficacy. *Cancer Cell* (2019) 36(2):168–78.e4. doi: 10.1016/j.ccell.2019.06.008
20. Li CW, Lim SO, Chung EM, Kim YS, Park AH, Yao J, et al. Eradication of Triple-Negative Breast Cancer Cells by Targeting Glycosylated PD-L1. *Cancer Cell* (2018) 33(2):187–201.e10. doi: 10.1016/j.ccell.2018.01.009
21. Sun L, Li CW, Chung EM, Yang R, Kim YS, Park AH, et al. Targeting Glycosylated PD-1 Induces Potent Antitumor Immunity. *Cancer Res* (2020) 80(11):2298–310. doi: 10.1158/0008-5472.can-19-3133
22. Liu Y-C, Yen H-Y, Chen C-Y, Chen C-H, Cheng P-F, Juan Y-H, et al. Sialylation and Fucosylation of Epidermal Growth Factor Receptor Suppress Its Dimerization and Activation in Lung Cancer Cells. *Proc Natl Acad Sci USA* (2011) 108(28):11332–7. doi: 10.1073/pnas.1107385108
23. Mereiter S, Magalhães A, Adamczyk B, Jin C, Almeida A, Drici L, et al. Glycomic Analysis of Gastric Carcinoma Cells Discloses Glycans as Modulators of RON Receptor Tyrosine Kinase Activation in Cancer. *Biochim Biophys Acta* (2016) 1860(8):1795–808. doi: 10.1016/j.bbagen.2015.12.016
24. Wichert B, Milde-Langosch K, Galatenko V, Schmalfeldt B, Oliveira-Ferrer L. Prognostic Role of the Sialyltransferase ST6GAL1 in Ovarian Cancer. *Glycobiology* (2018) 28(11):898–903. doi: 10.1093/glycob/cwy065
25. Myojin Y, Kodama T, Maesaka K, Motooka D, Sato Y, Tanaka S, et al. ST6GAL1 Is a Novel Serum Biomarker for Lenvatinib-Susceptible FGF19-Driven Hepatocellular Carcinoma. *Clin Cancer Res* (2021) 27(4):1150–61. doi: 10.1158/1078-0432.ccr-20-3382
26. Jin Y, Kim SC, Kim HJ, Ju W, Kim YH, Kim HJ. Increased Sialylation and Reduced Fucosylation of Exfoliated Cervical Cells Are Potential Markers of Carcinogenesis in the Cervix. *Clin Chem Lab Med* (2016) 54(11):1811–9. doi: 10.1515/cclm-2015-1014
27. Rivera-Juarez Mde L, Rosas-Murrieta NH, Mendieta-Carmona V, Hernandez-Pacheco RE, Zamora-Ginez I, Rodea-Avila C, et al. Promoter Polymorphisms of ST3GAL4 and ST6GAL1 Genes and Associations With Risk of Premalignant and Malignant Lesions of the Cervix. *Asian Pac J Cancer Prev* (2014) 15(3):1181–6. doi: 10.7314/apjcp.2014.15.3.1181
28. Zeng Q, Zhao RX, Chen J, Li Y, Li XD, Liu XL, et al. O-Linked GlcNAcylation Elevated by HPV E6 Mediates Viral Oncogenesis. *Proc Natl Acad Sci USA* (2016) 113(33):9333–8. doi: 10.1073/pnas.1606801113
29. Wang PH, Lee WL, Lee YR, Juang CM, Chen YJ, Chao HT, et al. Enhanced Expression of Alpha 2,6-Sialyltransferase ST6Gal I in Cervical Squamous Cell Carcinoma. *Gynecol Oncol* (2003) 89(3):395–401. doi: 10.1016/s0090-8258(03)00127-6
30. Wang J, Xiang F, Liu X, Ma X, Cai X, Yang Y, et al. HPV E7 Affects the Function of Cervical Cancer Cells via the TAL1/lnc–EBIC/KLHDC7B Axis. *Oncol Rep* (2021) 45(5):51. doi: 10.3892/or.2021.8002
31. Xiang F, Guan Q, Liu X, Xiao H, Xia Q, Liu X, et al. Distribution Characteristics of Different Human Papillomavirus Genotypes in Women in Wuhan, China. *J Clin Lab Anal* (2018) 32(8):e22581. doi: 10.1002/jcla.22581
32. Xiang T, Yuan C, Guo X, Wang H, Cai Q, Xiang Y, et al. The Novel ZEB1-Upregulated Protein PRTG Induced by Helicobacter Pylori Infection Promotes Gastric Carcinogenesis Through the cGMP/PKG Signaling Pathway. *Cell Death Dis* (2021) 12(2):150. doi: 10.1038/s41419-021-03440-1
33. Qin Y, Zhong Y, Zhu M, Dang L, Yu H, Chen Z, et al. Age- and Sex-Associated Differences in the Glycopatterns of Human Salivary Glycoproteins and Their Roles Against Influenza A Virus. *J Proteome Res* (2013) 12(6):2742–54. doi: 10.1021/pr400096w
34. Tang XL, Yuan CH, Ding Q, Zhou Y, Pan Q, Zhang XL. Selection and Identification of Specific Glycoproteins and Glycan Biomarkers of Macrophages Involved in Mycobacterium Tuberculosis Infection. *Tuberculosis (Edinb)* (2017) 104:95–106. doi: 10.1016/j.tube.2017.03.010
35. Zhang X, Pan C, Zhou L, Cai Z, Zhao S, Yu D. Knockdown of ST6Gal-I Increases Cisplatin Sensitivity in Cervical Cancer Cells. *BMC Cancer* (2016) 16(1):949. doi: 10.1186/s12885-016-2981-y
36. Klutzny S, Anurin A, Nicke B, Regan JL, Lange M, Schulze L, et al. PDE5 Inhibition Eliminates Cancer Stem Cells via Induction of PKA Signaling. *Cell Death Dis* (2018) 9(2):192. doi: 10.1038/s41419-017-0202-5
37. Gong L, Lei Y, Tan X, Dong Y, Luo Z, Zhang D, et al. Propranolol Selectively Inhibits Cervical Cancer Cell Growth by Suppressing the cGMP/PKG Pathway. *BioMed Pharmacother* (2019) 111:1243–8. doi: 10.1016/j.biopha.2019.01.027
38. Chen X, Loo JX, Shi X, Xiong W, Guo Y, Ke H, et al. E6 Protein Expressed by High-Risk HPV Activates Super-Enhancers of the EGFR and C-MET Oncogenes by Destabilizing the Histone Demethylase KDM5C. *Cancer Res* (2018) 78(6):1418–30. doi: 10.1158/0008-5472.can-17-2118
39. Basukala O, Sarabia-Vega V, Banks L. Human Papillomavirus Oncoproteins and Post-Translational Modifications: Generating Multifunctional Hubs for Overriding Cellular Homeostasis. *Biol Chem* (2020) 401(5):585–99. doi: 10.1515/hsz-2019-0408
40. Niebler M, Qian X, Höfler D, Kogosov V, Kaewprag J, Kaufmann AM, et al. Post-Translational Control of IL-1β via the Human Papillomavirus Type 16 E6 Oncoprotein: A Novel Mechanism of Innate Immune Escape Mediated by the E3-Ubiquitin Ligase E6-AP and P53. *PloS Pathog* (2013) 9(8):e1003536. doi: 10.1371/journal.ppat.1003536
41. Pinho SS, Reis CA. Glycosylation in Cancer: Mechanisms and Clinical Implications. *Nat Rev Cancer* (2015) 15(9):540–55. doi: 10.1038/nrc3982
42. Lai TY, Chen IJ, Lin RJ, Liao GS, Yeo HL, Ho CL, et al. Fucosyltransferase 1 and 2 Play Pivotal Roles in Breast Cancer Cells. *Cell Death Discov* (2019) 5:74. doi: 10.1038/s41420-019-0145-y
43. Yoshida H, Koodie L, Jacobsen K, Hanzawa K, Miyamoto Y, Yamamoto M. B4GALNT1 Induces Angiogenesis, Anchorage Independence Growth and Motility, and Promotes Tumorigenesis in Melanoma by Induction of Ganglioside GM2/GD2. *Sci Rep* (2020) 10(1):1199. doi: 10.1038/s41598-019-57130-2
44. Jiang T, Wu H, Lin M, Yin J, Tan L, Ruan Y, et al. B4GALNT1 Promotes Progression and Metastasis in Lung Adenocarcinoma Through JNK/c-Jun/Slug Pathway. *Carcinogenesis* (2021) 42(4):621–30. doi: 10.1093/carcin/bgaa141
45. Chen Y, Su L, Huang C, Wu S, Qiu X, Zhao X, et al. Galactosyltransferase B4GALT1 Confers Chemoresistance in Pancreatic Ductal Adenocarcinomas by Upregulating N-Linked Glycosylation of CDK11(P110). *Cancer Lett* (2021) 500:228–43. doi: 10.1016/j.canlet.2020.12.006
46. Shi S, Gu S, Han T, Zhang W, Huang L, Li Z, et al. Inhibition of MAN2A1 Enhances the Immune Response to Anti-PD-L1 in Human Tumors. *Clin Cancer Res* (2020) 26(22):5990–6002. doi: 10.1158/1078-0432.ccr-20-0778
47. Cisneros-Ramírez D, Martínez-Laguna Y, Martínez-Morales P, Aguilar-Lemarroy A, Jave-Suárez LF, Santos-López G, et al. Glycogene Expression Profiles From a HaCaT Cell Line Stably Transfected With HPV16 E5 Oncogene. *Mol Med Rep* (2020) 22(6):5444–53. doi: 10.3892/mmr.2020.11630
48. Webb Strickland S, Brimer N, Lyons C, Vande Pol SB. Human Papillomavirus E6 Interaction With Cellular PDZ Domain Proteins Modulates YAP Nuclear Localization. *Virology* (2018) 516:127–38. doi: 10.1016/j.virol.2018.01.003
49. He C, Mao D, Hua G, Lv X, Chen X, Angeletti PC, et al. The Hippo/YAP Pathway Interacts With EGFR Signaling and HPV Oncoproteins to Regulate Cervical Cancer Progression. *EMBO Mol Med* (2015) 7(11):1426–49. doi: 10.15252/emmm.201404976
50. Jones RB, Dorsett KA, Hjelmeland AB, Bellis SL. The ST6Gal-I Sialyltransferase Protects Tumor Cells Against Hypoxia by Enhancing HIF-1α Signaling. *J Biol Chem* (2018) 293(15):5659–67. doi: 10.1074/jbc.RA117.001194
51. Duarte HO, Rodrigues JG, Gomes C, Hensbergen PJ, Ederveen ALH, de Ru AH, et al. ST6Gal1 Targets the Ectodomain of ErbB2 in a Site-Specific Manner and Regulates Gastric Cancer Cell Sensitivity to Trastuzumab. *Oncogene* (2021) 40(21):3719–33. doi: 10.1038/s41388-021-01801-w
52. Zammataro L, Lopez S, Bellone S, Pettinella F, Bonazzoli E, Perrone E, et al. Whole-Exome Sequencing of Cervical Carcinomas Identifies Activating ERBB2 and PIK3CA Mutations as Targets for Combination Therapy. *Proc Natl Acad Sci USA* (2019) 116(45):22730–6. doi: 10.1073/pnas.1911385116

53. Liu N, Mei L, Fan X, Tang C, Ji X, Hu X, et al. Phosphodiesterase 5/Protein Kinase G Signal Governs Stemness of Prostate Cancer Stem Cells Through Hippo Pathway. *Cancer Lett* (2016) 378(1):38–50. doi: 10.1016/j.canlet.2016.05.010

Conflict of Interest: The authors declare that the research was conducted in the absence of any commercial or financial relationships that could be construed as a potential conflict of interest.

Publisher's Note: All claims expressed in this article are solely those of the authors and do not necessarily represent those of their affiliated organizations, or those of the publisher, the editors and the reviewers. Any product that may be evaluated in this article, or claim that may be made by its manufacturer, is not guaranteed or endorsed by the publisher.

Copyright © 2021 Wang, Liu, Liu, Cai, Yao, Chen, Song, Yuan, Tan, Hu, Xiang and Xiang. This is an open-access article distributed under the terms of the Creative Commons Attribution License (CC BY). The use, distribution or reproduction in other forums is permitted, provided the original author(s) and the copyright owner(s) are credited and that the original publication in this journal is cited, in accordance with accepted academic practice. No use, distribution or reproduction is permitted which does not comply with these terms.

frontiers in Oncology

ORIGINAL RESEARCH
published: 16 November 2021
doi: 10.3389/fonc.2021.787198

The Surgeon's Proficiency Affected Survival Outcomes of Minimally Invasive Surgery for Early-Stage Cervical Cancer: A Retrospective Study of 851 Patients

Ying Yang[1,2], *Yue Huang*[1,2] *and Zhengyu Li*[1,2*]

[1] *Department of Gynecology and Obstetrics, West China Second University Hospital, Sichuan University, Chengdu, China,* [2] *Key Laboratory of Pediatric Diseases and Birth Defects of Ministry of Education, West China Second University Hospital, Sichuan University, Chengdu, China*

OPEN ACCESS

Edited by:
Robert Vierkant,
Mayo Clinic, United States

Reviewed by:
Valerio Gallotta,
Catholic University of the Sacred Heart, Italy
Vito Andrea Capozzi,
University Hospital of Parma, Italy

***Correspondence:**
Zhengyu Li
zhengyuli01@126.com

Specialty section:
This article was submitted to Gynecological Oncology, a section of the journal Frontiers in Oncology

Received: *30 September 2021*
Accepted: *29 October 2021*
Published: *16 November 2021*

Citation:
Yang Y, Huang Y and Li Z (2021) The Surgeon's Proficiency Affected Survival Outcomes of Minimally Invasive Surgery for Early-Stage Cervical Cancer: A Retrospective Study of 851 Patients. Front. Oncol. 11:787198. doi: 10.3389/fonc.2021.787198

Purpose: To compare the clinical outcomes of patients with early-stage cervical cancer who underwent minimally invasive surgery (MIS) by surgeons in different phases and evaluate whether the proficiency of surgeons affects the survival outcomes.

Materials and Methods: A total of 851 patients with early-stage cervical cancer who underwent radical hysterectomy between January 2008 and June 2018 (every year from January to June) at a tertiary hospital were retrospectively analyzed. We categorized patients into four phases according to their sequence (phase one, 1-10 cases; phase two: 11-20 cases; phase three: 21-30 cases; phase four: > 30 cases). Demographics and clinical and pathological data were collected and analyzed.

Results: There were no statistical differences between the open surgery and MIS groups regarding three- and five-year overall survival (OS) and disease-free survival (DFS). The OS and DFS of patients in the MIS group in phase one were significantly lower than those in later phases and those in the open surgery group after adjustment (OS, $P = 0.009$; HR, 2.896; 95%CI, 1.303-6.435; DFS, $P = 0.009$; HR, 2.712; 95%CI, 1.289-5.706). Survival outcomes were not statistically significant when comparing different surgeons.

Conclusion: The phase one cases of MIS had lower OS and DFS than those in later phases and those in the open surgery group. Thus, we suggest that the proficiency of surgeons is associated with survival outcomes of MIS. Favorable outcomes can be obtained after a certain number of MIS cases.

Keywords: early-stage cervical cancer, minimally invasive surgery, open surgery, surgeon's proficiency, survival outcomes

INTRODUCTION

According to statistics from the International Agency for Research on Cancer, the incidence of cervical cancer was 604,000 in 2020, making it the fourth most common gynecological cancer worldwide (1). Radical hysterectomy (RH) with lymphadenectomy remains one of the preferred treatments for patients with cervical cancer diagnosed at the International Federation of Gynecology and Obstetrics (FIGO) stage IA-IIA (2). In recent decades, minimally invasive surgery (MIS) has become more common, displacing the use of traditional open surgery for early-stage cancer. However, the Laparoscopic Approach to Cervical Cancer (LACC) trial observed that disease-free survival (DFS) at 4.5 years and overall survival (OS) at three years of MIS were significantly lower than those of open surgery among women with stage IA1-IB1 cervical cancer, which remains controversial (3). Potential explanations include increasing tumor spillage due to the application of a uterine manipulator, the effect of CO_2 insufflation, the volume of surgery, and the surgeon's proficiency (4–7). Several studies have focused on the correlation between surgeon proficiency and clinical outcomes in recent years. Lan Ying Li et al. found that compared to open surgery, more cases were required for surgeons performing minimally invasive RH to reach an acceptable five-year DFS (8). Kim et al. demonstrated that surgeons' proficiency in the MIS group significantly affected progression-free survival (PFS) (9). Liu et al. concluded that the learning curve could be a probable reason for poor outcomes of MIS by analyzing stage IB cervical cancer patients treated with RH by one surgeon for 15 years (10). Nevertheless, existing studies have limitations such as low sample sizes, incomplete follow-up information, and the absence of clinicopathological features of patients. There is still insufficient evidence regarding whether a surgeon's proficiency is associated with survival outcomes in MIS. We aimed to explore the effects of surgeons' proficiency in MIS on short- and long-term clinical outcomes and whether it accounts for the clinical outcomes of MIS.

MATERIALS AND METHODS

Study Design and Participants

This study was approved by the Institutional Ethics Committee of West China Second University Hospital, and all participants provided their written informed consent to participate in this study. Cervical cancer patients with consecutive FIGO (2009) stage IA-IIA treated with RH between January 2008 and June 2018 (every year from January to June) were retrospectively analyzed. The inclusion criteria were: (1) patients with FIGO stage IA1 with lymphovascular space invasion (LVSI), IA2, IB, and selected IIA cervical cancer; (2) patients who underwent standard surgical treatment, which was performed by five specific surgeons according to the National Comprehensive Cancer Network guidelines, a modified RH (Type B of the Querleu and Morrow (Q-M) surgical classification system) with pelvic lymphadenectomy (PLND) in stage IA1 with LVSI and stage IA2, and an RH (Type C of the Q-M surgical classification system) with PLND with/without para-aortic lymphadenectomy in stage IB to IIA (2, 11, 12). (3) Patients with histological subtypes of squamous cell carcinoma, adenocarcinoma, or adenosquamous carcinoma, regardless of histological grading. The exclusion criteria were as follows: (1) patients with incomplete data or complete loss to follow-up; (2) patients with severe fundamental diseases such as immune deficiency or other malignant tumors; and (3) patients with cervical cancer in pregnancy.

Complete information, including demographics and clinical and pathological information, was extracted from the hospital information system by two investigators (Y.Y. and Y.H.). The demographics extracted included age, menstruation (menopause or not), and body mass index (BMI). The clinical information extracted included diagnosis, FIGO (2009) stage, surgical approach, surgeon name, date of surgery, hospital stay, duration of surgery, estimated blood loss, CO_2 pneumoperitoneum in MIS, number of resected lymph nodes, pre- and post-operative treatment, and imaging data. Pathological information included histologic subtype, grading, LVSI, stromal invasion depth, parametrial involvement, vaginal margin involvement, and lymph node metastasis. Recurrence was confirmed by clinical findings, radiological examinations, and pathology reports. OS and DFS were the primary outcomes of this study. OS was defined as the time interval between the date of surgery and the date of death. DFS was defined as the time interval between the date of surgery and either the date of the first recurrence or death.

Statistical Analysis

The data were analyzed using the Statistical Package for the Social Sciences software version 22.0 (IBM Corp, Armonk, NY, USA). Missing values were statistically imputed by multiple imputations using logistic regression and predictive mean matching (13). The enumeration data were analyzed using the chi-square test. The measurement data were analyzed *via* t-test and Mann-Whitney U test between two groups, while an analysis of variance and Kruskal-Wallis H test were used to compare multiple groups. Survival curves were generated using the Kaplan-Meier method and analyzed using the log-rank test and multivariable Cox proportional hazards regression models. All the *P*-values reported are two-sided. A *P*-value of < 0.05 was considered statistically significant.

RESULTS

Study Population

A total of 851 patients were included in the study: 510 in the open surgery group and 341 in the MIS group (no robotic RH). Their general characteristics are summarized in **Table 1**. The mean age of the patients was 46.51 years (range 18-73 years; standard deviation [SD] 9.33), and most patients (471, 55.35%) were diagnosed with stage IB1. There were no significant differences between the open surgery and MIS groups in terms

TABLE 1 | General characteristics of the study population stratified by surgical approach.

Characteristic	Open surgery (n=510, %)	Minimally invasive surgery (n=341, %)	*P* value
Age (year) (mean ± SD)	46.70 ± 9.39	46.22 ± 9.25	0.456
Menopause	170 (33.3)	114 (33.4)	0.976
BMI (kg/m2) (mean ± SD)	22.58 ± 2.80	23.06 ± 4.36	0.074
Histologic subtype			0.297
squamous-cell carcinoma	417 (81.8)	284 (83.3)	
adenocarcinoma	65 (12.7)	46 (13.5)	
adenosquamous carcinoma	28 (5.5)	11 (3.2)	
FIGO stage			<0.001
IA	24 (4.7)	17 (5.0)	
IB1	234 (45.9)	237 (69.5)	
IB2-IIA	252 (49.4)	87 (25.5)	
Histologic grading			0.149
G1	21 (4.1)	17 (5.0)	
G2	62 (12.2)	42 (12.3)	
G3	378 (74.1)	233 (68.3)	
Gx	49 (9.6)	49 (14.4)	
Stromal invasion depth			<0.001
<1/2	203 (39.8)	170 (49.9)	
≥1/2	307 (60.2)	171 (50.1)	
LVSI	308 (60.4)	208 (61.0)	0.860
Parametrial invasion	63 (12.4)	43 (12.6)	0.911
Positive vaginal margin	92 (18.0)	45 (13.2)	0.060
Lymph node metastasis	99 (19.4)	73 (21.4)	0.477
Hospital stay, median (range, days)	8 (3-30)	7 (3-21)	<0.001
Duration of surgery, median (range, min)	200 (85-510)	240 (75-450)	<0.001
Estimated blood loss, median (range, ml)	400 (50-2500)	200 (10-4500)	<0.001
Postoperative adjuvant treatment	399 (78.2)	285 (83.6)	0.054

BMI, body-mass index; FIGO, International Federation of Gynecology and Obstetrics; LVSI, lymph-vascular space invasion.

of age, menopause, BMI, histologic subtype, and grading. Advanced FIGO stage and deep cervical stromal invasion were more frequent in the open surgery group. The median length of hospital stay was eight days (range 3-30) in the open surgery group and seven days (range 3-21) in the MIS group ($P < 0.001$). The median duration of surgery was 200 minutes (range 85-510) in the open surgery group and 240 minutes (range 75-450) in the MIS group ($P < 0.001$), and the median volume of blood loss was 400 mL (range, 50-2500 mL) in the open surgery group and 200 mL (range, 10-4500 mL) in the MIS group ($P < 0.001$).

Clinical Outcomes in Different Surgical Approaches

The median follow-up duration was 88.6 and 62.2 months in the open surgery and MIS groups, respectively. With regard to the three- and five-year OS and DFS, statistically significant differences were not observed (three-year OS, 94.5% *vs*. 96.4%; five-year OS, 93.4% *vs*. 96.0%; $P = 0.291$; three-year DFS: 94.4% *vs*. 94.6%, five-year DFS: 92.8% *vs*. 94.2%, $P = 0.585$). After adjusting for age, BMI, FIGO stage, histologic subtype, and grading, identical results were obtained using multivariable Cox proportional hazards regression models [OS: $P = 0.894$, HR 1.039, 95%CI (0.593, 1.820); DFS, $P = 0.647$; HR, 0.891; 95% CI (0.544, 1.460); **Figure 1**]. In addition, we analyzed the survival outcomes of the open surgery and MIS groups for every surgeon and found that the survival outcomes were still not statistically significant (all *p*-values > 0.05).

Survival Outcomes in Different Phases and Surgeons

For every surgeon, we categorized patients who underwent surgery into four phases according to their sequence (phase one, 1-10 cases; phase two, 11-20 cases; phase three, 21-30 cases; phase four, more than 30 cases). Considering open surgery as an advanced technique, we did not categorize patients in this group into different phases. When stratified by surgical phases, the OS and DFS of the MIS group in phase one were significantly lower than those in later phases and in the open surgery group after adjusting for age, BMI, FIGO stage, histologic subtype, and grading. The three-year OS was 91.8% (45/49), and the five-year OS was 87.8% (43/49) in phase one of the MIS group ($P = 0.009$; HR, 2.896; 95%CI, 1.303-6.435). The three-year DFS was 91.8% (45/49) and the five-year DFS was 85.7% (42/49) in phase one of the MIS group ($P = 0.009$; HR, 2.712; 95%CI, 1.289-5.706; **Figure 2**). We obtained similar results when analyzing the surgeons separately (**Table 2**). Statistical differences were observed in the median number of resected lymph nodes ($p < 0.001$). There were no significant differences among the four phases with respect to perioperative characteristics, including hospital stay, duration of surgery, volume of blood loss, and volume of CO_2 pneumoperitoneum after adjustment (**Table 3**).

When comparing different surgeons, the survival outcomes were not statistically significant after adjustment. Furthermore, the subgroup analysis in the corresponding phases showed the same result (all $P > 0.05$; **Figure 3**).

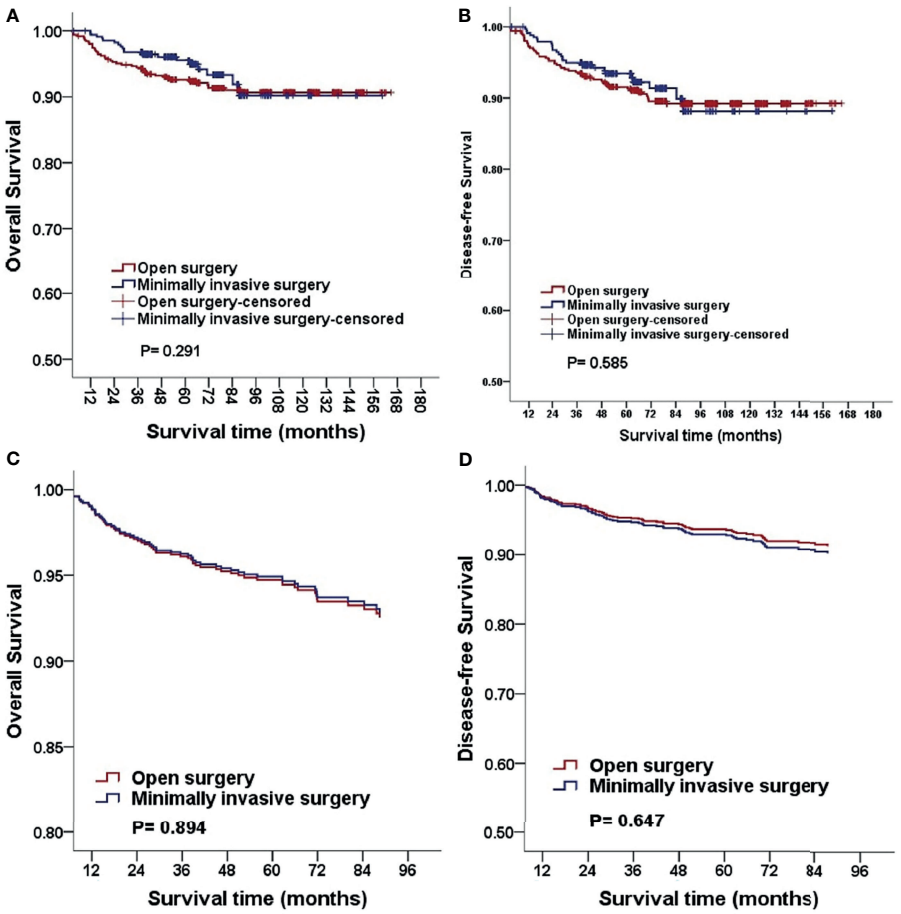


FIGURE 1 | Kaplan-Meier analysis of the OS and DFS for patients stratified by surgical approach **(A, B)**. The OS and DFS adjusted for clinicopathological factors for patients stratified by surgical approach **(C, D)**. MIS, minimally invasive surgery.

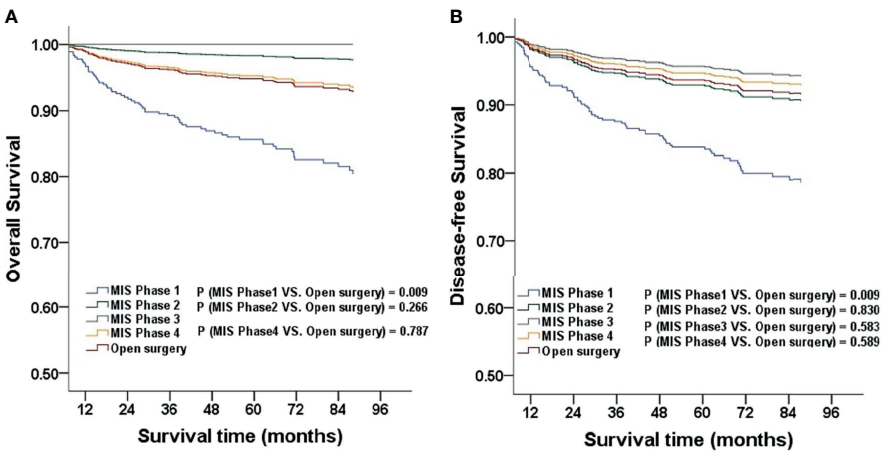


FIGURE 2 | The OS and DFS adjusted for clinicopathological factors for patients stratified by phase **(A, B)**. MIS, minimally invasive surgery.

TABLE 2 | Survival outcomes of different surgeons in different phases in minimally invasive surgery.

Variable		Overall survival				Disease-free survival			
		3-year (%)	5-year (%)	HR (95% CI)	*P* value	3-year (%)	5-year (%)	HR (95% CI)	*P* value
Open surgery		94.3	92.4	1 (ref.)	–	93.4	91.3	1 (ref.)	–
Surgeon A	P1	100	90	1.834 (0.237-14.17)	0.561	90	80	3.464 (0.792-15.162)	0.099
	P2	100	100	–	–	100	100	–	–
	P3	100	100	–	–	100	100	–	–
	P4	100	100	–	–	100	100	–	–
Surgeon B	P1	100	100	–	–	100	100	–	–
	P2	100	100	–	–	100	90	1.567 (0.199-12.341)	0.670
	P3	100	100	–	–	90	90	2.627 (0.336-20.542)	0.357
	P4	100	100	–	–	100	100	–	–
Surgeon C	P1	90	80	2.595 (0.732-9.197)	0.140	90	80	2.397 (0.698-8.226)	0.165
	P2	100	100	–	–	88.9	88.9	1.368 (0.183-10.231)	0.760
	P3	100	100	–	–	88.9	88.9	1.501 (0.202-11.126)	0.691
	P4	97.9	93.4	0.742 (0.263-2.094)	0.573	96.8	93.7	0.617 (0.220-1.725)	0.357
Surgeon D	P1	77.8	77.8	5.866 (1.301-26.441)	**0.021**	77.8	77.8	4.696 (1.061-20.776)	**0.042**
	P2	100	90	1.273 (0.164-9.901)	0.817	90	90	1.261 (0.165-9.662)	0.823
	P3	100	100	–	–	100	100	–	–
	P4	91.8	91.8	1.420 (0.585-3.446)	0.439	91.7	89.3	1.407 (0.621-3.187)	0.414
Surgeon E	P1	90	78.8	5.020 (1.106-22.790)	**0.037**	90	78.8	4.256 (0.951-19.037)	0.058
	P2	100	100	–	–	100	90	1.866 (0.247-14.102)	0.546
	P3	100	100	–	–	100	100	–	–
	P4	100	100	–	–	100	100	–	–
Total	P1	91.8	87.8	2.896 (1.303-6.435)	**0.009**	91.8	85.7	2.712 (1.289-5.706)	**0.009**
	P2	100	96.7	0.321 (0.043-2.381)	0.266	93.9	91.6	1.122 (0.392-3.213)	0.830
	P3	100	100	–	–	94.9	94.9	0.671 (0.162-2.782)	0.583
	P4	96	92.1	0.907 (0.446-1.843)	0.787	95.5	91.6	0.831 (0.426-1.624)	0.589

P values < 0.05 are in bold. P, phase; HR, hazard ratio; CI, confidence interval; ref, reference.

DISCUSSION

The World Health Organization proposed that patients with cervical cancer must be managed appropriately to accelerate the elimination of the disease, prompting more attention to the treatment of cervical cancer in recent years. Previous studies demonstrated that MIS and open surgery had comparable oncological outcomes (14–16). In contrast, several recent studies showed poorer oncological outcomes, especially lower DFS in patients treated with MIS (3, 17–19). As the findings were conflicting, the superiority or inferiority of MIS remains unclear. In our study, there were no statistical differences in the MIS and open surgery groups with regard to three- and five-year OS and DFS, and the subgroup analysis performed by different surgeons reached the same conclusion. However, when we compared different phases in MIS with open surgery, the OS and DFS of phase one were in line with those of the LACC trial. The perioperative outcomes such as hospital stay and blood loss were significantly better in the MIS group, whereas the duration of surgery was significantly shorter in the open surgery group, which is in accordance with many other studies.

According to the NCCN guideline (2), the standard approach for RH is the open surgery, and the oncologic risks of MIS should be informed carefully to patients given the findings of poorer survival outcomes of MIS recently. The development of MIS was affected by relevant research works. Therefore, it is essential to clear the reasonable application of MIS to achieve maximum benefits for patients. Pedestrian et al. showed that patients with tumor dimension less than two centimeters still suitable for MIS, but more studies are needed to refine on criteria (20).

Several potential reasons may explain the limitations of MIS, such as the use of a uterine manipulator, insufflation gas, intracorporeal colpotomy under CO_2 pneumoperitoneum, and the proficiency of the surgeon (7, 21–23). Gynecologic

TABLE 3 | Perioperative outcomes in different phases in minimally invasive surgery.

Characteristic	Minimally invasive surgery				
	Phase 1	Phase 2	Phase 3	Phase 4	*P* value
Hospital stay (days) (mean ± SD)	7.88 ± 2.88	7.32 ± 2.33	7.50 ± 2.39	7.15 ± 2.14	0.235
Duration of surgery (min) (mean ± SD)	252.73 ± 50.85	25.72 ± 56.88	238.89 ± 45.39	245.37 ± 62.08	0.659
Estimated blood loss, median (range, ml)	175 (20-800)	200 (40-600)	200 (80-4500)	200 (10-1000)	0.479
CO2 pneumoperitoneum, median (range, L)	590 (80-1200)	483.5 (160-1090)	669 (255-1200)	684 (100-1300)	0.123
No. of lymph nodes resected, median (range)	18.5 (4-33)	19 (3-57)	17.5 (6-50)	23 (2-53)	<0.001

SD, standard deviation.

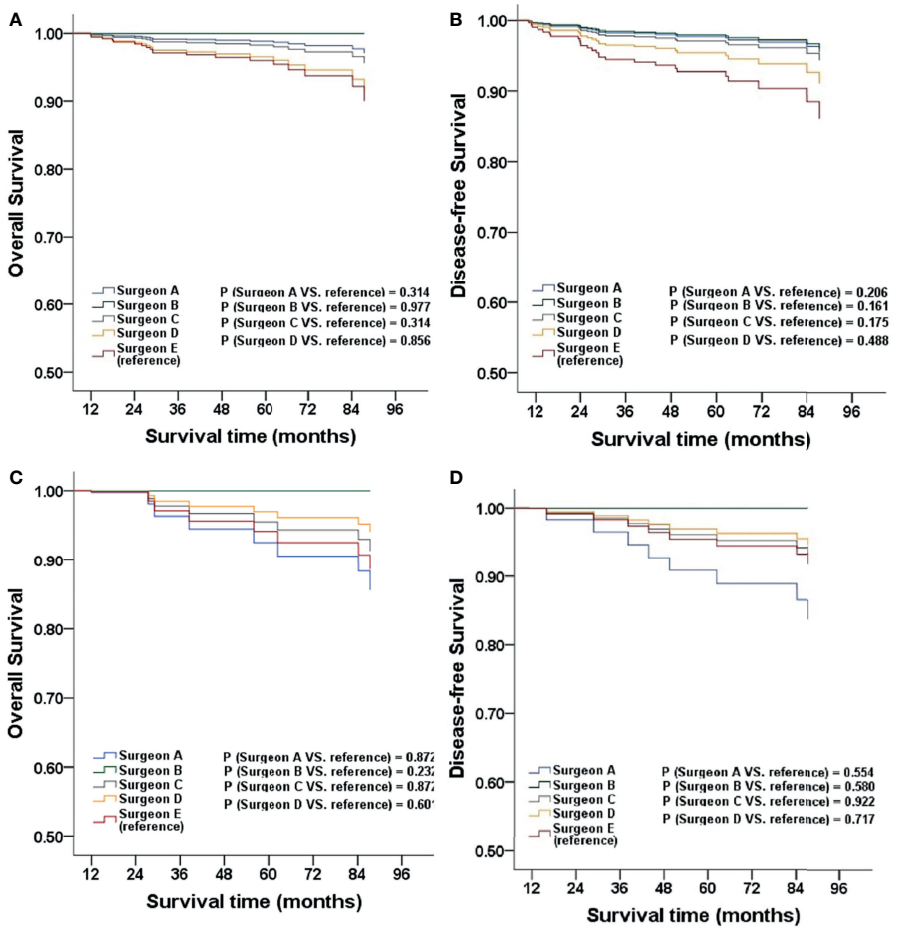


FIGURE 3 | The OS and DFS adjusted for clinicopathological factors for patients stratified by surgeon **(A, B)**, patients stratified by surgeon in MIS phase one **(C, D)**.

oncologists have designed innovative techniques and devices to reduce the potential negative consequences of these risks in recent years. For example, Hiroyuki Kanao et al. devised the "no-look, no-touch" technique for preventing intraoperative tumor spillage (24). Moreover, Peng Yuan et al. performed abdominal uterine manipulation and enclosed colpotomy (23). However, prospective studies are needed to evaluate the effects of these surgical techniques on oncological outcomes.

Previous studies have examined the learning curve in terms of some clinical parameters, such as the number of cases needed to reach a stable operation duration or to obtain a relatively low hemorrhage volume (25). Survival outcomes have rarely been reported. A recent study by Kim et al. concluded that improvement of surgical performance could be achieved after 13 cases of MIS (9). Pedestrian et al. demonstrated that the peak of reduction of the recurrence risk was the 19th MIS (26). Sert et al. showed that there was a higher number of recurrences in the first 50 cases (27). In this regard, our findings were in line with the results of previous studies that the first ten cases were significantly inferior to subsequent cases. Moreover, favorable survival outcomes observed after the first ten cases also demonstrated the effect of surgeon proficiency. There was no statistical significance when comparing the different surgeons, indicating that favorable outcomes can be obtained by practicing the MIS technique after a certain number of cases. Based on our findings, we offer the following suggestions. First, surgeons should undergo standardized training to improve their surgical skills (28). Second, surgeons performing MIS should have some standard qualification. For example, surgeons can only perform laparoscopic surgery after completing a certain number of virtual surgeries through surgery simulators. Third, beginners should be overseen by experienced surgeons, particularly for the first dozen or so cases.

The main strength of this study is the large sample size. In addition, compared with other studies, we analyzed more clinical parameters, making our results more robust and applicable to a larger population. However, our study has several limitations. Due to its retrospective nature, there could be bias in the patient selection. Furthermore, we did not evaluate the effect of different surgical techniques and devices in different phases. More studies on specific surgical approaches and techniques, including conventional multiport laparoscopic and laparo-endoscopic

single-site surgery with/without technological innovations, are needed. Although there was no robotic case in our study, some relevant studies showed that robotic and laparoscopic approaches were similar in perioperative and postoperative outcomes (29), future studies could consider this aspect.

In conclusion, our retrospective study demonstrated that phase one cases of MIS had lower OS and DFS than those in later phases or that underwent open surgery. Thus, we suggest that the proficiency of the operating surgeon is associated with the survival outcomes of MIS. More favorable outcomes can be obtained after a certain number of MIS cases have been performed.

DATA AVAILABILITY STATEMENT

The original contributions presented in the study are included in the article/supplementary material. Further inquiries can be directed to the corresponding author.

ETHICS STATEMENT

The studies involving human participants were reviewed and approved by the Institutional Ethics Committee of West China Second University Hospital. The patients/participants provided their written informed consent to participate in this study.

AUTHOR CONTRIBUTIONS

YY and ZYL contributed to data collection and study design. YY and YH contributed to data analysis. All authors contributed to the article and approved the submitted version.

FUNDING

This study was supported by grants from the Sichuan Youth Foundation of Science of Technology (Grant number: 2015JQ0026).

ACKNOWLEDGMENTS

The authors are grateful to the Department of Gynecology and Obstetrics, West China Second University Hospital, for supplying the data and all the patients.

REFERENCES

1. World Health Organization. WHO Guideline for Screening and Treatment of Cervical Precancer Lesions for Cervical Cancer Prevention (2021). Available at: https://wwwwhoint/publications/i/item/9789240030824.
2. Koh WJ, Abu-Rustum NR, Bean S, Bradley K, Campos SM, Cho KR, et al. Cervical Cancer, Version 3.2019, NCCN Clinical Practice Guidelines in Oncology. *J Natl Compr Canc Netw* (2019) 17:64–84. doi: 10.6004/jnccn.2019.0001
3. Ramirez PT, Frumovitz M, Pareja R, Lopez A, Vieira M, Ribeiro R, et al. Minimally Invasive *Versus* Abdominal Radical Hysterectomy for Cervical Cancer. *N Engl J Med* (2018) 379:1895–904. doi: 10.1056/NEJMoa1806395
4. Mowat A, Maher C, Ballard E. Surgical Outcomes for Low-Volume *vs* High-Volume Surgeons in Gynecology Surgery: A Systematic Review and Meta-Analysis. *Am J Obstet Gynecol* (2016) 215:21–33. doi: 10.1016/j.ajog.2016.02.048
5. Nezhat FR, Ananth CV, Vintzileos AM. The Two Achilles Heels of Surgical Randomized Controlled Trials: Differences in Surgical Skills and Reporting of Average Performance. *Am J Obstet Gynecol* (2019) 221:230–2. doi: 10.1016/j.ajog.2019.05.017
6. Casarin J, Buda A, Bogani G, Fanfani F, Papadia A, Ceccaroni M, et al. Predictors of Recurrence Following Laparoscopic Radical Hysterectomy for Early-Stage Cervical Cancer: A Multi-Institutional Study. *Gynecol Oncol* (2020) 159:164–70. doi: 10.1016/j.ygyno.2020.06.508
7. Chen S, Zheng Y, Tong L, Zhao X, Chen L, Wang Y. Laparoendoscopic Single-Site Radical Hysterectomy With Vaginal Closure and Without Uterine Manipulator for FIGO IB1 Cervical Cancer. *J Minim Invasive Gynecol* (2020) 27:1471–2. doi: 10.1016/j.jmig.2020.01.003
8. Li LY, Wen LY, Park SH, Nam EJ, Lee JY, Kim S, et al. Impact of the Learning Curve on the Survival of Abdominal or Minimally Invasive Radical Hysterectomy for Early-Stage Cervical Cancer. *Cancer Res Treat* (2021) 53:243–51. doi: 10.4143/crt.2020.063
9. Kim S, Min KJ, Lee S, Hong JH, Song JY, Lee JK, et al. Learning Curve Could Affect Oncologic Outcome of Minimally Invasive Radical Hysterectomy for Cervical Cancer. *Asian J Surg* (2021) 44:174–80. doi: 10.1016/j.asjsur.2020.05.006
10. Liu Y, Li L, Wu M, Ma S, Tan X, Zhong S, et al. The Impact of the Surgical Routes and Learning Curve of Radical Hysterectomy on the Survival Outcomes in Stage IB Cervical Cancer: A Retrospective Cohort Study. *Int J Surg* (2019) 68:72–7. doi: 10.1016/j.ijsu.2019.06.009
11. Querleu D, Morrow CP. Classification of Radical Hysterectomy. *Lancet Oncol* (2008) 9:297–303. doi: 10.1016/s1470-2045(08)70074-3
12. Cibula D, Abu-Rustum NR, Benedetti-Panici P, Köhler C, Raspagliesi F, Querleu D, et al. New Classification System of Radical Hysterectomy: Emphasis on a Three-Dimensional Anatomic Template for Parametrial Resection. *Gynecol Oncol* (2011) 122:264–8. doi: 10.1016/j.ygyno.2011.04.029
13. Austin PC, White IR, Lee DS, van Buuren S. Missing Data in Clinical Research: A Tutorial on Multiple Imputation. *Can J Cardiol* (2020) 37:13227–31. doi: 10.1016/j.cjca.2020.11.010
14. Shah CA, Beck T, Liao JB, Giannakopoulos NV, Veljovich D, Paley P. Surgical and Oncologic Outcomes After Robotic Radical Hysterectomy as Compared to Open Radical Hysterectomy in the Treatment of Early Cervical Cancer. *J Gynecol Oncol* (2017) 28:e82. doi: 10.3802/jgo.2017.28.e82
15. Wallin E, Floter Radestad A, Falconer H. Introduction of Robot-Assisted Radical Hysterectomy for Early Stage Cervical Cancer: Impact on Complications, Costs and Oncologic Outcome. *Acta Obstet Gynecol Scand* (2017) 96:536–42. doi: 10.1111/aogs.13112
16. Mendivil AA, Rettenmaier MA, Abaid LN, Brown JV3rd, Micha JP, Lopez KL, et al. Survival Rate Comparisons Amongst Cervical Cancer Patients Treated With an Open, Robotic-Assisted or Laparoscopic Radical Hysterectomy: A Five Year Experience. *Surg Oncol* (2016) 25:66–71. doi: 10.1016/j.suronc.2015.09.004
17. Uppal S, Gehrig PA, Peng K, Bixel KL, Matsuo K, Vetter MH, et al. Recurrence Rates in Patients With Cervical Cancer Treated With Abdominal *Versus* Minimally Invasive Radical Hysterectomy: A Multi-Institutional Retrospective Review Study. *J Clin Oncol* (2020) 38:1030–40. doi: 10.1200/jco.19.03012
18. Chao X, Li L, Wu M, Ma S, Tan X, Zhong S, et al. Efficacy of Different Surgical Approaches in the Clinical and Survival Outcomes of Patients With Early-Stage Cervical Cancer: Protocol of a Phase III Multicentre Randomised Controlled Trial in China. *BMJ Open* (2019) 9:e029055. doi: 10.1136/bmjopen-2019-029055
19. Melamed A, Margul DJ, Chen L, Keating NL, Del Carmen MG, Yang J, et al. Survival After Minimally Invasive Radical Hysterectomy for Early-Stage Cervical Cancer. *N Engl J Med* (2018) 379:1905–14. doi: 10.1056/NEJMoa1804923

20. Pedestrian Anchora L, Turco LC, Bizzarri N, Capozzi VA, Lombisani A, Chiantera V, et al. How to Select Early-Stage Cervical Cancer Patients Still Suitable for Laparoscopic Radical Hysterectomy: A Propensity-Matched Study. *Ann Surg Oncol* (2020) 27(6):1947–55. doi: 10.1245/s10434-019-08162-5
21. Klapdor R, Hertel H, Hillemanns P, Röttger M, Soergel P, Kuehnle E, et al. Peritoneal Contamination With ICG-Stained Cervical Secretion as Surrogate for Potential Cervical Cancer Tumor Cell Dissemination: A Proof-of-Principle Study for Laparoscopic Hysterectomy. *Acta Obstet Gynecol Scand* (2019) 98:1398–403. doi: 10.1111/aogs.13681
22. Kampers J, Gerhardt E, Sibbertsen P, Flock T, Klapdor R, Hertel H, et al. Protective Operative Techniques in Radical Hysterectomy in Early Cervical Carcinoma and Their Influence on Disease-Free and Overall Survival: A Systematic Review and Meta-Analysis of Risk Groups. *Arch Gynecol Obstet* (2021) 304:577–87. doi: 10.1007/s00404-021-06082-y
23. Yuan P, Liu Z, Qi J, Yang X, Hu T, Tan H. Laparoscopic Radical Hysterectomy With Enclosed Colpotomy and Without the Use of Uterine Manipulator for Early-Stage Cervical Cancer. *J Minim Invasive Gynecol* (2019) 26:1193–8. doi: 10.1016/j.jmig.2019.01.016
24. Kanao H, Matsuo K, Aoki Y, Tanigawa T, Nomura H, Okamoto S, et al. Feasibility and Outcome of Total Laparoscopic Radical Hysterectomy With No-Look No-Touch Technique for FIGO IB1cervical Cancer. *J Gynecol Oncol* (2019) 30:e71. doi: 10.3802/jgo.2019.30.e71
25. Heo YJ, Kim S, Min KJ, Lee S, Hong JH, Lee JK, et al. The Comparison of Surgical Outcomes and Learning Curves of Radical Hysterectomy by Laparoscopy and Robotic System for Cervical Cancer: An Experience of a Single Surgeon. *Obstet Gynecol Sci* (2018) 61:468–76. doi: 10.5468/ogs.2018.61.4.468
26. Pedestrian Anchora L, Bizzarri N, Gallotta V, Chiantera V, Fanfani F, Fagotti A, et al. Impact of Surgeon Learning Curve in Minimally Invasive Radical Hysterectomy on Early Stage Cervical Cancer Patient Survival. *Facts Views Vis Obgyn* (2021) 13(3):233–44. doi: 10.52054/FVVO.13.3.035
27. Hoogendam JP, Verheijen RH, Wegner I, Zweemer RP. Oncological Outcome and Long-Term Complications in Robot-Assisted Radical Surgery for Early Stage Cervical Cancer: An Observational Cohort Study. *Bjog* (2014) 121:1538–45. doi: 10.1111/1471-0528.12822
28. Moulton CA, Dubrowski A, Macrae H, Graham B, Grober E, Reznick R. Teaching Surgical Skills: What Kind of Practice Makes Perfect?: A Randomized, Controlled Trial. *Ann Surg* (2006) 244:400–9. doi: 10.1097/01.sla.0000234808.85789.6a
29. Gallotta V, Conte C, Federico A, Vizzielli G, Gueli Alletti S, Tortorella L, et al. Robotic *Versus* Laparoscopic Radical Hysterectomy in Early Cervical Cancer: A Case Matched Control Study. *Eur J Surg Oncol* (2018) 44(6):754–9. doi: 10.1016/j.ejso.2018.01.092

Conflict of Interest: The authors declare that the research was conducted in the absence of any commercial or financial relationships that could be construed as a potential conflict of interest.

Publisher's Note: All claims expressed in this article are solely those of the authors and do not necessarily represent those of their affiliated organizations, or those of the publisher, the editors and the reviewers. Any product that may be evaluated in this article, or claim that may be made by its manufacturer, is not guaranteed or endorsed by the publisher.

Copyright © 2021 Yang, Huang and Li. This is an open-access article distributed under the terms of the Creative Commons Attribution License (CC BY). The use, distribution or reproduction in other forums is permitted, provided the original author(s) and the copyright owner(s) are credited and that the original publication in this journal is cited, in accordance with accepted academic practice. No use, distribution or reproduction is permitted which does not comply with these terms.

frontiers in Oncology

ORIGINAL RESEARCH
published: 26 November 2021
doi: 10.3389/fonc.2021.732443

An Assessment of Ovarian Cancer Histotypes Across the African Diaspora

Sophia H. L. George[1,2,3], Ayodele Omotoso[3,4], Andre Pinto[3,5], Aisha Mustapha[3,6], Alex P. Sanchez-Covarrubias[1], Usman Aliyu Umar[3,7], Ali Bala Umar[3,7], Timothy Abiola Oluwasola[3,8], Clement Abu Okolo[3,9], Umeh Uchenna Anthony[3,11], Francis Ikechukwu Ukekwe[3,11], Maisaratu A. Bakari[3,12], Aminu M. C. Dahiru[3,12], Habiba Ibrahim Abdullahi[3,13], Bawa Ahmed Abimiku[3,13], Aisha Abdurrahman[3,10], Asmau Usman[3,10], Saad Aliyu Ahmed[3,14], Hadiza Abdullahi Usman[3,15], Abba Kabir[3,15], George Uchenna Eleje[3,16], Michael Emeka Chiemeka[3,17], Emily Nzeribe[3,18], Ikechukwu Nweke[3,18], SaiduAbubakar Kadas[3,19], Dauda E. Suleiman[3,19], Etim Ekanem[3,4], Umemmuo Maureen Uche[3,20], Jibrin Paul[3,20], Uzoma Maryrose Agwu[3,21], Felix O. Edegbe[3,21], Rose I. Anorlu[3,22], Adekunbiola Banjo[3,22], Kayode Olusegun Ajenifuja[3,23], Adegboyega Adisa Fawole[3,24], Ibrahim O. O. Kazeem[3,24], Francis Magaji[3,25], Olugbenga Silas[3,25], Boma Precious Athanasius[3,26], Nyengidiki Kennedy Tamunomie[3,27], Emem Bassey[3,28], Kunle Abudu[3,28], Ibrahim G. Ango[3,29], Kabiru Abdullahi[3,29], Ishak Lawal[3,30], Suleiman Aliyu Kabir[3,30], Victor Ekanem[3,31], Michael Ezeanochie[3,32], Usman Rahman Yahaya[3,33], Melissa Nicole Castillo[1], Vishal Bahall[34], Vikash Chatrani[35], Ian Brambury[2,36], Saida Bowe[2,37], Darron Halliday[2,37], George Bruney[37], Raleigh Butler[2,37], Camille Ragin[2,38], Folakemi Odedina[2,39], Srikar Chamala[40], Matthew Schlumbrecht[1,2,3*] and Bala Audu[3,15,16*]*

[1] Department of Obstetrics, Gynecology and Reproductive Sciences, Division of Gynecologic Oncology, Sylvester Comprehensive Cancer Center, University of Miami Miller School of Medicine, Miami, FL, United States, [2] African Caribbean Cancer Consortium, Philadelphia, PA, United States, [3] Transatlantic Gynecologic Cancer Research Consortium, Bauchi, Nigeria, [4] Department of Pathology, University of Calabar Teaching Hospital, Calabar, Nigeria, [5] Department of Pathology, University of Miami Miller School of Medicine, Miami, FL, United States, [6] Department of Obstetrics and Gynecology, Gynecologic Oncology Unit, Ahmadu Bello University Teaching Hospital, Zaria, Nigeria, [7] Department of Pathology, Aminu Kano Teaching Hospital, Kano, Nigeria, [8] Department of Obstetrics and Gynecology, Gynecological Oncology Unit, College of Medicine, University of Ibadan, Ibadan, Nigeria, [9] Department of Pathology, College of Medicine, University of Ibadan, Ibadan, Nigeria, [10] Federal Medical Centre Katsina, Katsina, Nigeria, [11] Department of Obstetrics and Gynecology and Department of Pathology, University of Nigeria Teaching Hospital Enugu, Enugu, Nigeria, [12] Department of Obstetrics and Gynecology and Department of Pathology, Federal Medical Center Yola, Yola, Nigeria, [13] Department of Obstetrics and Gynecology and Department of Pathology, University of Abuja Teaching Hospital, Gwagwalada, Nigeria, [14] Department of Pathology, Ahmadu Bello University Teaching Hospital, Zaria, Nigeria, [15] Department of Obstetrics and Gynecology, University of Maiduguri Teaching Hospital, Maiduguri, Nigeria, [16] Department of Obstetrics and Gynecology, Nnamdi Azikiwe University Teaching Hospital, Nnewi, Nigeria, [17] Department of Anatomic Pathology and Forensic Medicine, Nnamdi Azikiwe University Teaching Hospital, Nnewi, Nigeria, [18] Department of Obstetrics and Gynecology and Department of Pathology, Federal Medical Center, Owerri, Nigeria, [19] Department of Obstetrics and Gynecology and Department of Pathology, Abubakar Tafawa Balewa University Teaching Hospital, Bauchi, Nigeria, [20] Department of Obstetrics and Gynecology and Department of Pathology, National Hospital, Abuja, Nigeria, [21] Department of Obstetrics and Gynecology and Department of Pathology, Alex Ekwueme Federal University Teaching Hospital Abakaliki, Abakaliki, Nigeria, [22] Department of Obstetrics and Gynecology and Department of Pathology, Lagos University Teaching Hospital, Lagos, Nigeria, [23] Department of Obstetrics and Gynecology and Department of Pathology, Obafemi Awolowo University Teaching Hospital, Ile-Ife, Nigeria, [24] Department of Obstetrics and Gynecology and Department of Pathology, niversity of Ilorin Teaching Hospital, Ilorin, Nigeria, [25] Department of Obstetrics and Gynecology and Department of Pathology, Jos University Teaching Hospital, Jos, Nigeria, [26] Department of Anatomical Pathology, University of Port Harcourt Teaching Hospital, Port Harcourt, Nigeria, [27] Department of Obstetrics and Gynaecology, University of Port Harcourt Teaching Hospital, Port Harcourt, Nigeria, [28] Department of Obstetrics and Gynecology and Department of Pathology, University of Uyo Teaching Hospital, Uyo, Nigeria,

OPEN ACCESS

Edited by:
Tonya J. Webb,
University of Maryland, Baltimore, United States

Reviewed by:
Yu Yu,
Curtin University, Australia
Cara Mathews,
Women & Infants Hospital of Rhode Island, United States

***Correspondence:**
Sophia H. L. George
sophia.george@med.miami.edu
Matthew Schlumbrecht
mschlumbrecht@miami.edu
Bala Audu
balaaudu19@gmail.com

Specialty section:
This article was submitted to Gynecological Oncology, a section of the journal Frontiers in Oncology

Received: 29 June 2021
Accepted: 28 October 2021
Published: 26 November 2021

[29] Department of Obstetrics and Gynecology and Department of Pathology, smanu Danfodiyo University Teaching Hospital Sokoto, Sokoto, Nigeria, [30] Department of Obstetrics and Gynecology and Department of Pathology, Federal Medical Center - Birnin Kebbi, Birnin Kebbi, Nigeria, [31] Department of Anatomic Pathology, University of Benin Teaching Hospital, Benin City, Nigeria, [32] Department of Obstetrics and Gynecology, University of Benin Teaching Hospital, Benin City, Nigeria, [33] Department of Obstetrics and Gynecology, Federal Teaching Hospital Gombe, Gombe, Nigeria, [34] Department of Gynecologic Oncology, University of West Indies, Port-of-Spain, Trinidad and Tobago, [35] Faculty of Medical Sciences, Department of Gynecologic Oncology, University of West Indies-Cave Hill, Bridgetown, Barbados, [36] Department of Obstetrics and Gynecology, University of West Indies-Mona, Kingston, Jamaica, [37] Princess Margaret Hospital, University of the West Indies, School of Clinical Medicine and Research, Nassau, Bahamas, [38] Cancer Prevention and Control Program, Fox Chase Cancer Center, Philadelphia, PA, United States, [39] Department of Pharmacotherapy and Translational Research, University of Florida, Orlando, FL, United States, [40] Department of Pathology, Immunology and Laboratory Medicine, University of Florida, Gainesville, FL, United States

Objective: Ovarian cancer in Black women is common in many West African countries but is relatively rare in North America. Black women have worse survival outcomes when compared to White women. Ovarian cancer histotype, diagnosis, and age at presentation are known prognostic factors for outcome. We sought to conduct a preliminary comparative assessment of these factors across the African diaspora.

Methods: Patients diagnosed with ovarian cancer (all histologies) between June 2016-December 2019 in Departments of Pathology at 25 participating sites in Nigeria were identified. Comparative population-based data, inclusive of Caribbean-born Blacks (CBB) and US-born Blacks (USB), were additionally captured from the International Agency for Research on Cancer and Florida Cancer Data Systems. Histology, country of birth, and age at diagnosis data were collected and evaluated across the three subgroups: USB, CBB and Nigerians. Statistical analyses were done using chi-square and student's t-test with significance set at $p<0.05$.

Results: Nigerians had the highest proportion of germ cell tumor (GCT, 11.5%) and sex-cord stromal (SCST, 16.2%) ovarian cancers relative to CBB and USB ($p=0.001$). CBB (79.4%) and USB (77.3%) women were diagnosed with a larger proportion of serous ovarian cancer than Nigerians (60.4%) ($p<0.0001$). Nigerians were diagnosed with epithelial ovarian cancers at the youngest age (51.7± 12.8 years) relative to USB (58.9 ± 15.0) and CBB (59.0± 13.0,$p<0.001$). Black women [CBB (25.2 ± 15.0), Nigerians (29.5 ± 15.1), and USB (33.9 ± 17.9)] were diagnosed with GCT younger than White women (35.4 ± 20.5, $p=0.011$). Black women [Nigerians (47.5 ± 15.9), USB (50.9 ± 18.3) and CBB (50.9 ± 18.3)] were also diagnosed with SCST younger than White women (55.6 ± 16.5, $p<0.01$).

Conclusion: There is significant variation in age of diagnosis and distribution of ovarian cancer histotype/diagnosis across the African diaspora. The etiology of these findings requires further investigation.

Keywords: ovarian cancer, black women, germ cell, Caribbean, Nigeria, sex cord stromal, epithelial ovarian cancer (EOC)

INTRODUCTION

Globally, ovarian cancer remains a deadly disease (1). In 2021, GLOBOCAN estimates there will be 313,959 new diagnoses of ovarian cancer worldwide (2, 3). Ovarian cancer is a heterogeneous disease with three major histologic types: epithelial ovarian cancer (EOC), germ cell tumors (GCT), and sex cord stromal tumors (SCST). EOC is the most diagnosed histologic type and high-grade serous ovarian carcinoma (HGSC) is the most common epithelial tumor. EOCs like HGSC are aggressive and are usually diagnosed at advanced stages with poor overall survival. GCTs and SCSTs are rare, diagnosed at early stages and have relatively better overall survival. Women of African ancestry have a low incidence of ovarian cancer (1, 4–6). Unfortunately, like many other cancer diagnoses, Women of West African ancestry (Black women) with

ovarian cancer experience worse outcomes than White women. In the US, Black women have higher morbidity and mortality rates and higher un-staged or unclassified tumors compared with White women, resulting in undertreatment with subsequent compromise in progression-free survival (5, 7, 8). The 5-year ovarian cancer survival rate is 51% for Black women under 65 years of age and 22% for those 65 years and older. In contrast, among White women, these rates go up to 60% and 29% respectively (5, 9). Between 2005 and 2014, the age-adjusted incidence of ovarian cancer decreased by 1.4% in non-Hispanic Whites, but was stable in Blacks, Hispanics, American Indians and other ethnic groups (10). In addition to differential outcomes, recent data suggest that there are differences in the proportion of ovarian cancer histologies diagnosed in Black women in general (8, 11).

The Transatlantic slave trade was the largest forced immigration in history, transporting Africans to the US and the Caribbean (10). In the US, non-Hispanic Blacks comprise the second-largest racial/ethnic minority group and are disproportionately affected by high cancer mortality and morbidity. The Black population in the US is polylithic and is composed of both US native-born Black (UBB) and immigrant Black populations from the Caribbean (CBB) and Africa. Blacks from the US and the Caribbean have predominant West African ancestry, the majority from Nigeria, Ghana, and Benin (12). Understanding the global distribution of ovarian cancer histologic types among women of African ancestry is important to identify modifiers of disease etiology as well as opportunities for therapeutic interventions; both can improve ovarian cancer outcomes in a number of different treatment environments.

Notwithstanding the social, economic and health inequities linked to ovarian cancer outcomes in women of African descent in the US, we proceeded to study the prevalence of ovarian cancer histologies and age at diagnosis across the African diaspora. In this pilot study, our two-fold objective is first, to evaluate population-level patterns of ovarian cancer in Black women both globally and locally, and second, to describe the correlative patterns between age and histologic distribution in our TAGCReC-member cohorts. Such data may suggest variable etiologies of disease and generate hypotheses regarding global biologic variations in ovarian cancer in Black women.

METHODS

Ethical Approval

This study was approved by the University of Miami Institutional Review Board (IRB) (Protocols 2015-1022, 2018-0822, 2019-0756) and the National Health Research Ethics Committee of Nigeria (NHREC/01/01/2007- 23/08/2019).

Study Population

All women diagnosed with ovarian cancer between 2005 and 2017 (in Florida) and July 2016-July 2019 (in Nigeria) were identified through the state cancer registry (Florida) or each institution's Department of Pathology (Nigeria), respectively. Only data for cases with self-identification as non-Hispanic White, non-Hispanic Black, referred to as Caribbean-born Black or US-born Black in this report, were included.

Categories for histologic type included: EOC (serous, clear cell, endometrioid, mucinous and carcinosarcoma); germ cell tumors (immature teratoma, dysgerminoma, endodermal sinus tumor [yolk sac tumor], choriocarcinoma and carcinoid); SCST (granulosa cell and Sertoli-Leydig cell tumors). Histology and grade were reviewed by consortia lead Pathologists (AP and AO) to ensure consistency, with tumors being segregated into low-grade (low/moderately differentiated) or high-grade (poorly differentiated), when applicable. Borderline ovarian cancer histotypes were not included. If the grade and histology were inconsistent (e.g. carcinosarcoma classified as low-grade), they were adjusted through pathologist review to meet WHO classifications of the ovary.

In Nigeria, data extracted from pathology reports were captured in REDCap, a mature, secure web application which is encrypted, HIPAA-compliant, and hosted on a server at the University of Miami. Variables obtained included date of diagnosis, age of diagnosis in years, treatment facility (by country and state, if relevant), tumor grade and histology when available. Age was recorded as a continuous variable. Patients' country of birth was classified as US-born, Caribbean-born, or West African-born. Country of birth, race, and ethnicity were all self-reported.

Consortium

The Transatlantic Gynecologic Cancer Research Consortium (TAGCReC) was established to facilitate gynecologic cancer research across the nations that represent African diaspora people. TAGCReC's primary mission is to take a comprehensive approach to gynecologic oncology challenges across this population and to leverage opportunities present at our different institutions. The consortium's focus areas include cancer prevention, treatment, and survivorship, with transnational education opportunities. We have used this platform to interrogate race, genetics, environment, and health care practices to address health and health disparities in Africa and across the diaspora. Currently, the consortium is comprised of members in Nigeria, the USA, and the Caribbean; members include gynecologists with an interest in gynecologic oncology, board certified gynecologic oncologists, general and gynecologic pathologists, molecular geneticists, epidemiologists, and behavioral and basic scientists. The members were linked initially through existing African diasporic consortia and societies in Nigeria (Gynecological Oncology Society of Nigeria), the Caribbean (Caribbean Gynecologic Cancer Society), and USA (African Cancer Consortium – AC3).

Data Sources

Data from the Surveillance, Epidemiology and End Results (SEER) (13) were used to capture nationwide ovarian data cancer data for comparison. Variables obtained from SEER included race/ethnicity, age ranges, tumor characteristics such as stage at diagnosis, histology, and grade. Country of birth is not an accessible variable. The age range categories provided in SEER were used to compare Nigerians, Black and White populations in the US by cancer histotype.

Florida Cancer Data System (FCDS) is the legislatively mandated, population-based central cancer registry for Florida. Cases are abstracted from patient medical records in hospitals, free-standing

ambulatory surgical facilities, radiation therapy facilities, private physicians, and death certificates codes (14, 15). Variables obtained from FCDS included age, race/ethnicity, patients' country of birth, and tumor characteristics such as stage at diagnosis, histology, and grade. Race/ethnicity was based on self-identification and was present in nearly all (more than 98%) of the health records. These data are de-identified and therefore exempt from IRB approval. Women were included if they self-identified as Black and were born in the United States or one of the English- or French speaking Caribbean nations (Anguilla, Antigua, Bahamas, Barbados, Belize, British Virgin Islands, Cayman Islands, Cuba, Dominica, British Guyana, Grenada, Haiti, Jamaica, St. Kitts and Nevis, St. Lucia, St. Vincent, Trinidad Tobago, Turks and Caicos Islands, Suriname, US Virgin Islands or West Indies). Women who were born in Africa were excluded from the analysis due to low representation (1 Algeria, 1 Kenya, 1 Morocco, 2 Nigeria, 1 Tanzania, 2 Uganda and 1 South Africa).

The ovarian cancer cases were identified using International Classification of Diseases for Oncology, *Tenth Revision* (ICD-10). Tumor site and histology codes included in the analysis were as follows: primary site (C56.9, C57.0) classified as malignant tumors; serous (8050, 8120, 8122, 8130, 8140, 8201, 8260, 8440–8442, 8450, 8452, 8460–8463, 9014); clear cell (8005, 8310, 8313, 8443, 8444); endometrioid (8290, 8380–8383); carcinosarcoma (8575, 8950, 8951, 8980, 8981); mucinous (8144, 8384, 8470–8472, 8480–8482, 9015); mixed, undifferentiated, unspecified carcinoma (other/NOS; 8000–8004, 8010, 8020–8022, 8030–8033, 8046, 8052, 8070–8072, 8074, 8084, 8230, 8255, 8261–8263, 8323, 8560, 8562, 8570, 8574, 8940, 9000) (16). Non-epithelial histologic types; GCT - 9060, 9070, 9071, 9082, 9100, and SCST – 8620-8623, 8630-8633) were also included. Similarly to SEER, we used FCDS data to compare age range categories in Nigerians, Caribbean born blacks, US born blacks and US born whites. We also used age numerical values to create boxplots comparing these four groups. Finally, the percentages of tumor histotypes across four groups were compared: Epithelial ovarian cancer types between Nigerians, CB Blacks and USB Blacks (Serous vs Non-serous).

GLOBOCAN

GLOBOCAN 2020 provides cancer incidence estimates across 185 countries or territories by sex and age. For ovarian cancer, incidence and mortality data were available for World Health Organization (WHO) regions as well as individual countries and territories. We selected ovarian cancer incidence and mortality data for Africa, Latin America, and the Caribbean, and extracted age-standardized rates; data on cancer histotype were not available (17).

Statistics

Statistical analyses were performed using STATA IC 14.2 (StataCorp, College Station, TX); SAS software 9.4 (SAS Institute Inc., Cary, NC) and Prism 9.1.2 (Graphpad Prism LLC). The R packages ggpubr and ggplot2 (16) were used to create line charts and boxplots showing the age at cancer diagnosis distribution across subgroups. Summary statistics were used to describe the patient cohorts. Wilcoxon rank-sum was used for continuous variables in nonparametric distributions. Associations between categorical covariates and continuous variables were assessed with chi-squared tests and independent sample *t*-tests, respectively. Differences across means in all subgroups were tested using the analysis of variance (ANOVA). All tests were 2-tailed and p-value of < 0.05 was statistically significant.

RESULTS

Interrogation of the WHO GLOBOCAN 2020 data showed that globally, 313 959 incident ovarian cancer cases were forecasted in 2020. These numbers are expected to increase by 86.8% in Africa and 49.6% in Latin America and the Caribbean by 2040, compared to 25.9% in North America and 9.6% in Europe (**Figure 1A**). In Africa, ovarian cancer has the 5th highest incidence rate among cancers in women (3.8%) (ASR, 5.4/100,000), whereas in the Caribbean (26 countries) and the US, new ovarian cancer cases rank 9th (4.6/100,000) and 11th (8.0/100,000) respectively. The mortality to incidence ratio is high both in African and Caribbean countries when compared to North America countries such as the United States and Canada. In Africa, the age-standardized incidence rate (ASR) is highest in Ghana at 8.6/100,000, 5.6/100,000 in Nigeria and lowest in Mozambique at 1.8/100,000. In the Caribbean, the ASR was highest in Trinidad and Tobago (11.6/100,000) and lowest

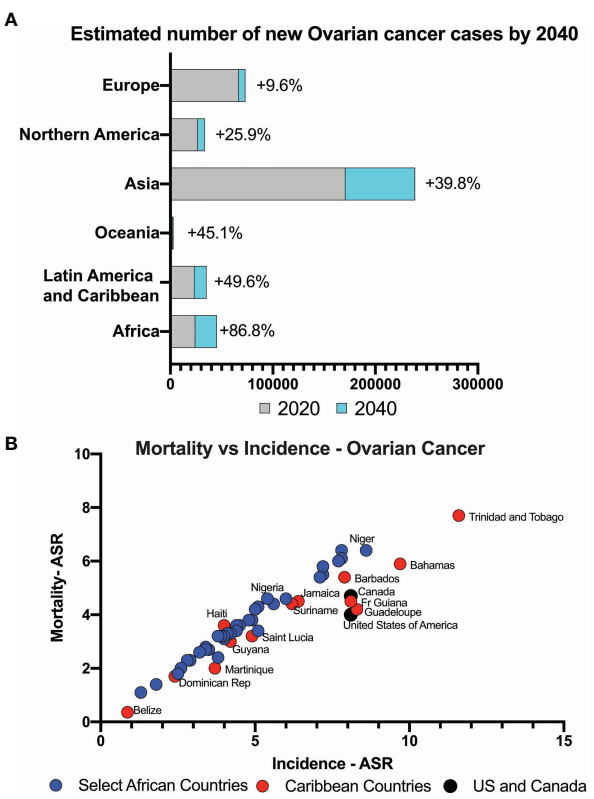


FIGURE 1 | **(A)** Estimated number of ovarian cancer cases expected globally. Low- and middle-income countries expect to see significant increase in newly diagnosed cases. **(B)** Mortality versus incidence rates of ovarian cancer in countries with majority Black women compared to USA and Canada.

in Belize (0.87/100.000). The ratio of mortality to incidence in West and East African countries is high at 0.97, similar to the Caribbean ratio of 0.92 (**Figure 1B**).

In Nigeria, data were collected in two phases. During Phase I, members were asked to identify within their institutions all ovarian cancer cases diagnosed within a 12-month period (June 2018-July 2019), with reported age and histotype. Twenty-one (21) sites across 6 political geographic regions in Nigeria provided data. In Phase II, in which 16 sites (12 from Phase I and 4 additional sites) participated, an independent pathology review of available archival tissue from ovarian cancer cases diagnosed between 2017-2019 was performed (**Supplementary Table 1** and **Figure 2A**). In total, 621 cases were identified. Of these, 594 cases had a confirmatory pathology report and/or tissue blocks. Epithelial tumors were the most common (**Figure 2B**), comprising 64.7% of cases, followed by SCST (16.2%), GCT (11.5%), sarcoma (0.8%) and other (lymphoma, Brenner and undefined tumors, 6.9%)). Epithelial tumors were serous (n=232, 60.4%); mucinous (n=97, 25.2%); endometrioid (n=12, 3.1%); clear cell (n=9,2.3%); carcinosarcoma (n=5, 1.3%) and undefined (7.6%). There were differences in the proportions of tumor types reported by regions across Nigeria (**Supplementary Table 1**). Nigerians had a higher proportion of GCT relative to the other groups assessed from the African diaspora (**Figure 3A**). Of the epithelial ovarian cancer (EOC) cases, Nigerians (60.4%) had the smallest proportion of serous cancers, compared to Caribbean-born Blacks (CBB, 79.4%) and US-born Blacks (USB, 77.4%) cases, p<0.0001 (**Figure 3B** and **Supplementary Table 2**).

Age at diagnosis for the three major histologic types – epithelial, sex cord stromal, and germ cell – varied significantly across Nigerian, CBB, USB and US White women (**Table 1** and **Figures 4A**–**F**). In our comparative analysis of the FCDS and Nigerian ovarian cohorts, the mean age of EOC patients in Nigeria was significantly younger, 51.7± 12.8 years (95% CI 17-80), than USB (58.9 years, 95% CI 21-88) and CBB (59.0 years, 95% CI 23-87) (p<0.001). SEER data showed a similar trend where Nigerians diagnosed with EOCs skewed to the left of US Black and White EOC patients (**Supplementary Figure 1**). Whereas there were non-significant differences amongst the ethnic minorities, Black women, independent of country of birth (West Africa, USA, or the Caribbean), were diagnosed at a younger age with both germ cell (p=0.011) and SCST compared to White women (p<0.01) (**Table 1** and **Figure 4C**–**E**). We assessed stage at presentation of incident ovarian cancer cases in Florida. The rare histologic tumors, germ cells and sex cord stromal tumors, there were no significant difference at stage at presentation. However, with epithelial ovarian cancers, there was a significant difference in stage at diagnosis amongst the three groups: CBB, USB and majority White EOC population. Both CBB and USB EOC patients had higher proportions of stage 3-4 and unstaged diagnoses (p=0.0006, **Supplementary Table 3**).

DISCUSSION

In 2020, ovarian cancer will account for about 313,000 cases worldwide, representing 3.4% of global cancer incidence in women, but 4.7% of cancer-related deaths. Our analysis of GLOBOCAN data revealed that the burden of ovarian cancer is increasing annually. By 2040, there is an expected 49.6-86.8% increase in ovarian cancer incidence in Africa, Latin America,

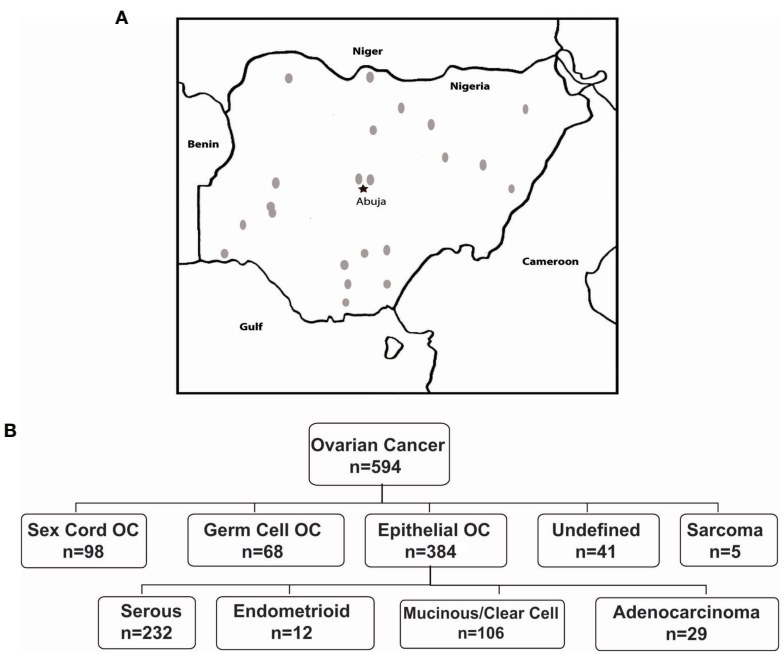


FIGURE 2 | **(A)** Study sites across Nigeria that participated in study. **(B)** Distribution of ovarian cancer cases by histology in Nigeria.

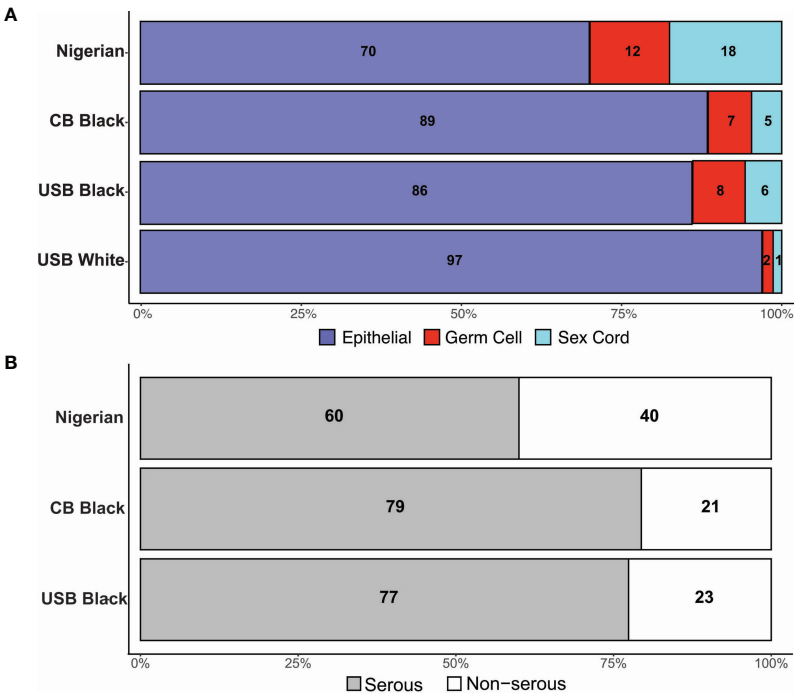


FIGURE 3 | **(A)** Distribution of tumor histology by cohort. **(B)** Distribution of Serous tumor types in Black women.

TABLE 1 | Distribution by age at diagnosis and ovarian histotype across groups.

	Number of Cases	Mean Age (± SD)	Median	p-value[a]
Epithelial Ovarian Tumor				Overall <0.001
Nigerian	316	51.7 ± 12.8	53	Ref
CBB	301	59.0 ± 13.0	59	<0.001
USB	906	58.9 ± 15.0	59	<0.001
US White NH	33377	65 ± 13.4	66	<0.001
Germ Cell Tumor				Overall <0.001
Nigerian	51	29.5 ± 15.1	28	Ref
CBB	23	33.9 ± 17.9	28	0.31
USB	86	25.2 ± 15.0	22	0.11
US White NH	560	35.4 ± 20.5	30	0.011
Sex Cord Stromal Tumor				Overall < 0.001
Nigerian	80	47.5 ± 15.9	46	Ref
CBB	16	50.9 ± 18.3	49	0.5
USB	60	48.8 ± 18.3	47	0.67
US White NH	461	55.6 ± 16.5	56	<0.011

[a]*ANOVA. CBB, Caribbean-born Black; USB, US-born Black; NH, non-Hispanic.*

and the Caribbean, which is much greater than the modest 9.6-25.9% increase expected among the predominantly White regions of Europe and North America.

Black women in Africa and the African diaspora develop distinct proportions of ovarian cancer histotypes across ancestry, ethnicity, and geography. The geographic regions in this study represent both indigenous Africans and diasporic Africans through forced immigration and enslavement, and now including voluntary emigration. As a result of this movement of people, African diaspora populations are genetically admixed (12, 18, 19). In the US, substantial demographic data collected on cancer patients demonstrate health disparities among people of African ancestry. Black women in the US have lower incidence of ovarian cancer but continue to experience worse outcomes. Smaller studies in West African countries such as Nigeria have documented similar poor survival in women diagnosed with ovarian cancer (20, 21).

Known factors that both modify and predict development of ovarian cancer include family history of breast and/or ovarian cancer; fertility factors such as decreased parity, earlier onset of menses, smaller family size, later age at time of first pregnancy, reproductive behavior; and environment. Risk factors associated

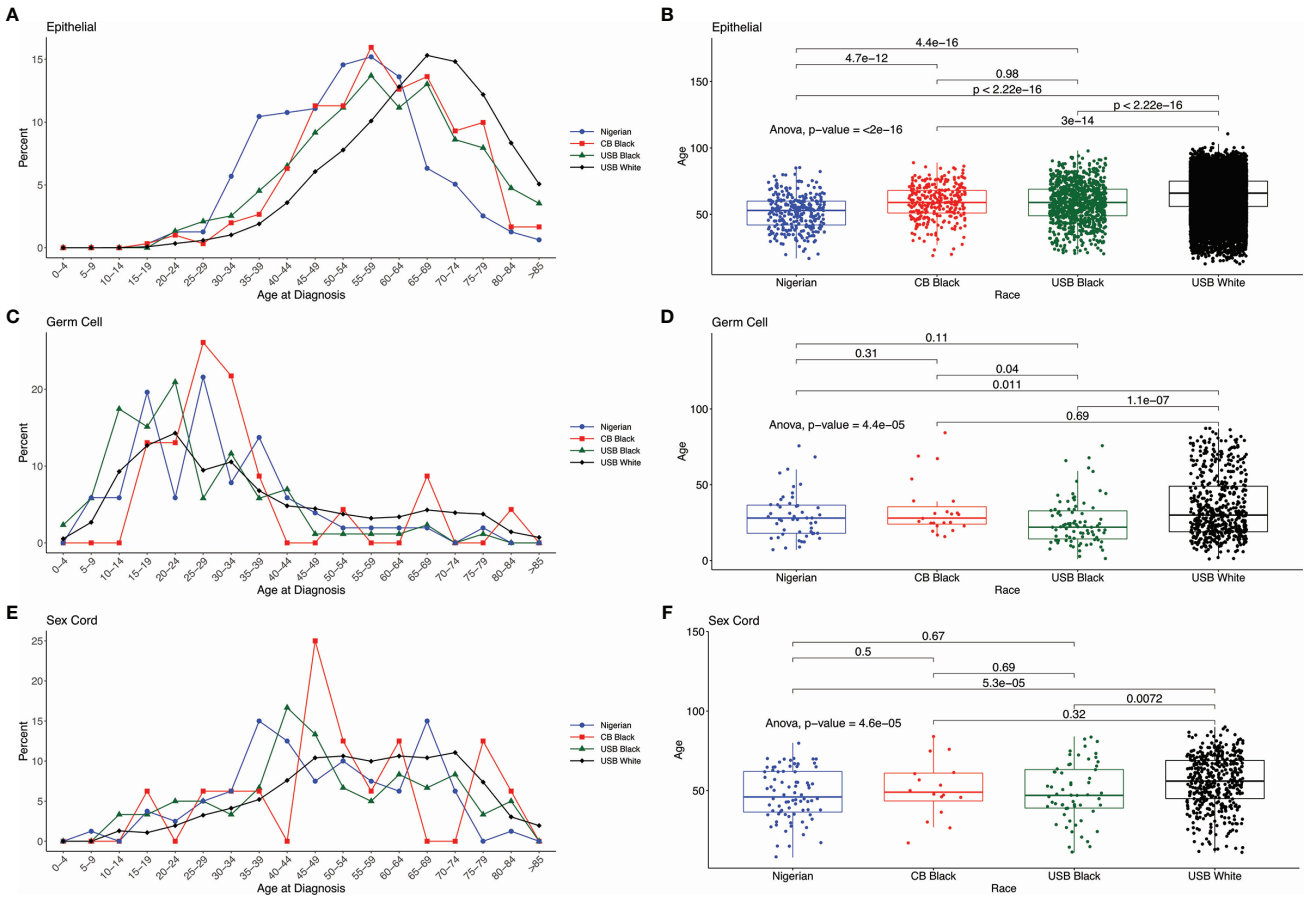


FIGURE 4 | Distribution of cases by age across the comparative groups. **(A, C, E)** Histograms by histologic type EOC, Germ Cell and Sex Cord Stromal tumors. **(B, D, F)** ANOVA comparing mean age at cancer diagnosis across different cohorts and histologic type.

with race and ethnicity are less well defined. Among populations with West or East African ancestry, these risk factors are poorly understood or in some cases not known at all. Our data collected in Nigeria represent a large-scale collection from the 7th most populated country in the world with a population of 206 million people, in which there are over 250 ethnic groups.

Our data show that there was a significant difference in the proportions of serous cancer across the three international cohorts. In addition, Black women diagnosed with EOC are diagnosed at more advanced stages, as have been shown in larger SEER data (11, 22). Nigerian women had a lower proportion of EOC cases, an observation previously published in a single institutional study (23–25). Further, differences in reported ovarian histotypes across Nigeria potentially suggest different cultural – health behavioral practices and thus exposures that may influence risk of ovarian cancer histologic development. Additionally, there may be unknown genetic, reproductive, and biologic influences (e.g. unreported prevalence of endometriosis, a precursor to clear cell and endometrioid ovarian cancers) as contributors to ovarian cancer histotypes. In the US, sex cord stromal tumors (SCST) only represent approximately 1% of ovarian cancer cases in White women, but a higher percentage in USB (6%) and CBB (5%) women; Nigerian women have the highest percentage (18%).

In Nigeria, 1 in 8 women diagnosed with breast cancer has hereditary breast and ovarian cancer syndrome (HBOC) (26). Women with HBOC develop cancers at younger ages that are typically high-grade, and of serous histology. Among CBB, the percentage of women with breast or ovarian cancer who have HBOC is variable: the Bahamas, 24%, with a pathogenic variant in *BRCA1, BRCA2* or *RAD51C*; Trinidad and Tobago, 12%; and Jamaica, 3% (27–30). No such data about ovarian cancer risk specifically in women in Africa are currently available; at present it is unknown if the histologic prevalence described here is representative of variations in HBOC or other hereditary cancer syndromes.

Reproductive factors like gravidity, parity and age at pregnancies influence ovarian cancer risks and etiology. A Norwegian study reported that pregnancy and age at the first and last births are sometimes associated with an differential risks of developing non-EOC malignancies (31). More specifically for SCST a decrease in risk was observed with increasing age at last

birth. In contrast, increasing age at first and last births was associated with an increased risk for GCT. The total fertility rate (TFR, the average number of children per woman) in Nigeria is 5.3. This ranged from 3.9 in the southwest to 6.6 in the northwest. The lowest rate was Lagos state with 3.4, and the highest was Katsina state with 7.3. On average in Nigeria, women aged 45-49 years have given birth to 6.4 children, with 2% never having given birth at all (infertile rather than voluntarily childless) (32). Total fertility rates in the Caribbean range from 2.96 in Haiti to 1.44 in St. Lucia, a steady decline from the 1950s when the TFR was 5.4 for the entire region (33). Similarly, in the USA, Black women have experienced a decrease in TFR to 1.8, compared to 1.7 in US White women (34). These differences in TFRs may suggest fertility correlations with non-EOC tumors, although more data are required to substantiate observations about higher incidence of these rare ovarian tumors in all Black women.

Women in Nigeria were also diagnosed at a younger age with EOC compared to Black women in the US and the Caribbean. There are reproductive factors such as age at first pregnancy and number of pregnancies that may account for this observation. Additionally, broadly in Western Africa life expectancy is 61 years compared to 75 years in the Caribbean and 83 years in the USA. Early age at menarche, multiparous and shorter lifespan, as opposed to living longer and having the opportunity to age into developing higher-risk disease, may explain, in part, the 10-year shift in EOC age at diagnosis among Nigerian women, CBB, and USB. A recent report from northern Nigeria (Zaria) reported that 80% of patients with ovarian cancer were pre-menopausal (24). Environmental factors such as air quality, and social determinants of health including housing, access to healthy food, equitable and proper health infrastructure, and systemic racism (in the US) are variables that can influence ovarian cancer etiology across the three regions studied. These variables are known to modulate genetic expression through epigenetics and will be important to assess disease pathogenesis in future investigations (35). The differences in the proportion of ovarian cancer histotypes between USB, CBB, and Nigerians undoubtedly involve a complex underpinning of genetic, epigenetic, lifestyle, and reproductive factors, which must be explored.

Limitations

As a pilot study, this work includes data from only one West African country. The findings may not necessarily be applicable to other geographic locations and should be considered hypothesis-generating. There is a selection bias in that the US-based cohort was drawn from Florida, which may not be representative of other North American regions. Further the cohort in Nigeria will only capture women who had resources (financial and social) to attend the clinics in participating sites. Comprehensive clinicopathologic data on each case were not available for all patients during the pilot study interval. There is limited chronological overlap between the US and Nigerian cohorts which may influence incident cases between the regions. A more thorough medical chart review, currently ongoing, is expected to reveal additional reproductive, familial, and epidemiologic factors associated with different types of ovarian cancers observed in these populations, and perhaps can better explain our preliminary observations.

CONCLUSION

Ovarian cancer in some West African and Caribbean countries is highly prevalent. The differences in prevalence and type are more pronounced in West African ovarian cancer cases for which genetics (familial), environmental, and reproductive factors may influence the etiology and pathogenesis in the spectra of ovarian cancer histotypes observed. Further, the exponential increase in ovarian cases expected by 2040 in Africa and the Caribbean, regions with low- to middle-income countries, highlights the need not only for robust health system infrastructure to decrease the mortality burden, for comprehensive studies to better understand the complex etiologies of this disease. Currently, there are no screening guidelines for ovarian cancer beyond risk-reduction surgeries and opportunistic salpingo-oophorectomies. It will be important to study both epidemiology and genetic factors influencing ovarian cancer pathogenesis in the diverse group of women across the African diaspora to identify factors contributing to both higher incidence and mortality. Such research will ultimately inform strategies for cancer prevention, early detection, and treatment optimization for these routinely underserved populations.

DATA AVAILABILITY STATEMENT

The original contributions presented in the study are included in the article/**Supplementary Material**. Further inquiries can be directed to the corresponding authors.

ETHICS STATEMENT

The studies involving human participants were reviewed and approved by University of Miami and the National Health Research Ethics Committee of Nigeria. Written informed consent for participation was not required for this study in accordance with the national legislation and the institutional requirements.

AUTHOR CONTRIBUTIONS

Design and Conduct of the Study: SG, BA, MS, AP, and AO. Provision of study materials or patients: All authors. Collection and assembly of data: SG, AO, AP, MC, AM, MS, BA. Data analysis and interpretation: SG, AO, AP, BA, MS, AM, AS-C. Preparation and review Manuscript: All authors. Accountable for all aspects of the work: All authors. All authors contributed to the article and approved the submitted version.

FUNDING

The study was partially funded by the HERI Foundation (BA, SG, MS, AP) and Sylvester Comprehensive Cancer Center. Research reported in this publication was supported by the National Cancer Institute of the National Institutes of Health under Award Number P30CA240139. The funders had no specific role in design and conduct of the study; collection, management, analysis, and interpretation of the data; preparation, review, or approval of the manuscript; and decision to submit the manuscript for publication.

ACKNOWLEDGMENTS

Staff of the Pathology Core at University of Miami Hospital and Biospecimen Shared Resource (BSSR) at Sylvester Comprehensive Cancer Center, the staff in the Department of Pathology, University of Calabar, Nigeria. SG, BA, AM, AO, AP, AS-C, and MNC, and MS had full access to all the data in the study and takes responsibility for the integrity of the data and the accuracy of the data analysis.

SUPPLEMENTARY MATERIAL

The Supplementary Material for this article can be found online at: https://www.frontiersin.org/articles/10.3389/fonc.2021.732443/full#supplementary-material

Supplementary Figure 1 | Distribution of cases by age across comparative groups using SEER data. Black, White, and Nigerian cohorts. **(A)**. Nigerian women diagnosed with EOC skew left of both Black and White women using SEER categorical age distribution. **(B)**. No observed differences in age at diagnosis between Nigerian women Germ Cell versus women in the US. **(C)**. No observed differences in age at diagnosis between Nigerian women Sex Cord Stromal tumors versus women in the US.

REFERENCES

1. Chornokur G, Amankwah EK, Schildkraut JM, Phelan CM. Global Ovarian Cancer Health Disparities. *Gynecol Oncol* (2013) 129(1):258–64. doi: 10.1016/j.ygyno.2012.12.016
2. Bray F, Ferlay J, Soerjomataram I, Siegel RL, Torre LA, Jemal A. Global Cancer Statistics 2018: GLOBOCAN Estimates of Incidence and Mortality Worldwide for 36 Cancers in 185 Countries. *CA Cancer J Clin* (2018) 68 (6):394–424. doi: 10.3322/caac.21492
3. Sung H, Ferlay J, Siegel RL, Laversanne M, Soerjomataram I, Jemal A, et al. Global Cancer Statistics 2020: GLOBOCAN Estimates of Incidence and Mortality Worldwide for 36 Cancers in 185 Countries. *CA Cancer J Clin* (2021) 71(3):209–49. doi: 10.3322/caac.21660
4. Cote ML, Ruterbusch JJ, Olson SH, Lu K, Ali-Fehmi R. The Growing Burden of Endometrial Cancer: A Major Racial Disparity Affecting Black Women. *Cancer Epidemiol Biomarkers Prev* (2015) 24(9):1407–15. doi: 10.1158/1055-9965.EPI-15-0316
5. DeSantis CE, Siegel RL, Sauer AG, Miller KD, Fedewa SA, Alcaraz KI, et al. Cancer Statistics for African Americans, 2016: Progress and Opportunities in Reducing Racial Disparities. *CA Cancer J Clin* (2016) 66(4):290–308. doi: 10.3322/caac.21340
6. Siegel RL, Miller KD, Jemal A. Cancer Statistics, 2018. *CA Cancer J Clin* (2018) 68(1):7–30. doi: 10.3322/caac.21442
7. Siegel RL, Fedewa SA, Miller KD, Goding-Sauer A, Pinheiro PS, Martinez-Tyson D, et al. Cancer Statistics for Hispanics/Latinos, 2015. *CA Cancer J Clin* (2015) 65(6):457–80. doi: 10.3322/caac.21314
8. Torre LA, Trabert B, DeSantis CE, Miller KD, Samimi G, Runowicz CD, et al. Ovarian Cancer Statistics, 2018. *CA Cancer J Clin* (2018) 68(4):284–96. doi: 10.3322/caac.21456
9. AmericanCancerSociety. Cancer Facts & Figures 2018 - Special Section: Ovarian Cancer. *ACS* (2018). Available at: https://www.cancer.org/research/cancer-facts-statistics/all-cancer-facts-figures/cancer-facts-figures-2018.html.
10. Rotimi CN, Tekola-Ayele F, Baker JL, Shriner D. The African Diaspora: History, Adaptation and Health. *Curr Opin Genet Dev* (2016) 41:77–84. doi: 10.1016/j.gde.2016.08.005
11. American Cancer Society. *Key Statistics for Ovarian Cancer*. Atlanta, GA: American Cancer Society (2019).
12. Montinaro F, Busby GB, Pascali VL, Myers S, Hellenthal G, Capelli C. Unravelling the Hidden Ancestry of American Admixed Populations. *Nat Commun* (2015) 6:6596. doi: 10.1038/ncomms7596
13. Siegel RL, Miller KD, Fuchs HE, Jemal A. Cancer Statistics, 2021. *CA Cancer J Clin* (2021) 71(1):7–33. doi: 10.3322/caac.21654
14. Siegel RL, Miller KD, Jemal A. Cancer Statistics, 2020. *CA Cancer J Clin* (2020) 70(1):7–30. doi: 10.3322/caac.21590
15. Berek JS, Kehoe ST, Kumar L, Friedlander M. Cancer of the Ovary, Fallopian Tube, and Peritoneum. *Int J Gynecol Obstetrics* (2018) 143(S2):59–78. doi: 10.1002/ijgo.12614
16. Kahle D, Wickham H. Ggmap: Spatial Visualization With Ggplot2. *R J* (2013) 5(1):144–61. doi: 10.32614/RJ-2013-014
17. J F, M E, F L, et al. *Global Cancer Observatory: Cancer Today (GLOBOCAN)* (2021). International Agency for Research on Cancer. Available at: https://gco.iarc.fr/today (Accessed 01 15 2021).
18. Pew Research Center. Modern Immigration Wave Brings 59 Million to U.S., Driving Population Growth and Change Through 2065: Views of Immigration's Impact on U.S. Society Mixed. Washington, D.C. (2015) Available at: https://www.pewresearch.org/hispanic/wp-content/uploads/sites/5/2015/09/2015-09-28_modern-immigration-wave_REPORT.pdf.
19. Beiki O, Hall P, Ekbom A, Moradi T. Breast Cancer Incidence and Case Fatality Among 4.7 Million Women in Relation to Social and Ethnic Background: A Population-Based Cohort Study. *Breast Cancer Res* (2012) 14(1):R5. doi: 10.1186/bcr3086
20. Okunade KS, Adejimi AA, Ohazurike EO, Salako O, Osunwusi B, Adenekan MA, et al. Predictors of Survival Outcomes After Primary Treatment of Epithelial Ovarian Cancer in Lagos, Nigeria. *JCO Glob Oncol* (2021) 7:89–98. doi: 10.1200/GO.20.00450
21. Okunade KS, Adetuyi IE, Adenekan M, Ohazurike E, Anorlu RI. Risk Predictors of Early Recurrence in Women With Epithelial Ovarian Cancer in Lagos, Nigeria. *Pan Afr Med J* (2020) 36:272. doi: 10.11604/pamj.2020.36.272.17827
22. DeSantis CE, Miller KD, Goding Sauer A, Jemal A, Siegel RL. Cancer Statistics for African Americans, 2019. *CA Cancer J Clin* (2019) 69(3):211–33. doi: 10.3322/caac.21555
23. Ibrahim HM, Ijaiya MA. Pattern of Gynaecological Malignancies at the University of Ilorin Teaching Hospital, Ilorin, Nigeria. *J Obstet Gynaecol* (2013) 33(2):194–6. doi: 10.3109/01443615.2012.738717
24. Zayyan MS, Ahmed SA, Oguntayo AO, Kolawole AO, Olasinde TA. Epidemiology of Ovarian Cancers in Zaria, Northern Nigeria: A 10-Year Study. *Int J Womens Health* (2017) 9:855–60. doi: 10.2147/IJWH.S130340
25. Forae GD, Aligbe JU. Ovarian Tumors Among Nigerian Females: A Private Practice Experience in Benin-City, Nigeria. *Adv BioMed Res* (2016) 5:61. doi: 10.4103/2277-9175.179183
26. Zheng Y, Walsh T, Gulsuner S, Casadei S, Lee MK, Ogundiran TO, et al. Inherited Breast Cancer in Nigerian Women. *J Clin Oncol* (2018) 36 (28):2820–5. doi: 10.1200/JCO.2018.78.3977
27. Donenberg T, Lunn J, Curling D, Turnquest T, Krill-Jackson E, Royer R, et al. A High Prevalence of BRCA1 Mutations Among Breast Cancer Patients From the Bahamas. *Breast Cancer Res Treat* (2011) 125(2):591–6. doi: 10.1007/s10549-010-1156-9
28. Akbari MR, Donenberg T, Lunn J, Curling D, Turnquest T, Krill-Jackson E, et al. The Spectrum of BRCA1 and BRCA2 Mutations in Breast Cancer Patients in the Bahamas. *Clin Genet* (2014) 85(1):64–7. doi: 10.1111/cge.12132

29. Trottier M, Lunn J, Butler R, Curling D, Turnquest T, Francis W, et al. Prevalence of Founder Mutations in the BRCA1 and BRCA2 Genes Among Unaffected Women From the Bahamas. *Clin Genet* (2016) 89(3):328–31. doi: 10.1111/cge.12602
30. George SHL, Donenberg T, Alexis C, DeGennaro V Jr, Dyer H, Yin S, et al. Gene Sequencing for Pathogenic Variants Among Adults With Breast and Ovarian Cancer in the Caribbean. *JAMA Network Open* (2021) 4(3):e210307–e210307. doi: 10.1001/jamanetworkopen.2021.0307
31. Albrektsen G, Heuch I, Kvåle G. Full-Term Pregnancies and Incidence of Ovarian Cancer of Stromal and Germ Cell Origin: A Norwegian Prospective Study. *Br J Cancer* (1997) 75(5):767–70. doi: 10.1038/bjc.1997.136
32. National Population Commission NPC, Icf. *Nigeria Demographic and Health Survey 2018 - Final Report*. Abuja, Nigeria: NPC and ICF (2019).
33. United Nations Department of Economic and Social Affairs, Population Division. *Total Fertility by Region, Subregion and Country, 1950-2100 (Live Births Per Woman)*. United Nations (2019). Available at: https://population.un.org/wpp/DataQuery/
34. Tj M, Be H. *Total Fertility Rates by State and Race and Hispanic Origin: United States, 2017*. Hyattsville, MD: National Center for Health Statistics (2018).
35. Palmer RC, Ismond D, Rodriquez EJ, Kaufman JS. Social Determinants of Health: Future Directions for Health Disparities Research. *Am J Public Health* (2019) 109(S1):S70–1. doi: 10.2105/AJPH.2019.304964

Conflict of Interest: The authors declare that the research was conducted in the absence of any commercial or financial relationships that could be construed as a potential conflict of interest.

Publisher's Note: All claims expressed in this article are solely those of the authors and do not necessarily represent those of their affiliated organizations, or those of the publisher, the editors and the reviewers. Any product that may be evaluated in this article, or claim that may be made by its manufacturer, is not guaranteed or endorsed by the publisher.

Citation: *George SHL, Omotoso A, Pinto A, Mustapha A, Sanchez-Covarrubias AP, Umar UA, Umar AB, Oluwasola TA, Okolo CA, Anthony UU, Ukekwe FI, Bakari MA, Dahiru AMC, Abdullahi HI, Abimiku BA, Abdurrahman A, Usman A, Ahmed SA, Usman HA, Kabir A, Eleje GU, Chiemeka ME, Nzeribe E, Nweke I, Kadas SA, Suleiman DE, Ekanem E, Uche UM, Paul J, Agwu UM, Edegbe FO, Anorlu RI, Banjo A, Ajenifuja KO, Fawole AA, Kazeem IOO, Magaji F, Silas O, Athanasius BP, Tamunomie NK, Bassey E, Abudu K, Ango IG, Abdullahi K, Lawal I, Kabir SA, Ekanem V, Ezeanochie M, Yahaya UR, Castillo MN, Bahall V, Chatrani V, Brambury I, Bowe S, Halliday D, Bruney G, Butler R, Ragin C, Odedina F, Chamala S, Schlumbrecht M and Audu B (2021) An Assessment of Ovarian Cancer Histotypes Across the African Diaspora. Front. Oncol. 11:732443. doi: 10.3389/fonc.2021.732443*

Copyright © 2021 George, Omotoso, Pinto, Mustapha, Sanchez-Covarrubias, Umar, Umar, Oluwasola, Okolo, Anthony, Ukekwe, Bakari, Dahiru, Abdullahi, Abimiku, Abdurrahman, Usman, Ahmed, Usman, Kabir, Eleje, Chiemeka, Nzeribe, Nweke, Kadas, Suleiman, Ekanem, Uche, Paul, Agwu, Edegbe, Anorlu, Banjo, Ajenifuja, Fawole, Kazeem, Magaji, Silas, Athanasius, Tamunomie, Bassey, Abudu, Ango, Abdullahi, Lawal, Kabir, Ekanem, Ezeanochie, Yahaya, Castillo, Bahall, Chatrani, Brambury, Bowe, Halliday, Bruney, Butler, Ragin, Odedina, Chamala, Schlumbrecht and Audu. This is an open-access article distributed under the terms of the Creative Commons Attribution License (CC BY). The use, distribution or reproduction in other forums is permitted, provided the original author(s) and the copyright owner(s) are credited and that the original publication in this journal is cited, in accordance with accepted academic practice. No use, distribution or reproduction is permitted which does not comply with these terms.

frontiers in Oncology

ORIGINAL RESEARCH
published: 14 December 2021
doi: 10.3389/fonc.2021.749114

MRI Radiomic Features: A Potential Biomarker for Progression-Free Survival Prediction of Patients With Locally Advanced Cervical Cancer Undergoing Surgery

Mengting Cai[1], Fei Yao[1], Jie Ding[1], Ruru Zheng[2], Xiaowan Huang[2], Yunjun Yang[1], Feng Lin[2†] and Zhangyong Hu[1*†]*

[1] Department of Radiology, The First Affiliated Hospital of Wenzhou Medical University, Wenzhou, China, [2] Department of Gynecology, The First Affiliated Hospital of Wenzhou Medical University, Wenzhou, China

OPEN ACCESS

Edited by:
Jian-Jun Wei, Northwestern University, United States

Reviewed by:
Raffaella Ergasti, Università Cattolica del Sacro Cuore, Italy
Anthony Magliocco, Protean BioDiagnostics Inc., United States

***Correspondence:**
Zhangyong Hu
huzy@21cn.com
Feng Lin
lin801026@163.com

†These authors have contributed equally to this work

Specialty section:
This article was submitted to Gynecological Oncology, a section of the journal Frontiers in Oncology

Received: *29 July 2021*
Accepted: *19 November 2021*
Published: *14 December 2021*

Citation:
Cai M-T, Yao F, Ding J, Zheng R-R, Huang X-W, Yang Y-J, Lin F and Hu Z-Y (2021) MRI Radiomic Features: A Potential Biomarker for Progression-Free Survival Prediction of Patients With Locally Advanced Cervical Cancer Undergoing Surgery. Front. Oncol. 11:749114. doi: 10.3389/fonc.2021.749114

Objectives: To investigate the prognostic role of radiomic features based on pretreatment MRI in predicting progression-free survival (PFS) of locally advanced cervical cancer (LACC).

Methods: All 181 women with histologically confirmed LACC were randomly divided into the training cohort (n = 126) and the validation cohort (n = 55). For each patient, we extracted radiomic features from whole tumors on sagittal T2WI and axial DWI. The least absolute shrinkage and selection operator (LASSO) algorithm combined with the Cox survival analysis was applied to select features and construct a radiomic score (Rad-score) model. The cutoff value of the Rad-score was used to divide the patients into high- and low-risk groups by the X-tile. Kaplan–Meier analysis and log-rank test were used to assess the prognostic value of the Rad-score. In addition, we totally developed three models, the clinical model, the Rad-score, and the combined nomogram.

Results: The Rad-score demonstrated good performance in stratifying patients into high- and low-risk groups of progression in the training (HR = 3.279, 95% CI: 2.865–3.693, $p < 0.0001$) and validation cohorts (HR = 2.247, 95% CI: 1.735–2.759, $p < 0.0001$). Otherwise, the combined nomogram, integrating the Rad-score and patient's age, hemoglobin, white blood cell, and lymph vascular space invasion, demonstrated prominent discrimination, yielding an AUC of 0.879 (95% CI, 0.811–0.947) in the training cohort and 0.820 (95% CI, 0.668–0.971) in the validation cohort. The Delong test verified that the combined nomogram showed better performance in estimating PFS than the clinical model and Rad-score in the training cohort ($p = 0.038$, $p = 0.043$).

Conclusion: The radiomics nomogram performed well in individualized PFS estimation for the patients with LACC, which might guide individual treatment decisions.

Keywords: locally advanced cervical cancer, magnetic resonance imaging, radiomics, progression-free survival, MRI

INTRODUCTION

Cervical cancer is one of the most common cancer in women worldwide and an important cause of cancer-related death among women (1). In developing countries, screening has not yet been fully universal, and the incidence and mortality of cervical cancer are still on the rise. In China, most cervical cancer patients are at advanced stages when diagnosed (2). Radical hysterectomy or concurrent chemoradiotherapy is the standard treatment protocol for locally advanced cervical cancer (LACC) (3). Nevertheless, recurrence or metastasis frequently occurred in these patients, with only 50% ~60% 5-year survival rate. Thence, pretreatment prediction for the high-risk recurrence or distant metastasis is important for the development of individualized treatment protocols.

Several clinical factors have already been identified as risk factors in cervical cancer patients, including International Federation of Gynecology and Obstetrics (FIGO) stage, lymph node metastasis (LNM), lymph vascular space invasion (LVSI), and depth of invasion (4, 5). Nevertheless, even if the clinical stage and treatment plan of the patient are similar, the clinical outcome can vary widely. These findings imply that the present prognostic model could not provide adequate prognostic information and correctly assess the intrinsic heterogeneity of tumors. Hence, new prognostic biomarkers are required for individual treatment.

Pretreatment magnetic resonance imaging (MRI) can supply more details about tumor heterogeneity than tissue samples and assist in determining the tumor size, location, degree of invasion into adjacent organs, and LNM (6, 7). The emerging radiomics holds great potential for facilitating better clinical decision-making. Radiomics refers to the conversion of medical images into mineable high-dimensional data *via* automatic high-throughput extraction of data characterization algorithms (8, 9). The main function of radiomics is that the image data-mining method can detect the intrinsic heterogeneity of tumors, unidentifiable by radiologists, and provide decision support noninvasively for oncology at low cost (10, 11). According to previous studies, radiomics features could predict the survival outcomes and recurrence, evaluate tumor subtype and stage, monitor therapeutic response, and detect LNM or distant metastasis (12–14). It is unknown whether radiomics signatures of pretreatment MRI can predict progression-free survival (PFS) in LACC patients who received radical hysterectomy without preoperative neoadjuvant chemotherapy.

Therefore, the purpose of our study is to develop and validate a noninvasive radiomics signature based on pretreatment MRI for the PFS prediction in patients with LACC.

MATERIALS AND METHODS

Patients

We identified 181 consecutive women with LACC who underwent surgeries following pretreatment MRI using a 3.0-T scanner at our institution between January 2011 and February 2017 (to ensure a minimum follow-up of 3 years). The inclusion criteria were as follows (**Supplementary Figure S1**): (i) patients who underwent radical hysterectomies and pelvic lymphadenectomies; (ii) patients who have not received treatment before surgery and the clinicopathological data are complete; and (iii) sagittal T2-weighted imaging (T2WI) and axial diffusion-weighted imaging (DWI) were performed less than the 2-week period before surgery. The exclusion criteria were as follows: (i) lesions invisible on axial DWI or sagittal T2WI; (ii) poor image quality due to the movement of the patient during examination or the chemical shift artifact of the gas in the colorectum; (iii) patients who underwent preoperative therapies; and (iv) patients with other cancers at the same time.

Follow-Up and Prognosis Evaluation

Information was collected from telephone consultations, outpatient medical records, and social security death indices. In our study, the endpoint event was PFS, which was defined as the time from the date of surgery until any recurrence (local or distant recurrence, metastasis). Clinical follow-up was every 3 months for the first 2 years, every 6 months for the next 3 years, and annually thereafter. Gynecological examinations, cervical cytology, and imaging tools such as computed tomography (CT), MR, and positron emission tomography (PET)/CT imaging were used to evaluate the patients during the follow-up.

MRI Scan Acquisition and Tumor Segmentation

All patients underwent pelvic 3.0-T MRI scans (Signa EXCITE; GE Medical Systems, 3200N, Grandview Blvd, Waukesha, WI 53188, USA; or Achieva, Philips Healthcare, The Netherlands), using a 16-channel phased-array encoding abdominal coil. The scanning range was set to cover the entire pelvis from the level of the anterior superior iliac spine to the inferior level of the symphysis pubis. Patients had to fast at least 6 h before the examination. The standard pelvic MR scan protocol was used in this retrospective study, including multiple b-value DWI (repetition time (TR)/echo time (TE) = 3,625/74 ms, field of view (FOV): 420 × 420 mm, matrix: 256 × 128, slice thickness/gap = 5 mm/6 mm, b-values: 0.700 s/mm^2), sagittal T2-weighted fat suppression (FS) images: (TR/TE = 3,200/106 ms, FOV = 320 × 320 mm, matrix = 320 × 224, slice thickness/gap = 4 mm/5 mm); axial T2-weighted fat suppression (FS) images: (TR/TE = 3,600/104 ms, FOV = 380 × 380 mm, matrix = 320 × 224. slice thickness/gap = 5 mm/6 mm); coronal T2-weighted fat suppression (FS) images: (TR/TE = 3,400/107 ms, FOV = 360 × 360 mm, matrix = 320 × 192, slice thickness/gap = 4 mm/5 mm); and axial T1-weighted imaging (T1WI): (TR/TE = 245 ms/2 ms, FOV: 380 × 380 mm, matrix: 384 × 180, slice thickness/gap = 5 mm/6 mm).

Pelvic MRI Digital Imaging and Communications in Medicine (DICOM) original images of all patients were downloaded from the Picture Archiving and Communication System (PACS) and uploaded into the ITK-SNAP (open source software; www.itksnap.org) for three-dimensional manual segmentation of MR images (15). The regions of interest (ROIs) of the entire tumor were manually outlined layer by layer by a radiologist with 5 years of experience in gynecological imaging, and the results were verified by a senior radiologist with 15 years of work experience. The radiomics workflow is displayed in **Figure 1**.

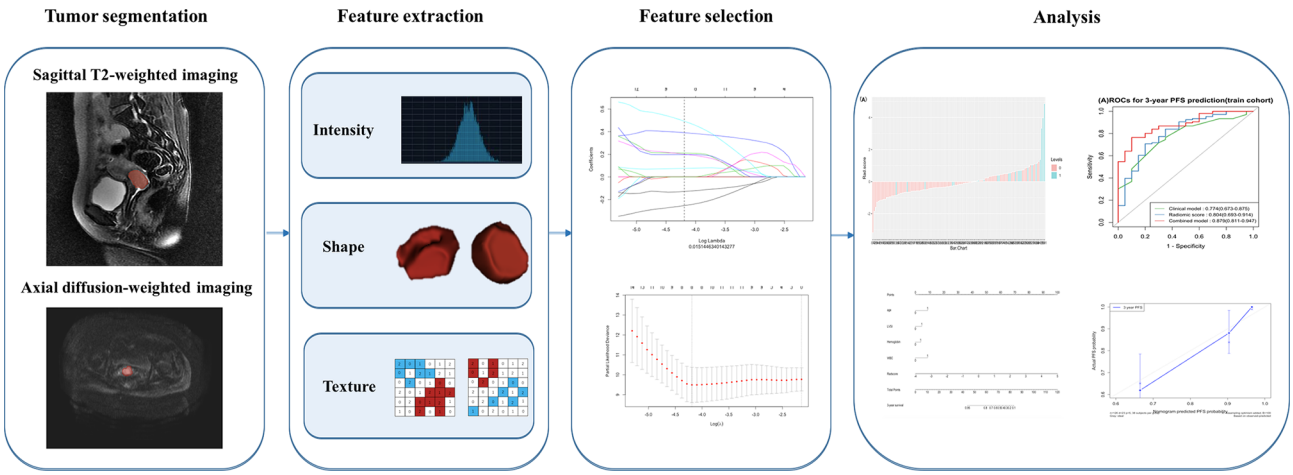


FIGURE 1 | The radiomics workflow.

Feature Extraction

Before feature extraction, the image was preprocessed, including resampling the MR image to a 1 × 1 × 1-mm^3 voxel size and normalizing the image gray scale to 0 to 255. The purpose of image preprocessing is to reduce heterogeneity bias caused by different equipments and scanning parameters. Radiomic feature extraction was implemented in Artificial Intelligence Kit Version 3.0.0.R, which is a commercial software of GE Healthcare. We extracted 396 radiomic features of tumor on T2WI and DWI, respectively, and a total of 792 quantitative features for each patient. The features were divided into four groups: (I) intensity histogram (n = 84), (II) morphology (n = 40) and (III) texture (n = 668), including (a) gray-level co-occurrence matrix (GLCM, n = 288), (b) gray-level run length matrix (GLRLM, n = 344), and (c) Haralick (n = 36).

Feature Selection

High-dimensional extraction produced various radiomic features, but not all of them were significantly associated with PFS in LACC. To develop the radiomics model, we designed a two-step procedure for dimensionality reduction and selection of radiomic features. We applied the least absolute shrinkage and selection operator (LASSO) algorithm jointly with the Cox survival analysis to select the importantly prognostic features in the training cohort (16, 17). Then, the multiple-feature-based radiomic signatures were created for predicting patients' PFS in the training cohort. The LASSO Cox regression model analysis was completed by the "glmnet" package (18, 19).

Building and Validation of the Radiomics Signature

The radiomics score (Rad-score, which was defined as the radiomics signature in the current study) was computed in the training cohort by the LASSO Cox regression model analysis. Above all, we evaluated the potential relationship of the Rad-score with PFS in the training cohort and then tested it in the validation cohort. In addition, all patients were divided into high-risk and low-risk groups according to the optimum cutoff value of the Rad-score by applying X-tile software (20). The relationship of the radiomic risk score with PFS was assessed in the training cohort and then verified in the validation cohort by using Kaplan–Meier analysis and log-rank test.

Construction of an Individualized PFS Prediction Model

The univariate Cox analysis was used to determine clinicopathologic factors associated with PFS in all patients (n = 181). LASSO Cox regression model analysis was applied to select variables with a p value < 0.1 in the univariate Cox analysis. Except the Rad-score, a clinical model which incorporated only the independent clinicopathologic risk factors was also built to predict the 3-year PFS. The prognostic performance of the models was measured by Harrell's concordance index (C-index), C-index = 0.5 describes a random prediction, and C-index = 1.0 implies a perfect prediction ability (21). Since the C-index method may be wrong when predicting a fixed time point (22), we also use the time-dependent area under the receiver operating characteristic (ROC) analysis to assess the t-year risk of an event (23, 24).

To provide the clinician with a quantitative approach to predict patients' probability of 3-year PFS, and to show the incremental value of the Rad-score to the clinicopathologic risk factors, we further built a combined nomogram (combined model) as an individualized PFS prediction model that incorporated both the Rad-score and clinicopathologic risk factors for PFS prediction. The prognostic performance of the nomogram was estimated by C-index and ROC analysis. Besides, calibration curves were used to compare the predicted PFS with the actual PFS.

Statistical Analysis

Statistical analysis was executed by R software (version 3.6.3) and SPSS (version 23.0). Rad-scores were divided into two groups according to the cutoff value selected by X-tile. In addition, the continuous clinical variables were converted into categorical variables on the basis of cutoff values, which were determined by ROC analysis or routine cutoff points (for size). Differences in

distributions between the training and validation cohorts were assessed with the chi-squared test as appropriate. A quantitative comparison of the area under the curve (AUC) was made with the Delong test (25). The glmnet package was adopted for running LASSO–Cox. The survival package was adopted for building the Cox proportional risk model, drawing the Kaplan–Meier analysis, and calculating the C-index. The rms package was used for nomograms and calibration curves. All two-sided *p* values less than 0.05 were considered significant.

RESULTS

Patient Characteristics

The clinicopathologic factors of all patients are summarized in **Table 1**. Of the 181 patients included in the study, the mean age of the patients was 50.67 ± 10.81 years. Disease recurred in 33 of 181 patients (18.2%). The median follow-up time was 50.5 months (40.75–66.0) for the training cohort and 48.0 months (40.0–66.0) for the validation cohort. There were no significant differences between the training cohort and the validation cohort in clinicopathologic features (p = 0.146–0.714).

Feature Selection, Radiomics Signature Building and Validation

The LASSO Cox regression model was used to build a prognostic Rad-score. Eight potential predictors, six features from T2WI, and two features from DWI were included in the training cohort. Finally, the Rad-score was constructed based on the eight features, and the calculation formula is as follows: Rad-score = -0.253 × T2WI_MinIntensity + 0.210 × T2WI_ClusterShade + 0.076 × T2WI_GLCM-IDM + 0.201 × T2WI_RLM-

TABLE 1 | Patient characteristics in the training and validation cohorts.

Characteristics	Training cohort (n = 126)	Validation cohort (n = 55)	p value
Age (years)			0.714
≥54.50	65 (51.59%)	30 (54.55%)	
<54.50	61 (48.41%)	25 (45.45%)	
FIGO stage			0.357
IB1	43 (34.13%)	24 (43.64.09%)	
IB2	10 (7.93%)	6 (10.91%)	
IIA1	54 (42.86%)	16 (29.09%)	
IIA2	19 (15.08%)	9 (16.36%)	
Size(cm)			0.539
2~4	97 (76.98%)	40 (72.73%)	
>4	29 (23.02%)	15 (27.27%)	
LVSI			0.360
Positive	35 (27.78%)	19 (34.55%)	
Negative	91 (72.22%)	36 (65.45%)	
PLN			0.409
Positive	21 (16.67%)	12 (21.82%)	
Negative	105 (83.33%)	43 (78.18%)	
Differentiation			0.758
Low grade	5 (3.97%)	1 (1.82%)	
Middle grade	51 (40.48%)	23 (41.82%)	
High grade	70 (55.56%)	31 (56.36%)	
Pathological type			0.260
SCC	110 (87.30%)	52 (94.54%)	
Adenocarcinoma	10 (7.94%)	1 (1.82%)	
Other	6 (4.76%)	2 (3.64%)	
SCCA(μg/L)			0.887
≥2.05	70 (58.33%))	28 (57.14%)	
<2.05	50 (41.67%	21 (42.86%)	
Albumin (g/L)			0.215
≥41.25	104 (82.54%)	41 (74.55%)	
<41.25	22 (17.46%)	14 (25.45%)	
Hemoglobin (g/L)			0.409
≥145.5	11 (8.73%)	7 (12.73%)	
<145.5	115 (91.27%)	48 (87.27%)	
Platelet (10^9/L)			0.653
≥296	29 (23.02%)	11 (20%)	
<296	97 (76.98%)	44 (80%)	
WBC (10^9/L)			0.236
≥7.465	39 (30.95%)	22 (40%)	
<7.465	87 (69.05%)	33 (60%)	

FIGO, International Federation of Gynecology and Obstetrics; LVSI, lymph vascular space invasion; LNM, lymph node metastasis; SCC, squamous cell carcinoma; SCCA, squamous cell carcinoma antigen; WBC, white blood cell.

LongRunEmphasis × T2WI_RLM-LongRunHighGreyLevel Emphasis + 0.391 × T2WI_LowIntensityLargeAreaEmphasis + 0.198 × DWI_HighIntensitySmallAreaEmphasis + 0.493 × DWI_SmallAreaEmphasis. Distributions of the Rad-score in the training and validation cohorts are displayed in **Supplementary Figure S2**.

The optimum cutoff generated by X-tile was 0.543. According to the optimal cutoff value, patients were classified into high-risk (Rad-score ≥ 0.543) and low-risk (Rad-score < 0.543) groups. A Kaplan–Meier analysis (**Figure 2**) was demonstrated that the patients in the high-risk group had shorter PFS than did the low-risk group in the training [hazard ratio (HR) = 3.279, 95% CI: 2.865–3.693, $p < 0.0001$] and validation cohorts (HR = 2.247, 95% CI: 1.735–2.759, $p < 0.0001$). **Figure 3** shows typical patients who had similar clinicopathological characteristics, but their PFS time was significantly different (9 vs. 37 months). The Rad-score of patient 2 was significantly higher than that of patient 1 (1.380 vs. 0.029). In the LASSO Cox regression analysis, the Rad-score yielded a C-index of 0.778 [95% confidence interval (CI): 0.699–0.858] for the training cohort (**Table 2**). The favorable prognostic performance of the Rad-score was further confirmed in the validation cohort (C-index, 0.816; 95% CI: 0.673–0.958).

Univariate Cox Analysis of the Risk Factors for PFS

In addition to Rad-score, we included a total of 12 clinicopathologic factors into the univariate analysis (**Table 3**), and the results showed that age (HR = 0.511, 95% CI: 0.247–1.053, $p = 0.069$), LVSI (HR = 2.286, 95% CI: 1.151–4.538, $p = 0.018$), squamous cell carcinoma antigen (HR = 0.427, 95% CI:

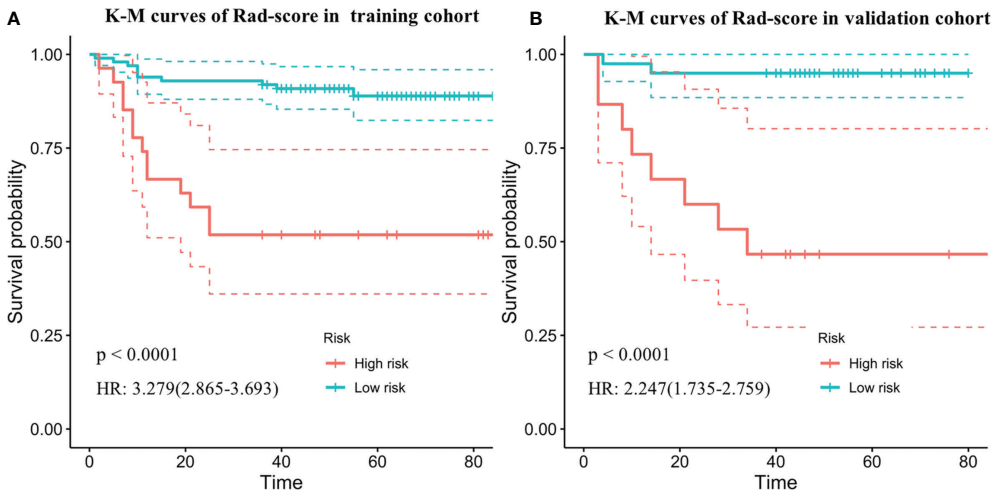


FIGURE 2 | Kaplan–Meier survival curves of progression-free survival according to the Rad-score in the training cohorts **(A)** and independent validation data set **(B)**. Shadows represent 95% confidence interval. HR, hazard ratio.

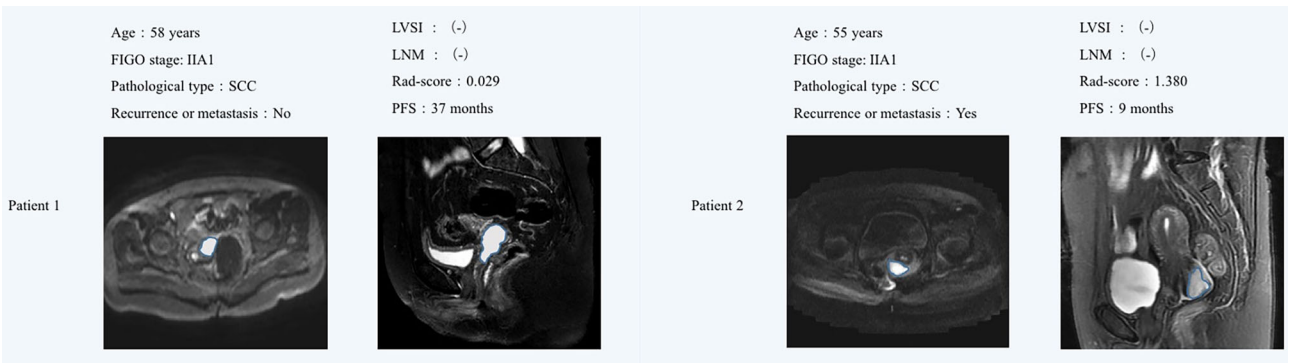


FIGURE 3 | MR images showed that the sagittal T2WI and axial DWI lesions were cervical cancer. Although patient 1 and patient 2 had similar clinicopathological characteristics, their Rad-score were significantly different. Patient 1 did not find obvious signs of recurrence or metastasis after 37 months of postoperative follow-up, while the Patient 2 relapsed 9 months after surgery. The Rad-score of patient 2 was significantly higher than that of patient 1. FIGO, International Federation of Gynecology and Obstetrics; LVSI, lymph vascular space invasion; LNM, lymph node metastasis; SCC, squamous cell carcinoma; PFS, progression-free survival.

TABLE 2 | Model performance on predicting 3-year PFS.

Models	Cohorts	C-index (95% CI)	AUC (95% CI)	ACC (95% CI)	Sensitivity (95% CI)	Specificity (95% CI)
Clinical model	Training	0.778 (0.699–0.858)	0.774 (0.673–0.875)	0.714 (0.711–0.717)	0.717 (0.631–0.803)	0.700 (0.499–0.901)
	Validation	0.816 (0.673–0.958)	0.707 (0.513–0.902)	0.764 (0.757–0.770)	0.800 (0.683–0.917)	0.600 (0.296–0.904)
Radiomic score	Training	0.756 (0.650–0.861)	0.804 (0.693–0.914)	0.722 (0.719–0.725)	0.708 (0.621–0.794)	0.800 (0.625–0.975)
	Validation	0.803 (0.690–0.915)	0.795 (0.653–0.937)	0.764 (0.757–0.770)	0.756 (0.630–0.881)	0.800 (0.552–1.048)
Combined model	Training	0.821 (0.746–0.896)	0.879 (0.811–0.947)	0.786 (0.783–0.788)	0.764 (0.683–0.845)	0.900 (0.769–1.031)
	Validation	0.829 (0.699–0.959)	0.82 (0.668–0.971)	0.855 (0.850–0.859)	0.867 (0.767–0.966)	0.800 (0.552–1.048)

PFS, progression-free survival; C-index, Harrell's concordance indices; CI, confidence interval; AUC, area under the curve; ACC, accuracy.

0.182–1.005, $p = 0.051$), albumin (HR = 0.530, 95% CI: 0.252–1.113, $p = 0.091$), hemoglobin (HR = 5.393, 95% CI: 2.560–11.363, $p < 0.0001$), white blood cell (WBC) (HR = 2.233, 95% CI: 1.128–4.420, $p = 0.021$), and Rad-score (HR = 2.647, 95% CI: 2.002–3.501, p < 0.0001), would be identified as candidate risk factors ($p < 0.1$) into the LASSO Cox regression analysis.

Assessment the Performances of Various Models in 3-Year PFS Prediction

The LASSO Cox regression model analysis showed that age, LVSI, hemoglobin, and WBC were finally selected and integrated into a clinical model (**Figure 4**). The performance of the clinical model for 3-year PFS prediction yielded a C-index value of 0.778

TABLE 3 | Univariate Cox analysis of risk factors for PFS in all patients.

Characteristics	Univariate analysis		
	Hazard ratio	95% CI	p value
Age			
≥54.5 years versus <54.5 years	0.511	0.247–1.053	0.069
Size			
2~4 cm versus >4 cm	0.851	0.396–1.831	0.680
FIGO stage			
IB1	Reference		
IB2	0.352	0.045–2.724	0.317
IIA1	1.337	0.614–2.912	0.464
IIA2	1.369	0.506–3.701	0.536
LVSI			
positive versus negative	2.286	1.151–4.538	0.018
PLN			
positive versus negative	1.748	0.813–3.762	0.153
Differentiation			
Low grade	Reference		
Middle grade	0.779	0.105–5.791	0.807
High grade	0.653	0.315–1.355	0.253
Pathological type			
SCC	Reference		
Adenocarcinoma	0.473	0.064–3.473	0.462
Other	2.469	0.751–8.112	0.137
SCCA (μg/L)			
≥2.05 versus <2.05	0.427	0.182–1.005	0.051
Albumin (g/L)			
≥41.25 versus <41.25	0.530	0.252–1.113	0.094
Hemoglobin (g/L)			
≥145.5 versus <145.5	5.393	2.560–11.363	<0.0001
Platelet (10^9/L)			
≥296 versus <296	1.088	0.472–2.508	0.843
WBC (10^9/L)			
≥7.465 versus <7.465	2.233	1.128–4.420	0.021
Rad-score	2.647	2.002–3.501	<0.0001

PFS, progression-free survival; FIGO, International Federation of Gynecology and Obstetrics; LVSI, lymph vascular space invasion; LNM, lymph node metastasis; SCC, squamous cell carcinoma; SCCA, squamous cell carcinoma antigen; WBC, white blood cell; CI, confidence interval.

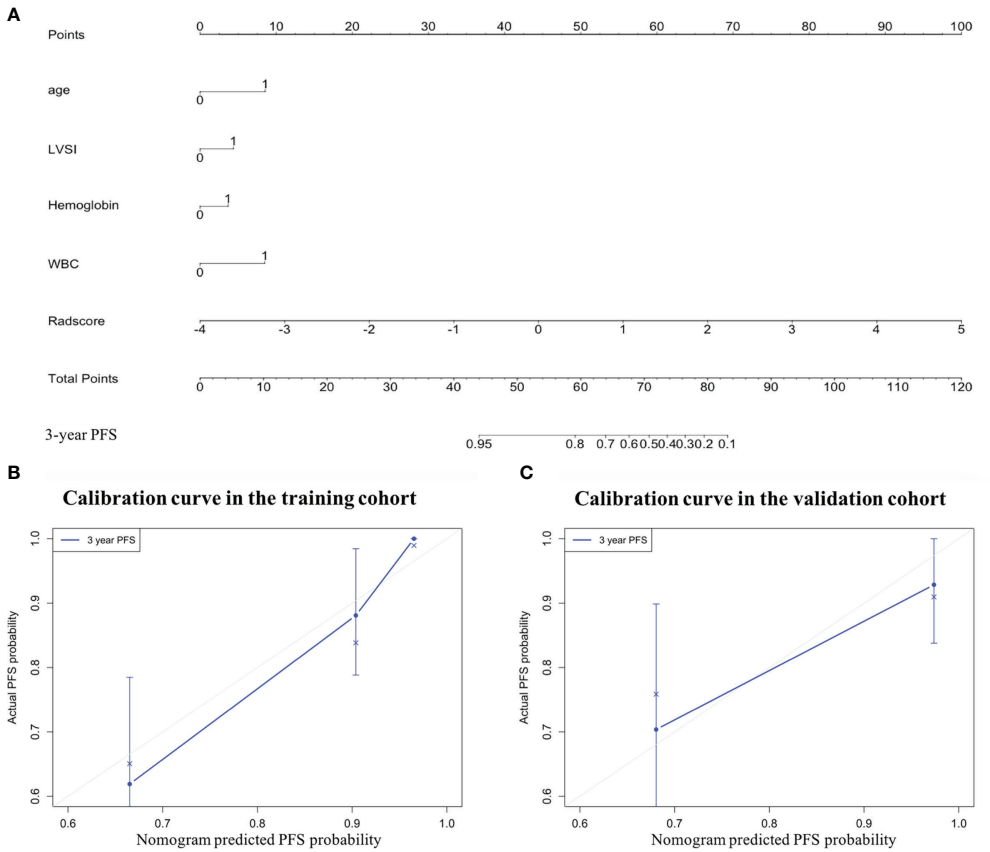


FIGURE 4 | The combined nomogram was developed to predict the risk of 3-year progression-free survival (PFS) of patients with locally advanced cervical cancer undergoing surgery. **(A)** The combined nomogram that integrates the Rad-score with the clinicopathologic features in the training data set. Calibration curves of the combined nomogram in the **(B)** training and **(C)** validation cohorts. The diagonal gray line represents a perfect evaluation, while the blue line represents the actual performance of the nomogram. A closer fit to the diagonal gray line indicates a better assessment. LVSI, lymph vascular space invasion; WBC, white blood cell.

(95% CI: 0.699–0.858) in the training cohort and 0.816 (95% CI: 0.673–0.958) in the validation cohort (**Table 2**). The combined nomogram (**Figure 4**) integrating the radiomic score and the above four clinicopathologic factors demonstrated a better discrimination both in the training (C-index, 0.821; 95% CI: 0.746–0.896) and in the validation cohort (C-index, 0.829; 95% CI: 0.699–0.959) when compared with radiomic score or clinical model alone (**Table 2**).

In the training cohort (**Table 2** and **Figure 5A**), the radiomics score (AUC, 0.804 [95% CI: 0.693–0.914]) showed a comparable prognostic performance with the clinical model (AUC, 0.774 [95% CI: 0.673–0.875]), with a p value of 0.719 (**Figure 6**). The combined nomogram was shown to be with the highest AUC value (0.879, [95% CI: 0.811–0.947]), demonstrating a significant improvement in PFS prediction compared to the clinical model or the radiomics score (p = 0.038, p = 0.043, respectively) (**Figure 6**). In the validation cohort (**Table 2** and **Figure 5B**), the clinical model yielded an AUC of 0.707 (95% CI: 0.513–0.902). Although the radiomics score (AUC, 0.795 [95% CI: 0.653–0.937]) showed improvement compared with the clinical model, the Delong test found that no significant difference was shown between the AUCs (p = 0.458) (**Figure 6**). The combined nomogram (AUC, 0.820 [95% CI: 0.668–0.971]) also showed improvement over the clinical model or the radiomics score for the PFS prediction in the validation cohort. However, the difference was not significant (p = 0.150, p = 0.684, respectively) (**Figure 6**).

DISCUSSION

In this study, we developed and validated an MRI-based Rad-score for noninvasive PFS prediction in patients with LACC undergoing surgery. The study demonstrated that the Rad-score was significantly related with 3-year PFS in both the training and validation cohorts. The Rad-score stratified the patients into low-risk and high-risk groups, and the Kaplan–Meier analysis showed that the patients in the high-risk group portended a worse prognosis with shorter PFS than did the low-risk group in the training (HR = 3.279, 95% CI: 2.865–3.693, $p < 0.0001$) and validation cohorts (HR = 2.247, 95% CI: 1.735–2.759, $p < 0.0001$). The performance of the combined nomogram which

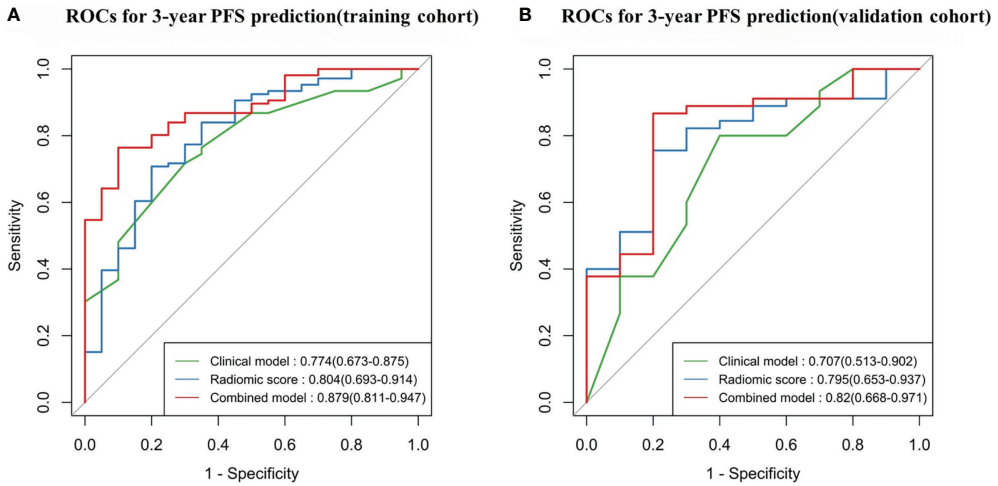


FIGURE 5 | Time-dependent receiver operating characteristic (ROC) curves comparing the predictive capacity of the three models. **(A)** Training cohort, N = 126. **(B)** Validation cohort, N = 55. PFS, progression-free survival.

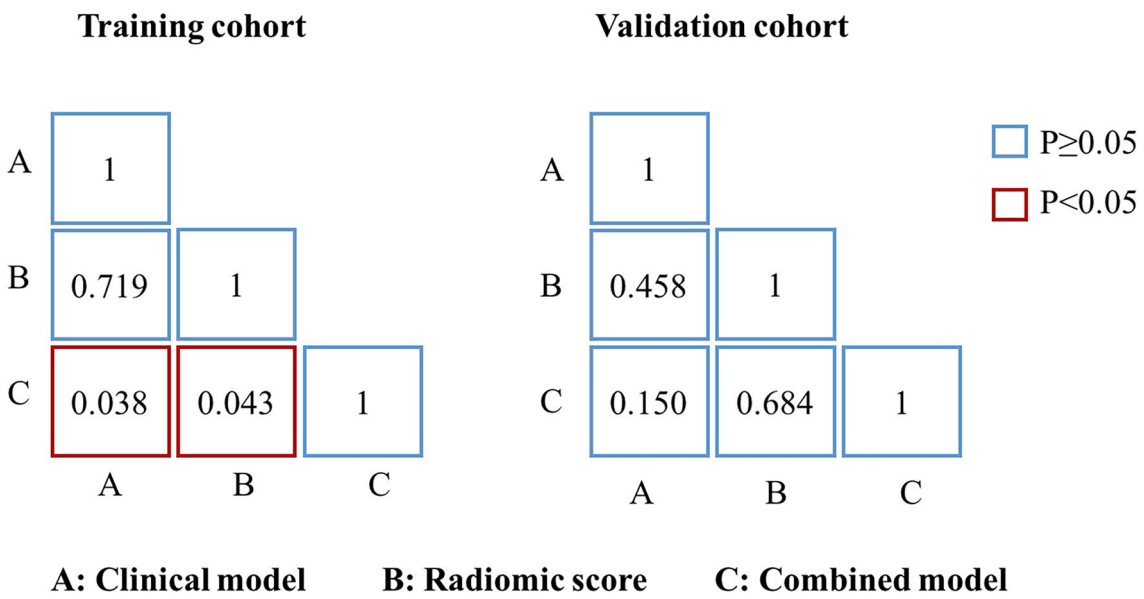


FIGURE 6 | Delong test between different models. p-value of the Delong test between any two models.

integrated Rad-score and significant clinicopathologic parameters was demonstrated to have better performance than the Rad-score or clinical model alone in the PFS prediction. Furthermore, the nomogram showed a satisfactory discrimination performance, with C-indexes of 0.821 and 0.829 in the training and validation cohorts.

Cox regression analysis was used to build the clinical model for PFS prediction. Four clinical features including age, hemoglobin, WBC, and LVSI were found to be correlated with PFS. Inflammation is an important part of the tumor microenvironment and plays a key role in the initiation, promotion, progression, invasion, and metastasis of the tumor (26). Systemic inflammation biomarkers such as C-reactive protein (CRP), platelet count, hemoglobin, and WBC had already been shown to have prognostic values in different tumors (27, 28). In our study, hemoglobin and WBC were also identified as important prognostic factors for PFS which was coherent with the results of the previous studies. In addition, lymph-vascular space invasion is considered to be a crucial factor in the tumor cell dissemination (29) and is identified as an unfavorable prognostic factor in cervical cancer (30, 31), which is consistent with our study.

Radiomics analysis has developed as a non-invasive method to visualize and quantify intra-tumor heterogeneity by high-throughput quantitative characteristic extraction from medical images, thereby providing prognostic information in medical decision making (8). In the recent years, researchers have used radiomics in the prediction of pathological features, LNM, and response to neoadjuvant chemotherapy in cervical cancer (12–14, 32), rather than clinical outcomes such as PFS and overall survival (OS). Jin et al. reported that MRI-based radiomics signature was an independent predictor of DFS in patients with early-stage cervical cancer treated with radical hysterectomy, and their study demonstrated that the Rad-score yielded a C-index of 0.753 (95% CI: 0.696-0.805) on 3-year DFS prediction, which were higher than either clinical model or combined model (33). However, these studies focused on early-stage (IB-IIA) cervical cancer treated by surgery. Only two clinicopathological features (LNM and LVSI) were included in their clinical model, which did not contain another hematological parameter. Some previous studies applied PET/CT radiomics to evaluate patients' responses to chemoradiotherapy with LACC (34, 35). Although PET/CT demonstrated good discrimination ability, its high cost and high radiation limited its wide use. The role of MRI-based radiomic signatures to evaluate PFS in patients with LACC who have surgical indicators has not yet been investigated. Therefore, in this context, it is necessary for us to do this research.

The LASSO-Cox-based method was used to construct the Rad-score, which derived from the joint T2WI and DWI. Wang et al. have published two articles about using Rad-score based on the joint T2WI and DWI for prediction of LNM or parametrial invasion (PMI) in patients with early cervical cancer (36, 37). These studies demonstrated that the Rad-score from the combined T2WI and DWI has a significant improvement performance for prediction of LNM or PMI, compared with the Rad-score from T2WI or DWI alone. The advantage of T2WI is that it can clearly show the anatomical features of tumors in the cervical cancer patients, and as a functional imaging, DWI can provide microscopic motion of water molecules in tissues and subsequently detect early pathological changes based on water diffusion properties (38). Therefore, the combination of T2WI and DWI could balance the shortcomings and gain more precise and comprehensive information about the tumors. In our study, the radiomic score that combined T2WI and DWI showed good performance for prediction of 3-year PFS in patients with LACC, which yielded a C-index of 0.803 (95% CI, 0.690–0.915) and an AUC of 0.795 (95% CI: 0.653-0.937) in the validation cohort.

To provide a clinically suitable and quantitative approach for the individual prediction of PFS in patients with LACC, a nomogram could enable gynecologists to evaluate the survival of patients based on their clinical and image characteristics. In the current study, a combined nomogram that combined both the Rad-score and other important clinicopathologic features was established for the 3-year PFS evaluation in patients with LACC for the first time. The combined nomogram was shown to have a significant improvement performance for the 3-year PFS prediction, compared with the Rad-score or clinical model alone (C-index of 0.821 vs. 0.778 and 0.816 in the training cohort; 0.829 vs. 0.816 and 0.803 in the validation cohort). This result was also verified by the conclusions of the ROC analysis. It indicated that the radiomics signature may contain information that is complementary to clinical factors, reflecting changes of human tissues at the molecular and genetic levels (9, 33). Another interesting finding of our research was that the Rad-score could serve as a marker in discriminating low-risk and high-risk patients. Patients with higher Rad-scores have the worse PFS. These results provided a new insight into the future treatment protocols in patients with LACC. For instance, LACC patients at high risk of recurrence and metastasis could be considered for preoperative neoadjuvant chemotherapy, whereas patients at low risk of recurrence could directly select surgeries, thereby avoiding unnecessary chemotherapy-related toxicities and disease progression due to delays in effective treatment. Therefore, the Rad-score may be used as an effective biomarker to improve the prognostic ability of pretreatment.

Our research has the following limitations. Firstly, its retrospective design and single-institution study may lead to inevitable selection bias. Prospective multicenter studies with larger populations will be required to confirm the robustness and reproducibility of the current research. Secondly, imaging data were collected by different MR scanners or imaging protocols. Although all the imaging data were normalized to reduce bias before extraction, the performance of the radiomics signature will be significantly improved by normalization of the imaging data. Finally, due to the limited number of patients with genetic data, we did not provide genomic characteristics in our study. In the future study, how to integrate genomic features, radiomics signature, and clinical characteristics together will become increasingly important.

CONCLUSION

We developed and validated a Rad-score as a non-invasive method for a preoperative evaluation of PFS in patients with LACC. The combined nomogram, which integrated the Rad-score and clinicopathologic factors, showed significant improvement in the prediction of PFS and may serve as a potential tool to guide individual treatment plans for patients with LACC.

DATA AVAILABILITY STATEMENT

The raw data supporting the conclusions of this article will be made available by the authors, without undue reservation.

ETHICS STATEMENT

The studies involving human participants were reviewed and approved by the First Affiliated Hospital of Wenzhou Medical University, Wenzhou, China. Written informed consent for participation was not required for this study in accordance with the national legislation and the institutional requirements.

AUTHOR CONTRIBUTIONS

MTC wrote the manuscript. MTC, YJY, ZYH, and FL: conception and design. MTC, FY, JD, RRZ, and XWH:

collection and assembly of data. ZYH, MTC, FY, JD, RRZ, and XWH: development of methodology. MTC, ZYH, FY: data analysis and interpretation.All authors contributed to the article and approved the submitted version.

FUNDING

This paper was financially supported by the Science and Technology Planning Projects of Wenzhou (Grant No. Y20180112), Health Foundation for Creative Talents in Zhejiang Province, China (No: 2016) and Project Foundation for the College Young and Middle-aged Academic Leader of Zhejiang Province, China (No: 2017).

SUPPLEMENTARY MATERIAL

The Supplementary Material for this article can be found online at: https://www.frontiersin.org/articles/10.3389/fonc.2021.749114/full#supplementary-material

REFERENCES

1. Siegel RL, Miller KD, Jemal A. Cancer Statistics, 2015. *CA Cancer J Clin* (2015) 65(1):5–29. doi: 10.3322/caac.21254
2. Serkies K, Jassem J. Systemic Therapy for Cervical Carcinoma - Current Status. *Chin J Cancer Res* (2018) 30(2):209–21. doi: 10.21147/j.issn.1000-9604.2018.02.04
3. Bhatla N, Aoki D, Sharma DN, Sankaranarayanan R. Cancer of the Cervix Uteri. *Int J Gynaecol Obstet* (2018) 143(Suppl 2):22–36. doi: 10.1002/ijgo.12611
4. Halle MK, Ojesina AI, Engerud H, Woie K, Tangen IL, Holst F, et al. Clinicopathologic and Molecular Markers in Cervical Carcinoma: A Prospective Cohort Study. *Am J Obstet Gynecol* (2017) 217(4):432.e1–.e17. doi: 10.1016/j.ajog.2017.05.068
5. Rose PG, Java J, Whitney CW, Stehman FB, Lanciano R, Thomas GM, et al. Nomograms Predicting Progression-Free Survival, Overall Survival, and Pelvic Recurrence in Locally Advanced Cervical Cancer Developed From an Analysis of Identifiable Prognostic Factors in Patients From NRG Oncology/Gynecologic Oncology Group Randomized Trials of Chemoradiotherapy. *J Clin Oncol* (2015) 33(19):2136–42. doi: 10.1200/jco.2014.57.7122
6. Ng SH, Chang TC, Ko SF, Yen PS, Wan YL, Tang LM, et al. Nasopharyngeal Carcinoma: MRI and CT Assessment. *Neuroradiology* (1997) 39(10):741–6. doi: 10.1007/s002340050499
7. Kusmirek J, Robbins J, Allen H, Barroilhet L, Anderson B, Sadowski EA. PET/CT and MRI in the Imaging Assessment of Cervical Cancer. *Abdom Imaging* (2015) 40(7):2486–511. doi: 10.1007/s00261-015-0363-6
8. Gillies RJ, Kinahan PE, Hricak H. Radiomics: Images Are More Than Pictures, They Are Data. *Radiology* (2016) 278(2):563–77. doi: 10.1148/radiol.2015151169
9. Aerts HJ, Velazquez ER, Leijenaar RT, Parmar C, Grossman P, Carvalho S, et al. Decoding Tumour Phenotype by Noninvasive Imaging Using a Quantitative Radiomics Approach. *Nat Commun* (2014) 5:4006. doi: 10.1038/ncomms5006
10. Lambin P, Rios-Velazquez E, Leijenaar R, Carvalho S, van Stiphout RG, Granton P, et al. Radiomics: Extracting More Information From Medical Images Using Advanced Feature Analysis. *Eur J Cancer (Oxf Engl 1990)* (2012) 48(4):441–6. doi: 10.1016/j.ejca.2011.11.036
11. Bartoschek M, Oskolkov N, Bocci M, Lövrot J, Larsson C, Sommarin M, et al. Spatially and Functionally Distinct Subclasses of Breast Cancer-Associated Fibroblasts Revealed by Single Cell RNA Sequencing. *Nat Commun* (2018) 9(1):5150. doi: 10.1038/s41467-018-07582-3
12. Erbay G, Onal C, Karadeli E, Guler OC, Arica S, Koc Z. Predicting Tumor Recurrence in Patients With Cervical Carcinoma Treated With Definitive Chemoradiotherapy: Value of Quantitative Histogram Analysis on Diffusion-Weighted MR Images. *Acta Radiol (Stockholm Sweden 1987)* (2017) 58(4):481–8. doi: 10.1177/0284185116656492
13. Schob S, Meyer HJ, Pazaitis N, Schramm D, Bremicker K, Exner M, et al. ADC Histogram Analysis of Cervical Cancer Aids Detecting Lymphatic Metastases-A Preliminary Study. *Mol Imaging Biol* (2017) 19(6):953–62. doi: 10.1007/s11307-017-1073-y
14. Liu Y, Zhang Y, Cheng R, Liu S, Qu F, Yin X, et al. Radiomics Analysis of Apparent Diffusion Coefficient in Cervical Cancer: A Preliminary Study on Histological Grade Evaluation. *J Magn Reson Imaging* (2019) 49(1):280–90. doi: 10.1002/jmri.26192
15. Yushkevich PA, Piven J, Hazlett HC, Smith RG, Ho S, Gee JC, et al. User-Guided 3D Active Contour Segmentation of Anatomical Structures: Significantly Improved Efficiency and Reliability. *NeuroImage* (2006) 31(3):1116–28. doi: 10.1016/j.neuroimage.2006.01.015
16. Zhang JX, Song W, Chen ZH, Wei JH, Liao YJ, Lei J, et al. Prognostic and Predictive Value of a microRNA Signature in Stage II Colon Cancer: A microRNA Expression Analysis. *Lancet Oncol* (2013) 14(13):1295–306. doi: 10.1016/s1470-2045(13)70491-1
17. Jiang Y, Yuan Q, Lv W, Xi S, Huang W, Sun Z, et al. Radiomic Signature of (18)F Fluorodeoxyglucose PET/CT for Prediction of Gastric Cancer Survival and Chemotherapeutic Benefits. *Theranostics* (2018) 8(21):5915–28. doi: 10.7150/thno.28018
18. Friedman J, Hastie T, Tibshirani R. Regularization Paths for Generalized Linear Models *via* Coordinate Descent. *J Stat Softw* (2010) 33(1):1–22. doi: 10.18637/jss.v033.i01
19. Simon N, Friedman J, Hastie T, Tibshirani R. Regularization Paths for Cox's Proportional Hazards Model *via* Coordinate Descent. *J Stat Softw* (2011) 39(5):1–13. doi: 10.18637/jss.v039.i05
20. Camp RL, Dolled-Filhart M, Rimm DL. X-Tile: A New Bio-Informatics Tool for Biomarker Assessment and Outcome-Based Cut-Point Optimization. *Clin Cancer Res* (2004) 10(21):7252–9. doi: 10.1158/1078-0432.Ccr-04-0713
21. Harrell FEJr., Califf RM, Pryor DB, Lee KL, Rosati RA. Evaluating the Yield of Medical Tests. *Jama* (1982) 247(18):2543–6. doi: 10.1001/jama.247.18.2543
22. Blanche P, Kattan MW, Gerds TA. The C-Index Is Not Proper for the Evaluation of T-Year Predicted Risks. *Biostatistics (Oxf Engl)* (2019) 20(2):347–57. doi: 10.1093/biostatistics/kxy006
23. Heagerty PJ, Zheng Y. Survival Model Predictive Accuracy and ROC Curves. *Biometrics* (2005) 61(1):92–105. doi: 10.1111/j.0006-341X.2005.030814.x
24. Chambless LE, Diao G. Estimation of Time-Dependent Area Under the ROC Curve for Long-Term Risk Prediction. *Stat Med* (2006) 25(20):3474–86. doi: 10.1002/sim.2299
25. DeLong ER, DeLong DM, Clarke-Pearson DL. Comparing the Areas Under Two or More Correlated Receiver Operating Characteristic Curves: A Nonparametric Approach. *Biometrics* (1988) 44(3):837–45. doi: 10.2307/2531595
26. Mantovani A, Allavena P, Sica A, Balkwill F. Cancer-Related Inflammation. *Nature* (2008) 454(7203):436–44. doi: 10.1038/nature07205
27. Barkati M, Fortin I, Mileshkin L, Bernshaw D, Carrier JF, Narayan K. Hemoglobin Level in Cervical Cancer: A Surrogate for an Infiltrative Phenotype. *Int J Gynecol Cancer* (2013) 23(4):724–9. doi: 10.1097/IGC.0b013e31828a0623
28. Wang L, Jia J, Lin L, Guo J, Ye X, Zheng X, et al. Predictive Value of Hematological Markers of Systemic Inflammation for Managing Cervical Cancer. *Oncotarget* (2017) 8(27):44824–32. doi: 10.18632/oncotarget.14827
29. Kikuchi E, Margulis V, Karakiewicz PI, Roscigno M, Mikami S, Lotan Y, et al. Lymphovascular Invasion Predicts Clinical Outcomes in Patients With Node-Negative Upper Tract Urothelial Carcinoma. *J Clin Oncol* (2009) 27(4):612–8. doi: 10.1200/jco.2008.17.2361
30. Yu Q, Lou XM, He Y. Prediction of Local Recurrence in Cervical Cancer by a Cox Model Comprised of Lymph Node Status, Lymph-Vascular Space Invasion, and Intratumoral Th17 Cell-Infiltration. *Med Oncol (Northwood Lond Engl)* (2014) 31(1):795. doi: 10.1007/s12032-013-0795-1

31. Twu NF, Ou YC, Liao CI, Chang WY, Yang LY, Tang YH, et al. Prognostic Factors and Adjuvant Therapy on Survival in Early-Stage Cervical Adenocarcinoma/Adenosquamous Carcinoma After Primary Radical Surgery: A Taiwanese Gynecologic Oncology Group (TGOG) Study. *Surg Oncol* (2016) 25(3):229–35. doi: 10.1016/j.suronc.2016.05.028
32. Downey K, Riches SF, Morgan VA, Giles SL, Attygalle AD, Ind TE, et al. Relationship Between Imaging Biomarkers of Stage I Cervical Cancer and Poor-Prognosis Histologic Features: Quantitative Histogram Analysis of Diffusion-Weighted MR Images. *AJR Am J Roentgenol* (2013) 200(2):314–20. doi: 10.2214/ajr.12.9545
33. Fang J, Zhang B, Wang S, Jin Y, Wang F, Ding Y, et al. Association of MRI-Derived Radiomic Biomarker With Disease-Free Survival in Patients With Early-Stage Cervical Cancer. *Theranostics* (2020) 10(5):2284–92. doi: 10.7150/thno.37429
34. Ho KC, Fang YH, Chung HW, Yen TC, Ho TY, Chou HH, et al. A Preliminary Investigation Into Textural Features of Intratumoral Metabolic Heterogeneity in (18)F-FDG PET for Overall Survival Prognosis in Patients With Bulky Cervical Cancer Treated With Definitive Concurrent Chemoradiotherapy. *Am J Nucl Med Mol Imaging* (2016) 6(3):166–75.
35. Lucia F, Visvikis D, Desseroit MC, Miranda O, Malhaire JP, Robin P, et al. Prediction of Outcome Using Pretreatment (18)F-FDG PET/CT and MRI Radiomics in Locally Advanced Cervical Cancer Treated With Chemoradiotherapy. *Eur J Nucl Med Mol Imaging* (2018) 45(5):768–86. doi: 10.1007/s00259-017-3898-7
36. Wang T, Gao T, Yang J, Yan X, Wang Y, Zhou X, et al. Preoperative Prediction of Pelvic Lymph Nodes Metastasis in Early-Stage Cervical Cancer Using Radiomics Nomogram Developed Based on T2-Weighted MRI and Diffusion-Weighted Imaging. *Eur J Radiol* (2019) 114:128–35. doi: 10.1016/j.ejrad.2019.01.003
37. Wang T, Gao T, Guo H, Wang Y, Zhou X, Tian J, et al. Preoperative Prediction of Parametrial Invasion in Early-Stage Cervical Cancer With MRI-Based Radiomics Nomogram. *Eur Radiol* (2020) 30(6):3585–93. doi: 10.1007/s00330-019-06655-1
38. Harry VN. Novel Imaging Techniques as Response Biomarkers in Cervical Cancer. *Gynecol Oncol* (2010) 116(2):253–61. doi: 10.1016/j.ygyno.2009.11.003

Conflict of Interest: The authors declare that the research was conducted in the absence of any commercial or financial relationships that could be construed as a potential conflict of interest.

Publisher's Note: All claims expressed in this article are solely those of the authors and do not necessarily represent those of their affiliated organizations, or those of the publisher, the editors and the reviewers. Any product that may be evaluated in this article, or claim that may be made by its manufacturer, is not guaranteed or endorsed by the publisher.

Copyright © 2021 Cai, Yao, Ding, Zheng, Huang, Yang, Lin and Hu. This is an open-access article distributed under the terms of the Creative Commons Attribution License (CC BY). The use, distribution or reproduction in other forums is permitted, provided the original author(s) and the copyright owner(s) are credited and that the original publication in this journal is cited, in accordance with accepted academic practice. No use, distribution or reproduction is permitted which does not comply with these terms.

frontiers in Oncology

ORIGINAL RESEARCH
published: 06 January 2022
doi: 10.3389/fonc.2021.746571

Homologous Recombination Deficiency Associated With Response to Poly (ADP-ribose) Polymerase Inhibitors in Ovarian Cancer Patients: The First Real-World Evidence From China

Jing Ni[1†], Wenwen Guo[2†], Qian Zhao[1†], Xianzhong Cheng[1], Xia Xu[3], Rui Zhou[1], Hongyuan Gu[1], Chen Chen[1] and Xiaoxiang Chen[1]*

[1] Department of Gynecologic Oncology, The Affiliated Cancer Hospital of Nanjing Medical University, Jiangsu Cancer Hospital, Jiangsu Institute of Cancer Research, Nanjing, China, [2] Department of Pathology, The Second Affiliated Hospital of Nanjing Medical University, Nanjing, China, [3] Department of Chemotherapy, Jiangsu Cancer Hospital, Jiangsu Institute of Cancer Research, The Affiliated Cancer Hospital of Nanjing Medical University, Nanjing, China

OPEN ACCESS

Edited by:
Shannon Neville Westin,
University of Texas MD Anderson Cancer Center, United States

Reviewed by:
Sarah Taylor,
University of Pittsburgh, United States
Min Deng,
Mayo Clinic, United States

***Correspondence:**
Xiaoxiang Chen
cxxxxcyd@gmail.com

[†]These authors have contributed equally to this work

Specialty section:
This article was submitted to Gynecological Oncology, a section of the journal Frontiers in Oncology

Received: 24 July 2021
Accepted: 08 December 2021
Published: 06 January 2022

Citation:
Ni J, Guo W, Zhao Q, Cheng X, Xu X, Zhou R, Gu H, Chen C and Chen X (2022) Homologous Recombination Deficiency Associated With Response to Poly (ADP-ribose) Polymerase Inhibitors in Ovarian Cancer Patients: The First Real-World Evidence From China. Front. Oncol. 11:746571. doi: 10.3389/fonc.2021.746571

Homologous recombination deficiency (HRD) is an approved predictive biomarker for Poly (ADP-ribose) polymerase inhibitors (PARPi) in ovarian cancer. However, the proportion of positive HRD in the real world and the relationship between HRD status and PARPi in Chinese ovarian cancer patients remain unknown. A total of 67 ovarian cancer patients who underwent PARPi, either olaparib or niraparib, were enrolled and passed inclusion criteria from August 2018 to January 2021 in the Affiliated Cancer Hospital of Nanjing Medical University. HRD status correlation with Progression-free survival (PFS) was analyzed and summarized with a log-rank test. Univariate and multiple cox-regression analyses were conducted to investigate all correlated clinical factors. Approximately 68.7% (46/67) patients were HRD positive and the rest 31.3% (21/67) were HRD negative. The PFS among HRD-positive patients was significantly longer than those HRD-negative patients (medium PFS 9.4 m vs 4.1 m, hazard ratio [HR]: 0.52, 95% CI: [0.38–0.71], p <0.001). Univariate cox-regression found that HRD status, Eastern Cooperative Oncology Group (ECOG) status, BRCA status, previous treatment lines, secondary cytoreductive surgery and R0 resection were significantly associated with PFS after PARPi treatment. After multiple regression correction, HRD status and ECOG were the independent factors to predict PFS (HR: 0.67, 95% CI: [0.49–0.92], p = 0.01; HR: 2.20, 95% CI: [1.14–4.23], p = 0.02, respectively). In platinum sensitivity evaluable subgroup (N = 49), HRD status and platinum sensitivity status remain significant to predict PFS after multiple regression correction (HR: 0.71, 95% CI: [0.51–0.98], p = 0.04; HR: 0.49, 95% CI: [0.24–1.0], p = 0.05, respectively). This is the first real-world study of HRD status in ovarian cancer patients in China, and we demonstrate that HRD is an

independent predictive biomarker for PARP inhibitors treatment in Chinese ovarian cancer patients.

Keywords: HRD, PARPi, predictive biomarker, ovarian cancer, Chinese population

INTRODUCTION

Ovarian cancer is the most lethal gynecological malignancy (1). Approximately 70% of the patients with ovarian cancer are diagnosed at an advanced stage. Most ovarian cancers patients are sensitive to platinum-based chemotherapy (2). How to prolong the platinum-free interval (PFI) is an important issue in ovarian cancer treatment. PARPi has changed the treatment pattern of ovarian cancer. Many clinical trials and real-world studies have confirmed that PARPi can significantly prolong the PFI of patients with ovarian cancer (3–6).

Poly (ADP-ribose) polymerase (PARP) plays an important role in DNA repair, maintenance of genome integrity, and regulation of various metabolic and signal transduction processes. PARP1 and PARP2 enzymes are activated after DNA damage that manifests mainly as single-strand breaks (SSBs), double-strand breaks (DSBs) or replication fork stalling (7); they also recognize and bind to the DNA fracture site and mediate DNA single-strand damage repair in tumor cells. In HRD-positive tumor cells, such as the BRCA mutation (BRCAmt) or other germline mutations in homologous recombination repair (HRR) pathway genes (e.g., RAD51 and ATM), single-strand DNA damage cannot be repaired, forming a synthetic lethal effect (8). Therefore, BRCAmt or HRD-positive tumor cells are more sensitive to PARPi (9). Previous studies also demonstrated that HRD-positive ovarian cancer patients had more significant clinical benefits from PARPi treatment (4, 6, 10).

At present, the FDA approved two commercial kits for HRD detection: FoundationFocus®CDx BRCA LOH (integrated to FoundationOne®CDx, shortened as F1CDx) and Myriad myChoice®CDx. The determination of HRD status is based on genomic scars. Cells with HRD had DNA repair dysfunction, which will lead to genome damage and leave genomic scars. FoundationFocus®CDx mainly evaluates HRD by loss of heterozygosity (LOH) with 16% as the threshold value that has been used for companion diagnostic (CDx) of rucaparib (11), while Myriad myChoice®CDx includes LOH, telomere allele imbalance (TAI), and large fragment migration (LST) with 42 as the threshold value that has been widely applied for CDx of niraparib and olaparib (4, 6, 10, 12). Approximately 50% of patients with high-grade serous ovarian cancer are HRD positive in the western population (13, 14).

In China, although four PARPi, namely, Olaparib, Niraparib, Pamiparib, and Fluzoparib, have been approved in ovarian cancer, HRD status has not been approved as a CDx biomarker, and there is no National Medical Products Administration (NMPA)-approved kit for HRD detection yet. Thus, the correlation of HRD status with PARPi therapeutic outcomes could be retrospectively studied in the real world. Our study aimed to perform HRD testing of ovarian cancer in the real world in China and correlate HRD status and clinical characteristics with therapeutic outcomes.

MATERIALS AND METHODS

Study Population

Between August 2018 and January 2021, a total of 79 ovarian cancer or fallopian tube cancer patients were treated with PAPRi for more than four weeks, including olaparib and niraparib in the Affiliated Cancer Hospital of Nanjing Medical University, were recruited (NCT:05044091). If patients experienced serious adverse events (Grades 3–4), the dose reduction and interruption would be done according to drug instruction of olaparib or niraparib. Treatment continued until the occurrence of radiological progression, as assessed by the Response Evaluation Criteria in Solid Tumors 1.1 (RECIST 1.1), unacceptable adverse events or death. Five patients with no qualified FFPE samples or no signed informed consent forms were excluded. Seven patients with failure of quality control of experimental or sequencing data or lost follow-up clinic information were further removed for data analysis. All methods were performed in accordance with the relevant guidelines and regulations by the ethics committee of the Affiliated Cancer Hospital of Nanjing Medical University. The study flowchart is shown in **Figure 1**.

HRD Testing

The formalin fixation and paraffin embedding (FFPE) samples from cytoreductive surgery were obtained with the patients' informed consent. DNA was extracted from FFPE biopsy/surgical specimens by MagPure FFPE DNA LQ kit (Kit# D6323). A total of 100 ng DNA (minimum 50 ng if the total DNA is less than 100 ng) was applied for library construction and 500 ng libraries were used for hybrid capture with an AmoyDx® HRD panel, which selected coding sequences (CDS) regions for 54 genes and 72,000 single nucleotide polymorphisms (SNPs). The list of 54 genes is shown in **Supplementary Table 1**. The selected libraries were pooled and sequenced on the Illumina Novaseq6000 with >500× unique coverage for 54 genes and >100× for SNP loci.

Sequence data were processed using a customized analysis pipeline designed to accurately detect multiple classes of genomic

Abbreviations: HRD, homologous recombination deficiency; PARPi, Poly (ADP-ribose) polymerase inhibitors; PFI, platinum free interval; LOH, loss of heterozygosity; TAI, telomeric allelic imbalance; LST, large-scale state transitions; NGS, next generation sequencing; PFS, progression free survival; SCS, secondary cytoreductive surgery; ECOG PS, Eastern Cooperative Oncology Group performance status; FIGO, International Federation of Gynecology and Obstetrics; R0, no macroscopic disease after surgery; R1, 1 cm or less macroscopic disease after surgery; R2, more than 1 cm macroscopic disease after surgery; PDS, primary debulking surgery; IDS, interval debulking surgery; NACT, Neoadjuvant chemotherapy; VUS, variants of unknown significance.

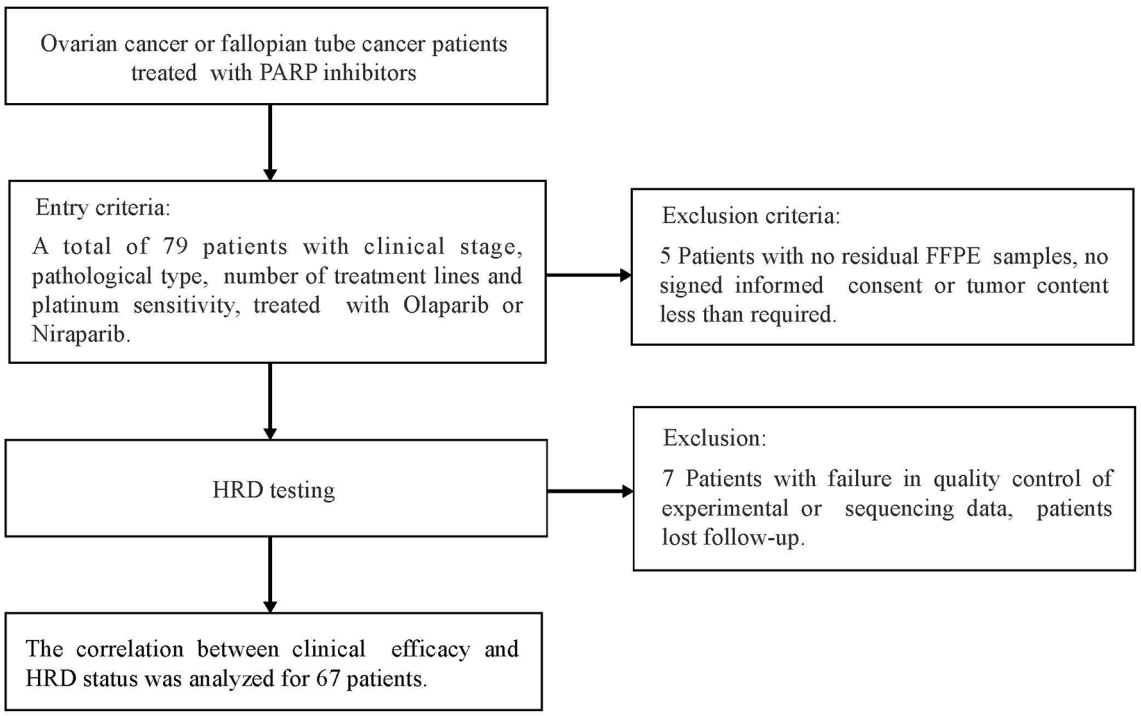


FIGURE 1 | Flow Diagram for the Real world PARPi treatment data cohort, patient inclusion and exclusion criteria of patients used for validation.

alterations: base substitutions, short insertions/deletions with detection sensitivity at variant allele frequency (VAF) ≥5%. Detected mutations for the 54 genes were annotated according to the American College of Medical Genetics (ACMG) guideline and classified as pathogenic, likely pathogenic, variants of unknown significance (VUS), likely benign and benign (15).

BRCA mutation positive (BRCAmt) was defined as BRCA1 and or BRCA2 pathogenic or likely pathogenic mutation was detected in patients and otherwise is BRCA wildtype (BRCAwt). HRR mutation positive was defined as pathogenic and likely pathogenic mutations in the following 15 HRR pathway genes as BRCA1, BRCA2, ATM, BARD1, BRIP1, CDK12, CHEK1, CHEK2, FANCL, PALB2, PPP2R2A, RAD51B, RAD51C, RAD51D, RAD54L, HDAC2, and FANCA. HRD score was calculated by the sum of three types of genomically unstable events, namely, LOH, TAI, and LST as defined by (16–19). HRD score cut-off was validated by BRCAness status and maintained the same as Myriad myChoice®CDx cut-off 42 (19). HRD-positive was defined by BRCA mutation positive and/or HRD score ≥42.

Clinical Assessments

All enrolled subjects received PARP inhibitor treatment, namely, olaparib or niraparib. Basic characteristics and follow-up information after PARPi treatment were collected. Serum CA125 and imaging examinations *via* computed tomography were performed on each patient at baseline, followed by a monthly examination of CA125 and bimonthly imaging examinations.

Adverse events (AEs) were graded according to the Common Terminology Criteria Adverse Events (CTCAE) V 5.0 to modulate the dosage. Progression-free survival was defined as the interval from the date of PARPi treatment to the date of disease progression or death from any cause, whichever occurred first.

Statistical Analysis

The Fisher exact test was used to test the difference of categorical variables, namely, BRCA mutation status and HRR mutation status, and the odds ratios (ORs) and 95% confidence intervals (CIs) were also calculated. For progression-free survival (PFS) analysis, Kaplan–Meier curves were compared by using a log-rank test, and the hazard ratio (HR) was determined through a Cox proportional hazards regression model to test the correlations between different variables and PFS. Baseline variables that achieved a level of significance of $P < 0.2$ in the univariable analysis were entered into multivariable models. All reported P-values were 2-tailed, and $P < 0.05$ was considered to be statistically significant. Statistical analyses were performed with python lifelines package version 0.22.3.

RESULTS

Patient Characteristics

In total, 65 ovarian cancer patients and 2 fallopian tube cancer patients were enrolled. The median age of patients was 55 years (range 31–80 years), and most of them were high-grade serous

carcinoma (86.6%). In total, 49 patients were diagnosed with FIGO III stage (73.1%) and thirteen patients had FIGO IV stage (19.4%). Twenty-nine patients were R0 resected with no macroscopic disease (43.3%). Thirty-seven patients were Eastern Cooperative Oncology Group performance status (ECOG PS) 0 (55.2%). Twenty-three patients underwent neoadjuvant chemotherapy (NACT) (34.3%). Approximately 26.9% of patients underwent secondary cytoreductive surgery. A total of 27 patients have done ≤2 lines of therapy before PARPi therapy (40.3%). Platinum sensitivity status was evaluable in 49 (73.1%) of the patients. In total, 47 patients (70.1%) were treated with olaparib, and the remaining patients (29.9%) were treated with niraparib. The median follow-up time was 7.9 months. Patients' clinic and pathological characteristics are summarized in **Table 1**.

TABLE 1 | Baseline characteristics of patients with HRD test. Values are reported as frequency (n [%]) or as mean (range).

Characteristic	Patient number (percent, %)
Age, years	
<55	33 (49.3)
≥55	34 (50.7)
Primary tumor site	
Ovary	65 (97.0)
Fallopian tube	2 (3.0)
FIGO stage	
I	1 (1.5)
II	4 (6.0)
III	49 (73.1)
IV	13 (19.4)
Histological type	
High-grade serous	58 (86.6)
Endometrioid	5 (7.5)
Low-grade serous	1 (1.5)
Clear cell carcinoma	1 (1.5)
Carcinosarcoma	1 (1.5)
Well-differentiated papillary mesothelioma	1 (1.5)
Residual disease after primary surgery	
R0	29 (43.3)
R1	32 (47.8)
R2	6 (9.0)
ECOG PS	
0	37 (55.2)
1	30 (44.8)
Neoadjuvant chemotherapy	
Yes	23 (34.3)
No	44 (65.7)
Treatment lines	
≤2	27 (40.3)
≥3	40 (59.7)
Treatment categories	
First-line maintenance therapy	8 (11.9)
Second-line maintenance therapy	6 (9.0)
Multi-line monotherapy	21 (31.3)
Exploratory therapy	
First-line monotherapy	2 (3.0)
First-line maintenance therapy	5 (7.5)
Second-line monotherapy	4 (6.0)
Second-line maintenance therapy	2 (3.0)
Multi-line monotherapy	19 (28.4)
Secondary cytoreductive surgery	
Yes	18 (26.9)
No	49 (73.1)
Family history	
Yes	24 (35.8)
No	43 (64.2)
BRCA status	
BRCAm	24 (35.8)
BRCAw	43 (64.2)

(Continued)

HRD Status Association With BRCA Mutation, HRR Mutation in Ovarian Cancer Patients

Approximately 35.8% (24/67) patients were BRCA mutation positive, and 41.8% (28/67) were HRR mutation positive. Approximately 68.7% (46/67) of the patients were HRD positive and the rest of the 31.3% (21/67) were HRD negative. Among the HRD positive patients, 52.2% (24/46) were BRCA mutation positive and 47.8% (22/46) were BRCA mutation negative. Both the HRD-positive and BRCA-positive populations are higher than the western population reported in QUADRA, PRIMA, and PAOLA-1 trials where the HRD-positive patients represent around 50% of western ovarian cancer patients (6, 10, 12). Meanwhile, recently, the ASCO2021 reported the L-MOCA: an open-label study of olaparib maintenance monotherapy in platinum-sensitive relapsed ovarian cancer in Chinese and Malaysian patients, where 47.3% (106/224) of the patients were BRCA mutation positive (20).

Further, we analyzed whether HRD score above cut-off (HRD score ≥42) patients were enriched in some patients with specific BRCA mutation or HRR pathway mutation. The results showed that patients with high HRD scores tend to be enriched in BRCA mutation and HRR mutation. However, the P-value is not significant due to the small sample size. The detailed results are shown in **Supplementary Table 2**.

HRD Status and Clinical Outcomes of Ovarian Cancer Patients Treated With PARPi

To unravel whether HRD status could identify patients benefiting from PARPi treatment, we compared the PFS difference between HRD positive patients (HRD score ≥42 or BRCA mutation positive, n = 46) and HRD negative patients (HRD score <42, n = 21). The PFS among HRD positive patients was significantly longer than those HRD negative patients (medium PFS 9.4 months *vs* 4.1 months, HR: 0.52, 95% CI [0.38–0.71], p <0.001) (**Figure 2A**). We further defined

TABLE 1 | Continued

Characteristic	Patient number (percent, %)
HRD status	
positive	46 (68.7)
negative	21 (31.3)
Platinum sensitivity	
Yes	17 (25.4)
No	32 (47.8)
Unknown	18 (26.9)
PARP inhibitor	
Olaparib	47 (70.1)
Niraparib	20 (29.9)

HRD, homologous recombination deficiency; FIGO, International Federation of Gynecology and Obstetrics; ECOG PS, Eastern Cooperative Oncology Group performance status; R0, no macroscopic disease; R1, 1 cm or less; R2, more than 1 cm; PDS, primary debulking surgery; IDS, interval debulking surgery; NACT, Neoadjuvant chemotherapy.

the HRD-positive group as having two subgroups: the BRCA mutation group (N = 24) and BRCA wildtype HRD positive (N = 22). We can see that both the BRCA mutation group and BRCA wildtype HRD-positive group showed significant higher PFS than the HRD-negative group (BRCAm: medium PFS 9.8 months vs 4.1 months, HR: 0.29, 95% CI[0.14–0.61], p = 0.001 and BRCAw HRD positive: medium PFS 9.2 months vs 4.1 months, HR: 0.52, 95% CI[0.36–0.76], p <0.001, respectively). The PFS difference between the BRCA mutation group and the BRCA wildtype HRD-positive group is not significant (PFS 9.8 months vs 9.2 months, HR: 0.85, 95% CI [0.40–1.80], p = 0.67) (**Figure 2B**).

In the univariable Cox proportional hazards regression model, in addition to the HRD status, Eastern Cooperative Oncology Group (ECOG) were also associated with PFS (ECOG: HR, 2.49; 95% CI [1.39–4.44]; p = 0.002). We further explored the association between HRD status and PFS in different ECOG statuses. The HRs and P-values still remained significant in better ECOG performance group (medium PFS 12.0 months *vs* 4.9 months; HR: 0.36; 95% CI [0.22–0.59]; p <0 .001) while the PFS in worse ECOG performance group were generally poor regardless of HRD status (medium PFS 4.5 months *vs* 3.2 months; HR: 0.79; 95% CI [0.52–1.18]; p = 0.23) (**Supplementary Figures 1A–C**).

Treatment lines, BRCA status, secondary cytoreductive surgery and R0 resection or not also tend to be associated with PFS (treatment lines: HR, 1.58; 95% CI [0.87–2.87]; P = 0 .13; BRCA status: HR, 0.66; 95% CI [0.36–1.23]; P = 0.19; Secondary cytoreductive surgery: HR, 1.59; 95% CI [0.85–2.98]; P = 0 .15; R0 resection or not: HR, 1.54; 95% CI [0.86–2.77]; P = 0 .15). Baseline variables that achieved a level of significance of P < 0.2 in the univariable analysis were entered into multivariable models. In the multivariate Cox proportional hazards regression model that included the above six factors, the association between HRD status and ECOG status remained significant (HRD status: HR: 0.67; 95% CI, [0.49–0.92]; p = 0.01; ECOG: HR: 2.20; 95% CI, [1.14–4.23]; p = 0.02) (**Table 2** and **Supplementary Figure 2**).

Since HRD score was the sum of LOH, TAI or LST, we further analyzed that LOH, TAI or LST independently correlated with PFS status. Each median score of LOH, TAI or LST was used as the threshold, with the PFS among high LST score group was significantly longer than those low LST score group (medium PFS 10.1 months *vs* 5.6 months, HR: 0.95, 95% CI [0.93–0.98], logRank p = 0.02) (**Supplementary Figure 3A** and **Supplementary Table 3**). There was a trend that PFS among high TAI or LOH score group was longer than those low TAI or LOH score group, although the p-value is not significant (**Supplementary Figures 3B, C**). Univariable Cox proportional hazards regression model showed that LOH, TAI, and LST were all associated with PFS (LOH: HR, 0.95; 95% CI [0.90–0.99]; p = 0 .026; TAI: HR, 0.95; 95% CI [0.91–0.98]; p = 0 .005; LST: HR, 0.95; 95% CI [0.93–0.98]; p <0 .001) (**Supplementary Table 3**). However, after multivariate regression correction, only LST status association with PFS remained significant (HR: 0.95; 95% CI [0.90–0.996]; p = 0.03) (**Supplementary Table 3**). From this dataset, we found that LOH, TAI and LST are not independent variables correlated with PFS and LST was the most significant.

Platinum Sensitivity Evaluable Subgroup Analysis

In the subgroup PARPi treated as first-line maintenance therapy and some exploratory therapy, platinum sensitivity status was not evaluable. However, platinum sensitivity status was recognized as a clinical marker to predict PARPi response in the second-line maintenance therapy. Thus we chose the platinum sensitivity evaluable subgroup (N = 49) to further analyze the HRD status, platinum sensitivity and other clinical factors associated with PFS of PARPi treatment. In the univariable Cox proportional hazards regression model, the HRD status, ECOG and platinum sensitivity were associated with PFS (HRD: HR, 0.70; 95% CI [0.51–0.96]; p = 0.03; ECOG: HR, 1.87; 95% CI [0.99–3.51]; p = 0.05; platinum sensitivity: HR, 0.47; 95% CI [0.24–0.94]; p = 0 .03). R0 resection or not tended to be associated with PFS (HR: 1.70; 95% CI [0.89–3.24]; p = 0 .11). In the multivariate Cox proportional hazards regression model that included the above four factors, the association between HRD status, and platinum sensitivity status remained significant (HRD status: HR, 0.71; 95% CI, [0.51–0.98]; p = 0.04; platinum sensitivity: HR, 0.49; 95% CI, [0.24–1.0]; p = 0.05) (**Table 3** and **Supplementary Figure 4**).

DISCUSSION

Epithelial ovarian cancer (EOC) has the highest mortality and morbidity in ovarian cancer (1). Germline pathogenic variants in EOC susceptibility genes, namely, those involved in homologous recombination and mismatch repair pathways are present in approximately 22 to 25% of EOC (21). High-grade serous ovarian cancer (HGSOC) is the most common type of EOC, accounting for 75% of all EOC, 15–20% of which western patients have germline BRCA1 or BRCA2 mutations. The BRCA mutation

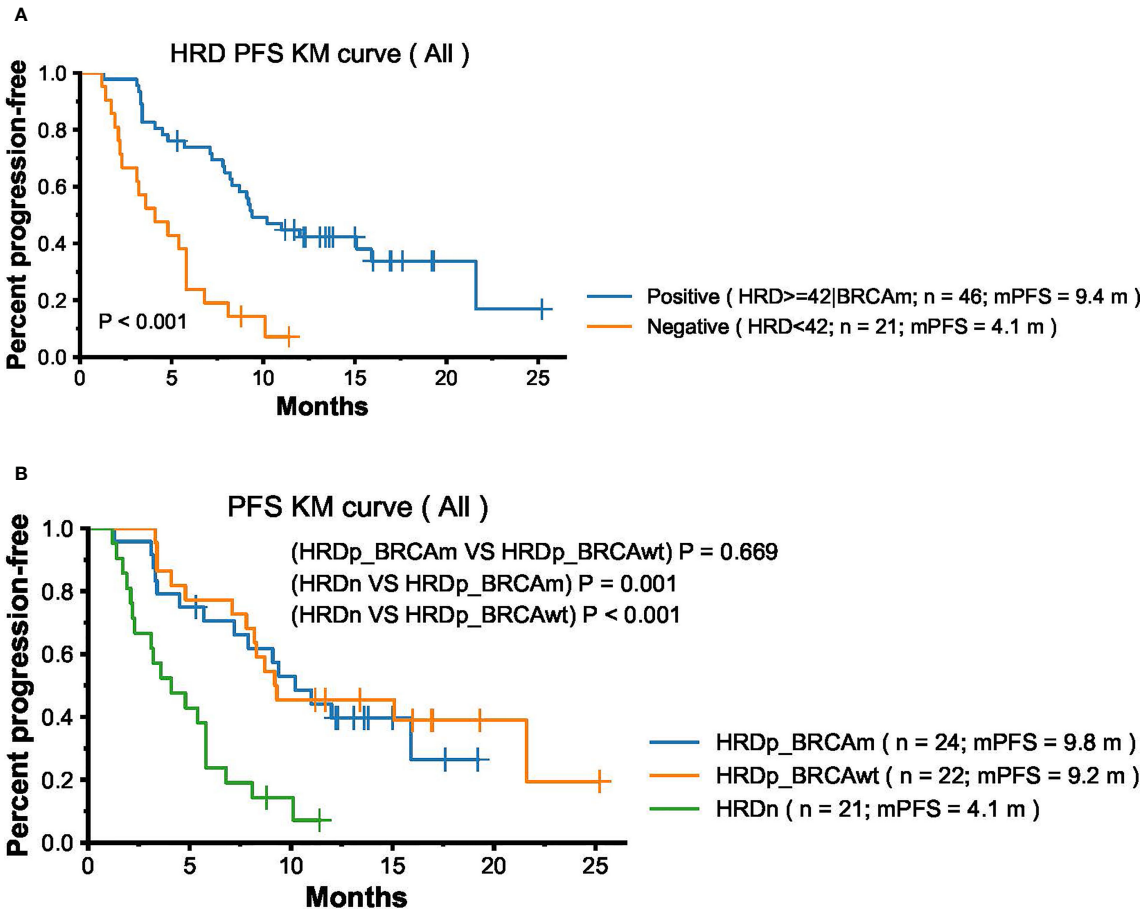


FIGURE 2 | Association Between HRD status and PFS in Ovarian Cancer Patients treated with PARPi olaparib and niraparib. **(A)** Progression-free survival (PFS) by HRD status positive (N = 46) and negative (N = 21). **(B)** Progression-free survival (PFS) by three group: BRCA mutation HRD positive group (N = 24), BRCA wildtype HRD positive (N = 22), and HRD negative (N = 21).

rate observed in our cohort was 35.8%, which was near the higher boundary of the previously reported range of 5 to 35% (14, 22). Similar to other studies, we also observed BRCA1 mutations occurring more frequently than BRCA2 mutations in Chinese ovarian cancer patients (23, 24). HRD is the first phenotypically defined predictive marker for therapy with PARP inhibitors in EOC (25). Genomic analyses show that homologous recombination is defective in nearly half of HGSOC (13, 14). To our knowledge, our study is the first real world study of NGS-based HRD in Chinese ovarian cancer and fallopian tube cancer patients. The proportion of HGSOC patients with HRD observed in our enrolled cohort was 68.7%, which was higher than the HRD positive proportion reported in western countries (50–60%) (14). Homologous recombination repair (HRR), namely, BRCA1, BRCA2, ATM, BARD1, BRIP1, CHEK1, CHEK2, RAD51C, and RAD51D, is an important pathway for normal cells to repair DNA DSB. HRR related mutations can induce HRD. Our results demonstrated that patients with high HRD scores tended to enrich in BRCA mutation and HRR mutation.

In our study, the HRD score was calculated by the Myriad myChoice®CDx test method, which was the sum of three HRD events: LOH, TAI, and LST. An HRD score cut-off of 42 represented the 95th percentile of BRCAness samples. BRCAness was defined as the set of known BRCA deficiency including the following three events: (i) one deleterious mutation in BRCA1 or BRCA2, with LOH in the wild-type copy, (ii) two deleterious mutations in the same gene, or (iii) promoter methylation of BRCA1 with LOH in the wild-type copy (26). From AmoyDx assay validation data, HRD score cut-off of 42 represented the 93th percentile of the set of BRCAness in Chinese ovarian cancer patients (N = 200) (Data was not shown in this paper). Previous studies demonstrated that LOH, TAI, and LST all proved to be useful markers in predicting response to a variety of therapeutic strategies exploiting defective DNA repair (19). Univariable Cox proportional hazards regression model showed that LOH, TAI, and LST were all associated with PFS and LST status association with PFS remaining the most significant after multiple regression correction.

TABLE 2 | Univariable and Multivariable Analysis of Progression-Free Survival for the total 67 patient cohort (N = 67).

Parameter	Univariable Analysis		Multivariable Analysis	
	HR (95% CI)	*P*-Value	HR (95% CI)	*P*-Value
HRD Status	0.60 (0.45–0.82)	<0.001	0.67 (0.49–0.92)	0.01
HRR mutation status	0.84 (0.47–1.50)	0.55	NA	NA
BRCA mutation status	0.66 (0.36–1.23)	0.19	0.74 (0.39–1.42)	0.37
ECOG	2.49 (1.39–4.44)	0.002	2.20 (1.14–4.23)	0.02
NACT	1.45 (0.81–2.61)	0.21	NA	NA
Treatment Lines	1.58 (0.87–2.87)	0.13	1.16 (0.61–2.20)	0.64
Family History	0.71 (0.39–1.32)	0.28	NA	NA
Secondary cytoreductive surgery	1.59 (0.85–2.98)	0.15	1.80 (0.91–3.53)	0.09
R0 resection or not	1.54 (0.86–2.77)	0.15	1.75 (0.96–3.26)	0.07
Stage	0.72 (0.42–1.23)	0.23	NA	NA

ECOG, Eastern Cooperative Oncology Group; ECOG performance status ≥2 vs 1 or 0; NACT, New Adjuvant Chemo Therapy yes or no; HR, hazard ratio; Treatment lines, lines ≤2 as 0, ≥3 lines as 1; NA, not applicable. Baseline variables that achieved a level of significance of P <0 .2 in the univariable analysis were entered into multivariable models.

TABLE 3 | Univariable and Multivariable Analysis of Progression-Free Survival for the platinum sensitivity status evaluable subgroup (N = 49).

Parameter	Univariable Analysis		Multivariable Analysis	
	HR (95% CI)	*P* Value	HR (95% CI)	*P* Value
HRD Status	0.70 (0.51–0.96)	0.03	0.71 (0.51–0.98)	0.04
HRR mutation status	0.75 (0.39–1.43)	0.38	NA	NA
BRCA mutation status	0.68 (0.35–1.33)	0.26	NA	NA
ECOG	1.87 (0.99–3.51)	0.05	1.55 (0.81–2.97)	0.18
NACT	1.39 (0.73–2.62)	0.31	NA	NA
Treatment Lines	1.30 (0.70–2.44)	0.41	NA	NA
Family History	0.81 (0.41–1.60)	0.55	NA	NA
Secondary cytoreductive surgery	1.31 (0.68–2.51)	0.42	NA	NA
R0 resection or not	1.70 (0.89–3.24)	0.11	1.69 (0.87–3.27)	0.12
Stage	0.87 (0.40–1.91)	0.73	NA	NA
Platinum sensitivity	0.47 (0.24–0.94)	0.03	0.49 (0.24–1.0)	0.05

ECOG, Eastern Cooperative Oncology Group; ECOG performance status ≥2 vs 1 or 0; NACT, New Adjuvant Chemo Therapy yes or no; HR, hazard ratio; Treatment lines, lines ≤2 as 0, ≥3 lines as 1; NA, not applicable. Baseline variables that achieved a level of significance of P <0 .2 in the univariable analysis were entered into multivariable models.

The approval of PARPi is an important milestone in the treatment of ovarian cancer patients. Many clinical studies have confirmed that ovarian cancer patients with BRCAmt and HRD positive can benefit from PARPi. Olaparib as maintenance treatment significantly increased PFS for patients with BRCAmt in SOLO1 and SOLO2 study (5, 27). Both NOVA and PRIMA studies found that patients with HRD positive could get more profit from niraparib as maintenance treatment (4, 6). The QUADRA study demonstrated that niraparib works among women with heavily pretreated ovarian cancer, especially in patients with HRD-positive platinum-sensitive disease, which included not only patients with BRCA mutation but also the population with BRCA wild-type (10). In the Chinese population, the NORA study found that niraparib maintenance treatment reduced the risk of disease progression or death by 68% and prolonged PFS in patients with platinum-sensitive recurrent ovarian cancer (28). However, a limited number of studies have investigated the relationship between HRD status and efficacy of PAPRi in the Chinese population. Our study performed the largest retrospective study to detect HRD status from Chinese ovarian cancer patients and correlate HRD status and clinical characteristics with PARPi therapeutic outcomes. However, PARP inhibitors have been available in China not for a long time, most of the patients we enrolled were taking it as multi-line monotherapy, which led to shorter PFS of our cohort.

Very consistent results were observed in both our cohort and the western population; whereby Chinese ovarian cancer patients with positive HRD had significantly better PFS after PARPi treatment. The single variant Cox proportional hazards regression analysis showed that the efficacy of PARPi was closely related to HRD status, ECOG score, treatment lines, BRCA mutation status, secondary tumor cell reduction and R0 resection or not. The multivariable analysis highlighted that HRD and ECOG were independent factors affecting the prognosis. Further analysis showed that the PFS in better ECOG performance group was significantly higher in HRD positive population while the PFS in worse ECOG performance group were generally poor regardless of HRD status. In the subgroup with the platinum sensitivity evaluable, HRD and platinum sensitivity were consistently significant to predict PFS no matter in univariable or multivariant regression analysis. However, BRCAmt was only significant to predict PFS in the univariable analysis. It was not statistically significant to the association between BRCAmt and PFS in the multivariate analysis, which

may be due to a small cohort and more patients with multi-line monotherapy that underpowered statistical procedure.

In conclusion, our study highlights several important considerations. We firstly elucidated the HRD status of ovarian cancer patients from China in the real world. Chinese ovarian cancer patients with HRD positive also had a better response to PARPi therapy and our cohort also found other clinical characteristics that could affect the efficacy of PARPi. Studies with larger cohorts are needed to validate these observations to expand its therapeutic markers.

DATA AVAILABILITY STATEMENT

The data and materials used in this manuscript is available from the corresponding author on reasonable requests.

ETHICS STATEMENT

The studies involving human participants were reviewed and approved by The Affiliated Cancer Hospital of Nanjing Medical University. The patients/participants provided their written informed consent to participate in this study.

AUTHOR CONTRIBUTIONS

JN and WG participated in the design of the present study and drafted the manuscript. QZ carried out the case recruitment of the present study. XZC and XX participated in the case recruitment of the present study. RZ and HG carried out statistical analysis. WG and CC participated in the statistical analysis. XXC designed of the study, performed the statistical analysis and revised the manuscript. All authors contributed to the article and approved the submitted version

FUNDING

This study was supported by grants from the National Natural Science Foundation of China 353 (No. 81472441, 81501205), Natural Science Foundation of Youth Fund Projects of Jiangsu Province (SBK2021040731), Jiangsu Provincial Scientific research and Health Project for Women and Children (No. F202004), Institute level project of Jiangsu Cancer Hospital (No. 355 ZM201804) and Beijing Kanghua Foundation for the Development of Traditional Chinese and Western Medicine -Le Fund (KH-2020-LJJ-021, KH-2021-LLZX-058).

ACKNOWLEDGMENTS

We sincerely thank Hua Dong et al. from Amoy Diagnostics Co., Ltd. for their technical assistance.

SUPPLEMENTARY MATERIAL

The Supplementary Material for this article can be found online at: https://www.frontiersin.org/articles/10.3389/fonc.2021.746571/full#supplementary-material

Supplementary Figure 1 | Comparison of Progression-Free Survival Between **(A)** ECOG score. Comparison of Progression-Free Survival Between HRD positive and negative group in **(B)** ECOG score=0 subgroup; **(C)** ECOG score=1 subgroup.

Supplementary Figure 2 | Figure presentation of the multivariate Cox proportional hazards regression model log(HR) and 95% Confidence Interval from the six factors associated with PFS (N=67).

Supplementary Figure 3 | Comparison of Progression-Free Survival Between Patients in the **(A)** LST high and LST low group; **(B)** TAI high and TAI low group; **(C)** LOH high and LOH low group. Each median score of LOH, TAI or LST was used as the threshold.

Supplementary Figure 4 | Figure presentation of the multivariate Cox proportional hazards regression model log(HR) and 95% Confidence Interval from the four factors associated with PFS in the platinum sensitivity evaluable subgroup (N=49).

REFERENCES

1. Siegel RL, Miller KD, Fuchs HE, Jemal A. Cancer Statistics, 2021. *CA: Cancer J Clin* (2021) 71(1):7–33. doi: 10.3322/caac.21654
2. Coleridge SL, Bryant A, Kehoe S, Morrison J. Chemotherapy Versus Surgery for Initial Treatment in Advanced Ovarian Epithelial Cancer. *Cochrane Database Syst Rev* (2021) 2:CD005343. doi: 10.1002/14651858.CD005343.pub5
3. Lee YY, Choi MC, Park JY, Suh DH, Kim JW. Major Clinical Research Advances in Gynecologic Cancer in 2020. *J Gynecol Oncol* (2021) 32(4):e53. doi: 10.3802/jgo.2021.32.e53
4. Mirza MR, Monk BJ, Herrstedt J, Oza AM, Mahner S, Redondo A, et al. Niraparib Maintenance Therapy in Platinum-Sensitive, Recurrent Ovarian Cancer. *N Engl J Med* (2016) 375(22):2154–64. doi: 10.1056/NEJMoa1611310
5. Ledermann J, Harter P, Gourley C, Friedlander M, Vergote I, Rustin G, et al. Olaparib Maintenance Therapy in Platinum-Sensitive Relapsed Ovarian Cancer. *N Engl J Med* (2012) 366(15):1382–92. doi: 10.1056/NEJMoa1105535
6. Gonzalez-Martin A, Pothuri B, Vergote I, DePont Christensen R, Graybill W, Mirza MR, et al. Niraparib in Patients With Newly Diagnosed Advanced Ovarian Cancer. *N Engl J Med* (2019) 381(25):2391–402. doi: 10.1056/NEJMoa1910962
7. Lord CJ, Ashworth A. The DNA Damage Response and Cancer Therapy. *Nature* (2012) 481(7381):287–94. doi: 10.1038/nature10760
8. Murai J, Huang SY, Das BB, Renaud A, Zhang Y, Doroshow JH, et al. Trapping of PARP1 and PARP2 by Clinical PARP Inhibitors. *Cancer Res* (2012) 72(21):5588–99. doi: 10.1158/0008-5472.CAN-12-2753
9. Tangutoori S, Baldwin P, Sridhar S. PARP Inhibitors: A New Era of Targeted Therapy. *Maturitas* (2015) 81(1):5–9. doi: 10.1016/j.maturitas.2015.01.015
10. Moore KN, Secord AA, Geller MA, Miller DS, Cloven N, Fleming GF, et al. Niraparib Monotherapy for Late-Line Treatment of Ovarian Cancer (QUADRA): A Multicentre, Open-Label, Single-Arm, Phase 2 Trial. *Lancet Oncol* (2019) 20(5):636–48. doi: 10.1016/S1470-2045(19)30029-4
11. Coleman RL, Oza AM, Lorusso D, Aghajanian C, Oaknin A, Dean A, et al. Rucaparib Maintenance Treatment for Recurrent Ovarian Carcinoma After Response to Platinum Therapy (ARIEL3): A Randomised, Double-Blind, Placebo-Controlled, Phase 3 Trial. *Lancet* (2017) 390(10106):1949–61. doi: 10.1016/S0140-6736(17)32440-6
12. Ray-Coquard I, Pautier P, Pignata S, Perol D, Gonzalez-Martin A, Berger R, et al. Olaparib Plus Bevacizumab as First-Line Maintenance in Ovarian Cancer. *N Engl J Med* (2019) 381(25):2416–28. doi: 10.1056/NEJMoa1911361

13. Cancer Genome Atlas Research N. Integrated Genomic Analyses of Ovarian Carcinoma. *Nature* (2011) 474(7353):609–15. doi: 10.1038/nature10166
14. Ngoi NYL, Tan DSP. The Role of Homologous Recombination Deficiency Testing in Ovarian Cancer and Its Clinical Implications: Do We Need It? *ESMO Open* (2021) 6(3):100144. doi: 10.1016/j.esmoop.2021.100144
15. Richards S, Aziz N, Bale S, Bick D, Das S, Gastier-Foster J, et al. Standards and Guidelines for the Interpretation of Sequence Variants: A Joint Consensus Recommendation of the American College of Medical Genetics and Genomics and the Association for Molecular Pathology. *Genet Med Off J Am Coll Med Genet* (2015) 17(5):405–24. doi: 10.1038/gim.2015.30
16. Abkevich V, Timms KM, Hennessy BT, Potter J, Carey MS, Meyer LA, et al. Patterns of Genomic Loss of Heterozygosity Predict Homologous Recombination Repair Defects in Epithelial Ovarian Cancer. *Br J Cancer* (2012) 107(10):1776–82. doi: 10.1038/bjc.2012.451
17. Birkbak NJ, Wang ZC, Kim JY, Eklund AC, Li Q, Tian R, et al. Telomeric Allelic Imbalance Indicates Defective DNA Repair and Sensitivity to DNA-Damaging Agents. *Cancer Discov* (2012) 2(4):366–75. doi: 10.1158/2159-8290.CD-11-0206
18. Popova T, Manie E, Rieunier G, Caux-Moncoutier V, Tirapo C, Dubois T, et al. Ploidy and Large-Scale Genomic Instability Consistently Identify Basal-Like Breast Carcinomas With BRCA1/2 Inactivation. *Cancer Res* (2012) 72 (21):5454–62. doi: 10.1158/0008-5472.CAN-12-1470
19. Timms KM, Abkevich V, Hughes E, Neff C, Reid J, Morris B, et al. Association of BRCA1/2 Defects With Genomic Scores Predictive of DNA Damage Repair Deficiency Among Breast Cancer Subtypes. *Breast Cancer Res BCR* (2014) 16 (6):475. doi: 10.1186/s13058-014-0475-x
20. Gao QL, Zhu JQ, Zhao WD, Huang Y, An RF, Zheng H, et al. L-MOCA: An Open-Label Study of Olaparib Maintenance Monotherapy in Platinum-Sensitive Relapsed Ovarian Cancer. *J Clin Oncol* (2021) 39(10):1165–84. doi: 10.1200/JCO.2021.39.15_suppl.e17526
21. Flaum N, Crosbie EJ, Edmondson RJ, Smith MJ, Evans DG. Epithelial Ovarian Cancer Risk: A Review of the Current Genetic Landscape. *Clin Genet* (2020) 97(1):54–63. doi: 10.1111/cge.13566
22. Ahmed N, Kadife E, Raza A, Short M, Jubinsky PT, Kannourakis G. Ovarian Cancer, Cancer Stem Cells and Current Treatment Strategies: A Potential Role of Magmas in the Current Treatment Methods. *Cells* (2020) 9(3):719. doi: 10.3390/cells9030719
23. Zhang S, Royer R, Li S, McLaughlin JR, Rosen B, Risch HA, et al. Frequencies of BRCA1 and BRCA2 Mutations Among 1,342 Unselected Patients With Invasive Ovarian Cancer. *Gynecol Oncol* (2011) 121(2):353–7. doi: 10.1016/j.ygyno.2011.01.020
24. Wu X, Wu L, Kong B, Liu J, Yin R, Wen H, et al. The First Nationwide Multicenter Prevalence Study of Germline BRCA1 and BRCA2 Mutations in Chinese Ovarian Cancer Patients. *Int J Gynecol Cancer Off J Int Gynecological Cancer Soc* (2017) 27 (8):1650–7. doi: 10.1097/IGC.0000000000001065
25. Ledermann JA, Drew Y, Kristeleit RS. Homologous Recombination Deficiency and Ovarian Cancer. *Eur J Cancer* (2016) 60:49–58. doi: 10.1016/j.ejca.2016.03.005
26. Telli ML, Timms KM, Reid J, Hennessy B, Mills GB, Jensen KC, et al. Homologous Recombination Deficiency (HRD) Score Predicts Response to Platinum-Containing Neoadjuvant Chemotherapy in Patients With Triple-Negative Breast Cancer. *Clin Cancer Res* (2016) 22(15):3764–73. doi: 10.1158/1078-0432.CCR-15-2477
27. Moore K, Colombo N, Scambia G, Kim BG, Oaknin A, Friedlander M, et al. Maintenance Olaparib in Patients With Newly Diagnosed Advanced Ovarian Cancer. *N Engl J Med* (2018) 379(26):2495–505. doi: 10.1056/NEJMoa1810858
28. Wu XH, Zhu JQ, Yin RT, Yang JX, Liu JH, Wang J, et al. Niraparib Maintenance Therapy in Patients With Platinum-Sensitive Recurrent Ovarian Cancer Using an Individualized Starting Dose (NORA): A Randomized, Double-Blind, Placebo-Controlled Phase III Trial. *Ann Oncol Off J Eur Soc Med Oncol* (2021) 32(4):512–21. doi: 10.1016/j.annonc.2020.12.018

Conflict of Interest: The authors declare that the research was conducted in the absence of any commercial or financial relationships that could be construed as a potential conflict of interest.

Publisher's Note: All claims expressed in this article are solely those of the authors and do not necessarily represent those of their affiliated organizations, or those of the publisher, the editors and the reviewers. Any product that may be evaluated in this article, or claim that may be made by its manufacturer, is not guaranteed or endorsed by the publisher.

Copyright © 2022 Ni, Guo, Zhao, Cheng, Xu, Zhou, Gu, Chen and Chen. This is an open-access article distributed under the terms of the Creative Commons Attribution License (CC BY). The use, distribution or reproduction in other forums is permitted, provided the original author(s) and the copyright owner(s) are credited and that the original publication in this journal is cited, in accordance with accepted academic practice. No use, distribution or reproduction is permitted which does not comply with these terms.

frontiers in Oncology

ORIGINAL RESEARCH
published: 11 January 2022
doi: 10.3389/fonc.2021.774558

Prognostic Signatures Based on Ferroptosis- and Immune-Related Genes for Cervical Squamous Cell Carcinoma and Endocervical Adenocarcinoma

Chaoqun Xing[1,2†], *Huiming Yin*[1,2†], *Zhi-Yong Yao*[1] *and Xiao-Liang Xing*[1*]

[1] School of Public Health and Laboratory Medicine, Hunan University of Medicine, Huaihua, China, [2] The First Affiliated Hospital of Hunan University of Medicine, Huaihua, China

OPEN ACCESS

Edited by:
Priya Ranjit Bhosale, University of Texas MD Anderson Cancer Center, United States

Reviewed by:
Jinyi Lang, Sichuan Cancer Hospital, China
Pierluigi Giampaolino, University of Naples Federico II, Italy

***Correspondence:**
Xiao-Liang Xing
xiaoliangxinghnm@126.com

[†]*These authors have contributed equally to this work*

Specialty section:
This article was submitted to Gynecological Oncology, a section of the journal Frontiers in Oncology

Received: *12 September 2021*
Accepted: *09 December 2021*
Published: *11 January 2022*

Citation:
Xing C, Yin H, Yao Z-Y and Xing X-L (2022) Prognostic Signatures Based on Ferroptosis- and Immune-Related Genes for Cervical Squamous Cell Carcinoma and Endocervical Adenocarcinoma. Front. Oncol. 11:774558. doi: 10.3389/fonc.2021.774558

Cervical squamous cell carcinoma and endocervical adenocarcinoma (CESC) are among the most common malignancies of the female genital tract. Ferroptosis and immunity regulate each other and play important roles in the progression of CESC. The present study aimed to screen ferroptosis- and immune-related differentially expressed genes (FI-DEGs) to identify suitable prognostic signatures for patients with CESC. We downloaded the RNAseq count data and corresponding clinical information of CESC patients from The Cancer Genome Atlas database; obtained recognized ferroptosis- and immune-related genes from the FerrDb and ImmPort databases, respectively; and screened for suitable prognostic signatures using a series of bioinformatics analyses. We identified eight FI-DEGs (*CALCRL*, *CHIT1*, *DES*, *DUOX1*, *FLT1*, *HELLS*, *SCD*, and *SDC1*) that were independently correlated with the overall survival of patients with CESC. The prediction model constructed using these eight FI-DEGs was also independently correlated with overall survival. Both the sensitivity and specificity of the prediction model constructed using these eight signatures were over 60%. The comprehensive index of ferroptosis and immune status was significantly correlated with the immunity of patients with CESC. In conclusion, the risk assessment model constructed with these eight FI-DEGs predicted the CESC outcomes. Therefore, these eight FI-DEGs could serve as prognostic signatures for CESC.

Keywords: CESC, DEGs, ferroptosis, immune, prognosis

INTRODUCTION

Cervical cancer is the fourth most frequently diagnosed cancer and the fourth leading cause of cancer-related death in women (1). There were almost 600,000 new cases and 340,000 deaths worldwide in 2020 (1). The risk of death from cervical cancer in women in developing countries is 0.9%, which is higher than that in developed countries (0.3%) (2). Despite a series of advances in the

prevention, screening, and treatment of cervical cancer, there has been no significant improvement in outcome (3, 4). The main treatments for patients with cervical cancer include surgery or postoperative concurrent chemoradiotherapy, such as T-cell therapy and checkpoint inhibitors (5). However, once local invasion and distant metastasis occur, the survival rate is significantly reduced, and complications significantly increase, which means that the efficacy of radiotherapy is diminished. Patients with metastatic or recurrent cervical cancer have a poor prognosis, with a 5-year overall survival (OS) rate of only 17% (2). Cervical squamous cell carcinoma and endocervical adenocarcinoma (CESC) account for approximately 15% of cancer deaths in women, with the second-highest mortality rate (6). Therefore, it is necessary to identify suitable signatures to predict the outcomes of patients with CESC.

Ferroptosis is a novel type of cell death that was first proposed by Dixon in 2012 (7). Ferroptosis can be activated by diverse physiological conditions and pathological stress (8). Numerous studies have demonstrated that dysregulation of ferroptosis is involved in several cancers, including CESC (9–12). Immunotherapy is a new type of cancer treatment that boosts the immune system. Immunotherapy has shown promising advantages in terms of treatment efficiency and long-term patient survival (13). Previous studies have documented that immune cells and immune-related factors can regulate ferroptosis, thus achieving the antitumor effects of immunotherapy. For example, Wang et al. found that $CD8^+$ T cells induce ferroptosis by downregulating *SLC3A2* and *SLC7A11*. The induction of ferroptosis effectively improves the antitumor effects of immunotherapy, which suggests that immunotherapy may be achieved by regulating ferroptosis. Additionally, previous studies have indicated that ferroptosis can regulate the immune system. The lipid metabolites released by ferroptotic cells can exert immunomodulatory effects on adjacent immune cells and induce an immune response (14). Therefore, to improve cancer diagnosis and prognosis, it is necessary to investigate the comprehensive network of ferroptosis- and immune-related genes.

Based on the currently known ferroptosis- and immune-related genes, and open public databases like The Cancer Genome Atlas (TCGA), it is hypothesized that prognostic signatures associated with ferroptosis and immune response might help to distinguish subgroups of CESC patients with distinct ferroptosis and immune phenotypes and survival profiles.

MATERIAL AND METHODS

Data Acquisition and Processing

RNAseq counts data (3 controls and 304 cancers) and the corresponding clinical information (**Supplementary Table 1**) was obtained from TCGA database. DESeq2 package in R 3.6.2 was used to screen the differentially expressed genes (DEGs). We utilized the specific criteria as following padj < 0.05, $|\log FC| \geq 2.0$, and basemean > 500 to filter the DEGs.

Generation of Ferroptosis-Related Differentially Expressed Genes and Immune-Related Differentially Expressed Genes

Recognized lists of ferroptosis and immune-related genes were obtained FerrDb (http://zhounan.org/ferrdb) and ImmPort database (http://immport.org), respectively. There were 259 ferroptosis-related genes (FR-Genes), including 108 ferroptosis driver genes, 69 ferroptosis suppressor genes, and 111 ferroptosis marker genes. There were 1,793 immune-related (IR-Genes).

Development of the Comprehensive Index of Ferroptosis and Immune Status

The ferroptosis and/or immune-related DEGs were first subjected to univariate Cox regression. The genes significantly related to the OS of patients with CESC were filtered by least absolute shrinkage and selection operator (LASSO) Cox regression analysis. Then, the candidate DEGs were then filtered by multivariate Cox regression analysis. The filtered candidate signatures were used for the risk assessment model construction, as follows: Risk score = βgene1 * Expgene1 + βgene2 * Expgene2 + ··· + βgenen * Expgenen (15). The β value was obtained from the multivariate Cox regression analysis. The expression values were obtained by DESeq2 analysis. The comprehensive index of ferroptosis and immune status (CIFI) value of each patient was calculated by using the risk score of the patient subtracted by the minimum risk score of the cohort, which was then divided by the maximum risk score of the cohort, namely, CIFI = (Risk score − Min)/Max (15).

Immune Profile Analysis

The ESTIMATE package in R software (3.6.2) was performed to calculate the stromal score, immune score, tumor purity, and ESTIMATE scores by using the genes expression data. We downloaded the calculated data of immune cell infiltration of patients with CESC from the Tumor Immune Estimation Resource (TIMER) and carried out correlation analysis for the ESTIMATE value and candidate prognosis signatures.

Principal Component Analysis

Principal component analysis (PCA) was conducted to reduce dimension and visualize the CESC patients with different CIFI values by 3 ferroptosis-related DEGs (FR-DEGs), 6 immune-related DEGs (IR-DEGs), and 8 ferroptosis- and immune-related DEGs (FI-DEGs) filtered by univariate Cox, LASSO analysis, and multivariate Cox analysis.

Statistical Analysis

A repeated-measures ANOVA followed by unpaired two-tailed Student's t-test was used as indicated. All results are expressed as mean ± SEM.

RESULTS

Identification of Candidate Prognostic Signatures

A total of 307 TCGA samples were included in the present study. The DESeq2 package in R 3.6.2 was used to screen the DEGs. There were 1,295 DEGs (969 upregulated and 326 downregulated) (**Figure 1A**). Of these, 25 were FR-DEGs (21 upregulated and 4 downregulated) (**Figure 1B**), and 129 were IR-DEGs (83 upregulated and 46 downregulated) (**Figure 1C**). Through univariate Cox regression and LASSO analysis, five FR-DEGs were significantly related to the OS of patients with CESC (**Figure 1D** and **Supplementary Figures 1A, B**). Then, multivariate Cox regression analysis of the five FR-DEGs was performed, and three FR-DEGs were determined to be independently related to the OS of patients with CESC (**Figure 1E**). Similarly, 6 out of 17 IR-DEGs were significantly independently related to the OS of patients with CESC (**Figures 1F, G** and **Supplementary Figures 1C, D**).

Additionally, we performed a comprehensive combined analysis of the 25 FR-DEGs and 129 IR-DEGs and found that 8 out of 18 FI-DEGs were independently related to the OS of patients with CESC (**Figures 1H, I** and **Supplementary Figures 1E, F**). The expression of these candidate prognostic signatures is shown in **Supplementary Figure 2**.

Construction of the Comprehensive Index of Ferroptosis and Immune Status Classifier

The risk assessment scores were calculated by multiplying the gene expression of independent prognostic signatures and their corresponding coefficients, which were obtained by multivariate Cox regression analysis. A comprehensive index of ferroptosis and immune status (CIFI) values was calculated using the formula mentioned in the *Materials and Methods* section. The optimal cutoff value (Youden's index) was used to regroup CESC patients (**Figures 2A, E, I**).

In the CIFI classifier constructed using the three FR-DEGs, 169 and 135 patients were classified as having high and low CIFI values, respectively. The CIFI values and survival time of the 304 patients in the model based on three FR-DEGs are displayed in **Figure 2B**. CESC patients with low CIFI values exhibited significantly better OS (**Figure 2C**). PCA indicated that CESC patients with low CIFI values could be clearly distinguished from those with high CIFI values (**Figure 2D**). We also constructed two more CIFI classifiers using the six IR-DEGs or eight FI-DEGs and performed the same analysis. Similar results were obtained for these two CIFI classifiers (**Figures 2E–L**).

We then plotted receiver operating characteristic (ROC) curves and found that the area under the curve (AUC) values

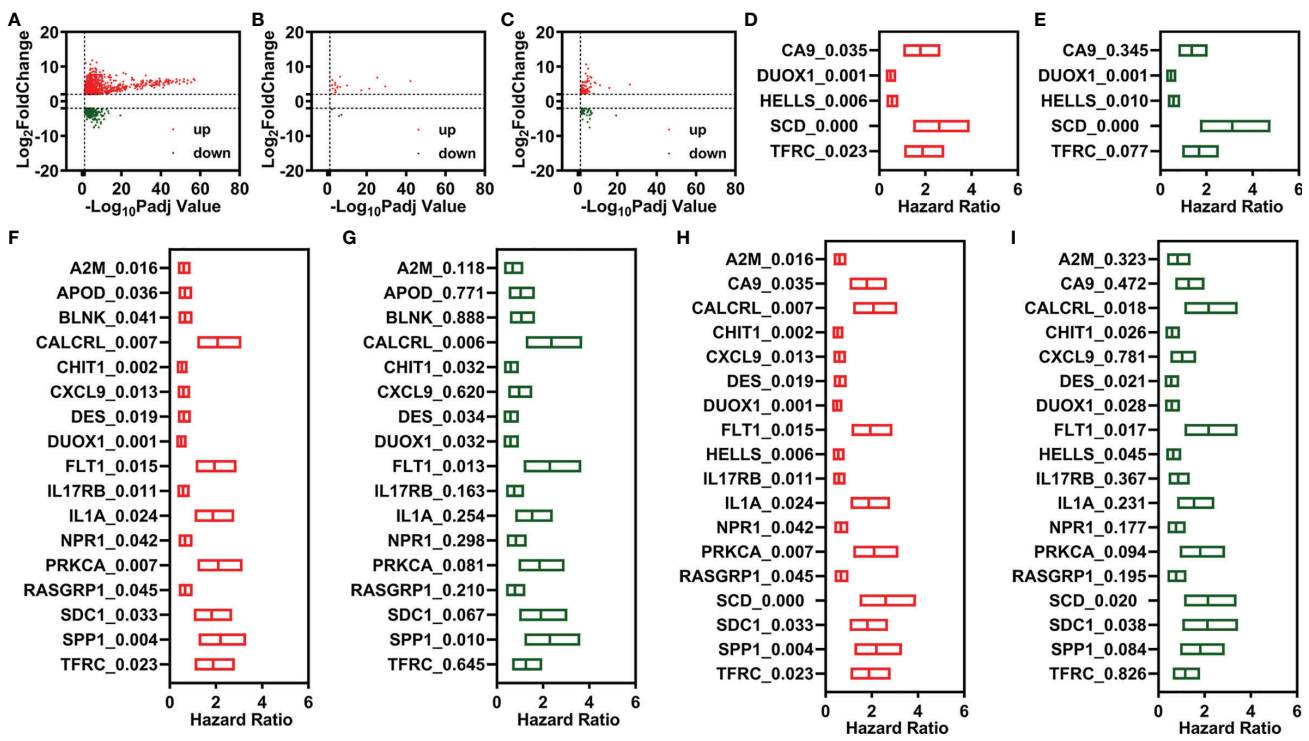


FIGURE 1 | Identification of candidate prognostic signatures. **(A–C)** Volcano plot of DEGs, FR-DEGs, and IR-DEGs for CESC. **(D, E)** Univariate **(D)** and multivariate **(C)** Cox regression analyses illustrate 3 FR-DEGs independently associated with the OS of CESC. **(F, G)** Univariate **(F)** and multivariate **(G)** Cox regression analyses illustrate 6 IR-DEGs independently associated with the OS of CESC. **(H, I)** Univariate **(H)** and multivariate **(I)** Cox regression analyses illustrate 8 FI-DEGs independently associated with the OS of CESC. DEGs, differentially expressed genes; FR-DEGs, ferroptosis-related DEGs; IR-DEGs, immune-related DEGs; CESC, cervical squamous cell carcinoma and endocervical adenocarcinoma; OS, overall survival.

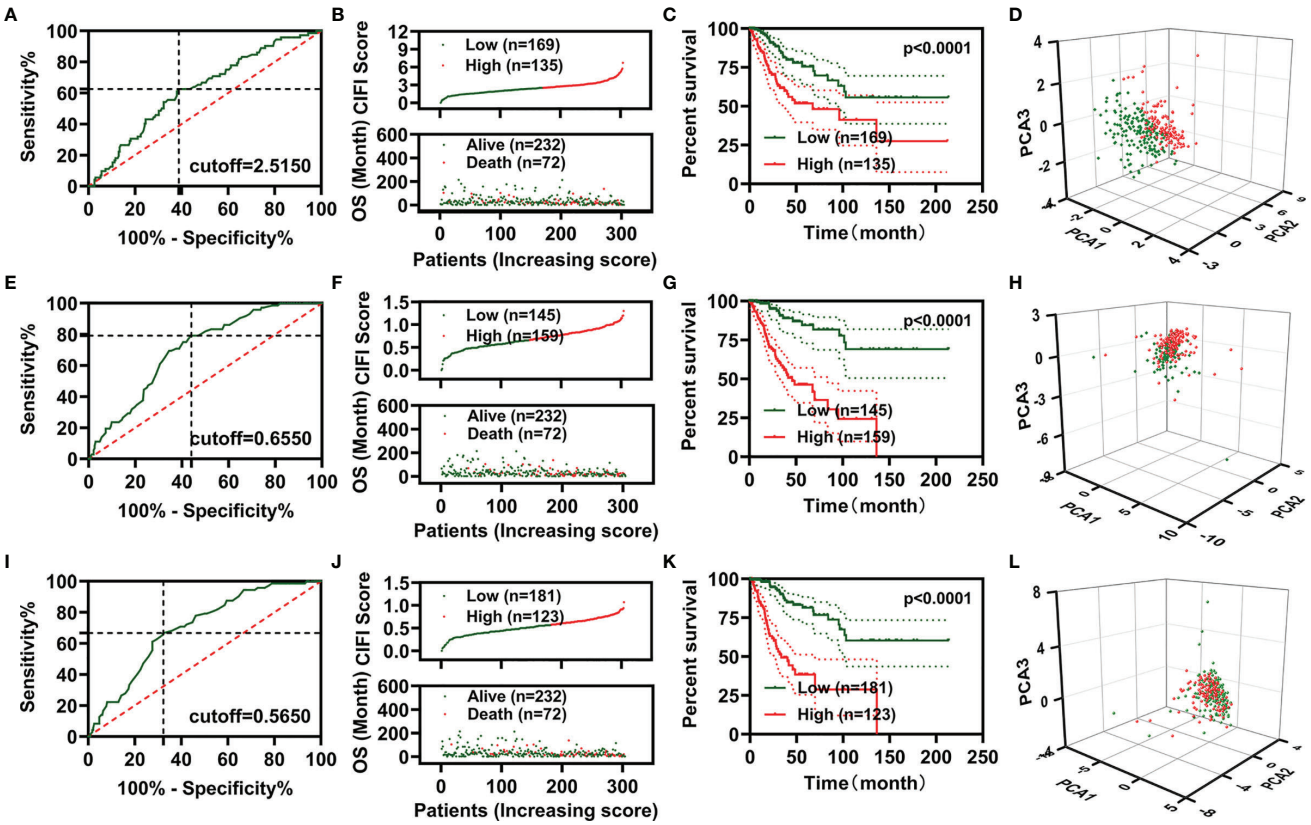


FIGURE 2 | Development of prognostic signatures based on FR-DEGs, IR-DEGs, and FI-DEGs. **(A–D)** Optimal cutoff value **(A)**, distribution of the CIFI values (up) and survival status (down) **(B)**, overall survival curves **(C)**, and PCA plot **(D)** of the prognosis model constructed by three FR-DEGs. **(E–H)** Optimal cutoff value **(E)**, distribution of the CIFI values (up) and survival status (down) **(F)**, overall survival curves **(G)**, and PCA plot **(H)** of the prognosis model constructed by six IR-DEGs. **(I–L)** Optimal cutoff value **(I)**, distribution of the CIFI values (up) and survival status (down) **(J)**, overall survival curves **(K)**, and PCA plot **(L)** of the prognosis model constructed by eight FI-DEGs. DEGs, differentially expressed genes; FR-DEGs, ferroptosis-related DEGs; IR-DEGs, immune-related DEGs; FI-DEGs, ferroptosis- and immune-related DEGs; CIFI, comprehensive index of ferroptosis and immune status; PCA, principal component analysis.

of the two CIFI models constructed using the six IR-DEGs or eight FI-DEGs were comparable with each other and higher than those of the CIFI model constructed using the three FR-DEGs (**Figures 3A–C**). All AUC values of the three prognosis models at 1, 3, 5, and 10 years were over 0.6 (**Figures 3A–C**).

We compared the expression of candidate signatures between the high and low CIFI groups in the corresponding models (**Figures 3D–F**). The correlation analysis indicated that three FR-DEGs (*DUOX1*, *HELLS*, and *SCD*) were significantly correlated with the CIFI value of the FR model (**Figure 3G**), two IR-DEGs (*FLT1* and *DUOX1*) were significantly correlated with the CIFI value of the IR model (**Figure 3H**), and two FI-DEGs (*DUOX1* and *SCD*) were significantly correlated with the CIFI value of the FI model (**Figure 3I**).

Independent Prognostic Value of the Comprehensive Index of Ferroptosis and Immune Status Classifier

To determine whether these CIFI models could serve as independent prognosis models for patients with CESC, clinical features (including age and pathological TNM) and the three CIFI models were used to perform univariate Cox regression analysis. As illustrated in **Figures 4A–C**, the clinical features and three CIFI models were significantly correlated with the OS of CESC patients (**Figures 4A–C**). Then, multivariate Cox regression analysis was performed, and the results indicated that the models based on six IR-DEGs or eight FI-DEGs were still correlated with OS (**Figures 4D–F**).

Moreover, the AUC values of the CIFI models based on six IR-DEGs or eight FI-DEGs were higher than those of the model based on clinical features (**Figures 3B, C, 4G–J**). The AUC values for the three CIFI models were 0.6226, 0.7008, and 0.7006, with sensitivities of 0.6250, 0.7917, and 0.6667 and specificities of 0.6121, 0.5603, and 0.6767, respectively (**Table 1**). The sensitivity and specificity of the model based on eight FI-DEGs were higher than those of the model based on three FR-DEGs. The sensitivity of the model based on six IR-DEGs was the highest, but the specificity was less than 0.6. Comparatively, the CIFI model based on the eight FI-DEGs may be the most suitable. Therefore, we used only this model in the following analysis.

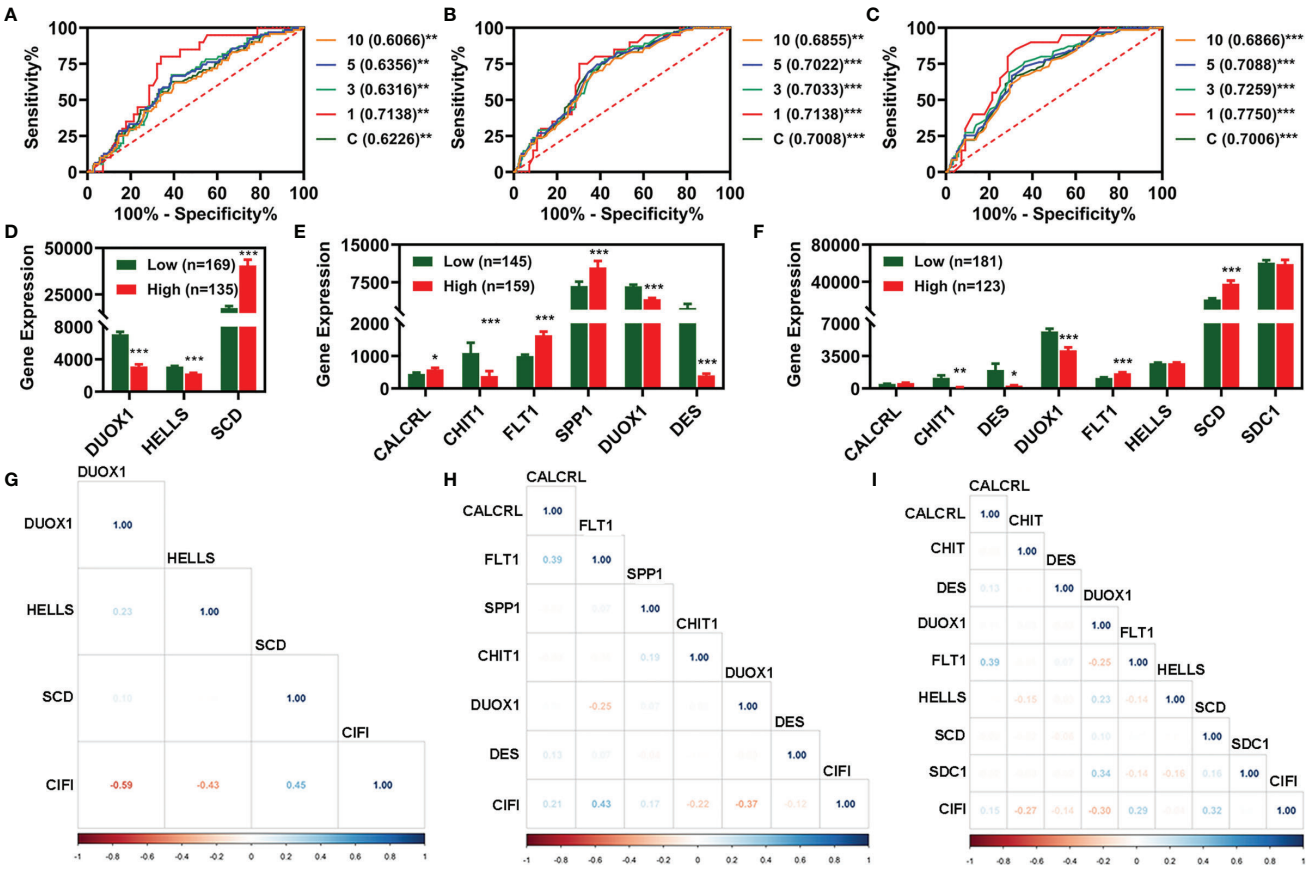


FIGURE 3 | Evaluation of the three prognosis models constructed based on FR-DEGs, IR-DEGs, and FI-DEGs. **(A–C)**, ROC plot analysis for FR-DEG model **(A)**, IR-DEG model **(B)**, and FI-DEG model **(C)**. **(D–F)** The expression profile of the candidate prognosis biomarkers in different models. **(D)** FR-DEG model. **(E)** IR-DEG model. **(F)** FI-DEG models. **(G–I)** Correlation analysis of the CIFI value of the model with the candidate prognosis biomarkers. **(G)** FR-DEG model. **(H)** IR-DEG model. **(I)** FI-DEG models. *p < 0.05, **p < 0.01, ***p < 0.001. DEGs, differentially expressed genes; FR-DEGs, ferroptosis-related DEGs; IR-DEGs, immune-related DEGs; FI-DEGs, ferroptosis- and immune-related DEGs; ROC, receiver operating characteristic; CIFI, comprehensive index of ferroptosis and immune status.

We investigated how different clinical features were associated with the expression of candidate prognostic signatures and the CIFI values of the FI-DEG model. As illustrated in **Figure 5**, *SDC1* expression was significantly different between N0 and N1 patients with CESC. The CIFI values were significantly different between the T1+2 and T3+4 groups.

Association Between Tumor Immune Infiltration and Comprehensive Index of Ferroptosis and Immune Status

To characterize the relationship between the CIFI value and tumor immune infiltration, we utilized the ESTIMATE package in R 3.6.2 to calculate the stromal score, immune score, and tumor purity. As illustrated in **Figures 6A–D**, the stromal score, tumor purity, and ESTIMATE score were significantly different between the normal group and the patients with CESC. Moreover, the stromal score, immune score, and tumor purity were significantly correlated with the ESTIMATE score (**Figure 7A**).

Compared with CESC patients with low CIFI values, those with high CIFI values exhibited significantly decreased stromal scores, immune scores, and ESTIMATE scores, as well as significantly increased tumor purity (**Figures 6E–H**). The CIFI value was significantly correlated with the immune score, tumor purity, and ESTIMATE score (**Figure 7B**).

Since we initially examined the DEGs correlated with ferroptosis and immunity, we then investigated the correlation between CIFI and levels of tumor-infiltrating immune cells and immune-related factors. We found that the levels of 26 tumor-infiltrating immune cells and immune-related factors were different between the normal group and CESC patients (**Supplementary Table 2**), and 12 of the 26 were different between CESC patients with high and low CIFI values (**Figure 6I**). We found that the microenvironment score_XCELL was significantly correlated with CIFI (**Figure 7C**).

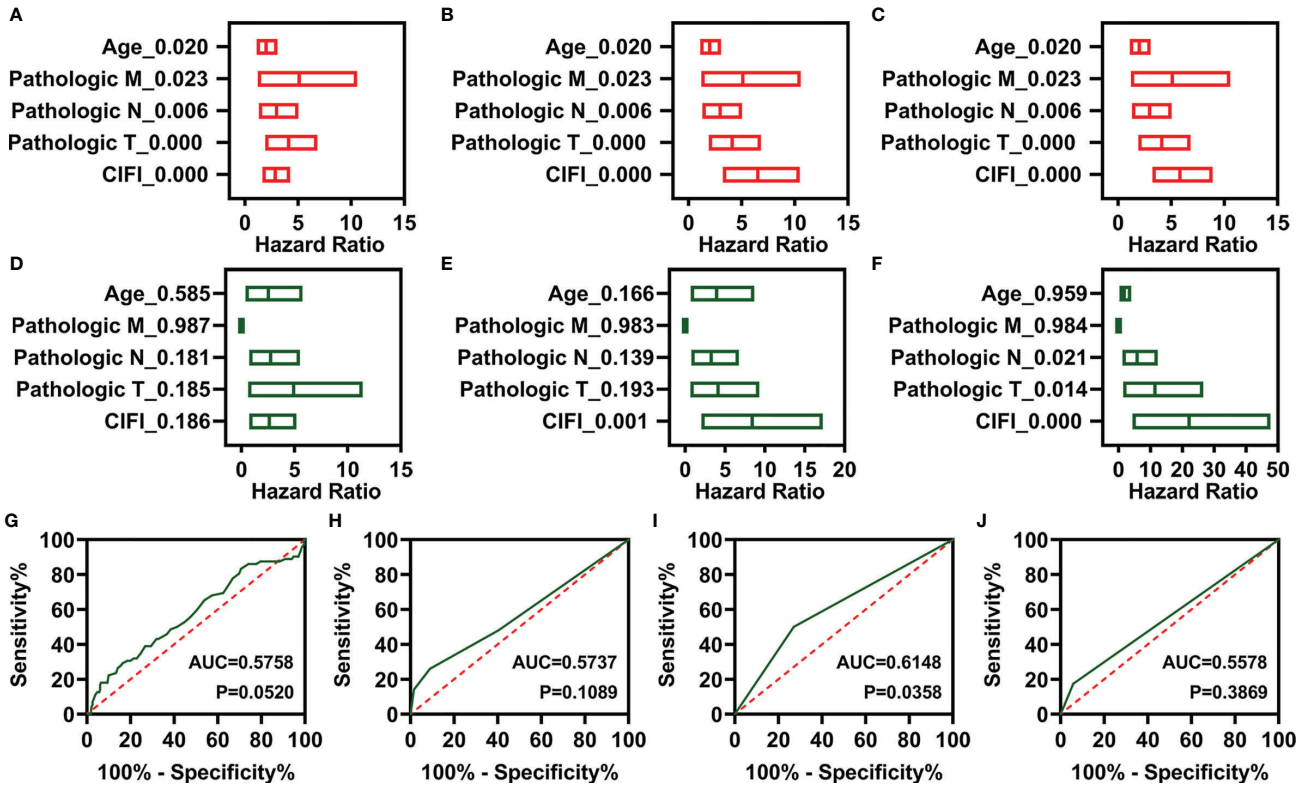


FIGURE 4 | Independent prognostic factors of overall survival. **(A–C)** Univariate Cox regression of prognostic factors in three different models. **(A)** FR-DEG model. **(B)** IR-DEG model. **(C)** FI-DEG models. **(D–F)** Multivariate Cox regression of prognostic factors in three different models. **(D)** FR-DEG model. **(E)** IR-DEG model. **(F)** FI-DEG models. **(G–J)** ROC curve plot of CESC patients with different clinical features. **(G)** Age. **(H)** Pathological T. **(I)** Pathological N. **(J)** Pathological M. DEGs, differentially expressed genes; FR-DEGs, ferroptosis-related DEGs; IR-DEGs, immune-related DEGs; FI-DEGs, ferroptosis- and immune-related DEGs; ROC, receiver operating characteristic; CESC, cervical squamous cell carcinoma and endocervical adenocarcinoma.

DISCUSSION

Cervical cancer is the fourth most frequently diagnosed cancer and the fourth leading cause of cancer-related deaths in women (1). Despite a series of advances in the prevention, screening, and treatment of cervical cancer, there has been no significant improvement in the improvement of cervical cancer outcomes (3, 4). Patients with metastatic or recurrent cervical cancer have a poor prognosis, with a 5-year OS rate of only 17% (2). Almost 15% of cervical cancers are CESC (6). Therefore, it is important to find suitable biomarkers that can predict the occurrence or prognosis of CESC. Previous studies have demonstrated that the dysregulation of ferroptosis and immunity could play an important role in the progression of CESC. In the present study, we aimed to screen FI-DEGs to identify suitable prognostic biomarkers for CESC. The prognosis model constructed using eight FI-DEGs performed better than the models constructed using three FR-DEGs or six IR-DEGs. The

TABLE 1 | Prognosis models for distinguishing patients with CESC from alive patients.

	FR-DEG CIFI model		IR-DEG CIFI model		FI-DEG CIFI model	
	Real death	Real alive	Real death	Real alive	Real death	Real alive
Predicted death	45	90	57	102	48	75
Predicted alive	27	142	15	130	24	157
Total	72	232	72	232	72	232
Correct	45	142	57	130	48	157
Sensitivity	0.6250		0.7917		0.6667	
Specificity		0.6121		0.5603		0.6767

CESC, cervical squamous cell carcinoma and endocervical adenocarcinoma; FR-DEG, ferroptosis-related differentially expressed gene; CIFI, comprehensive index of ferroptosis and immune status; IR-DEG, immune-related differentially expressed gene; FI-DEG, ferroptosis- and immune-related differentially expressed gene.

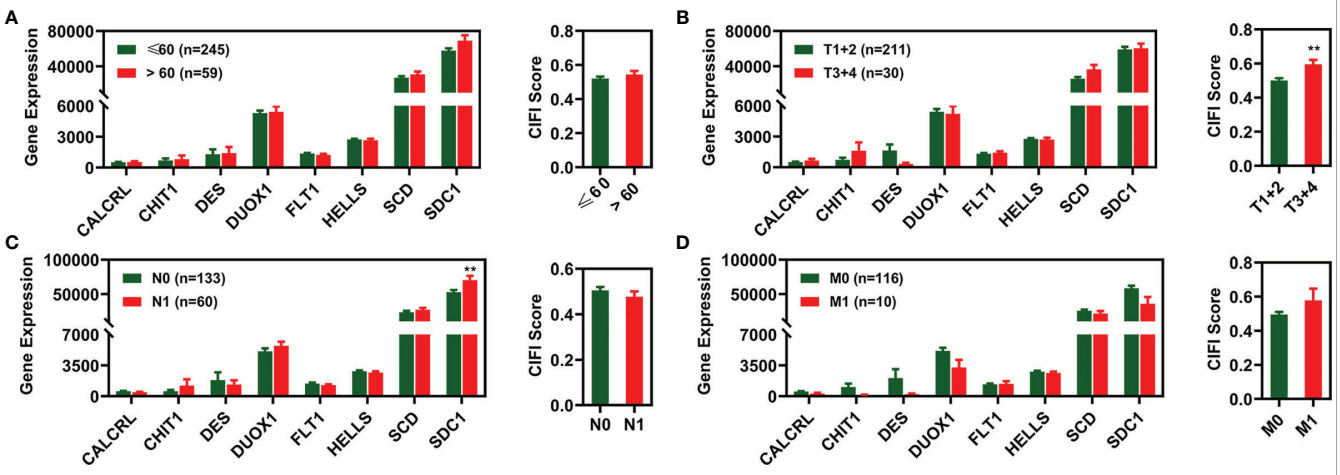


FIGURE 5 | Expression profile of 8 FI-DEGs (left) and CIFI value (right) in different clinical features. **(A)** Age. **(B)** Pathological T. **(C)** Pathological N. **(D)** Pathological M. **p < 0.01. DEGs, differentially expressed genes; FI-DEGs, ferroptosis- and immune-related DEGs; CIFI, comprehensive index of ferroptosis and immune status.

FI-DEG prognosis model independently predicted the outcome of CESC.

In CESC patients, the expression of *CHIT1*, *DUOX1*, *HELLS*, *SCD*, and *SDC1* was increased significantly, while that of *CALCRL*, *DES*, and *FLT1* was decreased significantly, compared with that in the normal group. Chitotriosidase (CHIT1), encoded by *CHIT1* gene, is a member of the chitinase family. Li et al. found that the variations rs61745299 and rs35920428 within the CDS region of *CHIT1* were associated with the risk of colorectal cancer (CRC). These two variations significantly increased the expression of *CHIT1* and were associated with CRC (16).

Dual oxidase 1 (DUOX1) is a member of the protein family of nicotinamide adenine dinucleotide phosphate oxidases. Previous evidence has shown that *DUOX1* is frequently downregulated in lung and liver cancers. However, Zhang et al. found that knockdown of *DUOX2* inhibited the invasion and migration of CRC cells by affecting the ubiquitination status of the ribosomal protein uL3 (17). In the present study, we found that *DUOX1* expression was increased in patients with CESC, which is consistent with Cho's previous report (18). These results suggest that *DUOX1* may play different roles in different cancers, and it is also possible that the abnormal *DUOX1* expression was only the result of CESC, rather than the cause.

Helicase, lymphoid-specific (HELLS) is a chromatin remodeling enzyme. Overexpression of *HELLS* was correlated with more aggressive clinical–pathological features and poorer prognosis (19). In retinoblastoma, Zocchi et al. found that downregulation of *HELLS* could drastically reduce the ectopic division of differentiating cells in Rb1/p107-null retinae, significantly decrease the incidence of retinoblastoma, delay tumor progression, and increase OS (20). However, in pancreatic cancer, Hou found that *HELLS* is upregulated; downregulation leads to tumor growth arrest and increased sensitivity to cisplatin (21). Additionally, Zhu et al. found that *HELLS* levels are increased in lung cancer. Overexpression of *HELLS* is correlated with the prognosis of lung cancer, indicating that *HELLS* may be a potential diagnostic biomarker for lung cancer (22). In the present study, we found that *HELLS* expression was upregulated. Patients with high *HELLS* expression displayed a better OS. These results indicate that *HELLS* plays different roles in the progression of different cancers.

Stearoyl-CoA desaturase (SCD) is an enzyme that catalyzes the rate-limiting step in monounsaturated fatty acid synthesis. *SCD* is highly expressed in ovarian cancer tissues and cell lines and inhibits SCD-induced cell death (23). The results from the study by Tesfay indicated that SCD inhibition could be an effective component of antitumor therapy (23). Other studies have also shown that SCD can promote cancer cell proliferation, migration, and metastasis (24, 25).

SDC1 is a transmembrane heparan sulfate proteoglycan and a member of the syndecan proteoglycan family. Previous studies have demonstrated that SDC1 has different effects in different cancers. For example, reduced expression of *SDC1* could lead to advanced stages of gastric cancer and CRC, while increased expression could promote the growth and proliferation of pancreatic and breast cancers (26). Regardless of its inhibitory or activating effects, these studies indicate that SDC1 plays a pivotal role in cancer. Moreover, *SDC1* could serve as a prognostic biomarker for various cancers, such as hepatocellular carcinoma, gastric cancer, laryngeal cancer, and squamous cell lung carcinoma (27–29). In the present study, we found that *SDC1* was upregulated in CESC patients, and those with high expression of *SDC1* displayed worse OS. The correlation between *SDC1* expression and the OS of CESC patients was independent. Our results indicated that *SDC1* could be a diagnostic and prognostic biomarker for CESC.

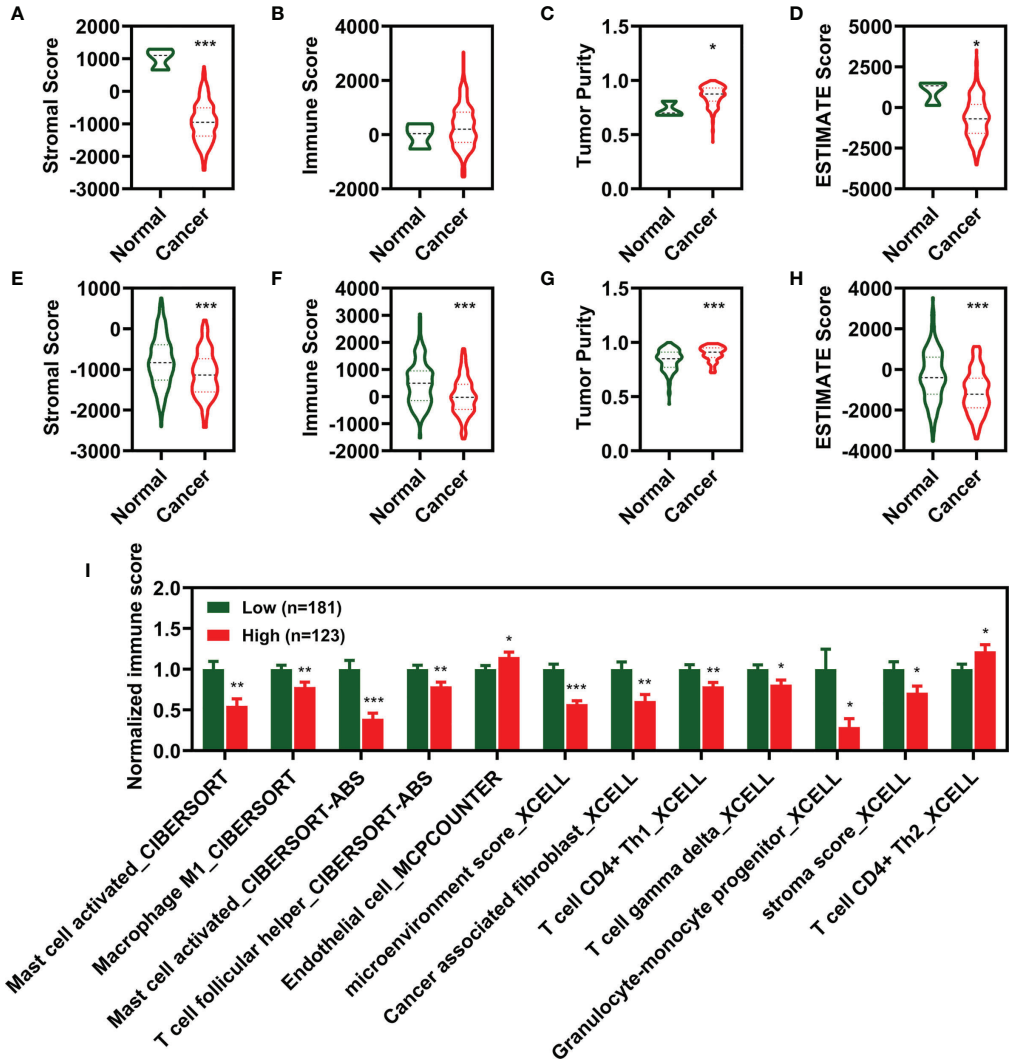


FIGURE 6 | Estimation of the immunity in different groups. **(A–D)** Score of stromal **(A)**, Immune **(B)**, tumor purity **(C)**, and ESTIMATE **(D)** between normal and cancer. **(E–H)** Score of stromal **(E)**, Immune **(F)**, tumor purity **(G)**, and ESTIMATE **(H)** between low CIFI group and high CIFI group of eight FI-DEG models. **(I)** Identified immune molecules and factors verified by differential analysis between low CIFI group and high CIFI group. *p < 0.05, **p < 0.01, ***p < 0.001. CIFI, comprehensive index of ferroptosis and immune status; DEG, differentially expressed genes; FI-DEG, ferroptosis- and immune-related DEG.

Calcitonin receptor-like (CALCRL) is a G-protein-coupled neuropeptide receptor. CALCRL was increased in some tumor types, such as acute myeloid leukemia, Kaposi's sarcoma, and Ewing sarcoma (30–32). High expression of *CALCRL* has been shown to be associated with poor prognosis in acute myeloid leukemia. Angenendt et al. found that knockout of *CALCRL* significantly impaired colony formation in human myeloid leukemia cell lines, indicating that CALCRL may be a potential therapeutic target in AML (33). Additionally, Larrue et al. found that CALCRL depletion reduces leukemic stem cell frequency in relapse-initiating cells post-chemotherapy *in vivo* (34). These results indicate that *CALCRL* is closely associated with cancer. In the present study, we found that *CALCRL* expression was decreased in CESC patients, although those with low *CALCRL* expression displayed a better OS. Although the results of our study are inconsistent with those of previous studies of other cancers, they further support a close relationship between *CALCRL* and cancer. Our results also suggest that CALCRL may play different roles in different cancers.

FLT-1, also known as vascular endothelial growth factor receptor 1 (VEGFR-1), is a high-affinity tyrosine kinase receptor for VEGF. Previous studies have demonstrated that *FLT1* expression is significantly correlated with OS in several cancers, including CRC, cholangiocarcinoma, and esophageal cancer (35–37). Additionally, Han et al. found that FLT1-rs9513111 was associated with a decreased risk of cervical

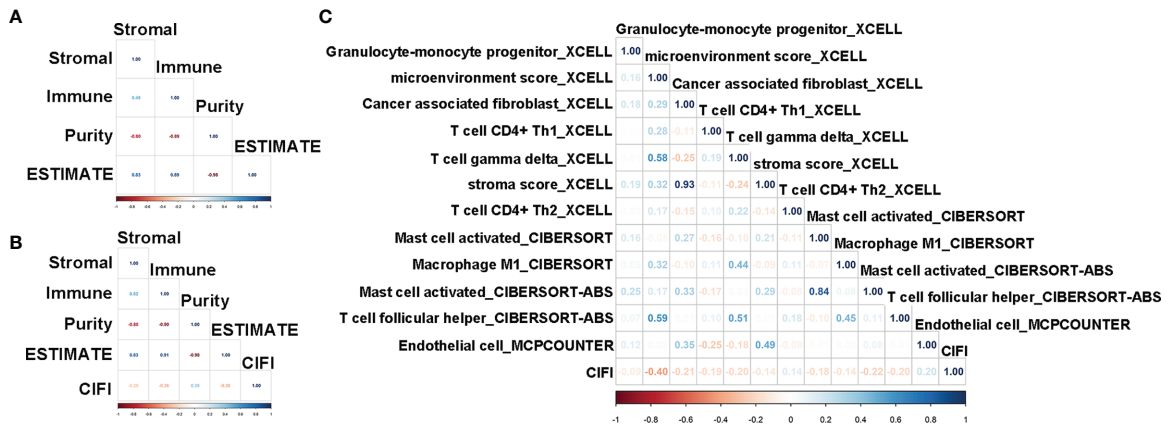


FIGURE 7 | Correlation analysis of CIFI value with the ESTIMATE score and immune molecular and factors. **(A, B)** Correlation of the ESTIMATE scores with stromal, immune, and tumor purity in the sample of normal and CESC **(A)** in the CESC patients **(B)**. **(C)** Correlation of the CIFI value with different immune molecular and factors. CIFI, comprehensive index of ferroptosis and immune status; CESC, cervical squamous cell carcinoma and endocervical adenocarcinoma.

cancer (38). Lv et al. found that the expression of *FLT1* was significantly correlated with the proliferation and invasion of trophoblast cells (39). FLT1 can inhibit proliferation, migration, and invasion of several cell types, such as CRC cells and trophoblast cells (39, 40). In the present study, we found that *FLT1* expression was independently correlated with the OS of CESC patients and could be used as a biomarker for CESC. Our present study reinforced that FLT1 may play an important role in the progression of CESC.

Arentz found that desmin (*DES*) expression was significantly increased in stage I and III tumors. In pancreatobiliary studies, Shin et al. found that *DES* could be used as a prognostic biomarker. We found that *DES* was downregulated in CESC patients. CESC patients with low *DES* expression had poorer survival than those with high expression.

CONCLUSION

We found that the expression of eight FI-DEGs was independently correlated with the OS of CESC patients. The model constructed using these eight FI-DEGs was correlated with the OS of CESC patients and effectively predicted outcomes. These results indicated that the eight FI-DEGs may serve as prognostic and diagnostic biomarkers for CESC. However, further research is needed to determine how these genes affect CESC progression by ferroptosis and immunity regulation and whether they can be used for clinical prognosis.

DATA AVAILABILITY STATEMENT

The original contributions presented in the study are included in the article/**Supplementary Material**. Further inquiries can be directed to the corresponding author.

AUTHOR CONTRIBUTIONS

X-LX conceived and designed the experiments. CX and HY performed the analysis. Z-YY helped to analyze the data. X-LX wrote the paper. All authors contributed to the article and approved the submitted version.

FUNDING

This project is financially supported by the Doctor Foundation of Hunan University of Medicine (2020122004), Hunan Provincial Science and Technology Department (2020SK51202), China Postdoctoral Science Foundation (2020TQ0365), and the Education Department of Hunan Province (20B417).

SUPPLEMENTARY MATERIAL

The Supplementary Material for this article can be found online at: https://www.frontiersin.org/articles/10.3389/fonc.2021.774558/full#supplementary-material

REFERENCES

1. Sung H, Ferlay J, Siegel RL, Laversanne M, Soerjomataram I, Jemal A, et al. Global Cancer Statistics 2020: GLOBOCAN Estimates of Incidence and Mortality Worldwide for 36 Cancers in 185 Countries. *CA Cancer J Clin* (2021) 71:209–49. doi: 10.3322/caac.21660
2. Ouyang D, Yang P, Cai J, Sun S, Wang Z. Comprehensive Analysis of Prognostic Alternative Splicing Signature in Cervical Cancer. *Cancer Cell Int* (2020) 20:221. doi: 10.1186/s12935-020-01299-4
3. Chargari C, Soria JC, Deutsch E. Controversies and Challenges Regarding the Impact of Radiation Therapy on Survival. *Ann Oncol* (2013) 24:38–46. doi: 10.1093/annonc/mds217

4. Zeng H, Chen W, Zheng R, Zhang S, Ji JS, Zou X, et al. Changing Cancer Survival in China During 2003-15: A Pooled Analysis of 17 Population-Based Cancer Registries. *Lancet Glob Health* (2018) 6:e555–67. doi: 10.1016/S2214-109X(18)30127-X
5. Small W Jr, Bacon MA, Bajaj A, Chuang LT, Fisher BJ, Harkenrider MM, et al. Cervical Cancer: A Global Health Crisis. *Cancer* (2017) 123:2404–12. doi: 10.1002/cncr.30667
6. Ojesina AI, Lichtenstein L, Freeman SS, Pedamallu CS, Imaz-Rosshandler I, Pugh TJ, et al. Landscape of Genomic Alterations in Cervical Carcinomas. *Nature* (2014) 506:371–5. doi: 10.1038/nature12881
7. Dixon SJ. Ferroptosis: Bug or Feature? *Immunol Rev* (2017) 277:150–7. doi: 10.1111/imr.12533
8. Dixon SJ, Lemberg KM, Lamprecht MR, Skouta R, Zaitsev EM, Gleason CE, et al. Ferroptosis: An Iron-Dependent Form of Nonapoptotic Cell Death. *Cell* (2012) 149:1060–72. doi: 10.1016/j.cell.2012.03.042
9. Wang L, Chen Y, Mi Y, Qiao J, Jin H, Li J, et al. ATF2 Inhibits Ani-Tumor Effects of BET Inhibitor in a Negative Feedback Manner by Attenuating Ferroptosis. *Biochem Biophys Res Commun* (2021) 558:216–23. doi: 10.1016/j.bbrc.2020.08.113
10. Wang R, Xing R, Su Q, Yin H, Wu D, Lv C, et al. Knockdown of SFRS9 Inhibits Progression of Colorectal Cancer Through Triggering Ferroptosis Mediated by GPX4 Reduction. *Front Oncol* (2021) 11:683589. doi: 10.3389/fonc.2021.683589
11. Wu P, Li C, Ye DM, Yu K, Li Y, Tang H, et al. Circular RNA Circepsti1 Accelerates Cervical Cancer Progression *via* miR-375/409-3P/515-5p-SLC7A11 Axis. *Aging (Albany NY)* (2021) 13:4663–73. doi: 10.18632/aging.202518
12. Xiaofei J, Mingqing S, Miao S, Yizhen Y, Shuang Z, Qinhua X, et al. Oleanolic Acid Inhibits Cervical Cancer Hela Cell Proliferation Through Modulation of the ACSL4 Ferroptosis Signaling Pathway. *Biochem Biophys Res Commun* (2021) 545:81–8. doi: 10.1016/j.bbrc.2021.01.028
13. Vonderheide RH, Domchek SM, Clark AS. Immunotherapy for Breast Cancer: What Are We Missing? *Clin Cancer Res* (2017) 23:2640–6. doi: 10.1158/1078-0432.CCR-16-2569
14. Shi L, Liu Y, Li M, Luo Z. Emerging Roles of Ferroptosis in the Tumor Immune Landscape: From Danger Signals to Anti-Tumor Immunity. *FEBS J* (2021). doi: 10.1111/febs.16034
15. Liu Y, Zhang X, Zhang J, Tan J, Li J, Song Z. Development and Validation of a Combined Ferroptosis and Immune Prognostic Classifier for Hepatocellular Carcinoma. *Front Cell Dev Biol* (2020) 8:596679. doi: 10.3389/fcell.2020.596679
16. Li FF, Yan P, Zhao ZX, Liu Z, Song DW, Zhao XW, et al. Polymorphisms in the CHIT1 Gene: Associations With Colorectal Cancer. *Oncotarget* (2016) 7:39572–81. doi: 10.18632/oncotarget.9138
17. Zhang X, Han J, Feng L, Zhi L, Jiang D, Yu B, et al. DUOX2 Promotes the Progression of Colorectal Cancer Cells by Regulating the AKT Pathway and Interacting With RPL3. *Carcinogenesis* (2021) 42:105–17. doi: 10.1093/carcin/bgaa056
18. Cho SY, Kim S, Son MJ, Kim G, Singh P, Kim HN, et al. Dual Oxidase 1 and NADPH Oxidase 2 Exert Favorable Effects in Cervical Cancer Patients by Activating Immune Response. *BMC Cancer* (2019) 19:1078. doi: 10.1186/s12885-019-6202-3
19. Law CT, Wei L, Tsang FH, Chan CY, Xu IM, Lai RK, et al. HELLS Regulates Chromatin Remodeling and Epigenetic Silencing of Multiple Tumor Suppressor Genes in Human Hepatocellular Carcinoma. *Hepatology* (2019) 69:2013–30. doi: 10.1002/hep.30414
20. Zocchi L, Mehta A, Wu SC, Wu J, Gu Y, Wang J, et al. Chromatin Remodeling Protein HELLS Is Critical for Retinoblastoma Tumor Initiation and Progression. *Oncogenesis* (2020) 9:25. doi: 10.1038/s41389-020-0210-7
21. Hou X, Yang L, Wang K, Zhou Y, Li Q, Kong F, et al. HELLS, a Chromatin Remodeler Is Highly Expressed in Pancreatic Cancer and Downregulation of It Impairs Tumor Growth and Sensitizes to Cisplatin by Reexpressing the Tumor Suppressor TGFBR3. *Cancer Med* (2021) 10:350–64. doi: 10.1002/cam4.3627
22. Zhu W, Li LL, Songyang Y, Shi Z, Li D. Identification and Validation of HELLS (Helicase, Lymphoid-Specific) and ICAM1 (Intercellular Adhesion Molecule 1) as Potential Diagnostic Biomarkers of Lung Cancer. *PeerJ* (2020) 8:e8731. doi: 10.7717/peerj.8731
23. Tesfay L, Paul BT, Konstorum A, Deng Z, Cox AO, Lee J, et al. Stearoyl-CoA Desaturase 1 Protects Ovarian Cancer Cells From Ferroptotic Cell Death. *Cancer Res* (2019) 79:5355–66. doi: 10.1158/0008-5472.CAN-19-0369
24. Han S, Wang Y, Ma J, Wang Z, Wang HD, Yuan Q. Sulforaphene Inhibits Esophageal Cancer Progression *via* Suppressing SCD and CDH3 Expression, and Activating the GADD45B-MAP2K3-P38-P53 Feedback Loop. *Cell Death Dis* (2020) 11:713. doi: 10.1038/s41419-020-02859-2
25. Xu X, Ding Y, Yao J, Wei Z, Jin H, Chen C, et al. miR-215 Inhibits Colorectal Cancer Cell Migration and Invasion *via* Targeting Stearoyl-CoA Desaturase. *Comput Math Methods Med* (2020) 11:713. doi: 10.1155/2020/5807836
26. Liao S, Liu C, Zhu G, Wang K, Yang Y, Wang C. Relationship Between SDC1 and Cadherin Signalling Activation in Cancer. *Pathol Res Pract* (2020) 216:152756. doi: 10.1016/j.prp.2019.152756
27. Bonnomet A, Syne L, Brysse A, Feyereisen E, Thompson EW, Noel A, et al. A Dynamic *In Vivo* Model of Epithelial-to-Mesenchymal Transitions in Circulating Tumor Cells and Metastases of Breast Cancer. *Oncogene* (2012) 31:3741–53. doi: 10.1038/onc.2011.540
28. Nieto MA. Epithelial Plasticity: A Common Theme in Embryonic and Cancer Cells. *Science* (2013) 342:1234850. doi: 10.1126/science.1234850
29. Zhang S, Qing Q, Wang Q, Xu J, Zhi F, Park PW, et al. Syndecan-1 and Heparanase: Potential Markers for Activity Evaluation and Differential Diagnosis of Crohn's Disease. *Inflamm Bowel Dis* (2013) 19:1025–33. doi: 10.1097/MIB.0b013e318280298f
30. Hagner S, Stahl U, Grimm T, Sturzl M, Lang RE. Expression of Calcitonin Receptor-Like Receptor in Human Vascular Tumours. *J Clin Pathol* (2006) 59:1104–7. doi: 10.1136/jcp.2005.026930
31. Dallmayer M, Li J, Ohmura S, Alba Rubio R, Baldauf MC, Holting TLB, et al. Targeting the CALCB/RAMP1 Axis Inhibits Growth of Ewing Sarcoma. *Cell Death Dis* (2019) 10:116. doi: 10.1038/s41419-019-1372-0
32. Gluexam T, Grandits AM, Schlerka A, Nguyen CH, Etzler J, Finkes T, et al. CGRP Signaling *via* CALCRL Increases Chemotherapy Resistance and Stem Cell Properties in Acute Myeloid Leukemia. *Int J Mol Sci* (2019) 20. doi: 10.3390/ijms20235826
33. Angenendt L, Bormann E, Pabst C, Alla V, Gorlich D, Braun L, et al. The Neuropeptide Receptor Calcitonin Receptor-Like (CALCRL) Is a Potential Therapeutic Target in Acute Myeloid Leukemia. *Leukemia* (2019) 33:2830–41. doi: 10.1038/s41375-019-0505-x
34. Larrue C, Guiraud N, Mouchel PL, Dubois M, Farge T, Gotanegre M, et al. Adrenomedullin-CALCRL Axis Controls Relapse-Initiating Drug Tolerant Acute Myeloid Leukemia Cells. *Nat Commun* (2021) 12:422. doi: 10.1038/s41467-020-20717-9
35. Rades D, Golke H, Schild SE, Kilic E. Impact of VEGF and VEGF Receptor 1 (FLT1) Expression on the Prognosis of Stage III Esophageal Cancer Patients After Radiochemotherapy. *Strahlenther Onkol* (2008) 184:416–20. doi: 10.1007/s00066-008-1850-2
36. Hoffmann AC, Goekkurt E, Danenberg PV, Lehmann S, Ehninger G, Aust DE, et al. EGFR, FLT1 and Heparanase as Markers Identifying Patients at Risk of Short Survival in Cholangiocarcinoma. *PloS One* (2013) 8:e64186. doi: 10.1371/journal.pone.0064186
37. Slattery ML, Lundgreen A, Wolff RK. VEGFA, FLT1, KDR and Colorectal Cancer: Assessment of Disease Risk, Tumor Molecular Phenotype, and Survival. *Mol Carcinog* (2014) 531):E140–150. doi: 10.1002/mc.22058
38. Han L, Husaiyin S, Ma C, Wang L, Niyazi M. TNFAIP8L1 and FLT1 Polymorphisms Alter the Susceptibility to Cervical Cancer Amongst Uyghur Females in China. *Biosci Rep* (2019) 39. doi: 10.1042/BSR20191155
39. Lv Y, Lu X, Li C, Fan Y, Ji X, Long W, et al. miR-145-5p Promotes Trophoblast Cell Growth and Invasion by Targeting FLT1. *Life Sci* (2019) 239:117008. doi: 10.1016/j.lfs.2019.117008
40. Jinjun W, Zhaowei W, Qiang L, Zhijun X, Juanzi Z, Lin L, et al. sFLT-1 Inhibits Proliferation, Migration, and Invasion of Colorectal Cancer SW480 Cells Through Vascular Mimicry Formation Suppression. *Tumour Biol* (2017) 39:1010428317698339. doi: 10.1177/1010428317698339

Conflict of Interest: The authors declare that the research was conducted in the absence of any commercial or financial relationships that could be construed as a potential conflict of interest.

Publisher's Note: All claims expressed in this article are solely those of the authors and do not necessarily represent those of their affiliated organizations, or those of the publisher, the editors and the reviewers. Any product that may be evaluated in

this article, or claim that may be made by its manufacturer, is not guaranteed or endorsed by the publisher.

Copyright © 2022 Xing, Yin, Yao and Xing. This is an open-access article distributed under the terms of the Creative Commons Attribution License (CC BY). The use, distribution or reproduction in other forums is permitted, provided the original author(s) and the copyright owner(s) are credited and that the original publication in this journal is cited, in accordance with accepted academic practice. No use, distribution or reproduction is permitted which does not comply with these terms.

frontiers in Oncology

SYSTEMATIC REVIEW
published: 24 January 2022
doi: 10.3389/fonc.2021.762921

Comparison of Minimally Invasive Versus Abdominal Radical Hysterectomy for Early-Stage Cervical Cancer: An Updated Meta-Analysis

Mengting Zhang[1†], Wei Dai[1†], Yuexiu Si[2], Yetan Shi[1], Xiangyuan Li[1], Ke Jiang[1], Jingyi Shen[1] and Liying Ying[3]*

[1] The Second Clinical Medical College, Zhejiang Chinese Medical University, Hangzhou, China, [2] School of Basic Medical Sciences, Zhejiang Chinese Medical University, Hangzhou, China, [3] Department of Obstetrics and Gynecology, Ningbo Yinzhou No. 2 Hospital, Ningbo, China

OPEN ACCESS

Edited by:
Stefano Restaino, Ospedale Santa Maria della Misericordia di Udine, Italy

Reviewed by:
Luigi Pedone Anchora, Agostino Gemelli University Polyclinic (IRCCS), Italy
Gunnar Kristensen, Oslo University Hospital, Norway

***Correspondence:**
Liying Ying
zmtccmit@163.com

[†]*These authors have contributed equally to this work and share first authorship*

Specialty section:
This article was submitted to Gynecological Oncology, a section of the journal Frontiers in Oncology

Received: *23 August 2021*
Accepted: *30 December 2021*
Published: *24 January 2022*

Citation:
Zhang M, Dai W, Si Y, Shi Y, Li X, Jiang K, Shen J and Ying L (2022) Comparison of Minimally Invasive Versus Abdominal Radical Hysterectomy for Early-Stage Cervical Cancer: An Updated Meta-Analysis. Front. Oncol. 11:762921. doi: 10.3389/fonc.2021.762921

Background: Although minimally invasive surgery (MIS) was commonly used to treat patients with early-stage cervical cancer, its efficacy remained controversial.

Methods: We systematically searched PubMed, Web of Science, and Cochrane Library databases until March 2021 to compare the prognosis of early-stage cervical cancer patients who underwent MIS (laparoscopic or robot-assisted radical hysterectomy) or ARH. The primary outcomes included rates of 3- and 5-year disease-free survival (DFS) and overall survival (OS). The study protocol was registered in PROSPERO: CRD42021258116.

Results: This meta-analysis included 48 studies involving 23346 patients (11220, MIS group; 12126, ARH group). The MIS group had a poorer medium-term (3-year) DFS (HR=1.08, 95% CI: 1.01-1.16, p=0.031) than the ARH group, without significant difference in medium-term OS as well as long-term (5-year) DFS and OS. Subgroup analysis of 3-year prognosis revealed that although patients in Western countries who underwent MIS had shorter DFS than those who underwent ARH (HR=1.10, p=0.024), no difference was observed in DFS among those in Asian countries. Moreover, MIS was linked to poorer 3-year DFS in patients with stage I cervical cancer (HR=1.07, p=0.020). Notably, subgroup analysis of 5-year prognosis revealed that patients with tumor size ≥2 cm undergoing MIS exhibited a shorter DFS than those who underwent ARH (HR=1.65, p=0.041).

Conclusion: Patients with early-stage cervical cancer undergoing MIS may have a poorer prognosis than those undergoing ARH. Therefore, applying MIS in early-stage cervical cancer patients should be conducted with caution.

Systematic Review Registration: The study protocol was registered in PROSPERO: CRD42021258116.

Keywords: abdominal radical hysterectomy, early-stage cervical cancer, prognosis, meta-analysis, minimally invasive surgery

INTRODUCTION

Cervical cancer was ranked as the fourth most frequently diagnosed cancer and the fourth leading cause of cancer death in women. Most of these cases occurred in sub-Saharan Africa, Melanesia, South America, and South-Eastern Asia, with the highest morbidity and mortality rates in sub-Saharan African (1). Surgery was the primary treatment option for early-stage cervical cancer to treat stage IA, IB1, and selected IIA1 cases (2). Conization alone or simple hysterectomy was an appropriate treatment option for patients with stage IA disease, whereas radical hysterectomy was the preferred treatment modality for stage IB1 or IIA1 patients (3). Abdominal radical hysterectomy (ARH) was a standard and historical treatment for early-stage cervical cancer (4, 5). As the research progressed, minimally invasive surgery (MIS) became the preferred treatment option for early-stage cervical cancer over the past two decades (6, 7).

The feasibility and safety of MIS (laparoscopic or robot-assisted radical hysterectomy) were gradually widely accepted (7, 8). Several retrospective studies and reviews (9–11) highlighted MIS benefits in reducing blood loss, shortening hospital stay, accelerating recovery time, and reducing the risk of postoperative complications, with equal survival outcomes as ARH. Nevertheless, preliminary results from a phase 3 multicenter randomized controlled trial (RCT) (12), presented at the Society of Gynecological Oncology (SGO) meeting in March 2018, indicated that early-stage cervical cancer patients undergoing MIS had a lower disease-free survival (DFS) and overall survival (OS) than those undergoing ARH. The RCT results were unexpected and sparked a huge debate (2). Since then, the guidelines from National Comprehensive Cancer Network (NCCN) (2) and International Federation of Gynecology and Obstetrics (FIGO) (13) have been revised to indicate that ARH remains the gold standard for treating early-stage cervical cancer.

Consequently, the comparison of prognosis between MIS and ARH in patients with early-stage cervical cancer remains controversial. Then, some clinical trials and reviews (14–17) demonstrated that patients with early-stage cervical cancer who underwent MIS or ARH had similar OS, but those who underwent MIS exhibited shorter DFS. Therefore, we performed a meta-analysis of available evidence to compare and evaluate medium- (3-year) and long-term (5-year) survival outcomes in patients with early-stage cervical cancer who underwent MIS or ARH.

METHODS

Search Strategy

We conducted a systematic search of PubMed, Web of Science, and Cochrane Library to identify relevant reports published from inception until March 2021. The search terms included (uterine cervical neoplasms OR cervical cancer OR cervix cancer OR cervical carcinoma) AND (minimally invasive OR laparoscopic OR robotic OR robot-assisted OR Davinci) AND (open OR abdominal OR traditional) AND (radical hysterectomy OR surgery OR hysterectomy OR surgical procedure OR operation). Additionally, potential studies were identified by manually searching the references of included articles. From the initial search to the final selection of studies, the entire review process was mapped using the Preferred Reporting Items for Systematic Reviews and Meta-analyses (PRISMA) flow diagram. The study protocol was registered in PROSPERO: CRD42021258116.

Eligible Criteria

The included studies met the following criteria: (1) the articles were observational studies or RCTs comparing patients with early-stage cervical cancer who underwent MIS (laparoscopic and/or robot-assisted radical hysterectomy) or ARH. (2) The studies contained detailed data on prognosis (DFS and OS) for patients with early-stage cervical cancer. (3) At least 3-year survival data was provided in the study. (4) The articles were published in English.

The exclusion criteria were as follows: (1) there was no extractable data for the study. (2) The studies included patients treated with preoperative neoadjuvant therapy or fertility-saving surgery (such as cervical resection). (3) Patients with distant metastases or those who underwent non-radical hysterectomy were investigated. (4) When a publication has been continuously updated or is duplicated, the highest-quality article is selected.

Data Extraction and Quality Assessment

Two independent researchers extracted data from each relevant article, and a third researcher arbitrated disagreements. We recorded information on author, year of publication, country, age, number of patients, study design, MIS type, primary FIGO tumor stage, tumor size, pathologic type, lymph node metastasis, lymph-vascular space invasion, tumor differentiation, and follow-up time. Additionally, this meta-analysis used medium- and long-term prognosis endpoints, including 3- and 5-year DFS and OS. Following that, the methodological quality of included RCTs and observational studies was assessed using Cochrane Collaboration's tool and Newcastle-Ottawa Quality Assessment Scale, respectively.

Statistical Analysis

All statistical analyses were performed using Stata 12.0 (18). Medium- and long-term prognoses in MIS and ARH groups were analyzed using a hazard ratio (HR) with a 95% confidence interval (95% CI) (19). Moreover, heterogeneity of HR was assessed based on I^2 statistics. Due to differences in study design and surgical treatment, a random-effects model was used to improve the credibility of results. Furthermore, Egger's test used $p<0.05$ as the significance level to evaluate publication bias (20). Sensitivity analysis for the stability of results was performed. All statistical tests were two-sided, and $p<0.05$ was considered statistically significant.

Abbreviations: MIS, minimally invasive surgery; ARH, Abdominal radical hysterectomy; OS, overall survival; DFS, disease-free survival; HR, hazard ratio; CI, confidence interval; FIGO, International Federation of Gynecology and Obstetrics; RCT, randomized controlled trial.

RESULTS

Characteristics of Eligible Research

The initial search resulted in 2600 relevant studies from different electronic databases. Following screening, 48 studies (10–12, 14–17, 21–61) encompassing 23346 patients fulfilled the inclusion criteria. The detailed screening process of articles is summarized in **Figure 1**. The basic characteristics of selected studies are listed in **Table 1**. Two studies were RCTs (12, 29), and the remaining were observational studies (10, 11, 14–17, 21–28, 30–61) (n=46). Three treatment modalities were adopted by contrast: MIS (laparoscopic radical hysterectomy plus robot-assisted radical hysterectomy) versus ARH (n=10), laparoscopic radical hysterectomy versus ARH (involved 31 studies), and robot-assisted radical hysterectomy versus ARH (involved 10 studies). Of 48 studies, 23 were conducted in Asian countries and 24 in Western countries. The remaining study was conducted in both Asian and Western countries. Among the studies conducted in Asian countries, 11 were conducted in China, 10 in Korea, 1 in Singapore, and 1 in Turkey. Of the studies conducted in Western countries, 7 were conducted in America, 1 in Brazil, 1 in Canada, 1 in Denmark, 1 in France, 4 in Italy, 3 in multicenters, 2 in the Netherlands, 1 in Poland, 1 in Spain, 1 in Sweden, and 1 in the United Kingdom. All studies were published between 2004 and 2021. In these eligible studies, the number of patients was a minimum of 14 and a maximum of 1305. Almost all patients were diagnosed with FIGO stage IA-IIA cervical cancer. In addition, the proportion of patients with tumor size ≥2 cm ranged from a minimum of 18.8% to a maximum of 78.6%. Squamous cell carcinoma was the most common pathological type of cervical cancer in our study. Additional details of included studies are presented in **Supplementary Table 1**.

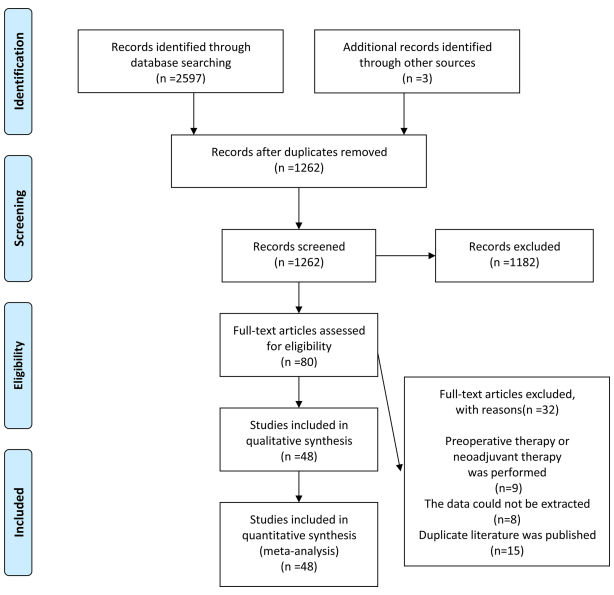


FIGURE 1 | A schematic flow for the selection of articles included in this meta-analysis.

Quality Assessment

Cochrane collaboration's tool was employed to assess the quality of RCT enrolled in the study. For observational studies, quality assessment was performed based on the Newcastle-Ottawa Quality Assessment Scale, and only high-quality studies with a total score ≥6 were included in the final analysis. Details on quality assessment are displayed in **Supplementary Table 2**.

Prognostic Analysis

Random effect analysis of 14 of 48 reports on 3-year DFS encompassing 7003 patients with early-stage cervical cancer revealed a statistically significant difference, suggesting that the MIS group had a shorter 3-year DFS than the ARH group (HR=1.08, 95% CI: 1.01-1.16, p=0.031; **Figure 2**). Besides, 14 studies involving 7118 patients with early-stage cervical cancer were assessed for 3-year OS, without observing a significant difference in 3-year OS between MIS and ARH groups (HR=1.09, 95% CI: 0.99-1.20, p=0.082; **Figure 3**).

There were 32 studies that provided 5-year DFS, including 13025 patients with early-stage cervical cancer. Among them, there were 6471 cases in the MIS group and 6312 cases in the ARH group. The results revealed that MIS had no significant effect on long-term DFS in patients with early-stage cervical cancer compared with ARH (HR=1.02, 95% CI: 0.98-1.07, p=0.266; **Figure 4**). Moreover, 15551 patients were evaluated for 5-year OS in 32 studies. The results illustrated that long-term OS of patients undergoing MIS was similar to that of patients undergoing ARH (HR=1.01, 95% CI: 0.97-1.05, p=0.795; **Figure 5**).

Subgroup Analysis of 3- and 5-Year Survival

Of 14 studies that provided 3-year DFS, a subgroup analysis was performed on cervical cancer stage, including nine studies for stage I (HR=1.07, 95% CI: 1.01-1.14, p=0.020) and five studies for IA-IB1 (HR=1.23, 95% CI: 1.02-1.49, p=0.034). Patients with stages I and IA-IB1 who underwent MIS had a poorer 3-year DFS than those with ARH. Additionally, five studies were conducted in Western countries (HR=1.10, 95% CI: 1.01-1.20, p=0.024), whereas eight studies were conducted in Asian countries (HR=1.04, 95% CI: 0.96-1.12, p=0.381). Overall, the pooled subgroup results demonstrated that in Western countries, patients treated with MIS exhibited a significantly shorter 3-year DFS than those treated with ARH. Nevertheless, in studies of Asian countries, no difference in DFS was observed between MIS and ARH groups. Regarding patients with tumor size <2 cm, a subgroup analysis revealed no statistically significant difference in 3-year DFS between both groups (HR=1.04, 95% CI: 0.98-1.09, p=0.186) (**Table 2**).

Likewise, there were 14 studies that reported 3-year OS, with nine reporting stage I (HR=1.06, 95% CI: 0.99-1.14, p=0.096), five reporting stage IA-IB1 (HR=1.42, 95% CI: 0.71-2.85, p=0.321) and three reporting stage IB1-II (HR=1.02, 95% CI: 0.92-1.13, p=0.689). The subgroup analysis indicated that compared with patients undergoing ARH, no statistical difference was observed in 3-year OS in patients with stage I, IA-IB1, and IB1-II cervical

TABLE 1 | Characteristics of all studies included in the meta-analysis.

Author	Year	Group	Country	Tumor stage (FIGO)	Patients number		Tumor size (%) ≥2cm		Pathologic type(%)							
					MIS	Control	MIS	Control	MIS				Control			
									SCC	ACC	ASC	Other	SCC	ACC	ASC	Other
Li	2021	MIS vs.ARH	Korea	IA-IIA	282	280	51.8	59.6	62.4	31.6	3.9	2.1	68.6	24.6	4.6	2.1
Kim	2021	MIS vs.ARH	Korea	IA1-IIA1	67	22	34.3	31.8	76.1	22.4	1.5	0.0	68.2	27.3	4.5	0.0
Kim	2021	MIS vs.ARH	Korea	IB1-IIA2	110	38	NA	NA	70.0	25.5	4.5	0.0	71.1	26.3	2.6	0.0
Zaccarini	2021	MIS vs.ARH	French	IA2-IIB	223	41	NA	NA	66.4	26.9	0.0	6.7	63.4	24.4	0.0	12.2
Chiva	2020	MIS vs.ARH	European	IB1	291	402	43.3	60.2	NA	NA	NA	NA	NA	NA	NA	NA
Levine	2020	MIS vs.ARH	America	IA2-IB1	82	44	42.7	54.5	43.9	47.6	8.5	0.0	65.9	27.3	6.8	0.0
Uppal	2020	MIS vs.ARH	America	IA1-IB1	560	255	18.8	31.0	55.0	40.7	4.3	0.0	60.0	35.7	4.3	0.0
Gil-Moreno	2019	MIS vs.ARH	Spain	IA1-IIB	112	76	NA	NA	60.7	33.9	0.0	5.4	61.8	30.2	0.0	7.8
Cusimano	2019	MIS vs.ARH	Canada	IA-II	473	485	NA	NA	51.6		48.4		56.1		43.9	
Ramirez[a]	2018	MIS vs.ARH	multicenter	IA1-IB1	319	312	42.3	42.9	67.10	27.30	2.80	2.80	67.30	25.60	1.90	5.10
Campos[a]	2021	LRH vs.ARH	Brazil	IA2-IIA	16	14	NA	NA	NA	NA	NA	NA	NA	NA	NA	NA
Rodriguez	2021	LRH vs.ARH	multicenter	IA1-IB1	681	698	26.5	27.8	65.0	31.1	3.9	0.0	67.0	28.1	4.9	0.0
Li	2021	LRH vs.ARH	China	IB1	574	574	NA	NA	82.4	15.2	2.4	0.0	85.2	11.5	3.3	0.0
Dai	2020	LRH vs.ARH	China	IB	213	213	NA	NA	75.6	22.5	1.9	0.0	68.5	27.2	4.2	0.0
Abel[#]	2020	LRH vs.ARH	America	II	410	1305	76.6	78.6	NA	NA	NA	NA	NA	NA	NA	NA
Kwon	2020	LRH vs.ARH	Korea	IA2-IB2	252	258	NA	NA	73.4	24.6	0.0	2.0	69.8	27.1	0.0	3.1
Qin	2020	LRH vs.ARH	China	IA2-IB1	172	84	29.7	35.7	76.8	20.3	2.9	0.0	85.7	9.5	4.8	0.0
Hu	2020	LRH vs.ARH	China	IA2-IB1/IIA1	406	406	59.1	62.1	88.0	9.1	1.7	1.2	88.9	8.4	1.5	1.2
Chen	2020	LRH vs.ARH	China	IB1	129	196	NA	NA	79.8	14.7	3.1	2.3	84.2	11.7	3.1	1.0
Wenzel	2020	LRH vs.ARH	Netherlands	IA2-IIA1	369	740	36.0	62.0	67.0	29.0	4.0	0.0	66.0	29.0	5.0	0.0
Pedone Anchora	2020	LRH vs.ARH	Italy	IA-IIB	206	217	33.5	47.5	67.5		32.5		65.0		35.0	
Wang	2019	LRH vs.ARH	China	IB2-IIB	217	179	NA	NA	86.6	11.5	1.8	0.0	89.4	5.0	5.6	0.0
Yuan	2019	LRH vs.ARH	China	IA2-IIA2	99	99	50.5	53.5	82.8	14.1	3.1	0.0	82.8	13.1	4.1	0.0
Kim	2019	LRH vs.ARH	Korea	IB	222	222	43.7	45.5	66.7	27.9	5.4	0.0	75.2	18.9	5.9	0.0
Paik	2019	LRH vs.ARH	Korea	IB1-IIA1	119	357	NA	NA	68.9	31.1	0.0	0.0	72.0	28.0	0.0	0.0
Liu	2019	LRH vs.ARH	China	IB	271	135	NA	NA	80.1	15.9	4.0	0.0	88.1	8.9	3.0	0.0
Lim	2019	LRH vs.ARH	Singapore	IA-IIA	51	85	NA	NA	41.2	49.0	3.9	5.9	58.8	31.8	3.5	5.9
Guo	2018	LRH vs.ARH	China	IA-IIA	412	139	NA	NA	82.5		17.5		79.1		20.9	
Corrado*	2018	LRH vs.ARH	Italy	IB1	152	101	NA	NA	72.3	24.3	0.0	3.4	67.3	22.8	5.9	4.0

(Continued)

TABLE 1 | Continued

Author	Year	Group	Country	Tumor stage (FIGO)	Patients number		Tumor size (%) ≥2cm		Pathologic type(%)							
					MIS	Control	MIS	Control	MIS				Control			
									SCC	ACC	ASC	Other	SCC	ACC	ASC	Other
Wang	2016	LRH vs.ARH	China	IA2-IIA2	203	203	NA	NA	84.7	11.8	3.5	0.0	76.9	18.7	4.4	0.0
Park	2016	LRH vs.ARH	Korea	IA2-IIA	196	107	52.2	27.7	NA	NA	NA	NA	NA	NA	NA	NA
Mendivil[$]	2016	LRH vs.ARH	America	IA2-IIB	49	39	NA	NA	77.6	18.4	2.0	2.0	69.2	12.8	10.3	7.7
Ditto	2015	LRH vs.ARH	Italy	IA2/IB1	60	60	NA	NA	60.0		40.0		58.0		42.0	
Toptas	2014	LRH vs.ARH	Turkey	IA2-IB1	22	46	31.8	67.4	81.8	4.6	13.6	0.0	63.0	10.9	21.7	4.4
Kong	2014	LRH vs.ARH	Korea	IB-IIA	40	48	NA	NA	75.0	17.5	7.5	0.0	81.3	14.6	4.2	0.0
van de Lande	2012	LRH vs.ARH	Netherlands	IB1	76	93	NA	NA	73.7	23.7	2.5	0.0	72.0	23.7	4.3	0.0
Choi	2012	LRH vs.ARH	Korea	IA-IIA	194	99	NA	NA	77.4	21.6	1.0	0.0	71.7	25.3	3.0	0.0
Lee	2011	LRH vs.ARH	Korea	I-II	24	48	NA	NA	79.2	16.7	4.1	0.0	79.2	16.7	4.1	0.0
Sobiczewski	2009	LRH vs.ARH	Poland	IA1-IIA	22	58	NA	NA	91.0	9.0	0.0	0.0	86.0	12.0	0.0	2.0
Malzoni	2009	LRH vs.ARH	Italy	IA1-IB1	65	62	NA	NA	86.2	10.8	3.0	0.0	85.5	9.7	4.8	0.0
Jackson	2004	LRH vs.ARH	United Kingdom	IB1	50	50	NA	NA	66.0	34.0	0.0	0.0	66.0	34.0	0.0	0.0
Abel[#]	2020	RRH vs.ARH	America	II	1234	1305	78.0	78.6	NA	NA	NA	NA	NA	NA	NA	NA
Chen	2020	RRH vs.ARH	China	IA-IIA2	879	879	NA	NA	94.1	5.2	0.7	0.0	94.3	5.2	0.0	0.0
Yang	2020	RRH vs.ARH	America	IA2-IIA	150	181	65.9	68.7	50.0	45.8	4.3	0.0	48.7	47.9	3.4	0.0
Doo	2019	RRH vs.ARH	America	IB1	49	56	39.0	62.0	61.0	33.0	6.0	0.0	57.0	36.0	7.0	0.0
Alfonzo	2019	RRH vs.ARH	Sweden	IA1-IB1	232	232	31.5	35.3	61.6	32.8	5.6	0.0	61.2	33.2	5.6	0.0
Corrado*	2018	RRH vs.ARH	Italy	IB1	88	101	NA	NA	64.8	26.1	5.8	3.3	67.3	22.8	5.9	4.0
Shah	2017	RRH vs.ARH	America	IA1-IB2	109	202	NA	NA	38.0	55.0	6.0	2.0	55.0	36.0	5.0	5.0
Sert	2016	RRH vs.ARH	Norway, America	IB1-IIA	259	232	NA	NA	57.0	36.0	3.0	4.0	59.0	35.0	3.0	3.0
Mendivil[$]	2016	RRH vs.ARH	America	IA2-IIB	58	39	NA	NA	62.1	22.4	10.3	5.2	69.2	12.8	10.3	7.7
Jensen	2020	RRH vs.ARH	Denmark	IA2-IB1	595	530	45.9	54.4	64.2	32.1	3.7	0.0	68.3	28.7	3.0	0.0

MIS, Minimally invasive surgery; ARH, Abominal radical hysterectomy; LRH, Laparoscopic radical hysterectomy; RRH, Robot-assisted radical hysterectomy; FIGO, International Federation of Gynecology and Obstetrics; RCT, Randomized controlled trial; POBS, Prospective observational study; ROBSs, Retrospective observational studies; SCC, Squamous cell carcinoma; ACC, Adenocarcinoma; ASC, Adenosquamous carcinoma; NA, Not available.

[a]*These two studies were RCTs, and the rest were observational studies (including 1 POBS and 45 ROBSs.).*

[#]*Both were from the same study.*

[*]*Both were from the same study.*

[$]*Both were from the same study.*

cancer undergoing MIS. In addition, six studies were conducted in Western countries (HR=1.04, 95% CI: 0.95-1.14, p=0.36), while the remaining seven were conducted in Asian countries (HR=1.12, 95% CI: 0.96-1.31, p=0.134). Additionally, a subgroup analysis based on tumor size revealed that compared with patients undergoing ARH, those with early-stage cervical cancer undergoing MIS included tumor size <2 cm (HR=1.01, 95% CI: 0.98-1.05, p=0.441) and tumor size ≥2 cm (HR=2.26, 95% CI: 0.64-7.94, p=0.203), but no statistically significant difference was observed in 3-year OS (**Table 2**).

Of 32 studies on 5-year DFS, 16 were for stage I cervical cancer (HR=1.03, 95% CI: 0.98-1.09, p=0.247), 13 were for

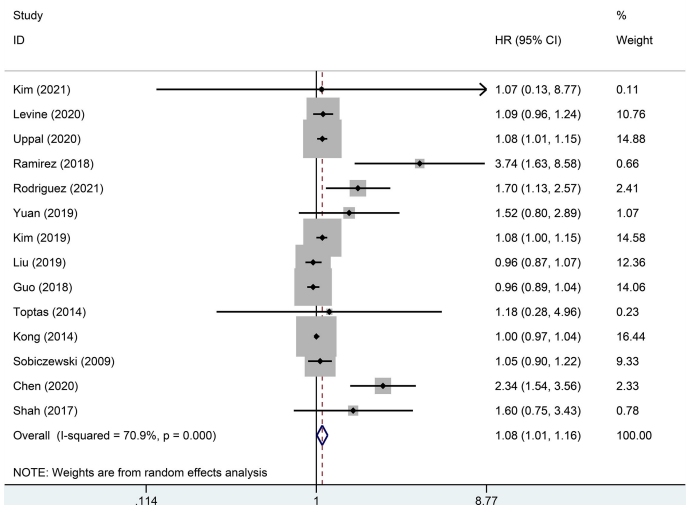


FIGURE 2 | Forest plot of the 3-year disease-free survival (DFS) of patients with early-stage cervical cancer on minimally invasive surgery (MIS) (p=0.031).

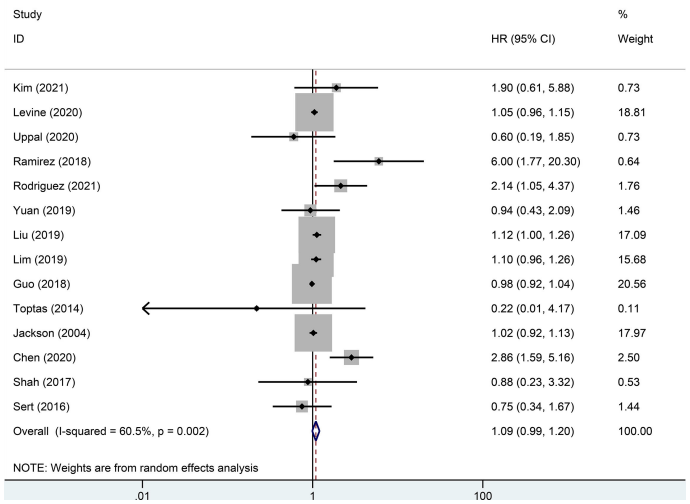


FIGURE 3 | Forest plot of the 3-year overall survival (OS) of early-stage cervical cancer patients on minimally invasive surgery (MIS) (p=0.082).

stage IA-IB1 (HR=1.04, 95% CI: 0.99-1.09, p=0.157), and 12 were for stage IB1-II (HR=1.06, 95% CI: 0.99-1.13, p=0.111). A total of 17 of 32 studies were conducted in Western countries (HR=1.03, 95% CI: 0.98-1.07, p=0.243), whereas 15 studies were conducted in Asian countries (HR=1.03, 95% CI: 0.92-1.17, p=0.577). Furthermore, nine studies evaluated 5-year DFS in patients with tumor size <2 cm (HR=0.86, 95% CI: 0.54-1.37, p=0.53). All above subgroup analyses revealed that MIS was not linked to long-term DFS in patients with early-stage cervical cancer. Notably, for early-stage cervical cancer patients with tumor size ≥2 cm, the pooled results disclosed that the MIS group may have a significantly shorter 5-year DFS than ARH group (HR=1.65, 95% CI: 1.02-2.66, p=0.041) (**Table 2**).

5-year OS was assessed in 32 studies, including 16 for stage I cervical cancer (HR=1.01, 95%CI: 0.96-1.06, p=0.665), 13 for stage IA-IB1 (HR=1.01, 95% CI: 0.97-1.05, p=0.626), 14 for stage IB1-II (HR=1.01, 95% CI: 0.97-1.06, p=0.606), and 2 for stage II (HR=1.03, 95% CI: 0.88-1.20, p=0.745). Moreover, 18 of 32 studies were performed in Western countries (HR=1.02, 95% CI: 0.95-1.10, p=0.597), while the remaining studies (n=14) were conducted in Asian countries (HR=1.00, 95% CI: 0.96-1.04,

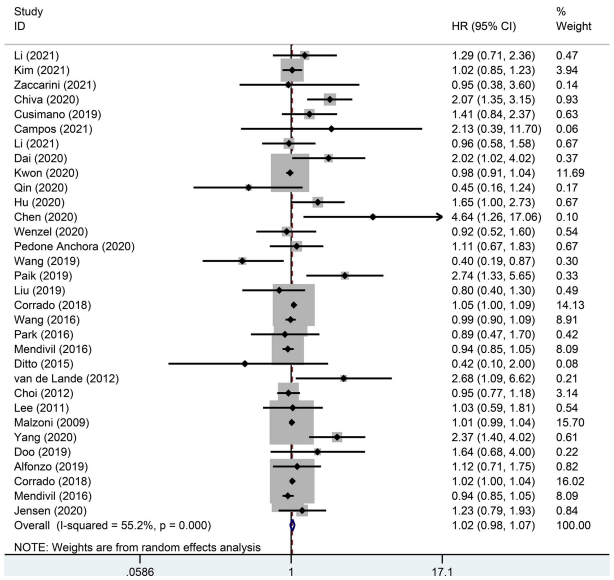


FIGURE 4 | Forest plot for the 5-year disease-free survival (DFS) of early-stage cervical cancer patients on minimally invasive surgery (MIS) (p=0.266).

p=0.9). Briefly, in the above subgroup analyses, the results revealed that MIS was not correlated with 5-year OS in patients with early-stage cervical cancer. Additionally, subgroup analyses of 5-year OS were performed for patients with various tumor sizes. According to the results for patients with tumor size <2 cm, long-term OS was not statistically different between the MIS and ARH groups (HR=1.03, 95% CI: 0.98-1.07, *p*=0.25). Although patients with tumor size ≥2 cm undergoing MIS had a poorer long-term OS than those undergoing ARH, the difference was not statistically significant (HR=1.76, 95% CI: 0.97-3.19, *p*=0.063) (**Table 2**).

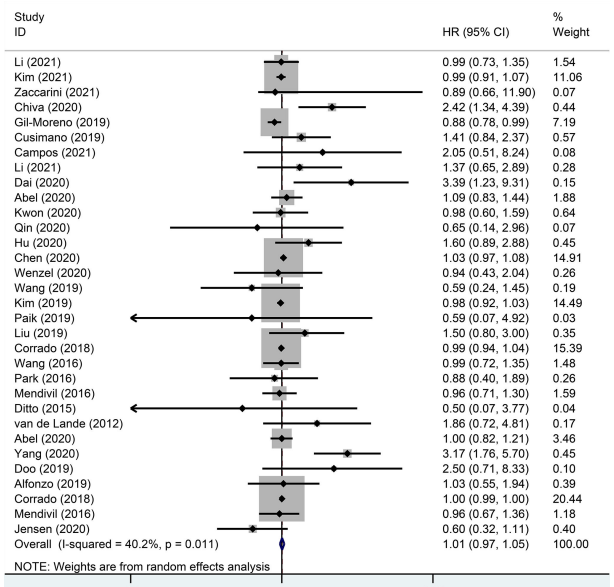


FIGURE 5 | Forest plot for the 5-year overall survival (OS) of early-stage cervical cancer patients on minimally invasive surgery (MIS) (p=0.795).

Publication Bias and Sensitivity Analysis of 3- and 5-Year Survival

Egger's test revealed no significant publication bias in this meta-analysis (*p*>0.05). Additionally, sensitivity analysis of 3- and 5-year survival rates revealed that the results remained stable.

DISCUSSION

Academics had cast doubt on previous surgical findings following the publication of 2018 Laparoscopic Approach to Cervical Cancer (LACC) trial. Additionally, the impact of MIS and ARH on the prognosis of patients with early-stage cervical cancer has been controversial. The RCT findings (12) revealed that MIS was associated with poorer DFS and OS than ARH, but some limitations were found. On the one hand, the trial of patients in the MIS group was terminated prematurely, and some patients received insufficient follow-up time. On the other hand, the results were inapplicable to assessing survival outcomes in "low-risk" cervical cancer patients. Moreover, the trial lacked specific preoperative imaging and central pathology (62). As a result, this meta-analysis systematically evaluated and compared prognosis (3- and 5-year DFS and OS) of patients with early-stage cervical cancer in MIS and ARH groups, and subgroup analyses of associated factors were conducted.

Our meta-analysis included 48 studies with 23346 patients. Based on evaluating 3-year prognosis, the results revealed that patients with early-stage cervical cancer undergoing MIS had a poorer 3-year DFS than those undergoing ARH, without observing a statistical difference in 3-year OS. In a multi-institution retrospective study, Uppal et al. (15) indicated that patients undergoing MIS had a poorer DFS, but no difference was observed in OS compared to those undergoing ARH, consistent with our findings. Meanwhile, subgroup analyses of tumor stage, region, and tumor size were performed on a 3-year prognosis. The pooled results of 3-year prognosis revealed that patients with stage I cervical cancer undergoing MIS exhibited poorer DFS than those undergoing ARH. Similarly, the pooled results in 3-year DFS demonstrated that patients with stage IA-IB1 and Western countries undergoing MIS indicated a shorter DFS than those undergoing ARH. Besides, no significant difference was observed in other subgroup analyses. For patients with stage I and IA-IB1, the poor results may be influenced by the frequency of the use of postoperative adjuvant therapy. In a Norwegian study (63), the incidence of postoperative radiotherapy was low in the MIS and ARH groups (6.1% vs. 12.5%). This study indicated that early-stage cervical cancer patients with stage IB1 and tumor size ≤2 cm who

TABLE 2 | Subgroup analysis of the 3- and 5-year survival of early-stage cervical cancer patients.

	No. of studies	HR	95%CI	*p*	Heterogeneity (I^2) (%)
3-year disease-free survival					
I	9	1.07	1.01-1.14	*0.020*	59.6
IA-IB1	5	1.23	1.02-1.49	*0.034*	69.2
Western	5	1.10	1.01-1.20	*0.024*	30.9
Asia	8	1.04	0.96-1.12	0.381	69.3
Tumor size<2cm	3	1.04	0.98-1.09	0.186	0.0
3-year overall survival					
I	9	1.06	0.99-1.14	0.096	48.4
IA-IB1	5	1.42	0.71-2.85	0.321	70.4
IB1-II	3	1.02	0.92-1.13	0.689	0.0
Western	6	1.04	0.95-1.14	0.360	13.0
Asia	7	1.12	0.96-1.31	0.134	69.4
Tumor size<2cm	3	1.01	0.98-1.05	0.441	17.4
Tumor size≥2cm	2	2.26	0.64-7.94	0.203	71.1
5-year disease-free survival					
I	16	1.03	0.98-1.09	0.247	68.5
IA-IB1	13	1.04	0.99-1.09	0.157	65.0
IB1-II	12	1.06	0.99-1.13	0.111	73.2
Western	17	1.03	0.98-1.07	0.243	58.3
Asia	15	1.03	0.92-1.17	0.577	54.4
Tumor size<2cm	9	0.86	0.54-1.37	0.530	50.9
Tumor size≥2cm	6	1.65	1.02-2.66	*0.041*	69.6
5-year overall survival					
I	16	1.01	0.96-1.06	0.665	56.2
IA-IB1	13	1.01	0.97-1.05	0.626	37.2
IB1-II	14	1.01	0.97-1.06	0.606	51.4
II	2	1.03	0.88-1.20	0.745	0.0
Western	18	1.02	0.95-1.10	0.597	55.1
Asia	14	1.00	0.96-1.04	0.900	6.3
Tumor size<2cm	9	1.03	0.98-1.07	0.250	0.0
Tumor size≥2cm	5	1.76	0.97-3.19	0.063	65.1

underwent MIS had significantly worse DFS than those with ARH. Nevertheless, a population-based study from Denmark (FIGO Stage IA2-IB1) (61) and a population-based study from Sweden (FIGO Stage IA1-IB1) (58) indicated a relatively high incidence of adjuvant therapy in the MIS and ARH groups (21.9% vs. 31.9%; 30.6% vs. 31.9%, respectively), with no difference in survival outcomes between the two groups. Since there was no difference in surgical techniques among the 3 closely related countries, it was tempting to speculate that the use of adjuvant radiotherapy had an impact on the survival outcomes. This speculation needs to be further confirmed. For patients from Western countries, DFS of MIS group was obviously inferior to that of ARH group. There was no clear explanation for this result. We suspected that it may be related to the different types of adjuvant therapy available in different geographic areas. Additionally, the frequency of use of adjuvant treatment in a study may influence the result. The relatively high number of patients receiving adjuvant therapy was likely to reduce the difference in survival between the two groups. NCCN guidelines (2) stated that for patients with stage IA2, IB1, or IIA1 who had negative lymph nodes after surgery but had other risk factors, pelvic external-beam radiation therapy was recommended with (or without) concurrent chemotherapy. A multicenter retrospective study from some Western countries (30) implicated that the incidence of postoperative adjuvant therapy was lower in the MIS group and the ARH group (29.2% vs. 30.7%), and the MIS group had worse prognosis after adjuvant therapy adjustment. By contrast, in a multi-center retrospective study from China (31), postoperative adjuvant therapy consisted of chemotherapy, radiotherapy or chemoradiotherapy. The study implicated that the incidence of postoperative adjuvant therapy was relatively high in the MIS and ARH groups (57.7% vs. 59.6%), with no significant difference between the two groups. Unfortunately, additional confirmation is required due to the scarcity of studies on adjuvant therapy and prognosis.

Likewise, 5-year prognosis was assessed in patients with early-stage cervical cancer. The results demonstrated no statistically significant difference between MIS and ARH groups. Brandt et al. (43) evaluated 196 cases and presented similar results that MIS had no association with a 5-year prognosis in patients with early-stage cervical cancer. Additionally, Abel et al. (33) revealed that stage II cervical cancer undergoing MIS or ARH revealed comparable 5-year survival rates. Nonetheless, some recent studies have demonstrated that early-stage patients undergoing MIS had poorer DFS and OS than those undergoing ARH. According to Dai et al. (32), patients with stage IB undergoing ARH had better DFS and OS than those undergoing MIS (5-year

DFS rate, 94.1% vs. 87.5%; 5-year OS rate, 98.1% vs. 92.3%). Chiva et al. (25) reported in an international European cohort observational study that early-stage cervical cancer patients undergoing MIS increased the risk of recurrence and death compared with those undergoing ARH. In addition, we observed that in many retrospective studies (28, 30, 33, 41, 47, 51, 57, 59), the MIS group had a shorter follow-up time than that of the ARH group. In order to objectively evaluate the effect of MIS and ARH on the prognosis of patients with early-stage cervical cancer, more adequate follow-up time is needed. Furthermore, 5-year prognosis subgroups were analyzed based on tumor stage, region, and tumor size. Except for tumor size ≥2 cm, no statistical difference was observed in other subgroup analyses. The lack of discrepancy in stage II may be due to the relatively small number of studies.

Specifically, the pooled results revealed that patients with tumor size ≥2 cm treated with MIS had a poorer long-term prognosis than those treated with ARH. Consistent with the results of Li et al. (21) and Chen et al. (64), patients with tumor size ≥2 cm undergoing MIS had a shorter DFS than those treated with ARH. The following reasons may be responsible for poorer DFS in patients with tumor size ≥2 cm undergoing MIS: (1) Wagner et al. (65) pointed out that tumor size was an independent prognostic factor for each stage and greatly influenced the prognosis of cervical cancer patients. Larger tumors have a higher risk of lymphatic metastasis (66–69), requiring greater tumor resection (66). However, MIS might be less thoroughly resected than ARH. (2) Pressing the tumor while using a uterine manipulator may spread cancer or increase lymphatic vascular space infiltration (70–72). The SUCCOR study (25) indicated that the risk of recurrence was 2.76-fold higher in patients undergoing MIS with a uterine manipulator compared to those undergoing ARH. (3) When tumors are large, selection bias of surgical methods may affect the results (73). MIS probably brings some surgical difficulties to surgeons (21, 22, 66, 70, 74), reducing the surgical effect. (4) Pneumoperitoneum environment may be a prognostic factor in patients undergoing MIS. An *in vitro* study (75) demonstrated that when cervical cancer cells were stimulated in CO_2 pneumoperitoneum environment *in vitro*, their proliferation ability was enhanced following a short period of inhibition. A retrospective analysis by Kong et al. (76) found that patients with early-stage cervical cancer undergoing MIS in pneumoperitoneal conditions increased the risk of recurrence and intraperitoneal tumor spread. In addition, the SUCCOR study (25) proposed that implementing a preoperative protective vaginal closure in patients undergoing MIS dramatically reduced the risk of recurrence and peritoneal metastasis compared to those undergoing ARH.

Compared with other studies, the strengths of this meta-analysis included the division of patients' prognoses into medium- (3-year) and long-term (5-year) categories, as well as subgroup analyses for various factors such as tumor stage, region, and tumor size. Indeed, our meta-analysis had several limitations. First, only two of the included studies were RCTs, while the remaining were observational studies, resulting in inevitable risks such as selection bias. Second, the baseline characteristics of studies varied, such as tumor stage and surgical procedure. Besides, sentinel lymph node and adjuvant therapy assessments were not performed due to limited data. Furthermore, the sample size of our study was impacted by language restrictions associated with included literature. Finally, the retrieval time span was relatively long, allowing for MIS technology development, resulting in studies that may not accurately reflect changes in survival outcomes over time.

CONCLUSION

In patients with Western countries and stage I cervical cancer, MIS was linked to a shorter medium-term DFS, particularly in stage IA-IB1. Regarding long-term prognosis, patients with tumor size ≥2 cm were unsuitable for MIS and had shorter DFS than ARH. Accordingly, MIS should be chosen with caution in patients with early-stage cervical cancer. Nevertheless, more large-scale RCTs, including two ongoing trials (NCT03739944, NCT03719547), and clinical studies are required to provide relevant data.

DATA AVAILABILITY STATEMENT

The original contributions presented in the study are included in the article/**Supplementary Material**. Further inquiries can be directed to the corresponding author.

AUTHOR CONTRIBUTIONS

Each author contributed significantly to concept and development of the present paper. LYY and MZ designed the research process. WD and MZ searched the database for corresponding articles and extracted useful information from the articles above. YXS and YTS used statistical software for analysis. XL, KJ, and JS drafted the meta-analysis. All authors had read and approved the manuscript and ensured that this was the case.

SUPPLEMENTARY MATERIAL

The Supplementary Material for this article can be found online at: https://www.frontiersin.org/articles/10.3389/fonc.2021.762921/full#supplementary-material

Supplementary Table 1 | Characteristics of all studies included in the meta-analysis.

Supplementary Table 2 | Quality assessment of included studies in this meta-analysis.

REFERENCES

1. Sung H, Ferlay J, Siegel RL, Laversanne M, Soerjomataram I, Jemal A, et al. Global Cancer Statistics 2020: GLOBOCAN Estimates of Incidence and Mortality Worldwide for 36 Cancers in 185 Countries. *CA: A Cancer J Clin* (2021) 71(3):209–49. doi: 10.3322/caac.21660
2. Koh WJ, Abu-Rustum NR, Bean S, Bradley K, Campos SM, Cho KR, et al. Cervical Cancer, Version 3.2019, NCCN Clinical Practice Guidelines in Oncology. *J Natl Compr Canc Netw* (2019) 17(1):64–84. doi: 10.6004/jnccn.2019.0001
3. Cibula D, Pötter R, Planchamp F, Avall-Lundqvist E, Fischerova D, Haie Meder C, et al. The European Society of Gynaecological Oncology/European Society for Radiotherapy and Oncology/European Society of Pathology Guidelines for the Management of Patients With Cervical Cancer. *Radiother Oncol* (2018) 127(3):404–16. doi: 10.1016/j.radonc.2018.03.003
4. Nezhat CR, Burrell MO, Nezhat FR, Benigno BB, Welander CE. Laparoscopic Radical Hysterectomy With Paraaortic and Pelvic Node Dissection. *Am J Obstetrics Gynecology* (1992) 166(3):864–5. doi: 10.1016/0002-9378(92)91351-A
5. Abu-Rustum NR, Hoskins WJ. Radical Abdominal Hysterectomy. *Surg Clin North Am* (2001) 81(4):815–28. doi: 10.1016/S0039-6109(05)70167-5
6. Spirtos NM, Eisenkop SM, Schlaerth JB, Ballon SC. Laparoscopic Radical Hysterectomy (Type III) With Aortic and Pelvic Lymphadenectomy in Patients With Stage I Cervical Cancer: Surgical Morbidity and Intermediate Follow-Up. *Am J Obstet Gynecol* (2002) 187(2):340–8. doi: 10.1067/mob.2002.123035
7. Stewart KI, Fader AN. New Developments in Minimally Invasive Gynecologic Oncology Surgery. *Clin Obstet Gynecol* (2017) 60(2):330–48. doi: 10.1097/GRF.0000000000000286
8. Koh WU, Greer BE, Abu-Rustum NR, Apte SM, Campos SM, Cho KR, et al. Cervical Cancer, Version 2.2015. *J Natl Compr Cancer Network JNCCN* (2015) 13(4):395–404. doi: 10.6004/jnccn.2015.0055
9. Clayton RD. Hysterectomy. *Best Pract Res Clin Obstet Gynaecol* (2006) 20(1):73–87. doi: 10.1016/j.bpobgyn.2005.09.007
10. Wenzel HHB, Smolders RGV, Beltman JJ, Lambrechts S, Trum HW, Yigit R, et al. Survival of Patients With Early-Stage Cervical Cancer After Abdominal or Laparoscopic Radical Hysterectomy: A Nationwide Cohort Study and Literature Review. *Eur J Cancer* (2020) 133:14–21. doi: 10.1016/j.ejca.2020.04.006
11. Yuan Z, Cao D, Yang J, Yu M, Shen K, Yang J, et al. Laparoscopic vs. Open Abdominal Radical Hysterectomy for Cervical Cancer: A Single-Institution, Propensity Score Matching Study in China. *Front Oncol* (2019) 9:1107. doi: 10.3389/fonc.2019.01107
12. Ramirez PT, Frumovitz M, Pareja R, Lopez A, Vieira M, Ribeiro R, et al. Minimally Invasive Versus Abdominal Radical Hysterectomy for Cervical Cancer. *N Engl J Med* (2018) 379(20):1895–904. doi: 10.1056/NEJMoa1806395
13. Committee FGO. FIGO Statement on Minimally Invasive Surgery in Cervical Cancer. *Int J Gynaecol Obstet* (2020) 149(3):264. doi: 10.1002/ijgo.13141
14. Wang W, Li L, Wu M, Ma S, Tan X, Zhong S. Laparoscopic vs. Abdominal Radical Hysterectomy for Locally Advanced Cervical Cancer. *Front Oncol* (2019) 9:1331. doi: 10.3389/fonc.2019.01331
15. Uppal S, Gehrig PA, Peng K, Bixel KL, Matsuo K, Vetter MH, et al. Recurrence Rates in Patients With Cervical Cancer Treated With Abdominal Versus Minimally Invasive Radical Hysterectomy: A Multi-Institutional Retrospective Review Study. *J Clin Oncol Off J Am Soc Clin Oncol* (2020) 38(10):1030–40. doi: 10.1200/JCO.19.03012
16. Kim SI, Lee M, Lee S, Suh DH, Kim HS, Kim K, et al. Impact of Laparoscopic Radical Hysterectomy on Survival Outcome in Patients With FIGO Stage IB Cervical Cancer: A Matching Study of Two Institutional Hospitals in Korea. *Gynecol Oncol* (2019) 155(1):75–82. doi: 10.1016/j.ygyno.2019.07.019
17. Paik ES, Lim MC, Kim MH, Kim YH, Song ES, Seong SJ, et al. Comparison of Laparoscopic and Abdominal Radical Hysterectomy in Early Stage Cervical Cancer Patients Without Adjuvant Treatment: Ancillary Analysis of a Korean Gynecologic Oncology Group Study (KGOG 1028). *Gynecol Oncol* (2019) 154(3):547–53. doi: 10.1016/j.ygyno.2019.06.023
18. Gu L, Huang X, Li S, Mao D, Shen Z, Khadaroo PA, et al. A Meta-Analysis of the Medium- and Long-Term Effects of Laparoscopic Sleeve Gastrectomy and Laparoscopic Roux-En-Y Gastric Bypass. *BMC Surg* (2020) 20(1):30. doi: 10.1186/s12893-020-00695-x
19. Gu L, Du N, Jin Q, Li S, Xie L, Mo J, et al. Magnitude of Benefit of the Addition of Poly ADP-Ribose Polymerase (PARP) Inhibitors to Therapy for Malignant Tumor: A Meta-Analysis. *Crit Rev Oncol Hematol* (2020) 147:102888. doi: 10.1016/j.critrevonc.2020.102888
20. Gu L, Chen M, Guo D, Zhu H, Zhang W, Pan J, et al. PD-L1 and Gastric Cancer Prognosis: A Systematic Review and Meta-Analysis. *PloS One* (2017) 12(8):e0182692. doi: 10.1371/journal.pone.0182692
21. Li LY, Wen LY, Park SH, Nam EJ, Lee JY, Kim S, et al. Impact of the Learning Curve on the Survival of Abdominal or Minimally Invasive Radical Hysterectomy for Early-Stage Cervical Cancer. *Cancer Res Treat* (2021) 53(1):243–51. doi: 10.4143/crt.2020.063
22. Kim S, Min KJ, Lee S, Hong JH, Song JY, Lee JK, et al. Learning Curve Could Affect Oncologic Outcome of Minimally Invasive Radical Hysterectomy for Cervical Cancer. *Asian J Surg* (2021) 44(1):174–80. doi: 10.1016/j.asjsur.2020.05.006
23. Kim SI, Lee J, Hong J, Lee SJ, Park DC, Yoon JH. Comparison of Abdominal and Minimally Invasive Radical Hysterectomy in Patients With Early Stage Cervical Cancer. *Int J Med Sci* (2021) 18(5):1312–7. doi: 10.7150/ijms.55017
24. Zaccarini F, Santy A, Dabi Y, Lavoue V, Carcopino X, Bendifallah S, et al. Comparison of Survival Outcomes Between Laparoscopic and Abdominal Radical Hysterectomy for Early-Stage Cervical Cancer: A French Multicentric Study. *J Gynecol Obstet Hum Reprod* (2021) 50(2):102046. doi: 10.1016/j.jogoh.2020.102046
25. Chiva L, Zanagnolo V, Querleu D, Martin-Calvo N, Arévalo-Serrano J, Căpîlna ME, et al. SUCCOR Study: An International European Cohort Observational Study Comparing Minimally Invasive Surgery Versus Open Abdominal Radical Hysterectomy in Patients With Stage IB1 Cervical Cancer. *Int J Gynecol Cancer* (2020) 30(9):1269–77. doi: 10.1136/ijgc-2020-001506
26. Levine MD, Brown J, Crane EK, Tait DL, Naumann RW. Outcomes of Minimally Invasive Versus Open Radical Hysterectomy for Early Stage Cervical Cancer Incorporating 2018 FIGO Staging. *J Minim Invasive Gynecol* (2021) 28(4):824–8. doi: 10.1016/j.jmig.2020.07.021
27. Gil-Moreno A, Carbonell-Socias M, Salicrú S, Centeno-Mediavilla C, Franco-Camps S, Colas E, et al. Radical Hysterectomy: Efficacy and Safety in the Dawn of Minimally Invasive Techniques. *J Minim Invasive Gynecol* (2019) 26(3):492–500. doi: 10.1016/j.jmig.2018.06.007
28. Cusimano MC, Baxter NN, Gien LT, Moineddin R, Liu N, Dossa F, et al. Impact of Surgical Approach on Oncologic Outcomes in Women Undergoing Radical Hysterectomy for Cervical Cancer. *Am J Obstet Gynecol* (2019) 221(6):619 e1–619 e24. doi: 10.1016/j.ajog.2019.07.009
29. Campos L, Limberger LF, Stein AT, Caldas JM. Survival After Laparoscopic Versus Abdominal Radical Hysterectomy in Early Cervical Cancer: A Randomized Controlled Trial. *Asian Pacific J Cancer Prev* (2021) 22(1):93–7. doi: 10.31557/APJCP.2021.22.1.93
30. Rodriguez J, Rauh-Hain JA, Saenz J, Isla DO, Rendon Pereira GJ, Odetto D, et al. Oncological Outcomes of Laparoscopic Radical Hysterectomy Versus Radical Abdominal Hysterectomy in Patients With Early-Stage Cervical Cancer: A Multicenter Analysis. *Int J Gynecol Cancer* (2021) 31(4):504–11. doi: 10.1136/ijgc-2020-002086
31. Li P, Chen L, Ni Y, Liu J, Li D, Guo J, et al. Comparison Between Laparoscopic and Abdominal Radical Hysterectomy for Stage IB1 and Tumor Size <2 Cm Cervical Cancer With Visible or Invisible Tumors: A Multicentre Retrospective Study. *J Gynecol Oncol* (2021) 32(2):e17. doi: 10.3802/jgo.2021.32.e17
32. Dai D, Huang H, Feng Y, Wan T, Liu Z, Tong C, et al. Minimally Invasive Surgery vs Laparotomy for Early Stage Cervical Cancer: A Propensity Score-Matched Cohort Study. *Cancer Med* (2020) 9(24):9236–45. doi: 10.1002/cam4.3527
33. Abel MK, Chan JK, Chow S, Darcy K, Tian C, Kapp DS, et al. Trends and Survival Outcomes of Robotic, Laparoscopic, and Open Surgery for Stage II Uterine Cancer. *Int J Gynecol Cancer* (2020) 30(9):1347–55. doi: 10.1136/ijgc-2020-001646
34. Kwon BS, Roh HJ, Lee S, Yang J, Song YJ, Lee SH, et al. Comparison of Long-Term Survival of Total Abdominal Radical Hysterectomy and Laparoscopy-Assisted Radical Vaginal Hysterectomy in Patients With Early Cervical Cancer: Korean Multicenter, Retrospective Analysis. *Gynecol Oncol* (2020) 159(3):642–8. doi: 10.1016/j.ygyno.2020.09.035
35. Qin M, Siyi L, Huang HF, Li Y, Gu Y, Wang W, et al. A Comparison of Laparoscopies and Laparotomies for Radical Hysterectomy in Stage IA1-IB1

Cervical Cancer Patients: A Single Team With 18 Years of Experience. *Front Oncol* (2020) 10:1738. doi: 10.3389/fonc.2020.01738
36. Hu TWY, Huang Y, Li N, Nie D, Li Z. Comparison of Laparoscopic Versus Open Radical Hysterectomy in Patients With Early-Stage Cervical Cancer: A Multicenter Study in China. *Int J Gynecol Cancer* (2020) 30(8):1143–50. doi: 10.1136/ijgc-2020-001340
37. Chen X, Zhao N, Ye P, Chen J, Nan X, Zhao H, et al. Comparison of Laparoscopic and Open Radical Hysterectomy in Cervical Cancer Patients With Tumor Size </=2 Cm. *Int J Gynecol Cancer* (2020) 30(5):564–71. doi: 10.1136/ijgc-2019-000994
38. Pedone Anchora L, Turco LC, Bizzarri N, Capozzi VA, Lombisani A, Chiantera V, et al. How to Select Early-Stage Cervical Cancer Patients Still Suitable for Laparoscopic Radical Hysterectomy: A Propensity-Matched Study. *Ann Surg Oncol* (2020) 27(6):1947–55. doi: 10.1245/s10434-019-08162-5
39. Liu Y, Li L, Wu M, Ma S, Tan X, Zhong S, et al. The Impact of the Surgical Routes and Learning Curve of Radical Hysterectomy on the Survival Outcomes in Stage IB Cervical Cancer: A Retrospective Cohort Study. *Int J Surg* (2019) 68:72–7. doi: 10.1016/j.ijsu.2019.06.009
40. Lim TYK, Lin KKM, Wong WL, Aggarwal IM, Yam PKL. Surgical and Oncological Outcome of Total Laparoscopic Radical Hysterectomy Versus Radical Abdominal Hysterectomy in Early Cervical Cancer in Singapore. *Gynecol Minim Invasive Ther* (2019) 8(2):53–8. doi: 10.4103/GMIT.GMIT_43_18
41. Guo J, Yang L, Cai J, Xu L, Min J, Shen Y, et al. Laparoscopic Procedure Compared With Open Radical Hysterectomy With Pelvic Lymphadenectomy in Early Cervical Cancer: A Retrospective Study. *Onco Targets Ther* (2018) 11:5903–8. doi: 10.2147/OTT.S156064
42. Corrado G, Vizza E, Legge F, Pedone Anchora L, Sperduti I, Fagotti A, et al. Comparison of Different Surgical Approaches for Stage IB1 Cervical Cancer Patients: A Multi-Institution Study and a Review of the Literature. *Int J Gynecol Cancer* (2018) 28(5):1020–8. doi: 10.1097/IGC.0000000000001254
43. Brandt B, Sioulas V, Basaran D, Kuhn T, LaVigne K, Gardner GJ, et al. Minimally Invasive Surgery Versus Laparotomy for Radical Hysterectomy in the Management of Early-Stage Cervical Cancer: Survival Outcomes. *Gynecol Oncol* (2020) 156(3):591–7. doi: 10.1016/j.ygyno.2019.12.038
44. Park JY, Kim D, Suh DS, Kim JH, Kim YM, Kim YT, et al. The Role of Laparoscopic Radical Hysterectomy in Early-Stage Adenocarcinoma of the Uterine Cervix. *Ann Surg Oncol* (2016) 23(Suppl 5):825–33. doi: 10.1245/s10434-016-5489-4
45. Mendivil AA, Rettenmaier MA, Abaid LN, Brown JV 3rd, Micha JP, Lopez KL, et al. Survival Rate Comparisons Amongst Cervical Cancer Patients Treated With an Open, Robotic-Assisted or Laparoscopic Radical Hysterectomy: A Five Year Experience. *Surg Oncol* (2016) 25(1):66–71. doi: 10.1016/j.suronc.2015.09.004
46. Ditto A, Martinelli F, Bogani G, Gasparri ML, Di Donato V, Zanaboni F, et al. Implementation of Laparoscopic Approach for Type B Radical Hysterectomy: A Comparison With Open Surgical Operations. *Eur J Surg Oncol* (2015) 41(1):34–9. doi: 10.1016/j.ejso.2014.10.058
47. Toptas T, Simsek T. Total Laparoscopic Versus Open Radical Hysterectomy in Stage IA2-IB1 Cervical Cancer: Disease Recurrence and Survival Comparison. *J Laparoendosc Adv Surg Tech A* (2014) 24(6):373–8. doi: 10.1089/lap.2013.0514
48. Kong TW, Chang SJ, Lee J, Paek J, Ryu HS, et al. Comparison of Laparoscopic Versus Abdominal Radical Hysterectomy for FIGO Stage IB and IIA Cervical Cancer With Tumor Diameter of 3 Cm or Greater. *Int J Gynecol Cancer* (2014) 24(2):280–8. doi: 10.1097/IGC.0000000000000052
49. van de Lande J, von Mensdorff-Pouilly S, Lettinga RG, Piek JM, Verheijen RH. Open Versus Laparoscopic Pelvic Lymph Node Dissection in Early Stage Cervical Cancer: No Difference in Surgical or Disease Outcome. *Int J Gynecol Cancer* (2012) 22(1):107–14. doi: 10.1097/IGC.0b013e31822c273d
50. Choi CH, Lee JW, Lee YY, Kim HJ, Song T, Kim MK, et al. Comparison of Laparoscopic-Assisted Radical Vaginal Hysterectomy and Laparoscopic Radical Hysterectomy in the Treatment of Cervical Cancer. *Ann Surg Oncol* (2012) 19(12):3839–48. doi: 10.1245/s10434-012-2406-3
51. Lee EJ, Kang H, Kim DH. A Comparative Study of Laparoscopic Radical Hysterectomy With Radical Abdominal Hysterectomy for Early-Stage Cervical Cancer: A Long-Term Follow-Up Study. *Eur J Obstet Gynecol Reprod Biol* (2011) 156(1):83–6. doi: 10.1016/j.ejogrb.2010.12.016
52. Sobiczewski P, Bidzinski M, Derlatka P, Panek G, Danska-Bidzinska A, Gmyrek L, et al. Early Cervical Cancer Managed by Laparoscopy and Conventional Surgery: Comparison of Treatment Results. *Int J Gynecol Cancer* (2009) 19(8):1390–5. doi: 10.1111/IGC.0b013e3181ba5e88
53. Malzoni M, Tinelli R, Cosentino F, Fusco A, Malzoni C. Total Laparoscopic Radical Hysterectomy Versus Abdominal Radical Hysterectomy With Lymphadenectomy in Patients With Early Cervical Cancer: Our Experience. *Ann Surg Oncol* (2009) 16(5):1316–23. doi: 10.1245/s10434-009-0342-7
54. Jackson KS, Das N, Naik R, Lopes AD, Godfrey KA, Hatem MH, et al. Laparoscopically Assisted Radical Vaginal Hysterectomy vs. Radical Abdominal Hysterectomy for Cervical Cancer: A Match Controlled Study. *Gynecol Oncol* (2004) 95(3):655–61. doi: 10.1016/j.ygyno.2004.07.055
55. Chen B, Ji M, Li P, Liu P, Zou W, Zhao Z, et al. Comparison Between Robot-Assisted Radical Hysterectomy and Abdominal Radical Hysterectomy for Cervical Cancer: A Multicentre Retrospective Study. *Gynecol Oncol* (2020) 157(2):429–36. doi: 10.1016/j.ygyno.2020.02.019
56. Yang J, Mead-Harvey C, Polen-De C, Magtibay P, Butler K, Cliby W, et al. Survival Outcomes in Patients With Cervical Cancer Treated With Open Versus Robotic Radical Hysterectomy: Our Surgical Pathology Interrogation. *Gynecol Oncol* (2020) 159(2):373–80. doi: 10.1016/j.ygyno.2020.08.031
57. Doo DW, Kirkland CT, Griswold LH, McGwin G, Huh WK, Leath CA 3rd, et al. Comparative Outcomes Between Robotic and Abdominal Radical Hysterectomy for IB1 Cervical Cancer: Results From a Single High Volume Institution. *Gynecol Oncol* (2019) 153(2):242–7. doi: 10.1016/j.ygyno.2019.03.001
58. Alfonzo E, Wallin E, Ekdahl L, Staf C, Rådestad AF, Reynisson P, et al. No Survival Difference Between Robotic and Open Radical Hysterectomy for Women With Early-Stage Cervical Cancer: Results From a Nationwide Population-Based Cohort Study. *Eur J Cancer* (2019) 116:169–77. doi: 10.1016/j.ejca.2019.05.016
59. Shah CA, Beck T, Liao JB, Giannakopoulos NV, Veljovich D, Paley P, et al. Surgical and Oncologic Outcomes After Robotic Radical Hysterectomy as Compared to Open Radical Hysterectomy in the Treatment of Early Cervical Cancer. *J Gynecol Oncol* (2017) 28(6):e82. doi: 10.3802/jgo.2017.28.e82
60. Sert BM, Boggess JF, Ahmad S, Jackson AL, Stavitzski NM, Dahl AA, et al. Robot-Assisted Versus Open Radical Hysterectomy: A Multi-Institutional Experience for Early-Stage Cervical Cancer. *Eur J Surg Oncol* (2016) 42(4):513–22. doi: 10.1016/j.ejso.2015.12.014
61. Jensen PT, Schnack TH, Frøding LP, Bjørn SF, Lajer H, Markauskas A, et al. Survival After a Nationwide Adoption of Robotic Minimally Invasive Surgery for Early-Stage Cervical Cancer – A Population-Based Study. *Eur J Cancer* (2020) 128:47–56. doi: 10.1016/j.ejca.2019.12.020
62. Naumann RW. Minimally Invasive Radical Hysterectomy Has Many Benefits Compared With Open Radical Hysterectomy: Will the LACC Trial Cause the Premature Demise of This Procedure? *J Minim Invasive Gynecol* (2019) 26(3):379–80. doi: 10.1016/j.jmig.2019.01.002
63. Sert BM, Kristensen GB, Kleppe A, Dørum A. Long-Term Oncological Outcomes and Recurrence Patterns in Early-Stage Cervical Cancer Treated With Minimally Invasive Versus Abdominal Radical Hysterectomy: The Norwegian Radium Hospital Experience. *Gynecol Oncol* (2021) 162(2):284–91. doi: 10.1016/j.ygyno.2021.05.028
64. Chen C, Fang Z, Wang Q, Li W, Li P, Wang L, et al. Comparative Study on the Oncological Prognosis of Laparoscopy and Laparotomy for Stage IIA1 Cervical Squamous Cell Carcinoma. *Eur J Surg Oncol* (2021) 47(2):346–52. doi: 10.1016/j.ejso.2020.07.016
65. Wagner AE, Pappas L, Ghia AJ, Gaffney DK. Impact of Tumor Size on Survival in Cancer of the Cervix and Validation of Stage IIA1 and IIA2 Subdivisions. *Gynecol Oncol* (2013) 129(3):517–21. doi: 10.1016/j.ygyno.2013.03.008
66. Armbrust R, Chen F, Richter R, Muallem MZ, Mustea A, Holthaus B, et al. Results of a German Wide Survey Towards Current Surgical Approach in Early Stage Cervical Cancer NOGGO MONITOR 11. *Sci Rep* (2021) 11(1):9774. doi: 10.1038/s41598-021-89071-0
67. Fagotti A, Pedone Anchora L, Conte C, Chiantera V, Vizza E, Tortorella L, et al. Beyond Sentinel Node Algorithm. Toward a More Tailored Surgery for Cervical Cancer Patients. *Cancer Med* (2016) 5(8):1725–30. doi: 10.1002/cam4.722
68. Gulseren V, Kocaer M, Gungorduk O, Ozdemir IA, Gokcu M, Mart EM, et al. Preoperative Predictors of Pelvic and Para-Aortic Lymph Node Metastases in

Cervical Cancer. *J Cancer Res Ther* (2019) 15(6):1231–4. doi: 10.4103/jcrt.JCRT_467_17
69. Casarin J, Buda A, Bogani G, Fanfani F, Papadia A, Ceccaroni M, et al. Predictors of Recurrence Following Laparoscopic Radical Hysterectomy for Early-Stage Cervical Cancer: A Multi-Institutional Study. *Gynecol Oncol* (2020) 159(1):164–70. doi: 10.1016/j.ygyno.2020.06.508
70. Eoh KJ, Lee JY, Nam EJ, Kim S, Kim SW, Kim YT. The Institutional Learning Curve is Associated With Survival Outcomes of Robotic Radical Hysterectomy for Early-Stage Cervical Cancer-a Retrospective Study. *BMC Cancer* (2020) 20(1):152. doi: 10.1186/s12885-020-6660-7
71. Wang Y, Li B, Ren F, Song Z, Ouyang L, Liu K. Survival After Minimally Invasive vs. Open Radical Hysterectomy for Cervical Cancer: A Meta-Analysis. *Front Oncol* (2020) 10:1236. doi: 10.3389/fonc.2020.01236
72. Nica A, Kim SR, Gien LT, Covens A, Bernardini MQ, Bouchard-Fortier G, et al. Survival After Minimally Invasive Surgery in Early Cervical Cancer: Is the Intra-Uterine Manipulator to Blame? *Int J Gynecol Cancer* (2020) 30 (12):1864–70. doi: 10.1136/ijgc-2020-001816
73. Kim JH, Kim K, Park SJ, Lee JY, Kim K, Lim MC, et al. Comparative Effectiveness of Abdominal Versus Laparoscopic Radical Hysterectomy for Cervical Cancer in the Postdissemination Era. *Cancer Res Treat* (2019) 51 (2):788–96. doi: 10.4143/crt.2018.120
74. Schermerhorn SMV, Christman MS, Rocco NR, Abdul-Muhsin H, L'Esperance JO, Castle EP, et al. Learning Curve for Robotic-Assisted Laparoscopic Retroperitoneal Lymph Node Dissection. *J Endourol* (2021) 35:1483–9. doi: 10.1089/end.2020.0549
75. Lin F, Pan L, Li L, Li D, Mo L. Effects of a Simulated CO2 Pneumoperitoneum Environment on the Proliferation, Apoptosis, and Metastasis of Cervical Cancer Cells In Vitro. *Med Sci Monit* (2014) 20:2497–503. doi: 10.12659/MSM.891179
76. Kong TW, Chang SJ, Piao X, Paek J, Lee Y, Lee EJ, et al. Patterns of Recurrence and Survival After Abdominal Versus Laparoscopic/Robotic Radical Hysterectomy in Patients With Early Cervical Cancer. *J Obstet Gynaecol Res* (2016) 42(1):77–86. doi: 10.1111/jog.12840

Conflict of Interest: The authors declare that the research was conducted in the absence of any commercial or financial relationships that could be construed as a potential conflict of interest.

Publisher's Note: All claims expressed in this article are solely those of the authors and do not necessarily represent those of their affiliated organizations, or those of the publisher, the editors and the reviewers. Any product that may be evaluated in this article, or claim that may be made by its manufacturer, is not guaranteed or endorsed by the publisher.

Copyright © 2022 Zhang, Dai, Si, Shi, Li, Jiang, Shen and Ying. This is an open-access article distributed under the terms of the Creative Commons Attribution License (CC BY). The use, distribution or reproduction in other forums is permitted, provided the original author(s) and the copyright owner(s) are credited and that the original publication in this journal is cited, in accordance with accepted academic practice. No use, distribution or reproduction is permitted which does not comply with these terms.

frontiers in Oncology

ORIGINAL RESEARCH
published: 24 January 2022
doi: 10.3389/fonc.2021.802068

MRVI1 and NTRK3 Are Potential Tumor Suppressor Genes Commonly Inactivated by DNA Methylation in Cervical Cancer

Huihui Ji[1†], Kehan Li[1†], Wenxiao Jiang[1], Jingwei Li[2], Jian-an Zhang[1] and Xueqiong Zhu[1,2]*

[1] Center of Uterine Cancer Diagnosis & Therapy Research of Zhejiang Province, Department of Obstetrics and Gynecology, the Second Affiliated Hospital of Wenzhou Medical University, Wenzhou, China, [2] Department of Obstetrics and Gynecology, Taizhou Woman and Children's Hospital of Wenzhou Medical University, Taizhou, China

OPEN ACCESS

Edited by:
Ram N. Ganapathi,
Carolinas Healthcare System,
United States

Reviewed by:
Chandraditya Chakraborty,
Dana-Farber Cancer Institute and Harvard Medical School, United States
Stephanie M. McGregor,
University of Wisconsin-Madison,
United States

***Correspondence:**
Xueqiong Zhu
wzzxq@wzhealth.com

[†]These authors have contributed equally to this work

Specialty section:
This article was submitted to Gynecological Oncology, a section of the journal Frontiers in Oncology

Received: 26 October 2021
Accepted: 24 December 2021
Published: 24 January 2022

Citation:
Ji H, Li K, Jiang W, Li J, Zhang J-a and Zhu X (2022) MRVI1 and NTRK3 Are Potential Tumor Suppressor Genes Commonly Inactivated by DNA Methylation in Cervical Cancer. Front. Oncol. 11:802068. doi: 10.3389/fonc.2021.802068

The abnormally methylated tumor suppressor genes (TSGs) associated with cervical cancer are unclear. DNA methylation data, RNA-seq expression profiles, and overall survival data were downloaded from TCGA CESC database. DMGs and DEGs were obtained through CHAMP and DESeq packages, respectively. TSGs were downloaded from TSGene 2.0. Candidate hypermethylated/down-regulated TSGs were further evaluated and pyrosequencing was used to confirm their difference in methylation levels of selected TSGs in cervical cancer patients. A total of 25946 differentially methylated CpGs corresponding to 2686 hypermethylated genes and 4898 hypomethylated genes between cervical cancer and adjacent normal cervical tissues were found in this study. Besides, 693 DEGs (109 up-regulated and 584 down-regulated) were discovered in cervical cancer tissues. Then, 192 hypermethylated/down-regulated genes were obtained in cervical cancer compared to adjacent tissues. Interestingly, 26 TSGs were found in hypermethylated/down-regulated genes. Among these genes, low expression of *MRVI1* and *NTRK3* was associated with poor overall survival in cervical cancer. Moreover, GEO data showed that *MRVI1* and *NTRK3* were significantly decreased in cervical cancer tissues. The expression levels of *MRVI1* and *NTRK3* were negatively correlated with the methylation levels of their promoter CpG sites. Additionally, elevated methylation levels of *MRVI1* and *NTRK3* promoter were further verified in cervical cancer tissues by pyrosequencing experiments. Finally, the ROC results showed that the promoter methylation levels of *MRVI1* and *NTRK3* had the ability to discriminate cervical cancer from healthy samples. The study contributes to our understanding of the roles of *MRVI1* and *NTRK3* in cervical cancer.

Keywords: *MRVI1*, *NTRK3*, cervical cancer, TSGs, DNA methylation

INTRODUCTION

Cervical cancer is the fourth most common cancer and the fourth leading cause of cancer death in women (1). The prognosis varies depending on the stage of cervical cancer. Compared with patients with early stage of cervical cancer, the five-year survival period of patients with advanced cervical cancer is much shorter (2). Therefore, the identification predictive biomarkers can help effective targeted therapy and treatment decisions.

Epigenetic processes can be reversed and this principle makes it a potential target for therapeutic intervention (3). Epigenetic variations could change the expression of tumor suppressor genes (TSGs) in cervical cancer (4). DNA methylation is an important part of epigenetics (5, 6) and the regulatory effect of DNA methylation on gene expression has been studied extensively (7, 8). DNA methylation levels could be detected by techniques, including pyrosequencing, methylation-specific polymerase chain reaction, methylation-sensitive high-resolution melting, multiplex ligation-dependent probe amplification (MLPA), and Combined bisulfite restriction analysis (COBRA) and MethyLight (9). Aberrant methylation of TSGs could silence the expression of TSGs to consequently promote tumor formation (10). During recent decades, there have been a massive number of studies about TSGs in cervical cancer (11–13). For example, compared with the control samples, the promoter methylation frequency of TSG (including *RARB*, *CADM1*, *PAX1*, and *DAPK1*) in patients with invasive cervical cancer is higher (14). The silencing of TSGs is thought to be an early, driving event in the oncogenic process. Even after human papilloma virus (HPV) clearance, the silencing of TSGs by DNA hypermethylation could trigger carcinogenesis of the cervix (15). However, changes in DNA methylation and related abnormal TSGs expression have not been systematically elucidated in cervical cancer.

Gene methylation profiling and gene expression profiling have been utilized to investigate DNA methylation and gene expression in the molecular mechanism, biological process, and biomarker (16–18). Combined analysis of gene expression and DNA methylation data may contribute to identifying potential biomarkers of cervical cancer for treatment. Therefore, in this study, Illumina HumanMethylation450K methylation data and RNA-seq expression profiles from the Cancer Genome Atlas-Cervical Cancer (TCGA-CESC) were integrated for identifying the DMGs and DEGs in cervical cancer. First, TSGs among hypermethylated/down-regulated genes were found. Second, cervical cancer prognosis-related genes were selected and used as candidate cervical cancer-related TSGs. Then, expression levels of these TSGs were subsequently verified in three independent data sets from the Gene Expression Omnibus (GEO) database. Moreover, cervical cancer tissues and paired adjacent normal cervical tissues were collected to verify the methylation levels of these TSGs. Finally, receiver operating characteristic (ROC) curve analysis was used to assess the development of candidate cervical cancer related TSGs. This study aims to find prognostic and diagnostic TSGs related to cervical cancer through data analysis and experimental verification.

RESULTS

Differential Methylation and Expression Analysis

The workflow of our study is displayed in **Figure 1**. TCGA-CESC was used to identify aberrantly methylation-regulated genes. 12611 hypermethylated CpG sites, which were correspond to 2686 genes, were found in cervical cancer than that in adjacent normal cervical tissues. On the contrary, 13335 hypomethylated CpG sites, which were correspond to 4898 genes, were discovered in cervical cancer compared to adjacent normal cervical tissues (**Figures 2A, B**). Additionally, a total of 693 DEGs (109 up-regulated and 584 down-regulated) were obtained from TCGA-CESC (**Figures 2C, D**). Then, 192 hypermethylated/down-regulated genes (**Figure 2E**) and 60 hypomethylated/up-regulated genes (**Figure 2F**) were identified. Hypermethylated/down-regulated genes were particularly focused in the current study.

GO and KEGG Pathway Enrichment of the Down-Regulated DEGs With Hypermethylation

The top 15 significant GO enrichments of biological processes were illustrated in **Figure 3A**, including extracellular structure organization, multicellular organismal signaling, extracellular matrix organization, and actin filament-based process. There were 13 enrichment pathways, such as vascular smooth muscle contraction, cGMP-PKG signaling pathway, calcium signaling pathway, focal adhesion, ECM-receptor interaction, proteoglycans in cancer, apelin signaling pathway (**Figure 3B**).

Identification of Candidate TSGs

26 TSGs were discovered in hypermethylated/down-regulated genes (**Figure 4A**). A total of 2361 cervical cancer survival-related genes were found by Kaplan–Meier analysis using RNA expression data. After integrated TSGs and survival-related genes, 2 overlapping genes (*MRVI1* and *NTRK3*) were discovered and considered as the cervical cancer candidate TSGs (**Figure 4B**).

Survival Analysis and Validation of *MRVI1* and *NTRK3* Expression

The expression levels of *MRVI1* and *NTRK3* genes were obtained in this study (**Figure 5A**). As shown in **Figures 5B, C**, the expression levels of *MRVI1* ($P = 0.002$) and *NTRK3* ($P = 0.029$) were significantly lower in cervical cancer than those in adjacent normal cervical tissues. In addition, patients with low expression of *MRVI1* ($P = 0.026$) and *NTRK3* ($P = 0.025$) had significantly worse survival rates (**Figures 5D, E**).

Validation of *MRVI1* and *NTRK3* Expression Levels by the GEO Database

MRVI1 and *NTRK3* levels were all significantly lower in cervical cancers compared to normal cervical tissues in three cervical cancer related datasets ($p < 0.05$, **Figures 6A–F**). The ROC curves of *MRVI1* and *NTRK3* gene expression levels to determine cervical

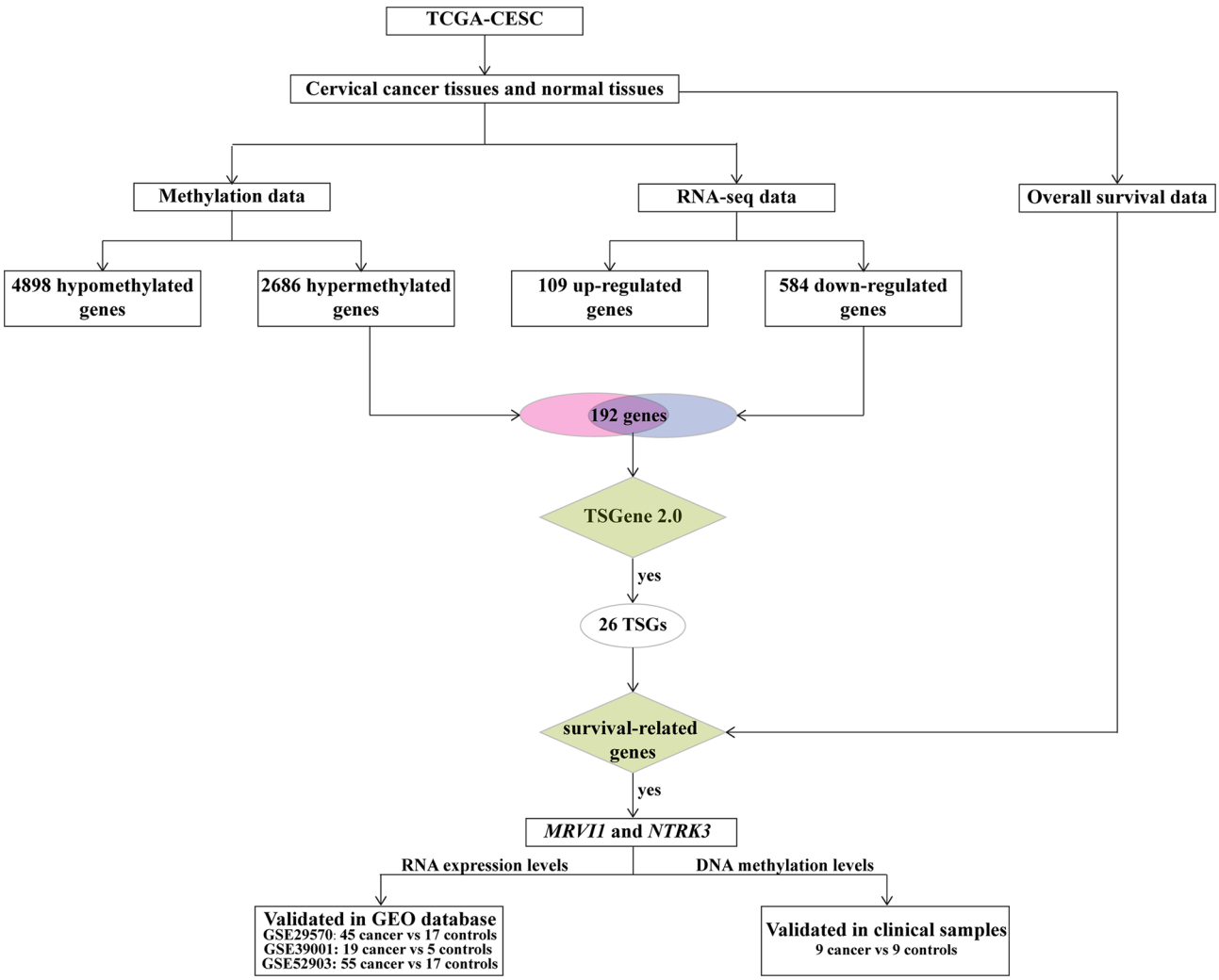


FIGURE 1 | Flow chart of data collection and analysis. TSGs, tumor suppressor genes.

cancer were presented in **Figures 6G–O**. The ROC curve indicated that *MRVI1* exhibited high diagnostic efficiency for cervical cancer in normal cervical controls in three datasets (AUC > 0.937). The AUC of the prediction model for *NTRK3* was greater than 0.653 in these datasets. The AUC of the combined prediction model of *MRVI1* and *NTRK3* (AUC > 0.947) was higher than that of the *MRVI1* (AUC > 0.937) and *NTRK3* (AUC > 0.653) (**Figures 6G–O** and **Table 1**). These results suggested that the expression levels of *MRVI1* and *NTRK3* could distinguish between cervical cancer patients and healthy controls.

Correlation Analysis of Promoter Region Methylation Level and Gene Expression Level

A total of 5 CpG sites were located in the promoter regions of *MRVI1* (cg24365867, cg24541550, cg16014606, and cg15283950) and *NTRK3* (cg14384532) (**Figure 7A**). The methylation levels of these CpG sites were up-regulated in cervical tumors compared to controls ($p < 0.05$, **Figures 7B–F**). Further correlation analysis showed that the methylation levels of these CpG sites were negatively associated with gene expression for these two genes ($p < 0.05$, **Figure 8**).

Verification of Differences in Promoter Methylation Levels of *MRVI1* and *NTRK3* by Pyrosequencing Experiments

In order to verify the differential methylation levels of *MRVI1* and *NTRK3* between cervical cancer and adjacent normal cervical tissues, pyrosequencing experiments were conducted. As shown in **Table 2** and **Figure 9A**, the methylation levels of cg24365867, cg24541550, cg16014606, and cg15283950 of *MRVI1* gene in cervical cancer were significantly higher than that in adjacent normal cervical tissues ($p < 0.05$). Compared with adjacent normal tissues, a significantly elevated methylation level of cg14384532 on *NTRK3* was also found in cervical cancer tissues ($p < 0.05$, **Table 2** and **Figure 9A**). In addition, ROC

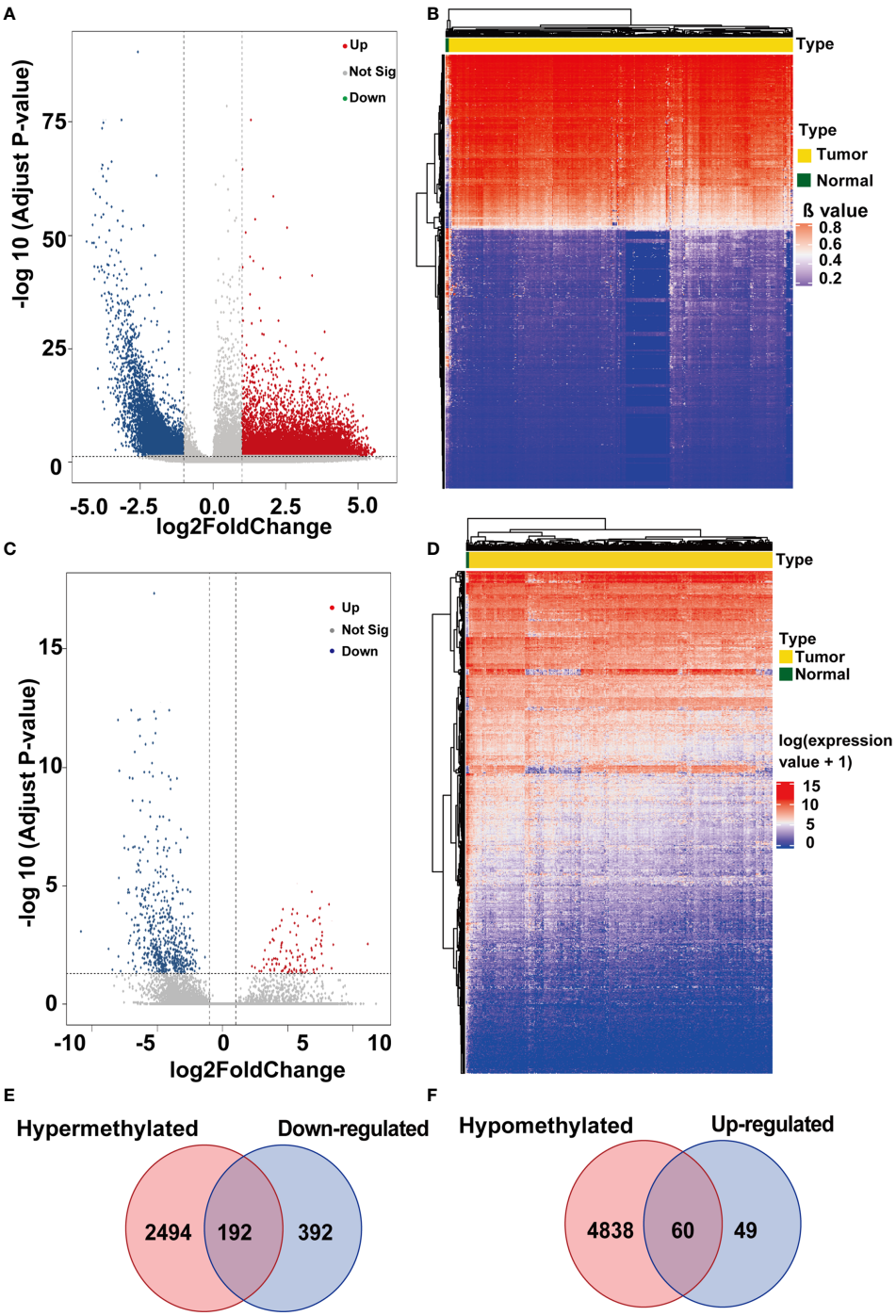


FIGURE 2 | The differentially methylated genes (DMGs) and differentially expression genes (DEGs) from TCGA-CESC database. **(A)** The volcano plot was constructed using log2fold change and –log10 (padj) values. Red plots represent the up-regulated CpG sites, green plots represent the down-regulated CpG sites, and black plots show those CpG sites that are not differentially expressed. **(B)** Heatmap of methylation values for top 1000 CpG sites methylated in cervical cancer patients. CpG sites are shown in the vertical columns and the cervical cancer samples in the horizontal rows. High methylation levels are displayed in red and low methylation levels in blue, according to the scale bar in the right of figure. **(C)** The volcano plot was constructed using log2 fold change and –log10 (padj) values. Red plots represent the up-regulated genes, green plots represent the down-regulated genes, and black plots show those genes that are not differentially expressed. **(D)** Heatmap of methylation values for DEGs in cervical cancer patients. The genes are displayed in the vertical columns and the cervical cancer samples in the horizontal rows. High expression levels are shown in red and low expression levels in blue, according to the scale bar in the right of the figure. **(E)** Venn diagrams of the genes relevant to hypermethylated/down-regulated genes. **(F)** Venn diagrams of the genes relevant to hypormethylated/up-regulated genes.

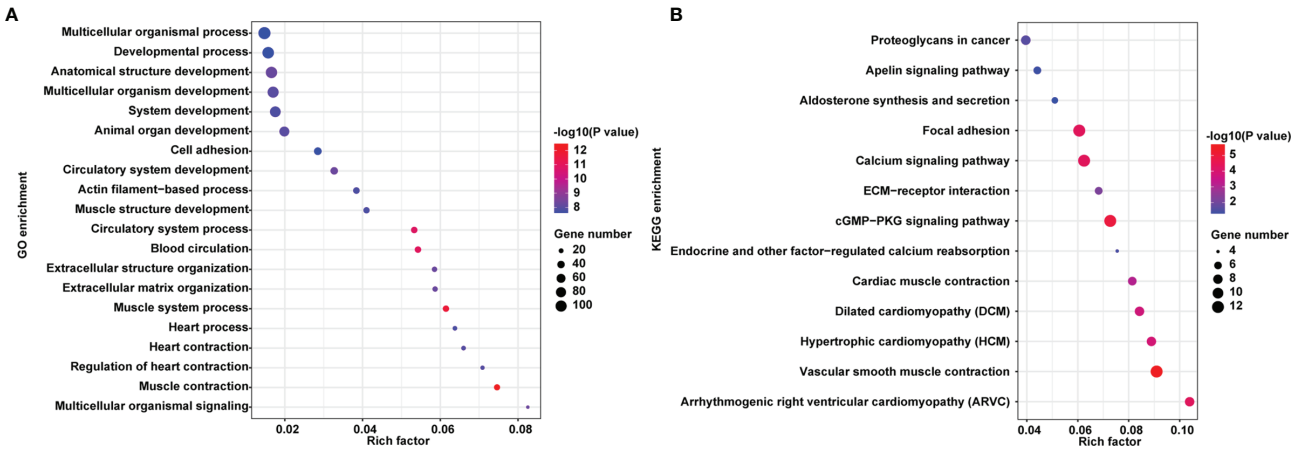


FIGURE 3 | GO and KEGG pathway of the genes relevant to hypermethylation/low expression genes. **(A)** GO of hypermethylated/down-regulated genes. Names of the top 15 items are indicated by the y-axis. The size of the colored dots is the enriched number of genes in each GO classification. The red dots indicate high enrichment and the blue dots indicate low enrichment. FDR value is expressed by the color order on the right edge. **(B)** KEGG pathway enrichment of hypermethylated/down-regulated genes. The size of the dot in the KEGG pathway bubble plot shows the enriched genes. High enriched represented by red, otherwise, by blue.

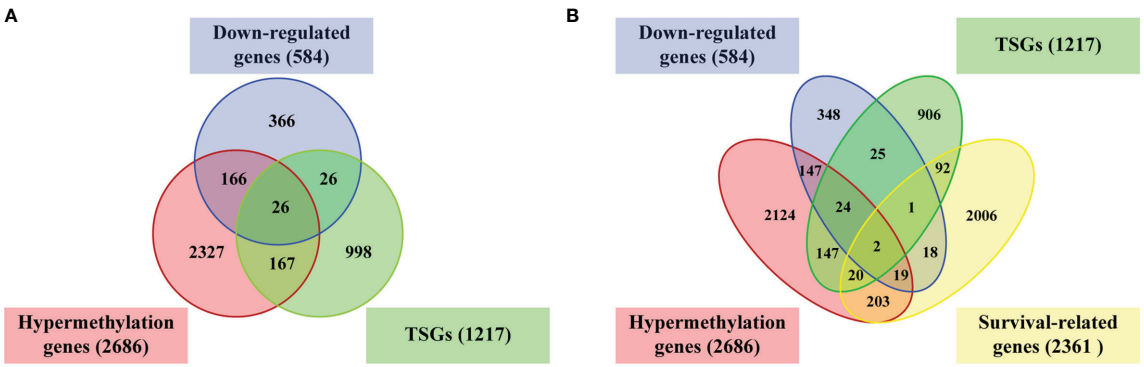


FIGURE 4 | Venn diagram of overlapping genes. **(A)** Venn diagram of overlapping genes in down-regulated genes (blue circle), and hypermethylation genes (red circle), and TSGs (green circle). **(B)** Venn diagram of overlapping genes in down-regulated genes (blue circle), and hypermethylation genes (red circle), TSGs (green circle), and survival-related genes (yellow circle). TSGs, tumor suppressor genes.

analysis was performed and AUC was calculated to assess the potential diagnostic value of *MRVI1* and *NTRK3* using the methylation levels of CpG sites on promoter regions. As shown in **Figures 9B–G**, five CpG sites had excellent diagnostic performance for discriminating cervical cancer from healthy cervical samples (cg24365867, p = 0.003, AUC = 0.901; cg24541550, p= 0.003, AUC = 0.901; cg16014606, p = 0.002, AUC = 0.914; cg15283950, p = 0.003, AUC = 0.901; cg14384532, p = 0.014, AUC = 0.840; Combined, p = 0.0002, AUC = 1.000).

DISCUSSION

Cervical cancer is one of the most common types of cancer and represents a major global health challenge (1). Since aberrant DNA methylation occurs very early during tumorigenesis (19), it could therefore be used as an early diagnostic biomarker (20). In this study, hypermethylated and significantly lower expressions of TSGs *MRVI1* and *NTRK3* were discovered in cervical cancers than that in normal cervical tissues using the bioinformatics. The differences of *MRVI1* and *NTRK3* expressions between cervical cancer specimens and normal cervical tissues were further verified *via* three GEO datasets. Besides, the low expression of *MRVI1* and *NTRK3* was negatively associated with high methylation levels of promoter CpG sites. Moreover, promoter hypermethylation levels of *MRVI1* and *NTRK3* were also found in our clinical cervical cancer samples. ROC curve analyses proved the diagnostic value of *MRVI1* and *NTRK3* in cervical cancer. Furthermore, low expression of *MRVI1* and *NTRK3* was associated with poor prognosis of cervical cancer. These results

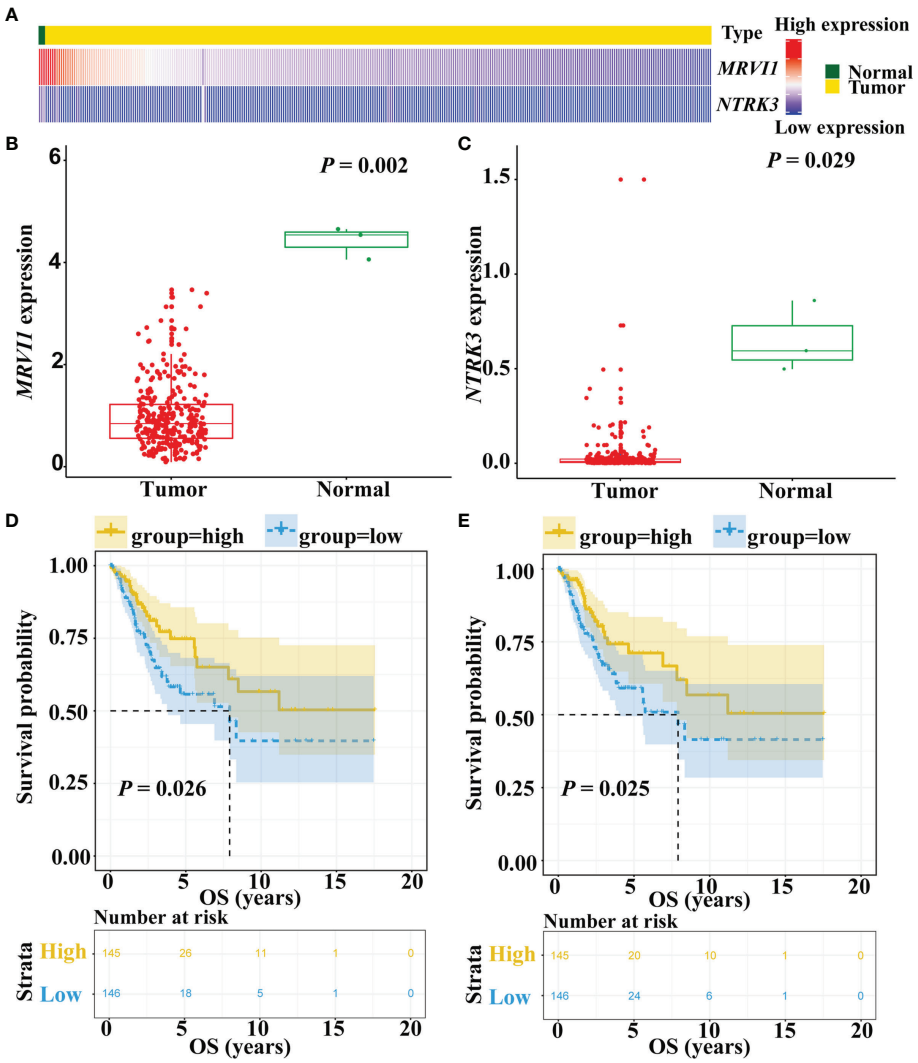


FIGURE 5 | Prognostic values of *MRVI1* and *NTRK3*. **(A)** Hierarchical clustering of *MRVI1* and *NTRK3*; Expression of *MRVI1* **(B)** and *NTRK3* **(C)** in 304 cervical cancer patients and 3 normal cervical tissues. The *MRVI1* and *NTRK3* expression levels (log2(FPKM+1)) are significantly decreased in cervical cancer patients compared with the normal controls. **(D, E)** Kaplan–Meier curves show that low expression of *MRVI1* and *NTRK3* have worse prognosis than that of the high expression of *MRVI1* and *NTRK3*.

enhanced our understanding of the DNA methylation pattern of TSGs in cervical cancer.

MRVI1 is a protein-coding gene, which has been widely studied in cancer (21, 22). *MRVI1* was reported to regulate the cellular release of calcium signal (23), which plays an important role in cancer cell proliferation invasiveness (24). One study discovered that MRVI1 was transcriptionally activated by p53, and p53-induced inhibition of colorectal cancer prognosis was depended on MRVI1 (25). Zhu et al. found that the *MRVI1*-AS1/ATF3 signalling pathway could increase paclitaxel chemosensitivity by modulating the Hippo-TAZ signalling pathway in nasopharyngeal cancer (21). Another research found that miR-940 could promote proliferation and metastasis of endometrial carcinoma through the regulation of *MRVI1* (22). High expression of *MRVI1* had a better prognosis than that of the low expression of *MRVI1* in endometrial carcinoma (22). Unfortunately, the role of *MRVI1* in cervical cancer has not yet been reported. In the current study, the overall survival of cervical cancer patients with low *MRVI1* expression was also significantly shorter than those with high *MRVI1* expression, which is consistent with previous endometrial carcinoma study.

NTRK3 encodes the TrkC protein, a member of neurotrophic tropomyosin receptor kinase (Trk) family, which autophosphorylates and motivates various signalling pathways such as MAPK and PI3K/AKT pathways (26). Trk aberrations, including gene fusion, gene overexpression, and single nucleotide variation, are involved in the pathogenesis of many cancers, among which NTRK3 gene fusion is extremely confirmed for oncogenic event (27). Unusual activation of

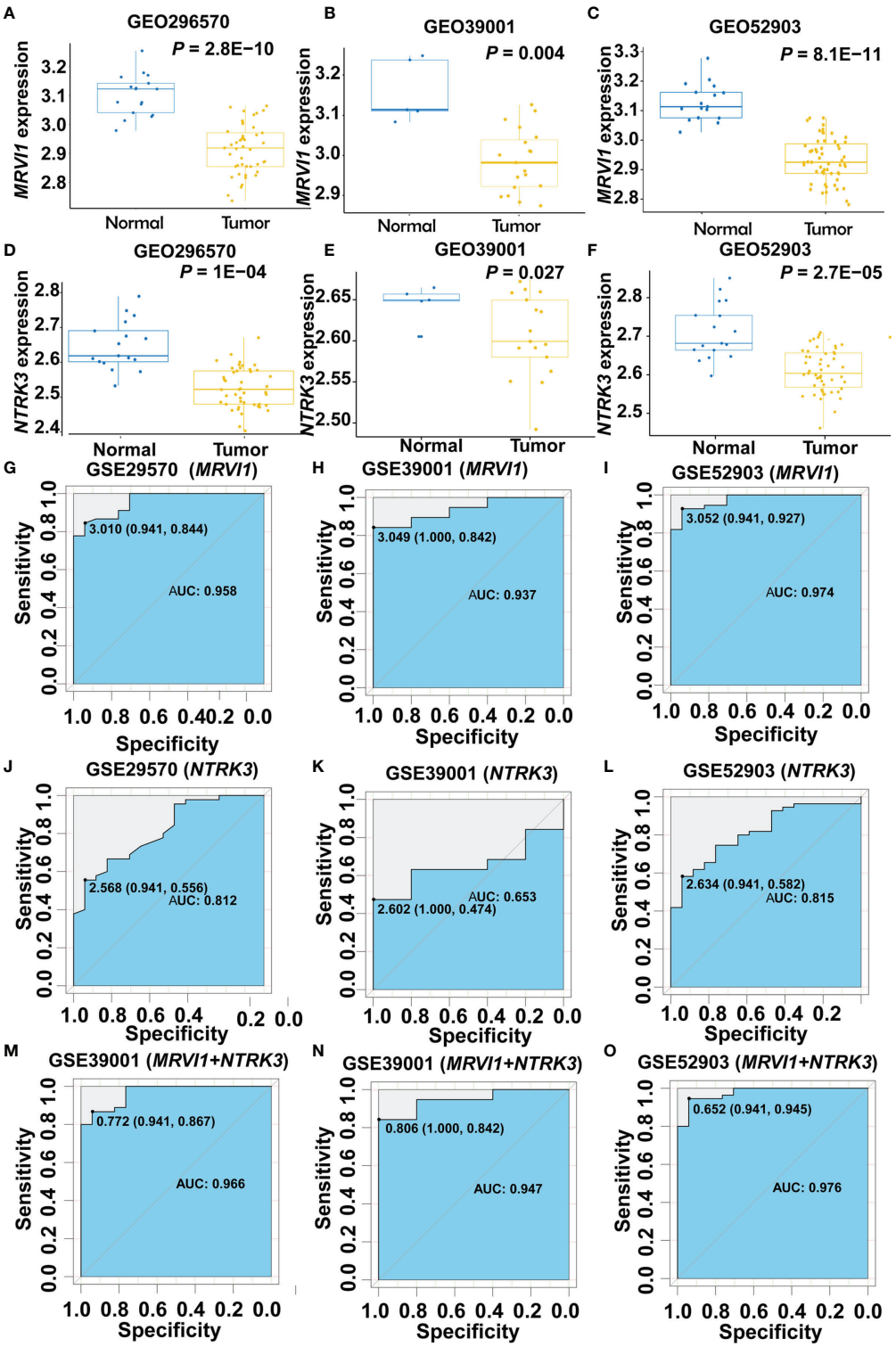


FIGURE 6 | Confirmed expression levels and ROC curve analyses for the prediction of cervical cancer. **(A–F)** Boxplots of gene expression levels in three GEO databases for *MRVI1* and *NTKR3*. The left y-axis shows the mRNA expression levels for *MRVI1* or *NTRK3*. The x-axis represents the two groups (normal tissue and cervical tumor). Each panel represents a different GEO database (GSE29570, GSE39001, and GSE52903). ROC curve of *MRVI1* **(G–I)**, *NTRK1* **(J–L)**, and combined expression **(M–O)** for distinguishing between cervical cancer and non-tumor tissues in individual GEO datasets. AUC, the area under the ROC curve; GEO, Gene Expression Omnibus; ROC, receiver operating characteristics.

TABLE 1 | Accuracy of *MRVI1* and *NTRK3* for predicting the prognosis of cervical cancer patients.

	GEO	AUC	95% CI	Cut off point	Sensitivity	Specificity
MRVI1	GSE29570	0.958	0.914-1.000	3.010	0.844	0.941
	GSE39001	0.937	0.842-1.000	3.049	0.842	1.000
	GSE52903	0.974	0.944-1.000	3.052	0.927	0.941
NTRK3	GSE29570	0.812	0.698-0.925	2.568	0.556	0.941
	GSE39001	0.653	0.432-0.872	2.602	0.474	1.000
	GSE52903	0.815	0.711-0.919	2.634	0.582	0.941
Combination	GSE29570	0.966	0.928-1.000	0.772	0.867	0.941
	GSE39001	0.947	0.861-1.000	0.806	0.842	1.000
	GSE52903	0.976	0.947-1.000	0.652	0.945	0.941

AUC, area under curve; 95% CI, 95% confidence interval.

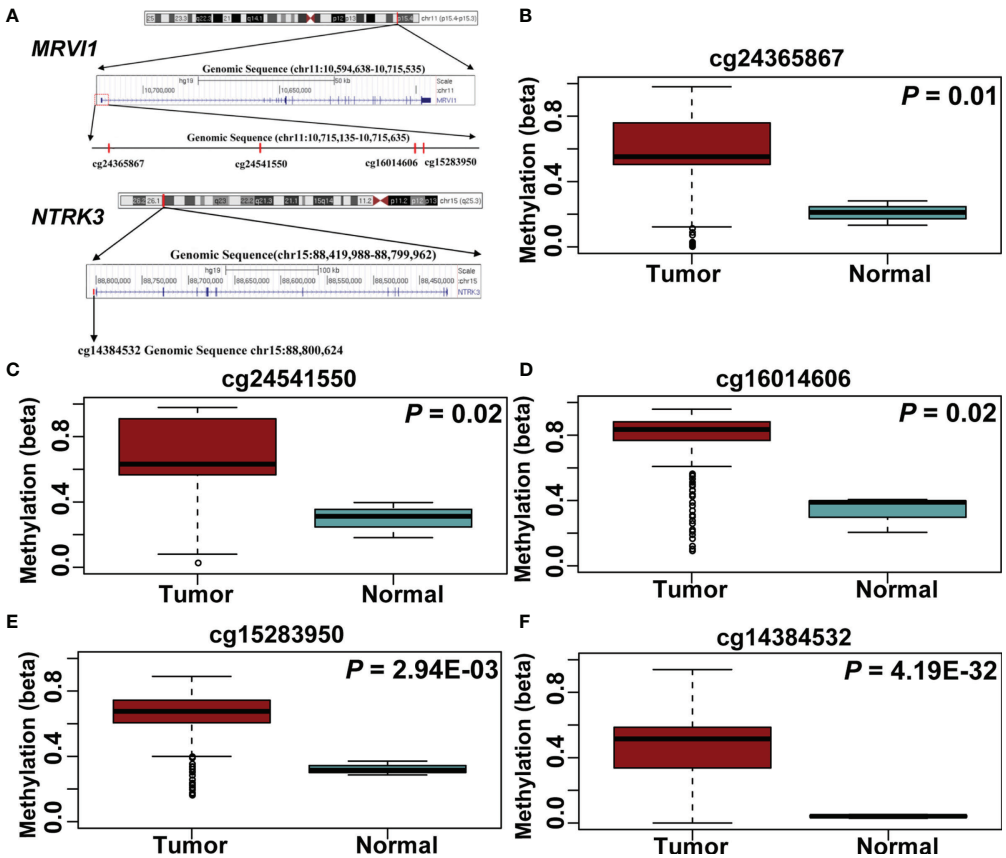


FIGURE 7 | Five CpG sites in *MRVI1* and *NTRK3* promoter regions. **(A)** The locations of CpG sites. The level of *MRVI1* promoter DNA methylation **(B–E)** and *NTRK3* promoter DNA methylation **(F)** presented as a box plot in the cervical cancer and normal cervical tissues.

NTRK3 and its fusion proteins may balance the epithelial–mesenchymal transition (EMT), oncogenicity, and tumor growth rate *via* triggering various signalling pathways (28). *ETV6-NTRK3* gene fusion acted as a potent oncogene driver and had been presented in the majority of cases of infantile fibrosarcoma (29). Oncogenic fusions in *NTRK* family receptor tyrosine kinases had been identified in several cancers and could serve as therapeutic targets, for instance in spitz tumors (30), fibrosarcoma (31), gastrointestinal stromal tumors (32), and inflammatory myofibroblastic tumors (33). Conversely, *NTRK3* expression was a good prognosis factor in a variety of cancers and more specifically in melanomas (34), neuroblastomas (35), and colorectal cancer (36). *NTRK3* expression and activation had been shown to trigger apoptosis in medulloblastoma cells (37). In recent years, *SPECC1L-NTRK3* gene fusion was found in cervical sarcoma patients (38). However, the research on *NTRK3* gene in cervical cancer is rare. Depending on the present study, *NTRK3*

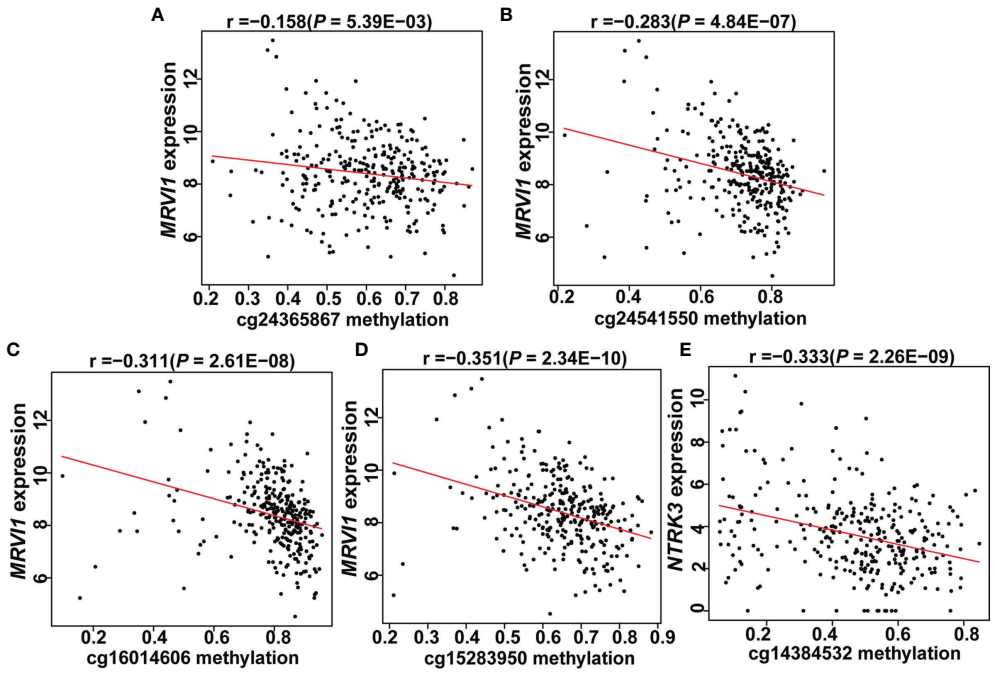


FIGURE 8 | Expression of two genes correlated with promoter CpG site methylation in cervical tissues. **(A–D)** *MRVI1* gene expression was negatively correlated with DNA methylation levels of cg24365867, cg24541550, cg16014606, and cg15283950. **(E)** *NTRK3* gene expression was negatively correlated with DNA methylation level of cg14384532. x-axis: DNA methylation levels; y-axis: relative gene expression levels; red line: linear regression.

TABLE 2 | Association between *MRVI1* and *NTRK3* methylation status and cervical cancer.

		Tumor	Non-tumor	*P* value
MRVI1	CG24365867	51.21 ± 18.44	25.30 ± 7.47	0.002
	CG24541550	70.54 ± 22.47	33.37 ± 10.04	0.001
	CG16014606	50.81 ± 13.95	24.19 ± 7.27	0.0003
	CG15283950	51.26 ± 16.02	23.69 ± 6.81	0.001
NTRK3	CG14384532	31.47 ± 23.43	5.62 ± 1.73	0.010

expression was significantly lower in cervical cancer specimens than that in normal cervical tissues, and low *NTRK3* expression was associated with a poor prognosis. These findings suggested that *NTRK3* might likewise serve as a tumor suppressor gene in cervical cancer.

In present study, two TSGs (*MRVI1* and *NTRK3*) were identified *via* bioinformatics. Nevertheless, a total of 26 hypermethylated/down-regulated TSGs have been discovered, the rest TSGs should be further studied. Although, the hypermethylation levels of *MRVI1* and *NTRK3* were verified in 9 cervical cancer tissues by pyrosequencing, the large number of clinical samples should be collected in further study. Hypermethylated and down-regulated expression levels of TSGs *MRVI1* and *NTRK3* have been identified in the current study; however, the detail epigenetic regulatory mechanism under cervical cancer still needs further investigation. In summary, our results revealed that hypermethylation in the promoter regions of *MRVI1* and *NTRK3* genes might lead to low expression in cervical cancer. Low expression levels of *MRVI1* and *NTRK3* were associated with poor prognosis of cervical cancer. The methylation levels and expression levels of *MRVI1* and *NTRK3* had the ability to effectively discriminate cervical cancer from healthy samples. Therefore, *MRVI1* and *NTRK3* genes may play important roles in the occurrence and prognosis of cervical cancer. It could be further explored and validated as a therapeutic target for cervical cancer. In conclusion, the down-regulation of *MRVI1* and *NTRK3* may drive cervical cancer through hypermethylation of their promoters. Further studies are needed to draw more attention to the roles of these TSGs in cervical cancer.

MATERIALS AND METHODS

Data Resources for DNA Methylation, RNA-Seq Data and Clinical Information

Illumina Infinium HumanMethylation450K and RNA-seq expression profiles were downloaded from TCGA-CESC

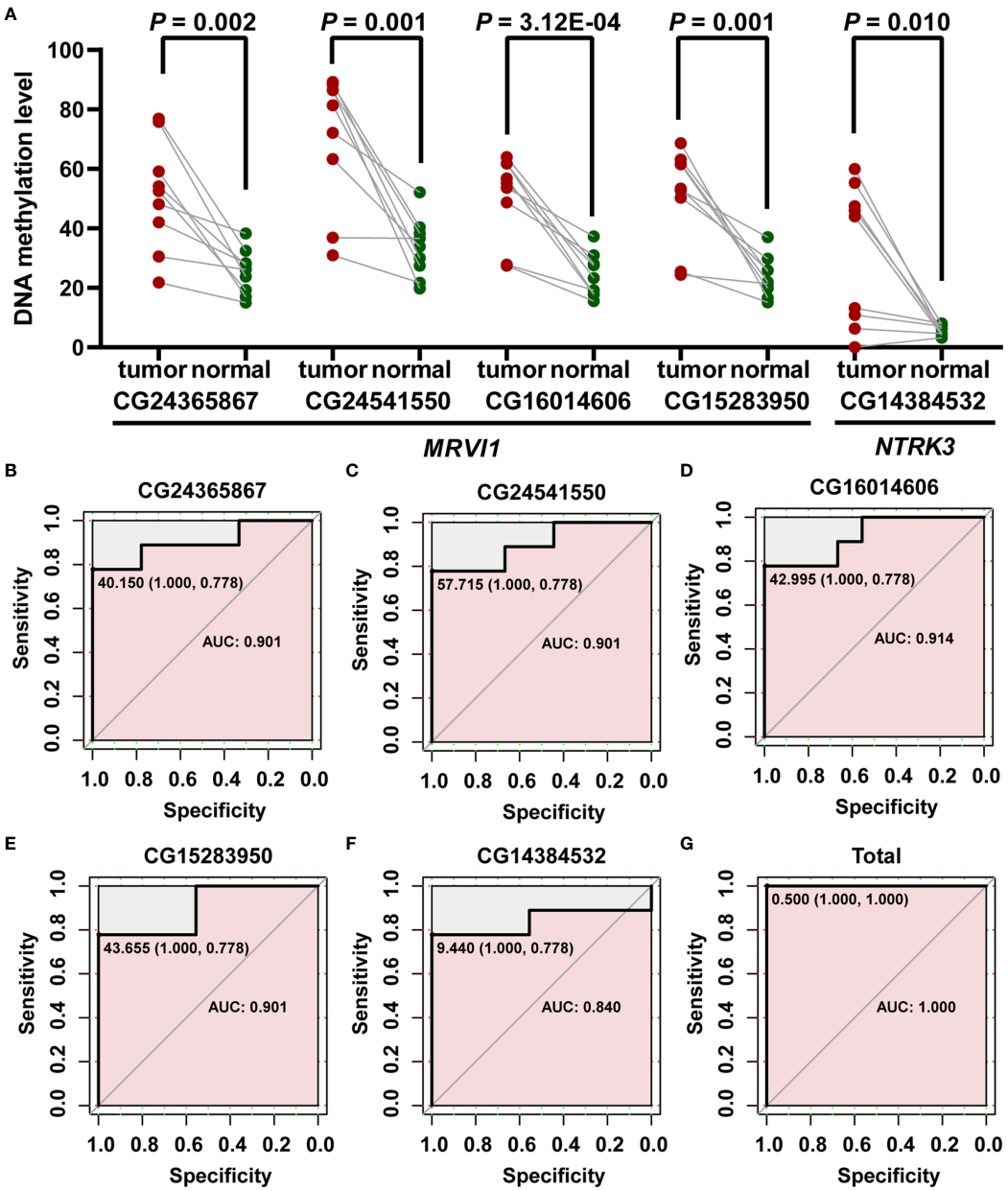


FIGURE 9 | Confirmed methylation levels and ROC curve analyses for the prediction of cervical cancer. **(A)** The methylation levels of *MRVI1* and *NTRK3* were significantly higher in cervical cancer tissues than in adjacent normal tissues. ROC curve of methylation levels of *MRVI1* **(B–E)**, *NTRK1* **(F)**, and combined methylation levels of five CpGs **(G)** for distinguishing between cervical cancer and non-tumor cervical tissues. AUC, the area under the ROC curve; ROC, receiver operating characteristics.

(https://cancergenome.nih.gov/). Methylation data of 307 cervical cancer and 3 normal cervical tissues were collected in the present study. The probes were annotated by using the Bioconductor package with the human genome assembly GRCh37 (hg19). Gene expression profile corresponding to abnormally methylated genes was also download. In addition, the corresponding clinical overall survival data of 291 samples were included. Besides, 3 cervical cancer-related expression datasets (GSE29570, GSE39001, and GSE52903) were obtained from the GEO database. GSE29570 (39) includes the expression data from 17 healthy female exocervix samples and 45 cervical cancer samples, GSE39001 (40) contains data from 5 healthy female cervical samples and 19 cervical cancer samples, and GSE52903 (41) contains expression profiles from a discovery cohort of 17 healthy female cervical samples and 55 cervical cancer samples.

TABLE 3 | Primers used for the pyrosequencing assay.

Gene	Forward primer (5' to 3')	Reverse primer (5' to 3')	Sequencing primer (5' to 3')
MRVI1	GGGGATTGTTATTTGTTGTGTGGATAT	Biotin- AAACTCCTCTAAAAACCCCACTC	AGGGGTTTAGGGTGA
	TGGGGAGTTTTTATTATTTAAGGTTAATG	Biotin- TAAATCCCAACCCCTCTCAAA	AGGTTAATGTTATATTTGGTTT
	AAGTATGTGAGTTTGGAGAAGA	Biotin- TCTCCCAAACCATTCTCTCTAAC	GGTAGGGGTTGTTTTTA
NTRK3	GGAAATGAGTGTTATTTAGATTAAGGAT	Biotin- ACCCCAAAAAAACACCCA	AGTGTTATTTAGATTAAGGATT

Differential Methylation and Gene Expression Analysis

Between cervical cancer tissues and normal cervical tissues, significant DMGs and DEGs were identified using DESeq package (42) and CHAMP package of R (43), respectively. The false discovery rate (FDR) was adopted to avoid the occurrence of false-positive results. FDR < 0.05 and |Log2 Fold change (Log2FC)| > 1 were used to select significant DMG or DEG.

Gene Ontology (GO) and KEGG Pathway Analysis

GO and KEGG pathway enrichment analysis of hypermethylated/down-regulated genes was performed using the g:Profiler program (44).

Searching for TSGs Associated With Cervical Cancer

Among hypermethylated/down-regulated genes, TSGs were identified based on TSGene 2.0 (45). With the median expression level as the demarcation point, 291 patients with clinical data in TCGA were divided into low-risk group and high-risk group. Kaplan-Meier analysis in the survival package of R (46) was used to compare the difference in overall survival between the two groups. Prognostic-related TSGs were considered as candidate genes for cervical cancer. To solve the problem of a small number of normal tissues in TCGA-CESC, the expression levels of cervical cancer candidate TSGs in three GEO datasets (GSE29570, GSE39001, and GSE52903) were further compared by T test using R.

Pyrosequencing Experiment

Nine pairs of cervical cancer specimens and adjacent normal cervical tissues were obtained from the Second Affiliated Hospital of Wenzhou Medical University. Cervical cancer patients were diagnosed by experienced pathologists based on the results of surgically removed specimens (**Supplementary Table 1**). Human genomic DNA was extracted from tissue samples using the Genomic DNA Extraction Kit (Qiagen, Dusseldorf, Germany). DNA concentrations were determined by the Infinite F200 Tecan microplate reader (Tecan, männedorf, Switzerland). Primers were designed using the PyroMark Assay Design Software 2.0 and bisulfite-treated DNA PCR-amplified using the PyroMark PCR kit prior to analysis on a PyroMark Q96 according to manufacturer's instruction (Qiagen, Dusseldorf, Germany). Sequences of the PCR primers were shown in **Table 3**. Amplification was carried out as follows: 95°C for 3 min, followed by 40 cycles of 94°C for 30 s, 56°C for 30 s, and 72°C for 1 min, with a final elongation step at 72°C for 7 min. Raw data were analyzed using PyroMark Q96 software (Qiagen, Dusseldorf, Germany). The research protocol was approved by the Ethics Committee of the Second Affiliated Hospital of Wenzhou Medical University. Written informed consents were obtained from all subjects.

Statistical Analysis

Pearson correlation coefficient was used to correlate promoter methylation levels with candidate TSGs expression levels. ROC curves were used to compare the sensitivity and specificity of the candidate TSGs expression levels and promoter methylation levels in the prediction of cervical cancer. All the data were analyzed using R scripts. A two-tailed p value < 0.05 was considered statistically significant.

DATA AVAILABILITY STATEMENT

The raw data supporting the conclusions of this article will be made available by the authors, without undue reservation.

AUTHOR CONTRIBUTIONS

Conceptualization, HJ and XZ. Methodology, KL. Formal analysis, KL, WJ, JL, J-aZ. Investigation and writing, HJ and XZ. Visualization and supervision, XZ. All authors have read and agreed to the published version of the manuscript.

FUNDING

This work was supported by the grant from the Subject of Integrated Traditional Chinese and Western Medicine in Zhejiang Province (2017-XK-A42). The study sponsors had no involvement in the collection, analysis, and interpretation of data, or in the writing of the manuscript.

SUPPLEMENTARY MATERIAL

The Supplementary Material for this article can be found online at: https://www.frontiersin.org/articles/10.3389/fonc.2021.802068/full#supplementary-material

REFERENCES

1. Sung H, Ferlay J, Siegel RL, Laversanne M, Soerjomataram I, Jemal A, et al. Global Cancer Statistics 2020: GLOBOCAN Estimates of Incidence and Mortality Worldwide for 36 Cancers in 185 Countries. *CA Cancer J Clin* (2021) 71:209–49. doi: 10.3322/caac.21660
2. Sakuragi N. Refining Insight Into Cervical Cancer Progression. *Lancet Oncol* (2014) 15:371–2. doi: 10.1016/S1470-2045(14)70085-3
3. Mathers JC, Strathdee G, Relton CL. Induction of Epigenetic Alterations by Dietary and Other Environmental Factors. *Adv Genet* (2010) 71:3–39. doi: 10.1016/B978-0-12-380864-6.00001-8
4. Zhao S. Specific Type Epigenetic Changes in Cervical Cancers. *Methods Mol Biol* (2015) 1238:733–49. doi: 10.1007/978-1-4939-1804-1_38
5. Teschendorff AE, Relton CL. Statistical and Integrative System-Level Analysis of DNA Methylation Data. *Nat Rev Genet* (2018) 19:129–47. doi: 10.1038/nrg.2017.86
6. Xie XL, Yu Y, Yuan ZF, Yang J, Ma PP, Li DC, et al. Comparative Analysis on Content and Distribution of CpG Sites in Milk Production Traits and Mastitis-Related Genes in Dairy Cattle. *Yi Chuan* (2012) 34:437–44. doi: 10.3724/SP.J.1005.2012.00437
7. Husquin LT, Rotival M, Fagny M, Quach H, Zidane N, McEwen LM, et al. Exploring the Genetic Basis of Human Population Differences in DNA Methylation and Their Causal Impact on Immune Gene Regulation. *Genome Biol* (2018) 19:222. doi: 10.1186/s13059-018-1601-3
8. Long MD, Smiraglia DJ, Campbell MJ. The Genomic Impact of DNA CpG Methylation on Gene Expression; Relationships in Prostate Cancer. *Biomolecules* (2017) 7. doi: 10.3390/biom7010015
9. Quillien V, Lavenu A, Karayan-Tapon L, Carpentier C, Labussiere M, Lesimple T, et al. Comparative Assessment of 5 Methods (Methylation-Specific Polymerase Chain Reaction, MethyLight, Pyrosequencing, Methylation-Sensitive High-Resolution Melting, and Immunohistochemistry) to Analyze O6-Methylguanine-DNA-Methyltranferase in a Series of 100 Glioblastoma Patients. *Cancer* (2012) 118:4201–11. doi: 10.1002/cncr.27392
10. Kazanets A, Shorstova T, Hilmi K, Marques M, Witcher M. Epigenetic Silencing of Tumor Suppressor Genes: Paradigms, Puzzles, and Potential. *Biochim Biophys Acta* (2016) 1865:275–88. doi: 10.1016/j.bbcan.2016.04.001
11. Sin STK, Li Y, Liu M, Ma S, Guan XY. TROP-2 Exhibits Tumor Suppressive Functions in Cervical Cancer by Dual Inhibition of IGF-1R and ALK Signaling. *Gynecol Oncol* (2019) 152:185–93. doi: 10.1016/j.ygyno.2018.10.039
12. Qin Y, Tang X, Liu M. Tumor-Suppressor Gene NBPF1 Inhibits Invasion and PI3K/mTOR Signaling in Cervical Cancer Cells. *Oncol Res* (2016) 23:13–20. doi: 10.3727/096504015X14410238486766
13. Guerrero-Setas D, Perez-Janices N, Blanco-Fernandez L, Ojer A, Cambra K, Berdasco M, et al. RASSF2 Hypermethylation is Present and Related to Shorter Survival in Squamous Cervical Cancer. *Mod Pathol* (2013) 26:1111–22. doi: 10.1038/modpathol.2013.32
14. Tawe L, Grover S, Zetola N, Robertson ES, Gaseitsiwe S, Moyo S, et al. Promoter Hypermethylation Analysis of Host Genes in Cervical Cancer Patients With and Without Human Immunodeficiency Virus in Botswana. *Front Oncol* (2021) 11:560296. doi: 10.3389/fonc.2021.560296
15. Rogeri CD, Silveira HCS, Causin RL, Villa LL, Stein MD, de Carvalho AC, et al. Methylation of the hsa-miR-124, SOX1, TERT, and LMX1A Genes as Biomarkers for Precursor Lesions in Cervical Cancer. *Gynecol Oncol* (2018) 150:545–51. doi: 10.1016/j.ygyno.2018.06.014
16. Li Z, Heng J, Yan J, Guo X, Tang L, Chen M, et al. Integrated Analysis of Gene Expression and Methylation Profiles of 48 Candidate Genes in Breast Cancer Patients. *Breast Cancer Res Treat* (2016) 160:371–83. doi: 10.1007/s10549-016-4004-8
17. van den Dungen MW, Murk AJ, Kok DE, Steegenga WT. Comprehensive DNA Methylation and Gene Expression Profiling in Differentiating Human Adipocytes. *J Cell Biochem* (2016) 117:2707–18. doi: 10.1002/jcb.25568
18. Zhou R, Man Y. Integrated Analysis of DNA Methylation Profiles and Gene Expression Profiles to Identify Genes Associated With Pilocytic Astrocytomas. *Mol Med Rep* (2016) 13:3491–7. doi: 10.3892/mmr.2016.4943
19. Hao X, Luo H, Krawczyk M, Wei W, Wang W, Wang J, et al. DNA Methylation Markers for Diagnosis and Prognosis of Common Cancers. *Proc Natl Acad Sci USA* (2017) 114:7414–9. doi: 10.1073/pnas.1703577114
20. Kim MS, Lee J, Sidransky D. DNA Methylation Markers in Colorectal Cancer. *Cancer Metastasis Rev* (2010) 29:181–206. doi: 10.1007/s10555-010-9207-6
21. Zhu Y, He D, Bo H, Liu Z, Xiao M, Xiang L, et al. The MRVI1-AS1/ATF3 Signaling Loop Sensitizes Nasopharyngeal Cancer Cells to Paclitaxel by Regulating the Hippo-TAZ Pathway. *Oncogene* (2019) 38:6065–81. doi: 10.1038/s41388-019-0858-7
22. Zhou Z, Xu YP, Wang LJ, Kong Y. miR-940 Potentially Promotes Proliferation and Metastasis of Endometrial Carcinoma Through Regulation of MRVI1. *Biosci Rep* (2019) 39. doi: 10.1042/BSR20190077
23. Schlossmann J, Ammendola A, Ashman K, Zong X, Huber A, Neubauer G, et al. Regulation of Intracellular Calcium by a Signalling Complex of IRAG, IP3 Receptor and cGMP Kinase Ibeta. *Nature* (2000) 404:197–201. doi: 10.1038/35004606
24. Bong AHL, Monteith GR. Calcium Signaling and the Therapeutic Targeting of Cancer Cells. *Biochim Biophys Acta Mol Cell Res* (2018) 1865:1786–94. doi: 10.1016/j.bbamcr.2018.05.015
25. Ma L, Wang H, Sun Y, Yang D, Pu L, Zhang X. P53-Induced MRVI1 Mediates Carcinogenesis of Colorectal Cancer. *Scand J Gastroenterol* (2020) 55:824–33. doi: 10.1080/00365521.2020.1782465
26. Okamura R, Boichard A, Kato S, Sicklick JK, Bazhenova L, Kurzrock R. Analysis of NTRK Alterations in Pan-Cancer Adult and Pediatric Malignancies: Implications for NTRK-Targeted Therapeutics. *JCO Precis Oncol* (2018) 2018. doi: 10.1200/PO.18.00183
27. Khotskaya YB, Holla VR, Farago AF, Mills Shaw KR, Meric-Bernstam F, Hong DS. Targeting TRK Family Proteins in Cancer. *Pharmacol Ther* (2017) 173:58–66. doi: 10.1016/j.pharmthera.2017.02.006
28. Jin W. Roles of TrkC Signaling in the Regulation of Tumorigenicity and Metastasis of Cancer. *Cancers (Basel)* (2020) 12. doi: 10.3390/cancers12010147
29. Bielack SS, Cox MC, Nathrath M, Apel K, Blattmann C, Holl T, et al. Rapid, Complete and Sustained Tumour Response to the TRK Inhibitor Larotrectinib in an Infant With Recurrent, Chemotherapy-Refractory Infantile Fibrosarcoma Carrying the Characteristic ETV6-NTRK3 Gene Fusion. *Ann Oncol* (2019) 30:viii31–5. doi: 10.1093/annonc/mdz382
30. Yeh I, Tee MK, Botton T, Shain AH, Sparatta AJ, Gagnon A, et al. NTRK3 Kinase Fusions in Spitz Tumours. *J Pathol* (2016) 240:282–90. doi: 10.1002/path.4775
31. Church AJ, Calicchio ML, Nardi V, Skalova A, Pinto A, Dillon DA, et al. Recurrent EML4-NTRK3 Fusions in Infantile Fibrosarcoma and Congenital Mesoblastic Nephroma Suggest a Revised Testing Strategy. *Mod Pathol* (2018) 31:463–73. doi: 10.1038/modpathol.2017.127
32. Shi E, Chmielecki J, Tang CM, Wang K, Heinrich MC, Kang G, et al. FGFR1 and NTRK3 Actionable Alterations in "Wild-Type" Gastrointestinal Stromal Tumors. *J Transl Med* (2016) 14:339. doi: 10.1186/s12967-016-1075-6
33. Yamamoto H, Yoshida A, Taguchi K, Kohashi K, Hatanaka Y, Yamashita A, et al. ALK, ROS1 and NTRK3 Gene Rearrangements in Inflammatory Myofibroblastic Tumours. *Histopathology* (2016) 69:72–83. doi: 10.1111/his.12910
34. Xu X, Tahan SR, Pasha TL, Zhang PJ. Expression of Neurotrophin Receptor Trk-C in Nevi and Melanomas. *J Cutan Pathol* (2003) 30:318–22. doi: 10.1034/j.1600-0560.2003.00068.x
35. Bouzas-Rodriguez J, Cabrera JR, Delloye-Bourgeois C, Ichim G, Delcros JG, Raquin MA, et al. Neurotrophin-3 Production Promotes Human Neuroblastoma Cell Survival by Inhibiting TrkC-Induced Apoptosis. *J Clin Invest* (2010) 120:850–8. doi: 10.1172/JCI41013
36. Luo Y, Kaz AM, Kanngurn S, Welsch P, Morris SM, Wang J, et al. NTRK3 is a Potential Tumor Suppressor Gene Commonly Inactivated by Epigenetic Mechanisms in Colorectal Cancer. *PloS Genet* (2013) 9:e1003552. doi: 10.1371/journal.pgen.1003552
37. Kim JY, Sutton ME, Lu DJ, Cho TA, Goumnerova LC, Goritchenko L, et al. Activation of Neurotrophin-3 Receptor TrkC Induces Apoptosis in Medulloblastomas. *Cancer Res* (1999) 59:711–9.
38. Hodgson A, Pun C, Djordjevic B, Turashvili G. NTRK-Rearranged Cervical Sarcoma: Expanding the Clinicopathologic Spectrum. *Int J Gynecol Pathol* (2021) 40:73–7. doi: 10.1097/PGP.0000000000000669
39. Guardado-Estrada M, Medina-Martinez I, Juarez-Torres E, Roman-Bassaure E, Macias L, Alfaro A, et al. The Amerindian mtDNA Haplogroup B2 Enhances the Risk of HPV for Cervical Cancer: De-Regulation of Mitochondrial Genes may be Involved. *J Hum Genet* (2012) 57:269–76. doi: 10.1038/jhg.2012.17

40. Espinosa AM, Alfaro A, Roman-Basaure E, Guardado-Estrada M, Palma I, Serralde C, et al. Mitosis is a Source of Potential Markers for Screening and Survival and Therapeutic Targets in Cervical Cancer. *PloS One* (2013) 8: e55975. doi: 10.1371/journal.pone.0055975
41. Medina-Martinez I, Barron V, Roman-Bassaure E, Juarez-Torres E, Guardado-Estrada M, Espinosa AM, et al. Impact of Gene Dosage on Gene Expression, Biological Processes and Survival in Cervical Cancer: A Genome-Wide Follow-Up Study. *PloS One* (2014) 9:e97842. doi: 10.1371/journal.pone.0097842
42. Anders S, Huber W. Differential Expression Analysis for Sequence Count Data. *Genome Biol* (2010) 11:R106. doi: 10.1186/gb-2010-11-10-r106
43. Tian Y, Morris TJ, Webster AP, Yang Z, Beck S, Feber A, et al. ChAMP: Updated Methylation Analysis Pipeline for Illumina BeadChips. *Bioinformatics* (2017) 33:3982–4. doi: 10.1093/bioinformatics/btx513
44. Reimand J, Arak T, Adler P, Kolberg L, Reisberg S, Peterson H, et al. G: Profiler-A Web Server for Functional Interpretation of Gene Lists (2016 Update). *Nucleic Acids Res* (2016) 44:W83–9. doi: 10.1093/nar/gkw199
45. Zhao M, Kim P, Mitra R, Zhao J, Zhao Z. TSGene 2.0: An Updated Literature-Based Knowledgebase for Tumor Suppressor Genes. *Nucleic Acids Res* (2016) 44:D1023–31. doi: 10.1093/nar/gkv1268
46. Bland JM, Altman DG. Survival Probabilities (the Kaplan-Meier Method). *BMJ* (1998) 317:1572. doi: 10.1136/bmj.317.7172.1572

Conflict of Interest: The authors declare that the research was conducted in the absence of any commercial or financial relationships that could be construed as a potential conflict of interest.

Publisher's Note: All claims expressed in this article are solely those of the authors and do not necessarily represent those of their affiliated organizations, or those of the publisher, the editors and the reviewers. Any product that may be evaluated in this article, or claim that may be made by its manufacturer, is not guaranteed or endorsed by the publisher.

Copyright © 2022 Ji, Li, Jiang, Li, Zhang and Zhu. This is an open-access article distributed under the terms of the Creative Commons Attribution License (CC BY). The use, distribution or reproduction in other forums is permitted, provided the original author(s) and the copyright owner(s) are credited and that the original publication in this journal is cited, in accordance with accepted academic practice. No use, distribution or reproduction is permitted which does not comply with these terms.

frontiers in Oncology

ORIGINAL RESEARCH
published: 27 January 2022
doi: 10.3389/fonc.2021.812033

Noninvasive Predictor for Premalignant and Cancerous Lesions in Endometrial Polyps Diagnosed by Ultrasound

Jianying Xu[1], Xuan Rao[1], Weiguo Lu[1,2,3], Xing Xie[1], Xinyu Wang[1,2] and Xiao Li[1,2,4*]*

[1] Department of Gynecologic Oncology, Women's Hospital, School of Medicine Zhejiang University, Hangzhou, China, [2] Cancer Center, Zhejiang University, Hangzhou, China, [3] Center for Uterine Cancer Diagnosis & Therapy Research of Zhejiang Province, Hangzhou, China, [4] Zhejiang Provincial Key Laboratory of Precision Diagnosis and Therapy for Major Gynecological Diseases, Women's Hospital, Zhejiang University School of Medicine, Hangzhou, China

Background: There was no consensus for management of asymptomatic endometrial polyps (EPs) up to date.

Objective: The aim of present study was to determine the risk factors of malignant lesions in EPs diagnosed by ultrasound and establish a noninvasive predictor to decrease unnecessary hysteroscopy for EPs.

Study Design: We reviewed the records of all consecutive patients who underwent hysteroscopy for EPs in the Women's Hospital School of Medicine Zhejiang University between January 1, 2001 and December 31, 2018. The patients with histological diagnoses of atypical hyperplasia or cancer were defined as malignancy, while the patients with histological diagnoses of benign lesions were randomly selected as benign group according to the ratio of 1:4 (malignancy:benign), matching by age and year of hospitalization. Logistic regression analysis was used to analyze the clinical parameters for predicting malignancy of EPs. A Chi-squared automatic interaction detection (CHAID) decision tree analysis was performed to find a noninvasive predictor. The sensitivity, specificity, and the receiver operating characteristic curve (ROC) were used for assess the efficacy of the noninvasive predictor. New diagnosed EPs patients received in 2019 were used for verifying the accuracy of the noninvasive predictor.

Results: The age in 15,790 cases of benign lesions was significantly younger than that in 230 malignancy cases (41.97 ± 11.53 year vs 53.31 ± 11.61 years, p <0.001). AUB (OR 7.306, 95%CI 4.927–10.835), large EPs (OR 2.595, 95%CI 1.662–4.052), and blood flow signal in EPs (OR 2.690, 95%CI 1.872–3.866) were independent predictive factors of malignancy in all enrolled patients. A noninvasive predictor for malignancy of EPs was established, through combining with AUB, large polyps and blood flow signal. This predictor presented excellent sensitivity and NPV (91.3 and 95.8%), with acceptable specificity and AUC (0.801). Further validation in new diagnosed EPs also suggested excellent sensitivity and reasonable specificity (100 and 58.5%) of the predictor. Factors such as thickened endometrial thickness, menopause shorter than 10 years,

OPEN ACCESS

Edited by:
Stefano Restaino, Ospedale Santa Maria della Misericordia di Udine, Italy

Reviewed by:
Komsun Suwannarurk, Thammasat University, Thailand
Vito Andrea Capozzi, University Hospital of Parma, Italy

***Correspondence:**
Xiao Li
5198008@zju.edu.cn
Xinyu Wang
wangxy@zju.edu.cn

Specialty section:
This article was submitted to Gynecological Oncology, a section of the journal Frontiers in Oncology

Received: *09 November 2021*
Accepted: *30 December 2021*
Published: *27 January 2022*

Citation:
Xu J, Rao X, Lu W, Xie X, Wang X and Li X (2022) Noninvasive Predictor for Premalignant and Cancerous Lesions in Endometrial Polyps Diagnosed by Ultrasound. Front. Oncol. 11:812033. doi: 10.3389/fonc.2021.812033

hypertension, obesity and nulliparous were also validated as independent predictors of malignancy in different subgroup analysis.

Conclusions: The noninvasive predictor combined with other risk factors from subgroup analysis would be reliable to distinguish the benign lesions from malignancy for EPs diagnosed by ultrasound.

Keywords: endometrial polyps, hysteroscopy, malignancy, noninvasive predictor, ultrasound

INTRODUCTION

Endometrial polyps (EPs) are defined as localized exophytic overgrowth occurring on the surface of the endometrium that may contain glands, fibrous tissue, and blood vessels in variable amounts (1, 2). With the widespread use of ultrasound in routine gynecological examination, the prevalence of EPs increased significantly, especially asymptomatic EPs (3). EPs may spontaneously regress in approximately 25% of cases, especially smaller polyps (<1.0 cm) (4). But the clinical manifestations of EPs were similar to early stage endometrial malignancy (3). The American Association of Gynecologic Laparoscopists (AAGL) estimated that the prevalence of cancerous and premalignant lesions of EPs range from 0 to 12.9%, depending on the subgroup (5). Thus, the fear of malignancy might inevitably entail overtreatment of EPs, which would bring unnecessary surgery related risks and lead to low cost-effectiveness ratio.

A number of studies have attempted to define the risk factors for cancerous and premalignant lesions of EPs diagnosed by ultrasound. Older age has been validated as a high-risk factor associated with malignancy. Previous reports suggested that the risk of malignancy increased over the age of 50, while younger age might be a protective factor (6, 7). Other studies also found that the incidence of malignancy increased 2.41–2.8 folds in women ≥60 years compared with those <60 years (1, 8). Abnormal uterine bleeding (AUB) is the most common symptom in EPs, with the incidence ranging from 23 to 75% (3, 9, 10). Previous studies also suggested that EPs patients with AUB presented an increased risk of malignancy (3, 11). For postmenopausal EPs, the women with AUB displayed an increased risk of malignancy ranging from 3.67 to 31.1 folds compared with asymptomatic women (1, 12), while for premenopausal EPs, AUB was not an independent risk factor for malignancy (1, 7, 13). Nevertheless, in order to relieve symptoms of AUB, surgical removal of EPs was recommended for symptomatic EPs patients in clinical practice, no matter whether for postmenopausal or premenopausal patients (5, 14).

The AAGL guidelines stated that expectant management was reasonable for small EPs in asymptomatic women (5). But the standard clinical management for asymptomatic EPs is still unclear to date (1, 7, 15). Moreover, studies about the relationship between obesity, diabetes mellitus (DM), hypertension, polycystic ovary syndrome (PCOS), menopause hormone replacement therapy (HRT), and malignancy of EPs also brought conflicting results (1, 9, 11, 13, 16, 17). So it is necessary to further comprehensively evaluate the risk factors related with malignant lesions in the EPs and create a more applicable strategy for clinical management of EPs. In the present study, we thoroughly analyzed the epidemiological and clinical parameters related to premalignant and cancerous lesions in EPs through various subgroup analyses, and firstly established a noninvasive comprehensive predictor which might be helpful to identify the malignant possibility of EPs patients. It is hoped to bring an excellent balance between missed diagnosis of the malignant lesions and unnecessary surgical complications and financial burden in EPs patients.

MATERIALS AND METHODS

We reviewed the records of all consecutive patients who underwent hysteroscopy for EPs in the Women's Hospital School of Medicine Zhejiang University between January 1, 2001 and December 31, 2018. The enrolled patients should meet all the following inclusion criteria: EPs diagnosed by ultrasound preoperatively, EPs treated by hysteroscopy, histological diagnosis confirmed by Paraffin Section and used as gold standard for final definite diagnosis, clinical and demographic data were available. Patients with missing data were excluded. Clinical and demographic data were extracted from the medical records, namely, age at diagnosis, height and weight, gravidity and parity, menopausal status, AUB, the largest dimension and blood flow signal of the EPs in latest preoperative transvaginal sonography (TVS), past history such as hypertension, DM, breast cancer, Lynch syndrome, PCOS, family history of endometrial cancer and previous EPs confirmed by histology, the usage of HRT and tamoxifen, and the number and appearance of EPs observed by hysteroscopy, namely, size, shape, texture, surface vascular conditions and ulcerative conditions of the polyps. For postmenopausal women, the following variables were further collected, namely, age of menopause, the time after menopause (years), estrogen level, and endometrial thickness (ET) of single layer measured by TVS. The patients with histological diagnoses of atypical hyperplasia or cancer were defined as malignancy group, and further nominated as premalignant group and cancerous group respectively, while the patients with histological diagnoses of benign lesions were randomly selected as benign group according to the ratio of 1:4 (malignancy:benign), matching by age and year of hospitalization. Patients in the benign and malignancy groups were used as a training set for the modeling of the noninvasive predictor.

Furthermore, we retrieved all records of consecutive patients who underwent hysteroscopy for EPs in our hospital from January 1, 2019 to December 31, 2019. The inclusion and exclusion criteria were the same as mentioned above. The data collected were used as a validation set for verifying the noninvasive predictor. The present study was approved by the Medical Research Ethics Review Board of the Women's Hospital School of Medicine Zhejiang University (IRB-20190016-R).

Ultrasound was carried out by the experienced sonographers with ultrasound systems equipped with a 5–9 MHz transvaginal probe. Body mass index (BMI) was calculated using weight divided by height squared (kg/m^2). BMI ≥28 kg/m^2 was defined as obesity. Women were considered menopause if they reported a period of amenorrhea of at least 12 months. Late menopause was defined as menopausal age >53 years. The appearance of EPs with crisp, prone to bleeding, irregular surfaces, ulcerative, and vascular abundance during hysteroscopy were considered as malignant signs (18).

Statistical analysis was carried out by Statistical Package for the Social Sciences (SPSS) software (version 24.0). Conditional univariate and multivariate logistic regression analyses were used to analyze the variable for predicting malignancy, and nonconditional univariate and multivariate logistic regression analysis were further used in subgroup analysis. Quantitative variables were presented as means ± standard deviation and compared by Student's t-test. Qualitative variables were presented as number (percentage) and compared by Chi-square test. An alpha level <0.05 was considered statistically significant. The Chi-squared automatic interaction detection (CHAID) algorithm was used to perform decision tree analysis. The patients in the benign and malignancy groups were the training set. The groups created by the model of decision tree analysis were further divided into 3 subgroups according to the risk of malignancy: low-risk (≤5%), intermediate-risk (>5 to ≤20%), and high-risk (>20%). A noninvasive predictor was established based on decision tree analysis. The validation set was used to verify the accuracy of the noninvasive predictor. The sensitivity, specificity, positive predictive value (PPV), and negative predictive value (NPV) of the noninvasive predictor and direct judgment by hysteroscopy were calculated and compared for malignancy judgment. The area under the curve (AUC) with 95% CI was calculated using the receiver operating characteristic (ROC) curve.

RESULTS

The Demographic and Clinical Data of Patients With EPs Diagnosed by Ultrasound

From January 1, 2001 to December 31, 2018, a total of 16,020 cases with clinical diagnosis of EPs were admitted for hysteroscopy in our hospital. Among them, 230 cases were histological diagnosed as malignancy, namely, 50 atypical hyperplasia and 180 cancers, while 920 patients with benign histological diagnoses were randomly selected as benign group, and 2 patients among them were further excluded due to a lack of sufficient information. The detailed histological results of all enrolled patients are listed in **Table 1**.

As shown in **Table 2**, the age between malignancy and benign groups has no significantly difference due to age matched. But the age in 15,790 cases of benign lesions was significantly younger than that in malignancy (41.97 ± 11.53 years vs 53.31 ± 11.61 years, p <0.001). This result was consistent with previous reports (1, 7, 8). The incidence of AUB in benign group was significantly lower than that in malignancy (35.1% vs 82.2%, p <0.001). The dimension of EPs in benign group was smaller than malignancy (1.34 ± 0.71 cm vs 1.91 ± 1.00 cm, p <0.001), with 588 cases of large EPs (the largest dimension ≥1 cm) in benign group and 199 cases in malignancy. The ratio of blood flow signal detected by TVS in benign group was also significantly lower than that in malignancy (35.2% vs 64.3%, p <0.001).

Due to the clinical significance of AUB and menopause in EPs, the demographic and clinical data were further listed according 4 subgroups which included postmenopausal women with and without AUB, premenopausal women with and without AUB (**Appendix Table 1**). HRT, tamoxifen therapy, Lynch syndrome, PCOS and family history of endometrial cancer were excluded in further data analysis due to the very small sample size.

Independent Risk Factors for Predicting Malignancy in Patients With EPs

As shown in **Table 3**, univariate analysis demonstrated that AUB, large EPs, blood flow signal in EPs and late menopause were significantly related with malignancy. Multivariate analysis further validated that AUB (OR 7.306, 95%CI 4.927–10.835), large EPs (OR 2.595, 95%CI 1.662–4.052), and blood flow signal in EPs (OR 2.690, 95%CI 1.872–3.866) were independent predictive factors of malignancy in all enrolled patients. When benign and premalignant patients were respectively compared with cancerous group, both postmenopause and AUB were validated as independent risk factors of cancer (**Appendix Tables 2.1**, **2.2**).

Due to the menopause status and AUB were both important impact factors for clinical manage in EPs patients, subgroup

TABLE 1 | Postoperative histological results of EPs diagnosed by ultrasound in training set.

Diagnosis	Number (%)
Premalignant and cancerous	230
Atypical hyperplasia	50 (21.74%)
Endometrial carcinoma	165 (71.74%)
Serous carcinoma	7 (3.04%)
Clear cell carcinoma	5 (2.17%)
Carcinosarcoma	3 (1.30%)
Benign	918
Endometrial polyps	880 (95.86%)
Simple hyperplasia	15 (1.63%)
Complex hyperplasia	6 (0.65%)
Uterine myoma	2 (0.22%)
Endometrial	15 (1.63%)

EPs, endometrial polyps.

TABLE 2 | Demographic and clinical data in benign and malignancy group in training set.

Variables	Benign	Malignancy	Premalignant	Cancerous
Total	918	230	50	180
Age, y[a]	53.31 ± 11.59	53.31 ± 11.61	45.66 ± 11.95	55.44 ± 10.60
BMI, kg/m^2[a]	23.38 ± 3.37	24.20 ± 3.65	23.95 ± 3.04	24.26 ± 3.80
Gravidity[a]	2.53 ± 1.41	2.58 ± 1.45	2.00 ± 1.26	2.74 ± 1.47
Parity[a]	1.54 ± 1.03	1.52 ± 1.05	0.98 ± 0.84	1.67 ± 1.06
Postmenopausal	574 (62.5%)	145 (63.0%)	15 (30.0%)	130 (72.2%)
Age of menopause, y[a,b]	50.37 ± 3.26	51.49 ± 3.50	52.53 ± 2.45	51.37 ± 3.59
The time after menopause, y[a,b]	10.00 ± 6.49	8.79 ± 7.01	6.13 ± 4.94	9.09 ± 7.16
Estrogen value ≥37pmol/l[b]	168 (29.3%)	40 (27.6%)	3 (20.0%)	37 (28.5%)
Late menopause	120 (13.1%)	49 (21.3%)	12 (24.0%)	37 (20.6%)
AUB	322 (35.1%)	189 (82.2%)	33 (66.0%)	156 (86.7%)
Largest dimension of EPs, cm[a]	1.34 ± 0.71	1.91 ± 1.00	1.59 ± 0.81	2.00 ± 1.03
Have blood flow signal	323 (35.2%)	148 (64.3%)	29 (58.0%)	119 (66.1%)
ET ≥0.2 cm[b]	103 (17.9%)	40 (27.6%)	7 (46.7%)	33 (25.4%)
Hypertension	258 (28.1%)	75 (32.6%)	15 (30.0%)	60 (33.3%)
DM	48 (5.2%)	12 (5.2%)	0 (0.0%)	12 (6.7%)
HRT	6 (0.7%)	1 (0.4%)	1 (2.0%)	0 (0.0%)
Breast cancer	25 (2.7%)	1 (0.4%)	0 (0.0%)	1 (0.6%)
Tamoxifen use	9 (1.0%)	0 (0.0%)	0 (0.0%)	0 (0.0%)
Lynch syndrome	0 (0.0%)	0 (0.0%)	0 (0.0%)	0 (0.0%)
PCOS	1 (0.1%)	3 (1.3%)	2 (4.0%)	1 (0.6%)
Family history of endometrial cancer	3 (0.3%)	0 (0.0%)	0 (0.0%)	0 (0.0%)
Previous EPs	72 (7.8%)	12 (5.2%)	6 (12.0%)	6 (3.3%)
Multiple polyps	424 (46.2%)	120 (52.2%)	35 (70.0%)	85 (47.2%)
Malignant sign by hysteroscopy	17 (1.9%)	98 (42.6%)	7 (14.0%)	91 (50.6%)

BMI, body mass index; AUB, abnormal uterine bleeding; EPs, endometrial polyps; ET, endometrial thickness; DM, diabetes mellitus; HRT, hormone replacement therapy; PCOS, polycystic ovary syndrome.

[a]*It was expressed in terms of mean ± standard deviation.*

[b]*This variable was calculated only for postmenopausal patients.*

analyses were conducted (**Tables 4**, **5** and **Appendix Tables 3, 4**). In addition to AUB, large EPs and blood flow signal, univariate and multivariate analyses suggested that ET ≥0.2 cm (OR 1.914, 95%CI 1.126–3.254) was an independent predictor of malignancy for postmenopausal patients, while hypertension (OR 5.891, 95%CI 1.392–24.937) was an independent predictor of malignancy for premenopausal patients (**Tables 4**, **5**). For postmenopausal patients without AUB, menopause <10 y (OR 3.205, 95%CI 1.024–10.000), blood flow signal (OR 2.865, 95%CI 1.143–7.177), and ET ≥0.2 cm (OR 3.624, 95%CI 1.397–9.397) were found to be independent predictors of malignancy. For premenopausal patients without AUB, nulliparous (OR 6.494, 95%CI 2.088–20.000), obesity (OR 8.867, 95%CI 1.512–52.008), large EPs (OR 4.180, 95%CI 1.283–13.616), and hypertension (OR 5.891, 95%CI 1.392–24.937) were found to be independent predictors of malignancy.

TABLE 3 | Univariate and multivariate analysis of demographic and clinical data between benign and malignancy groups in training set.

	Variables	OR	95%CI	p-Value
Univariate	Obesity	1.483	0.960–2.291	0.076
	Gravidity (0 vs ≥1)	1.264	0.654–2.445	0.484
	Parity (0 vs ≥1)	1.475	0.821–2.653	0.193
	Postmenopausal	1.125	0.590–2.143	0.721
	Late menopause	1.996	1.328–2.999	0.001
	AUB	8.369	5.706–12.275	<0.001
	Large EPs	3.705	2.463–5.573	<0.001
	Have blood flow signal	3.675	2.659–5.078	<0.001
	Hypertension	1.286	0.918–1.802	0.144
	DM	1.000	0.520–1.925	1.000
	Breast cancer	0.147	0.020–1.104	0.062
	Previous EPs	0.639	0.338–1.207	0.168
	Multiple polyps	1.313	0.963–1.790	0.085
Multivariate	Late menopause	1.414	0.860–2.325	0.172
	AUB	7.306	4.927–10.835	<0.001
	Large EPs	2.595	1.662–4.052	<0.001
	Have blood flow signal	2.690	1.872–3.866	<0.001

CI, confidence interval; AUB, abnormal uterine bleeding; EPs, endometrial polyps; DM, diabetes mellitus.

TABLE 4 | Univariate and multivariate analysis of demographic and clinical data between benign and malignancy groups in postmenopausal patients in training set.

	Variables	OR	95%CI	p-Value
Univariate	Obesity	1.336	0.802–2.224	0.266
	Gravidity (0 vs ≥1)	0.655	0.145–2.959	0.582
	Parity (0 vs ≥1)	0.787	0.225–2.755	0.708
	The time after menopause <10 y	1.449	1.000–2.101	0.050
	Estrogen value ≥37 pmol/l	0.953	0.636–1.427	0.814
	Late menopause	2.104	1.370–3.232	0.001
	AUB	14.889	9.059–24.469	<0.001
	Large EPs	3.647	2.075–6.408	<0.001
	Have blood flow signal	4.270	2.918–6.249	<0.001
	ET ≥0.2 cm	1.742	1.142–2.657	0.010
	Hypertension	1.019	0.703–1.476	0.922
	DM	1.087	0.558–2.115	0.806
	Breast cancer	0.183	0.024–1.371	0.098
	Previous EPs	0.875	0.354–2.160	0.771
	Multiple polyps	1.228	0.840–1.794	0.288
multivariate	Late menopause	1.696	0.996–2.889	0.052
	AUB	13.630	8.140–22.822	<0.001
	Large EPs	2.944	1.539–5.630	0.001
	Have blood flow signal	3.264	2.058–5.176	<0.001
	ET ≥0.2 cm	1.914	1.126–3.254	0.017

CI, confidence interval; AUB, abnormal uterine bleeding; EPs, endometrial polyps; DM, diabetes mellitus; ET, endometrial thickness.

TABLE 5 | Univariate and multivariate analysis of demographic and clinical data between benign and malignancy groups in premenopausal patients in training set.

	Variables	OR	95%CI	p-Value
Univariate	Obesity	2.130	0.880–5.157	0.148
	Gravidity (0 vs ≥1)	1.343	0.733–2.460	0.415
	Parity (0 vs ≥1)	1.486	0.867–2.551	0.190
	Late menopause	1.155	0.529–2.521	0.837
	AUB	3.781	2.195–6.516	<0.001
	Large EPs	3.706	2.068–6.644	<0.001
	Have blood flow signal	2.609	1.537–4.430	<0.001
	Hypertension	2.722	1.392–5.325	0.005
	DM	0.988	0.977–1.000	0.712
	Breast cancer	0.988	0.977–1.000	0.712
	Previous EPs	0.505	0.208–1.225	0.138
	Multiple polyps	1.568	0.897–2.743	0.143
multivariate	AUB	3.403	1.937–5.978	<0.001
	Large EPs	2.697	1.464–4.996	0.001
	Have blood flow signal	3.506	2.352–5.226	0.002
	Hypertension	2.744	1.297–5.804	0.008

CI, confidence interval; AUB, abnormal uterine bleeding; EPs, endometrial polyps; DM, diabetes mellitus.

The Efficacy of Noninvasive Predictor in Predicting of Malignancy in EPs Diagnosed by TVS

As high risk factors for malignancy in EPs, AUB, large EPs and blood flow signal were further inputted into the model of decision tree analysis. The model created six groups which were further divided into low, intermediate, and high-risk subgroups for malignancy (**Figure 1**). The overall accuracy of decision tree analysis for correctly identifying malignant lesions in EPs was 82.4%. For internal validation, a misclassification risk of 18.3% ± 1.1% (standard error) was calculated using the 10-fold cross-validation method. Thus, EPs with AUB, or TVS showed large EPs and blood flow signal at same time were designated as noninvasive predictor, since they were created in the high-risk or intermediate-risk subgroups. When compared with the direct judgment by hysteroscopy, the predictor had significantly higher sensitivity (91.3% vs 42.6%, p <0.001) and NPV (95.8% vs 87.2%, p = 0.040) for malignancy. The AUC of the predictor was also higher than direct judgment by hysteroscopy (0.801 vs 0.704) (**Table 6** and **Figure 2**). Although the predictor showed lower PPV (31.1% vs 85.2%, p <0.001) and specificity (49.3% vs 98.1%, p <0.001), we thought it was reasonable as a primary screening test, especially in postmenopausal group (PPV = 35.0%, specificity = 56.6%). Furthermore, we also did the external validation of the decision tree model. We used the data of new diagnosed EPs in 2019 to verify the efficacy of the noninvasive predictor. A total of 1,863 EPs were diagnosed by ultrasound and underwent hysteroscopy in 2019. Among them, the malignancy group were 25 cases, namely, 12 atypical hyperplasia and 13 cancers. All the 25 patients had AUB or large EPs with blood flow

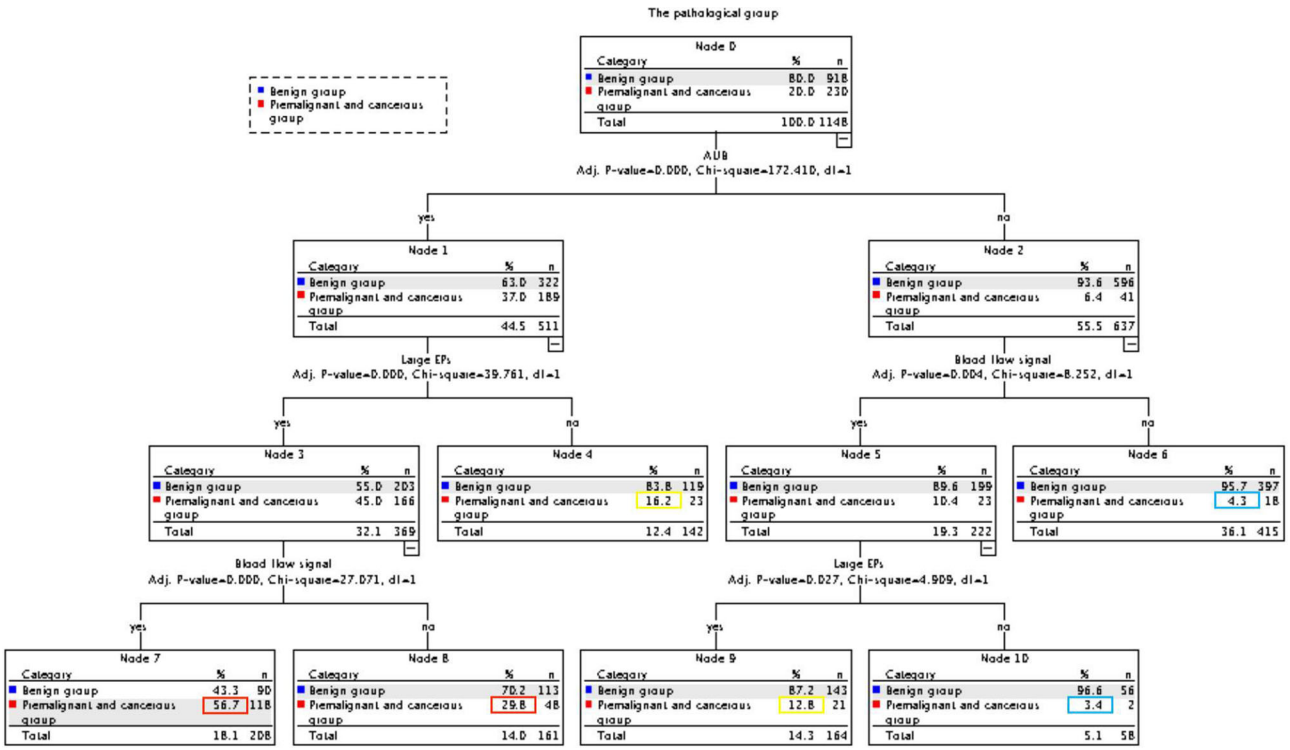


FIGURE 1 | CHAID decision tree analysis on the risk of malignancy in EPs (Nodes 6 and 10 are classified as low-risk groups, 4 and 9 as intermediate-risk groups, 7 and 8 as a high-risk group).

signal. The average age in the validation set was consistent with that of 16,020 cases between January 1, 2001 and December 31, 2018 (40.61 ± 11.94 years vs 42.14 ± 11.94, p = 0.073). For external validation, the overall accuracy for identifying malignant lesions in EPs was 89.2%, while the misclassification risk was 10.8% ± 0.7% (standard error). Our predictor still presented excellent screening value in different subgroups, with specificity of 58.5% in total population and 71.6% in postmenopausal group (**Table 6**). These results suggested that the adoption of the predictor would lead to at least 40% reduction in unnecessary surgeries.

COMMENT

As we know, hysteroscopy is recommended for EPs as both a diagnostic and therapeutic intervention (5). In the present study, all enrolled patients with EPs were subjected to hysteroscopy,

TABLE 6 | The diagnostic value of direct judgment by hysteroscopy and noninvasive predictor.

Set	Method	Groups	Sensitivity (%)	Specificity (%)	PPV (%)	NPV (%)	AUC
Set 1	A	total	42.6	98.1	85.2	87.2	0.704
		premenopausal	23.5	98.3	76.9	83.9	0.609
		postmenopausal	53.8	98.1	87.6	89.4	0.759
	B	total	91.3	49.3	31.1	95.8	0.801
		premenopausal	89.4	37.2	26.0	93.4	0.731
		postmenopausal	92.4	56.6	35.0	96.7	0.843
Set 2	A	total	36.0	99.9	90.0	99.1	0.680
		premenopausal	21.4	99.9	75.0	99.3	0.607
		postmenopausal	54.5	100	100	98.5	0.773
	B	total	100	58.5	3.2	100	0.801
		premenopausal	100	55.6	2.0	100	0.774
		postmenopausal	100	71.6	10.5	100	0.899

Set 1, Training Set; Set 2, Validation Set; Method A, Direct judgment by hysteroscopy; Method B, Noninvasive predictor; PPV, positive predictive value; NPV, negative predictive value; AUC, area under the curve.

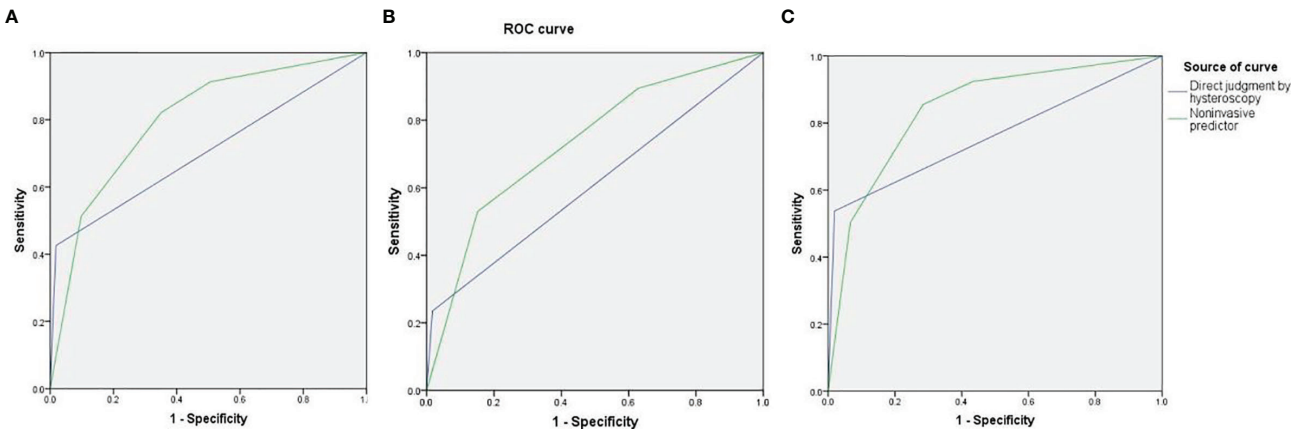


FIGURE 2 | The area under the curve (AUC) of direct judgment by hysteroscopy and noninvasive predictor in total patients **(A)**, premenopausal patients **(B)**, and postmenopausal patients **(C)**.

which allowed us to assess the final diagnosis of the "EPs" accurately by histology results. We found that 4.14% of the patients with "EPs" in benign group were validated as other diseases by histology, namely, myomas, endometrium, etc., which suggested that TVS findings were not specific (5, 19, 20). More importantly, 1.44% of the patients with clinical diagnosis of EPs were finally diagnosed as malignancy. These results suggested that the indications of hysteroscopy should be developed carefully to balance missed diagnosis and overtreatment of EPs better. The challenge is how to choose the favorable opportunity to perform hysteroscopy.

Consistent with previous studies (1, 7, 8), our results suggested that age was a high risk factor for malignancy in "EPs" patients. The mean age of malignancy was about 11 years older than benign patients. In addition to age, other factors, namely, obesity and ultrasonic instruments can also worsen the diagnostic accuracy of transvaginal ultrasound (21, 22), so we matched the age and the year of hospitalization in training set in order to better evaluate other risk factors. Our results suggested that AUB, large EPs, and blood flow signal were independent predictive factors for malignancy, no matter in all enrolled EPs patients, postmenopausal group or premenopausal group. In addition, postmenopause and AUB were both found as independent risk factors for cancer, when compared with benign and premalignant patients respectively.

Among the risk factors for malignancy mentioned above, AUB was the most significant one (1, 3, 11, 12). The malignant risk of premenopausal patients with AUB was 3.403 folds higher than those without AUB in present study, which was discordant with previous reports (1, 7, 13). This could be attributed to different study populations and sample sizes. For example, the study by Uglietti enrolled 803 premenopausal patients with only 6 malignancies (7). Nevertheless, symptomatic EPs were suggested to be removed, because evidences reported that AUB would be resolving in 75–100% of cases (5, 14, 23). Reports from Ben-arie and Ferrazzi suggested that the largest diameter of EP larger than 1.5 and 1.8 cm were risk indicators for malignancy (24, 25), while our results suggested that the diameter of EP ≥1 cm was high risk factor (OR = 2.595), which was in accord with the study by Wang (2). There are limited data and even opposed opinion to support Doppler ultrasound aiding in the differentiation of hyperplasia and malignancy in polyps (5, 26–29), but our results suggested that blood flow signal detected by TVS increased the prevalence of malignancy (OR = 2.690).

Multiple studies reported that thickened ET in postmenopausal patients was related with malignancy in "EPs" patients (30–32), with the cutoff value ranging from 0.5 to 1.1 cm (double layer). Similarly, the present study found the prevalence of malignancy in postmenopausal patients with ET ≥0.2 cm (single layer) was higher (OR 1.914) than others, which supported that thickened ET should also be alerted. Furthermore, premenopausal patients with hypertension should be ruled out malignancy, due to the OR of hypertension was 5.891. Costa-Paiva and Baiocchi also reported that hypertension was a risk factor of malignant EPs (12, 15). Although the intrinsic mechanism was not clear, hypertension has been reported that it was closely associated with hormone-dependent tumors (33).

There was no consensus for management of asymptomatic EPs up to date (1, 7, 15, 25). Thus, we further analyzed the risk factors in patients without AUB. In addition to thickened ET and blood flow signal, menopause shorter than 10 years was validated as an independent predictor of malignancy for postmenopausal patients without AUB, while in addition to large EPs and hypertension, obesity and nulliparous were considered as high risk factors for premenopausal patients without AUB. These results would help gynecologists make clinical decision for "EPs" upon certain circumstance.

Based on our encouraging data, we established a noninvasive predictor for malignancy of EPs, through combining with AUB, large EPs, and blood flow signal. Compared with the direct judgment by hysteroscopy, this predictor presented excellent sensitivity and NPV, with reasonable specificity. The AUC of this predictor reached 0.801. Further validation using new data also

suggested that noninvasive predictors were valuable as a screening indicator. Thus, the newly noninvasive predictor would undoubtedly contribute to rational clinical management for "EPs".

To our best knowledge, this was the largest scale study to evaluate the risk factors related with malignancy of "EPs", with more than 200 cases of malignancy (1, 7, 15, 25, 34–38). The large sample size permitted us to comprehensively assess the association between risk factors and malignancy through various subgroup analyses. Due to the retrospective nature of the present study, some potential risk factors might not be fully evaluated. Further prospective studies are warranted to verify the related predictor of malignancy in "EPs" patients.

CONCLUSIONS

The present study validated that AUB, large EPs and blood flow signal were important independent high risk factors for malignancy of EPs. We firstly presented a noninvasive predictor, which included AUB, large EPs (≥1 cm), and blood flow signal shown by TVS. The predictor could effectively predict the malignancy in EPs diagnosed by TVS and help gynecologist accurately choose hysteroscopy for high risk patients. As the complement to the noninvasive predictor, thickened ET in postmenopausal patients, menopause shorter than 10 years in postmenopausal patients without AUB, hypertension in premenopausal patients, obesity and nulliparous in premenopausal patients without AUB should be a concern for the possibility of malignancy. With the predictor taken with the complements together, it would be reliable to distinguish the benign lesions from malignancy for EPs diagnosed by TVS.

DATA AVAILABILITY STATEMENT

The raw data supporting the conclusions of this article will be made available by the authors, without undue reservation.

AUTHOR CONTRIBUTIONS

JX: Data curation, formal analysis, software, and writing-original draft. XR: Data curation, methodology, writing-original draft. WL: Supervision, validation and writing-review and editing. XX: Supervision, and writing-review and editing. XW, XL: Conceptualization, supervision, and writing-review and editing. All authors contributed to the article and approved the submitted version.

SUPPLEMENTARY MATERIAL

The Supplementary Material for this article can be found online at: https://www.frontiersin.org/articles/10.3389/fonc.2021.812033/full#supplementary-material

REFERENCES

1. Ricciardi E, Vecchione A, Marci R, Schimberni M, Frega A, Maniglio P, et al. Clinical Factors and Malignancy in Endometrial Polyps. Analysis of 1027 Cases. *Eur J Obstet Gynecol Reprod Biol* (2014) 183:121–4. doi: 10.1016/j.ejogrb.2014.10.021
2. Wang JH, Zhao J, Lin J. Opportunities and Risk Factors for Premalignant and Malignant Transformation of Endometrial Polyps: Management Strategies. *J Minim Invasive Gynecol* (2010) 17(1):53–8. doi: 10.1016/j.jmig.2009.10.012
3. Uglietti A, Buggio L, Farella M, Chiaffarino F, Dridi D, Vercellini P, et al. The Risk of Malignancy in Uterine Polyps: A Systematic Review and Meta-Analysis. *Eur J Obstet Gynecol Reprod Biol* (2019) 237:48–56. doi: 10.1016/j.ejogrb.2019.04.009
4. DeWaay DJ, Syrop CH, Nygaard IE, Davis WA, Van Voorhis BJ. Natural History of Uterine Polyps and Leiomyomata. *Obstet Gynecol* (2002) 100(1):3–7. doi: 10.1016/s0029-7844(02)02007-0
5. American Association of Gynecologic Laparoscopists. AAGL Practice Report: Practice Guidelines for the Diagnosis and Management of Endometrial Polyps. *J Minim Invasive Gynecol* (2012) 19(1):3–10. doi: 10.1016/j.jmig.2011.09.003
6. Yuk JS, Shin JY, Moon HS, Lee JH. The Incidence of Unexpected Uterine Malignancy in Women Undergoing Hysteroscopic Myomectomy or Polypectomy: A National Population-Based Study. *Eur J Obstet Gynecol Reprod Biol* (2018) 224:12–6. doi: 10.1016/j.ejogrb.2018.03.003
7. Uglietti A, Mazzei C, Deminico N, Somigliana E, Vercellini P, Fedele L. Endometrial Polyps Detected at Ultrasound and Rate of Malignancy. *Arch Gynecol Obstet* (2014) 289(4):839–43. doi: 10.1007/s00404-013-3037-z
8. Sasaki LMP, Andrade KRC, Figueiredo ACMG, Wanderley MDS, Pereira MG. Factors Associated With Malignancy in Hysteroscopically Resected Endometrial Polyps: A Systematic Review and Meta-Analysis. *J Minim Invasive Gynecol* (2018) 25(5):777–85. doi: 10.1016/j.jmig.2018.02.004
9. Kilicdag EB, Haydardedeoglu B, Cok T, Parlakgumus AH, Simsek E, Bolat FA. Polycystic Ovary Syndrome and Increased Polyp Numbers as Risk Factors for Malignant Transformation of Endometrial Polyps in Premenopausal Women. *Int J Gynaecol Obstet* (2011) 112(3):200–3. doi: 10.1016/j.ijgo.2010.10.014
10. Shushan A, Revel A, Rojansky N. How Often are Endometrial Polyps Malignant? *Gynecol Obstet Invest* (2004) 58(4):212–5. doi: 10.1159/000080189
11. Litta P, Di Giuseppe J, Moriconi L, Delli Carpini G, Piermartiri MG, Ciavattini A. Predictors of Malignancy in Endometrial Polyps: A Multi-Institutional Cohort Study. *Eur J Gynaecol Oncol* (2014) 35(4):382–6.
12. Costa-Paiva L, Godoy CE Jr, Antunes A Jr, Caseiro JD, Arthuso M, Pinto-Neto AM. Risk of Malignancy in Endometrial Polyps in Premenopausal and Postmenopausal Women According to Clinicopathologic Characteristics. *Menopause* (2011) 18(12):1278–82. doi: 10.1097/gme.0b013e31821e23a1
13. Elfayomy AK, Soliman BS. Risk Factors Associated With the Malignant Changes of Symptomatic and Asymptomatic Endometrial Polyps in Premenopausal Women. *J Obstet Gynaecol India* (2015) 65(3):186–92. doi: 10.1007/s13224-014-0576-6
14. Lieng M, Istre O, Sandvik L, Engh V, Qvigstad E. Clinical Effectiveness of Transcervical Polyp Resection in Women With Endometrial Polyps: Randomized Controlled Trial. *J Minim Invasive Gynecol* (2010) 17(3):351–7. doi: 10.1016/j.jmig.2010.01.019
15. Baiocchi G, Manci N, Pazzaglia M, Giannone L, Burnelli L, Giannone E, et al. Malignancy in Endometrial Polyps: A 12-Year Experience. *Am J Obstet Gynecol* (2009) 201(5):462.e1–462.e4624. doi: 10.1016/j.ajog.2009.05.055
16. Gambadauro P, Martínez-Maestre MÁ, Schneider J, Torrejón R. Endometrial Polyp or Neoplasia? A Case-Control Study in Women With Polyps at Ultrasound. *Climacteric* (2015) 18(3):399–404. doi: 10.3109/13697137.2014.967673
17. Pergialiotis V, Prodromidou A, Siotos C, Frountzas M, Perrea D, Vlachos GD. Systemic Hypertension and Diabetes Mellitus as Predictors of Malignancy Among Women With Endometrial Polyps: A Meta-Analysis of Observational Studies. *Menopause* (2016) 23(6):691–7. doi: 10.1097/GME.0000000000000602
18. Ngo YG, Fu HC, Chu L, Tseng C, Chen C, Lee C, et al. Specific Hysteroscopic Findings can Efficiently Distinguish the Differences Between Malignant and Benign Endometrial Polyps. *Taiwan J Obstet Gynecol* (2020) 59(1):85–90. doi: 10.1016/j.tjog.2019.11.013

19. Bernard JP, Rizk E, Camatte S, Robin F, Taurelle R, Lecuru F. Saline Contrast Sonohysterography in the Preoperative Assessment of Benign Intrauterine Disorders. *Ultrasound Obstet Gynecol* (2001) 17(2):145–9. doi: 10.1046/j.1469-0705.2001.00336.x
20. Nalaboff KM, Pellerito JS, Ben-Levi E. Imaging the Endometrium: Disease and Normal Variants. *Radiographics* (2001) 21(6):1409–24. doi: 10.1148/radiographics.21.6.g01nv211409
21. Fischerova D, Frühauf F, Zikan M, Pinkavova I, Kocián R, Dundr P, et al. Factors Affecting Sonographic Preoperative Local Staging of Endometrial Cancer. *Ultrasound Obstet Gynecol* (2014) 43(5):575–85. doi: 10.1002/uog.13248
22. Capozzi VA, Merisio C, Rolla M, Pugliese M, Morganelli G, Cianciolo A, et al. Confounding Factors of Transvaginal Ultrasound Accuracy in Endometrial Cancer. *J Obstet Gynaecol* (2021) 41(5):779–84. doi: 10.1080/01443615.2020.1799342
23. Nathani F, Clark TJ. Uterine Polypectomy in the Management of Abnormal Uterine Bleeding: A Systematic Review. *J Minim Invasive Gynecol* (2006) 13(4):260–8. doi: 10.1016/j.jmig.2006.03.015
24. Ben-Arie A, Goldchmit C, Laviv Y, Levy R, Caspi B, Huszar M, et al. The Malignant Potential of Endometrial Polyps. *Eur J Obstet Gynecol Reprod Biol* (2004) 115(2):206–10. doi: 10.1016/j.ejogrb.2004.02.002
25. Ferrazzi E, Zupi E, Leone FP, Savelli L, Omodei U, Moscarini M, et al. How Often are Endometrial Polyps Malignant in Asymptomatic Postmenopausal Women? A Multicenter Study. *Am J Obstet Gynecol* (2009) 200(3):235. doi: 10.1016/j.ajog.2008.09.876
26. Alcázar JL, Castillo G, Mínguez JA, Galán MJ. Endometrial Blood Flow Mapping Using Transvaginal Power Doppler Sonography in Women With Postmenopausal Bleeding and Thickened Endometrium. *Ultrasound Obstet Gynecol* (2003) 21(6):583–8. doi: 10.1002/uog.143
27. Vuento MH, Pirhonen JP, Mäkinen JI, Tyrkkö JE, Laippala PJ, Grönroos M, et al. Screening for Endometrial Cancer in Asymptomatic Postmenopausal Women With Conventional and Colour Doppler Sonography. *Br J Obstet Gynaecol* (1999) 106(1):14–20. doi: 10.1111/j.1471-0528.1999.tb08079.x
28. de Kroon CD, Hiemstra E, Trimbos JB, Jansen FW. Power Doppler Area in the Diagnosis of Endometrial Cancer. *Int J Gynecol Cancer* (2010) 20(7):1160–5. doi: 10.1111/igc.0b013e3181f0df98
29. Goldstein SR, Monteagudo A, Popiolek D, Mayberry P, Timor-Tritsch I. Evaluation of Endometrial Polyps. *Am J Obstet Gynecol* (2002) 186(4):669–74. doi: 10.1067/mob.2002.122128
30. Zhang Y, Chen M, Guo YS, Duan H. Clinical Characters of Pre-Malignant and Malignant Polyp in Postmenopausal Women and the Diagnostic Value of Hysteroscopy. *Zhonghua Fu Chan Ke Za Zhi* (2016) 51(05):366–70. doi: 10.3760/cma.j.issn.0529-567X.2016.05.009
31. Tofiloska V, Velik-Stefanovska V, Dimitrov G. The Connection Between the Endometrial Thickness and the Risk of Endometrial Malignancy in Postmenopausal Women. *Open Access Maced J Med Sci* (2019) 7(14):2263–6. doi: 10.3889/oamjms.2019.639
32. Smith-Bindman R, Kerlikowske K, Feldstein VA, Subak L, Scheidler J, Segal M, et al. Endovaginal Ultrasound to Exclude Endometrial Cancer and Other Endometrial Abnormalities. *JAMA* (1998) 280(17):1510–7. doi: 10.1001/jama.280.17.1510
33. Hamet P. Cancer and Hypertension: A Potential for Crosstalk? *J Hypertens* (1997) 15(12 Pt 2):1573–7. doi: 10.1097/00004872-199715120-00058
34. Lasmar BP, Lasmar RB. Endometrial Polyp Size and Polyp Hyperplasia. *Int J Gynaecol Obstet* (2013) 123(3):236–9. doi: 10.1016/j.ijgo.2013.06.027
35. Lenci MA, Nascimento VA, Grandini A, Fahmy W, Depes D, Baracat F, et al. Premalignant and Malignant Lesions in Endometrial Polyps in Patients Undergoing Hysteroscopic Polypectomy. *Einstein (Sao Paulo)* (2014) 12(1):16–21. doi: 10.1590/s1679-45082014ao2764
36. Kuribayashi Y, Nakagawa K, Sugiyama R, Motoyama H, Sugiyama R. Frequency of Endometrial Cancer and Atypical Hyperplasia in Infertile Women Undergoing Hysteroscopic Polypectomy. *J Obstet Gynaecol Res* (2017) 43(9):1465–71. doi: 10.1111/jog.13408
37. Gambadauro P, Martínez-Maestre MÁ, Schneider J, Torrejón R. Malignant and Premalignant Changes in the Endometrium of Women With an Ultrasound Diagnosis of Endometrial Polyp. *J Obstet Gynaecol* (2014) 34(7):611–5. doi: 10.3109/01443615.2014.916255
38. Golan A, Cohen-Sahar B, Keidar R, Condrea A, Ginath S, Sagiv R. Endometrial Polyps: Symptomatology, Menopausal Status and Malignancy. *Gynecol Obstet Invest* (2010) 70(2):107–12. doi: 10.1159/000298767

Conflict of Interest: The authors declare that the research was conducted in the absence of any commercial or financial relationships that could be construed as a potential conflict of interest.

Publisher's Note: All claims expressed in this article are solely those of the authors and do not necessarily represent those of their affiliated organizations, or those of the publisher, the editors and the reviewers. Any product that may be evaluated in this article, or claim that may be made by its manufacturer, is not guaranteed or endorsed by the publisher.

Copyright © 2022 Xu, Rao, Lu, Xie, Wang and Li. This is an open-access article distributed under the terms of the Creative Commons Attribution License (CC BY). The use, distribution or reproduction in other forums is permitted, provided the original author(s) and the copyright owner(s) are credited and that the original publication in this journal is cited, in accordance with accepted academic practice. No use, distribution or reproduction is permitted which does not comply with these terms.

frontiers in Oncology

ORIGINAL RESEARCH
published: 28 January 2022
doi: 10.3389/fonc.2022.748403

PFKFB3 Regulates Chemoresistance, Metastasis and Stemness *via* IAP Proteins and the NF-κB Signaling Pathway in Ovarian Cancer

Yu-xin Jiang[1,2†], Michelle K. Y. Siu[1†], Jing-jing Wang[1], Thomas H. Y. Leung[1], David W. Chan[1], Annie N. Y. Cheung[3], Hextan Y. S. Ngan[1] and Karen K. L. Chan[1]*

[1] Department of Obstetrics and Gynaecology, University of Hong Kong, Hong Kong, Hong Kong SAR, China,
[2] Department of Gynaecology, The First Affiliated Hospital of Nanjing Medical University, Jiangsu, China,
[3] Department of Pathology, University of Hong Kong, Hong Kong, Hong Kong SAR, China

OPEN ACCESS

Edited by:
Ram N. Ganapathi, Carolinas Healthcare System, United States

Reviewed by:
Dong-Joo (Ellen) Cheon, Albany Medical College, United States
Carrie D. House, San Diego State University, United States

***Correspondence:**
Karen K. L. Chan
kklchan@hku.hk

†These authors have contributed equally to this work

Specialty section:
This article was submitted to Gynecological Oncology, a section of the journal Frontiers in Oncology

Received: *27 July 2021*
Accepted: *03 January 2022*
Published: *28 January 2022*

Citation:
Jiang Y-x, Siu MKY, Wang J-j, Leung THY, Chan DW, Cheung ANY, Ngan HYS and Chan KKL (2022) PFKFB3 Regulates Chemoresistance, Metastasis and Stemness via IAP Proteins and the NF-κB Signaling Pathway in Ovarian Cancer. Front. Oncol. 12:748403. doi: 10.3389/fonc.2022.748403

Glycolysis has been reported to be critical for cancer stem cells (CSCs), which are associated with tumor chemoresistance, metastasis and recurrence. Thus, selectively targeting glycolytic enzymes may be a potential therapy for ovarian cancer. 6-phosphofructo-2-kinase/fructose-2,6-biphosphatase 3 (PFKFB3), the main source of fructose-2,6-bisphosphate, controls the first committed step in glycolysis. We investigate the clinical significance and roles of PFKFB3 in ovarian cancer using *in vitro* and *in vivo* experiments. We demonstrate that PFKFB3 is widely overexpressed in ovarian cancer and correlates with advanced stage/grade and poor outcomes. Significant up-regulation of PFKFB3 was found in ascites and metastatic foci, as well as CSC-enriched tumorspheres and ALDH+CD44+ cells. 3PO, a PFKFB3 inhibitor, reduced lactate level and sensitized A2780CP cells to cisplatin treatment, along with the modulation of inhibitors of apoptosis proteins (c-IAP1, c-IAP2 and survivin) and an immune modulator CD70. Blockade of PFKFB3 by siRNA approach in the CSC-enriched subset led to decreases in glycolysis and CSC properties, and activation of the NF-κB cascade. PFK158, another potent inhibitor of PFKFB3, impaired the stemness of ALDH+CD44+ cells *in vitro* and *in vivo*, whereas ectopic expression of PFKFB3 had the opposite results. Overall, PFKFB3 was found to mediate metabolic reprogramming, chemoresistance, metastasis and stemness in ovarian cancer, possibly *via* the modulation of inhibitors of apoptosis proteins and the NF-κB signaling pathway; thus, suggesting that PFKFB3 may be a potential therapeutic target for ovarian cancer.

Keywords: PFKFB3, stemness, PFK158, therapeutic target, ovarian cancer

INTRODUCTION

Ovarian cancer is the leading cause of death in gynecologic malignancies with 75% of patients presenting late at the advanced stages. Optimal treatment involves primary cytoreductive surgery followed by adjuvant chemotherapy with cisplatin. Unfortunately, the prognosis is not optimistic due to chemoresistance and frequent relapse. Identifying the related molecular mechanisms can

help to develop alternative therapeutic strategies for ovarian cancer (1). Unlike other tumors, ovarian cancer has a unique pattern of metastasis. Because of the lack of an anatomical barrier, ovarian cancer cells are likely to separate from the primary lesion, shed and flow into the abdominal cavity and spread *via* the peritoneal fluid which allows cancer cells to spread into the distant organs (2). Most advanced ovarian cancer patients are diagnosed with accumulation of peritoneal fluid (also known as ascites fluid). Previous studies have indicated that "spheroids" or "tumorspheres" can be enriched in ascites from patients with ovarian cancer with enhanced tumorigenesis and cancer stem cell (CSC) properties (3, 4). Accumulating evidence suggests that CSCs or tumor-initiating cells may be the source of all tumor cells and a cause of metastasis, chemoresistance and recurrence (5). Thus, targeting CSCs may be a novel therapeutic strategy for ovarian cancer.

Accumulating evidence suggests that glycolysis is critical for CSC maintenance (6). Pyruvate dehydrogenase (PDH), a key enzyme responsible for switching pyruvate toward the tricarboxylic acid cycle in mitochondria and away from glycolysis, is diminished in CD44+/MyD88+ ovarian CSCs (7). A subset of radio-resistant ovarian cancer cells has been identified with CSC-like aggressive properties, up-regulated glucose transporter 1 (GLUT1) expression and an elevated extracellular acidification rate. Moreover, 188Re-Liposome, an anti-cancer drug, has been found to suppress tumor growth by shifting glycolysis toward oxidative phosphorylation (OXPHOS) (8). With metabolic assays, spheroids have been derived from ascites with enhanced glycolytic influx and resistance to oxygen deprivation (3). These studies have indicated the crucial role of glycolysis in ovarian CSCs regulation, although the underlying mechanism remains unknown.

Phosphofructokinase 1 (PFK1), a key enzyme in glycolysis, is regulated by fructose-2,6-bisphosphate (F-2,6-BP). F-2,6-BP is induced by 6-phosphofructo-2-kinase/fructose-2,6-biphosphatase 3 (PFKFB3) *via* its kinase activity, thereby enhancing glycolysis. PFKFB3 has been reported to be up-regulated in malignant tumors compared with normal tissue in leukemia and several human cancers, including colorectal, breast, lung, thyroid and nasopharyngeal cancer (9–13). Up-regulation of PFKFB3 expression in nasopharyngeal (12) and breast (13) cancers promotes tumor cell proliferation, metastasis and angiogenesis. Beyond glycolysis, PFKFB3 has been revealed to be involved in the cell cycle in breast cancer cells by degrading p27, which inhibits G1/S transition and promotes apoptosis (14). A recent study has suggested that high expression of PFKFB3 indicates poor prognosis and enhances the self-renewal capacity of CSCs by *in vivo* extreme limiting dilution assays in breast cancer (15). However, the role of PFKFB3 in tumorigenesis, CSCs regulation of ovarian cancer, remains to be further elucidated.

Firstly, the clinical significance of PFKFB3 in ovarian cancer was assessed. We then investigated the effects and mechanism of PFKFB3 on ovarian cancer metabolic switch and regulation of chemoresistance to cisplatin using one of its inhibitors 3PO. In our recent study, we found that ALDH+CD44+ cells isolated from ascites-derived tumor cells show enhanced CSC properties (16). Here, we isolated tumorspheres or an ALDH+CD44+ cell subset from ascites or ascites-originating ovarian cancer cell lines (SKOV3 and OVCAR3) and compared the PFKFB3 expression between the CSC-enriched subpopulation and non-CSCs. Functional assays were conducted, and the downstream signaling pathway through which PFKFB3 affects stemness in the CSC-enriched subpopulation was studied using siRNA approach and treatment with another PFKFB3 inhibitor, PFK 158. Our *in vitro* and *in vivo* results show that PFKFB3 was overexpressed in ovarian cancer, ascites-derived tumor cells and CSC-enriched subpopulations. Knockdown of PFKFB3 or blocking PFKFB3 with 3PO/PFK158 reduced lactate production, sensitized resistant cells to cisplatin treatment and inhibited CSC properties and tumor growth. In contrast, overexpression of PFKFB3 led to the opposite effects. The mechanisms involve inhibition of apoptosis and activation of NF-κB signaling pathway. Thus, PFKFB3 might be used as a potential therapeutic target in treating ovarian cancer.

MATERIALS AND METHODS

Clinical Samples and Cell Lines

A tissue microarray analysis (TMA, OVC1021; Biomax) with 102 cores from four normal benign and 97 ovarian cancer tissues was performed in duplicate. Number of samples in each categories were shown in **Figure 1B**. Clinicopathological characteristics of 97 samples were shown in **Supplementary Table S1**. Archived formalin-fixed, paraffin-embedded (FFPE) samples from 13 pairs of advanced-stage high-grade serous primary ovarian cancer tissues and their matched metastatic foci from the Queen Mary Hospital (University of Hong Kong) were used for this study. Fresh ascitic fluid and primary tissue samples were obtained from patients underwent tumor-debulking surgery for serous, clear cell and endometrioid ovarian cancer, followed by chemotherapy. Primary cancer cells and matched ascites cancer cells were from serous ovarian cancer. Tumorsphere/monolayer cancer cells derived from ascites were from serous and clear cell ovarian cancers. Ascites cancer cells used for functional assays after transient knockdown of PFKFB3 were from serous and endometrioid ovarian cancers. Ascitic fluid and tissue samples were isolated into single cells. Briefly, solid tumor tissues were finely minced with scissors, incubated with $Ca2^{+}$/$Mg2^{+}$-free PBS containing 1 mg/mL collagenase/dispase (Roche, UK) at 37°C for 80 min, filtered through a sterile cell strainer (40 μm; Corning, NY, USA), and centrifuged at 100 g for 10 min. The ascitic fluid was centrifuged at 100 g for 10 min, the supernatant fraction was discarded, and the cell pellet was collected. To exclude erythrocytes, we purified the obtained single cells with various solutions of NaCl. The isolated cells were cultured in 1:1 mixture of MCDB 105 medium and Medium 199 (Sigma-Aldrich) with 10% fetal bovine serum (Gibco) and 1% penicillin-streptomycin. The use of patient samples was approved by the Institution Ethical Review Board of the University of Hong Kong (UW 16-107). The normal human ovarian surface epithelial cell line HOSE 11-12 was provided by Professor SW Tsao (School of Biomedical Sciences, University of Hong Kong). Three human ovarian cancer cell lines, SKOV3,

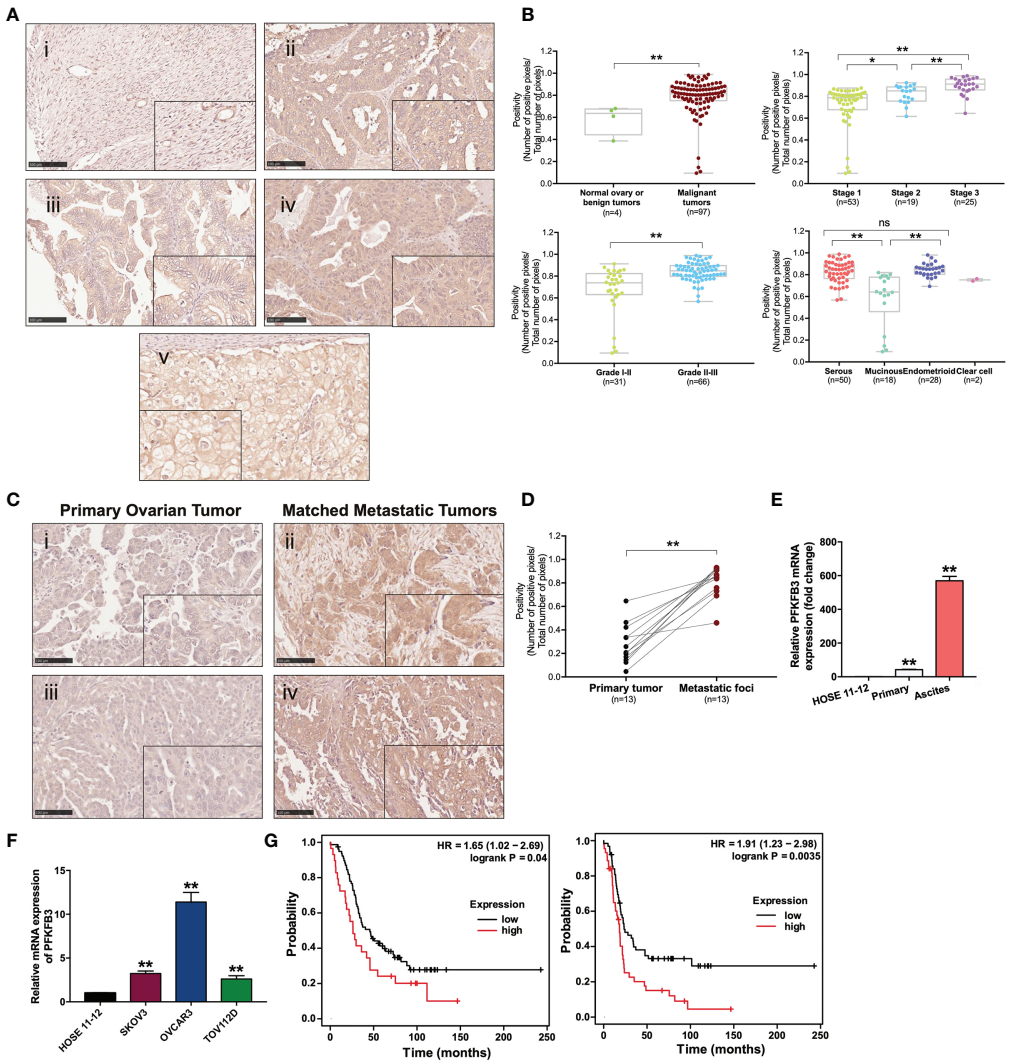


FIGURE 1 | Overexpression of PFKFB3 in ovarian cancer is correlated with metastasis and poor prognosis. **(A)** Representative images of PFKFB3 expression in (i) normal ovarian tissue, (ii) serous, (iii) mucinous, (iv) endometrioid and (v) clear cell subtypes of tumor samples on ovarian cancer TMA (OVC1021, Biomax) by IHC staining (scale bar, 100 μm). The insets highlight regions with higher magnification. **(B)** Association of PFKFB3 with stage/grade/histotype in ovarian cancer. The graphs for stage and grade encompass all four histotypes. **(C)** Representative images of IHC staining for PFKFB3 expression in ovarian primary tumors (i, iii) and their metastatic foci (ii, iv; scale bar, 100 μm). **(D)** Bar chart showing PFKFB3 staining in 13 pairs of tissues. **(E)** Relative PFKFB3 mRNA expression in HOSE 11-12, primary cancer cells and matched ascites cancer cells from high-grade serous ovarian cancer, determined by qPCR. **(F)** PFKFB3 expression in HOSE 11-12 and ovarian cancer cell lines (SKOV3, OVCAR3, and TOV112D) at the mRNA level, determined by qPCR. **(G)** (left) Overall and (right) progression-free survival rates were analyzed with the log-rank test for PFKFB3 high/low groups of ovarian cancer patients obtained from GSE26193 (n = 107), by using the Kaplan-Meier plotter. (*$p < 0.05$, **$p < 0.01$; n.s., not significant).

OVCAR3 and TOV112D, were purchased from ATCC (Manassas, VA, USA). A2780S, a cisplatin chemosensitive cell line, and its chemoresistant counterpart A2780CP, were provided by Prof. Benjamin B.K. Tsang (Department of Obstetrics & Gynaecology and Cellular & Molecular Medicine, University of Ottawa).

Tumorsphere Culture

Single cells were seeded into six-well ultra-low attachment plates at a density of 2000–5000 cells/well containing serum-free DMEM/F12 (1:1) (Gibco, MD, USA) supplemented with 10 ng/mL basic fibroblast growth factor (Sigma-Aldrich, MO, USA), 20 ng/mL human epidermal growth factor (Sigma-Aldrich) and 5 μg/mL insulin. Every 2 days, fresh medium was added to each well without removal of the old medium. Tumorspheres, defined as multicellular cell aggregates floating in the medium 7-14 days after culture, were used for mRNA and protein extraction, as well as for functional assays.

Fluorescence-Activated Cell Sorting

Fluorescence-activated cell sorting (FACS) was used to isolate the ALDH and CD44 double-positive/double-negative

subpopulation. Briefly, cells were suspended and incubated in ALDEFLUOR™ Assay Buffer containing ALDEFLUOR™ reagent (StemCell Technologies, Canada) at 37°C for 30 min and centrifuged for 10 min at 300 g; the supernatant was then discarded. APC-conjugated CD44 antibody (Miltenyi Biotec, Germany) was added to the cells resuspended in Flow Buffer (Miltenyi Biotec, Germany) with the FcR Blocking Reagent. Then the mixture was incubated in the dark for 30 min at 4°C. Cells were stained with the ALDH inhibitor diethylaminobenzaldehyde (DEAB), and anti-IgG-APC was used as a negative control for flow cytometry gating.

Transient Transfection of PFKFB3

For transient knockdown, two commercially obtained PFKFB3 siRNA (Cat#: 4427038; siRNA #1 ID:s10357; siRNA #2 ID: s10359; Ambion; USA) (transfected as duplexes) and control siRNA (Cat#: 4390846; Ambion; USA) were introduced into cancer cells *via* SilentFect reagent (Bio-Rad, Canada). For transient overexpression, PFKFB3 (Cat#: RC22748L2) and control vector (Cat#: PS100071) plasmids (GFP-tagged; OriGene, MD, USA) were introduced into cancer cells with Lipofectamine 3000 reagent (Invitrogen, Canada). For transfection in tumorspheres, spheres were dissociated into single cells and seeded into six-well ultra-low attachment plates 24 h before transfection (17). The cells were harvested and plated for the subsequent functional assays 48 h after transfection.

Drug Treatment

For cisplatin treatment, A2780S and A2780CP cells were plated 24 h before treatment with cisplatin (0, 2.5, 5 and 10 μM) (Invitrogen, Canada) for 48 h. For 3PO and cisplatin co-treatment, A2780CP cells were plated 24 h before treatment with cisplatin (20 μM) and 3PO (10 μM) (Sigma, USA). ddH2O and DMSO were used as vehicle for cisplatin and 3PO, respectively. For PFK158 treatments, ALDH+CD44+ SKOV3 cells were plated 12 h before treatment with PFK158 (0.5, and 1.0 μM) (Axon Medchem, Holland) or control vehicle (ddH2O) for 48 h.

Immunohistochemistry

Immunohistochemistry (IHC) analysis of TMA and FFPE-tissue sections was performed according to the manufacturer's instructions. Briefly, the sections were incubated with anti-PFKFB3 antibody (rabbit anti-PFKFB3, 1:100; Cat. #AP8145b, ABGENT, San Diego, USA) at 4°C overnight in the dark and then incubated with Labelled Polymer-HRP solution (Dako, CA, USA) and 1% 3, 3-diaminobenzidine-hydrogen peroxide (Sigma-Aldrich). The expression was analyzed with a positive pixel count algorithm by ImageScope software (www.aperio.com). According to positive and negative control tissues. the color saturation threshold, with the peak (1.0) and bottom (0) limits for the strongest and weakest pixel settings was set by the software. Based on the intensity and quantity of positive pixels, which was normalized to the number of pixels counted in the selected representative areas, positive pixel counting (positivity) was calculated automatically. Five representative areas were selected and an average score obtained for each core of TMA and sample tissue section. Negative control with primary antibody replaced with PBS was performed.

Real-Time PCR

Total RNA was extracted from ovarian cancer cells with a NucleoSpin® RNA Kit (Macherey-Nagel, Germany) and used to generate cDNA with SuperScript VILO™ Master Mix (Invitrogen) according to the manufacturer's instructions. The expression levels of mRNAs were quantified with the ABI Prism 7700 platform (Life Technologies) with SYBR Green qPCR Master Mix (ExCell, China). The relative mRNA expression levels were assessed with the comparative Ct method with GAPDH as the reference gene. The primers used in this study are as follows: GAPDH forward 5′ to 3′ TCCATGACAACT TTGGTATCGTG, reverse 5′ to 3′ ACAGTCTTCTGGGTG GCAGTG; PFKFB3 forward 5′ to 3′ CAGTTGTGGCCTCCA ATATC, reverse 5′ to 3′ GCTTCATAGCAACTGATCC; KLF4 forward 5′ to 3′ GGGAGAAGACACTGCGTCAA, and reverse 5′ to 3′ GGAAGTCGCTTCATGTGGGA.

Human Apoptosis RT^2 Profiler PCR Array

To examine the apoptotic pathways by which 3PO inhibits the chemoresistant phenotype of cancer cells, the expression of 84 apoptosis-related genes in cisplatin (20 μM) and 3PO (10 μM) treatment was evaluated using the human apoptosis RT^2 profiler PCR array (PAHS-012Z, Qiagen, Germany). qPCR was performed on a real-time PCR System (ABI Vii7 Fast, Life Technologies). Data analysis was performed by the RT^2 profiler PCR array software with normalization genes automatically selected from the full plate.

Immunoblot Analysis

Protein was prepared by lysing cells in CelLyticTM M solution (Sigma-Aldrich) with a protease inhibitor cocktail. After protein quantification with a NanoDrop 2000/2000c spectrophotometer (Thermo Scientific, US), equal amounts of protein lysates were loaded and resolved by SDS-PAGE and transferred to a polyvinylidene difluoride membrane. Protein signals were immunodetected with the appropriate antibodies (rabbit anti-PFKFB3, 1:1000, ABGENT, AP8145b; rabbit anti-PARP, 1:1000, CST, #9542; rabbit anti-c-IAP1, 1:1000, CST #7065; rabbit anti-c-IAP2, 1:1000, CST #3130; and rabbit anti-survivin, 1:1000, CST #2808; PARP, 1:1000, CST, #9542; rabbit anti-KLF4, 1:1000, CST, #4038; rabbit anti-BMI1, 1:1000, CST, #58565; rabbit anti-p-p65, 1:1000, CST, #3033; rabbit anti-p65, 1:1000, CST, #4765; and mouse anti-Actin, 1:50, 000, Abcam, ab6276).

Metabolic Assays

Lactate levels and oxygen consumption rate were measured with a Lactate Colorimetric Assay Kit II (BioVision, Canada) and Extracellular Oxygen Consumption Assay (Abcam), according to the manufacturers' instructions and normalized to cell number.

Annexin-V-FLUOS Staining

The apoptosis status of cells after 3PO treatment with or without cisplatin treatment was evaluated by Annexin-V-FLUOS Staining Kit (Roche) following the protocol provided by the

manufacturer. Briefly, the harvested single cells were incubated with FITC-conjugated annexin-V reagent and PI and detected by flow cytometry analysis. Early apoptosis (annexin V+PI-) and late apoptosis (annexin V+PI+) were included into apoptotic cells.

Transwell Migration and Invasion Assays

Transwell migration and invasion assays were conducted to measure cellular capacity to migrate and invade *in vitro*. For migration and invasion assays using tumorspheres, spheres were dissociated into single cells before cell plating. Briefly, an equal quantity (1.25×10^5) of cells cultured in serum-free medium was transferred to the top chamber with an 8.0 μm pore polycarbonate membrane for migration and a Matrigel-coated membrane for invasion. The lower chamber was filled with 10% fetal bovine serum medium. The assays continued for 12–24 h, and cells that had migrated/invaded were fixed, stained with 0.5% crystal violet and imaged. The migration/invasion capacity was normalized to that of control cells.

Clonogenic Assays

Cancer cells were serially diluted and seeded in triplicate into a six-well plate at a density of 500 cells/well and colony formation was performed over 10 to 14 days. Then, cells were stained with 0.05% crystal violet, and colonies of >50 cells were counted.

Sphere Formation Assays

Sphere formation assays were conducted by culturing cancer cells with CSC medium in six-well ultra-low attachment plates at a density of 2000–5000 cells/well and allowing the cells to grow for 7–14 days. Then, 300 μl fresh CSC medium was added to the plates every second day. Spheres with diameters >50 μm were counted.

In Vivo Tumorigenicity Analysis *via* Subcutaneous Implantation and Limiting Dilution Assays

For *in vivo* tumorigencity analysis, BALB/c nude mice (7–8 weeks) with T cell-deficiency were used, according to protocols approved by the Committee of the Use of Live Animals in Teaching and Research (CULATR) under an approved license (No. 4598-18). FACS-sorted ALDH+CD44+ SKOV3 cells were pre-treated with PFK158 (1.0 μM) or control vehicle (ddH_2O) for 3 days, collected, suspended in a mixture of RPMI medium and Matrigel (High Concentration, Corning), and subcutaneously injected into the flanks of mice after serial dilution (3×10^5, 1×10^4, 5×10^3, or 2.5×10^3 cells) (18). Each group consisted of five mice, and tumor incidence was recorded. The estimated frequency of CSCs was calculated *via* Extreme Limiting Dilution Analysis software (http://bioinf.wehi.edu.au/software/elda/). For the group injected with 3×10^5 cells, tumor formation time, size and weight were recorded every 3 to 5 days for 28 days. The mice were euthanized at 28 days post tumor inoculation with 150 mg/kg pentobarbital after the experiment.

Cancer Genome Atlas Dataset (TCGA) and Gene Expression Profiling Interactive Analysis (GEPIA)

The online software GEPIA (www.gepia.cancer-pku.cn) was used to analyze the correlation between target genes and PFKFB3 in ovarian cancer on the basis of the TCGA database.

Statistical Analysis

The data are shown as the means ± SEM of triplicate experiments. GraphPad Prism 7.0 software was used for data analysis with a two-tailed t-test or one-way ANOVA. The survival rate was analyzed with Kaplan-Meier Plotter (www.kmplot.com), and hazard ratios and log-rank P-values were calculated automatically on the basis of the optimal cutoff value auto-selected in the software. Differences were considered statistically significant at $p < 0.05$ (* represents $p<0.05$ and ** $p<0.01$).

RESULTS

Overexpression of PFKFB3 in ovarian cancer correlates with metastasis and poor prognosis to study the role of PFKFB3 in ovarian cancer, we analyzed two independent microarray databases from Oncomine. Statistical up-regulation of PFKFB3 was observed in ovarian cancer tissues compared with normal ovary tissues (**Table 1**). TMA analysis was used to study the expression of PFKFB3 in ovarian cancer tissues. In the cytoplasm, PFKFB3 was found to be more highly expressed in malignant tumors than in normal tissues/benign tumors (**Figure 1A**). Specifically, PFKFB3 was significantly up-regulated in higher grades and stages (**Figure 1B**). For histologic subtypes, serous and endometrioid subtypes had significantly higher expression than the mucinous subtype (**Figure 1B**). Since the sample number of clear cell subtype is small (n=2), we have not used this subtype for statistical analysis. In addition, 13 pairs of FFPE tissue sections composed of metastatic foci and matched primary ovarian tumors were examined through PFKFB3 staining with IHC (**Figure 1C**). Statistically higher expression of PFKFB3 was observed in the metastatic foci (**Figure 1D**). No staining was observed in negative control with primary antibody replaced with PBS (**Supplementary Figure 1**). PFKFB3 was further detected to be up-regulated in ascites-derived tumor cells compared with

TABLE 1 | Detailed information about the 3 public expression datasets of Oncomine database about PFKFB3 in ovarian cancer.

Datasets (sample size)	Comparison Groups	Fold Change	P value	Overexpression Gene Rank
Lu Ovarian (50)	Ovarian Serous Adenocarcinoma vs. Normal	1.596	0.007	2184 (in top 13%)
	Ovarian Mucinous Adenocarcinoma vs. Normal	2.015	0.011	1224 (in top 7%)
Welsh Ovarian (32)	Ovarian Serous Surface Papillary Carcinoma vs. Normal	2.079	0.008	1478 (in top 28%)

primary tumor cells (**Figure 1E**) by qPCR; thus, suggesting that PFKFB3 is associated with metastasis in ovarian cancer. Moreover, Real-time PCR (qPCR) revealed up-regulation of PFKFB3 in ovarian cancer cell lines (SKOV3, OVCAR3 and TOV112D) compared with the HOSE 11-12 cell line (**Figure 1F**).

To investigate the prognostic value of PFKFB3 in ovarian cancer at the mRNA level, we analyzed a clinical database (GSE26193) containing data from 107 patients, by using Kaplan-Meier Plotter with the auto-selected best cutoff. Higher PFKFB3 was associated with poorer overall (p=0.04) and progression-free (p=0.0035) survival; thus, suggesting a correlation between PFKFB3 and poor outcomes in ovarian cancer (**Figure 1G**).

PFKFB3 Regulates Chemoresistance in Ovarian Cancer

To study the effect of PFKFB3 on chemoresistance of ovarian cancer, we first detected PFKFB3 expression in A2780S and A2780CP cells after cisplatin treatment (0, 2.5, 5 and 10 μM) for 48 h. Our findings of decreased PFKFB3 protein expression in A2780S cells but not in A2780CP cells after cisplatin treatment (**Figure 2A**), suggesting a differential regulation of PFKFB3 expression between sensitive and resistant ovarian cancer cells by cisplatin treatment. We further detected that treatment of chemoresistant A2780CP cells with 3-(3-pyridinyl)-1-(4-pyridinyl)-2-propen-1-one (3PO), the first compound for PFKFB3 inhibition (20), could decrease lactate production (**Figure 2B**). Then, we investigated if 3PO would abolish drug resistance of A2780CP by treating cells with 3PO and cisplatin for 48 h. Cisplatin (20 μM) treatment without 3PO caused 14.8% apoptotic cells, whereas cisplatin (20 μM) and 3PO (10 μM) combined treatment caused 31.55% (**Figure 2C**), suggesting that 3PO enhanced the effect of cisplatin in treating cancer cells. Moreover, increased cleavage of PARP was observed in cisplatin and 3PO combined treatment (**Figure 2D**).

It is generally believed that chemoresistance is in part contributed by the inability of cells to undergo apoptosis. To determine the apoptotic pathways by which 3PO attenuates the

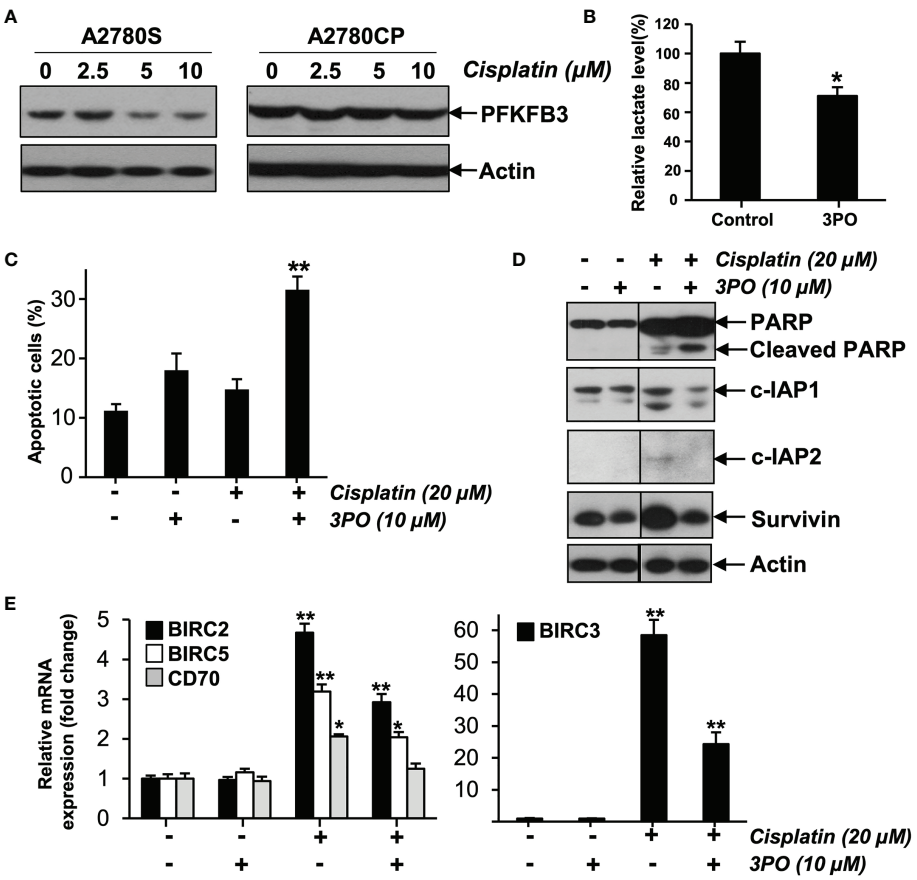


FIGURE 2 | PFKFB3 regulates chemoresistance in ovarian cancer. **(A)** Protein levels of PFKFB3 in A2780S and A2780CP cells treated with cisplatin (0, 2.5, 5 and 10 μM) for 48 h, determined by immunoblotting. **(B)** Relative lactate production level of A2780CP cells treated with 3PO (0, 10 μM), determined by Lactate Colorimetric Assay Kit II. **(C)** A2780CP cells treated with 3PO (0 and 10 μM) and cisplatin (0 and 20 μM) for 48 h, cell apoptosis was detected by Annexin V- FLUOS staining. **(D)** Protein expression of PARP, cleaved PARP, c-IAP1, c-IAP2 and survivin in A2780CP cells treated with 3PO (0 and 10 μM) and cisplatin (0 and 20 μM) for 48 h, determined by immunoblotting. **(E)** Bar chart of BIRC2, BIRC3, BIRC5 and CD70 genes mRNA expression in A2780CP cells treated with 3PO (0 and 10 μM) and cisplatin (0 and 20 μM) for 48 h, determined by the human apoptosis RT^2 profiler PCR array. (n = 3; *p < 0.05; **p < 0.01).

chemoresistant phenotype of cancer cells, the expression of 84 apoptosis-related genes in cisplatin and 3PO treatment was evaluated using the human apoptosis RT^2 profiler PCR array (**Figure 2E**). We found cisplatin induced mRNA expression of the inhibitors of apoptosis (IAP) proteins including BIRC2 (c-IAP1), BIRC3 (c-IAP2) and BIRC5 (survivin) and an immune modulator CD70 (TNFSF7) in A2780CP cells. We further detected same pattern of c-IAP1, c-IAP2 and survivin in protein levels (**Figure 2D**), suggesting 3PO could sensitize ovarian cancer cells *via* altering expression of c-IAP1, c-IAP2, survivin and CD70.

PFKFB3 Shifts CSCs Metabolism in Ovarian Cancer

Besides chemoresistance, stemness also play vital roles in the progression of ovarian cancer. In the present study, we applied two methods for enriching CSCs from ascites of ovarian cancer. One method involved maintaining tumorspheres in ultra-low attachment plates with serum-free medium. The other method involved sorting the top 5% brightest staining cells with stem cell markers (ALDH and CD44) by FACS, on the basis of our recent findings that ALDH+CD44+ cells isolated from ascites-derived tumor cells show enhanced CSC properties (16). Compared with that in monolayer or ALDH-CD44- cancer cells, significantly higher PFKFB3 mRNA expression was clearly detected in tumorspheres derived from ascites and ascites-derived cell lines (SKOV3 and OVCAR3) or ALDH+CD44+ cells sorted from SKOV3 and OVCAR3 cells (**Figure 3A**). Moreover, greater protein expression of PFKFB3 was found in tumorspheres or ALDH+CD44+ cells than monolayer/ALDH-CD44- SKOV3 cells (**Figure 3B**). There results indicated high expression of PFKFB3 in CSC-enriched subsets derived from ascites in ovarian cancer.

We have recently found that tumorspheres/ALDH+CD44+ cells favor glycolysis more than OXPHOS (16). To study the role of PFKFB3 in altered CSC metabolism in ovarian cancer, we performed metabolic assays using tumorspheres/ALDH+CD44+ cells transfected with siPFKFB3 duplexes and ALDH-CD44- cells transfected with PFKFB3. First, qPCR (**Figure 3C**) and western blot (**Figure 3D**) analyses were performed to validate the transfection efficiency. We then found that PFKFB3 knockdown led to decreased lactate production (**Figure 3E**) and an increased oxygen consumption rate (**Figure 3F**) in ALDH+CD44+ cells, whereas PFKFB3 overexpression resulted in increased lactate production and decreased the oxygen consumption rate in ALDH-CD44- cells. These data suggested that PFKFB3 could increase glycolytic influx and decrease OXPHOS activity in ALDH+CD44+ cells.

PFKFB3 Promotes Stemness in Ovarian Cancer, Probably Through the NF-κB Signaling Pathway

Next, we studied the role of PFKFB3 in regulating CSCs in ovarian cancer. We found that siPFKFB3-transfected tumorspheres/ALDH+CD44+ cells exhibited significantly less migration/invasion (**Figure 4A**) and formation of colonies (**Figure 4B**) and spheres (**Figure 4C**) than groups transfected with control siRNA. Moreover, transient overexpression of PFKFB3 in ALDH-CD44- cells led to the opposite effects (**Figures 4A–C**). GEPIA was used to predict the positive correlation between PFKFB3 and the stemness genes, NANOG, OCT4, SOX2, KLF4 and BMI1. A significant albeit very weak correlation was detected between high expression of PFKFB3 and upregulation of KLF4 and BMI1 (**Supplementary Figure 2**), suggesting KLF4 and BMI1 as the potential downstream targets of PFKFB3 on CSC properties in ovarian cancer. No significant correlation was found between PFKFB3 and NANOG, OCT4 and SOX2 (data not shown). We further found that decreased KLF4 and BMI1 mRNA and/or protein expression was observed in PFKFB3 suppressed tumorspheres/ALDH+CD44+ cells, whereas increased KLF4 and BMI1 expression was found in PFKFB3 overexpressing ALDH-CD44- cells (**Figures 4D, E**).

Numerous pathways are involved in CSC regulation in ovarian cancer, including NF-κB pathways (20). Phosphorylation of p65 at S536 (p-RelA) is one of the canonical NF-κB activation indicators (21). We further found that p-p65 was decreased in ALDH+CD44+ SKOV3 cells transfected with siPFKFB3 as compared with control cells (**Figure 4E**). Conversely, PFKFB3-overexpressing ALDH-CD44- SKOV3 cells had higher expression of p-p65 (**Figure 4E**). In addition, to assess the effect of NF-κB on stemness mediated by PFKFB3, we treated both ALDH-CD44-SKOV3 cells with ectopic PFPFB3 expression and control cells with the NF-κB inhibitor, dimethylaminoparthenolide (DMAPT), for 48 h. DMAPT inhibited the increased sphere formation capacity induced by the PFKFB3 plasmid in ALDH-CD44 cells but had no effects on the ALDH-CD44- cells transfected with the control plasmid (**Figure 4F**). Together, our results indicated that PFKFB3 regulates CSC properties in ovarian cancer, possibly through the NF-κB signaling pathway.

PFK158 Suppresses Stemness in Ovarian Cancer

PFK158 is a PFKFB3 inhibitor that mimics genetic inhibition of PFKFB3 in malignant pleural mesothelioma (22). Here, ALDH+CD44+ cells were treated with PFK158 and examined with functional assays to evaluate the effects of PFK158 on the CSC subpopulation in SKOV3 cells. PFKFB3 inhibited migration/invasion (**Figure 5A**) and sphere formation (**Figure 5B**) capacity in ALDH+CD44+ SKOV3 cells. Moreover, KLF4 mRNA expression decreased in ALDH+CD44+ cells suppressed by PFK158 (**Figure 5C**). To determine the effect of PFK158 on tumorigenesis *in vivo*, we injected control or PFK158-pretreated ALDH+CD44+ SKOV3 cells into the flanks of nude mice. The number of days of tumor formation and tumor sizes were recorded. After 28 days, tumors were dissected and weighed. PFK158-pretreated ALDH+CD44+ cells formed smaller tumors, and the tumor formation time was prolonged from an average of 9.4 days to 17.4 days (**Figure 5D**). Moreover, tumor size and weight were significantly lower in the PFK158-pretreated group than the control group (**Figure 5E**). We used *in vivo* limiting

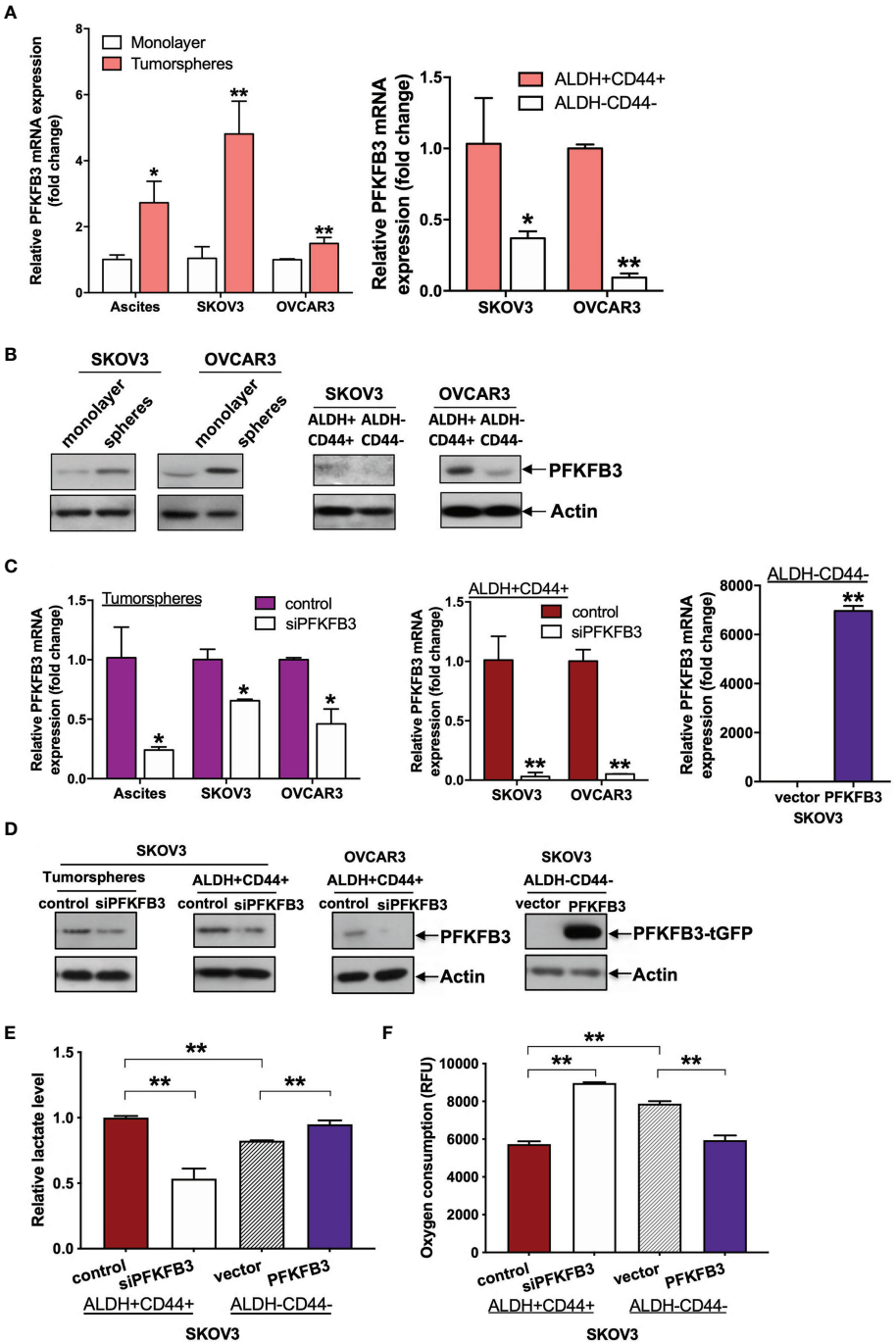


FIGURE 3 | PFKFB3 shifts CSC metabolism in ovarian cancer. **(A)** Relative mRNA expression of PFKFB3 in tumorsphere/monolayer and ALDH+CD44+/ALDH-CD44- cells *via* qPCR. **(B)** Protein expression of PFKFB3 in tumorsphere/monolayer and ALDH+CD44+/ALDH-CD44- cells, determined *via* immunoblotting; Relative PFKFB3 **(C)** mRNA and **(D)** protein expression in tumorspheres and ALDH+CD44+ cells transfected with control siRNA or siPFKFB3 duplexes and PFKFB3-overexpressing ALDH-CD44- cells, determined by qPCR and immunoblotting, respectively. **(E)** Relative lactate production and **(F)** oxygen consumption rate of PFKFB3-suppressing ALDH+CD44+ cells and PFKFB3-overexpressing ALDH-CD44- cells after 24 h incubation. (n = 3; *p < 0.05, **p < 0.01).

dilution assays with a serial dilution of PFK158/control-pretreated ALDH+CD44+ SKOV3 cells to determine the effect of PFK158 on tumor-initiating properties. Tumor-incidence declined from 100% to 60% in the 10^4-cell group, 100% to 40% in the 5000-cell group, and 80% to 40% in the 2500-cell group with PFK158-pretreated ALDH+CD44+ SKOV3 cells (**Figure 5F**). These findings suggested that PFK158 suppresses stemness in ovarian cancer.

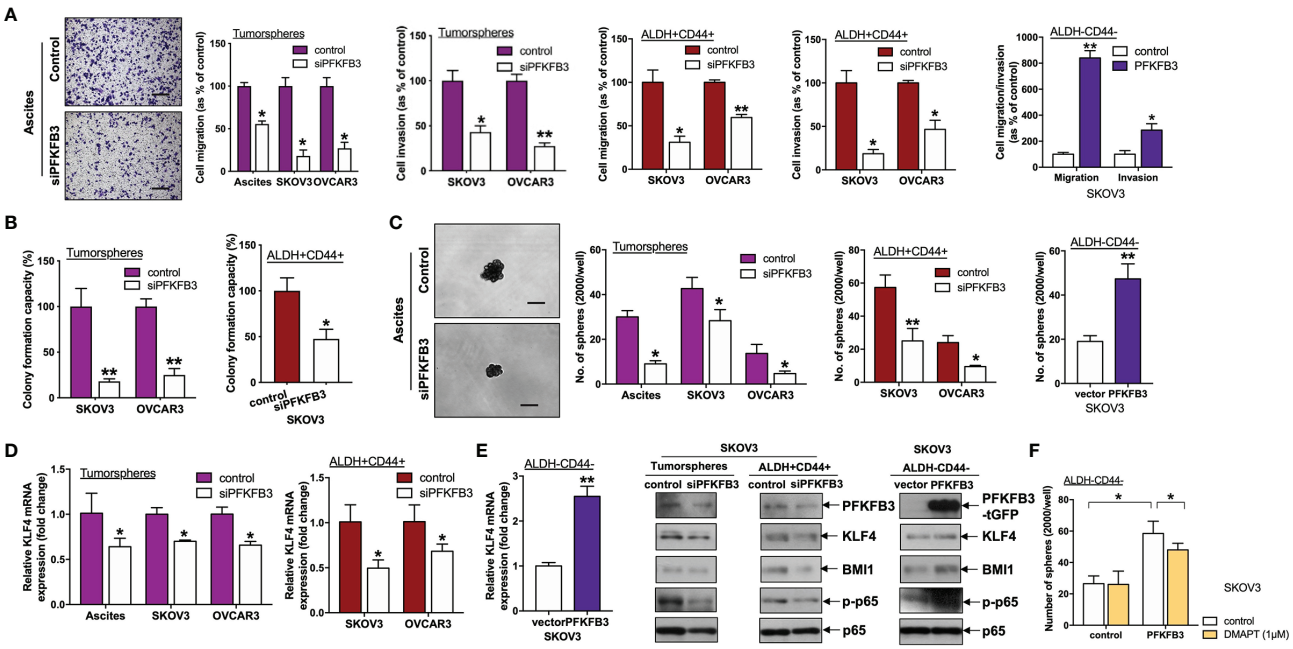


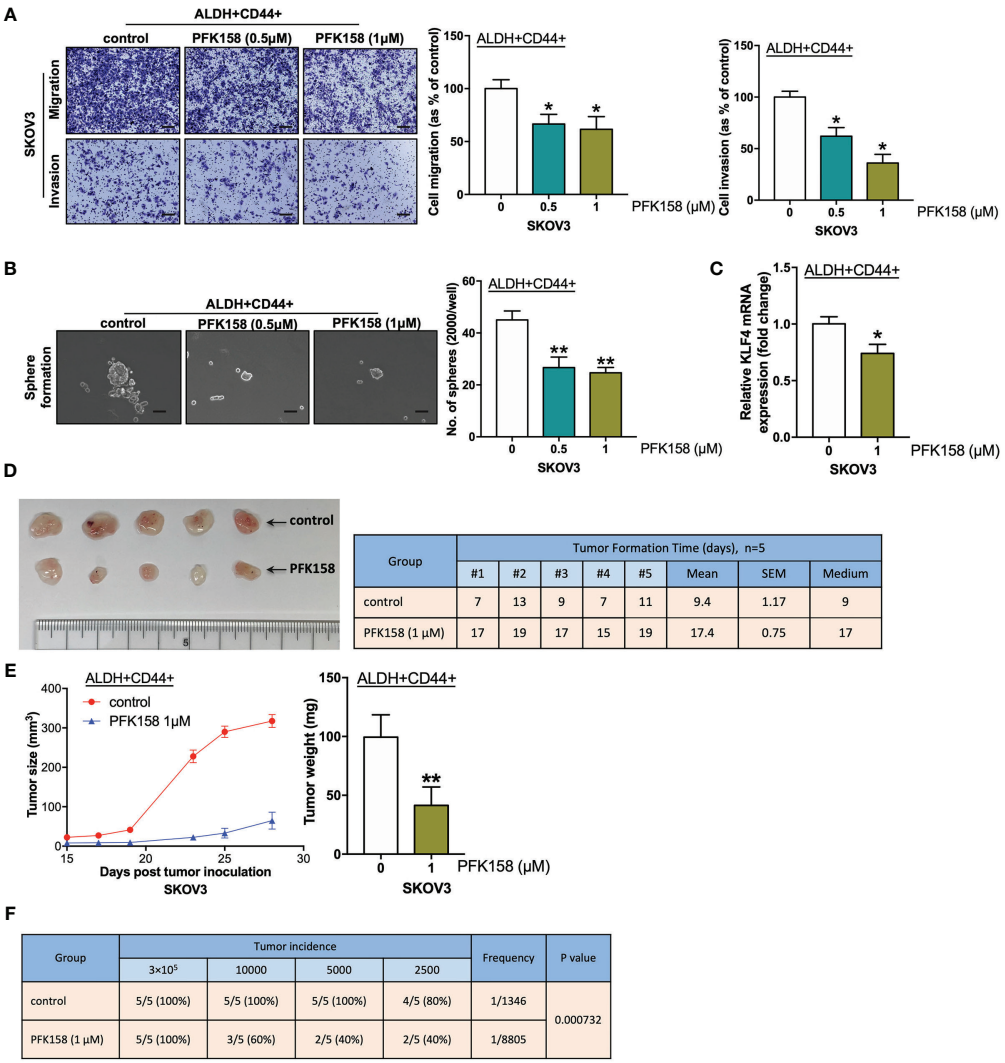
FIGURE 4 | PFKFB3 promotes stemness in ovarian cancer. **(A)** Transwell migration/invasion assays of PFKFB3-suppressing tumorspheres and ALDH+CD44+ cells and PFKFB3-overexpressing ALDH-CD44- cells. Representative images of migrating tumorspheres with transient knockdown of PFKFB3 (left; scale bar, 100 μm). **(B)** Clonogenic assay of tumorspheres and ALDH+CD44+ cells transfected with control and siPFKFB3 duplexes cells. **(C)** Sphere formation assay of PFKFB3-suppressing tumorspheres and ALDH+CD44+ cells and PFKFB3-overexpressing ALDH-CD44- cells. Representative images of sphere-forming cells with transient knockdown of PFKFB3 (left; scale bar, 100 μm). **(D)** Relative KLF4 mRNA expression of PFKFB3-suppressing tumorspheres and ALDH+CD44+ cells and PFKFB3-overexpressing ALDH-CD44- cells, determined by qPCR. **(E)** Protein expression of PFKFB3, KLF4, BMI1, p-p65 and p65 in PFKFB3-knockdown tumorspheres (left) ALDH+CD44+ (middle) SKOV3 cells and PFKFB3-overexpressing ALDH-CD44- (right) SKOV3 cells, determined by immunoblotting. **(F)** After DMAPT (1 μM) treatment of PFKFB3-overexpressing ALDH-CD44- cells for 48 h, sphere formation assays were conducted and analyzed. (n = 3; *p < 0.05, **p < 0.01).

DISCUSSION

We found through IHC analysis that PFKFB3 was markedly higher in ovarian cancer tissues than normal ovary tissues, a finding consistent with Oncomine analysis results. PFKFB3 was also associated with tumor stage, grade and serous subtype. Moreover, higher expression of PFKFB3 decreased the survival rate and correlated with metastasis, thus, suggesting that PFKFB3 may be a novel prognostic marker for ovarian cancer. Concordantly, PFKFB3 is correlated with the aggressive features of breast cancer and indicates poorer prognosis in breast cancer and hepatocellular carcinoma (15, 23). In gastric cancer, PFKFB3 is preferentially expressed in tumors with lymph node metastasis (24). In the present study, we demonstrate for the first time to the best of our knowledge that PFKFB3 is preferentially expressed in metastatic foci and ascites in ovarian cancer, suggesting that PFKFB3 could be associated with metastasis in ovarian cancer.

Here, blocking PFKFB3 by 3PO could inhibit lactate production and enhance the sensitivity of A2780CP cells to cisplatin. Further, we noticed cisplatin induced IAPs mRNA/protein expression including c-IAP1, c-IAP2 and survivin and an immune modulator CD70 in A2780CP cells, whereas 3PO could abolish their mRNA/protein induction, suggesting 3PO could sensitize ovarian cancer cells to cisplatin possibly through the modulation of c-IAP1, c-IAP2, survivin and CD70 mRNA expression. Increase expression of c-IAP1, c-IAP2 and survivin after cisplatin treatment in resistant cells has been documented (25, 26), suggesting their roles on cisplatin resistance (27, 28). Blocking survivin through knockout or inhibitor could suppress metastasis and chemoresistance (29). Also, the association between CD70 and clinical cisplatin resistance and poor prognosis of advanced ovarian cancer has been recorded (30, 31), yet the precise mechanism remains to be elucidated. These results strongly supported PFKFB3 as a mediator of cisplatin resistance in ovarian cancer.

Recent studies have suggested that CSCs show an altered energy balance, with glycolysis being the major metabolic phenotype in cancers of the liver, breast and colon (6). In ovarian cancer, anaerobic glycolysis is enhanced in tumorspheres derived from cancer cells (3). In our recent study, we further discovered that tumorspheres/ALDH+CD44+ cells favor glycolysis more than OXPHOS (16). Here, we found that PFKFB3, another key enzyme in promoting glycolysis, was up-regulated in ascites-derived cancer cells. Furthermore, tumorspheres and the ALDH+CD44+ cell subset originating from ascites had greater expression of PFKFB3 than differentiated cancer cells. These findings further support that CSC-enriched subpopulations such as in ALDH+CD44+ cell subset derived from ascites favor glycolysis over OXPHOS.



Group	Tumor Formation Time (days), n=5							
	#1	#2	#3	#4	#5	Mean	SEM	Medium
control	7	13	9	7	11	9.4	1.17	9
PFK158 (1 μM)	17	19	17	15	19	17.4	0.75	17

F

Group	Tumor incidence				Frequency	P value
	3×10^5	10000	5000	2500		
control	5/5 (100%)	5/5 (100%)	5/5 (100%)	4/5 (80%)	1/1346	0.000732
PFK158 (1 μM)	5/5 (100%)	3/5 (60%)	2/5 (40%)	2/5 (40%)	1/8805	

FIGURE 5 | PFK158 suppresses stemness in ovarian cancer. **(A)** Transwell migration and invasion (scale bar, 100 μM) and **(B)** sphere formation (scale bar, 100 μM) of ALDH+ CD44+ SKOV3 cells pretreated with control and PFK158 (0.5 and 1.0 μM) for 48 h. **(C)** Relative KLF4 mRNA expression of ALDH+CD44+ SKOV3 cells treated with 1.0 μM PFK158, determined by qPCR. (n=3; *p < 0.05, **p < 0.01). **(D)** After inoculation of 3×10^5 ALDH+CD44+ SKOV3 cells pretreated with control (n = 5) and PFK158 (1.0μM, n = 5) into the right/left flanks of mice, images of dissected tumors and tumor formation days were recorded. **(E)** Line chart showing the tumor growth and bar chart showing the weights of tumors derived from the mice injected with 3×10^5 control and PFK158-pretreated ALDH+CD44+ SKOV3 cells. **(F)** Tumor incidence and estimated frequency from *in vivo* limiting dilution assays with injection of a limiting dilution (3×10^5, 10×10^3, 5×10^3, or 2.5×10^3 cells) of control and PFK158-pretreated ALDH+CD44+ SKOV3 cells into the flanks of mice.

Functionally, knockdown of PFKFB3 results in a reduced migration rate of gastric cancer cells (24), a result consistent with our finding that manipulation of PFKFB3 in CSC-enriched/differentiated subsets affected the migration/invasion capacity of ovarian cancer *in vitro*. Silencing of PFKFB3 decreases glucose consumption and inhibits DNA repair; thus, suppressing tumor growth in hepatocellular carcinoma (23). Our study not only found upregulated PFKFB3 in CSC-enriched ovarian cancer cells, but also revealed that PFKFB3 promoted clonogenicity and sphere-formation, and induced KLF4 and BMI1 expression in ovarian cancer cells.

In terms of downstream signaling, PFKFB3 binds and activates CDK4, a kinase controlling the G1/S transition, thus, promoting cell cycle progression (32). Moreover, silencing of PFKFB3 deactivates CDK1 and stabilizes p27 protein expression, thereby leading to G1/S arrest and enhanced apoptosis in HeLa cells (14). A recent study revealed that up-regulation of PFKFB3 promoted immune evasion and tumorigenesis by inducing PD-L1 expression through NF-κB activation in hepatocellular carcinoma (33). NF-κB pathways have also been suggested to be involved in CSC regulation of ovarian cancer (20). Here, we observed that silencing of PFKFB3 decreased NF-κB activation,

whereas ectopic expression of PFKFB3 up-regulated NF-κB activation. Not all functional assays (overexpression studies) were performed in all cell lines and SKOV3 may not be a representative of the most common high-grade serous ovarian cancer, the use of other ovarian cancer cell lines for performing function assays after overexpression of PFKFB3 would be examined in further studies.

We further evaluated the therapeutic potential of targeting PFKFB3. The compound 3PO has been identified to be an inhibitor of PFKFB3 (19) and has been reported to attenuate glycolytic activity and attenuate tumor growth in bladder, liver, breast (11) and colon cancers (34). Blockade of PFKFB3 by 3PO in mutant JAK2-driven myeloproliferative neoplasms alters redox homeostasis through inhibiting glycolysis, thus, resulting in accumulation of reactive oxygen species and increased apoptosis (35). In ovarian cancer, 3PO blocks glycolysis, thus, causing increased extracellular glucose and impeded lactate secretion, induces apoptosis (36) and enhances the sensitivity of tumor cells to platinum therapy (37). However, 3PO has not been applied clinically because of its poor water solubility (11). Another potent selective PFKFB3 inhibitor, PFK158, is the first PFKFB3 inhibitor being approved by the U.S. Food and Drug Administrator (FDA) to undergo clinical trial in patients with various malignancies including ovarian, prostate, lung, melanoma, breast and pancreatic cancers (http://www.advancedcancertherapeutics.com). In combination with immune checkpoint inhibitors, PFK158 has been found to decrease tumor growth in a preclinical mouse model in melanoma (38). A previous study has suggested that PFK158 combined with chemotherapy increases apoptosis in melanoma cells (39). As a small molecular antagonist of PFKFB3, PFK158 can mimic genetic inhibition of PFKFB3 (thus inhibiting glycolytic activity), arrest tumor cells in G0/G1 phase, and promote cell death as well as enhance chemotherapy in malignant pleural mesothelioma (22). Recently, PFK158 has been reported to inhibit glucose metabolism and enhance the sensitivity of tumor cells to carboplatin in ovarian and cervical cancer cells (40). Here, we extended the function of PFK158 to CSC-enriched subpopulations. Our study showed that PFK158 attenuates sphere formation, migration/invasion and KLF4 mRNA expression, and enhances the sensitivity of ALDH +CD44+ cancer cells. Moreover, PFK158 impedes tumorigenesis and tumor-initiation *in vivo*.

CONCLUSIONS

In conclusion, we demonstrated that overexpression of PFKFB3 in ovarian cancer cells, especially in the CSC subpopulation, correlates with metastasis and patient survival. PFKFB3 could induce lactate production, chemoresistance, CSC properties and tumor growth in ovarian cancer through inhibition of apoptosis and NF-κB signaling pathway. Moreover, our evidence suggests the therapeutic potential of PFK158 as an inhibitor of PFKFB3 in targeting ovarian cancer.

DATA AVAILABILITY STATEMENT

The original contributions presented in the study are included in the article/**Supplementary Material**. Further inquiries can be directed to the corresponding author.

ETHICS STATEMENT

The use of patient samples was approved by the Institution Ethical Review Board of the University of Hong Kong (UW 16-107). The patients/participants provided their written informed consent to participate in this study. This study was approved by the Committee of the Use of Live Animals in Teaching and Research (CULATR) under an approved license (No. 4598-18).

AUTHOR CONTRIBUTIONS

Y-xJ, MS, and KC conceived the project. Y-xJ, MS, and J-jJ performed the experiments. TL, DC, and AC contributed new reagents/analytic tools. Y-xJ, MS, HN, and KC analysed the data. Y-xJ and MS wrote the manuscript. MS and KC supervised the study. All authors provided critical revision and approved the final manuscript.

FUNDING

The work was jointly funded by the University of Hong Kong (201411159066) and by the Hong Kong Research Grants Council General Research Fund (HKU 17101414), and the Research Fund from the Department of Obstetrics and Gynaecology.

SUPPLEMENTARY MATERIAL

The Supplementary Material for this article can be found online at: https://www.frontiersin.org/articles/10.3389/fonc.2022.748403/full#supplementary-material

REFERENCES

1. Lengyel E. Ovarian Cancer Development and Metastasis. *Am J Pathol* (2010) 177:1053–64. doi: 10.2353/ajpath.2010.100105
2. Nieman KM, Kenny HA, Penicka CV, Ladanyi A, Buell-Gutbrod R, Zillhardt MR, et al. Adipocytes Promote Ovarian Cancer Metastasis and Provide Energy for Rapid Tumor Growth. *Nat Med* (2011) 17:1498–503. doi: 10.1038/nm.2492
3. Liao J, Qian F, Tchabo N, Mhawech-Fauceglia P, Beck A, Qian Z, et al. Ovarian Cancer Spheroid Cells With Stem Cell-Like Properties Contribute to Tumor Generation, Metastasis and Chemotherapy Resistance Through Hypoxia-Resistant Metabolism. *PloS One* (2014) 9:e84941. doi: 10.1371/journal.pone.0084941

4. Ahmed N, Stenvers KL. Getting to Know Ovarian Cancer Ascites: Opportunities for Targeted Therapy-Based Translational Research. *Front Oncol* (2013) 3:256. doi: 10.3389/fonc.2013.00256
5. Pattabiraman DR, Weinberg RA. Tackling the Cancer Stem Cells - What Challenges Do They Pose? *Nat Rev Drug Discov* (2014) 13:497–512. doi: 10.1038/nrd4253
6. Wong TL, Che N, Ma S. Reprogramming of Central Carbon Metabolism in Cancer Stem Cells. *Biochim Biophys Acta* (2017) 1863:1728–38. doi: 10.1016/j.bbadis.2017.05.012
7. Alvero AB, Chen R, Fu HH, Montagna M, Schwartz PE, Rutherford T, et al. Molecular Phenotyping of Human Ovarian Cancer Stem Cells Unravels the Mechanisms for Repair and Chemoresistance. *Cell Cycle* (2009) 8:158–66. doi: 10.4161/cc.8.1.7533
8. Shen YA, Lan KL, Chang CH, Lin LT, He CL, Chen PH, et al. Intraperitoneal (188)Re-Liposome Delivery Switches Ovarian Cancer Metabolism From Glycolysis to Oxidative Phosphorylation and Effectively Controls Ovarian Tumour Growth in Mice. *Radiother Oncol* (2016) 119:282–90. doi: 10.1016/j.radonc.2016.02.007
9. Mor I, Cheung EC, Vousden KH. Control of Glycolysis Through Regulation of PFK1: Old Friends and Recent Additions. *Cold Spring Harb Symp Quant Biol* (2011) 76:211–6. doi: 10.1101/sqb.2011.76.010868
10. Li X, Liu J, Qian L, Ke H, Yao C, Tian W, et al. Expression of PFKFB3 and Ki67 in Lung Adenocarcinomas and Targeting PFKFB3 as a Therapeutic Strategy. *Mol Cell Biochem* (2018) 445(1–2):123–4. doi: 10.1007/s11010-017-3258-8
11. Shi L, Pan H, Liu Z, Xie J, Han W. Roles of PFKFB3 in Cancer. *Signal Transduct Target Ther* (2017) 2:17044. doi: 10.1038/sigtrans.2017.44
12. Gu M, Li L, Zhang Z, Chen J, Zhang W, Zhang J, et al. PFKFB3 Promotes Proliferation, Migration and Angiogenesis in Nasopharyngeal Carcinoma. *J Cancer* (2017) 8:3887–96. doi: 10.7150/jca.19112
13. Peng F, Li Q, Sun JY, Luo Y, Chen M, Bao Y. PFKFB3 Is Involved in Breast Cancer Proliferation, Migration, Invasion and Angiogenesis. *Int J Oncol* (2018) 52:945–54. doi: 10.3892/ijo.2018.4257
14. Yalcin A, Clem BF, Imbert-Fernandez Y, Ozcan SC, Peker S, O'Neal J, et al. 6-Phosphofructo-2-Kinase (PFKFB3) Promotes Cell Cycle Progression and Suppresses Apoptosis *via* Cdk1-Mediated Phosphorylation of P27. *Cell Death Dis* (2014) 5:e1337. doi: 10.1038/cddis.2014.292
15. La Belle Flynn A, Calhoun BC, Sharma A, Chang JC, Almasan A, Schiemann WP. Autophagy Inhibition Elicits Emergence From Metastatic Dormancy by Inducing and Stabilizing Pfkfb3 Expression. *Nat Commun* (2019) 10:3668. doi: 10.1038/s41467-019-11640-9
16. Jiang Y-X, Siu MK-Y, Wang J-J, Mo X-T, Leung TH-Y, Chan DW, et al. Ascites-Derived ALDH+CD44+ Tumour Cell Subsets Endow Stemness, Metastasis and Metabolic Switch *via* PDK4-Mediated STAT3/AKT/NF-κb/IL-8 Signalling in Ovarian Cancer. *Br J Cancer* (2020) 123:275–87. doi: 10.1038/s41416-020-0865-z
17. Chen X, Wei B, Han X, Zheng Z, Huang J, Liu J, et al. LGR5 Is Required for the Maintenance of Spheroid-Derived Colon Cancer Stem Cells. *Int J Mol Med* (2014) 34:35–42. doi: 10.3892/ijmm.2014.1752
18. Li J, Condello S, Thomes-Pepin J, Ma X, Xia Y, Hurley TD, et al. Lipid Desaturation Is a Metabolic Marker and Therapeutic Target of Ovarian Cancer Stem Cells. *Cell Stem Cell* (2017) 20:303–14.e5. doi: 10.1016/j.stem.2016.11.004
19. Clem B, Telang S, Clem A, Yalcin A, Meier J, Simmons A, et al. Small-Molecule Inhibition of 6-Phosphofructo-2-Kinase Activity Suppresses Glycolytic Flux and Tumor Growth. *Mol Cancer Ther* (2008) 7:110–20. doi: 10.1158/1535-7163.MCT-07-0482
20. House CD, Jordan E, Hernandez L, Ozaki M, James JM, Kim M, et al. NFkappaB Promotes Ovarian Tumorigenesis *via* Classical Pathways That Support Proliferative Cancer Cells and Alternative Pathways That Support ALDH(+) Cancer Stem-Like Cells. *Cancer Res* (2017) 77:6927–40. doi: 10.1158/0008-5472.CAN-17-0366
21. Bradford JW, Baldwin AS. IKK/nuclear factor-kappaB and Oncogenesis: Roles in Tumor-Initiating Cells and in the Tumor Microenvironment. *Adv Cancer Res* (2014) 121:125–45. doi: 10.1016/B978-0-12-800249-0.00003-2
22. Sarkar Bhattacharya S, Thirusangu P, Jin L, Roy D, Jung D, Xiao Y, et al. PFKFB3 Inhibition Reprograms Malignant Pleural Mesothelioma to Nutrient Stress-Induced Macropinocytosis and ER Stress as Independent Binary Adaptive Responses. *Cell Death Dis* (2019) 10:725. doi: 10.1038/s41419-019-1916-3
23. Shi WK, Zhu XD, Wang CH, Zhang YY, Cai H, Li XL, et al. PFKFB3 Blockade Inhibits Hepatocellular Carcinoma Growth by Impairing DNA Repair Through AKT. *Cell Death Dis* (2018) 9:428. doi: 10.1038/s41419-018-0435-y
24. Han J, Meng Q, Xi Q, Wang H, Wu G. PFKFB3 Was Overexpressed in Gastric Cancer Patients and Promoted the Proliferation and Migration of Gastric Cancer Cells. *Cancer Biomark* (2017) 18:249–56. doi: 10.3233/CBM-160143
25. Tirro E, Consoli ML, Massimino M, Manzella L, Frasca F, Sciacca L, et al. Altered Expression of C-IAP1, Survivin, and Smac Contributes to Chemotherapy Resistance in Thyroid Cancer Cells. *Cancer Res* (2006) 66:4263–72. doi: 10.1158/0008-5472.CAN-05-3248
26. Cohen S, Bruchim I, Graiver D, Evron Z, Oron-Karni V, Pasmanik-Chor M, et al. Platinum-Resistance in Ovarian Cancer Cells Is Mediated by IL-6 Secretion *via* the Increased Expression of its Target cIAP-2. *J Mol Med (Berl)* (2013) 91:357–68. doi: 10.1007/s00109-012-0946-4
27. Fulda S, Vucic D. Targeting IAP Proteins for Therapeutic Intervention in Cancer. *Nat Rev Drug Discov* (2012) 11:109–24. doi: 10.1038/nrd3627
28. Singh N, Krishnakumar S, Kanwar RK, Cheung CH, Kanwar JR. Clinical Aspects for Survivin: A Crucial Molecule for Targeting Drug-Resistant Cancers. *Drug Discov Today* (2015) 20:578–87. doi: 10.1016/j.drudis.2014.11.013
29. Zhao G, Wang Q, Wu Z, Tian X, Yan H, Wang B, et al. Ovarian Primary and Metastatic Tumors Suppressed by Survivin Knockout or a Novel Survivin Inhibitor. *Mol Cancer Ther* (2019) 18:2233–45. doi: 10.1158/1535-7163.MCT-19-0118
30. Liu N, Sheng X, Liu Y, Zhang X, Yu J. Increased CD70 Expression Is Associated With Clinical Resistance to Cisplatin-Based Chemotherapy and Poor Survival in Advanced Ovarian Carcinomas. *Onco Targets Ther* (2013) 6:615–9. doi: 10.2147/OTT.S44445
31. Aggarwal S, He T, Fitzhugh W, Rosenthal K, Feild B, Heidbrink J, et al. Immune Modulator CD70 as a Potential Cisplatin Resistance Predictive Marker in Ovarian Cancer. *Gynecol Oncol* (2009) 115:430–7. doi: 10.1016/j.ygyno.2009.08.031
32. Jia W, Zhao X, Zhao L, Yan H, Li J, Yang H, et al. Non-Canonical Roles of PFKFB3 in Regulation of Cell Cycle Through Binding to CDK4. *Oncogene* (2018) 37:1685–98. doi: 10.1038/s41388-017-0072-4
33. Chen DP, Ning WR, Jiang ZZ, Peng ZP, Zhu LY, Zhuang SM, et al. Glycolytic Activation of Peritumoral Monocytes Fosters Immune Privilege *via* the PFKFB3-PD-L1 Axis in Human Hepatocellular Carcinoma. *J Hepatol* (2019) 71:333–43. doi: 10.1016/j.jhep.2019.04.007
34. Klarer AC, O'Neal J, Imbert-Fernandez Y, Clem A, Ellis SR, Clark J, et al. Inhibition of 6-Phosphofructo-2-Kinase (PFKFB3) Induces Autophagy as a Survival Mechanism. *Cancer Metab* (2014) 2:2. doi: 10.1186/2049-3002-2-2
35. Nageswara Rao T, Hansen N, Hilfiker J, Rai S, Majewska JM, Lekovic D, et al. JAK2 Mutant Hematopoietic Cells Display Metabolic Alterations That Can be Targeted to Treat Myeloproliferative Neoplasms. *Blood* (2019) 134(21):1832–46. doi: 10.1182/blood.2019000162
36. Xintaropoulou C, Ward C, Wise A, Marston H, Turnbull A, Langdon SP. A Comparative Analysis of Inhibitors of the Glycolysis Pathway in Breast and Ovarian Cancer Cell Line Models. *Oncotarget* (2015) 6:25677–95. doi: 10.18632/oncotarget.4499
37. Xintaropoulou C, Ward C, Wise A, Queckborner S, Turnbull A, Michie CO, et al. Expression of Glycolytic Enzymes in Ovarian Cancers and Evaluation of the Glycolytic Pathway as a Strategy for Ovarian Cancer Treatment. *BMC Cancer* (2018) 18:636. doi: 10.1186/s12885-018-4521-4
38. Chesney JA TS, Yaddanapudi K, Grewal JS. Targeting 6-Phosphofructo-2-Kinase (PFKFB3) as an Immunotherapeutic Strategy. *J Clin Oncol* (2016) 34. doi: 10.1200/JCO.2016.34.15_suppl.e14548
39. Gustafsson NMS, Farnegardh K, Bonagas N, Ninou AH, Groth P, Wiita E, et al. Targeting PFKFB3 Radiosensitizes Cancer Cells and Suppresses Homologous Recombination. *Nat Commun* (2018) 9:3872. doi: 10.1038/s41467-018-06287-x
40. Mondal S, Roy D, Sarkar Bhattacharya S, Jin L, Jung D, Zhang S, et al. Therapeutic Targeting of PFKFB3 With a Novel Glycolytic Inhibitor PFK158

Promotes Lipophagy and Chemosensitivity in Gynecologic Cancers. *Int J Cancer* (2019) 144:178–89. doi: 10.1002/ijc.31868

Conflict of Interest: The authors declare that the research was conducted in the absence of any commercial or financial relationships that could be construed as a potential conflict of interest.

Publisher's Note: All claims expressed in this article are solely those of the authors and do not necessarily represent those of their affiliated organizations, or those of the publisher, the editors and the reviewers. Any product that may be evaluated in this article, or claim that may be made by its manufacturer, is not guaranteed or endorsed by the publisher.

Copyright © 2022 Jiang, Siu, Wang, Leung, Chan, Cheung, Ngan and Chan. This is an open-access article distributed under the terms of the Creative Commons Attribution License (CC BY). The use, distribution or reproduction in other forums is permitted, provided the original author(s) and the copyright owner(s) are credited and that the original publication in this journal is cited, in accordance with accepted academic practice. No use, distribution or reproduction is permitted which does not comply with these terms.

frontiers in Oncology

SYSTEMATIC REVIEW
published: 10 February 2022
doi: 10.3389/fonc.2022.814989

Assessing Post-Treatment Pathologic Tumor Response in Female Genital Tract Carcinomas: An Update

*Frediano Inzani[1], Damiano Arciuolo[1], Giuseppe Angelico[1], Angela Santoro[1], Antonio Travaglino[1], Nicoletta D'Alessandris[1], Giulia Scaglione[1], Michele Valente[1], Federica Cianfrini[1], Antonio Raffone[3,4] and Gian Franco Zannoni[1,2]**

[1] Unità di Ginecopatologia e Patologia Mammaria, Dipartimento Scienze della Salute della Donna, del Bambino e di Sanità Pubblica, Fondazione Policlinico Universitario A. Gemelli IRCCS, Rome, Italy, [2] Istituto di Anatomia Patologica, Università Cattolica del Sacro Cuore, Rome, Italy, [3] Gynecology and Obstetrics Unit, Department of Neuroscience, Reproductive Sciences and Dentistry, School of Medicine, University of Naples Federico II, Naples, Italy, [4] Division of Gynaecology and Human Reproduction Physiopathology, Department of Medical and Surgical Sciences (DIMEC), IRCCS Azienda Ospedaliero-Univeristaria di Bologna. S. Orsola Hospital, University of Bologna, Bologna, Italy

OPEN ACCESS

Edited by:
Jian-Jun Wei,
Northwestern University,
United States

Reviewed by:
Federica Perelli,
Santa Maria Annunziata Hospital, Italy
Diego Raimondo,
University of Bologna, Italy

***Correspondence:**
Gian Franco Zannoni
gianfranco.zannoni@policlinicogemelli.itpoliclinicogemelli.it

Specialty section:
This article was submitted to Gynecological Oncology, a section of the journal Frontiers in Oncology

Received: 14 November 2021
Accepted: 05 January 2022
Published: 10 February 2022

Citation:
Inzani F, Arciuolo D, Angelico G, Santoro A, Travaglino A, D'Alessandris N, Scaglione G, Valente M, Cianfrini F, Raffone A and Zannoni GF (2022) Assessing Post-Treatment Pathologic Tumor Response in Female Genital Tract Carcinomas: An Update. Front. Oncol. 12:814989. doi: 10.3389/fonc.2022.814989

In the last decades, several new therapeutic strategies have been introduced in the field of gynecologic oncology. These include neoadjuvant chemotherapy for high-grade serous tubo-ovarian carcinoma, hormonal fertility-sparing strategies for endometrial cancer, pressurized intraperitoneal aerosol chemotherapy (PIPAC) for surgically incurable peritoneal metastasis, and neoadjuvant treatments for locally advanced cervical carcinomas. All these recent advances lead to the development of novel scoring systems for the evaluation of pathological response related to specific treatments. In this regard, pathological evaluation of the morphological modifications related to these treatments and the definition of a tumor regression grading score have been introduced in clinical practice in order to achieve a more efficient prognostic stratification of patients affected by gynecological malignancies. The aim of the present paper is to provide a detailed review on the post-treatment pathological scoring systems in patients affected by gynecological malignancies.

Keywords: neoadjuvant chemotherapy, histological tumor regression grading, ovarian cancer, endometrial cancer, cervical cancer, pressurized intraperitoneal aerosol chemotherapy

INTRODUCTION

With the introduction of neoadjuvant therapeutic strategies in the field of gynecologic oncology, pathological evaluation of the morphological modifications related to chemotherapy has become a crucial step in order to establish the treatment response and to achieve a prognostic stratification of patients.

Several tumor regression grading (TRG) systems have been introduced in clinical practice. TRG systems according to Mandard (1), Dworak (2), and Becker (3) were the first tumor regression grading systems applied in the gastrointestinal (GI) tract (4). Moreover, assessment of the changes in tumor burden, according to the Response Evaluation Criteria in Solid Tumors (RECIST), represents an additional tool to evaluate a patient's response to chemotherapy (5). Even if with

different criteria, ranking, and number of categories, all these systems are based on the evaluation of the residual tumor cells and regressive changes in the tumor bed. These systems were firstly utilized to evaluate chemotherapy response in primary tumors; later, similar scoring systems showing a good prognostic stratification were introduced for metastatic lesions arising from colon in liver and peritoneum (6–8). The introduction of TRG systems in gynecologic oncology is more recent than the GI tract and still not well standardized in some cases. Herein, we present a detailed review on the post-treatment pathological scoring systems in patients affected by gynecological malignancies.

HIGH-GRADE OVARIAN SEROUS CARCINOMA TREATED WITH NEOADJUVANT THERAPY

Ovarian carcinomas represent the second commonest gynecological cancer in Western countries after endometrial cancer and most cases are diagnosed at the advanced stage where the recommended treatment consists of a debulking surgery with the aim of an optimal cytoreduction; in cases where this is not feasible because of the advanced stage or clinical contraindications, neoadjuvant chemotherapy (NACT) followed by surgery has been introduced to reduce the tumor volume and to enhance the surgical results (9, 10).

McCluggage et al., in 2002 (9), described for the first time the histological regressive features in ovarian carcinoma after NACT (9). They pointed out that both the epithelial and stroma component showed morphological changes with a general decrease of gland-to-stroma ratio. The neoplastic cells following NACT are usually arranged in small groups or in single cells and show nuclear enlargement with hyperchromatism, chromatin clumping or smudging, and cytoplasm with intense eosinophilia, vacuolation, or foam-cell changes. Stromal alterations include fibrosis, inflammation, foamy histiocytes, cholesterol cleft formation, fat necrosis, and dystrophic calcifications including free psammoma bodies. Mitotic figures are often inconspicuous. According to the abovementioned morphological alterations observed following NACT, a correct nosological classification of ovarian cancer following chemotherapy may be extremely difficult. However, immunohistochemistry could be useful in establishing the presence of minimal residual neoplastic cells and in the diagnosis of the nature of the tumor (9). The pathological prognostic value in the assessment of post-NACT tubo-ovarian high-grade serous carcinoma was attempted by Bohm et al. in 2015 (11). At first, a six-tier scoring system was proposed and assessed on the two most frequent involved sites that are routinely removed at surgery: omentum and adnexa. This system was called "chemotherapy response score" (CRS) and was set as follows: CRS0—no evidence of tumor response (no fibroinflammatory changes, no evidence of chemotherapy response) with viable tumor only; CRS1—minimal regression-associated fibroinflammatory changes, mainly viable tumor; CRS2—minor (focal or diffuse) regression-associated fibroinflammatory changes, predominantly extensive viable tumor (fibrosis to tumor ratio <1:1 or viable tumor nodules of 5 mm or more); CRS3—extensive regression-associated fibroinflammatory changes with focal viable degenerate tumor (multifocal tumor deposits that individually are <5 mm and/or fibrosis-to-tumor ratio >1:1); CRS4—mainly regression-associated fibroinflammatory changes with minimal tumor (very few individual tumor cells or tumor cell groups); CRS5—no viable invasive tumor identified. This score showed a good prognostic value in terms of progression-free survival (PFS) and overall survival (OS) when it was applied to the omentum, with a significant difference between the best (CRS4–5) and intermediate (CRS2–3) responders, while on the adnexa, it did not reach any significant results and it did not stratify the prognosis. According to the result obtained in the omentum, the authors grouped the 6-tier scoring system in a simpler 3-tier system: (i) CRS1: absence or minimal presence of tumor response; mainly viable tumor with no or minimal regression-associated fibroinflammatory changes, limited to a few foci; (ii) CRS2: appreciable tumor response in which viable tumor foci are readily identifiable; tumor is regularly distributed, ranging from multifocal or diffuse regression-associated fibroinflammatory changes with viable tumor arranged in sheets, streaks, or nodules to extensive regression-associated fibroinflammatory changes with multifocal residual tumor easily identifiable yet; and (iii) CRS3: complete or near-complete response to treatment with no residual tumor or minimal irregularly scattered tumor foci seen as individual cells, cell groups, or nodules up to 2 mm in maximum size. Switching from a 6- to a 3-tier scoring system has improved the interobserver reproducibility and showed a significant difference in PFS between CRS1–2 and CRS3. The prognostic value of the 3-tier CRS was confirmed and reinforced in further studies (12–15) and by a meta-analysis (16). Detailed pathological images of CRS system are depicted in **Figure 1**. In relation to the slight prognostic differences observed between omental CRS1 and CRS2, some authors (17) have suggested a binary prognostication system (CRS3 vs. CRS1/2) as opposed to a 3-tier score. If this system had a great value in the prognosis when it is applied on the omentum, the authors did not find any clinical meaning when applied the 3-tier score system to the adnexa. After these results, other studies have investigated the prognostic value of CRS not only in omentum, but also on the adnexal sites (18, 19). From these works, it appears that CRS, when used on the omentum, adnexa, and as a combined score (omental and adnexal), was significantly associated with PFS but not with OS; adnexal CRS1/2 are more likely to develop platinum-resistant disease. Recently, the modified 2-tier CRS (CRS1/2 versus CRS3) was significantly associated with survival (OS and PFS), independent of scoring site (omental vs. adnexal). Additional morphological features (oncocytic change, inflammation, and desmoplasia) can also predict patient outcomes (20). Given these contrasting results, further studies on larger cohorts are needed to confirm the prognostic value of the CRS in the adnexa. Currently, the 3-tier Böhm's score applied on the omentum is recommended in the main oncological guidelines (21, 22) given its role as a biomarker in therapeutic decision-making.

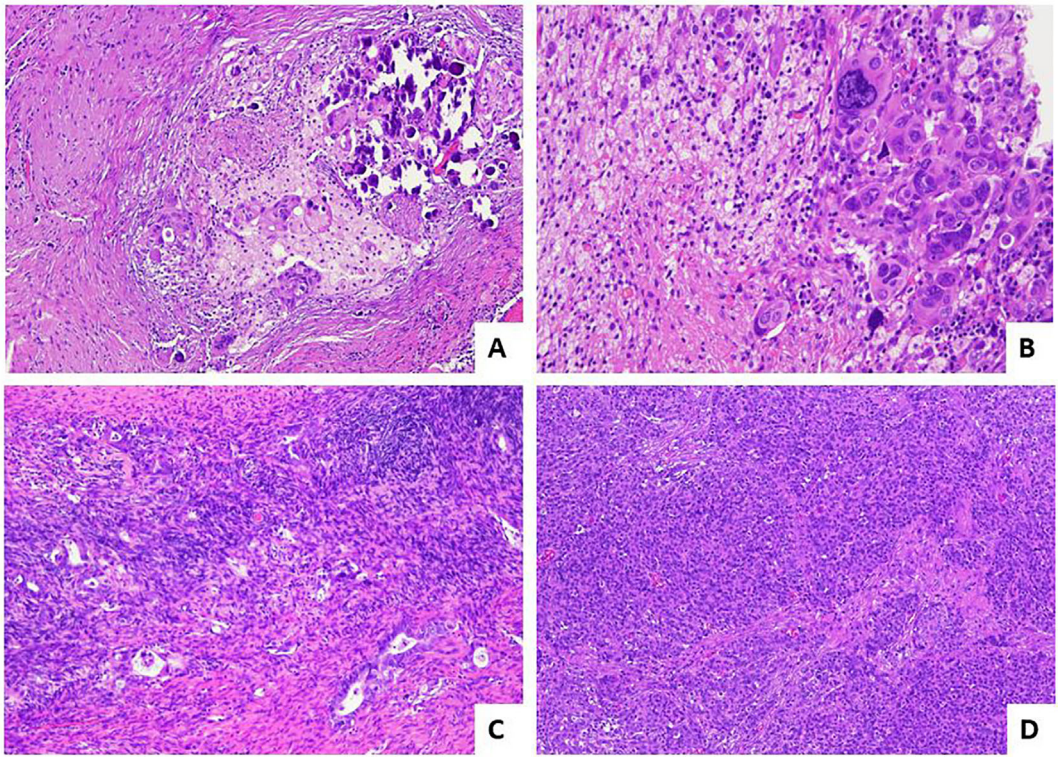


FIGURE 1 | Pathological response score for post-NACT high-grade serous tubo-ovarian carcinoma. **(A)** Example of CRS3 score: diffuse regressive fibro-inflammatory changes with small residual foci of neoplasms <2 mm [hematoxylin and eosin-stained sections (H&E); 10×]. **(B)** Higher magnification of image in A, with evidence of residual marked atypical neoplastic cells.(H&E; 40×). **(C)** Example of CRS2 score with appreciable response: residual tumor easily identifiable, >2 mm, with diffuse regression-associated fibro-inflammatory changes (H&E; 10×). **(D)** Example of CRS1 score with absent response: tumor without evidence of regression (H&E; 4×).

TUBO-OVARIAN CARCINOMA TREATED WITH PRESSURIZED INTRAPERITONEAL AEROSOL CHEMOTHERAPY (PIPAC)

In 2013, a new treatment called pressurized intraperitoneal aerosol chemotherapy (PIPAC) has been introduced for treatment of peritoneal metastases. This technique delivers drugs into the abdominal cavity as an aerosol under pressure in patients with advanced stages of peritoneal metastases from all kinds of tumors, including those with a gynecological origin. This system maximizes exposure of peritoneal tumor implants to chemotherapy agents, with favorable pharmacokinetics and biodistribution (23). Several PIPAC procedures, usually at least three times, are performed at 6 ± 2-week intervals. According to the treatment regimens, the abdomen is accessed through one 10- to 12-mm (nebulizer) and one 5-mm (optical) trocar. Ascites is quantified and sampled for cytological examination, or if ascites is not present, a peritoneal flushing is performed. The abdominal cavity is then explored with documentation of the peritoneal cancer index (PCI). Before each drug's injection, at least 4 representative biopsies, sized 3–5 mm, are taken using biopsy forceps at suspect localizations and, if possible, in the four different quadrants of abdominal cavity, for assessment of pathological response (24). A 4-tiered pathological scoring system, namely, the peritoneal regression grading score (PRGS), was proposed by Solass in 2016 (25): PRGS1, complete response (no tumor cells with only regressive features); PRGS2, major response (predominant regression features with rare groups of residual cancer cells are observed); PRGS3, minor response (predominant vital neoplastic component with evident regressive features); PRG4, no response (neoplastic mass without signs of regression). PRGS is not a specific system for tubo-ovarian carcinoma, but is a system proposed for monitoring the response of peritoneal metastasis of several origins in patients who undergo PIPAC. Pathological images illustrating different response scores for post-PIPAC peritoneal metastases are provided in **Figure 2**.

It must be pointed out that multiple peritoneal biopsies in different sites may show different PRG scores. The meaning of this heterogeneity is unknown; it could be related to different clones with different chemosensitivity or to a different drug's distribution. By now, reporting both the highest and the mean PRGS has been proposed.

PRGS has a good rational base, but its prognostic significance is still debated. A relevant bias is related to the sampling procedures and the consequent assessment of a TRG on a small bioptic sample compared to an excisional surgical resection, on which an extensive sampling and histological examination could be done by the pathologist. Moreover, Solass et al. in 2018 (26) at 11th PSOGI (Peritoneal Surface Oncology Group International)

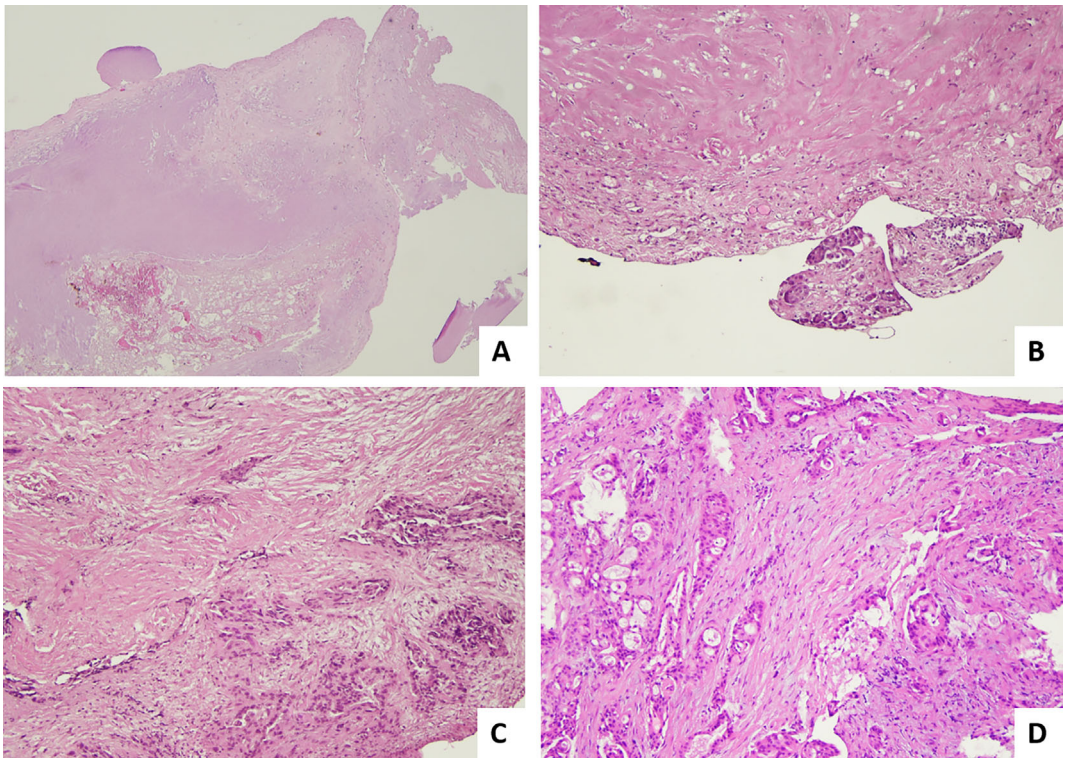


FIGURE 2 | Pathological response score for post-PIPAC peritoneal metastasis. **(A)** Example of PRGS1 or complete response: regressive sclero-necrotic changes without evidence of residual tumor cells (H&E; 2×). **(B)** Example of PRGS2 or major response; regressive sclerotic changes predominant over few aggregates of residual tumor cells (H&E; 20×). **(C)** Another area of the case illustrated in B (PRGS2) (H&E; 4×). **(D)** Example of PRGS3 or minor response: tumor cells predominant over regressive fibrotic changes (H&E; 20×).

presented an abstract with a univariate analysis that showed for the first time a prognostic trend of PRGS for overall survival (p = 0.08) in a prospective cohort of 49 patients with peritoneal metastasis of several origins including tubo-ovarian carcinoma (26). In another study by Benzerdjeb et al., highest and mean PRGS alone did not show prognostic value at PFS and OS in a cohort of 112 patients with peritoneal metastases from different origins, including ovarian carcinoma, treated with PIPAC. In detail, the difference between PRGS at the first PIPAC procedure and at the third PIPAC procedure was considered to define the increase of PRGS, used as a comparison parameter. However, when the increase of highest PRGS was combined with peritoneal cytology (positive and negative for neoplastic cells) in a combined progression index, it acquired a significant prognostic value at OS and PFS (27). Concerning the reproducibility of a 4-tier PRGS, Solass et al. conducted a study on 33 patients with peritoneal metastases from a different origin, with a total of 331 biopsies (28). Eight pathologists with different levels of experience in the peritoneal pathology and PRGS system were involved. Statistical analysis by intraclass correlation coefficients (ICCs) and Krippendorff's alpha revealed a moderate to good interobserver variability and a good to excellent intraobserver variability. The study also showed that PRGS could be used by younger pathologists without loss of accuracy. Finally, another potential utility of the bioptic samples obtained during PIPAC treatments could be the possibility to perform molecular analyses. As shown in the paper by Rezniczek et al., several changes in gene expression profile during repeated PIPAC procedures are associated with better clinical treatment response (29). Therefore, molecular analyses might be utilized in the near future for refining individual treatment.

ENDOMETRIAL CARCINOMA

Endometrial carcinoma represents the most common gynecologic malignancy in developed countries (30) and is mostly treated by surgery. Some studies analyzed retrospectively and prospectively clinical results of NACT followed by interval debulking surgery (IDS) in locally advanced endometrial carcinoma (31–36); however, only a single study on 40 patients with advanced endometrial cancer attempted to apply the CRS system to omental and adnexal metastases with promising results (37). The main field, where pathological assessment of treatment response is currently performed on endometrial neoplasms, is represented by hormonal fertility-sparing treatment. The standard treatment for atypical hyperplasia (AH) and well-differentiated endometrial adenocarcinoma (WDC) is surgery. However, in case

of AH or in case of WDC (FIGO G1) limited to the endometrium in the absence of suspicious of myometrial invasion or metastatic disease, the possibility of fertility-sparing strategies could be taken into consideration for the women with contraindications to surgery or especially for young women strongly desirous of offspring with the main purpose of postponing surgery after a pregnancy has been completed (38, 39). For moderately differentiated endometrioid endometrial (FIGO G2) tumors, data concerning the efficacy of fertility-sparing approach are still very limited. However, according to a recent paper, fertility-sparing treatment seems to be feasible even in a higher than G1 risk category of EC patients, with efficacy similar to those observed in G1 patients (40).

Different strategies based on the use of oral or topical intrauterine progestins could be used. In terms of remission, recurrence, and pregnancy rates, several studies revealed that treatments based on levonorgestrel-releasing intrauterine device may be more effective than systemic therapy for women with complex atypical hyperplasia, particularly in morbidly obese women, allowing to achieve complete response rates (38–40). On the other hand, Masciullo et al. found that hysteroscopic resection of AH and WDC in combination with oral progestin therapy (megestrol acetate) was significantly associated with shorter treatment duration to achieve complete response and longer time to relapse, compared to patients treated with progestin therapy alone (41). The histological monitoring in fertility-sparing strategies is well defined and consists in a descriptive approach (**Figure 3**) (42). In brief, after the first bioptic diagnosis, patients start the therapy and are monitored with repeated endometrial biopsies usually at 3-monthly intervals (42). Related to the risk of later recurrence, the long-term follow-up with biopsy at 6- to 12-monthly intervals could continue until surgical treatment is considered. Pathological modifications on the endometrium treated by progestins involve both the stromal and glandular components (43): the most frequent finding is represented by atrophic glands, with decreased atypia (nuclear rounding, and smudged, homogenized, fine nuclear chromatin), decreased mitotic activity, and decreased gland-to-stroma ratio, associated with pseudodecidualized stroma, often with intracytoplasmic vacuolations, hemosiderin depositions, foci of necrosis, calcifications, and presence of inflammatory elements (foamy histiocytes or plasma cells). Other less frequent features include myxoid-like alterations, sclero-hyaline nodules, micropapillary/papillary and cribriform architectures, reactive atypia or metaplastic changes of the superficial epithelium (being mucinous, secretory, eosinophilic, and squamous), and sometimes even ulceration and erosions. These morphological changes are related to the release of

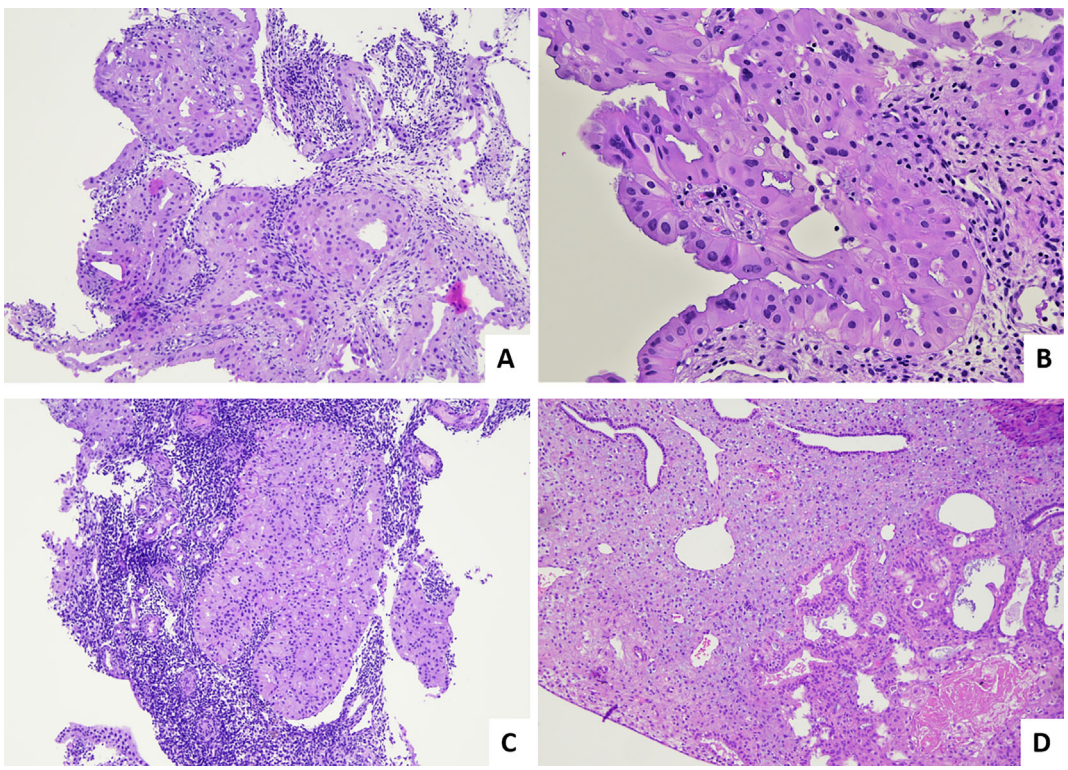


FIGURE 3 | Pathological evaluation of post hormonal fertility-sparing therapy bioptical samples for AH and WDC. **(A)** Fragment of endometrial tissue with persistence of AH such as on the previous biopsy (H&E; 4×). **(B)** Higher magnification of sample in A, with evidence of residual nuclear atypia and presence of abundant eosinophilic cytoplasm (H&E; 40×). **(C)** Fragment of endometrial tissue with persistence of EEC such as on the previous biopsy (H&E; 4×). **(D)** Endometrial tissue with a focus of residual AH, in a context with pseudodecidualized stroma (H&E; 10×).

progestins and also to the physical presence of the device releasing the hormone.

The same alterations are also found in the context of AH and WDC. Range of possible response to treatment is wide and is based on evaluation of the last biopsy and its comparison with the previous one. The main possibilities are the following: (i) total response/Resolution: the last specimen shows proliferative, secretory, inactive, or atrophic pattern endometrium, without evidence of atypia and hyperplastic features; (ii) partial response/ Regression: the last specimen shows hyperplasia without atypia; (iii) persistence: AH was present in both the pretreatment and final specimen or if the pretreatment sample shows WDC and the final shows AH or WDC; (iv) progression: the last biopsy shows WDC when the pretreatment one showed AH or if the final specimen shows moderately or poorly differentiated carcinoma when the pretreatment biopsy showed WDC; and (v) recurrence: a lesion that had either resolved or regressed during the course of treatment and then reappears.

However, even cases of persistence of WDC or AH may often show some treatment-associated changes (43). Biopsies with persistence of disease may be characterized by areas of AH intermingled with areas of atrophic endometrium. Persisting WDCs itself may often show a general decrease of mitotic activity, decrease of glandular/stromal ratio, and diffuse eosinophilic cytoplasmic metaplasia. Post-treatment biopsies in patients with AH may maintain complex glandular structures but without cytological atypia. In particular, nuclear atypia should be the main parameter for our evaluation and the more powerful predictor because some architectural abnormalities such as papillary proliferations or glandular confluency/crowding and cribriform structures without nuclear atypia should be considered morphological changes related to progestins therapy on the initial lesion (44). Moreover, studies concerning fertility-sparing strategies have pointed out the following pieces of advice (45): (i) the pathologist should review the pretreatment biopsy specimen and all subsequent post-treatment biopsy specimens; (ii) progestin treatment should be continued until there is no evidence of "residual disease"; and (iii) if cytologic atypia is detected after 6 months of treatment, definitive surgical treatment (hysterectomy) should be considered.

Some clinical and pathologic parameters have been demonstrated to be a good predictor of response to progestin therapy in premenopausal women with AH and WDC, such as body mass index (BMI), patient's age, pretreatment architectural histological pattern, and the pathological response in the first follow-up specimen post-therapy (46, 47).

Several immunohistochemical markers have also been demonstrated as predictive biomarkers of response to therapy with progestins (48). In particular, in a meta-analysis, 43 immunohistochemical markers that seem to correlate with treatment response were evaluated. Results indicate that high expression of estrogen receptor (ER) and progesterone receptor (PR) has a good response in different studies. The assessment of ER and PR also appeared relevant in follow-up: in some studies, PR and ER showed a downregulation in good responders (49). Moreover, the PR isoforms and the stromal PR expression appear to be relevant (50). Recently, it has been shown that abnormal mismatch repair (MMR) protein expression can predict poor response to progestins and/or higher rate of recurrence in young women with AH or FIGO 1 carcinoma (51). Finally, other authors reported that another biomarker, FGFR2c, appears to be strongly associated with progestin treatment failure, with low overall response rate to levonorgestrel intrauterine device treatment (52).

CARCINOMA OF THE UTERINE CERVIX

In cases of locally advanced cervical carcinomas (LACC), platinum-based chemoradiotherapy and brachytherapy are the preferred treatment. In some centers, radical surgery is performed after neoadjuvant treatment, although this approach remains controversial in the guidelines (53).

Similar to other anatomical districts, morphological changes are observed on both neoplastic and non-neoplastic tissue (54). In cases with total or partial response, residual tumor cells show the following modifications: (i) neoplastic nuclei show enlargement in size with irregular outlines; (ii) the cytoplasm is either intensely eosinophilic or clear with vacuolated or foamy appearance; and (iii) multinucleated giant cells (foreign body-like) may be observed.

Morphological changes in tumor stroma include (i) dense fibrosis; (ii) collections of foamy histiocytes, (iii) cholesterol clefts, (iv) necrosis, (v) calcifications, and (vi) myointimal thickening of the blood vessels related to a marked deposition of fibrous acellular material. Erosive cervicitis and glandular atypia of non-neoplastic endocervical epithelium can simulate malignant changes, but they lack epithelial stratification, severe nuclear atypia, and significant mitotic activity, typical of invasive and *in situ* adenocarcinoma.

Regarding tumor regression grading systems in cervical cancer, a 3-tier system has been proposed by Zannoni et al. in 2008 (54); briefly, it was based on the size of the residual tumors cells: pR2 was defined by the presence of foci more than 3 mm, pR1 (microscopic residual) if the foci were less than 3 mm, and pR0 was defined as the absence of neoplasm (**Figure 4**).

The system was assessed on a group of 50 women affected by advanced uterine cervical cancer who underwent radiotherapy and chemotherapy and subsequent surgical resection; a significant response (pR0 and pR1) was described in most cases (76%). Prognostic value was not studied in the original proposal paper; only recently a good prognostic value was revealed in our series of about 100 cases (our unpublished data).

An additional 5-tier system has been proposed by Takatori et al. (55): grade 0, no evidence of effect; grade 1a, neoplastic cells occupy >2/3 of the tumor bed; grade 1b, the cells remain in >1/3 but <2/3; grade 2, tumor cells remain in <1/3; and grade 3, there are no tumor cells. Cases with a score of 2 and 3 showed a better survival than patients with a score of 1a and 1b.

Other authors proposed a system based on the maximum infiltration of the neoplastic residual cells after neoadjuvant treatment with the threshold of 3 mm, regardless of the size of the tumor or regression ratio (56–58). This system appears to be

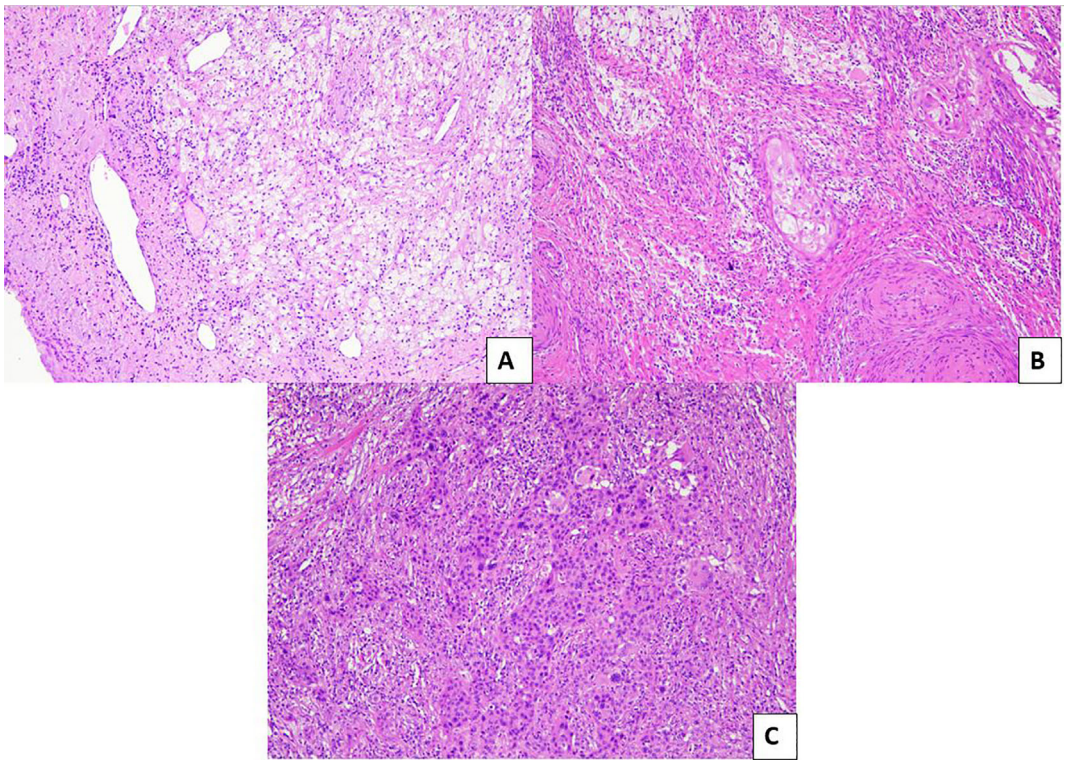


FIGURE 4 | Pathological evaluation of post neoadjuvant LACCs. **(A)** Example of pR0: no residual tumor is evident in the surgical specimen (H&E; 10×). **(B)** Example of pR1: microscopic residual tumor (<3 mm) with intermingled inflammatory infiltrate (H&E; 10×). **(C)** Example of pR2: macroscopic residual tumor (>3 mm) with minimal inflammatory response (H&E; 10×).

objective, easily applicable, reproducible, and based on quantitatively measurable parameters.

Several systems adopt the threshold of 3 mm of depth of invasion, with some peculiar differences, e.g., Huang et al. and Buda et al. defined CR as the complete response, absence of the tumor, and negative nodes; PR1, residual disease with depth <3 mm of stromal invasion, including *in situ* carcinoma with or without lymphatic metastasis; PR2, residual disease with depth > 3 mm of stromal invasion (57, 58).

Gadducci et al. defined 4 categories: (i) "overall optimal (absence of the tumor cells with negative nodes); (ii) "optimal partial response" (residual disease with <3 mm stromal invasion including *in situ* carcinoma and negative nodes); (iii) "suboptimal response" (intra-cervical residual disease or extra-cervical residual disease with positive nodes or extra-cervical residual disease with negative nodes); and (iv) "no responders" (56).

All the systems adopting the threshold of 3 mm showed good prognostic stratification, suggesting that a residual with <3 mm of stromal invasion is prognostically similar to a complete response as confirmed in our recent metanalysis (59) and appeared more reproducible than other classical systems based on the ratio residual cancer cells/tumor bed that could be influenced by a subjective evaluation.

Finally, recent studies analyzed the role of immune microenvironment in cervical cancer, focusing on the connection between tumor-infiltrating lymphocytes (TILs) and response to therapy (60, 61). According to these preliminary results, cervical cancer represents a potential target for immunotherapy, also in the neoadjuvant setting (60). Moreover, neutrophil-to-lymphocyte ratio (NLR), platelet-to-lymphocyte ratio (PLR), tumor-infiltrating lymphocytes (TILs), and PD-L1 expression have been shown to correlate with the response of LACC patients to NACT (61).

CONCLUSIONS

In the present paper, we provided a detailed review on the most relevant and prognostically significant pathological scoring systems in gynecological tumors, which are schematically summarized in **Table 1**.

Pathological assessment of treatment response in gynecological malignancies has important prognostic and therapeutic implications in the following circumstances: (i) post-NACT surgical resections of ovarian and cervical cancer; (ii) peritoneal metastases treated with PIPAC; and (iii) endometrial carcinoma treated with fertility-sparing therapeutic strategies.

CRS system applied on the omental tissue is mandatory in our pathological reports according to current guidelines (20, 21) to evaluate the response of post-neoadjuvant high-grade serous

TABLE 1 | Key points on definition of tumor response for main gynecological neoplasms.

Type of Treatment: NACT on high-grade serous tubo-ovarian carcinoma.
Pathological evaluation: CRS evaluated on surgical resection of omentum localization; validated system, mandatory in the evaluation of post-NACT ovarian carcinoma.
CRS1 no or minimal response (tumor without evidence of regression or with few foci of regression-associated fibro-inflammatory changes).
CRS2 appreciable response (residual tumor easily identifiable >2 mm with diffuse regression-associated fibro-inflammatory changes)
CRS3 complete or near-complete response (diffuse regressive fibro-inflammatory changes with small residual foci of neoplasms <2 mm or no residual tumor identified)
Type of Treatment: Post-PIPAC peritoneal metastasis.
Pathological evaluation: PRGS evaluated on multiple bioptic samples made during each PIPAC procedure; proposed, under validation.
PRGS1 complete response (regressive changes without evidence of tumor cells)
PRGS2 major response (regressive changes predominant over tumor cells)
PRGS3 minor response (tumor cells predominant over regressive changes)
PRGS4 no response (tumor without evidence of regressive changes)
Type of Treatment: Hormonal Fertility-sparing therapy for AH and WDC.
Pathological evaluation: descriptive approach on bioptic endometrial samples made at 3 monthly interval control, compared with the previous sample.
Total response/Resolution: the last specimen shows endometrium without atypia or hyperplastic features.
- **Partial response/Regression**: the last specimen shows hyperplasia without atypia.
- **Persistence**: the last specimen with persistence of AH or WDC, such as on the previous biopsy.
-**Progression**: the last specimen with WDC when the pretreatment one showed AH or with carcinoma with a higher grade than the previous biopsy.
- **Recurrence**: reappearance of a lesion resolved/regressed during the treatment.
Type of Treatment: neoadjuvant therapy of LACC.
Pathological evaluation: several systems have been proposed based on different criteria; these systems are under validation.
System based on size of residual tumor: pR0 no residual tumor; **pR1** microscopic residual tumor (<3 mm); **pR2** macroscopic residual tumor (>3 mm)
System based on depth of invasion: CR complete response without residual tumor; **PR1** residual tumor with less than 3 mm stromal invasion; **PR2** residual tumor with less than 3 mm stromal invasion.
System based on ratio residual tumor/regressive changes: grade 0 no evidence of effect; grade 1a neoplastic cells occupy >2/3 of the tumor bed; grade 1b the cells remain in >1/3 but <2/3; grade 2 tumor cells remain in <1/3; grade 3 there are no tumor cells.

carcinoma. PIPAC has emerged in recent years as a novel method of intraperitoneal drug administration to treat inoperable peritoneal metastasis from different origins, also including gynecologic carcinomas mainly represented by ovarian cancer. A 4-degree system called PRGS has been proposed to monitor histological response on biopsies made during PIPAC procedures. Its prognostic value has not yet been defined but its use is suggested, also for research purposes, in centers where PIPAC technology is available (24).

Fertility-sparing treatments, based on progestins, for atypical hyperplasia/endometrial carcinoma are not standard treatments, and when chosen, they require a very close follow-up and biopsies should be examined by pathologists with good experience in gynecopathology. A score system has not been defined, but the identification of persistence of atypia represents a crucial point to define therapeutic management (39).

Finally, for locally advanced cervical carcinomas subjected to the controversial and debated neo-adjuvant chemotherapy, different systems have been proposed to evaluate histological response on surgical samples. Several systems based on the depth of infiltration with the threshold of 3 mm appear to be an easily applicable and well-reproducible approach, and they would currently seem to be the most promising among those proposed for prognostic value (53).

DATA AVAILABILITY STATEMENT

The original contributions presented in the study are included in the article/supplementary material. Further inquiries can be directed to the corresponding author.

AUTHOR CONTRIBUTIONS

FI and GZ: study design and acquisition of pathological data. AS and GA: acquisition of pathological data and writing of the manuscript. AT, AR and DA: acquisition of clinical data and software analysis. MV and GS: revised the paper critically for important intellectual content. FC and ND'A: critical review of the manuscript. All authors contributed to the article and approved the submitted version.

REFERENCES

1. Mandard AM, Dalibard F, Mandard JC, Marnay J, Henry-Amar M, Petiot JF, et al. Pathologic Assessment of Tumor Regression After Preoperative Chemoradiotherapy of Esophageal Carcinoma. Clinicopathologic Correlations. *Cancer* (1994) 73:2680–6. doi: 10.1002/1097-0142(19940601)73:11<2680::AID-CNCR2820731105>3.0.CO;2-C
2. Dworak O, Keilholz L, Hoffmann A. Pathological Features of Rectal Cancer After Preoperative Radiochemotherapy. *Int J Colorectal Dis* (1997) 12:19–23. doi: 10.1007/s003840050072
3. Fan Z, Li H, Hu R, Liu Y, Liu X, Gu L. Fertility-Preserving Treatment in Young Women With Grade 1 Presumed Stage IA Endometrial Adenocarcinoma: A Meta-Analysis. *Int J Gynecol Cancer* (2018) 28:385–93. doi: 10.1097/IGC.0000000000001164

4. Becker K, Mueller JD, Schulmacher C, Ott K, Fink U, Busch R, et al. Histomorphology and Grading of Regression in Gastric Carcinoma Treated With Neoadjuvant Chemotherapy. *Cancer* (2003) 98:1521–30. doi: 10.1002/cncr.11660
5. Eisenhauer EA, Therasse P, Bogaerts J, Schwartz LH, Sargent D, Ford R, et al. New Response Evaluation Criteria in Solid Tumours: Revised RECIST Guideline (Version 1.1). *Eur J Cancer* (2009) 45:228–47. doi: 10.1016/j.ejca.2008.10.026
6. Thies S, Langer R. Tumor Regression Grading of Gastrointestinal Carcinomas After Neoadjuvant Treatment. *Front Oncol* (2013) 3:262. doi: 10.3389/fonc.2013.00262
7. Blazer DG3rd, Kishi Y, Maru DM, Kopetz S, Chun YS, Overman MJ, et al. Pathologic Response to Preoperative Chemotherapy: A New Outcome End Point After Resection of Hepatic Colorectal Metastases. *J Clin Oncol* (2008) 26:5344–51. doi: 10.1200/JCO.2008.17.5299
8. Passot G, You B, Boschetti G, Fontaine J, Isaac S, Decullier E, et al. Pathological Response to Neoadjuvant Chemotherapy: A New Prognosis Tool for the Curative Management of Peritoneal Colorectal Carcinomatosis. *Ann Surg Oncol* (2014) 21:2608–14. doi: 10.1245/s10434-014-3647-0
9. McCluggage WG, Lyness RW, Atkinson RJ, Dobbs SP, Harley I, McClelland HR, et al. Morphological Effects of Chemotherapy on Ovarian Carcinoma. *J Clin Pathol* (2002) 55:27–31. doi: 10.1136/jcp.55.1.27
10. Miller K, Price JH, Dobbs SP, McClelland RH, Kennedy K, McCluggage WG. An Immunohistochemical and Morphological Analysis of Post-Chemotherapy Ovarian Carcinoma. *J Clin Pathol* (2008) 61:652–7. doi: 10.1136/jcp.2007.053793
11. Böhm S, Faruqi A, Said I, Lockley M, Brockbank E, Jeyarajah A. Chemotherapy Response Score: Development and Validation of a System to Quantify Histopathologic Response to Neoadjuvant Chemotherapy in Tubo-Ovarian High-Grade Serous Carcinoma. *J Clin Oncol* (2015) 1(33):2457–63. doi: 10.1200/JCO.2014.60.5212
12. Coghlan E, Meniawy TM, Munro A, Bulsara M, Stewart CJ, Tan A, et al. Prognostic Role of Histological Tumor Regression in Patients Receiving Neoadjuvant Chemotherapy for High-Grade Serous Tubo-Ovarian Carcinoma. *Int J Gynecol Cancer* (2017) 27:708–13. doi: 10.1097/IGC.0000000000000945
13. Ditzel HM, Strickland KC, Meserve EE, Stover E, Konstantinopoulos PA, Matulonis UA, et al. Assessment of a Chemotherapy Response Score (CRS) System for Tubo-Ovarian High-Grade Serous Carcinoma (HGSC). *Int J Gynecol Pathol* (2019) 38:230–40. doi: 10.1097/PGP.0000000000000513
14. Lee JY, Chung YS, Na K, Kim HM, Park CK, Nam EJ. External Validation of Chemotherapy Response Score System for Histopathological Assessment of Tumor Regression After Neoadjuvant Chemotherapy in Tubo-Ovarian High-Grade Serous Carcinoma. *J Gynecol Oncol* (2017) 28:e73. doi: 10.3802/jgo.2017.28.e73
15. Singh P, Kaushal V, Rai B, Rajwanshi A, Gupta N, Dey P, et al. The Chemotherapy Response Score is a Useful Histological Predictor of Prognosis in High-Grade Serous Carcinoma. *Histopathology* (2018) 72:619–25. doi: 10.1111/his.13399
16. Cohen PA, Powell A, Böhm S, Gilks CB, Stewart CJR, Meniawy TM, et al. Pathological Chemotherapy Response Score is Prognostic in Tubo-Ovarian High-Grade Serous Carcinoma: A Systematic Review and Meta-Analysis of Individual Patient Data. *Gynecol Oncol* (2019) 154:441–8. doi: 10.1016/j.ygyno.2019.04.679
17. Rajkumar S, Polson A, Nath R, Lane G, Sayasneh A, Jakes A, et al. Prognostic Implications of Histological Tumor Regression (Böhm's Score) in Patients Receiving Neoadjuvant Chemotherapy for High Grade Serous Tubal & Ovarian Carcinoma. *Gynecol Oncol* (2018) 151:264–8. doi: 10.1016/j.ygyno.2018.08.042
18. Santoro A, Angelico G, Piermattei A, Inzani F, Valente M, Arciuolo D, et al. Pathological Chemotherapy Response Score in Patients Affected by High Grade Serous Ovarian Carcinoma: The Prognostic Role of Omental and Ovarian Residual Disease. *Front Oncol* (2019) 9:778. doi: 10.3389/fonc.2019.00778
19. Lawson BC, Euscher ED, Bassett RL, Liu J, Ramalingam P, Zhong Y, et al. A 3-Tier Chemotherapy Response Score for Ovarian/Fallopian Tube/Peritoneal High-Grade Serous Carcinoma: Is it Clinically Relevant? *Am J Surg Pathol* (2020) 44:206–13. doi: 10.1097/PAS.0000000000001391
20. Zhong Y, Liu J, Li X, Westin SN, Malpica A, Lawson BC, et al. A Modified 2 Tier Chemotherapy Response Score (CRS) and Other Histopathologic Features for Predicting Outcomes of Patients With Advanced Extrauterine High-Grade Serous Carcinoma After Neoadjuvant Chemotherapy. *Cancers* (2021) 13:704. doi: 10.3390/cancers13040704
21. *College of American Pathologist Protocol for the Examination of Specimens From Patients With Primary Tumors of the Ovary, Fallopian Tube, or Peritoneum* . Available at: http://www.cap.org.
22. NCCN clinical practice guidelines in Oncology (NCCN Guidelines®). . Available at: http://www.nccn.org/guidelines/category.
23. Di Giorgio A, Sgarbura O, Rotolo S, Schena CA, Bagalà C, Inzani F, et al. Pressurized Intraperitoneal Aerosol Chemotherapy With Cisplatin and Doxorubicin or Oxaliplatin for Peritoneal Metastasis From Pancreatic Adenocarcinoma and Cholangiocarcinoma. *Ther Adv Med Oncol* (2020) 12:1758835920940887. doi: 10.1177/1758835920940887
24. Alyami M, Hübner M, Grass F, Bakrin N, Villeneuve L, Laplace N, et al. Pressurised Intraperitoneal Aerosol Chemotherapy: Rationale, Evidence, and Potential Indications. *Lancet Oncol* (2019) 20:e368–77. doi: 10.1016/S1470-2045(19)30318-3
25. Solass W, Sempoux C, Detlefsen S, Carr NJ, Bibeau F. Peritoneal Sampling and Histological Assessment of Therapeutic Response in Peritoneal Metastasis: Proposal of the Peritoneal Regression Grading Score (PRGS). *Pleura Peritoneum* (2016) 1:99–107. doi: 10.1515/pp-2016-0011
26. Solass W, Kurtz F, Struller F, A. Staebler, Bosmuller H, Konigsrainer A, et al. Prognostic Value of Peri- Toneal Grading Regression Score (PRGS) in Peritoneal Metastasis: An Exploratory Analysis on Registry Data. *Pleura Peritoneum* (2018) Suppl. S1:sA27.
27. Benzerdjeb N, Durieux E, Tantot J, Isaac S, Fontaine J, Harou O, et al. Prognostic Impact of Combined Progression Index Based on Peritoneal Grading Regression Score and Peritoneal Cytology in Peritoneal Metastasis. *Histopathology* (2020) 77:548–59. doi: 10.1111/his.14092
28. Solass W, Sempoux C, Carr NJ, Bibeau F, Neureiter D, Jäger T, et al. Reproducibility of the Peritoneal Regression Grading Score for Assessment of Response to Therapy in Peritoneal Metastasis. *Histopathology* (2019) 74(7):1014–24. doi: 10.1111/his.13829
29. Rezniczek GA, Jüngst F, Jütte H, Tannapfel A, Hilal Z, Hefler LA, et al. Dynamic Changes of Tumor Gene Expression During Repeated Pressurized Intraperitoneal Aerosol Chemotherapy (PIPAC) in Women With Peritoneal Cancer. *BMC Cancer* (2016) 16:654. doi: 10.1186/s12885-016-2668-4
30. Concin N, Creutzberg CL, Vergote I, Cibula D, Mirza MR, Marnitz S, et al. ESGO/ESTRO/ESP Guidelines for the Management of Patients With Endometrial Carcinoma. *Virchows Arch* (2021) 478:153–90. doi: 10.1007/s00428-020-03007-z
31. de Lange NM, Ezendam NPM, Kwon JS, Vandenput I, Mirchandani D, Amant F, et al. Neoadjuvant Chemotherapy Followed by Surgery for Advanced-Stage Endometrial Cancer. *Curr Oncol* (2019) 26:e226–32. doi: 10.3747/co.26.4655
32. Bogani G, Ditto A, Leone Roberti Maggiore U, Scaffa C, Mosca L, Chiappa V, et al. Neoadjuvant Chemotherapy Followed by Interval Debulking Surgery for Unresectable Stage IVB Serous Endometrial Cancer. *Tumori* (2019) 105:92–7. doi: 10.1177/0300891618784785
33. Boisen MM, Vargo JA, Beriwal S, Sukumvanich P, Olawaiye AB, Kelley JL, et al. Surgical Outcomes of Patients Undergoing Extrafascial Hysterectomy After Neoadjuvant Radiotherapy With or Without Chemotherapy for Locally Advanced Endometrial Cancer Clinically Extending to the Cervix or Parametria. *Int J Gynecol Cancer* (2017) 27:1149–54. doi: 10.1097/IGC.0000000000000614
34. Iheagwara UK, Vargo JA, Chen KS, Burton DR, Taylor SE, Berger JL, et al. Neoadjuvant Chemoradiation Therapy Followed by Extrafascial Hysterectomy in Locally Advanced Type II Endometrial Cancer Clinically Extending to Cervix. *Pract Radiat Oncol* (2019) 9:248–56. doi: 10.1016/j.prro.2019.02.007
35. Khouri OR, Frey MK, Musa F, Muggia F, Lee J, Boyd L, et al. Neoadjuvant Chemotherapy in Patients With Advanced Endometrial Cancer. *Cancer Chemother Pharmacol* (2019) 84:281–5. doi: 10.1007/s00280-019-03838-x

36. Vandenput I, Van Calster B, Capoen A, Leunen K, Berteloot P, Neven P, et al. Neoadjuvant Chemotherapy Followed by Interval Debulking Surgery in Patients With Serous Endometrial Cancer With Transperitoneal Spread (Stage IV): A New Preferred Treatment? *Br J Cancer* (2009) 101:244–9. doi: 10.1038/sj.bjc.6605157
37. Jani I, Lastra RR, Brito KS, Liao C, Lazo I, Lee NK, et al. Chemotherapy Response Score as a Prognostic Tool in Patients With Advanced Stage Endometrial Carcinoma Treated With Neoadjuvant Chemotherapy. *Int J Gynecol Cancer* (2021) 31:852–8. doi: 10.1136/ijgc-2020-002202
38. Cavaliere AF, Perelli F, Zaami S, D'Indinosante M, Turrini I, Giusti M, et al. Fertility Sparing Treatments in Endometrial Cancer Patients: The Potential Role of the New Molecular Classification. *Int J Mol Sci* (2021) 22:12248. doi: 10.3390/ijms222212248
39. Falcone F, Leone Roberti Maggiore U, Di Donato V, Perrone AM, Frigerio L, Bifulco G, et al. Fertility-Sparing Treatment for Intramucous, Moderately Differentiated, Endometrioid Endometrial Cancer: A Gynecologic Cancer Inter-Group (GCIG) Study. *J Gynecol Oncol* (2020) 31:e74. doi: 10.3802/jgo.2020.31.e74
40. Mandelbaum RS, Ciccone MA, Nusbaum DJK, Khoshchehreh M, Purswani H, Morocco EB, et al. Progestin Therapy for Obese Women With Complex Atypical Hyperplasia: Levonorgestrel-Releasing Intrauterine Device vs Systemic Therapy. *Am J Obstet Gynecol* (2020) 223(1):103.e1–103.e13. doi: 10.1016/j.ajog.2019.12.273
41. Masciullo V, Trivellizzi N, Zannoni G, Catena U, Moroni R, Fanfani F, et al. Prognostic Impact of Hysteroscopic Resection of Endometrial Atypical Hyperplasia-Endometrioid Intraepithelial Neoplasia and Early-Stage Cancer in Combination With Megestrol Acetate. *Am J Obstet Gynecol* (2021) 04 (224):408–10. doi: 10.1016/j.ajog.2020.12.1210
42. Williams AT, Ganesan R. Role of the Pathologist in Assessing Response to Treatment of Ovarian and Endometrial Cancers. *Histopathology* (2020) 76:93–101. doi: 10.1111/his.13994
43. Hejmadi RK, Chaudhri S, Ganesan R, Rollason TP. Morphologic Changes in the Endometrium Associated With the Use of the Mirena Coil: A Retrospective Study of 106 Cases. *Int J Surg Pathol* (2007) 15:148–54. doi: 10.1177/1066896906299120
44. Mentrikoski MJ, Shah AA, Hanley KZ, Atkins KA. Assessing Endometrial Hyperplasia and Carcinoma Treated With Progestin Therapy. *Am J Clin Pathol* (2012) 138:524–34. doi: 10.1309/AJCPM2TSDDF1MHBZ
45. Wheeler DT, Bristow RE, Kurman RJ. Histologic Alterations in Endometrial Hyperplasia and Well-Differentiated Carcinoma Treated With Progestins. *Am J Surg Pathol* (2007) 31:988–98. doi: 10.1097/PAS.0b013e31802d68ce
46. Penner KR, Dorigo O, Aoyama C, Ostrzega N, Balzer BL, Rao J, et al. Predictors of Resolution of Complex Atypical Hyperplasia or Grade 1 Endometrial Adenocarcinoma in Premenopausal Women Treated With Progestin Therapy. *Gynecol Oncol* (2012) 124:542–8. doi: 10.1016/j.ygyno.2011.11.004
47. Zakhour M, Cohen JG, Gibson A, Walts AE, Karimian B, Baltayan A, et al. Abnormal Mismatch Repair and Other Clinicopathologic Predictors of Poor Response to Progestin Treatment in Young Women With Endometrial Complex Atypical Hyperplasia and Well-Differentiated Endometrial Adenocarcinoma: A Consecutive Case Series. *BJOG* (2017) 124:1576–83. doi: 10.1111/1471-0528.14491
48. Travaglino A, Raffone A, Saccone G, Insabato L, Mollo A, De Placido G, et al. Immunohistochemical Predictive Markers of Response to Conservative Treatment of Endometrial Hyperplasia and Early Endometrial Cancer: A Systematic Review. *Acta Obstet Gynecol Scand* (2019) 98:1086–99. doi: 10.1111/aogs.13587
49. Vereide AB, Kaino T, Sager G, Arnes M, Ørbo A. Effect of Levonorgestrel IUD and Oral Medroxyprogesterone Acetate on Glandular and Stromal Progesterone Receptors (PRA and PRB), and Estrogen Receptors (ER-Alpha and ER-Beta) in Human Endometrial Hyperplasia. *Gynecol Oncol* (2006) 101:214–23. doi: 10.1016/j.ygyno.2005.10.030
50. Kim JJ, Chapman-Davis E. Role of Progesterone in Endometrial Cancer. *Semin Reprod Med* (2010) 28:081–90. doi: 10.1055/s-0029-1242998
51. Raffone A, Catena U, Travaglino A, Masciullo V, Spadola S, Della Corte L, et al. Mismatch Repair-Deficiency Specifically Predicts Recurrence of Atypical Endometrial Hyperplasia and Early Endometrial Carcinoma After Conservative Treatment: A Multi-Center Study. *Gynecol Oncol* (2021) 161:795–801. doi: 10.1016/j.ygyno.2021.03.029
52. Sengal AT, Smith D, Rogers R, Snell CE, Williams ED, Pollock PM. Fibroblast Growth Factor Receptor 2 Isoforms Detected *via* Novel RNA ISH as Predictive Biomarkers for Progestin Therapy in Atypical Hyperplasia and Low-Grade Endometrial Cancer. *Cancers (Basel)* (2021) 13:1703. doi: 10.3390/cancers13071703
53. Cibula D, Pötter R, Planchamp F, Avall-Lundqvist E, Fischerova D, Haie Meder C, et al. The European Society of Gynaecological Oncology/European Society for Radiotherapy and Oncology/European Society of Pathology Guidelines for the Management of Patients With Cervical Cancer. *Virchows Arch* (2018) 472:919–36. doi: 10.1007/s00428-018-2362-9
54. Zannoni GF, Vellone VG, Carbone A. Morphological Effects of Radiochemotherapy on Cervical Carcinoma: A Morphological Study of 50 Cases of Hysterectomy Specimens After Neoadjuvant Treatment. *Int J Gynecol Pathol* (2008) 27:274–81. doi: 10.1097/PGP.0b013e31815b1263
55. Takatori E, Shoji T, Omi H, Kagabu M, Miura F, Takeuchi S, et al. Analysis of Prognostic Factors for Patients With Bulky Squamous Cell Carcinoma of the Uterine Cervix Who Underwent Neoadjuvant Chemotherapy Followed by Radical Hysterectomy. *Int J Clin Oncol* (2015) 20:345–50. doi: 10.1007/s10147-014-0702-6
56. Gadducci A, Sartori E, Maggino T, Zola P, Cosio S, Zizioli V, et al. Pathological Response on Surgical Samples is an Independent Prognostic Variable for Patients With Stage Ib2-IIb Cervical Cancer Treated With Neoadjuvant Chemotherapy and Radical Hysterectomy: An Italian Multicenter Retrospective Study (CTF Study). *Gynecol Oncol* (2013) 131:640–4. doi: 10.1016/j.ygyno.2013.09.029
57. Huang K, Sun H, Chen Z, Li X, Wang S, Zhao X, et al. Optimal Pathological Response Indicated Better Long-Term Outcome Among Patients With Stage IB2 to IIB Cervical Cancer Submitted to Neoadjuvant Chemotherapy. *Sci Rep* (2016) 6:28278. doi: 10.1038/srep28278
58. Buda A, Fossati R, Colombo N, Fei F, Floriani I, Gueli Alletti D, et al. Randomized Trial of Neoadjuvant Chemotherapy Comparing Paclitaxel, Ifosfamide, and Cisplatin With Ifosfamide and Cisplatin Followed by Radical Surgery in Patients With Locally Advanced Squamous Cell Cervical Carcinoma: The SNAP01 (Studio Neo-Adjuvante Portio) Italian Collaborative Study. *J Clin Oncol* (2005) 23(18):4137–45. doi: 10.1200/JCO.2005.04.172
59. Zannoni GF, Travaglino A, Raffone A, Arciuolo D, D'Alessandris N, Scaglione G, et al. Depth of Stromal Invasion as the Most Prognostically Relevant Regression System in Locally Advanced Cervical Cancer After Neoadjuvant Treatment: A Systematic Review and Meta-Analysis Grading. *Diagnostics* (2021) 11:1772. doi: 10.3390/diagnostics11101772
60. D'Alessandris N, Palaia I, Pernazza A, Tomao F, Di Pinto A, Musacchio L, et al. PD-L1 Expression Is Associated With Tumor Infiltrating Lymphocytes That Predict Response to NACT in Squamous Cell Cervical Cancer. *Virchows Arch* (2021) 478:517–25. doi: 10.1007/s00428-020-02922-5
61. Palaia I, Tomao F, DI Pinto A, Pernazza A, Santangelo G, D'Alessandris N, et al. Response to Neoadjuvant Chemotherapy in Locally Advanced Cervical Cancer: The Role of Immune-Related Factors. *In Vivo*. (2021) 35:1277–83. doi: 10.21873/invivo.12379

Conflict of Interest: The authors declare that the research was conducted in the absence of any commercial or financial relationships that could be construed as a potential conflict of interest.

Publisher's Note: All claims expressed in this article are solely those of the authors and do not necessarily represent those of their affiliated organizations, or those of the publisher, the editors and the reviewers. Any product that may be evaluated in this article, or claim that may be made by its manufacturer, is not guaranteed or endorsed by the publisher.

Copyright © 2022 Inzani, Arciuolo, Angelico, Santoro, Travaglino, D'Alessandris, Scaglione, Valente, Cianfrini, Raffone and Zannoni. This is an open-access article distributed under the terms of the Creative Commons Attribution License (CC BY). The use, distribution or reproduction in other forums is permitted, provided the original author(s) and the copyright owner(s) are credited and that the original publication in this journal is cited, in accordance with accepted academic practice. No use, distribution or reproduction is permitted which does not comply with these terms.

frontiers in Oncology

ORIGINAL RESEARCH
published: 11 February 2022
doi: 10.3389/fonc.2022.823018

DLC1 Is a Prognosis-Related Biomarker Correlated With Tumor Microenvironment Remodeling in Endometrial Carcinoma

Yalan Wu[1†], *Li-e Zheng*[1†], *Shumin Chen*[1], *Chengyu Lv*[2] *and Yuxiu Huang*[1*]

[1] Department of Gynecology, The Affiliated First Hospital of Fujian Medical University, Fuzhou, China, [2] Department of Obstetrics and Gynecology, Fujian Maternity and Child Health Hospital, Affiliated Hospital of Fujian Medical University, Fuzhou, China

OPEN ACCESS

Edited by:
Priya Ranjit Bhosale, University of Texas MD Anderson Cancer Center, United States

Reviewed by:
Ziheng Wang, Affiliated Hospital of Nantong University, China
Luca Falzone, G. Pascale National Cancer Institute Foundation (IRCCS), Italy

***Correspondence:**
Yuxiu Huang
yxhuang@fjmu.edu.cn

[†]These authors have contributed equally to this work and share first authorship

Specialty section:
This article was submitted to Gynecological Oncology, a section of the journal Frontiers in Oncology

Received: 26 November 2021
Accepted: 14 January 2022
Published: 11 February 2022

Citation:
Wu Y, Zheng L, Chen S, Lv C and Huang Y (2022) DLC1 Is a Prognosis-Related Biomarker Correlated With Tumor Microenvironment Remodeling in Endometrial Carcinoma. Front. Oncol. 12:823018. doi: 10.3389/fonc.2022.823018

Background and Aim: Deleted in liver cancer 1 (DLC1) is confirmed as a metastasis suppressor gene in endometrial carcinoma (EC). However, its functional mechanisms remain unclear. This study aimed to explore the relationship between DLC1 expression and EC.

Methods: The Cancer Genome Atlas database was used for evaluating the expression of DLC1 in pan-cancer. CIBERSORT was used to assess the relationship between DLC1 and tumor immune infiltration. We applied real-time quantitative polymerase chain reaction to determine the expression of DLC1 in EC and adjacent normal tissue samples. The targeting endogenous protein levels were assessed using the dataset from the cBioPortal database.

Results: DLC1 expression negatively correlated with the clinical characteristics (clinical stage, histologic grade) and positively correlated with the survival of patients with uterine corpus EC (UCEC). The gene set enrichment analysis displayed that the low-expression DLC1 group was enriched in metabolic pathways. Concomitantly, the high-expression DLC1 group was enriched in tumor immune-related activities. The CIBERSORT analysis showed that the number of resting memory CD4 T cells and resting mast cells positively correlated with DLC1 expression, while the number of macrophages M2 had a negative correlation, indicating that DLC1 played a key role in mediating immune cell infiltration. The target gene validation confirmed that DLC1 expression was downregulated in tumor samples. The target protein level was consistently downregulated in tumor samples.

Conclusions: DLC1 levels might be useful in predicting the prognosis of patients with UCEC and especially governing the status of tumor microenvironment transition from immune-dominant to metabolic-dominant. The findings shed a different light on the immune therapeutics of UCEC.

Keywords: deleted in liver cancer 1 (DLC1), endometrial neoplasms, prognosis-related biomarker, tumor microenvironment remodeling, metastasis suppressor gene, macrophages M2, immune cell infiltration

INTRODUCTION

Endometrial carcinoma (EC) is the most common gynecological malignancy with an increasing incidence in developed countries (1, 2). With the development of medicine, a variety of treatments are applied in clinical practice, including surgical resection, chemotherapy, radiotherapy, hormonal therapy, and immunotherapy (3, 4). However, the estimated number of new EC cases in the USA in 2021 is 66,570 with 12,940 deaths according to the American Cancer Society (1). Hence, novel treatment options are urgently needed as the prognosis has not improved over these years.

Many studies have shown that the tumor microenvironment (TME) plays a crucial role in cancer development (5–8). The TME is composed of extracellular matrix, blood or lymphatic vessels, fibroblasts, inflammatory cells, immune cells, and extracellular metabolites. Tumor-infiltrating immune cells (TICs) play a vital role in modulating the TME status of EC (9). Hence, TICs can predict the prognosis of patients with EC. In the TME, tumor cells create a toxic milieu for TICs through metabolism to suppress immunity (10). A study proved that the high-immunity TME might prevent the progression of EC (11). Unfortunately, the concrete mechanism is uncertain. Programmed death-1 signaling was proved to be associated with the activation of tumor-infiltrating CD4 and CD8 T cells in the TME. Based on this, targeting this pathway seems to be a promising immunotherapeutic strategy to be applied in clinical studies (12). A recent study demonstrated a cross talk between tumor cells and tumor-associated macrophages (TAMs) *via* SIGLEC1, CCL8, and CSF1, suggesting that the gene signature of TAMs correlated with poor clinical outcomes (13). These results suggested that the immune response within the TME might be of much importance in the development of EC. Therefore, the dynamic modulation of the immune and stromal components in the TME can be examined through an appropriate precise genetic analysis.

Deleted in liver cancer 1 (DLC1) was initially identified in a primary human hepatocellular carcinoma (HCC) in 1998. It acts as a switch by promoting the conversion of the active RhoGTP into the inactive RhoGDP to affect the cytoskeleton, focal adhesion, and cell migration (14, 15). DLC1 was considered as a metastasis suppressor gene in EC, but its functional mechanisms remain unclear. We speculated that DLC1 was relevant to the prognosis of EC through immune infiltrates. In this study, we conducted a comprehensive assessment of the relationship between DLC1 and patient prognosis using The Cancer Genome Atlas (TCGA) database. We further investigated the link between DLC1 and immune cell infiltration of tumors using CIBERSORT to investigate the aforementioned assumptions. Our results offered novel insights into the functional role of DLC1 in EC, thereby highlighting a potential mechanistic basis whereby DLC1 influenced immune cell interaction with tumors. The restoration of DLC1 expression in cancer cells induced apoptosis and senescence; inhibited cell growth, migration, and invasiveness; and reduced tumor formation (16).

Immunotherapy basically involves stimulating the endogenous immune response specifically against tumor cells and represents the most promising therapeutic approach in EC. DLC1 might be an attractive target for tumor immunotherapy in EC.

MATERIALS AND METHODS

Data Collection

A total of 33 selected cancer types with the corresponding expression profiles and clinical data were downloaded from the TCGA database (https://portal.gdc.cancer.gov/). A dataset of 543 cases of EC was obtained from the TCGA database. We also extracted detailed clinical information, as shown in **Table 1**,

TABLE 1 | TCGA endometrial carcinoma patient characteristics.

Clinical characteristics		Total (543)	%
Age at diagnosis (years)		64 (31–90)	
Histologic grade	G1	98	18.0
	G2	120	22.1
	G3	325	59.9
Histology	Endometrioid adenocarcinoma	401	73.9
	Serous cystadenocarcinoma	137	25.2
	The other	5	0.9
Stage	I	339	62.4
	II	51	9.4
	III	124	22.8
	IV	29	5.4
Diabetes	Yes	99	27.2
	No	265	72.8
BMI	≤30	302	59.0
	>30	210	41.0
Menopause status	Pre	35	7.1
	Peri	445	89.5
	Post	17	3.4
Race	White	372	74.7
	Black or African American	106	21.3
	Asian	20	4.0

including age, histologic grade, histology, clinical stage, diabetes, body mass index (BMI), menopause status, and race. A dataset of a study [Endometrial Cancer (MSK, 2012)] including 95 patients with UCEC (83 endometrioid and 12 serous tumors), with the clinical information and expression profiles, was obtained from the cBioPortal database (http://www.cbioportal.org/). Seventeen pairs of matched EC and adjacent normal tissues were collected from 17 patients with EC who underwent surgery at The Affiliated First Hospital of Fujian Medical University from January 2018 to September 2018. The clinical sample collection cohorts included 17 patients. Reverse transcription-quantitative polymerase chain reaction was carried out to determine the relative expression of DLC1.The patients from the TCGA database were defined as a training cohort, while the dataset from the cBioPortal and the results of PCR were used for external validation.

Gene Set Enrichment Analysis

KEGG and C7 gene set v7.4 collections were downloaded from the Molecular Signatures Database as the target sets. Gene set enrichment analysis (GSEA) was performed using the software GSEA-4.1 downloaded from the Broad Institute. We used the GSEA to determine the correlation between DLC1 expression and signaling pathway. The whole transcription of all tumor samples was used for GSEA, and only gene sets supplied with NOM $P < 0.05$ and FDR $q < 0.07$ were considered significant.

TIC Profile

The CIBERSORT computational method was applied for estimating the TIC abundance profile in all tumor samples, followed by quality filtering. Only 319 tumor samples with $P < 0.05$ were selected for the following analysis.

TIMER Database Analysis

TIMER (https://cistrome.shinyapps.io/timer/) is a database designed for analyzing immune cell infiltrates in multiple types of cancers. We assessed how DLC1 expression correlated with the expression of the markers of particular immune-infiltrating cell subsets.

Real-Time Quantitative PCR

RT-qPCR was performed using 17 pairs of matched EC and adjacent normal tissues from 17 patients with EC who underwent surgery at The Affiliated First Hospital of Fujian Medical University from January 2018 to September 2018. The study was approved by an institutional review board. All methods were performed following the regulations and relevant guidelines. The written informed consent was obtained before clinical sample collection. The histology of all samples was centrally reviewed by a pathologist. None of the patients had received therapeutic medications or previous surgical interventions before sample collection.

Total RNA from the EC and adjacent normal tissues was extracted using an E.Z.N.A. Total RNA Kit I kit (Omega, Shanghai, China) and then reverse-transcribed into cDNA using a Evo M-MLV reverse transcription reagent kit (Accurate Biology, Hunan, China). The relative expression levels of DLC1 were determined by RT-qPCR using an SYBR Premix Ex Taq kit (TaKaRa, Shanghai, China) in a real-time PCR system. Finally, the threshold cycle (Ct) of the target gene and reference gene was obtained. All samples were set for two replicates, and the final results were averaged. The primer sequences used for amplification are shown in **Table 2**. GAPDH was used as the endogenous controls.

Statistical Analysis

We used R (v.4.0.2) and SPSS 23.0 statistical software to perform statistical analysis. Box plot and violin plot were produced using R language with the ggpubr package. The gene expression difference of DLC1 was analyzed using the Wilcoxon rank-sum test. The survival analysis and clinical characteristic analysis were performed using R language. The survival curve was plotted by the Kaplan–Meier method and log-rank test as the statistical significance test; a P-value <0.05 indicated a statistically significant difference. The relationship between clinical characteristics and DLC1 expression level was evaluated using the Wilcoxon rank-sum or Kruskal–Wallis rank-sum test. The cutoff value of DLC1 expression was determined by its median value. We used $2-\Delta\Delta Ct$ to analyze the outcome of PCR. The distribution of paired sample difference disobeying a normality test was found. The median (interquartile range) was used for statistical description of DLC1 expression. The difference of DLC1 expression between matched EC and adjacent normal tissues was analyzed using the Wilcoxon signed-rank test. A P-value of less than 0.05 indicated a statistically significant difference.

RESULTS

Assessment of DLC1 Expression in Different Cancer and Normal Tissues

We first analyzed the expression of DLC1 in multiple tumor and normal tissue types using the TCGA database to explore DLC1

TABLE 2 | The primer sequences used for amplification.

Primer name	Primer sequences	Primer length (nt)	Product length (bp)	Annealing temperature (°C)
DLC1 F	AAACAGTATGGCACCTCA	18	164	51.72
DLC1 R	CAATCAAATACCTGGACAA	19		
β-Actin F	TGGCACCCAGCACAATGAA	19	186	60.80
β-Actin R	CTAAGTCATAGTCCGCCTAGAAGCA	25		

expression in cancer and normal tissues. The analysis displayed that DLC1 expression significantly declined in normal controls in thyroid carcinoma. In contrast, DLC1 expression significantly decreased in bladder urothelial carcinoma, breast invasive carcinoma, cervical squamous cell carcinoma and endocervical adenocarcinoma (CESC), cholangiocarcinoma (CHOL), kidney chromophobe, kidney renal papillary cell carcinoma (KIRP), liver hepatocellular carcinoma, lung adenocarcinoma, lung squamous cell carcinoma, prostate adenocarcinoma, rectum adenocarcinoma, and uterine corpus EC (UCEC) tissues compared with normal control tissues.

The expression of DLC1 in tumor and normal adjacent tissue samples in the TCGA dataset is displayed in **Figure 1**.

Relationship Between DLC1 Expression and Cancer Patient Prognosis

The study next analyzed the correlation between DLC1 expression and cancer patient prognosis. We employed the TCGA database to assess how DLC1 expression was related to prognosis by analyzing 33 TCGA cancer types. We demonstrated that the increase in DLC1 expression was related to a worse prognosis in ACC [overall survival (OS): $P = 0.007$, hazard ratio (HR) = 1.777, 95% CI = 1.166–2.708; disease-specific survival (DSS): $P = 0.002$, HR = 2.017, 95% CI = 1.306–3.115; progression-free interval (PFI): $P < 0.001$, HR = 2.156, 95% CI = 1.544–3.011] and LGG (OS: $P < 0.001$, HR = 2.431, 95% CI = 1.875–3.152; DSS: $P < 0.001$, HR = 2.765, 95% CI = 2.091–3.655; PFI: $P < 0.001$, HR = 2.178, 95% CI = 1.740–2.725). On the contrary, we found a relationship between decreased DLC1 expression and better patient prognosis in KIRC (OS: $P < 0.001$, HR = 0.682, 95% CI = 0.564–0.826; DSS: $P < 0.001$, HR = 0.618, 95% CI = 0.491–0.777; PFI: $P = 0.001$, HR = 0.738, 95% CI = 0.612–0.890), UVM (OS: $P < 0.001$, HR = 0.287, 95% CI = 0.154–0.537; DSS: $P < 0.001$, HR = 0.259, 95% CI = 0.131–0.513; PFI: $P = 0.001$, HR = 0.417, 95% CI = 0.244–0.713), and UCEC (OS: $P = 0.002$, HR = 0.556, 95% CI = 0.383–0.806; DSS: $P = 0.006$, HR = 0.544, 95% CI = 0.353–0.837; PFI: $P = 0.007$, HR = 0.676, 95% CI = 0.509–0.898) (**Supplement Table 4**).

These findings clearly demonstrated that DLC1 expression conspicuously correlated with the outcome of multiple tumor types (**Figures 2**, **3**).

Decreased Expression of DLC1 in EC Predicts a Poorer Prognosis

We focused on DLC1 expression in UCEC for a subsequent set of analyses, including DLC1 expression and clinical characteristic correlation analysis, survival analysis, and Cox logistic regression analysis.

After excluding normal UCEC samples, DLC1 expression data of 543 patients with EC and clinical data were preserved from the TCGA database (**Table 1**).

In this study, the Wilcoxon rank-sum test displayed that the DLC1 expression significantly decreased in the tumor samples compared with normal ones (**Figure 4A**). Similar results were observed in the pairing analysis between the normal and tumor tissues that originated from the same patients (**Figure 4B**). Next, using the Wilcoxon rank-sum test and the Kruskal–Wallis test, we discovered that the reduced expression of DLC1 was significantly related to tumor histological types (EEA vs. SEA, $P = 8.2e{-}05$), histological grade (G2 vs. G3, $P = 0.03$), clinical

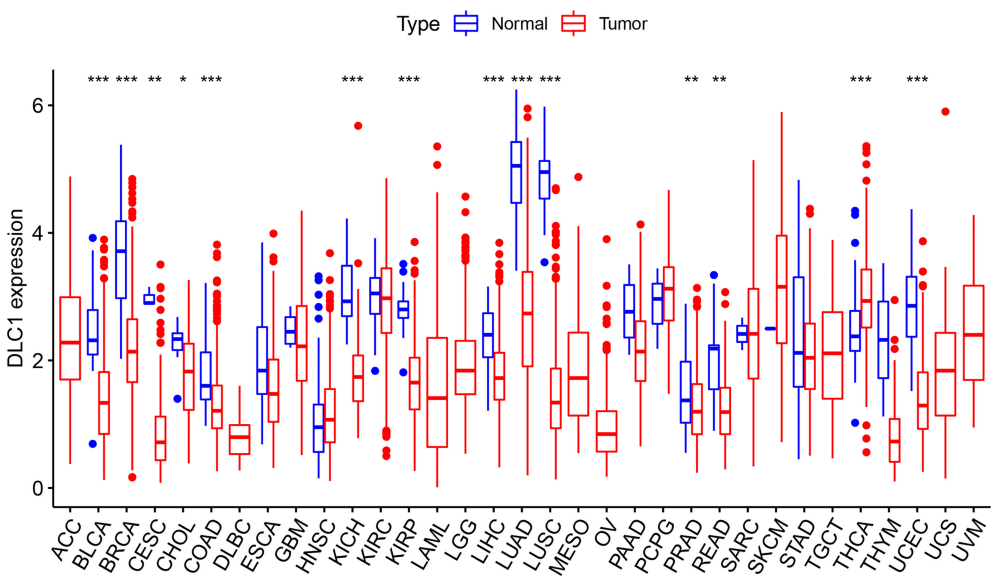


FIGURE 1 | Expression level of deleted in liver cancer 1 (DLC1) in different types of tumor and normal tissues in The Cancer Genome Atlas (TCGA) database (*$P <$ 0.05, **$P < 0.01$, ***$P < 0.001$).

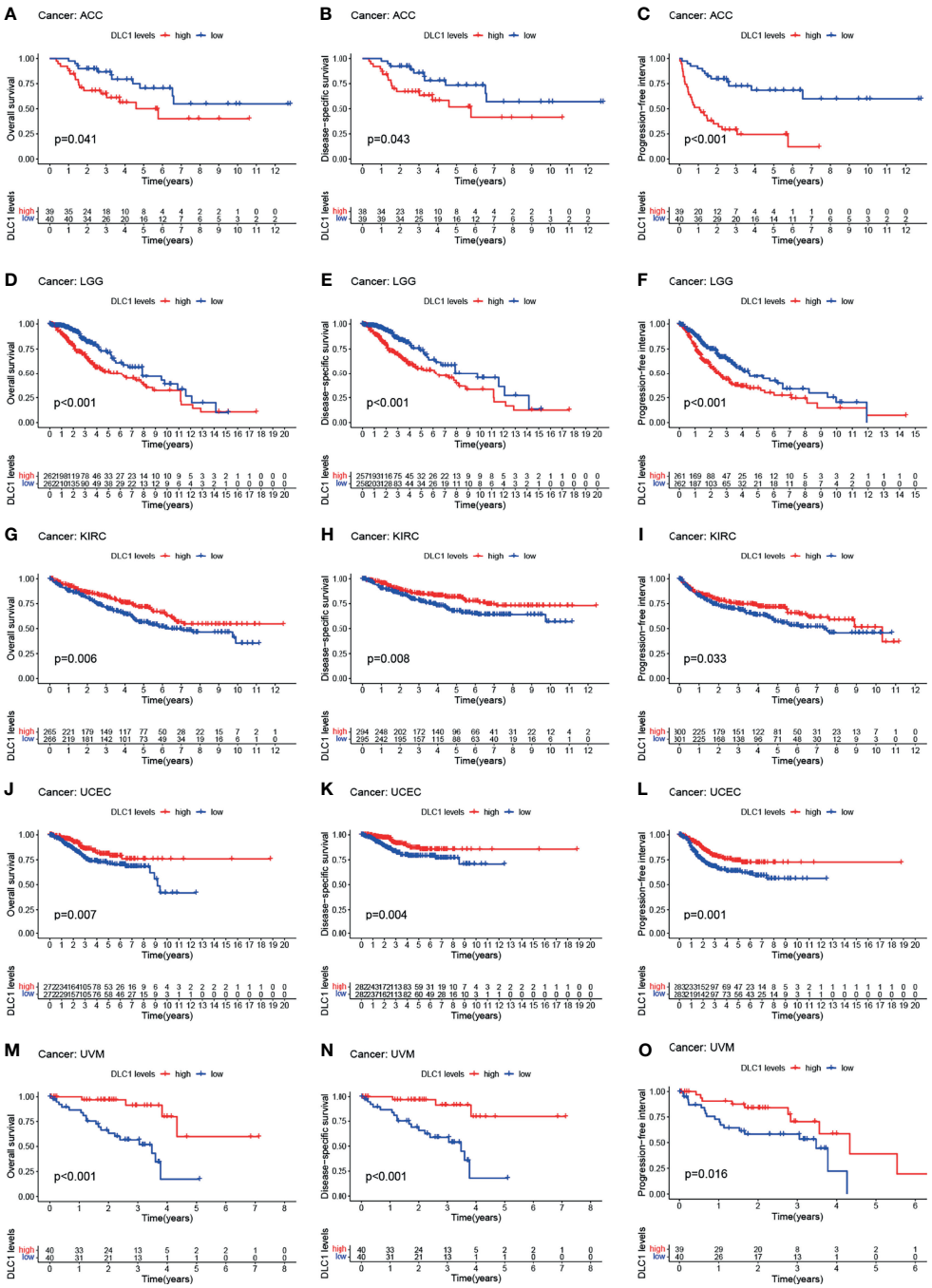


FIGURE 2 | Relationship between DLC1 expression and prognosis of various types of cancer in the TCGA database **(A–O)**. Patients were divided into high-expression and low-expression groups depending on the comparison with the median expression level using the log-rank test. OS, overall survival; DSS, disease-specific survival; PFI, progression-free interval.

stage (P = 0.047), BMI (P = 0.036), diabetes (P = 0.018), event (P = 0.004), and menopause status (P = 8.6e−07) (**Figures 4D–I**). As shown in **Table 3**, age, stage, grade, and DLC1 expression were demonstrated as independent prognostic indicators for patients with UCEC (P < 0.05). Multivariate Cox analysis displayed that poor OS had a significant correlation with age (P < 0.001, HR = 1.047, 95% CI = 1.019–1.076), stage (P < 0.001, HR = 1.859, 95% CI = 0.538–2.325), grade (P = 0.001, HR = 2.569, 95% CI = 1.458–4.525), and DLC1 expression (P = 0.003, HR = 0.695, 95% CI = 0.547–0.882).

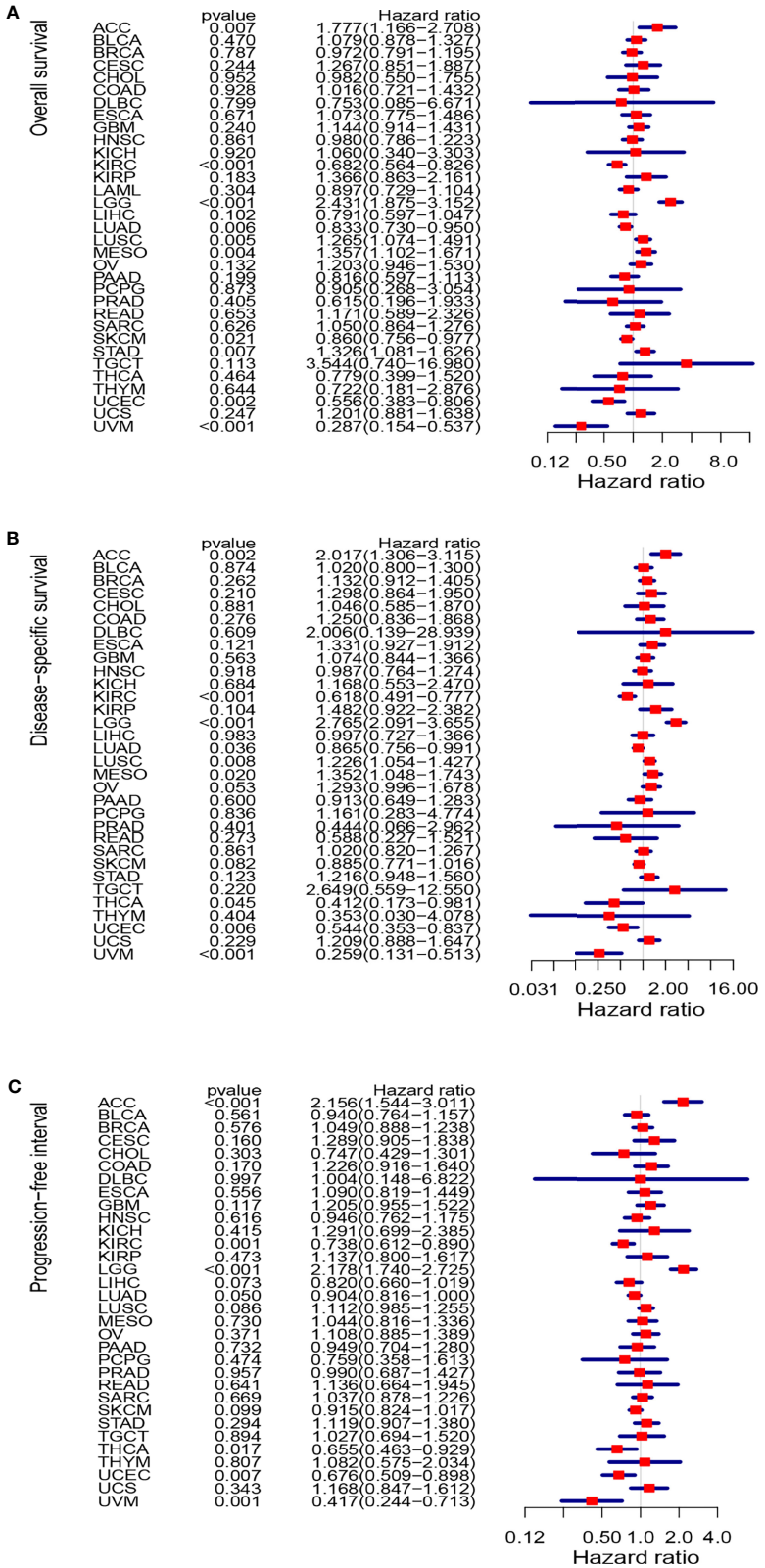


FIGURE 3 | Forest plots of studies investigating the correlation between DLC1 expression and prognosis of various types of cancer in the TCGA database. **(A)** Forest plots for overall survival; **(B)** forest plots for disease-specific survival; **(C)** forest plot for progression-free interval. HR, hazard ratio; CI, confidence interval.

DLC1 Might Be Associated With the Immune and Stromal Components in the TME

Given the DLCI expression was associated with the survival and clinical characteristics of patients with UCEC, GSEA was performed in the high-expression and low-expression groups relative to the median level of DLCI expression. The tumor immunity- and inflammation-related activities, such as Wnt signaling pathway, leukocyte transendothelial migration, and JAK–STAT signaling pathway, were mainly enriched in the high-DLC1 expression group (**Figure 5A**).

In the low-DLC1 expression group, the metabolic pathways that were enriched included pyrimidine metabolism, pyruvate metabolism, alanine aspartate and glutamate metabolism, and oxidative phosphorylation (**Figure 5B**). Regarding the C7 collection defined by MSigDB, multiple immune functional gene sets were predominantly enriched in the high-DLC1 expression group (**Figure 5C**). Nevertheless, no gene sets were enriched in the low-DLC1 expression group. Based on the aforementioned results, we postulated that DLC1 might be associated with the immune and stromal components in the TME.

Relationship Between DLC1 and the Proportion of TICs

The study further verified the relationship between DLC1 expression and the immune microenvironment. We applied the CIBERSORT algorithm to analyze the proportion of tumor-infiltrating immune subsets and constructed a profile including 21 kinds of immune cells in UCEC samples (**Figure 6**). A total of three kinds of TICs were associated with DLC1 expression, as detected by the difference and correlation analyses (**Figure 7**).

Among these, the proportion of resting memory CD4 T cells and resting mast cells positively correlated with DLC1 expression. However, the number of macrophages M2 had a negative correlation. The results confirmed that the expression levels of DLC1 influenced the immune activity of the TME.

Target Gene Expression Validation

As shown in **Figure 4**, we found DLC1 with lower expression levels in tumor samples (**Figures 4A, B**); patients with the high expression of DLC1 exhibited prolonged survival (**Figures 2J–L**). We then collected 17 UCEC samples and adjacent normal tissue samples to validate the expression of DLC1 in patients with

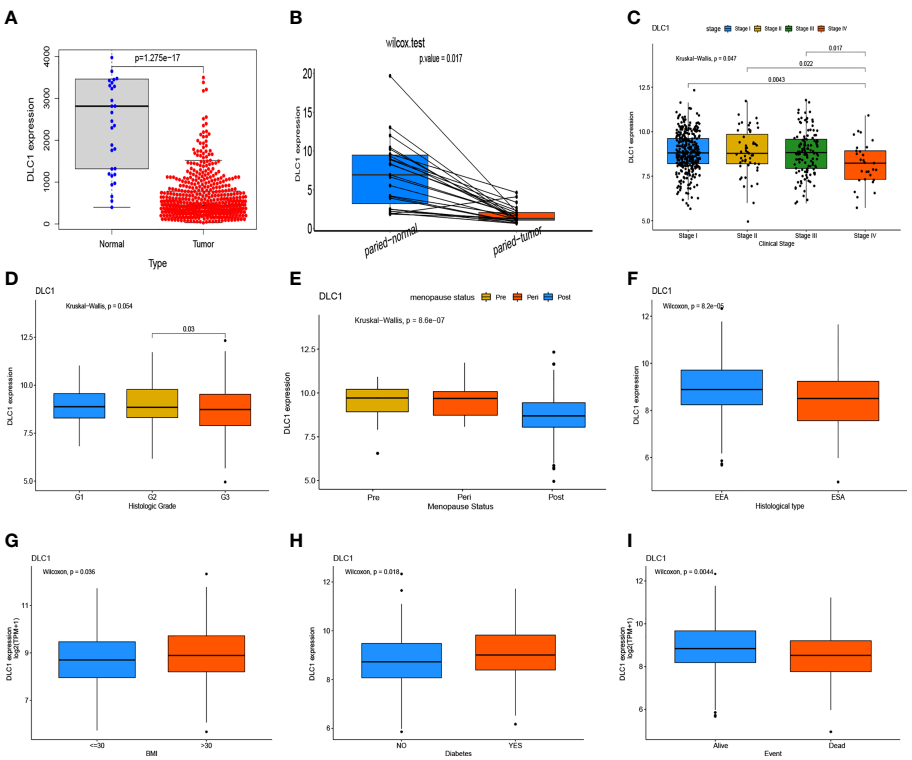


FIGURE 4 | Expression level of DLC1 in samples and its correlation with the clinical characteristics and survival of patients with uterine corpus endometrial carcinoma (UCEC). **(A)** DLC1 expression in the normal and tumor samples. Analyses were performed across all normal and tumor samples with *P*-value close to zero using the Wilcoxon rank-sum test. **(B)** Paired differentiation analysis for the DLC1 expression in the normal and tumor samples derived from the same patient (*P* = 5.572602e−05) using the Wilcoxon signed-rank test. **(C–I)** Relationship between DCL1 expression and clinical characteristics and survival. The statistical significance was calculated using the Kruskal–Wallis rank-sum test or Wilcoxon rank-sum test.

TABLE 3 | Univariate analysis and multivariate analysis of the correlation of DLC1 expression with OS among endometrial carcinoma patients.

Parameter	Univariate analysis			Multivariate analysis		
	HR	95% CI	*P*	HR	95% CI	*P*
Age	1.041	1.020–1.062	**<0.001**	1.047	1.019–1.076	**<0.001**
Stage	1.976	1.641–2.381	**<0.001**	1.859	0.538–2.325	**<0.001**
BMI	0.99	0.968–1.013	0.405	1.015	0.987–1.043	0.304
Grade	2.718	1.792–4.123	**<0.001**	2.569	1.458–4.525	**0.001**
Diabetes	1.176	0.685–2.016	0.557	1.118	0.618–2.023	0.713
DLC1	0.827	0.690–0.992	**0.041**	0.695	0.547–0.882	**0.003**

Bold values indicate P <0.05.
HR, hazard ratio; CI, confidence interval.

UCEC. The expression of DLC1 was consistently downregulated in tumor samples (**Figure 8A**).

Target Protein Expression Validation

We download a dataset [Endometrial Cancer (MSK, 2012)] of 95 patients with UCEC (83 endometrioid and 12 serous tumors) from the cBioPortal database to investigate the endogenous protein levels of DLC1. The target protein level was consistently downregulated in tumor samples. Survival analysis demonstrated that the decrease in DLC1 protein level was related to a worse prognosis ($P = 0.04$) (**Figure 8B, C**).

DISCUSSION

This study sought to find out the correlation between DLC1 expression and EC prognosis through TCGA database and subsequently explore its related mechanism. DLC1 is associated with immune activity. Importantly, a series of bioinformatics analyses suggested that DLC1 might be an essential regulator of the TME status for patients with EC.

In this study, we assessed the expression of DLC1 in 33 different types of cancers using the TCGA database, so as to reveal the differences between tumor and normal tissue expression of DLC1 in many cancers. We explored the

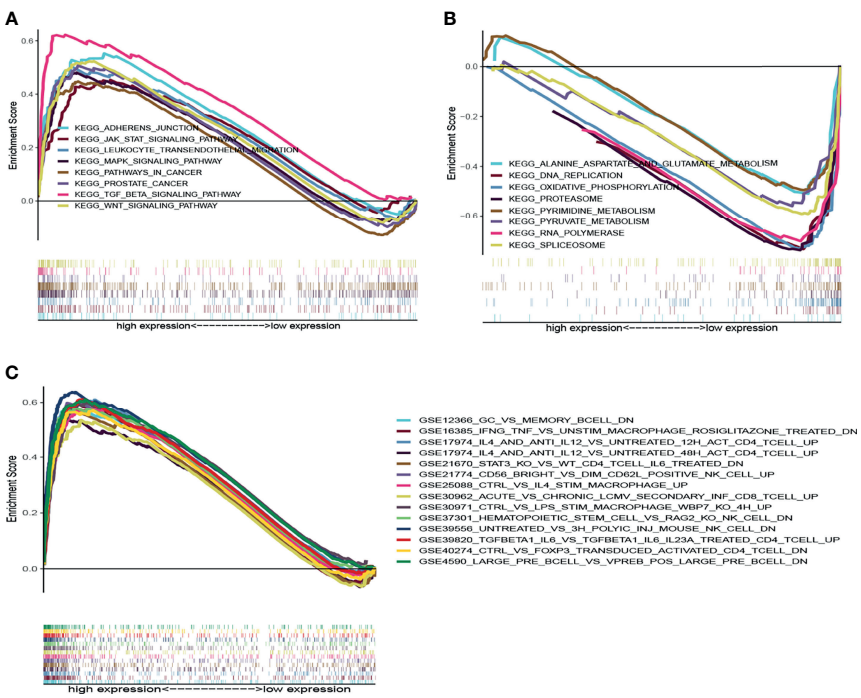


FIGURE 5 | GSEA for samples with high-DLC1 and low-DLC1 expression. **(A)** Enriched gene sets in the KEGG collection of the high-DLC1 expression sample. Each line is uniquely colored demonstrating one particular gene set. Upregulated genes are located on the left approaching the origin of the coordinates, while the downregulated ones lay on the right of the *x*-axis. Only gene sets satisfied with NOM *P* <0.05 and FDR *q* <0.07 were considered significant. In the plot, only leading gene sets are presented. **(B)** Enriched gene sets in the KEGG collection of low-DLC1 expression sample. **(C)** Enriched gene sets in C7 collection and the immunologic gene sets in the high-DLC1 expression sample. Only leading gene sets are displayed in the plot.

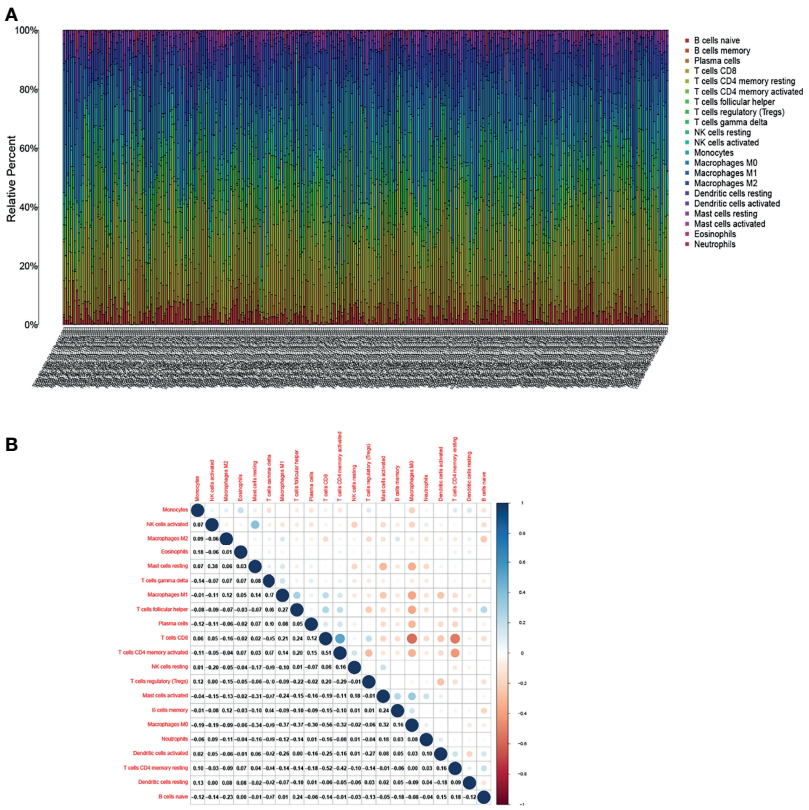


FIGURE 6 | Tumor-infiltrating immune cell (TIC) profile in tumor samples and correlation analysis. **(A)** Proportion of 21 kinds of TICs in UCEC tumor samples is displayed by a ballot plot. Column names of the plot correspond to sample ID. **(B)** Heatmap presenting the relationship between 21 kinds of TICs and numeric in each tiny box representing the association *P*-value between two kinds of cells. The shade of each tiny color box indicates the corresponding association value between two cells. The significance test was displayed using Pearson correlation coefficient.

prognostic relation between the expression of DLC1 and 33 different types of cancers, indicating the correlation between lower DLC1 expression and a poor UCEC prognosis. DLC1 is viewed as a potential tumor suppressor. A study showed that restoring DLC1 expression in cancer cells induced apoptosis and senescence, inhibited migration and invasiveness, and reduced tumor formation (16). Suppressing DLC1 degradation could inhibit the migration through the DLC1/RhoA pathway in breast cancer (17). The upregulated expression of DLC1 could inhibit the migration from 32.5% to 11.5% in HCC cells, and its post-translational modification was mediated by PI3K/Akt signaling (18). The restoration of DLC1 expression in gallbladder cancer cells resulted in caspase-3-mediated apoptosis (19). DLC1 may mediate cell apoptosis and suppress the growth and invasion through regulating the Wnt/β-catenin signaling pathway (20). Despite a series of studies focusing on DCL1, the mechanism of its influence on cancer cells has not yet been completely elucidated.

We further explored whether the expression of DLC1 was related to histological type, histological grade, clinical stage, BMI, diabetes, event, and menopause status. DLC1 expression was significantly lower in the late stages than in the early stages of cancer. These results suggested that DLC1 might serve as a prognostic marker of EC. A report showed that DLC1 was often lost in cancer cells. It remained within the stromal components and was concentrated in proximity to endothelial (CD34 positive) cells (21). Therefore, we further analyzed the relationship between DLC1 expression and TME. The GSEA results showed that the metabolic pathways including pyrimidine metabolism, pyruvate metabolism, alanine aspartate and glutamate metabolism, and oxidative phosphorylation were enriched in the low-DLC1 expression group. A study suggested that stroma-associated pancreatic stellate cells supported malignant cells by providing nutrients such as alanine and lipids to the TME (22). This might be part of the mechanisms underlying the relationship between DLC1 and tumor prognosis. In the high-DLC1 expression group, tumor immunity-related signaling pathways, such as Wnt signaling pathway, leukocyte transendothelial migration, and JAK–STAT signaling pathway, were markedly enriched. Our study found that the balance between typical tumor pathways and metabolism affected the immunity status to a certain degree. Accordingly, the downregulation of DLC1 with the advancing stage of UCEC and the conversion of TME from immune-predominant into

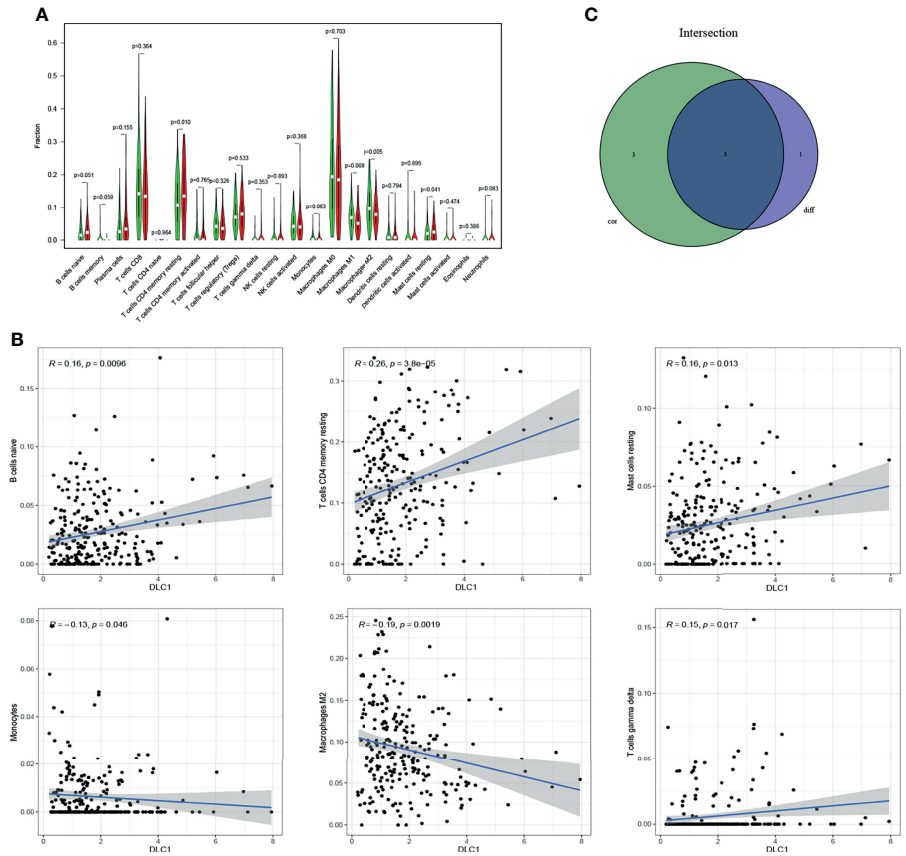


FIGURE 7 | Relationship between TIC proportion and DLC1 expression. **(A)** Differentiation of 21 kinds of immune cells in UCEC tumor samples with low- or high-DLC1 expression compared with the median of DLC1 expression level was shown by a violin plot. The significance test was displayed using Wilcoxon rank-sum. **(B)** Scatter plot showed the relationship between six kinds of TICs in proportion with the DLC1 expression ($P < 0.05$). The blue line in each plot was fitted into a linear model indicating the proportion of tropism of the immune cells along with DLC1 expression; the correlation test was displayed using the Pearson correlation coefficient. **(C)** Venn plot presented three kinds of TICs relative to DLC1 expression co-determined by difference and correlation tests indicated in violin and scatter plots, respectively.

metabolic-dominant status indicated that DLC1 might be a potential tumor suppressor in UCEC.

The CIBERSORT analysis for the proportion of TICs revealed that the number of macrophages M2 negatively correlated with DLC1 expression in patients with UCEC. Different TAM subsets play a role in the inhibition of tumor progression. The levels of anti-inflammatory cytokines, scavenging receptors, angiogenesis factors, and protease were higher in M2-like macrophages than in M1-like macrophages. Therefore, TAMs were deemed to promote tumor progression. Cytokines are highly dynamic in the TAM compartment. The macrophage-centric treatments include transformation into M1-like macrophages. A recent study demonstrated a cross talk between tumor cells and TAMs *via* SIGLEC1, CCL8, and CSF1 (13). We concluded that the expression of DLC1 negatively correlated with SIGLEC1 and CCL8 expression using the TIMER website, which further proved that DLC1 expression was negatively related to M2-like macrophages (**Supplement Table 3**). Therefore, our findings might offer new ideas for macrophage-related treatments in EC.

TAMs can be polarized into M2-like or M1-like macrophages (distinct TAM subsets) that can induce or repress antitumor immunity, angiogenesis, and cell migration (23). M2-like macrophages express higher levels of anti-inflammatory cytokines, scavenging receptors, angiogenesis factors, and proteases compared with M1-type macrophages (23, 24). In consequence, TAMs are confirmed to stimulate tumor progression. Cytokines within the TME compartment, which is highly dynamic, can manipulate immune functions (6, 25). TAM-centered therapeutic approaches include inducing TAMs to form M1-like macrophages (26).

Studies showed that a multidisciplinary approach to the study of tumors could better identify novel diagnostic and prognostic biomarkers based on the analysis of high-quality biobanks, as well as help formulate better management (27–30). In the final part of the study, we applied real-time quantitative PCR to determine the expression of DLC1 in EC and adjacent normal tissue samples. Then, the DLC1 protein level was assessed using a dataset from the cBioPortal database for final

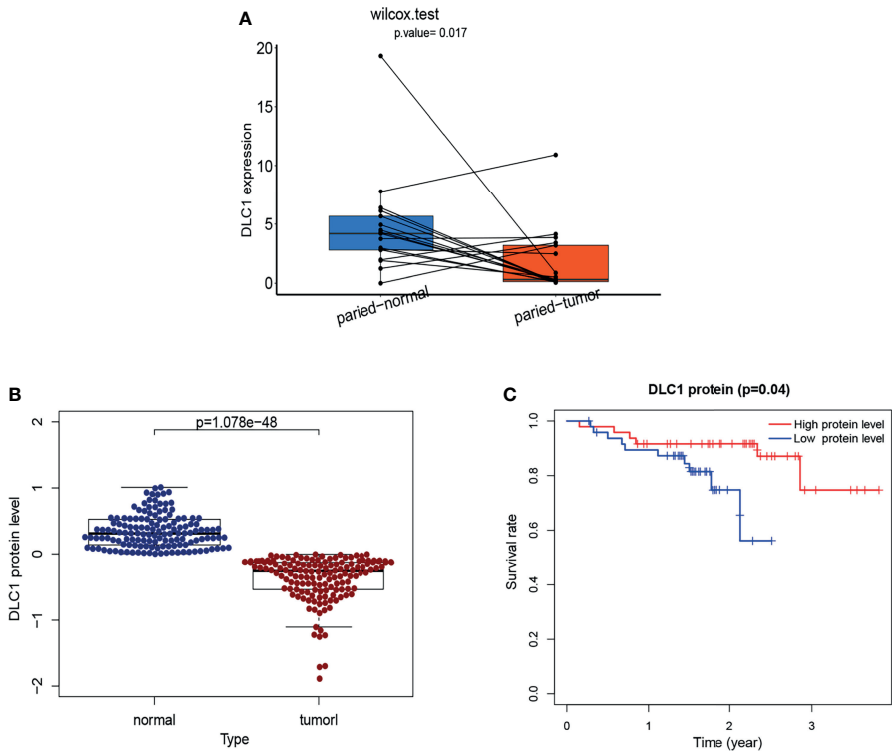


FIGURE 8 | Validation of the target gene by RT-qPCR analysis and validation of DLC1 protein expression based on a dataset from cBioPortal. **(A)**Tumor tissues and paired normal tissues were derived from 17 patients with EC, and Wilcoxon signed-rank test was used for evaluating the statistical significance of differences. **(B)** Relationship between DLC1 protein expression and prognosis of EC in the cBioPortal database. Patients were divided into high-target protein expression or low-target protein expression group depending on the comparison with the median expression level using the log-rank test. **(C)** DLC1 protein expression in the normal and tumor samples. Analyses were performed across all normal and tumor samples with *P*-value close to zero using the Wilcoxon rank-sum test.

verification. Therefore, DLC1 is a valuable prognostic biomarker correlated with TME remodeling in EC. Finding an efficient method to upregulate DLC1 expression may provide an adjuvant treatment for patients with UCEC who are deficient in DLC1 expression.

CONCLUSIONS

Our study first analyzed the expression of DLC1 in multiple tumor and normal tissue types using the TCGA database, displaying that DLC1 expression significantly declined in UCEC. We concentrated on DLC1 in UCEC for a subsequent set of analyses. We discovered that the decreased expression of DLC1 in EC predicted a poorer prognosis. GSEA was performed to further investigate the mechanism. The tumor immunity- and inflammation-related activities were mainly enriched in the high-DLC1 expression group, while metabolic pathways were enriched in the low-DLC1 expression group. Therefore, we postulated that DLC1 might be associated with the immune and stromal components in the TME. We applied for the CIBERSORT algorithm and discovered that resting memory CD4 T cells and resting mast cells positively correlated with DLC1 expression, but the number of macrophages M2 had a negative correlation. Finally, we applied real-time quantitative PCR to determine the expression of DLC1 in EC and adjacent normal tissue samples for further verification. Then, the DLC1 protein level was assessed using a dataset from the cBioPortal database for final verification. These results allowed a more comprehensive understanding of the mechanism of DLC1 affecting the EC prognosis, shedding a different light on the immune therapeutics of UCEC. However, the study had certain limitations in terms of the small number of human samples and the lack of functional studies on EC. More human samples and the corresponding clinical data should be collected to confirm the findings based on the databases.

DATA AVAILABILITY STATEMENT

The datasets presented in this study can be found in online repositories. The names of the repository/repositories and accession number(s) can be found in the article/**Supplementary Material**.

ETHICS STATEMENT

The studies involving human participants were reviewed and approved by the Medical Ethics Committee of The Affiliated First Hospital of Fujian Medical University. The patients/participants provided their written informed consent to participate in this study.

AUTHOR CONTRIBUTIONS

YH and YW conceived of the presented idea. YW developed the theory and performed the computations. YW and SC collected samples. CL performed the real-time quantitative PCR. YW verified the analytical methods. LZ encouraged SC to investigate and supervise the findings of this work. YW and LZ wrote the manuscript with input from all authors. All authors contributed to the design and implementation of the research, to the analysis of the results, and to the writing of the manuscript.

ACKNOWLEDGMENTS

We thank The Cancer Genome Atlas (TCGA) project, TIMER, CIBERSORT, and cBioPortal databases and their contributors for the valuable public datasets used in this study. We thank the seventeen patients with EC who underwent surgery at The Affiliated First Hospital of Fujian Medical University in this study. And we also would like to express our appreciation to the fund, Natural Science Fundation of Fujian Province (No.2016J01530).

SUPPLEMENTARY MATERIAL

The Supplementary Material for this article can be found online at: https://www.frontiersin.org/articles/10.3389/fonc.2022.823018/full#supplementary-material

REFERENCES

1. Siegel RL, Miller KD, Fuchs HE, Jemal A. Cancer Statistics, 2021. *CA Cancer J Clin* (2021) 711:10–13. doi: 10.3322/caac.21654
2. Sung H, Ferlay J, Siegel RL, Laversanne M, Soerjomataram I, Jemal A, et al. Global Cancer Statistics 2020: GLOBOCAN Estimates of Incidence and Mortality Worldwide for 36 Cancers in 185 Countries. *CA Cancer J Clin* (2021) 713:293. doi: 10.3322/caac.21660
3. Concin N, Matias-Guiu X, Vergote I, Cibula D, Mirza MR, Marnitz S, et al. ESGO/ESTRO/ESP Guidelines for the Management of Patients With Endometrial Carcinoma. *Radiother Oncol* (2021) 154:564–74. doi: 10.1016/j.radonc.2020.11.018
4. Paulino E, De Melo AC. Adjuvant Treatment of Endometrial Cancer in Molecular Era: Are We Ready to Move on? *Crit Rev Oncol Hematol* (2020) 153:4. doi: 10.1016/j.critrevonc.2020.103016
5. Quail DF, Joyce JA. Microenvironmental Regulation of Tumor Progression and Metastasis. *Nat Med* (2013) 1911:1–2. doi: 10.1038/nm.3394
6. Hinshaw DC, Shevde LA. The Tumor Microenvironment Innately Modulates Cancer Progression. *Cancer Res* (2019) 7918:1–8. doi: 10.1158/0008-5472.CAN-18-3962
7. Brassart-Pasco S, Brezillon S, Brassart B, Ramont L, Oudart JB, Monboisse JC. Tumor Microenvironment: Extracellular Matrix Alterations Influence Tumor Progression. *Front Oncol* (2020) 10:397. doi: 10.3389/fonc.2020.00397
8. Napoli S, Scuderi C, Candido S, Basile MS, Gattuso G, Bella VD, et al. Functional Roles of Matrix Metalloproteinases and Their Inhibitors in Melanoma. *Cells* (2020). doi: 10.3390/cells9051151
9. Meng Y, Yang Y, Zhang Y, Yang X, Li X, Hu C. The Role of an Immune Signature for Prognosis and Immunotherapy Response in Endometrial Cancer. *Am J Transl Res* (2021) 13(2):1943–8141/AJTR0113797. Original Article.
10. Lim AR, Rathmell WK, Rathmell JC. The Tumor Microenvironment as a Metabolic Barrier to Effector T Cells and Immunotherapy. *Elife* (2020) 9:5–6. doi: 10.7554/eLife.55185
11. Liu J, Nie S, Wu Z, Jiang Y, Wan Y, Li S, et al. Exploration of a Novel Prognostic Risk Signatures and Immune Checkpoint Molecules in Endometrial Carcinoma Microenvironment. *Genomics* (2020) 1125:3131. doi: 10.1016/j.ygeno.2020.05.022
12. Di Tucci C, Capone C, Galati G, Iacobelli V, Schiavi MC, Di Donato V, et al. Immunotherapy in Endometrial Cancer: New Scenarios on the Horizon. *J Gynecol Oncol* (2019) 303:3–5. doi: 10.3802/jgo.2019.30.e46
13. Cassetta L, Fragkogianni S, Sims AH, Swierczak A, Forrester LM, Zhang H, et al. Human Tumor-Associated Macrophage and Monocyte Transcriptional Landscapes Reveal Cancer-Specific Reprogramming, Biomarkers, and Therapeutic Targets. *Cancer Cell* (2019) 354:1. doi: 10.1016/j.ccell.2019.02.009
14. Barras D, Chevalier N, Zoete V, Dempsey R, Lapouge K, Olayioye MA, et al. A WXW Motif is Required for the Anticancer Activity of the TAT-RasGAP317-326 Peptide. *J Biol Chem* (2014) 28934:1. doi: 10.1074/jbc.M114.576272
15. Yuan B-Z, Miller MJ, Keck CL, Zimonjic DB, Thorgeirsson SS, Popescua NC. Cloning, Characterization, and Chromosomal Localization of a Gene Frequently Deleted in Human Liver Cancer (DLC-1) Homologous to Rat RhoGAP. *Cancer Res* (1998).
16. Yam JW, Tse EY, Ng IO. Role and Significance of Focal Adhesion Proteins in Hepatocellular Carcinoma. *J Gastroenterol Hepatol* (2009) 244:524–5. doi: 10.1111/j.1440-1746.2009.05813.x
17. Zhu W, Ma L, Yang B, Zheng Z, Chai R, Liu T, et al. Flavone Inhibits Migration Through DLC1/RhoA Pathway by Decreasing ROS Generation in Breast Cancer Cells. *In Vitro Cell Dev Biol Anim* (2016) 525:3–4. doi: 10.1007/s11626-016-0010-8
18. Chai R, Fu H, Zheng Z, Liu T, Ji S, Li G. Resveratrol Inhibits Proliferation and Migration Through SIRT1 Mediated Posttranslational Modification of PI3K/AKT Signaling in Hepatocellular Carcinoma Cells. *Mol Med Rep* (2017) 166:8041. doi: 10.3892/mmr.2017.7612
19. Qin Y, Chu B, Gong W, Wang J, Tang Z, Shen J, et al. Inhibitory Effects of Deleted in Liver Cancer 1 Gene on Gallbladder Cancer Growth Through Induction of Cell Cycle Arrest and Apoptosis. *J Gastroenterol Hepatol* (2014) 295:966–7, 71. doi: 10.1111/jgh.12486
20. Wang C, Wang J, Liu H, Fu Z. Tumor Suppressor DLC-1 Induces Apoptosis and Inhibits the Growth and Invasion of Colon Cancer Cells Through the Wnt/beta-Catenin Signaling Pathway. *Oncol Rep* (2014) 315:2270, 6. doi: 10.3892/or.2014.3057
21. Wolosz D, Walczak A, Wilczynski GM, Szparecki G, Wilczek E, Gornicka B. Deleted in Liver Cancer 1 Expression and Localization in Hepatocellular Carcinoma Tissue Sections. *Oncol Lett* (2014) 82:286. doi: 10.3892/ol.2014.2216
22. Sousa CM, Biancur DE, Wang X, Halbrook CJ, Sherman MH, Zhang L, et al. Pancreatic Stellate Cells Support Tumour Metabolism Through Autophagic Alanine Secretion. *Nature* (2016). doi: 10.1038/nature19084
23. Yang L, Zhang Y. Tumor-Associated Macrophages: From Basic Research to Clinical Application. *J Hematol Oncol* (2017) 101:1, 3. doi: 10.1186/s13045-017-0430-2
24. Mantovani A, Sozzani S, Locati M, Allavena P, Sica A. Macrophage Polarization:Tumor-Associated Macrophages as a Paradigm for Polarized M2 Mononuclear Phagocytes. *Trends Immunol* (2002) 23:549–55. doi: 10.1016/s1471-4906(02)02302-5

25. Vitale I, Manic G, Coussens LM, Kroemer G, Galluzzi L. Macrophages and Metabolism in the Tumor Microenvironment. *Cell Metab* (2019) 301:37. doi: 10.1016/j.cmet.2019.06.001
26. Mantovani A, Marchesi F, Malesci A, Laghi L, Allavena P. Tumour-Associated Macrophages as Treatment Targets in Oncology. *Nat Rev Clin Oncol* (2017) 147:1. doi: 10.1038/nrclinonc.2016.217
27. Falzone L, Scandurra G, Lombardo V, Gattuso G, Lavoro A, Distefano AB, et al. A Multidisciplinary Approach Remains the Best Strategy to Improve and Strengthen the Management of Ovarian Cancer (Review). *Int J Oncol* (2021) 591:1. doi: 10.3892/ijo.2021.5233
28. Dondi G, Coluccelli S, De Leo A, Ferrari S, Gruppioni E, Bovicelli A, et al. An Analysis of Clinical, Surgical, Pathological and Molecular Characteristics of Endometrial Cancer According to Mismatch Repair Status. A Multidisciplinary Approach. *Int J Mol Sci* (2020) 2119:14. doi: 10.3390/ijms21197188
29. Adishesh M, Hapangama DK. Enriching Personalized Endometrial Cancer Research With the Harmonization of Biobanking Standards. *Cancers (Basel)* (2019) 1111:1. doi: 10.3390/cancers11111734
30. Wong HS-C, Hsu Y-W, Juan Y-S, Chen H-H, Wu M-S, Liu W-M, et al. Integrative Bioinformatic Analyses of an Oncogenomic Profile Reveal the Biology of Endometrial Cancer and Guide Drug Discovery. *Oncotarget* (2015) 7:5909–23. doi: 10.18632/oncotarget.6716

Conflict of Interest: The authors declare that the research was conducted in the absence of any commercial or financial relationships that could be construed as a potential conflict of interest.

Publisher's Note: All claims expressed in this article are solely those of the authors and do not necessarily represent those of their affiliated organizations, or those of the publisher, the editors and the reviewers. Any product that may be evaluated in this article, or claim that may be made by its manufacturer, is not guaranteed or endorsed by the publisher.

Copyright © 2022 Wu, Zheng, Chen, Lv and Huang. This is an open-access article distributed under the terms of the Creative Commons Attribution License (CC BY). The use, distribution or reproduction in other forums is permitted, provided the original author(s) and the copyright owner(s) are credited and that the original publication in this journal is cited, in accordance with accepted academic practice. No use, distribution or reproduction is permitted which does not comply with these terms.

frontiers in Oncology

ORIGINAL RESEARCH
published: 21 March 2022
doi: 10.3389/fonc.2022.761219

Early Cervical Lesions Affecting Ovarian Reserve and Reproductive Outcomes of Females in Assisted Reproductive Cycles

Qiyu Yang[1], Juan Hu[1], Meng Wang[1], Zhou Li[1], Bo Huang[1], Lixia Zhu[1], Qingsong Xi[2]* and Lei Jin[1]**

[1] Reproductive Medicine Center, Tongji Hospital, Tongji Medical College, Huazhong University of Science and Technology, Wuhan, China, [2] Oncology Center, Tongji Hospital, Tongji Medical College, Huazhong University of Science and Technology, Wuhan, China

OPEN ACCESS

Edited by:
Scott Christley,
University of Texas Southwestern Medical Center, United States

Reviewed by:
Clarissa Polen-De,
Mayo Clinic, United States
Antonio Simone Laganà,
University of Insubria, Italy

***Correspondence:**
Lixia Zhu
zhulixia027@163.com
Qingsong Xi
xiqingsong@gmail.com
Lei Jin
leijintongjih@qq.com

Specialty section:
This article was submitted to Gynecological Oncology, a section of the journal Frontiers in Oncology

Received: 19 August 2021
Accepted: 28 February 2022
Published: 21 March 2022

Citation:
Yang Q, Hu J, Wang M, Li Z, Huang B, Zhu L, Xi Q and Jin L (2022) Early Cervical Lesions Affecting Ovarian Reserve and Reproductive Outcomes of Females in Assisted Reproductive Cycles. Front. Oncol. 12:761219. doi: 10.3389/fonc.2022.761219

To estimate the effects of early cervical lesions (ECL) on female reproductive function and IVF/ICSI cycle outcomes, a retrospective cohort study involving 111 infertile women from 2014 to 2019 was performed. Thirty-seven women with a history of ECL and seventy-four controls, undergoing IVF/ICSI cycles, were included in the ECL group and comparison group respectively. Demographic characteristics, ovarian reserve, and IVF/ICSI cycle outcomes of both groups were collected. Basal serum FSH level, AMH level, AFC, number of oocytes retrieved and matured, normal fertilization rate, embryo available rate, blastocyst formation rate, implantation rate, pregnancy rate, and cumulative live birth rate (CLBR) were assessed and compared. We observed that while both groups were similar concerning baseline features, significantly more women in the ECL group were diagnosed as poor ovarian response (POR), compared with those in the comparison group (27.0% *vs.* 10.8%, P=0.003). The pregnancy rate and LBR for a complete cycle were both significantly lower in the ECL group (38.5% *vs.* 58.8%, P=0.021; 28.9% *vs.* 48.2%, P=0.025, respectively). The conservative and optimal CLBRs for up to four complete cycles in the ECL group were also lower than those in the comparison group (40.5% *vs.* 55.4%, P=0.140; 45.9% *vs.* 67.6%, P=0.028). Longer time intervals (over one year) between ECL diagnosis/treatment and assisted reproductive technology (ART) cycle start negatively affected the pregnancy rate and LBR. In conclusion, female patients with ECL history seemingly have a lower ovarian reserve, reduced pregnancy rate, and decreased live birth rate (LBR), compared with age-matched women undergoing IVF/ICSI.

Keywords: cervical intraepithelial neoplasia, cervical cancer, ovarian reserve, assisted reproductive technology, cumulative live birth rate

INTRODUCTION

Cervical cancer remains the fourth most common cancer in women (1). With the development and popularization of screening methods, patients with cervical lesions can be early diagnosed and receive fertility-sparing treatment (2, 3). Cervical intraepithelial neoplasia (CIN), or squamous intraepithelial lesion (SIL), known as the pathological diagnosis of cervical precancerous lesion, was classified into low-grade lesion (CIN1) and high-grade lesions (CIN2 and CIN3), based on the different morphological characteristics and clinicopathological processes. CIN1 is attributed to active human papillomavirus (HPV) infection and usually regresses without treatment, while the high-grade SIL and early invasive cervical cancer, may need surgical treatments, such as conization, loop electrosurgical excision procedure (LEEP), and trachelectomy (4, 5).

The fecundability and obstetric outcomes of the patients with a history of early cervical lesions (ECL), including CIN and early invasive cancer, were analyzed previously. A case-control study showed a 2-fold increase in risk of infertility for women after CIN treatments compared with untreated women (6), while other studies involving larger samples demonstrated no evident adverse effects of CIN history and treatments on fertility (7, 8). As for early invasive cervical cancer, previous studies mainly focused on obstetric outcomes following different-type surgeries, such as abdominal, vaginal, or robot-assisted radical trachelectomy, aiming to prove the feasibility and safety of surgeries (9–12). Generally, most studies indicated that no significant negative effect of ECL and related surgical treatment on female fertility was observed.

But like the non-oncology population, even if the treatment of the cervix does not increase the prevalence of infertility, some patients are unable to conceive spontaneously for various reasons and require assisted reproductive technology (ART) to obtain offspring (7, 13). Whether the infertile patients with an ECL history would experience worse ART outcomes remains to be explored. In the current study, by retrospective analyses of the patients with ECL history undergoing ART in our center, the ovarian reserve, ovarian response, embryo development, and obstetrical outcomes were compared with those of the comparison group, to estimate the effect of ECL on female reproductive function and *in vitro* fertilization (IVF)/intracytoplasmic sperm injection (ICSI) outcomes.

MATERIALS AND METHODS

Study Population

All women undergoing IVF/ICSI cycles from January 2014 to December 2019 at the Reproductive Medicine Center of Tongji Hospital in Wuhan, China were reviewed. Thirty-seven women who were noted to have a history of pathologically confirmed ECL were included in the ECL group. For each patient, two age-matched controls with similar body mass index (BMI) and infertility type during the same period were included in the comparison group. Women with other benign or malignant tumors, polycystic ovarian syndrome (PCOS), endometriosis, congenital abnormality, previous ovarian surgery, oocyte donors, and preimplantation genetic diagnosis cycles were excluded from the analyses in both groups.

The original study was approved by the Ethical Committee of Tongji Hospital, Tongji Medicine College, Huazhong University of Science and Technology on 24 April 2019 (#[2019]S964). Each of the patients had given written informed consent at the time of treatment for the future use of their clinical data.

Ovarian Stimulation Protocol, Oocyte Retrieval, and Embryo Transfer

Ovarian stimulation protocols have been processed as previously described (14, 15). Briefly, pituitary suppression was achieved by injection of GnRH agonist starting in the mid-luteal phase of the previous cycle or GnRH antagonist starting with the existence of follicles measuring 13-14 mm in diameter. The dosage and duration of recombinant follicle-stimulating hormone (FSH) were adjusted based on individual ovarian responses. When two to three leading follicles reached a mean diameter of 18 mm, intramuscular injection of recombinant human chorionic gonadotropin (hCG) was performed, and oocytes were retrieved by guided transvaginal ultrasound 36-38h after hCG administration. The IVF or ICSI were performed as appropriate, and embryo transfer was performed on day 3 after oocyte retrieval. The surplus available embryos were frozen on day 3 or further cultured to day 5 or 6 for cryopreservation. Transfer with cryopreserved embryos was performed after priming the uterus with estrogen.

Data Collection

Demographic characteristics, including age at cycle start, BMI, infertility duration, infertility type, and causes of infertility, were collected. Basal serum FSH level, antimüllerian hormone (AMH) level, and antral follicle count (AFC) were extracted for assessment of ovarian reserve. IVF/ICSI cycle information extracted included the amount of gonadotropin used, total days of ovarian stimulation, estradiol (E2) level, number of large follicles on hCG trigger day, number of oocytes retrieved and matured, available embryos, blastocysts, embryos transferred, pregnancies, and live births. For the ECL group, detailed information about cervical lesion type, treatment, and time from diagnosis/treatment of cervical lesion to cycle start was recorded.

Criteria of Assessment

Women with poor ovarian response (POR) were classified with at least two of the three following features: advanced maternal age (≥40 years) or any other risk factor for POR; a previous POR (≤3 oocytes with a conventional ovarian stimulation protocol); and an abnormal ovarian reserve test (i.e. AFC <5–7 or AMH <0.5–1.1 ng/ml), according to the Bologna criteria (16). The normal fertilization rate was defined as the number of 2PN zygotes divided by the number of matured oocytes; the cleavage rate was defined as the number of cleaved embryos divided by the number of fertilized oocytes; the available embryo rate was defined as the number of embryos available for transfer, freezing, and extended culture divided by the number of normally-fertilized and cleaved embryos (including the late-

cleaved embryos); the blastocyst formation rate was the number of blastocysts divided by the number of day 3 embryos for extended culture; the good-quality blastocyst formation rate was the blastocysts available for cryopreservation divided by the number of day 3 embryos for extended culture. Implantation rate referred to the ratio of the number of gestational sacs to the number of embryos transferred. Clinical pregnancy was confirmed if an intrauterine fetal heartbeat could be observed by transvaginal ultrasound. The live birth was defined as the birth of at least one live child after 28 weeks of gestation. Deliveries of multiple pregnancies were counted as one live birth.

For first-cycle cumulative live birth rate (CLBR) assessment, live birth rates (LBR) were calculated following every embryo-transfer procedure during the first complete cycle. For multiple cycles, two kinds of CLBRs were calculated. The conservative CLBR was calculated based on the assumption that women who discontinued ART treatment would not have achieved live birth if they had continued, while the optimal CLBR assumed that women who discontinued treatment would have had the same chance of live birth with continued ART as those who did continue (17). Women were considered to have discontinued ART treatment if they failed to have a treatment-dependent live birth and did not return for further ART cycles until 31 December 2019.

Statistical Analysis

Data were analyzed and presented using SPSS software (SPSS Inc, version 22.0) and Graphpad Prism (version 8.0). Continuous data were analyzed with Kruskal-Wallis nonparametric method and expressed as median (interquartile range [IQR]), or with a Student t-test if data were normally distributed. Categorical data were presented as the number of cases and frequency (percentage), with a Chi-Square test to assess between-group differences. Logistic regression was performed to explore the influencing factors of cycle outcomes. The conservative CLBR estimate was calculated as the number of live births up to and including a specific treatment cycle, divided by the number of women who started their first ART cycle during the study period. The optimal estimate of CLBR was calculated by the Kaplan-Meier method upon inclusion of all treatment cycles in the analysis. Log-rank test and Kaplan-Meier curves with live birth considered as an event were used to illustrate differences between groups (14). Wald P-values were two-sided; $P<0.05$ was considered to be significant.

RESULTS

Baseline Characteristics

Thirty-seven women with a history of ECL, involving fifty-three IVF/ICSI cycles, were identified and included in the ECL group. Age-matched women were included in the comparison group at a ratio of 1:2, with eighty-six IVF/ICSI cycles. The median age of women commencing ART in both groups was 34 years. Other baseline features, including BMI, infertility type and duration, and infertility cause, were also similar between the two groups (**Table 1**).

Among the 37 patients with ECL history, 31 (83.8%) have been diagnosed as CIN and others as cervical cancer, based on pathological evidence. Four CIN1 patients and two CIN2 patients have received no treatment but regular follow-up, and three patients with CIN3 or early-stage cancer have undergone trachelectomy, with different extents of resection. Most patients (75.7%) have been treated with conization or LEEP. All patients underwent the re-examination of HPV infection and Thinprep cytologic test (TCT) regularly after cervical surgeries and specially prior to ART treatment, to exclude recurrence. Nearly half of the patients (45.9%) started the ART cycles within one year after ECL diagnosis or treatment, while 29.7% did not choose ART until two years later (**Supplementary Table S1**).

Ovarian Reserve and Response

According to our observation, the ECL group had higher basal FSH level (median: 8.9 *vs.* 7.3 mIU/mL, $P<0.001$), lower AMH

TABLE 1 | Demographic characteristics of the ECL and comparison groups.

Characteristics	ECL patients	Comparison	P-value
Number of patients, n	37	74	/
Number of ART cycles, n	53	86	/
Female age at cycle start (y)	34 (31–39)	34 (31-39)	0.712
BMI (kg/m^2)	21.8 (19.8-23.4)	21.5 (19.8-23.3)	0.700
Infertility duration (y)	3 (1-5)	3 (2-4.3)	0.659
Infertility type, n (%)			0.841
Primary	16 (43.2%)	30 (40.5%)	
Secondary	21 (56.8%)	44 (59.5%)	
Infertility cause, n (%)			0.733
Female factors only	26 (70.3%)	46 (62.2%)	
Tubal	16 (43.2%)	33 (44.6%)	
DOR	5 (13.5%)	11 (14.9%)	
Tubal +DOR	5 (13.5%)	2 (2.7%)	
Male factors only	2 (5.4%)	7 (9.5%)	
Combined male and female factors	4 (10.8%)	12 (16.2%)	
Unexplained	5 (13.5%)	9 (12.2%)	

Values are median (IQR) for continuous variables and n (%) for categorical variables.
ECL, early cervical lesions; ART, assisted reproductive technology; BMI, body mass index; DOR, diminished ovarian reserve.

level (2.0 *vs.* 3.2 ng/mL, P=0.009), and fewer AFC (8.0 *vs.* 11.0, P<0.001) than the comparison group (**Table 2**). After stimulation, the ECL group reached significantly lower E2 levels and fewer large follicles on hCG trigger days, consequently fewer oocytes were obtained (6.0 *vs.* 9.0, P=0.015), although the oocyte maturation rates were similar between the two groups. Based on the Bologna criteria, more women with a history of ECL were diagnosed as POR compared with those without cervical lesion history (27.0% *vs.* 10.8%, P=0.003).

IVF/ICSI Results, Obstetric and Neonatal Outcomes

As for the IVF/ICSI results, no significant differences were observed in normal fertilization rate, cleavage rate, available embryo rate, blastocyst formation rate, and good-quality blastocyst formation rate between the two groups. For fresh-embryo transfer cycles, the average numbers of transferred embryos were 1.26 and 1.41 in the ECL and comparison group, respectively (P>0.05). However, we found that the implantation rate, pregnancy rate, and LBR following fresh embryo transfer in the ECL group were all significantly lower than those in the comparison group (20.7% *vs.* 53.9%, P=0.002; 26.1% *vs.* 61.1%, P=0.005; 21.7% *vs.* 50.0%, P=0.021, respectively).

All pregnant women were followed up until a live birth was achieved or abortion occurred after their last IVF/ICSI cycles. For one complete cycle, which encompasses the outcomes from fresh and all frozen/thawed embryo transfers following one ovarian stimulation, the pregnancy rate and LBR of the ECL group were also significantly lower than those of the comparison group (38.5% *vs.* 58.8%, P=0.021; 28.9% *vs.* 48.2%, P=0.025, respectively) (**Table 3**).

For the first complete cycle, the CLBR following every embryo-transfer procedure rose from 27.0% to 35.1% in the ECL group, and from 39.2% to 51.4% in the comparison group (P=0.113), shown in **Figure 1**. The conservative and optimal CLBRs for up to four complete cycles were presented in **Figure 2**. Overall, the CLBR was 35.1% for the first complete cycle of the ECL group, rising to 40.5% (conservative) and 45.9% (optimal) for the second cycle, while in the comparison group, the CLBR rose from 51.4% for the first cycle to 55.4% (conservative) and 67.6% (optimal) for the second cycle. The difference of optimal CLBRs between the two groups was significant (P=0.033). CLBRs did not increase from the third cycle in either group.

Considering the significantly lower pregnancy rate and LBR in the ECL group, factors such as age, BMI, lesion type, treatment, and the time interval between ECL diagnosis/treatment and IVF/ICSI cycle, were included in multivariate logistic regression for analysis (**Supplementary Table S2**). The results showed that higher BMI negatively affected the pregnancy rate but not the LBR. The pregnancy rate and LBR were both significantly reduced in patients with a time interval of more than one year between ECL diagnosis/treatment and IVF/ICSI, compared with the ones who started cycles within one year (pregnancy rate: 45.0% *vs.* 65.7%, OR: 0.087 [0.008-0.963], P=0.047; LBR: 30.0% *vs.* 52.9%, OR: 0.022 [0.001-0.623], P=0.027), although the median ages at cycle start were similar (33.5 *vs.* 34.0 years).

Of all the live births obtained by single embryo transfer in both groups, none were preterm delivery. All preterm births occurred during the course of twin pregnancies, and the incidence of preterm births and neonatal weight did not differ significantly between the two groups. Very few women in either group have maternal complications, including gestational diabetes, hypertensive disorder, and placental abnormalities. There were no cases of neonatal defects in both groups (**Table 3**).

DISCUSSION

As mentioned before, nowadays cervical lesions could be detected in early stage, and the risk of pre-invasive to invasive lesions shift might be predicted, based on the evaluation of some biomarkers, such as $p16^{ink}4a$, p16, E-cadherin, Ki67, pRb, and p53 (18). Moreover, through the application of sentinel lymph

TABLE 2 | Ovarian reserve and response to stimulation in the ECL and comparison groups.

Reproductive results	ECL patients	Comparison	P-value
Ovarian reserve			
Day3 FSH (mIU/mL)	8.9 (7.0-13.2)	7.3 (6.1-8.4)	**<0.001**
Day3 AFC	8.0 (4.0-10.0)	11.0 (7.0-16.0)	**<0.001**
AMH (ng/mL)	2.0 (1.1-4.0)	3.2 (1.8-5.8)	**0.009**
Ovarian response			
Total dose of gonadotropins (IU)	2400.0 (1875.5-3075.0)	2437.5 (1887.5-3018.8)	0.919
Days of gonadotropins use (d)	9.0 (8.0-10.5)	10.0 (8.8-11.0)	0.150
E2 on hCG trigger day (pg/mL)	1454.0 (694.4- 2329.5)	2084.0 (1356.5-3518.5)	**0.001**
No. of large follicles on hCG day	6 (4-10)	8 (6-13)	**0.008**
No. of oocytes retrieved	6 (3-11)	9 (5-15)	**0.015**
No. of MII oocytes	5 (3-8)	8 (4-13)	**0.021**
Maturation rate	89.1%	85.7%	0.213
Incidence of POR	27.0%	10.8%	**0.003**

ECL, early cervical lesions; FSH, follicle-stimulating hormone; AFC, antral follicle count; AMH, antimüllerian hormone; E2, estradiol; hCG, human chorionic gonadotropin; POR, poor ovarian response. Bold fonts were statistically significant.

TABLE 3 | IVF/ICSI results and obstetric outcomes of ECL and comparison groups.

IVF/ICSI outcomes		ECL patients	Comparison	P-value
Normal fertilization rate		74.0% (267/361)	73.1% (542/741)	0.302
Cleavage rate		97.3% (323/332)	97.2% (649/668)	0.904
Available embryo rate		85.0% (243/286)	87.4% (514/588)	0.318
Blastocyst formation rate		73.6% (131/178)	69.5% (285/410)	0.560
Good-quality blastocyst formation rate		43.3% (77/178)	44.6% (183/410)	0.797
Fresh embryo transfer (ET)				
No. of fresh ET cycles		23	54	
Average no. of fresh embryos transferred		1.26	1.41	0.211
Implantation rate in fresh ET cycles		20.7% (6/29)	53.9% (41/76)	**0.002**
Pregnancy rate in fresh ET cycles		26.1% (6/23)	61.1% (33/54)	**0.005**
Single ET cycles		23.5% (4/17)	56.3% (18/32)	**0.028**
Double ET cycles		33.3% (2/6)	68.2% (15/22)	0.128
Live birth rate in fresh ET cycles		21.7% (5/23)	50.0% (27/54)	**0.021**
Pregnancy rate per complete cycle		38.5% (20/52)	58.8% (50/85)	**0.021**
LBR per complete cycle		28.9% (15/52)	48.2% (41/85)	**0.025**
Obstetric outcomes				
Preterm birth rate	Single ET cycle	0% (0/12)	0% (0/22)	1.000
	Double ET cycle	33.3% (1/3)	42.1% (8/19)	0.779
Newborns weight (g)		3347.5± 511.3	2998.1± 668.9	0.060
Maternal complications, n				/
Gestational diabetes		1	2	
Placental abnormalities		1	2	
Hypertensive disorder		0	1	
Neonatal defects		0	0	

ECL, early cervical lesions; LBR, live birth rate.
Bold fonts were statistically significant.

node (SLN) mapping, the surgical treatment of cervical lesions also became more accurate (19). All these advances in technologies and concepts dramatically increased the fertility sparing opportunity for patients with cervical lesions, and also highlighted the necessity of reproductive evaluation and fertility guidance for these patients.

The results of this study suggest that female patients with CIN or early cervical cancer history have lower ovarian reserve, reduced pregnancy rate, and decreased CLBR, compared with age-matched women undergoing IVF/ICSI. Although the infertility rate and IVF delivery proportion of patients with ECL history were not increased according to previous studies (7, 8), it appears that those infertile patients do not have an optimal outcome in seeking ART treatment. Moreover, the time interval between ECL diagnosis/treatment and ART cycle start is seemingly associated with the pregnancy rate and LBR.

The deleterious impact of ECL history on the ovarian reserve is unexpected because lesions were localized and all treatments

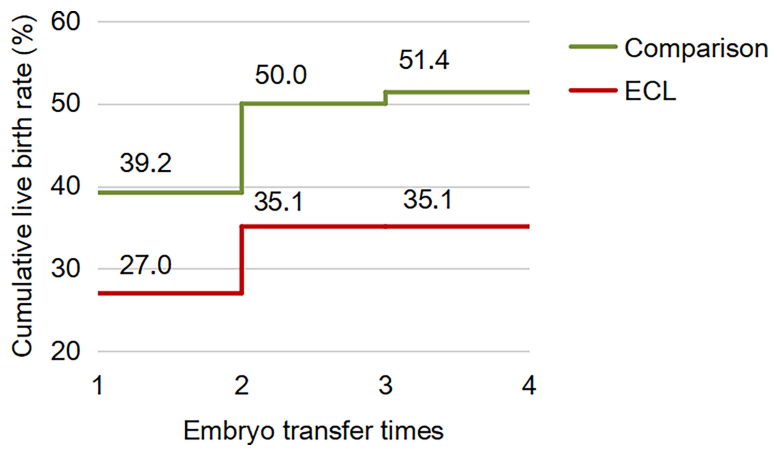


FIGURE 1 | The CLBR following every embryo-transfer procedure for the first complete cycle. For each complete cycle, the LBR following every embryo-transfer procedure rose from 27.0% to 35.1% in the ECL group (red line), and from 39.2% to 51.4% in the comparison group (green line). The difference between the two groups was not significant (P=0.113).

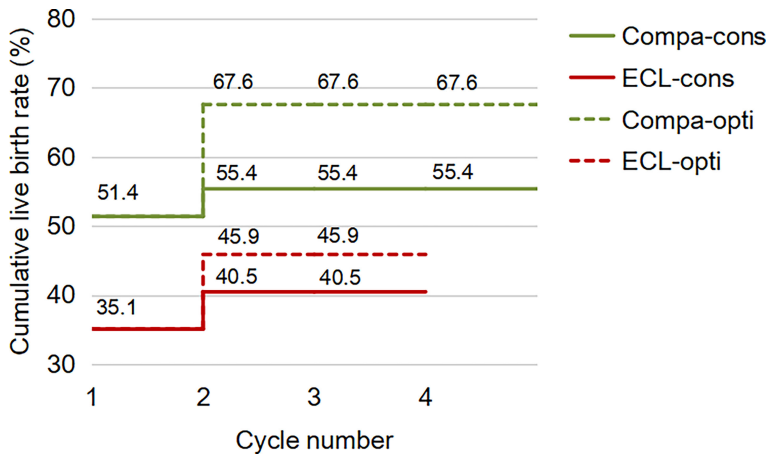


FIGURE 2 | The conservative and optimal CLBRs for up to four complete cycles in both groups. The CLBR was 35.1% for the first complete cycle of the ECL group, rising to 40.5% (conservative) and 45.9% (optimal) for the second cycle. In the comparison group, the CLBR rose from 51.4% for the first cycle to 55.4% (conservative) and 67.6% (optimal) for the second cycle. The difference of optimal CLBRs between the two groups was significant (P=0.033), although not significant for conservative CLBRs (P=0.139). CLBRs did not increase from the third cycle in either group.

did not seem to directly involve the ovaries. The underlying mechanisms probably involve cervical treatments, HPV infection, and the potential reproductive damaging effects of the tumor itself:

The various cervical treatments reportedly caused different pregnancy results (20), while very little literature investigated their effects on ovarian reserve. Spracklen et al. reported that women with a history of LEEP required more time to conceive a pregnancy resulting in live birth when compared to similar women with no history of cervical surgery (6), but Sklavos et al., attempting to clarify the mechanism, found that the delayed time to pregnancy is likely not due to a LEEP-associated decrease in ovarian reserve as measured by AMH (21). Another study involving eighteen patients undergoing abdominal radical trachelectomy found no significant differences in AMH levels between surgery group and control group (22). However, the conclusions require further verification due to the small sample size. In the current study, the effect of cervical treatments was not evaluated specifically considering the limited number of untreated patients and possible inconsistency in surgical operations.

As for HPV infection, the majority in the ECL group (67.6%) were with clear evidence of HPV positive when they were diagnosed as ECL, but more information regarding HPV types was regrettably missing. A most recent study investigated the long-term impact of being diagnosed with high risk (HR)-HPV-positive and HR-HPV-negative lesions in a large group of women treated with conization for high-grade cervical dysplasia, and found that HR-HPV-positive patients experienced a 8-fold increase risk of recurrence than HR-HPV-negative counterpart (23). We speculated the HR-HPV infection might have a more sustained impact on patients. However, there is a lack of studies regarding HPV effects on female hormones or oocyte production, while more attention has been focused on the impact of HPV vaccines on ovarian reserve (24). Although a causal conclusion cannot be confirmed by now, six case reports indicated a possible association between the 4-valent HPV vaccine and primary ovarian insufficiency (POI) (25, 26). We hypothesized that HPV, which contains more active biological substances than its vaccine, may be more likely to be detrimental to ovarian function. More research regarding the long-term effect of HPV infection or 2-, 4-, 9-valent vaccines on ovarian reserve is required.

Additionally, the impact of the tumor itself on reproductive function should not be ignored. A meta-analysis reviewed seven studies that evaluated the ovarian performance of patients with cancers, including breast cancer, lymphoma or leukemia, gynecologic cancer, or other malignancies. The result showed that, even before radio/chemotherapy, the number of retrieved oocytes among patients with cancer was significantly lower compared with age-matched healthy IVF patients (27). In a recent study exploring the impact of cancer type on ovarian response to stimulation for fertility preservation, a lower ovarian response in patients with gynecologic cancers was identified (28). However, the conclusion remains controversial, based on the conflicting results of other studies (29, 30), and more studies are also needed to reveal the mechanisms.

Simultaneously, the ART outcomes of ECL patients in our study were also unsatisfactory. Two kinds of CLBRs in the ECL group were lower than those in the comparison group, with a statistical significance in optimal CLBRs difference. The conservative CLBR is pessimistic, while the optimal CLBR is probably overly optimistic, based on their computational principles. As the prognosis-adjusted CLBRs were closer to the optimal than the conservative estimate (17), we have more reason to believe that the ECL group did suffer from a lower CLBR.

HPV infection may be involved. Spandorfer et al. have reported significantly decreased pregnancy rates in IVF cycles

in women with cervical HPV infection (without cytological abnormalities) who were undergoing IVF compared with those who were HPV negative (23.0% *vs.* 57.0%, respectively), and no significant difference in the miscarriage rates was found (31). Another study of 199 infertile couples, however, showed a marked increase in the risk of pregnancy loss when HPV infection was diagnosed (32). Importantly, a cervical lesion requiring treatment is more complex than a simple HPV infection, and the different treatments could affect ART outcomes, as shortened cervical length and abnormal cervical function are likely to increase the risk of miscarriage or preterm delivery (7, 33). The current study firstly presented a reduced pregnancy rate and CLBR in patients with cervical lesions undergoing ART treatment, while the impact on preterm delivery rate was not significant.

Our study took the ovarian reserve of ECL patients into consideration, which has usually been ignored by other researchers assessing the effect of HPV or cervical treatment on ART outcomes. In addition, the CLBRs were calculated both conservatively and optimistically to present the ART outcomes that patients are most concerned about. Limitations of this study include its retrospective and single-center nature, with a rather small sample size. The influence of treatment methods was not assessed specifically as the patients received surgeries in different centers.

In conclusion, we have shown that a history of early cervical lesion among infertile women may have a significantly negative impact on the ovarian reserve and IVF/ICSI outcomes, with a higher incidence of POR and lower live birth rate. This study provides data support for further exploration of the effects of cervical cancer and other tumors on fertility and also advocates that oncologists and reproductive physicians pay more attention to these patients. Comprehensive ovarian function assessment, individualized fertility guidance, and planned follow-up by professionals are recommended for patients with early cervical lesions history.

DATA AVAILABILITY STATEMENT

The original contributions presented in the study are included in the article/**Supplementary Material**. Further inquiries can be directed to the corresponding authors.

AUTHOR CONTRIBUTIONS

QY, JH, MW, QX, and LZ collected the clinical data. QY, LZ, ZL, and BH analyzed the data. QY, LZ, and MW composed the manuscript. QX and LJ were responsible for the concept and study design. All authors contributed to the interpretation, discussion and editing of the manuscript. All authors contributed to the article and approved the submitted version.

FUNDING

This work was supported by the research grants from National Key Research and Development Project (2018YFC1002103) and the Health Commission of Hubei Province Scientific Research Project (WJ2021M110).

SUPPLEMENTARY MATERIAL

The Supplementary Material for this article can be found online at: https://www.frontiersin.org/articles/10.3389/fonc.2022.761219/full#supplementary-material

REFERENCES

1. Arbyn M, Weiderpass E, Bruni L, de Sanjosé S, Saraiya M, Ferlay J, et al. Estimates of Incidence and Mortality of Cervical Cancer in 2018: A Worldwide Analysis. *Lancet Glob Health* (2020) 8:e191–203. doi: 10.1016/S2214-109X(19)30482-6
2. Fontham ETH, Wolf AMD, Church TR, Etzioni R, Flowers CR, Herzig A, et al. Cervical Cancer Screening for Individuals at Average Risk: 2020 Guideline Update From the American Cancer Society. *CA Cancer J Clin* (2020) 70:321–46. doi: 10.3322/caac.21628
3. Curry SJ, Krist AH, Owens DK, Barry MJ, Caughey AB, Davidson KW, et al. Screening for Cervical Cancer: US Preventive Services Task Force Recommendation Statement. *JAMA* (2018) 320:674–86. doi: 10.1001/jama.2018.10897
4. Schiffman M, Doorbar J, Wentzensen N, de Sanjosé S, Fakhry C, Monk BJ, et al. Carcinogenic Human Papillomavirus Infection. *Nat Rev Dis Primers* (2016) 2:16086. doi: 10.1038/nrdp.2016.86
5. Souho T, Benlemlih M, Bennani B. Human Papillomavirus Infection and Fertility Alteration: A Systematic Review. *PloS One* (2015) 10:e0126936. doi: 10.1371/journal.pone.0126936
6. Spracklen CN, Harland KK, Stegmann BJ, Saftlas AF. Cervical Surgery for Cervical Intraepithelial Neoplasia and Prolonged Time to Conception of a Live Birth: A Case-Control Study. *BJOG* (2013) 120:960–5. doi: 10.1111/1471-0528.12209
7. Jakobsson M, Gissler M, Tiitinen A, Paavonen J, Tapper AM. Treatment for Cervical Intraepithelial Neoplasia and Subsequent IVF Deliveries. *Hum Reprod* (2008) 23:2252–5. doi: 10.1093/humrep/den271
8. Wise LA, Willis SK, Perkins RB, Wesselink AK, Klann A, Crowe HM, et al. A Prospective Study of Treatments for Cervical Intraepithelial Neoplasia and Fecundability. *Am J Obstet Gynecol* (2019) 223:96.e1–15. doi: 10.1016/j.ajog.2019.12.017
9. Nishio H, Fujii T, Sugiyama J, Kuji N, Tanaka M, Hamatani T, et al. Reproductive and Obstetric Outcomes After Radical Abdominal Trachelectomy for Early-Stage Cervical Cancer in a Series of 31 Pregnancies. *Hum Reprod* (2013) 28:1793–8. doi: 10.1093/humrep/det118
10. Johansen G, Lönnerfors C, Falconer H, Persson J. Reproductive and Oncologic Outcome Following Robot-Assisted Laparoscopic Radical Trachelectomy for Early Stage Cervical Cancer. *Gynecol Oncol* (2016) 141:160–5. doi: 10.1016/j.ygyno.2016.01.028
11. Li X, Xia L, Li J, Chen X, Ju X, Wu X. Reproductive and Obstetric Outcomes After Abdominal Radical Trachelectomy (ART) for Patients With Early-Stage Cervical Cancers in Fudan, China. *Gynecol Oncol* (2020) 157:418–22. doi: 10.1016/j.ygyno.2020.02.016
12. Shinkai S, Ishioka S, Mariya T, Fujibe Y, Kim M, Someya M, et al. Pregnancies After Vaginal Radical Trachelectomy (RT) in Patients With Early Invasive Uterine Cervical Cancer: Results From a Single Institute. *BMC Pregnancy Childbirth* (2020) 20:248. doi: 10.1186/s12884-020-02949-1
13. Nezhat C, Roman RA, Rambhatla A, Nezhat F. Reproductive and Oncologic Outcomes After Fertility-Sparing Surgery for Early Stage Cervical Cancer: A Systematic Review. *Fertil Steril* (2020) 113:685–703. doi: 10.1016/j.fertnstert.2020.02.003

14. Xu B, Chen Y, Geerts D, Yue J, Li Z, Zhu G, et al. Cumulative Live Birth Rates in More Than 3,000 Patients With Poor Ovarian Response: A 15-Year Survey of Final *In Vitro* Fertilization Outcome. *Fertil Steril* (2018) 109:1051–9. doi: 10.1016/j.fertnstert.2018.02.001
15. Geng Y, Xun Y, Hu S, Lai Q, Jin L. GnRH Antagonist Versus Follicular-Phase Single-Dose GnRH Agonist Protocol in Patients of Normal Ovarian Responses During Controlled Ovarian Stimulation. *Gynecol Endocrinol* (2019) 35:309–13. doi: 10.1080/09513590.2018.1528221
16. Ferraretti AP, La Marca A, Fauser BC, Tarlatzis B, Nargund G, Gianaroli L. ESHRE Working Group on Poor Ovarian Response Definition. ESHRE Consensus on the Definition of 'Poor Response' to Ovarian Stimulation for *In Vitro* Fertilization: The Bologna Criteria. *Hum Reprod* (2011) 26:1616–24. doi: 10.1093/humrep/der092
17. Chambers GM, Paul RC, Harris K, Fitzgerald O, Boothroyd CV, Rombauts L, et al. Assisted Reproductive Technology in Australia and New Zealand: Cumulative Live Birth Rates as Measures of Success. *Med J Aust* (2017) 207:114–8. doi: 10.5694/mja16.01435
18. Valenti G, Vitale SG, Tropea A, Biondi A, Laganà AS. Tumor Markers of Uterine Cervical Cancer: A New Scenario to Guide Surgical Practice? *Updates Surg* (2017) 69:441–9. doi: 10.1007/s13304-017-0491-3
19. Rossetti D, Vitale SG, Tropea A, Biondi A, Laganà AS. New Procedures for the Identification of Sentinel Lymph Node: Shaping the Horizon of Future Management in Early Stage Uterine Cervical Cancer. *Updates Surg* (2017) 69:383–8. doi: 10.1007/s13304-017-0456-6
20. Rob L, Skapa P, Robova H. Fertility-Sparing Surgery in Patients With Cervical Cancer. *Lancet Oncol* (2011) 12:192–200. doi: 10.1016/S1470-2045(10)70084-X
21. Sklavos MM, Spracklen CN, Saftlas AF, Pinto LA. Does Loop Electrosurgical Excision Procedure of the Uterine Cervix Affect Anti-Müllerian Hormone Levels? *BioMed Res Int* (2014) 2014:875438. doi: 10.1155/2014/875438
22. Muraji M, Sudo T, Iwasaki S, Ueno S, Wakahashi S, Yamaguchi S, et al. The Effect of Abdominal Radical Trachelectomy on Ovarian Reserve: Serial Changes in Serum Anti-Müllerian Hormone Levels. *J Cancer* (2012) 3:191–5. doi: 10.7150/jca.4316
23. Bogani G, Sopracordevole F, Di Donato V, Ciavattini A, Ghelardi A, Lopez S, et al. High-Risk HPV-Positive and -Negative High-Grade Cervical Dysplasia: Analysis of 5-Year Outcomes. *Gynecol Oncol* (2021) 161:173–8. doi: 10.1016/j.ygyno.2021.01.020
24. Christianson MS, Wodi P, Talaat K, Halsey N. Primary Ovarian Insufficiency and Human Papilloma Virus Vaccines: A Review of the Current Evidence. *Am J Obstet Gynecol* (2020) 222:239–44. doi: 10.1016/j.ajog.2019.08.045
25. Little DT, Ward HRG. Adolescent Premature Ovarian Insufficiency Following Human Papillomavirus Vaccination: A Case Series Seen in General Practice. *J Investig Med High Impact Case Rep* (2014) 2:2324709614556129. doi: 10.1016/j.ajog.2019.08.045
26. Colafrancesco S, Perricone C, Tomljenovic L, Shoenfeld Y. Human Papilloma Virus Vaccine and Primary Ovarian Failure: Another Facet of the Autoimmune/Inflammatory Syndrome Induced by Adjuvants. *Am J Reprod Immunol* (2013) 70:309–16. doi: 10.1111/aji.12151
27. Friedler S, Koc O, Gidoni Y, Raziel A, Ron-El R. Ovarian Response to Stimulation for Fertility Preservation in Women With Malignant Disease: A Systematic Review and Meta-Analysis. *Fertil Steril* (2012) 97:125–33. doi: 10.1016/j.fertnstert.2011.10.014
28. Alvarez RM, Ramanathan P. Fertility Preservation in Female Oncology Patients: The Influence of the Type of Cancer on Ovarian Stimulation Response. *Hum Reprod* (2018) 33:2051–9. doi: 10.1093/humrep/dew158
29. Robertson AD, Missmer SA, Ginsburg ES. Embryo Yield After *In Vitro* Fertilization in Women Undergoing Embryo Banking for Fertility Preservation Before Chemotherapy. *Fertil Steril* (2011) 95:588–91. doi: 10.1016/j.fertnstert.2010.04.028
30. Tulandi T, Holzer H. Effects of Malignancies on the Gonadal Function. *Fertil Steril* (2012) 98:813–5. doi: 10.1016/j.fertnstert.2012.05.010
31. Spandorfer SD, Bongiovanni AM, Fasioulotis S, Rosenwaks Z, Ledger WJ, Witkin SS. Prevalence of Cervical Human Papillomavirus in Women Undergoing *In Vitro* Fertilization and Association With Outcome. *Fertil Steril* (2006) 86:765–7. doi: 10.1016/j.fertnstert.2006.01.051
32. Perino A, Giovannelli L, Schillaci R, Ruvolo G, Fiorentino FP, Alimondi P, et al. Human Papillomavirus Infection in Couples Undergoing *In Vitro* Fertilization Procedures: Impact on Reproductive Outcomes. *Fertil Steril* (2011) 95:1845–8. doi: 10.1016/j.fertnstert.2010.11.047
33. Pinborg A, Ortoft G, Loft A, Rasmussen SC, Ingerslev HJ. Cervical Conization Doubles the Risk of Preterm and Very Preterm Birth in Assisted Reproductive Technology Twin Pregnancies. *Hum Reprod* (2015) 30:197–204. doi: 10.1093/humrep/deu260

Conflict of Interest: The authors declare that the research was conducted in the absence of any commercial or financial relationships that could be construed as a potential conflict of interest.

Publisher's Note: All claims expressed in this article are solely those of the authors and do not necessarily represent those of their affiliated organizations, or those of the publisher, the editors and the reviewers. Any product that may be evaluated in this article, or claim that may be made by its manufacturer, is not guaranteed or endorsed by the publisher.

Copyright © 2022 Yang, Hu, Wang, Li, Huang, Zhu, Xi and Jin. This is an open-access article distributed under the terms of the Creative Commons Attribution License (CC BY). The use, distribution or reproduction in other forums is permitted, provided the original author(s) and the copyright owner(s) are credited and that the original publication in this journal is cited, in accordance with accepted academic practice. No use, distribution or reproduction is permitted which does not comply with these terms.

frontiers in Oncology

ORIGINAL RESEARCH
published: 29 March 2022
doi: 10.3389/fonc.2022.817250

Machine Learning-Assisted Ensemble Analysis for the Prediction of Response to Neoadjuvant Chemotherapy in Locally Advanced Cervical Cancer

*Yibao Huang†, Qingqing Zhu†, Liru Xue, Xiaoran Zhu, Yingying Chen and Mingfu Wu**

Department of Gynecology, National Clinical Research Center for Obstetrical and Gynecological Diseases, Key Laboratory of Cancer Invasion and Metastasis, Ministry of Education, Tongji Hospital, Tongji Medical College, Huazhong University of Science and Technology, Wuhan, China

OPEN ACCESS

Edited by:
Stefano Restaino, Ospedale Santa Maria della Misericordia di Udine, Italy

Reviewed by:
Anna Myriam Perrone, Sant'Orsola-Malpighi Polyclinic, Italy
Carlo Ronsini, Università degli Studi della Campania "Luigi Vanvitelli", Italy

***Correspondence:**
Mingfu Wu
wu_mingfu@tjh.tjmu.edu.cn

†These authors have contributed equally to this work and share first authorship

Specialty section:
This article was submitted to Gynecological Oncology, a section of the journal Frontiers in Oncology

Received: *17 November 2021*
Accepted: *28 February 2022*
Published: *29 March 2022*

Citation:
Huang Y, Zhu Q, Xue L, Zhu X, Chen Y and Wu M (2022) Machine Learning-Assisted Ensemble Analysis for the Prediction of Response to Neoadjuvant Chemotherapy in Locally Advanced Cervical Cancer. Front. Oncol. 12:817250. doi: 10.3389/fonc.2022.817250

The clinical benefit of neoadjuvant chemotherapy (NACT) before concurrent chemoradiotherapy (CCRT) vs. adjuvant chemotherapy after CCRT is debated. Non-response to platinum-based NACT is a major contributor to poor prognosis, but there is currently no reliable method for predicting the response to NACT (rNACT) in patients with locally advanced cervical cancer (LACC). In this study we developed a machine learning (ML)-assisted model to accurately predict rNACT. We retrospectively analyzed data on 636 patients diagnosed with stage IB2 to IIA2 cervical cancer at our hospital between January 1, 2010 and December 1, 2020. Five ML-assisted models were developed from candidate clinical features using 2-step estimation methods. Receiver operating characteristic curve (ROC), clinical impact curve, and decision curve analyses were performed to evaluate the robustness and clinical applicability of each model. A total of 30 candidate variables were ultimately included in the rNACT prediction model. The areas under the ROC curve of models constructed using the random forest classifier (RFC), support vector machine, eXtreme gradient boosting, artificial neural network, and decision tree ranged from 0.682 to 0.847. The RFC model had the highest predictive accuracy, which was achieved by incorporating inflammatory factors such as platelet-to-lymphocyte ratio, neutrophil-to-lymphocyte ratio, neutrophil-to-albumin ratio, and lymphocyte-to-monocyte ratio. These results demonstrate that the ML-based prediction model developed using the RFC can be used to identify LACC patients who are likely to respond to rNACT, which can guide treatment selection and improve clinical outcomes.

Keywords: locally advanced cervical cancer, neoadjuvant chemotherapy, machine learning analysis, predictive model, pathology response

INTRODUCTION

Cervical cancer is a malignant tumor and major cause of morbidity and mortality, with an estimated 500,000 new cases and 300,000 deaths each year (1, 2). Over the past decade, substantial progress has been made in the early diagnosis and treatment of locally advanced cervical cancer (LACC) (3). The standard treatments for LACC are surgery, radiation therapy, and chemotherapy (CT) (3), but none of these are optimal. Local residual disease following chemoradiotherapy (CRT) can be treated by salvage surgery; however, this is associated with various complications (4, 5). Additionally, the response of LACC patients to radical surgery after radiotherapy and CT is generally poor, while radiotherapy may not be a treatment option in low-income countries (6, 7). As such, there is a need for more effective and accessible treatment options for LACC.

As a potential alternative therapy, platinum-based neoadjuvant (NA)CT has been shown to reduce tumor volume (3, 8). According to the International Federation of Gynecology and Obstetrics (FIGO) classification system of 2009, NACT can be considered for patients with stage IB2 to IIA2 LACC, especially before radical hysterectomy (9–11). Cisplatin-based NACT is associated with improved long-term survival rates in LACC (12–14). However, there are currently no models that can accurately predict the pathologic response to NACT in these patients, although this could facilitate clinical management. Machine learning (ML) is a data analysis method with applications in healthcare (15). Compared to conventional statistical models, ML-based ensemble analysis can ensure robustness of a statistical model and improve its predictive accuracy through iterative algorithms.

There is no consensus on the cutoff for optimal response to NACT (rNACT) in patients with LACC, with overall response rates to NACT ranging from 52 to 95% (16, 17). In this study, we applied ML-based algorithms to establish a model to accurately predict rNACT in LACC patients by using preoperative clinical parameters and inflammatory markers.

METHODS

Patient Selection

Patients who were diagnosed with FIGO stage IB2–IIA2 cervical cancer at the Tongji Hospital of Tongji Medical College, Huazhong University of Science and Technology (Wuhan, China) between January 2010 and December 2020 were retrospectively enrolled in this study. The inclusion criteria for patients were as follows: (i) received platinum-based NACT, without adverse effects; (ii) received a standard cycle of NACT before the operation with no other treatment; (iii) underwent systematic physical examination before the operation, including peripheral blood monitoring and imaging examination; and (iv) a complete set of medical data was available. We excluded patients who had severe organ injuries or incomplete clinical parameters, laboratory test results, and imaging findings in their medical records. The study protocol was in compliance with the provisions of the Helsinki Declaration (2013 revision) and was approved by the Institutional Review Committee of Tongji Hospital, Tongji Medical College, Huazhong University of Science and Technology (TJ-IRB20210631). All information of the patients was strictly confidential and informed consent was waived due to its traceability. The workflow for LACC patient selection and model construction is summarized in **Figure 1**. The study was approved by the Institutional Review Committee of Tongji Hospital, Tongji Medical College, Huazhong University of Science and Technology (TJ-IRB20210631).

Data Collection and Quality Assessment

The following data were collected for all patients: age, body mass index, histology, FIGO stage, tumor size before NACT, histologic grade, lymph node metastasis, lymph vascular space invasion, parametrial involvement, surgical margin, neutrophil count (10^9/l), lymphocyte count (10^9/l), platelet count (10^9/l), monocyte count (10^9/l), hemoglobin, albumin, globulin, and tumor markers. For variables with missing values, the median was typically used. If ≥10% of values were missing for a given variable, it was excluded from variable screening for the final model.

Evaluation Criteria for NACT

For pathologic response assessment, all patients who received NACT were independently examined by 2 pathologists. rNACT was evaluated according to the Response Evaluation Criteria in Solid Tumors (RECIST) v1.1 criteria (18), and was categorized into the following 4 levels according to the presence or absence of

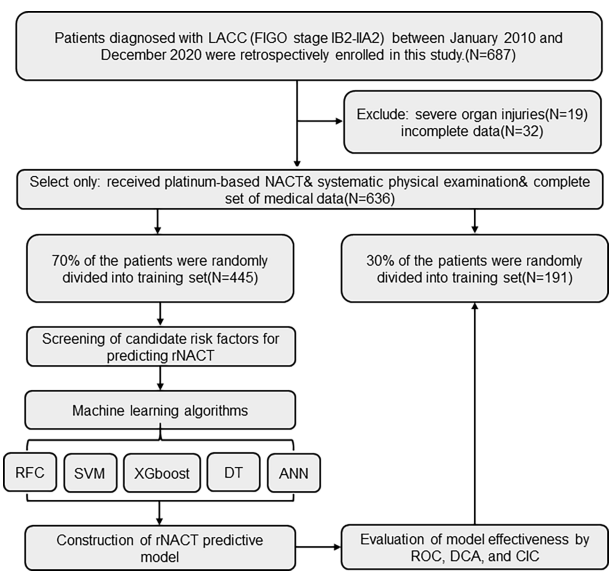


FIGURE 1 | Flow diagram of patient selection and data processing. ANN, artificial neural network; CIC, clinical impact curve; DCA, decision curve analysis; DT, decision tree; FIGO, International Federation of Gynecology and Obstetrics; RFC, random forest classifier; ROC, receiver operating characteristic; SVM, support vector machine; XGboost, eXtreme gradient boosting.

pathologic response: (i) complete response (CR), almost complete disappearance of cancer lesions; (ii) partial response (PR), ≥30% decrease in total maximum diameter of cancer lesions; (iii) progressive disease (PD), ≥20% decrease in total maximum diameter of cancer lesions; and (iv) stable disease (SD), total maximum diameter of cancer lesions defined as either insufficient contraction in line with PR or increased compliance with PD. LACC patients were considered to be rNACT if they were determined as having CR or PR following NACT treatment; meanwhile, patients with SD or PD were regarded as non-rNACT.

Development and Validation of ML-Based Models

Four ML-based algorithms were used to build predictive models. We used the Classification and Regression Training (caret) package to randomly divide the dataset into 2 parts, 70% for model training and 30% for model validation. A total of 5 ML-based algorithms were evaluated for the predictive model. The model variables were screened by 2-step estimation (19) according to the following formula.

$$\widehat{m} = \widehat{m}_3 \cap \widehat{m}_4$$

The characteristic variable was X and the target variable was Y; these were evenly divided into 2 parts—namely, X1, Y1 and X2, Y2. Through univariate screening, the variable quantum set m^1 was screened on X1 and Y1, and m^2 was filtered by X2 and Y2. A lasso was then used to re-fit the model, and the filtered variables were marked as m^3 and m^4. The optimal subset for modeling was obtained based on the intersection of the variable sets. The model was evaluated by inspection, discrimination, and calibration. A receiver operating characteristic (ROC) curve was used to assess the predictive accuracy of the model in the training and validation sets. The discriminatory ability of each model was quantified by the area under the ROC curve (AUC), decision curve analysis (DCA), and clinical impact curve (CIC) analysis.

Statistical Analysis

Median (interquartile range) and frequencies (%) were described for continuous and categorical variables, respectively. The chi-squared test or Mann–Whitney U test was used to compare baseline clinical characteristics between the rNACT and non-rNACT cohorts as appropriate. All analyses were performed using Python v3.9.2 (https://www.python.org/) and R v4.0.4 (http://www.r-project.org/). All tests were 2-sided, and $p < 0.05$ was considered statistically significant.

RESULTS

Baseline Characteristics of the Study Population and rNACT

The detailed clinical characteristics and pathologic baseline data of 636 patients with LACC are shown in **Table 1**. All patients received platinum-based NACT, with no serious adverse reactions. For internal validation, patients were randomly divided into a training set (N = 445, 70%) and validation set (N = 191, 30%) using the caret package. According to the RECIST criteria, 396 (88.9%) and 162 (84.8%) patients showed rNACT in the training and validation sets, respectively, indicating that these patients were sensitive to NACT. Follow-up treatment was determined according to the condition of the patients and included radical surgery, radiation, and concurrent (C)CRT. Of these patients, 614 (96.6%) underwent radical surgery and 91 (14.3%) received radiotherapy or CCRT.

Selection of Candidate Variables Using Different ML-Based Algorithms

Candidate covariates of each algorithm were filtered and 30 were included in the correlation analysis between outcome and independent variables. rNACT was significantly correlated with inflammatory factors and clinical variables, namely, platelet-to-lymphocyte ratio (PLR), neutrophil-to-lymphocyte ratio (NLR), neutrophil-to-albumin ratio (NAR), lymphocyte-to-monocyte ratio (LMR), and tumor size (**Figure 2A**). PLR, LMR, and NAR were important factors in the ML-based model (**Figure 2B**). Consistent with the results of correlation analysis, the 5 top-ranked predictors were PLR, NLR, NAR, LMR, and tumor size.

Construction of ML-Based rNACT Predictive Model

Random forest classifier (RFC) and decision tree (DT) are commonly used ML-based algorithms in supervised learning. The RFC model was constructed using the formula $I(X = x_i) = -\log_2 P(x_i)$, where I(X) is the information for candidate variables and $P(x_i)$ is the probability of x_i (**Figure 3A**). Thirty variables were ordered according to the mean decrease in Gini index (**Supplementary Table 1**); the top 10 ranked variables were used to construct the optimal RFC prediction model, which included PLR, NLR, NAR, LMR, and tumor size. Inflammatory factors, PLR, LMR, and tumor size served as irreplaceable weights at DT branches (**Figure 3B**). Using the iterative algorithm of supervised learning, both RFC and DT models were used for rNACT prediction.

Comparison Among ML-Based Models

Based on the iterative analysis of baseline characteristics, we used 5 supervised learning models for NACT risk assessment and to optimize predictive performance. As expected, the RFC model was better able to distinguish between LACC patients in the rNACT and non-rNACT cohorts. The AUCs of the RFC model reached a plateau when *** variables were introduced, indicating that the RFC model had the highest predictive accuracy, followed by DT, artificial neural network (ANN), support vector machine (SVM), and eXtreme gradient boosting (XGBoost) models (**Figure 4A**). The predictive performance of ML-based models is summarized in **Table 2**. Consistent with the results of the ROC analysis, the RFC model also showed a robust predictive performance in the DCA (**Figure 4B**).

TABLE 1 | Baseline demographic and clinicopathologic features of patients with LACC with and without a diagnosis of rNACT.

Variables	Overall	Training set		P-value	Testing set		P-value
	N = 636	Responders (N = 396)	Non-responders (N = 49)		Responders (N = 162)	Non-responders (N = 29)	
Age, years	47.00 [42.00, 52.00]	47.00 [42.75, 52.00]	49.00 [41.00, 54.00]	0.713	47.00 [43.00, 52.00]	45.00 [37.00, 52.00]	0.229
Weight, kg	55.44 [50.00, 60.00]	55.44 [50.00, 60.00]	55.44 [49.00, 59.00]	0.563	55.44 [50.00, 60.00]	55.00 [53.00, 60.00]	0.642
Height, m	157.40 [154.00, 160.00]	157.40 [154.00, 160.62]	157.40 [155.00, 160.00]	0.86	157.40 [155.00, 160.00]	158.00 [154.00, 160.00]	0.934
Smoking							
Yes	34 (5.3)	22 (5.6)	1 (2.0)	0.48	10 (6.2)	1 (3.4)	0.883
No	602 (94.7)	374 (94.4)	48 (98.0)		152 (93.8)	28 (96.6)	
FIGO stage							
Ib	4 (0.6)	2 (0.5)	1 (2.0)	0.356	1 (0.6)	0 (0.0)	0.845
Ib2	402 (63.2)	256 (64.6)	28 (57.1)		99 (61.1)	19 (65.5)	
IIa	12 (1.9)	7 (1.8)	2 (4.1)		3 (1.9)	0 (0.0)	
IIa2	218 (34.3)	131 (33.1)	18 (36.7)		59 (36.4)	10 (34.5)	
Histology							
SCC	542 (85.2)	340 (85.9)	44 (89.8)	0.235	134 (82.7)	24 (82.8)	0.921
ADC	68 (10.7)	42 (10.6)	3 (6.1)		19 (11.7)	4 (13.8)	
AdCa	9 (1.4)	5 (1.3)	2 (4.1)		2 (1.2)	0 (0.0)	
Other	17 (2.7)	9 (2.3)	0 (0.0)		7 (4.3)	1 (3.4)	
Tumor grade							
G1	37 (5.8)	28 (7.1)	1 (2.0)	0.063	7 (4.3)	1 (3.4)	0.04
G2	278 (43.7)	186 (47.0)	19 (38.8)		64 (39.5)	9 (31.0)	
G3	241 (37.9)	138 (34.8)	26 (53.1)		59 (36.4)	18 (62.1)	
Unknown	80 (12.6)	44 (11.1)	3 (6.1)		32 (19.8)	1 (3.4)	
Tumor size	3.60 [2.50, 4.10]	3.50 [2.30, 4.00]	6.00 [5.00, 7.00]	<0.001	3.50 [2.50, 4.00]	6.00 [5.00, 7.00]	<0.001
Lymphatic invasion							
Yes	85 (13.4)	56 (14.1)	12 (24.5)	0.152	13 (8.0)	4 (13.8)	0.597
No	528 (83.0)	326 (82.3)	36 (73.5)		142 (87.7)	24 (82.8)	
Unknown	23 (3.6)	14 (3.5)	1 (2.0)		7 (4.3)	1 (3.4)	
Parametrial invasion							
Yes	38 (6.0)	21 (5.3)	7 (14.3)	0.033	7 (4.3)	3 (10.3)	0.374
No	598 (94.0)	375 (94.7)	42 (85.7)		155 (95.7)	26 (89.7)	
Pelvic lymph metastasis							
Yes	103 (16.2)	56 (14.1)	22 (44.9)	<0.001	18 (11.1)	7 (24.1)	0.159
No	510 (80.2)	326 (82.3)	26 (53.1)		137 (84.6)	21 (72.4)	
Unknown	23 (3.6)	14 (3.5)	1 (2.0)		7 (4.3)	1 (3.4)	
Paraortic lymph metastasis							
Yes	18 (2.8)	11 (2.8)	4 (8.2)	0.128	3 (1.9)	0 (0.0)	0.74
No	595 (93.6)	371 (93.7)	44 (89.8)		152 (93.8)	28 (96.6)	
Unknown	23 (3.6)	14 (3.5)	1 (2.0)		7 (4.3)	1 (3.4)	
SCC	4.30 [0.80, 4.30]	4.30 [0.80, 4.30]	2.20 [0.60, 4.30]	0.041	4.30 [1.12, 4.30]	1.30 [0.70, 4.30]	0.028
P53							
Positive	32 (5.0)	16 (4.0)	1 (2.0)	0.382	11 (6.8)	4 (13.8)	0.282
Negative	14 (2.2)	11 (2.8)	0 (0.0)		2 (1.2)	1 (3.4)	
Unknown	590 (92.8)	369 (93.2)	48 (98.0)		149 (92.0)	24 (82.8)	
CEA	5.15 [3.44, 5.15]	5.15 [3.10, 5.15]	5.15 [3.61, 5.15]	0.705	5.15 [4.16, 5.15]	5.15 [5.15, 5.15]	0.96
CA125	42.00 [42.00, 42.00]	42.00 [42.00, 42.00]	42.00 [42.00, 42.00]	0.008	42.00 [28.73, 42.00]	42.00 [42.00, 42.00]	0.289
CA199	32.19 [32.19, 32.19]	32.19 [32.19, 32.19]	32.19 [32.19, 32.19]	0.605	32.19 [28.69, 32.19]	32.19 [32.19, 32.19]	0.521
CCRT							
Yes	91 (14.3)	16 (4.0)	44 (89.8)	<0.001	9 (5.6)	22 (75.9)	<0.001
No	530 (83.3)	371 (93.7)	5 (10.2)		147 (90.7)	7 (24.1)	
Unknown	15 (2.4)	9 (2.3)	0 (0.0)		6 (3.7)	0 (0.0)	
Surgical method							
Laparoscopy	485 (76.3)	300 (75.8)	38 (77.6)	0.888	127 (78.4)	20 (69.0)	0.424
Open	129 (20.3)	83 (21.0)	10 (20.4)		28 (17.3)	8 (27.6)	
Unknown	22 (3.5)	13 (3.3)	1 (2.0)		7 (4.3)	1 (3.4)	
Surgical margin							
Positive	11 (1.7)	4 (1.0)	2 (4.1)		4 (2.5)	1 (3.4)	
Negative	603 (94.8)	379 (95.7)	46 (93.9)	0.194	151 (93.2)	27 (93.1)	0.935
Positive	22 (3.5)	13 (3.3)	1 (2.0)		7 (4.3)	1 (3.4)	
LND	31.00 [25.00, 38.00]	31.00 [25.00, 38.00]	32.00 [27.00, 37.00]	0.309	32.00 [25.00, 39.75]	30.00 [26.00, 34.00]	0.302

(Continued)

TABLE 1 | Continued

Variables	Overall	Training set		P-value	Testing set		P-value
	N = 636	Responders (N = 396)	Non-responders (N = 49)		Responders (N = 162)	Non-responders (N = 29)	
Platelet count	251.50 [209.00, 276.40]	239.00 [204.75, 276.40]	327.00 [301.00, 370.00]	<0.001	245.50 [204.50, 276.00]	347.00 [318.00, 386.00]	<0.001
Leukocyte count	6.30 [4.92, 7.43]	6.36 [5.03, 7.43]	5.15 [4.17, 7.43]	0.01	6.37 [4.89, 7.43]	6.02 [5.14, 6.53]	0.351
Lymphocyte count	1.63 [1.27, 1.77]	1.63 [1.28, 1.82]	1.40 [0.99, 1.63]	0.006	1.63 [1.33, 1.76]	1.48 [1.26, 1.65]	0.54
Monocyte count	0.43 [0.30, 0.47]	0.43 [0.31, 0.46]	0.37 [0.24, 0.45]	0.059	0.45 [0.32, 0.51]	0.41 [0.25, 0.47]	0.576
Hemoglobin	112.00 [102.00, 122.00]	112.00 [102.00, 122.00]	112.00 [102.00, 119.00]	0.455	112.00 [103.00, 123.00]	114.00 [112.00, 123.00]	0.311
Neutrophil count	3.98 [2.84, 4.74]	4.06 [2.90, 4.92]	3.20 [2.23, 4.38]	0.025	4.06 [2.82, 4.62]	3.62 [2.97, 4.49]	0.564
NLR	2.67 [1.74, 3.47]	2.37 [1.63, 2.97]	10.00 [9.00, 11.00]	<0.001	2.35 [1.72, 2.82]	11.00 [9.00, 12.00]	<0.001
PLR	156.52 [123.27, 180.89]	146.19 [118.82, 171.15]	280.00 [230.00, 356.00]	<0.001	149.72 [119.02, 168.10]	253.00 [222.22, 314.00]	<0.001
LMR	6.80 [4.66, 9.18]	7.22 [5.30, 9.41]	2.91 [1.64, 3.75]	<0.001	7.59 [5.60, 9.41]	3.72 [2.63, 4.66]	<0.001
PNR	63.11 [49.17, 85.37]	63.11 [46.68, 79.01]	104.06 [76.35, 140.00]	<0.001	63.11 [50.83, 78.84]	97.71 [70.83, 122.36]	<0.001
Fibrinogen	4.28 [3.14, 5.56]	3.95 [3.01, 5.00]	6.72 [6.13, 7.18]	<0.001	4.11 [2.99, 5.25]	6.39 [6.05, 7.04]	<0.001
Albumin	39.40 [36.50, 41.20]	39.40 [36.30, 41.00]	39.30 [36.20, 40.80]	0.822	39.40 [37.23, 41.20]	40.10 [38.30, 42.20]	0.343
GGT	23.00 [15.00, 29.55]	22.00 [15.00, 29.55]	29.55 [19.00, 37.00]	0.012	24.00 [15.00, 29.55]	20.00 [15.00, 29.55]	0.42
Globulin	31.20 [28.50, 33.02]	31.20 [28.48, 33.00]	31.30 [29.40, 34.90]	0.165	31.20 [28.52, 32.27]	31.20 [28.70, 32.30]	0.887
A/G	1.26 [1.15, 1.39]	1.26 [1.15, 1.39]	1.26 [1.11, 1.32]	0.343	1.26 [1.19, 1.41]	1.29 [1.21, 1.39]	0.823
PNI	47.55 [43.50, 49.66]	47.55 [43.50, 49.75]	47.20 [42.00, 48.00]	0.245	47.55 [43.60, 50.44]	48.10 [46.10, 49.85]	0.52
NAR	0.26 [0.17, 0.34]	0.23 [0.15, 0.31]	1.27 [0.98, 1.51]	<0.001	0.25 [0.15, 0.32]	1.12 [0.58, 1.44]	<0.001

Data are shown as median [interquartile range] or n (%).

ADC, adenocarcinoma; AdCa, adenosquamous carcinoma; A/G, albumin-to-globulin ratio; CA125, cancer antigen 125; CA199, cancer antigen 199; CCRT, concurrent chemoradiotherapy; CEA, carcinoembryonic antigen; FBG, fasting blood glucose; FIGO, International Federation of Gynecology and Obstetrics; GGT, γ-glutamyltransferase; IQR, interquartile range; LMR, lymphocyte-to-monocyte ratio; LND, lymph node dissection; NAR, neutrophil-to-albumin ratio; NLR, neutrophil-to-lymphocyte ratio; PLR, platelet-to-lymphocyte ratio; PNI, prognostic nutrition index; PNR, platelet-to-neutrophil ratio; SCC, squamous cell carcinoma.

Internal Validation of the Optimal Predictive Model

To further validate the performance of the RFC model, we also used CIC to evaluate predictive accuracy. The CIC analysis revealed rNACT stratification in the training set (**Figure 5A**). This was supported by the risk factors for rNACT identified in the validation set (**Figure 5B**), indicating that the selected features were highly relevant to rNACT.

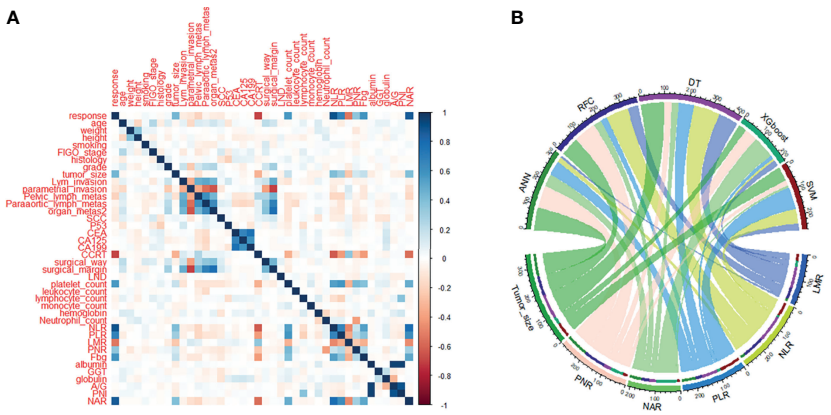


FIGURE 2 | Variable screening and weight allocation. **(A)** Correlation matrix analysis of candidate features. **(B)** Weight distribution of the candidate variables of each ML-based model. ADC, denocarcinoma; A/G, albumin-to-globulin ratio; ANN, artificial neural network; CA125, cancer antigen 125; CA199, cancer antigen 199; CCRT, concurrent chemoradiotherapy; CEA, carcinoembryonic antigen; CIC, clinical impact curve; DCA, decision curve analysis; DT, decision tree; FIGO, International Federation of Gynecology and Obstetrics; GGT, serum γ-glutamyltransferase; LMR, lymphocyte-to-monocyte ratio; LND, lymph node dissection; NAR, neutrophil-to-albumin ratio; NLR, neutrophil-to-lymphocyte ratio; PLR, platelet-to-lymphocyte ratio; PNI, prognostic nutrition index; PNR, platelet-to-neutrophil ratio; RFC, random forest classifier; ROC, receiver operating characteristic curve; SCC, squamous cell carcinoma; SVM, support vector machine; XGboost, eXtreme gradient boosting.

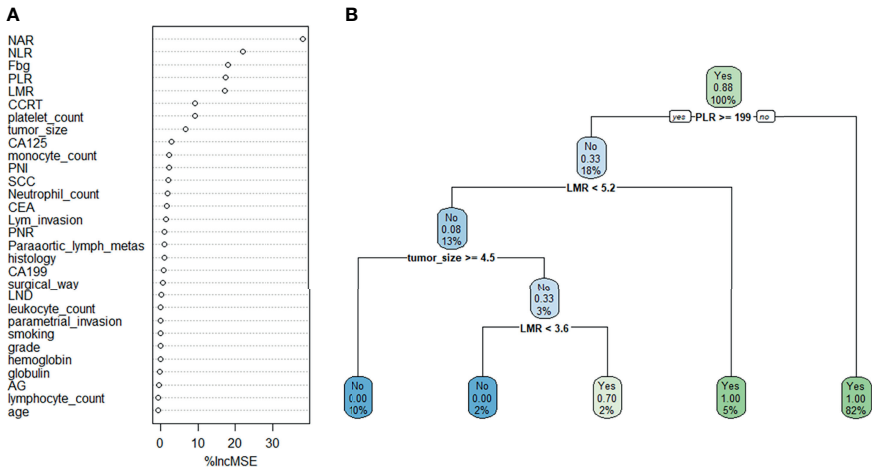


FIGURE 3 | Visualization of the predictive model based on ML-based algorithm. **(A)** RFC model. **(B)** DT model. Candidate factors associated with rNACT were ordered using the RFC algorithm **(A)**, and the prediction node and weight were allocated with the DT algorithm **(B)**.

DISCUSSION

Inaccurate risk stratification of cancer patients can affect clinical decision-making and outcomes. Given the excellent performance of ML-based algorithms in the classification of rNACT, the RFC, DT, ANN, XGboost, and SVM algorithms were used in our study to establish a predictive model for rNACT in LACC patients. There were 2 major findings to our study. First, we achieved accurate risk stratification of LACC patients who received NACT based on markers of systemic inflammation. Second, we developed and validated a novel ML-based predictive model that is superior to existing prediction algorithms to identify LACC patients who would benefit from NACT.

Systemic inflammation plays a critical role in promoting the progression and metastasis of many cancers (20–23), and was shown to be associated with the development, progression, and metastasis of cervical cancer (24). We therefore examined pre-NACT treatment peripheral blood-related inflammatory marker levels in patients with LACC, and the results were consistent with previous findings (13). As expected, systemic inflammatory markers such as neutrophils, lymphocytes, and platelets and also albumin, C-reactive protein, and other biochemical markers were useful in predicting rNACT in LACC patients. NACT effectively reduces serum levels of tumor markers and NLR and prolongs survival time (25). We compared patients who responded to NACT with those who did not respond and found that in the former, the levels of inflammatory biomarkers were significantly altered compared to before NACT treatment whereas in non-responders, there were no differences between pre- and post-treatment levels. Additionally, we found that PLR, prognostic nutrition index, and LMR were significantly associated with rNACT. Thus, changes in the level of preoperative inflammatory factors can predict the response of LACC patients to NACT.

rNACT was related to NAR and the concentration of fibrinogen, a coagulation factor. The latter has prognostic value

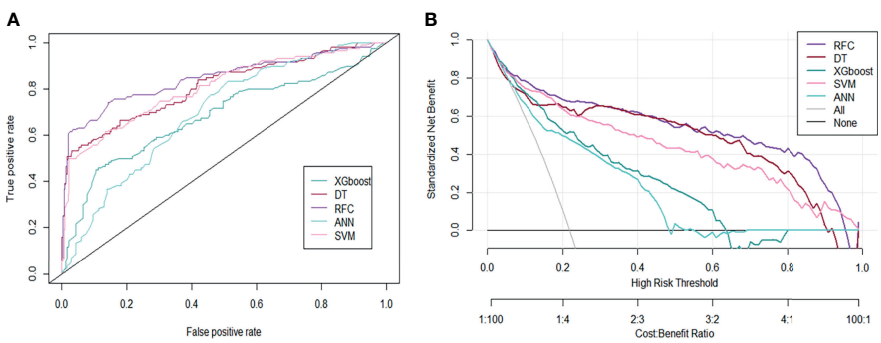


FIGURE 4 | Predictive performance of candidate models based on the ML-based algorithm. **(A)** Area under the ROC curve for 5 ML-based models. **(B)** DCA for the 5 ML-based models. ANN, artificial neural network; DT, decision tree; RFC, random forest classifier; SVM, support vector machine; XGboost, eXtreme gradient boosting.

TABLE 2 | Receiver operating characteristic curve analysis for predicting response to neoadjuvant chemotherapy in each machine learning-based model.

Model	AUC		Number of candidate variables
	Mean	95% CI	
RFC	0.847	0.286–1.408	8
SVM	0.811	0.245–1.377	9
DT	0.807	0.225–1.389	8
ANN	0.682	0.118–1.246	7
XGboost	0.697	0.113–1.281	9

ANN, artificial neutral network; AUC, area under the receiver operating characteristic curve; CI, confidence interval; DT, decision tree; RFC, random forest classifier; SVM, support vector machine; XGboost, eXtreme gradient boosting.

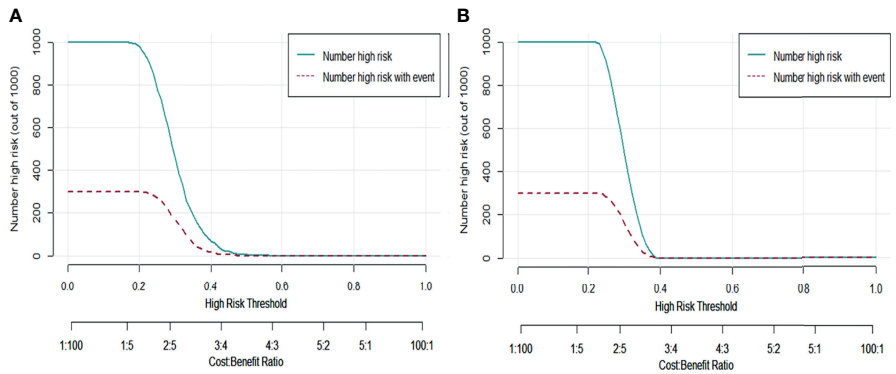


FIGURE 5 | Predictive performance of the RFC model evaluated with the CIC. **(A)** Training set. **(B)** Validation set. The dark green line predicts the probability of poor rNACT, and the purple line shows the number of patients at high risk of non-rNACT.

in many cancer types, namely, hepatocellular carcinoma (26), gastrointestinal stromal tumors (27), and colorectal cancer (28), and was found to predict the levels of inflammatory factors in our study. In the weighting of the prediction model, it was an index that optimized the accuracy and robustness of rNACT prediction by the RFC model.

Our ML-based model incorporated clinical parameters and laboratory test results according to previous reports (12–14); clinical indicators including larger tumor size and earlier stage were shown to be independent predictors of rNACT (12). We therefore evaluated the predictive accuracy of the models and found that systemic inflammatory markers had a large weight in each model. The RFC model allowed calculation of risk level based on all variables collected from medical records, and yielded the highest predictive accuracy. The RFC uses the bootstrapping resampling technique to reduce variance (29). DCA and CIC analysis were used to assess the predictive performance of the RFC model, and the results showed that the model was able to discriminate between rNACT and non-rNACT cohorts. Thus, the model can be used to identify LACC patients who may benefit from NACT before surgery.

There were some limitations to this study. First, there was selection bias as only patients from a tertiary referral hospital were included. Second, although the predictive model was validated in our study, it may not be applicable to other patient populations; therefore, it must be tested using external data. Third, the ML-based model was only for patients with stage Ib2 to IIa2 LACC; further research is needed to determine whether it can be applied to patients at different stages.

CONCLUSION

We developed a ML-based algorithm to identify factors that can predict rNACT in patients with LACC. The model constructed using the RFC had the highest predictive accuracy, with PLR, NLR, NAR, LMR, and tumor size being the most important predictors. Thus, a combination of clinical data and systemic inflammatory markers may aid clinicians in individual risk assessment of rNACT.

DATA AVAILABILITY STATEMENT

The datasets presented in this study can be found in online repositories. The names of the repository/repositories and accession number(s) can be found in the article/**Supplementary Material**.

ETHICS STATEMENT

The studies involving human participants were reviewed and approved by The Institutional Review Committee of Tongji

Hospital, Tongji Medical College, Huazhong University of Science and Technology. Written informed consent for participation was not required for this study in accordance with the national legislation and the institutional requirements. Written informed consent was obtained from the individual(s) for the publication of any potentially identifiable images or data included in this article.

AUTHOR CONTRIBUTIONS

YBH and QQZ: study conception and planning, statistical analysis, data interpretation, manuscript drafting, and final approval of manuscript. LRX, XRZ, and YYC: data interpretation and final approval of the manuscript. MFW: study conception and planning, statistical analysis, data interpretation, manuscript drafting, and final approval of the manuscript All authors listed have made a substantial, direct, and intellectual contribution to the work and approved it for publication.

FUNDING

This research was supported by the Applied Basic Research Program of WMBST (no. 2019020701011436).

ACKNOWLEDGMENTS

The authors thank all study participants for consenting to the use of their medical records, and the staff members of Tongji Hospital for their assistance with data collection.

SUPPLEMENTARY MATERIAL

The Supplementary Material for this article can be found online at: https://www.frontiersin.org/articles/10.3389/fonc.2022.817250/full#supplementary-material

REFERENCES

1. Wang L, Zhao Y, Wang Y, Wu X. The Role of Galectins in Cervical Cancer Biology and Progression. *BioMed Res Int* (2018) 2018:2175927. doi: 10.1155/2018/2175927
2. Arbyn M, Weiderpass E, Bruni L, de Sanjosé S, Saraiya M, Ferlay J, et al. Estimates of Incidence and Mortality of Cervical Cancer in 2018: A Worldwide Analysis. *Lancet Glob Health* (2020) 8:e191–203. doi: 10.1016/s2214-109x(19)30482-6
3. Klyuchko KO, Gargin VV. Influence of Neoadjuvant Chemoradiotherapy for Locally Advanced Cervical Cancer. *Pol Merkur Lekarski* (2020) 48:406–9.
4. van Kol KGG, Ebisch RMF, Piek JMJ, Zusterzeel PLM, Vergeldt TFM, Bekkers RLM. Salvage Surgery for Patients With Residual Disease After Chemoradiation Therapy for Locally Advanced Cervical Cancer: A Systematic Review on Indication, Complications, and Survival. *Acta Obstet Gynecol Scand* (2021) 100:1176–85. doi: 10.1111/aogs.14093
5. Horeweg N, Mittal P, Gradowska PL, Boere I, Chopra S, Nout RA. Adjuvant Systemic Therapy After Chemoradiation and Brachytherapy for Locally Advanced Cervical Cancer: A Systematic Review and Meta-Analysis. *Cancers* (2021) 13:1880. doi: 10.3390/cancers13081880
6. Ferrandina G, Gallotta V, Federico A, Fanfani F, Ercoli A, Chiantera V, et al. Minimally Invasive Approaches in Locally Advanced Cervical Cancer Patients Undergoing Radical Surgery After Chemoradiotherapy: A Propensity Score Analysis. *Ann Surg Oncol* (2021) 28:3616–26. doi: 10.1245/s10434-020-09302-y
7. Yin M, Zhao F, Lou G, Zhang H, Sun M, Li C, et al. The Long-Term Efficacy of Neoadjuvant Chemotherapy Followed by Radical Hysterectomy Compared With Radical Surgery Alone or Concurrent Chemoradiotherapy on Locally Advanced-Stage Cervical Cancer. *Int J Gynecol Cancer* (2011) 21:92–9. doi: 10.1111/IGC.0b013e3181fe8b6e
8. Voinea S, Herghelegiu CG, Sandru A, Ioan RG, Bohilțea RE, Bacalbașa N, et al. Impact of Histological Subtype on the Response to Chemoradiation in Locally Advanced Cervical Cancer and the Possible Role of Surgery. *Exp Ther Med* (2021) 21:93. doi: 10.3892/etm.2020.9525
9. Lapresa M, Parma G, Portuesi R, Colombo N. Neoadjuvant Chemotherapy in Cervical Cancer: An Update. *Expert Rev Anticancer Ther* (2015) 15:1171–81. doi: 10.1586/14737140.2015.1079777
10. Li R, Lu ST, Si JG, Liu B, Wang H, Mei YY, et al. Prognostic Value of Responsiveness of Neoadjuvant Chemotherapy Before Surgery for Patients With Stage IB(2)/IIA(2) Cervical Cancer. *Gynecol Oncol* (2013) 128:524–9. doi: 10.1016/j.ygyno.2012.11.006
11. Feng X, Chen H, Li L, Gao L, Wang L, Bai X. Postoperative Adjuvant Chemotherapy Improved the Prognosis in Locally Advanced Cervical Cancer Patients With Optimal Response to Neoadjuvant Chemotherapy. *Front Oncol* (2020) 10:608333:608333. doi: 10.3389/fonc.2020.608333
12. Huang Y, Liu L, Cai J, Yang L, Sun S, Zhao J, et al. The Efficacy and Response Predictors of Platinum-Based Neoadjuvant Chemotherapy in Locally Advanced Cervical Cancer. *Cancer Manag Res* (2020) 12:10469–77. doi: 10.2147/CMAR.S270258
13. Chen W, Wang B, Zeng R, Wang T. Development and Validation of a Nomogram for the Estimation of Response to Platinum-Based Neoadjuvant Chemotherapy in Patients With Locally Advanced Cervical Cancer. *Cancer Manag Res* (2021) 13:1279–89. doi: 10.2147/CMAR.S293268
14. Ou Z, Zhao D, Li B, Wang Y, Liu S, Zhang Y. A Preoperative Nomogram for Predicting Chemoresistance to Neoadjuvant Chemotherapy in Patients With Locally Advanced Cervical Squamous Carcinoma Treated With Radical Hysterectomy. *Cancer Res Treat* (2021) 53:233–42. doi: 10.4143/crt.2020.159
15. Beniczky S, Karoly P, Nurse E, Ryvlin P, Cook M. Machine Learning and Wearable Devices of the Future. *Epilepsia* (2021) 62:S116–24. doi: 10.1111/epi.16555
16. Dueñas-Gonzalez A, López-Graniel C, González-Enciso A, Cetina L, Rivera L, Mariscal I, et al. A Phase II Study of Multimodality Treatment for Locally Advanced Cervical Cancer: Neoadjuvant Carboplatin and Paclitaxel Followed by Radical Hysterectomy and Adjuvant Cisplatin Chemoradiation. *Ann Oncol* (2003) 14:1278–84. doi: 10.1093/annonc/mdg333
17. Gupta S, Maheshwari A, Parab P, Mahantshetty U, Hawaldar R, Sastri Chopra S, et al. Neoadjuvant Chemotherapy Followed by Radical Surgery Versus Concomitant Chemotherapy and Radiotherapy in Patients With Stage IB2, IIA, or IIB Squamous Cervical Cancer: A Randomized Controlled Trial. *J Clin Oncol* (2018) 36:1548–55. doi: 10.1200/jco.2017.75.9985
18. Eisenhauer EA, Therasse P, Bogaerts J, Schwartz LH, Sargent D, Ford R, et al. New Response Evaluation Criteria in Solid Tumours: Revised RECIST Guideline (Version 1). *Eur J Cancer* (2009) 45:228–47. doi: 10.1016/j.ejca.2008.10.026
19. Fan J, Lv J. A Selective Overview of Variable Selection in High Dimensional Feature Space. *Stat Sin* (2010) 20:101–48.
20. Rossi S, Basso M, Strippoli A, Schinzari G, D'Argento E, Larocca M, et al. Are Markers of Systemic Inflammation Good Prognostic Indicators in Colorectal Cancer? *Clin Colorectal Cancer* (2017) 16:264–74. doi: 10.1016/j.clcc.2017.03.015
21. Jensen TO, Riber-Hansen R, Schmidt H, Hamilton-Dutoit SJ, Steiniche T. Tumor and Inflammation Markers in Melanoma Using Tissue Microarrays: A Validation Study. *Melanoma Res* (2011) 21:509–15. doi: 10.1097/CMR.0b013e32834a3899
22. Busch EL, Whitsel EA, Kroenke CH, Yang YC. Social Relationships, Inflammation Markers, and Breast Cancer Incidence in the Women's Health Initiative. *Breast* (2018) 39:63–9. doi: 10.1016/j.breast.2018.03.013

23. Terlikowska KM, Dobrzycka B, Terlikowski R, Sienkiewicz A, Kinalski M, Terlikowski SJ. Clinical Value of Selected Markers of Angiogenesis, Inflammation, Insulin Resistance and Obesity in Type 1 Endometrial Cancer. *BMC Cancer* (2020) 20:921. doi: 10.1186/s12885-020-07415-x
24. Vitkauskaite A, Urboniene D, Celiesiute J, Jariene K, Skrodeniene E, Nadisauskiene RJ, et al. Circulating Inflammatory Markers in Cervical Cancer Patients and Healthy Controls. *J Immunotoxicol* (2020) 17:105–9. doi: 10.1080/1547691x.2020.1755397
25. Wang X, Chen J, Sun W, Zhu M, Li D, Chen G. Influences of Neoadjuvant Chemotherapy on Clinical Indicators, Prognosis and Neutrophil/Lymphocyte Ratio of Stage IB2–IIB Cervical Cancer. *J BUON* (2020) 25:757–63.
26. Gan W, Yi Y, Fu Y, Huang J, Lu Z, Jing C, et al. Fibrinogen and C-Reactive Protein Score is a Prognostic Index for Patients With Hepatocellular Carcinoma Undergoing Curative Resection: A Prognostic Nomogram Study. *J Cancer* (2018) 9:148–56. doi: 10.7150/jca.22246
27. Lu J, Chen S, Li X, Qiu G, He S, Wang H, et al. Gastrointestinal Stromal Tumors: Fibrinogen Levels are Associated With Prognosis of Patients as Blood-Based Biomarker. *Medicine* (2018) 97:e0568. doi: 10.1097/md.0000000000010568
28. Tang L, Liu K, Wang J, Wang C, Zhao P, Liu J. High Preoperative Plasma Fibrinogen Levels are Associated With Distant Metastases and Impaired Prognosis After Curative Resection in Patients With Colorectal Cancer. *J Surg Oncol* (2010) 102:428–32. doi: 10.1002/jso.21668
29. Rigatti SJ. Random Forest. *J Insur Med* (2017) 47:31–9. doi: 10.17849/insm-47-01-31-39.1

Conflict of Interest: The authors declare that the research was conducted in the absence of any commercial or financial relationships that could be construed as a potential conflict of interest.

Publisher's Note: All claims expressed in this article are solely those of the authors and do not necessarily represent those of their affiliated organizations, or those of the publisher, the editors and the reviewers. Any product that may be evaluated in this article, or claim that may be made by its manufacturer, is not guaranteed or endorsed by the publisher.

Copyright © 2022 Huang, Zhu, Xue, Zhu, Chen and Wu. This is an open-access article distributed under the terms of the Creative Commons Attribution License (CC BY). The use, distribution or reproduction in other forums is permitted, provided the original author(s) and the copyright owner(s) are credited and that the original publication in this journal is cited, in accordance with accepted academic practice. No use, distribution or reproduction is permitted which does not comply with these terms.

frontiers in Oncology

ORIGINAL RESEARCH
published: 30 March 2022
doi: 10.3389/fonc.2022.809159

Risk Factor Assessment of Lymph Node Metastasis in Patients With FIGO Stage IB1 Cervical Cancer

Mu Xu[1†], Xiaoyan Xie[1†], Liangzhi Cai[1], Yongjin Xie[1], Qiao Gao[1] and Pengming Sun[1,2]*

[1] Department of Gynecology, Fujian Maternity and Child Health Hospital, Affiliated Hospital of Fujian Medical University, Fuzhou, China, [2] Laboratory of Gynecologic Oncology, Fujian Maternal and Child Health Hospital, Affiliated Hospital of Fujian Medical University, Fuzhou, China

Objectives: To assess the risk factors of lymph node metastasis (LNM) in patients with FIGO stage (2009) IB1 cervical cancer (CC).

Methods: Patients with FIGO stage IB1 CC who underwent radical resection between 2012 and 2018 were recruited. The risk factors for LNM were analysed. A recursive partitioning analysis (RPA) was used to divide the patients into risk groups and assess their risk of LNM.

Results: The 5-year overall survival rate was 91.72%, while 80.0% and 93.5% for patients with or without LNM (P<0.05). Multivariable logistic regression analysis showed that lymphovascular invasion (LVI), depth of invasion (DI), tumour size (TS), squamous cell carcinoma (SCC) antigen level were independent risk factors (all P<0.05). Patients were divided into low-risk (no LVI, DI <1/2, TS <2 cm), intermediate-risk (no LVI, DI <1/2, TS ≥2 cm; no LVI, DI ≥1/2, normal SCC level; LVI, DI <1/2, TS <2 cm), and high-risk (no LVI, DI ≥1/2, SCC level ≥1.5 ng/ml; LVI, TS <2 cm, DI ≥1/2; LVI, TS ≥2 cm) groups by RPA according to these four factors. The incidence of LNM among the three groups was 0.00%, 4.40%, and 24.10%, respectively (all P<0.001). The 5-year overall survival rates differed among the groups (98.2%, 92.7%, 83.0%, respectively, P=0.001).

Conclusions: LNM affects the prognosis of patients with FIGO stage IB1 CC. Lymphadenectomy may be avoided for patients in the low-risk group and recommended for those in the high-risk group. Whether dissection is performed in the intermediate-risk group depends on the lymph node biopsy results.

Keywords: cervical cancer, lymph node metastasis, lymph node dissection, risk factor, prognosis

OPEN ACCESS

Edited by:
Patrice Mathevet, Centre Hospitalier Universitaire Vaudois (CHUV), Switzerland

Reviewed by:
Valerio Gallotta, Agostino Gemelli University Polyclinic (IRCCS), Italy
Ozan Cem Guler, Başkent University, Turkey

****Correspondence:***
Pengming Sun
sunfemy@hotmail.com

[†]These authors have contributed equally to this work

Specialty section:
This article was submitted to Gynecological Oncology, a section of the journal Frontiers in Oncology

Received: *04 November 2021*
Accepted: *07 March 2022*
Published: *30 March 2022*

Citation:
Xu M, Xie X, Cai L, Xie Y, Gao Q and Sun P (2022) Risk Factor Assessment of Lymph Node Metastasis in Patients With FIGO Stage IB1 Cervical Cancer. Front. Oncol. 12:809159. doi: 10.3389/fonc.2022.809159

INTRODUCTION

Cervical cancer (CC), the most common gynaecologic malignancy in women worldwide, has the highest incidence and mortality in China and threatens women's lives and health (1, 2). Lymph node metastasis (LNM) is a critical risk factor for the survival of patients with CC (3, 4). The survival in patients with LNM is obviously worse than that of patients without LNM in the same International Federation of Gynecology and Obstetrics (FIGO) stage. The 5-year overall survival

(OS) rate is 90% for early-stage CC without versus less than 50% with LNM (5). According to the 2019 National Comprehensive Cancer Network (NCCN) guideline, radical hysterectomy and pelvic lymph node dissection ± para-aortic lymph node dissection are the standard surgical treatment for FIGO IB1 CC patients without fertility requirements. Fertility-sparing surgery (Radical trachelectomy and pelvic lymph node dissection ± para-aortic lymph node dissection) for stage IB1 has been most validated for tumors ≤2 cm (6). Nevertheless, some patients experience sequelae after lymphadenectomy, such as vascular or nerve injury, pelvic lymphocysts, and lower-limb lymphedema, which can be life-threatening, increase length of hospital stay, and affect quality of life (7–9). The incidence of LNM in early-stage CC is reportedly 15–20% (10, 11) and even lower in FIGO stage IB1 patients at 7–17.4% (12–14). Therefore, exploring the risk factors of LNM in FIGO stage IB1 and classifying patients into different groups to avoid the risk caused by lymph node dissection for low-risk patients is of great clinical significance. Current predictive models for the simultaneous assessment of LNM risk in patients with FIGO stage IB1 CC have not been reported. Therefore, this study explored the available factors for LNM in FIGO stage IB1 CC and stratified the risk of LNM based on recursive partitioning analysis (RPA) to provide a reference for the selection of surgical treatment for early CC.

MATERIALS AND METHODS

Study Population

A total of 284 patients with CC who underwent radical resection at Fujian Provincial Maternity and Children's Hospital between January 2012 and December 2018 were recruited. The following inclusion criteria were applied: (1) histologically confirmed CC; (2) FIGO stage IB1 with no evidence of tumours invading adjacent organs or distant metastasis; (3) having undergone radical hysterectomy with pelvic lymphadenectomy; and (4) patients had completed fertility or without fertility requirements. The risk of surgery had been fully informed and all patients signed informed consent before operation and required radical hysterectomy. The study excluded patients who had distant metastases in the liver, lung, or peritoneum/pelvic cavity diagnosed before or during the surgery, those who underwent preoperative neoadjuvant radiotherapy and/or chemotherapy, or those whose medical records were incomplete/inaccurate. FIGO staging criteria (2009) were used for tumour staging. According to the postoperative pathological examination results, supplementary chemotherapy, radiotherapy, or concurrent chemoradiotherapy should be performed in cases of high-risk factors such as worse pathological differentiation degree, positive pelvic LNM, parametrial involvement, deep muscle layer infiltration, positive lymphovascular invasion (LVI), or positive surgical resection margins.

Follow-Up Investigation

A postoperative follow-up assessment was performed every 3 months for 2 years and then every 6 months during years 3–5. Most routine follow-up appointments included a physical examination, vaginal examination, laboratory testing (including cancer antigen 125 (Ca125) and squamous cell carcinoma (SCC) antigen), chest radiography, and pelvic ultrasonography. Lung computed tomography or pelvic magnetic resonance imaging was performed when necessary. OS was defined as the time from surgery to death of any cause or to the time of censoring on the date of the last follow-up. The final follow-up evaluation was conducted in December 2020. The median follow-up period was 54.3 (range, 6.4–97.1) months.

Statistical Analysis

The chi-square test or Fisher's exact probability method was used to compare the classified variables. A t-test or the Mann-Whitney U test was used to analyse differences in numerical variables. Survival curves were constructed according to the Kaplan–Meier method, and differences between curves were analysed using the log-rank test. Variables with values of $P<0.05$ on univariate analysis were subjected to a multivariate logistic regression analysis. According to those results, recursive partitioning analysis (RPA) was used to divide the patients into different risk groups. The groups with a similar incidence of LNM were reintegrated into a single risk group. Finally, the low-risk, intermediate-risk, and high-risk groups were determined with the incidence of LNM increasing in turn. The statistical analyses were performed using SPSS for Windows version 26.0 (SPSS Inc., Chicago, IL, USA) and R x64 ver. 4.1.0 (R Foundation for Statistical Computing, Vienna, Austria). All tests were two-sided, and statistical significance was determined at values of $P<0.05$.

RESULTS

Clinicopathological Characteristics

A total of 284 patients were included in the study. Their clinicopathological features are presented in **Table 1**. The incidence of LNM was 8.4%. The median patient age was 46 (range, 24–66) years. A body mass index (BMI) of <24 and ≥24 was observed in 188 (66.2%) and 96 (33.8%) cases, respectively. Squamous, adenoma, and adenosquamous carcinomas were observed in 214 (75.4%), 59 (20.8%), and 11 (3.9%) cases, respectively. Invasion depths of <1/2 and ≥ 1/2 of the stroma were observed in 168 (59.2%) and 116 (40.8%) cases, respectively. There were 77 (27.1%) and 207 (72.9%) cases of positive LVI versus no LVI, respectively. There were 178 (62.7%) and 106 (37.3%) patients with a tumour size (TS) <2 cm and ≥2 cm, respectively. There were 163 (57.4%) and 121 (42.6%) cases with a normal or high Ca125 level, respectively. There were 187 (65.8%) and 97 (34.2%) cases of a normal and high SCC level, respectively (**Table 1**).

Impact of LNM on Survival Outcomes

The median follow-up time was 54.3 (range, 6.4–97.1) months. The 5-year OS rate of all patients and in those with and without LNM were 91.72%, 80.0%, and 93.5%, respectively ($P=0.009$) (**Figure 1**).

TABLE 1 | Patient Demographics and Clinical Characteristics of CC Patients by LNM.

Parameters	Total	LNM		P value
	(n=284) n (%)	Absent (n=260) n (%)	Present (n=24) n (%)	
Age (y)				0.088
<45	119 (41.9)	105 (40.4)	14 (58.3)	
≥45	165 (58.1)	155 (59.6)	10 (41.7)	
BMI (kg/m^2)				0.341
<24	188 (66.2)	170 (65.4)	18 (75.0)	
≥24	96 (33.8)	90 (34.6)	6 (25.0)	
Surgery				0.829
Open	148 (52.1)	136 (52.3)	12 (50.0)	
Laparoscopy	136 (47.9)	124 (47.7)	12 (50.0)	
Histological type				0.069
Squamous	214 (75.4)	193 (74.2)	21 (87.5)	
Adenocarcinoma	59 (20.8)	58 (22.3)	1 (4.2)	
Adenosquamous	11 (3.9)	9 (3.5)	2 (8.3)	
Depth of invasion				<0.001
<1/2	168 (59.2)	165 (63.5)	3 (12.5)	
≥1/2	116 (40.8)	95 (36.5)	21 (87.5)	
Lymphovascular invasion				<0.001
No	207 (72.9)	200 (76.9)	7 (29.2)	
Yes	77 (27.1)	60 (23.1)	17 (70.8)	
Tumor Size (cm)				<0.001
<2	178 (62.7)	172 (66.2)	6 (25.0)	
≥2	106 (37.3)	88 (33.8)	18 (75.0)	
Ca125 (U/ml)				0.039
<35	163 (57.4)	154 (59.2)	9 (37.5)	
≥35	121 (42.6)	106 (40.8)	15 (62.5)	
SCC (ng/ml)				<0.001
<1.5	187 (65.8)	180 (69.2)	7 (29.2)	
≥1.5	97 (34.2)	80 (30.8)	17 (70.8)	

CC, cervical cancer; LNM, lymph node metastasis; BMI, body mass index; Ca125, cancer antigen 125; SCC, squamous cell carcinoma antigen.

Risk Factor Analysis of LNM

The univariate analysis showed that TS, depth of invasion (DI), LVI, SCC antigen level, and Ca125 level were associated with LNM (all P<0.05) (**Table 1**). In the multivariate logistic regression analysis, TS (odds ratio (OR), 0.351; 95% confidence interval (CI), 0.123–0.992; P=0.044), DI (OR, 0.205; 95% CI, 0.054–0.772; P=0.019), LVI (OR, 0.281; 95% CI, 0.100–0.785; P=0.015), SCC antigen level (OR, 0.338; 95% CI, 0.123–0.924; P=0.035) were independent factors for LNM (**Table 2**).

Risk Groups of LNM by RPA

Based on the results of the multivariable analysis, RPA using the four independent risk factors was performed to classify the patients into different risk groups. The group was divided into subgroups according to the R software prioritisation of the binary variables. Finally, the patients were reclassified into nine groups. Patients with a similar incidence of LNM were merged. The patients were ultimately divided into low-risk, intermediate-risk, and high-risk groups (**Figure 2**). In the model, there were 110 low-risk patients (38.7%) (no LVI, DI <1/2, TS <2 cm), 91 intermediate-risk patients (32.1%) (no LVI, DI <1/2, TS ≥2 cm; no LVI, DI ≥1/2, normal SCC antigen level; LVI, DI <1/2, TS <2 cm), and 83 high-risk patients (29.2%) (no LVI, DI ≥1/2, SCC antigen level ≥1.5 ng/mL; LVI, TS <2 cm, DI ≥1/2; LVI, TS ≥2 cm).

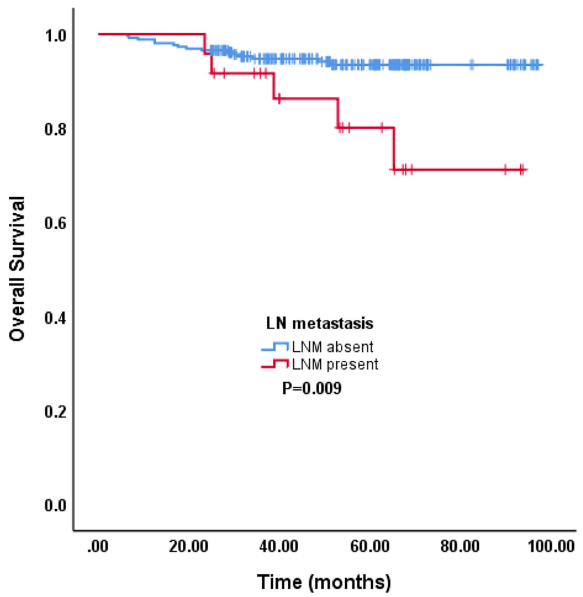


FIGURE 1 | The survival between LNM absent and LNM present.

TABLE 2 | Multivariable Binary Logistic Regression Analysis of CC for the LNM.

	Multivariable Analysis			
	Odds Ratio	95%CI		P
Tumor Size (cm)				0.044
<2	Ref			
≥2	0.351	0.123	0.992	
Depth of invasion				0.019
<1/2	Ref			
≥1/2	0.205	0.054	0.772	
Lymphovascular invasion				0.015
No	Ref			
Yes	0.281	0.100	0.785	
Ca125(U/ml)				0.189
<35	Ref			
≥35	0.523	0.199	1.375	
SCC(ng/ml)				0.035
<1.5	Ref			
≥1.5	0.338	0.123	0.924	

CC, cervical cancer; LNM, lymph node metastasis; SCC, squamous cell carcinoma.

Difference in LNM Rate and Prognosis by RPA Findings

The incidence of LNM was 0.00%, 4.40%, and 24.10% in the low-risk, intermediate-risk, and high-risk groups, respectively (all P<0.001; **Figure 3**). The 5-year OS rates were 98.2%, 92.7%, and 82.0%, respectively, which were also significantly different (P=0.001; **Figure 4**).

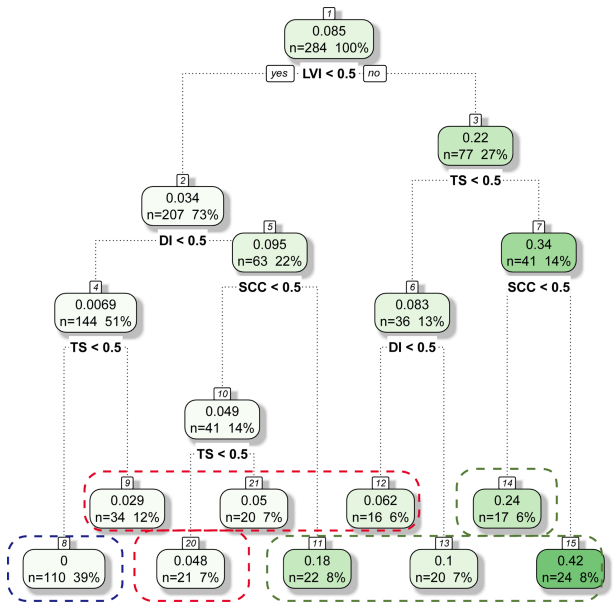


FIGURE 2 | Classification Tree for LNM Status. Blue line, Red line, Green line represents Low-Risk Group, Intermediate-Risk Group and High-Risk Group, respectively.

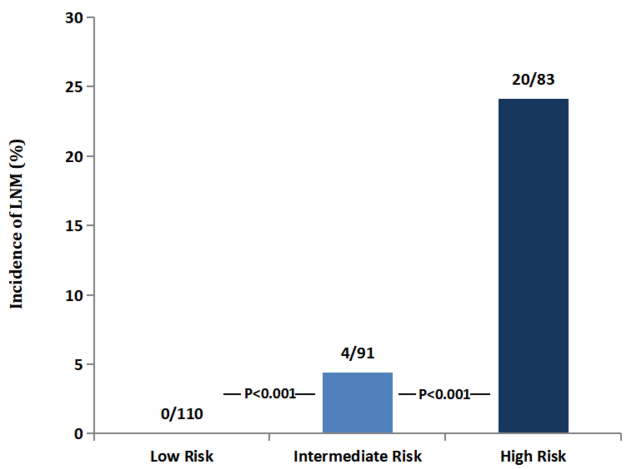


FIGURE 3 | The number of LNM according to RPA risk stratifications.

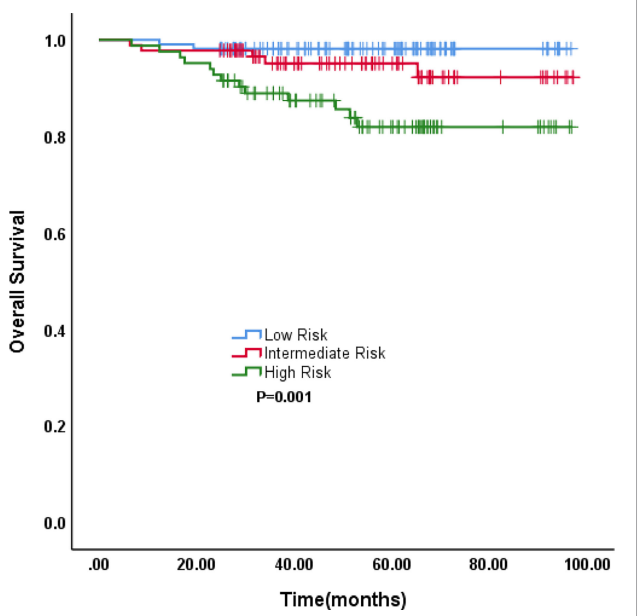


FIGURE 4 | The survival according to RPA risk stratifications.

DISCUSSION

CC is a common gynaecologic malignant tumour for which postoperative recurrence and metastasis are the main causes of death (15, 16). Patients with early-stage CC always have a better prognosis after surgery (2) but worse prognosis when proven to be metastatic. LNM, as the main mode of metastasis in patients with CC, is a high-risk factor for recurrence and greatly impacts treatment and prognosis (3, 4). LNM was also formally included in the FIGO staging system in 2018 (17). Therefore, pelvic lymph node dissection is important. According to the NCCN, the standard surgical treatment is radical hysterectomy and pelvic lymphadenectomy in patients with FIGO stage IB1 CC without fertility requirements (6). However, some patients experience sequelae from this procedure (such as vascular or nerve injury, pelvic lymphocyst, and lower-limb lymphedema), which may increase the length of hospital stay and affect quality of life (7–9). In addition, the rate of LNM in FIGO stage IB1 patients was 7–17.4% (12–14). Lymphadenectomy may not have a survival benefit, but it may increase the incidence of postoperative complications in LNM-negative patients. LNM-positive patients not treated with lymphadenectomy may experience recurrence within a short period postoperative. Therefore, it is of great significance to explore the risk factors influencing LNM and conduct a risk assessment in patients with FIGO stage IB1 CC.

This study showed an 8.4% (24/284) rate of LNM in patients with FIGO stage IB1 CC, a finding that is in accordance with those of other studies (12–14). The 5-year OS rate in patients with LNM was significant lower than patients without LNM. As the patients were selected from January 2012 to December 2018 before the results of LACC trails (18), a certain proportion of patients underwent radical hysterectomy *via* laparoscopy. However, the results showed no prognostic differences between patients *via* laparoscopy or not (**Supplementary Figure 1**). This result needed further confirmation in future studies. The rate of LNM also showed no significant difference between the open and laparoscopic surgery in the study. In addition, with the development of technology, robotic surgery has been gradually applied in clinical. Previous studies showed the equivalence of robotic and laparoscopic approaches to radical surgery of early CC patients (19), so did the salvage lymphadenectomy (20).

Therefore, it also may be a good choice in clinical practice in the future.

The multivariable logistic regression analysis showed that LVI, DI, TS, and SCC antigen level were independent risk factors, which is also consistent with previous reports (4, 21–23). LVI is closely associated with LNM in CC. Invasion into the space between lymphatic endothelial cells is an indispensable step for the metastasis of cancer cells; thus, it often predicts a poor prognosis. The larger the tumour diameter and the deeper the musculature invasion, the more likely tumour cells will invade the intravascular system, and thus the more likely the development of LNM. The SCC antigen is a specific serum tumour marker for CC that was first discovered by Kato in 1977 (24). The higher the SCC antigen level, the more aggressive the tumour and the higher the probability of LNM (25, 26). However, previous studies (4, 21) analysed only the independent risk factors affecting LNM without further risk grouping, resulting in some limitations in determining whether lymphadenectomy should also be performed. This study was the first to report a risk stratification by RPA based on these factors, and it provides a reference for whether lymphadenectomy should be performed simultaneously in patients with early-stage CC.

RPA is a statistical method for multivariable analyses that divides groups into subgroups according to the priority of several binary independent variables to correctly classify the members of a group. As a result, a concise decision tree is generated intuitively to determine decision rules with higher sensitivity and specificity (27). This method is widely used in medical decision-making. The RPA was first used by Goldman to establish a decision tree for the diagnosis of patients with acute chest pain in 1982 (28). It was also used to group patients with acute decompensated heart failure by Fonarow (29). In this study, the rate of LNM was 0.00% in patients with no LVI, a DI <1/2, and a TS <2 cm (low-risk group) according to the RPA. The negative LVI, less tumor size and less depth of invasion meant the less invasion in the intravascular system and parametrial involvement, leading to the less possibility of LNM (21–23, 30). Lymphadenectomy may be avoided in these patients to reduce postoperative complications. The LNM rate was as high as 24.10% in high-risk patients, including: those with no LVI, a DI ≥ 1/2, and an SCC antigen level ≥1.5 ng/mL; those with LVI, a TS <2 cm, and a DI ≥1/2; and those with LVI and a TS ≥2 cm. Therefore, simultaneous lymphadenectomy is recommended.

Sentinel lymph node biopsy (SLNB) has recently been used in patients with early-stage CC. Compared to pelvic lymph node dissection, SLNB reduces the incidence of postoperative complications and improves quality of life without affecting the survival prognosis (31–34). SLNB could be applied in the intermediate-risk group (no LVI, DI <1/2, TS ≥2 cm; no LVI, DI ≥1/2, normal SCC level; LVI, DI <1/2, TS <2 cm) as the rate of LNM was 4.40%. Whether to perform simultaneous lymphadenectomy could be determined based on the SLNB results. In addition, the LNM rate differed significantly between the three groups here and also on the survival analysis, indicating that risk grouping based on these four risk factors has a certain reference significance in clinical decision-making.

This study had several limitations. First, it was retrospective in design, which inevitably involves data selection bias. Second, the research was conducted in a single centre with small case numbers, and our findings require further confirmation in prospective multicentre studies. However, to our knowledge, this study is the first to explore the risk factors affecting LNM in patients with FIGO stage IB1 CC. Furthermore, the RPA was used to classify the risk groups to make the model more clinically useful. Based on these findings, we have proposed recommendations for lymphadenectomy for different risk groups with early CC, which will aid surgeons make better clinical decisions, showing the important clinical significance of our study.

DATA AVAILABILITY STATEMENT

The raw data supporting the conclusions of this article will be made available by the authors, without undue reservation.

ETHICS STATEMENT

The present study was approved by the Ethics Committee of the Fujian Provincial Maternity and Children's Hospital. Written informed consent was obtained from all participants. The patients/participants provided their written informed consent to participate in this study.

AUTHOR CONTRIBUTIONS

MX and XX designed, conceived this study, and wrote the paper. YX and QG contributed to the literature search and collect the data. LC was involved in data extraction and analyzed the data. PS revised the paper. All authors have approved the final edition of the manuscript.

FUNDING

This study was funded by Fujian Provincial Maternity and Children's Hospital Natural Science Foundation (Grant No. YCXM 20–03).

SUPPLEMENTARY MATERIAL

The Supplementary Material for this article can be found online at: https://www.frontiersin.org/articles/10.3389/fonc.2022.809159/full#supplementary-material

Supplementary Figure 1 | The survival between laparoscopic surgery and open surgery.

REFERENCES

1. Song B, Ding C, Chen W, Sun H, Zhang M, Chen W. Incidence and Mortality of Cervical Cancer in China, 2013. *Chin J Cancer Res* (2017) 29(6):471–6. doi: 10.21147/j.issn.1000-9604.2017.06.01
2. Siegel RL, Miller KD, Jemal A. Cancer Statistics, 2018. *CA Cancer J Clin* (2018) 68(1):7–30. doi: 10.3322/caac.21442
3. Mabuchi S, Isohashi F, Yokoi T, Takemura M, Yoshino K, Shiki Y, et al. A Phase II Study of Postoperative Concurrent Carboplatin and Paclitaxel Combined With Intensity-Modulated Pelvic Radiotherapy Followed by Consolidation Chemotherapy in Surgically Treated Cervical Cancer Patients With Positive Pelvic Lymph Nodes. *Gynecol Oncol* (2016) 141 (2):240–6. doi: 10.1016/j.ygyno.2016.02.011
4. Nanthamongkolkul K, Hanprasertpong J. Predictive Factors of Pelvic Lymph Node Metastasis in Early-Stage Cervical Cancer. *Oncol Res Treat* (2018) 41 (4):194–8. doi: 10.1159/000485840
5. Aoki Y, Sasaki M, Watanabe M, Sato T, Tsuneki I, Aida H, et al. High-Risk Group in Node-Positive Patients With Stage IB, IIA, and IIB Cervical Carcinoma After Radical Hysterectomy and Postoperative Pelvic Irradiation. *Gynecol Oncol* (2000) 77(2):305–9. doi: 10.1006/gyno.2000.5788
6. Koh WJ, Abu-Rustum NR, Bean S, Bradley K, Campos SM, Cho KR, et al. Cervical Cancer, Version 3. 2019, NCCN Clinical Practice Guidelines in Oncology. *J Natl Compr Canc Netw* (2019) 17(1):64–84. doi: 10.6004/jnccn.2019.0001
7. Ferrandina G, Pedone Anchora L, Gallotta V, Fagotti A, Vizza E, Chiantera V, et al. Can We Define the Risk of Lymph Node Metastasis in Early-Stage Cervical Cancer Patients? A Large-Scale, Retrospective Study. *Ann Surg Oncol* (2017) 24(8):2311–8. doi: 10.1245/s10434-017-5917-0
8. Yahata H, Kobayashi H, Sonoda K, Kodama K, Yagi H, Yasunaga M, et al. Prognostic Outcome and Complications of Sentinel Lymph Node Navigation Surgery for Early-Stage Cervical Cancer. *Int J Clin Oncol* (2018) 23(6):1167–72. doi: 10.1007/s10147-018-1327-y
9. Zhao J, Cai J, Wang H, Dong W, Zhang Y, Wang S, et al. Region-Specific Risk Factors for Pelvic Lymph Node Metastasis in Patients With Stage IB1 Cervical Cancer. *J Cancer* (2021) 12(9):2624–32. doi: 10.7150/jca.53215
10. Salvo G, Ramirez PT, Levenback CF, Munsell MF, Euscher ED, Soliman PT, et al. Sensitivity and Negative Predictive Value for Sentinel Lymph Node Biopsy in Women With Early-Stage Cervical Cancer. *Gynecol Oncol* (2017) 145(1):96–101. doi: 10.1016/j.ygyno.2017.02.005
11. Tanaka T, Sasaki S, Tsuchihashi H, Terai Y, Yamamoto K, Yamada T, et al. Which Is Better for Predicting Pelvic Lymph Node Metastases in Patients With Cervical Cancer: Fluorodeoxyglucose-Positron Emission Tomography/Computed Tomography or a Sentinel Node Biopsy? A Retrospective Observational Study. *Med (Baltimore)* (2018) 97(16):e0410. doi: 10.1097/MD.0000000000010410
12. Wang Y, Yao T, Yu J, Li J, Chen Q, Lin Z. Can Pelvic Lymphadenectomy be Omitted in Patients With Stage IA2, IB1, and IIA1 Squamous Cell Cervical Cancer? *Springerplus* (2016) 5(1):1262. doi: 10.1186/s40064-016-2927-5
13. Zhou J, Ran J, He ZY, Quan S, Chen QH, Wu SG, et al. Tailoring Pelvic Lymphadenectomy for Patients With Stage IA2, IB1, and IIA1 Uterine Cervical Cancer. *J Cancer* (2015) 6(4):377–81. doi: 10.7150/jca.10968
14. Rob L, Robova H, Chmel R, Komar M, Halaska M, Skapa P. Surgical Options in Early Cervical Cancer. *Int J Hyperthermia* (2012) 28(6):489–500. doi: 10.3109/02656736.2012.675116
15. Twu NF, Ou YC, Liao CI, Chang WY, Yang LY, Tang YH, et al. Prognostic Factors and Adjuvant Therapy on Survival in Early-Stage Cervical Adenocarcinoma/Adenosquamous Carcinoma After Primary Radical Surgery: A Taiwanese Gynecologic Oncology Group (TGOG) Study. *Surg Oncol* (2016) 25(3):229–35. doi: 10.1016/j.suronc.2016.05.028
16. Jeong SY, Park H, Kim MS, Kang JH, Paik ES, Lee YY, et al. Pretreatment Lymph Node Metastasis as a Prognostic Significance in Cervical Cancer: Comparison Between Disease Status. *Cancer Res Treat* (2020) 52(2):516–23. doi: 10.4143/crt.2019.328
17. Bhatla N, Aoki D, Sharma DN, Sankaranarayanan R. Cancer of the Cervix Uteri. *Int J Gynaecol Obstet* (2018) 143(Suppl 2):22–36. doi: 10.1002/ijgo.12611
18. Ramirez PT, Frumovitz M, Pareja R, Lopez A, Vieira M, Ribeiro R, et al. Minimally Invasive Versus Abdominal Radical Hysterectomy for Cervical Cancer. *N Engl J Med* (2018) 379(20):1895–904. doi: 10.1056/NEJMoa1806395
19. Gallotta V, Conte C, Federico A, Vizzielli G, Alletti SG, Tortorella L, et al. Robotic Versus Laparoscopic Radical Hysterectomy in Early Cervical Cancer: A Case Matched Control Study. *Eur J Surg Oncol* (2018) 44(6):754–9. doi: 10.1016/j.ejso.2018.01.092
20. Gallotta V, Giudice MT, Conte C, Sarandeses AV, D'Indinosante M, Federico A, et al. Minimally Invasive Salvage Lymphadenectomy in Gynecological Cancer Patients: A Single Institution Series. *Eur J Surg Oncol* (2018) 44 (10):1568–72. doi: 10.1016/j.ejso.2018.08.006
21. Huang BX, Fang F. Progress in the Study of Lymph Node Metastasis in Early-Stage Cervical Cancer. *Curr Med Sci* (2018) 38(4):567–74. doi: 10.1007/s11596-018-1915-0
22. Zhou Z, Li W, Zhang F, Hu K. The Value of Squamous Cell Carcinoma Antigen (Scca) to Determine the Lymph Nodal Metastasis in Cervical Cancer: A Meta-Analysis and Literature Review. *PLoS One* (2017) 12(12):e0186165. doi: 10.1371/journal.pone.0186165
23. Yang H, Hu H, Gou Y, Hu Y, Li H, Zhao H, et al. Combined Detection of Twist1, Snail1 and Squamous Cell Carcinoma Antigen for the Prognostic Evaluation of Invasion and Metastasis in Cervical Squamous Cell Carcinoma. *Int J Clin Oncol* (2018) 23(2):321–8. doi: 10.1007/s10147-017-1210-2
24. Kato H, Torigoe T. Radioimmunoassay for Tumor Antigen of Human Cervical Squamous Cell Carcinoma. *Cancer* (1977) 40(4):1621–8. doi: 10.1002/1097-0142(197710)40:4<1621::aid-cncr2820400435>3.0.co;2-i
25. Salvatici M, Achilarre MT, Sandri MT, Boveri S, Vanna Z, Landoni F. Squamous Cell Carcinoma Antigen (SCC-Ag) During Follow-Up of Cervical Cancer Patients: Role in the Early Diagnosis of Recurrence. *Gynecol Oncol* (2016) 142(1):115–9. doi: 10.1016/j.ygyno.2016.04.029
26. Xu F, Li Y, Fan L, Ma J, Yu L, Yi H, et al. Preoperative SCC-Ag and Thrombocytosis as Predictive Markers for Pelvic Lymphatic Metastasis of Squamous Cervical Cancer in Early FIGO Stage. *J Cancer* (2018) 9(9):1660–6. doi: 10.7150/jca.24049
27. Breiman L. *Classification and Regression Trees*. Boca Raton: Chapman & Hall/CRC (1984).
28. Goldman L, Weinberg M, Weisberg M, Olshen R, Cook EF, Sargent RK, et al. A Computer-Derived Protocol to Aid in the Diagnosis of Emergency Room Patients With Acute Chest Pain. *N Engl J Med* (1982) 307(10):588–96. doi: 10.1056/NEJM198209023071004
29. Fonarow GC, Adams KFJr, Abraham WT, Yancy CW, Boscardin WJ. ADHERE Scientific Advisory Committee, Et Al. Risk Stratification for in-Hospital Mortality in Acutely Decompensated Heart Failure: Classification and Regression Tree Analysis. *JAMA* (2005) 293(5):572–80. doi: 10.1001/jama.293.5.572
30. Kato T, Takashima A, Kasamatsu T, Nakamura K, Mizusawa J, Nakanishi T, et al. Clinical Tumor Diameter and Prognosis of Patients With FIGO Stage IB1 Cervical Cancer (JCOG0806-A). *Gynecol Oncol* (2015) 137(1):34–9. doi: 10.1016/j.ygyno.2015.01.548
31. Lennox GK, Covens A. Can Sentinel Lymph Node Biopsy Replace Pelvic Lymphadenectomy for Early Cervical Cancer? *Gynecol Oncol* (2017) 144 (1):16–20. doi: 10.1016/j.ygyno.2016.08.337
32. Togami S, Kubo R, Kawamura T, Yanazume S, Kamio M, Kobayashi H. Comparison of Lymphatic Complications Between Sentinel Node Navigation Surgery and Pelvic Lymphadenectomy in Patients With Cervical Cancer. *Jpn J Clin Oncol* (2020) 50(5):543–7. doi: 10.1093/jjco/hyaa001
33. Guani B, Dorez M, Magaud L, Buenerd A, Lecuru F, Mathevet P. Impact of Micrometastasis or Isolated Tumor Cells on Recurrence and Survival in Patients With Early Cervical Cancer: SENTICOL Trial. *Int J Gynecol Cancer* (2019) 29(3):447–52. doi: 10.1136/ijgc-2018-000089
34. Stany MP, Stone PJ, Felix JC, Amezcua CA, Groshen S, Ye W, et al. Lymph Node Micrometastases in Early-Stage Cervical Cancer Are Not Predictive of Survival. *Int J Gynecol Pathol* (2015) 34(4):379–84. doi: 10.1097/PGP.0000000000000188

Conflict of Interest: The authors declare that the research was conducted in the absence of any commercial or financial relationships that could be construed as a potential conflict of interest.

Publisher's Note: All claims expressed in this article are solely those of the authors and do not necessarily represent those of their affiliated organizations, or those of the publisher, the editors and the reviewers. Any product that may be evaluated in

this article, or claim that may be made by its manufacturer, is not guaranteed or endorsed by the publisher.

Copyright © 2022 Xu, Xie, Cai, Xie, Gao and Sun. This is an open-access article distributed under the terms of the Creative Commons Attribution License (CC BY). The use, distribution or reproduction in other forums is permitted, provided the original author(s) and the copyright owner(s) are credited and that the original publication in this journal is cited, in accordance with accepted academic practice. No use, distribution or reproduction is permitted which does not comply with these terms.

frontiers in Oncology

SYSTEMATIC REVIEW
published: 31 March 2022
doi: 10.3389/fonc.2022.732322

Association Between Endometriosis and Prognosis of Ovarian Cancer: An Updated Meta-Analysis

Peng Chen and Chi-Yuan Zhang *

Department of Obstetrics and Gynecology, Shengjing Hospital of China Medical University, Shenyang, China

Objective: Increased risk of ovarian cancer (OC) among endometriosis patients has been proposed. However, the association between endometriosis and prognosis of OC remains controversial. This study evaluated whether endometriosis had influence on the survival outcomes of OC through a meta-analysis.

Methods: Relevant studies were retrieved from PubMed, Embase, and Web of Science databases and were evaluated using the Newcastle-Ottawa Quality Assessment Scale. Effect size was presented as hazard ratio (HR) and 95% confidence interval (CI). Heterogeneity test evaluation was performed using Cochran's Q test and I^2 statistics. Publication bias was determined using Egger's test. Statistical analysis was performed using Stata 12.0 software.

Results: Twenty-one studies involving 38641 patients were included. For the total OC, there were significant differences in overall survival (OS) [HR (95% CI)=0.67 (0.55, 0.80), P<0.001] and progression-free survival (PFS) [HR (95% CI)=0.58 (0.42, 0.81), P=0.001] between endometriosis-associated ovarian cancer (EAOC) and non-EAOC patients in the random-effects models (P<0.05). For ovarian clear cell cancer, there were significant differences in terms of OS [HR (95% CI)=0.63 (0.48, 0.83), P=0.001] and PFS [HR (95% CI)=0.67 (0.52, 0.87), P=0.002] between EAOC and non-EAOC patients in the fixed-effects models (P>0.05). Subgroup analysis suggested no significant differences between EAOC and non-EAOC in OS and PFS in the univariate analysis per subgroup, and PFS in the American subgroup (P>0.05).

Conclusion: EAOC patients tended to have better OS and PFS than non-EAOC patients. Conducting higher quality prospective cohort studies with large sample sizes is recommended to confirm the authenticity of the current study's results.

Systematic Review Registration: https://inplasy.com/inplasy-2022-3-0109/.

Keywords: endometriosis, ovarian cancer, prognosis, meta-analysis, overall survival, progression-free survival

OPEN ACCESS

Edited by:
Stefano Restaino, Ospedale Santa Maria della Misericordia di Udine, Italy

Reviewed by:
Farr Nezhat, Nezhat Surgery for Gyn/Onc, United States
Guangchuan Wang, Center for Excellence in Molecular Cell Science (CAS), China

***Correspondence:**
Chi-Yuan Zhang
zcysjcmu@163.com

Specialty section:
This article was submitted to Gynecological Oncology, a section of the journal Frontiers in Oncology

Received: *28 June 2021*
Accepted: *07 March 2022*
Published: *31 March 2022*

Citation:
Chen P and Zhang C-Y (2022) Association Between Endometriosis and Prognosis of Ovarian Cancer: An Updated Meta-Analysis. Front. Oncol. 12:732322. doi: 10.3389/fonc.2022.732322

INTRODUCTION

Endometriosis is a type of estrogen-dependent chronic inflammatory disease and is a common gynecological condition affecting 5-10% of reproductive-aged women in the world. It is defined as the ectopic growth of endometrial glands and stroma, causing dysmenorrhea, pelvic pain and infertility (1). Although endometriosis is benign lesion, it exhibits malignant biological behaviors

similar to cancer, such as local invasion, metastasis, invasion, and easy recurrence (2), and malignant transformation of endometriosis has been proposed as early as 1925 (3). Under the influence of multiple factors, ectopic ovarian endometrial cells with malignant potential gradually change their normal ectopic endometrial cystic epithelium to atypical ectopic endometrial epithelium and invasive carcinoma, which is then called endometriosis associated ovarian cancer (EAOC). Endometriosis may be a precursor lesion to specific subtypes of OC, and prevalence studies show that ovarian clear cell cancer (OCCC) and endometrioid ovarian cancer (EOC) are predominate in women with endometriosis (3–6).

Studies have shown that patients with endometriosis are at higher risk of developing ovarian cancer (OC) (7). Endometriosis is reported to be a risk factor for epithelial OC, which is associated with a 50% increase in epithelial OC risk (8). A meta-analysis of 13 case-control studies suggested that patients with endometriosis had a significantly elevated risk of specific histological subtypes of OC, including OCCC, EOC and low-grade serous OC (9). OC is the seventh most common cancer in women (10) and the 2nd gynecologic cause of cancer deaths in women worldwide (11), with a 5-year survival rate of 47.4%. Prognosis for OC patients is directly associated with tumor stage at the time of diagnosis, ranging from approximately 90% in stage I-tumors to 25% in metastatic tumors (10).

Several studies based on meta-analyses have revealed an association between endometriosis and prognosis of OC in 2014 to 2015, but inconsistent conclusions were found among them (12–14). In recent years, additional studies have been reported the differences of the prognosis of OC patients with or without endometriosis. For example, a retrospective nationwide cohort study of 32,419 women indicated that OC patients with endometriosis had longer overall survival than those without endometriosis, even after adjusting for confounding factors (15). Li et al. indicated that patients with EAOC had longer overall survival (109.8 months) than those with non-EAOC (47.4 months) (16). However, no associations between endometriosis and prognosis of OC were found in the study of Ju et al. (17). Therefore, to obtain a more comprehensive and objective result, we performed a meta-analysis to uncover the differences in terms of progression-free survival (PFS) and overall survival (OS) within EAOC and non-EAOC patients.

METHODS

Search Strategy

According to a pre-established retrieval strategy, the relevant studies were systematically retrieved from PubMed, Embase, Web of Science databases with the retrieval time up to May 11, 2021 and without language restrictions. The search terms contained three categories: research object ("ovarian neoplasm", "ovarian cancer", "ovary neoplasm", "ovary cancer", "ovarian carcinoma", "ovary carcinoma"), exposure factors ("endometriosis", "endometrioses") and outcomes ("mortality", "survival", "prognosis"). Two search terms in the same category are combined with "OR", while "AND" was used between two search terms of different categories. The detailed retrieval strategies for different databases are listed in **Table S1**. Additionally, manual retrieval was carried out for the paper version of the relevant studies, and the references of the relevant reviews and included studies were also retrieved.

Inclusion and Exclusion Criteria

Studies were included in this meta-analysis if they met the following criteria: (1) patients who were pathologically and histologically diagnosed as epithelial ovarian cancer were included; (2) PFS or OS of OC patients with or without endometriosis were reported; (3) they were retrospective or prospective cohort studies or nested case-control studies; and (4) the crude or multivariable adjusted hazard ratio (HR) and 95% confidence interval (CI) for PFS and OS were reported. Studies were excluded from this analysis if they were: (1) non-original articles, such as reviews, conference abstracts and comments; (2) the studies that provide only a figure but not a detailed HR (95% CI) to show the results of survival analysis; (3) duplicate studies or multiple studies involving the same data, with only the one with the most complete information included. On the basis of the above selection criteria, study retrieval was carried out by two independent investigators.

Data Extraction and Quality Evaluation

Data extraction was conducted independently in accordance with the form pre-designed by two investigators. The following data were extracted, including the first author's name, region of research, year of publication, when the study subjects were recruited, subject information, including: sample size, age, histological subtypes, adjuvant treatment, outcomes, and other confounding factors. The extracted data were exchanged and reviewed, and disagreements were settled through a thorough discussion. The methodological quality evaluation for the included studies, which involved the selection, comparability, and exposure of the included study subjects, were conducted with reference to the Newcastle-Ottawa Quality Assessment Scale (NOS) (18), which includes 8 scoring items with a full score of 9. Studies with a final score ranging from 7 to 9 are regarded as high quality, while those with a final score ranging from 4 to 6 or less than 4 are regarded as medium quality or low quality, respectively.

Statistical Analysis

All statistical analyses were completed using Stata 12.0 software. HR and 95% CI were utilized as effect size indicators to evaluate the differences on PFS and OS of EAOC vs. non-EAOC. Cochran's Q test and I^2 test (19) were used to assess the heterogeneity among studies. Significant heterogeneity was determined with $P<0.05$ or $I^2>50\%$, and a random-effects model was utilized. A fixed-effects model was utilized when no significant heterogeneity was observed ($P\geq0.05$ and $I^2 \leq 50\%$). The effect of region, confounding factors adjusted or not for heterogeneity, and the pooled results were evaluated with a subgroup analysis. Publication bias evaluation was conducted using Egger's test. If there was significant publication bias, the

stability of the results of the meta-analysis was evaluated using the trim-and-fill method. The stability of the results was also evaluated using the method of elimination one by one.

RESULTS

Study Retrieval

In total, 1931 studies, including 702 studies from PubMed, 713 studies from Embase, and 516 studies from the Web of Science database were retrieved. Among these studies, 549 duplicate studies were first removed. Of the 1382 remaining studies, 1345 irrelevant studies were excluded after title/abstract reading. After full-text reading, 16 studies were further excluded, including 11 studies without detailed HR (95% CI) to show the results, 3 reviews, and 2 studies without detailed information of PFS or OS. Finally, 21 studies (12, 15–17, 20–36) were included in the current meta-analysis (**Figure 1**).

Characteristics of Studies

A total of 38641 cases were included in these 21 studies. **Table 1** shows the detailed characteristics of the 21 included studies. All the studies were retrospective cohort studies except for the study of Erzen et al. (23), which was a nested case-control study. The included patients had Stage I-IV OC in all studies except for the study of Ju et al. (17), in which the included patients had Stage I-III OC (data not shown). These studies were published from 1989 to 2021, and were conducted in 8 countries, such as China, South Korea, USA, Japan, and Italy. In addition, the ages of the included cases were not reported in the study of Katagiri et al. (24), but the ages of all the cases were mentioned in three studies (20, 21, 26). The remaining 17 studies reported the ages of cases in the EAOC and non-EAOC groups, and among these studies, significant differences were found between the cases belonging to different EAOC and non-EAOC age groups in ten studies (12, 15, 16, 22, 29, 31–35).

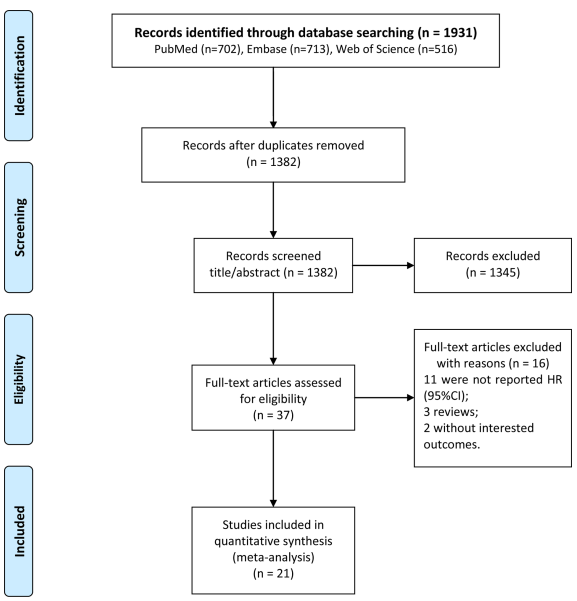


FIGURE 1 | Flow chart of the patient selection process.

Quality Evaluation

The methodological quality evaluation for the 21 included studies was conducted with reference to NOS, and the results are shown in **Table 2**. The NOS scores of the 21 studies ranged from 5 to 8 points, of which 5 points was evaluated for one study (23), 6 points for five studies (21, 22, 24, 33, 36), 7 points for six studies (16, 20, 25, 28, 29, 31) and 8 points for nine studies (12, 15, 17, 26, 27, 30, 32, 34, 35). Overall, the methodological quality of the included studies was moderate. Recall bias and confounding bias were the primary bias.

Meta-Analysis and Subgroup Analysis

The impact of endometriosis on the prognosis of total OC was presented in **Figure 2**. Eighteen studies reported the pooled results for OS of patients, and significant heterogeneity among studies were observed (I^2 = 41.9%, P = 0.032). A random-effects model was utilized to pool the results. As shown in **Figure 2**, there was a significant difference in terms of OS within EAOC and non-EAOC groups [HR (95% CI) = 0.67 (0.55, 0.80), P < 0.001], suggesting that EAOC patients had better OS than non-EAOC patients. Similarly, EAOC patients had better PFS than non-EAOC patients [HR (95% CI) = 0.58 (0.42, 0.81), P = 0.001] in the random-effects model (I^2 = 53.4%, *P*= 0.014) (**Figure 2**). Subgroup analysis indicated that no differences in OS were found between the OC patients with or without endometriosis [HR (95% CI) = 0.73 (0.38, 1.39), P = 0.332] in the univariate analysis subgroup. The results of other subgroups were consistent with the total pooled results. Subgroup analysis for PFS suggested that there was a statistically significant difference in Asian (P=0.005) and multivariate analysis subgroups (P=0.001), while there was no statistically significant difference in the America (P=0.169) and univariate analysis subgroups (P=0.260). In addition, whether confounding factors were adjusted or not was found to be one of the sources of significant heterogeneity for OS (**Table 3**).

The impact of endometriosis on OCCC prognosis is presented in **Figure 3**. There was no significant heterogeneity between the studies for OS (I^2 = 0.0%, P = 0.589) and PFS (I^2 = 40.2%, P = 0.123) therefore, fixed-effects models were used. Similarly, EAOC patients were associated with a better OS [HR (95% CI) = 0.63 (0.48, 0.83), P = 0.001] (**Figure 3**) and PFS [HR (95% CI) = 0.67 (0.52, 0.87), P = 0.002] (**Figure 3**) in comparison with non-EAOC patients. Subgroup analysis did not detect any significant difference in OS between the OCCC patients with or without endometriosis in the Europe [HR (95% CI) = 0.68 (0.28, 1.67), P =0.339] and univariate analysis subgroups [HR (95% CI) = 1.38 (0.61, 3.11), P =0.444]. The results of other subgroups were consistent with the total pooled results. Subgroup analysis for PFS suggested that there was statistical significance in the Asian (P=0.003) and multivariate analysis subgroups (P=0.001), while

TABLE 1 | Characteristics of the included studies.

Study	Area	Period of enrollment	Age, years, (EAOC/non-EAOC)	Histological subtype	n, EAOC/ non-EAOC	Adjuvant treatment	Outcomes	Adjusted factors
Barreta, A 2018 (20)	Brazil	1995-2016	56.8±11.9	OCCC, EOC	50, 40/10	NR	PFS, OS	Histology, CA-125, Stage
Crozier, MA 1989 (21)	USA	1959-1985	51 (28-77)	OCCC	59, 13/46	Radiotherapy or PBC	PFS, OS	Crude
Dinkelspiel, HE 2016 (22)	USA	2000-2013	52 (47-57)/ 61 (55-70) *	Serous, mucinous, OCCC, EOC, mixed	139, 49/90	PBC	PFS, OS	Crude
Erzen, M 2001 (23)	Slovenia	1990-1999	54.5±11.5/54.7±11.7	Serous, mucinous, OCCC, EOC, others	290, 58/232	NR	OS	Crude
Hermens, M 2021 (15)	the Netherlands	1990-2015	56 (49-63)/ 66 (56-75) *	Serous, mucinous, OCCC, EOC, others	35530, 2008/33522	Chemo- therapy	OS	Age, Surgery, Chemotherapy, stage, Histological Subtype, grade.
Ju, UC 2019 (17)	Korea	2004-2016	49.0±12.7/53.4±13.6	OCCC, EOC	119, 30/89	Chemo- therapy	PFS, OS	Stage, Grade, Laterality of tumor, LN metastasis, RD
Katagiri, A 2012 (24)	Japan	NR	NR	OCCC	60, 28/32	PBC	PFS, OS	Crude
Kim, HS 2014 (13)	Korea	1997-2012	31(<55), 16(≥55)/ 26(<55), 36(≥55) *	OCCC	109, 47/62	Taxane/PBC	PFS, OS	Age, FIGO stage, histology, optimal debulking, adjuvant treatment
Kumar, S 2011 (25)	USA	1992-2002	54/59	Serous, mucinous, OCCC, EOC	226, 42/184	NR	OS	Age, Race, Stage, Grade, treatment
Lee, HY 2020 (26)	Korea	1995-2015	51 (25-81)	OCCC	308, 107/201	PBC	PFS, OS	Age, ECOG PS, Grade, Stage, chemotherapy, Optimal debulking
Li, QW 2019 (16)	China	2002-2017	48.65±8.98/54.39±9.05 *	OCCC, EOC	128, 34/94	NR	OS	Serum CA125, RD, Ascites, Stage, Histological type, Chemo-resistance
Lu, J 2017 (27)	China	1995-2010	49.6(47.6-51.7)/51.1 (49.5-52.7)	OCCC, EOC, Mixed	196, 58/138	PBC	PFS, OS	Age, Histology, Stage, ECOG PS, LNM, RD, ascites, CA125
Noli, S 2013 (28)	Italy	1990-2010	51.4±9.8/54.3±11.2	OCCC, EOC	113, 36/77	NR	OS	Stage
Orezzoli, JP 2008 (29)	USA	1975-2002	45-61/54-63 *	OCCC	84, 41/43	PBC	OS	Age, stage, RD, chemotherapy, peritoneal washings
Paik, ES 2018 (30)	Korea	2002-2015	45.1±7.0/46.7±10.3	OCCC, EOC	224, 41/183	Taxane/PBC	PFS, OS	Age, CA-125, FIGO stage, Grade, RD
Park, JY 2018 (31)	Korea	1991-2012	48 (29-69)/51 (28-79) *	OCCC	155, 78/77	PBC	PFS, OS	CA-125, FIGO stage, Ovarian surface involvement, Optimal debulking
Ren, T 2017 (32)	China	2000-2012	45 (40-49.5)/52 (44-62) *	OCCC, EOC	304, 68/236	PBC	PFS, OS	Age, Menopause, Stage, Histotype, LNM, RD, CA125, Tumor side, Chemotherapy, Chemoresistance
Scarfone, G 2014 (33)	Italy	1990-2012	51.4±10.0/58.4±11.2 *	OCCC	73, 27/46	NR	OS	Stage
Wang, S 2013 (34)	China	2000-2012	45.8±11.2/51.2±12.7 *	EOC	188, 32/156	PBC	PFS	Age, Menopausal status, Stage, RD, Grade, Clear cell mixed, EC
Ye, S 2014 (35)	China	2000-2012	46 (30-60)/54 (30-74) *	OCCC	200, 79/131	PBC	PFS, OS	Age, CA 125, Stage, RD, Menopausal status, Gravidity
Zhu, CC 2021 (36)	China	2010-2020	45.50±6.19/50.09±10.40	OCCC	86, 16/70	Paclitaxel and platinum	PFS, OS	Crude

EAOC, Endometriosis-associated ovarian carcinoma; EOC, endometrioid ovarian carcinoma; LNM, Lymph node metastasis; OCCC, ovarian clear cell carcinoma; OS, Overall survival; PBC, Platinum-based chemotherapy; PFS, Progression-free survival; RD, Residual disease; USA, the United States of America.

**means significant differences were found between the EAOC and non-EAOC groups.*

TABLE 2 | Quality assessment of the included studies.

Study	Representativeness of the exposed cohort	Selection of the unexposed cohort	Ascertainment of exposure	Outcome of interest not present at start of study	Control for important factor or additional factor	Outcome assessment	Follow-up long enough for outcomes to occur	Adequacy of follow-up of cohorts	Total quality scores
Barreta, A 2018 (20)	☆	☆	☆	–	☆	☆	☆	☆	7
Crozier, MA 1989 (21)	☆	☆	☆	–	–	☆	☆	☆	6
Dinkelspiel, HE 2016 (22)	☆	☆	☆	–	–	☆	☆	☆	6
Erzen, M 2001 (23)	☆	☆	☆	–	–	–	☆	☆	5
Hermens, M 2021 (15)	☆	☆	☆	–	☆☆	☆	☆	☆	8
Ju, UC 2019 (17)	☆	☆	☆	–	☆☆	☆	☆	☆	8
Katagiri, A 2012 (24)	☆	☆	☆	–	–	☆	☆	☆	6
Kim, HS 2014 (13)	☆	☆	☆	–	☆☆	☆	☆	☆	8
Kumar, S 2011 (25)	☆	☆	☆	–	☆	☆	☆	☆	7
Lee, HY 2020 (26)	☆	☆	☆	–	☆☆	☆	☆	☆	8
Li, QW 2019 (16)	☆	☆	☆	–	☆	☆	☆	☆	7
Lu, J 2017 (27)	☆	☆	☆	–	☆☆	☆	☆	☆	8
Noli, S 2013 (28)	☆	☆	☆	–	☆	☆	☆	☆	7
Orezzoli, JP 2008 (29)	☆	☆	☆	–	☆	☆	☆	☆	7
Paik, ES 2018 (30)	☆	☆	☆	–	☆☆	☆	☆	☆	8
Park, JY 2018 (31)	☆	☆	☆	–	☆	☆	☆	☆	7
Ren, T 2017 (32)	☆	☆	☆	–	☆☆	☆	☆	☆	8
Scarfone, G 2014 (33)	☆	☆	☆	–	–	☆	☆	☆	6
Wang, S 2013 (34)	☆	☆	☆	–	☆☆	☆	☆	☆	8
Ye, S 2014 (35)	☆	☆	☆	–	☆☆	☆	☆	☆	8

there was no statistical significance in the America (P=0.270) and univariate analysis subgroups (P=0.892) (**Table 4**).

Publication Bias and Sensitivity Analysis

Egger's test found no significant publication bias among the studies for PFS (P=0.945) of total OC patients, as well as the studies for OS (P=0.523) and PFS (P=0.728) of OCCC patients. There was significant publication bias among studies that reported the OS of total OC patients (P=0.002). The stability of the pooled results of the meta-analysis was evaluated using the trim-and-fill method, and the results found a significant difference in terms of OS within EAOC and non-EAOC groups, indicating stable results.

In addition, sensitivity analysis revealed that the variation ranges of pooled results for OS [HR (95% CI) = 0.63 (0.50, 0.79) to 0.70 (0.59, 0.83), P < 0.05, **Figure 4**] and PFS [HR (95% CI) = 0.53 (0.39, 0.73) to 0.64 (0.47, 0.86), P < 0.05, **Figure 4**] of total OC patients were not significantly reversed. Similarly, the variation ranges of pooled results for OS [HR (95% CI) = 0.56 (0.42, 0.76) to 0.66 (0.49, 0.91), P < 0.05, **Figure 5**] and PFS [HR (95% CI) = 0.62 (0.47, 0.81) to 0.73 (0.55, 0.97), P < 0.05, **Figure 5**] of OCCC patients were not significantly reversed. These results suggest that the pooled results for all outcomes were stable and not significantly altered by any single study.

DISCUSSION

The prevalence of OC was 2.0-17.0% endometriosis patients, while the prevalence of endometriosis was 3.4-52.6% OC patients (37). A Nationwide Population-Based 14-year Cohort Study suggested that the prevalence of EOC in endometriosis patients ranged from 1.9 per 10000 in recalled endometriosis patients to 18.7 per 10000 in tissue-confirmed endometrioma (38). These data suggested that endometriosis was closely related to OC. EAOC is not a homogeneous group of malignancies and includes several histological subtypes. A previous study suggested that patients with endometriosis had specific histological subtypes of OC, including OCCC, EOC and low-grade serous OC, but not with mucinous or high-grade serous OC or borderline OC (9).

In this meta-analysis, we found that EAOC patients had a better OS in comparison to non-EAOC patients in both total OC and OCCC cohorts. Although there was significant publication bias among studies in terms of OS in the total OC cohort, the results of both the trim-and-fill method and the one-by-one elimination method suggested stability of the results of this meta-analysis. Consistent with our results, a higher OS rate in EAOC patients were also reported in the meta-analysis of Yang et al. (14) and Kim et al. (13). In addition, endometriosis-associated higher OS rates were also observed in the OCCC and mixed-subtype of OC subgroups in the meta-analysis of Yang et al. (14). However, another meta-analysis suggested that endometriosis had no influence on the OS of OCCC patients (12). Additionally, we also found that EAOC patients had better PFS than non-EAOC patients. However, no significant differences in terms of PFS within EAOC and non-EAOC patients were observed in

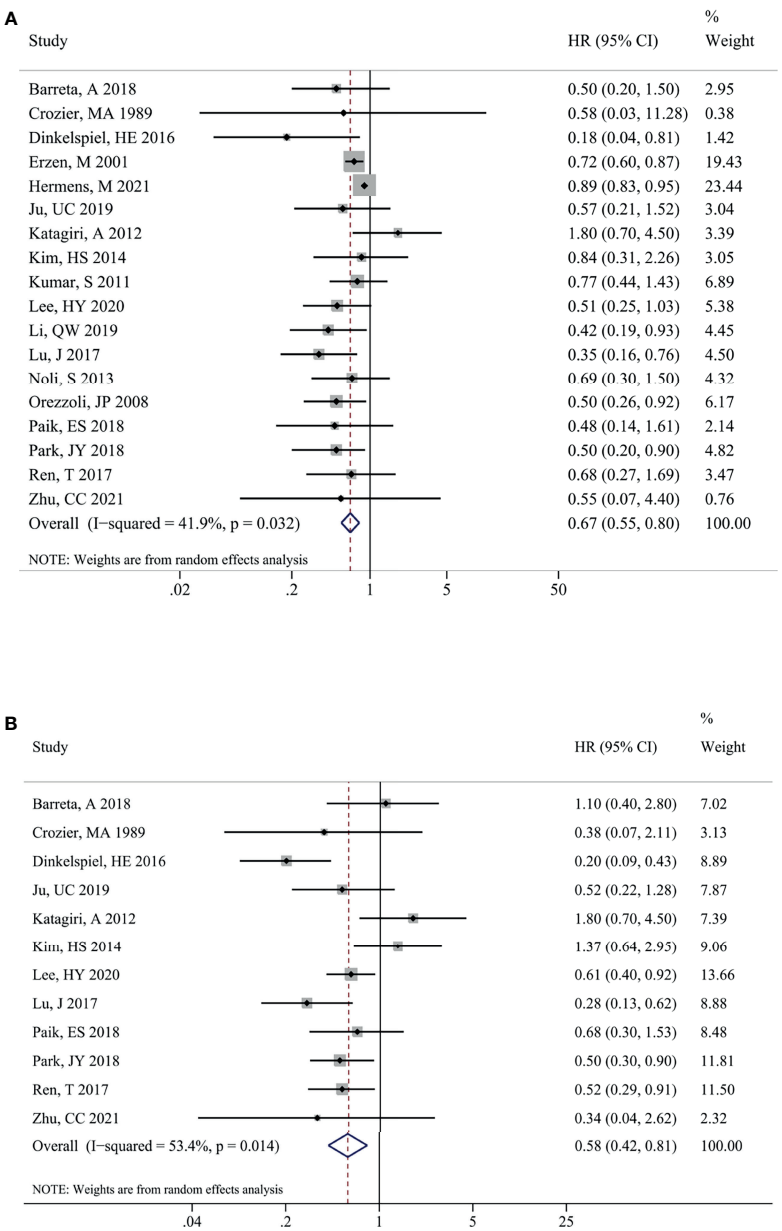


FIGURE 2 | Impact of endometriosis on the prognosis of total OC. Forest plots showing the pooled results for endometriosis on overall survival **(A)** and progression-free survival **(B)** of total OC patients. OC, ovarian cancer.

previous meta-analyses (12–14). In these meta-analyses, less studies (4, 4 and 6 studies) in terms of PFS were included, while 12 studies were included in our study to explore the differences within EAOC and non-EAOC patients. More recent studies ranging from 2016 to 2021 were included. This might explain the reason for the different results in our meta-analysis and previous meta-analyses. For example, a recent study suggested that a significantly longer DFS was found in EAOC patients (51.9 months) than in non-EAOC patients (30.5 months) (39).

There was no significant difference in terms of PFS between EAOC and non-EAOC patients in the American subgroup in our study, suggesting that the study area might have influence on the results. Among the 21 included studies, the study of Hermens et al. (15) involved large amount of Dutch population-based cohort, and they suggested that patients with endometriosis had better OS than the patients without endometriosis. Similar results were observed in Asia and America populations in our study. Despite most of patients from the study of Hermens et al. (15), sensitivity analysis indicated that pooled results for all

TABLE 3 | Outcomes of the subgroup analysis (total ovarian cancer patients).

Model	No. of studies	Heterogeneity test		Effect size	
		I^2 (%)	P_H	OR (95% CI)	*P* value
OS	18	41.9	0.032	0.67 (0.55, 0.80)	<0.001
Area					
Asia	10	0	0.443	0.57 (0.43, 0.76)	<0.001
America	5	0	0.486	0.56 (0.38, 0.82)	0.003
Europe	3	57.7	0.094	0.81 (0.68, 0.97)	0.023
Multivariate analysis					
Yes	13	38.1	0.080	0.62 (0.49, 0.79)	<0.001
No	5	43.3	0.133	0.73 (0.38, 1.39)	0.332
PFS	12	53.4	0.014	0.58 (0.42, 0.81)	0.001
Area					
Asia	9	44.5	0.071	0.63 (0.45, 0.87)	0.005
America	3	72.1	0.028	0.43 (0.13, 1.43)	0.169
Multivariate analysis					
Yes	8	31.9	0.173	0.60 (0.45, 0.80)	0.001
No	4	76.5	0.005	0.48 (0.14, 1.71)	0.260

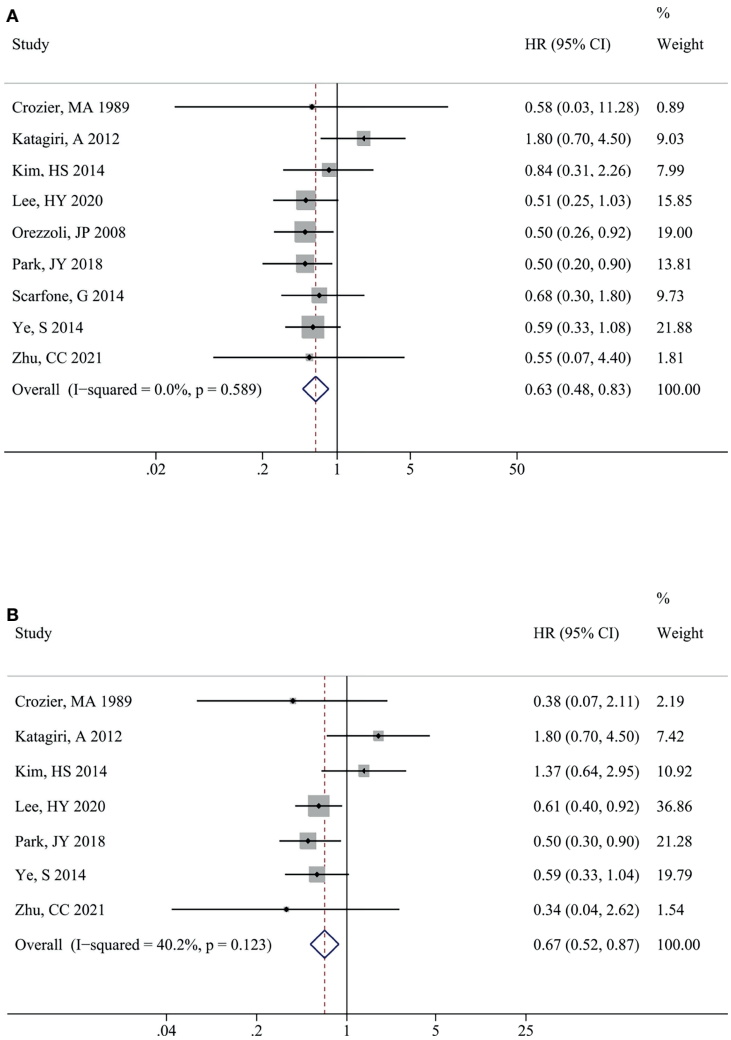


FIGURE 3 | Impact of endometriosis on the prognosis of OCCC. Forest plots showed the pooled results for endometriosis on overall survival **(A)** and progression-free survival **(B)** of OCCC patients. OCCC, ovarian clear cell cancer.

TABLE 4 | Outcomes of the subgroup analysis (OCCC patients).

Model	No. of studies	Heterogeneity test		Effect size	
		I^2 (%)	P_H	OR (95% CI)	*P* value
OS	9	0	0.589	0.63 (0.48, 0.83)	0.001
Area					
Asia	6	15.4	0.315	0.66 (0.47, 0.92)	0.015
America	2	0	0.924	0.50 (0.27, 0.94)	0.032
Europe	1	NA	NA	0.68 (0.28, 1.67)	0.399
Multivariate analysis					
Yes	6	0	0.951	0.57 (0.42, 0.76)	<0.001
No	3	0	0.497	1.38 (0.61, 3.11)	0.444
PFS	7	40.2	0.123	0.67 (0.52, 0.87)	0.002
Area					
Asia	6	47.9	0.087	0.68 (0.53, 0.88)	0.003
America	1	NA	NA	0.38 (0.07, 2.11)	0.270
Multivariate analysis					
Yes	4	36.2	0.195	0.64 (0.49, 0.83)	0.001
No	4	47.4	0.149	1.05 (0.49, 2.25)	0.892

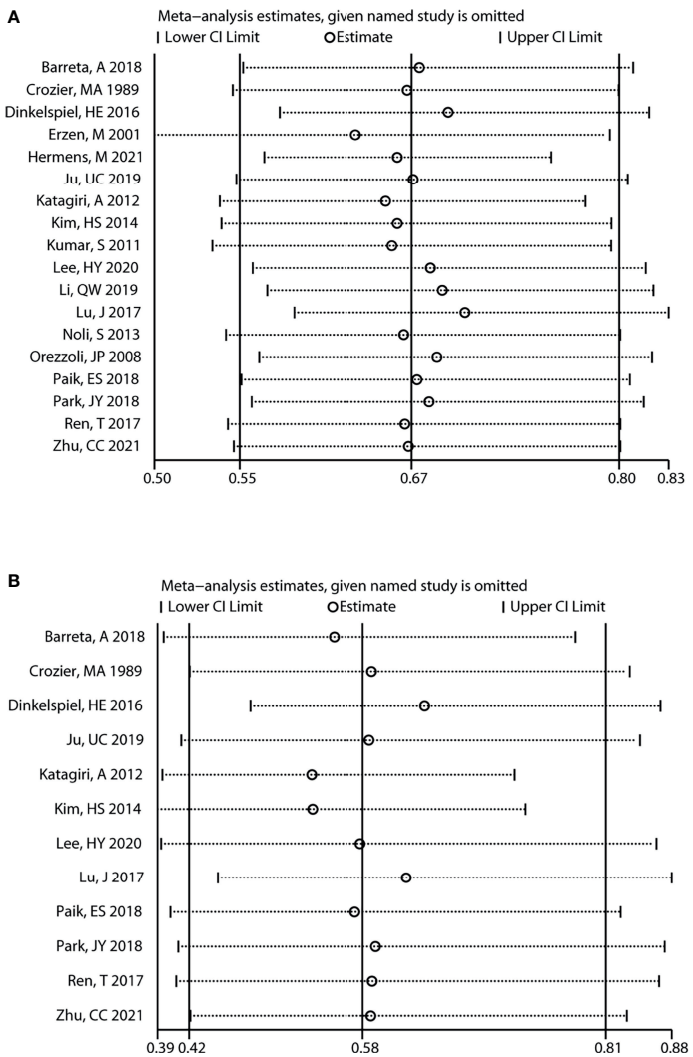


FIGURE 4 | Sensitivity analysis for the results of total OC. Sensitivity analysis to evaluate the stability of the pooled results for the impact of endometriosis on overall survival **(A)** and progression-free survival **(B)** of total OC patients. OC, ovarian cancer.

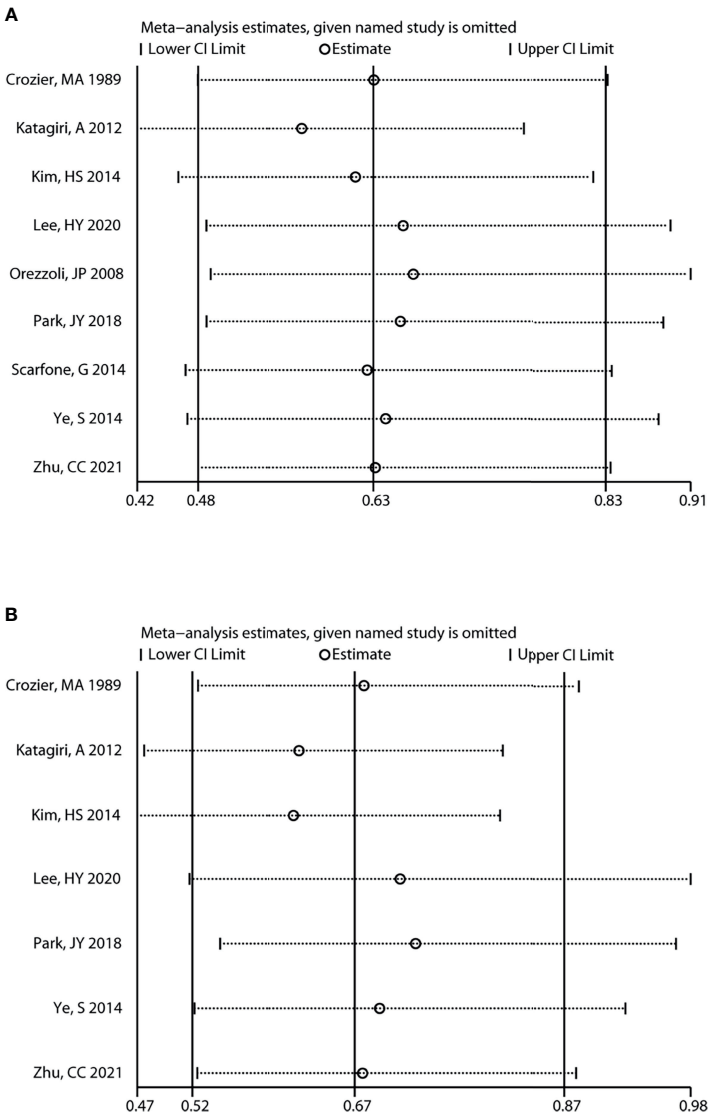


FIGURE 5 | Sensitivity analysis for the results of OCCC. Sensitivity analysis to evaluate the stability of the pooled results for assessing the impact of endometriosis on the overall survival **(A)** and progression-free survival **(B)** of OCCC patients. OCCC, ovarian clear cell cancer.

outcomes were stable and not significantly altered by their study. Additionally, we found that patients with endometriosis had better PFS than the patients without endometriosis in Asia population but not in America population. While PFS was not mentioned in the study of Hermens et al. (15).It was reported that OC patients with endometriosis were usually younger, and were usually diagnosed at an early stage (39). Significant differences between early stages (stages I and II, 73.8% vs. 41.8%, $P < 0.00001$) and low histological grades (grade I, 33.3% vs. 19.3%, $P < 0.001$) were found between EAOC and non-EAOC patients, suggesting a significant association of endometriosis with low tumor grades and early stage tumors (14). These might explain the better prognosis of EAOC patients, in that early-stage cancer might be a driver for better prognosis of EAOC patients rather than an association with endometriosis, as suggested in the study of Li et al. (16). However, Sharfrir et al. found a 29% decreased risk of death among OC patients who pre-diagnostic endometriosis, and association was stable after adjustment for FIGO stage, tumor histology, tumor characteristics and chemotherapy (40). Further studies should be performed to investigate the associations of endometriosis with prognosis of OC in age and stage matched studies. Women with endometriosis are more aware of physical discomfort, so they are more likely to see a doctor earlier, and may require more frequent gynecological ultrasound. This may explain the reason why OC patients with endometriosis were usually diagnosed at

an early stage. On the other hand, the treatment of endometriosis involves continuous oral contraceptive use, which has been reported to reduce the risk of OC (41).

There were still some limitations in the current meta-analysis. (1) The adjuvant therapy regimens were not uniform among the included studies, which might affect the association between endometriosis and OS and PFS in OC patients. (2) The pooled results showed no statistical significance among studies that reported the crude HR, probably because that there was no significant difference in terms of OS or PFS of EAOC vs. non-EAOC in the univariate analysis of these studies and were therefore not included in the multivariate analysis. On the contrary, studies with statistical significance in univariate analysis and further implementation of multivariate analysis to correct for the influence of confounders on survival risk, endometriosis was more likely to be significantly associated with OS and PFS in OC patients. This might allow the pooled results of meta-analysis to overstate the strength of the association between endometriosis and risk of death. (3) All the included studies were retrospective studies; thus, recall and confounding biases were common and inevitable biases among them. Although multivariate analysis was performed in most studies to correct for the influence of confounding factors on the results, the inconsistency of correction factors might also affect the accuracy of the results.

In conclusion, this meta-analysis suggested that endometriosis was significantly associated with the OS and PFS of OC patients. EAOC patients tended to have longer OS and PFS than non-EAOC patients. Conducting higher quality prospective cohort studies with larger sample sizes are recommended to confirm the authenticity of the results.

DATA AVAILABILITY STATEMENT

The raw data supporting the conclusions of this article will be made available by the authors, without undue reservation.

AUTHOR CONTRIBUTIONS

PC acquired funding, collected data, conducted the statistical analysis, created tables and figures, and wrote the manuscript. C-YZ designed the study and helped in writing the manuscript. All authors contributed to the article and approved the submitted version.

FUNDING

The present study was supported by The Natural Science Foundation of Liaoning Province (grant no. 2018010551–301) and the Shengjing Hospital of China Medical University (grant no. MF95). These funding supported in data analysis of the study and in writing the manuscript.

SUPPLEMENTARY MATERIAL

The Supplementary Material for this article can be found online at: https://www.frontiersin.org/articles/10.3389/fonc.2022.732322/full#supplementary-material

REFERENCES

1. Chapron C, Marcellin L, Borghese B, Santulli P. Rethinking Mechanisms, Diagnosis and Management of Endometriosis. *Nat Rev Endocrinol* (2019) 15 (11):666–82. doi: 10.1038/s41574-019-0245-z
2. Kajiyama H, Suzuki S, Yoshihara M, Tamauchi S, Yoshikawa N, Niimi K, et al. Endometriosis and Cancer. *Free Radic Biol Med* (2019) 133:186–92. doi: 10.1016/j.freeradbiomed.2018.12.015
3. Nezhat F, Apostol R, Mahmoud M, el Daouk M. Malignant Transformation of Endometriosis and its Clinical Significance. *Fertil Steril* (2014) 102(2):342–4. doi: 10.1016/j.fertnstert.2014.04.050
4. Herreros-Villanueva M, Chen CC, Tsai EM, Er TK. Endometriosis-Associated Ovarian Cancer: What Have We Learned So Far? *Clin Chim Acta* (2019) 493:63–72. doi: 10.1016/j.cca.2019.02.016
5. Nezhat FR, Pejovic T, Reis FM, Guo SW. The Link Between Endometriosis and Ovarian Cancer: Clinical Implications. *Int J Gynecol Cancer* (2014) 24 (4):623–8. doi: 10.1097/IGC.0000000000000100
6. Nezhat F, Datta MS, Hanson V, Pejovic T, Nezhat C, Nezhat C. The Relationship of Endometriosis and Ovarian Malignancy: A Review. *Fertil Steril* (2008) 90(5):1559–70. doi: 10.1016/j.fertnstert.2008.08.007
7. Králíčková M, Laganà AS, Ghezzi F, Vetvicka V. Endometriosis and Risk of Ovarian Cancer: What do We Know? *Arch Gynecol Obstet* (2020) 301(1):1–10. doi: 10.1007/s00404-019-05358-8
8. Vercellini P, Viganò P, Somigliana E, Fedele L. Endometriosis: Pathogenesis and Treatment. *Nat Rev Endocrinol* (2014) 10(5):261–75. doi: 10.1038/nrendo.2013.255
9. Pearce CL, Templeman C, Rossing MA, Lee A, Near AM, Webb PM, et al. Association Between Endometriosis and Risk of Histological Subtypes of Ovarian Cancer: A Pooled Analysis of Case-Control Studies. *Lancet Oncol* (2012) 13(4):385–94. doi: 10.1016/S1470-2045(11)70404-1
10. Stewart C, Ralyea C, Lockwood S. Ovarian Cancer: An Integrated Review. *Semin Oncol Nurs* (2019) 35(2):151–6. doi: 10.1016/j.soncn.2019.02.001
11. Lheureux S BM, Oza AM. Epithelial Ovarian Cancer: Evolution of Management in the Era of Precision Medicine. *CA Cancer J Clin* (2019) 69 (4):280–304. doi: 10.3322/caac.21559
12. Kim HS, Kim MA, Lee M, Suh DH, Kim K, No JH, et al. Effect of Endometriosis on the Prognosis of Ovarian Clear Cell Carcinoma: A Two-Center Cohort Study and Meta-Analysis. *Ann Surg Oncol* (2015) 22(8):2738–45. doi: 10.1245/s10434-014-4319-9
13. Kim HS, Kim TH, Chung HH, Song YS. Risk and Prognosis of Ovarian Cancer in Women With Endometriosis: A Meta-Analysis. *Br J Cancer* (2014) 110(7):1878–90. doi: 10.1038/bjc.2014.29
14. Yang B, Wang D, Chen H, Yang F. The Association Between Endometriosis and Survival Outcomes of Ovarian Cancer: Evidence-Based on a Meta-Analysis. *Niger J Clin Pract* (2015) 18(5):577–83. doi: 10.4103/1119-3077.158941
15. Hermens M, van Altena AM, van der Aa M, Bulten J, van Vliet H, Siebers AG, et al. Ovarian Cancer Prognosis in Women With Endometriosis: A Retrospective Nationwide Cohort Study of 32,419 Women. *Am J Obstet Gynecol* (2021) 224(3):284.e1–10. doi: 10.1016/j.ajog.2020.08.056
16. Li Q, Sun Y, Zhang X, Wang L, Wu W, Wu M, et al. Endometriosis-Associated Ovarian Cancer is a Single Entity With Distinct Clinicopathological Characteristics. *Cancer Biol Ther* (2019) 20(7):1029–34. doi: 10.1080/15384047.2019.1595278
17. Ju UC, Kang WD, Kim SM. The Effect of Concurrent Endometriosis on the Prognosis of Women With Ovarian Clear Cell or Endometrioid Carcinoma. *Int J Gynaecol Obstet* (2019) 146(2):177–83. doi: 10.1002/ijgo.12861
18. Wells G, Shea B, O'Connell D, Peterson J, Welch V, Losos M. *The Newcastle-Ottawa Scale (NOS) for Assessing the Quality of Nonrandomised Studies in Meta-Analyses* (2014). Available at: http://www.ohri.ca/programs/clinical_epidemiology/oxford.asp.

19. Higgins JP, Thompson SG, Deeks JJ, Altman DG. Measuring Inconsistency in Meta-Analyses. *BMJ* (2003) 327(7414):557–60. doi: 10.1136/bmj.327.7414.557
20. Barreta A, Sarian L, Ferracini AC, Eloy L, Brito ABC, de Angelo Andrade L, et al. Endometriosis-Associated Ovarian Cancer: Population Characteristics and Prognosis. *Int J Gynecol Cancer* (2018) 28(7):1251–7. doi: 10.1097/IGC.0000000000001317
21. Crozier MA, Copeland LJ, Silva EG, Gershenson DM, Stringer CA. Clear Cell Carcinoma of the Ovary: A Study of 59 Cases. *Gynecol Oncol* (1989) 35 (2):199–203. doi: 10.1016/0090-8258(89)90043-7
22. Dinkelspiel HE, Matrai C, Pauk S, Pierre-Louis A, Chiu YL, Gupta D, et al. Does the Presence of Endometriosis Affect Prognosis of Ovarian Cancer? *Cancer Invest* (2016) 34(3):148–54. doi: 10.3109/07357907.2016.1139716
23. Erzen M, Rakar S, Klancnik B, Syrjänen K. Endometriosis-Associated Ovarian Carcinoma (EAOC): An Entity Distinct From Other Ovarian Carcinomas as Suggested by a Nested Case-Control Study. *Gynecol Oncol* (2001) 83(1):100–8. doi: 10.1006/gyno.2001.6382
24. Katagiri A, Nakayama K, Rahman MT, Rahman M, Katagiri H, Nakayama N, et al. Loss of ARID1A Expression is Related to Shorter Progression-Free Survival and Chemoresistance in Ovarian Clear Cell Carcinoma. *Mod Pathol* (2012) 25(2):282–8. doi: 10.1038/modpathol.2011.161
25. Kumar S, Munkarah A, Arabi H, Bandyopadhyay S, Semaan A, Hayek K, et al. Prognostic Analysis of Ovarian Cancer Associated With Endometriosis. *Am J Obstet Gynecol* (2011) 204(1):63.e1–7. doi: 10.1016/j.ajog.2010.08.017
26. Lee HY, Hong JH, Byun JH, Kim HJ, Baek SK, Kim JY, et al. Clinical Characteristics of Clear Cell Ovarian Cancer: A Retrospective Multicenter Experience of 308 Patients in South Korea. *Cancer Res Treat* (2020) 52 (1):277–83. doi: 10.4143/crt.2019.292
27. Lu J, Tao X, Zhou J, Lu Y, Wang Z, Liu H, et al. Improved Clinical Outcomes of Patients With Ovarian Carcinoma Arising in Endometriosis. *Oncotarget* (2017) 8(4):5843–52. doi: 10.18632/oncotarget.13967
28. Noli S, Cipriani S, Scarfone G, Villa A, Grossi E, Monti E, et al. Long Term Survival of Ovarian Endometriosis Associated Clear Cell and Endometrioid Ovarian Cancers. *Int J Gynecol Cancer* (2013) 23(2):244–8. doi: 10.1097/IGC.0b013e31827aa0bb
29. Orezzoli JP, Russell AH, Oliva E, Del Carmen MG, Eichhorn J, Fuller AF, et al. Prognostic Implication of Endometriosis in Clear Cell Carcinoma of the Ovary. *Gynecol Oncol* (2008) 110(3):336–44. doi: 10.1016/j.ygyno.2008.05.025
30. Paik ES, Kim TJ, Choi CH, Kim BG, Bae DS, Lee JW, et al. Clinical Outcomes of Patients With Clear Cell and Endometrioid Ovarian Cancer Arising From Endometriosis. *J Gynecol Oncol* (2018) 29(2):e18. doi: 10.3802/jgo.2018.29.e18
31. Park JY, Kim DY, Suh DS, Kim JH, Kim YM, Kim YT, et al. Significance of Ovarian Endometriosis on the Prognosis of Ovarian Clear Cell Carcinoma. *Int J Gynecol Cancer* (2018) 28(1):11–8. doi: 10.1097/IGC.0000000000001136
32. Ren T, Wang S, Sun J, Qu JM, Xiang Y, Shen K, et al. Endometriosis is the Independent Prognostic Factor for Survival in Chinese Patients With Epithelial Ovarian Carcinoma. *J Ovarian Res* (2017) 10(1):67. doi: 10.1186/s13048-017-0363-y
33. Scarfone G, Bergamini A, Noli S, Villa A, Cipriani S, Taccagni G, et al. Characteristics of Clear Cell Ovarian Cancer Arising From Endometriosis: A Two Center Cohort Study. *Gynecol Oncol* (2014) 133(3):480–4. doi: 10.1016/j.ygyno.2014.03.017
34. Wang S, Qiu L, Lang JH, Shen K, Huang HF, Pan LY, et al. Prognostic Analysis of Endometrioid Epithelial Ovarian Cancer With or Without Endometriosis: A 12-Year Cohort Study of Chinese Patients. *Am J Obstet Gynecol* (2013) 209(3):241.e1–9. doi: 10.1016/j.ajog.2013.05.032
35. Ye S, Yang J, You Y, Cao D, Bai H, Lang J, et al. Comparative Study of Ovarian Clear Cell Carcinoma With and Without Endometriosis in People's Republic of China. *Fertil Steril* (2014) 102(6):1656–62. doi: 10.1016/j.fertnstert.2014.08.008
36. Zhu C, Zhu J, Qian L, Liu H, Shen Z, Wu D, et al. Clinical Characteristics and Prognosis of Ovarian Clear Cell Carcinoma: A 10-Year Retrospective Study. *BMC Cancer* (2021) 21(1):322. doi: 10.1186/s12885-021-08061-7
37. Heidemann LN, Hartwell D, Heidemann CH, Jochumsen KM. The Relation Between Endometriosis and Ovarian Cancer - a Review. *Acta Obstet Gynecol Scand* (2014) 93(1):20–31. doi: 10.1111/aogs.12255
38. Lee WL, Chang WH, Wang KC, Guo CY, Chou YJ, Huang N, et al. The Risk of Epithelial Ovarian Cancer of Women With Endometriosis May be Varied Greatly If Diagnostic Criteria Are Different: A Nationwide Population-Based Cohort Study. *Med (Baltimore)* (2015) 94(39):e1633. doi: 10.1097/MD.0000000000001633
39. Bassiouny D, El-Baz MA, Gamil TM, Shams N, Ismiil N, Dubé V, et al. Endometriosis-Associated Ovarian Cancer is a Subset With a More Favorable Outcome and Distinct Clinical-Pathologic Characteristics. *Int J Gynecol Pathol* (2019) 38(5):435–42. doi: 10.1097/PGP.0000000000000533
40. Shafrir AL, Babic A, Tamimi RM, Rosner BA, Tworoger SS, Terry KL, et al. Reproductive and Hormonal Factors in Relation to Survival and Platinum Resistance Among Ovarian Cancer Cases. *Br J Cancer* (2016) 115(11):1391–9. doi: 10.1038/bjc.2016.316
41. Schrijver LH, Antoniou AC, Olsson H, Mooij TM, Roos-Blom MJ, Azarang L, et al. Oral Contraceptive Use and Ovarian Cancer Risk for BRCA1/2 Mutation Carriers: An International Cohort Study. *Am J Obstet Gynecol* (2021) 225 (1):51.e1–17. doi: 10.1016/j.ajog.2021.01.014

Conflict of Interest: The authors declare that the research was conducted in the absence of any commercial or financial relationships that could be construed as a potential conflict of interest.

Publisher's Note: All claims expressed in this article are solely those of the authors and do not necessarily represent those of their affiliated organizations, or those of the publisher, the editors and the reviewers. Any product that may be evaluated in this article, or claim that may be made by its manufacturer, is not guaranteed or endorsed by the publisher.

Copyright © 2022 Chen and Zhang. This is an open-access article distributed under the terms of the Creative Commons Attribution License (CC BY). The use, distribution or reproduction in other forums is permitted, provided the original author(s) and the copyright owner(s) are credited and that the original publication in this journal is cited, in accordance with accepted academic practice. No use, distribution or reproduction is permitted which does not comply with these terms.

frontiers | Frontiers in Oncology

ORIGINAL RESEARCH
published: 08 April 2022
doi: 10.3389/fonc.2022.818613

VEGF-D Serum Level as a Potential Predictor of Lymph Node Metastasis and Prognosis in Vulvar Squamous Cell Carcinoma Patients

Antonella Ravaggi[1,2,3†], Angela Gambino[1,2†], Federico Ferrari[2], Alessandro Olivari[1], Laura Zanotti[1,3], Chiara Romani[3], Laura Ardighieri[4], Paolo Antonelli[5], Giorgia Garganese[6,7], Daniela Gallo[7,8], Giovanni Scambia[7,8], Eliana Bignotti[2,3], Enrico Sartori[1,2], Stefano Calza[5,9‡] and Franco Odicino[1,2‡]*

[1] Department of Clinical and Experimental Sciences, Division of Obstetrics and Gynecology, University of Brescia, Brescia, Italy, [2] Division of Obstetrics and Gynecology, Azienda Socio Sanitaria Territoriale Spedali Civili di Brescia, Brescia, Italy, [3] 'Angelo Nocivelli' Institute of Molecular Medicine, University of Brescia—Azienda Socio Sanitaria Territoriale Spedali Civili, Brescia, Italy, [4] Department of Pathology, Azienda Socio Sanitaria Territoriale Spedali Civili di Brescia, Brescia, Italy, [5] Unit of Biostatistics and Bioinformatics, Department of Molecular and Translational Medicine, University of Brescia, Brescia, Italy, [6] Gynecology and Breast Care Center, Mater Olbia Hospital, Olbia, Italy, [7] Dipartimento Universitario Scienze della Vita e Sanità Pubblica, Sezione di Ginecologia ed Ostetricia, Università Cattolica del Sacro Cuore, Rome, Italy, [8] Dipartimento Scienze della Salute della Donna, del Bambino e di Sanità Pubblica, Fondazione Policlinico Universitario A. Gemelli, Istituto di Ricovero e Cura a Carattere Scientifico, Rome, Italy, [9] BDbiomed, Big & Open Data Innovation Laboratory, University of Brescia, Brescia, Italy

Background: Radical surgical resection of the primary tumor with mono/bilateral inguinofemoral lymph node dissection is the standard treatment for invasive vulvar squamous cell carcinoma (VSCC) and is frequently related to severe morbidity. Tailoring surgical treatment is of paramount importance, and a comprehensive preoperative evaluation is mandatory. Vascular endothelial growth factor D (VEGF-D) is considered a regulator of lymphangiogenesis involved in tumor spread *via* lymphatic vessels. The aim of this study was to evaluate the potential of VEGF-D in the prediction of inguinofemoral lymph node metastasis.

Methods: We analyzed the preoperative levels of serum VEGF-D (sVEGF-D) from two independent cohorts of patients with VSCC by enzyme-linked immunosorbent assay and its protein expression on tumor tissue by immunohistochemistry. Logistic regression was performed to identify the independent risk factors for lymph node metastasis, and Cox proportional hazard model was used for survival analysis.

Results: High levels of sVEGF-D, but not tissue VEGF-D, significantly correlated with positive groin nodes and a more advanced International Federation of Gynecologists and Obstetricians (FIGO) stage. In multivariable analysis, a high sVEGF-D level was an independent predictor of lymph node metastasis and worse prognosis. A prediction model based on sVEGF-D, tumor grade assessed on biopsy, tumor diameter, and lymph

OPEN ACCESS

Edited by:
Chiara Mazziotta,
University of Ferrara, Italy

Reviewed by:
Matteo Morotti,
Centre Hospitalier Universitaire Vaudois (CHUV), Switzerland
Luigi Turco,
Mater Olbia Hospital, Italy
Jacobus Van Der Velden,
University of Amsterdam, Netherlands

***Correspondence:**
Antonella Ravaggi
antonella.ravaggi@unibs.it
orcid.org/0000-0003-4661-9979

†These authors share first authorship

‡These authors share last authorship

Specialty section:
This article was submitted to Gynecological Oncology, a section of the journal Frontiers in Oncology

Received: 19 November 2021
Accepted: 14 March 2022
Published: 08 April 2022

Citation:
Ravaggi A, Gambino A, Ferrari F, Olivari A, Zanotti L, Romani C, Ardighieri L, Antonelli P, Garganese G, Gallo D, Scambia G, Bignotti E, Sartori E, Calza S and Odicino F (2022) VEGF-D Serum Level as a Potential Predictor of Lymph Node Metastasis and Prognosis in Vulvar Squamous Cell Carcinoma Patients. Front. Oncol. 12:818613. doi: 10.3389/fonc.2022.818613

node clinical evaluation was able to predict lymph node metastasis, reaching C-index values of 0.79 and 0.73 in the training and validation cohorts, respectively.

Conclusions: The preoperative sVEGF-D level might be a reliable biomarker for the prediction of lymph node metastasis and prognosis in patients with VSCC, supporting better clinical/surgical decision. Multicenter prospective studies are required to confirm our findings.

Keywords: vulvar squamous cell carcinoma, VEGF-D, lymph node metastasis, prognosis, serum

INTRODUCTION

Vulvar carcinoma is a rare gynecologic cancer with an annual incidence of 2.4 every 100,000 women based on cases in 2014–2018 (1). In 2021, approximately 6,120 new cases of vulvar cancer have been predicted in the United States, and about 1,550 women are expected to die of this cause (2). The incidence is higher among women aged 70 years or older; however, recently, an increasing frequency of vulvar cancer in young women has been observed (3, 4).

For patients with invasive vulvar squamous cell carcinoma (VSCC), the most common type of vulvar cancer, the standard treatment in clinical early-stage disease is radical resection of the tumor with bilateral inguinofemoral lymphadenectomy or sentinel lymph node (SLN) biopsy, when appropriate. In the absence of clinical suspicious lymph nodes (cN0), the SLN procedure should be considered the preferred procedure instead of radical dissection only within narrow selection criteria, including: unifocal lesions of <4 cm, not completely excised at diagnostic biopsy, and never undergone previous vulvar/groin surgery or neoadjuvant treatments (5–7). Furthermore, the SLN procedure should be performed only in centers with high-level experience in order to minimize false-negative rates. Therefore, a large cohort of cN0 patients is currently not submitted to the SLN procedure and instead referred to radical lymphadenectomy. This procedure showed no evidence of lymph node metastasis at final histology in 70% of cases, with increased postoperative physical and psychological morbidity rates (8). For this reason, many efforts are being made to optimize clinical management in order to avoid overtreatment of patients without lymph node metastasis and to ensure a high diagnostic sensitivity in identifying patients with positive groin nodes (9).

In this context, the identification of circulating or tissue biomarkers involved in the aggressiveness of tumor cells and in the metastasis process could be an important tool to guide and/or refine the surgical decision.

One of the most studied molecular systems in the regulation of tumor lymphangiogenesis is based on the interaction between vascular endothelial growth factor D (VEGF-D) and the corresponding VEGF receptor 3 (VEGFR-3), commonly expressed on the surface of lymphatic endothelial cells (10, 11). VEGF-D is a member of the VEGF family, which also includes VEGF-A, VEGF-B, VEGF-C, and placental growth factor (PlGF), and it is an important key regulator of both physiological and pathological angiogenesis and lymphangiogenesis (11). VEGF-D promotes lymphatic metastasis by inducing tumor-associated lymphangiogenesis in a mouse tumor model (12), and its over expression was associated with lymphatic tumor spread and poor patient prognosis in several human cancers (13–16). To the best of our knowledge, only one study evaluated the expressions of VEGF-D and VEGFR-3 using immunohistochemistry (IHC) in VSCC (17). Further investigations are required to clarify the clinical significance of these markers in patients with VSCC.

In the present study, we investigated the role of VEGF-D in predicting inguinofemoral lymph node metastasis. For the first time, the preoperative levels of serum VEGF-D (sVEGF-D) were quantified and correlated with the clinicopathological characteristics and prognosis of patients affected by VSCC.

METHODS

Study Design

This retrospective study aimed to investigate the significance of VEGF-D in the clinical setting of VSCC patients and, in particular, in the preoperative prediction of lymph node metastasis. To this intent, two groups of patients with VSCC were recruited. Cohort A was used to analyze the correlations between sVEGF-D levels or the tissue expressions of VEGF-D and VEGFR-3 with the clinic opathological features and prognosis. Moreover, more importantly, cohort A was used as a training set to design a predictive algorithm for lymph node metastases. Three different models for the preoperative prediction of lymph node involvement were built using logistic regression: *base model*, including only clinical/radiological lymph node status; *clinical model*, including the clinicopathological characteristics available before surgery (e.g., tumor diameter, tumor grade from biopsy, and clinical lymph node status); and *extended model*, built with the addition of the sVEGF-D level to the clinical model.

Cohort B was kept external and independent and was used as a validation set to evaluate the performance of the extended model in the prediction of lymph node metastasis.

Patients and Samples

A retrospective study was performed on a total of 135 patients with VSCC divided into two independent cohorts, hereafter called A and B, comprising 80 and 55 women, respectively.

The inclusion criteria were as follows: histologically confirmed VSCC, tumor depth of invasion of at least 1 mm,

surgical treatment performed in the enrolling centers, availability of frozen serum samples collected prior to surgery, and/or availability of formalin-fixed paraffin-embedded (FFPE) tumor tissue samples surgically obtained from the primary tumor site. For cohort B, only serum samples were required. Patients with synchronous cancer or with a history of malignancy in the 5 years prior to the VSCC diagnosis were excluded from the study of circulating sVEGF-D.

The eligible patients of cohort A were consecutively enrolled between January 2003 and August 2019 at the Division of Obstetrics and Gynecology of "ASST-Spedali Civili di Brescia" (Brescia, Italy). The eligible patients of cohort B were consecutively enrolled between May 2012 and October 2018 at the Division of Gynecologic Oncology of "Fondazione Policlinico Universitario A. Gemelli IRCCS" (Rome, Italy).

All patients were preoperatively assessed by expert gynecologic oncologists and dedicated specialists for primary tumor histology, obtained by incisional biopsy, and lymph node status evaluation, obtained by clinical exam and dedicated imaging (ultrasound and/or PET). A positive clinical lymph node status was defined in the presence of at least one suspicious lymph node at imaging.

All patients were surgically treated by complete surgical tumor resection (partial or radical vulvectomy) and inguinal lymph node dissection, performed mono- or bilaterally, as appropriate, on the base of the distance of the primary tumor from the midline, according to international guidelines (5, 6) at the time of the study.

All 80 patients from cohort A underwent radical lymphadenectomy. Among the 55 patients in cohort B, 12 underwent exclusive SLN, 9 underwent combined SLN and inguinofemoral lymphadenectomy, and 34 underwent inguinofemoral lymphadenectomy.

The stage of disease was assessed in accordance with the International Federation of Gynecologists and Obstetricians (FIGO) revised staging system of 2009, in use during the enrollment period.

Adjuvant treatment was administered to 24 out of 80 patients in cohort A (radiotherapy, chemotherapy, or chemoradiotherapy to 21, 2, and 1 patient, respectively). Fifty-one patients did not receive adjuvant therapies, and for 5 patients, this information was missing. All patients in cohort A were followed from the time of their confirmed diagnosis until death or March 2021. Follow-up data were not required for the patients in cohort B. Clinical and histopathological data were acquired from the original reports.

The characteristics of the patients in the two cohorts are summarized in **Table 1**.

The study was performed following the set of principles in the Declaration of Helsinki and was approved by the Research Review Board–Ethics Committee of the ASST Spedali Civili, Brescia, Italy (study reference no. NP3512) and of the Fondazione Policlinico Universitario "A. Gemelli" IRCCS—Università Cattolica del Sacro Cuore, Rome, Italy (study reference no. ID2844). Written informed consent for the collection and use of personal records and biological material for health research was obtained from all patients enrolled. All data were collected in an electronic database and managed in accordance with privacy regulations.

VEGF-D Serum Concentration Measurement

In both cohorts, fasting blood samples were drawn from patients strictly before surgery. Serum was separated by centrifugation at 1,500 × *g* for 10 min within 1 h, frozen in liquid nitrogen, and then stored at −80°C until analysis. Sample analysis was centralized in Brescia Hospital laboratory and carried out without any prior knowledge of the patients' clinical status.

The sVEGF-D levels were analyzed with enzyme-linked immunosorbent assay (ELISA) using the immunoassay Human VEGF-D Quantikine ELISA (R&D Systems, Minneapolis, MN, USA) following the manufacturer's instructions. Briefly, 50 ml of standards, controls, and serum samples were analyzed in duplicate, and plates were read at 450 nm, setting a wavelength correction to 570 nm, on an automatic plate reader (Spectramax 340 PC; Molecular Devices Corporation, Sunnyvale, CA, USA). As declared by the manufacturer, the dynamic range of VEGF-D detection goes from 125 to 4,000 pg/ml, with intra-assay and inter-assay imprecision (coefficient of variation, CV) values ranging from 2.4% to 6.2% and from 7.2% to 8.0%, respectively.

Immunohistochemical Staining of VEGF-D and VEGFR-3 on Formalin-Fixed Tumor Tissues

To evaluate the protein expression levels of VEGF-D and VEGFR-3, IHC staining was performed on VSCC tissue samples from cohort A at the Department of Pathology, "ASST-Spedali Civili of Brescia." Whole tissue sections (2 μm) were obtained from FFPE blocks, stained with hematoxylin and eosin, and analyzed by a staff surgical pathologist. IHC analyses were performed on 4-μm tissue sections using the Leica Bond III fully automated IHC Stainer (Leica Biosystems, New Castle upon Tyne, UK). No antigen retrieval was carried out. The sections were incubated with the primary antibodies anti-VEGF-D diluted 1:200 (clone 78923; R&D Systems) for 15 min and anti-VEGFR-3 diluted 1:50 (clone NCL-L-VEGFR-3; Leica Biosystems) for 30 min. The reaction was revealed using the automated Leica BOND system by the Bond Polymer Refine Detection Kit (DS9800; Leica Biosystems), which consisted of sequential incubation with post-primary and horseradish peroxidase (HRP)–polymer for 8 min each, followed by diaminobenzidine as chromogen and by hematoxylin as nuclear counterstain.

Cellular staining was graded for intensity (0, negative staining; 1, weak staining; 2, moderate staining; and 3, strong staining) and percentage of positive cells (0, 0%; 1, 1%–20%; 2, 11%–50%; and 3, 51%–100%). A single IHC scale with scores 0–9 was calculated by multiplying the intensity and the percentage staining scores. Then, four total scores (0, 1, 2, 3) were obtained, grouping score 0 in total score 0, scores 1–3 in total score 1, scores 4 and 6 in total score 2, and score 9 in total score 3.

TABLE 1 | Clinical characteristics of vulvar squamous cell carcinoma (VSCC) patients.

Clinical annotations	Cohort A	Cohort B	Total
No. of patients	80	55	135
Age (years)			
Mean (SD)	70.2 (11.7)	71.4 (11.4)	70.7 (11.5)
Median (Q1–Q3)	70.5 (63.0–79.0)	74.0 (64.0–80.0)	73.0 (63.0–80.0)
Clinical lymph node status			
Negative	43 (60.6%)	28 (50.9%)	71 (56.3%)
Positive	28 (39.4%)	27 (49.1%)	55 (43.7%)
Missing	9	0	9
Tumor grade on biopsy			
G1	30 (38.5%)	12 (30.8%)	42 (35.9%)
G2–G3	48 (61.5%)	27 (69.2%)	75 (64.1%)
Missing	2	16	18
Diameter (mm)			
Mean (SD)	34.5 (17.5)	37.8 (20.2)	35.8 (18.6)
Median (Q1–Q3)	30.0 (22.0–45.8)	32.5 (19.5–57.0)	30 (20.0–50.0)
Missing	0	1	
FIGO stage			
I	43 (53.8%)	28 (50.9%)	71 (52.6%)
II	3 (3.7%)	2 (3.6%)	5 (3.7%)
III	33 (41.3%)	23 (41.8%)	56 (41.5%)
IV	1 (1.2%)	2 (3.7%)	3 (2.2%)
Tumor grade			
G1	18 (22.5%)	4 (7.3%)	22 (16.3%)
G2	50 (62.5%)	40 (72.7%)	90 (66.7%)
G3	12 (15.0%)	11 (20.0%)	23 (17.0%)
Depth of invasion (mm)			
Mean (SD)	9.9 (8.5)	7.8 (5.1)	9.0 (7.4)
Median (Q1–Q3)	8.0 (5.0–13.0)	6.0 (4.0–10.5)	7.0 (4.0–12.0)
Missing	1	2	3
Vascular invasion			
Absent	57 (71.3%)	29 (61.7%)	86 (67.7%)
Present	23 (28.7%)	18 (38.3%)	41 (32.3%)
Missing	0	8	8
Perineural invasion			
Absent	49 (62.0%)	42 (87.5%)	91 (71.7%)
Present	30 (38.0%)	6 (12.5%)	36 (28.3%)
Missing	1	7	8
Lymph node metastasis			
Absent	46 (57.5%)	30 (54.5%)	76 (56.3%)
Present	34 (42.5%)	25 (45.5%)	59 (43.7%)
Surgical margins			
Negative	65 (82.3%)	52 (94.5%)	117 (87.3%)
Positive	14 (17.7%)	3 (5.5%)	17 (12.7%)
Missing	1	0	1

Q1, first quartile; Q3, third quartile; SD, standard deviation.

Statistical Methods

The association between the levels of sVEGF-D and the clinicopathological characteristics in cohort A was evaluated using univariable linear models after transforming the sVEGF-D levels on a $\log_2$ scale.

The role of sVEGF-D as a predictor of lymph node involvement was evaluated using a logistic regression model including the clinicopathological characteristics available before radical vulvectomy: estimated tumor diameter, tumor grade assessed on biopsy, and lymph node status from clinical/radiological evaluation. The results were reported as odds ratios (ORs) and 95% confidence intervals (95%CIs).

The discrimination performance of the models was quantified with the concordance index (C-index), which is equivalent to the area under the receiver operating characteristic (ROC) curve (AUC). The 95%CI for the C-index was obtained after 200 bootstrap resampling (18). Model calibration was evaluated graphically and reporting scaled Brier scores (the bigger the better) (19) and the Hosmer–Lemeshow test (20). Unreliability test (testing the H_0 for a calibration line with slope = 1 and intercept = 0) was performed using a chi-squared test with 2 *df* (21).

Penalized maximum likelihood was used to obtain more stable coefficients through shrinkage in order to achieve better performance for prediction (22, 23). Selection of the optimal penalization parameter was performed based on Hurvich and Tsai's corrected Akaike's information criterion (AIC) (24).

Progression-free survival (PFS) was defined as the time from surgery to progression or recurrence, while disease-specific survival (DSS) was defined as the time from surgery to cancer-

related death. Univariable and multivariable Cox proportional hazard models were used for modeling PFS and DSS.

For display purposes, the sVEGF-D values were dichotomized using maximally selected rank statistics (25), both for DSS and PFS. Briefly, this procedure searches for the optimal threshold that maximizes the log-rank statistic, accounting for test multiplicity. Binary-coded sVEGF-D values were used in the multivariable models accounting for stage, grade, and vascular and perineural invasion, and the corresponding survival curves were displayed using the Kaplan–Meier method.

All tests were two-sided and assumed a 5% significance level. All statistical analyses were performed with the program R Core Team (version 4.1.1).

RESULTS

VEGF-D Serum Level Correlates With Lymph Node Metastasis and FIGO Stage

Preoperative serum samples from 62 out of 80 patients in cohort A were suitable to analyze the sVEGF-D levels using ELISA. The median and the mean values of sVEGF-D were 456.0 pg/ml (range = 370.9–573.5) and 483.4 pg/ml (SD = 178.5), respectively. As shown in **Table 2**, high levels of sVEGF-D significantly correlated with lymph node metastasis (p = 0.023) and higher FIGO stage (III–IV *vs.* I–II, p = 0.023). No other significant correlations with the clinicopathological factors were evident.

In 49 out of 80 patients, FFPE tumor tissue samples surgically obtained from the primary tumor site were available to evaluate the tissue protein expression of VEGF-D and its receptor VEGFR-3. A pattern of positive cytoplasmic expression for VEGF-D and VEGFR-3 was found in 92% and 94% of the VSCC patients, respectively (**Supplementary Figure S1**). No correlation was found between the expression of VEGF-D or VEGFR-3 and the clinicopathological characteristics of the tumor (**Supplementary Table S1**); therefore, the next steps of the study were conducted considering exclusively serum VEGF-D.

For 31 out of 80 patients, matched tissue and serum samples were available. The serum VEGF-D level was only partially correlated with the tissue VEGF-D protein score, with a borderline statistical significance (r_s = 0.317, p = 0.082).

High Level of sVEGF-D Correlates With Poor Prognosis

In cohort A, 79 out of 80 patients were considered for survival analysis (median follow-up = 101.1 months, IQR = 58.0–150.5 months). Forty-one (51.9%) had disease recurrence or progression. At the time of the last follow-up, 36 patients

TABLE 2 | Vascular endothelial growth factor D (VEGF-D) serum levels and correlation with the clinicopathological characteristics of vulvar squamous cell carcinoma (VSCC) patients from cohort A (N = 62).

Characteristics	Levels (*N*)	sVEGF-D (pg/ml)			
		Mean (SD)	Median	Q1–Q3	*p*-value[a]
Age (years)	<72 (31)	485.3 (116.4)	474.8	406.8–558.9	0.933
	≥72 (31)	481.4 (226.3)	408.9	344.8–604.8	
FIGO stage	I–II (36)	440.0 (135.1)	420.2	360.3–542.3	**0.023**
	III–IV (26)	543.4 (213.9)	476.9	410.1–666.7	
Tumor grade	G1 (16)	490.8 (259.9)	436.8	310.0–601.1	0.435
	G2 (38)	465.2 (146.8)	428.8	374.7–534.5	
	G3 (8)	554.7 (106.5)	527.2	477.5–598.6	
Tumor diameter (mm)	≤20 (16)	495.8 (141.2)	471.8	414.0–586.8	0.428
	21–40 (26)	449.6 (133.9)	428.8	355.3–564.6	
	>40 (20)	517.3 (245.1)	465.1	382.5–571.0	
Depth of invasion (mm)	≤8 (29)	489.9 (149.3)	482.8	383.2–615.9	0.771
	>8 (32)	476.3 (206.0)	429	368.5–493.2	
	NA (1)				
Vascular invasion	No (43)	491.7 (193.8)	456.7	372.2–574.5	0.587
	Yes (19)	464.6 (140.9)	455.4	378.6–528.4	
Perineural invasion	No (40)	492.0 (203.4)	464.8	360.3–591.1	0.572
	Yes (21)	464.3 (125.7)	438.4	386.3–518.6	
	NA (1)				
Lymph node metastasis	No (36)	440.0 (135.1)	420.2	360.3–542.3	**0.023**
	Yes (26)	543.4 (213.9)	476.9	410.1–666.7	
Recurrence	No (29)	444.6 (167.6)	438.4	320.8–540.6	0.115
	Yes (32)	517.4 (186.3)	464.1	392.3–618.6	
	NA (1)				
Adjuvant treatment	No (42)	461.3 (158.3)	429.8	363.7–545.8	0.465
	Yes (18)	492.8 (136.2)	465.1	405.3–574.2	
	NA (2)				

Significant p-values are indicated in bold.

FIGO, International Federation of Gynecologists and Obstetricians; Q1, first quartile; Q3, third quartile; NA, not available.

[a]*Linear model ANOVA on log2-transformed sVEGF-D values.*

(45.6%) were alive, 30 (38.0%) were dead of disease, and 13 (16.4%) died of other causes.

In the univariable analysis for DSS, higher preoperative sVEGF-D levels (log scale) were significantly associated with worse prognosis [hazard ratio (HR) = 2.70, $p = 0.02$] and with other traditional prognostic factors, such as advanced FIGO stage (HR = 9.43, $p < 0.01$), perineural invasion (HR = 2.17, $p = 0.03$), lymphovascular invasion (HR = 2.55, $p = 0.01$), and lymph node metastasis (HR = 9.43, $p < 0.01$) (**Figure 1A** and **Supplementary Table S2**).

In addition, in the univariable analysis for PFS, higher preoperative sVEGF-D levels (HR = 2.15, $p = 0.036$), lymph node metastasis (HR = 3.20, $p < 0.01$), lymphovascular invasion (HR = 1.95, $p = 0.04$), and advanced FIGO stage (HR = 3.20, $p < 0.01$) were significantly associated with a high risk of recurrence (**Figure 1B** and **Supplementary Table S2**).

In the multivariable analysis, the preoperative sVEGF-D levels (entered as a restricted cubic spline with 3 knots, i.e., a quadratic trend) were demonstrated to be independent prognostic factors for poor DSS (likelihood ratio test: $\chi^2_2 = 7.30$, $p = 0.026$) (**Table 3** and **Figure 1A**). Similarly, in the multivariable analysis for PFS, sVEGF-D (linear trend) was marginally significant ($p = 0.047$) (**Table 3** and **Figure 1B**).

Association Between Lymph Node Metastasis and Clinicopathological Characteristics

In order to assess the factors associated with lymph node metastasis and to build a predictive algorithm, pathological lymph node status was compared with the clinicopathological variables available before and after surgery. As reported in **Supplementary Table S3**, lymph node metastasis was significantly associated with positive/suspicious clinical lymph node status ($p = 0.002$), increased tumor diameter ($p = 0.029$), higher sVEGF-D levels ($p = 0.027$), greater depth of stromal invasion ($p = 0.024$), and the presence of vascular ($p = 0.012$) and perineural ($p = 0.005$) invasion.

sVEGF-D Represents an Independent Marker of Lymph Node Involvement

As described above in the *Study Design*, three different models for preoperative prediction of lymph node involvement were built using logistic regression (**Table 4**).

The base model, including only the clinical/radiological lymph node status, showed a moderate adjusted C-index (C-index$_{adj}$) of 0.70 (95%CI = 0.57–0.80); the clinical model, including the clinicopathological characteristics available before surgery (e.g., tumor diameter, tumor grade evaluated on biopsy, and clinical/radiological lymph node status), showed good discrimination, with C-index$_{adj}$ of 0.74 (95%CI = 0.62–0.88), and good calibration (scaled Brier score = 0.23) (**Supplementary Figure S2A**). The extended model, built by adding the sVEGF-D level to the clinical model, resulted in a significant improvement of the fit (likelihood ratio test: $\chi^2_1 = 4.35$, $p = 0.037$), suggesting an independent association between sVEGF-D and lymph node involvement. Both discrimination and calibration showed a slight improvement, with higher C-index$_{adj}$ (0.79, 95%CI = 0.64–0.92) and scaled Brier score (0.34) (**Supplementary Figure S2B**).

sVEGF-D Confirms Its Predictive Role in an Independent VSCC Cohort

The extended model applied to cohort B (validation set) showed a reasonably high C-index (0.73, 95%CI = 0.54–0.87). Comparison of the probabilities predicted by the extended model between the two groups of patients divided according to the presence of positive lymph nodes showed good separation with a discrimination slope of 0.78 and an acceptable agreement between the observed and predicted proportions of lymph node metastasis (Hosmer–Lemeshow test, $p = 0.08$) (**Supplementary Figure S3**).

Finally, we evaluated the performance of the extended model on the entire cohort of patients (A + B) in comparison with the base model. The model with sVEGF-D showed a significantly superior performance compared to the clinical/radiological

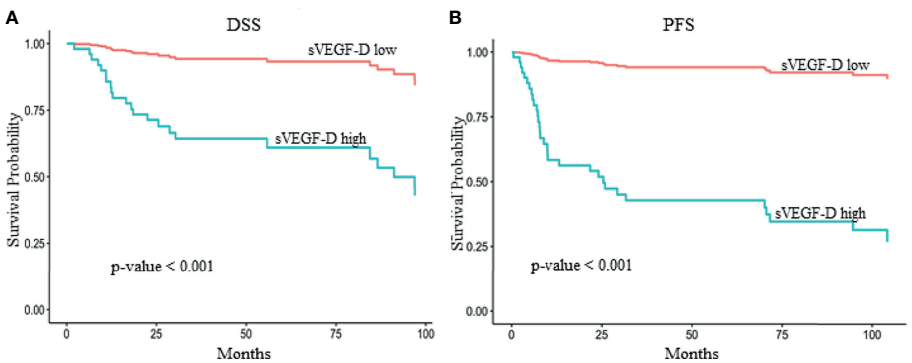


FIGURE 1 | Kaplan–Meier survival curves showing the effect of serum vascular endothelial growth factor D (sVEGF-D) level in multivariate models adjusted for stage, grade, and vascular and perineural invasion. The optimal threshold for sVEGF-D categorization was determined by maximally selected rank statistics. The reported *p*-values were adjusted for multiple testing. Higher sVEGF-D levels [>393 and >329 pg/ml for disease-specific survival (DSS) and progression-free survival (PFS), respectively] exhibited a significant association with reduced DSS **(A)** ($p < 0.001$) and PFS **(B)** ($p < 0.001$) in 61 patients with vulvar squamous cell carcinoma (VSCC) from cohort A.

TABLE 3 | Multivariable survival analysis for both disease-specific survival (DSS) and progression-free survival (PFS) on 61 VSCC patients from cohort A.

Variables	DSS		PFS	
	HR (95%CI)	*p*-value	HR (95%CI)	*p*-value
FIGO stage				
III–IV *vs*. I–II	10.5 (3.28–33.55)	**<0.001**	2.25 (0.99–5.14)	0.053
Tumor grade				
G2–G3 *vs*. G1	0.68 (0.20–2.30)	0.540	0.46 (0.19–1.15)	0.098
Vascular invasion				
Yes *vs*. no	1.88 (0.68–5.20)	0.220	2.08 (0.84–5.15)	0.116
Perineural invasion				
Yes *vs*. no	1.63 (0.56–4.75)	0.370	1.58 (0.62–4.01)	0.339
sVEGF-D				
Q3 *vs*. Q2	3.15 (1.21–8.23)	**0.026**[a]	1.86 (1.09–3.17)	**0.047**[a]

Significant p-values are indicated in bold.
HR, hazard ratio; FIGO, International Federation of Gynecologists and Obstetricians; sVEGF-D, serum vascular endothelial growth factor D; Q2, second quartile; Q3, third quartile.
[a]*Likelihood ratio test-based p-value.*

evaluation of the lymph nodes (ROC-AUCs of 0.792 and 0.685, respectively, $p = 0.008$) (**Table 5**). At the optimal cutoff value (Youden), the specificity, sensitivity, positive predictive value (PPV), negative predictive value (NPV), false-negative rate (FNR), and false-positive rate (FPR) of the extended model were 83.0%, 74.4%, 76.3%, 80.4%, 25.6%, and 17.0%, respectively.

DISCUSSION

Lymph node status is the most important prognostic factor for patients with VSCC, and failure to remove metastatic lymph nodes has serious consequences due to its high mortality (26). On the other hand, removal of lymph nodes can cause both short- and long-term serious side effects (8). For these reasons, a diagnostic test with an optimal sensitivity and specificity would be needed to safely avoid lymphadenectomy. Special attention seems to be focused on high-performance imaging modalities in the prediction of lymph node status, such as ultrasound (27, 28) and ^{18}F-FDG-PET/CT (PET) (29–31), in order to better select cN0 patients and identify before surgery those with nodal metastases, even with not palpable nodes. However, to date, imaging cannot diagnose small metastases prior to surgery when their size is below the resolution limits of the available imaging techniques (32).

In this context, circulating biomarkers could offer a valid contribution in the design of a predictive algorithm. For several different tumors such as breast (13), colon (14), ovarian (15), endometrial (16), cervical (33), bladder (34), thyroid (35), gastric (36), esophageal (37), and gallbladder (38) cancers, a strong association between an increased expression of VEGF-D and the presence of lymph node metastases has already been demonstrated by IHC (13–16, 33) or at serum level (34–38); however, investigations on this biomarker regarding VSCC are lacking. To the best of our knowledge, this is the first study investigating the role of sVEGF in VSCC.

In the present study, our findings indicated that an increased serum VEGF-D level is an independent predictor for the presence of metastatic disease in the lymph nodes and an independent risk factor of poor outcomes in terms of both DSS and PFS. In addition, a predictive model adding sVEGF-D to other clinicopathological parameters significantly improved the prediction of nodal metastasis.

Higher levels of sVEGF-D in cancer patients compared to healthy controls or benign pathologies have been detected for some tumor types (36–38) and not for others (34, 35), but

TABLE 4 | Logistic regression model estimates for association with prediction of lymph node in cohort A.

Variables	LN clinical evaluation (base model)		Clinical variables (clinical model)		Clinical + sVEGF-D (extended model)		Shrunk coefficients[a]
	OR (95%CI)	*p*-value	OR (95%CI)	*p*-value	OR (95%CI)	*p*-value	
sVEGF-D levels							
(pg/ml), log2 scale	–	–	–	–	4.63 (1.10–19.47)	0.037	3.11
Clinical lymph node status							
Positive *vs*. negative	5.24 (1.86–14.71)	0.002	4.48 (1.46–13.69)	0.009	3.82 (1.07–13.60)	0.039	2.62
Tumor diameter (mm)	–	–	1.03 (1.00–1.06)	0.078	1.04 (1.00–1.08)	0.057	1.03
Tumor grade on biopsy							
G2–G3 *vs*. G1	–	–	2.94 (0.94–9.26)	0.065	3.84 (1.06–13.96)	0.041	2.55
No. of patients	71		70		61		
C-index$_{adj}$ (95%CI)	0.695 (0.565–0.803)		0.743 (0.622–0.882)		0.788 (0.637–0.924)		

Results are reported as odds ratio (OR) and 95% confidence interval (CI). C-index was adjusted for optimism using bootstrap. 95% CI was computed via bootstrap.
LN, lymph node; sVEGF-D, serum vascular endothelial growth factor D; C-index$_{adj}$, adjusted C-index.
[a]*Coefficients computed using penalized maximum likelihood for the extended model.*

TABLE 5 | Metrics assessing the performance of the proposed methods for the prediction of lymph node metastasis.

Metrics (95%CI)	LN clinical evaluation	Extended model
AUC	0.685 (0.602–0.768)	0.792 (0.700–0.884)
Specificity (%)	72.2 (61.1–81.9)	83.9 (62.5–92.9)
Sensitivity (%)	64.8 (51.9–77.8)	74.4 (58.1–90.7)
Accuracy (%)	69.0 (61.1–77.0)	78.8 (70.7–85.9)
PPV (%)	63.8 (54.2–73.8)	76.7 (63.6–88.9)
NPV (%)	73.5 (65.8–81.5)	80.4 (72.1–90.9)
FNR (%)	35.2 (22.2–48.1)	25.6 (9.3–41.9)
FPR (%)	27.8 (18.1–38.9)	16.1 (7.1–37.5)
p-value (DeLong test)	0.008	

Comparison was made between the performance of the extended model and the base model (LN clinical evaluation) in the whole cohort (A and B). All 95%CIs were calculated using bootstrap (B = 2,000).

LN, lymph node; AUC, area under the curve; PPV, positive predictive value; NPV, negative predictive value; FNR, false-negative rate; FPR, false-positive rate.

regardless of this, a positive correlation with lymph node metastasis has been demonstrated in all studies.

VEGF-C and VEGF-D are key stimulators of both angiogenesis, *via* the activation of VEGFR-2, and lymphangiogenesis, *via* the activation of VEGFR-3, constitutively expressed by lymphatic endothelial cells, promoting growth and remodeling of lymphatic vessels (10, 39, 40). In animal models, VEGF-D-driven lymphatic metastasis has been attributed to both the growth of new lymphatics adjacent to the tumor and the enlargement of preexisting collecting lymphatic vessels (41). In addition to VEGF-D and VEGF-C, VEGF-A, fibroblast growth factor-2, and hepatocyte growth factor have been reported to exert lymphangiogenic activity either directly or indirectly, mediated by the VEGF-C/VEGF-D/VEGFR-3 signaling pathway (42–44).

Tumor spread through the lymphatics is known to be a negative prognosticator, but the molecular mechanisms of VEGF-D as an independent prognostic factor in many types of cancers are still unclear (13–16, 38). One possible hypothesis is that VEGF-D is a mitogenic and morphogenic effector of the proto-oncogene c-Fos and, consequently, may be involved in c-Fos-induced tumor transformation and progression (45, 46).

We found, for the first time, that high circulating levels of sVEGF-D correlate with lymph node metastasis and advanced stage in VSCC patients, as already shown for other malignancies (34–38). On the other hand, the tissue expressions of VEGF-D and VEGFR-3 by IHC did not correlate with any clinicopathological characteristics, as demonstrated by a previous study showing a positive IHC staining for VEGF-D and VEGFR-3 in 100% and 90% of VSCC cases, respectively, and no correlation with the presence of lymph node metastases (17).

According to previous literature (47–49), our study showed that clinical lymph node status, tumor diameter, vascular and perineural invasion, and depth of invasion significantly correlated with inguinofemoral lymph node metastasis. With the aim of providing a useful tool for a tailored surgical approach, we focused our attention on the variables available before surgery: tumor diameter, tumor grade evaluated on biopsy, clinical lymph node status, and sVEGF-D level. The extended model based on these four covariates showed good performance, demonstrated by the C-index of discrimination equal to 0.788. Notably, the performance of the extended model was significantly superior compared to that of the clinical model including only clinical predictors, but excluding sVEGF-D, and to that of the base model based on clinical/radiological evaluation of lymph nodes. The results, validated on an external independent cohort of VSCC patients, confirmed the ability of the extended model to classify patients with respect to lymph node positivity. It is well known that the performance of a predictive model is always lower in the validation group compared to that in the cohort of samples used for its development. The slight difference in the C-index values between our training and validation sets could be explained by the non-homogeneity of the two cohorts as they differed in the surgical approach used to assess lymph nodal status.

Only one previous study proposed two predictive models for groin node metastases based on four parameters (depth of infiltration, grade of differentiation, tumor diameter, and EGFR), but only the first two were independent predictors (50). The two models have not been validated in independent cohorts of patients and their performance is unclear.

Our study provided encouraging preliminary evidence for further investigations on sVEGF-D in association with other clinicopathological variables available preoperatively in the prediction of lymph node metastasis in patients with VSCC. The limits of the present study, which can be mainly attributed to the rarity of this tumor, are mainly related to the relatively small number of cases, the retrospective design, and the prolonged time interval of enrollment, during which many things have changed. The most important evolution concerned the improvement of imaging performance in the prediction of lymph node status due to technological development, the availability of more experienced examiners, and the increased knowledge of this rare pathology obtained by dedicated studies. Currently, imaging provides higher NPV, which in fact is the favored predictive driver since failing to recognize a metastasis and missing the surgical removal could significantly impair prognosis. On the other hand, sVEGF-D could potentially support a higher PPV with other diagnostic tools, being associated with the presence of lymph node metastasis.

In conclusion, it will be essential to validate these retrospective results in larger multicenter prospective studies to identify a threshold value that can achieve FNR and NPV values in accordance with the guidelines of the Gynecologic Cancer Group of the European Organization for Research and

Treatment of Cancer (EORTC) (5) and to update the sVEGF-D predictive model integrated with current high-performance imaging methods.

DATA AVAILABILITY STATEMENT

The raw data supporting the conclusions of this article will be made available by the authors, without undue reservation.

ETHICS STATEMENT

The studies involving human participants were reviewed and approved by Comitato Etico di Brescia, ASST Spedali Civili, Brescia, Italy, and Comitato Etico Policlinico Universitario "A. Gemelli" IRCCS—Università Cattolica del Sacro Cuore, Rome, Italy. The patients/participants provided written informed consent to participate in this study.

AUTHOR CONTRIBUTIONS

AR, AG, and FO conceived and designed the study. AR and LA performed the experiments. PA and SC executed the statistical analysis. AO, EB, LZ, CR, and DG collected data. FO, ES, EB, FF, GG, and GS contributed to the analyses and interpretation of data. AR and SC wrote the first drafts of the manuscript. All authors contributed to the article and approved the submitted version.

FUNDING

AG and FO were supported by local research grants from the University of Brescia. SC was supported by a research grant from the Italian Ministry of Education, University and Research (PRIN project no. 20178S4EK9).

ACKNOWLEDGMENTS

We wish to thank all the physicians and the nurses working in the Department of Obstetrics and Gynecology, ASST Spedali Civili, University of Brescia, particularly to Mrs. Maria Teresa Pedretti for the assistance in collecting blood samples. This paper is dedicated to the memory of our colleague, Dr. Anna Benetti, who recently passed away.

SUPPLEMENTARY MATERIAL

The Supplementary Material for this article can be found online at: https://www.frontiersin.org/articles/10.3389/fonc.2022.818613/full#supplementary-material

Supplementary Table 1 | Protein expression of VEGF-D and VEGFR-3 on vulvar cancer tissues and correlation with clinicopathological characteristics (49 VSCC patients from Cohort A).

Supplementary Table 2 | Univariable survival analysis for both disease specific survival (DSS) and progression free survival (PFS) on VSCC patients from Cohort A.

Supplementary Table 3 | Clinicopathologic characteristics of VSCC patients from Cohort A in relation to pathologic lymph node status.

Supplementary Figure 1 | Representative immunohistochemical staining for VEGF-D and VEGFR-3 in vulvar invasive squamous cell carcinoma. Magnification 20x.

Supplementary Figure 2 | Calibration curves for prediction models. **(A)** Calibration curve for the *clinical model*. **(B)** Calibration curve for the *extended model*.

Supplementary Figure 3 | Calibration curve for the *penalized extended model* applied to the validation cohort B.

REFERENCES

1. National cancer Institute. *Cancer Stat Facts: Vulvar Cancer*. (2021). Available at: http://www.seer.cancer.gov/statfacts/html/vulva.html.
2. Siegel RL, Miller KD, Fuchs HE, Jemal A. Cancer Statistics, 2021. *CA Cancer J Clin* (2021) 71(1):7–33. doi: 10.3322/caac.21654
3. Lai J, Elleray R, Nordin A, Hirschowitz L, Rous B, Gildea C, et al. Vulval Cancer Incidence, Mortality and Survival in England: Age-Related Trends. *BJOG* (2014) 121(6):728–38. doi: 10.1111/1471-0528.12459
4. Meltzer-Gunnes CJ, Smastuen MC, Kristensen GB, Trope CG, Lie AK, Vistad I. Vulvar Carcinoma in Norway: A 50-Year Perspective on Trends in Incidence, Treatment and Survival. *Gynecol Oncol* (2017) 145(3):543–8. doi: 10.1016/j.ygyno.2017.03.008
5. Oonk MHM, Planchamp F, Baldwin P, Bidzinski M, Brannstrom M, Landoni F, et al. European Society of Gynaecological Oncology Guidelines for the Management of Patients With Vulvar Cancer. *Int J Gynecol Cancer* (2017) 27 (4):832–7. doi: 10.1097/IGC.0000000000000975
6. Koh WJ, Greer BE, Abu-Rustum NR, Campos SM, Cho KR, Chon HS, et al. Vulvar Cancer, Version 1.2017, NCCN Clinical Practice Guidelines in Oncology. *J Natl Compr Canc Netw* (2017) 15(1):92–120. doi: 10.6004/jnccn.2017.0008
7. Collarino A, Fuoco V, Garganese G, Pereira Arias-Bouda LM, Perotti G, Manca G, et al. Lymphoscintigraphy and Sentinel Lymph Node Biopsy in Vulvar Carcinoma: Update From a European Expert Panel. *Eur J Nucl Med Mol Imaging* (2020) 47(5):1261–74. doi: 10.1007/s00259-019-04650-8
8. Hinten F, van den Einden LC, Hendriks JC, van der Zee AG, Bulten J, Massuger LF, et al. Risk Factors for Short- and Long-Term Complications After Groin Surgery in Vulvar Cancer. *Br J Cancer* (2011) 105(9):1279–87. doi: 10.1038/bjc.2011.407
9. Garganese G, Collarino A, Fragomeni SM, Rufini V, Perotti G, Gentileschi S, et al. Groin Sentinel Node Biopsy and (18)F-FDG PET/CT-Supported Preoperative Lymph Node Assessment in Cn0 Patients With Vulvar Cancer Currently Unfit for Minimally Invasive Inguinal Surgery: The GroSNaPET Study. *Eur J Surg Oncol* (2017) 43(9):1776–83. doi: 10.1016/j.ejso.2017.06.018
10. Achen MG, Jeltsch M, Kukk E, Makinen T, Vitali A, Wilks AF, et al. Vascular Endothelial Growth Factor D (VEGF-D) is a Ligand for the Tyrosine Kinases VEGF Receptor 2 (Flk1) and VEGF Receptor 3 (Flt4). *Proc Natl Acad Sci USA* (1998) 95(2):548–53. doi: 10.1073/pnas.95.2.548
11. Achen MG, Stacker SA. Vascular Endothelial Growth Factor-D: Signaling Mechanisms, Biology, and Clinical Relevance. *Growth Factors* (2012) 30 (5):283–96. doi: 10.3109/08977194.2012.704917
12. Stacker SA, Caesar C, Baldwin ME, Thornton GE, Williams RA, Prevo R, et al. VEGF-D Promotes the Metastatic Spread of Tumor Cells *via* the Lymphatics. *Nat Med* (2001) 7(2):186–91. doi: 10.1038/84635
13. Nakamura Y, Yasuoka H, Tsujimoto M, Yang Q, Imabun S, Nakahara M, et al. Prognostic Significance of Vascular Endothelial Growth Factor D in Breast Carcinoma With Long-Term Follow-Up. *Clin Cancer Res* (2003) 9(2):716–21.

14. White JD, Hewett PW, Kosuge D, McCulloch T, Enholm BC, Carmichael J, et al. Vascular Endothelial Growth Factor-D Expression is an Independent Prognostic Marker for Survival in Colorectal Carcinoma. *Cancer Res* (2002) 62 (6):1669–75.
15. Yokoyama Y, Charnock-Jones DS, Licence D, Yanaihara A, Hastings JM, Holland CM, et al. Vascular Endothelial Growth Factor-D is an Independent Prognostic Factor in Epithelial Ovarian Carcinoma. *Br J Cancer* (2003) 88 (2):237–44. doi: 10.1038/sj.bjc.6600701
16. Yokoyama Y, Charnock-Jones DS, Licence D, Yanaihara A, Hastings JM, Holland CM, et al. Expression of Vascular Endothelial Growth Factor (VEGF)-D and its Receptor, VEGF Receptor 3, as a Prognostic Factor in Endometrial Carcinoma. *Clin Cancer Res* (2003) 9(4):1361–9.
17. Jach R, Dyduch G, Radon-Pokracka M, Przybylska P, Mika M, Dulinska-Litewka J, et al. Expression of Vascular Endothelial Growth Factors VEGF- C and D, VEGFR-3, and Comparison of Lymphatic Vessels Density Labeled With D2-40 Antibodies as a Prognostic Factors in Vulvar Intraepithelial Neoplasia (VIN) and Invasive Vulvar Cancer. *Neuro Endocrinol Lett* (2011) 32 (4):530–9.
18. McGeechan K, Macaskill P, Irwig L, Liew G, Wong TY. Assessing New Biomarkers and Predictive Models for Use in Clinical Practice: A Clinician's Guide. *Arch Intern Med* (2008) 168(21):2304–10. doi: 10.1001/archinte.168.21.2304
19. Steyerberg EW, Vickers AJ, Cook NR, Gerds T, Gonen M, Obuchowski N, et al. Assessing the Performance of Prediction Models: A Framework for Traditional and Novel Measures. *Epidemiology* (2010) 21(1):128–38. doi: 10.1097/EDE.0b013e3181c30fb2
20. Hosmer DW, Hosmer T, Le Cessie S, Lemeshow S. A Comparison of Goodness-of-Fit Tests for the Logistic Regression Model. *Stat Med* (1997) 16(9):965–80. doi: 10.1002/(sici)1097-0258(19970515)16:9<965::aid-sim509>3.0.co;2-o
21. Harrell FE, Lee KL. Using Logistic Model Calibration to Assess the Quality of Probability of Predictions. (1991). pp. 1–24. Available from: https://biostat.app.vumc.org/wiki/pub/Main/FrankHarrell/logistCal.pdf.
22. Copas JB. Regression, Prediction and Shrinkage. *J R Stat Soc B* (1983) 45 (3):311–54. doi: 10.1111/j.2517-6161.1983.tb01258.x
23. Draper NR, Smith H. *Applied Regression Analysis. 3rd Ed* Vol. xvii. . New York: Wiley (1998). p. 706.
24. Hurvich CM, Tsai CL. Regression and Time-Series Model Selection in Small Samples. *Biometrika* (1989) 76(2):297–307. doi: 10.2307/2336663
25. Hothorn T, Zeileis A. Generalized Maximally Selected Statistics. *Biometrics* (2008) 64(4):1263–9. doi: 10.1111/j.1541-0420.2008.00995.x
26. Raspagliesi F, Hanozet F, Ditto A, Solima E, Zanaboni F, Vecchione F, et al. Clinical and Pathological Prognostic Factors in Squamous Cell Carcinoma of the Vulva. *Gynecol Oncol* (2006) 102(2):333–7. doi: 10.1016/j.ygyno.2005.12.027
27. Garganese G, Fragomeni SM, Pasciuto T, Leombroni M, Moro F, Evangelista MT, et al. Ultrasound Morphometric and Cytologic Preoperative Assessment of Inguinal Lymph-Node Status in Women With Vulvar Cancer: MorphoNode Study. *Ultrasound Obstet Gynecol* (2020) 55(3):401–10. doi: 10.1002/uog.20378
28. Garganese G, Bove S, Fragomeni S, Moro F, Triumbari EKA, Collarino A, et al. Real-Time Ultrasound Virtual Navigation in 3D PET/CT Volumes for Superficial Lymph-Node Evaluation: Innovative Fusion Examination. *Ultrasound Obstet Gynecol* (2021) 58(5):766–72. doi: 10.1002/uog.23613
29. Collarino A, Garganese G, Fragomeni SM, Pereira Arias-Bouda LM, Ieria FP, Boellaard R, et al. Radiomics in Vulvar Cancer: First Clinical Experience Using (18)F-FDG PET/CT Images. *J Nucl Med* (2018) 60(2):199–206. doi: 10.2967/jnumed.118.215889
30. Rufini V, Garganese G, Ieria FP, Pasciuto T, Fragomeni SM, Gui B, et al. Diagnostic Performance of Preoperative [(18)F]FDG-PET/CT for Lymph Node Staging in Vulvar Cancer: A Large Single-Centre Study. *Eur J Nucl Med Mol Imaging* (2021) 48(10):3303–14. doi: 10.1007/s00259-021-05257-8
31. Triumbari EKA, de Koster EJ, Rufini V, Fragomeni SM, Garganese G, Collarino A. 18f-FDG PET and 18F-FDG PET/CT in Vulvar Cancer: A Systematic Review and Meta-Analysis. *Clin Nucl Med* (2021) 46(2):125–32. doi: 10.1097/RLU.0000000000003411
32. Fischerova D, Garganese G, Reina H, Fragomeni SM, Cibula D, Nanka O, et al. Terms, Definitions and Measurements to Describe Sonographic Features of Lymph Nodes: Consensus Opinion From the Vulvar International Tumor Analysis (VITA) Group. *Ultrasound Obstet Gynecol* (2021) 57(6):861–79. doi: 10.1002/uog.23617
33. Dai Y, Tong R, Guo H, Yu T, Wang C. Association of CXCR4, CCR7, VEGF-C and VEGF-D Expression With Lymph Node Metastasis in Patients With Cervical Cancer. *Eur J Obstet Gynecol Reprod Biol* (2017) 214:178–83. doi: 10.1016/j.ejogrb.2017.04.043
34. Benoit T, Keller EX, Wolfsgruber P, Hermanns T, Gunthart M, Banzola I, et al. High VEGF-D and Low MMP-2 Serum Levels Predict Nodal-Positive Disease in Invasive Bladder Cancer. *Med Sci Monit* (2015) 21:2266–74. doi: 10.12659/MSM.894383
35. Lai CW, Duh QY, Chen CW, Chuang FJ, Chang YJ, Lin MT, et al. VEGF-D and A Preoperative Serum Levels Predict Nodal and Distant Metastases in Differentiated Thyroid Cancer Patients. *World J Surg* (2015) 39(7):1742–9. doi: 10.1007/s00268-015-3016-6
36. Tsirlis TD, Kostakis A, Papastratis G, Masselou K, Vlachos I, Papachristodoulou A, et al. Predictive Significance of Preoperative Serum VEGF-C and VEGF-D, Independently and Combined With Ca19-9, for the Presence of Malignancy and Lymph Node Metastasis in Patients With Gastric Cancer. *J Surg Oncol* (2010) 102(6):699–703. doi: 10.1002/jso.21677
37. Kozlowski M, Kowalczuk O, Milewski R, Chyczewski L, Niklinski J, Laudanski J. Serum Vascular Endothelial Growth Factors C and D in Patients With Oesophageal Cancer. *Eur J Cardiothorac Surg* (2010) 38(3):260–7. doi: 10.1016/j.ejcts.2010.01.061
38. Liu MC, Jiang L, Hong HJ, Meng ZW, Du Q, Zhou LY, et al. Serum Vascular Endothelial Growth Factors C and D as Forecast Tools for Patients With Gallbladder Carcinoma. *Tumour Biol* (2015) 36(8):6305–12. doi: 10.1007/s13277-015-3316-3
39. Joukov V, Pajusola K, Kaipainen A, Chilov D, Lahtinen I, Kukk E, et al. A Novel Vascular Endothelial Growth Factor, VEGF-C, is a Ligand for the Flt4 (VEGFR-3) and KDR (VEGFR-2) Receptor Tyrosine Kinases. *EMBO J* (1996) 15(2):290–98. doi: 10.1002/j.1460-2075.1996.tb00359.x
40. Stacker SA, Williams SP, Karnezis T, Shayan R, Fox SB, Achen MG. Lymphangiogenesis and Lymphatic Vessel Remodelling in Cancer. *Nat Rev Cancer* (2014) 14(3):159–72. doi: 10.1038/nrc3677
41. Karnezis T, Shayan R, Caesar C, Roufail S, Harris NC, Ardipradja K, et al. VEGF-D Promotes Tumor Metastasis by Regulating Prostaglandins Produced by the Collecting Lymphatic Endothelium. *Cancer Cell* (2012) 21(2):181–95. doi: 10.1016/j.ccr.2011.12.026
42. Cao R, Bjorndahl MA, Gallego MI, Chen S, Religa P, Hansen AJ, et al. Hepatocyte Growth Factor is a Lymphangiogenic Factor With an Indirect Mechanism of Action. *Blood* (2006) 107(9):3531–6. doi: 10.1182/blood-2005-06-2538
43. Chang LK, Garcia-Cardena G, Farnebo F, Fannon M, Chen EJ, Butterfield C, et al. Dose-Dependent Response of FGF-2 for Lymphangiogenesis. *Proc Natl Acad Sci USA* (2004) 101(32):11658–63. doi: 10.1073/pnas.0404272101
44. Cursiefen C, Chen L, Borges LP, Jackson D, Cao J, Radziejewski C, et al. VEGF-A Stimulates Lymphangiogenesis and Hemangiogenesis in Inflammatory Neovascularization *via* Macrophage Recruitment. *J Clin Invest* (2004) 113(7):1040–50. doi: 10.1172/JCI20465
45. Orlandini M, Marconcini L, Ferruzzi R, Oliviero S. Identification of a C-Fos-Induced Gene That is Related to the Platelet-Derived Growth Factor/Vascular Endothelial Growth Factor Family. *Proc Natl Acad Sci USA* (1996) 93 (21):11675–80. doi: 10.1073/pnas.93.21.11675
46. Marconcini L, Marchio S, Morbidelli L, Cartocci E, Albini A, Ziche M, et al. C-Fos-Induced Growth Factor/Vascular Endothelial Growth Factor D Induces Angiogenesis *in vivo* and *in vitro*. *Proc Natl Acad Sci USA* (1999) 96(17):9671–6. doi: 10.1073/pnas.96.17.9671
47. Homesley HD, Bundy BN, Sedlis A, Yordan E, Berek JS, Jahshan A, et al. Prognostic Factors for Groin Node Metastasis in Squamous Cell Carcinoma of the Vulva (a Gynecologic Oncology Group Study). *Gynecol Oncol* (1993) 49 (3):279–83. doi: 10.1006/gyno.1993.1127
48. Smyczek-Gargya B, Volz B, Geppert M, Dietl J. A Multivariate Analysis of Clinical and Morphological Prognostic Factors in Squamous Cell Carcinoma of the Vulva. *Gynecol Obstet Invest* (1997) 43(4):261–7. doi: 10.1159/000291869
49. Ferrari F, Forte S, Ardighieri L, Bonetti E, Fernando B, Sartori E, et al. Multivariate Analysis of Prognostic Factors in Primary Squamous Cell Vulvar Cancer: The Role of Perineural Invasion in Recurrence and Survival. *Eur J Surg Oncol* (2019) 45(11):2115–9. doi: 10.1016/j.ejso.2019.07.029
50. Oonk MH, de Bock GH, van der Veen DJ, Ten Hoor KA, de Hullu JA, Hollema H, et al. EGFR Expression is Associated With Groin Node Metastases

in Vulvar Cancer, But Does Not Improve Their Prediction. *Gynecol Oncol* (2007) 104(1):109–13. doi: 10.1016/j.ygyno.2006.07.035

Conflict of Interest: The authors declare that the research was conducted in the absence of any commercial or financial relationships that could be construed as a potential conflict of interest.

The reviewer LT declared a shared affiliation with one of the authors GG to the handling editor at the time of review.

Publisher's Note: All claims expressed in this article are solely those of the authors and do not necessarily represent those of their affiliated organizations, or those of the publisher, the editors and the reviewers. Any product that may be evaluated in this article, or claim that may be made by its manufacturer, is not guaranteed or endorsed by the publisher.

Copyright © 2022 Ravaggi, Gambino, Ferrari, Olivari, Zanotti, Romani, Ardighieri, Antonelli, Garganese, Gallo, Scambia, Bignotti, Sartori, Calza and Odicino. This is an open-access article distributed under the terms of the Creative Commons Attribution License (CC BY). The use, distribution or reproduction in other forums is permitted, provided the original author(s) and the copyright owner(s) are credited and that the original publication in this journal is cited, in accordance with accepted academic practice. No use, distribution or reproduction is permitted which does not comply with these terms.

frontiers | Frontiers in Oncology

REVIEW
published: 08 April 2022
doi: 10.3389/fonc.2022.805613

Current Prognostic and Predictive Biomarkers for Endometrial Cancer in Clinical Practice: Recommendations/Proposal from the Italian Study Group

Gian Franco Zannoni[1,2], Emma Bragantini[3], Francesca Castiglione[4], Matteo Fassan[5], Giancarlo Troncone[6], Frediano Inzani[1], Anna Pesci[7], Angela Santoro[1] and Filippo Fraggetta[8,9]*

[1] Unità di Ginecopatologia e Patologia Mammaria, Dipartimento Scienze della Salute della Donna, del Bambino e di Sanità Pubblica, Fondazione Policlinico Universitario A. Gemelli Istituto di Ricerca e Cura a Carattere Scientifico (IRCCS), Rome, Italy, [2] Istituto di Anatomia Patologica, Università Cattolica del Sacro Cuore, Rome, Italy, [3] Department of Surgical Pathology, Ospedale S. Chiara, Trento, Italy, [4] Histopathology and Molecular Diagnostics, Careggi University Hospital, Florence, Italy, [5] Department of Medicine - DIMED, University of Padova, Padova, Italy, [6] Department of Public Health, University of Naples Federico II, Naples, Italy, [7] Department of Pathology, Sacred Heart Hospital Don Calabria Negrar, Verona, Italy, [8] Pathology Unit, "Cannizzaro" Hospital, Catania, Italy, [9] Pathology Unit, "Gravina" Hospital, Caltagirone, Italy

Endometrial carcinoma (EC) is the most common gynecological malignant disease in high-income countries, such as European countries and the USA. The 2020 edition of the World Health Organization (WHO) Classification of Tumors of the Female Genital Tract underlines the important clinical implications of the proposed new histomolecular classification system for ECs. In view of the substantial genetic and morphological heterogeneity in ECs, both classical pthological parameters and molecular classifiers have to be integrated in the pathology report. This review will focus on the most commonly adopted immunohistochemical and molecular biomarkers in daily clinical characterization of EC, referring to the most recent published recommendations, guidelines, and expert opinions.

Keywords: endometrial cancer, prognostic markers, histomolecular classification, pathological guidelines, prognostic stratification

OPEN ACCESS

Edited by:
Priya Ranjit Bhosale, University of Texas MD Anderson Cancer Center, United States

Reviewed by:
Shujie Yang, The University of Iowa, United States
LianCheng Zhu, ShengJing Hospital of China Medical University, China
Atif Ali Hashmi, Liaquat National Medical College, Pakistan

***Correspondence:**
Gian Franco Zannoni
gianfranco.zannoni@unicatt.it

Specialty section:
This article was submitted to Gynecological Oncology, a section of the journal Frontiers in Oncology

Received: *30 October 2021*
Accepted: *11 March 2022*
Published: *08 April 2022*

Citation:
Zannoni GF, Bragantini E, Castiglione F, Fassan M, Troncone G, Inzani F, Pesci A, Santoro A and Fraggetta F (2022) Current Prognostic and Predictive Biomarkers for Endometrial Cancer in Clinical Practice: Recommendations/Proposal from the Italian Study Group. Front. Oncol. 12:805613. doi: 10.3389/fonc.2022.805613

INTRODUCTION

Endometrial carcinoma (EC) is the most common gynecological malignancy in Western countries. It represents the sixth most commonly diagnosed cancer and the 14th leading cause of cancer death in women worldwide (1). The 5th edition of the WHO of Tumors of the Female Genital Tract, published in 2020, considers the molecular classification system for ECs as an additional tool to

integrate traditional histopathological criteria [histological type and grade, pattern of myometrial involvement, lymphovascular involvement (LVSI) and FIGO stage] (2). The aim of this integrated histomolecular approach is to unify both classical pathological parameters and molecular data in one pathology report and correlate them to the clinical risk groups, for a better multidisciplinary definition of patient outcomes (3).

AIM

This overview will focus to enlighten and summarize the histological features (**Figure 1**) and the immunohistochemical and molecular biomarkers useful to perform a right and complete characterization of endometrial cancer.

Considering the important insights into the biological characterization and clinical management of EC, the Italian Society of Pathological Anatomy and Cytopathology (SIAPEC) and members of PAGINE (Italian Group of Gynaecological Pathology) worked on a collaborative project to draft consensus specific recommendations on the (i) most important definitions related to the 2013 The Cancer Genome Atlas (TGCA) histomolecular classifications; (ii) methods of POLE, MSI, p53 testing on cancer tissue (**Figure 2**); and (iii) methods of other (optional) prognostic marker evaluation on cancer tissue (**Figure 3** and **Tables 1**-**8**). Members of the working group have been selected among professionals with high standard records on scientific activity and routine pathological and clinical work on gynecological pathology and molecular testing of cancers, comprising 10 pathologists/molecular pathologists.

FROM 2013 TCGA REVOLUTION TO THE MOLECULAR SURROGATES FOR EC BIOLOGICAL CHARACTERIZATION

In 2013, TCGA Research Network reported a large-scale, integrated genomic, transcriptomic, and proteomic analysis of 373 ECs, including 307 endometrial endometrioid carcinomas (EECs), 53 serous endometrial carcinomas (SECs), and 13 mixed cases, showing that EC could be stratified into four prognostically relevant molecular groups: POLE/ultramutated (7%) with excellent prognosis with no recurrence regardless of the FIGO grade, the microsatellite-instability/hypermutated (28%) and the copy-number-low/endometrioid (39%) characterized by intermediate prognosis, and the copy-number-high/serous like (26%) characterized by SECs and showing poor prognosis (4).

As the molecular classification proposed by the TCGA used cost prohibitive methods for group assignment in routine clinical practice, subsequent studies, in particular the Leiden/PORTEC group and the Vancouver/ProMisE group, developed and validated a molecular surrogates based on immunohistochemistry expression of p53 protein and mismatch repair (MMR) proteins and POLE sequencing. The four groups identified with such approach, i.e., POLE-mutant (POLEmut), MMR-deficient (dMMR), p53-abnormal (p53abn), and no specific molecular profile (NSMP), have been recently integrated in the European guidelines for endometrial cancer management (5, 6) with important clinical implications as the following:

- all POLEmut carcinomas up to FIGO stage II are included in the low-risk group and can be managed by observation alone

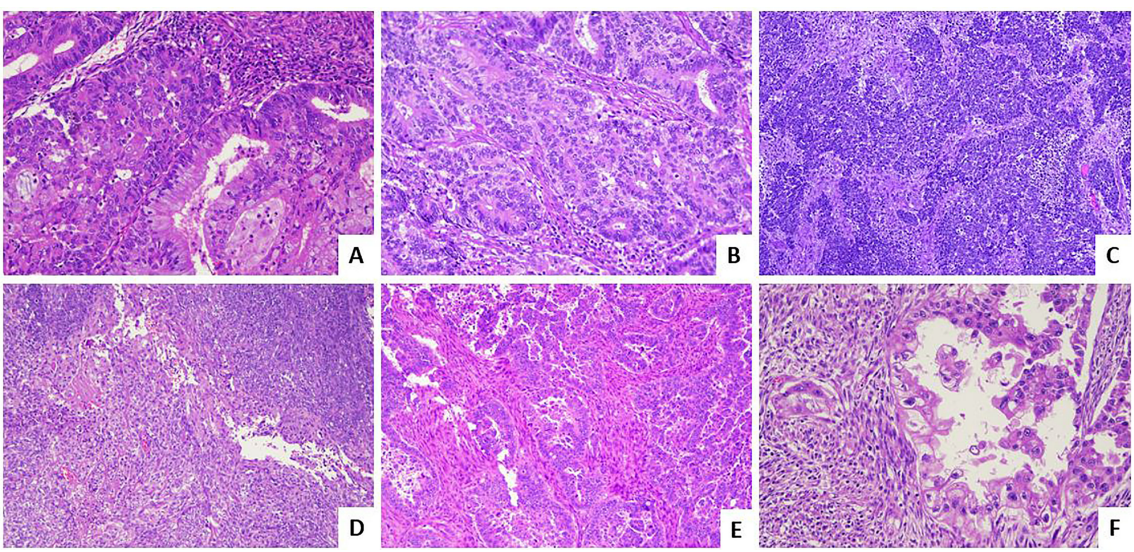


FIGURE 1 | Histological subtypes of endometrial carcinoma: an overview. **(A)** An endometrioid carcinoma G1 FIGO with mucinous features (LSAB, 10×). **(B)** An endometrioid carcinoma G2 FIGO (LSAB, 10×). **(C)** An endometrioid carcinoma G3 FIGO with basaloid features (LSAB, 4×). **(D)** An endometrioid carcinoma G3 FIGO with spindle cell features (LSAB, 4×). **(E)** A serous carcinoma (LSAB, 10×). **(F)** A clear cell carcinoma (LSAB, 20×).

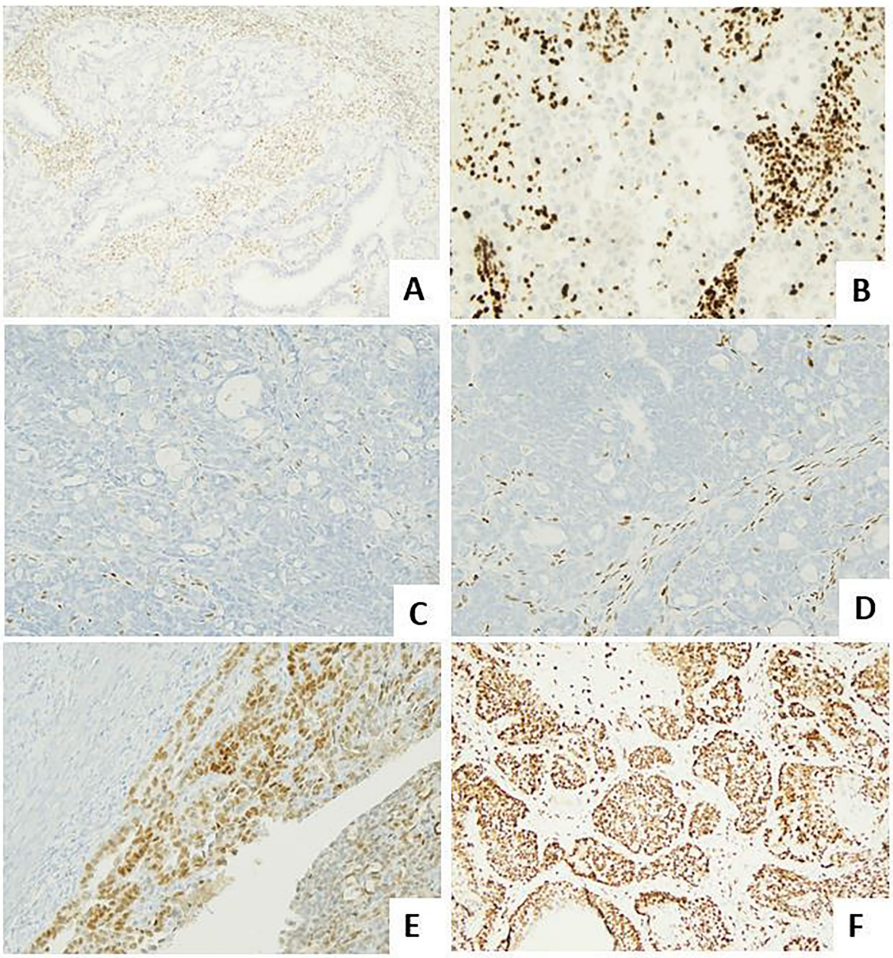


FIGURE 2 | Molecular landscape of endometrial carcinoma: the role of the immunohistochemical surrogates. **(A)** An endometrioid carcinoma G2 FIGO with loss of MLH1 expression (LSAB, 10×). **(B)** An endometrioid carcinoma G2 FIGO with loss of MSH2 expression (LSAB, 10×). **(C, D)** An endometrioid carcinoma G3 FIGO with loss of ER (LSAB, 10×) and PR (LSAB, 10×). **(E)** An endometrioid carcinoma G2 FIGO with expression of ER in 80% of neoplastic cells, with a 2+ score intensity (LSAB, 10×). **(F)** A serous carcinoma with overexpressed aberrant pattern of p53 (LSAB, 4×).

- p53mut EECs are lumped together with non-endometrioid carcinomas in the high-risk group and, in the absence of myometrial invasion, are considered at intermediate risk (7).

POLE SUBGROUP

Clinical Definition and Therapeutical Implications

The POLE1–4 genes encode for one of the four subunits that form Polϵ (DNA polymerase epsilon). POLE gene contains both the catalytic active site and the proofreading exonuclease domain (8). Polϵ is a protein responsible for the polymerization of the leading strand during DNA replication. It also possesses 3' to 5' exonuclease capability to repair misincorporated nucleotides during DNA replication and it is also involved in DNA repair pathways such as MMR, base excision repair (BER), nucleotide excision repair (NER), or double-strand break repair (9).

A few missense germline mutations in the proofreading domain of POLE affecting the exonuclease repair of Polϵ have been shown to be pathogenic such as W347C, N363K, D368V, L424V, P436S, or Y458F. These mutations hence result in a mutation rate increase of about 100-fold. Accordingly, these tumors are usually called ultramutated (10).

Pathogenic somatic mutations in the proofreading domain of POLE have been found in some tumor types, such as endometrial tumors (8%) and at lower frequencies in colorectal, glioblastoma, ovary, prostate, breast, or gastric cancer (9, 11–14). These mutations seem to confer similar phenotypes regardless of the tumor tissue type. These are missense, heterozygous mutations where no second hit by either mutation or LOH seems to be required, and they are very early events, possibly initiating. Some mutations are hotspots such as P286R, S297F, V411L, or S459F,

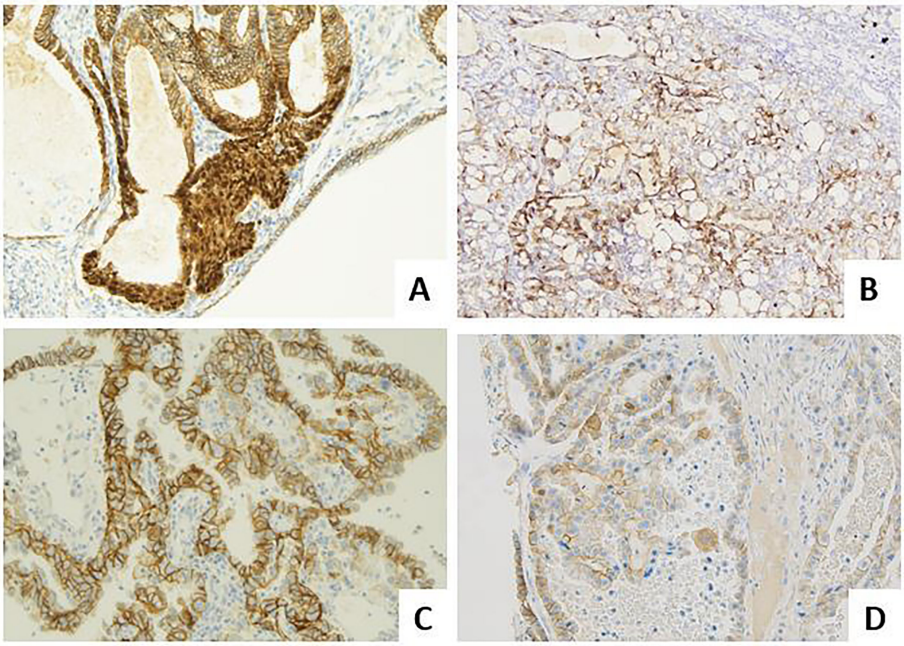


FIGURE 3 | Molecular landscape of endometrial carcinoma: the role of other immunohistochemical markers. **(A)** An endometrioid carcinoma G1 FIGO with nuclear beta-catenin expression in foci of morular metaplasia (LSAB, 20×). **(B)** An endometrioid carcinoma G2 FIGO with L1CAM over-expression (>10%) (LSAB, 4×). **(C)** A serous carcinoma with HER2 score 3+, according to the 2007 modified ASCO CAP scoring method (LSAB, 20×). **(D)** A clear cell carcinoma with HER2 score 2+, according to the 2007 modified ASCO CAP scoring method (LSAB, 20×).

but other rarer mutations have also been identified (e.g., P286H/L, S297Y, F367S, L424V/I, P436R, M444K, and A456P). These mutations result in ultramutation with an over-representation of C>A (15). Moreover, POLE tumors are hardly ever concomitant with MSI, although a few tumors with both phenotypes have been described, but they do not seem to show chromosomal instability as their karyotype is nearly diploid (16). Patients with somatic POLE driver mutations are younger on average and the prognosis is excellent in the early stage (15).

In EC, the POLE mt group is characterized by somatic mutations in the exonuclease domain of POLE, which encodes the catalytic subunit of DNA polymerase epsilon. Ultramutated tumors have an extraordinarily high mutation rate (232×10^{-6} mutations per megabase), included both low-grade (uncommonly) and high-grade EECs (significantly) and consistently showed the most favorable prognosis with no recurrence and this excellent outcome appears to be maintained across the several histotypes, regardless of the

TABLE 1 | POLE: recommendations and comments from the working group.

Recommendations
A) No surrogate for POLE mutation still exists but the targeted sequencing for the common mutations in this gene could be used rather than whole genome or panel testing (mutation analysis of the exonuclease domain of POLE exons 9, 11, 13, and 14). Comments The mutational analysis of the exonuclease domain of POLE should be considered in the following cases: - EEC G3 and other high-grade histologies (UEC/DEC, clear cell, carcinosarcoma) - rare histotypes (neuroendocrine tumors) - abundance in TIL and/or peritumoral lymphocytes - mixed cases - ambiguous morphologies - ambiguous immunophenotype (possible multiple classifiers) - subclonal p53 at IHC Mutational analysis should be carried out only in selected experienced centers. Minimal requirement is the adequate assessment of the 5 more frequent occurring POLE hotspot variants. Unknown variants or VUS should be discussed at the Tumor Board.

TABLE 2 | MSI: recommendations and comments from the working group.

Recommendations
A) The first method for MSI testing is represented by MMR IHC, a widely available laboratory test, utilizing antibodies against MLH1, MSH2, MSH6, and PMS2.
B) MSI-PCR-based molecular testing is indicated in case of indeterminate IHC results (disagreement or interpretative difficulties). The five poly-A panel is the recommended panel given its higher sensitivity and specificity.
C) As a novel alternative tool for MSI testing, NGS should be carried out only in selected centers experienced in these techniques.
Comments
- Use the IHC approach for detecting the four MMR proteins and assessing MMRd in any sporadic cancer type belonging to the spectrum of cancers found in Lynch Syndrome, so including EC.
- Standardize pre-analytical and analytical protocol of testing
- IHC can be performed on biopsies or surgical specimens if available, preferring the best-preserved sample as first choice
The main advantages of performing IHC on biopsies are the following:
(i) the better degree of fixation of biopsies
(ii) the early knowledge of MSI status in a pre-operative setting
The main advantages of performing IHC on surgical samples are the following:
(i) larger amount of tumoral representative tissue; (ii) the possibility to select the best specimen for IHC testing; (iii) the possibility to overcome tumor heterogeneity.
- The presence of an internal positive control is mandatory for interpretation of results.
- Move to MSI-PCR or NGS (in selected centers) as a confirmatory test or whenever there is any doubt in IHC interpretation. In particular, in the following events:
- Indeterminate/equivocal/ambiguous IHC results
- False-negative MMR immunostainings mainly caused by pre-analytical poor tissue fixation
- Aberrant staining patterns such as cytoplasmic, dot-like, or perinuclear staining
– Loss of only one heterodimer subunit (e.g., only MLH1 or only PMS2 and not both)

TABLE 3 | P53: recommendations and comments from the working group.

Recommendations
A) The first method for p53 testing is represented by IHC, a widely available laboratory test, utilizing antibodies against p53.
B) Genetic testing (Sanger sequencing or NGS) is indicated in case of indeterminate IHC results (disagreement or interpretative difficulties).
C) Genetic testing should be carried out only in selected centers experienced in these techniques.
Comments
- Use the IHC approach for detecting p53 pattern of expression
- Standardize pre-analytical and analytical protocol of testing
- IHC can be performed on biopsies or surgical specimens if available, preferring the best-preserved sample as first choice
The main advantages of performing IHC on biopsies are the following:
(i) the better degree of fixation of biopsies
(ii) the early knowledge of p53 status in a pre-operative setting
The main advantages of performing IHC on surgical sample are the following:
(i) larger amount of tumoral representative tissue; (ii) the possibility to select the best specimen for IHC testing; (iii) the possibility to overcome tumor heterogeneity.
- The presence of an internal positive control is mandatory for interpretation of results.
- Move to genetic testing as a confirmatory test or whenever there is any doubt in IHC interpretation.
We retain that undoubtedly diagnostic interpretative challenges by p53 immunohistochemistry are possible events, but we are also aware that equally there are similar issues around quality assurance for genetic testing of TP53 mutation (Sanger sequencing or NGS) that may not be totally reliable.

TABLE 4 | Hormonal receptors: comments from the working group.

Comments
- ER and PR are affordable immunohistochemical markers, available in all pathological laboratories worldwide and thus this scoring system could be easily implemented in routine practice.
- Scoring for ER and PR adds relevant prognostic information to current clinical practice
- Correlation between ER/PR expression in preoperative and postoperative material could be investigated also in EC, as well as already test in breast cancer
- Reporting of percentages in the form of continuous or semicontinuous values for ER/PR expression, avoiding dichotomous values (e.g., positive, negative) is recommended
- Reporting of intensity score is also advised
- Immunohistochemical analysis for ER and PR expression can be performed manually or by digital image analysis that could provide a more objective and reproducible evaluation

TABLE 5 | L1CAM: comment from the working group.

Comment
Similarly to beta-catenin, since ESGO/ESTRO/ESP recent guidelines do not consider L1CAM in EC molecular risk stratification, but considering that L1CAM could represent an additional marker to personalize patient treatment, we propose to introduce the use of L1CAM only with a scientific intent.

TABLE 6 | Beta-catenin: comment from the working group.

Comment
Since there is still scientific debate to introduce the use of beta-catenin immunohistochemistry in the prognostic stratification of EC, we propose to analyze it only with a research purpose.

TABLE 7 | PDL1: comments from the working group.

Comments
- To date, immunohistochemistry is the gold standard for PD-L1 expression assessment
- Pathologists should be aware that this analysis is significantly affected by several factors:
(i) different standardization protocols of PD-L1 assays
(ii) different immunohistochemical commercially available antibody clones used among the different institutions
(iii) different scoring algorithms evaluating PD-L1 positivity in tumor cells (TCs) and/or in immune cells (ICs) separately or in combination (combined positive score, CPS)
(iv) use of different cutoffs
(v) possible intratumoral heterogeneity of PD-L1 expression
- An adequate immunohistochemical PDL1 evaluation should consider positive (lung macrophages, placental, spleen, and tonsil) and negative controls (alveolar cells, hepatocytes, and normal squamous epithelium)
- In particular, in EC, it seems that CPS has shown methodological advantages over cell type-specific scoring systems (TPS and ICS)

FIGO grade and other clinicopathological factors (17). According to the recent ESGO/ESTRO/ESP guidelines, all POLEmut carcinomas up to FIGO stage II, regardless of FIGO grade, histotype, or LVSI, are included in the low-risk group and could be managed by observation alone, with no need for adjuvant treatment (7).

For the very high immunogenicity (abundance of pre-existing tumor-antigen-restricted CD8+T-cells), with upregulation of immune checkpoint and other immunosuppressive genes, the POLEmut ECs together with MSI ECs, as "hot tumors", are promising candidates for checkpoint blockade immunotherapy, being considered the best molecular types that can respond to anti-PD-1/PDL1 treatment (16). They may also be sensitive to treatment with nucleoside analogs as they increase the mutation burden to a level where tumor cells are not viable.

TABLE 8 | HER2: comments from the working group.

Comments
- Consider HER2 testing in advanced/recurrent endometrial serous carcinoma and in the mixed forms with serous component
- In mixed carcinomas, HER2 testing should be performed on a tissue block containing the highest amount of serous component
- For other high-grade histologies, we propose to introduce HER2 testing only with a scientific intent
- The first method for HER2 testing is represented by HER2 IHC
- Molecular reflex test (FISH/SISH) is indicated in case of equivocal (2+) IHC results
- Standardize pre-analytical and analytical protocol of testing
- IHC can be performed on biopsies or surgical specimens if available, preferring the best-preserved sample as first choice
The main advantages of performing IHC on biopsies are the following:
(i) the better degree of fixation of biopsies
(ii) the early knowledge of HER2 status in a pre-operative setting
The main advantages of performing IHC on surgical sample are the following:
(i) larger amount of tumoral representative tissue
(ii) the possibility to select the best specimen for IHC testing
(iii) the possibility to overcome tumor heterogeneity

Pathological Features

Typical histopathological features of a POLE mut ECs are as follows:

- endometrioid histotype
- high grade, with foci demonstrating severe nuclear atypia and giant cells
- high mitotic index
- abundance in tumor-infiltrating lymphocytes (TILs) and/or peritumoral lymphocytes
- morphological heterogeneity and ambiguity
- substantial LVSI
- subclonal p53 at immunohistochemistry (IHC)

Interpretation Issues

Currently, there is no surrogate markers for POLE mutation and targeted sequencing for the common mutations or whole genome or panel testing must be used (mutation analysis of the exonuclease domain of POLE exons 9, 11, 13, 14). Not all POLE mutations impact prognosis as nearly all (>95%) POLE mutations outside the exonuclease domain are not associated with a ultramutated phenotype, and part of the mutations inside the exonuclease domain are not pathogenetic (18). For the five most common POLE mutations (P286R, V411L, S297F, A456P, and S459F), pathogenicity (in this sense meaning causal for tumor ultramutation) has been confirmed (18); however, the classification of other, less frequent POLE variants is currently challenging and variants of unknown significance (VUS) include the following: A465V, L424V, T278M, and A428T (18).

DEFECTIVE DNA MISMATCH REPAIR COMPLEX AS SURROGATE OF MICROSATELLITE INSTABILITY

Clinical Definition and Therapeutical Implications

MMR is a highly conserved protein complex for recognizing and repairing erroneous short insertion, short deletion, and misincorporation/mismatches of bases that can arise during DNA replication and recombination, as well as repairing some forms of DNA damage. The most important MMR players include MLH1 (mutL homologue 1), MSH2 (mutS homologue 2), MSH6 (mutS homologue 6), and PMS2 (postmeiotic segregation increased) (19).

These four proteins function in heterodimers: MLH1-PMS2 and MSH2-MSH6 43,44 (where MLH1 and MSH2 are obligatory partners of these heterodimers) (20, 21). An alteration in MLH1 and MSH2 results in subsequent proteolytic degradation of the mutated protein and its secondary partner (21). Conversely, mutations in secondary PMS2 or MSH6 may not result in proteolytic degradation of their primary partners, as MSH6 can be substituted in the heterodimer by MSH3, and PMS2 by PMS1 or MLH3. Consequently, the PMS2 antibody detects all cases that harbor either MLH1 or PMS2 abnormalities (22), and the MSH6 antibody detects all cases that harbor either MSH2 or MSH6 abnormality. MLH1 and MSH2 alone do not recognize cases with PMS2 or MSH6 abnormalities.

The inactivation of these genes (i.e., DMMR) can occur due to germline and/or somatic mutations or epigenetic silencing, resulting in the accumulation of frame-shift mutations (either through insertions or deletions) with a subsequent increased mutational burden, especially within repetitive stretches of DNA, called microsatellites (short tandem repeats, generally of a sequence that ranges from one to six bases), being distributed along the genome of both coding and non-coding regions and particularly sensitive to DNA mismatching errors during DNA replication or iatrogenic damage; this manifests as microsatellite instability (MSI). Thus, MSI is a condition of genetic hypermutability resulting from defective DNA MMR, and the two terms are often used interchangeably (22).

Germline mutation(s) of the MMR genes is the hallmark of constitutional mismatch repair deficiency (CMMRD) (23). CMMRD is due to a biallelic MMR gene mutation in which MMR defects are inherited from both parents. Mutations occur in well-characterized MMR genes including MLH1, PMS2, PMS1, MSH2, and MSH6 (24). This leads to a rare childhood cancer predisposition syndrome with recessive inheritance. The spectrum of CMMRD tumors is broad and CDMMR patients possess a high risk of multiple cancers, including hematological, brain, and intestinal tumors (25).

Lynch syndrome (LS) is an autosomal dominant disorder resulting from:

- constitutional germline mutations, affecting the DNA MMR genes MLH1, MSH2, MSH6, and PMS2
- constitutional MLH1 methylation
- 3' end truncating EPCAM deletion, causing allele-specific epigenetic silencing of the neighboring DNA mismatch repair gene MSH2 and subsequent hypermethylation of its CpG island promoter in tissues expressing EPCAM (26). In this context cancers can arise in the colo-rectum, endometrium, ovary, stomach, small bowel, gallbladder, hepatobiliary tract, pancreas, renal pelvis and/or ureter, bladder, kidney, brain, or prostate. Generally, the MLH1 variant is correlated with the highest risk of colorectal cancer, while the MSH2 variant is correlated with the highest risk of other cancers. ECs occurring in this setting represent 3%–5% of cases and often arise in younger women (45–55 years). EC is the index cancer in slightly more than 50% of cases.

Also, a substantial proportion (25%–30%) of non-LS endometrial carcinomas (sporadic ECs) have dMMR (27). Most are due to:

- sporadic somatic biallelic hypermethylation of the MLH1 gene promoter
- two somatic mismatch repair gene mutations

- one somatic mutation with LOH of the other allele
- alternatively, secondary epigenetic silencing of MSH6 is observed after neoadjuvant radio-chemotherapeutic treatments (28, 29).

Clinical and Pathological Associated Features

The MSI/hypermutated group is characterized by a high mutational rate (18×10^{-6} mutations per megabase) and included both low-grade and high-grade EEC.

Clinically, regarding patients with dMMR ECs, their prognosis seems to consistently remain intermediate. In particular, in early-stage, low-grade EECs, which usually have a good prognosis, dMMR appears as a risk factor for relapses (30, 31). In high-grade EECs, generally characterized by an intermediate prognosis between low-grade EEC and non-endometrioid carcinomas, dMMR is similarly associated to an intermediate prognosis (32). In the dMMR group of EEC, both LVSI and deep myometrial invasion were found as independent prognostic factors, while a high FIGO grade was not (33). DMMR EECs with MLH1 promoter methylation seem to have a worse prognosis than dMMR EEC with the mutation of MMR genes (33), offering a possible substratification of the dMMR group.

In non-endometrioid carcinomas, which have a poor prognosis, dMMR is a favorable prognostic factor (34–38). So, it is possible to consider the DMMR group as an intermediate-risk group regardless of the histotype. An exception could be represented by undifferentiated/dedifferentiated EC (UEC/DEC), in which a loss of SWI/SNF proteins expression seems to be associated with aggressive behavior even in the case of a dMMR signature

Moreover, dMMR ECs are unlikely to respond to conservative hormonal treatment and show a high likelihood of lymphovascular space invasion justifying a sentinel or other nodal procedure, and have not shown significant survival benefit by a chemotherapeutical approach. On the other hand, they seem to respond well to radiotherapy.

From a pathological point of view, dMMR/MSI ECs are more frequently characterized by the following distinctive gross and histological features:

- Lower uterine segment origin
- Significant peritumoral and intratumoral infiltrating lymphocytes (≥40 TIL/10HPFs), with more CD8+, CD45RO+, and PD1+ T cells at the invasive margin in LS —endometrial cancers compared with sporadic dMMR endometrial neoplasms (39).
- Synchronous ovarian cancer (clear cell or endometrioid variants)
- Higher grade with undifferentiated component
- Phenotypic heterogeneity (defined as two morphologically distinct tumor populations)
- > LVSI
- > Deep myoinvasion
  (higher prevalence of MSH2 MSH6 loss in MELF+ EECs has also been reported) (40)
- > Stage

Thus, morphology can significantly improve the efficacy of dMMR/MSI detection, because pathologists, on the basis of peculiar histopathological features often associated with a genetic profile, could identify "sentinel case", with high suspicion for LS.

However, Mills et al. showed that more than half of the LS-related endometrial tumors (58%) did not have the classical pathological MSI tumor features (41). On this wave, pathological features are not always specific except for an endometroid histology and studies show contradicting results. In conclusion, to support a morphologic suspicion, in order to detect LS-related endometrial cancers, a universal screening is recommended.

Reasons for MMR Testing in EC

MMR screening/MSI testing has several important clinical implications:

- screening for LS: it is estimated that one in 250–300 people are affected by LS and EC is often the first or sentinel cancer and can precede subsequent cancers such as colorectal carcinoma by approximately a decade. The identification of LS in a family allows surveillance and preventive measures in order to reduce the mortality from subsequent LS-related cancers.
- histomolecular diagnosis of EC: the TCGA classification and the recent ESGO/ESTRO/ESP guidelines require MMR testing of all cases for identification of the hypermutated dMMR/MSI EC group, with important management implications;
- predictive testing: dMMR tumors are eligible for targeted treatment with immune checkpoint inhibitors and are also characterized by overexpression of PD-1/PD-L1 (42).

In particular, recently, anti-PD1 antibody dostarlimab (Jemperli) has been approved by EMA and FDA to treat patients with dMMR or MSI-high (MSI-H) recurrent or advanced EC that has progressed after platinum-based chemotherapy.

Laboratory Diagnostic Tests

Detection of dMMR can be carried out by IHC for the MMR proteins or through MSI testing. The two methods have comparable sensitivity and show approximately 96% concordance.

MMR protein IHC is the highly accurate surrogate of MSI molecular testing in EC. It is the recommended test to assess the presence or absence of MLH1, PMS2, MSH2, and MSH6 (alone or in combination with MSI testing) (**Supplementary Figure**). IHC analysis is usually preferred over MSI testing, for the following advantages:

- it is cheaper
- it has a lower turnaround time

- it is easily available
- it needs only a limited amount of tissue (i.e., 4 tissue slides)
- it is amenable to IHC external quality assurance schemes
- it allows correlation with morphology
- it enables the rapid identification of the defective protein, thus guiding downstream testing

Although a combination of only two antibodies MSH6 and PMS2 may reduce the cost without a significant decrease in the diagnostic accuracy as proposed by some paper, we discourage the use of a two-antibody (i.e., PMS2 and MSH6) approach (21). MMR protein expression in normal tissues is seen as nuclear staining, with uniform or variable intensity, according to the proliferative cell activity. In cancer cells, generally characterized by higher proliferation rates than normal tissue, the staining intensity is typically stronger and higher than that seen in the background stroma, normal glands, or inflammatory cells (internal control). Nuclear expression of all 4 mismatch repair proteins on IHC suggests MSS. Loss of nuclear staining for any of the proteins with an internal positive control indicates MSI.

There are 4 typical abnormal MMR IHC patterns:

i. loss of both MLH1 and PMS2; this occurs in MLH1 deficiency (mutation/methylation)
ii. loss of both MSH2 and MSH6; this occurs in MSH2 deficiency (mutation)
iii. isolated loss of MSH6; this occurs in MSH6 somatic deficiency
iv. isolated loss of PMS2; this occurs in PMS2 somatic deficiency

It is important to note that MMR IHC loss with absence of MLH1 promoter methylation does not equate to LS, and only about half of the cases will be proven to have an inherited defect. The majority of these occur due to biallelic somatic loss of an MMR protein (27).

Problems and Pitfalls in MMR IHC Interpretation

IHC can be considered valuable only in presence of a well-identifiable positive internal control (background stroma, normal glands, or inflammatory cells).

However, in some instances, a pathologist could run into the following problems or diagnostic pitfalls (43) (**Supplementary Table**):

- MMR IHC is very fixation-sensitive. Poorly fixed areas typically show negative staining in the absence of stromal staining, with a gradual decrease of intensity from positive areas. It is necessary that well-fixed areas are examined when reporting MMR IHC, to avoid erroneous interpretation. For this reason, MMR IHC should be carried out on better-preserved samples (biopsies or surgical samples). When the testing is performed in a preoperative setting, there is the added advantage that this molecular information is available at the time of EC diagnosis.

- Very weak/very focal expression may be seen in the presence of DMMR. As already stated, the expression of MMR proteins is generally strong and diffuse compared to the internal control, so that any deviation from this, including very weak/focal expression in the presence of an unequivocal positivity in stromal cells, should be noted and reported either as defective or equivocal/indeterminate. For example, weak focal/patchy immunoreactivity for MSH6 can be seen with MSH2 loss of expression/germline mutations. Repeating the staining on a different section or on biopsy specimen could solve some of these issues.
- Subclonal expression, defined as a focal loss of expression by tumor cells (at least 10% of the tumoral area, to assign tumor to the dMMR group); in order to distinguish it from variable expression as a result of a fixation artifact, normal staining must be seen in the internal control in the area showing expression loss in tumor cells. The cutoff of 10% is suggested to avoid reporting this pattern in cases where it is extremely focal and of unlikely clinical significance. Subclonal expression (generally subclonal MSH6 loss) is believed to occur as an acquired secondary (non-germline) defect, a "passenger mutation" arising from an underlying dMMR (in particular MLH1 defect) or in the presence of pathogenic POLE mutations. Subclonal MSH6 loss is sometimes accompanied by variable expression of MSH2. When subclonal MSH6 loss occurs with another defect, the reporting terminology should be as for the underlying defect. When subclonal MSH6 loss occurs as an isolated abnormality, this should be reported as abnormal as it may indicate an underlying germline abnormality, most likely in a gene other than MSH6. The behavior of these cases with regard to prognosis and responses to treatment is unknown.

- Punctate nuclear expression in a low proportion of MLH1 loss cases. This pattern should be reported as loss of expression and is thought to be a technical artifact, seen with the MLH1 (M1) clone (Roche Diagnostics)
- Cytoplasmic/dot-like/membranous staining should be reported as abnormal. It is possibly related to technical reasons
- Geographical loss of MLH1 and PMS2 due to heterogeneous hypermethylation within the tumor
- Loss of 3 or all proteins (total loss)
- Discordance or heterogeneity between MMR IHC and MSI:
  - MSS with loss of MMR protein expression due to MLH1 promoter hypermethylation or somatic MMR variants
  - MSI with retained/proficient MMR protein expression (6%–7%) due to POLE variants or determined by catalytically inactive mutated MMR proteins (missense mutation) that retain their antigenic integrity

MSI testing is based on PCR amplification of microsatellite markers. The pentaplex panel of five poly-A mononucleotide repeats (BAT-25, BAT-26, NR-21, NR-24, and NR-27) is the recommended panel given its higher sensitivity and specificity (44). Historically, loss of stability in 1 of the five microsatellite markers was defined as MSI-low and loss of stability in ≥2 as MSI-high. Currently, MSI-low tumors should be included within MSS tumors (45).

In selected experienced centers, NGS can represent an alternative novel molecular test to assess MSI, especially in non-Lynch-associated tumors (46), with the main advantage consisting in coupling MSI analysis with the determination of tumor mutational burden (TMB), along with other possibly targetable alterations.

Subsequent testing for MLH1 hypermethylation in order to identify a MLH1/PMS2-negative tumor as sporadic and (in the absence of a germline mutation) somatic mutations should be used to further evaluate the risk of subsequent cancers

P53 IHC AS SURROGATE OF TP53 MUTATION

Clinical Definition and Therapeutical Implications

p53 protein was discovered in 1979 as a 53-kilodalton protein from SV40 transformed cells (47) and was recognized as a tumor suppressor protein in 1992 (48). Mainly acting as a transcriptional factor, it plays important roles in the regulation of cell proliferation, DNA repair, apoptosis, genomic stability, senescence, and metabolic homeostasis (49). When DNA is damaged, p53 induces the expression of p21, a cyclin-dependent kinase (CDK) inhibitor that suppresses cyclin–CDK complexes, resulting in cell cycle arrest in the G1 phase, in this way allowing DNA repair before replication at S1 (50, 51). If the cells cannot repair the DNA damage, p53 induces apoptosis by activating apoptosis signal genes, such as BAX, PUMA, Noxa, and PERP (52). Loss of p53 function allows abnormal cell dysregulated proliferation, and this phenomenon is closely associated with carcinogenesis. Dysfunction of p53 has been observed in many malignant tumors (53, 54), mainly due to the inactivation of p53 protein by binding proteins or TP53 mutations. Majority of p53 mutations in cancer are missense mutations, leading to the expression of full-length mutant p53 (p53abn) protein. Many tumor-associated p53abn proteins not only lose the tumor-suppressive function of wild-type p53 but also gain new activities to promote tumorigenesis and tumoral progression, termed gain of function.

In endometrial cancer, the copy-number high/serous-like group is characterized by low mutational rate (2.3×10^{-6} mutation per megabase) but extensive SCNA somatic copy-number alteration (SCNA), with TP53 mutation in 90% of cases (17).The copy-number high/serous like group mainly includes high-grade tumors, in particular SECs and UCSs. Although accounting for only 15% of all ECs, it is responsible for 50%–70% of endometrial cancer mortality, showing a poor outcome in all histotypes and justifying the classification of all carcinomas with a p53abn phenotype in the high-risk category irrespectively of other factors (30, 38, 55, 56). However, prognostic differences between different histotypes may still exist, due to the simultaneity of other unfavorable clinicopathological factors (57).

For instance, p53abn SC might be more aggressive than p53abn EEC and p53abn CC-EC but less aggressive than p53abn UCS (58), but until now, it is not well known if these differences can justify different types of clinical treatment. Moreover, we have to remember that also a small percentage (2%–5%) of low-grade EECs shares TP53 mutations, exhibiting a mutation-type immunoreactivity.

Recent evidence has shown improved survival outcomes with the addition of chemotherapy compared with radiation alone in p53abn ECs. Targeted therapy for p53abn ECs also exists with a proportion of p53abn ECs known to have homologous recombination deficiency (HRD), DNA damage, high PARP-1 expression, or human epidermal growth factor 2 (HER2) overexpression/amplification (see later in the text). In fact, PARP inhibitors and anti-HER-2 targeted therapy with trastuzumab have shown promising results in these tumors (59).

Immunohistochemical Interpretation

Only a validated optimized laboratory protocol including appropriate "high expressor" positive control (HGSC), low-expressing (e.g., tonsil), and negative control tissues (colon) together with a correct pathological interpretation of p53 immunohistochemical staining are fundamental to achieve high diagnostic accuracy in predicting the presence of TP53 mutation and to obtain high interlaboratory concordance (60).

A 4-tier system (61, 62), recommended for p53 IHC interpretation, in the presence of a well-recognizable positive internal (non-neoplastic cells such as lymphocytes, fibroblasts, or endothelial cells) consists of:

1. abnormal/aberrant/mutation type—overexpression: diffuse and uniformly strong nuclear expression of p53 in virtually 100% of tumor cell nuclei in a well-fixed case and at least 75% of tumor cell nuclei in a less well-fixed case, generally due to non-synonymous missense mutations
2. abnormal/aberrant/mutation type—complete absence, due to nonsense mutations
3. abnormal/aberrant/mutation type—cytoplasmic expression (with a variable nuclear staining), generally associated to loss-of-function mutations disrupting the nuclear localization domain of p53
4. normal—wild type: nuclear p53 expression is observable in <80% of cells and/or with variable intensity, in absence of TP53 mutation, but we have to keep in mind that in about 5% of cases, a mutator genotype due to some splice site mutations or truncating mutations can also result in detectable, nonfunctional p53 protein with a wild-type staining pattern.

Cases without a positive internal control must be reported as uninterpretable.

Problems and Pitfalls in p53 IHC Interpretation

- Wild-type different grading: depending on the cellular differentiation and the proliferative activity, the normal wild-type pattern can show a wide range of staining, from only very few scattered tumor cell nuclei positive (low wild-type) to the majority of nuclei being positive (high wild-type).

- Heterogeneous p53 expression/subclonal TP53 mutation: a proportion of G3 EEC or ambiguous carcinomas with an ultramutated or hypermutated genotype (either POLEmut or DMMR) can acquire a TP53 mutation later in the tumoral course, developing a subclonal TP53 mutation that may result in heterogenous p53 expression, with a combination of normal wild-type and abnormal patterns (overexpression and/or 'null' phenotype and/or cytoplasmic staining). In these cases (generally defined multiple classifiers, as DMMR/p53abn ECs—64%; POLEmut/p53abn ECs—31%), an experienced gynecopathologist together with an optimized immunohistochemical protocol are necessary to assess such patterns (63), differentiating them from mixed cancers or from the possibility of a "wild-type variability" and "p53 mosaic patterns". We retain that in case the morphologic features suggestive of POLE mutations (see later in the text) are present and p53 staining pattern is abnormal, it may be useful to repeat the stain on a different tumor section.
- Mosaic patterns of p53: generally due to preanalytical factors (delayed fixation with antigen degradation) or to rare molecular alterations (splice site mutation or low allelic frequency of TP53 mutation in some tumor areas) that determine variable intensity of the staining (some staining strong, some moderate, some weak, few negative).
- Nonspecific nuclear blush due to technical artifacts, could be misinterpreted as wild type in cases of true complete absence.
- Nonspecific cytoplasmic blush due to technical artifacts, could be misinterpreted as p53abn. It represents an equivocal blush, which may be ignored.
- Mixed abnormal patterns (complete absence and overexpression) indicating either different clonal origin or tumor progression with acquisition of a different type of TP53 mutation.
- p53 overexpression in a subset of EECs (without an underlying mutation) can be explained by dysregulation of other factors such as ERβ and MDM2.

NO SPECIFIC MOLECULAR PROFILE SURROGATE OF THE COPY NUMBER LOW/ENDOMETRIOID GROUP

The copy-number-low/endometrioid group is characterized by low mutational rate (2.9×10^{-6} mutations per megabase), with no specific molecular profile (NMSP; no MSI or POLE mutations) and with a low degree of somatic copy-number alteration (SCNA, no p53 mutations) (17). Consistently lacking of molecular signatures, the NSMP also lacks a univocal prognostic significance.

Generally, the NSMP group shows a good-to-intermediate prognosis in low-grade EEC, an intermediate outcome in high-grade EEC, and poor prognosis in non-endometrioid carcinomas (30, 32, 35, 37, 38, 56).

The NSMP group may further be stratified based on histological (i.e., tumor grade and histotype, LVSI, depth of myometrial invasion), immunohistochemical (i.e., L1CAM expression), or molecular (i.e., CTNNB1 mutation) features (64).

Beta-Catenin as a Surrogate of CTNNB1 Mutation?

Beta-catenin is a multifunctional protein expressed on the surface of epithelial cells, acting as a structural component of the E-cadherin-related cell adhesion system (65). This molecule has a crucial role in maintenance of epithelial stability by regulating cell growth and intercellular adhesion. Beta-catenin also plays other important functional roles, including control of cell polarization, differentiation, "stemness," and cell motility (66). At the cellular level, beta-catenin is the key mediator of the Wnt canonical pathway (67, 68). Constitutive activation of the Wnt signaling is a major etiological factor for many cancers (69, 70).

In the resting state of Wnt signaling, beta-catenin is phosphorylated by glycogen synthase kinase 3ββ (GSK3-β) within a protein complex including casein kinase 1, adenomatous polyposis coli (APC), and Axin. Phosphorylated beta-catenin is immediately degraded *via* the ubiquitin–proteasome pathway. In the active state, WNT binds to Frizzled (Fz), activating (Dsh), which inhibits the activity of GSK3-β, resulting in dephosphorylation and stabilization of beta-catenin, in this way enabling accumulation within the nucleus. A stable beta-catenin translates WNT signal into the transient transcription of a TCF/LEF (T-cell factor/lymphocyte enhancer factor) gene program, governing cell fate, proliferation, and other processes in several types of cancer (71, 72). Stabilized molecule could be considered a cause of genomic instability, promoting tumor development and aggressiveness. Numerous studies have shown that CTNNB1, the gene of beta-catenin, together with APC and Axin are frequently mutated in different types of human cancers and that the nuclear accumulation of beta-catenin could be considered the final step of constitutive activation of WNT signaling (73).

In particular, in EC, it has been described that a subset of low-grade, early-stage EECs (about 50% of NSMP EECs and almost 20% of all ECs) can harbor CTNNB1 exon 3 mutations, and when this happens, prognosis in terms of OS and recurrence-free survival is worse (31, 70, 74), overall intermediate, although their frequent clinic–pathological characteristics are commonly associated with lower risk of recurrence (younger age, squamous differentiation, low TILs, less incidence of deep myometrial invasion, and less incidence of LVSI, with a low number of other concurrent mutations, such as KRAS and FGFR2 mutation) (64).

Nuclear accumulation of beta-catenin, well detectable by immunohistochemistry, has been assessed as a possible surrogate for sequencing to identify CTNNB1-mutant cases, resulting in conflicting data, varying from an overall good agreement between protein nuclear staining and CTNNB1 status (70, 75, 76) to high discordance.

It seems that nuclear accumulation of beta-catenin in EEC implies the presence of CTNNB1 mutation, but not *vice versa* (76, 77). Furthermore, no standardized criteria for interpretation of beta-catenin immunostaining have been defined in order to consider its expression normal vs. aberrant. It seems that even a minimal percentage of beta-catenin positive nuclei should be

considered significant, while only a nuclear expression being at least moderate should be considered of diagnostic significance.

Finally, in most cases, nuclear beta-catenin in EEC is limited to the morular metaplasia foci, not present in all CTNNB1-mutant cases and not clearly correlated to prognosis (76–79).

MULTIPLE MOLECULAR CLASSIFIERS AND INTERPRETATION ISSUES

Multiple classifier EC is defined as a tumor harboring more than one molecular classifying feature:

- dMMR/p53abn
- POLE mut/p53abn
- dMMR/POLE mut/p53abn
- dMMR/POLE mut

The simultaneous presence of two or three molecular signatures is encountered in 3% of ECs and outcomes correspond to those predicted by the driver molecular subtype; in particular, the POLEmut signature, when characterized by a pathogenic status, prevails over the other signatures, conferring a good prognosis regardless of MMR and p53 status, while the dMMR signature prevails over the p53abn signature (18). These findings support:

- the classification of tumors with a pathogenic POLE EDM and dMMR and/or p53abn as single classifier POLEmut ECs
- the classification of tumors with a wild-type POLE and dMMR and/or p53abn as single classifier DMMR
- the classification of tumors with a dMMR and p53abn as single classifier DMMR ECs

In this way, in the context of dMMR EC or POLEmut ECs, passenger secondary events such as the occurrence of TP53 mutation, do not affect biological behavior and should not prompt intensified treatment.

OPEN QUESTIONS AND PERSPECTIVES FROM THE CONSENSUS PANEL

Hormonal Receptor Status

Clinical Definition and Immunohistochemical Interpretation

ER and PR belong to the superfamily of steroid receptors, regulating the hormonal activity in the different phases of the endometrial cycle (80). Binding to its ligand, the hormonal receptor leads to translocation of the ligand–receptor complex to the nucleus where receptor dimers bind specific hormone-responsive DNA elements of target genes (81). In the endometrium, estrogen determines proliferation, while progesterone inhibits estrogen-induced endometrial proliferation (82).

The nuclear presence of ER and PR in tumor tissue is routinely evaluated by IHC in different organs, and also in pathological–neoplastic conditions. Immunohistochemical loss of ER and PR expression in tumor tissue is associated with a higher risk of node metastases and poor prognosis (reduced disease-free survival and disease-specific survival) and with poor response to hormonal therapy (63, 83–86). Scoring systems, based on percentage alone or on combinations of percentages and intensity of staining are used frequently (87–89), although the percentage score has been retained more relevant than staining intensity scores as confirmed by recent studies (90, 91).

However, the cutoff value for ER and PR positivity with the strongest prognostic value for clinical outcome in EC is still unclear (83, 90, 92). Over time, different cutoff values have been proposed: 1% or 10% of positive tumor nuclei, or a staining-intensity index of 3 (on a 0–9 scale) (87, 93–97).

Recently, the ENITEC collaboration study has proposed an EC-specific classification for ER and PR expression categorized into three groups: a high-risk group–low HR expressing (ER/PR expression: 0%–10%), with unfavorable outcome (5-year DSS 75.9%–83.3%); an intermediate-risk group (ER/PR expression: 20%–80%) with intermediate outcome (5-year DSS 93.0%–93.9%); and a low-risk group–high HR expressing (ER/PR expression: 90%–100%) with a favorable outcome (5-year DSS 97.8%–100%). In this study, at the first cutoff value of 10%, ER had a higher specificity, indicating that ER ≤10% is more able to identify high-risk cases; at the cutoff value of 80%, PR had a higher sensitivity, suggesting that PR is more able to identify a low-risk population (98). Contradictory results regarding the prognostic value of ER/PR expression within TGCA molecular subgroups have been reported, due to application of multiple cutoff values for ER/PR expression (64, 99)

L1CAM as a Tool to Further Clinically Stratify NMSP EECs?

L1, also known as L1CAM, is a transmembrane cell surface glycoprotein member of the L1 protein family, encoded by the L1CAM gene, sited in the long arm of the X chromosome in Xq28 position. This protein, of 200-220 kDa, is a neuronal cell adhesion molecule with important roles in cell migration, adhesion, and neuronal differentiation (100). It is normally expressed in neuronal and non-neuronal cells and also overexpressed in multiple tumor cells, making them more aggressive and chemo-resistant. In this way, this upregulation is associated with tumor progression, acquisition of EMT phenotype, and metastasis, causing poor prognosis (101–104).

Regarding EC, some authors have found significant association between L1CAM (>10%) and p53-mutant, both related to risk recurrence for EC patients (105). According to another recent work, L1CAM detection has been used as a surrogate of LVSI, and so lymph node involvement, with the advantage of also a possible preoperative evaluation (106).

Moreover, it has been demonstrated that L1CAM stratifies patients with NSMP: high L1CAM immunohistochemical expression (>10%) was associated to highly aggressive tumors, characterized by poor differentiation, NE histology, and worse prognosis independently from age of patients (higher risk of distant recurrences and pelvic lymph-node involvement) (107, 108).

PDL1

Definition and Therapeutic Implications

Programmed death-ligand 1 (PD-L1, CD247, or B7-H1) is one of the ligands of the programmed cell death 1 (PD-1) receptor, a dominant negative regulator of antitumor T-cell effector function (56). It is induced by inflammation and expressed by tumor microenvironment and tumor cells (20). The blockade of the PD-1–PD-L1 binding by the use of selected specific antibodies has become a novel therapeutic tool in tumors overexpressing PD-L1 or in tumors with activated T-cell immunoresponse and high tumoral mutation burden. Anti-PD-1/PD-L1 therapies determine T-cell proliferation and infiltration into the tumoral area, promoting an increased cytotoxic T-cell response, leading to an evident tumor response (109, 110).

Regarding EC, since the high mutational load and abundance in neoantigens, the POLEmut and DMMR groups are considered optimal candidates to respond to anti-PD-1/PDL1 treatment (immune checkpoint blockade therapy) and the assessment of PDL-1 expression may be reasonable in these tumors (42, 111).

The recent ESGO/ESTRO/ESP guidelines of EC have approved dMMR/MSI as the selection criteria for the second-line standard of care anti-PD-1/PD-L1 immune therapy with pembrolizumab. In MMR stable ECs, a combined second-line therapy consisting of pembrolizumab+lenvatinib, a multi-tyrosine kinase inhibitor, could be considered as a possible option (7).

Clinical and Pathological Associated Features

Regarding EC, considerable variations in PD-L1 positivity frequencies (from 0.9% to 44.3%) have been reported (16, 112–123). Moreover different PD-L1 expression profiles between molecular subclasses, histologic subtypes, and tumoral stage have been described, with the POLE mutant, the dMMR, the non-endometrioid types, and the advanced endometrial cancers displaying the highest PD-L1 levels in TCs and ICs, and CPS (111).

Regarding the association between PDL1 and prognosis, data are still unclear. Some authors showed that high PD-L1 in tumor cells (TCs) was associated with better OS and longer treatment-free interval (TFI) after primary chemotherapy in recurrent cases, whereas high PD-L1 in tumor-infiltrating immune cells (TICs) was associated with worse OS as well as MSI (124). On the other hand, a recent meta-analysis showed that in EC, PD-L1 expression seems to be not associated with poor prognosis (OS and PFS), while it is positively correlated with poor differentiation and advanced tumor stage (125).

HER2

Her2 (human epidermal growth factor receptor 2) or HER2/neu, also known as receptor tyrosine-protein kinase erbB-2, or CD340, or ERBB2, is an oncogenic protein encoded by the ERBB2 proto-oncogene, located at the long arm of human chromosome 17 (17q12) (126). It is a member of the human epidermal growth factor receptor (HER/EGFR/ERBB) family that is involved in the activation of different signaling pathways, such as mitogen-activated protein kinase (MAPK), phosphoinositide 3-kinase (PI3K/Akt), protein kinase C (PKC), and signal transducer and activator of transcription (STAT), generally promoting cell proliferation and inhibiting the apoptosis process (127). Normal tissues have a low complement of HER2 membrane protein. Its amplification/overexpression plays an important role in the development and progression of 15%–30% of breast cancers and 7%–34% of gastric cancers, conferring worse biological behavior and clinical outcome (128), although the protein has become an important biomarker for targeted molecular therapy (129).

Over-expression also occurs in approximately 25% to 30% of endometrial serous carcinomas, with over 50% of HER2-positive tumors showing marked intratumoral HER2 immunohistochemical or genic heterogeneity (130).

With particular regard to endometrial serous carcinoma, nowadays there is a growing demand for new-targeted therapies for this aggressive tumor type, characterized by the highest recurrence rate and considered responsible for 40% of endometrial cancer mortality, with an overall 5-year survival rate of only 45% (131–133).

Recently, promising clinical results have been obtained from a multi-institutional, randomized phase 2 clinical trial, demonstrating that the addition of trastuzumab to standard chemotherapy resulted in significant improvement in progression-free and overall survival in HER2-positive advanced stage and recurrent endometrial serous carcinoma (59). This therapeutical approach limited to serous tumor subtype, either pure or as a component of mixed EC, was endorsed by the National Comprehensive Cancer Network (NCCN) Uterine Neoplasm Guidelines (134). On this wave, the pathologic testing and scoring of tumoral HER2 protein expression and gene amplification may be considered a critical part of patient selection for this type of targeted therapy.

It is well known that distinct characteristics of HER2 protein expression and gene amplification can be observed in different tumors of different organ systems (135, 136). Thus, similarly to breast and gastric cancer, based on evidence from the recent successful clinical trial and 2 comprehensive pre-trial pathologic studies (137, 138), a new set of HER2 testing algorithm and scoring criteria have been proposed for routine pathological evaluation of endometrial serous carcinoma. Scoring categories have been classified as follows (139–141) (**Figure 4**):

- 0 HER2 NEGATIVE: No staining in tumor cells
- 1+ HER2 NEGATIVE: Faint/barely perceptible, incomplete membrane staining in any proportion, or weak complete staining in <10% of tumor cells
- 2+ HER2 EQUIVOCAL: Strong complete or basolateral/lateral membrane staining in ≤30%, or weak to moderate complete or basolateral/lateral staining in ≥10% of tumor cells
- 3+ HER2 POSITIVE: Strong complete or basolateral/lateral membrane staining in >30% of tumor cells (modified 2007 American Society of Clinical Oncology/College of American Pathologists [ASCO/CAP] breast criteria).

FISH should be performed only on tumors with a 2+ immunohistochemical score on a large tumor area in direct

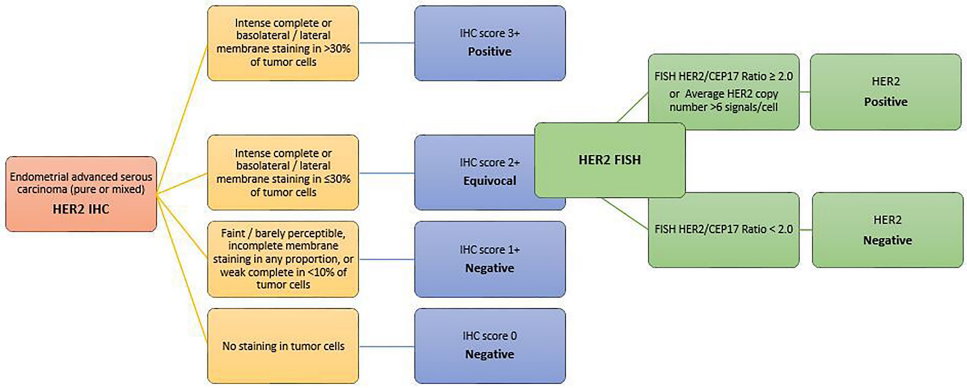


FIGURE 4 | HER2 scoring method in endometrial carcinomas A set of HER2 testing algorithm and scoring criteria have been proposed for routine pathological evaluation of endometrial serous carcinoma. Scoring categories have been classified according to the modified 2007 American Society of Clinical Oncology/College of American Pathologists [ASCO/CAP] breast criteria.

correlation with the HER2 immunostained slide, and a HER2/CEP17 ratio of ≥2.0 can be considered amplified. However, until more data become available to define whether HER2 amplification could be considered equal or superior to INC in predicting clinical therapeutical response, tumors with HER2/CEP17 ratio <2 and average HER2 copy number ≥6.0/nucleus should also be included in the HER2 amplified category.

Future studies are necessary to resolve a number of practical pathological issues.

Currently, there are only limited data available on optimal specimen type (biopsy versus hysterectomy) for HER2 testing in uterine serous cancer.

Recently, discordant HER2 status has also been observed between primary and metastatic endometrial tumors, in particular in heterogeneous cancers (142, 143).

Furthermore, another laboratory practical problem is represented by the optimal HER2 testing algorithm (IHC as primary test vs. FISH as reflex test), depending on the correlation between test type and therapeutic response.

Similarly to breast and gastric cancers, further clinicopathologic studies will be essential to define the pathological concept and the clinical impact of intratumoral heterogeneity and its correlation to therapeutic response (144). Only fewer data are available regarding HER2 positivity rates in early-stage endometrial serous carcinoma: only a recent study showed a statistically significant association between HER2 positivity and poor prognosis in terms of DFS and OS (145).

Finally, there is a strong clinical interest in expanding targeted HER2 therapy to other high-grade EC in the future, due to the recently identified similarities in HER2 protein expression/gene amplification between endometrial serous carcinoma and endometrial carcinosarcomas (146–148).

Preoperative Setting

Nowadays, an intriguing challenge is represented by the application and validation of TCGA classification in small diagnostic biopsies/endometrial curetting, in order to decide the adequate surgical/clinical approach. Recent studies suggest highly concordant results between diagnostic biopsies and hysterectomy specimens, in particular for MMR loss, MSI high, and p53 wild and aberrant types, in contrast to moderate levels of agreement reported for the classical histomorphological parameters (grade, histotype). In this way, in the setting of an adequate technical and medical training, with well-experienced professional figures and well-defined laboratory protocols, molecular classification preoperatively applied seems to provide earlier and more reliable prognostic information to guide clinical management (149).

The bioptical specimen, being immediately placed in formalin compared with hysterectomy specimens that may sit for several hours before processing, allows a better tissue fixation and a superior antigen preservation consequently may assure a more reproducible and adequate biological characterization (150) in cases in which endometrium on surgical sample is sub-optimally preserved for immunostains.

Other possible applications of molecular categorization on bioptical samples could consider the role of MSI status in predicting resistance to progestins for early-stage EECs and the overall unfavorable prognostic significance of MMR deficiency in conservatively treated EECs (151).

Nevertheless, the potential limit derived from the adoption of the molecular TGCA classification to small biopsies in daily practice could derive from the occurrence of intratumoral heterogeneity, with possible molecular discrepancies between the initial endometrial biopsy and the hysterectomy specimen.

Optimal Tissue Handling and Sectioning Requirements for Interlaboratory Reproducibility

The increasing clinical demand for a histomolecular approach in classifying ECs should prompt pathology laboratories to implement specific protocols for specimen handling and fixation. We must be aware that molecular and IHC testing can be affected by:

- Pre-analytical variables: specimen collection and handling, tissue fixation (uniformity, time, and type) and protocol of processing
- Analytical variables: choice of immunohistochemistry protocol, reagent variability, antigen retrieval technique, and technician training/expertise
- Post-analytical variables: evaluation of positive/negative controls, morphological correlations, diagnostic and prognostic significance, correlation with other data, interpretation and reporting of results, and experience/expertise of the pathologist.

The goal consists in ensuring reproducibility, obtaining high quality of stained sections with minimal inter-observer variability in the diagnostic report and in promoting inter-laboratory standardization, which are all synonyms of quality assurance. We retain that it can be achieved only by the application of automated systems (e.g., Ventana and Dako systems) and FDA-approved kits or validated laboratory platforms and tests (152, 153).

In particular:

- Time from tissue acquisition to fixation should be as short as possible (cold ischemia time of less than 1 h)
- Samples for molecular/IHC testing should be fixed in 10% neutral buffered formalin for 6–72 h for both endometrial biopsy and hysterectomy specimens
- Samples should be sliced at 5- to 10-mm intervals after appropriate gross inspection and margin designation and placed in a sufficient volume of neutral buffered formalin. Any exceptions to this process must be included in the report.
- Sections should ideally not be used for IHC testing if cut >6 weeks earlier; this may vary with primary fixation or storage conditions
- Optimal internal validation procedure of the test must be performed before test is offered

CONCLUSIONS

For the correct assignment of ECs to one of the 4 molecular subgroups, a correct interpretation of molecular and immunohistochemical data is fundamental.

Currently, there is no surrogate markers for POLE mutation, and targeted sequencing for the common mutations or whole genome or panel testing must be used.

In order to support a morphologic suspicion and/or to detect LS-related endometrial cancers, a universal screening is recommended for MMR testing in EC, with important management and therapeutical implications.

Similarly to MMR deficiency detection by IHC, a validated optimized laboratory protocol together with a correct pathological interpretation of p53 immunohistochemical staining are fundamental to achieve high diagnostic accuracy in predicting the presence of TP53 mutation, in this way selecting candidate patients for targeted therapy with PARP inhibitors.

Considering the NSMP group, it may be stratified based on histological (i.e., tumor grade and histotype, LVSI, and depth of myometrial invasion), immunohistochemical (i.e., L1CAM expression), or molecular (i.e., CTNNB1 mutation) features. Up-to-date contradictory results regarding the prognostic value of ER/PR expression within all the TGCA molecular subgroups have been reported.

Considerable variations in PD-L1 positivity frequencies have been reported and data regarding the association between PDL1 and prognosis are still unclear.

Based on the modified 2007 ASCO/CAP guidelines for breast cancer, a new set of HER2 testing algorithm and scoring criteria have been proposed for routine pathological evaluation of endometrial serous carcinoma, helping to select patients eligible for antiHER2 therapies.

Considering all these advances in the EC molecular landscape, we retain that, in the personalized medicine era, although molecular classification of ECs is going to open a new interesting scenario by introducing novel molecularly driven treatment choices for EC, pathology is still crucial for clinical management. In this new context, molecular classifiers should be combined with clinical risk groups and pathological parameters in an integrated histo-molecular approach, able to better discriminate outcomes for different patients.

AUTHOR CONTRIBUTIONS

All authors contributed to the study conception and design. AS, FI, AP, MF, and EB performed the literature search. FF, FC, GT, and AS performed data analysis. AS, GZ, and FI drafted and/or critically revised the work. All authors contributed to the article and approved the submitted version.

SUPPLEMENTARY MATERIAL

The Supplementary Material for this article can be found online at: https://www.frontiersin.org/articles/10.3389/fonc.2022.805613/full#supplementary-material

Supplementary Figure | Flow chart for Lynch Syndrome triage, by the use of IHC for 4 MMR proteins as a first choice test

REFERENCES

1. Lortet-Tieulent J, Ferlay J, Bray F, Jemal A. International Patterns and Trends in Endometrial Cancer Incidence 1978–2013. *J Natl Cancer Inst* (2017) 110:354–61. doi: 10.1093/jnci/djx214
2. WHO Classification of Tumours Editorial Board. *Female Genital Tumours. 5th ed* Vol. 4. Lyon: IARC (2020).
3. Murali R, Grisham RN, Soslow RA. The Roles of Pathology in Targeted Therapy of Women With Gynecologic Cancers. *Gynecol Oncol* (2018) 148 (1):213–21. doi: 10.1016/j.ygyno.2017.11.020

4. Cancer Genome Atlas Research Network, Kandoth C, Schultz N, Cherniack AD, Akbani R, Liu Y, et al. Integrated Genomic Characterization of Endometrial Carcinoma. *Nature* (2013) 497:67–73. doi: 10.1038/nature12113
5. Bae HS, Kim H, Kwon SY, Kim K-R, Song JY, Kim I. Should Endometrial Clear Cell Carcinoma Be Classified as Type IIEndometrial Carcinoma? *Int J Gynecol Pathol* (2015) 34:74–84. doi: 10.1097/PGP.0000000000000111
6. Colombo N, Creutzberg C, Amant F, Bosse T, González-Martín A, Ledermann J, et al. ESMO-ESGO-ESTRO Consensus Conference on Endometrial Cancer: Diagnosis, Treatment and Follow-Up. *Ann Oncol* (2015) 27:16–41. doi: 10.1093/annonc/mdv484
7. Concin N, Matias-Guiu X, Vergote I, Cibula D, Mirza MR, Marnitz S, et al. ESGO/ESTRO/ESP Guidelines for the Management of Patients With Endometrial Carcinoma. *Virchows Arch* (2021) 478:153–90. doi: 10.1007/s00428-020-03007-z
8. Bellido F, Pineda M, Aiza G, Valdés-Mas R, Navarro M, Puente DA, et al. POLE and POLD1 Mutations in 529 Kindred With Familial Colorectal Cancer and/or Polyposis: Review of Reported Cases and Recommendations for Genetic Testing and Surveillance. *Genet Med* (2016) 18(4):325–32. doi: 10.1038/gim.2015.75
9. Church DN, Briggs SE, Palles C, Domingo E, Kearsey SJ, Grimes JM, et al. DNA Polymerase and δ Exonuclease Domain Mutations in Endometrial Cancer. *Hum Mol Genet* (2013) 22(14):2820–8. doi: 10.1093/hmg/ddt131
10. Campbell BB, Light N, Fabrizio D, Zatzman M, Fuligni F, de Borja R, et al. Comprehensive Analysis of Hypermutation in Human. *Cancer Cell* (2017) 171(5):1042–56. doi: 10.1016/j.cell.2017.09.048
11. Church DN, Stelloo E, Nout RA, Valtcheva N, Depreeuw J, ter Haar N, et al. Prognostic Significance of POLE Proofreading Mutations in Endometrial Cancer. *J Natl Cancer Inst* (2014) 107(1):402. doi: 10.1093/jnci/dju402
12. Domingo E, Freeman-Mills L, Rayner E, Glaire M, Briggs S, Vermeulen L, et al. Somatic POLE Proofreading Domain Mutation, Immune Response, and Prognosis in Colorectal Cancer: A Retrospective, Pooled Biomarker Study. *Lancet Gastroenterol Hepatol* (2016) 1(3):207–16. doi: 10.1016/S2468-1253(16)30014-0
13. Rayner E, van Gool IC, Palles C, Kearsey SE, Bosse T, Tomlinson I. Church DNA Panoply of Errors: Polymerase Proofreading Domain Mutations in Cancer. *Nat Rev Cancer* (2016) 16(2):71–81. doi: 10.1038/nrc.2015.12
14. Erson-Omay EZ, alayan AO, Schultz N, Weinhold N, Omay SB, Özduman K, et al. Günel M Somatic POLE Mutations Cause an Ultramutated Giant Cell High-Grade Glioma Subtype With Better Prognosis. *Neuro Oncol* (2015) 17(10):1356–64. doi: 10.1093/neuonc/nov027
15. Temko D, Van Gool IC, Rayner E, Glaire M, Makino S, Brown M, et al. Tomlinson I Somatic POLE Exonuclease Domain Mutations are Early Events in Sporadic Endometrial and Colorectal Carcinogenesis, Determining Driver Mutational Landscape, Clonal Neoantigen Burden and Immune Response. *J Pathol* (2018) 245(3):283–96. doi: 10.1002/path.5081
16. Eggink FA, Van Gool IC, Leary A, Pollock PM, Crosbie EJ, Mileshkin L, et al. Immunological Profiling of Molecularly Classified High-Risk Endometrial Cancers Identifies POLE-Mutant and Microsatellite Unstable Carcinomas as Candidates for Checkpoint Inhibition. *Oncoimmunology* (2016) 6(2):e1264565. doi: 10.1080/2162402X.2016.1264565
17. Santoro A, Angelico G, Travaglino A, Inzani F, Arciuolo D, Valente M, et al. New Pathological and Clinical Insights in Endometrial Cancer in View of the Updated ESGO/ESTRO/ESP Guidelines. *Cancers* (2021) 13:2623. doi: 10.3390/cancers13112623
18. León-Castillo A, Britton H, McConechy MK, McAlpine JN, Nout R, Kommoss S, et al. Interpretation of Somatic POLE Mutations in Endometrial Carcinoma. *J Pathol* (2020) 250:323–35. doi: 10.1002/path.5372
19. Boland CR, Goel A. Microsatellite Instability in Colorectal Cancer. *Gastroenterology* (2010) 138(6):2073–87 e3. doi: 10.1053/j.gastro.2009.12.064
20. Fassan M, Scarpa A, Remo A, De Maglio G, Troncone G, Marchetti A, et al. Current Prognostic and Predictive Biomarkers for Gastrointestinal Tumors in Clinical Practice. *Pathologica* (2020) 112(3):248–59. doi: 10.32074/1591-951X-158
21. Luchini C, Bibeau F, Ligtenberg MJL, Singh N, Nottegar A, Bosse T, et al. ESMO Recommendations on Microsatellite Instability Testing for Immunotherapy in Cancer, and Its Relationship With PD-1/PD-L1 Expression and Tumour Mutational Burden: A Systematic Review-Based Approach. *Ann Oncol* (2019) 30:1232–43. doi: 10.1093/annonc/mdz116
22. Ma J, Setton J, Lee NY, Riaz N, Powell SN. The Therapeutic Significance of Mutational Signatures From DNA Repair Deficiency in Cancer. *Nat Commun* (2018) 9:3292. doi: 10.1038/s41467-018-05228-y
23. Galuppini F, Opocher E, Tabori U, Mammi I, Edwards M, Campbell B, et al. Concomitant IDH Wildtype Glioblastoma and IDH1-Mutant Anaplastic Astrocytoma in a Patient With Constitutional Mismatch Repair Deficiency Syndrome. *Neuropathol Appl Neurobiol* (2018) 44:233–9. doi: 10.1111/nan.12450andofLynchsyndrome
24. Abedalthagafi M. Constitutional Mismatch Repair-Deficiency: Current Problems and Emerging Therapeutic Strategies. *Oncotarget* (2018) 9(83):35458–69. doi: 10.18632/oncotarget.26249
25. Wimmer K, Kratz CP, Vasen HF, Caron O, Colas C, Entz-Werle N, et al. Diagnostic Criteria for Constitutional Mismatch Repair Deficiency Syndrome: Suggestions of the European Consortium 'Care for CDMMR' (C4CDMMR). *J Med Genet* (2014) 51:355–65. doi: 10.1136/jmedgenet-2014-102284
26. Li X, Liu G, Wu W. Recent Advances in Lynch Syndrome. *Exp Hematol Oncol* (2021) 10:37. doi: 10.1186/s40164-021-00231-4
27. Leclerc J, Vermaut C, Buisine MP. Diagnosis of Lynch Syndrome and Strategies to Distinguish Lynch-Related Tumors From Sporadic MSI/dMMR Tumors. *Cancers (Basel)* (2021) 13(3):467. doi: 10.3390/cancers13030467
28. Indraccolo S, Lombardi G, Fassan M, Pasqualini L, Giunco S, Marcato R, et al. Genetic, Epigenetic, and Immunologic Profiling of MMR-Deficient Relapsed Glioblastoma. *Clin Cancer Res* (2019) 25:1828–37. doi: 10.1158/1078-0432.CCR-18-1892
29. Bao F, Panarelli NC, Rennert H, Sherr DL, Yantiss RK. Neoadjuvant Therapy Induces Loss of MSH6 Expression in Colorectal Carcinoma. *Am J Surg Pathol* (2010) 34:1798–804. doi: 10.1097/PAS.0b013e3181f906cc
30. Bosse T, Nout RA, McAlpine JN, McConechy MK, Britton H, Hussein YR, et al. Molecular Classification of Grade 3 Endometrioid Endometrial Cancers Identifies Distinct Prognostic Subgroups. *Am J Surg Pathol* (2018) 42:561–8. doi: 10.1097/PAS.0000000000001020
31. Moroney MR, Davies KD, Wilberger AC, Sheeder J, Post MD, Berning AA, et al. Molecular Markers in Recurrent Stage I, Grade 1 Endometrioid Endometrial Cancers. *Gynecol Oncol* (2019) 153:517–20. doi: 10.1016/j.ygyno.2019.03.100
32. Joehlin-Price A, Van Ziffle J, Hills NK, Ladwig N, Rabban JT, Garg K. Molecularly Classified Uterine FIGO Grade 3 Endometrioid Carcinomas Show Distinctive Clinical Outcomes But Overlapping Morphologic Features. *Am J Surg Pathol* (2021) 45:421–9. doi: 10.1097/PAS.0000000000001598
33. Pasanen A, Loukovaara M, Bützow R. Clinicopathological Significance of Deficient DNA Mismatch Repair and MLH1 Promoter Methylation in Endometrioid Endometrial Carcinoma. *Mod Pathol* (2020) 33:1443–52. doi: 10.1038/s41379-020-0501-8
34. Conlon N, Da Cruz Paula A, Ashley CW, Segura S, De Brot L, da Silva EM, et al. Endometrial Carcinomas With a "Serous" Component in Young Women Are Enriched for DNA Mismatch Repair Deficiency, Lynch Syndrome, and POLE Exonuclease Domain Mutations. *Am J Surg Pathol* (2020) 44:641–8. doi: 10.1097/PAS.0000000000001461
35. Kim SR, Cloutier BT, Leung S, Cochrane D, Britton H, Pina A, et al. Molecular Subtypes of Clear Cell Carcinoma of the Endometrium: Opportunities for Prognostic and Predictive Stratification. *Gynecol Oncol* (2020) 158:3–11. doi: 10.1016/j.ygyno.2020.04.043
36. Delair DF, Burke KA, Selenica P, Lim RS, Scott SN, Middha S, et al. The Genetic Landscape of Endometrial Clear Cell Carcinomas. *J Pathol* (2017) 243:230–41. doi: 10.1002/path.4947
37. McConechy MK, Hoang LN, Chui MH, Senz J, Yang W, Rozenberg N, et al. In-Depth Molecular Profiling of the Biphasic Components of Uterine Carcinosarcomas. *J Pathol Clin Res* (2015) 1:173–85. doi: 10.1002/cjp2.18
38. Cherniack AD, Shen H, Walter V, Stewart C, Murray BA, Bowlby R, et al. Integrated Molecular Characterization of Uterine Carcinosarcoma. *Cancer Cell* (2017) 31:411–23. doi: 10.1016/j.ccell.2017.02.010
39. Ramchander NC, Ryan NAJ, Walker TDJ, Harries L, Bolton J, Bosse T, et al. Distinct Immunological Landscapes Characterize Inherited and Sporadic Mismatch Repair Deficient Endometrial Cancer. *Front Immunol* (2019) 10:3023. doi: 10.3389/fimmu.2019.03023

40. Santoro A, Angelico G, Inzani F, Spadola S, Arciuolo D, Valente M, et al. Pathological Features, Immunoprofile and Mismatch Repair Protein Expression Status in Uterine Endometrioid Carcinoma: Focus on MELF Pattern of Myoinvasion. *Eur J Surg Oncol* (2021) 47(2):338–45. doi: 10.1016/j.ejso.2020.06.041
41. Mills AM, Liou S, Ford JM, Berek JS, Pai RK, Longacre TA. Lynch Syndrome Screening Should be Considered for All Patients With Newly Diagnosed Endometrial Cancer. *Am J Surg Pathol* (2014) 38:1501–9. doi: 10.1097/PAS.0000000000000321
42. Marabelle A, Fakih M, Lopez J, Shah M, Shapira-Frommer R, Nakagawa K, et al. Association of Tumour Mutational Burden With Outcomes in Patients With Advanced Solid Tumours Treated With Pembrolizumab: Prospective Biomarker Analysis of the Multicohort, Open-Label, Phase 2 KEYNOTE-158 Study. *Lancet Oncol* (2020) 21:1353–65. doi: 10.1016/S1470-2045(20)30445-9
43. Singh N, Wong R, Tchrakian N, Allen S-G, Clarke B, Gilks CB. Interpretation and Reporting Terminology for Mismatch Repair Protein Immunohistochemistry in Endometrial Cancer. BAGP Guidance Document: MMR Immunohistochemistry interpretation and terminology. *Modern Pathol* (2020) 34(5):1–2. doi: 10.1038/s41379-020-00680-y
44. Goel A, Nagasaka T, Hamelin R, Boland CR. An Optimized Pentaplex PCR for Detecting DNA Mismatch Repair-Deficient Colorectal Cancers. *PloS One* (2010) 5:e9393. doi: 10.1371/journal.pone.0009393
45. Umar A, Boland CR, Terdiman JP, Syngal S, de la Chapelle A, Rüschoff J, et al. Revised Bethesda Guidelines for Hereditary Nonpolyposis Colorectal Cancer (Lynch Syndrome) and Microsatellite Instability. *J Natl Cancer Inst* (2004) 96:261–8. doi: 10.1093/jnci/djh034
46. Nowak JA, Yurgelun MB, Bruce JL, Rojas-Rudilla V, Hall DL, Shivdasani P, et al. Detection of Mismatch Repair Deficiency and Microsatellite Instability in Colorectal Adenocarcinoma by Targeted Next-Generation Sequencing. *J Mol Diagn* (2017) 19:84–91. doi: 10.1016/j.jmoldx.2016.07.010
47. Linzer DI, Levine AJ. Characterization of a 54K Dalton Cellular SV40 Tumor Antigen Present in SV40-Transformed Cells and Uninfected Embryonal Carcinoma Cells. *Cell* (1979) 17:43–52. doi: 10.1016/0092-8674(79)90293-9
48. Lane DP. P53, Guardian of the Genome. *Nature* (1992) 358:15–6. doi: 10.1038/358015a0
49. Chen J. The Cell-Cycle Arrest and Apoptotic Functions of P53 in Tumor Initiation and Progression. *Cold Spring Harb Perspect Med* (2016) 6(3):a026104. doi: 10.1101/cshperspect.a026104
50. Al Bitar S, Gali-Muhtasib H. The Role of the Cyclin Dependent Kinase Inhibitor P21cip1/Waf1 in Targeting Cancer: Molecular Mechanisms and Novel Therapeutics. *Cancers (Basel)* (2019) 11(10):1475. doi: 10.3390/cancers11101475
51. Abbas T, Dutta A. P21 in Cancer: Intricate Networks and Multiple Activities. *Nat Rev Cancer* (2009) 9(6):400–14. doi: 10.1038/nrc2657
52. Riley T, Sontag E, Chen P. Levine A Transcriptional Control of Human P53-Regulated Genes. *Nat Rev Mol Cell Biol* (2008) 9(5):402–12. doi: 10.1038/nrm2395
53. Petitjean A, Mathe E, Kato S, Ishioka C, Tavtigian SV, Hainaut P, et al. Impact of Mutant P53 Functional Properties Ontp53mutation Patterns and Tumor Phenotype: Lessons From Recent Developments in the IARC TP53 Database. *Hum Mutat* (2007) 28:622–9. doi: 10.1002/humu.20495
54. Olivier M, Hollstein M, Hainaut P. TP53 Mutations in Human Cancers: Origins, Consequences, and Clinical Use. Cold Spring Harb. *Perspect Biol* (2010) 2(1):a001008. doi: 10.1101/cshperspect.a001008
55. Stelloo E, Bosse T, Nout RA, Mackay HJ, Church DN, Nijman HW, et al. Refining Prognosis and Identifying Targetable Pathways for High-Risk Endometrial Cancer; a TransPORTEC Initiative. *Mod Pathol* (2015) 28:836–44. doi: 10.1038/modpathol.2015.43
56. Santoro A, Angelico G, Travaglino A, Raffone A, Arciuolo D, D'Alessandris N, et al. Clinico-Pathological Significance of TCGA Classification and SWI/SNF Proteins Expression in Undifferentiated/Dedifferentiated Endometrial Carcinoma: A Possible Prognostic Risk Stratification. *Gynecol Oncol* (2021) 161:629–35. doi: 10.1016/j.ygyno.2021.02.029
57. Raffone A, Travaglino A, Mascolo M, Carbone L, Guida M, Insabato L, et al. TCGA Molecular Groups of Endometrial Cancer: Pooled Data About Prognosis. *Gynecol Oncol* (2019) 155:374–83. doi: 10.1016/j.ygyno.2019.08.019
58. Prueksaritanond N, Chantape W. Comparative Survival Outcomes of Uterine Papillary Serous Carcinoma, Clear Cell Carcinoma, Grade 3 Endometrioid Adenocarcinoma, and Carcinosarcoma of Endometrial Cancer in Rajavithi Hospital. *J Med Assoc Thail Chotmaihet Thangphaet* (2016) 99:75–83.
59. Fader AN, Roque DM, Siegel E, Buza N, Hui P, Abdelghany O, et al. Randomized Phase II Trial of Carboplatin-Paclitaxel Versus Carboplatin-Paclitaxel-Trastuzumab in Uterine Serous Carcinomas That Overexpress Human Epidermal Growth Factor Receptor 2/Neu. *J Clin Oncol* (2018) 36:2044–51. doi: 10.1200/JCO.2017.76.5966
60. Köbel M, Ronnett BM, Singh N, Soslow RA, Gilks CB, McCluggage WG. Interpretation of P53 Immunohistochemistry in Endometrial Carcinomas: Toward Increased Reproducibility International. *J Gynecol Pathol* (2019) 38:S123–31. doi: 10.1097/PGP.0000000000000488
61. Köbel M, Reuss A, du BA, Kommoss S, Kommoss F, Gao D, et al. The Biological and Clinical Value of P53 Expression in Pelvic High-Grade Serous Carcinomas. *J Pathol* (2010) 222:191–8. doi: 10.1002/path.2744
62. Koübel M, Piskorz AM, Lee S, Lui S, LePage C, Marass F, et al. Optimized P53 Immunohistochemistry Is an Accurate Predictor of TP53 Mutation in Ovarian Carcinoma. *J Pathol Clin Res* (2016) 2:247–58. doi: 10.1002/cjp2.53
63. van Weelden WJ, Massuger L, Enitec JMA, Pijnenborg AR. Anti-Estrogen Treatment in Endometrial Cancer: A Systematic Review. *Front Oncol* (2019) 9:359. doi: 10.3389/fonc.2019.00359
64. Stelloo E, Nout RA, Osse EM, Juergenliemk-Schulz IJ, Jobsen JJ, Lutgens LC, et al. Improved Risk Assessment by Integrating Molecular and Clinicopathological Factors in Early-Stage Endometrial Cancer—Combined Analysis of the PORTEC Cohorts. *Clin Cancer Res* (2016) 22:4215–24. doi: 10.1158/1078-0432.CCR-15-2878
65. Nelson WJ, Nusse R. Convergence of Wnt, Beta-Catenin, and Cadherin Pathways. *Science* (2004) 303:1483–847. doi: 10.1126/science.1094291
66. Ring A, Kim YM, Kahn M. Wnt/catenin Signaling in Adult Stem Cell Physiology and Disease. *Stem Cell Rev Rep* (2014) 10(4):512–25. doi: 10.1007/s12015-014-9515-2
67. Bovolenta P, Rodriguez J, Esteve P. Nfrizzled/RIK Mediated Signalling in Axon Guidance. *Development* (2006) 133:4399–408. doi: 10.1242/dev.02592
68. MacDonald BT, Tamai K, He X. Wnt/beta-Catenin Signaling: Components, Mechanisms, and Diseases. *Dev Cell* (2009) 17(1):9–26. doi: 10.1016/j.devcel.2009.06.016
69. Polakis P. The Many Ways of WNT in Cancer. *Curr Opin Gen Dev* (2007) 17:45–51. doi: 10.1016/j.gde.2006.12.007
70. Zannoni GF, Angelico G, Santoro A. Aberrant Non-Canonical WNT Pathway as Key-Driver of High-Grade Serous Ovarian Cancer Development. *Virchows Arch* (2020) 477:321–2. doi: 10.1007/s00428-020-02760-5
71. Wu D, Pan W. GSK3: A Multifaceted Kinase in Wnt Signaling. *Trends Biochem Sci* (2010) 35(3):161–8. doi: 10.1016/j.tibs.2009.10.002
72. Lecarpentier Y, Schussler O, Hébert J-L, Vallée A. Multiple Targets of the Canonical WNT/β-Catenin Signaling in Cancers. *Front Oncol* (2019) 9:1248. doi: 10.3389/fonc.2019.01248
73. Zhan T, Rindtorff N, Boutros M. Wnt Signaling in Cancer. *Oncogene* (2017) 36:1461–73. doi: 10.1038/onc.2016.304
74. Kurnit K, Kim GN, Fellman BM, Urbauer DL, Mills GB, Zhang W, et al. CTNNB1 (Beta-Catenin) Mutation Identifies Low Grade, Early Stage Endometrial Cancer Patients at Increased Risk of Recurrence. *Mod Pathol* (2017) 30:1032–41. doi: 10.1038/modpathol.2017.15
75. Travaglino A, Raffone A, Saccone G, De Luca C, Mollo A, Mascolo M, et al. Immunohistochemical Nuclear Expression of β-Catenin as a Surrogate of CTNNB1 Exon 3 Mutation in Endometrial Cancer. *Am J Clin Pathol* (2019) 151:529–38. doi: 10.1093/ajcp/aqy178
76. Kim G, Kurnit K, Djordjevic B, Singh C, Munsell MF, Wang W-L, et al. Nuclear β-Catenin Localization and Mutation of the CTNNB1 Gene: A Context-Dependent Association. *Mod Pathol* (2018) 31:1553–9. doi: 10.1038/s41379-018-0080-0
77. Meljen VT, Mittenzwei R, Wong J, Puechl A, Whitaker R, Broadwater G, et al. Endometrial Adenocarcinomas With No Specific Molecular Profile. *Int J Gynecol Pathol* (2021) 40(6):587–96. doi: 10.1097/PGP.0000000000000747
78. Costigan DC, Dong F, Nucci MR, Howitt BE. Clinicopathologic and Immunohistochemical Correlates of CTNNB1 Mutated Endometrial

Endometrioid Carcinoma. *Int J Gynecol Pathol* (2020) 39:119–27. doi: 10.1097/PGP.0000000000000583
79. Travaglino A, Raffone A, Gencarelli A, Raimondo D, Moretta P, Pignatiello S, et al. Relationship Between Morular Metaplasia and Squamous Differentiation in Endometrial Carcinoma. *Pathol Res Pr* (2021) 217:153307. doi: 10.1016/j.prp.2020.153307
80. Yaşar P, Ayaz G, User SD, Güpür G, Muyan M. Molecular Mechanism of Estrogen-Estrogen Receptor Signaling. *Reprod Med Biol* (2016) 16(1):4–20. doi: 10.1002/rmb2.12006
81. Fuentes N, Silveyra P. Estrogen Receptor Signaling Mechanisms. *Adv Protein Chem Struct Biol* (2019) 116:135–70. doi: 10.1016/bs.apcsb.2019.01.001
82. Marquardt RM, Kim TH, Shin JH, Jeong JW. Progesterone and Estrogen Signaling in the Endometrium: What Goes Wrong in Endometriosis? *Int J Mol Sci* (2019) 20(15):3822. doi: 10.3390/ijms20153822
83. Trovik J, Wik E, Werner HM, Krakstad C, Helland H, Vandenput I, et al. Hormone Receptor Loss in Endometrial Carcinoma Curettage Predicts Lymph Node Metastasis and Poor Outcome in Prospective Multicentre Trial. *Eur J Canc* (2013) 49:3431–41. doi: 10.1016/j.ejca.2013.06.016
84. van der Putten LJM, Visser NCM, van de Vijver K, Santacana M, Bronsert P, Bulten J, et al. Added Value of Estrogen Receptor, Progesterone Receptor, and L1 Cell Adhesion Molecule Expression to Histology-Based Endometrial Carcinoma Recurrence Prediction Models: An ENITEC Collaboration Study. *Int J Gynecol Canc* (2018) 28:514–23. doi: 10.1097/IGC.0000000000001187
85. Zannoni GF, Monterossi G, De Stefano I, Gargini A, Salerno MG, Farulla I, et al. The Expression Ratios of Estrogen Receptor Alpha (ERalpha) to Estrogen Receptor Beta1 (ERbeta1) and ERalpha to ERbeta2 Identify Poor Clinical Outcome in Endometrioid Endometrial Cancer. *Hum Pathol* (2013) 44:1047–54. doi: 10.1016/j.humpath.2012.09.007
86. Ethier JL, Desautels DN, Amir E, MacKay H. Is Hormonal Therapy Effective in Advanced Endometrial Cancer? A Systematic Review and Meta-Analysis. *Gynecol Oncol* (2017) 147:158–66. doi: 10.1016/j.ygyno.2017.07.002
87. Jongen V, Briet J, de Jong R, ten Hoor K, Boezen M, van der Zee A, et al. Expression of Estrogen Receptor-Alpha and -Beta and Progesterone Receptor-A and -B in a Large Cohort of Patients With Endometrioid Endometrial Cancer. *Gynecol Oncol* (2009) 112:537–42. doi: 10.1016/j.ygyno.2008.10.032
88. Krakstad C, Trovik J, Wik E, Engelsen IB, Werner HM, Birkeland E, et al. Loss of GPER Identifies New Targets for Therapy Among a Subgroup of ERalpha-Positive Endometrial Cancer Patients With Poor Outcome. *Br J Canc* (2012) 106:1682–8. doi: 10.1038/bjc.2012.91
89. Singh M, Zaino RJ, Filiaci VJ, Leslie KK. Relationship of Estrogen and Progesterone Receptors to Clinical Outcome in Metastatic Endometrial Carcinoma: A Gynecologic Oncology Group Study. *Gynecol Oncol* (2007) 106:325–33. doi: 10.1016/j.ygyno.2007.03.042
90. Wang Y, Ma X, Wang Y, Liu Y, Liu C. Comparison of Different Scoring Systems in the Assessment of Estrogen Receptor Status for Predicting Prognosis in Endometrial Cancer. *Int J Gynecol Pathol* (2019) 38:111–8. doi: 10.1097/PGP.0000000000000490
91. Allison KH, Hammond MEH, Dowsett M, McKernin SE, Carey LA, Fitzgibbons PL, et al. Estrogen and Progesterone Receptor Testing in Breast Cancer: ASCO/CAP Guideline Update. *J Clin Oncol* (2020) 38 (12):1346–66. doi: 10.1200/JCO.19.02309
92. Palmer DC, Muir IM, Alexander AI, Cauchi M, Bennett RC, Quinn MA. The Prognostic Importance of Steroid Receptors in Endometrial Carcinoma. *Obstet Gynecol* (1988) 72:388–93.
93. Yi M, Huo L, Koenig KB, Mittendorf EA, Meric-Bernstam F, Kuerer HM, et al. Which Threshold for ER Positivity? A Retrospective Study Based on 9639 Patients. *Ann Oncol* (2014) 25:1004–11. doi: 10.1093/annonc/mdu053
94. Wik E, Raeder MB, Krakstad C, Trovik J, Birkeland E, Hoivik EA, et al. Lack of Estrogen Receptor-Alpha Is Associated With Epithelial-Mesenchymal Transition and PI3K Alterations in Endometrial Carcinoma. *Clin Canc Res* (2013) 19:1094–105. doi: 10.1158/1078-0432.CCR-12-3039
95. Guan J, Xie L, Luo X, Yang B, Zhang H, Zhu Q, et al. The Prognostic Significance of Estrogen and Progesterone Receptors in Grade I and II Endometrioid Endometrial Adenocarcinoma: Hormone Receptors in Risk Stratification. *J Gynecol Oncol* (2019) 30:e13. doi: 10.3802/jgo.2019.30.e13
96. Huvila J, Talve L, Carpen O, Edqvist PH, Ponten F, Grenman S, et al. Progesterone Receptor Negativity is an Independent Risk Factor for Relapse in Patients With Early Stage Endometrioid Endometrial Adenocarcinoma. *Gynecol Oncol* (2013) 130:463–9. doi: 10.1016/j.ygyno.2013.06.015
97. Mylonas I. Prognostic Significance and Clinical Importance of Estrogen Receptor Alpha and Beta in Human Endometrioid Adenocarcinomas. *Oncol Rep* (2010) 24:385–93. doi: 10.3892/or_00000871
98. van Weelden WJ, Reijnen C, V N H, Vandevelde K, Bulten J, Bult P, et al. The Cutoff for Estrogen and Progesterone Receptor Expression in Endometrial Cancer Revisited: A European Network for Individualized Treatment of Endometrial Cancer Collaboration Study. *Hum Pathol* (2021) 109:80–91. doi: 10.1016/j.humpath.2020.12.003
99. Karnezis AN, Leung S, Magrill J, McConechy MK, Yang W, Chow C, et al. Evaluation of Endometrial Carcinoma Prognostic Immunohistochemistry Markers in the Context of Molecular Classification. *J Pathol Clin Res* (2017) 3:279–93. doi: 10.1002/cjp2.82
100. Djabali M, Mattei MG, Nguyen C, Roux D, Demengeot J, Denizot F, et al. The Gene Encoding L1, a Neural Adhesion Molecule of the Immunoglobulin Family, Is Located on the X Chromosome in Mouse and Man. *Genomics* (1990) 7(4):587–93. doi: 10.1016/0888-7543(90)90203-7
101. Rathjen FG, Schachner M. Immunocytological and Biochemical Characterization of a New Neuronal Cell Surface Component (L1 Antigen) Which is Involved in Cell Adhesion. *EMBO J* (1984) 3:1–10. doi: 10.1002/j.1460-2075.1984.tb01753.x
102. Brümmendorf T, Kenwrick S, Rathjen FG. Neural Cell Recognition Molecule L1: From Cell Biology to Human Hereditary Brain Malformations. *Curr Opin Neurobiol* (1998) 8:87–97. doi: 10.1016/S0959-4388(98)80012-3
103. Patzke C, Acuna C, Giam LR, Wernig M, Südhof TC. Conditional Deletion of L1CAM in Human Neurons Impairs Both Axonal and Dendritic Arborization and Action Potential Generation. *J Exp Med* (2016) 213:499–515. doi: 10.1084/jem.20150951
104. Schmid RS, Maness PF. L1 and NCAM Adhesion Molecules as Signaling Coreceptors in Neuronal Migration and Process Outgrowth. *Curr Opin Neurobiol* (2008) 18:245–50. doi: 10.1016/j.conb.2008.07.015
105. Van Gool IC, Stelloo E, Nout RA, Nijman HW, Edmondson RJ, Church DN, et al. Prognostic Significance of L1CAM Expression and Its Association With Mutant P53 Expression in High-Risk Endometrial Cancer. *Mod Pathol* (2016) 29(2):174–81. doi: 10.1038/modpathol.2015.147
106. de Freitas D, Aguiar FN, Anton C, Bacchi CE, Carvalho JP, Carvalho FM. L1 Cell Adhesion Molecule (L1CAM) Expression in Endometrioid Endometrial Carcinomas: A Possible Pre-Operative Surrogate of Lymph Vascular Space Invasion. *PloS One* (2018) 13(12):e0209294. doi: 10.1371/journal.pone.0209294
107. Kommoss FK, Karnezis AN, Kommoss F, Talhouk A, Taran FA, Staebler A, et al. L1CAM Further Stratifies Endometrial Carcinoma Patients With No Specific Molecular Risk Profile. *Br J Cancer* (2018) 119:480–6. doi: 10.1038/s41416-018-0187-6
108. Corrado G, Laquintana V, Loria R, Carosi M, de Salvo L, Sperduti I, et al. Endometrial Cancer Prognosis Correlates With the Expression of L1CAM and Mir34a Biomarkers. *J Exp Clin Cancer Res* (2018) 637(1):139. doi: 10.1186/s13046-018-0816-1
109. Kim ST, Cristescu R, Bass AJ, Kim KM, Odegaard JI, Kim K, et al. Comprehensive Molecular Characterization of Clinical Responses to PD-1 Inhibition in Metastatic Gastric Cancer. *Nat Med* (2018) 24:1449–58. doi: 10.1038/s41591-018-0101-z
110. Baumeister SH, Freeman GJ, Dranoff G, Sharpe AH. Coinhibitory Pathways in Immunotherapy for Cancer. *Annu Rev Immunol* (2016) 34:539–73. doi: 10.1146/annurev-immunol-032414-112049
111. Pasanen A, Ahvenainen T, Pellinen T, Vahteristo P, Loukovaara M, Bützow R. PD-L1 Expression in Endometrial Carcinoma Cells and Intratumoral Immune Cells: Differences Across Histologic and TCGA-Based Molecular Subgroups. *Am J Surg Pathol* (2020) 44:174–81. doi: 10.1097/PAS.0000000000001395
112. Howitt BE, Shukla SA, Sholl LM, Ritterhouse LL, Watkins JC, Rodig S, et al. Association of Polymerase E-Mutated and Microsatellite-Instable Endometrial Cancers With Neoantigen Load, Number of Tumor-Infiltrating Lymphocytes, and Expression of PD-1 and PD-L1. *JAMA Oncol* (2015) 1:1319–23. doi: 10.1001/jamaoncol.2015.2151
113. Mo Z, Liu J, Zhang Q, Chen Z, Mei J, Liu L, et al. Expression of PD-1, PD-L1 and PD-L2 is Associated With Differentiation Status and Histological Type of Endometrial Cancer. *Oncol Lett* (2016) 12:944–50. doi: 10.3892/ol.2016.4744

114. Bregar A, Deshpande A, Grange C, Zi T, Stall J, Hirsch H, et al. Characterization of Immune Regulatory Molecules B7-H4 and PD-L1 in Low and High Grade Endometrial Tumors. *Gynecol Oncol* (2017) 145:446–52. doi: 10.1016/j.ygyno.2017.03.006
115. Yamashita H, Nakayama K, Ishikawa M, Nakamura K, Ishibashi T, Sanuki K, et al. Microsatellite Instability Is a Biomarker for Immune Checkpoint Inhibitors in Endometrial Cancer. *Oncotarget* (2017) 9:5652–64. doi: 10.18632/oncotarget.23790
116. Sloan EA, Ring KL, Willis BC, Modesitt SC, Mills AM. PD-L1 Expression in Mismatch Repair-Deficient Endometrial Carcinomas, Including Lynch Syndrome-Associated and MLH1 Promoter Hypermethylated Tumors. *Am J Surg Pathol* (2017) 41:326–33. doi: 10.1097/PAS.0000000000000783
117. Li Z, Joehlin-Price AS, Rhoades J, Ayoola-Adeola M, Miller K, Parwani AV, et al. Programmed Death Ligand 1 Expression Among 700 Consecutive Endometrial Cancers: Strong Association With Mismatch Repair Protein Deficiency. *Int J Gynecol Cancer* (2018) 28:59–68. doi: 10.1097/IGC.0000000000001120
118. Kim J, Kim S, Lee HS, Yang W, Cho H, Chay DB, et al. Prognostic Implication of Programmed Cell Death 1 Protein and Its Ligand Expressions in Endometrial Cancer. *Gynecol Oncol* (2018) 149:381–7. doi: 10.1016/j.ygyno.2018.02.013
119. Asaka S, Yen TT, Wang TL, Shih IM, Gaillard S. T Cell-Inflamed Phenotype and Increased Foxp3 Expression in Infiltrating T-Cells of Mismatch-Repair Deficient Endometrial Cancers. *Mod Pathol* (2019) 32:576–84. doi: 10.1038/s41379-018-0172-x
120. Crumley S, Kurnit K, Hudgens C, Fellman B, Tetzlaff MT, Broaddus R, et al. Identification of a Subset of Microsatellite-Stable Endometrial Carcinoma With High PD-L1 and CD8+ Lymphocytes. *Mod Pathol* (2019) 32:396–404. doi: 10.1038/s41379-018-0148-x
121. Kucukgoz Gulec U, Kilic Bagir E, Paydas S, Guzel AB, Gumurdulu D, Vardar MA, et al. Programmed Death-1 (PD-1) and Programmed Death-Ligand 1 (PD-L1) Expressions in Type 2 Endometrial Cancer. *Arch Gynecol Obstet* (2019) 300:377–82. doi: 10.1007/s00404-019-05180-2
122. Talhouk A, Derocher H, Schmidt P, Leung S, Milne K, Gilks CB, et al. Molecular Subtype Not Immune Response Drives Outcomes in Endometrial Carcinoma. *Clin Cancer Res* (2018) 25:2537–48. doi: 10.1158/1078-0432.CCR-18-3241
123. Herzog TJ, Arguello D, Reddy SK, Gatalica Z. PD-1, PD-L1 Expression in 1599 Gynecological Cancers: Implications for Immunotherapy. *Gynecol Oncol* (2015) 137:204–5. doi: 10.1016/j.ygyno.2015.01.514
124. Zhang S, Minaguchi T, Xu C, Qi N, Itagaki H, Shikama A, et al. PD-L1 and CD4 Are Independent Prognostic Factors for Overall Survival in Endometrial Carcinomas. *BMC Cancer* (2020) 20:127. doi: 10.1186/s12885-020-6545-9
125. Lu L, Li Y, Luo R, Xu J, Feng J, Wang M. Prognostic and Clinicopathological Role of PD-L1 in Endometrial Cancer: A Meta-Analysis. *Front Oncol* (2020) 10:632. doi: 10.3389/fonc.2020.00632
126. Brandt-Rauf PW, Pincus MR, Carney WP. The c-erbB-2 Protein in Oncogenesis: Molecular Structure to Molecular Epidemiology. *Crit Rev Oncogenesis* (1994) 5(2-3):313–29. doi: 10.1615/CritRevOncog.v5.i2-3.100
127. Riese DJ, Stern DF. Specificity Within the EGF Family/ErbB Receptor Family Signaling Network. *BioEssays* (1998) 20:41–8. doi: 10.1002/(SICI)1521-1878(199801)20:1<41::AID-BIES7>3.0.CO;2-V
128. Iqbal N, Iqbal N. Human Epidermal Growth Factor Receptor 2 (HER2) in Cancers: Overexpression and Therapeutic Implications. *Mol Biol Int* (2014) 2014:852748. doi: 10.1155/2014/852748
129. Twomey JD, Brahme NN, Zhang B. Drug-Biomarker Co-Development in Oncology - 20 Years and Counting. *Drug Resist Updat* (2017) 30:48–62. doi: 10.1016/j.drup.2017.02.002
130. Santin AD, Bellone S, Van Stedum S, Bushen W, De Las Casas LE, Korourian S, et al. Determination of HER2/neu Status in Uterine Serous Papillary Carcinoma: Comparative Analysis of Immunohistochemistry and Fluorescence *In Situ* Hybridization. *Gynecol Oncol* (2005) 98(1):24–30. doi: 10.1016/j.ygyno.2005.03.041
131. Hamilton CA, Cheung MK, Osann K, Chen L, Teng NN, Longacre TA, et al. Uterine Papillary Serous and Clear Cell Carcinomas Predict for Poorer Survival Compared to Grade 3 Endometrioid Corpus Cancers. *Br J Cancer* (2006) 94(5):642–6. doi: 10.1038/sj.bjc.6603012
132. de Boer SM, Powell ME, Mileshkin L, Katsaros D, Bessette P, Haie-Meder C, et al. Adjuvant Chemoradiotherapy Versus Radiotherapy Alone in Women With High-Risk Endometrial Cancer (PORTEC-3): Patterns of Recurrence and Post-Hoc Survival Analysis of a Randomised Phase 3 Trial. *Lancet Oncol* (2019) 20(9):1273–85. doi: 10.1016/S1470-2045(19)30395-X
133. Homesley HD, Filiaci V, Gibbons SK, Long HJ, Cella D, Spirtos NM, et al. A Randomized Phase III Trial in Advanced Endometrial Carcinoma of Surgery and Volume Directed Radiation Followed by Cisplatin and Doxorubicin With or Without Paclitaxel: A Gynecologic Oncology Group Study. *Gynecol Oncol* (2009) 112(3):543–52. doi: 10.1016/j.ygyno.2008.11.014
134. National Comprehensive Cancer Network. *Uterine Neoplasms (Version 4.2019)*. Available at: https://www.nccn.org/professionals/physician_gls/pdf/uterine.pdf (Accessed October, 2019).
135. Wolff AC, Hammond MEH, Allison KH, Harvey BE, Mangu PB, Bartlett JMS, et al. Human Epidermal Growth Factor Receptor 2 Testing in Breast Cancer: American Society of Clinical Oncology/ College of American Pathologists Clinical Practice Guideline Focused Update. *Arch Pathol Lab Med* (2018) 142:1364–82. doi: 10.5858/arpa.2018-0902-SA
136. Bartley AN, Washington MK, Ventura CB, Ismaila N, Colasacco C, Benson AB3rd, et al. HER2 Testing and Clinical Decision Making in Gastroesophageal Adenocarcinoma: Guideline From the College of American Pathologists, American Society for Clinical Pathology, and American Society of Clinical Oncology. *Arch Pathol Lab Med* (2016) 140:1345–63. doi: 10.5858/arpa.2016-0331-CP
137. Buza N, English DP, Santin AD, Hui P. Toward Standard HER2 Testing of Endometrial Serous Carcinoma: 4-Year Experience at a Large Academic Center and Recommendations for Clinical Practice. *Mod Pathol* (2013) 26(12):1605–12. doi: 10.1038/modpathol.2013.113
138. Buza N, Hui P. Marked Heterogeneity of HER2/NEU Gene Amplification in Endometrial Serous Carcinoma. *Genes Chromosomes Cancer* (2013) 52(12):1178–86. doi: 10.1002/gcc.22113
139. Buza N, Euscher ED, Matias-Guiu X, McHenry A, Oliva E, Ordulu Z, et al. Reproducibility of Scoring Criteria for HER2 Immunohistochemistry in Endometrial Serous Carcinoma: A Multi-Institutional Interobserver Agreement Study. *Modern Pathol* (2021) 34:1194–202. doi: 10.1038/s41379-021-00746-5
140. Buza N. HER2 Testing in Endometrial Serous Carcinoma Time for Standardized Pathology Practice to Meet the Clinical Demand. *Arch Pathol Lab Med* (2021) 145(6):687–91. doi: 10.5858/arpa.2020-0207-RA
141. Buza N. HER2 Testing and Reporting in Endometrial Serous Carcinoma: Practical Recommendations for HER2 Immunohistochemistry and Fluorescent *In Situ* Hybridization: Proceedings of the ISGyP Companion Society Session at the 2020 USCAP Annual Meeting. *Int J Gynecol Pathol* (2021) 40(1):17–23. doi: 10.1097/PGP.0000000000000711
142. Rottmann D, Assem H, Matsumoto N, Wong S, Hui P, Buza N. Does Specimen Type Have an Impact on HER2 Status in Endometrial Serous Carcinoma? Discordant HER2 Status of Paired Endometrial Biopsy and Hysterectomy Specimens in the Presence of Frequent Intratumoral Heterogeneity. *Int J Gynecol Pathol* (2021) 40(3):263–71. doi: 10.1097/PGP.0000000000000690
143. Halle MK, Tangen IL, Berg HF, Hoivik EA, Mauland KK, Kusonmano K, et al. HER2 Expression Patterns in Paired Primary and Metastatic Endometrial Cancer Lesions. *Br J Cancer* (2018) 118(3):378–87. doi: 10.1038/bjc.2017.422
144. Wakatsuki T, Yamamoto N, Sano T, Chin K, Kawachi H, Takahari D, et al. Clinical Impact of Intratumoral HER2 Heterogeneity on Trastuzumab Efficacy in Patients With HER2-Positive Gastric Cancer. *J Gastroenterol* (2018) 53(11):1186–95. doi: 10.1007/s00535-018-1464-0
145. Erickson BK, Najjar O, Klein M, Shahi M, Dolan M, Cimino-Mathews A, et al. Human Epidermal Growth Factor 2 (HER2) in Early Stage Uterine Serous Carcinoma: A Multi-Institutional Cohort. *Fader J Clin Oncol* (2020) 38(15_suppl):6084–4. doi: 10.1200/JCO.2020.38.15_suppl.6084
146. Rottmann D, Snir OL, Wu X, Wong S, Hui P, Santin AD, et al. HER2 Testing of Gynecologic Carcinosarcomas: Tumor Stratification for Potential Targeted Therapy. *Mod Pathol* (2020) 33(1):118–27. doi: 10.1038/s41379-019-0358-x
147. Menderes G, Bonazzoli E, Bellone S, Black J, Predolini F, Pettinella F, et al. SYD985, a Novel Duocarmycinbased HER2-Targeting Antibody-Drug

Conjugate, Shows Antitumor Activity in Uterine and Ovarian Carcinosarcoma With HER2/Neu Expression. *Clin Cancer Res* (2017) 23 (19):5836–45. doi: 10.1158/1078-0432.CCR-16-2862

148. Guzzo F, Bellone S, Buza N, Hui P, Carrara L, Varughese J, et al. HER2/neu as a Potential Target for Immunotherapy in Gynecologic Carcinosarcomas. *Int J Gynecol Pathol* (2012) 31(3):211–21. doi: 10.1097/PGP.0b013e31823bb24d
149. Abdulfatah E, Wakeling E, Sakr S, Al-Obaidy K, Bandyopadhyay S, Morris R, et al. Molecular Classification of Endometrial Carcinoma Applied to Endometrial Biopsy Specimens: Towards Early Personalized Patient Management. *Gynecol Oncol* (2019) 154:467–74. doi: 10.1016/j.ygyno.2019.06.012
150. Plotkin A, Kuzeljevic B, De Villa V, Thompson EF, Gilks CB, Clarke BA, et al. Interlaboratory Concordance of ProMisE Molecular Classification of Endometrial Carcinoma Based on Endometrial Biopsy Specimens. *Int J Gynecol Pathol* (2019) 39(6):537–45. doi: 10.1097/PGP.0000000000000654
151. Chung YS, Woo HY, Lee JY, Park E, Nam EJ, Kim S, et al. Mismatch Repair Status and Progestin Therapy in Endometrial Cancer. *Am J Obstet Gynecol* (2021) 224(4):370.e1–370.e13. doi: 10.1016/j.ajog.2020.10.003
152. Clive R, Taylor MD. DPhil. The Total Test Approach to Standardization of Immunohistochemistry. Arch Pathol Lab Med—Vol 124, July 2000 Editorials. 51. Walker RA. Quantification of Immunohistochemistry–Issues Concerning Methods, Utility and Semiquantitative Assessment I. *Histopathology* (2006) 49:406–10. doi: 10.1111/j.1365-2559.2006.02514.x
153. Angelico G, Santoro A, Inzani F, Straccia P, Spadola S, Arciuolo D, et al. An Emerging Anti-P16 Antibody-BC42 Clone as an Alternative to the Current E6H4 for Use in the Female Genital Tract Pathological Diagnosis: Our Experience and a Review on P16ink4a Functional Significance, Role in Daily-Practice Diagnosis, Prognostic Potential, and Technical Pitfalls. *Diagnostics* (2021) 11:713. doi: 10.3390/diagnostics11040713

Conflict of Interest: The authors declare that the research was conducted in the absence of any commercial or financial relationships that could be construed as a potential conflict of interest.

Publisher's Note: All claims expressed in this article are solely those of the authors and do not necessarily represent those of their affiliated organizations, or those of the publisher, the editors and the reviewers. Any product that may be evaluated in this article, or claim that may be made by its manufacturer, is not guaranteed or endorsed by the publisher.

Copyright © 2022 Zannoni, Bragantini, Castiglione, Fassan, Troncone, Inzani, Pesci, Santoro and Fraggetta. This is an open-access article distributed under the terms of the Creative Commons Attribution License (CC BY). The use, distribution or reproduction in other forums is permitted, provided the original author(s) and the copyright owner(s) are credited and that the original publication in this journal is cited, in accordance with accepted academic practice. No use, distribution or reproduction is permitted which does not comply with these terms.

frontiers | Frontiers in Oncology

ORIGINAL RESEARCH
published: 11 April 2022
doi: 10.3389/fonc.2022.782030

Prognostic Effect of Primary Recurrence Patterns in Squamous Cervical Carcinoma After Radical Surgery

Zongkai Zhang[1†], *Long Jiang*[2†], *Rui Bi*[1,3], *Xiaohua Wu*[1,4], *Guihao Ke*[1,4] *and Jun Zhu*[1,4*]

[1] Department of Oncology, Shanghai Medical College, Fudan University, Shanghai, China, [2] Department of Anesthesia, Zhongshan Hospital Fudan University Shanghai Cancer Center, Shanghai, China, [3] Department of Pathology, Fudan University Shanghai Cancer Center, Shanghai, China, [4] Department of Gynecologic Oncology, Fudan University Shanghai Cancer Center, Shanghai, China

Objective: To examine the effect of primary recurrence patterns on the prognosis of squamous cervical cancer after initial treatment.

Methods: Primary recurrence patterns and prognostic factors were examined in stage IB-IIA cervical cancer patients after initial treatment. Recurrence site (locoregional recurrence and distant metastasis or in-field and out-field recurrence for patients receiving adjuvant radiotherapy) and subtype (nodal and organ recurrence) were examined. Clinicopathological characteristics and survival rates were evaluated to generate a prognostic nomogram.

Results: A total of 472 patients were included. The median follow-up period, 5-year overall (OS) rate, and median OS were 59.1 months, 33.7%, and 24.0 months, respectively. Overall, 38.8% and 61.2% of the patients had locoregional recurrence and distant metastasis, respectively, and survival rates were comparable in these groups. Patients with nodal recurrence had better OS than those with organ recurrence (38.3% vs 30.7%, respectively; P = 0.001). Patients not receiving adjuvant radiotherapy had increased risk of pelvic recurrence [odds ratio (OR) = 0.148; 95% confidence interval [(CI): 0.075–0.291, $P = 0.000$]. Positive lymph-vascular space invasion (OR= 1.928; 95% CI: 1.151–3.229, $P = 0.013$) and no chemotherapy (OR = 0.521; 95% CI: 0.317–0.733, $P = 0.040$) increased the risk of distant metastasis. Positive lymph node status after initial treatment were associated with nodal recurrence (OR = 3.729; 95% CI: 1.838–7.563, $P = 0.000$), while elevated preoperative squamous cell carcinoma antigen (SCC-Ag) levels were associated with organ recurrence (OR = 1.642; 95% CI: 1.325–2.265, $P = 0.002$). Recurrence subtype, therapy for relapse, the International Federation of Gynecology and Obstetrics stage, adjuvant radiotherapy, preoperative SCC-Ag levels, and risk subgroup were independently associated with OS.

Conclusions: Primary recurrence patterns were associated with specific clinicopathological characteristics of cervical cancer. Recurrent cervical cancer prognosis was mainly affected by recurrence location and subtype.

Keywords: cervical cancer, recurrence patterns, therapy for relapse, locoregional recurrence, distant metastasis

OPEN ACCESS

Edited by:
Stefano Restaino, Ospedale Santa Maria della Misericordia di Udine, Italy

Reviewed by:
Clarissa Polen-De, Mayo Clinic, United States
Jinluan Li, Fujian Provincial Cancer Hospital, China

***Correspondence:**
Jun Zhu
dragonzld@163.com

[†]*These authors have contributed equally to this work*

Specialty section:
This article was submitted to Gynecological Oncology, a section of the journal Frontiers in Oncology

Received: *23 September 2021*
Accepted: *16 March 2022*
Published: *11 April 2022*

Citation:
Zhang Z, Jiang L, Bi R, Wu X, Ke G and Zhu J (2022) Prognostic Effect of Primary Recurrence Patterns in Squamous Cervical Carcinoma After Radical Surgery. Front. Oncol. 12:782030. doi: 10.3389/fonc.2022.782030

INTRODUCTION

Cervical cancer is the fourth most common gynecologic cancer worldwide and a leading cause of cancer-related deaths in developing countries (1). The incidence of cervical cancer has decreased owing to extensive screening and vaccination programs, with the latter targeting patients with high-risk human papilloma virus genotypes (2, 3). Standard treatment for early-stage cervical cancer [International Federation of Gynecology and Obstetrics (FIGO 2009) stage IB-IIA] includes radical surgery with or without adjuvant radiotherapy (RT) (4, 5). Consecutive editions of clinical guidelines have improved cervical cancer management, thus increasing remission rates and decreasing the risk of relapse; these changes have resulted in recently reported 5-year overall survival (OS) rates of early stage cervical cancer in the range of 70%–90% (6, 7). This progress notwithstanding, approximately 10%–15% of patients with early-stage disease experience recurrence (8).

Cervical cancer recurrence patterns may vary; however, they generally include locoregional recurrence (LR) and distant metastasis (DM). Recurrent disease management requires a personalized approach depending on the site of recurrence, which may determine prognosis. Previous studies have shown that patient prognosis after initial treatment was associated with clinicopathological characteristics, recurrence patterns, and relapse therapy type (9–11). However, few studies have examined risk factors for recurrence and the relationship between different recurrence patterns and prognosis. This study aimed to examine patients experiencing cervical cancer recurrence to identify their clinicopathological characteristics, recurrence patterns, and treatment type received, and to evaluate the relationship between different clinicopathological characteristics and recurrence patterns; this study aimed to examine the impact of recurrence patterns on prognosis.

MATERIALS AND METHODS

We retrospectively extracted data of 472 patients with recurrent cervical cancer who underwent standard abdominal radical hysterectomy and pelvic lymph node (LN) dissection at the Department of Gynecologic Oncology, Fudan University Shanghai Cancer Center, China, between May 2006 and January 2014. All included patients had histologically confirmed squamous cell carcinoma and the 2009 FIGO stage IB–IIA disease after initial treatment. All patients provided consent for their data to be used for research purposes. Data on clinicopathological and prognostic characteristics, including age at diagnosis, the FIGO stage, postoperative pathological findings[histological type, tumor grade, lymph-vascular space invasion (LVSI) status, tumor volume, and LN status], treatment modalities, date and type of recurrence, and date of death or last follow-up, were collected. The study was approved by the Ethics Committee of Fudan University Shanghai Cancer Center, Shanghai, China.

Adjuvant Therapy

Patients with intermediate-risk factors that met the Sedlis criteria, including tumor diameter, depth of stromal invasion (DSI), or LVSI status, and patients with more than one high-risk factor (including parametrial involvement, positive LN, or positive surgical margins) received adjuvant RT (ART) or concurrent chemoradiotherapy. Patients received pelvic intensity-modulated radiotherapy with computed tomography (CT) planned. Target delineation was based on the Radiation Therapy Oncology Group Consensus Guidelines (12, 13). Concurrent cisplatin was administered weekly at a dose of 40 mg/m^2. Brachytherapy was administered among patients with vaginal margin invasion. Patients with one or more high-risk factors received 4–6 cycles of paclitaxel (135 mg/m^2) and carboplatin (AUC = 5) on day 1.

Recurrence Classification and Treatment

Recurrence was confirmed based on findings from biopsy and/or imaging-based examinations such as CT, magnetic resonance imaging (MRI), or positron emission tomography (PET) scanning, obtained ahead of treatment planning. LR was defined as isolated pelvic recurrence, including vaginal recurrence with or without pelvic LN recurrence. DM was defined as distant site failure at either an organ or LN site. Multiple-site recurrence was defined as recurrence both inside and outside the pelvis; this type of recurrence was classified as DM. In-field and out-field recurrences were defined as recurrence inside or outside the pelvis for patients after ART. LN recurrence (LNR) included bilateral upper neck, supraclavicular, mediastinal, celiac, and pelvic and inguinal regions. Organ recurrence included recurrences in the vagina and other organs. Therapy for relapse included external beam radiation therapy and brachytherapy, surgery, and systemic chemotherapy. RT and surgery were classified as local therapy.

Statistical Analyses

Patients' demographic and clinicopathological characteristics and treatments for recurrent disease were reported as frequencies. Univariable survival curves were created using the Kaplan-Meier method. Between-group comparisons were performed using the log-rank test. Cox proportional hazards regression was used for univariate and multivariate analyses. Variables with p-values of <0.10 in univariate analysis were included in multivariate analyses. For all statistical tests, two-tailed p-values of <0.05 were considered significant. A prognostic nomogram was generated based on multivariable analysis results. Harrel's concordance index (C-index) and a calibration curve were used to evaluate nomogram performance. The accuracy and reliability of the recurrence model were evaluated based on time-dependent receiver operating characteristic curves. All statistical analyses were performed in SPSS version 25.0 (SPSS, Chicago, IL) and R software ver. 4.0.5.

RESULTS

This study included 472 women who underwent pelvic LN dissection for cervical squamous cell carcinoma with FIGO stages IB-IIA. The patients' median age was 47 (range: 22–77) years. All tumors were pathologically staged after radical surgery and included stages IB1 (n = 112, 23.7%), IB2 (n = 61, 12.9%), IIA1 (n = 162, 34.3%), and IIA2 (n = 137, 29.0%). Preoperative squamous cell carcinoma antigen (SCCA) levels of ≥2.55 ng/mL,

bulky tumor size of ≥4 cm, DSI greater than 1/2 thickness, positive LVSI, and parametrial invasion were observed in 62.0% (n = 240), 56.8% (n = 268), 85.8% (n = 400), 63.0% (n = 289), and 14.4% (n = 64) of the patients, respectively. Thirty-eight (8.5%) patients had positive vaginal margins. Positive LN (PLN) was detected in 224 (50.3%) patients. The median number of harvested LNs was 23 (range: 7–77); a single (range: 0–37) PLN was harvested. A total of 356 (75.4%) patients underwent ART. Among 305 (85.0%) patients who underwent chemotherapy, 204 (64.2%) received concurrent chemotherapy (**Table 1**).

Recurrence Patterns and Prognostic Factors

LR and DM accounted for 38.8% (183/472) and 61.2% (289/472) of recurrence cases, respectively. A total of 26.1% (n = 123) and 73.9% (n = 349) of failures were LNR and organ recurrence, respectively (**Table 2**).

RT, systemic chemotherapy, and surgery for relapse accounted for 44.0% (54/123), 41.5% (51/123), and 13.8% (17/123) of therapies for LNR, respectively. The corresponding rates for organ recurrence were 26.6% (93/349), 64.2% (224/349), and 9.2% (32/349), respectively (**Table 1**).

In univariate analysis, PLNs, SCCA levels of ≥2.55 ng/mL, tumor size of ≥4 cm, DSI, positive LVSI, parametrial invasion, and no ART were predictors of LR and DM (**Table 2**). In multivariate analysis, DSI (odds ratio [OR] = 1.494; 95% confidence interval [CI]: 1.286–2.853, $P = 0.011$) and ART (OR = 0.148; 95% CI: 0.075–0.291, $P = 0.000$) were independently associated with LR. LVSI (OR= 1.928; 95% CI: 1.151–3.229, $P = 0.013$) and adjuvant chemotherapy (OR = 0.521; 95% CI: 0.317–0.733, $P = 0.040$) were independently associated with DM. In addition, PLNs (OR = 3.729; 95% CI: 1.838–7.563, $P = 0.000$) and ART (OR = 0.470; 95% CI: 0.176–0.843, $P = 0.003$) were independently associated with LNR. SCCA levels of ≥2.55 ng/mL (OR = 1.642; 95% CI: 1.325–2.265, $P = 0.002$) and LVSI (OR = 1.462; 95% CI: 1.203–2.048, $P = 0.005$) were independently associated with organ recurrence (**Table 3**).

Survival and Stratification Analyses

For cases of disease recurrence, the median follow-up time was 59.1 (range 1.9–146.6) months. The 5-year OS rate was 33.7%, and the median OS was 24.0 months. Patients with LR (5-year OS rate, 28.1%; median OS = 40 months) and those with DM (5-year OS rate, 38.9%; median OS = 37 months) ($P = 0.755$) had similar survival rates (**Figure 1A**). However, the prognosis was poorer for patients with LR with ART than for those without ART (**Figure 1B**). LNR (5-year OS rate, 38.3%; median OS = 51 months) had a better survival than organ recurrence (5-year OS rate, 30.7%; median OS = 34 months) ($P = 0.001$) (**Figure 1C**). Prognosis associated with pelvic LNR (5-year OS rate, 18.3%; median OS = 37 months) was poorer than that associated with LNR outside of the pelvis (5-OS rate, 36.9%; median OS = 50 months) ($P = 0.019$) (**Figure 1D**). Among patients with organ recurrence only, lung metastasis (5-year OS rate, 32.5%; median OS = 48 months) was associated with survival rates that were

TABLE 1 | Baseline characteristic.

	N (%)
Age	
<60	422 (89.4%)
≥60	50 (10.6%)
Menopause	
Yes	173 (36.7%)
No	299 (63.3%)
FIGO Stage	
IB1	112 (23.7%)
IB2	61 (12.9%)
IIA1	162 (34.3%)
IIA2	137 (29.0%)
ECOG	
0~1	430 (91.1%)
2~3	42 (8.9%)
SCCA	
<2.55	147 (38.0%)
≥2.55	240 (62.0%)
Tumor size	
<4cm	204 (43.2%)
≥4cm	268 (56.8%)
Invasion depth	
<1/2	66 (14.2%)
≥1/2	400 (85.8%)
LVSI	
Positive	289 (63.0%)
Negative	170 (37.0%)
Parametrium	
Positive	64 (14.4%)
Negative	379 (85.6%)
Surgery margin	
Positive	38 (8.5%)
Negative	409 (91.5%)
Risk	
Intermediate	188 (41.8%)
High	262 (58.2%)
Adjuvant radiotherapy	
Yes	356 (75.4%)
No	116 (24.6%)
Chemotherapy	
Yes	305 (85.0%)
No	54 (15.0%)
Positive lymph nodes	
Yes	224 (50.3%)
No	221 (49.7%)
Recurrence location	
LR	183 (38.8%)
DM	289 (61.2%)
Pelvic with distant recurrence	45 (9.5%)
Recurrent type	
Lymphatic	123 (26.1%)
Organic	349 (73.9%)
Lymphatic recurrence site	
Supraclavicular nodes	39 (8.3%)
Mediastinal nodes	28 (5.9%)
Para aortic nodes	24 (5.1%)
Retroperitoneal nodes	35 (7.4%)
Inguinal nodes	20 (4.2%)
Organic recurrence site	
Vaginal	264 (55.9%)
Liver	25 (5.3%)
Lung	119 (25.3%)
Bone	79 (16.7%)

(Continued)

TABLE 1 | Continued

	N (%)
Treatment for lymph nodes	
Radiotherapy	54 (44.0%)
Chemotherapy	51 (41.5%)
Surgery	17 (13.8%)
Treatment for metastatic organ	
Radiotherapy	93 (26.6%)
Chemotherapy	224 (64.2%)
Surgery	32 (9.2%)

ECOG, The Eastern Cooperative Oncology Group; SCCA, serum squamous cell carcinoma antigen; LVSI, lymph-vascular space invasion; LR, locoregional recurrence; DM, distant metastasis.

better than those associated with other organ recurrence sites (5-year OS rate, 19.7%; median OS = 34 months) (P = 0.039) (**Figure 1E**). Patients with vaginal recurrence (5-year OS rate, 31.7%; median OS = 34 months) had a worse prognosis than did those without vaginal recurrence (5-year OS rate, 46.0%; median OS = 51 months) (P = 0.001) (**Figure 1F**). According to ART stratification, in-field recurrence was associated with poorer prognosis (5-year OS rate, 24.9%; median OS = 29 months) than out-field recurrence (5-year OS rate, 30.8%; median OS = 42 months) (P = 0.024) (**Figure 1B**). For all recurrent cases, surgery was associated with 5-year OS rates that were better than those associated with RT and chemotherapy (5-year OS rate of surgery, RT and chemotherapy: 56.9%, 35.7% and 27.3%; median OS: NA, 46 months and 32 months, respectively, P < 0.001). For in-field recurrence only, surgery (5-year OS rate, 36.5%; median OS = 36 months) was associated with OS that was better than that associated with secondary RT (5-year OS rate, 12.2%; median OS = 24 months) (P = 0.047). In patients with LR, LNR, and organ recurrence, outcomes associated with surgery and RT were better than those associated with systemic chemotherapy (P = 0.011).

Predictive Factors for OS and Nomogram

In multivariate analysis, type of recurrence, therapy for relapse, the FIGO stage, ART, baseline serum SCCA levels, and risk factor subgroup were independently associated with prognosis after recurrence (**Table 4**). All relevant predictors were used to construct a prognostic nomogram, and points were assigned based on corresponding factor coefficients; the total score was used to predict 5-year OS rates. The C-index of the nomogram was 0.724 (95% CI, 0.679–0.769) in the internal validation set (**Figure 2A**). Calibration curves are presented in **Figure 2B**. The results indicated that the nomogram was well-calibrated. In addition, this nomogram was compared to commonly used risk prediction methods, including the FIGO stage and Sedlis criteria and other previously used models. The AUC of our nomogram was greater than those of models previously used (0.846 vs. 0.720 vs. 0.677, P < 0.001) (**Figure 2C**).

DISCUSSION

In the present study, primary recurrence patterns were associated with the prognosis of squamous cervical cancer after initial

TABLE 2 | Univariate logistic regression models for different recurrence sites and subtypes.

Subgroup	Reference	LR		DM		LNR		Organ recurrence	
		OR (95CI)	P	OR (95CI)	P	OR (95CI)	P	OR (95CI)	P
Age									
>=60	<60	1.291 (0.717~2.324)	0.395	0.860 (0.475~1.560)	0.620	0.508 (0.232~1.116)	0.092	1.967 (0.896~4.315)	0.092
FIGO stage									
IIA	IB	0.949 (0.653~1.380)	0.784	1.207 (0.823~1.770)	0.334	1.004 (0.655~1.538)	0.986	1.004 (0.655~1.538)	0.986
Tumor size									
>=4cm	<4cm	1.488 (1.032~2.145)	0.033	1.381 (0.951~2.007)	0.090	1.593 (1.040~2.440)	0.032	1.593 (1.040~2.440)	0.032
Lymph nodes									
N+	N–	1.939 (1.330~2.826)	0.001	2.346 (1.586~3.473)	<0.001	4.630 (2.871~7.466)	<0.001	4.630 (2.871~7.466)	<0.001
SCCA									
>=2.55	<2.55	1.704 (1.466~2.063)	0.010	1.555 (1.023~2.365)	0.039	2.440 (1.469~4.052)	0.001	2.440 (1.469~4.052)	0.001
DSI									
>=1/2	<1/2	2.096 (1.223~3.593)	0.007	2.857 (1.674~4.877)	<0.001	1.944 (0.982~3.850)	0.056	1.944 (0.982~3.850)	0.056
LVSI									
Positive	Negative	2.506 (1.697~3.700)	<0.001	2.373 (1.606~3.506)	<0.001	4.984 (2.859~8.689)	<0.001	4.975 (2.857~8.696)	<0.001
Parametrial									
Positive	Negative	2.102 (1.202~3.678)	0.009	2.236 (1.210~4.130)	0.010	2.462 (1.424~4.255)	0.001	2.462 (1.424~4.255)	0.001
Surgical margin									
Positive	Negative	0.668 (0.339~1.318)	0.245	0.965 (0.489~1.906)	0.919	1.150 (0.551~2.398)	0.710	1.150 (0.551~2.398)	0.710
ART									
Yes	No	0.161 (0.098~0.265)	<0.001	0.733 (0.403~1.332)	0.308	0.282 (0.152~0.524)	<0.001	0.518 (0.250~1.074)	0.077
Chemotherapy									
Yes	No	0.645 (0.361~1.152)	0.139	0.193 (0.123~0.304)	<0.001	1.930 (0.931~4.000)	0.077	0.282 (0.152~0.524)	<0.001

SCCA, squamous cell carcinoma antigen; LVSI, lymph-vascular space invasion; DSI, deep stromal invasion; ART, adjuvant radiotherapy.

TABLE 3 | Multivariate logistic regression models for different recurrence sites and subtypes.

Subgroup	Reference	LR		DM		LNR		Organ recurrence	
		OR (95CI)	P	OR (95CI)	P	OR (95CI)	P	OR (95CI)	P
Tumor size									
>=4cm	<4cm	1.308 (0.808~2.118)	0.274			1.012 (0.558~1.835)	0.970	1.016 (0.563~1.833)	0.958
Lymph nodes									
N+	N–	1.159 (0.670~2.005)	0.598	1.622 (0.962~2.735)	0.070	3.729 (1.838~7.563)	<0.001	1.559 (0.791~3.072)	0.200
SCCA									
>=2.55	<2.55	1.265 (0.739~2.164)	0.392	1.127 (0.678~1.872)	0.645	1.509 (0.762~2.991)	0.238	3.690 (1.838~7.407)	<0.001
DSI									
>=1/2	<1/2	2.026 (1.172~3.502)	0.011	1.792 (0.908~3.534)	0.093	1.698 (0.509~5.682)	0.388	1.743 (0.532~5.709)	0.358
LVSI									
Positive	Negative	1.747 (0.763~4.001)	0.187	1.931 (1.153~3.235)	0.012	2.140 (0.936~4.893)	0.071	2.367 (1.154~4.919)	0.002
Parametrial									
Positive	Negative	1.293 (0.671~2.490)	0.443	1.212 (0.618~2.377)	0.576	1.191 (0.591~2.397)	0.625	1.143 (0.572~2.287)	0.705
ART									
Yes	No	0.148 (0.075~0.291)	<0.001			2.401 (1.470~4.543)	<0.001	0.650 (0.212~1.993)	0.451
Chemotherapy									
Yes	No			0.519 (0.31~0.869)	0.043	1.078 (0.373~3.114)	0.890	0.895 (0.312~2.567)	0.837

SCCA, squamous cell carcinoma antigen; LVSI, lymph-vascular space invasion; DSI, deep stromal invasion; ART, adjuvant radiotherapy.

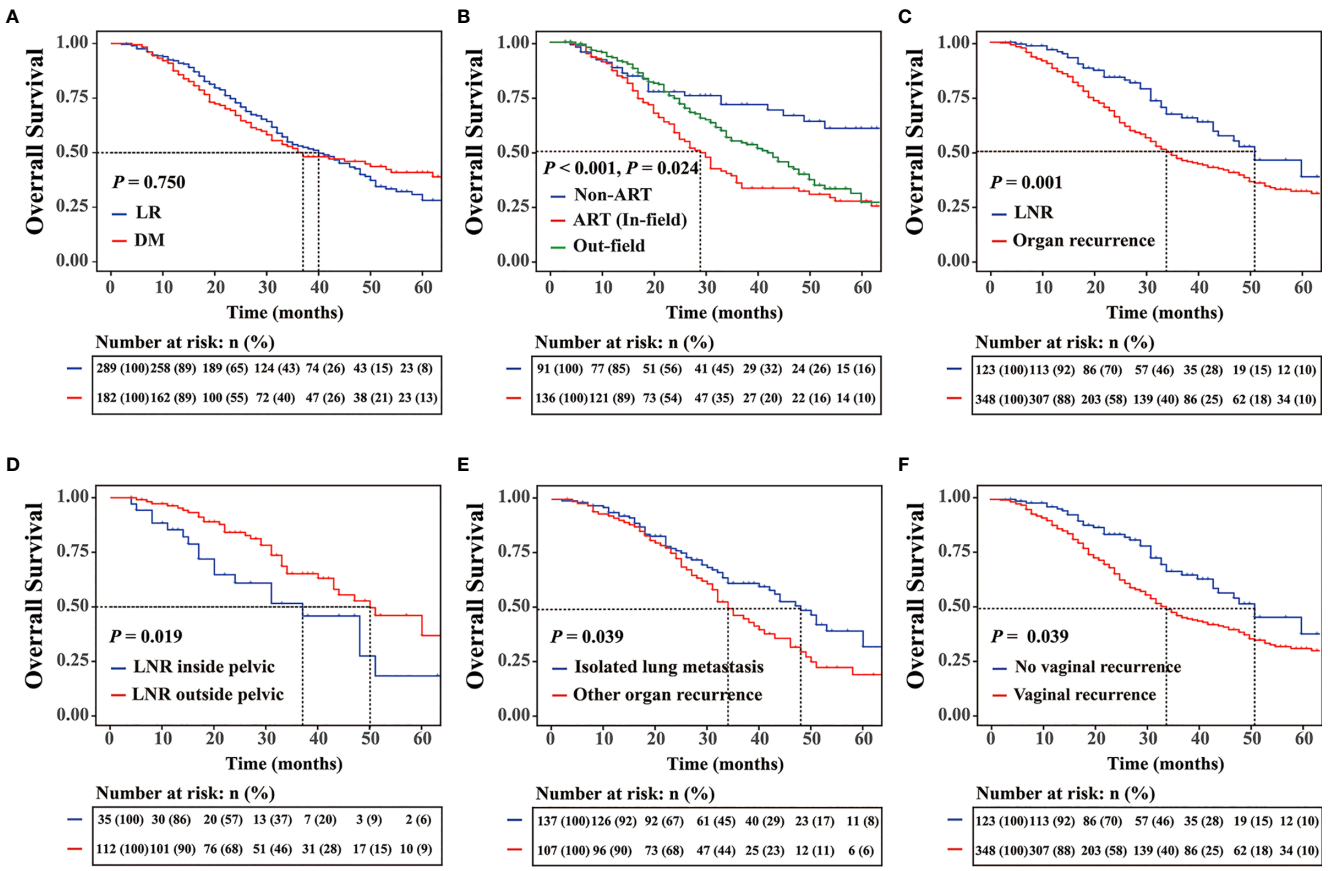


FIGURE 1 | **(A)** Five-year overall survival (OS) rates for different recurrence sites. **(B)** OS rates for patients with locoregional recurrence (LR) with or without adjuvant radiotherapy (ART) and the OS for patients with the out-field recurrence. **(C)** Five-year OS rates for patients with different recurrence subtypes, **(D)** patients with lymph node recurrence, **(E)** patients with or without isolated lung metastasis, and **(F)** patients with or without vaginal stump.

TABLE 4 | Multivariate Cox proportional hazards models for 5-year overall survival.

Subgroup	Reference	HR	95 CI	*P* Value
Recurrence type				
Organ recurrence	Lymph nodes recurrence	1.917	1.151-3.193	0.012
Vaginal recurrence		2.448	1.661-3.609	<0.001
Therapy for relapse				
Chemotherapy	Radiotherapy	1.105	0.786-1.553	0.567
Surgery		0.500	0.275-0.907	0.023
FIGO stage				
IB2	IB1	2.193	1.292-3.721	0.004
IIA1		1.526	0.995-2.342	0.053
IIA2		2.043	1.331-3.138	0.001
ART				
Yes	No	0.567	0.404-0.795	0.001
Risk group				
Intermediate	None	2.073	1.653-4.036	0.002
High		2.155	1.649-4.470	0.003
SCCA				
>=2.55	<2.55	1.568	1.098-2.238	0.013

SCCA, squamous cell carcinoma antigen; ART, adjuvant radiotherapy.

treatment. The patterns of recurrence in cervical cancer vary, and thus, different treatments for relapse may result in different prognoses. The National Comprehensive Cancer Network Guidelines recommend individualized therapy for relapse, including surgery, RT, and chemotherapy. For localized recurrence after initial treatment, radical retreatment, including RT and/or chemotherapy, and surgery may be administered. However, radical retreatment options may vary among recurrence sites; for example, patients with regional LN recurrence may be suitable candidates for radical surgery and RT. In such cases, patients eligible for radical treatment may achieve long-term disease-free survival rates of approximately 40% (14). Most previous studies evaluated prognosis based on patients' clinicopathological features and recurrence sites. However, few studies have examined the relationship between specific parameters and recurrence patterns. The present study examined the prognostic relevance of recurrence patterns and subtypes, and that of clinicopathological factors.

In our cohort, there were more cases of DM than LR (61.2% vs. 38.8%). Furthermore, the incidence of organ recurrence was higher than that of LNR. Vaginal recurrence was the most common recurrence site, followed by the lung and bone. Previous population-based studies reported vaginal recurrence as the most common local recurrence site in patients with cervical cancer; meanwhile, the lung and bone were the common sites of distant metastases (15, 16). In our study, LNR was a particular kind of recurrence pattern; in addition, approximately 12.5% and 8.3% of recurrence cases were

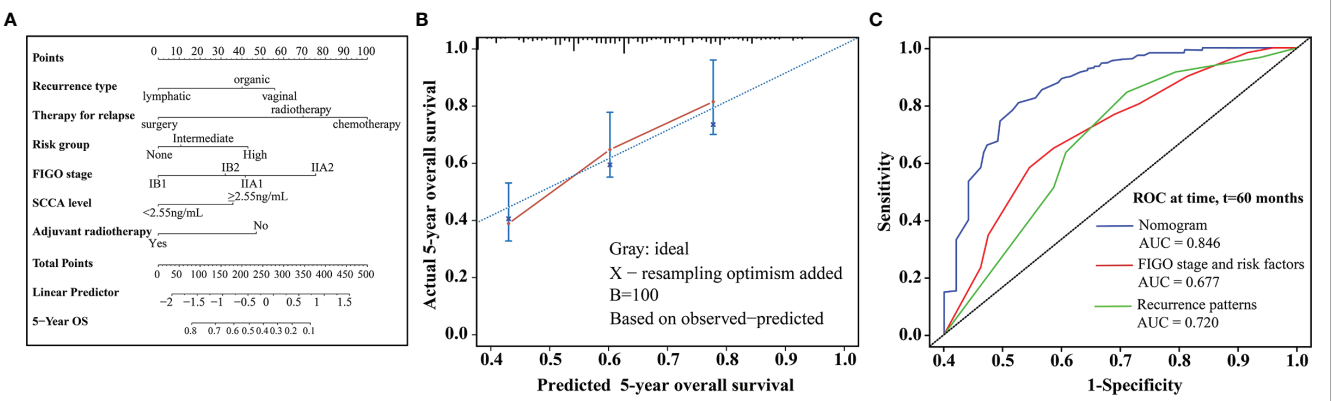


FIGURE 2 | **(A)** Nomogram predicting 5-year OS rates for patients with relapse after initial treatment. The nomogram was based on scores corresponding to each independent variable. The total score (bottom of the scale) indicates the probabilities of 5-year OS rates. **(B)** The predicted and observed 5-year OS rates were used for model calibration. The x-axis displays nomogram-predicted probability, while the y-axis displays observed survival rates estimated using the Kaplan-Meier method. The dotted line indicates excellent model calibration, with good concordance between the predicted and observed survival rates. The vertical bars represent 95% confidence intervals. **(C)** Receiver operating characteristic curves with area under the curve values compare nomogram and traditional model discrimination. The blue lines represent survival rates predicted by the nomogram.

observed at para-aortic and supraclavicular LNs, respectively. The para-aortic lymphatic system is connected to the cervix and pelvic LNs, resulting in a high recurrence rate in para-aortic LNs (17, 18). Kim et al. reported rates of 59.5% and 40.5% for distant and pelvic recurrence, respectively (combined: 21.5%, central: 10.7%, pelvic 8.3%) (19). Pamela et al. used PET scans to detect recurrences in para-aortic LNs and reported a rate of 18.7%, which was consistent with the present study findings (20). Tae et al. reported a 5.4% recurrence rate in the supraclavicular region after radical hysterectomy in patients with early-stage cervical cancer (21).

Common prognostication methods include the FIGO staging system and the Peters and Sedlis criteria. However, these models fail to account for the effects of recurrence patterns. When patients experience disease recurrence, little attention is given to baseline clinical characteristics, which may help assess the risk of recurrence. Studies on the relevance of recurrence patterns and initial treatment types to the risk of relapse are rare. Nevertheless, baseline clinicopathological characteristics may help inform treatment as these factors may affect the risk of relapse. Consequently, we examined the associations among baseline clinicopathological characteristics, recurrence patterns, therapy for relapse, and prognosis to establish a predictive model to inform clinical practice.

In the present study, approximately half of the patients with recurrence had elevated serum SCCA levels at diagnosis and half had positive LN status after surgery. All cases with recurrence presented with intermediate- or high-risk factors or both at baseline. Different recurrence patterns may be associated with specific clinicopathological characteristics at initial treatment. According to univariate and multivariate analyses, DSI and the absence of ART were associated with a high risk of LR. Patients who did not receive adjuvant chemotherapy but had LVSI were more likely to experience DM than their counterparts. PLN status after initial treatment or lack of ART may result in LNR. Preoperative serum SCCA levels and positive LVSI findings were independent predictive factors for organ recurrence. Jeong et al. reported that approximately 59% of recurrence cases had elevated serum SCCA levels at diagnosis (22). Serum SCCA levels are biomarkers commonly used for auxiliary diagnosis and surveillance in cervical cancer; elevated serum SCCA levels are associated with the extent of the disease (23, 24). However, no previous study has examined the association between serum SCCA levels and specific recurrence patterns. According to the Sedlis criteria, DSI is an intermediate risk factor for recurrence in cervical cancer; we have previously shown that DSI may be independently associated with both DFS and OS (25). The effect of LVSI on early-stage cervical cancer remains controversial, and previous studies have yielded conflicting results. Balaya and Obrzut found that LVSI may be associated with decreased 5-year DFS and 10-year OS (26, 27). Meanwhile, Creasman et al. have suggested that LVSI may not be a prognostic factor (28). In the present study, patients with positive LVSI had increased risk of DM, specifically, at distant organs. The present study model was superior to previous models for disease prognostication (29–31).

The prognosis associated with LR was comparable to that associated with DM. More specifically, cases of LNR had better prognosis than cases of organ recurrence; however, pelvic LNR had poor overall prognosis. Isolated LNR may be radically treated with either surgery or RT; in contrast, organ recurrence is difficult to treat with any radical approach. For patients with organ recurrence, vaginal recurrence was associated with poor prognosis; meanwhile, isolated lung metastasis was associated with better OS rates compared to those associated with the other sites of organ recurrence. Isolated lung disease may be treatable with surgery or RT, which may improve prognosis. Previous studies have shown that patients who benefit from aggressive local therapy for oligometastatic disease include those with nodal or lung metastases (32). Nevertheless, pelvic recurrence was associated with poor prognosis in patients with LR after ART. The palliation of pelvic recurrences is difficult at previously irradiated sites that are not amenable to local pain control techniques or surgical resection. These sites are generally not responsive to chemotherapy; consequently, affected patients are often advised to undergo pelvic exenteration or receive systematic chemotherapy; however, pelvic exenteration is a complex procedure susceptible to complications, which may affect prognosis. Thus, the National Comprehensive Cancer Network guidelines recommend pelvic exenteration for very select patients. Moreover, secondary RT is not feasible due to the high risk of adverse effects and dose-limiting toxicity (33, 34). Chemotherapy is often recommended for patients with extra-pelvic metastases or recurrent disease who are not candidates for RT or exenterative surgery.

This study had some limitations that should be considered when interpreting its findings. First, it was a retrospective study, which makes it subject to the effects of selection bias and confounding factors. Second, nodal metastasis has been redefined in the 2018 FIGO staging system; however, this study dataset and the included citations refer mostly to the 2009 FIGO staging system. Finally, although local treatment status emerged as a prognostic factor for OS, the lack of precise information on recurrence treatment may impact the specificity of the present results.

CONCLUSION

Recurrent cervical cancer is associated with poor prognosis in cases of in-field recurrence. Different clinicopathological characteristics are associated with different recurrence sites and subtypes. The present findings suggest that patients with DSI and absence of ART are at a high risk of LR. Patients who did not receive adjuvant chemotherapy and presented with LVSI were more likely to experience DM than their counterparts. PLNs after initial treatment or lack of ART may increase the risk of LNR. Preoperative serum SCCA levels and positive LVSI status increased the risk of organ recurrence. Recurrent cervical cancer prognosis is associated with recurrence location and subtype.

DATA AVAILABILITY STATEMENT

The raw data supporting the conclusions of this article will be made available by the authors, without undue reservation.

ETHICS STATEMENT

Written informed consent was obtained from the individual(s) for the publication of any potentially identifiable images or data included in this article.

AUTHOR CONTRIBUTIONS

Conception and design: ZZ, LJ, and JZ. Collection and assembly of data: ZZ and LJ. Data analysis and interpretation: ZZ, LJ, and JZ. Pathological slides reviewing: RB. Manuscript writing: ZZ and LJ. Final approval of manuscript: ZZ, LJ, RB, XW, GK, and JZ. All authors contributed to the article and approved the submitted version.

FUNDING

The present study was supported by the National Natural Science Foundation of China (Youth Fund no. 81902640).

ACKNOWLEDGMENTS

We thank all the faculty members in our department and all the patients, and their families involved in the current study.

REFERENCES

1. Bray F, Ferlay J, Soerjomataram I, Siegel RL, Torre LA, Jemal A. Global Cancer Statistics 2018: GLOBOCAN Estimates of Incidence and Mortality Worldwide for 36 Cancers in 185 Countries. *CA Cancer J Clin* (2018) 68 (6):394–424. doi: 10.3322/caac.21492
2. Lees BF, Erickson BK, Huh WK. Cervical Cancer Screening: Evidence Behind the Guidelines. *Am J Obstet Gynecol* (2016) 214(4):438–43. doi: 10.1016/j.ajog.2015.10.147
3. Lei T, Mao WM, Lei TH, Dai LQ, Fang L, Chen WQ, et al. Incidence and Mortality Trend of Cervical Cancer in 11 Cancer Registries of China. *Chin J Cancer Res* (2011) 23(1):10–4. doi: 10.1007/s11670-011-0010-x
4. American College of O, Gynecologists. ACOG Practice Bulletin. Diagnosis and Treatment of Cervical Carcinomas. Number 35, May 2002. American College of Obstetricians and Gynecologists. *Int J Gynaecol Obstet* (2002) 78 (1):79–91. doi: 10.1016/s0020-7292(02)90092-5
5. Gaffney DK, Erickson-Wittmann BA, Jhingran A, Mayr NA, Puthawala AA, Moore D, et al. ACR Appropriateness Criteria(R) on Advanced Cervical Cancer Expert Panel on Radiation Oncology-Gynecology. *Int J Radiat Oncol Biol Phys* (2011) 81(3):609–14. doi: 10.1016/j.ijrobp.2010.11.005
6. Peters WA 3rd, Liu PY, Barrett RJ 2nd, Stock RJ, Monk BJ, Berek JS, et al. Concurrent Chemotherapy and Pelvic Radiation Therapy Compared With Pelvic Radiation Therapy Alone as Adjuvant Therapy After Radical Surgery in High-Risk Early-Stage Cancer of the Cervix. *J Clin Oncol* (2000) 18(8):1606–13. doi: 10.1200/JCO.2000.18.8.1606
7. Wenzel HHB, Smolders RGV, Beltman JJ, Lambrechts S, Trum HW, Yigit R, et al. Survival of Patients With Early-Stage Cervical Cancer After Abdominal or Laparoscopic Radical Hysterectomy: A Nationwide Cohort Study and Literature Review. *Eur J Cancer* (2020) 133:14–21. doi: 10.1016/j.ejca.2020.04.006
8. van der Velden J, Mom CH, van Lonkhuijzen L, Tjiong MY, Westerveld H, Fons G. Analysis of Isolated Loco-Regional Recurrence Rate in Intermediate Risk Early Cervical Cancer After a Type C2 Radical Hysterectomy Without Adjuvant Radiotherapy. *Int J Gynecol Cancer* (2019) 29:874–8. doi: 10.1136/ijgc-2019-000445
9. Gee MS, Atri M, Bandos AI, Mannel RS, Gold MA, Lee SI. Identification of Distant Metastatic Disease in Uterine Cervical and Endometrial Cancers With FDG PET/CT: Analysis From the ACRIN 6671/GOG 0233 Multicenter Trial. *Radiology* (2018) 287(1):176–84. doi: 10.1148/radiol.2017170963
10. Salani R, Khanna N, Frimer M, Bristow RE, Chen LM. An Update on Post-Treatment Surveillance and Diagnosis of Recurrence in Women With Gynecologic Malignancies: Society of Gynecologic Oncology (SGO) Recommendations. *Gynecol Oncol* (2017) 146(1):3–10. doi: 10.1016/j.ygyno.2017.03.022
11. Yoneda JY, Braganca JF, Sarian LO, Borba PP, Conceicao JC, Zeferino LC. Surgical Treatment of Microinvasive Cervical Cancer: Analysis of Pathologic Features With Implications on Radicality. *Int J Gynecol Cancer* (2015) 25 (4):694–8. doi: 10.1097/IGC.0000000000000416
12. Small W Jr, Bosch WR, Harkenrider MM, Strauss JB, Abu-Rustum N, Albuquerque KV, et al. NRG Oncology/RTOG Consensus Guidelines for Delineation of Clinical Target Volume for Intensity Modulated Pelvic Radiation Therapy in Postoperative Treatment of Endometrial and Cervical Cancer: An Update. *Int J Radiat Oncol Biol Phys* (2021) 109(2):413–24. doi: 10.1016/j.ijrobp.2020.08.061
13. Small W Jr, Mell LK, Anderson P, Creutzberg C, De Los Santos J, Gaffney D, et al. Consensus Guidelines for Delineation of Clinical Target Volume for Intensity-Modulated Pelvic Radiotherapy in Postoperative Treatment of Endometrial and Cervical Cancer. *Int J Radiat Oncol Biol Phys* (2008) 71 (2):428–34. doi: 10.1016/j.ijrobp.2007.09.042
14. Thomas GM, Dembo AJ, Myhr T, Black B, Pringle JF, Rawlings G. Long-Term Results of Concurrent Radiation and Chemotherapy for Carcinoma of the Cervix Recurrent After Surgery. *Int J Gynecol Cancer* (1993) 3(4):193–8. doi: 10.1046/j.1525-1438.1993.03040193.x
15. Zhang Y, Guo Y, Zhou X, Wang X, Wang X. Prognosis for Different Patterns of Distant Metastases in Patients With Uterine Cervical Cancer: A Population-Based Analysis. *J Cancer* (2020) 11(6):1532–41. doi: 10.7150/jca.37390
16. Zhou S, Peng F. Patterns of Metastases in Cervical Cancer: A Population-Based Study. *Int J Clin Exp Pathol* (2020) 13(7):1615–23.
17. Bae BK, Park SH, Jeong SY, Chong GO, Kim MY, Kim JC. Mapping Patterns of Para-Aortic Lymph Node Recurrence in Cervical Cancer: A Retrospective Cohort Analysis. *Radiat Oncol* (2021) 16(1):128. doi: 10.1186/s13014-021-01856-9
18. Eifel PJ, Winter K, Morris M, Levenback C, Grigsby PW, Cooper J, et al. Pelvic Irradiation With Concurrent Chemotherapy Versus Pelvic and Para-Aortic Irradiation for High-Risk Cervical Cancer: An Update of Radiation Therapy Oncology Group Trial (RTOG) 90-01. *J Clin Oncol* (2004) 22(5):872–80. doi: 10.1200/JCO.2004.07.197
19. Kim TH, Kim MH, Kim BJ, Park SI, Ryu SY, Cho CK. Prognostic Importance of the Site of Recurrence in Patients With Metastatic Recurrent Cervical Cancer. *Int J Radiat Oncol Biol Phys* (2017) 98(5):1124–31. doi: 10.1016/j.ijrobp.2017.03.029
20. Peters PN, Pierson WE, Chen LM, Westphalen AC, Chapman JS, Hsu IC. PET-Detected Asymptomatic Recurrence Is Associated With Improved Survival in Recurrent Cervical Cancer. *Abdom Radiol (NY)* (2021) 46 (1):341–50. doi: 10.1007/s00261-020-02633-0
21. Kong TW, Son JH, Paek J, Chang SJ, Ryu HS. Prognostic Factors Influencing Pelvic, Extra-Pelvic, and Intraperitoneal Recurrences in Lymph Node-Negative Early-Stage Cervical Cancer Patients Following Radical Hysterectomy. *Eur J Obstet Gynecol Reprod Biol* (2020) 252:94–9. doi: 10.1016/j.ejogrb.2020.06.030

22. Jeong BK, Huh SJ, Choi DH, Park W, Bae DS, Kim BG. Prognostic Value of Different Patterns of Squamous Cell Carcinoma Antigen Level for the Recurrent Cervical Cancer. *Cancer Res Treat* (2013) 45(1):48–54. doi: 10.4143/crt.2013.45.1.48
23. Fu J, Wang W, Wang Y, Liu C, Wang P. The Role of Squamous Cell Carcinoma Antigen (SCC Ag) in Outcome Prediction After Concurrent Chemoradiotherapy and Treatment Decisions for Patients With Cervical Cancer. *Radiat Oncol* (2019) 14(1):146. doi: 10.1186/s13014-019-1355-4
24. Salvatici M, Achilarre MT, Sandri MT, Boveri S, Vanna Z, Landoni F. Squamous Cell Carcinoma Antigen (SCC-Ag) During Follow-Up of Cervical Cancer Patients: Role in the Early Diagnosis of Recurrence. *Gynecol Oncol* (2016) 142(1):115–9. doi: 10.1016/j.ygyno.2016.04.029
25. Zhu J, Cao L, Wen H, Bi R, Wu X, Ke G. The Clinical and Prognostic Implication of Deep Stromal Invasion in Cervical Cancer Patients Undergoing Radical Hysterectomy. *J Cancer* (2020) 11(24):7368–77. doi: 10.7150/jca.50752
26. Balaya V, Guani B, Magaud L, Bonsang-Kitzis H, Ngo C, Mathevet P, et al. Validation of the 2018 FIGO Classification for Cervical Cancer: Lymphovascular Space Invasion Should Be Considered in IB1 Stage. *Cancers (Basel)* (2020) 12(12):3554. doi: 10.3390/cancers12123554
27. Obrzut B, Semczuk A, Narog M, Obrzut M, Krol P. Prognostic Parameters for Patients With Cervical Cancer FIGO Stages IA2-IIB: A Long-Term Follow-Up. *Oncology* (2017) 93(2):106–14. doi: 10.1159/000471766
28. Creasman WT, Kohler MF. Is Lymph Vascular Space Involvement an Independent Prognostic Factor in Early Cervical Cancer? *Gynecol Oncol* (2004) 92(2):525–9. doi: 10.1016/j.ygyno.2003.11.020
29. Ryu SY, Kim MH, Nam BH, Lee TS, Song ES, Park CY, et al. Intermediate-Risk Grouping of Cervical Cancer Patients Treated With Radical Hysterectomy: A Korean Gynecologic Oncology Group Study. *Br J Cancer* (2014) 110(2):278–85. doi: 10.1038/bjc.2013.716
30. Sedlis A, Bundy BN, Rotman MZ, Lentz SS, Muderspach LI, Zaino RJ. A Randomized Trial of Pelvic Radiation Therapy Versus No Further Therapy in Selected Patients With Stage IB Carcinoma of the Cervix After Radical Hysterectomy and Pelvic Lymphadenectomy: A Gynecologic Oncology Group Study. *Gynecol Oncol* (1999) 73(2):177–83. doi: 10.1006/gyno.1999.5387
31. Ramirez PT, Pareja R, Rendon GJ, Millan C, Frumovitz M, Schmeler KM. Management of Low-Risk Early-Stage Cervical Cancer: Should Conization, Simple Trachelectomy, or Simple Hysterectomy Replace Radical Surgery as the New Standard of Care? *Gynecol Oncol* (2014) 132(1):254–9. doi: 10.1016/j.ygyno.2013.09.004
32. Im JH, Yoon HI, Kim S, Nam EJ, Kim SW, Yim GW, et al. Tailored Radiotherapeutic Strategies for Disseminated Uterine Cervical Cancer Patients. *Radiat Oncol* (2015) 10:77. doi: 10.1186/s13014-015-0373-0
33. Sardain H, Lavoue V, Redpath M, Bertheuil N, Foucher F, Leveque J. Curative Pelvic Exenteration for Recurrent Cervical Carcinoma in the Era of Concurrent Chemotherapy and Radiation Therapy. A Systematic Review. *Eur J Surg Oncol* (2015) 41(8):975–85. doi: 10.1016/j.ejso.2015.03.235
34. Llewelyn M, Taylor A. Re-Irradiation of Cervical and Endometrial Cancer. *Curr Opin Oncol* (2017) 29(5):343–50. doi: 10.1097/CCO.0000000000000392

Conflict of Interest: The authors declare that the research was conducted in the absence of any commercial or financial relationships that could be construed as a potential conflict of interest.

Publisher's Note: All claims expressed in this article are solely those of the authors and do not necessarily represent those of their affiliated organizations, or those of the publisher, the editors and the reviewers. Any product that may be evaluated in this article, or claim that may be made by its manufacturer, is not guaranteed or endorsed by the publisher.

Copyright © 2022 Zhang, Jiang, Bi, Wu, Ke and Zhu. This is an open-access article distributed under the terms of the Creative Commons Attribution License (CC BY). The use, distribution or reproduction in other forums is permitted, provided the original author(s) and the copyright owner(s) are credited and that the original publication in this journal is cited, in accordance with accepted academic practice. No use, distribution or reproduction is permitted which does not comply with these terms.

frontiers | Frontiers in Oncology

SYSTEMATIC REVIEW
published: 14 April 2022
doi: 10.3389/fonc.2022.844801

How Immunotherapy Modified the Therapeutic Scenario of Endometrial Cancer: A Systematic Review

Brigida Anna Maiorano[1,2], Mauro Francesco Pio Maiorano[3], Gennaro Cormio[3], Annamaria Maglione[4], Domenica Lorusso[5,6] and Evaristo Maiello[1]*

[1] Oncology Department, Fondazione Casa Sollievo della Sofferenza IRCCS, San Giovanni Rotondo, Italy, [2] Department of Translational Medicine and Surgery, Catholic University of the Sacred Heart, Rome, Italy, [3] Obstetrics and Gynecology Unit, Department of Biomedical Sciences and Human Oncology, University of Bari "Aldo Moro", Bari, Italy, [4] Obstetrics and Gynecology Department, Fondazione Casa Sollievo della Sofferenza IRCCS, San Giovanni Rotondo, Italy, [5] Department of Women and Child Health, Division of Gynaecologic Oncology, Fondazione Policlinico Universitario "A. Gemelli" IRCCS, Rome, Italy, [6] Scientific Directorate, Fondazione Policlinico Universitario "A. Gemelli" IRCCS, Rome, Italy

Background: Endometrial cancer (EC) represents the sixth most common female tumor. In the advanced setting, the prognosis is dismal with limited treatment options. Platinum-based chemotherapy represents the actual standard of care in first-line chemotherapy, but no standard second-line chemotherapy is approved, with less than 1/4 of patients responding to second-line chemotherapy. In the last 10 years, immune checkpoint inhibitors (ICIs) have changed the treatment landscape of many solid tumors.

Methods: The review was conducted according to the PRISMA guidelines. We searched EMBASE, MEDLINE, Cochrane Database, and conference abstracts from international societies, up to November 2021. Clinical trials employing ICIs in advanced EC, written in English, were included. Reviews, letters, and commentaries were excluded. The overall response rate (ORR), progression-free survival (PFS), overall survival (OS), and safety (number and grade of treatment-related adverse events [TRAEs]) were evaluated.

Results: 15 studies, for a total of 1,627 patients, were included: 14 non-randomized phase I/II trials and 1 randomized phase III trial. Anti-PD1 (pembrolizumab, nivolumab, dostarlimab) and anti-PD-L1 agents (avelumab, atezolizumab, durvalumab) were administered as single agents; pembrolizumab and nivolumab were combined with the tyrosine-kinase inhibitors (TKI) lenvatinib and cabozantinib, respectively; and durvalumab was associated with anti-CTLA4 tremelimumab. 4 studies selected only MSI patients. Single agents determined an ORR from 26.7% to 58% among MSI patients, from 3% to 26.7% among MSS patients. DCR ranged from 53.5% to 88.9% in MSI, 31.4% to 35.2% in MSS patients. The combination of TKI and ICIs determined 32% to 63.6% of ORR in all-comers, 32%–36.2% in MSS patients. 54.2% to 76% of patients developed TRAEs. The combination of ICIs and TKI achieved a higher toxicity rate than single agents (≥G3 TRAEs 88.9%).

Conclusion: ICIs represent an effective option for pretreated advanced EC patients with a tolerable profile. Given the encouraging results in MSI patients, every woman diagnosed with EC should be investigated for MS status. In MSS women, the combination of ICIs and

OPEN ACCESS

Edited by:
Marcia Hall,
Mount Vernon Cancer Centre, United Kingdom

Reviewed by:
Athina Christopoulou,
General University Hospital of Patras, Greece
Gian Paolo Spinelli,
Sapienza University of Rome, Italy

****Correspondence:***
Brigida Anna Maiorano
b.maiorano@operapadrepio.it

Specialty section:
This article was submitted to Gynecological Oncology, a section of the journal Frontiers in Oncology

Received: *28 December 2021*
Accepted: *21 March 2022*
Published: *14 April 2022*

Citation:
Maiorano BA, Maiorano MFP, Cormio G, Maglione A, Lorusso D and Maiello E (2022) How Immunotherapy Modified the Therapeutic Scenario of Endometrial Cancer: A Systematic Review. Front. Oncol. 12:844801. doi: 10.3389/fonc.2022.844801

TKI is more effective than monotherapy, notwithstanding safety concerns. PD-L1 cannot predict ICI response, whereas other biomarkers such as MSI and tumor mutational burden seem more accurate. Ongoing randomized trials will further clarify the role of these therapeutic options.

Systematic Review Registration: PROSPERO, CRD42021293538.

Keywords: endometrial cancer (EC), immune checkpoint inhibitors (ICI), immunotherapy, pembrolizumab, lenvatinib, dostarlimab, PD1, microsatellite instability (MSI)

1 INTRODUCTION

With an incidence of approximately 10.8 cases/100,000/year, endometrial cancer (EC) represents the sixth most common cancer among women, accounting for 4.5% of all new cancer diagnoses. The incidence rises with age, being very uncommon before 40 years and reaching 35.2 cases/100,000/year among >50-year-old women, with a median age at diagnosis of 63 years (1–3). Several risk factors for EC have been identified: age, familiar history, previous radiation therapy, obesity, diabetes, metabolic disease, diet, exercise, and general lifestyle (4). Furthermore, menopause, tamoxifen use, birth control pills, intrauterine devices, pregnancy, polycystic ovarian syndrome, and history of endometrial hyperplasia, while affecting circulating sex hormone levels, might contribute to EC development (5). EC represents the 13th cause of cancer-related deaths among women, with a mortality rate of 2.5/100,000/year (1). The 5-year survival rate dramatically drops from 94.9% for localized diseases to 17.8% for the metastatic stage, representing 9% of total diagnoses (2). In the localized setting, surgery is the first-choice treatment, also combined with radiotherapy, whereas chemotherapy represents the cornerstone for the high-risk and advanced diseases. The current standard of care (SOC) for first-line advanced/recurrent EC is the combination of carboplatin and paclitaxel, which guarantees a median overall survival (mOS) of 37 months and a median progression-free survival (mPFS) of 13 months (6). However, there is currently no SOC after platinum progression (7). Response rates (RRs) with single-agent chemotherapy (mainly ifosfamide, docetaxel, doxorubicin, weekly paclitaxel), and endocrine therapy, range from 8% to 24%, with less than 1 year of OS (8, 9). Recent findings have suggested the efficacy of platinum derivatives in "platinum-sensitive" patients (10). However, while platinum rechallenge might be an option in recurrent EC with a long recurrence-free interval, there is clearly a need for new therapeutic options (7, 9, 10).

The Cancer Genome Atlas (TCGA) described at least 4 molecular subtypes of EC: polymerase ϵ (POLE)-mutant, microsatellite instable-high (MSI-H), copy number low, and copy number high. The first two subtypes are associated with a better prognosis. Effectively, up to 30% of EC are MSI-H, characterized by defective proteins that repair DNA through the mismatch repair (MMR) mechanism. MMR-deficient (MMRd) EC accumulates errors in areas of repetitive DNA sequences called microsatellites, developing a high mutational load due to the release of a significant number of neo-antigens, which has been associated with immunotherapy response (11). Indeed, immunotherapy, particularly immune-checkpoint inhibitors (ICIs), represents the current cutting-edge therapy for many solid tumors, including gynecological malignancies (12). It is worthy of note that the Food and Drug Administration (FDA) granted two accelerated approvals of ICIs for pretreated EC patients: pembrolizumab for MSI-H tumors in 2017, and pembrolizumab plus lenvatinib for MS-stable (MSS) disease in 2019 (13, 14). Moreover, in 2021, the European Medial Agency (EMA) approved pembrolizumab and lenvatinib for pretreated EC patients, and dostarlimab for MSI-H EC (15, 16).

We hereby systematically reviewed the clinical trials regarding ICIs for the treatment of advanced EC to evaluate how they might change the clinical approach to this malignancy and future directions for tailored trials. To the best of our knowledge, this is the first systematic review to synthesize the efficacy and safety of clinical trials employing ICIs in EC.

2 MATERIALS AND METHODS

2.1 Protocol Registration

We registered the protocol for this systematic review with PROSPERO (CRD42021293538).

2.2 Search Strategy and Data Extraction

This systematic review was carried out following the Preferred Reporting Items for Systematic Reviews and Meta-Analysis (PRISMA) statement (17). Two authors (BM and MM) independently performed a literature search of the databases PubMed, EMBASE, and Cochrane Central Register of Controlled Trials, in November 2021. The search terms ("endometrial neoplasms" OR ("endometrial" AND "neoplasms") OR "endometrial cancer" OR ("endometrial" AND "cancer") OR "uterine cancer" OR ("uterine" AND "cancer") AND ["immune checkpoint inhibitors" OR "ICIs" OR "avelumab" OR "nivolumab" OR "atezolizumab" OR "pembrolizumab" OR "durvalumab" OR "tremelimumab" OR "ipilimumab" or "dostarlimab")] were used. An additional search for conference abstracts from the American Association of Clinical Oncology (ASCO), European Society of Medical Oncology (ESMO), and Society of Gynecologic Oncology (SGO) was also performed. Article citations were manually checked for additional references.

2.3 Inclusion and Exclusion Criteria, Population, Intervention, and Outcomes

We included phase I–IV clinical trials reporting efficacy and safety data of ICIs (single agents or combinations) in advanced/

recurrent EC patients, written in the English language. From multi-cohort trials, the number and data of EC patients were identified. Meta-analyses, reviews, case reports, correspondences, personal opinions, and *in vitro*/animal studies were excluded. For the selected studies, the following data were collected: trial name, first author, year of publication, phase, number of treated patients, administered drugs and dosage, and primary and secondary endpoints. We specifically addressed the following efficacy outcomes: overall response rate (ORR), disease control rate (DCR), progression-free survival (PFS), and overall survival (OS); for safety, number and grade of treatment-related adverse events (TRAEs).

2.4 Risk of Bias

Two reviewers independently assessed the risk of bias. In case of disagreement, a third reviewer was consulted. The Risk Of Bias In Non-randomised Studies - of Interventions (ROBINS-I) tool was used to assess the risk of bias, including eight domains: confounding bias; selection bias; classification bias; deviation from intended interventions bias; missing data; measure outcome bias; selection of the reported results; and overall bias (18).

3 RESULTS

A total of 104 studies were identified from the electronic search. After duplicate removal and title/abstract screening, 75 studies were eligible. After checking inclusion and exclusion criteria, we removed 4 studies for being written in languages other than English, 33 among case reports, reviews, correspondences, personal opinions, or commentaries; in 1 study, the complete text was not available, and 22 reports were removed for focusing on different topics. At the end of the screening, a total of 15 studies were included in our review (**Figure 1**).

3.1 Characteristics of the Included Studies

The included studies were 14 phase I/II clinical trials and 1 randomized phase III trial (19–33). No phase IV trial was found. Anti-PD1 agents were used in 11 studies; 4 studies employed anti-PD-L1 agents (in 1 study, anti-CTLA4 was associated). Among PD1, 8 studies used pembrolizumab, 2 nivolumab, and 1 dostarlimab (19–29). Anti-PD-L1 agents consisted of avelumab (1 study), atezolizumab (1 study), and durvalumab (2 studies) (30–33). Anti-PD1 was administered as a single agent in 7 studies (19–23, 27, 29). Pembrolizumab was combined with the tyrosine-kinase inhibitor (TKI) lenvatinib in 3 studies, nivolumab with the TKI cabozantinib in 1 study (24–26, 28). Anti-PD-L1 was administered as monotherapy in 3 studies (30–32). Durvalumab was associated with anti-CTLA-4 tremelimumab in 1 study (33). No study of single-agent anti-CTLA-4 was found. Pembrolizumab was administered every 3 weeks (q3w) at the fixed dosage of 200 mg in 5 studies, 10 mg/kg in 3 studies; nivolumab was administered at the flat dose of 240 mg every 2 weeks (q2w), and in 1 study the shift to 480 mg every 4 weeks (q4w) was planned; atezolizumab was administered either at 1,200 mg or at 15 mg/kg q3w; the avelumab dosage was 10 mg/kg q2w, and dostarlimab was started at the dosage of 500 mg q3w then continued at 1,500 mg every 6 weeks (q6w); and durvalumab was administered at the fixed dosage of 1,500 mg q4w alone or combined with tremelimumab 75 mg q4w. 1,627 patients were treated, ranging from 9 to 827. The overall response rate (ORR) was the most frequent primary endpoint (11 studies): it was defined as the percentage of patients achieving a complete response (CR) or a partial response (PR) (19–24, 26, 27, 29, 30, 33). In one study, the primary endpoint was defined as objective tumor response rate (OTRR—defined as the sum of complete and partial responses divided for the total number of patients) (32). Progression-free survival (PFS)—defined as the time from randomization to disease progression or death, whichever occurred first—was the primary endpoint in 4 studies (20, 25, 28, 30). Overall survival (OS)—defined as the time from randomization to death—was assessed as a co-primary endpoint with PFS in the only selected phase III study (25). PFS, OS, duration of response (DOR), and safety were most commonly investigated among secondary endpoints. Quality of life was addressed as the secondary endpoint only in one study (25). **Table 1** shows the main characteristics of the included studies. No serious risk of bias emerged (**Figure 1**, **Supplementary Material**).

Overall, ORR ranged from 3% to 63.6%. When considering only MSI patients, ORR to single agents ranged from 26.7% to 58% (median 48%), while when including only MSS patients, ORR was 3% to 26.7% (median 14.8%). In the combination ICI-TKI studies, ORR was 32% to 63.6%; KEYNOTE-146 reported an ORR of 63.6% in MSI patients (n = 11), whereas MSS patients reached an ORR of 32% to 36.2% in KEYNOTE-146 and -775. 12 studies reported DCR, ranging from 26.1% to 95.6% in all-comers, with peaks in MSI patients treated with single agents (53.5% to 88.9%), and patients receiving the combination of pembrolizumab/lenvatinib (90.9% in MSI, 84% in MSS patients). No additional benefit derived from the dual-ICI combination, as durvalumab plus tremelimumab determined an ORR of 11.1%. Considering the types of responses, 35% of patients developed a PD, and 27% PR, 26% SD, and 7% of CR were observed (**Figure 2**).

11 studies reported mPFS that ranged from 1.7 to 18.9 months. Among MSI groups, mPFS to ICI monotherapy was 8.1 months (range 5.5–13.1 mos). With combination ICI–TKI, mPFS ranged from 7.2 to 8.7 mos in all-comers, with similar benefits in MSS patients (6.6–7.4 months), reaching 18.9 months among 11 MSI patients in KEYNOTE-146. mOS was available only for 5 studies, ranging from 9.6 to 18.3 months (**Figure 3**).

With ICI monotherapy, 54.2% to 76% of patients developed TRAEs, of which 6.8% to 27.7% were ≥G3. The combination of ICIs and TKI achieved a higher toxicity rate than single agents (≥G3 TRAEs 67%–88.9%). The dual anti-PD1/anti-CTLA4 inhibition determined 44% of serious TRAEs (**Table 1**).

3.2 ICIs Targeting PD1

3.2.1 Pembrolizumab

Pembrolizumab monotherapy was investigated in 5 trials, 1 of which was a phase Ib study and 4 were phase II studies, for a total of 150 patients (range 9–79) (19–23). Pembrolizumab was administered at the dosage of 10 mg/kg q3w in all studies except for KEYNOTE-158 and NCT02899793, which used the flat dose of

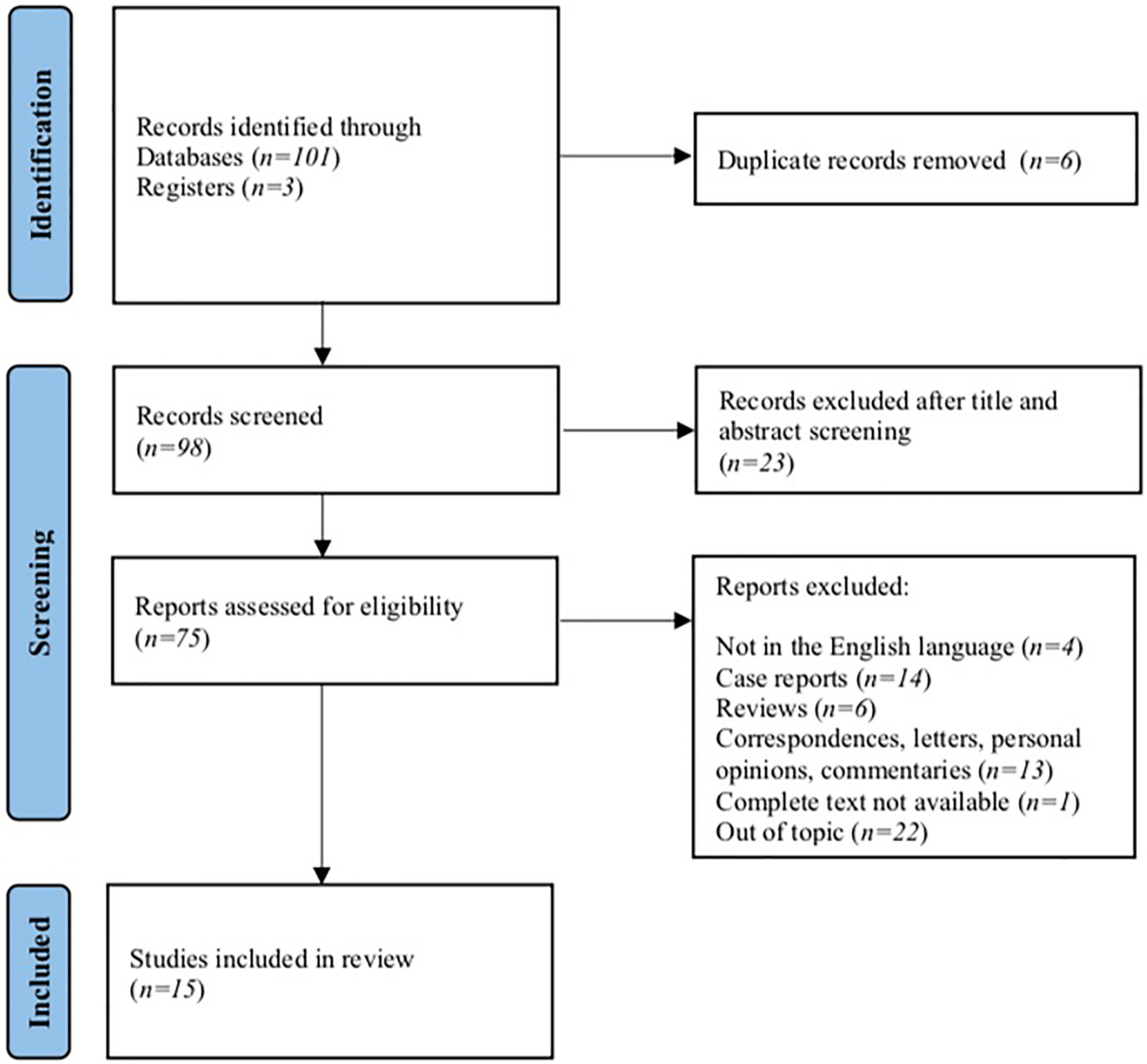


FIGURE 1 | PRISMA flowchart for study selection of the systematic review.

200 mg q3w. Patients were selected for MSI-H/MMRd status in 4 studies (19–22). Among them, NCT02899793 was a pilot study comparing MSI-H patients with Lynch syndrome versus sporadic MLH1 mutations (22). In KEYNOTE-028, patients were included in case of PD-L1 positivity (cutoff 1% on tumor or inflammatory cells or in the stroma) (23).

Cohorts D/K of the KEYNOTE-158 phase II trial (NCT02628067) included 79 MSI-H EC patients. The primary endpoint was ORR; DOR, PFS, and OS were secondary endpoints. ORR was 48% (95% confidence interval [CI], 36.7%–59.6%), DCR 83.5%. mPFS was 13.1 months (95% CI, 4.3–34.4 mos), mOS not reached (NR; 95% CI, 27.2 mos-NR). 14 CR were recorded (of note, EC recorded one of the highest CR rates among the solid tumors included in the study). TRAEs were reported in 76% of patients, with no grade 5 events (19). Similar results were achieved in 15 MMRd and 9 MSI-H EC patients in two phase II trials, with—primary endpoint—ORRs of 55% and 56% and DCRs 73.3% and 88.9%, respectively. In the first study, mOS was 148.8 weeks. ≥G3 toxicities were reported in 27.7% of MMRd patients, but no ≥G3 TRAE was recorded among 9 MSI-H patients (20, 21). In the pilot phase II NCT02899793 study, 24 MSI-H EC patients were treated with pembrolizumab, reaching an ORR of 58% (95% CI, 36.6%–77.9%), which was 100% in patients with Lynch syndrome, versus 44% of sporadic cases ($p = 0.024$). Patients with Lynch syndrome ($n = 6$) were all alive after 3 years, whereas in sporadic patients ($n = 18$), 3-year PFS

TABLE 1 | Trials of ICIs in advanced/recurrent EC.

Author	Study name	Phase	Target population *(number of pts)*	Administered drugs	Primary EP	Secondary EP	Results				
							ORR	DCR	PFS	OS	Safety
Marabelle et al. (19)	KEYNOTE-158 (NCT02628067)—cohorts D/K	II	MSI EC (n = 79)	Pembrolizumab 200 mg q3w	ORR	DOR, PFS, OS	ORR 48% (95% CI, 36.7–59.6%)	DCR 83.5%	mPFS 13.1 mos (95% CI, 4.3–34.4 mos)	mOS NR (95% CI, 27.2 mos-NR)	TRAEs 76%, no G5
Le et al. (20)	NCT01876511—cohort C	II	MSI EC (n = 15)	Pembrolizumab 10 mg/kg q2w	20w-irPFS, 28-mos ORR, 20w-PFS	4y-OS, 28w-irPFS, 28w-PFS, 28-mos DCR	ORR 55%	DCR 73.3%	20w-irPFS 67% 20w-PFS 68% (56-83)	mOS 148.8 wks (94.7-NA)	≥G3 TRAEs 27.7%
Fader et al. (21)	NA	II	MSI EC of endometrioid histology (n = 9)	Pembrolizumab 10 mg/kg q2w	ORR	NA	ORR 56% (95% CI, 21–86%)	DCR 88.9%	NA	mOS NR (12 mos OS 89%)	No ≥G3 TRAEs
Roque et al. (22)	NCT02899793	II	MSI-H EC with Lynch syndrome (n = 6) or sporadic MLH1 mutations (n = 18)	Pembrolizumab 200 mg q3w	ORR, safety	PFS, OS	ORR 58% (95% CI, 36.6–77.9%) ORR 100% (Lynch) vs. 44% (sporadic) (p = 0.024)	NA	3-yr PFS 30% (sporadic) (p = 0.017)	3-yr OS 100% (Lynch), 43% (sporadic) (p = 0.043)	≥G3 TRAEs 6.8%
Ott et al. (23)	KEYNOTE-028 (NCT02054806)	Ib	PD-L1^{+} EC (n = 23)	Pembrolizumab 10 mg/kg q2w	ORR	DOR, PFS, OS, safety	ORR 13% (95% CI, 2.8% to 33.6%)	DCR 26.1%	mPFS 1.8 mos (95% CI, 1.6–2.7 mos)	mOS NR (95% CI, 4.3 mos-NR)	TRAEs 54.2%, G3 16.7%, no G4
Makker et al. (24)	KEYNOTE-146/Study 111 (NCT02501096)	Ib/II	EC (n = 108) Stratification: MSI (n = 11) MSS (n = 94)	Pembrolizumab 200mg q3w + lenvatinib 20 mg daily	ORR24w	DOR, PFS, OS	ORR24w 38.0% (95% CI, 28.8%–47.8%)	DCR 84.7% (95% CI, 77.1%–90.5%)	mPFS 7.4 mos (95% CI, 5.3–8.7 mos)	mOS 16.7 mos (95% CI,15.0 mos-NR)	≥G3 TRAEs 69.4%
							MSI subgroup: ORR24w 63.6% (95% CI, 30.8%–89.1%)	MSI subgroup: DCR 90.9% (95% CI, 58.7%–99.8%)	MSI subgroup: mPFS 18.9 mos (95% CI, 4-NR)	MSI subgroup: NR	
							MSS subgroup: ORR24w 36.2% (95% CI, 26.5-46.7%)	MSS subgroup: DCR 84% (95% CI, 75%-90.8%)	MSS subgroup: mPFS 7.4 mos (95% CI, 5-8.7 mos)	MSS subgroup: mOS 16.7 mos (95% CI, 15–NR)	

(Continued)

TABLE 1 | Continued

Author	Study name	Phase	Target population *(number of pts)*	Administered drugs	Primary EP	Secondary EP	Results				
							ORR	DCR	PFS	OS	Safety
Makker et al. (25)	KEYNOTE-775/Study 309 (NCT03517449)	III	EC (n = 827), randomized: Exp: n = 411 Ctrl: n = 416 MSS: n = 697	Pembrolizumab 200 mg q3w plus lenvatinib 20 mg daily or TPC (doxorubicin 60 mg/m^2 q3w or paclitaxel 80 mg/m2, 3 weeks on, 1 week off)	PFS OS	ORR, safety, QoL	MSS subgroup: ORR 30% (95% CI, 26%–36%) vs. 15% (95% CI, 12%–19%, p<0.0001)	NA	MSS subgroup: mPFS 6.6 mos (95% CI, 5.6–7.4 mos) vs. 3.8 mos (95% CI, 3.6–5.0 mos); HR 0.6 (95% CI, 0.50–0.72; p < 0.0001)	MSS subgroup: mOS 17.4 mos (95% CI, 14.2–19.9 mos) vs. 12 mos (95% CI, 10.8–13.3 mos); HR 0.68 (95% CI, 0.56–0.84; p = 0.0001)	≥G3 TRAEs 88.9% (P+L arm) and 72.7% (CTX arm); combo arm: 30.8% discontinued pembrolizumab, 18.7% discontinued lenvatinib, 14% discontinued both pembro and lenvatinib
			MSI: n = 130				All-comers: ORR 31.9% vs. 14.7%		All-comers: mPFS 7.2 vs. 3.8 mos; HR 0.56	All-comers: mOS 18.3 vs. 11.4 months; HR 0.62	
Taylor et al. (26)	NCT02501096—EC cohort	Ib/II	EC - not selected for biomarkers (n = 23)	Pembrolizumab 200 mg q3w plus lenvatinib 20 mg daily	ORR24w	ORR, PFS, DOR, DCR	ORR24w and overall ORR 52% (95% CI, 30.6%–73.2%)	DCR 95.6%	mPFS 9.7 mos (95% CI, 4.2 mos-NR)	NA	TRAEs 97%, ≥G3 TRAEs 67%, 2 TR-deaths
Tamura et al. (27)	JapicCTI-163212	II	EC—not selected for biomarkers (n = 22)	Nivolumab 240 mg q2w	ORR	OS, PFS, DCR, safety	ORR 23% (95% CI, 11%–38%)	DCR 68.2%	mPFS 3.4 mos (95% CI, 2.0–5.4 mos)	NA	TRAEs 61%, ≥G3 TRAEs 17%
Lheureux et al. (28)	NCT03367741	II	EC—not selected for biomarkers, randomized (n = 76)	Arm A: nivolumab 240 mg q2w (480 mg q4w after 4 cycles) + cabozantinib 40 mg daily	PFS	OS, ORR, safety	ORR 25% (Arm A), 16.7% (Arm B)	DCR 69.4% (Arm A), 27.8% (Arm B)	Arm A: mPFS 5.3 mos (95% CI, 3.5–9.5 mos)	NA	Most common AEs (>G1/G2): diarrhea (47.2%), hypertransaminasemia (44.4%), fatigue (38.9%), nausea (30.6%)
			Arm A: n = 36 Arm B: n = 18 Exploratory Arm C (carcinosarcoma or EC progressive to immunotherapy): n = 29	Arm B: nivolumab 240 mg Arm C: nivolumab + cabozantinib					Arm B: mPFS 1.9 mos (95% CI, 1.6–3.8 mos)		
Oaknin et al. (29)	GARNET (NCT02715284)	I/II	103 MSI EC, 142 MSS EC	Dostarlimab 500 mg q3w x 4 → 1,000 mg q6w	ORR	DOR, DCR	MSI: ORR 44.7% (95% CI, 34.9%–54.8%)	MSI: DCR 57.3%	MSI: mPFS 8.1 months (95% CI, 3.0–18.0 months)	mOS NR	TRAEs: 63.5% (MSI), 71.7% (MSS); serious TRAEs: 13.5% (MSI), 19.3% (MSS)
							MSS: ORR 13.4% (95% CI,	MSS: DCR 35.2%			

(Continued)

TABLE 1 | Continued

Author	Study name	Phase	Target population *(number of pts)*	Administered drugs	Primary EP	Secondary EP	Results				
							ORR	DCR	PFS	OS	Safety
							8.3%–20.1%)				
Kostantinopoulos et al. (30)	NCT02912572	II	MSI/*POLE* mutated cohort (n = 15) MSS cohort (n = 16) → closed for futility	Avelumab 10 mg/kg q2w	PFS6, ORR	PFS, OS, safety	MSI cohort: ORR 26.7% (95% CI, 7.8%–55.1%)	DCR 53.3%	MSI cohort: PFS6 40% (95% CI, 16.3%–66.7%)	MSI cohort: mOS NR	TRAEs 71%, G3 TRAEs 19.4%
Fleming et al. (31)	NCT01375842	Ia	PD-L1^{+} EC, then amended to all patients (n = 15)	Atezolizumab 1,200 mg or 15 mg/kg q3w	Safety, clinical activity	NA	ORR 13%	DCR 26.7%	mPFS 1.7 mos (95% CI, 0.6–11 mos)	mOS 9.6 mos (95% CI, 0.6–11.8 mos)	47% TRAEs, no G4-5 TRAEs
Antill et al. (32)	PHAEDRA (ANZGOG1601/ ACTRN12617000106336)	II	EC (n = 71): 36 MSI 35 MSS	Durvalumab 1,500 mg q4w	OTRR (iRECIST)	PFS, OS	MSI: OTRR 47% (95% CI 32%–63%)	MSI: DCR 63.9%	MSI: mPFS 8.3 mos	MSI: mOS NR 12-mos OS 71%	NA
							MSS: OTRR 3% (95% CI 1%–15%)	MSS: DCR 31.4%	MSS: mPFS 1.8 mos	MSS: mOS 11.5 mos 12-mos OS 51%	
Rubinstein et al. (33)	NCT03015129	II	EC (>10 MSI or carcinosarcoma per arm) (n = 54; D: n = 27, D+T: n = 27)	Durvalumab 1,500 mg q4w or plus tremelimumab 75 mg q4w → durvalumab 1,500 mg q4w	ORR	NA	D arm: ORR 14.8% (90% CI, 6.6%–100%)	NA	D arm: mPFS 7.6w PFS24w 13.3% (95% CI, 6.1%–100%)	NA	D arm: 7% G3, 4% G4 TRAEs
							DT arm: ORR 11.1% (90% CI, 4.2%–100%)		DT arm: mPFS 8.1w PFS24w 18.5% (95% CI, 10.1%–100%)		DT arm: 32% G3, 11% G4 TRAEs

AEs, adverse events; CI, confidence interval; CR, complete response; CTX, chemotherapy; DCR, disease control rate; DOR, duration of response; EC, endometrial cancer; HR, hazard ratio; irORR, immune-related objective response rate; irPFS, immune-related progression free survival; mDOR, median duration of response; mOS, median overall survival; mPFS, median progression free survival; MSI, microsatellite instability; MSS, microsatellite stability; NA, not available; NR, not reached; ORR, objective response rate; ORR24w, objective response rate at 24 weeks; OS, overall survival; OTRR, objective tumor response rate; PD-L1, programmed death-ligand 1; PFS, progression free survival; PFS24w, progression free survival at 24 weeks; PFS6, progression-free survival at 6 months; POLE, polymerase epsilon; PR, partial response; QoL, quality of life; SD, stable disease; TPC, treatment of physician's choice; TRAE, treatment-related adverse event.

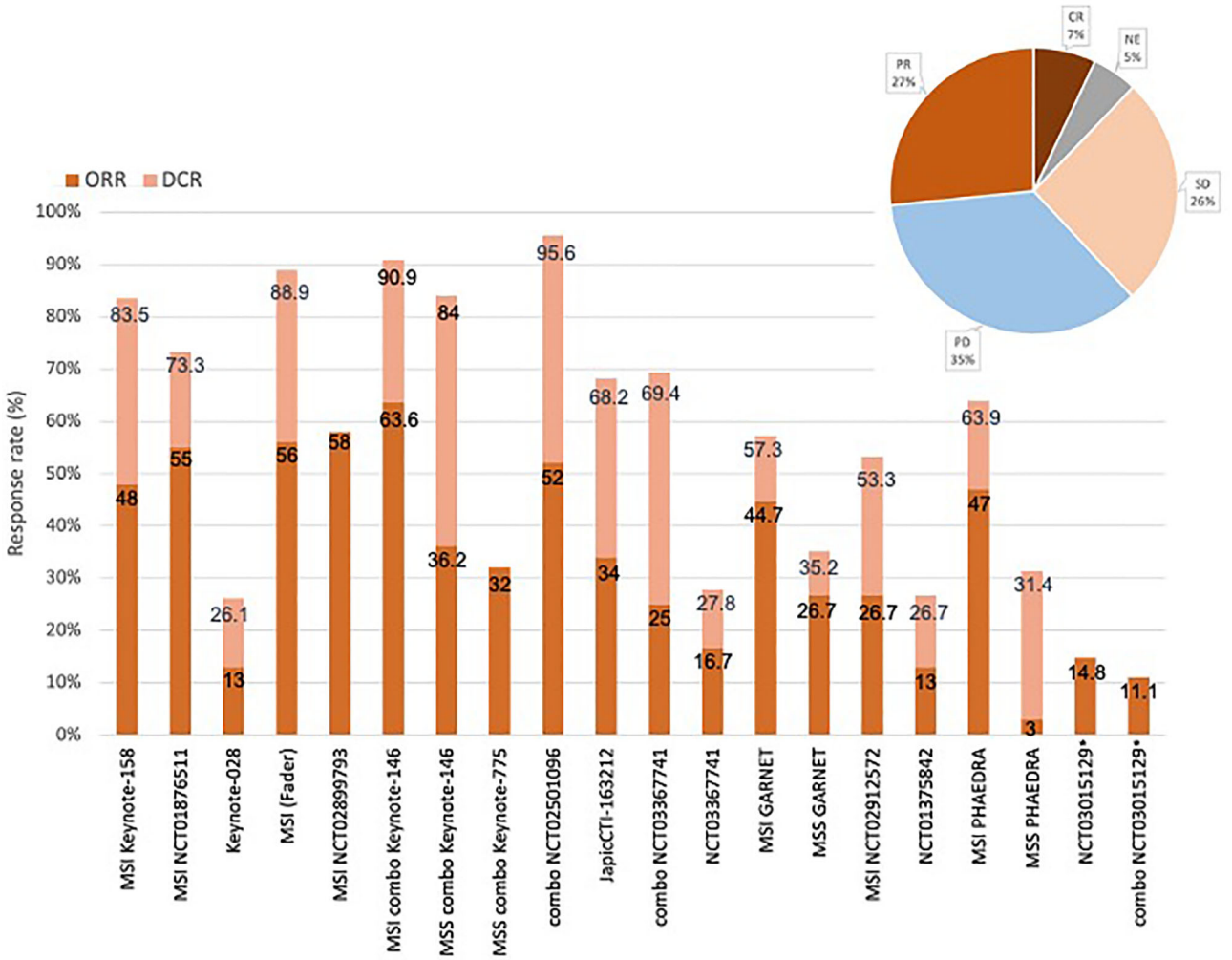


FIGURE 2 | Responses and response rates of the included studies. Overall response rate (ORR) ranged from 3% to 58%. ORR to single agents ranged from 26.7% to 58% for MSI patients, 3% to 26.7% for MSS patients (studies that selected MSI and MSS patients are indicated in the figure). In the combination ICIs-TKI studies ("combo" in the figure), ORR was 32% to 52%, reaching 36.2% in MSS patients, 63.6% in MSI patients. DCR ranged from 26.1% to 95.6% in all studies, with peaks in MSI patients (around 90% as single agents or combinations) and MSS patients in case of combination (84%). Objective tumor response rate (OTRR—marked with *) to the combo durvalumab plus tremelimumab was 11.1%. Types of responses recorded in the studies were: 35% progressive disease (PD), 27% partial response (PR), 26% stable disease (SD), 7% complete response (CR).

and 3-year OS were 30% (p = 0.017) and 43% (p = 0.043), respectively. 6.8% ≥G3 TRAEs were recorded (22). In the multi-cohort phase Ib KEYNOTE-028 study (NCT02054806), patients with locally advanced or metastatic PD-L1-positive solid tumors were enrolled. ORR was the primary endpoint; secondary endpoints included safety, DOR, PFS, and OS. 23 EC patients were included in the efficacy analysis, with an ORR of 13.0% (95% CI, 2.8%–33.6%), DCR of 26.1%, mPFS of 1.8 months (95% CI, 1.6–2.7 mos), and mOS NR. Among these patients, only one was POLE-mutant and one MSI-H; the remaining were stable or not evaluable for MSI. The only POLE-mutant patients achieved a PR, and the MSI patient had PD; among all patients, 3 PR, 3 SD, and 13 PD were recorded. 13 TRAEs and 4 G3 TRAEs, but no G4 AEs, occurred (23).

The combination of pembrolizumab 200 mg q3w and lenvatinib 20 mg daily was evaluated in 3 studies enrolling pretreated EC patients (24–26). There were 2 phase Ib/II trials investigating ORR (24 weeks after treatment starting) as the primary endpoint, and a phase III trial with PFS and OS as co-primary endpoints. Overall, 542 patients received the combination. In the phase Ib/II KEYNOTE-146/Study111 (NCT02501906), 108 patients were included. The study demonstrated a 24-week ORR (primary endpoint) of 38.0% (95% CI, 28.8%–47.8%), ranging from 36.2% (26.5%–46.7%) in patients with MSS tumors (n = 94) to 63.6% (95% CI, 30.8%–89.1%) in patients with MSI-H tumors (n = 11). DCR was 84.7% (95% CI, 77.1%–90.5%) in all-comers, 84% (95% CI, 75%–90.8%) in MSS patients, and 90.9% (95% CI, 58.7%–99.8%) in MSI

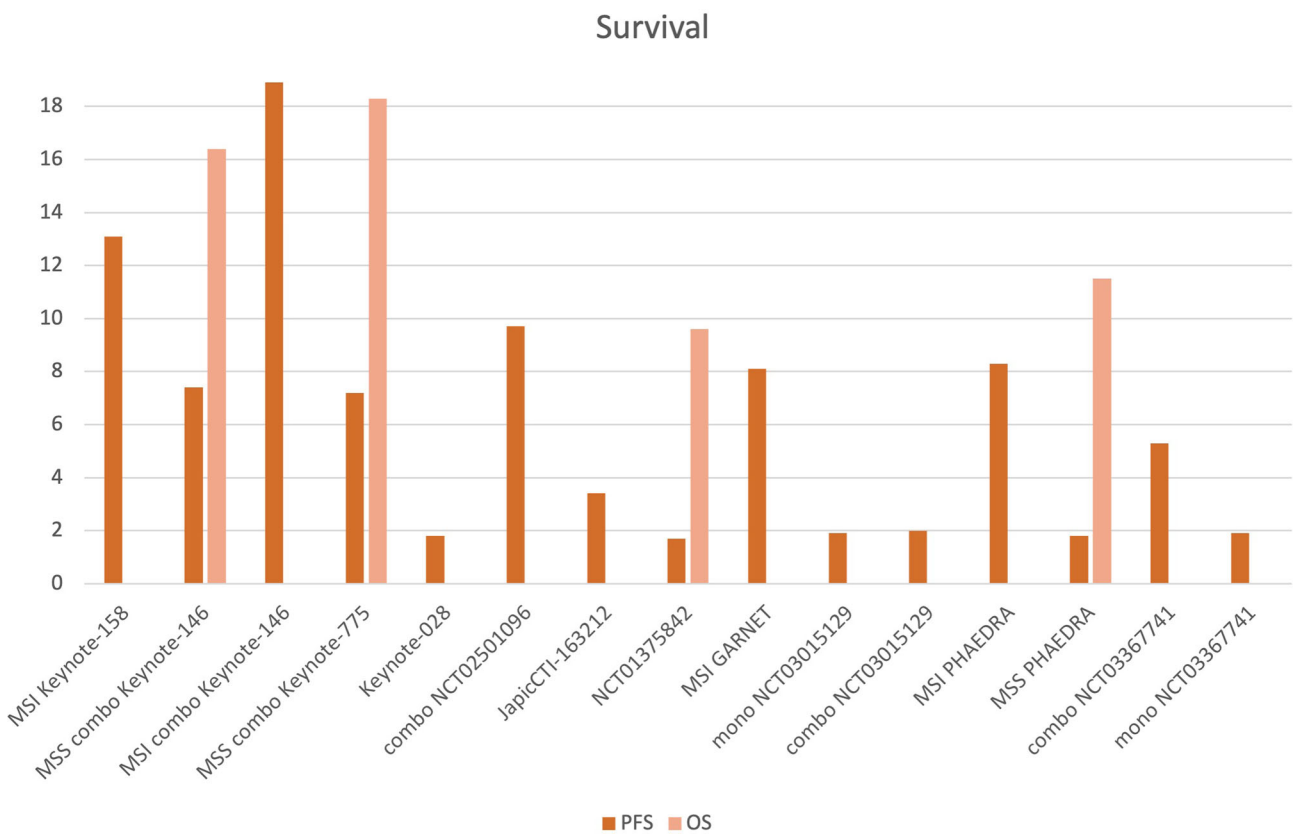


FIGURE 3 | Progression-free survival (PFS) and overall survival (OS) of the included studies. 11 studies reported mPFS, which ranged from 1.7 to 18.9 months. Among MSI patients treated with ICI monotherapy, mPFS was 8.1 months (5.6–13.1 mos). With combination ICIs-TKI, mPFS ranged from 7.2 to 18.9 mos (among the 11 MSI patients of Keynote-146), ranging from 6.6 to 7.4 months for MSS patients. mOS was available for 5 studies, ranging from 9.6 to 18.3 mos (MSI, MSS groups and combination—"combo" studies are indicated.

patients. mDOR was 21.2 months. mPFS was similar between all-comers (7.4 months; 95% CI, 5.3–8.7 mos) and MSS patients (7.4 mos; 95% CI, 5.0–7.6 mos) and reached 18.9 months in MSI patients (95% CI, 4 mos-NR). mOS was 16.7 months in all patients (95% CI, 15 mos-NR), 16.4 months in MSS (95% CI, 13.5-25.9 mos), and NR in MSI patients. 69.4% of women experienced ≥G3 TRAEs, most frequently hypothyroidism (47.6%). 6 treatment-related deaths were reported (24). This study led the FDA to grant breakthrough therapy designation to the combination of pembrolizumab and lenvatinib for pretreated MSS EC women (14). The KEYNOTE-775/Study309 (NCT03517449) is the phase III confirmatory trial for KEYNOTE-146. 827 women were randomized to receive lenvatinib 20 mg plus pembrolizumab 200 mg q3w (n = 411) versus treatment of physician choice (doxorubicin or weekly paclitaxel) (n = 416). PFS and OS were the co-primary endpoints, while ORR, safety, and quality of life were secondary endpoints. In all-comers, ORR was 32% vs. 15%, mPFS was 7.2 vs. 3.8 mos (HR 0.56), and mOS was 18.3 vs. 11.4 months (HR 0.62), respectively. In the MSS cohort, ORR was 30% vs. 15%, mPFS was 6.6 vs. 3.8 mos (HR 0.6; 95% CI, 0.50–0.72; $p < 0.0001$), and mOS was 17.4 vs. 12 mos (HR 0.68; 95% CI, 0.56–0.84; $p = 0.0001$), respectively. ≥G3 TRAEs were observed in almost 89% of the lenvatinib/pembrolizumab arm (most commonly hypertension) and 72.7% of the chemotherapy arm, with 30.8% discontinuing pembrolizumab, 18.7% discontinuing lenvatinib, and 14% discontinuing both pembro and lenvatinib in the combination arm (25). 23 EC patients were treated in the phase Ib/II NCT02501096 trial. The—primary endpoint—24-week ORR was 52% (95% CI, 30.6%–73.2%), with 2 CR and 10 PR, and DCR was 95.6%. mPFS was 9.7 months (95% CI, 4.2 mos-NR). ≥G3 TRAEs occurred in 67% of patients, hypertension, fatigue (12%), diarrhea (9%), proteinuria (8%), and increased lipase levels (7%) being the most common. 2 treatment-related deaths were recorded (26).

3.2.2 Nivolumab

As monotherapy, nivolumab was tested in the JapicCTI-163212 phase II trial on the Japanese population. 22 patients in the EC cohort received nivolumab 240 mg q2w, with ORR as the primary endpoint, and OS, PFS, DOR, and safety as secondary endpoints. ORR was 23% (95% CI, 11%–38%), mPFS 3.4 months (95% CI, 2.0–5.4 mos). DCR was 68.2%, with no CR observed. 61% of patients developed a TRAE, which was >G3 in 17% of

cases. Exploratory biomarker analysis included PD-L1$^+$ and MSI-H patients: similar ORRs were recorded between PD-L1-positive and -negative patients; none of the 6 MSS-stable patients and both 2 MSI women responded to nivolumab (27).

Nivolumab was tested in combination with cabozantinib in the randomized three-cohort phase II NCT03367741 trial. Patients were eligible if they had recurrent EC progressing to at least 1 platinum-based chemotherapy in the first two cohorts; a third exploratory cohort included patients with carcinosarcoma or progressive patients to previous immunotherapy. 76 women were randomized to receive nivolumab (240 mg q2w for the first 4 cycles, followed by 480 mg q4w) plus cabozantinib 40 mg daily (arm A; n = 36) or nivolumab monotherapy (arm B; n = 18); the exploratory cohort (cohort C) of 9 carcinosarcoma and 20 ICI-progressing EC patients received nivolumab plus cabozantinib. PFS was the primary endpoint. OS, ORR, and safety were assessed as secondary endpoints. mPFS was 5.3 months (95% CI, 3.5–9.5 mos) in arm A, and 1.9 months (95% CI, 1.6–3.8 mos) in arm B. ORR was 25% and 16.7% in arms A and B, respectively. DCR was 69.4% in arm A, 27.8% in arm B. Diarrhea (47.2%), transaminase increase (44.4%), fatigue (38.9%), and nausea (30.6%) were the most common TRAEs. In the exploratory cohort, among 9 patients with carcinosarcoma, 1 PR and 4 SD were observed; among the 20 immunotherapy-progressive EC women, 6 responses and 8 SD were recorded (28).

3.2.3 Dostarlimab

In the phase I/II GARNET study, 103 women with MSI and 142 with MSS advanced/recurrent EC received 500 mg of dostarlimab q3w for 4 doses and then 1,000 mg q6w. The primary endpoint was ORR; DCR and DOR were secondary endpoints. Dostarlimab showed a meaningful clinical benefit, with an ORR of 44.7% (95% CI, 34.9%–54.8%) in MSI, and 13.4% (95% CI, 8.3%–20.1%) in MSS women. DCR was 57.3% and 35.2% in the MSI and MSS groups, respectively. 63.5% MSI and 71.7% MSS patients developed TRAEs, of which 13.5% and 19.3% were serious AEs (29).

3.3 ICIs Targeting PD-L1

3.3.1 Avelumab

In a single-arm phase II study (NCT02912572), two cohorts of EC patients (15 MSI and 16 MSS) were treated with avelumab 10 mg/kg q2w until progression or unacceptable toxicity. The co-primary endpoints were the frequency of patients with a PFS of at least 6 months after initiating therapy (PFS6), and ORR. Secondary endpoints were PFS, OS, and safety. The MSS cohort was closed after meeting futility criteria, whereas MSI patients exhibited an ORR of 26.7% (95% CI, 7.8%–55.1%) and a PFS6 rate of 40% (95% CI, 16.3%–66.7%), regardless of PD-L1 status. DCR was 53.3%. 71% of patients developed a TRAE, of which 19.4% were G3 TRAEs (30).

3.3.2 Atezolizumab

Atezolizumab 1,200 mg or 15 mg/kg q3w was administered during a phase Ia study (NCT01375842) to 15 patients with advanced/recurrent EC, 93% of which progressed to ≥2 prior systemic therapies. 7/15 patients were MSS, 1 was MSI-H, and 7 had MS-unknown status. Patients were initially evaluated for PD-L1 status (with a cutoff for positivity of 5%); the study was then extended to all patients independently from PD-L1. Atezolizumab clinical benefit seemed to be highly related to PD-L1 expression and MSI. ORR was 13%, DCR 26.7%; 2 PR were observed, 1 in a MSI patient, 1 in a patient with 70% of TIL infiltration, both of which were PD-L1 positive. mPFS was 1.7 months (95% CI, 0.6–11 mos), mOS 9.6 months (95% CI, 0.6–11.8 mos). 47% of patients developed a TRAE, but no G4-G5 events were recorded (31).

3.3.3 Durvalumab

In the phase II PHAEDRA (ANZGOG1601) trial, durvalumab 1,500 mg q4w was administered to 71 patients with MSS (n = 35) or MSI (n = 36) advanced EC. The objective tumor response (OTR, including CR and PR by RECIST criteria) rate was the primary endpoint while PFS and OS were secondary endpoints. Among MSI, the OTR rate was 47% (95% CI, 32%–63%), with 6 CR and 11 PR, and DCR was 63.9%. mPFS was 8.3 mos, and mOS was NR with a 12-mos OS rate of 71%. In the MSS subgroup, the OTR rate was 3% (95% CI, 1%–15%), DCR was 31.4%, with only 1 PR and 10 SD observed, and mPFS was 1.8 mos, mOS 11.5 mos, and 12-mos with an OS rate of 51% (32). In the NCT03015129 phase II trial, EC patients were randomized to receive durvalumab 1,500 mg q4w with or without tremelimumab 75 mg q4w for 4 cycles, followed by durvalumab maintenance, until progression or unacceptable toxicity. ORR was the primary endpoint. At least 10 patients with carcinosarcoma or MSI per arm were planned: as 2 patients were excluded due to early death, 27 patients per arm were considered. 5 patients were MSI, 48 MSS; in 3 cases, the MS status was unknown. In the single-agent arm, there were 1 CR (MSS) and 3 PR (2 MSS and 1 MSI), reaching an ORR of 14.8% (90% CI, 6.6%–100%). mPFS was 7.6 weeks, PFS24wks was 13.3% (90% CI, 6.1%–100%), and mDOR was 16 wks. Regarding the combination arm, 2 CR (1 MSI, 1 MSS) and 1 PR (MSS) were found. ORR was 11.1% (90% CI, 4.2%–100%), mPFS was 8.1 wks, and PFS24wks was 18.5% (90% CI, 10.1%–100%). As for safety, G3 TRAEs occurred in 7% of patients in the single-agent arm and 32% of patients in the double-agent arm, with fatigue and diarrhea as the most common TRAEs. G4 TRAEs occurred in 4% of single-agents and 11% of combination groups (33).

4 DISCUSSION

EC profoundly impacts women's health in terms of morbidity and mortality, and dismal results are reported in platinum-progressing patients (1–3, 7). Therefore, the search for effective treatments beyond the first line represents one of the most important unmet needs for this malignancy (7). In the last 10 years, ICIs have brought a paradigm shift in the therapy of many solid tumors. Effectively, EC represents a unicum among gynecological tumors, as ICI approvals have already occurred in pretreated patients (13–16). The results of our systematic review confirm that ICIs are effective in patients with pretreated

advanced EC. ORR ranges from 3% to 63.6%, DCR ranges from 26.1% to 95.6%. Overall, response to ICIs is tripartite: 1/3 of progressing patients, 1/3 of responding patients (CR+PR), and 1/3 of disease stability. Therefore, 2 out of 3 women might benefit from ICIs. The impressive results of the KEYNOTE-158 (cohorts D/K) and GARNET trials justify the use of anti-PD-1 in MSI-H tumors, confirming the FDA and EMA approvals (19, 29). The results of the other trials corroborate the efficacy of single-agent ICIs in MSI-H patients, as ORR ranges from 26.7% to 58% (19–22, 29, 30, 32). The efficacy is far more limited in MSS patients, with ORRs ranging from 3% to 26.7% (29, 32). However, another effective approved therapy for those patients is represented by the double association of pembrolizumab and the TKI lenvatinib, with ORRs of 32%–36.2% (24–26, 28). Besides ORR, the amount of disease stability is considerable, with DCRs from 26.1% to 95.6%, in line with the effect of ICIs: effectively, since ICIs restore a tumor-specific immune response, novel patterns of response are observed after immunotherapy that differ from chemotherapy and target therapies, such as durable responses that not always start rapidly but can persist even after ICI interruption (34). OS results are incomplete for most studies, however—as previously described in other solid tumors, the ICI effect is prolonged and OS is improved beyond PFS. This is in line with studies conducted in other solid tumors, as—once established—the immune response persists in the long run (**Figure 2**).

Despite these premises, we should point out that at least 1 out of 3 EC patients progresses to ICIs. Therefore, the search for predictive biomarkers is of utmost importance for better patient selection and treatment strategy definition. Regarding PD1 and PD-L1, EC shows the highest rates of expression among gynecological tumors, with PD1 positivity reported in around 75% of cases, and PD-L1 positivity ranging from 25% to 100% of EC specimens (especially in the endometrioid subtype), associated with advanced stages and poor prognosis (35). Controversial data regard the correlation between PD-L1 expression and MS status, with evidence of higher PD-L1 levels in MSI than MSS EC in some cases, but no differences in other reports (36–38). Moreover, results regarding the predictive role of PD-L1 for ICIs are inconsistent (23, 27). Differently from PD-L1, tumor mutational burden (TMB) seems useful for identifying a subgroup of patients who could better respond to ICIs (39, 40). In a biomarker analysis of KEYNOTE-158, 790 patients were evaluable for TMB: 102 patients (13%) were TMB high (having >10 mutations per megabase) and reached an ORR of 29% versus 6% of the non-TMB-high group (40). We should deepen the predictive role of TMB in EC, especially POLE-mutant and MSI tumors, which are associated with high TMB (39). A high number of tumor-infiltrated lymphocytes (TILs) are associated with a more favorable prognosis of EC, as if a more robust immune response against tumor was activated (41). A substantial TIL infiltrate, with a high $CD8^+/FOXP3^+$ ratio, has been indicated as a possible biomarker of response to ICIs also in EC (38, 41). On the contrary, infiltration of immune-suppressive elements in the tumor microenvironment (TME)—such as tumor-associated macrophages (TAMs)—correlates with advanced stages, higher aggressivity, and shorter survival (42). Among the other potential biomarkers, it has been evidenced that cyclooxygenase-2 (COX-2) is inversely correlated with $CD8^+$ infiltration, playing a potential predictive role for ICIs. It is known that COX-2 expression relates to EC development and aggressiveness, playing a negative prognostic role (43–45). *Homo sapiens* AT-rich interactive domain 1A (ARID1A) mutations have been correlated with higher infiltrations of $CD8^+$ and $CD4^+$ T-cells, B cells, neutrophils, macrophages, and dendritic cells (DCs), representing potential predictive biomarkers for ICI efficacy (46).

The most recent TCGA classification could represent a starting point for better understanding the genomic and immunological features of EC in order to guide the best treatment selection: POLE-ultra-mutated tumors represent 8%–10% of endometrioid subtype and are characterized by mutation of a catalytic subunit of epsilon DNA polymerase; MSI-H tumors have high mutation rate and are found in sporadic and inherited EC; copy number-low included the majority of endometrioid subtype, having a low mutation rate and frequent mutations of phosphatase and tensin homolog (PTEN), phosphoinositide 3-kinase (PI3KCA), ARID1A, Kirsten rat sarcoma virus (KRAS), and catenin beta-1 (CTNNB1) genes; copy number-high included serous and 25% of endometrioid tumors, having a high copy number variation but low mutation rate, TP53 mutations, low hormone receptor expression, very similar to triple-negative breast cancer, and serous ovarian cancer (11). The classification of TCGA is intriguing, as POLE-mutant and MSI-H EC correspond to specific phenotypes with signs of immune activation, such as high TMB, PD1/PD-L1 overexpression, and high $CD3^+$ and $CD8^+$ TIL infiltrates (38, 41). Some cases are described of good response in POLE-mutant or MSI-H EC, also in histologic subtypes different from endometrioid, such as clear cells or serous—for which evidence is far more limited (47). Even if MSI seems an effective predictive marker for guiding patients' selection so far, further investigation is needed. As emerged from the pilot NCT02899793 study, defects of MMR genes leading to MSI could differ from each other: in the study, germline mutations were associated with a meaningfully higher response to pembrolizumab than sporadic mutations. Moreover, Lynch-like versus sporadic MSI, as well as the different genetic alterations, also has a prognostic significance (22, 48). Effectively, whether mechanisms underlying MSI characterize ICI sensitivity is unclear, and pathways leading to ICI resistance remain unknown. Therefore, future studies should evaluate ICIs and their combinations in different subtypes of MSI patients but also resistance mechanisms to ICIs and treatment after progression. Combination of ICIs with drugs having a different mechanism of action could be helpful to overcome ICI resistance, as preliminary results of the exploratory cohort of the NCT03367741 trial show: among the 20 immunotherapy-progressive women, 6 responses and 8 SD to nivolumab plus cabozantinib were recorded (28). Far less is known about the role of POLE mutation for ICI response, which should be further investigated. A single patient reaching an SD after pembrolizumab was reported in the KEYNOTE-028 trial, and other good responses to ICIs are described, but with limited data

TABLE 2 | Ongoing trials of ICI combinations in EC.

clinicaltrials.gov registration	Phase	Setting	ICIs	Combination (drug class)
Advanced/recurrent EC				
NCT03276013 (TOPIC)	II	Pretreated EC	Pembrolizumab	Doxorubicin
NCT03914612	III	Untreated EC	Pembrolizumab	Paclitaxel, carboplatin
NCT03835819	II	Pretreated MSS FRalpha+ EC	Pembrolizumab	Mirvetuximab soravtansine/IMGN853 (ADC)
NCT02549209	II	Untreated or platinum-sensitive EC	Pembrolizumab	Carboplatin, paclitaxel
NCT04014530 (ATAPEMBRO)	I-II	Pretreated MMRd EC	Pembrolizumab	Ataluren (anti non-sense mutations of DNA)
NCT05036681	II	Untreated or pre-treated MSS EC	Pembrolizumab	Futibatinib (anti-FGFR)
NCT04652076 (GYNET)	I-II	Pretreated EC	Pembrolizumab	Carboplatin, paclitaxel, NP-137 (anti-Netrin1)
NCT04865289 (ENGOT-en9/MK-7902-001, LEAP-001)	III	Untreated EC	Pembrolizumab	Carboplatin, paclitaxel, lenvatinib (TKI)
NCT04781088	II	Pretreated EC	Pembrolizumab	Paclitaxel, lenvatinib (TKI)
NCT02646748	I	Pretreated EC	Pembrolizumab	Itacitinib/INCB050465 (JAK inhibitor)
NCT03454451	I	Pretreated EC	Pembrolizumab	Ciforadenant/CPI-006 (anti-CD73 antibody)
NCT05039801	I	Pretreated EC	Pembrolizumab	IPN60090 (glutaminase inhibitor)
NCT03849469	I	Pretreated EC	Pembrolizumab	XmAb22841 (bi-specific anti-CTLA4/anti-LAG3 antibody)
NCT04278144	I-II	HER-2$^+$ pre-treated EC	Pembrolizumab	BDC-1001 (anti-HER2)
NCT04460456	I	HER-2$^+$ pre-treated EC	Pembrolizumab	SBT6050 (anti-HER2)
NCT03367741	II	Pretreated EC	Nivolumab	Cabozantinib (TKI)
NCT04106414	II	Pretreated EC	Nivolumab	BMS-986205 (IDO inhibitor)
NCT04423029	I-II	Pretreated EC	Nivolumab	DF6002 (anti-IL12 receptor)
NCT03667716	I	Pretreated EC	Nivolumab	COM701 (PVRIG inhibitor)
NCT03508570	I	Pretreated EC	Nivolumab, Ipilimumab	Double ICIs (anti-PD1/anti-CTLA4)
NCT04570839	I-II	Pretreated EC	Nivolumab	COM701 (PVRIG inhibitor), BMS-986207 (anti-TIGIT)
NCT04042116	I-II	Pretreated EC	Nivolumab	Lucitanib (anti-VEGFR1-3)
NCT03126110	I-II	Pretreated EC	Nivolumab, Ipilimumab	INCAGN01876 (anti-GITR)
NCT02912572	II	Pretreated EC	Avelumab	Talazoparib (PARP inhibitor), axitinib (TKI)
NCT03503786 (MITO END-3)	II	Pretreated EC	Avelumab	Carboplatin, paclitaxel
NCT03603184 (AtTEnd)	III	Untreated EC	Avelumab	Carboplatin, paclitaxel
NCT03526432	II	Pretreated EC	Atezolizumab	Bevacizumab (anti-VEGF)
NCT04486352	I-II	Pretreated EC	Atezolizumab	Bevacizumab (anti-VEGF), ipatasertib (AKT inhibitor), talazoparib (PARP inhibitor)
NCT03694262 (EndoBARR)	II	Pretreated EC	Atezolizumab	Rucaparib (PARP inhibitor), bevacizumab (anti-VEGF)
NCT03170960	I-II	Pretreated EC	Atezolizumab	Cabozantinib (TKI)
NCT04269200	III	Untreated EC	Durvalumab	Carboplatin, paclitaxel, olaparib (PARP inhibitor) maintenance
NCT04444193	NA	Untreated EC	Durvalumab	Lenvatinib (TKI)
NCT03951415 (DOMEC)	II	Untreated or pretreated EC	Durvalumab	Olaparib (PARP inhibitor)
NCT03660826	II	Pretreated EC	Durvalumab	Capivasertib (AKT inhibitor), cediranib (anti-VEGFR), olaparib (PARP inhibitor)
NCT03277482	I	Pretreated EC	Durvalumab, Tremelimumab	RT
NCT03983954	I	Pretreated EC	Durvalumab	Obinutuzumab (anti-CD20), naptumomab estafenatox (anti-5T4)
NCT03981796	III	Untreated EC	Dostarlimab	Carboplatin, paclitaxel-niraparib
Adjuvant EC				
NCT03694834	I	Neoadjuvant/adjuvant EC	Pembrolizumab	Single dose before surgery, then combined with adjuvant CT
NCT03932409 (FIERCE)	I	Neoadjuvant/adjuvant EC	Pembrolizumab	Single dose before RT (brachytherapy), then combined with adjuvant CT
NCT04214067	III	Adjuvant EC	Pembrolizumab	Plus RT vs. RT alone, stage II/III MSI
NCT04634877 (Keynote-B21)	III	Adjuvant EC	Pembrolizumab	Added to adjuvant CT +/- RT

ADC, antibody–drug conjugate; AKT, AK strain transforming; CD, cluster of differentiation; CT, chemotherapy; FGFR, fibroblast growth factor receptor; FR, folate receptor; GITR, glucocorticoid-induced tumor necrosis factor receptor; HER-2, human epidermal growth factor receptor 2; IDO, indoleamine 2,3-dioxygenase; IL, interleukin; JAK, Janus kinase; LAG-3, lymphocyte-activation gene 3; MMRd, mismatch-repair deficient; MSS, microsatellite stable; NA, not applicable; PARP, poly(ADP-ribose) polymerase; PVRIG, poliovirus receptor-related immunoglobulin domain containing; RT, radiation therapy; TIGIT, T-cell immunoreceptor with Ig and ITIM domains; TKI, tyrosine-kinase inhibitor; VEGF, vascular endothelial growth factor; VEGFR, VEGF-receptor.

(44, 45). Effectively, nivolumab induced an ORR of 50% in patients with pathogenic POLE mutations and MMRp treated with nivolumab in the exonucleasic domain-mutated (ed) POLE cohort of the phase II NCT03012581 trial, of which 4/16 were diagnosed with EC (46–49). The integration of molecular and immune classification could be helpful to guide best patients' selection.

Regarding MSS EC, the combination of ICIs and TKIs seems effective. Multikinase TKIs have been associated with a decrease in immunosuppressive elements such as TAMs and increase in $CD8^+$ T cells, inducing immune activation, and they upregulate PD-L1 and Tregs that, in turn, promote angiogenesis (50–52). However, after these studies, concerns about the safety profile have emerged, as 2 out of 3 patients developed serious adverse events (24–26, 28). Like other tumor subtypes, combination treatments represent future options for EC, and currently, studies are focusing on the association with other drugs. Many trials are ongoing, most frequently regarding the combination of ICIs and chemotherapy, radiotherapy, PARP inhibitors, and tyrosine-kinase inhibitors; also, some studies are targeting the adjuvant setting. Effectively, chemotherapy holds immunomodulant properties: for example, platinum compounds can upregulate the class I major histocompatibility complex (MHC), recruit effector T cells and stimulate their cytotoxicity, and downregulate immuno suppressive elements of the TME (53). Antiangiogenics directly influence TME, increasing TILs, favoring dendritic cell maturations and T-cell infiltration (54). PARP inhibitors increase $CD4^+$ and $CD8^+$ T-cells, class II MHC, and immune mediators such as PD1, interferon (IFN) gamma and tumor necrosis factor (TNF) alpha, decreasing inhibitory elements such as T-cell immunoglobulin domain and mucin domain 3 (Tim-3), lymphocyte-activation gene 3 (LAG-3), and PD1 (55). Finally, other immunomodulant pathways such as LAG-3, indoleamine 2,3-dioxygenase (IDO), and Janus kinase (JAK) represent complementary axes for improving immune response and potentiate anti-PD/PD-L1 (**Table 2**). Another potential combination is with radiotherapy, which indeed holds a central role for treating EC both with curative intent in the localized stage and as symptom palliation in the metastatic setting (7). In fact, radiation causes cancer cell damage, exposing tumor antigens and activating immune response after priming T cells. Moreover, radiotherapy modulates TME, favoring the infiltration of immune cells at tumor sites (56). Therefore, the combination of ICIs and RT is under evaluation, especially in the localized setting (**Table 2**). All the studies we included in our systematic review have been conducted in pretreated patients. Nonetheless, it could be of interest to evaluate if an earlier ICI start is feasible and effective for advanced EC patients, for planning a correct sequence strategy. Currently, studies of ICIs and chemotherapy or PARP inhibitors combinations are ongoing in naïve patients (**Table 2**).

Our analysis has several potential limitations. First is the heterogeneity of the included trials, in terms of treated patients, biomarker selection, and endpoints. We did not conduct a quantitative comparative meta-analysis due to the non-comparative design of the almost totality of included trials, and therefore the conclusions drawn about the efficacy and safety of ICIs in EC from our work are only descriptive. Moreover, OS data are incomplete: a longer follow-up is needed to clarify the real impact on survival of ICIs for EC patients. Furthermore, in many studies, safety data are partially reported. Data from randomized trials comparing ICIs with other treatments are warranted to validate efficacy and safety outcomes.

5 CONCLUSIONS

The results of our systematic review demonstrate that ICIs are effective and well-tolerated in patients with pretreated advanced/recurrent EC. To the best of our knowledge, it is the first systematic review focusing on this topic. With single agents, the highest responses are observed among MSI patients. MSS patients benefit more from the combination of pembrolizumab and lenvatinib, notwithstanding with worse toxicity than ICIs alone. So far, no advantages have derived from the double PD1/CTLA4 blocking. Randomized clinical trials are expected. Given the exciting results in MSI-H patients, MMR status should be investigated in every advanced EC patient at diagnosis. On the contrary, PD-L1 as a unique biomarker cannot predict ICI response in EC. For sure, accurate predictive biomarkers are warranted, as well as further studies investigating resistance mechanisms and treatment after ICI progression. So far, clinical trials have focused on pretreated patients, but the impact of ICIs both as single agents and as combinations should be investigated in naïve patients.

DATA AVAILABILITY STATEMENT

The original contributions presented in the study are included in the article/**Supplementary Material**. Further inquiries can be directed to the corresponding author.

AUTHOR CONTRIBUTIONS

BM: conceptualization, methodology, formal analysis, software, investigation, data curation, original draft preparation, review, editing. MM: software, investigation, data curation, original draft preparation. GC: validation, supervision, visualization. AM: visualization. DL: manuscript review, validation, supervision, visualization. EM: editing, validation, supervision, visualization. All authors contributed to the article and approved the submitted version.

SUPPLEMENTARY MATERIAL

The Supplementary Material for this article can be found online at: https://www.frontiersin.org/articles/10.3389/fonc.2022.844801/full#supplementary-material

REFERENCES

1. GLOBOCAN. *Uterus* (2020). Available at: https://gco.iarc.fr/today/data/factsheets/cancers/24-Corpus-uteri-fact-sheet.pdf (Accessed 1 December 2021).
2. SEER. *Uterine Cancer*. Available at: https://seer.cancer.gov/statfacts/html/corp.html (Accessed 1 December 2021).
3. Siegel RL, Miller KD, Fuchs HE, Jemal A. Cancer Statistics, 2021. *CA Cancer J Clin* (2021) 71(1):7–33. doi: 10.3322/caac.21654
4. Esposito K, Chiodini P, Capuano A, Bellastella G, Maiorino MI, Giugliano D. Metabolic Syndrome and Endometrial Cancer: A Meta-Analysis. *Endocrine* (2014) 45:28–36. doi: 10.1007/s12020-013-9973-3
5. Raglan O, Kalliala I, Markozannes G, Cividini S, Gunter MJ, Nautiyal J, et al. Risk Factors for Endometrial Cancer: An Umbrella Review of the Literature. *Int J Cancer* (2018) 145:1719–30. doi: 10.1002/ijc.31961
6. Miller DS, Filiaci VL, Mannel RS, Cohn DE, Matsumoto T, Tewari KS, et al. Carboplatin and Paclitaxel for Advanced Endometrial Cancer: Final Overall Survival and Adverse Event Analysis of a Phase III Trial (NRG Oncology/Gog0209). *J Clin Oncol* (2020) 38:3841–50. doi: 10.1200/JCO.20.01076
7. Concin N, Matias-Guiu X, Vergote I, Cibula D, Mirza MR, Marnitz S, et al. ESGO/ESTRO/ESP Guidelines for the Management of Patients With Endometrial Carcinoma. *Int J Gynecol Cancer* (2021) 31:12–39. doi: 10.1136/ijgc-2020-002230
8. Humber CE, Tierney JF, Symonds RP, Collingwood M, Kirwan J, Williams C, et al. Chemotherapy for Advanced, Recurrent or Metastatic Endometrial Cancer: A Systematic Review of Cochrane Collaboration. *Ann Oncol* (2007) 18:409–20. doi: 10.1093/annonc/mdl417
9. Fleming GF. Second-Line Therapy for Endometrial Cancer: The Need for Better Options. *JCO* (2015) 33:3535–40. doi: 10.1200/JCO.2015.61.7225
10. Nagao S, Nishio S, Michimae H, Tanabe H, Okada S, Otsuki T, et al. Applicability of the Concept of "Platinum Sensitivity" to Recurrent Endometrial Cancer: The SGSG-012/GOTIC-004/Intergroup Study. *Gynecol Oncol* (2013) 131:567–73. doi: 10.1016/j.ygyno.2013.09.021
11. Levine DA. Integrated Genomic Characterization of Endometrial Carcinoma. *Nature* (2013) 497:67–73. doi: 10.1038/nature12113
12. Maiorano BA, Maiorano MFP, Lorusso D, Maiello E. Ovarian Cancer in the Era of Immune Checkpoint Inhibitors: State of the Art and Future Perspectives. *Cancers (Basel)* (2021) 13:4438. doi: 10.3390/cancers13174438
13. Marcus L, Lemery SJ, Keegan P, Pazdur R. FDA Approval Summary: Pembrolizumab for the Treatment of Microsatellite Instability-High Solid Tumors. *Clin Cancer Res* (2019) 25(13):3753–8. doi: 10.1158/1078-0432.CCR-18-4070
14. FDA. *FDA Grants Regular Approval to Pembrolizumab and Lenvatinib for Advanced Endometrial Carcinoma*. Available at: https://www.fda.gov/drugs/resources-information-approved-drugs/fda-grants-regular-approval-pembrolizumab-and-lenvatinib-advanced-endometrial-carcinoma (Accessed 1 December 2021).
15. Merck. *European Commission Approves KEYTRUDA® (Pembrolizumab) Plus LENVIMA® (Lenvatinib) for Patients With Certain Types of Endometrial Carcinoma*. Available at: https://www.merck.com/news/european-commission-approves-keytruda-pembrolizumab-plus-lenvima-lenvatinib-for-patients-with-certain-types-of-endometrial-carcinoma/ (Accessed 1 December 2021).
16. ESMO. *EMA Recommends Granting a Conditional Marketing Authorisation for Dostarlimab*. Available at: https://www.esmo.org/oncology-news/ema-recommends-granting-a-conditional-marketing-authorisation-for-dostarlimab (Accessed 1 December 2021).
17. Moher D, Liberati A, Tetzlaff J, Altman DG, Group TP. Preferred Reporting Items for Systematic Reviews and Meta-Analyses: The PRISMA Statement. *PloS Med* (2009) 6:e1000097. doi: 10.1371/journal.pmed.1000097
18. Sterne JA, Hernán MA, Reeves BC, Savović J, Berkman ND, Viswanathan M, et al. ROBINS-I: A Tool for Assessing Risk of Bias in Non-Randomised Studies of Interventions. *BMJ* (2016) 355:i4919. doi: 10.1136/bmj.i4919
19. Marabelle A, Le DT, Ascierto PA, Di Giacomo AM, De Jesus-Acosta A, Delord J-P, et al. Efficacy of Pembrolizumab in Patients With Noncolorectal High Microsatellite Instability/Mismatch Repair–Deficient Cancer: Results From the Phase II KEYNOTE-158 Study. *J Clin Oncol* (2020) 38:1–10. doi: 10.1200/JCO.19.02105
20. Le DT, Durham JN, Smith KN, Wang H, Bartlett BR, Aulakh LK, et al. Mismatch Repair Deficiency Predicts Response of Solid Tumors to PD-1 Blockade. *Science* (2017) 357:409–13. doi: 10.1126/science.aan6733
21. Fader AN, Diaz LA, Armstrong DK, Tanner EJ, Uram J, Eyring A, et al. Preliminary Results of a Phase II Study: PD-1 Blockade in Mismatch Repair–Deficient, Recurrent or Persistent Endometrial Cancer. *Gynecol Oncol* (2016) 141:206–7. doi: 10.1016/j.ygyno.2016.04.532
22. Roque DM, Bellone S, Siegel ER, Buza N, Bonazzoli E, Guglielmi A, et al. A Phase II Evaluation of Pembrolizumab in Recurrent Microsatellite Instability-High (MSI-H) Endometrial Cancer Patients With Lynch-Like Versus MLH-1 Methylated Characteristics (NCT02899793). *JCO* (2021) 39:5523–3. doi: 10.1200/JCO.2021.39.15_suppl.5523
23. Ott PA, Bang Y-J, Berton-Rigaud D, Elez E, Pishvaian MJ, Rugo HS, et al. Safety and Antitumor Activity of Pembrolizumab in Advanced Programmed Death Ligand 1-Positive Endometrial Cancer: Results From the KEYNOTE-028 Study. *J Clin Oncol* (2017) 35:2535–41. doi: 10.1200/JCO.2017.72.5952
24. Makker V, Taylor MH, Aghajanian C, Oaknin A, Mier J, Cohn AL, et al. Lenvatinib Plus Pembrolizumab in Patients With Advanced Endometrial Cancer. *J Clin Oncol* (2020) 38:2981–92. doi: 10.1200/JCO.19.02627
25. Makker V, Colombo N, Casado Herráez A, Santin A, Colomba E, Miller D. Society of Gynecologic Oncology 2021 Virtual Annual Meeting on Women's Cancer. A Multicenter, Open-Label, Randomized Phase 3 Study to Compare the Efficacy and Safety of Lenvatinib in Combination With Pembrolizumab vs Treatment of Physician's Choice in Patients With Advanced Endometrial Cancer: Study 309/KEYNOTE-775. *Int J Gynec Canc* (2021) 31:A4–5.
26. Taylor MH, Lee C-H, Makker V, Rasco D, Dutcus CE, Wu J, et al. Phase IB/II Trial of Lenvatinib Plus Pembrolizumab in Patients With Advanced Renal Cell Carcinoma, Endometrial Cancer, and Other Selected Advanced Solid Tumors. *J Clin Oncol* (2020) 38:1154–63. doi: 10.1200/JCO.19.01598
27. Tamura K, Hasegawa K, Katsumata N, Matsumoto K, Mukai H, Takahashi S, et al. Efficacy and Safety of Nivolumab in Japanese Patients With Uterine Cervical Cancer, Uterine Corpus Cancer, or Soft Tissue Sarcoma: Multicenter, Open-Label Phase 2 Trial. *Cancer Sci* (2019) 110(9):2894–904. doi: 10.1111/cas.14148
28. Lheureux S, Matei D, Konstantinopoulos PA, Block MS, Jewell A, Gaillard S, et al. A Randomized Phase II Study of Cabozantinib and Nivolumab Versus Nivolumab in Recurrent Endometrial Cancer. *JCO* (2020) 38:6010–0. doi: 10.1200/JCO.2020.38.15_suppl.6010
29. Oaknin A, Duska LR, Sullivan RJ, Pothuri B, Ellard SL, Leath CA, et al. Preliminary Safety, Efficacy, and Pharmacokinetic/Pharmacodynamic Characterization From GARNET, A Phase I/II Clinical Trial of the Anti–PD-1 Monoclonal Antibody, TSR-042, in Patients With Recurrent or Advanced MSI-H and MSS Endometrial Cancer. *Gynecol Oncol* (2019) 154:17. doi: 10.1016/j.ygyno.2019.04.044
30. Konstantinopoulos PA, Luo W, Liu JF, Gulhan DC, Krasner C, Ishizuka JJ, et al. Phase II Study of Avelumab in Patients With Mismatch Repair Deficient and Mismatch Repair Proficient Recurrent/Persistent Endometrial Cancer. *J Clin Oncol* (2019) 37:2786–94. doi: 10.1200/JCO.19.01021
31. Fleming GF, Emens LA, Eder JP, Hamilton EP, Liu JF, Liu B, et al. Clinical Activity, Safety and Biomarker Results From a Phase Ia Study of Atezolizumab (Atezo) in Advanced/Recurrent Endometrial Cancer (rEC). *JCO* (2017) 35:5585–5. doi: 10.1200/JCO.2017.35.15_suppl.5585
32. Antill Y, Kok PS, Stockler MR, Robledo K, Yip S, Parry M, et al. Australia New Zealand Gynaecological Oncology Group (ANZGOG). Clinical Activity of Durvalumab for Patients With Advanced Mismatch Repair-Deficient and Repair-Proficient Endometrial Cancer. A Nonrandomized Phase 2 Clinical Trial. *J Immunother Cancer* (2021) 9:e002255. doi: 10.1136/jitc-2020-002255
33. Rubinstein MM, Caird I, Zhou Q, Iasonos A, Friedman CF, Cadoo KA, et al. A Phase II Trial of Durvalumab With or Without Tremelimumab in Patients With Persistent or Recurrent Endometrial Carcinoma and Endometrial Carcinosarcoma. *JCO* (2019) 37:5582–2. doi: 10.1200/JCO.2019.37.15_suppl.5582
34. Borcoman E, Kanjanapan Y, Champiat S, Kato S, Servois V, Kurzrock R, et al. Novel Patterns of Response Under Immunotherapy. *Ann Oncol* (2019) 30:385–96. doi: 10.1093/annonc/mdz003
35. Lu L, Li Y, Luo R, Xu J, Feng J, Wang M. Prognostic and Clinicopathological Role of PD-L1 in Endometrial Cancer: A Meta-Analysis. *Front Oncol* (2020) 10:632. doi: 10.3389/fonc.2020.00632
36. Howitt BE, Shukla SA, Sholl LM, Ritterhouse LL, Watkins JC, Rodig S, et al. Association of Polymerase E-Mutated and Microsatellite-Instable Endometrial Cancers With Neoantigen Load, Number of Tumor-Infiltrating Lymphocytes, and Expression of PD-1 and PD-L1. *JAMA Oncol* (2015) 1:1319–23. doi: 10.1001/jamaoncol.2015.2151

37. Pakish JB, Zhang Q, Chen Z, Liang H, Chisholm GB, Yuan Y, et al. Immune Microenvironment in Microsatellite Instable Endometrial Cancers: Hereditary or Sporadic Origin Matters. *Clin Cancer Res* (2017) 23:4473–81. doi: 10.1158/1078-0432.CCR-16-2655
38. Vanderwalde A, Spetzler D, Xiao N, Gatalica Z, Marshall J. Microsatellite Instability Status Determined by Next-Generation Sequencing and Compared With PD-L1 and Tumor Mutational Burden in 11,348 Patients. *Cancer Med* (2018) 7:746–56. doi: 10.1002/cam4.1372
39. Chalmers ZR, Connelly CF, Fabrizio D, Gay L, Ali SM, Ennis R, et al. Analysis of 100,000 Human Cancer Genomes Reveals the Landscape of Tumor Mutational Burden. *Genome Med* (2017) 9:34. doi: 10.1186/s13073-017-0424-2
40. Marabelle A, Fakih M, Lopez J, Shah M, Shapira-Frommer R, Nakagawa K, et al. Association of Tumour Mutational Burden With Outcomes in Patients With Advanced Solid Tumours Treated With Pembrolizumab: Prospective Biomarker Analysis of the Multicohort, Open-Label, Phase 2 KEYNOTE-158 Study. *Lancet Oncol* (2020) 21:1353–65. doi: 10.1016/S1470-2045(20)30445-9
41. de Jong RA, Leffers N, HM B, ten Hoor KA, van der Zee AGJ, Hollema H, et al. Presence of Tumor-Infiltrating Lymphocytes Is an Independent Prognostic Factor in Type I and II Endometrial Cancer. *Gynecol Oncol* (2009) 114:105–10. doi: 10.1016/j.ygyno.2009.03.022
42. Kübler K, Ayub TH, Weber SK, Zivanovic O, Abramian A, Keyver-Paik M-D, et al. Prognostic Significance of Tumor-Associated Macrophages in Endometrial Adenocarcinoma. *Gynecol Oncol* (2014) 135:176–83. doi: 10.1016/j.ygyno.2014.08.028
43. Cao QJ, Einstein MH, Anderson PS, Runowicz CD, Balan R, Jones JG. Expression of COX-2, Ki-67, Cyclin D1, and P21 in Endometrial Endometrioid Carcinomas. *Int J Gynecol Pathol* (2002) 21:147–54. doi: 10.1097/00004347-200204000-00007
44. Ohno Y, Ohno S, Suzuki N, Kamei T, Inagawa H, Soma G-I, et al. Role of Cyclooxygenase-2 in Immunomodulation and Prognosis of Endometrial Carcinoma. *Int J Cancer* (2005) 114:696–701. doi: 10.1002/ijc.20777
45. Suemori T, Susumu N, Iwata T, Banno K, Yamagami W, Hirasawa A, et al. Intratumoral CD8+ Lymphocyte Infiltration as a Prognostic Factor and Its Relationship With Cyclooxygenase 2 Expression and Microsatellite Instability in Endometrial Cancer. *Int J Gynecol Cancer* (2015) 25:1165–72. doi: 10.1097/IGC.0000000000000482
46. Jiang T, Chen X, Su C, Ren S, Zhou C. Pan-Cancer Analysis of ARID1A Alterations as Biomarkers for Immunotherapy Outcomes. *J Cancer* (2020) 11:776–80. doi: 10.7150/jca.41296
47. Santin AD, Bellone S, Buza N, Choi J, Schwartz PE, Schlessinger J, et al. Regression of Chemotherapy-Resistant Polymerase ϵ (POLE) Ultra-Mutated and MSH6 Hyper-Mutated Endometrial Tumors With Nivolumab. *Clin Cancer Res* (2016) 22:5682–7. doi: 10.1158/1078-0432.CCR-16-1031
48. Post CCB, Stelloo E, Smit V, Ruano D, Tops CM, Vermij L, et al. Prevalence and Prognosis of Lynch Syndrome and Sporadic Mismatch Repair Deficiency in Endometrial Cancer. *JNCI* (2021) 113:1212–20. doi: 10.1093/jnci/djab029
49. Rousseau BJ-C, Bieche I, Pasmant E, Simmet V, Hamzaoui N, Masliah-Planchon J, et al. 526o High Activity of Nivolumab in Patients With Pathogenic Exonucleasic Domain POLE (edPOLE) Mutated Mismatch Repair Proficient (MMRp) Advanced Tumours. *Ann Oncol* (2020) 31:S463. doi: 10.1016/j.annonc.2020.08.640
50. Mittica G, Ghisoni E, Giannone G, Aglietta M, Genta S, Valabrega G. Checkpoint Inhibitors in Endometrial Cancer: Preclinical Rationale and Clinical Activity. *Oncotarget* (2017) 8:90532–44. doi: 10.18632/oncotarget.20042
51. Kato Y, Bao X, Macgrath S, Tabata K, Hori Y, Tachino S, et al. Lenvatinib Mesilate (LEN) Enhanced Antitumor Activity of a PD-1 Blockade Agent by Potentiating Th1 Immune Response. *Ann Oncol* (2016) 27(6suppl):VI1. doi: 10.1093/annonc/mdw362.02
52. Lee WS, Yang H, Chon HJ, Kim C. Combination of Anti-Angiogenic Therapy and Immune Checkpoint Blockade Normalizes Vascular-Immune Crosstalk to Potentiate Cancer Immunity. *Exp Mol Med* (2020) 52:1475–85. doi: 10.1038/s12276-020-00500-y
53. de Biasi AR, Villena-Vargas J, Adusumilli PS. Cisplatin-Induced Antitumor Immunomodulation: A Review of Preclinical and Clinical Evidence. *Clin Cancer Res* (2014) 20:5384–91. doi: 10.1158/1078-0432.CCR-14-1298
54. Shrimali RK, Yu Z, Theoret MR, Chinnasamy D, Restifo NP, Rosenberg SA. Antiangiogenic Agents can Increase Lymphocyte Infiltration Into Tumor and Enhance the Effectiveness of Adoptive Immunotherapy of Cancer. *Cancer Res* (2010) 70:6171–80. doi: 10.1158/0008-5472.CAN-10-0153
55. Ding L, Kim H-J, Wang Q, Kearns M, Jiang T, Ohlson CE, et al. PARP Inhibition Elicits STING-Dependent Antitumor Immunity in Brca1-Deficient Ovarian Cancer. *Cell Rep* (2018) 25:2972–80.e5. doi: 10.1016/j.celrep.2018.11.054
56. Wang Y, Deng W, Li N, Neri S, Sharma A, Jiang W, et al. Combining Immunotherapy and Radiotherapy for Cancer Treatment: Current Challenges and Future Directions. *Front Pharmacol* (2018) 9:185. doi: 10.3389/fphar.2018.00185

Conflict of Interest: The authors declare that the research was conducted in the absence of any commercial or financial relationships that could be construed as a potential conflict of interest.

Publisher's Note: All claims expressed in this article are solely those of the authors and do not necessarily represent those of their affiliated organizations, or those of the publisher, the editors and the reviewers. Any product that may be evaluated in this article, or claim that may be made by its manufacturer, is not guaranteed or endorsed by the publisher.

Copyright © 2022 Maiorano, Maiorano, Cormio, Maglione, Lorusso and Maiello. This is an open-access article distributed under the terms of the Creative Commons Attribution License (CC BY). The use, distribution or reproduction in other forums is permitted, provided the original author(s) and the copyright owner(s) are credited and that the original publication in this journal is cited, in accordance with accepted academic practice. No use, distribution or reproduction is permitted which does not comply with these terms.

frontiers | Frontiers in Oncology

ORIGINAL RESEARCH
published: 14 April 2022
doi: 10.3389/fonc.2022.800049

Discussion on the Treatment Strategy for Stage ⅡA1 Cervical Cancer (FIGO 2018)

Xiaolin Chen[1‡], Wentong Liang[2‡], Hui Duan[1‡], Minling Wu[1‡], Xuemei Zhan[3], Encheng Dai[4], Qiubo Lv[5], Qinghuang Xie[6], Ruilei Liu[4], Yan Xu[7], Xiaonong Bin[8], Jinghe Lang[9], Ping Liu[1] and Chunlin Chen[1*†]*

[1] Department of Obstetrics and Gynecology, Nanfang Hospital, Southern Medical University, Guangzhou, China, [2] Department of Obstetrics and Gynecology, Guizhou Provincial People's Hospital, Guizhou, China, [3] Department of Obstetrics and Gynecology, Jiangmen Central Hospital, Jiangmen, China, [4] Department of Obstetrics and Gynecology, Linyi People's Hospital, Linyi, China, [5] Department of Obstetrics and Gynecology, Beijing Hospital, Beijing, China, [6] Department of Gynecology, Foshan Maternal and Child Health Hospital, Foshan, China, [7] Department of Obstetrics and Gynecology, Pan Yu Central Hospital, Guangzhou, China, [8] Department of Epidemiology, College of Public Health, Guangzhou Medical University, Guangzhou, China, [9] Department of Obstetrics and Gynecology, Peking Union Medical College Hospital, Peking Union Medical College, Beijing, China

OPEN ACCESS

Edited by:
Sheng-Mou Hsiao, Far Eastern Memorial Hospital (FEMH), Taiwan

Reviewed by:
Hooman Soleymani majd, Oxford University Hospitals NHS Trust, United Kingdom
Juan Zhou, Xiamen University, China

***Correspondence:**
Ping Liu
lpivy@126.com
Chunlin Chen
ccl1@smu.edu.cn

†ORCID ID:
Chunlin Chen
orcid.org/0000-0002-1708-3047

‡These authors have contributed equally to this work and share first authorship

Specialty section:
This article was submitted to Gynecological Oncology, a section of the journal Frontiers in Oncology

Received: *22 October 2021*
Accepted: *18 March 2022*
Published: *14 April 2022*

Citation:
Chen X, Liang W, Duan H, Wu M, Zhan X, Dai E, Lv Q, Xie Q, Liu R, Xu Y, Bin X, Lang J, Liu P and Chen C (2022) Discussion on the Treatment Strategy for Stage ⅡA1 Cervical Cancer (FIGO 2018). Front. Oncol. 12:800049. doi: 10.3389/fonc.2022.800049

Objective: This study aimed to explore the best treatment strategy for International Federation of Gynecology and Obstetrics (FIGO) 2018 stage IIA1 cervical cancer patients by comparing the survival outcomes of two treatment methods: abdominal radical hysterectomy (ARH) with standard postoperative therapy and radio-chemotherapy (R-CT).

Methods: Patients with FIGO2018 stage IIA1 cervical cancer who underwent ARH or received R-CT were screened from the clinical diagnosis and treatment for cervical cancer in China (Four C) database. The recurrence cases between the two groups were analyzed. The 5-year overall survival (OS) and disease-free survival (DFS) of patients diagnosed with stage IIA1 cervical cancer in 47 hospitals in mainland China between 2004 and 2018 were compared by using propensity score matching (PSM).

Results: A total of 724 patients met the inclusion criteria. In the total study population, The R-CT group had higher recurrence (22.8% for the R-CT group and 11.2% for the ARH group, $P<0.001$) rates compared to the ARH group.The 5-year OS and DFS of the ARH group (n=658) were significantly higher than those of the R-CT group (n=66) (OS: 85.9% *vs*. 71.2%, $P=0.009$; DFS: 79.2%*vs*. 70.5%, $P=0.027$). R-CT was associated with worse 5-year OS (HR=3.19, 95% CI: 1.592-6.956, $P=0.001$) and DFS (HR=2.089, 95% CI: 1.194-3.656, $P=0.01$). After 1:2 PSM, the 5-year OS and DFS of the ARH group (n=126) were significantly higher than those of the R-CT group (n=64) (OS:88.9% *vs.* 70.1%, $P=0.04$; DFS:82.8% *vs.* 69.8%, $P=0.019$). R-CT was still associated with worse 5-year OS (HR=2.391, 95% CI: 1.051-5.633, $P=0.046$) and DFS (HR=2.6, 95% CI: 1.25-5.409, $P=0.011$).

Conclusion: Our study demonstrated that for stage FIGO2018 stage IIA1 cervical cancer patients, ARH offers better oncological outcomes than R-CT.

Keywords: cervical cancer, stage ⅡA1, overall survival, disease-free survival, treatment strategies

INTRODUCTION

All cases of lymph node metastasis were classified as newly established International Federation of Gynecology and Obstetrics (FIGO) 2018 stage IIIC (1, 2), so FIGO2018 stage IIA1 was redefined as follows: cancerous lesion with invasion that exceeded the cervix but did not reach 1/3 of the vagina or the pelvic wall; maximum tumour diameter of the cancerous stove ≤4 cm; and no metastasis to the pelvic lymph nodes. However, for the treatment of FIGO2018 stage IIA1 cervical cancer patients, surgical treatment or curative chemotherapy could be chosen (3). Since FIGO2018 stage IIA1 cervical cancer no longer includes lymph node metastasis, it was worth exploring whether the optimal treatment strategy has also changed. Based on the above questions, this study was intended to screen FIGO2018 stage IIA1 cervical cancer patients from the clinical diagnosis and treatment for cervical cancer in China (Four C) database. We compared the oncological outcomes of abdominal radical hysterectomy (ARH) with standard postoperative therapy and radio-chemotherapy (R-CT) to explore the best treatment strategies for patients with FIGO2018 stage IIA1 cervical cancer.

MATERIALS AND METHODS

Data Source

We systematically collected clinical data on 63,926 patients with cervical cancer at each stage in 47 hospitals in mainland China between 2004 and 2018 and tracked patients' long-term oncological outcomes. This study was a multi-centre retrospective cohort study approved by the Southern Hospital Ethics Committee of Southern Medical University (Ethics number NFEC-2017-135). The clinical trial identifier is CHiCTR1800017778 (International Clinical Trials Registry Platform Search Port, http://apps.who.int/trialsearch/). Data collection and follow-up were carried out by gynecologists who had received unified training. After the completion of data entry, two independent gynecologists double-entered the data and checked the information to ensure the accuracy of the data. Relevant data collection and database construction procedures can be found in papers published by our team (4–8). Among them, the cases in this database collected before 2009 were staged by FIGO 1994, and the cases collected after 2009 were staged by FIGO2009. All the cases were re-corrected according to the FIGO2018 cervical cancer staging system after being entered into the database.

Inclusion and Exclusion Criteria

In this study, the inclusion and exclusion criteria were as follows:

Inclusion criteria for the ARH with postoperative standard therapy group (ARH group): (1) age ≥18 years old; (2) cervical biopsy pathology diagnosis of cervical cancer; (3) postoperative histological types: squamous cell carcinoma, adenocarcinoma, and adenosquamous cell carcinoma; (4) clinical stage IIA1 (2018) disease; (5) no neoadjuvant chemotherapy or radiotherapy; (6) surgical approach: abdominal; (7) operation type: Querleu–Morrow type C hysterectomy + pelvic lymph node excision ± abdominal para-aortic lymph node excision/ biopsy; (8) complete postoperative pathological report and information on the lymph node status (negative pelvic lymph node and para-aortic lymph node metastases); (9) postoperative adjuvant treatment: standard; and (10) attending follow-up visits.

Inclusion criteria for the R-CT group: (1) age ≥18 years old; (2) cervical biopsy pathology diagnosis of cervical cancer; (3) histological types: squamous cell carcinoma, adenocarcinoma, and adenosquamous cell carcinoma; (4) FIGO2018 stage: stage IIA1; (5) pre-treatment MRI or CT examination and description of the lymph node status (negative for pelvic lymph node and para-aortic lymph node metastases); (6) initial treatment: R-CT, treatment including pelvic external beam radiotherapy+vaginal brachytherapy, with a radiotherapy dose≥85 Gy, including concurrent platinum-containing chemotherapy; and (7) attending follow-up visits.

The exclusion criteria were as follows: (1) did not meet the abovementioned admission criteria; and (2) pregnancy combined with cervical cancer, residual cancer, or another malignancy.

Observation Indicators

The observation endpoints were overall survival (OS) and disease-free survival (DFS), and the cut-off point for long-term oncological outcomes was 5-year. OS was defined as the date of diagnosis until death from any cause or the last effective follow-up, and DFS was defined as the date of diagnosis until death, recurrence, or the last effective follow-up.

Statistical Methods

SPSS software (Version 22.0, SPSS Inc., Chicago, IL, USA) was used for statistical analysis, and the PSM extension of SPSS 22.0 software was used to achieve propensity score matching (PSM). Measurement data are expressed as the mean ± standard deviation, and an independent sample t-test was used for comparisons between groups. Count data are expressed as percentages (%), and the chi-square test was used to compare intergroup rates. Kaplan-Meier curves were drawn to analyze survival, and log-rank tests were used to compare differences in the survival curves. Multivariate Cox regression was used to analyze and determine independent risk factors, the relevant risks, and confidence intervals. In this study, $P < 0.05$ was considered statistically significant.

RESULTS

Case Screening Results

This study screened 724 patients who met the inclusion criteria. The data screening process is shown in **Figure 1**.

Recurrence Patterns

The median follow-up was 58 months (1–152 months). Up to the last day of follow-up, 107patients developed neoplastic recurrence, and the recurrence rate was 14.8% for 5-year.

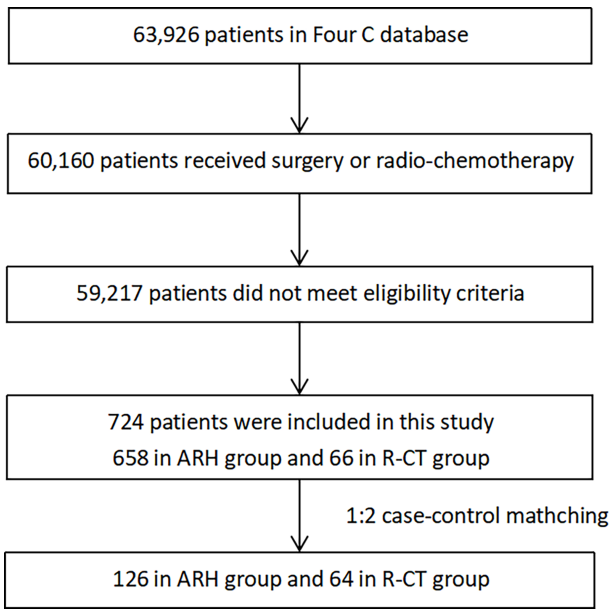


FIGURE 1 | Flow diagram of patient recruitment and exclusions.

14.1% of the ARH group patients and 21.2% in the R-CT group developed neoplastic recurrence. Besides, The R-CT group had shorter recurrence 16.43 ± 12.21 months for the R-CT group and 21.30 ± 13.74 months for the ARH group) time compared to the ARH group. Local recurrence was seen in 26 cases. Distant recurrence was seen in 34 cases. The recurrence pattern of the remaining 47 cases was unknown (**Table 1**).

Prognosis Comparison of the ARH Group and the R-CT Group Before and After Matching

A total of 724 patients met the inclusion criteria: 658 in the ARH group and 66 in the R-CT group (**Table 2**). Among the overall study population, Kaplan-Meier curve analysis showed that both the 5-year OS and DFS in the ARH group were significantly higher than those in the R-CT group (OS: 85.9% *vs.* 71.2%, *P*=0.009; DFS: 79.2% *vs.* 70.5%, *P*=0.027) (**Figures 2A, B**). Cox multivariate analysis showed a higher risk of death or recurrence in the R-CT group than in the ARH group (HR=3.19, 95% CI: 1.592-6.956, *P*=0.001) and worse DFS (HR=2.089, 95% CI: 1.194-3.656, *P*=0.01) (**Table 3**).

Due to differences in age between the ARH group and the R-CT group in the overall study population, 1:2 PSM was performed. After PSM, 126 patients were included in the ARH group, and 64 patients were included in the R-CT group (**Table 2**). These results were consistent with those of the whole study population. Kaplan-Meier curve analysis showed that both the 5-year OS and DFS in the ARH group were higher than those in the R-CT group (OS:88.9% *vs.* 70.1%, *P*=0.04; DFS:82.8% *vs.* 69.8%, *P*=0.019) (**Figures 2C, D**). Multivariate Cox analysis showed a higher risk of death or recurrence in the R-CT group than in the ARH group (HR=2.391, 95% CI: 1.051-5.633, *P*=0.046) and worse DFS (HR=2.6, 95% CI: 1.25-5.409, *P*=0.011) (**Table 4**).

DISCUSSION

According to the FIGO2018 staging system for cervical cancer, all patients with lymph node metastasis were classified as the newly established stage IIIC, and patients with stage IIA1 cervical cancer with lymph node metastasis were no longer included. However, the 2020 NCCN Guidelines for Cervical Cancer are consistent with the previous treatment principles of FIGO2009 stage IIA1 cervical cancer: (1) radical hysterectomy + pelvic lymphadenectomy (evidence level 1) ± para-aortic lymphadenectomy (evidence level 2B), and sentinel lymphadenography can be considered. (2) For patients with contraindications or refuse surgery, external pelvic irradiation + vaginal brachytherapy ± concurrent chemotherapy containing platinum is recommended (3). With changes in the principles of the FIGO2018 staging system, are the above treatments still suitable for patients with stage IIA1 cervical cancer? To answer this question, we conducted this multi-centre, large-sample retrospective study to compare long-term oncological outcomes in patients with FIGO2018 stage IIA1 cervical cancer who were cured by ARH and R-CT to obtain the optimal treatment strategy.

The oncological outcomes in the ARH group were better than those in the R-CT group in the overall study population. After controlling for confounding factors, such as age and histological type by 1:2 PSM, the 5-year OS and DFS of the ARH group were still higher than those of the R-CT group. In this study, the overall recurrence rate was 14.8%. The results are consistent with the recurrence rate of cervical cancer reported in previous studies (5%-40%). The R-CT group had a higher recurrence rate but shorter recurrence time compared to the ARH group, but there was no statistical difference between groups. Based on previous reports, we

TABLE 1 | Recurrence patterns of patients in the ARH and R-CT groups.

Characteristic	ARH group (n=658)	R-CT group (n=66)
Recurrence		
NO	565 (85.9%)	52 (78.8%)
YES	93 (14.1%)	14 (21.2%)
recurrence time	21.30 ± 13.74	16.43 ± 12.21
Patterns of recurrence		
Local recurrence	24 (25.8%)	2 (14.3%)
Distant metastases	32 (34.4%)	2 (14.3%)
Unknown	37 (39.8%)	10 (71.4%)

TABLE 2 | Clinicopathologic characteristics of patients in the ARH and R-CT groups.

Characteristic	Before propensity score matching			After propensity score matching		
	ARH group (n=658)	R-CT group (n=66)	P value	ARH group (n=126)	R-CT group (n=64)	P value
Age	52.13 ± 9.74	58.11 ± 8.54	<0.001	57.67 ± 8.35	57.67 ± 8.30	0.997
Tumor size	2.97 ± 0.89	3.16 ± 0.98	0.094	3.04 ± 0.81	3.19 ± 0.97	0.249
Histological type			0.320			0.619
Squamous cell carcinoma	605 (91.9%)	64 (97%)		118 (93.7%)	62 (96.9%)	
Adenocarcinoma	36 (5.5%)	1(1.5%)		5 (4%)	1 (1.6%)	
Adenosquamous carcinoma	17 (2.6%)	1 (1.5%)		3 (2.4%)	1 (1.6%)	

ARH, abdominal radical hysterectomy; R-CT, radio-chemotherapy; OS, overall survival; DFS, disease-free survival.

opted to combine cervical, vaginal vault, pelvic LN, and pelvic wall recurrences as LRR, and organ metastasis, peritoneal carcinomatosis and extra-pelvic LN recurrences as DR (9). Heterogeneity exists between different recurrence patterns in cervical cancer patients in previous studies (10–14). In our study, there was also statistical difference in recurrence modes between the two groups(P<0.05). In ARH group, the proportion of distant metastases (**34.4%**) was higher than that of local metastases (**25.8%**). Since 71.4% of the recurrence cases in the R-CT group had unknown metastasis sites, there were only 2 cases of local and distant metastasis respectively. However, additional information on the specific site of recurrence is needed for further research. This finding suggests that FIGO2018 stage IIA1 patients with cervical cancer may benefit from radical hysterectomy with standard postoperative therapy.

Previous articles comparing the oncological outcomes between ARH and R-CT in cervical cancer patients were based on the FIGO2009 staging system. In 2009, Bansal N (15) found that in stage IB1-IIA2 cervical cancer, the oncological outcome of patients with a tumor diameter < 6 cm receiving surgical treatment was better than that of the same patients receiving radiotherapy, and the study results of Rungruang B (16) were similar. In our study, 5-year OS and DFS were adopted as the observation outcome, so the results were more accurate. In addition, patients who received standard postoperative adjuvant treatment were included in this study, and the effects of non-standard postoperative treatment and other factors on the prognosis of patients were excluded. Moreover, the results and conclusions of this study were consistent with previous findings of our team (4).

However, findings from some studies are inconsistent with our findings. Landoni F (17, 18) found no difference between the survival outcomes of radiation therapy and surgical treatment in

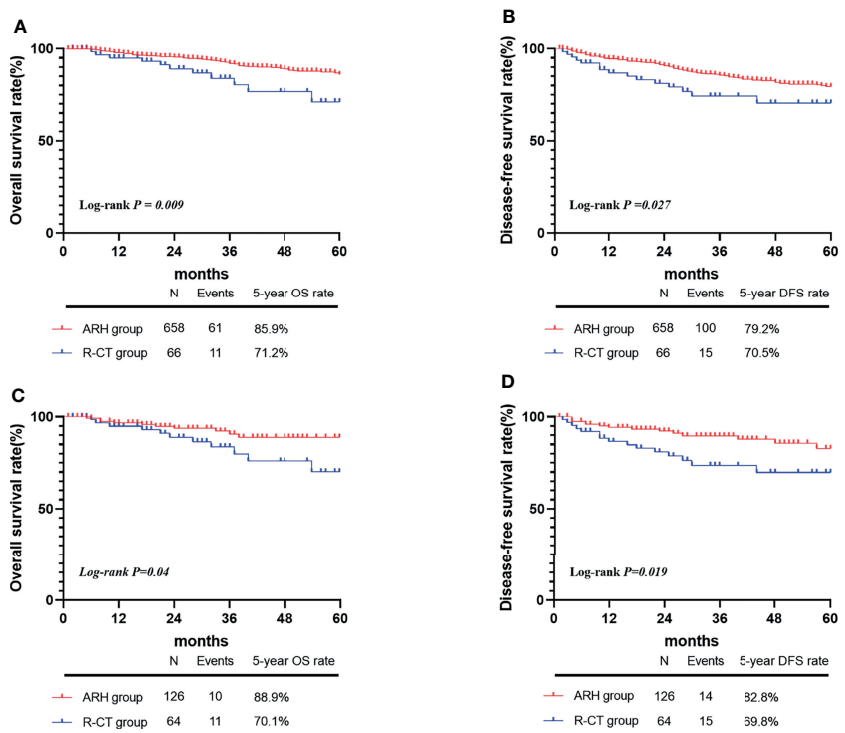


FIGURE 2 | The 5-year OS and DFS rates of the ARH group and R-CT groups before and after 1:2 matching. Before matching, panels **A** and **B**; after matching, panels **C** and **D**.

TABLE 3 | Cox multivariate survival analysis before propensity score matching.

Before propensity score matching	Multivariate analysis for 5-year OS			Multivariate analysis for 5-year DFS		
	P	HR	95% CI	P	HR	95% CI
ARH *vs.* R-CT	0.001	3.19	1.592-6.956	0.01	2.089	1.194-3.656
Age	0.025	0.97	0.944-0.996	0.134	0.984	0.963-1.005
Tumor size	0.478	0.918	0.724-1.164	0.478	0.918	0.724-1.164
Histological type	0.04			0.001		
Squamous cell carcinoma						
Adenocarcinoma		3.052	1.367-6.816		3.593	1.983-6.51
Adenosquamous carcinoma		1.928	0.598-6.215		1.306	0.412-4.142

ARH, abdominal radical hysterectomy; R-CT, radio-chemotherapy; OS, overall survival; DFS, disease-free survival; CI, confidence interval; HR, hazard ratio.

TABLE 4 | Cox multivariate survival analysis after propensity score matching.

After propensity score matching	Multivariate analysis for 5-year OS			Multivariate analysis for 5-year DFS		
	P	HR	95% CI	P	HR	95% CI
ARH *vs.* R-CT	0.046	2.391	1.051-5.633	0.011	2.6	1.25-5.409
Age	0.834	0.994	0.944-1.048	0.366	0.979	0.936-1.025
Tumor size	0.195	0.738	0.466-1.168	0.011	0.617	0.425-0.896
Histological type	0.982			0.513		
Squamous cell carcinoma						
Adenocarcinoma		2.426	1.582-6.049		2.364	0.549-10.176
Adenosquamous carcinoma		2.063	0.632-7.012		1.306	0.412-4.142

ARH, abdominal radical hysterectomy; R-CT, radio-chemotherapy; OS, overall survival; DFS, disease-free survival; CI, confidence interval; HR, hazard ratio.

patients with stage IB1-IIA2 cervical cancer, possibly due to factors such as the small sample size in their studies, non-standard postoperative assisted treatment, and uncontrolled bias. The same problem was also present in the research of Yamashita H, et al. (19) In 2017, Wu SG et al. (20) analyzed 3,653 patients who received RH and 116 patients who received R-CT, and the results of PSM showed no significant difference in the effect of the two treatment methods on the prognosis of patients with stage IB1 and stage IIA1 cervical cancer, but the study also included patients with stage 1B cervical cancer. Furthermore, there was a large difference in the number of patients between the two groups, and the reliability of the PSM results was relatively low.

Compared with previous reports or articles on the optimal treatment strategy for cervical cancer, this study has certain advantages. On the one hand, there is currently a lack of relevant literature reports on the treatment strategy for FIGO2018 stage IIA1 cervical cancer, and previous studies were based on the optimal treatment plan for FIGO2009 stage IIA1 cervical cancer. However, patients with lymph node metastasis were not excluded from those studies. This study supplemented the relatively new research results in this aspect. On the other hand, this study was a multi-centre retrospective study that covered the case information of 1070 cervical cancer patients from 47 hospitals in various regions of China. At present, the current project represents a relatively comprehensive perspective of cervical cancer clinical diagnosis and treatment on a large number of patients worldwide. Due to the sufficient number of samples, we conducted multi-angle, multi-level, and multi-azimuth analyses of each stage of cervical cancer and adopted PSM to balance the baseline differences, which made the results more reliable.

We acknowledge several limitations to this study. This was a retrospective study, and there may have been confounding factors and biases, but these differences were balanced to a large extent through PSM; Although this study did not completely cover all regions in China and there are different medical levels in different regions, this database still represents the most comprehensive database on the diagnosis and treatment of cervical cancer patients in China.

In conclusion, our study found that for stage IIA1 cervical cancer patients, abdominal radical hysterectomy (ARH) with postoperative standard therapy offers better overall survival and disease-free survival outcomes than radio-chemotherapy (R-CT). This finding is consistent with the treatment recommended by the 2021 NCCN guidelines. Of course, the treatment strategy for FIGO2018 stage IIA1 cervical cancer still requires further prospective studies for verification.

DATA AVAILABILITY STATEMENT

The original contributions presented in the study are included in the article/supplementary material. Further inquiries can be directed to the corresponding authors.

ETHICS STATEMENT

The studies involving human participants were reviewed and approved by Institutional Ethics Review Board of the Nanfang Hospital. Written informed consent for participation was not

required for this study in accordance with the national legislation and the institutional requirements.

AUTHOR CONTRIBUTIONS

Conception and design: CC, PL, WL, and HD. Administrative support: CC and PL. Provision of study materials or patients: XZ, ED, QL, QX, RL, YX, JL, PL, and CC. Collection and assembly of data: XC, WL, HD, and MW. Data analysis and interpretation: XC, WL, HD, MW, and XB. Manuscript writing: All authors. All authors contributed to the article and approved the submitted version.

FUNDING

This study received funding from the National Science and Technology Support Program of China (2 Grant No. 014BAI05B03), the National Natural Science Fund of Guangdong (Grant No. 2015A030311024), and the Science and Technology Plan of Guangzhou (Grant No. 158100075).

ACKNOWLEDGMENTS

We thank Min Hao (The Second Hospital of ShanXi Medical University), Bin Ling (China-Japan Friendship Hospital), Lixin Sun and Hongwei Zhao (Shanxi Cancer Hospital), Jihong Liu and Lizhi Liang (Sun Yat-sen University Cancer Center), Lihong Lin and Yu Guo (Anyang Tumor Hospital), Li Wang (The Affiliated Tumor Hospital of Zhengzhou University), Weidong Zhao (Anhui Provincial Cancer Hospital), Yan Ni (The Yuncheng Central Hospital of Shanxi Province), Wentong Liang and Donglin Li (Guizhou Provincial People`s Hospital), Xuemei Zhan and Mingwei Li (Jiangmen Central Hospital), Weifeng Zhang (Ningbo Women & Children's Hospital), Peiyan Du (The Affiliated Cancer Hospital and Institute of Guangzhou Medical University), Ziyu Fang (Liuzhou Workers' Hospital), Rui Yang (Shenzhen Hospital of Peking University), Long Chen (Qingdao Municipal Hospital), Encheng Dai and Ruilei Liu (Linyi People's Hospital), Yuanli He and Mubiao Liu (Zhujiang Hospital, Southern Medical University), Jilong Yao and Zhihua Liu (Shenzhen Maternity & Child Health Hospital), Xueqin Wang (The Fifth Affiliated Hospital of Southern Medical University), Anwei Lu (Maternal and Child Health Hospital of Guiyang Province), Shuangling Jin (Peace Hospital affiliated to Changzhi Medical College), Ben Ma (Guangzhou First People's Hospital), Zhonghai Wang (Shenzhen Nanshan People's Hospital), Lin Zhu (The Second Hospital of Shandong University), Hongxin Pan (The Third Affiliated Hospital of Shenzhen University), Qianyong Zhu (No. 153. Center Hospital of Liberation Army/Hospital No. 988 of the Chinese People's Liberation Army Joint Support Force), Dingyuan Zeng and Zhong Lin (Maternal and Child Health Care Hospital of Liuzhou), Xiaohong Wang (Laiwu People's Hospital/ Jinan City People's Hospital), and Bin Zhu (The Affiliated Yiwu Women and Children Hospital of Hangzhou Medical College) for their contribution during the data collection.

REFERENCES

1. Bhatla N, Berek JS, Fredes MC, Denny LA, Grenman S, Karunaratne K, et al. Revised FIGO Staging for Carcinoma of the Cervix Uteri. *Int J Gynecol Obstet* (2019) 145(1):129–35. doi: 10.1002/ijgo.12749
2. Neerja B, Daisuke A, Nand SD, Rengaswamy S. Cancer of the Cervix Uteri. *Int J Gynaecol Obstet* (2018) 143 Suppl:2. doi: 10.1002/ijgo.12611
3. Abu-Rustum N, Yashar CM, Bean S, Bradley K, Campos SM, Chon HS, et al. D: NCCN Guidelines Insights: Cervical Cancer, Version 1.2020. *J Natl Compr Cancer Netw: JNCCN* (2020) 18(6):660–6. doi: 10.6004/jnccn.2020.0027
4. Liu P, Lin L, Kong Y, Huo Z, Zhu L, Bin X, et al. Comparison of Survival Outcomes Between Radio-Chemotherapy and Radical Hysterectomy With Postoperative Standard Therapy in Patients With Stage IB1 to IIA2 Cervical Cancer: Long-Term Oncological Outcome Analysis in 37 Chinese Hospitals. *BMC Cancer* (2020) 20(1):189. doi: 10.1186/s12885-020-6651-8
5. Zhang W, Chen C, Liu P, Li W, Hao M, Zhao W, et al. Staging Early Cervical Cancer in China: Data From a Multicenter Collaborative. *Int J Gynecol Cancer* (2019) 29:869–73. doi: 10.1136/ijgc-2019-000263
6. Oncology - Cervical Cancer. Investigators at Southern Medical University Describe Findings in Cervical Cancer (Effects of Preoperative Radiotherapy or Chemoradiotherapy On Postoperative Pathological Outcome of Cervical Cancer-From the Large Database of 46,313 Cases of…). *Inf Technol Newsweekly* (2020) 46(1):148–54. doi: 10.1016/j.ejso.2019.09.188
7. Weifeng Z, Chunlin C, Ping L, Weili L, Min H, Weidong Z, et al. Impact of Pelvic MRI in Routine Clinical Practice on Staging of IB1-IIA2 Cervical Cancer. *Cancer Manage Res* (2019) 11:3603–9. doi: 10.2147/CMAR.S197496
8. Chunlin C, Wuliang W, Ping L, Pengfei L, Lu W, Shuangling J, et al. Survival After Abdominal Q-M Type B Versus C2 Radical Hysterectomy for Early-Stage Cervical Cancer. *Cancer Manage Res* (2019) 11:10909–19. doi: 10.2147/CMAR.S220212
9. Yang K, Park W, Huh SJ, Bae D-S, Kim B-G, Lee J-W. Clinical Outcomes in Patients Treated With Radiotherapy After Surgery for Cervical Cancer. *Radiat Oncol J* (2017) 35(1):39–47. doi: 10.3857/roj.2016.01893
10. Mazeron R, Gilmore J, Dumas I, Champoudry J, Goulart J, Vanneste B, et al. Adaptive 3D Image-Guided Brachytherapy: A Strong Argument in the Debate on Systematic Radical Hysterectomy for Locally Advanced Cervical Cancer. *Oncologist* (2013) 18(4):415–22. doi: 10.1634/theoncologist.2012-0367
11. Teh J, Yap SP, Tham I, Sethi VK, Chua EJ, Yeo R, et al. Concurrent Chemoradiotherapy Incorporating High-Dose Rate Brachytherapy for Locally Advanced Cervical Carcinoma: Survival Outcomes, Patterns of Failure, and Prognostic Factors. *Int J Gynecol Cancer* (2010) 20(3):428–33. doi: 10.1111/IGC.0b013e3181d4a0d1
12. Mazeron R, Castelnau-Marchand P, Dumas I, del Campo ER, Kom LK, Martinetti F, et al. Impact of Treatment Time and Dose Escalation on Local Control in Locally Advanced Cervical Cancer Treated by Chemoradiation and Image-Guided Pulsed-Dose Rate Adaptive Brachytherapy. *Radiother Oncol* (2015) 114(2):257–63. doi: 10.1016/j.radonc.2014.11.045
13. Parker K, Gallop-Evans E, Hanna L, Adams M. Five Years' Experience Treating Locally Advanced Cervical Cancer With Concurrent Chemoradiotherapy and High-Dose-Rate Brachytherapy: Results From a Single Institution. *Int J Radiat Oncol Biol Phys* (2009) 74(1):140–6. doi: 10.1016/j.ijrobp.2008.06.1920
14. Chen SW, Liang JA, Hung YC, Yeh LS, Chang WC, Lin WC, et al. Concurrent Weekly Cisplatin Plus External Beam Radiotherapy and High-Dose Rate Brachytherapy for Advanced Cervical Cancer: A Control Cohort Comparison With Radiation Alone on Treatment Outcome and Complications. *Int J Radiat Oncol Biol Phys* (2006) 66(5):1370–7. doi: 10.1016/j.ijrobp.2006.07.004

15. Bansal N, Herzog TJ, Shaw RE, Burke WM, Deutsch I, Wright JD. Primary Therapy for Early-Stage Cervical Cancer: Radical Hysterectomy vs Radiation. *Am J Obstet Gynecol* (2009) 201(5):485.e1-9. doi: 10.1016/j.ajog.2009.06.015
16. Rungruang B, Courtney-Brooks M, Beriwal S, Zorn KK, Richard SD, Olawaiye AB, et al. Surgery Versus Radiation Therapy for Stage IB2 Cervical Carcinoma: A Population-Based Analysis. *Int J Gynecol Cancer* (2012) 22 (3):484–9. doi: 10.1097/IGC.0b013e31823f890f
17. Landoni F, Maneo A, Colombo A, Placa F, Milani R, Perego P, et al. Randomised Study of Radical Surgery Versus Radiotherapy for Stage Ib-IIa Cervical Cancer. *Lancet* (1997) 350(9077). doi: 10.1016/S0140-6736(97)02250-2
18. Fabio L, Alessandro C, Rodolfo M, Franco P, Vanna Z, Costantino M. Randomized Study Between Radical Surgery and Radiotherapy for the Treatment of Stage IB-IIA Cervical Cancer: 20-Year Update. *J Gynecol Oncol* (2017) 28(3). doi: 10.3802/jgo.2017.28.e34
19. Yamashita H, Nakagawa K, Tago M, Shiraishi K, Nakamura N, Ohtomo K, et al. Comparison Between Conventional Surgery and Radiotherapy for FIGO Stage I–II Cervical Carcinoma: A Retrospective Japanese Study. *Gynecol Oncol* (2005) 97(3). doi: 10.1016/j.ygyno.2005.03.017
20. Wu S-G, Zhang W-W, He Z-Y, Sun J-Y, Wang Y, Zhou J. Comparison of Survival Outcomes Between Radical Hysterectomy and Definitive Radiochemotherapy in Stage IB1 and IIA1 Cervical Cancer. *Cancer Manage Res* (2017) 2017(default). doi: 10.2147/CMAR.S145926

Conflict of Interest: The authors declare that the research was conducted in the absence of any commercial or financial relationships that could be construed as a potential conflict of interest.

Publisher's Note: All claims expressed in this article are solely those of the authors and do not necessarily represent those of their affiliated organizations, or those of the publisher, the editors and the reviewers. Any product that may be evaluated in this article, or claim that may be made by its manufacturer, is not guaranteed or endorsed by the publisher.

Copyright © 2022 Chen, Liang, Duan, Wu, Zhan, Dai, Lv, Xie, Liu, Xu, Bin, Lang, Liu and Chen. This is an open-access article distributed under the terms of the Creative Commons Attribution License (CC BY). The use, distribution or reproduction in other forums is permitted, provided the original author(s) and the copyright owner(s) are credited and that the original publication in this journal is cited, in accordance with accepted academic practice. No use, distribution or reproduction is permitted which does not comply with these terms.

frontiers | Frontiers in Oncology

ORIGINAL RESEARCH
published: 28 April 2022
doi: 10.3389/fonc.2022.714663

Hypermethylated *CDO1* and *ZNF454* in Cytological Specimens as Screening Biomarkers for Endometrial Cancer

Lei Wang[1†], Lanlan Dong[2†], Jun Xu[2], Lin Guo[1,3], Yiran Wang[1], Kangkang Wan[2], Wei Jing[1,4], Lanbo Zhao[1], Xue Feng[1], Kailu Zhang[1], Miao Guo[1], Yuliang Zou[1], Lianglu Zhang[2,5] and Qiling Li[1*]*

[1] Department of Obstetrics and Gynecology, The First Affiliated Hospital of Xi'an Jiaotong University, Xi'an, China, [2] Wuhan ammunition Life-Tech Co., Ltd., Wuhan, China, [3] Department of Obstetrics and Gynecology, Tangdu Hospital, the Fourth Military Medical University, Xi'an, China, [4] Department of Gynecologic Oncology, Shaanxi Provincial Cancer Hospital, Xi'an, China, [5] State Key Laboratory of Virology, Department of Biochemistry and Molecular Biology, College of Life Sciences, Wuhan University, Wuhan, China

OPEN ACCESS

Edited by:
Jian-Jun Wei,
Northwestern University,
United States

Reviewed by:
Antonio Mollo,
University of Salerno, Italy
David Atallah,
Saint Joseph University, Lebanon

***Correspondence:**
Lianglu Zhang
zhangll@whammunition.com
Qiling Li
liqiling@mail.xjtu.edu.cn

[†]These authors have contributed equally to this work

Specialty section:
This article was submitted to Gynecological Oncology, a section of the journal Frontiers in Oncology

Received: 25 May 2021
Accepted: 28 March 2022
Published: 28 April 2022

Citation:
Wang L, Dong L, Xu J, Guo L, Wang Y, Wan K, Jing W, Zhao L, Feng X, Zhang K, Guo M, Zou Y, Zhang L and Li Q (2022) Hypermethylated CDO1 and ZNF454 in Cytological Specimens as Screening Biomarkers for Endometrial Cancer. Front. Oncol. 12:714663. doi: 10.3389/fonc.2022.714663

We aimed to estimate the diagnostic value of DNA methylation levels in cytological samples of endometrial cancer (EC) and atypical hyperplasia (AH). Two hypermethylated genes, namely, cysteine dioxygenase type 1 (*CDO1*) and zinc finger protein 454 (*ZNF454*), in patients with EC were identified from The Cancer Genome Atlas database. In 103 endometrial histological specimens (the training set), the methylation levels of candidate genes were verified by quantitative methylation-specific polymerase chain reaction (qMSP). The methylation levels of another 120 cytological specimens (the testing set) were evaluated. Sensitivity (Se), specificity (Sp), accuracy, and area under the curve (AUC) were determined, with diagnosis verified by histopathological results. *CDO1* and *ZNF454* verified hypermethylation in histological specimens of patients with EC and AH compared with those with benign and normal endometrium ($P < 0.001$). In cytological specimens, hypermethylated *CDO1* showed 86.36% Se and 90.79% Sp with the cutoff value of 6.0 to distinguish between malignant and benign groups; *ZNF454* showed 79.55% Se and 93.42% Sp with the cutoff value of 7.1. When the two genes were combined, Se increased to 90.91% and Sp was 86.84%. AUC reached 0.931 (95% CI: 0.885–0.976). The diagnostic accuracy with cytology had no significant difference with endometrial tissue ($P = 0.847$ for *CDO1*, $P = 0.108$ for *ZNF454*, and $P = 0.665$ for their combination). Hypermethylated *CDO1* and *ZNF454* in endometrial cytology showed high Se, Sp, and AUC to detect EC and AH. Methylation analysis of endometrial cytology is promising biomarker for the screening of EC and AH.

Keywords: cysteine dioxygenase type 1 (*CDO1*), endometrial cancer (EC), endometrial cytology test (ECT), zinc finger protein 454 (*ZNF454*), DNA methylation, screening, cytology

INTRODUCTION

Among female reproductive tract cancers, endometrial cancer (EC) is the most prevalent in developed countries (1). The 5-year survival rate of early diagnosed cases (stage I and stage II) ranges from approximately 96% to 74% (2, 3). However, approximately 15% of ECs are diagnosed in stages III–IV with a very poor prognosis (4). The risk of developing EC from endometrial hyperplasia without atypia is around 3% and increases up to 23% in endometrial atypical hyperplasia (AH) (5). It is very important to screen AH and early EC in women at high risks (6).

There are no highly sensitive and standardized screening methods for EC (7). Transvaginal ultrasound is a non-invasive diagnostic test but the cutoff value for endometrial thickness remains unclear. With a low specificity (Sp) of 24.3%–74%, transvaginal ultrasound cannot reliably identify malignant lesions (8, 9). Although traditional dilation and curettage (D&C) is relatively effective and hysteroscopic biopsy can be performed to make a definite diagnosis, these are invasive procedures to obtain endometrial tissues (10, 11). Hysteroscopic biopsy or D&C collects limited amount of endometrial tissue, which results in difficulty and disagreement for pathological diagnosis (12, 13). In addition, with a high false positive rate, DNA quantitative cytology test or sequencing of circulating tumor DNA had not been optimized enough in a large-scale screening either (14, 15). Limitations also exist in the endometrial cytology test (ECT) on early screening and in the diagnosis of EC, such as a lack of enough cytopathologists and a unified diagnostic standard (16).

More and more studies on epigenetics reveal a close association between DNA methylation and the progression of cancer. Some methylation biomarkers have been applied for early detection, diagnosis, and prognosis (17). They could differentiate cancerous tissue from normal tissue with >95% accuracy in common cancers (18). DNA methylation of cytological specimens, as a minimally or non-invasive biomarker, is explored extensively in solid tumors, such as cervical cancer using liquid-based cervical scrapes, urothelial tract carcinoma using urinary samples, and lung cancer using bronchoalveolar lavage fluid samples (19–21). Compared with the benign endometrium (BE), tissue specimens of EC and precancerous lesions show significant differences in methylation levels (22–24). There is an urgent need to find a comprehensive panel of methylation biomarkers for more minimally invasive, accurate, and economical screening methods of EC.

In the present study, we aimed to propose a novel method for the screening of EC. Two hypermethylated candidate genes, namely, cysteine dioxygenase type 1 (*CDO1*) and zinc finger protein 454 (*ZNF454*), were selected in patients with EC from The Cancer Genome Atlas (TCGA) database and literature. The sensitivity (Se) and Sp of the two genes were examined on endometrial cytology. The area under the curve (AUC) of receiver operating characteristic (ROC) of methylation assays were also detected to estimate the diagnostic value for EC and AH.

Abbreviations: AH, atypical hyperplasia; AUC, area under the curve; BE, benign endometrium; *CDO1*, cysteine dioxygenase type 1; Ct, cycle threshold; D&C, dilation and curettage; EC, endometrial cancer; ECT, endometrial cytology test; PCR, polymerase chain reaction; qMSP, quantitative methylation-specific polymerase chain reaction; ROC, receiver operating characteristic; Se, sensitivity; Sp, specificity; TCGA, The Cancer Genome Atlas; TSS, transcriptional start site; *ZNF454*, zinc finger protein 454.

MATERIALS AND METHODS

Identification of Candidate Biomarkers

To identify candidate genes, the DNA methylation data from a total of 431 EC tissue samples and 46 corresponding adjacent normal endometrial samples were obtained from TCGA database (http://cancergenome.nih.gov/), along with the corresponding clinical information (**Supplementary Table 1**). The methylation score for each CpG in genome-wide identification and validation was represented as a β-value and normalized, and the details were described previously (25). The β-value indicated a level of DNA methylation ranging from 0 (unmethylated) to 1 (fully methylated). Different cutoff values were defined as hypomethylation (β-value: 0.3–0.25) and hypermethylation (β-value: 0.7–0.5). The sex chromosome probes were removed, and the remaining CpG sites were analyzed in 22 pairs of chromosomes. Only the top 5% of genes with differences in hypermethylation from the mean β-values of tumor (β_T) minus the normal values (β_N) and Δβ (β_T-β_N) ≥ 0.3 were selected. We focused on probes of CpG sites located closest (≤2 kb) to the upstream of the transcriptional start site (TSS) of the coding genes. If several CpG sites, we would take the average value as the methylation value of the gene. Finally, we selected two hypermethylated candidates with ≥5 remaining CpG sites in the coding gene based on relevant literature, for further validation.

Then, the two genes were further confirmed hypermethylated in EC by first-generation sequencing using randomly collected specimens of cancerous and non-cancerous tissues after hysterectomy. The process of recruitment was the same as the patients in the training set.

Recruitment of Histological and Cytological Specimens

According to the method to calculate sample size in the diagnosis experiment (26) and the Se and Sp of candidate genes in relevant studies (22, 27, 28), a minimum of 41 cases in the malignant group and 57 cases in the benign group were required for our study (Se was taken as 0.88 and Sp was taken as 0.82 to predict results).

From June 2019 to January 2020, women with certain diagnosis, including EC, AH, or benign diseases, such as uterine myoma, adenomyosis, and uterine prolapse, underwent total hysterectomy in The First Affiliated Hospital of Xi'an Jiaotong University. Their endometrial tissues specimens obtained from surgical resections were formalin-fixed and paraffin-embedded, as a training set for histological DNA

methylation analysis. The histopathological diagnosis using hematoxylin and eosin staining was confirmed by two pathologists as the reference standard. Inclusion criteria were as follows: 1) patients were at 25–90 years old and 2) patients without systemic diseases or other malignant tumors except for EC. Exclusion criteria were as follows: clinical information was incomplete or non-traceable.

As a testing set, endometrial cytological samples were prospectively collected from patients in The First Affiliated Hospital of Xi'an Jiaotong University, Tangdu Hospital of the Fourth Military Medical University, and Shaanxi Provincial Cancer Hospital with Li brushes (Xi'an Meijiajia Medical Co., 20152660054) before hysterectomy or D&C. These patients were suspected of having EC, AH, or benign diseases. Specimens were sampled by professional gynecologists after standard training. The procedure of endometrial sampling using Li Brush was shown in our previous study (16). First, the patients were placed in the lithotomy position. After conventional perineal and vaginal disinfection (iodine), the uterine cervix was exposed by a sterile speculum and the uterine depth was detected with uterine probe. Second, the sampler was put into the fundus of uterus after the brush head was hidden in the drivepipe. The drivepipe was drawn out 5 mm to show the brush, and the handle was rotated 5–10 complete circles to gather cells of the uterine corpus. Third, the drivepipe was advanced 3 mm and the handle was again rotated to gather cells from the uterine fundus. Last, the brush was removed from uterine cavity after protecting the brush head under the casing. When sampling was complete, endometrial cells were collected in the preservation solution for DNA methylation test. Our previous study showed that cytology by Li brush had a lower insufficient sample rate than did D&C (29). All of the patients were pathologically diagnosed by their tissues or cells using hematoxylin and eosin staining. The pathological results were defined as gold standard and demographic data were well documented. Inclusion criteria were the same as described above in the training set. Exclusion criteria were as follows: 1) insufficient quantity of samples for methylation test and 2) clinical information was incomplete or non-traceable.

This article was approved by the Ethics Committee of The First Affiliated Hospital of Xi'an Jiaotong University (XJTU1AF2015LSL-007). Informed consent was obtained from every participant in this study. All participants were recruited randomly.

The test criteria included Se, Sp, and accuracy. Se was defined as the probability that a patient who was diagnosed as positive (EC and AH) by the gold standard showed a positive methylation result. Sp was defined as the probability that a person who was diagnosed as negative (BE) by the gold standard had a negative result for methylation test. Accuracy was the ratio when the methylation result and cytopathologic or histopathologic diagnoses were both positive or both negative.

Quantitative Methylation-Specific Polymerase Chain Reaction

Genomic DNA was extracted from paraffin-embedded endometrial tissue and cells specimens (from hysterectomy, D&C, and cytology) using the TIANamp Genomic DNA Kit (TIANGEN Biotech Co., DP304, Beijing, China). According to the manufacturer's instructions, tissues were prepared in a cell suspension and digested with Proteinase K at 56°C until being dissolved. The genomic DNA was dissolved in nuclease-free water and bisulfite converted using the DNA Bisulfite Conversion Kit (TIANGEN Biotech Co., DP215, Beijing, China). Two pairs of primers were designed, allowing separate amplification of populations representing methylated and unmethylated DNA fragments. To confirm the quality and quantity of bisulfite-modified DNA, ACTB was used to normalize the DNA input, thus allowing unbiased amplification. Primers to measure the amount of the non-CpG region of ACTB in each methylation-independent assay were designed as controls. These primers were designed by Oligo 7.0 Primer Analysis software (Molecular Biology Insights, Inc., Colorado Springs, CO, USA). Polymerase chain reaction (PCR) products were amplified with the LightCycler 480 SYBR Green I Master (Roche, Indianapolis, IN, USA) and performed using ABI7500 (Applied Biosystems, Thermo Fisher Scientific Corp., Waltham, MA, USA). A 25 μl of reaction contained 5 μl of bisulfite-converted DNA, 250 nmol/L each primer, and 10 μl of Master Mix. The reactions were conducted under the following thermal profiles: 95°C for 10 min, 45 cycles consisted of denaturing at 95°C for 20 s, annealing at 60°C for 30 s. The melt curve data were generated by increasing the temperature from 60°C to 90°C and recording fluorescence. All specimens conducted triplicate testing in each gene.

The cycle threshold (Ct)–values of the two PCR reactions were compared to determine the methylation level of the site. The lower the Ct-values, the higher the gene methylation status. The ACTB was used as an internal reference gene by amplifying non-CpG sequences. The DNA methylation level was estimated as the ΔCt by using the formula: Ct (target gene) − Ct (ACTB). The distribution of the dot plots represents the methylation levels, in terms of change in Ct (ΔCt-value) of each candidate gene. We generated the best cutoff values of ΔCt from the tissues or cells to distinguish between benign and cancerous subjects. Methylation was considered as positive when ΔCt-value ≤ the cutoff value (at least two replicates).

Statistical Analysis

Patients and tumor characteristics were tabulated. Normality test was used to determine whether the variance of the population was equal by Kolmogorov–Smirnov test, and age differences between groups as continuous variables were compared using Student's *t*-test (two-tailed). The significant differences of methylated CpG sites between cancerous and benign specimens were analyzed using the Mann–Whitney *U*-test. In addition, the differences between EC, AH, and BE were analyzed using the Kruskal–Wallis test ($P < 0.001$). ROC curves were generated to determine the ΔCt cutoff values of candidate gene methylation. The Se, Sp, and AUC of each gene, or genetic combination, were calculated. The differences of the accuracy between the training set and the testing set were considered significant if the *P*-value of Chi-squared test was < 0.05. Data were analyzed using SPSS version 20.0 software (SPSS Inc., Chicago, IL, USA).

RESULTS

Candidate Biomarkers

The data that support the findings of this study are available in TCGA database. As described in the above method, a total of 75 candidate biomarkers in the top 5% were selected, of which 17 were upstream genes. Six genes with ≥5 remaining CpG sites were further analyzed and two of them, namely, *CDO1* and *ZNF454*, were picked up by referring to relevant references (22, 27, 28). Their methylation data were showed in **Supplementary Table 2**, and the methylation levels, between cancerous and normal tissues, showed a significant difference ($P < 0.001$) (**Figure 1A**). ROC curve was determined on the basis of TCGA database (**Figure 1B**). To explore further the clinical relevance of DNA methylation level, we made comparisons between different age groups, stages, pathologic parameters, and grades. We found that methylation level of *CDO1* or *ZNF454* had no statistical difference between women aged ≤60 and >60 (**Figure 2A**) and between different stages (**Figure 2B**). Methylation status of *CDO1* had no statistical difference between different pathological types. However, *ZNF454* had a significant difference between endometrioid carcinoma and serous carcinoma ($P < 0.001$) and between serous carcinoma and mixed carcinoma ($P < 0.05$) (**Figure 2C**). In addition, methylation level of *CDO1* or *ZNF454* had statistical difference between different grades ($P < 0.01$) (**Figure 2D**).

Next, the Se, Sp, and accuracy of these two genes were calculated in the initial verification using first-generation sequencing (Sanger sequencing results were partially shown in **Supplementary Figures 1, 2**). Thirty-eight individual endometrial tissues were randomly collected from surgical resections in The First Affiliated Hospital of Xi'an Jiaotong University, including 25 cancerous and 13 normal tissues (**Table 1**). Se and Sp levels of *CDO1* were 92.00% and 92.31%, respectively. Se and Sp levels of *ZNF454* were 88.00% and 100.00%, respectively. In addition, their diagnostic accuracy levels were both above 92%. Therefore, the two genes, namely, *CDO1* and *ZNF454*, were determined for follow-up verification in training set.

Verification of Candidate Genes in Histological Specimens (Training Set)

A total of 103 specimens (21 EC, 20 AH, 41 BE, and 21 adjacent benign endometrial tissues) were included in the training set. Demographics related to the clinical samples were shown in **Supplementary Table 3**. There were 20 endometrioid carcinoma and one mucinous carcinoma among 21 EC. To assess methylation differences between malignant and BE, EC and AH were included in the malignant group, with a total of 41 patients. They both required early treatment and management in clinical. From the perspective of screening, we did not distinguish EC and AH respectively. BE and adjacent benign endometrial tissues were included in benign group, with a total of 62 patients. Women in malignant group were aged from 28 to 66 years (47.10 ± 8.22 years) and those in benign group were aged from 30 to 66 years (49.63 ± 7.54 years). Age was not significantly different between the two groups (P = 0.116).

Primer sequences for qMSP analysis were designed as **Supplementary Table 4**. To determine the amplification efficiency of primers, we used methylated primers to amplify the methylated or the unmethylated templates. As shown in **Supplementary Figure 3A**, the template was well amplified when the concentration of methylated template was only 1×10^2 copies/μl, whereas the unmethylated template had very low amplification even the concentration of unmethylated template reached 1×10^5 copies/μl. **Supplementary Figure 3B** shows the

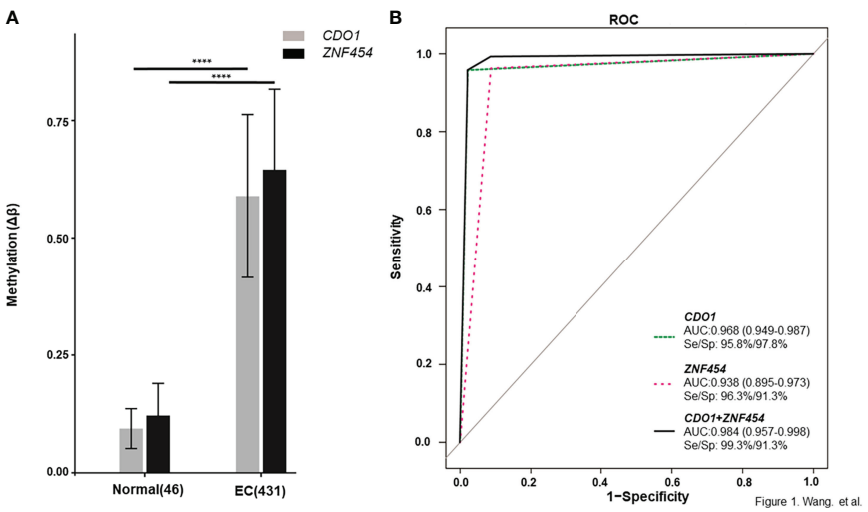


FIGURE 1 | DNA methylation levels of candidate genes from TCGA database. DNA methylation levels are displayed as Δβ-values for each candidate gene. **(A)** *CDO1* and *ZNF454* methylation levels between cancerous and normal tissues. **(B)** The area under the receiver operating characteristic curve (AUC-ROC) for the DNA methylation status of *CDO1* and *ZNF454*. ****$P < 0.0001$.

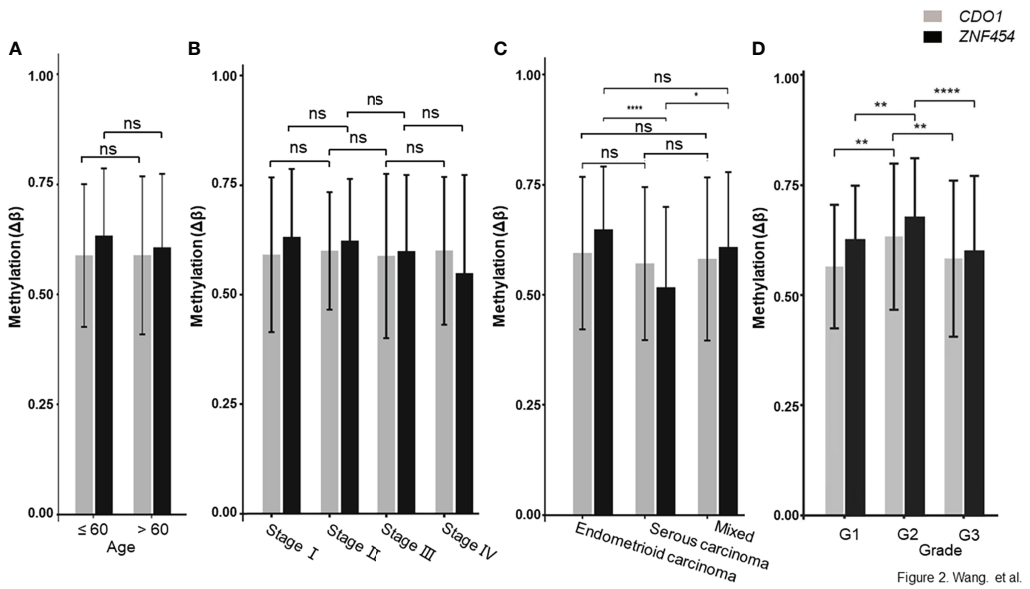


FIGURE 2 | DNA methylation level between different age groups, stages and pathologic types. **(A)** *CDO1 and ZNF454* methylation levels between women aged ≤60 and >60. **(B)** *CDO1* and *ZNF454* methylation levels between different stages. **(C)** *CDO1* and *ZNF454* methylation levels between different pathological types. **(D)** *CDO1* and *ZNF454* methylation levels between different grades. ****$P < 0.0001$; **$P < 0.01$; *$P < 0.05$; ns, no significance.

representative curves for 100% methylated DNA and fully unmethylated DNA along with different dilution of methylated and unmethylated DNA. The melting temperature (Tm) of the unmethylated template was lower than that of the methylated template in the melt curve (**Supplementary Figure 3C**). At 86.61°C, the methylated primers specifically amplified the methylated template.

As shown in **Figures 3A, B**, the mean methylation levels of *CDO1* and *ZNF454* in EC, AH, and BE were significantly different ($P < 0.001$). By using ROC curve and AUC analysis methods, the optimal cutoff values of ΔCt of *CDO1/ZNF454* were 9.8/11.4 when the Youden index (Se + Sp − 1) reached the maximum in the ROC curves. At the thresholds, in the malignant group, 33 cases of *CDO1* methylation were positive, and eight cases were negative. In the benign group, four cases were positive and 58 cases were negative. Thus, the diagnostic Se and Sp were 80.49% and 93.55%, respectively. AUC was 0.910 (95% CI: 0.851–0.968) (**Figure 3C**). Whereas 32 cases of *ZNF454* methylation were positive and nine cases were negative in the malignant group, 11 were positive and 51 were negative in the benign group. The Se and Sp levels of *ZNF454* were 78.05% and 82.26%, respectively. AUC was 0.838 (95% CI: 0.750–0.925) (**Figure 3D**). When the two genes were combined, the Se and Sp levels were 92.68% and 82.26%, respectively. AUC was 0.911 (95% CI: 0.854–0.968) (**Figure 3E**).

TABLE 1 | Se, Sp, and accuracy of DNA methylation of *CDO1* and *ZNF454* using first-generation sequencing.

Gene	True positive	False positive	Se (%)[a]	Sp (%)[b]	Accuracy (%)
CDO1	23/25	1/13	92.00	92.31	92.11
ZNF454	22/25	0/13	88.00	100.00	92.11

[a]*Se, sensitivity.*
[b]*Sp, specificity.*

Methylation Assays of Candidate Genes in Cytological Specimens (Testing Set)

A total of 174 cytological specimens were collected, of which 25 cases that did not have a sufficient number of endometrial cells for the methylation test and 29 cases that lacked detailed pathological information were successively excluded. The degree of satisfaction of sampling for the methylation test was 85.63% (149 of 174) and 120 cytological specimens were left in an independent testing set (42 EC, 2 AH, and 76 BE). Their demographics were shown in **Supplementary Table 3**, and one of the patients did not undergo hysterectomy for financial reasons, so her stage of EC was unknown. Among 42 EC, there were 38 endometrioid carcinoma, two mucinous carcinoma, one serous carcinoma, and one mixed serous and endometrioid carcinoma. Women in the malignant group (EC and AH) were aged from 28 to 74 years (51.48 ± 9.67 years), and those in the benign group were aged from 23 to 77 years (48.82 ± 10.11 years). Age was not significantly different between the two groups ($P = 0.161$).

As shown in **Figures 4A, B**, *CDO1* and *ZNF454* methylation levels were significantly different among EC, AH, and BE ($P < 0.001$). When the Youden index reached the maximum in the ROC curves, the cutoff ΔCt-values of *CDO1/ZNF454* were 6.0/7.1. Thus, in the malignant group, 38 cases of *CDO1* methylation were positive, and six cases were negative. In the benign group, seven cases were positive, and 69 cases were negative. Se level was 86.36%, and Sp level was 90.79%. AUC was 0.911 (95% CI:

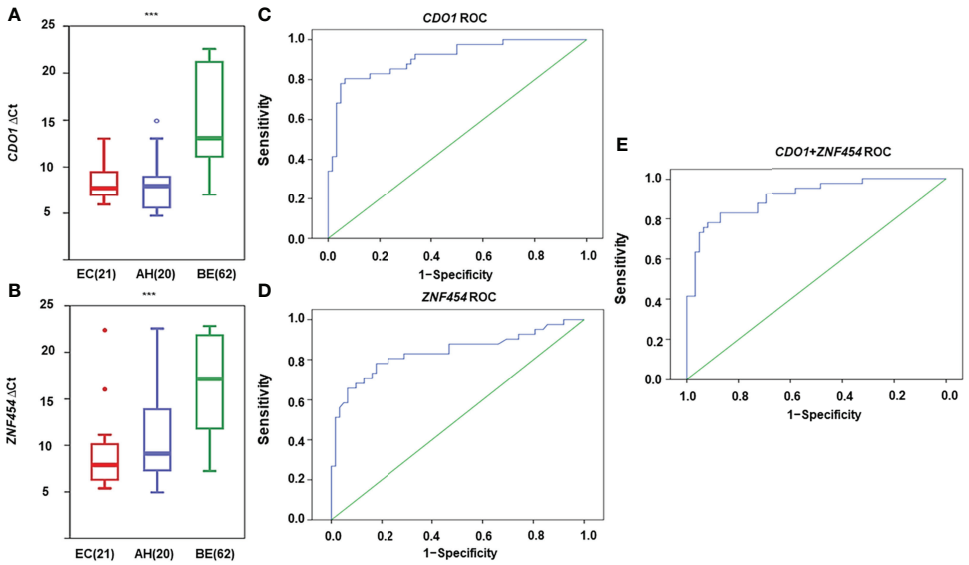


FIGURE 3 | DNA methylation levels for candidate genes detected by quantitative methylation-specific polymerase chain reaction (qMSP) in histological specimens. DNA methylation levels are displayed as the difference in cycle threshold (ΔCt)–values for **(A)** *CDO1* and **(B)** *ZNF454*. Horizontal bars in the middle indicate the average methylation levels. The area under the receiver operating characteristic curve (AUC-ROC) for the DNA methylation status of **(C)** *CDO1*, **(D)** *ZNF454*, and **(E)** combination of the two genes. ***$P < 0.001$.

0.850–0.973) (**Figure 4C**). Thirty-five cases of *ZNF454* methylation were positive, and nine cases were negative in the malignant group. Five cases of *ZNF454* methylation were positive, and 71 cases were negative in the benign group. Se and Sp levels were 79.55% and 93.42%, respectively. AUC was 0.905 (95% CI: 0.848–0.963) (**Figure 4D**). When the two genes were combined, Se and Sp levels were 90.91% and 86.84%, respectively. AUC increased to 0.931 (95% CI: 0.885–0.976) (**Figure 4E**). Compared with the indicators of individual genes, the Se and AUC were best but Sp was slightly lower.

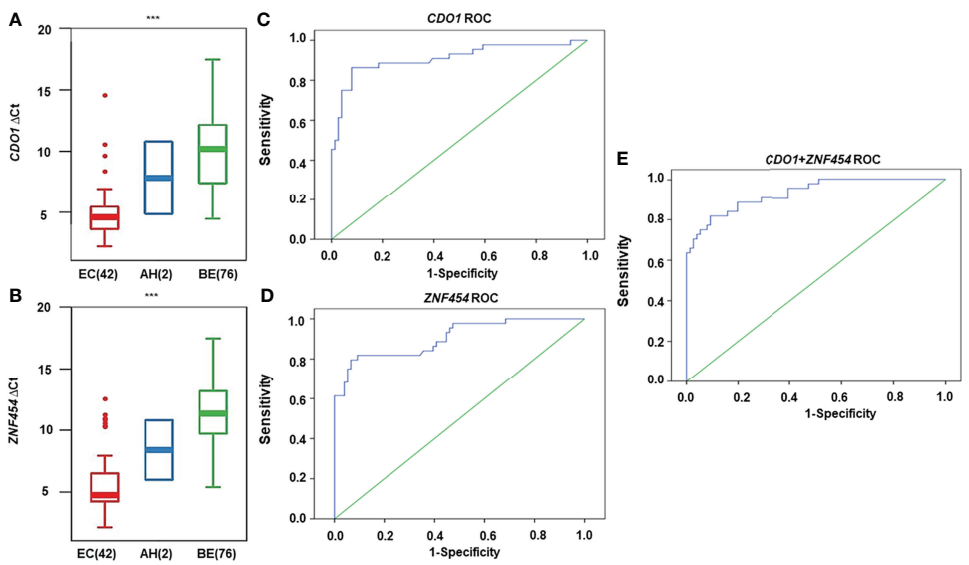


FIGURE 4 | DNA methylation levels for candidate genes detected by quantitative methylation-specific polymerase chain reaction (qMSP) in cytological specimens. DNA methylation levels are displayed as the difference in cycle threshold (ΔCt)–values for **(A)** *CDO1* and **(B)** *ZNF454*. Horizontal bars in the middle indicate the average methylation levels. The area under the receiver operating characteristic curve (AUC-ROC) for the DNA methylation status of **(C)** *CDO1*, **(D)** *ZNF454*, and **(E)** combination of the two genes. ***$P < 0.001$.

Comparison of the Accuracy of Histological and Cytological Methylation

The diagnostic accuracy of the genes was calculated in the detection of EC and AH from the training set and the testing set. The diagnostic accuracy of *CDO1*/*ZNF454* methylation had no statistical difference between cytological specimens and histological specimens (P = 0.847/P = 0.108). When the two genes were combined, the accuracy had no significant difference (P = 0.665) (**Table 2**). The diagnostic accuracy of the candidate genes methylation in cytological specimens was not worse than that in the histological samples.

The flow chart of this study is shown in **Figure 5**.

DISCUSSION

We proved a relatively high Se, Sp, and AUC of *CDO1* or *ZNF454* methylation test in the cytological detection of EC and AH. When the two candidate genes were combined, clinical performance was better because of lower missed diagnosed rate (1 − Se) and higher AUC. Diagnostic accuracy in cytological specimens had no significant difference compared with that in histological ones. It was of great help in scenarios of limited availability or quality of tissue.

Compared with relevant studies conducted by Wentzensen's team (30, 31), our research showed some advantages. First, our analysis demonstrated the Se and Sp in detail, with higher AUCs and a larger sample size. A total of 120 cytological specimens were collected for the diagnostic test and the methylation biomarker panel obtained an AUC of 0.931, with a 90.91% Se and an 86.84% Sp. Although Wentzensen et al. estimated an Sp of only > 50% and a summary AUC of 0.85 in 38 EC and 37 BE specimens, they found that among women with carcinoma, median methylation levels of most candidate genes in frozen carcinoma tissues and cell specimens seemed to be similar, but the *P*-value was not calculated (31). In their follow-up study, the methylation levels of candidate genes were compared in 38 EC and 28 BE. The best AUC for a single gene was 0.90. However, the Se and Sp were not calculated (30). A systematic review and meta-analysis including 22 studies showed that the pooled Se and Sp levels of DNA methylation in sporadic EC were 93% and 48%, respectively, and the AUC of summary ROC was 0.8834 (32). Apparently, we seem to have a better Sp and AUC using only two candidate genes. Second, *CDO1* and *ZNF454* were identified from the TCGA database and validated through a rigorous selection process, as described in Materials and Methods. *CDO1*, as a tumor suppressor gene, was also reported hypermethylated in cervical scrapings of patients with EC by Huang et al. (22, 33). *ZNF454* may be a tumor-suppressor gene with potential use as a prognostic indicator (27), but its methylation site was not previously reported in EC. Our study found that *ZNF454*, with relatively high Se, Sp, and AUC, was also a promising biomarker on EC screening. Although Wentzensen et al. investigated the diagnostic potential of seven genes (*ADCYAP1*, *ASCL2*, *CDH13*, *HS3ST2*, *HTR1B*, *MME*, and *NPY*), they identified hypermethylated in EC (31) and five other genes (*GTF2A1*, *HAAO*, *HOXA9*, *HSP2A*, and *RASSF1*) observed by other research studies (30). Third, endometrial sampling was performed by Li brushes in our study but Tao brushes (Cook Medical, Bloomington, IN, USA) in research studies of Wentzensen et al. Although our comparative analysis showed a high diagnostic accordance between the Li brush and Tao brush in evaluating EC and AH, Tao brush is more expensive and rarely available in China, which increases the screening cost (29). Considering social and economic benefits, Li brush may be a better choice in the screening program.

Our research provides a minimally invasive method for EC and AH screening. Considering the low EC prevalence, traditional invasive D&C to obtain endometrial tissue is redundant and unnecessary procedure in screening of large population (34). For high-risk population, such as those with Lynch syndrome and obesity (6), endometrial brush sampling brings less discomfort than invasive D&C (16). Cytological DNA methylation test reduces the workload of pathologists, which is of great value especially in countries with a shortage of cytopathologists. As a preliminary screening test, when its positive result occurs, gynecologists perform a further biopsy for a definite diagnosis.

Some studies proposed other minimally invasive and indirect methods to screen EC through the DNA methylation analysis, such as cervical scrapings, intravaginal tampons, and urine fractions (22, 30, 33, 35–37). Huang et al. revealed a Se level of between 87.0% and 91.8% and a Sp level of between 80.0% and 95.5% for EC detection by a three-gene panel in cervical scrapes (22, 33). Chang et al. reported a Se level of 83%–90% and a Sp level of 69%–88% using cervical scrapings in the detection of EC (36). In studies using intravaginal tampons, although Sp reached 100%, Se was only 37%–40%. The maximum AUC to distinguish malignant endometrial tumors was only 0.82 (35). Considering that only a tiny number of abnormal cells exfoliated from the uterine cavity could be captured in the early stage of EC, the detection with cervical scrapings during the Papanicolaou test or vaginal pool samples in tampons was opportunistic (38). DNA methylation analysis in urine provided an alternative for the

TABLE 2 | Comparison of gene methylation level on diagnostic accuracy.

	Accuracy (*CDO1*) (%)	Accuracy (*ZNF454*) (%)	Accuracy (*CDO1* + *ZNF454*) (%)
Histological (n = 103)	88.35	80.58	86.41
Cytological (n = 120)	89.17	88.33	88.33
χ^2	0.037	2.577	0.187
p	0.847	0.108	0.665

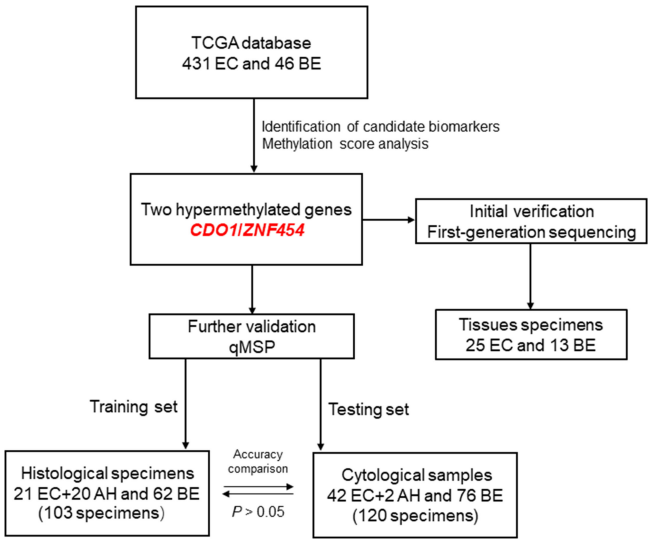


FIGURE 5 | The flow chart of this study. EC, endometrial cancer; BE, benign endometrium; AH, atypical hyperplasia; qMSP, quantitative methylation-specific polymerase chain reaction.

detection of EC. In all urine fractions (full void, sediment, and supernatant), three DNA methylation markers (*GHSR*, *SST*, and *ZIC1*) showed increased methylation levels in patients with EC as compared to controls, with AUC values ranging from 0.86 to 0.95 (37). The results seemed to be encouraging, but more exploration was needed. In our study, endometrial cells were collected directly from the uterine cavity, which achieved rather satisfactory results.

Despite some encouraging results, our research still had several limitations. We had not stratified our analysis based on the body mass index, categories of pathology, grades, or clinical developments (AH to EC). These factors could have been associated with distinct DNA methylation signatures (24, 39, 40). **Figures 2C, D** in the current study also suggested that DNA methylation status might be related to histopathology. As an extension of the current work, further validation in stratified, population-based studies should be conducted to determine more applicable cutoff values of DNA methylation of better biomarkers.

CONCLUSION

We conducted a series of identification and verification work to find DNA methylated biomarkers associated with abnormal endometrium (including EC and AH). As a preliminary screening test, *CDO1* and *ZNF454* methylation analysis in cytological specimens improved the screening procedures of EC and AH. It provided a valuable and minimally invasive method to distinguish women with EC and AH from the vast majority of women without neoplastic lesions.

DATA AVAILABILITY STATEMENT

The original contributions presented in the study are included in the article/**Supplementary Material**. Further inquiries can be directed to the corresponding authors.

ETHICS STATEMENT

The studies involving human participants were reviewed and approved by the Ethics Committee of the First Affiliated Hospital of Xi'an Jiaotong University. The patients/participants provided their written informed consent to participate in this study.

AUTHOR CONTRIBUTIONS

Conceptualization: LW, LLZ, and QL. Data curation, formal analysis, investigation, methodology, and visualization: LW, LD, JX, LG, YW, KW, WJ, LBZ, XF, KZ, MG and YZ. Project administration and resources: LW, LD, LG, YW, LBZ, and QL. Supervision and validation: LW, LD, JX, KW, and QL. Writing—original draft: LW, LD, and QL. Writing—review and editing: All authors. All authors contributed to the article and approved the submitted version.

FUNDING

This study was funded by the Clinical Research Award of The First Affiliated Hospital of Xi'an Jiaotong University (No.

XJTU1AF-CRF-2019-002) and the Key Research and Development Project of Shaanxi Provincial Science and Technology Department (No. 2019QYPY-138). The sponsors have no involvement in study design, data collection, analysis, and interpretation or in writing of the manuscript.

SUPPLEMENTARY MATERIAL

The Supplementary Material for this article can be found online at: https://www.frontiersin.org/articles/10.3389/fonc.2022.714663/full#supplementary-material

REFERENCES

1. Faizan U, Muppidi V. *Uterine Cancer*. Treasure Island, FL: StatPearls (2021).
2. Ortoft G, Hogdall C, Hansen ES, Dueholm M. Survival and Recurrence in Stage II Endometrial Cancers in Relation to Uterine Risk Stratification After Introduction of Lymph Node Resection and Omission of Postoperative Radiotherapy: A Danish Gynecological Cancer Group Study. *J Gynecol Oncol* (2020) 31:e22. doi: 10.3802/jgo.2020.31.e22
3. Miller KD, Nogueira L, Mariotto AB, Rowland JH, Yabroff KR, Alfano CM, et al. Cancer Treatment and Survivorship Statistics, 2019. *CA Cancer J Clin* (2019) 69:363–85. doi: 10.3322/caac.21565
4. Creasman WT, Odicino F, Maisonneuve P, Quinn MA, Beller U, Benedet JL, et al. Carcinoma of the Corpus Uteri. *Int J Gynaecol Obstet* (2006) 95(Suppl 1):S105–S43. doi: 10.1016/S0020-7292(06)60031-3
5. Daud S, Jalil SS, Griffin M, Ewies AA. Endometrial Hyperplasia - the Dilemma of Management Remains: A Retrospective Observational Study of 280 Women. *Eur J Obstet Gynecol Reprod Biol* (2011) 159:172–5. doi: 10.1016/j.ejogrb.2011.06.023
6. Gentry-Maharaj A, Karpinskyj C. Current and Future Approaches to Screening for Endometrial Cancer. *Best Pract Res Clin Obstet Gynaecol* (2020) 65:79–97. doi: 10.1016/j.bpobgyn.2019.12.006
7. Costas L, Frias-Gomez J, Guardiola M, Benavente Y, Pineda M, Pavon MA, et al. New Perspectives on Screening and Early Detection of Endometrial Cancer. *Int J Cancer* (2019) 145:3194–206. doi: 10.1002/ijc.32514
8. Park YR, Lee SW, Kim Y, Bae IY, Kim HK, Choe J, et al. Endometrial Thickness Cut-Off Value by Transvaginal Ultrasonography for Screening of Endometrial Pathology in Premenopausal and Postmenopausal Women. *Obstet Gynecol Sci* (2019) 62:445–53. doi: 10.5468/ogs.2019.62.6.445
9. Wong AS, Lao TT, Cheung CW, Yeung SW, Fan HL, Ng PS, et al. Reappraisal of Endometrial Thickness for the Detection of Endometrial Cancer in Postmenopausal Bleeding: A Retrospective Cohort Study. *BJOG* (2016) 123:439–46. doi: 10.1111/1471-0528.13342
10. van Hanegem N, Prins MM, Bongers MY, Opmeer BC, Sahota DS, Mol BW, et al. The Accuracy of Endometrial Sampling in Women With Postmenopausal Bleeding: A Systematic Review and Meta-Analysis. *Eur J Obstet Gynecol Reprod Biol* (2016) 197:147–55. doi: 10.1016/j.ejogrb.2015.12.008
11. Miyamoto T, Abiko K, Murakami R, Furutake Y, Baba T, Horie A, et al. Hysteroscopic Morphological Pattern Reflects Histological Grade of Endometrial Cancer. *J Obstet Gynaecol Res* (2019) 45:1479–87. doi: 10.1111/jog.13998
12. Visser NCM, Reijnen C, Massuger L, Nagtegaal ID, Bulten J, Pijnenborg JMA. Accuracy of Endometrial Sampling in Endometrial Carcinoma: A Systematic Review and Meta-Analysis. *Obstet Gynecol* (2017) 130:803–13. doi: 10.1097/AOG.0000000000002261
13. Ordi J, Bergeron C, Hardisson D, McCluggage WG, Hollema H, Felix A, et al. Reproducibility of Current Classifications of Endometrial Endometrioid Glandular Proliferations: Further Evidence Supporting a Simplified Classification. *Histopathol* (2014) 64:284–92. doi: 10.1111/his.12249
14. Maritschnegg E, Wang Y, Pecha N, Horvat R, Van Nieuwenhuysen E, Vergote I, et al. Lavage of the Uterine Cavity for Molecular Detection of Mullerian Duct Carcinomas: A Proof-Of-Concept Study. *J Clin Oncol* (2015) 33:4293–300. doi: 10.1200/JCO.2015.61.3083
15. Yang BH, Yu MX, Xu J, Su Y, Ai ZH. The Value of DNA Quantitative Cytology Test for the Screening of Endometrial Cancer. *Cancer Manag Res* (2019) 11:10383–91. doi: 10.2147/CMAR.S225672
16. Han L, Du J, Zhao L, Sun C, Wang Q, Tuo X, et al. An Efficacious Endometrial Sampler for Screening Endometrial Cancer. *Front Oncol* (2019) 9:67. doi: 10.3389/fonc.2019.00067
17. Pan Y, Liu G, Zhou F, Su B, Li Y. DNA Methylation Profiles in Cancer Diagnosis and Therapeutics. *Clin Exp Med* (2018) 18:1–14. doi: 10.1007/s10238-017-0467-0
18. Hao X, Luo H, Krawczyk M, Wei W, Wang W, Wang J, et al. DNA Methylation Markers for Diagnosis and Prognosis of Common Cancers. *Proc Natl Acad Sci USA* (2017) 114:7414–9. doi: 10.1073/pnas.1703577114
19. Schmitz M, Eichelkraut K, Schmidt D, Zeiser I, Hilal Z, Tettenborn Z, et al. Performance of a DNA Methylation Marker Panel Using Liquid-Based Cervical Scrapes to Detect Cervical Cancer and its Precancerous Stages. *BMC Cancer* (2018) 18:1197. doi: 10.1186/s12885-018-5125-8
20. Pierconti F, Martini M, Fiorentino V, Cenci T, Racioppi M, Foschi N, et al. Upper Urothelial Tract High-Grade Carcinoma: Comparison of Urine Cytology and DNA Methylation Analysis in Urinary Samples. *Hum Pathol* (2021) 118:42–8. doi: 10.1016/j.humpath.2021.09.007
21. Dong S, Li W, Wang L, Hu J, Song Y, Zhang B, et al. Histone-Related Genes Are Hypermethylated in Lung Cancer and Hypermethylated HIST1H4F Could Serve as a Pan-Cancer Biomarker. *Cancer Res* (2019) 79:6101–12. doi: 10.1158/0008-5472.CAN-19-1019
22. Huang RL, Su PH, Liao YP, Wu TI, Hsu YT, Lin WY, et al. Integrated Epigenomics Analysis Reveals a DNA Methylation Panel for Endometrial Cancer Detection Using Cervical Scrapings. *Clin Cancer Res* (2017) 23:263–72. doi: 10.1158/1078-0432.CCR-16-0863
23. Multinu F, Chen J, Madison JD, Torres M, Casarin J, Visscher D, et al. Analysis of DNA Methylation in Endometrial Biopsies to Predict Risk of Endometrial Cancer. *Gynecol Oncol* (2020) 156:682–8. doi: 10.1016/j.ygyno.2019.12.023
24. Cornel KMC, Wouters K, Van de Vijver KK, van der Wurff AAM, van Engeland M, Kruitwagen R, et al. Gene Promoter Methylation in Endometrial Carcinogenesis. *Pathol Oncol Res* (2019) 25:659–67. doi: 10.1007/s12253-018-0489-2
25. Cancer Genome Atlas Research N, Kandoth C, Schultz N, Cherniack AD, Akbani R, Liu Y, et al. Integrated Genomic Characterization of Endometrial Carcinoma. *Nature* (2013) 497:67–73. doi: 10.1038/nature12113
26. Malhotra RK, Indrayan A. A Simple Nomogram for Sample Size for Estimating Sensitivity and Specificity of Medical Tests. *Indian J Ophthalmol* (2010) 58:519–22. doi: 10.4103/0301-4738.71699
27. Zhu Q, Wang J, Zhang Q, Wang F, Fang L, Song B, et al. Methylationdriven Genes PMPCAP1, SOWAHC and ZNF454 as Potential Prognostic Biomarkers in Lung Squamous Cell Carcinoma. *Mol Med Rep* (2020) 21:1285–95. doi: 10.3892/mmr.2020.10933
28. Liu J, Wan Y, Li S, Qiu H, Jiang Y, Ma X, et al. Identification of Aberrantly Methylated Differentially Expressed Genes and Associated Pathways in Endometrial Cancer Using Integrated Bioinformatic Analysis. *Cancer Med* (2020) 9:3522–36. doi: 10.1002/cam4.2956
29. Lv S, Wang Q, Li Y, Zhao L, Wang Y, Feng X, et al. A Clinical Comparative Study of Two Different Endometrial Cell Samplers for Evaluation of Endometrial Lesions by Cytopathological Diagnosis. *Cancer Manag Res* (2020) 12:10551–7. doi: 10.2147/CMAR.S272755
30. Bakkum-Gamez JN, Wentzensen N, Maurer MJ, Hawthorne KM, Voss JS, Kroneman TN, et al. Detection of Endometrial Cancer *via* Molecular Analysis of DNA Collected With Vaginal Tampons. *Gynecol Oncol* (2015) 137:14–22. doi: 10.1016/j.ygyno.2015.01.552
31. Wentzensen N, Bakkum-Gamez JN, Killian JK, Sampson J, Guido R, Glass A, et al. Discovery and Validation of Methylation Markers for Endometrial Cancer. *Int J Cancer* (2014) 135:1860–8. doi: 10.1002/ijc.28843
32. Fan Y, Wang Y, Fu S, Yang L, Lin S, Fan Q, et al. The Diagnostic Role of DNA Methylation in Sporadic Endometrial Cancer: A Systematic Review and Meta-Analysis. *Oncotarget* (2018) 9:8642–52. doi: 10.18632/oncotarget.23480

33. Liew PL, Huang RL, Wu TI, Liao CC, Chen CW, Su PH, et al. Combined Genetic Mutations and DNA-Methylated Genes as Biomarkers for Endometrial Cancer Detection From Cervical Scrapings. *Clin Epigenetics* (2019) 11:170. doi: 10.1186/s13148-019-0765-3
34. den Helder RV, Wever BM, van Trommel JA, Ket JC, Bleeker MC, Steenbergen RD, et al. DNA Methylation Markers for Endometrial Cancer Detection in Minimally Invasive Samples: A Systematic Review. *Epigenomics* (2020) 12:1661–72. doi: 10.2217/epi-2020-0164
35. Sangtani A, Wang C, Weaver A, Hoppman NL, Kerr SE, Abyzov A, et al. Combining Copy Number, Methylation Markers, and Mutations as a Panel for Endometrial Cancer Detection *via* Intravaginal Tampon Collection. *Gynecol Oncol* (2020) 156:387–92. doi: 10.1016/j.ygyno.2019.11.028
36. Chang CC, Wang HC, Liao YP, Chen YC, Weng YC, Yu MH, et al. The Feasibility of Detecting Endometrial and Ovarian Cancer Using DNA Methylation Biomarkers in Cervical Scrapings. *J Gynecol Oncol* (2018) 29:e17. doi: 10.3802/jgo.2018.29.e17
37. van den Helder R, Wever BMM, van Trommel NE, van Splunter AP, Mom CH, Kasius JC, et al. Non-Invasive Detection of Endometrial Cancer by DNA Methylation Analysis in Urine. *Clin Epigenetics* (2020) 12:165. doi: 10.1186/s13148-020-00958-7
38. Gupta P, Gupta N, Dey P. Morphometric Analysis of Endometrial Cells in Liquid-Based Cervical Cytology Samples. *Cytopathol* (2017) 28:140–8. doi: 10.1111/cyt.12364
39. Kommoss FKF, Stichel D, Schrimpf D, Kriegsmann M, Tessier-Cloutier B, Talhouk A, et al. DNA Methylation-Based Profiling of Uterine Neoplasms: A Novel Tool to Improve Gynecologic Cancer Diagnostics. *J Cancer Res Clin Oncol* (2020) 146:97–104. doi: 10.1007/s00432-019-03093-w
40. Farkas SA, Sorbe BG, Nilsson TK. Epigenetic Changes as Prognostic Predictors in Endometrial Carcinomas. *Epigenetics* (2017) 12:19–26. doi: 10.1080/15592294.2016.1252891

Conflict of Interest: LD, JX, KW, and LLZ were employed by Wuhan ammunition Life-Tech Co., Ltd.

The remaining authors declare that the research was conducted in the absence of any commercial or financial relationships that could be construed as a potential conflict of interest.

Publisher's Note: All claims expressed in this article are solely those of the authors and do not necessarily represent those of their affiliated organizations, or those of the publisher, the editors and the reviewers. Any product that may be evaluated in this article, or claim that may be made by its manufacturer, is not guaranteed or endorsed by the publisher.

Copyright © 2022 Wang, Dong, Xu, Guo, Wang, Wan, Jing, Zhao, Feng, Zhang, Guo, Zou, Zhang and Li. This is an open-access article distributed under the terms of the Creative Commons Attribution License (CC BY). The use, distribution or reproduction in other forums is permitted, provided the original author(s) and the copyright owner(s) are credited and that the original publication in this journal is cited, in accordance with accepted academic practice. No use, distribution or reproduction is permitted which does not comply with these terms.

frontiers | Frontiers in Oncology

ORIGINAL RESEARCH
published: 09 May 2022
doi: 10.3389/fonc.2022.842703

30-Year Experience With 22 Cases of Malignant Transformation Arising From Ovarian Mature Cystic Teratoma: A Rare Disease

Yan Li[1†], Meng Qin[1†], Ying Shan[1†], Huan-wen Wu[2], Xiao-ding Liu[2], Jie Yin[1], Yu Gu[1], Wei Wang[1], Yong-xue Wang[1], Jia-yu Chen[1], Li Ma[3], Ying Jin[1] and Ling-ya Pan[1]*

[1] Department of Obstetrics and Gynecology, Peking Union Medical College Hospital, Chinese Academy of Medical Sciences and Peking Union Medical College, National Clinical Research Center for Obstetric & Gynecologic Diseases, Beijing, China, [2] Department of Pathology, Peking Union Medical College Hospital, Chinese Academy of Medical Sciences and Peking Union Medical College, Beijing, China, [3] Department of Anesthesiology, Peking Union Medical College Hospital, Chinese Academy of Medical Sciences and Peking Union Medical College, Beijing, China

OPEN ACCESS

Edited by:
Sarah M. Temkin, National Institutes of Health (NIH), United States

Reviewed by:
Komsun Suwannarurk, Thammasat University, Thailand
Stephanie M. McGregor, University of Wisconsin-Madison, United States

***Correspondence:**
Ying Jin
jinying@pumch.cn

[†]These authors have contributed equally to this work

Specialty section:
This article was submitted to Gynecological Oncology, a section of the journal Frontiers in Oncology

Received: *24 December 2021*
Accepted: *31 March 2022*
Published: *09 May 2022*

Citation:
Li Y, Qin M, Shan Y, Wu H-w, Liu X-d, Yin J, Gu Y, Wang W, Wang Y-x, Chen J-y, Ma L, Jin Y and Pan L-y (2022) 30-Year Experience With 22 Cases of Malignant Transformation Arising From Ovarian Mature Cystic Teratoma: A Rare Disease. Front. Oncol. 12:842703. doi: 10.3389/fonc.2022.842703

Objective: To investigate the clinical characteristics and survival outcomes of patients with malignant transformation arising from ovarian mature cystic teratoma (MT-MCT).

Methods: This retrospective study included patients with ovarian MCTs at Peking Union Medical College Hospital (PUMCH) during 1990.01-2020.12. When the pathologic histology was MT-MCT, detailed information was collected.

Results: Overall, 7229 ovarian MCT patients and 22 patients with MT-MCT were enrolled. The rate of malignant transformation of all ovarian MCTs was 0.30%. Most patients with MT-MCT were 51 (21–75) years old, and the tumor mass size was 10 (3–30) cm. The typical clinical symptoms were mainly abdominal pain and distension. The levels of tumor markers were elevated on preoperative examination. Early diagnosis could be made by ultrasonic examination, pelvic enhanced MRI and CT. Most patients underwent debulking surgery and adjuvant chemotherapy. The most common histological type to exhibit malignant transformation was squamous cell carcinoma (59.1%), followed by adenocarcinoma (13.6%), carcinoid (9.1%), and borderline tumor (18.2%). The 5-year RFS and OS rates were 54.5% and 81.8%, respectively. Patients with FIGO stage I had the best RFS (P=0.047) and OS (P=0.018), followed by those with FIGO stage II-IV.

Conclusion: MT-MCTs mainly occur in elderly females, are rare and have a poor prognosis. Advanced FIGO stage is a risk factor for survival. Although there is no standard treatment, cytoreductive debulking surgery and adjuvant chemotherapy could be considered. Perimenopausal and menopausal women with MCT should receive surgical treatment.

Keywords: ovarian mature cystic teratoma, malignant transformation, survival outcomes, squamous cell carcinoma, rare disease (RD)

INTRODUCTION

Ovarian germ cell tumors (OGCTs) are derived from ovarian primordial germ cells, including benign or malignant tumors. OGCTs account for approximately 20%-25% of all ovarian tumors but only approximately 5% of all ovarian malignant tumors (1, 2). OGCTs mainly occur in young women aged 10–30 years, accounting for 70% of female ovarian tumors in this age group (3). Mature cystic teratomas (MCTs), also referred to as dermoid cysts, are one of the most common benign OGCTs (4). The potential cells in teratomas can differentiate into a variety of tissues from the three layers of primordial germ cells.

When the components of MCTs develop into somatic malignant tumors, they can become malignant OGCTs, which is called malignant transformation arising from ovarian mature cystic teratomas (MT-MCTs) (5, 6). It is reported that the incidence of malignant transformation of MCTs is 0.2%-2% (6, 7), accounting for 2.9% of all malignant OGCTs (8). Any component of MCTs can progress to malignancy, but the most common malignant transformation type is squamous cell carcinoma (SCC) from the ectoderm (9, 10). MT-MCTs are not equal to ovarian immature teratomas (IT) (11). Immature teratomas are also known as malignant teratomas, teratoblastomas or embryonal teratomas (12) and account for less than 1% of ovarian teratomas but 35.6% of all malignant OGCTs. IT patients are often under 20 years of age (13), while MT-MCTs were more common in women of postmenopausal age (14).

The preoperative detection of MT-MCT is very challenging. The chief symptoms and positive tumor markers lack specificity and sensitivity (5). The early diagnosis of teratomas mainly relies on ultrasonic examination (15). The echo of MCT on ultrasound is obviously related to its structure. In addition, magnetic resonance imaging (MRI) and computed tomography (CT) scans have better efficacy and specificity in tumor location and qualitative diagnosis than ultrasound (16, 17). However, it is still difficult to distinguish MT-MCT from other benign and malignant ovarian tumors. A few studies ever reported that risk factors included age ≥45 years, tumor size >10 cm, rapid growth, and imaging findings (10, 18, 19). There are no standard treatment strategies about MT-MCT. Typical treatment is complete debulking surgery followed by adjuvant chemotherapy (19). When malignant transformation has occurred in the teratoma, the treatments always adjust according to the type of transformation (19).

However, as MT-MCT is a rare disease, there are almost no evidence-based studies. Therefore, we performed this retrospective study to explore the characteristics and clinical outcomes of patients with malignant transformation arising from ovarian mature cystic teratoma.

MATERIALS AND METHODS

Study Population

This retrospective study included all patients with ovarian MCTs between January 1990 and December 2020 at Peking Union Medical College Hospital (PUMCH). Patients with any of the following characteristics were excluded: 1) critical clinical or operation data were lacking; or 2) repeated specimen collection was required. All patients provided written informed consent under the approval of the Ethics Committee of PUMCH. All ethical standards, including ethics committee approval and the informed consent procedure, were in accordance with international guidelines.

Data Collection

The basic information and pathologic histology of ovarian MCT patients were extracted from the medical records from the Hospital Information System (HIS). When the pathologic histology revealed MT-MCT, detailed information was collected. For this retrospective analysis, the following data were extracted from HIS and through telephone interviews: patient information, clinical information, pathological characteristics, surgical outcomes, and survival outcomes. Two pathologists who have abundant experience in gynecologic pathology independently examined the slides with hematoxylin-eosin (HE) staining and immunohistochemistry for all included patients. A third reviewer was involved in a discussion to resolve differences. The standard tumor stage was defined by the International Federation of Gynecology and Obstetrics (FIGO) staging system in 2014. The recurrence-free survival (RFS) was defined as the time interval between the date of the first diagnosis and the date of ovarian cancer progression. The overall survival (OS) was defined as the time interval between the date of the first diagnosis and the date of death (20). RFS and OS were the survival prognosis indices for this study.

Statistical Analysis

All statistical analyses were performed using SPSS software (version 23.0; SPSS Inc., Chicago, IL, USA), and graphs were generated using GraphPad Prism software for Macbook (version 9.0; GraphPad software Inc., San Diego, USA). Student's t tests and Mann–Whitney U tests were used to compare continuous variables. Pearson's chi-squared tests and Fisher's exact tests were used to compare categorical variables (21). Survival analysis was performed using Kaplan–Meier curves and the log-rank test. Statistical significance was set at $P<0.050$.

RESULTS

Overall, 7229 ovarian MCT patients were diagnosed at PUMCH during the period from 1990.01-2020.12. According to the pathological histology results, 22 patients had malignant transformation arising from ovarian MCTs. The rate of malignant transformation in all ovarian MCTs was 0.30%. **Table 1** shows the clinicopathological characteristics and survival outcomes of each patient with MT-MCTs. **Table 2** shows a summary of the clinicopathological characteristics of all patients with MT-MCTs.

Clinical Characteristics of the Included Patients

The age of the included patients was 51 (21–75) years old. Half of the patients experience complications, mainly hypertension (HTN), diabetes mellitus (DM), nephritis, etc. The chief complaint was abdominal pain and distension for approximately 1–3 months in

TABLE 1 | The clinicopathological characteristics and survival outcomes of each patient with malignant transformation arising from ovarian mature cystic teratomas.

Case	Age (yr)	Gestation/ pregnancy	Complications	Symptoms	Tumor size (cm)	Positive tumor marker	Neoadjuvant chemotherapy	FIGOstage	Primary Surgery	Malignant transformation Histology	Tumor grade	Adjuvant treatment	Status	Follow-up time (Mo)
1	60	G7P7	None	Pelvic mass	5.0	None	No	III	Cytoreduction	AC-MCT	G1	Yes	Dead	120.6
2	35	G3P1	None	Abdominal distension	3.0	None	No	II	Cytoreduction	BD-MCT	NR	No	Alive	315.4
3	46	G2P2	None	Bellyache	12.0	None	No	IA	Cytoreduction	SCC-MCT	G2	No	Alive	197.7
4	65	G2P1	Nephritis	Bellyache	11.3	None	No	III	Cytoreduction	SCC-MCT	G1	No	Dead	145.4
5	55	G0P0	HTN	Pelvic mass	8.5	Ca125/CA199	Yes	III	Cytoreduction	Goiter-carcinoid	G1	Yes	Dead	41.2
6	71	G1P1	DM	Poor appetite	10.0	Ca125/CA199	No	IIB	Cytoreduction	SCC-MCT	G1	No	Dead	75.5
7	75	G2P2	HTN	Abdominal distension	15.0	CA125	Yes	IIB	Cytoreduction	AC-MCT	G3	Yes	Dead	85.6
8	64	G4P3	None	Pelvic mass	13.3	CA199	No	I	Cytoreduction	BD-MCT	NR	No	Alive	14.1
9	57	G3P1	None	Bellyache	10.0	Ca125/CA199	No	IIB	Cytoreduction	SCC-MCT	G3	Yes	Alive	133.2
10	45	G3P3	DM	Pelvic mass	8.1	Ca125/ SCCAg	No	IIIC	Cytoreduction	SCC-MCT	G3	Yes	Dead	16.8
11	41	G1P1	None	Pelvic mass	5.7	Ca125/ CA199/CEA	No	II	Oophorocystectomy	BD-MCT	NR	Yes	Recurrent but alive	119.6
12	60	G3P1	None	Vaginocele	12.0	None	No	II	Cytoreduction	SCC	G2	Yes	Dead	114.0
13	33	G2P0	HBV	Abdominal distension	30.0	CA125/CEA/ AFP	No	I	Staging Surgery	BD-MCT	NR	No	Alive	107.8
14	39	G5P1	None	Bellyache	8.2	CA199/CEA	No	IIC	Staging Surgery	SCC-MCT	G1	Yes	Dead	24.0
15	25	G0P0	Psoriasis	Bellyache	15.0	CA199	No	IA	Fertility preservation surgery	SCC-MCT	G1	Yes	Alive	12.5
16	21	G0P0	None	Menstrual disorder	7.0	None	No	IC	Fertility preservation surgery	CC-MCT	NR	No	Alive	59.9
17	64	G2P2	HTN	Bellyache	10.0	CA125/ CA199	No	II	Cytoreduction	SCC-MCT	G2	Yes	Alive	48.7
18	48	G2P1	Cerebral infarction	Bellyache	12.8	CA125/ CA199/ SCCAg/CEA	Yes	IV	Cytoreduction	SCC-MCT	G3	Yes	Dead	23
19	62	G3P1	Carotid plaque	Bellyache	8.7	CA125/ CA199/ SCCAg	No	IA	Staging Surgery	SCC-MCT	G2	Yes	Recurrent but alive	39.9
20	36	G0P0	IgA nephropathy	Bellyache	5.0	CA125/ SCCAg	No	IA	Staging Surgery	SCC-MCT	G2	Yes	Alive	11.8
21	62	G1P1	None	Pelvic mass	8.4	Ca125/CA199	No	II	Abdominal hysterectomy +bilateral salpingo-oophorectomy	SCC-MCT	G2	Yes	Alive	7.5
22	46	G2P1	None	Vaginal drainage	14.0	Ca125/ CA199/CEA	No	III	Cytoreduction	AC-MCT	G1	Yes	Alive	1.1

TABLE 2 | The clinicopathological characteristics summary of all patients with malignant transformation arising from ovarian mature cystic teratomas.

Variable	Number (N = 22)	%	Variable	Number (N = 22)	%
Age (year)	51 (21-75)		**Primary Surgery**		
<60	13	59.10%	Cytoreductive surgery	14	63.60%
≥60	9	40.90%	Staging Surgery	4	18.20%
Complications			Fertility preservation surgery	2	9.10%
No	11	50.00%	Others	2	9.10%
Yes	11	50.00%	**Reexplore laparotomy for complete stage**		
Menopause			No	18	81.80%
No	10	45.50%	Yes	4	18.2
Yes	12	54.50%	**Operation complication**		
Previous pregnancy			No	19	86.40%
No	4	18.20%	Yes	3	13.60%
Yes	18	81.80%	intestinal obstruction	1	4.50%
Previous delivery			infection	1	4.50%
No	5	22.70%	lymphedema	1	4.50%
Yes	17	77.30%	**Adjuvant treatment**		
Clinical symptoms			No	7	31.80%
Bellyache/abdominal distension	12	54.50%	Yes	15	68.20%
Pelvic mass	6	27.30%	TC	8	36.40%
Others	4	18.20%	TP	5	22.70%
Tumor mass size (cm)	10 (3-30)		PEB	1	4.50%
<10cm	10	45.50%	Others	1	4.50%
≥10cm	12	54.50%	**Malignant transformation Histology**		
Positive tumor marker			Squamous-cell carcinoma	13	59.10%
CA125	13	59.10%	Adenocarcinoma	3	13.60%
CA199	12	54.50%	Carcinoid	2	9.10%
SCCAg	4	18.20%	Borderline tumor	4	18.20%
CEA	5	22.70%	**Tumor grade**		
AFP	1	4.50%	G1	7	31.80%
Neoadjuvant chemotherapy			G2	6	27.30%
No	19	86.40%	G3	4	18.20%
Yes	3	13.60%	No report	5	22.70%
FIGO stage			**Recurrence**		
I	7	31.80%	No	12	54.50%
II	9	40.90%	Yes	11	50.00%
III	5	22.70%	Recurrent death	9	40.90%
IV	1	4.50%	Recurrent but alive	2	9.10%
			Follow-up time (Months)	54.3(12.0-315.4)	

Data are presented as number (%) or mean (±SD) or median (±IQR).

54.5% of patients; 27.3% patients visited a doctor due to a palpable abdominal mass. The tumor mass size of the MCT with malignant transformation was 10 (3–30) cm, which well explained the main symptoms. The tumor mass size of 54.5% of the patients was larger than 10 cm. Other symptoms included irregular menstruation and vaginal discharge. The level of tumor markers was elevated on preoperative examination and mainly included carbohydrate antigen 125 (CA125), carbohydrate antigen 199 (CA199), and squamous cell carcinoma antigen (SCCAg).

The typical imaging of patients with squamous cell carcinoma transformation in MCTs (SCC-MCTs) is shown in **Figure 1**. The ultrasound and enhanced CT images of case 18 were obtained. In addition, the pelvic enhanced MRI images of case 20 were collected. **Figure 1A** shows a pelvic ultrasound of SCC-MCT, revealing a moderate echo in the right adnexal area (10.5*7.9*8.3 cm) with an irregular shape and clear boundary. No echo or strip-shaped strong echo was observed in this area. CDFI: Striped arteriovenous blood flow is seen in the surrounding interior (PSV: 11.8 cm/s and RI: 0.35). In **Figure 1B**, the pelvic enhanced MRI of SCC-MCTs showed a lobulated cystic solid mass from the adnexal area with a high-low mixed signal located in the lower abdomen and pelvic cavity (13.8*8.8*10.5 cm) and compression changes in the adjacent bowel, bladder and uterus. In **Figure 1C**, enhanced CT of SCC-MCTs in the pelvis revealed a lobulated soft tissue density mass in the pelvic cavity (9.4*9.9 cm) with uneven internal density, spot-shaped high-density foci and fat density shadow. In addition, the plain CT value was approximately 37 HU. Uneven mild enhancement was observed on the enhanced scan. The boundary was not clear between this mass and the small intestine and anterior uterine edge in the pelvic cavity.

There were four histological types of MT-MCT exhibiting malignant transformation, namely, squamous cell carcinoma (SCC-MCT, 13/22, 59.1%), adenocarcinoma (AC-MCT, 3/22, 13.6%), carcinoid (CC-MCT, 2/22, 9.1%), and borderline tumor (BD-MCT, 4/22, 18.2%). CA125 and SCCAg were usually elevated in SCC-MCTs. The tumor differentiation grade included well differentiated (G1, 31.8%), moderately differentiated (G2, 27.3%) and poorly differentiated (G3, 18.2%). The tumor grade was not reported in CC-MCT and BD-MCT because of its pathological particularity. **Figure 1D** shows a typical pathological image of a patient (case 18) with SCC-MCT. In this case, the gray nodule (9*7*5 cm) appears cystic and solid. Hairs can be seen in the cystic

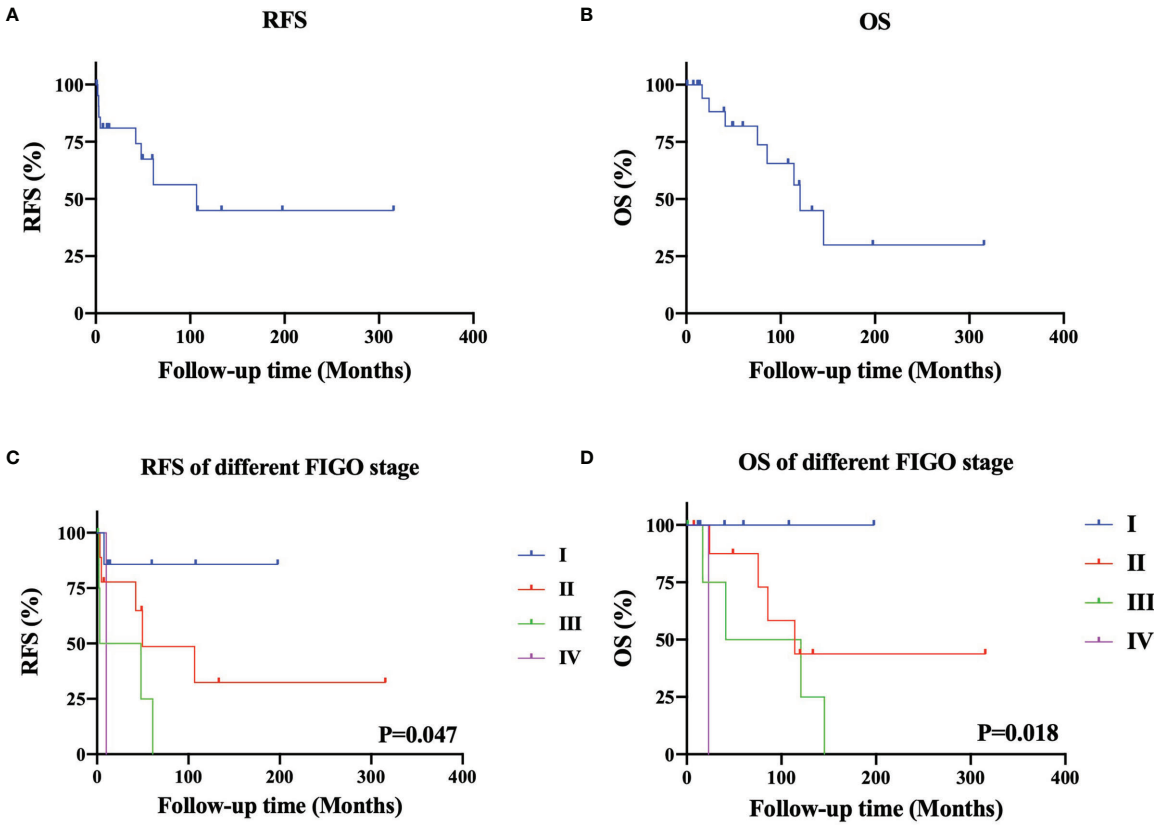


FIGURE 1 | Typical imaging and pathological image of patients with squamous cell carcinoma arising from ovarian mature cystic teretomas (SCC-MCTs). **(A)** [case 18]: Pelvic ultrasound of SCC-MCT showing that a moderate echo was observed in the right adnexal area (10.5*7.9*8.3 cm), with an irregular shape and clear boundry. No echo or strip-shaped strong echo was observed in this area. CDFI: Striped asteriovenous blood flow is seen in the surrounding interior PSV: 11.8 cm/s, RI: 0.35. **(B)** [case 20]: Pelvic enchanced MRI of SCC-MCTs showing a lobulated cystic solid mass from the adnexal area with a high-low mixed signal located in the lower abdomen and pelvic cavity (13.8*8.8*105cm) and compression changes in the adjacent bowel, bladder and uterus. **(C)** [case 18]: Pelvic enchance CT of SCC-MCTs showing a lobulated soft tissue density mass in the pelvic cavity (9.4*9.9cm), with uneven internal density, spot-shaped high-density foci and fat density shadows. In addition, the plain CT value was approximately 37HU. Uneven mild enhancement was observed on enchanced scan. The boundry was not clear between this mass and the small intestine and interior uterine edge in the pelvic cavity. **(D)** [case 18]: Pathological images showing that the gray nodule (9*7*5cm) on the section was cystic and solid. Hairs can be seen in the cystic area, while the solid area appears gray-yellow and solid with medium texture. The tumor consisted of 30-40% malignant components.)

area, while the solid area is gray–yellow and has medium texture. For this case, the tumor consisted of 30-40% malignant components. Most ovarian patients with MT-MCTs were in the early FIGO stage. The number of patients with FIGO stage I-IV disease was seven, nine, five, and one, respectively. One FIGO stage IV patient had bone and lung metastasis.

Treatments of the Included Patients

Three patients underwent neoadjuvant chemotherapy (NACT). Among them, two patients had extensive implant metastasis in the upper abdomen and a large tumor burden throughout the whole body in preoperative evaluation, thus receiving NACT to achieve a higher rate of satisfactory cytoreduction. The other one patient was at advanced age and had a poor performance status that could not tolerate primary cytoreduction. After receiving NACT, the tumor burden of all three patients were significantly reduced by CA125 and CT scans (22, 23). Among all 22 patients, 90.9% of patients underwent standard ovarian surgery, including cytoreductive surgery (63.6%), ovarian cancer staging surgery (18.2%), and fertility preservation staging surgery (9.1%). Only one patient underwent total abdominal hysterectomy and bilateral salpingo-oophorectomy, and the other one patient underwent oophorocystectomy. If it's highly suspected that the pelvic mass was malignant by preoperative evaluation, the immediate rapid pathological examination during operation was necessary. The rate of reexplore laparotomy for complete stage was 18.2%. A total of 13.6% of patients had operation complications, including intestinal obstruction (4.5%), infection (4.5%), and lymphedema (4.5%). A total of 68.2% of patients received adjuvant chemotherapy, including TC (taxol+carboplatin, 8/15), TP (taxol+cisplatin, 5/15), and PEB (cisplatin+ etoposide + bleomycin, 1/15).

Survival Outcomes of the Included Patients

The follow-up time was 54.3 (12.0-315.4) months. **Figures 2A**, **2B** show the RFS and OS of 22 patients with MT-MCT, respectively.

The 3-year and 5-year RFS rates were 72.7% and 54.5%, respectively. The 3-year and 5-year OS rates were 86.4% and 81.8%, respectively. Among all nine dead patients, eight patients were dead due to tumor recurrence, and one patient died of suicide. The recurrence sites were commonly in pelvic cavity and inguinal lymph nodes. In addition, we performed a subgroup analysis of the RFS and OS of 22 patients characterized by FIGO stage, as shown in **Figures 2C, D**. The results showed that patients with FIGO stage I disease had the best RFS, followed by those with FIGO stages II, III, and IV (P=0.047). Similarly, the patients with FIGO stage I disease had the best OS, followed by those with FIGO stage II, III, and IV (P=0.018). The 5-year RFS rates in patients with FIGO stages I, II, III, and IV were 85.7%, 55.6%, 20.0%, and 0%, respectively. The 5-year OS rates in patients with FIGO stages I, II, III, and IV were 100.0%, 88.9%, 60%, and 0%, respectively.

Table 3 showed the clinicopathological characteristics and survival outcomes of all included patients characterized by SCC-MT group and other histology group. There were no significant differences in all variables, including age, clinical symptoms, tumor mass size, the number of NACT and adjuvant treatment, FIGO stage, primary surgery type, and the number of recurrent patients. We performed a subgroup analysis of the RFS and OS outcomes of 22 patients characterized by different MT histology, as respectively shown in **Figures S1A, B**. The patients with BD-MCT tended to have better survival outcomes than those with SCC-MCT and AC-MCT/CC-MCT. However, there were no significant differences in RFS (P=0.220) and OS (P=0.163). The 5-year RFS rates were respectively 61.5% and 100% between SCC-MCT group and other histology group. The 5-year OS rates were respectively 76.9% and 77.7% between two groups.

DISCUSSION

MT-MCT is a rare type of malignant ovarian cancer (24). Ovarian MCTs mainly occur in women during the child-bearing years, while types that exhibit malignant transformation generally occur in women between 40 and 60 years old (25, 26). It has been

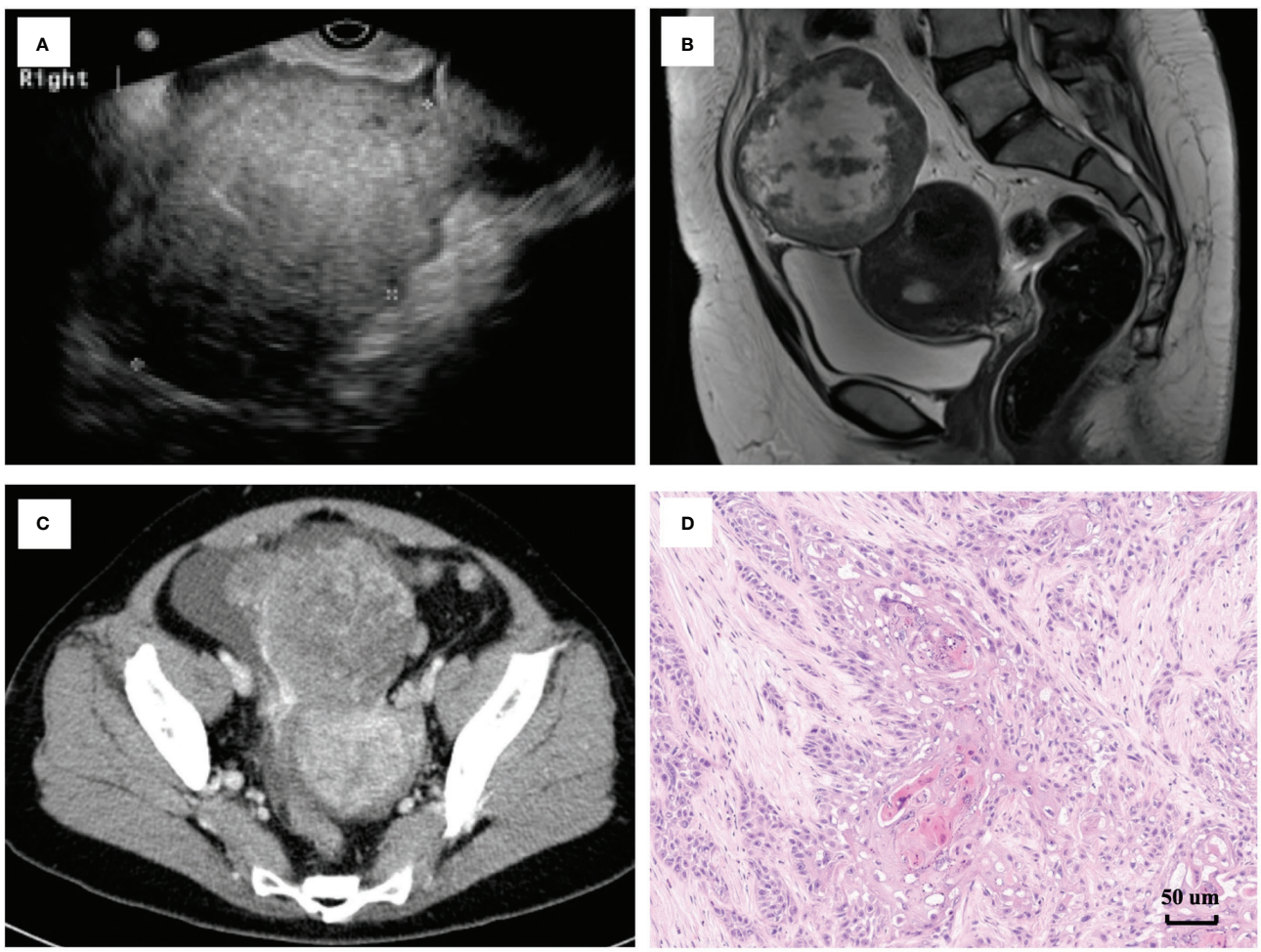


FIGURE 2 | The survival outcomes of patients with malignant transformation arising from ovarian mature cystic teratomas. The recurrence-free survival **(A)** and overall survival **(B)** of 22 patients with MT-MCT. The recurrence-free survival **(C)** and overall survival **(D)** of 22 patients characterized by different FIGO stage).

TABLE 3 | The clinicopathological characteristics and survival outcomes of all included patients characterized by different malignant transformation histology.

Variable	SCC-MT (N = 13)	Other Histology (N = 9)	*P* value
Age (year)			0.548
<60	7 (53.8%)	6 (66.7%)	
≥60	6 (46.2%)	3 (33.3%)	
Clinical symptoms			0.219
Bellyache/abdominal distension	9 (69.2%)	3 (33.3%)	
Pelvic mass	2 (15.4%)	4 (44.4%)	
Others	2 (15.4%)	2 (22.2%)	
Tumor mass size (cm)			0.429
<10cm	5 (38.5%)	5 (55.6%)	
≥10cm	8 (61.5%)	4 (44.4%)	
Neoadjuvant chemotherapy			0.329
No	12 (92.3%)	7 (77.8%)	
Yes	1 (7.7%)	2 (22.2%)	
FIGO stage			0.643
I	4 (30.8%)	3 (33.3%)	
II	6 (46.2%)	3 (33.3%)	
III	2 (15.4%)	3 (33.3%)	
IV	1 (7.7%)	0	
Primary Surgery			0.902
CRS	8 (61.5%)	6 (66.7%)	
Staging Surgery	3 (23.1%)	1 (11.1%)	
Fertility preservation surgery	1 (7.7%)	1 (11.1%)	
TAH+BSO	1 (7.7%)	1 (11.1%)	
Adjuvant treatment			0.29
No	3 (23.1%)	4 (44.4%)	
Yes	10 (76.9%)	5 (55.6%)	
Recurrence			0.665
No	6 (46.2%)	5 (55.6%)	
Yes	7 (53.8%)	4 (44.4%)	
Recurrent death	6 (85.7%)	3 (75.0%)	
Recurrent but alive	1 (14.3%)	1 (25.0%)	
5-year RFS rates	61.50%	100%	
5-year OS rates	76.90%	77.70%	

reported that the average age of patients with MT-MCTs is 50 years old, while the average age of patients with benign teratomas is 33 years old (9). MT-MCT tumors are typically located in one ovary but can involve both ovaries. The tumor mass size is usually large, most of which are 10 to 20 cm in diameter (27). The level of positive tumor markers is associated with MT-MCTs, and different tumor markers have different sensitivities for different histological types (28). Thus, it is difficult to identify these tumors using a single tumor marker. In this study, the clinical characteristics of patients with MT-MCTs were consistent with the findings from other literature reports, including age, symptoms, tumor mass size, and positive tumor markers.

Early diagnosis of MT-MCT relies on comprehensive imaging examinations including ultrasound, MRI, and CT (29). A large number of lipids, hair, cartilage and thyroid cells cause MCTs to exhibit obvious ultrasonic imaging characteristics, such as the dough sign, wall nipple sign and lipid stratification sign (18). However, lipid stratification and calcification are also present in MT-MCTs. MRI showed that the thickening of the cyst wall and the presence of intracapsular papilla and solid components can be important features in the diagnosis of malignant MCTs (16). In addition, direct invasion of the surrounding tissues or peritoneal implantation metastasis is observed in some cases. The distinguishing features of MT-MCT are the presence of components of benign teratoma (e.g., grease, hair, bone, etc.) and a combination of malignant tumor features (e.g., blood flow signals or enhanced solid components). Therefore, it is important to identify older patients with larger tumors or those who have tumors with malignant characteristics to exclude potential malignant transformation of MCTs (27). It is emphasized that surgical treatment should be performed for perimenopausal and postmenopausal patients with ovarian mature teratoma, even though almost all of them are benign.

The pathological diagnosis of MT-MCTs is difficult. Pathologists should have abundant experience in diagnosing gynecologic tumor pathologies. Finding a teratomatous component is critical. Malignant transformation may occur in the endodermal, mesodermal and exodermal components of teratomas (30). In terms of pathological characteristics, ovarian MCTs are generally large and solid, with or without a dermoid cyst. They may protrude into the cyst wall or form thickening of the wall (31). It is a grayish white, raised or nodular, lumpy, papillary and cauliflower mass. It is often brittle, accompanied by bleeding and necrosis (32). SCC is the most common malignant transformation histology of MCTs (33). SCC-MCT shows a varied morphology, ranging from G1 and keratinizing to G3 to anaplastic (31). One study reported that squamous carcinoma of MCT originates from squamous epithelial metaplasia, which may be related to HPV infection (30). AC-MCT most commonly arise from gastrointestinal-type epithelium and respiratory-type

epithelium. Low-grade mucinous epithelial neoplasms with mucin extravasation may arise in teratomas and mimic metastases (31). The tumor consisted of 10-40% malignant components, which depends on the histology type and tumor grade. Other rare types include thyroid-type papillary carcinoma, undifferentiated carcinoma, borderline tumor, melanoma, small cell carcinoma, and sarcomas (34–39). The immunophenotype of the malignant components is similar to that of malignancies occurring at classical sites. In addition, it is necessary to identify the difference between ovarian metastatic tumors and MT-MCTs. Doctors should exclude metastasis of cervical or vaginal squamous cell carcinoma, gastrointestinal adenocarcinoma, urothelial carcinoma of the urinary system, etc. (5). Clinical imaging and pathological diagnosis after surgical resection can help to identify the primary lesion (40). In addition, it is necessary to diagnose ovarian primary squamous cell carcinoma and endometrial adenocarcinoma with scale changes, as they lack hair and sebum components (41). Immunohistochemistry may also be helpful for diagnosis and differential diagnosis.27

To identify the molecular biological characteristics and genomic abnormalities of MT-MCT, deoxyribonucleic acid (DNA) and microribonucleic acid (miRNA) analyses were performed (42). Cooke et al. reported that a total of 244 abnormalities were identified in 79 genes in SCC-MCT. TP53 was the most frequently altered gene in SCC (80%), followed by PIK3CA (52%) and CDKN2A (44%). The gene mutation in TP53 was associated with improved overall survival (43). The overall mutational burden of SCC-MCT is high, but MCT has a low mutation burden. SCC-MCTs share similar mutation profiles to SCC (43). Yoshida et al. analyzed comprehensive miRNA sequencing in SCC-MCTs and normal ovarian and mature teratoma tissues. Two miRNAs (miR-151a-3p and miR-378a-3p) were markedly upregulated, and two miRNAs (miR-26a-5p and miR-99a-5p) were markedly downregulated in cancer tissues. In addition, these findings were validated in fresh cancer tissues of patient-derived xenograft (PDX) models (44). Gene analysis research on MT-MCTs can help us better understand the cause of malignant transformation from teratomas to provide innovative thinking related to treatment and drug research.

As MT-MCTs are very rare, there is no standard treatment at present. The basic principle is that surgical treatment, early detection and complete resection can improve the survival rate (25, 45). For perimenopausal or postmenopausal women, total abdominal hysterectomy with bilateral salpingo-oophorectomy, omentectomy, pelvic lymphadenectomy are recommended (46). For early-stage women who have fertility requirements, the uterus and normal ovary could be preserved (25). Adjuvant chemotherapy mainly depends on the malignant pathological type of MCT. TC and TP are the most commonly used chemotherapy regimens (14). It has been reported that the 5-year survival rate of MT-MCTs with FIGO stage I is 95%, which is much better than that of patients with advanced-stage disease (47). Ruey-jien et al. reported that the 5-year survival rates of stage I, II, III and IV patients were 75.5%, 33.8%, 20.6% and 0%, respectively, after a follow-up of 188 patients (45). In our study, the 5-year OS rates in patients with FIGO stages I, II, III, and IV were 100.0%, 88.9%, 60%, and 0%, respectively. Therefore, tumor stage and optimal debulking are critical to survival outcomes (45).

CONCLUSION

In conclusion, this retrospective study showed that the rate of malignant transformation in all ovarian MCTs was 0.30%. MT-MCTs mainly occur in elderly females, are rare and have a poor prognosis. Advanced FIGO stage is a risk factor for survival. Preoperative examination included positive tumor markers (CA125, CA199, and SCCAg), ultrasonic examination, pelvic enhanced MRI and CT. Although there is no standard treatment, cytoreductive debulking surgery and adjuvant chemotherapy could be considered. Perimenopausal and menopausal women with MCT should receive surgical treatment.

DATA AVAILABILITY STATEMENT

The raw data supporting the conclusions of this article will be made available by the authors, without undue reservation.

ETHICS STATEMENT

All patients provided written informed consent under the approval of the Ethics Committee of PUMCH. The patients/participants provided their written informed consent to participate in this study. Written informed consent was obtained from the individual(s) for the publication of any potentially identifiable images or data included in this article.

AUTHOR CONTRIBUTIONS

Study conceptualization: L-yP, YJ; Study design: YL, MQ, YJ; Data acquisition: YL, MQ, YG, WW, LM; Quality control of data and algorithms: JY, J-yC, YS; Data analysis and interpretation: YL, MQ, Y-xW, H-wW, X-dL; Statistical analysis: YL, MQ; Manuscript preparation: YL, MQ; Manuscript editing: all authors; Manuscript review: YJ. All authors contributed to the article and approved the submitted version.

FUNDING

This project was supported by the Non-profit Central Research Institute Fund of Chinese Academy of Medical Sciences (2021-PT320-001). Furthermore, this project was also supported by CAMS Innovation Fund for Medical Sciences (CIFMS-2017-I2M-1-002).

SUPPLEMENTARY MATERIAL

The Supplementary Material for this article can be found online at: https://www.frontiersin.org/articles/10.3389/fonc.2022.842703/full#supplementary-material

REFERENCES

1. Tewari K, Cappuccini F, Disaia PJ, Berman ML, Manetta A, Kohler MF. Malignant Germ Cell Tumors of the Ovary. *Obstet Gynecol* (2000) 95(1):128–33. doi: 10.1016/s0029-7844(99)00470-6
2. Sagae S, Kudo R. Surgery for Germ Cell Tumors. *Semin Surg Oncol* (2000) 19 (1):76–81. doi: 10.1002/1098-2388(200007/08)19:1<76::aid-ssu12>3.0.co;2-b
3. Zalel Y, Piura B, Elchalal U, Czernobilsky B, Antebi S, Dgani R. Diagnosis and Management of Malignant Germ Cell Ovarian Tumors in Young Females. *Int J Gynaecol Obstet* (1996) 55(1):1–10. doi: 10.1016/0020-7292(96)02719-1
4. Ayhan A, Bukulmez O, Genc C, Karamursel BS, Ayhan A. Mature Cystic Teratomas of the Ovary: Case Series From One Institution Over 34 Years. *Eur J Obstet Gynecol Reprod Biol* (2000) 88(2):153–7. doi: 10.1016/s0301-2115(99) 00141-4
5. Srisajjakul S, Prapaisilp P, Bangchokdee S. Imaging Features of Unusual Lesions and Complications Associated With Ovarian Mature Cystic Teratoma. *Clin Imaging* (2019) 57:115–23. doi: 10.1016/j.clinimag.2019.05.013
6. Gadducci A, Guerrieri ME, Cosio S. Squamous Cell Carcinoma Arising From Mature Cystic Teratoma of the Ovary: A Challenging Question for Gynecologic Oncologists. *Crit Rev Oncol Hematol* (2019) 133:92–8. doi: 10.1016/j.critrevonc.2018.10.005
7. Comerci JTJr., Licciardi F, Bergh PA, Gregori C, Breen JL. Mature Cystic Teratoma: A Clinicopathologic Evaluation of 517 Cases and Review of the Literature. *Obstet Gynecol* (1994) 84(1):22–8.
8. Smith HO, Berwick M, Verschraegen CF, Wiggins C, Lansing L, Muller CY, et al. Incidence and Survival Rates for Female Malignant Germ Cell Tumors. *Obstet Gynecol* (2006) 107(5):1075–85. doi: 10.1097/01.AOG.0000216004.22588.ce
9. Hackethal A, Brueggmann D, Bohlmann MK, Franke FE, Tinneberg H-R, Münstedt K. Squamous-Cell Carcinoma in Mature Cystic Teratoma of the Ovary: Systematic Review and Analysis of Published Data. *Lancet Oncol* (2008) 9:1173–80. doi: 10.1016/S1470-2045(08)70306-1
10. Dos Santos L, Mok E, Iasonos A, Park K, Soslow RA, Aghajanian C, et al. Squamous Cell Carcinoma Arising in Mature Cystic Teratoma of the Ovary: A Case Series and Review of the Literature. *Gynecol Oncol* (2007) 105(2):321–4. doi: 10.1016/j.ygyno.2006.12.008
11. Ahmed A, Lotfollahzadeh S. *Cystic Teratoma. StatPearls*. Treasure Island, FL: StatPearls Publishing Copyright (2021). StatPearls Publishing LLC.
12. Smith HO, Berwick M, Verschraegen CF, Wiggins C, Lansing L, Muller CY, et al. Incidence and Survival Rates for Female Malignant Germ Cell Tumors. *Obstet Gynecol* (2006) 107(5):1075–85. doi: 10.1097/01.AOG.0000216004.22588.ce
13. Faure-Conter C, Pashankar F. Immature Ovarian Teratoma: When to Give Adjuvant Therapy? *J Pediatr Hematol Oncol* (2017) 39(7):487–9. doi: 10.1097/ mph.0000000000000950
14. Qin L, Zhao T, Liu X, Wang H, Gu X, Chen D, et al. Malignant Transformation Arising From Mature Ovarian Cystic Teratoma: A Case Series. *Med (Baltimore)* (2021) 100(13):e24726. doi: 10.1097/md.0000000000024726
15. Rim SY, Kim SM, Choi HS. Malignant Transformation of Ovarian Mature Cystic Teratoma. *Int J Gynecol Cancer* (2006) 16(1):140–4. doi: 10.1111/ j.1525-1438.2006.00285.x
16. Şahin H, Akdoğan AI, Ayaz D, Karadeniz T, Sancı M. Utility of the "Floating Ball Sign" in Diagnosis of Ovarian Cystic Teratoma. *Turk J Obstet Gynecol* (2019) 16(2):118–23. doi: 10.4274/tjod.galenos.2019.67209
17. Lai PF, Hsieh SC, Chien JC, Fang CL, Chan WP, Yu C. Malignant Transformation of an Ovarian Mature Cystic Teratoma: Computed Tomography Findings. *Arch Gynecol Obstet* (2005) 271(4):355–7. doi: 10.1007/s00404-004-0676-0
18. Takagi H, Ichigo S, Murase T, Ikeda T, Imai A. Early Diagnosis of Malignant-Transformed Ovarian Mature Cystic Teratoma: Fat-Suppressed MRI Findings. *J Gynecol Oncol* (2012) 23(2):125–8. doi: 10.3802/jgo.2012.23.2.125
19. Oranratanaphan S, Khemapech N. Characteristics and Treatment Outcomes of Patients With Malignant Transformation Arising From Mature Cystic Teratoma of the Ovary: Experience at a Single Institution. *Asian Pac J Cancer Prev* (2013) 14(8):4693–7. doi: 10.7314/apjcp.2013.14.8.4693
20. Watanabe H, Okada M, Kaji Y, Satouchi M, Sato Y, Yamabe Y, et al. New Response Evaluation Criteria in Solid Tumours - Revised RECIST Guideline (Version 1.1). *Gan to kagaku ryoho Cancer Chemother* (2009) 36:2495–501.
21. du Prel J-B, Röhrig B, Hommel G, Blettner M. Choosing Statistical Tests: Part 12 of a Series on Evaluation of Scientific Publications. *Dtsch Arztebl Int* (2010) 107(19):343–8. doi: 10.3238/arztebl.2010.0343
22. Qin M, Jin Y, Ma L, Zhang YY, Pan LY. The Role of Neoadjuvant Chemotherapy Followed by Interval Debulking Surgery in Advanced Ovarian Cancer: A Systematic Review and Meta-Analysis of Randomized Controlled Trials and Observational Studies. *Oncotarget* (2018) 9(9):8614–28. doi: 10.18632/oncotarget.23808
23. Gu Y, Qin M, Jin Y, Zuo J, Li N, Bian C, et al. A Prediction Model for Optimal Primary Debulking Surgery Based on Preoperative Computed Tomography Scans and Clinical Factors in Patients With Advanced Ovarian Cancer: A Multicenter Retrospective Cohort Study. *Front Oncol* (2020) 10:611617. doi: 10.3389/fonc.2020.611617
24. Indulkar ST, Khare MS, Shah VB, Khade AL. Squamous Cell Carcinoma Arising in Mature Teratoma of the Ovary Masquerading as Abdominal Tuberculosis. *J Midlife Health* (2018) 9(1):44–6. doi: 10.4103/jmh.JMH_81_17
25. Li C, Zhang Q, Zhang S, Dong R, Sun C, Qiu C, et al. Squamous Cell Carcinoma Transformation in Mature Cystic Teratoma of the Ovary: A Systematic Review. *BMC Cancer* (2019) 19(1):217. doi: 10.1186/s12885-019-5393-y
26. Tokunaga H, Watanabe Y, Kaiho M, Yokoyama Y, Futagami M, Watanabe T, et al. Advanced Squamous Cell Carcinomas Arising From Mature Cystic Teratoma of the Ovary: A Retrospective Case Series at the Tohoku Gynecologic Cancer Unit. *Int Cancer Conf J* (2016) 5(3):146–9. doi: 10.1007/s13691-016-0246-x
27. Chiang AJ, Chen MY, Weng CS, Lin H, Lu CH, Wang PH, et al. Malignant Transformation of Ovarian Mature Cystic Teratoma Into Squamous Cell Carcinoma: A Taiwanese Gynecologic Oncology Group (TGOG) Study. *J Gynecol Oncol* (2017) 28(5):e69. doi: 10.3802/jgo.2017.28.e69
28. Choi EJ, Koo YJ, Jeon JH, Kim TJ, Lee KH, Lim KT. Clinical Experience in Ovarian Squamous Cell Carcinoma Arising From Mature Cystic Teratoma: A Rare Entity. *Obstet Gynecol Sci* (2014) 57(4):274–80. doi: 10.5468/ ogs.2014.57.4.274
29. An JS, Wu LY, Li XG, Zhang R, Song Y, Ma SK, et al. Clinical Analysis of 44 Cases With Malignant Transformation of Ovarian Mature Cystic Teratoma. *Zhonghua Fu Chan Ke Za Zhi* (2013) 48(2):123–8.
30. Araujo IB, Pinheiro MV, Zanvettor PH, Studart EJ, Filho DF, Coupland SE. High Frequency of Malignant Transformation of Ovarian Mature Teratoma Into Squamous Cell Carcinoma in Young Patients in Northeast Brazil. *Int J Gynecol Pathol* (2016) 35(2):176–84. doi: 10.1097/pgp.0000000000000225
31. WHO Classification of Tumors Editorial Board. Female Genital Tumors: WHO Classification of Tumors (2020). p. 138–9.
32. Khachatryan A. Malignant Tumors In Ovarian Mature Cystic Teratomas Intraoperative Diagnostic Basis. *Georgian Med News* (2016) Issue):22–8.
33. Mahe E, Sur M. Squamous Lesions of the Ovary. *Arch Pathol Lab Med* (2011) 135(12):1611–4. doi: 10.5858/arpa.2010-0640-RS
34. Kita N, Satoh T, Onuki-Tanabe M, Ainoya Y, Yamada N, Oki A, et al. Undifferentiated Carcinoma With Osteoclast-Like Multinucleated Giant Cells Arising in an Ovarian Mature Cystic Teratoma. *Gynecol Obstet Invest* (2003) 56(4):184–7. doi: 10.1159/000074283
35. Tanaka H, Sakakura Y, Kobayashi T, Yoshida K, Asakura T, Taniguchi H. A Case of Thyroid-Type Papillary Carcinoma Derived From Ovarian Mature Cystic Teratoma, Resected by Laparoscopic Surgery. *Asian J Endosc Surg* (2011) 4(2):86–9. doi: 10.1111/j.1758-5910.2011.00076.x
36. Kajo K, Masák L, Sorkovská D, Vallová M, Kajo M, Macháleková K, et al. Mucinous Carcinoma (Non-Intestinal Type) Arising in the Ovarian Mature Cystic Teratoma - A Case Report. *Cesk Patol* (2013) 49(4):141–5.
37. Lai J, Garvey KY, Li P, Azevedo RA. Primary Ovarian Melanoma Arising From a Mature Teratoma With Melanoma *In Situ* Present in the Ciliated Columnar and Squamous Epithelium in a Patient With Synchronous Skin Basal Cell Carcinoma. *Int J Gynecol Pathol* (2021) 40(4):383–90. doi: 10.1097/ pgp.0000000000000727
38. Pongsuvareeyakul T, Sukpan K, Chaicharoen S, Khunamornpong S. Leiomyosarcoma and Squamous Cell Carcinoma Arising in Mature Cystic Teratoma of the Ovary. *Case Rep Pathol* (2017) 2017:7907359. doi: 10.1155/ 2017/7907359
39. Ikota H, Kaneko K, Takahashi S, Kawarai M, Tanaka Y, Yokoo H, et al. Malignant Transformation of Ovarian Mature Cystic Teratoma With a Predominant Pulmonary Type Small Cell Carcinoma Component. *Pathol Int* (2012) 62(4):276–80. doi: 10.1111/j.1440-1827.2012.02804.x
40. Saleh M, Bhosale P, Menias CO, Ramalingam P, Jensen C, Iyer R, et al. Ovarian Teratomas: Clinical Features, Imaging Findings and Management. *Abdom Radiol (NY)* (2021) 46(6):2293–307. doi: 10.1007/s00261-020-02873-0

41. Saba L, Guerriero S, Sulcis R, Virgilio B, Melis G, Mallarini G. Mature and Immature Ovarian Teratomas: CT, US and MR Imaging Characteristics. *Eur J Radiol* (2009) 72(3):454–63. doi: 10.1016/j.ejrad.2008.07.044
42. Shen DH, Khoo US, Xue WC, Cheung AN. Ovarian Mature Cystic Teratoma With Malignant TransformationAn Interphase Cytogenetic Study. *Int J Gynecol Pathol* (1998) 17(4):351–7. doi: 10.1097/00004347-199810000-00009
43. Yoshida K, Yokoi A, Kagawa T, Oda S, Hattori S, Tamauchi S, et al. Unique miRNA Profiling of Squamous Cell Carcinoma Arising From Ovarian Mature Teratoma: Comprehensive miRNA Sequence Analysis of Its Molecular Background. *Carcinogenesis* (2019) 40(12):1435–44. doi: 10.1093/carcin/bgz135
44. Cooke SL, Ennis D, Evers L, Dowson S, Chan MY, Paul J, et al. The Driver Mutational Landscape of Ovarian Squamous Cell Carcinomas Arising in Mature Cystic Teratoma. *Clin Cancer Res* (2017) 23(24):7633–40. doi: 10.1158/1078-0432.Ccr-17-1789
45. Chen RJ, Chen KY, Chang TC, Sheu BC, Chow SN, Huang SC. Prognosis and Treatment of Squamous Cell Carcinoma From a Mature Cystic Teratoma of the Ovary. *J Formos Med Assoc* (2008) 107(11):857–68. doi: 10.1016/s0929-6646(08)60202-8
46. Abhilasha N, Bafna UD, Pallavi VR, Rathod PS, Krishnappa S. A Review of Squamous Cell Carcinoma Arising in Mature Cystic Teratoma of the Ovary. *Indian J Cancer* (2016) 53(4):612–4. doi: 10.4103/0019-509x.204763
47. Gadducci A, Giuliani D, Cosio S, Lissoni A, Ferrero AM, Landoni F. Clinical Outcome of Patients With Malignant Tumors Associated With Mature Cystic Teratomas of the Ovary: A Retrospective Multicenter Italian Study. *Anticancer Res* (2019) 39(5):2513–7. doi: 10.21873/anticanres.13372

Conflict of Interest: The authors declare that the research was conducted in the absence of any commercial or financial relationships that could be construed as a potential conflict of interest.

Publisher's Note: All claims expressed in this article are solely those of the authors and do not necessarily represent those of their affiliated organizations, or those of the publisher, the editors and the reviewers. Any product that may be evaluated in this article, or claim that may be made by its manufacturer, is not guaranteed or endorsed by the publisher.

Copyright © 2022 Li, Qin, Shan, Wu, Liu, Yin, Gu, Wang, Wang, Chen, Ma, Jin and Pan. This is an open-access article distributed under the terms of the Creative Commons Attribution License (CC BY). The use, distribution or reproduction in other forums is permitted, provided the original author(s) and the copyright owner(s) are credited and that the original publication in this journal is cited, in accordance with accepted academic practice. No use, distribution or reproduction is permitted which does not comply with these terms.

frontiers | Frontiers in Oncology

ORIGINAL RESEARCH
published: 19 May 2022
doi: 10.3389/fonc.2022.843278

Real-World Efficacy of Bevacizumab in Patients With Recurrent Epithelial Ovarian Cancer

Jo-Ni Hung[1], Shih-Tien Hsu[1,2,3], Lou Sun[1], Sheau-Feng Hwang[1], Chih-Ku Liu[1], Yu-Hsiang Shih[1], Ming-Jer Chen[1,4], Jun-Sing Wang[5,6,7,8†] and Chien-Hsing Lu[1,4,8,9*†]*

[1] Department of Obstetrics and Gynecology, Taichung Veterans General Hospital, Taichung, Taiwan, [2] Center for General Education, Ling Tung University, Taichung, Taiwan, [3] School of Medicine, China Medical University, Taichung, Taiwan, [4] Department of OB/GYN, School of Medicine, National Yang Ming Chiao Tung University, Taipei, Taiwan, [5] Department of Medicine, School of Medicine, National Yang Ming Chiao Tung University, Taipei, Taiwan, [6] Division of Endocrinology and Metabolism, Department of Internal Medicine, Taichung Veterans General Hospital, Taichung, Taiwan, [7] College of Medicine, National Chung-Hsing University, Taichung, Taiwan, [8] Ph.D. Program in Translational Medicine, Institute of Biomedical Sciences, National Chung-Hsing University, Taichung, Taiwan, [9] Rong-Hsing Research Center for Translational Medicine, National Chung-Hsing University, Taichung, Taiwan

OPEN ACCESS

Edited by:
Alberto Farolfi, Scientific Institute of Romagna for the Study and Treatment of Tumors (IRCCS), Italy

Reviewed by:
Valerio Gallotta, Agostino Gemelli University Polyclinic (IRCCS), Italy
Kai Ding, University of Oklahoma Health Sciences Center, United States

***Correspondence:**
Chien-Hsing Lu
chlu@vghtc.gov.tw
Jun-Sing Wang
jswang@vghtc.gov.tw

†These authors have contributed equally to this work and share senior authorship

Specialty section:
This article was submitted to Gynecological Oncology, a section of the journal Frontiers in Oncology

Received: *25 December 2021*
Accepted: *22 April 2022*
Published: *19 May 2022*

Citation:
Hung J-N, Hsu S-T, Sun L, Hwang S-F, Liu C-K, Shih Y-H, Chen M-J, Wang J-S and Lu C-H (2022) Real-World Efficacy of Bevacizumab in Patients With Recurrent Epithelial Ovarian Cancer. Front. Oncol. 12:843278. doi: 10.3389/fonc.2022.843278

Background: Bevacizumab in combination with chemotherapy prolonged the progression-free survival (PFS) of patients with recurrent epithelial ovarian cancer (EOC) in large-scale randomized controlled trials. However, real-world data for the use of bevacizumab in Asian patients with EOC is lacking. This study investigated the efficacy of adding bevacizumab to chemotherapy and compared it with that of chemotherapy alone in patients with recurrent EOC using real-world data from an Asian population.

Method: We conducted a retrospective cohort study using data from a tertiary medical center in central Taiwan. Patients who had EOC with first relapse between 2011 and 2019 were enrolled. Patients' medical histories, medication treatment, and relevant information were collected. The outcomes were PFS and overall survival (OS). The Kaplan-Meier plot was used to generate a survival curve for OS and PFS. Cox proportional hazard analysis was used to determine the associations of Bevacizumab treatment with OS and PFS with adjustment of relevant variables. Subgroup analyses were conducted to determine if there was a significant variation in the aforementioned associations.

Results: After a median follow-up of 23 months, 67% of patients in the Bevacizumab group and 81% of patients in the non-Bevacizumab group had disease progression or death. There was no significant between-group difference in OS (p = 0.475). The median duration of PFS was 18.9 and 9.6 months, respectively, favoring those who were treated with Bevacizumab. After multivariate adjustment, treatment with Bevacizumab was associated with a lower risk of disease progression (hazard ratio 0.33, 95% CI 0.13-0.85, p = 0.021). The improvement in PFS was consistent in the subgroups of different histological types, different disease stages at diagnosis, different treatment-free intervals, those undergoing or not undergoing secondary cytoreductive surgery, diverse chemotherapy regimens.

Conclusion: Our findings provided crucial insights into the efficacy of bevacizumab for the treatment of recurrent EOC in the real-world setting.

Keywords: recurrent epithelial ovarian cancer, bevacizumab (Avastin®), real-world study, progression, survival outcome

INTRODUCTION

Epithelial ovarian cancer (EOC) is the second most common and the most lethal gynecological cancer in developed countries (1). Most of the patients are diagnosed as having advanced stage disease and experience relapse of the disease despite achieving complete remission. Approximately 49% of patients die within 5 years (2). Resistance to chemotherapy is commonly observed in patients with recurrent EOC, and its treatment is considerably challenging. Therefore, the prognosis of recurrent EOC is poor, with a progression-free survival (PFS) of approximately 8–13 months (2–4). Asian countries had the largest number of incident cases (~171,000) and mortality (~113,000) of EOC in 2020 (5), and only a small proportion of Asian patients (<30%) were enrolled in previous clinical trials (2, 3).

Bevacizumab, a humanized monoclonal antibody against angiogenesis, has been approved by the US Food and Drug Administration for the treatment of recurrent EOC since 2016 (6–10). Bevacizumab in combination with chemotherapy prolonged the PFS of patients with primary (6, 8) or recurrent (7, 9) EOC in large-scale randomized controlled trials (RCTs). However, patient enrollment into RCTs is usually highly selective, and most of them are from Western countries. Moreover, differences in the histological types and prognosis of EOC between Asian and Caucasian patients have been reported (11). Therefore, real-world data for the use of bevacizumab in Asian patients with EOC (1, 12) are required, especially for those with recurrent EOC.

This study investigated the efficacy of adding bevacizumab to chemotherapy and compared it with that of chemotherapy alone in patients with recurrent EOC by using real-world data from an Asian population.

MATERIALS AND METHODS

Study Population and Data Collection

We conducted a retrospective cohort study by using data from a tertiary medical center in central Taiwan. The study protocol was approved by our institutional review board (CE21233B). We identified patients who were newly diagnosed as having EOC between 2011 and 2019 (n = 491, **Figure 1**). After excluding patients who had concurrent cancer (n = 22), did not undergo debulking surgery (n = 3), did not achieve disease remission after treatment (n = 58), did not experience disease recurrence (n = 241), had incomplete data (n = 28), and were lost to follow-up (n = 34), we identified 105 patients with surgically and pathologically proved EOC who had the first recurrence of the disease during the study period. Furthermore, we excluded patients who declined treatment (n = 24) and those who received poly (adenosine diphosphate–ribose) polymerase (PARP) inhibitors or immunotherapy (n = 14) for recurrent EOC. Finally, 67 patients with first recurrence of EOC were analyzed in this study, and they were divided into two groups based on whether they received bevacizumab treatment for the recurrent disease (**Figure 1**).

According to international guidelines, we determined chemotherapy regimens after recurrence based on the treatment-free survival durations of the patients. Women who had relapse less than 6 months after the end of front-line therapy were treated with nonplatinum chemotherapy, whereas those who had recurrence after 6 months were treated with the combination of platinum and nonplatinum drugs. Because bevacizumab was not reimbursed by our national health insurance system before May 2020 (13), the treatment doses and cycles of bevacizumab were affected by cost considerations.

Patients' medical history, medication treatment data, and relevant information were collected from electronic health records. We assessed our patients' socioeconomic status by ward fee payment (totally covered by the National Health Insurance or private insurance). The status of disease progression and survival was confirmed in April 2021. Disease progression was defined as an increase in the volume of tumors and the presence of new lesions or ascites on abdominal CT scans performed every 3 months. The primary outcome of this study was overall survival (OS) and PFS. OS was defined as the interval from the initiation of second-line treatment for recurrent EOC to the date of mortality or April 2021. PFS was defined as the interval from the initiation of second-line treatment for recurrent EOC to the date of disease progression, patient mortality, or April 2021.

Statistical Analysis

Differences in baseline characteristics between the two treatment groups were compared using the Mann–Whitney U test and chi-square test for continuous and categorical variables, respectively. The Kaplan–Meier method was used to generate survival curves for OS and PFS. Cox proportional hazard analysis was performed to determine the association of bevacizumab treatment with OS and PFS after adjustment for relevant variables. Subgroup analysis was conducted to determine if a significant variation was present in the aforementioned association. All statistical analyses were performed using the Statistical Package for Social Sciences (IBM SPSS version 22.0; International Business Machines Corp, NY, USA), and a p value of <0.05 was considered statistically significant.

RESULTS

Table 1 lists the characteristics of the study patients according to whether they received bevacizumab treatment for recurrent ovarian cancer. Overall, most of the patients had serous

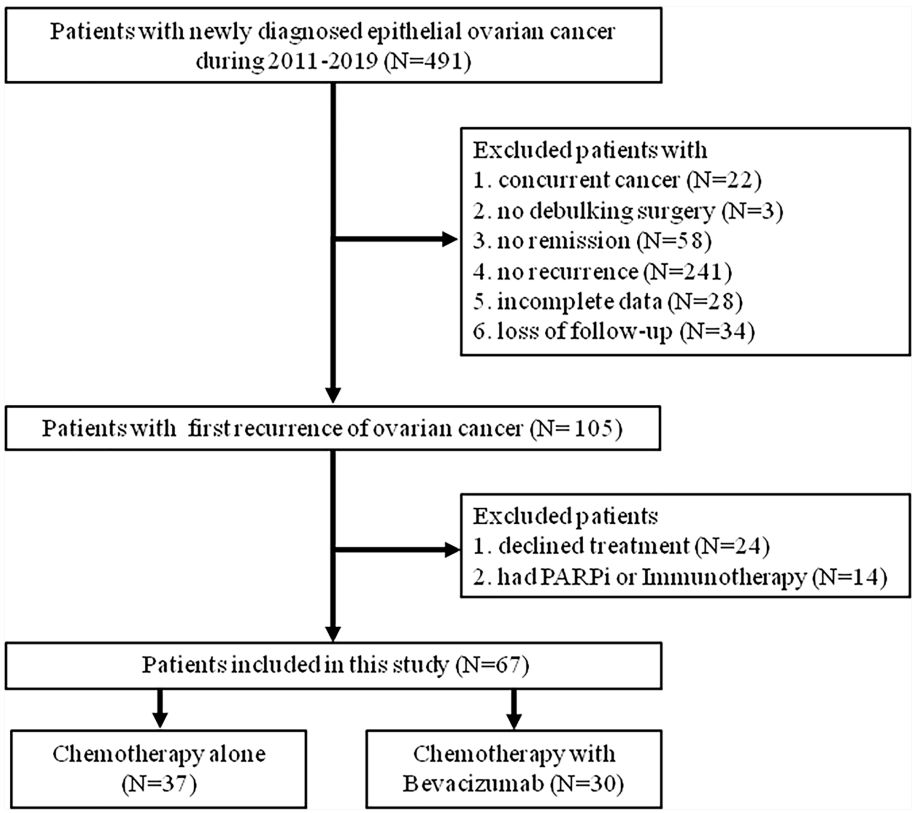


FIGURE 1 | Study flow chart for population selection.

TABLE 1 | Characteristics of study participants according to Bevacizumab treatment for recurrence.

Variables	Chemotherapy alone	Chemotherapy with Bevacizumab	P
Number of participants	37	30	
Age at diagnosis, years	59.0 (53.0-66.0)	56.5 (47.8-65.3)	0.316
Cell type, n (%)			1.000
Serous	28 (75.7)	23 (76.7)	
Non-serous	9 (24.3)	7 (23.3)	
Stage at diagnosis, n (%)			0.451
Stage I-II	3 (8.1)	5 (16.7)	
Stage III-IV	34 (91.9)	25 (83.3)	
Suboptimal debulking surgery, n (%)	5 (13.5)	3 (10.0)	0.722
Front-line Bevacizumab use, n (%)	7 (18.9)	4 (13.3)	0.742
Treatment free interval, n (%)			0.692
< 6 months	3 (8.1)	4 (13.3)	
≥ 6 months	34 (91.9)	26 (86.7)	
Cytoreductive surgery for recurrence, n (%)	14 (37.8)	8 (26.7)	0.480
Chemotherapy regimen for recurrence, n (%)			0.842
Platinum plus Paclitaxel or PLD	29 (78.4)	25 (83.3)	
Others	8 (21.6)	5 (16.7)	
Cycles of Chemotherapy	6.0 (5.0-9.5)	7.0 (6.0-9.0)	0.692
Cycles of Bevacizumab	0	8.5 (5.5-16.25)	
Socioeconomic status (ward fee payment), n (%)			0.001
Totally covered by National Health Insurance	29 (78.4)	19 (63.3)	
Private insurance	8 (21.6)	11 (36.7)	

Data are presented as median (interquartile range) or n (%). PLD, pegylated liposomal doxorubicin.

ovarian cancer (76.1%) with advanced stage (88.1%, stage III-IV) at diagnosis. Eight patients (11.9%) underwent suboptimal initial debulking surgery, whereas 11 (16.4%) patients received first-line bevacizumab treatment. Most of the patients (89.6%) had a treatment-free interval of ≥6 months. After disease recurrence, 22 (32.8%) patients underwent secondary cytoreductive surgery, with complete gross resection achieved in all patients, except in one patient in the bevacizumab group. All the patients received doublet chemotherapy, mainly with platinum plus paclitaxel (80.6%) or platinum plus pegylated liposomal doxorubicin. The dose of bevacizumab was 7.5 or 15 mg/kg every 3 weeks, and 76% (23/30) of the patients underwent more than 6 cycles of bevacizumab. The patients underwent fewer cycles due to economic reasons rather than adverse effects. No significant between-group differences were noted in these clinical variables except socioeconomic status (ward fee payment, **Table 1**).

Figure 2 shows the Kaplan–Meier curves of OS and PFS. After a median follow-up of 23 months, 67% of the patients in the bevacizumab group and 81% of the patients in the non-bevacizumab group exhibited disease progression or had died. No significant between-group difference was observed in OS ($p = 0.475$). The median durations of PFS were 18.9 and 9.6 months, respectively, in the bevacizumab and non-bevacizumab groups, respectively ($p = 0.070$, **Figure 2**).

Table 2 shows the findings of Cox regression analysis for OS and PFS after adjustment for relevant clinical variables. No significant association was observed between bevacizumab treatment and OS. After multivariate adjustment, bevacizumab treatment was associated with a lower risk of disease progression (hazard ratio: 0.33, 95% confidence interval [CI]: 0.13–0.85, $p = 0.021$). The benefit of bevacizumab treatment for the risk of disease progression was consistent across various subgroups, including subgroups of the cell type, cancer stage at diagnosis, treatment-free interval, secondary cytoreductive surgery, and chemotherapy regimen for recurrent disease (**Figure 3**, all p interaction > 0.05).

In terms of the significant adverse effects of bevacizumab treatment, two patients experienced new-onset hypertension, and one patient experienced brain infarction without visible brain metastasis on brain CT. Among patients not treated with bevacizumab, one patient developed rectovaginal fistula after bowel surgery and another patient experienced brain infarction with the evidence of brain metastasis. All other severe adverse effects other than hypertension occurred beyond the second progression.

DISCUSSION

The results of this study demonstrated a significant improvement in PFS with the addition of bevacizumab to chemotherapy for recurrent EOC (**Table 2**). The improvement in PFS was consistent in the subgroups of different histological types, different disease stages at diagnosis, different treatment-free intervals, those undergoing or not undergoing secondary cytoreductive surgery, and diverse chemotherapy regimens (**Figure 3**). Our findings provided crucial insights into the efficacy of bevacizumab for the treatment of recurrent EOC in the real-world setting.

The improvement in PFS (hazard ratio: 0.33, 95% CI: 0.13–0.85, $p = 0.021$) in our study was consistent with that observed in previous phase III RCTs. In patients with recurrent platinum-sensitive EOC, the addition of bevacizumab to carboplatin–gemcitabine and carboplatin–paclitaxel significantly improved PFS compared with chemotherapy alone in the Ocean trial (hazard ratio: 0.484, 95% CI: 0.388–0.605, $p < 0.001$) (7) and GOG0213 (hazard ratio: 0.628, 95% CI: 0.534–0.739, $p < 0.001$) (14). More recently, the ENGOT-ov 18 trial (15) reported that patients treated with bevacizumab–carboplatin–pegylated liposomal doxorubicin (PLD) had longer PFS than did those treated with different regimens established in the Ocean trial (7). In patients with recurrent platinum-resistant EOC, bevacizumab with a nonplatinum regimen (PLD, paclitaxel, or topotecan) demonstrated a PFS benefit in the Aurelia trial (hazard ratio: 0.48, 95% CI: 0.38–0.6, $p < 0.001$) (9). On the basis of these trials, the majority of our patients were treated with established treatment combinations. However, most of the RCTs include an almost homogenous group of participants, and patients may receive more focused care and follow-up compared with that typically observed in real-world practice. Moreover, the majority of patients enrolled in the previous trials were from Western countries (94% in OCEAN and 80% in GOG-0213) (7, 14). These factors may limit the extrapolation of results to other populations (16) such as Asian patients with recurrent EOC. Thus, real-world observational studies should be conducted to confirm the effectiveness of treatment under ordinary and often variable conditions.

Real-world data regarding the effectiveness of bevacizumab in Asian patients with recurrent EOC are scant. In a retrospective cohort study (17), the use of bevacizumab in addition to front-line chemotherapy was associated with an improvement in PFS and OS in patients with ovarian, tubal, and peritoneal cancer compared with chemotherapy alone. However, no data on the use of bevacizumab in the recurrent setting are available. In another cohort study, the outcomes of patients with recurrent EOC treated with bevacizumab were reported. However, no "control group" (patients without bevacizumab treatment) was included in that study. Therefore, the efficacy of bevacizumab in the setting of recurrent EOC should be explored. To our knowledge, this is the first real-world study exploring the benefit of bevacizumab treatment for recurrent EOC.

The prolonged PFS in our treatment group (median: 18.9 vs. 9.6 months, difference: 9.3 months) was longer than that reported in previous RCTs (difference: 3–4 months) (7, 14, 18). Uncertain problems regarding the treatment for recurrent ovarian cancer still exist, including those related to the optimal cycles of chemotherapy, combinations of chemotherapy, and dosage of bevacizumab. The cycles of chemotherapy were limited to 6–8 in GOG0213 (14) and 6 in the AGO-OVAR2.5 trial (15). By contrast, patients in real-world practice might receive more cycles of chemotherapy until no measurable disease is observed, tumor markers return to normal levels, or intolerable side effects

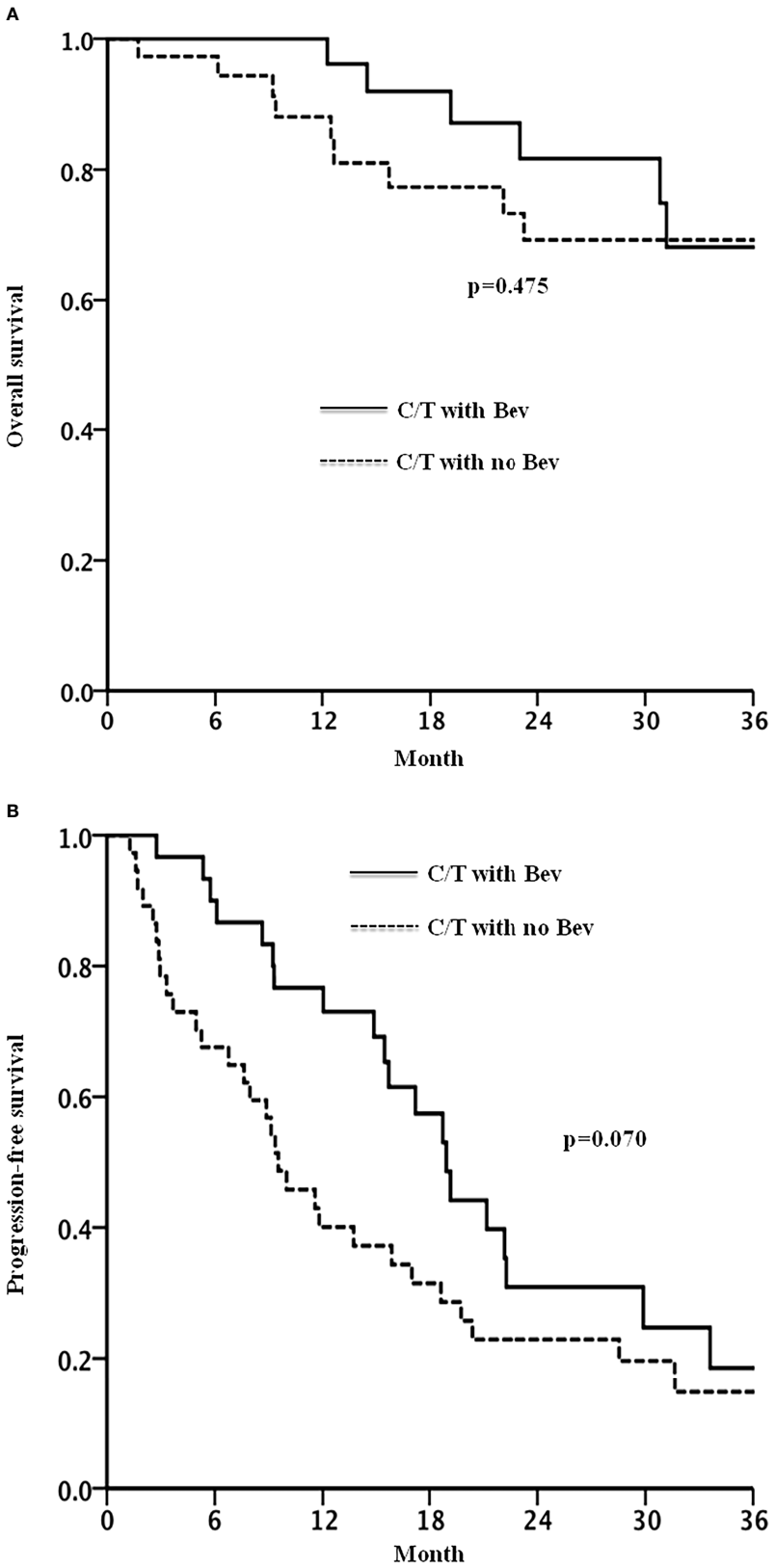


FIGURE 2 | Overall survival **(A)** and progression free survival **(B)** in patients with recurrent ovarian cancer treated with chemotherapy with or without bevacizumab.

TABLE 2 | Associations of Bevacizumab treatment for recurrent disease with overall and progression free survival.

	Overall survival		Progression free survival	
Bevacizumab (use vs. no use)	**Hazard ratio (95% CI)**	**P**	**Hazard ratio (95% CI)**	**P**
Univariate analysis	0.69 (0.24-1.93)	0.478	0.60 (0.34-1.05)	0.074
Multivariate analysis[a]	0.39 (0.08-1.92)	0.244	0.33 (0.13-0.85)	0.021

[a]*Adjusted for stage at diagnosis, histological subtype, suboptimal debulking surgery, front-line Bevacizumab use, cytoreductive surgery, chemotherapy regimen for recurrent disease, and socioeconomic status (ward fee payment).*

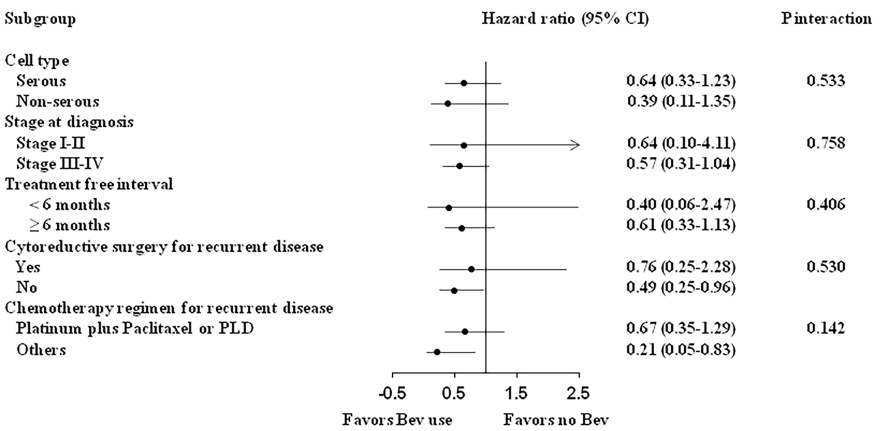


FIGURE 3 | Subgroup analysis of the efficacy of bevacizumab on progression-free survival.

are experienced. Overall, 40% of our patients received more than six cycles of chemotherapy. Whether more cycles of chemotherapy lead to more favorable outcomes for patients with recurrent EOC warrants further investigation. In addition, we had a higher proportion of patients undergoing secondary cytoreductive surgery (33% in our study) compared with that in the Ocean trial (11%) (7) and GOG 0213 (16%) (14), and almost all the patients had no visible tumor after surgery, which may have contributed to more favorable outcomes in our study.

In our study, treatment with bevacizumab reduced the risk of disease progression in the patients who did not undergo secondary cytoreductive surgery (hazard ratio: 0.49, 95% CI: 0.25–0.96, **Figure 3**) with a nonsignificant between-group difference (in patients who underwent secondary cytoreductive surgery, hazard ratio: 0.76, 95% CI: 0.25–2.28, p interaction=0.530). Theoretically, secondary surgery can act as a drug booster that enhances drug penetration and helps to overcome drug resistance in patients with poorly vascularized tumors. However, secondary surgery poses a risk of surgical complications for patients, and it might postpone bevacizumab treatment and increase its toxicity (such as fistula formation or wound dehiscence). The role of secondary cytoreductive surgery became controversial after the GOG0213 trial; this RCT that included 84% of the patients receiving bevacizumab reported that secondary surgery followed by chemotherapy did not significantly prolong survival compared with no surgery (14). Recently, the SOC-1 trial (19), an RCT conducted in China, demonstrated that secondary cytoreductive surgery could extend PFS to nearly 5 months. The findings are similar to those of the DESKTOPIII trial (20). Notably, the proportion of bevacizumab use was low in these two studies. Based on the aforementioned results, the PFS benefit of bevacizumab and secondary cytoreductive surgery might not be additive. Patients may have various presentations of tumor relapse (different recurrent anatomic sites and lymph nodes) and status of BRCA gene. These factors may also impact patients' outcomes after secondary cytoreductive surgery, as reported in previous studies (21, 22). Furthermore, new drugs are available (such as PARP inhibitor) for treatment of recurrent EOC. The role of surgical approach should be reconsidered, and individualized treatment is needed (21, 22). Therefore, real-world data on various study populations as a reference for treatment decision are clinically relevant. Considering that patients who are not a candidate for secondary surgery usually have larger tumor burden, extensive metastasis, or poorer prognosis compared with surgical candidates, treatment with bevacizumab in addition to chemotherapy may be an optimal choice for these patients.

This study has several limitations. First, the treatment dose of bevacizumab in our patients was lower than that administered in previous RCTs (7, 9, 14) likely due to financial reasons. We assessed and adjusted socioeconomic status (ward fee payment by National Health Insurance or private insurance) (23, 24), and the effect of bevacizumab on PFS was independent of this factor. More than half of our patients received a treatment dose of 7.5 mg/kg every 3 weeks compared with 15 mg/kg every 3 weeks in previous trials (7, 9, 14). Considering this limitation, bevacizumab treatment significantly improved PFS in our

patients. Second, the number of the patients included in our study was small. Finally, because this is not a randomized study, some confounders might exist. Hence, our findings should be confirmed in another study including a larger number of patients.

In conclusion, we demonstrated that treatment with bevacizumab in addition to commonly used chemotherapy significantly prolonged the PFS of patients with recurrent EOC in the real-world setting.

DATA AVAILABILITY STATEMENT

The raw data supporting the conclusions of this article will be made available by the authors, without undue reservation.

ETHICS STATEMENT

The studies involving human participants were reviewed and approved by Institutional Review Board of Taichung Veterans General Hospital. Written informed consent for participation was not required for this study in accordance with the national legislation and the institutional requirements.

AUTHOR CONTRIBUTIONS

J-NH and C-HL were accountable for conception and design of the study. J-NH, C-HL, S-TH, LS, S-FH, and C-KL performed acquisition of data. J-NH, Y-HS, and J-SW performed the statistical analysis. J-NH, Y-HS, C-HL, J-SW, and M-JC helped interpret the results and wrote the original draft of the manuscript. All authors were involved in the supervision and revision of the manuscript. All authors contributed to the article and approved the submitted version.

ACKNOWLEDGMENTS

The authors would like to thank the Biostatistics Task Force of Taichung Veterans General Hospital and Taiwan society of cancer registry for their assistance.

REFERENCES

1. Sung H, Ferlay J, Siegel RL, Laversanne M, Soerjomataram I, Jemal A, et al. Global Cancer Statistics 2020: GLOBOCAN Estimates of Incidence and Mortality Worldwide for 36 Cancers in 185 Countries. *CA Cancer J Clin* (2021) 71:209–49. doi: 10.3322/caac.21660
2. Parmar MKB, Ledermann JA, Colombo N, du Bois A, Delaloye J-F, Kristensen GB, et al. Paclitaxel Plus Platinum-Based Chemotherapy Versus Conventional Platinum-Based Chemotherapy in Women With Relapsed Ovarian Cancer: The ICON4/AGO-OVAR-2.2 Trial. *Lancet* (2003) 361:2099–106. doi: 10.1016/S0140-6736(03)13718-X
3. Pfisterer J, Plante M, Vergote I, Du Bois A, Hirte H, Lacave AJ, et al. Gemcitabine Plus Carboplatin Compared With Carboplatin in Patients With Platinum-Sensitive Recurrent Ovarian Cancer: An Intergroup Trial of the AGO-OVAR, the NCIC CTG, and the EORTC GCG. *J Clin Oncol* (2006) 24:4699–707. doi: 10.1200/JCO.2006.06.0913
4. Weng C-S, Wu C-C, Chen T-C, Chen J-R, Huang C-Y, Chang C-L. Retrospective Analysis Of Comparative Outcomes In Recurrent Platinum-Sensitive Ovarian Cancer Treated With Pegylated Liposomal Doxorubicin (Lipo-Dox) And Carboplatin Versus Paclitaxel And Carboplatin. *Cancer Manag Res* (2019) 11:9899–905. doi: 10.2147/CMAR.S217329
5. World Health Organization. Cancer Statistics. Who. (2018). Available at: https://gco.iarc.fr/today/data/factsheets/cancers/25-Ovary-fact-sheet.pdf.
6. Perren TJ, Swart AM, Pfisterer J, Ledermann JA, Pujade-Lauraine E, Kristensen G, et al. A Phase 3 Trial of Bevacizumab in Ovarian Cancer. *N Engl J Med* (2011) 365:2484–96. doi: 10.1056/nejmoa1103799
7. Aghajanian C, Blank SV, Goff BA, Judson PL, Teneriello MG, Husain A, et al. OCEANS: A Randomized, Double-Blind, Placebo-Controlled Phase III Trial of Chemotherapy With or Without Bevacizumab in Patients With Platinum-Sensitive Recurrent Epithelial Ovarian, Primary Peritoneal, or Fallopian Tube Cancer. *J Clin Oncol* (2012) 30:2039–45. doi: 10.1200/JCO.2012.42.0505
8. Burger RA, Brady MF, Bookman MA, Fleming GF, Monk BJ, Huang H, et al. Incorporation of Bevacizumab in the Primary Treatment of Ovarian Cancer. *Obstet Gynecol Surv* (2012) 67:289–90. doi: 10.1097/OGX.0b013e3182547170
9. Pujade-Lauraine E, Hilpert F, Weber B, Reuss A, Poveda A, Kristensen G, et al. Bevacizumab Combined With Chemotherapy for Platinum-Resistant Recurrent Ovarian Cancer: The AURELIA Open-Label Randomized Phase III Trial. *J Clin Oncol* (2014) 32:1302–8. doi: 10.1200/JCO.2013.51.4489
10. Officer CM. *Roche's Avastin (Bevacizumab) Plus Chemotherapy Receives FDA Approval for Platinum-Sensitive Recurrent Ovarian Cancer* (2016). Available at: https://www.roche.com/media/releases/med-cor-2016-12-07.htm.
11. Fuh KC, Java JJ, Chan JK, Kapp DS, Monk BJ, Burger RA, et al. Differences in Presentation and Survival of Asians Compared to Caucasians With Ovarian Cancer: An NRG Oncology/GOG Ancillary Study of 7914 Patients. *Gynecol Oncol* (2019) 154:420–5. doi: 10.1016/j.ygyno.2019.05.013
12. Chen W-C, Qiu JT, Lai C-H, Huang H-J, Lin C-T, Chen M-Y, et al. Outcomes and Prognoses of Patients With Ovarian Cancer Using Bevacizumab: 6-Year Experience in a Tertiary Care Hospital of Northern Taiwan. *PloS One* (2017) 12:e0175703. doi: 10.1371/journal.pone.0175703
13. National Health Insurance Administration Ministry of Health and Welfare-About NHI. Available at: https://www.nhi.gov.tw/English/Content_List.aspx?n=ED4A30E51A609E49&topn=ED4A30E51A609E49.
14. Coleman RL, Brady MF, Herzog TJ, Sabbatini P, Armstrong DK, Walker JL, et al. Bevacizumab and Paclitaxel–Carboplatin Chemotherapy and Secondary Cytoreduction in Recurrent, Platinum-Sensitive Ovarian Cancer (NRG Oncology/Gynecologic Oncology Group Study GOG-0213): A Multicentre, Open-Label, Randomised, Phase 3 Trial. *Lancet Oncol* (2017) 18:779–91. doi: 10.1016/S1470-2045(17)30279-6
15. Pfisterer J, Shannon CM, Baumann K, Rau J, Harter P, Joly F, et al. Bevacizumab and Platinum-Based Combinations for Recurrent Ovarian Cancer: A Randomised, Open-Label, Phase 3 Trial. *Lancet Oncol* (2020) 21:699–709. doi: 10.1016/S1470-2045(20)30142-X
16. Ware JH, Hamel MB. Pragmatic Trials — Guides to Better Patient Care? *N Engl J Med* (2011) 364:1685–7. doi: 10.1056/nejmp1103502
17. Wu P-Y, Cheng Y-M, Shen M-R, Chen Y-C, Huang Y-F, Chou C-Y. Real-World Study of Adding Bevacizumab to Chemotherapy for Ovarian, Tubal, and Peritoneal Cancer as Front-Line or Relapse Therapy (ROBOT): 8-Year Experience. *Front Oncol* (2020) 10:1095. doi: 10.3389/fonc.2020.01095
18. Haunschild CE, Tewari KS. Bevacizumab Use in the Frontline, Maintenance and Recurrent Settings for Ovarian Cancer. *Futur Oncol* (2020) 16:225–46. doi: 10.2217/fon-2019-0042
19. Shi T, Zhu J, Feng Y, Tu D, Zhang Y, Zhang P, et al. Secondary Cytoreduction Followed by Chemotherapy Versus Chemotherapy Alone in Platinum-Sensitive Relapsed Ovarian Cancer (SOC-1): A Multicentre, Open-Label, Randomised, Phase 3 Trial. *Lancet Oncol* (2021) 22:439–49. doi: 10.1016/S1470-2045(21)00006-1
20. Kuroki L, Guntupalli SR. Treatment of Epithelial Ovarian Cancer. *BMJ* (2020) 371:1–20. doi: 10.1136/bmj.m3773

21. Gallotta V, Bruno M, Conte C, Giudice MT, Davia F, Moro F, et al. Salvage Lymphadenectomy in Recurrent Ovarian Cancer Patients: Analysis of Clinical Outcome and BRCA1/2 Gene Mutational Status. *Eur J Surg Oncol* (2020) 46 (7):1327–33. doi: 10.1016/j.ejso.2020.01.035
22. Gallotta V, Conte C, D'Indinosante M, Capoluongo E, Minucci A, De Rose AM, et al. Prognostic Factors Value of Germline and Somatic Brca in Patients Undergoing Surgery for Recurrent Ovarian Cancer With Liver Metastases. *Eur J Surg Oncol* (2019) 45(11):2096–102. doi: 10.1016/j.ejso.2019.06.023
23. Moss J, Murphy J, Filiaci V, Wenzel L, Minasian L, Temkin S. Disparities in Health-Related Quality of Life in Women Undergoing Treatment for Advanced Ovarian Cancer: The Role of Individual-Level and Contextual Social Determinants. *Support Care Cancer* (2018) 27(2):531–8. doi: 10.1007/s00520-018-4340-9
24. Baandrup L, Dehlendorff C, Hertzum-Larsen R, Hannibal C, Kjaer S. Prognostic Impact of Socioeconomic Status on Long-Term Survival of Non-Localized Epithelial Ovarian Cancer - The Extreme Study. *Gynecol Oncol* (2021) 161(2):458–62. doi: 10.1016/j.ygyno.2021.01.042

Conflict of Interest: The authors declare that the research was conducted in the absence of any commercial or financial relationships that could be construed as a potential conflict of interest.

Publisher's Note: All claims expressed in this article are solely those of the authors and do not necessarily represent those of their affiliated organizations, or those of the publisher, the editors and the reviewers. Any product that may be evaluated in this article, or claim that may be made by its manufacturer, is not guaranteed or endorsed by the publisher.

Copyright © 2022 Hung, Hsu, Sun, Hwang, Liu, Shih, Chen, Wang and Lu. This is an open-access article distributed under the terms of the Creative Commons Attribution License (CC BY). The use, distribution or reproduction in other forums is permitted, provided the original author(s) and the copyright owner(s) are credited and that the original publication in this journal is cited, in accordance with accepted academic practice. No use, distribution or reproduction is permitted which does not comply with these terms.

frontiers | Frontiers in Oncology

ORIGINAL RESEARCH
published: 19 May 2022
doi: 10.3389/fonc.2022.810631

Molecular Classification in Patients With Endometrial Cancer After Fertility-Preserving Treatment: Application of ProMisE Classifier and Combination of Prognostic Evidence

Xuting Ran[1,2], *Tingwenyi Hu*[1,2] *and Zhengyu Li*[1,2]*

[1] *Department of Gynecology and Obstetrics, West China Second University Hospital, Sichuan University, Chengdu, China,* [2] *Key Laboratory of Birth Defects and Related Diseases of Women and Children (Sichuan University), Ministry of Education, Chengdu, China*

The Proactive Molecular Risk Classifier for Endometrial Cancer (ProMisE) is a molecular classification system that identifies endometrial cancer (EC) into four prognostically distinct subtypes: *POLE*-mutated, mismatch repair deficiency (MMR-D), p53 wild-type (p53wt), and p53 abnormal (p53abn). However, few reports have applied the ProMisE classifier to EC patients who underwent fertility-preserving treatment (FPT) so far. This study evaluated whether the ProMisE classifier predicted in early-stage EC patients after FPT. We first summarized the three reported outcomes of ProMisE applied to EC patients who received FPT. The hormone-treated patients with EC from 2010 to 2020 in our facility were then analyzed. By sequential immunohistochemistry and Sanger sequencing of *POLE* according to the ProMisE system, formalin-fixed paraffin-embedded blocks of patients before treatment were collected and classified into *POLE*-mutated, MMR-D, p53wt, and p53abn subtypes. The primary outcome was a complete response rate after FPT. Thirteen patients were enrolled from our facility, with 3 (3/13) MMR-D, 0 (0/13) POLE, 8 (8/13) p53wt, 1 (1/13) p53abn, and 1 (1/13) failed with DNA amplification. Six (6/8) patients with p53wt, 2 (2/3) patients with MMR-D, and 1 (1/1) patient with p53abn achieved a complete response in 6 months after treatment. The results of our study and the reported outcomes were finally combined. A total of 106 patients who underwent FPT were included. Of these, 23 (21.7%) were classified as MMR-D, 3 (2.8%) as *POLE*-mutated, 3 (2.8%) as p53abn, and 77 (72.6%) as p53wt. There was no significant difference in the complete response rate (P = 0.152) and recurrence rate (P = 0.174) between MMR-D and p53wt subtypes after FPT. Based on current data, we observed no prognostic significance of the ProMisE classifier in EC patients who underwent FPT. Larger prospective studies are needed to elucidate the precise prognostic meaning of this molecular classifier in these cases.

Keywords: molecular classification, endometrial cancer, fertility-preserving treatment, ProMisE classifier, progestin

OPEN ACCESS

Edited by:
Antonio Mollo,
University of Salerno, Italy

Reviewed by:
Federica Perelli,
Santa Maria Annunziata Hospital, Italy
Paolo Casadio,
University of Bologna, Italy

***Correspondence:**
Zhengyu Li
zhengyuli01@126.com

Specialty section:
This article was submitted to Gynecological Oncology, a section of the journal Frontiers in Oncology

Received: *07 November 2021*
Accepted: *14 April 2022*
Published: *19 May 2022*

Citation:
Ran X, Hu T and Li Z (2022) Molecular Classification in Patients With Endometrial Cancer After Fertility-Preserving Treatment: Application of ProMisE Classifier and Combination of Prognostic Evidence. Front. Oncol. 12:810631. doi: 10.3389/fonc.2022.810631

INTRODUCTION

Endometrial cancer (EC) is one of the most common gynecological malignancies worldwide, with approximately 417,000 cases diagnosed in 2020 (1). Almost 7% of new cases occur in women under age 44, and the incidence is increasing due to obesity and other risk factors (2). Although the gold standard treatment for patients with EC is total hysterectomy with bilateral salpingo-oophorectomy, fertility-preserving treatment (FPT) could be considered in FIGO stage IA, lesions confined to the endometrium or superficial myometrium, and grade 1 endometrioid EC patients who desire pregnancy in the future (3). Current FPT options include oral progestin agents (medroxyprogesterone acetate or megestrol acetate) or the levonorgestrel intrauterine system (LNG-IUS), with a 79.4% overall complete response rate in a recent meta-analysis (4).

Although fertility-sparing management for endometrial cancer has increasingly been investigated, the selection of patients suitable for FPT with pathologic examination and magnetic resonance imaging (MRI) still has shortfalls due to a lack of consensus among pathologists and an unreproducible diagnosis of histotype and grade of EC (5). Besides, although patients eligible for FPT are those younger than 40 years with well-differentiated, endometrioid EC clinically limited to the endometrium and no extra-uterine disease, these indications are not restricted in clinical practice. FPT appears to be feasible even in age > 40 years (6), with grade 2 endometrioid adenocarcinoma (7), or with minimal myometrial infiltration (8). In this scenario, a better tool of a molecular classifier is needed to help direct patient management and identify patients for whom conservative management is safe.

The Cancer Genome Atlas (TCGA) endometrial collaborative project discovered four distinct prognostic EC genomic subtypes (9). Since it was costly and complex for clinical application, the Proactive Molecular Risk Classifier for Endometrial Cancer (ProMisE), which is simple and suitable in clinical practice, was developed and stratified EC into 4 subgroups: (i) mismatch repair deficient (MMR-D), showing the loss of one or more mismatch repair protein(s); (ii) DNA polymerase epsilon (POLE), with mutations in the exonuclease domain in exons 9–14, is associated with very favorable outcomes; (iii) p53 abnormal (p53abn) demonstrating aberrant p53 immunohistochemical staining; and (iv) p53 wild type (p53wt) (10). This classifier has been validated and applied to EC patients who underwent standard surgical treatment. However, its application to EC patients who received FPT is relatively novel, and there are only a few studies tested on a cohort of EC patients who were conservatively treated, with differences in outcomes among these studies (11–13). This study further validated whether the ProMisE classifier could predict treatment response in women with endometrial cancer who underwent fertility-sparing treatment.

MATERIALS AND METHODS

Search Strategy, Data Extraction and Quality Assessment

First, we included original studies with primary data reporting the prognostic significance of the Proactive Molecular Risk Classifier for EC in the fertility-sparing management of endometrial cancer. We searched for peer-reviewed studies published before 1 November 2021, in the MEDLINE, Embase, and Google Scholar databases with various combinations of the following keywords: fertility-sparing treatments, progesterone, intrauterine devices, and early endometrial cancer. Studies were selected if the participants were women diagnosed histologically with early-stage EC, the intervention was fertility-sparing therapy, patients were classified according to the ProMisE for molecular subtypes, and a complete response (CR) rate, a partial response (PR) rate, a and relapse rate (RR) were included in the outcomes.

Studies were hand-searched and selected in a 2-stage process. First, the titles and abstracts from the electronic searches were scrutinized by 2 reviewers independently (XR and TH), and full manuscripts of all citations that met the pre-defined selection criteria were obtained. Second, final inclusion or exclusion decisions were made on the examination of the full manuscripts.

Data were extracted independently by 2 reviewers (XR and TH). We extracted data on the study population (number, age, BMI, percentage of molecular subtypes, and follow-up time), and the major outcomes. We assessed study quality using items from the Newcastle–Ottawa Quality Assessment Scale and the Quality Assessment of Diagnostic Accuracy Studies tool (14) (**Supplementary Table 1**).

Two reviewers (XR and TH) independently assessed the risk of bias of each study using the Quality in Prognosis Studies (QUIPS) tool, which contains several domains: study participation, study attrition, prognostic factor measurement, outcome measurement, study confounding, and statistical analysis and reporting. The risk of bias concerns were rated in each domain as "high risk of bias," "moderate risk of bias," or "low risk of bias." The overall risk of bias was considered low if ≤2 domains were rated as having a moderate risk of bias and all others were rated as having a low risk of bias. The overall risk of bias was considered moderate if >2 domains were rated as having a moderate risk of bias and all others were rated as having a low risk of bias. The overall risk of bias was considered high if ≥1 domain was rated a high risk of bias, irrespective of all other domains (15). Consensus was reached after classification by individual researchers (**Supplementary Table 2**).

Study Population

We retrospectively reviewed the data of young patients with endometrial cancer who had received FPT at the West China Second University Hospital, Sichuan University, during 2010–2020. The study was approved by the ethics committee of West China Second University Hospital, Sichuan University. The inclusion criteria were as follows (1): aged 18–40 years (2),

clinically presumed International Federation of Gynecology and Obstetrics (FIGO) stage IA (3), pathologically diagnosed grade 1, endometrioid adenocarcinoma, and (4) no contraindication for progestin treatment. Exclusion criteria include inadequate quality of tumor tissues, unclear medication history, or no tissue available at our institution. The primary outcome was the complete response rate after FPT for each molecular group. A complete response (CR) was defined as no evidence of residual EC or atypical hyperplasia (AH) at follow-up endometrial sampling, diagnosed by hysteroscopic biopsy. Time until CR was measured from the treatment start date. The other pathologic responses to progestin treatment were defined as follows: Partial regression (PR) was defined as the presence of atypical hyperplasia (AH) during follow-up endometrial sampling by hysteroscopic biopsy. Disease persistence was defined as no evidence of disease regression was observed within 6 months. Disease progression is a lesion of higher grade or clinically progressive disease, including myometrial invasion, extrauterine disease, or lymph node metastasis. Recurrence was defined as the presence of EC or AH during follow-up after an endometrial sample indicated treatment response. Time to recurrence was defined as from the date of the complete response. Patient follow-up data were gathered until the end of 2020.

The evaluation of response before achieving CR was performed using dilation and curettage (D&C) or hysteroscopic biopsy every 3 months during the initial treatment for 2 years, then 6-monthly. Unless there was any evidence of progression in the follow-up endometrial biopsies and/or imaging studies, patients continued to receive initial treatment until they achieved CR.

Application of the ProMisE Classifier to Endometrial Biopsy Specimens

The FFPE biopsies of patients were evaluated according to the ProMisE algorithm based on IHC for MMR proteins, sequencing for the presence of POLE exonuclease domain mutations, and IHC for p53 (5, 12, 16). Tumors were categorized into one of the four ProMisE molecular subgroups: POLE-mutated, mismatch repair deficient (MMR-D), p53 wild-type (p53wt), and p53-abnormal (p53abn).

IHC for MMR and P53 Proteins

In the first step of the algorithm, a representative FFPE block was evaluated for the expression of the MMR proteins, namely, MLH1, MSH2, MSH6, and PMS2 by IHC. Sections were cut at 4 mm thickness and de-waxed in xylene and ethanol before rehydration. Researchers then blocked endogenous peroxidase activity by incubating sections in a 3% H2O2 solution in methanol at room temperature for 10 min. After antigen retrieval with citric acid (pH 6.0) at 121°C for 15 min, the sections were blocked with 10% normal goat serum and incubated overnight at 4°C with four antibodies: anti-hMLH1 (1:1,000; ProteinTech Group, Chicago, IL); anti-hMSH2 (1:100; ProteinTech Group, Chicago, IL); anti-hMSH6 (1:100; ProteinTech Group, Chicago, IL); and anti-hPMS2 (1:1,000; ProteinTech Group, Chicago, IL). After washing with PBS, the sections were incubated with biotinylated rabbit anti-goat immunoglobulin antibody (ZSGB-Bio Ltd., Beijing, China), and the slides were visualized by staining with diaminobenzidine (Dako Ltd., Glostrup, Denmark) and counterstained with hematoxylin. Protein expression in appendix tissue served as an internal positive control. For p53 immunostaining, the slides were incubated with p53 primary antibody (1:100; ProteinTech Group, Chicago, IL). Slides of high-grade serous ovarian cancer were used as positive controls.

We performed image acquisition (BA400Digital; MOTIC China Group Co., Ltd.) and quantitative analysis (Halo 101-WL-HALO-1; Indica Labs, USA) of the slides. The tumor was classified into the MMR-D subtype if IHC demonstrated a loss of MMR protein nuclear expression. Immunostaining for p53 was considered abnormal when there was no staining of tumor cell nuclei or strong and diffuse staining (absent p53 protein or aberrant increased protein accumulation, respectively), while intermediate levels of expression were considered wild-type.

DNA Extraction, Targeted Sequencing for POLE Mutation

Genomic DNA (gDNA) was extracted from FFPE using the Ezup Column Animal Genomic DNA Purification Kit (Sangon Biotech (Shanghai) Co., Ltd.). gDNA was amplified with the forward and reverse primers. After purified PCR products were detected by agarose gel electrophoresis (150 V, 100 mA, 10–20 min), DNA was extracted from the agarose gel by a SanPrep Column DNA Gel Extraction Kit (Sangon Biotech (Shanghai) Co., Ltd.), and then Sanger-sequenced with the BigDye terminator v1.1 sequencing kit and a 3730xl automated sequencer (Applied Biosystems, Foster City, CA, USA). The results were analyzed by Variant reporter software version 2.1 (Applied Biosystems).

Statistical Analysis

Data were collected retrospectively through chart review. Summary statistics are provided. Normally distributed continuous variables (age and body mass index (BMI)) were compared using Student's t-test; nonparametric continuous factors were compared using the Wilcoxon rank-sum test and proportions were compared using a chi-square test. Analyses were conducted using SPSS 22.0 (IBM Corp., Armonk, NY, USA).

RESULTS

Literature Review of the Three Previous Studies

After literature searching, we found three studies that tested the PromisE classifier on EC patients who received FPT so far (11–13). The characteristics and outcome measures of each study are summarized in **Table 1**. A total of 94 EC patients who underwent hormone therapy were classified by ProMisE in 3 studies and distributed as follows: 20 (21.3%) MMR-D, 3 (3.2%) POLE, 2 (2.1%) p53abn, and 69 (73.4%) p53wt. In the study by Falcone et al. (12), three cases had more than one molecular feature: MMR-D + p53abn (n = 1); MMR-D + POLE-

TABLE 1 | Molecular characterization of patients with endometrial cancer underwent FPT and outcomes.

Study	Characteristics	MMR-D	*POLE*-Mutated	p53abn	p53wt	P^1	Total
Chung et al. (11)	**Number**	**9 (15.8)**	**2 (3.5)**	**1 (1.8)**	**45 (78.9)**	–	**57**
	Age at diagnosis (years)	33 (26–40)	27, 34	33	31 (19–45)	0.382	33 (19–45)
	BMI (kg/m^2)	24.6 (18.8–41.3)	40.5, 20.2	20.0	26.8 (17.8–39.9)	0.265	25.7 (17.8–41.3)
	CR rate at 6 months	1 (11.1)	1 (1/2)	1 (1/1)	24 (53.3)	0.010	27 (47.4)
	Best overall response of CR/PR rate	4 (44.4)	1 (1/2)	1 (1/1)	37 (82.2)	0.018	43 (75.4)
	Recurrence rate after CR	1 (25.0)	1 (1/2)	1 (1/1)	16 (43.2)	0.629	19 (44.2)
	Hysterectomy	4 (44.4)	2 (2/2)	0 (0/1)	22 (48.9)	1.000	28 (49.1)
Falcone et al. (12)	**Number**	**7 (46.7)**	**1 (6.7)**	**0 (0)**	**7 (46.7)**		**15**
	Age at diagnosis (years)	38 (28–39)	36	–	37 (25–40)	–	37 (25–40)
	BMI (kg/m^2)	29.0 (24.3–53.5)	38.3	–	24.2 (22.7–33.1)	–	26.3 (22.7–53.3)
	CR rate at 6 months	5 (5/7)	1 (1/1)	–	7 (7/7)	–	13 (13/15)
	Best overall response of CR/PR rate	5 (5/7)	1 (1/1)	–	7 (7/7)	–	13 (13/15)
	Recurrence rate after CR	1 (1/7)	0 (0/1)	–	2 (2/7)	–	3 (3/15)
	Hysterectomy	2 (2/7)	0 (0/1)	–	2 (2/7)	–	4 (4/15)
Puechl et al. (13)	**Number**	**4 (18.2)**	**0 (0)**	**1 (6.7)**	**17 (77.3)**	–	**22**
	CR rate at 6 months	3 (3/4)	–	0 (0/1)	13 (76.5)	–	–
	Best overall response of CR/PR rate	3 (3/4)	–	0 (0/1)	13 (76.5)	–	16 (72.7)
	Progression or required definitive treatment	1 (1/4)	–	1 (1/1)	4 (23.5)	–	6 (27.3)
	Hysterectomy	1 (1/4)	–	1 (1/1)	4 (23.5)	–	6 (100.0)
Summary of the 3 studies	**Number**	**20 (21.3)**	**3 (3.2)**	**2 (2.1)**	**69 (73.4)**	–	**94**
	CR rate at 6 months	9 (45.0)	2 (2/3)	1 (1/2)	44 (63.8)	0.195	56 (59.6)
	Best overall response of CR/PR rate	12 (60.0)	2 (2/3)	1 (1/2)	57 (82.6)	0.040	72 (76.6)
	Recurrence rate after CR	3 (15.0)	1 (1/3)	2 (2/2)	22 (31.9)	0.168	28 (29.8)
	Hysterectomy	7 (35.0)	2 (2/3)	1 (1/2)	28 (40.6)	0.796	38 (40.4)

Data are presented as median (range) or n (%). [1]Patients with POLE-mutated or p53abn were excluded.
MMR-D, mismatch repair deficient; abn, abnormal; wt, wild type; BMI, body mass index; CR, complete regression; PR, partial response; -, not available.

mutated subtypes (n = 2). The rest of all cases demonstrated one molecular feature.

The oncologic outcomes of the three studies are presented. Chung et al. reported the following CR rates at 6 months of the four ProMisE subtypes: 1 (11.1%) MMR-D, 1 (1/2) POLE, 1 (1/1) p53abn, and 24 (53.3%) p53wt; best overall response of CR/PR rate: 4 (44.4%) MMR-D and 37 (82.2%) p53wt; recurrence rate after CR: 1 (25.0%) MMR-D, 1 (1/2) POLE, 1 (1/1) p53abn, and 16 (43.2%) p53wt. Falcone et al. stated the CR rate at 6 months as follows: 5 (5/7) MMR-D, 1 (1/1) POLE, and 7 (7/7) p53wt; recurrence rate after CR: 1 (1/7) MMR-D and 2 (2/7) p53wt. Puechl et al. reported a CR rate at 6 months: 3 (3/4) MMR-D and 13 (76.5%) p53wt, with 1 (1/4) MMR-D, 1 (1/1) p53abn, and 4 (23.5) p53wt having progression or requiring definitive treatment. After combining the results of three studies, patients with MMR-D showed a lower overall response rate of CR/PR rate than those with the p53wt subtype (60.0% vs 82.6%, P = 0.040), which was consistent with the result of Chung et al. (11). The combined CR rate after 6 months of hormone therapy in the MMR-D group had no significant difference compared with p53wt subgroup, however, Chung et al. (11) reported a lower rate in MMR-D patients. Puechl et al. (13) reported that 1/4 of EC patients with MMR-D and 4/17 with p53wt developed progression or underwent definitive surgery after levonorgestrel intrauterine system (LNG-IUS) treatment. They also included 37 endometrial intraepithelial neoplasia (EIN) patients. After adding them to EC patients (n = 59), p53abn tumors exhibited the shortest time to progression or definitive therapy. Due to the small sample size, Falcone et al. (12) did not conclude that there were significant differences in outcomes among subtypes.

From combined studies, we found that, similar to the result of Chung et al. (11), the MMR-D subtype was associated with a worse overall response rate compared to the p53wt subtype in women with EC who underwent FPT. However, larger samples changed the comparison outcomes of the CR rate at 6 months after treatment between MMR-D and p53wt subtypes. Therefore, studies are needed to further test whether the MMR-D subtype could predict response in women with endometrial cancer treated conservatively. Besides, owing to the limited sample size, the POLE-mutated and p53abn subtypes in predicting hormone response also need to be further explored.

Results of the Current Study

Owing to the limited samples and changed outcomes after the combination of previous studies, we performed further exploration to test the prognostic ability of the ProMisE classifier in EC patients who underwent FPT. Thirteen patients with Grade 1 endometrioid adenocarcinoma who underwent FPT; pretreatment formalin-fixed, paraffin-embedded (FFPE) tissues in our institution were included. The study flowchart is shown in **Figure 1**. A total of 49 Grade 1 endometrioid adenocarcinoma (EAC) patients who underwent FPT between 2010 and 2020 in the West China University Hospital were first identified; 35 patients had their pre-treatment biopsies obtained in other hospitals, and 1 patient lost survival information. Finally, 13 patients were enrolled in the ProMisE algorithm application.

Immunohistochemistry (IHC) for MMR proteins was performed in the first step. Three cases exhibited a loss of MMR proteins and were categorized as MMR-D subtype. MMR-intact cases were then evaluated for POLE mutations by Sanger

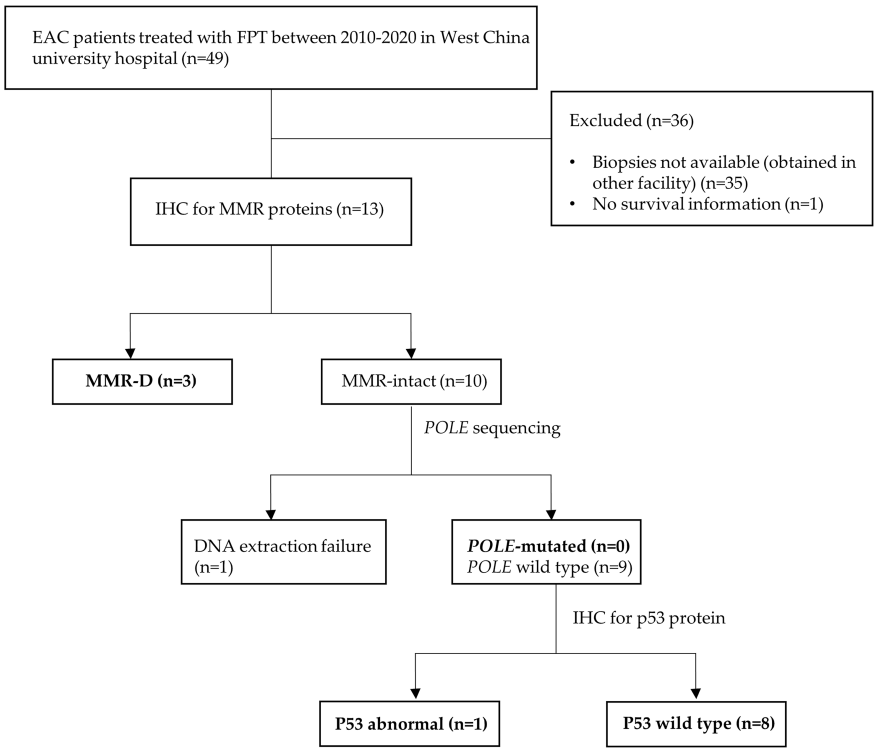


FIGURE 1 | Flow chart of patient selection and ProMise algorithm apllication.

sequencing. Nine cases showed POLE wild-type and one case failed DNA amplification. Then, POLE wild-type cases were subjected to IHC for p53, one case showed p53 overexpression and was classified as p53abn subtype. In summary, the molecular classification of the 13 cases presented the following ProMisE subtypes: 3 (3/13) MMR-D, 0 (0/13) POLE, 8 (8/13) p53wt, 1 (1/13) p53abn, and 1 (1/13) failed with DNA amplification. No cases showed more than one molecular feature. The detailed molecular features of all patients are summarized in **Table 2**.

The clinical–pathological characteristics, treatment, oncologic, and pregnancy outcomes of the patients are detailed in **Table 3**. The mean age of the cohort was 29.8 ± 4.3 years and the mean body mass index (BMI) was 25.4 ± 7.1 (kg/m^2). All patients had an initial diagnosis of Grade 1 endometrioid adenocarcinoma (EAC). Four of thirteen cases were diagnosed *via* hysteroscopy, and 9/13 *via* dilation and curettage (D&C). Patients received treatment, namely, megestrol acetate (MA), medroxyprogesterone acetate (MPA), goserelin acetate, and

TABLE 2 | Molecular classification by ProMisE algorithm of all the patients.

Patients (No.)	Age at diagnosis (years)	ProMisE subtype	MMR IHC abnormal	*POLE* mutation	p53 IHC
1	31	p53wt	–	–	p53wt
2	35	MMR-D	MSH6	–	p53wt
3	23	p53wt	–	–	p53wt
4	29	p53wt	–	–	p53wt
5	28	p53wt	–	–	p53wt
6	33	p53wt	–	–	p53wt
7	26	–	–	DNA amplification failure	p53wt
8	34	p53abn	–	–	p53abn
9	29	p53wt	–	–	p53wt
10	23	p53wt	–	–	p53wt
11	29	p53wt	–	–	p53wt
12	31	MMR-D	MSH6	–	p53wt
13	37	MMR-D	MSH2; MSH6	–	p53wt

IHC, immunohistochemistry; MMR, mismatch repair; MSH6, MutS homolog 6; MSH2, MutS homolog 2; MMR-D, mismatch repair deficient.

TABLE 3 | Demographics, clinical–pathological characteristics, treatment, oncologic outcomes of the EC patients who underwent FPT.

Patients (No.)	Age at diagnosis (years)	BMI (kg/m^2)	Pre-diagnosis GxPx	Pathology	Diagnostic method	Treatment, mg/day	Treatment duration, months
1	31	21.9	G0P0	G1 EAC	D&C	MA, 160 + MPA, 250	3 +3
2	35	20.4	G2P1	G1 EAC	Hysteroscopy	MA, 160	3
3	23	20.7	G0P0	G1 EAC	D&C	MA, 160	6
4	29	18.4	G1P0	G1 EAC	D&C	MA, 160	3
5	28	30.8	G0P0	G1 EAC	Hysteroscopy	MA, 160 + LNG-IUS	6 + 5
6	33	37.6	G0P0	G1 EAC	D&C	MA, 160 + LNG-IUS	6
7	26	26.6	G0P0	G1 EAC	Hysteroscopy	MPA, 250 + LNG-IUS	10
8	34	39.4	G2P0	G1 EAC	Hysteroscopy	MPA, 500	24
9	29	30.7	G0P0	G1 EAC	Hysteroscopy	LNG-IUS	12
10	23	24.8	G0P0	G1 EAC	Hysteroscopy	LNG-IUS	11
11	29	18.6	G0P0	G1 EAC	Hysteroscopy	MA, 160	3
12	31	20.4	G0P0	G1 EAC	Hysteroscopy	MPA, 250 + LNG-IUS	4
13	37	20.3	G0P0	G1 EAC	Hysteroscopy	MA, 160 + GnRH-A (i.m)	1month + 4 times

Patients (No.)	Follow-up duration, months	Oncologic outcome at 6 months	Final diagnosis	Recurrence (months)	Second cancer (months)	Hysterectomy	Current status	GxPx at the end of the treatment
1	138	CR	Normal	–	–	No	NED	G0P0
2	120	CR	Normal	–	–	No	NED	G2P1
3	123	CR	Normal	107	Ovarian cancer (107)	Yes	AWD	G0P0
4	84	CR	Normal	–	–	Yes	NED	G1P0
5	60	Progression[1]	EAC	–	–	Yes	NED	G0P0
6	48	CR	Normal	–	–	No	NED	G0P0
7	46	CR	Normal	–	–	No	NED	G0P0
8	27	PR	Normal	–	–	No	NED	G2P0
9	15	CR	Normal	–	–	No	NED	G0P0
10	11	CR	Normal	–	–	No	NED	G0P0
11	12	Persistent	EAC	–	–	Yes	NED	G0P0
12	15	CR	Normal	–	–	No	NED	G0P0
13	13	Persistent	EAC	–	–	Yes	NED	G0P0

[1]*Definitive surgery at 5 months.*

BMI, body mass index; G, gravida; P, para; G1, Grade 1; D&C, dilation and curettage; EAC, endometrioid adenocarcinoma; MA, megestrol acetate; MPA, medroxyprogesterone acetate; LNG-IUS, Levonorgestrel-releasing intrauterine system; GnRH-A, Gonadotropin-releasing hormone agonist; i.m, intramuscular injection; CR, complete response; AWD, alive with disease; NED, no evidence of disease.

levonorgestrel. The average time of the treatment was 7.7 months, ranging from 3 to 24 months. Ten of thirteen patients had a complete response after hormone treatment at 6 months. Patient No. 3 was found with disease progression and an ovarian mass after 107 months of complete response and was treated by definitive surgery, showing a stage IA G2 endometrioid ovarian cancer (OC) and synchronous asymptomatic endometrioid G2 EC.

Three patients had disease progression and persistent disease, respectively. Patient No. 5 had p53wt mutation-developed disease progression after 6 months of MA plus 5 months of LNG-IUS therapy. The final diagnosis showed stage IA G1 endometrioid EC. Patient No. 11 with p53wt mutation kept persistent after 3 months of MA treatment, then underwent definitive surgery immediately. Patient No. 13 with MMR-D underwent genetic testing and did not suggest Lynch syndrome. MRI of the patient showed minimal myometrial infiltration and it was not recommended to continue FPT after 1 month of MA treatment and 4 GnRH-A injections. Overall, 12 patients were alive and had no evidence of disease; 1 patient was alive with ovarian cancer at the end of the follow-up.

Finally, we combined our results with the three previous studies. The molecular characterization and outcomes are detailed in **Table 4**. A total of 106 EC patients who underwent hormone therapy were included after the combination of the 4 studies. p53wt was still the most common subtype and was observed in 77 cases (72.6%). MMR-D was found in 23 cases (21.7%) and was presented as the second most common subtype.

TABLE 4 | Molecular characterization and outcomes of the 4 studies.

Study	Characteristics	MMR-D	*POLE*-Mutated	p53abn	p53wt	*P*[1]	Total
Summary of the 4 studies	Number	23 (21.7)	3 (2.8)	3 (2.8)	77 (72.6)	–	106
	CR rate at 6 months	11 (47.8)	2 (2/3)	2 (2/3)	50 (64.9)	0.152	64 (60.4)
	Best overall response of CR/PR rate	14 (60.9)	2 (2/3)	2 (2/3)	62 (80.5)	0.092	80 (75.6)
	Recurrence rate after CR/Progression	3 (13.0)	1 (1/3)	2 (2/3)	23 (29.9)	0.174	29 (27.4)
	Hysterectomy	8 (34.8)	2 (2/3)	1 (1/3)	32 (41.6)	0.633	43 (40.6)

[1]*Patients with POLE-mutated (n = 3) or p53abn (n = 3) were excluded.*

Patients were classified as the following subtypes: 23 (21.7%) MMR-D, 3 (2.8%) POLE-mutated, 3 (2.8%) p53abn, and 77 (72.6%) p53wt. We compared the outcomes of the MMR-D subtype and the p53wt subtype, and we found there was no significant difference in the CR rate after treatment at 6 months between the two groups (47.8% vs. 64.9%, P = 0.152) and overall response of CR/PR rate (60.9% vs. 80.5%, P = 0.092). Recurrence rates were 13.0 and 29.9% in the MMR-D and p53wt subtypes, respectively, which also showed no significant difference (P = 0.174). Of 43 patients with treatment failure or progression who underwent hysterectomy, there was no significant difference between the two groups either.

DISCUSSION

This study evaluated the prognostic ability of the ProMisE classifier in early-stage EC patients after FPT. We found no significant difference in the CR rate (P = 0.152) between the MMR-D and p53wt subtypes after FPT. The other oncologic outcomes, including overall response, CR/PR rate, and recurrence rate, also showed no significant difference. Based on current results, we observed no prognostic significance for the ProMisE classifier in EC patients who underwent FPT.

Due to the inadequate ability to refine prognostication or assess treatment efficacy in the last decade, the traditional systems of histo-morphological classification and risk group stratification of EC have been challenged by molecular-based classification. The Cancer Genome Atlas (TCGA) endometrial collaborative project discovered four distinct prognostic EC subtypes based on genomic abnormalities, identifying four molecularly defined prognostic subgroups (10). Later, the analogous but simplified ProMisE classifier was developed and validated, showing high concordance between diagnostic and hysterectomy specimens (5, 17). A few previous studies have applied the ProMisE classifier to EC patients who were conservatively treated, and our study further tested the ProMisE molecular classification system on EC patients who underwent FPT. Our results showed a two-type molecular heterogeneity (MMR-D and p53wt subtypes) within a group of G1 EACs and relatively homogeneous good survival outcomes at present.

We found 3/13 cases of MMR-D at IHC analysis. Patient No. 13 with MMR-D did not suggest Lynch syndrome and had a hysterectomy due to persistent disease. The other two MMR-D patients had a good response to hormone therapy, and they did not undergo LS testing. Similar to the small sample study by Falcone et al. (12), they found about 50% (7/15) MMR defects at IHC analysis and clinical outcome, with 4 of 7 mutated patients showing EC persistence/progression or metachronous Lynch syndrome-associated tumors. The different distributions and outcomes were likely due to the study populations.

We finally combined the outcomes of four studies with the same purpose. The combined results showed four ProMisE subtype distributions as follows: 77 (72.6%) p53wt, 23 (21.7%) MMR-D, 3 (2.8%) POLE-mutated, and 3 (2.8%) p53abn. There were no significant differences in CR rate and recurrence rate between MMR-D and p53wt subtypes, which broke the hypotheses based on validated ProMisE in large cohorts of EC patients and indicated that MMR-D could predict good or poor responses to FPT in EC patients. Our results were different from the pre-combined study and opinions (11, 18–20). The reason for this difference may be attributed to the study population due to the lack of mechanism evidence between MMR deficiency and hormone therapy in EC patients. From previous clinical studies, we also found a controversial relationship between MMR-D and hormone-treated outcomes of EC. Britton et al. (18) first applied the ProMisE classifier to a large cohort of young EC women (<50 years of age) after ProMisE was validated in the non-age stratified cohorts (17) and reported that MMR-D is associated with poorer outcomes compared to p53wt, including overall, disease-specific, and progression-free survival. However, several studies hold different opinions about whether MMR-D can be a predictive biomarker for hormone therapy in EC women. Zakhour et al. (21) found 5/84 EAC patients with MMR-D who underwent progestin therapy and none of the MMR-D patients responded to progestin. Chung et al. (11) found MMR-D had poor outcomes after hormone therapy in early-stage EC. Gallos et al. (22) found no associations between MLH1 protein expression and regression/relapse of women with endometrial hyperplasia treated with LNG-IUS. A hypothesis indicated that MMR-deficient may reduce the function of progesterone receptor (23), however, its reaction to progesterone therapy remained unclear (24, 25). In this regard, further validation is needed to assess the relationship between MMR-D and progestin response in EC patients who received FPT.

Our results showed rare POLE mutated and p53abn subtypes and a much higher proportion of p53wt and MMR-D subtypes than the EC cohort <50 yo at diagnosis (18). A possible reason for this difference may be the loss of POLE patients during the selection of large volume tumor blocks for DNA extraction or population characteristics.

Other factors that have been studied to predict the efficacy of fertility sparing treatment of EC. Travaglino et al. (26) assessed the predictive significance of PTEN and found it seemed not to be useful as a predictive marker of response to conservative treatment of EC, suggesting that PTEN is not applicable as a stand-alone predictive marker. Raffone et al. (27) reported that mismatch repair protein deficiency appears as a highly specific predictor of recurrence of EEC after initial regression. Clinical factors, such as longer menstrual cycles and infrequent menstrual bleeding, also appeared as independent predictive factors for conservative treatment failure in EEC (28). Weak stromal expression of isoform B of the progesterone receptor (PRB) was also found as a highly sensitive predictive marker of both no response and recurrence of EEC conservatively treated (29). Besides, many of the non-coding RNAs (ncRNAs) also reported a prognosis prediction function and remarkable importance in defining the therapeutic and surveillance path of EC patients, such as lncRNA and sncRNA (30). Both lncRNA and sncRNA functionally interact with EC diagnostic and prognostic genes and may be a valuable alternative marker for risk evaluation to aid patient-tailored treatment and improve the

outcome of patients with EC (31). Further prospective studies, suggest that all of these factors, combined with the ProMisE classifiers, might represent valuable biomarkers to improve risk stratification for EC patients who underwent fertility sparing treatment.

This study combined the eligible outcomes of the FPT response with the implementation of ProMisE in EC patients. Based on current data, we observed no prognostic information from the classifier for conservatively treated patients. However, this study is limited by the lack of assessment of outcomes for POLE-mt and p53abn patients due to the limited sample size, retrospective nature, and heterogeneity in classification methods across a combination of several studies. Future evaluation is warranted to determine whether molecular classification predicts outcomes for patients considering hormone therapy for endometrial cancer.

DATA AVAILABILITY STATEMENT

The original contributions presented in the study are included in the article/**Supplementary Material**. Further inquiries can be directed to the corresponding author.

ETHICS STATEMENT

The studies involving human participants were reviewed and approved by the ethics committee of West China Second University Hospital, Sichuan University. The ethics committee waived the requirement of written informed consent for participation.

AUTHOR CONTRIBUTIONS

Methodology, formal analysis, investigation, writing—original draft preparation, XR. Methodology, formal analysis, investigation, TH. Conceptualization, formal analysis, investigation, resources, data curation, writing—review and editing, supervision, project administration, funding acquisition, ZL. All authors listed have made a substantial, direct, and intellectual contribution to the work and approved it for publication.

FUNDING

This research was funded by the Department of Science and Technology of Sichuan Province, grant number 2019YJ0072.

SUPPLEMENTARY MATERIAL

The Supplementary Material for this article can be found online at: https://www.frontiersin.org/articles/10.3389/fonc.2022.810631/full#supplementary-material

REFERENCES

1. Sung H, Ferlay J, Siegel RL, Laversanne M, Soerjomataram I, Jemal A, et al. Global Cancer Statistics 2020: GLOBOCAN Estimates of Incidence and Mortality Worldwide for 36 Cancers in 185 Countries. *CA Cancer J Clin* (2021) 71(3):209–49. doi: 10.3322/caac.21660
2. Corzo C, Barrientos Santillan N, Westin SN, Ramirez PT. Updates on Conservative Management of Endometrial Cancer. *J Minim Invasive Gynecol* (2018) 25(2):308–13. doi: 10.1016/j.jmig.2017.07.022
3. Koh WJ, Abu-Rustum NR, Bean S, Bradley K, Campos SM, Cho KR, et al. Uterine Neoplasms, Version 1.2018, NCCN Clinical Practice Guidelines in Oncology. *J Natl Compr Canc Netw* (2018) 16(2):170–99. doi: 10.6004/jnccn.2018.0006
4. Lucchini SM, Esteban A, Nigra MA, Palacios AT, Alzate-Granados JP, Borla HF. Updates on Conservative Management of Endometrial Cancer in Patients Younger Than 45 Years. *Gynecol Oncol* (2021) 161(3):802–9. doi: 10.1016/j.ygyno.2021.04.017
5. Talhouk A, McConechy MK, Leung S, Li-Chang HH, Kwon JS, Melnyk N, et al. A Clinically Applicable Molecular-Based Classification for Endometrial Cancers. *Br J Cancer* (2015) 113(2):299–310. doi: 10.1038/bjc.2015.190
6. Capozzi VA, Rosati A, Rumolo V, Ferrari F, Gullo G, Karaman E, et al. Novelties of Ultrasound Imaging for Endometrial Cancer Preoperative Workup. *Minerva Med* (2021) 112(1):3–11. doi: 10.23736/S0026-4806.20.07125-6
7. Mitsuhashi A, Habu Y, Kobayashi T, Kawarai Y, Ishikawa H, Usui H, et al. Long-Term Outcomes of Progestin Plus Metformin as a Fertility-Sparing Treatment for Atypical Endometrial Hyperplasia and Endometrial Cancer Patients. *J Gynecol Oncol* (2019) 30(6):e90. doi: 10.3802/jgo.2019.30.e90
8. Falcone F, Leone Roberti Maggiore U, Di Donato V, Perrone AM, Frigerio L, Bifulco G, et al. Fertility-Sparing Treatment for Intramucous, Moderately Differentiated, Endometrioid Endometrial Cancer: A Gynecologic Cancer Inter-Group (GCIG) Study. *J Gynecol Oncol* (2020) 31(5):e74. doi: 10.3802/jgo.2020.31.e74
9. Casadio P, La Rosa M, Alletto A, Magnarelli G, Arena A, Fontana E, et al. Fertility Sparing Treatment of Endometrial Cancer With and Without Initial Infiltration of Myometrium: A Single Center Experience. *Cancers (Basel)* (2020) 12(12):3571. doi: 10.3390/cancers12123571
10. Kandoth C, Schultz N, Cherniack AD, Akbani R, Liu Y, Shen H, et al. Integrated Genomic Characterization of Endometrial Carcinoma. *Nature* (2013) 497(7447):67–73. doi: 10.1038/nature12113
11. Chung YS, Woo HY, Lee JY, Park E, Nam EJ, Kim S, et al. Mismatch Repair Status Influences Response to Fertility-Sparing Treatment of Endometrial Cancer. *Am J Obstet Gynecol* (2021) 224(4):370.e1–370.e13. doi: 10.1016/j.ajog.2020.10.003
12. Falcone F, Normanno N, Losito NS, Scognamiglio G, Esposito Abate R, Chicchinelli N, et al. Application of the Proactive Molecular Risk Classifier for Endometrial Cancer (ProMisE) to Patients Conservatively Treated: Outcomes From an Institutional Series. *Eur J Obstet Gynecol Reprod Biol* (2019) 240:220–5. doi: 10.1016/j.ejogrb.2019.07.013
13. Puechl AM, Spinosa D, Berchuck A, Secord AA, Drury KE, Broadwater G, et al. Molecular Classification to Prognosticate Response in Medically Managed Endometrial Cancers and Endometrial Intraepithelial Neoplasia. *Cancers (Basel)* (2021) 13(11):2847. doi: 10.3390/cancers13112847
14. Whiting PF, Rutjes AW, Westwood ME, Mallett S, Deeks JJ, Reitsma JB, et al. QUADAS-2: A Revised Tool for the Quality Assessment of Diagnostic Accuracy Studies. *Ann Intern Med* (2011) 155(8):529–36. doi: 10.7326/0003-4819-155-8-201110180-00009
15. Ubachs J, Ziemons J, Minis-Rutten IJG, Kruitwagen RFPM, Kleijnen J, Lambrechts S, et al. Sarcopenia and Ovarian Cancer Survival: A Systematic Review and Meta-Analysis. *J Cachexia Sarcopenia Muscle* (2019) 10(6):1165–74. doi: 10.1002/jcsm.12468
16. Talhouk A, McConechy MK, Leung S, Yang W, Lum A, Senz J, et al. Confirmation of ProMisE: A Simple, Genomics-Based Clinical Classifier for Endometrial Cancer. *Cancer* (2017) 123(5):802–13. doi: 10.1002/cncr.30496

17. Kommoss S, McConechy MK, Kommoss F, Leung S, Bunz A, Magrill J, et al. Final Validation of the ProMisE Molecular Classifier for Endometrial Carcinoma in a Large Population-Based Case Series. *Ann Oncol* (2018) 29 (5):1180–8. doi: 10.1093/annonc/mdy058
18. Britton H, Huang L, Lum A, Leung S, Shum K, Kale M, et al. Molecular Classification Defines Outcomes and Opportunities in Young Women With Endometrial Carcinoma. *Gynecol Oncol* (2019) 153(3):487–95. doi: 10.1016/j.ygyno.2019.03.098
19. Stewart KI, Yates MS, Westin SN. Pushing the Envelope: Expanding Fertility Sparing Treatment of Endometrial Cancer. *J Gynecol Oncol* (2020) 31(5):e82. doi: 10.3802/jgo.2020.31.e82
20. Son J, Carr C, Yao M, Radeva M, Priyadarshini A, Marquard J, et al. Endometrial Cancer in Young Women: Prognostic Factors and Treatment Outcomes in Women Aged ≤40 Years. *Int J Gynecol Cancer* (2020) 30(5):631–9. doi: 10.1136/ijgc-2019-001105
21. Zakhour M, Cohen JG, Gibson A, Walts AE, Karimian B, Baltayan A, et al. Abnormal Mismatch Repair and Other Clinicopathologic Predictors of Poor Response to Progestin Treatment in Young Women With Endometrial Complex Atypical Hyperplasia and Well-Differentiated Endometrial Adenocarcinoma: A Consecutive Case Series. *Bjog* (2017) 124(10):1576–83. doi: 10.1111/1471-0528.14491
22. Gallos ID, Devey J, Ganesan R, Gupta JK. Predictive Ability of Estrogen Receptor (ER), Progesterone Receptor (PR), COX-2, Mlh1, and Bcl-2 Expressions for Regression and Relapse of Endometrial Hyperplasia Treated With LNG-IUS: A Prospective Cohort Study. *Gynecol Oncol* (2013) 130 (1):58–63. doi: 10.1016/j.ygyno.2013.04.016
23. Derbyshire AE, Ryan N, Crosbie EJ. Biomarkers Needed to Predict Progestin Response in Endometrial Cancer. *Bjog* (2017) 124(10):1584. doi: 10.1111/1471-0528.14490
24. Chen M, Jin Y, Li Y, Bi Y, Shan Y, Pan L. Oncologic and Reproductive Outcomes After Fertility-Sparing Management With Oral Progestin for Women With Complex Endometrial Hyperplasia and Endometrial Cancer. *Int J Gynaecol Obstet* (2016) 132(1):34–8. doi: 10.1016/j.ijgo.2015.06.046
25. Zhou R, Yang Y, Lu Q, Wang J, Miao Y, Wang S, et al. Prognostic Factors of Oncological and Reproductive Outcomes in Fertility-Sparing Treatment of Complex Atypical Hyperplasia and Low-Grade Endometrial Cancer Using Oral Progestin in Chinese Patients. *Gynecol Oncol* (2015) 139(3):424–8. doi: 10.1016/j.ygyno.2015.09.078
26. Travaglino A, Raffone A, Saccone G, Insabato L, Mollo A, De Placido G, et al. PTEN as a Predictive Marker of Response to Conservative Treatment in Endometrial Hyperplasia and Early Endometrial CancerA Systematic Review and Meta-Analysis. *Eur J Obstet Gynecol Reprod Biol* (2018) 231:104–10. doi: 10.1016/j.ejogrb.2018.10.025
27. Raffone A, Catena U, Travaglino A, Masciullo V, Spadola S, Della Corte L, et al. Mismatch Repair-Deficiency Specifically Predicts Recurrence of Atypical Endometrial Hyperplasia and Early Endometrial Carcinoma After Conservative Treatment: A Multi-Center Study. *Gynecol Oncol* (2021) 161 (3):795–801. doi: 10.1016/j.ygyno.2021.03.029
28. Raffone A, Travaglino A, Flacco ME, Iasevoli M, Mollo A, Guida M, et al. Clinical Predictive Factors of Response to Treatment in Patients Undergoing Conservative Management of Atypical Endometrial Hyperplasia and Early Endometrial Cancer. *J Adolesc Young Adult Oncol* (2021) 10(2):193–201. doi: 10.1089/jayao.2020.0100
29. Raffone A, Travaglino A, Zullo FM, Gencarelli A, Micheli M, Miranda S, et al. Predictive Accuracy of Progesterone Receptor B in Young Women With Atypical Endometrial Hyperplasia and Early Endometrial Cancer Treated With Hysteroscopic Resection Plus LNG-IUD Insertion. *J Minim Invasive Gynecol* (2021) 28(6):1244–53. doi: 10.1016/j.jmig.2020.10.009
30. Cavaliere AF, Perelli F, Zaami S, Piergentili R, Mattei A, Vizzielli G, et al. Towards Personalized Medicine: Non-Coding RNAs and Endometrial Cancer. *Healthcare (Basel)* (2021) 9(8):965. doi: 10.3390/healthcare9080965
31. Piergentili R, Zaami S, Cavaliere AF, Signore F, Scambia G, Mattei A, et al. Non-Coding RNAs as Prognostic Markers for Endometrial Cancer. *Int J Mol Sci* (2021) 22(6):3151. doi: 10.3390/ijms22063151

Conflict of Interest: The authors declare that the research was conducted in the absence of any commercial or financial relationships that could be construed as a potential conflict of interest.

Publisher's Note: All claims expressed in this article are solely those of the authors and do not necessarily represent those of their affiliated organizations, or those of the publisher, the editors and the reviewers. Any product that may be evaluated in this article, or claim that may be made by its manufacturer, is not guaranteed or endorsed by the publisher.

Copyright © 2022 Ran, Hu and Li. This is an open-access article distributed under the terms of the Creative Commons Attribution License (CC BY). The use, distribution or reproduction in other forums is permitted, provided the original author(s) and the copyright owner(s) are credited and that the original publication in this journal is cited, in accordance with accepted academic practice. No use, distribution or reproduction is permitted which does not comply with these terms.

frontiers | Frontiers in Oncology

SYSTEMATIC REVIEW
published: 25 May 2022
doi: 10.3389/fonc.2022.796983

Efficacy and Safety of Placebo During the Maintenance Therapy of Ovarian Cancer in Randomized Controlled Trials: A Systematic Review and Meta-analysis

Jin-feng Wang[1], Lan-bo Zhao[1], Ya-di Bin[1], Kai-lu Zhang[1], Chao Sun[1], Yi-ran Wang[1], Xue Feng[1], Jing Ji[1], Li-song He[2], Fang-yao Chen[3] and Qi-ling Li[1]**

[1] Department of Obstetrics and Gynecology, First Affiliated Hospital of Xi'an Jiaotong University, Xi'an, China, [2] School of Finance, Xi'an Eurasia University, Xi'an, China, [3] Department of Epidemiology and Biostatistics, School of Public Health, Xi'an Jiaotong University Health Science Center, Xi'an, China

Introduction: This meta-analysis evaluated the efficacy and safety of placebo during the maintenance therapy of ovarian cancer (OC) patients in randomized controlled trials (RCTs).

Methods: A comprehensive literature review was performed for RCTs published up to and including August 2020 from four electronic databases. We analyzed the efficacy and safety in the control arms of the maintenance therapy in advanced OC patients. Hazard ratios (HRs) and the corresponding 95% confidence intervals (CIs) of progression-free survival (PFS) and overall survival (OS) were estimated in the placebo arms and the observation arms, respectively, using the Frequency Framework method. We also calculated the incidences of common adverse effects (AEs) in the placebo arms.

Results: In total, 41 articles with 20,099 (4,787 in the placebo arms, 3,420 in the observation arms, and 11,892 in the experiment arms) patients were included in this meta-analysis. Compared with observation, placebo did not improve or reduce PFS (HR, 1.02; 95% CI, 0.87–1.20; $P = 0.81$) and OS (HR, 1.02; 95% CI, 0.89–1.16; $P = 0.76$) of OC patients, while other treatments, except for radiotherapy, significantly improved PFS and OS (all $P < 0.05$). The incidences of AEs produced by placebo were 94.03% in all grades and 20.22% in grade ≥3. The incidences of AEs were 29.75% in fatigue, 26.38% in nausea, 24.34% in abdominal pain, 18.92% in constipation, 16.65% in diarrhea, 14.55% in vomiting, 13.89% in hypertension, and 13.14% in headache.

Conclusions: Placebo did not improve or reduce the PFS and OS benefits of OC patients in RCTs but increased the incidences of AEs.

Keywords: ovarian cancer, maintenance therapy, efficacy, safety, placebo, randomized controlled trials

OPEN ACCESS

Edited by:
Cara Mathews, Women and Infants Hospital of Rhode Island, United States

Reviewed by:
Luigi Turco, Mater Olbia Hospital, Italy
Richard Penson, Harvard Medical School, United States

****Correspondence:***
Qi-ling Li
liqiling@mail.xjtu.edu.cn
Fang-yao Chen
chenfy@mail.xjtu.edu.cn

Specialty section:
This article was submitted to Gynecological Oncology, a section of the journal Frontiers in Oncology

Received: *18 October 2021*
Accepted: *22 April 2022*
Published: *25 May 2022*

Citation:
Wang J-f, Zhao L-b, Bin Y-d, Zhang K-l, Sun C, Wang Y-r, Feng X, Ji J, He L-s, Chen F-y and Li Q-l (2022) Efficacy and Safety of Placebo During the Maintenance Therapy of Ovarian Cancer in Randomized Controlled Trials: A Systematic Review and Meta-analysis. Front. Oncol. 12:796983. doi: 10.3389/fonc.2022.796983

INTRODUCTION

Ovarian cancer (OC) is one of the most common malignant reproductive tumors in women, with high recurrence rate and high mortality. Its median progression-free survival (PFS) and median overall survival (OS) range from 16 to 21 months and from 24 to 60 months, respectively (1). OC is the main cause of death among women in the USA and worldwide, accounting for the fifth and eighth, respectively (2, 3). In 2021, a total of 21,410 newly diagnosed cases and 13,770 deaths due to OC were estimated in America (2).

The standard first-line therapy of OC is debulking surgery in combination with chemotherapy based on paclitaxel and platinum, which can relieve the symptoms of the patients and achieve no evidence of disease progression temporarily. About 70% of the patients encounter a recurrence within 3 years (4). Therefore, many researchers put forward maintenance therapy, including extra-chemotherapy, immunotherapy, antiangiogenic inhibitors (AIs), selective small-module (SSM) inhibitors, and poly-ADP-ribose polymerase (PARP) inhibitors (4–8). All of them were added following complete or partial remission of chemotherapy in order to eschew disease progression and increase PFS and OS. Many randomized controlled trials (RCTs) further confirmed the efficacy and the safety of these maintenance therapies (4, 9–11). Some maintenance drugs, such as olaparib and niraparib, have shown significant positive effects on PFS and OS (4, 9). Most clinical trials on immunotherapy (7, 12–15), chemotherapy (6, 16–18), and SSM inhibitors (8) exhibited negative effects on PFS and OS, with a few studies gaining opposite results (16, 19). However, whether the control arms of RCTs, including placebo or observation, basically have effects on survival in the maintenance process is undefined. Until now, scarce reports have been published on the positive effects of placebo in RCTs.

Placebo, with a long history, mainly contains three forms: pharmacologic (a tablet), physical (a manipulation), and psychological (a conversation) (20). Recently, placebo tablets, an inert substance, have been administrated blindly to patients in clinical trials with an expectation for such to produce clinical benefits through the interaction with a caregiver and healthcare systems (21). The positive effects produced by placebo in clinical trials are not affected by its pharmacologic or physiologic properties (22). The positive effects are the evolution of the disease process altered in a positive direction (22). Researchers compared the differences between placebo and observation directly in the aspects of subjective and objective outcomes, including pain, psychopathy, hypertension, and so on (20). They found that placebo exhibited a few benefits on continuous subjective outcomes and the treatment of pain, but it did not have effects on objective or binary outcomes. Jonas et al. found that the placebo effect was related to the size, color, and label of tablets (23). I Požgain et al. showed that placebo in RCTs was effective for the health status of patients because of their own beliefs (24). Julia W. Haas et al. concerned about the effect of blindness caused by placebo on the treatment of patients with irritable bowel syndrome. The results found that patients with double-blind placebo possessed more enthusiasm; however, those with open-label placebo were contradicted, attributing the improvement of symptoms more to psychological function instead of the treatment itself (25). About 25% patients (26) and 19% healthy volunteers (27) taking a placebo experienced adverse events (AEs). Maxine de la Cruz et al. found that there was a placebo response in clinical trials about the treatment of fatigue in advanced cancer patients (28). However, no comparative study has been established to prove the differences between placebo and observation in the efficacy and AEs of the maintenance therapy of OC RCTs yet.

In this meta-analysis, we mainly compared the differences of median PFS and median OS between patients in the placebo and observation arms and illustrated the safety of placebo in RCTs with the maintenance therapy of advanced OC.

PATIENTS AND METHODS

Search Strategy

According to the Preferred Reporting Items for Systematic Review and Meta-analysis (PRISMA) guidelines (29), electronic databases (PubMed, Web of Science, Embase, and Cochrane Library) were searched from their inception to August 2020 to obtain relevant RCTs. The search terms included "ovarian cancer" or "ovarian neoplasms", "placebo" or "maintenance" or "consolidation" or "observation" or "natural history", and "randomized controlled trial". We also performed a manual search to find potential relative RCTs by using the reference lists of key articles. The language of all RCTs was limited to English.

Inclusion and Exclusion Criteria

The inclusion criteria were as follows: (1) population: patients with FIGO stage IIB–IV epithelial ovarian, fallopian tube, primary peritoneal cancer or platinum-sensitive recurrent ovarian cancer (ROC) who are receiving maintenance therapy; (2) study design and comparators: phase II or III RCTs with control arms, including placebo or observation; (3) interventions: no other anticancer treatments except for standard front-line chemotherapy added to placebo or observation arms; (4) outcomes: mature data of median PFS or median OS reported as hazard ratios (HRs) and 95% confidence intervals (CIs), the number of patients with common AEs in the placebo arm, and the total number of patients receiving placebo; and (5) the latest articles were applied when duplicate publications existed or when publications were continuously updated.

The exclusion criteria were as follows: (1) not RCTs, including abstract, meeting, case, editorial, review, and so on; (2) platinum-resistant advanced OC or ROC; (3) animal trials; (4) other antitumor agents in the control arms; (5) no long-term outcomes covered in the study; and (6) unavailable research data.

No ethical approval and patient consent were required because the meta-analysis was performed based on previously published studies.

Outcome Measures

The primary outcome of this meta-analysis was median PFS. Median OS and AEs were the secondary outcomes. The AEs were in accordance with the National Cancer Institute Common Terminology Criteria for Adverse Events, version 4.0.

Assessment of the Risk of Bias and Data Extraction

We assessed the potential risk of bias in the trials using the Cochrane Collaboration Risk of Bias Assessment tool, which involved the following domains: (1) random sequence generation (selection bias); (2) allocation concealment (selection bias); (3) blinding of participants, personnel, and outcome assessment (performance bias and detection bias); (4) incomplete outcome data (attrition bias); and (5) selective reporting data (reporting bias) (30). The risks were divided into three levels: high, unclear, and low. Two reviewers (Wang and Sun) completed the review independently. Disagreements were resolved by a discussion.

Two reviewers (Wang and Sun) independently extracted the baseline information from each study, including data on author, year of publication, RCT phase, and the number of experimental arms and control arms. The primary and secondary endpoints included median PFS, median OS, the corresponding HR and 95% CIs, and the number of common AEs.

Statistical Analysis

We indirectly compared the median PFS and median OS between the placebo arms and the observation arms by using HR and 95% CIs in view of the Frequency Framework method. We calculated the corresponding HR and 95% CIs by combining the HR with the 95% CIs of all subgroups in view of the generic inverse of variance method with a fixed-effect model (31). The incidences of common AEs were calculated by IBM SPSS Statistics (version 20.0) using the number of patients with common AEs in the placebo arms and the total number of patients receiving placebo. Heterogeneity among the studies was evaluated by the inconsistency index (I^2) value. If $I^2 \geq 50\%$ or $P < 0.1$, a random-effect model was used to reduce the heterogeneity and increase the reliability; if $I^2 < 50\%$ or $P > 0.1$, a fixed-effect model was used. All statistical tests were two-sided, $P < 0.05$ was considered statistically significant (22). We used Review Manager (version 5.3, the Cochrane library) for the assessment of the risk of bias and R software (version 3.4.4, the R Foundation for Statistical Computing) for network meta-analyses.

RESULTS

Study Selection and Characteristics

A total of 4,102 studies were retrieved through searching the electronic databases and other sources. Forty-one studies with 20,099 patients (experiment arms = 11,892; placebo arms = 4,787; observation arms = 3,420) that met the inclusion criteria were retained for comparison analysis. The PRISMA flow chart summarizing the process of evidence acquisition is shown in **Figure 1**. The flow chart mapped out the number of studies identified, screened, included, and excluded as well as the reasons for exclusions. The included studies were published between 2003 and 2020. The control arms of these RCTs consisted of 21 placebos (10 placebo maintenance after chemotherapy and 11 placebo through maintenance with and after chemotherapy) and 14 observations. Among 21 placebo studies (1, 5, 8, 9, 11, 12, 14, 15, 32–49), which all analyzed mature median PFS, 15 studies calculated the median OS, with 9 results being mature. There were 14 studies in the observation arms (6, 7, 13, 16–19, 50–57), all of which analyzed the mature median PFS and 13 studies analyzed the median OS, with 9 studies acquiring mature results. One study with secondary cytoreduction in the observation arms (57), one study with only a subgroup analysis (40), and one phase Ib/II study after extracting phase II data (8) were included in this meta-analysis. Except for one study (8), the other placebo arms with 2,665 patients all reported AEs in detail. The main characteristics and outcomes of the included RCTs are summarized in **Table 1**. **Figure 2** shows the results about the assessment of the risk of bias in the included RCTs according to the Cochrane Collaboration Risk of Bias Assessment tool. The network plots of the direct comparisons in the maintenance therapy of OC for PFS and OS are displayed in **Figures 3A, B**.

Progression-Free Survival

A total of 35 RCTs (4 RCTs: AIs with 1,058 patients; 10 RCTs: TC + AIs through with 3,990 patients; 1 RCT: TC + AIs current with 625 patients; 5 RCTs: PARPi with 1,566 patients; 2 RCTs: TC + PARPi through with 463 patients; 5 RCTs: immunotherapy with 890 patients; 1 RCT: TC + immunotherapy at 1.25 mg with 370 patients; 1 RCT: TC + immunotherapy at 2.5 mg with 366 patients; 6 RCTs: chemotherapy with 1,576 patients; 1 RCT: radiotherapy with 32 patients; 2 RCTs: TC + selective small-molecule inhibitor through with 117 patients; 21 RCTs: placebo with 4,606 patients; and 14 RCTs: observation with 3,420 patients) were included, which reported mature data on the PFS of OC patients with maintenance therapy. There was significant heterogeneity among RCTs (overall: $I^2 = 49.6\%$; $P = 0.002$), so the pooled HR was calculated by using a random-effect model. Except for placebo (HR, 1.02; 95% CI, 0.87–1.20; $P = 0.81$) and radiotherapy (HR, 0.59; 95% CI, 0.30–1.19; $P = 0.13$), other treatments significantly improved the PFS when compared with observation (all $P < 0.05$) (**Figure 4A**). Compared with PARP inhibitors indirectly, PFS was significantly improved in AIs (HR, 0.61; 95% CI, 0.48–0.77; $P < 0.001$), chemotherapy (HR, 0.57; 95% CI, 0.44–0.75; $P < 0.001$), immunotherapy (HR, 0.59; 95% CI, 0.46–0.75; $P < 0.001$), chemotherapy combined with AIs recurrent (HR, 0.61; 95% CI, 0.45–0.83; $P < 0.002$), chemotherapy combined with AIs through (HR, 0.70; 95% CI, 0.58–0.84; $P < 0.001$), chemotherapy combined with immunotherapy at 1.25 mg (HR, 0.56; 95% CI, 0.40–0.79; $P < 0.001$), and chemotherapy combined with immunotherapy at 2.5 mg (HR, 0.64; 95% CI, 0.45–0.91; $P = 0.012$) (**Figure 5**).

Overall Survival

Among 28 RCTs about median OS, 18 studies (3 RCTs: AIs with 935 patients; 7 RCTs: TC+AIs through with 2,861 patients;

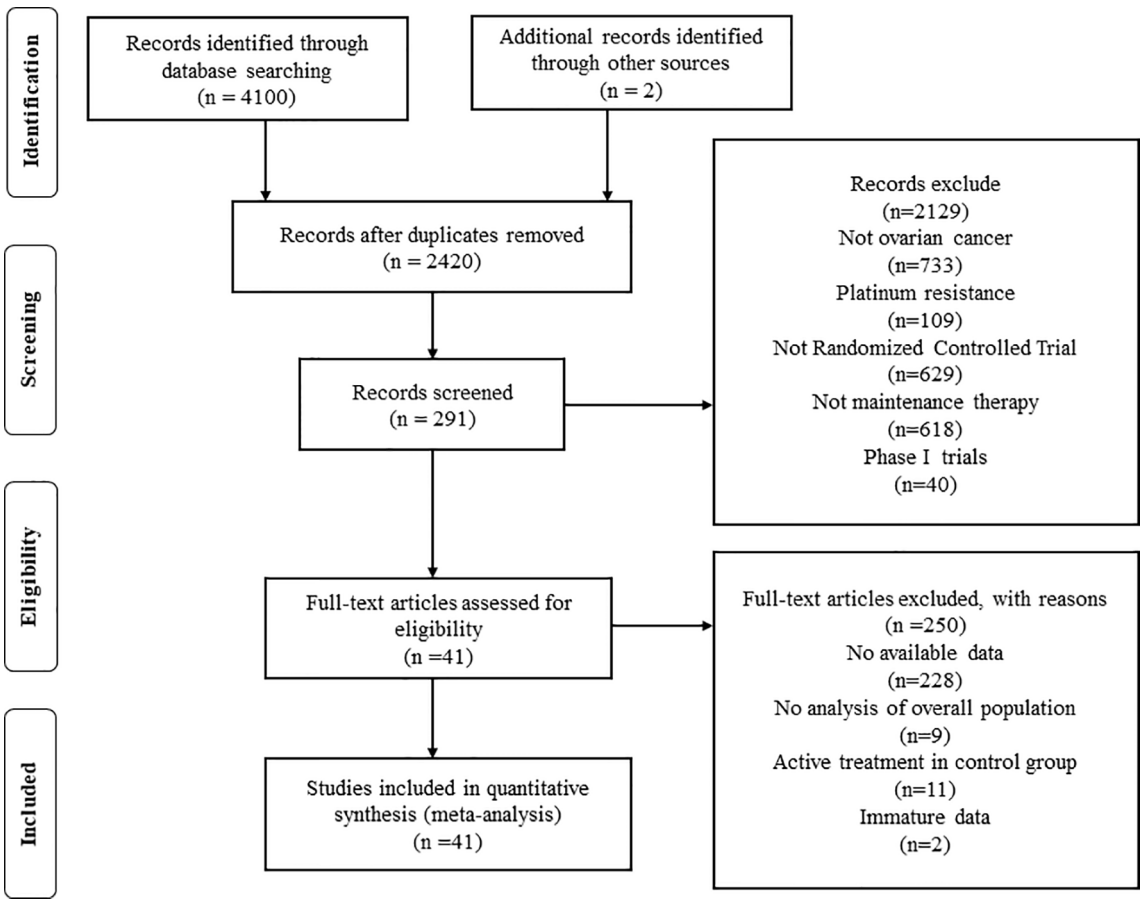


FIGURE 1 | Preferred Reporting Items for Systematic Review and Meta-analysis flow chart of the study selection process.

TABLE 1 | Baseline characteristics of the included studies.

Author	Phase	Treatment	Number	Primary endpoint	Second endpoint	Median progressive-free survival (months)	Hazard ratio (HR)	95% CI	Median overall survival (months)	HR	95% CI
Placebo arm in the control arm											
Jonathan S, 2004 (12)		Oregovomab	73	PFS		13.3	0.927	0.621–1.383			
		Placebo	72			10.3					
Paul Sabbatini, 2013, MIMOSA Study (14)	III	Abagovomab	593	PFS	OS	13.43	1.099	0.919–1.315	NR	1.15	0.872–1.518
		Placebo	295			13.4			NR		
Thomas J. Herzog, 2013 (11)	II	Sorafenib	123	PFS	OS	12.7	1.09	0.72–1.63	NR	1.49	0.69–3.23
		Placebo	123			15.7			NR		
Andreas du Bois/I. Vergote, 2014/2019, AGO-OVAR16 (38, 43)	III	Pazopanib	472	PFS	OS	17.9	0.77	0.64–0.91	59.1	0.96	0.805–1.145
		Placebo	468			12.3			64		
		Placebo	131			13.8			3 years OS rate: 80%		
A. González-Martín, 2019, PRIMA/ENGOT-OV26/GOG-3012 (9)	III	Niraparib	487	PFS	OS	13.8	0.62	0.5–0.76	2 years OS rate: 84%	0.7	0.44–1.11

(Continued)

TABLE 1 | Continued

Author	Phase	Treatment	Number	Primary endpoint	Second endpoint	Median progressive-free survival (months)	Hazard ratio (HR)	95% CI	Median overall survival (months)	HR	95% CI
		Placebo	246			8.2			2 years OS rate: 77%		
Robert A. Burger/Krishnansu S. Tewari, 2011/2019, GOG-0218 (35, 37)	III	(TC + bevacizumab) + bevacizumab	623	PFS	OS	14.1	0.717	0.625–0.824	43.4	0.96	0.85–1.09
		bevacizumab initiation treatment	625			11.2	0.908	0.795–1.040	40.8	1.06	0.94–1.2
		(TC + placebo) + placebo	625			10.3			41.1		
Ignace B. Vergote, 2013 (1)	II	(TC + enzastaurin) + enzastaurin	69	PFS		18.9	0.8	0.5–1.29			
		(TC + placebo) + placebo	73			15.2					
Andreas du Bois/Isabelle Ray-Coquard, 2015/2019, AGO-OVAR 12 (36)	III	(TC + nintedanib) + nintedanib	911	PFS	OS	17.6	0.86	0.75–0.98	62	0.99	0.83–1.17
		(TC + placebo) + placebo	455			16.6			62.8		
Ignace Vergote, 2019, TRINOVA-3/ENGOT-ov2/GOG-3001 (48)	III	(TC + trebananib) + trebananib	678	PFS		15.9	0.93	0.79–1.09	46.6	0.99	0.79–1.25
		(TC + placebo) + placebo	337			15			43.6		
Robert L. Coleman, 2019 (49)	III	(TC + veliparib) + veliparib	382	PFS	OS	23.5	0.68	0.56–0.83	NE		
		Veliparib combination only	383						NE		
		(TC + placebo) + placebo	375			17.3			NE		
Jonathan A. Ledermann, 2011 (45)	II	BIBF 1120	43	PFS	OS	36-week PFS rate: 16.3%	0.65	0.42–1.02	NE	0.84	0.51–1.39
		Placebo	40			36-week PFS rate: 5%			NE		
Jonathan Ledermann, MD/ Michael Friedlander, 2012/2018 (39)	II	Olaparib	136	PFS		8.4	0.35	0.25–0.49	29.8	0.73	0.55–0.95
		Placebo	129			4.8			27.8		
M.R. Mirza, 2016, ENGOT-OV16/NOVA trial (40)	III										
gBRCA cohort		Niraparib	138	PFS		21	0.27	0.17–0.41			
		Placebo	65			5.5					
Non-gBRCA cohort		Niraparib	234			9.3	0.45	0.34–0.61			
		Placebo	116			3.9					
Eric Pujade-Lauraine, 2017, SOLO2/ENGOT-Ov21 (42)	III	Olaparib	196	PFS	OS	19.1	0.3	0.22–0.41	NR	0.8	0.3–1.31
		Placebo	99			5.5			NR		
Prof. Robert L. Coleman, 2017, ARIEL3 (46)	III	Rucaparib	375	PFS		10.8	0.36	0.3–0.45			
		Placebo	189			5.4					
Carol Aghajanian, 2012/2015, OCEANS (5, 34)	III	(GC + bevacizumab) + bevacizumab	242	PFS	OS	12.4	0.484	0.388–0.605	33.6	0.95	0.77–1.18
		(GC + placebo) + placebo	242			8.4			32.9		
F. Cognetti, 2013, AGO-OVAR 2.14 (44)	II	(TC + zibotentan) + zibotentan	59	PFS	OS	7.6	1.46	80% CI: 1.1–1.94			

(Continued)

TABLE 1 | Continued

Author	Phase	Treatment	Number	Primary endpoint	Second endpoint	Median progressive-free survival (months)	Hazard ratio (HR)	95% CI	Median overall survival (months)	HR	95% CI
		(GC + placebo) + placebo	61			10					
Ignace Vergote, 2016 (15)	III	(TC + farletuzumab, 1.25 mg/kg) + farletuzumab, 1.25 mg/kg	370	PFS	OS	9.5	0.99	0.81–1.21	28.7	0.99	0.78–1.27
		(TC+ farletuzumab, 2.5 mg/kg) Farletuzumab, 2.5mg/kg	366			9.7	0.86	0.7–1.06	32.1	0.88	0.68–1.13
		(TC + placebo) + placebo	364			9			29.1		
Jonathan A. Ledermann, 2016, ICON6 (33)	III	(TC + cediranib) + cediranib	164	PFS	OS	11	0.56	0.44–0.72	26.3	0.77	0.55–1.07
		(TC + cediranib) + placebo	174			9.9	NR	NR			
		(TC + placebo) + placebo	118			8.7			21		
Ignace Vergote, 2020 (8)	Ib/II	(GC + ralimetinib) + ralimetinib	58	PFS	OS	10.25	0.773	90% CI: 0.535–1.117	29.17	0.83	90% CI: 0.538–1.27
		(GC + placebo) + placebo	52			7.92			25.1		
Amit M. Oza, 2020 (32)	II	(TC + adavosertib) + adavosertib	59	PFS	OS	9.9	0.55	0.32–0.95	NR	1	0.53–1.88
		(TC + placebo) + placebo	62			8			35.4		
Observation arm in the control arm											
B. Sorbe, 2003 (54)		Chemotherapy	35	PFS	OS	5 years: 36%; 37	0.72	0.4–1.3			
		Radiotherapy	32			5 years: 56%; 116	0.52	0.27–0.99		5 years: 69%	
		Observation	31			5 years: 35%; 32					
M.J. Piccart, 2003 (16)	III	Cisplatin	76	OS	PFS	4.625	0.89	0.59–1.33	6.96	0.82	0.52–1.29
		Observation	76			3.45			5.875		
Sabino De Placido, 2004 (6)	III	Topotecan	137	PFS	OS	18.2	1.18	0.86–1.63			
		Observation	136			28.4					
G.D. Hall, 2004 (7)	III	Interferon-alpha (INFa) 2a	149	PFS, OS		10.3	0.96	0.75–1.22	27	1.06	0.82–1.38
		Observation	149			10.4			32.7		
Ignace B. Vergote, 2014 (55)	III	Erlotinib	420	PFS	OS	12.7	1.05	0.9–1.23	50.8	0.99	0.81–1.2
		Observation	415			12.4			59.1		
Jun Liu, 2014 (50)		Autologous cytokine-induced killer cells	46	PFS	OS	37.7	0.493	0.302–0.807	61.5		
		Observation	46			22.2			55.9		
H.J. Gray, 2016 (13)	II	Cvac	29	PFS	OS	13	0.72	0.38–1.38	NR	0.38	Not shown
		Observation	27			9			NR		
Chyong-Huey Lai, 2019 (19)	III	Pegylated liposomal doxorubicin/ carboplatin	23	PFS	OS	55.5	0.4	0.19–0.87	NR	0.53	0.22–1.27
		Observation	21			9.2			95.1		

(Continued)

TABLE 1 | Continued

Author	Phase	Treatment	Number	Primary endpoint	Second endpoint	Median progressive-free survival (months)	Hazard ratio (HR)	95% CI	Median overall survival (months)	HR	95% CI
Andreas du Bois, 2006 (17)	III	(TC + epirubicin) + epirubicin	647	OS	PFS	18.4	0.95	0.83–1.07	45.8	0.93	0.81–1.08
		Observation	635			17.9			41		
Jacobus Pfifi Sterer, 2006 (18)	III	TC + topotecan	658	OS	PFS	18.2	0.97	0.85–1.1	43.1	1.01	0.86–1.18
		Observation	650			18.5			44.5		
Werner Meier, 2012 (51)	II	(TC + lonafarnib) + lonafarnib	53	NR	NR	14.2	0.78	0.5–1.2	34.4	0.62	0.4–1.1
		Observation	52			17.8			47.3		
Amit M. Oza/Timothy J. Perren, 2015, ICON7 (52)	III	(TC + bevacizumab) + bevacizumab	764	PFS	OS	19.8	0.87	0.77–0.99	58	0.99	0.85–1.14
		Observation	764			17.4			58.6		
Amit M. Oza, 2015 (53)	II	(TC + olaparib) + olaparib	81	PFS	OS	12.2	0.51	0.34–0.77	33.8	1.17	0.79–1.73
		Observation	81			9.6			37.6		
Robert L. Coleman, 2017, NRG Oncology/Gynecologic Oncology Group study GOG-0213 (57)	III	(TC + bevacizumab) + bevacizumab	337	OS	PFS	13.8	0.628	0.534–0.739	42.2	0.83	0.683–1.005
		Observation	337			10.4			37.3		

TC, paclitaxel and carboplatin; GC, gemcitabine and carboplatin; PFS, progression-free survival; OS, overall survival; HR, hazard ratio; 95% CI, 95% confidence interval.

1 RCT: TC + AIs recurrent with 625 patients; 1 RCT: PARPi with 136 patients; 1 RCT: TC + PARPi through with 81 patients; 1 RCT: immunotherapy with 149 patients; 1 RCT: TC + immunotherapy at 1.25 mg with 370 patients; 1 RCT: TC + immunotherapy at 2.5 mg with 366 patients; 3 RCTs: chemotherapy with 1,381 patients; 1 RCT: TC + selective small-molecule inhibitor through with 58 patients; 9 RCTs: placebo with 2,375 patients; 9 RCTs: observation with 3,159 patients) reported mature data on OS of OC patients with maintenance therapy. No significant heterogeneity existed in RCTs (overall: I^2 = 0%; P = 0.73), so the pooled HR was calculated by using a fixed-effect model. Except for placebo (HR, 1.02; 95% CI, 0.89–1.16; P = 0.76), other treatments significantly improved OS when compared with observation (all P <0.05) (**Figure 4B**). Compared with PARP inhibitors indirectly, OS was significantly improved in chemotherapy combined with AIs recurrent (HR, 0.72; 95% CI, 0.53–0.98; P = 0.036) (**Figure 5**).

AEs

Considering the accuracy of the results, we only analyzed the toxicity profiles of placebo maintenance therapy after completing chemotherapy to avoid its effect. Results regarding the patients' all grades and grade ≥ 3 toxicity profiles were pooled for only 10 placebo maintenance therapy in all included studies. Except for a study with grade ≥ 3 toxicity profiles (45), other RCTs reported all grades and grade ≥ 3 toxicity profiles in detail. Toxicity profiles were classified into total toxicity, hematological toxicities, gastrointestinal toxicities, and other toxicities. In all, 5 studies (9, 14, 41, 42, 46) with 954 patients reported the number of all grades AEs (897 patients) and 6 studies (9, 14, 41, 42, 45, 46) with 994 patients reported the number of grade ≥ 3 AEs (201 patients); the incidences of all grades AEs and grade ≥ 3 AEs were 94.03% (95% CI, 92.53%–95.53%) and 20.22% (95% CI, 17.72%–22.72%), respectively (**Table 2**).

Hematological Toxicities

We assessed three common hematological toxicities, including anemia, neutropenia, and thrombocytopenia, in this meta-analysis. The incidences of all grades and grade ≥ 3 toxicities were 9.65% (95% CI, 7.65%–11.65%) and 1.21% (95% CI, 0.38%–2.04%) in anemia, 6.38% (95% CI, 5.05%–7.71%) and 1.54% (95% CI, 0.87%–2.21%) in neutropenia, and 3.07% (95% CI, 2.08%–4.06%) and 0.68% (95% CI, 0.18%–1.18%) in thrombocytopenia, respectively (**Table 2**).

Gastrointestinal Toxicities

We also assessed several common gastrointestinal toxicities, such as nausea, abdominal pain, constipation, diarrhea, and vomiting. The incidences of all grades and grade ≥ 3 gastrointestinal toxicities were 26.38% (95% CI, 24.01%–28.75%) and 1.04% (95% CI, 0.13%–1.95%) in nausea, 24.34% (95% CI, 22.31%–26.37%) and 1.44% (95% CI, 0.83%–2.05%) in abdominal pain, 18.92% (95% CI, 16.44%–21.4%) and 2.65% (95% CI, 1.03%–4.27%) in constipation, 16.65% (95% CI, 14.79%–18.51%) and 1.62% (95% CI, 0.83%–2.41%) in diarrhea, and 14.55% (95% CI, 12.32%–16.78%) and 0.91% (95% CI, 0.28%–1.54%) in vomiting, respectively (**Table 2**).

Other Toxicities

Other toxicities like fatigue, hypertension, headache, insomnia, and dizziness were also analyzed in this meta-analysis. The incidences of all grades and grade ≥ 3 toxicities were 29.75% (95% CI, 27.63%–31.87%) and 1.19% (95% CI, 0.63%–1.75%) in fatigue, 13.89% (95% CI, 11.44%–

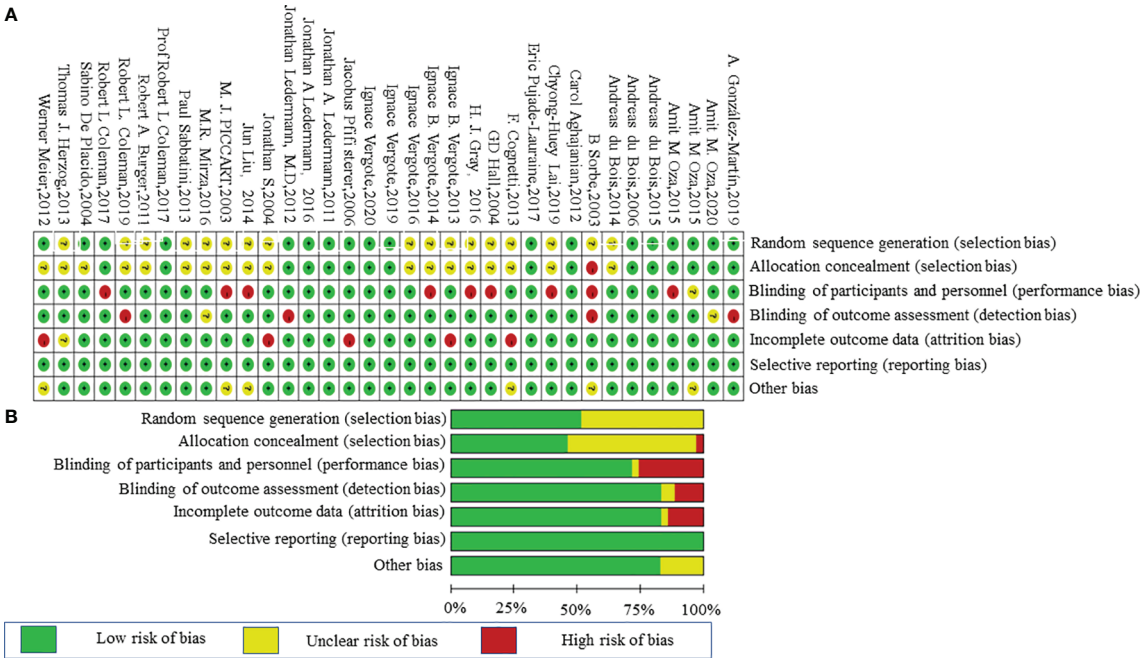


FIGURE 2 | Risk-of-bias graph. **(A)** Review authors' judgments about each risk-of-bias item presented as percentages across all included studies. **(B)** Review of authors' judgments about each risk-of-bias item for each included study.

16.34%) and 4.06% (95% CI, 2.66%–5.46%) in hypertension, 13.14% (95% CI, 11.57%–14.71%) and 0.64% (95% CI, 0.08%–1.2%) in headache, 10.29% (95% CI, 7.88%–12.7%) and 0.41% [95% CI, (-0.39%)-1.21%] in insomnia, and 7.06% (95% CI, 5.0%–9.12%) and 0.53% [95% CI, (-0.51%)-1.57%] in dizziness successively (**Table 2**).

DISCUSSION

Lots of meta-analyses about experimental drugs were performed to estimate the effect on survival. Ours was the first one concentrating on RCTs to assess the placebo effect of maintenance therapy in primary and recurrent OC settings. In

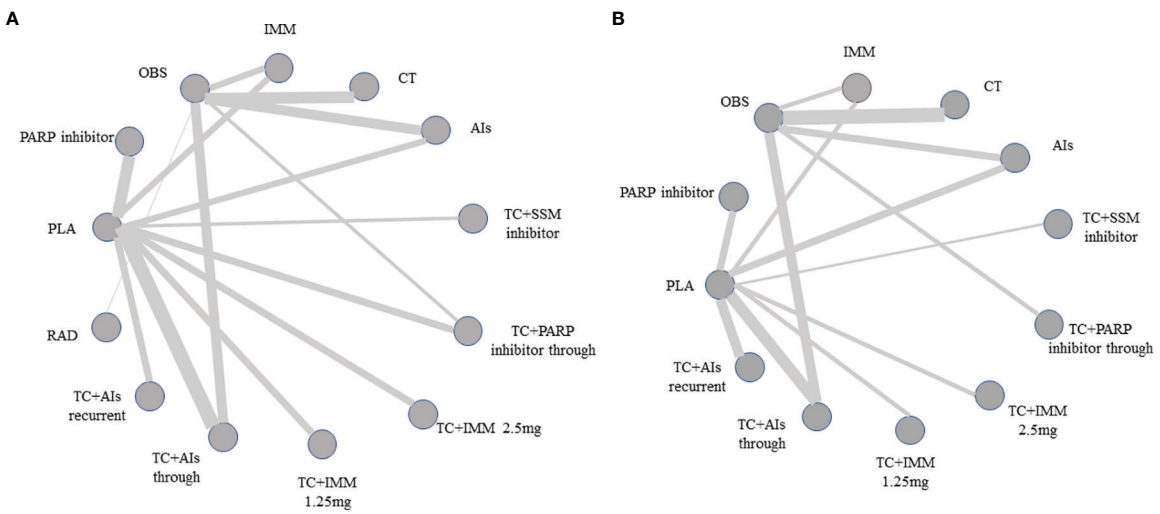


FIGURE 3 | Network of treatment comparisons for overall efficacy. **(A)** Network plot of treatment comparisons of progression-free survival. **(B)** Network of treatment comparisons of overall survival. Directly comparable treatments are linked with a line, the thickness of which corresponds to the number of trials that assessed the comparison. AIs, angiogenesis inhibitors; PLA, placebo; TC, platinum plus paclitaxel; CT, chemotherapy; OBS, observation; PARP inhibitors, poly (ADP-ribose) polymerase inhibitors; IMM, immunotherapy; RAD, radiotherapy; SSM inhibitors, selective small-module inhibitors.

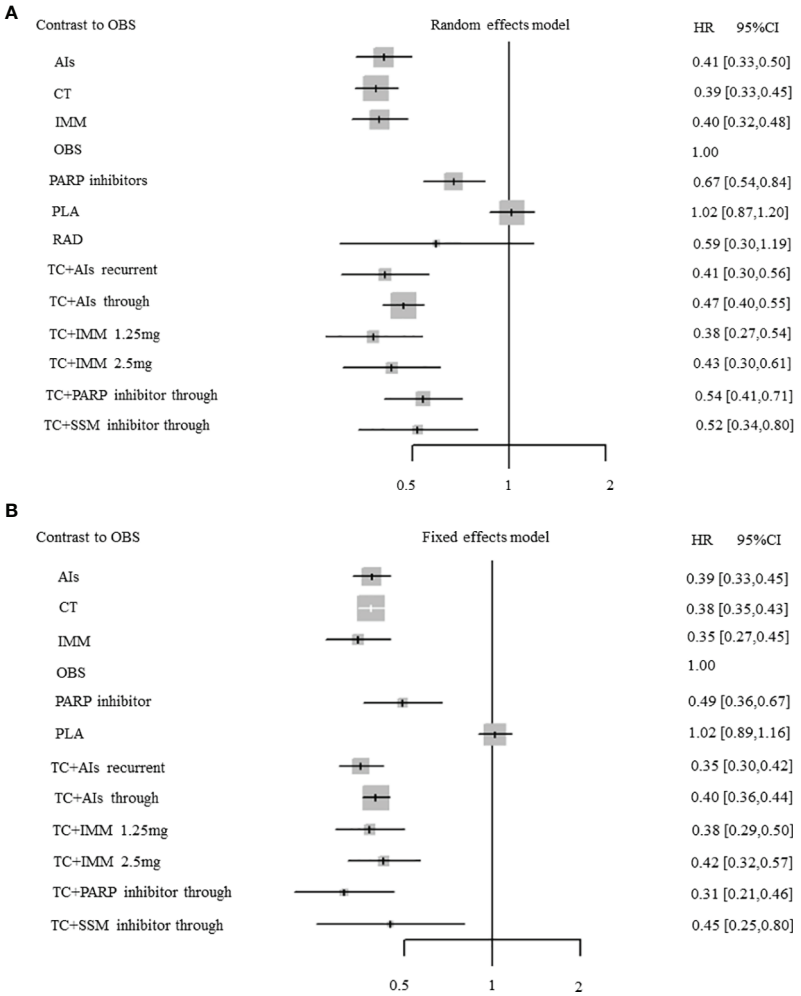


FIGURE 4 | Forest plots. **(A)** Progression-free survival (PFS). **(B)** Overall survival. Hazard ratios and 95% confidence intervals (95% CIs) of each treatment *versus* observation in the maintenance therapy of ovarian cancer. Central dots represent medians; lines represent 95% CIs.

this meta-analysis, we proved no statistically significant differences in the survival, whether PFS or OS, of OC patients between placebo and observation (all $P > 0.05$). Until now, no research has focused on this point. The National Comprehensive Cancer Network Guideline believes that participating in clinical trials for any cancer patients is the best management, which is positively encouraged (the corresponding website: nccn.org/clinical trials/member_institutions.aspx.). The ratios of the amount of participants between the experimental and the control arms of the included RCTs were 2:1 (9, 14, 36, 40, 42, 46, 48), 1:1 (1, 5–8, 11–13, 16–19, 32, 34, 38, 39, 41, 43–45, 50–53, 55–57, 58), or 1:1:1 (15, 35, 37, 49, 54). That implied that the participants had the opportunity of 1/3 or 1/2 to take placebo, but our results proved that it did not have an effect on survival. Therefore, it is safe to be ignored when designing patients' composition in RCTs.

However, placebo produced some AEs—the incidences of all grades and grade ≥ 3 were 94.03% (95% CI, 92.53%–95.53%) and 20.22% (95% CI, 17.72%–22.72%), respectively, which were higher than those of the observation arms and the study of Matías Rodrigo Chacón et al. (85.1% in all grades and 18% in grade ≥ 3) (59). The reason of the difference was that our study only included OC patients, while the study of Matías Rodrigo Chacón et al. contained cases of melanoma, non-small cell lung cancer, gastrointestinal stromal tumor, and renal cell carcinoma. $SOLO_2$ (42), focusing on OC, reported the incidences of placebo-related AEs as 94.95% in all grades and 18.18% in grade ≥ 3, which was similar to our results. Fatigue was the most common AEs, followed by gastrointestinal toxicities. A. Hrobjartsson et al. suggested that subjective symptoms, such as pain and anxiety, were affected more easily by placebo effect than objective measures like blood pressure (20). Julia W. Haas et al. found that patients with irritable bowel syndrome in a double-blind placebo experiment possessed more enthusiasm. However, those in an open-label placebo research were contradicted and thought that the improvement of symptoms rarely came from the

AIs	1.0555 (0.8205-1.3578)	1.0323 (0.8021-1.3287)	**0.408 (0.334-0.4984)**	**0.6062 (0.4768-0.7709)**	**0.4001 (0.3322-0.4819)**	0.6863 (0.3328-1.4155)	0.992 (0.7156-1.3753)	0.8685 (0.7088-1.0641)	1.0768 (0.7515-1.5428)	0.9455 (0.658-1.3586)	0.7554 (0.5543-1.0294)	0.7841 (0.5066-1.2136)
1.0051 (0.8391-1.204)	CT	0.9792 (0.7632-1.2563)	**0.3866 (0.3318-0.4504)**	**0.5744 (0.4393-0.7509)**	**0.3791 (0.304-0.4727)**	0.6502 (0.3189-1.3256)	0.9399 (0.6639-1.3305)	0.8228 (0.6647-1.0184)	1.0202 (0.6985-1.4899)	0.8958 (0.6117-1.3119)	**0.7156 (0.521-0.983)**	0.7429 (0.4724-1.1682)
1.1144 (0.8282-1.4995)	1.1088 (0.8411-1.4616)	IMM	**0.3953 (0.3236-0.4828)**	**0.5873 (0.4583-0.7525)**	**0.3876 (0.3186-0.4715)**	0.6648 (0.3223-1.3712)	0.961 (0.6892-1.3399)	0.8413 (0.6824-1.0372)	1.0431 (0.7242-1.5024)	0.9159 (0.6342-1.323)	0.7317 (0.5347-1.0014)	0.7596 (0.4887-1.1807)
0.3861 (0.3327-0.4481)	**0.3841 (0.3468-0.4254)**	**0.3465 (0.268-0.4479)**	OBS	**1.4858 (1.1922-1.8517)**	0.9806 (0.8363-1.1499)	1.682 (0.8389-3.3727)	**2.4313 (1.7794-3.3221)**	**2.1285 (1.8344-2.4698)**	**2.6391 (1.8662-3.732)**	**2.3173 (1.6338-3.2868)**	**1.8512 (1.4016-2.4451)**	**1.9218 (1.2551-2.9427)**
0.7843 (0.5723-1.0748)	0.7803 (0.5625-1.0825)	0.7038 (0.4702-1.0534)	**2.0314 (1.4885-2.7724)**	PARP inhibitor	**0.66 (0.5669-0.7684)**	1.1321 (0.5457-2.3484)	**1.6364 (1.2019-2.2278)**	**1.4326 (1.1845-1.7326)**	**1.7762 (1.2601-2.5036)**	**1.5597 (1.1032-2.205)**	1.246 (0.9227-1.6824)	1.2935 (0.847-1.9753)
0.378 (0.3292-0.434)	**0.3761 (0.3192-0.4431)**	**0.3392 (0.2545-0.452)**	0.979 (0.861-1.1131)	**0.4819 (0.363-0.6397)**	PLA	1.7153 (0.8402-3.5018)	**2.4794 (1.8955-3.243)**	**2.1706 (1.9362-2.4333)**	**2.6912 (1.9783-3.6611)**	**2.3632 (1.7313-3.2256)**	**1.8878 (1.4571-2.4459)**	**1.9598 (1.32-2.9096)**
-	-	-	-	-	-	RAD	1.4455 (0.6743-3.0986)	1.2654 (0.6213-2.5775)	1.569 (0.7212-3.4132)	1.3777 (0.6325-3.0011)	1.1006 (0.5203-2.3283)	1.1425 (0.5053-2.5833)
1.091 (0.9085-1.3101)	1.0854 (0.8857-1.3302)	0.979 (0.7172-1.3364)	**2.8257 (2.37-3.3689)**	**1.391 (1.0226-1.892)**	**2.8864 (2.5596-3.2548)**	-	TC+AIs recurrent	0.8755 (0.6539-1.1721)	1.0855 (0.7215-1.633)	0.9531 (0.6319-1.4376)	0.7614 (0.5243-1.1057)	0.7904 (0.4902-1.2746)
0.9685 (0.8363-1.1215)	0.9636 (0.8313-1.1168)	0.869 (0.6581-1.1476)	**2.5084 (2.2547-2.7906)**	1.2348 (0.9181-1.6608)	**2.5623 (2. 3479-2.7963)**	-	0.8877 (0.7652-1.0299)	TC+AIs through	1.2399 (0.8929-1.7217)	1.0887 (0.7816-1.5165)	0.8697 (0.661-1.1444)	0.9029 (0.5984-1.3624)
1.0172 (0.7723-1.3398)	1.0121 (0.7578-1.3516)	0.9128 (0.6285-1.3256)	**2.6346 (2.0098-3.4538)**	1.2969 (0.8957-1.8779)	**2.6912 (2.1205-3.4155)**	-	0.9324 (0.714-1.2176)	1.0503 (0.8149-1.3538)	TC+IMM 1.25mg	0.8781 (0.5699-1.3602)	0.7015 (0.4692-1.0488)	0.7282 (0.4413-1.2017)
0.9113 (0.6802-1.2208)	0.9066 (0.668-1.2306)	0.8177 (0.556-1.2027)	**2.3602 (1.7697-3.1478)**	1.1618 (0.7922-1.7039)	**2.4109 (1.8631-3.1197)**	-	0.8353 (0.6285-1.11)	0.9409 (0.7167-1.2352)	0.8958 (0.6306-1.2726)	TC+IMM 2.5mg	0.7989 (0.5329-1.1975)	0.8293 (0.5015-1.3713)
1.244 (0.8173-1.8934)	1.2377 (0.8248-1.8572)	1.1163 (0.6982-1.7847)	**3.222 (2.1754-4.7721)**	1.5861 (0.9611-2.6175)	**3.2912 (2.1772-4.9753)**	-	1.1403 (0.7415-1.7535)	1.2845 (0.855-1.9297)	1.2229 (0.759-1.9705)	1.3651 (0.8388-2.2217)	TC+PARP inhibitor through	1.0381 (0.6472-1.6651)
0.8642 (0.48-1.5559)	0.8598 (0.4744-1.5583)	0.7755 (0.4091-1.4701)	**2.2384 (1.246-4.0209)**	1.1019 (0.5823-2.0852)	**2.2864 (1.2911-4.0492)**	-	0.7922 (0.4417-1.4205)	0.8923 (0.5005-1.5909)	0. 8496 (0.4574-1.5781)	0.9484 (0.5066-1.7753)	0.6947 (0.3432-1.4064)	TC+SSM inhibitor through

FIGURE 5 | Hazard ratios (HRs) and 95% confidence intervals (95% CIs) of efficacy among the maintenance therapies of ovarian cancer patients between progression-free survival (PFS, up) and overall survival (OS, down). Comparisons between treatments should be read from left to right, and the estimate is in the cell in common between the column-defining treatment and the row-defining treatment. For efficacy, HR lower than 1 and 95% CI not including 1 favor the row-defining treatment of PFS or the column-defining treatment of OS. To obtain the HRs for comparisons in the opposite direction, reciprocals should be taken. Significant results are in bold and underlined.

treatment itself but that it was more like a psychological function (25).

The results compared with PARP inhibitors in this study were different from the study of Feng et al. (60), the only meta-analysis comparing PARP inhibitors, AIs, and chemotherapy, and showed that PARP inhibitors were superior to AIs and chemotherapy. We considered the following several reasons: (1) our study only included platinum-sensitive OC patients, while Feng's study included those cases which are platinum-sensitive and platinum-resistant; (2) comprehensive maintenance therapy models were illustrated in this meta-analysis, and the trials' numbers of immunotherapy were obviously less than those of other treatments, which might affect the weight of data; and (3) Feng's study merged placebo and observation into one arm, but some results continued to be debatable in the maintenance therapy of RCTs with OC—for example, immunotherapy did not improve the patients' survival, but PARP inhibitors did so, while in this indirect meta-analysis immunotherapy was prior to PARP inhibitors. We considered that sample sizes and the weight of data produced conflicting results. In the future, a large number of direct comparative clinical trials are needed to confirm the relation between immunotherapy and PARP inhibitors.

Several highlights existed in this meta-analysis, which are as follows: firstly, it was conducted according to PRISMA and included all well-designed and high-quality phase II or phase III RCTs to reduce the risk of bias among trials and increase the reliability of the results. Secondly, it included comprehensive models of maintenance treatment of OC, such as chemotherapy, AIs, PARP inhibitors, immunotherapy, and SSM inhibitors. Thirdly, network meta-analysis was used to indirectly compare the efficacy between placebo and observation and among experimental drugs due to no direct RCTs. Lastly, it firstly stated the incidences of AEs produced by placebo tablets in RCTs with OC and was not only limited to the fatigue in advanced cancer patients (28).

Some limitations were stated in our meta-analysis. First, performing a stratified pooled analysis to reduce the risk of bias among clinical trials according to disease setting (primary *vs*. recurrent OC) was difficult because of the limited clinical trials. Different endpoints existed in the studies, and the number of clinical trials of all kinds of maintenance therapies was less than 10. Second, the data used were based on the clinical trial level rather than the individual patient; data on survival and AEs were not assessed accurately or incorporated into the analysis due to lacking original data which were not available, which were supposed to be more sensitive for toxicity analysis. Third, we only evaluated the incidences of AEs in placebo arms without combination with chemotherapy, which could not better represent all patients included in the RCTs. Lastly, we did not calculate the relative risk ratio of AEs between placebo and observation due to insufficient data on AEs about observation.

TABLE 2 | Overall incidences (%) and 95% confidence intervals of common adverse events in patients with placebo maintenance.

Adverse events	Trials	All grades	Events (*n*)	Total (*n*)	Trials	Grade ≥ 3	Events (*n*)	Total (*n*)
Any	5	94.03 (92.53–95.53)	897	954	6	20.22 (17.72–22.72)	201	994
Hematological disorders								
Anemia	5	9.65 (7.65–11.65)	81	839	4	1.21 (0.38–2.04)	8	660
Neutropenia	6	6.38 (5.05–7.71)	83	1,300	6	1.54 (0.87–2.21)	20	1,300
Thrombocytopenia	5	3.07 (2.08–4.06)	36	1,172	5	0.68 (0.18–1.18)	7	1,023
Gastrointestinal disorders								
Nausea	8	26.38 (24.01–28.75)	350	1,327	2	1.04 (0.13–1.95)	5	482
Abdominal pain	8	24.34 (22.31–26.37)	418	1,717	8	1.44 (0.83–2.05)	21	1,463
Constipation	6	18.92 (16.44–21.40)	182	962	3	2.65 (1.03–4.27)	10	377
Diarrhea	8	16.65 (14.79–18.51)	257	1,544	5	1.62 (0.83–2.41)	16	990
Vomiting	6	14.55 (12.32–16.78)	140	962	6	0.91 (0.28–1.54)	8	879
Other toxicities								
Fatigue	9	29.75 (27.63–31.87)	532	1,788	7	1.19 (0.63–1.75)	17	1,423
Hypertension	3	13.89 (11.44–16.34)	106	763	3	4.06 (2.66–5.46)	31	763
Headache	9	13.14 (11.57–14.71)	235	1,788	3	0.64 (0.08–1.20)	5	778
Insomnia	3	10.29 (7.88–12.7)	63	612	1	0.41 [(-0.39) –1.21]	1	244
Dizziness	4	7.06 (5.0–9.12)	42	595	1	0.53 [(-0.51) –1.57]	1	189

CONCLUSIONS

This network meta-analysis indicated that the maintenance therapy of OC improved PFS and partial OS benefits. Compared with observation, placebo did not improve or reduce the PFS or OS benefits, but it increased the incidences of AEs in OC patients. In the future, more clinical trials should be designed to directly confirm the placebo effect.

DATA AVAILABILITY STATEMENT

The original contributions presented in the study are included in the article/supplementary material. Further inquiries can be directed to the corresponding authors.

AUTHOR CONTRIBUTIONS

QL conceived the study idea and wrote the manuscript. JW performed the search in the electronic databases, organized the data, and wrote the manuscript. LH and FC analyzed the data. CS performed the search in the electronic databases and organized the data. YW and XF checked the data again. LZ, YB, KZ, and JJ made modifications in the paper. All authors contributed to the article and approved the submitted version.

FUNDING

This work was supported by the Clinical Research Award of the First Affiliated Hospital of Xi'an Jiaotong University, China (XJTU1AF-2018-017 and XJTU1AF-CRF-2019-002), the Natural Science Basic Research Program of Shaanxi (2018JM7073 and 2017ZDJC-11), the Key Research and Development Program of Shaanxi (2017ZDXM-SF-068 and 2019QYPY-138), the Innovation Capability Support Program of Shaanxi (2017XT-026 and 2018XT-002), and the Medical Research Project of Xi'an Social Development Guidance Plan (2017117SF/YX011-3). The funders had no role in the study design, data collection and analysis, decision to publish, or preparation of the manuscript.

REFERENCES

1. Vergote IB, Chekerov R, Amant F, Harter P, Casado A, Emerich J, et al. Randomized, Phase II, Placebo-Controlled, Double-Blind Study With and Without Enzastaurin in Combination With Paclitaxel and Carboplatin as First-Line Treatment Followed by Maintenance Treatment in Advanced Ovarian Cancer. *J Clin Oncol* (2013) 31(25):3127–32. doi: 10.1200/JCO.2012.44.9116
2. Siegel RL, Miller KD, Fuchs HE, Jemal A. Cancer Statistics, 2021. *CA Cancer J Clin* (2021) 71(1):7–33. doi: 10.3322/caac.21654
3. Sung H, Ferlay J, Siegel RL, Laversanne M, Soerjomataram I, Jemal A, et al. Global Cancer Statistics 2020: GLOBOCAN Estimates of Incidence and Mortality Worldwide for 36 Cancers in 185 Countries. *CA Cancer J Clin* (2021) 71(3):209–49. doi: 10.3322/caac.21660
4. Moore K, Colombo N, Scambia G, Kim BG, Oaknin A, Friedlander M, et al. Maintenance Olaparib in Patients With Newly Diagnosed Advanced Ovarian Cancer. *N Engl J Med* (2018) 379(26):2495–505. doi: 10.1056/NEJMoa1810858
5. Aghajanian C, Blank SV, Goff BA, Judson PL, Teneriello MG, Husain A, et al. OCEANS: A Randomized, Double-Blind, Placebo-Controlled Phase III Trial of Chemotherapy With or Without Bevacizumab in Patients With Platinum-Sensitive Recurrent Epithelial Ovarian, Primary Peritoneal, or Fallopian Tube Cancer. *J Clin Oncol* (2012) 30(17):2039–45. doi: 10.1200/JCO.2012.42.0505
6. De Placido S, Scambia G, Di Vagno G, Naglieri E, Lombardi AV, Biamonte R, et al. Topotecan Compared With No Therapy After Response to Surgery and Carboplatin/Paclitaxel in Patients With Ovarian Cancer: Multicenter Italian Trials in Ovarian Cancer (MITO-1) Randomized Study. *J Clin Oncol* (2004) 22(13):2635–42. doi: 10.1200/JCO.2004.09.088
7. Hall GD, Brown JM, Coleman RE, Stead M, Metcalf KS, Peel KR, et al. Maintenance Treatment With Interferon for Advanced Ovarian Cancer: Results of the Northern and Yorkshire Gynaecology Group Randomised Phase III Study. *Br J Cancer* (2004) 91(4):621–6. doi: 10.1038/sj.bjc.6602037
8. Vergote I, Heitz F, Buderath P, Powell M, Sehouli J, Lee CM, et al. A Randomized, Double-Blind, Placebo-Controlled Phase 1b/2 Study of Ralimetinib, A P38 MAPK Inhibitor, Plus Gemcitabine and Carboplatin Versus Gemcitabine and Carboplatin for Women With Recurrent Platinum-Sensitive Ovarian Cancer. *Gynecol Oncol* (2020) 156(1):23–31. doi: 10.1016/j.ygyno.2019.11.006
9. González-Martín A, Pothuri B, Vergote I, DePont Christensen R, Graybill W, Mirza MR, et al. Niraparib in Patients With Newly Diagnosed Advanced Ovarian Cancer. *N Engl J Med* (2019) 381(25):2391–402. doi: 10.1056/NEJMoa1910962
10. Hirte H, Vergote IB, Jeffrey JR, Grimshaw RN, Coppieters S, Schwartz B, et al. A Phase III Randomized Trial of BAY 12-9566 (Tanomastat) as Maintenance Therapy in Patients With Advanced Ovarian Cancer Responsive to Primary Surgery and Paclitaxel/Platinum Containing Chemotherapy: A National Cancer Institute of Canada Clinical Trials Group Study. *Gynecol Oncol* (2006) 102(2):300–8. doi: 10.1016/j.ygyno.2005.12.020
11. Herzog TJ, Scambia G, Kim BG, Lhommé C, Markowska J, Ray-Coquard I, et al. A Randomized Phase II Trial of Maintenance Therapy With Sorafenib in Front-Line Ovarian Carcinoma. *Gynecol Oncol* (2013) 130(1):25–30. doi: 10.1016/j.ygyno.2013.04.011
12. Berek JS, Taylor PT, Gordon A, Cunningham MJ, Finkler N, Orr JJr., et al. Randomized, Placebo-Controlled Study of Oregovomab for Consolidation of Clinical Remission in Patients With Advanced Ovarian Cancer. *J Clin Oncol* (2004) 22(17):3507–16. doi: 10.1200/JCO.2004.09.016
13. Gray HJ, Benigno B, Berek J, Chang J, Mason J, Mileshkin L, et al. Progression-Free and Overall Survival in Ovarian Cancer Patients Treated With CVac, a Mucin 1 Dendritic Cell Therapy in a Randomized Phase 2 Trial. *J Immunother Cancer* (2016) 4:34. doi: 10.1186/s40425-016-0137-x
14. Sabbatini P, Harter P, Scambia G, Sehouli J, Meier W, Wimberger P, et al. Abagovomab as Maintenance Therapy in Patients With Epithelial Ovarian Cancer: A Phase III Trial of the AGO OVAR, COGI, GINECO, and GEICO–the MIMOSA Study. *J Clin Oncol* (2013) 31(12):1554–61. doi: 10.1200/JCO.2012.46.4057
15. Vergote I, Armstrong D, Scambia G, Teneriello M, Sehouli J, Schweizer C, et al. A Randomized, Double-Blind, Placebo-Controlled, Phase III Study to Assess Efficacy and Safety of Weekly Farletuzumab in Combination With Carboplatin and Taxane in Patients With Ovarian Cancer in First Platinum-Sensitive Relapse. *J Clin Oncol* (2016) 34(19):2271–8. doi: 10.1200/JCO.2015.63.2596
16. Piccart MJ, Floquet A, Scarfone G, Willemse PH, Emerich J, Vergote I, et al. Intraperitoneal Cisplatin Versus No Further Treatment: 8-Year Results of EORTC 55875, A Randomized Phase III Study in Ovarian Cancer Patients With a Pathologically Complete Remission After Platinum-Based Intravenous Chemotherapy. *Int J Gynecol Cancer* (2003) 13(Suppl 2):196–203. doi: 10.1136/ijgc-00009577-200311001-00012
17. du Bois A, Weber B, Rochon J, Meier W, Goupil A, Olbricht S, et al. Addition of Epirubicin as a Third Drug to Carboplatin-Paclitaxel in First-Line Treatment of Advanced Ovarian Cancer: A Prospectively Randomized Gynecologic Cancer Intergroup Trial by the Arbeitsgemeinschaft Gynaekologische Onkologie Ovarian Cancer Study Group and the Groupe D'investigateurs Nationaux Pour l'Etude Des Cancers Ovariens. *J Clin Oncol* (2006) 24(7):1127–35. doi: 10.1200/JCO.2005.03.2938
18. Pfisterer J, Weber B, Reuss A, Kimmig R, du Bois A, Wagner U, et al. Randomized Phase III Trial of Topotecan Following Carboplatin and Paclitaxel in First-Line Treatment of Advanced Ovarian Cancer: A Gynecologic Cancer Intergroup Trial of the AGO-OVAR and GINECO. *J Natl Cancer Inst* (2006) 98(15):1036–45. doi: 10.1093/jnci/djj296
19. Lai CH, Vallikad E, Lin H, Yang LY, Jung SM, Liu HE, et al. Maintenance of Pegylated Liposomal Doxorubicin/Carboplatin in Patients With Advanced Ovarian Cancer: Randomized Study of an Asian Gynecologic Oncology Group. *J Gynecol Oncol* (2020) 31(1):e5. doi: 10.3802/jgo.2020.31.e5
20. Hrobjartsson A, Gotzsche PC. Is the Placebo Powerless? An Analysis of Clinical Trials Comparing Placebo With No Treatment. *N Engl J Med* (2001) 344(21):1594–602. doi: 10.1056/NEJM200105243442106
21. Sheldon R, Opie-Moran M. The Placebo Effect in Cardiology: Understanding and Using it. *Can J Cardiol* (2017) 33(12):1535–42. doi: 10.1016/j.cjca.2017.09.017
22. Brody H. Meaning and an Overview of the Placebo Effect. *Perspect Biol Med* (2018) 61(3):353–60. doi: 10.1353/pbm.2018.0048
23. Jonas WB, Crawford C, Colloca L, Kaptchuk TJ, Moseley B, Miller FG, et al. To What Extent are Surgery and Invasive Procedures Effective Beyond a Placebo Response? A Systematic Review With Meta-Analysis of Randomised, Sham Controlled Trials. *BMJ Open* (2015) 5(12):e009655. doi: 10.1136/bmjopen-2015-009655
24. Požgain I, Požgain Z, Degmečić D. Placebo and Nocebo Effect: A Mini-Review. *Psychiatr Danub* (2014) 26(2):100–7.
25. Haas JW, Ongaro G, Jacobson E, Conboy LA, Nee J, Iturrino J, et al. Patients' Experiences Treated With Open-Label Placebo Versus Double-Blind Placebo: A Mixed Methods Qualitative Study. *BMC Psychol* (2022) 10(1):20. doi: 10.1186/s40359-022-00731-w
26. Shepherd M. The Placebo: From Specificity to the non-Specific and Back. *Psychol Med* (1993) 23(3):569–78. doi: 10.1017/S0033291700025356
27. Rosenzweig P, Brohier S, Zipfel A. The Placebo Effect in Healthy Volunteers: Influence of Experimental Conditions on the Adverse Events Profile During Phase I Studies. *Clin Pharmacol Ther* (1993) 54(5):578–83. doi: 10.1038/clpt.1993.190
28. de la Cruz M, Hui D, Parsons HA, Bruera E. Placebo and Nocebo Effects in Randomized Double-Blind Clinical Trials of Agents for the Therapy for Fatigue in Patients With Advanced Cancer. *Cancer* (2010) 116(3):766–74. doi: 10.1002/cncr.24751
29. Shamseer L, Moher D, Clarke M, Ghersi D, Liberati A, Petticrew M, et al. Preferred Reporting Items for Systematic Review and Meta-Analysis Protocols (PRISMA-P) 2015: Elaboration and Explanation. *BMJ* (2015) 350:g7647. doi: 10.1136/bmj.g7647
30. Ma J, Deng H, Li J, Hu S, Yang Y, Liu S, et al. Efficacy and Safety of Olaparib Maintenance Therapy in Platinum-Sensitive Ovarian Cancer Patients With BRCA Mutations: A Meta-Analysis on Randomized Controlled Trials. *Cancer Manag Res* (2019) 11:3061–78. doi: 10.2147/CMAR.S191107

31. Tomao F, Bardhi E, Di Pinto A, Sassu CM, Biagioli E, Petrella MC, et al. Parp Inhibitors as Maintenance Treatment in Platinum Sensitive Recurrent Ovarian Cancer: An Updated Meta-Analysis of Randomized Clinical Trials According to BRCA Mutational Status. *Cancer Treat Rev* (2019) 80:101909. doi: 10.1016/j.ctrv.2019.101909
32. Oza AM, Estevez-Diz M, Grischke EM, Hall M, Marmé F, Provencher D, et al. A Biomarker-Enriched, Randomized Phase II Trial of Adavosertib (AZD1775) Plus Paclitaxel and Carboplatin for Women With Platinum-Sensitive TP53-Mutant Ovarian Cancer. *Clin Cancer Res* (2020) 26(18):4767–76. doi: 10.1158/1078-0432.CCR-20-0219
33. Ledermann JA, Embleton AC, Raja F, Perren TJ, Jayson GC, Rustin GJS, et al. Cediranib in Patients With Relapsed Platinum-Sensitive Ovarian Cancer (ICON6): A Randomised, Double-Blind, Placebo-Controlled Phase 3 Trial. *Lancet* (2016) 387(10023):1066–74. doi: 10.1016/S0140-6736(15)01167-8
34. Aghajanian C, Goff B, Nycum LR, Wang YV, Husain A, Blank SV. Final Overall Survival and Safety Analysis of OCEANS, A Phase 3 Trial of Chemotherapy With or Without Bevacizumab in Patients With Platinum-Sensitive Recurrent Ovarian Cancer. *Gynecol Oncol* (2015) 139(1):10–6. doi: 10.1016/j.ygyno.2015.08.004
35. Tewari KS, Burger RA, Enserro D, Norquist BM, Swisher EM, Brady MF, et al. Final Overall Survival of a Randomized Trial of Bevacizumab for Primary Treatment of Ovarian Cancer. *J Clin Oncol* (2019) 37(26):2317–28. doi: 10.1200/JCO.19.01009
36. Ray-Coquard I, Cibula D, Mirza MR, Reuss A, Ricci C, Colombo N, et al. Final Results From GCIG/ENGOT/AGO-OVAR 12, A Randomised Placebo-Controlled Phase III Trial of Nintedanib Combined With Chemotherapy for Newly Diagnosed Advanced Ovarian Cancer. *Int J Cancer* (2020) 146 (2):439–48. doi: 10.1002/ijc.32606
37. Burger RA, Brady MF, Bookman MA, Fleming GF, Monk BJ, Huang H, et al. Incorporation of Bevacizumab in the Primary Treatment of Ovarian Cancer. *N Engl J Med* (2011) 365(26):2473–83. doi: 10.1056/NEJMoa1104390
38. Du Bois A, Floquet A, Kim JW, Rau J, del Campo JM, Friedlander M, et al. Incorporation of Pazopanib in Maintenance Therapy of Ovarian Cancer. *J Clin Oncol* (2014) 32(30):3374–82. doi: 10.1200/JCO.2014.55.7348
39. Friedlander M, Matulonis U, Gourley C, du Bois A, Vergote I, Rustin G, et al. Long-Term Efficacy, Tolerability and Overall Survival in Patients With Platinum-Sensitive, Recurrent High-Grade Serous Ovarian Cancer Treated With Maintenance Olaparib Capsules Following Response to Chemotherapy. *Br J Cancer* (2018) 119(9):1075–85. doi: 10.1038/s41416-018-0271-y
40. Mirza MR, Monk BJ, Herrstedt J, Oza AM, Mahner S, Redondo A, et al. Niraparib Maintenance Therapy in Platinum-Sensitive, Recurrent Ovarian Cancer. *N Engl J Med* (2016) 375(22):2154–64. doi: 10.1056/NEJMoa1611310
41. Ledermann J, Harter P, Gourley C, Friedlander M, Vergote I, Rustin G, et al. Olaparib Maintenance Therapy in Platinum-Sensitive Relapsed Ovarian Cancer. *N Engl J Med* (2012) 366(15):1382–92. doi: 10.1056/NEJMoa1105535
42. Pujade-Lauraine E, Ledermann JA, Selle F, Gebski V, Penson RT, Oza AM, et al. Olaparib Tablets as Maintenance Therapy in Patients With Platinum-Sensitive, Relapsed Ovarian Cancer and a BRCA1/2 Mutation (SOLO2/ENGOT-Ov21): A Double-Blind, Randomised, Placebo-Controlled, Phase 3 Trial. *Lancet Oncol* (2017) 18(9):1274–84. doi: 10.1016/S1470-2045(17)30469-2
43. Vergote I, Du Bois A, Floquet A, Rau J, Kim JW, Del Campo JM, et al. Overall Survival Results of AGO-OVAR16: A Phase 3 Study of Maintenance Pazopanib Versus Placebo in Women Who Have Not Progressed After First-Line Chemotherapy for Advanced Ovarian Cancer. *Gynecol Oncol* (2019) 155(2):186–91. doi: 10.1016/j.ygyno.2019.08.024
44. Cognetti F, Bagnato A, Colombo N, Savarese A, Scambia G, Sehouli J, et al. A Phase II, Randomized, Double-Blind Study of Zibotentan (ZD4054) in Combination With Carboplatin/Paclitaxel Versus Placebo in Combination With Carboplatin/Paclitaxel in Patients With Advanced Ovarian Cancer Sensitive to Platinum-Based Chemotherapy (AGO-OVAR 2.14). *Gynecol Oncol* (2013) 130(1):31–7. doi: 10.1016/j.ygyno.2012.12.004
45. Ledermann JA, Hackshaw A, Kaye S, Jayson G, Gabra H, McNeish I, et al. Randomized Phase II Placebo-Controlled Trial of Maintenance Therapy Using the Oral Triple Angiokinase Inhibitor BIBF 1120 After Chemotherapy for Relapsed Ovarian Cancer. *J Clin Oncol* (2011) 29 (28):3798–804. doi: 10.1200/JCO.2010.33.5208
46. Coleman RL, Oza AM, Lorusso D, Aghajanian C, Oaknin A, Dean A, et al. Rucaparib Maintenance Treatment for Recurrent Ovarian Carcinoma After Response to Platinum Therapy (ARIEL3): A Randomised, Double-Blind, Placebo-Controlled, Phase 3 Trial. *Lancet* (2017) 390(10106):1949–61. doi: 10.1016/S0140-6736(17)32440-6
47. Du Bois A, Kristensen G, Ray-Coquard I, Reuss A, Pignata S, Colombo N, et al. Standard First-Line Chemotherapy With or Without Nintedanib for Advanced Ovarian Cancer (AGO-OVAR 12): A Randomised, Double-Blind, Placebo-Controlled Phase 3 Trial. *Lancet Oncol* (2016) 17(1):78–89. doi: 10.1016/S1470-2045(15)00366-6
48. Vergote I, Scambia G, O'Malley DM, Van Calster B, Park SY, Del Campo JM, et al. Trebananib or Placebo Plus Carboplatin and Paclitaxel as First-Line Treatment for Advanced Ovarian Cancer (TRINOVA-3/ENGOT-Ov2/GOG-3001): A Randomised, Double-Blind, Phase 3 Trial. *Lancet Oncol* (2019) 20 (6):862–76. doi: 10.1016/S1470-2045(19)30178-0
49. Coleman RL, Fleming GF, Brady MF, Swisher EM, Steffensen KD, Friedlander M, et al. Veliparib With First-Line Chemotherapy and as Maintenance Therapy in Ovarian Cancer. *N Engl J Med* (2019) 381(25):2403–15. doi: 10.1056/NEJMoa1909707
50. Liu J, Li H, Cao S, Zhang X, Yu J, Qi J, et al. Maintenance Therapy With Autologous Cytokine-Induced Killer Cells in Patients With Advanced Epithelial Ovarian Cancer After First-Line Treatment. *J Immunother* (2014) 37(2):115–22. doi: 10.1097/CJI.0000000000000021
51. Meier W, du Bois A, Rau J, Gropp-Meier M, Baumann K, Huober J, et al. Randomized Phase II Trial of Carboplatin and Paclitaxel With or Without Lonafarnib in First-Line Treatment of Epithelial Ovarian Cancer Stage IIB-Iv. *Gynecol Oncol* (2012) 126(2):236–40. doi: 10.1016/j.ygyno.2012.04.050
52. Oza AM, Cook AD, Pfisterer J, Embleton A, Ledermann JA, Pujade-Lauraine E, et al. Standard Chemotherapy With or Without Bevacizumab for Women With Newly Diagnosed Ovarian Cancer (ICON7): Overall Survival Results of a Phase 3 Randomised Trial. *Lancet Oncol* (2015) 16(8):928–36. doi: 10.1016/S1470-2045(15)00086-8
53. Perren TJ, Swart AM, Pfisterer J, Ledermann JA, Pujade-Lauraine E, Kristensen G, et al. A Phase 3 Trial of Bevacizumab in Ovarian Cancer. *N Engl J Med* (2011) 365(26):2484–96. doi: 10.1056/NEJMoa1103799
54. Sorbe B. Consolidation Treatment of Advanced (FIGO Stage III) Ovarian Carcinoma in Complete Surgical Remission After Induction Chemotherapy: A Randomized, Controlled, Clinical Trial Comparing Whole Abdominal Radiotherapy, Chemotherapy, and No Further Treatment. *Int J Gynecol Cancer* (2003) 13(3):278–86. doi: 10.1046/j.1525-1438.2003.13193.x
55. Vergote IB, Jimeno A, Joly F, Katsaros D, Coens C, Despierre E, et al. Randomized Phase III Study of Erlotinib Versus Observation in Patients With No Evidence of Disease Progression After First-Line Platin-Based Chemotherapy for Ovarian Carcinoma: A European Organisation for Research and Treatment of Cancer-Gynaecological Cancer Group, and Gynecologic Cancer Intergroup Study. *J Clin Oncol* (2014) 32(4):320–6. doi: 10.1200/JCO.2013.50.5669
56. Oza AM, Cibula D, Benzaquen AO, Poole C, Mathijssen RH, Sonke GS, et al. Olaparib Combined With Chemotherapy for Recurrent Platinum-Sensitive Ovarian Cancer: A Randomised Phase 2 Trial. *Lancet Oncol* (2015) 16(1):87–97. doi: 10.1016/S1470-2045(14)71135-0
57. Coleman RL, Brady MF, Herzog TJ, Sabbatini P, Armstrong DK, Walker JL, et al. Bevacizumab and Paclitaxel-Carboplatin Chemotherapy and Secondary Cytoreduction in Recurrent, Platinum-Sensitive Ovarian Cancer (NRG Oncology/Gynecologic Oncology Group Study GOG-0213): A Multicentre, Open-Label, Randomised, Phase 3 Trial. *Lancet Oncol* (2017) 18(6):779–91. doi: 10.1016/S1470-2045(17)30279-6
58. Mannel RS, Brady MF, Kohn EC, Hanjani P, Hiura M, Lee R, et al. A Randomized Phase III Trial of IV Carboplatin and Paclitaxel × 3 Courses Followed by Observation Versus Weekly Maintenance Low-Dose Paclitaxel in Patients With Early-Stage Ovarian Carcinoma: A Gynecologic Oncology Group Study. *Gynecol Oncol* (2011) 122(1):89–94. doi: 10.1016/j.ygyno.2011.03.013
59. Chacon MR, Enrico DH, Burton J, Waisberg FD, Videla VM. Incidence of Placebo Adverse Events in Randomized Clinical Trials of Targeted and Immunotherapy Cancer Drugs in the Adjuvant Setting: A Systematic Review and Meta-Analysis. *JAMA Netw Open* (2018) 1(8):e185617. doi: 10.1001/jamanetworkopen.2018.5617
60. Feng Y, Huang H, Wan T, Zhang C, Tong C, Liu J. Comparison of PARPis With Angiogenesis Inhibitors and Chemotherapy for Maintenance in Ovarian

Cancer: A Network Meta-Analysis. *Adv Ther* (2019) 36(12):3368–80. doi: 10.1007/s12325-019-01106-1

Conflict of Interest: The authors declare that the research was conducted in the absence of any commercial or financial relationships that could be construed as a potential conflict of interest.

Publisher's Note: All claims expressed in this article are solely those of the authors and do not necessarily represent those of their affiliated organizations, or those of the publisher, the editors and the reviewers. Any product that may be evaluated in this article, or claim that may be made by its manufacturer, is not guaranteed or endorsed by the publisher.

Copyright © 2022 Wang, Zhao, Bin, Zhang, Sun, Wang, Feng, Ji, He, Chen and Li. This is an open-access article distributed under the terms of the Creative Commons Attribution License (CC BY). The use, distribution or reproduction in other forums is permitted, provided the original author(s) and the copyright owner(s) are credited and that the original publication in this journal is cited, in accordance with accepted academic practice. No use, distribution or reproduction is permitted which does not comply with these terms.

frontiers | Frontiers in Oncology

ORIGINAL RESEARCH
published: 01 June 2022
doi: 10.3389/fonc.2022.860900

Integration of scRNA-Seq and TCGA RNA-Seq to Analyze the Heterogeneity of HPV+ and HPV- Cervical Cancer Immune Cells and Establish Molecular Risk Models

Erdong Wei[1], *Amin Reisinger*[1], *Jiahua Li*[1], *Lars E. French*[1,2], *Benjamin Clanner-Engelshofen*[1†] *and Markus Reinholz*[1*†]

[1] Department of Dermatology and Allergy, Ludwig-Maximilians-Universität München (LMU) Munich, University Hospital, Munich, Germany, [2] Dr. Phillip Frost Department of Dermatology & Cutaneous Surgery, Miller School of Medicine, University of Miami, Miami, FL, United States

OPEN ACCESS

Edited by:
Makoto Tsuiji,
Hoshi University School of Pharmacy and Pharmaceutical Science, Japan

Reviewed by:
Yiran Li,
Tongji University, China
Leticia Rocha-Zavaleta,
National Autonomous University of Mexico, Mexico

***Correspondence:**
Markus Reinholz
Markus.Reinholz@med.uni-muenchen.de

[†]These authors have contributed equally to this work

Specialty section:
This article was submitted to Gynecological Oncology, a section of the journal Frontiers in Oncology

Received: 23 January 2022
Accepted: 02 May 2022
Published: 01 June 2022

Citation:
Wei E, Reisinger A, Li J, French LE, Clanner-Engelshofen B and Reinholz M (2022) Integration of scRNA-Seq and TCGA RNA-Seq to Analyze the Heterogeneity of HPV+ and HPV- Cervical Cancer Immune Cells and Establish Molecular Risk Models. Front. Oncol. 12:860900. doi: 10.3389/fonc.2022.860900

Background: Numerous studies support that Human papillomavirus (HPV) can cause cervical cancer. However, few studies have surveyed the heterogeneity of HPV infected or uninfected (HPV+ and HPV-) cervical cancer (CESC) patients. Integration of scRNA-seq and TCGA data to analyze the heterogeneity of HPV+ and HPV- cervical cancer patients on a single-cell level could improve understanding of the cellular mechanisms during HPV-induced cervical cancer.

Methods: CESC scRNA-seq data obtained from the Gene Expression Omnibus (GEO) database and the Seurat, Monocle3 package were used for scRNA-seq data analysis. The ESTIMATE package was used for single-sample gene immune score, CIBERSORT package was used to identify immune scores of cells, and the "WGCNA" package for the weighted correlation network analysis. Univariate Cox and LASSO regression were performed to establish survival and relapse signatures. KEGG and GO analyses were performed for the signature gene. Gene Expression Profiling Interactive Analysis was used for Pan-cancer analysis.

Results: In the HPV+ CESC group, CD8+ T cells and B cells were down-regulated, whereas T reg cells, CD4+ T cells, and epithelial cells were up-regulated according to scRNA-seq data. Survival analysis of TCGA-CESC revealed that increased expression of naive B cells or CD8+ T cells favors the survival probability of CESC patients. WGCNA, univariate Cox, and LASSO Cox regression established a 9-genes survival signature and a 7-gene relapse model. Pan-cancer analysis identified IKZF3, FOXP3, and JAK3 had a similar distribution and effects in HPV-associated HNSC.

Conclusion: Analysis of scRNA-seq and bulk RNA-seq of HPV+ and HPV- CESC samples revealed heterogeneity from transcriptional state to immune infiltration. Survival and relapse models were adjusted according to the heterogeneity of HPV+ and HPV- CESC immune cells to assess the prognostic risk accurately. Hub genes represent similar protection in HPV-associated HNSC while showing irrelevant to other potential HPV-related cancers.

Keywords: cervical cancer, HPV - human papillomavirus, scRNA seq, immune cells (ICs), gene signature, prognosis, carcinoma

INTRODUCTION

In 2020, the World Health Organization (WHO) reported 604,127 new cases of cervical cancer (CESC) and 341,831 CESC-related casualties (1). Seventy percent of patients of the CESC and CESC-related deaths were Human papillomavirus (HPV) type 16 and 18 positive (2). The HPV, a non-enveloped double-stranded DNA virus, is a well-studied transmitter of sexual infections worldwide (1). Many HPV infections have no symptoms, and 90% resolve spontaneously within two years (2). However, in some cases (3), HPV infections could result in warts or precancerous lesions, which increase the risk of cancer, including vulva, vagina, penis, and anus (4).

Single-cell RNA sequencing (scRNA-seq) is a technique used to define the global gene expression profile of a single cell utilizing optimized next-generation sequencing. This allows the exploration of previously hidden heterogeneity in a cell population (5). In previous studies, scRNA-seq was the technique of choice for investigating cancer and adjacent normal tissues. In Li`s study (6), scRNA-seq was performed to compare the expression differences between CESC-derived endothelial cells and normal endothelial cells revealing marker genes associated with cancer endothelial cells. In comparison with scRNA-seq, the advantage of The Cancer Genome Atlas (TCGA) data lies within the ability to integrate RNA samples and clinical information on a larger scale, which enables consecutive analysis of the clinical significance of genes. Bezzecchi et al. used TCGA RNA-seq to analyze the HPV+ and HPV- Neck squamous cell carcinoma (HNSC) revealing that the overexpression of histone fold domain subunits and NF-YAs is counteracting cancer progression in HPV+ patients (7).

We hypothesized that HPV has an effect at multiple levels. Hence, we aim to reveal the heterogeneity from transcriptional to immune infiltration between HPV+ and HPV- samples by scRNA-seq as well as bulk RNA sequencing. Then, we try to link the survival and relapse with genes based on the difference between HPV+ and HPV- samples. Further, we analyzed the role of hub genes in other potential HPV- associated cancers to know whether HPV infections have a consistent effect on different cancers.

METHODS

Data Collection and Processing

Single-cell RNA sequencing data of cervical cancer with HPV+ and HPV- (GSM5236544, GSM5236545, GSM5236546, GSM5236547) were downloaded from Gene Expression Omnibus (GEO) database (http://www.ncbi.nlm.nih.gov/geo/). Single-cell RNA sequencing data of HNSCC with HPV+ and HPV- (GSE139324) were downloaded from Gene Expression Omnibus (GEO) database Transcriptome profiling data and the corresponding clinical data were collected from GSE GEO database (GSE142583, GSE6791, GSE181805, GSE190224) and TCGA-CESC *via* the Sangerbox tools, a free online platform for data analysis (http://www.sangerbox.com/tool).

Single-Cell RNA Processing

The Seurat package was used to explore the transcriptional heterogeneity of cells within the HPV+ and HPV- tumor microenvironment for integration, pre-process, batch effect reduction, and non-linear dimension reduction of the datasets (8). The FindCluster () function was used to cluster cells. The Findmarkers () function was used to get marker genes in the clusters. SingleR was used to annotate cells automatically. The pseudotime trajectory analysis was performed using the Monocle3 package with default settings (9).

Immune Estimate

The immune score was estimated using ESTIMATE (Estimation of Stromal and Immune cells in Malignant Tumors using Expression data) (10). Immune cell proportions in the HPV+ and HPV- samples were analyzed utilizing cell type identification by calculating relative subsets of RNA transcripts (CIBERSORT) (11).

DeRNA and WGCNA

Differentially expressed RNA (DeRNA) among HPV+ and HPV- groups were screened out through Linear Models for Microarray Analysis (limma) package in R software (12). The cutoff values of screening were |fold change (FC)| >1.2 and $p < 0.05$. The "WGCNA" package was used for the weighted correlation network analysis (WGCNA) (13).

Molecular Risk Model Construction

The survival package's coxph () function was used to fit the Cox risk regression, and a p-value of 0.05 was considered survival/relapse related (14). The least absolute shrinkage and selection operator (LASSO) method is a compression estimation that creates a more refined model by generating a penalty function, compressing certain coefficients while simultaneously setting some values to zero. As a result, the benefit of subset shrinking is preserved. A biased estimation for multicollinear data processing allows for selecting variables when estimating parameters, allowing for a better solution to the multicollinearity problem in regression analysis. We utilized the glmnet package for analysis, and for model construction, we used 10-fold cross-validation and LASSO Cox regression (15).

Functional Enrichment Analysis

Gene Ontology (GO) and Kyoto Encyclopedia of Genes and Genomes (KEGG) enrichment analyses were performed to identify biological processes and pathways that were most related to hub genes with $p < 0.05$ as cutoff value (http://www.sangerbox.com/tool).

HPV-Associated Pan Cancer Analysis

Gene Expression Profiling Interactive Analysis 2021 (GEPIA2021), a web-based tool, analyzed the hub genes expressions and overall survival in HPV-associated cancers (16). ScRNA-seq and RNA expression profiling of HPV+ and HPV- HNSCC were analyzed like 2.1 and 2.4.

RESULT

Data Integration and scRNA-Seq Data Analysis

Patients' information was summarized from the corresponding clinical data in 46 samples with known HPV states (**Table 1**). Overall, the CESC patients in the HPV- group tended to be younger and more likely to have a lower tumor grade, but this is not significant (P=0.81) due to a massive number of high-grade patients in TCGA-CESC were excluded with incomplete HPV state.

In the scRNA analysis, 19 clusters were obtained by their gene expression patterns (11,899 marker genes) (**Figures 1A–C**). The annotation of cells by SingleR (**Figure 2A**) resulted in nine main immune cell type clusters based on their expression of immune cell markers. Based on the different abundance of marker genes expression in scRNA sequencing (**Figures 2B, C**), the dimension by UMAP and tSNE revealed reduced $CD8^+$ T cell and B cell clusters, while an increase in Treg -, $CD4^+$ T -, and epithelial cell clusters was observed within HPV+ CESC patients. Pseudotime trajectory analysis highlighted the heterogeneity of immune cell development between HPV+ and HPV- CESC patients (**Figures 2D, E**).

Immune Cell Analysis

The advantage of large-scale integration of paired clinical information in TCGA-CESE transcriptional RNA data allowed the analysis of immune signatures between HPV+ and HPV- CESC groups by using the ESTIMATE algorithm with TCGA RNA data input (**Figure 3A**). CIBERSORT enabled the estimation of the CESC patients' immune cell status (22 immune cell types) based on TCGA-CESE RNA count data (**Figure 3B**).

The performance of a survival analysis considering the immune status of the CESC patients revealed a low survival probability for patients with a smaller abundance of CD8+ T cells and naive B cells (**Figures 3C, D**). CD8+ T cells and naive B cells immune clusters were chosen as targets for subsequent analysis. Other immune cell clusters were excluded from subsequent analysis due to either not having significant expression between HPV+ and HPV- group or showed no statistical influence on the survival probability of CESC patients (**Supplementary Figure 1**). Genes in the cluster of epithelial cells were also excluded due to not being represented within the immune cell status (22 immune cells).

Differentially Expressed RNA and WGCNA Analysis

Since both the HPV+ and the HPV- group consists of CESC patients, the identification of DERNAs is aggravated. In contrast, the comparison of cancer and non-cancer groups allows a much simpler statistical analysis. To access the DERNAs between the HPV+ and HPV- CESC patients, an adjusted fold-change (1.2-fold change) and a standard p-value (<0.05) were set (**Figure 4A**) resulting in the identification of 6317 DERNAs. After creating a matrix containing the identified DERNAs, a WGCNA analysis (soft threshold = 5) was performed. The construction of a scale-free co-expression network enabled the identification of gene features related to CD8+ T cells and naive B cells. In total, 11 modules were generated (**Figure 4B**), of which the red had the highest correlation with the CD8+T score (r=0.46, P=2.8e−17, **Figure 4C**), and the black had the highest correlation with the naive B cells score (r=0.37, P=1.8e−11, **Figure 4C**). The results show that the important elements of the red module and black module represent CD8+ T cells and naive B cells respectively, finally obtaining 249 hub genes (MM>0.8 and GS>0.1 from the two modules.

Genetic Risk Model

Univariate Cox (proportional hazards model) proportional risk models were taken to analyze the hub genes, which related to CD8+ T cells, Naive B cells, and differently expressed between HPV+ and HPV- CESC. Two hundred genes were significantly associated with overall survival (log-rank test p<0.05, **Figure 5A**). In the survival univariate Cox proportional risk models, 39 genes (HR>1) were recognized as increased in hazard, 161 genes (HR<1) were recognized as reduction in hazard. Then, LASSO regression was used to solve the multicollinearity problem and minimize the number of genes in the risk model, as shown in **Figure 5B** LASSO Cox regression analysis, and each independent variable's change trajectory. Next, internal 10-fold cross-validation was performed after LASSO-cox regression to get a superior model (**Figure 5C**), When lambda = 0.0285755570440733, the model is optimum, and nine genes (IKZF3, APOBEC3H, JAK3, CLECL1, FOXP3, CD6, CLEC2D, LINC00158, PILRA) were chosen to build a survival risk model. The final 9-gene signature is as follows:

$$RiskScore = -0.110045311944626 * IKZF3 - 0.180200464406653 * APOBEC3H - 0.009738330408125074 * JAK3 - 0.100574502555081 * CLECL1 - 0.0109656212011594 * FOXP3 - 0.00569462037861635 * CD6 - 0.00590561916507251 * CLEC2D - 0.279175668959309 * LINC00158 - 0.00677990623712316 * PILRA$$

TABLE 1 | HPV+ and HPV- CESC patient information. The tumor stages and age information of HPV+ and HPV- CESC patients.

	HPV+ (N = 42)	HPV-(N = 4)	Total (N = 46)
Tumor Stage			
I	32 (69.57%)	3 (6.52%)	35 (76.09%)
II	5 (10.87%)	1 (2.17%)	6 (13.04%)
III	4 (8.70%)	0 (0.0e+0%)	4 (8.70%)
IV	1 (2.17%)	0 (0.0e+0%)	1 (2.17%)
Age			
Mean±SD	42.75 ± 11.47	37.00 ± 9.90	42.48 ± 11.36

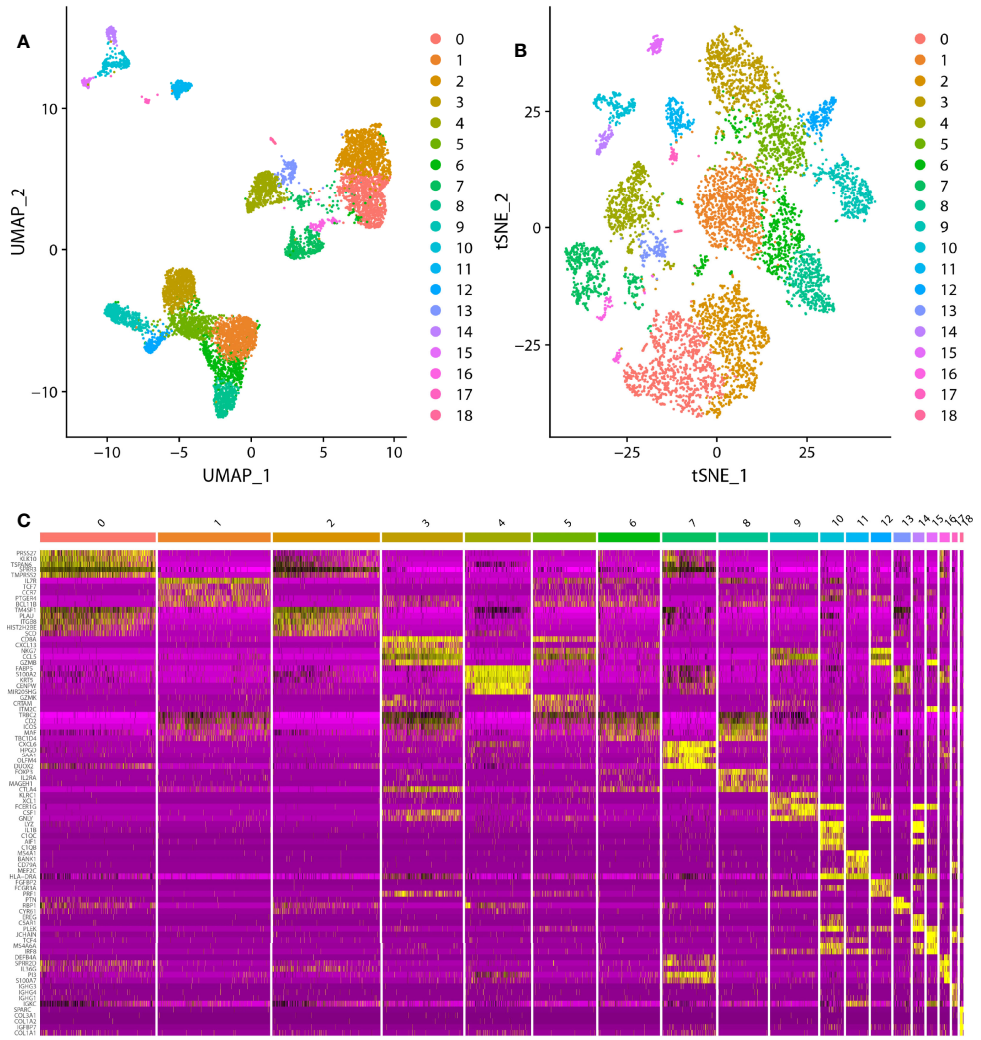


FIGURE 1 | The dimension reduction of CESC scRNA-seq. **(A)** Separate clusters according to UAMP. **(B)** Separate clusters according to tSNE. **(C)** Top five marker genes of each cluster.

Due to nine genes in the survival risk model having a negative coefficient, these genes could be considered as favorable, the higher these genes expression, the lower RiskScore will be calculated. The TCGA-CESC samples with corresponding survival state and survival time were classified as high or low risk with median standardization. The results of the KM (Kaplan–Meier estimator) curves revealed significant differences between the low- and high-risk groups (p=4.0e-5, **Figure 5D**). As shown in (**Figure 5E**), the TCGA-CESE data of the individual patients was assigned to low RiskScore or high RiskScore groups using the median RiskScore. The survival probability of patients with an elevated expression of IKZF3, APOBEC3H, JAK3, CLECL1, FOXP3, CD6, CLEC2D, LINC00158, and PILRA was increased. In addition, the application of receiver operating characteristic (ROC) curves verified the sensitivity and specificity of the overall survival model (**Figure 5F**). For the 1-, 3-, and 5-year prognoses, the present risk model predicted AUC values of 0.74, 0.68, and 0.71, respectively. This supported the accurate prediction of CESC patients' overall survival by the model.

The same method was performed again to get a relapse model. One hundred thirty-nine genes were significantly associated (log-rank test p<0.05, **Figure 6A**) with relapse, 54 genes increased in hazard (HR>1) while 85 genes reduced in hazard (HR<1). The relapse model is optimal when lambda = 0.0283647620242562, seven genes (ARHGAP30, DOK2, ICOS, JAK3, FOXP3, IKZF3, HEATR9) were chosen to construct a relapse risk model (**Figures 6B, C**). The final 7-gene signature is as follows:

$$RiskScore = -0.0210123392211442 * ARHGAP30 - 0.0139776933948472 * DOK2 - 0.0654058831289185 * ICOS - 0.00439045899467425 * JAK3 - 0.0303215128344747 * FOXP3 - 0.0203955365226131 * IKZF3 - 1.57542330970538 * HEATR9$$

An equal approach was used for the 7-gene relapse model utilizing the same models as for the survival model.

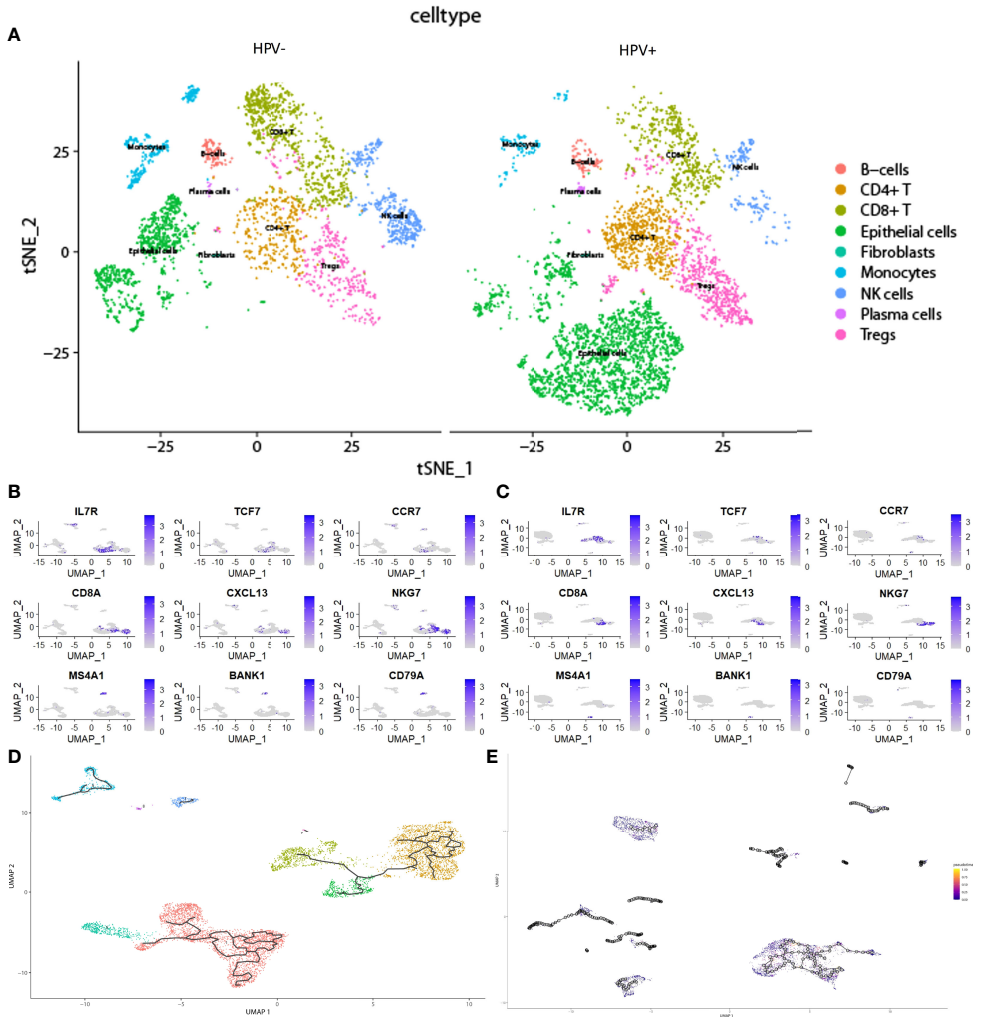


FIGURE 2 | The heterogeneity in HPV+ and HPV- CESC scRNA-seq. **(A)** Cell type annotation of HPV+ and HPV- group. **(B)** Top marker genes of CD8+T, CD4+T, and B cells in HPV- group. **(C)** Top marker genes of CD8+T, CD4+T, and B cells in HPV+ group. **(D)** Pseudotime and trajectory analysis of HPV- group. **(E)** Pseudotime and trajectory analysis of HPV+ group.

A significantly higher relapse probability of the high RiskScore group was observed than in the low RiskScore group (**Figure 6D**, p=0.01). The relapse probability of patients with a reduced expression of ARHGAP30, DOK2, ICOS, JAK3, FOXP3, IKZF3, and HEATR9 was increased identifying the down-regulation of these genes as potential risk factor of relapse (**Figure 6E**). AUC values of 0.76 (1-year relapse), 0.70 (3-year relapse), and 0.74 (5-year relapse) obtained from the ROC curves support the high accuracy of the model in predicting CESC patients' relapse (**Figure 6F**).

Gene Set Enrichment Analysis

To access the non-immunological function of the hub genes, which showed highest correlation to the CD8+ T cells or B cells according to WGCNA analysis, GO functional and KEGG pathway analysis were performed. The outcome was that genes relevant in the survival risk model and relapse risk model were predominantly enriched in biological processes associated with immunological function, while the influence on non-immunological processes could be neglected (**Figures 7A–C**). Due to the small number of genes in the relapse risk model, no hits in the KEGG pathway analysis were obtained.

HPV-Associated Pan Cancer Analysis

Since HPV infection is suspected to contribute to the emergence of other cancer types (Bladder Urothelial Carcinoma (BLCA), HNSC, Colon adenocarcinoma (COAD), Prostate Adenocarcinoma (PRAD)), an HPV-associated pan cancer analysis of IKZF3, FOXP3, and JAK3 was performed. Since these genes were represented in both risk models (survival and relapse), their potential impact on cancerogenesis was estimated higher than for genes appearing in only one model. The expressions of genes are shown in **Figure 8A**.

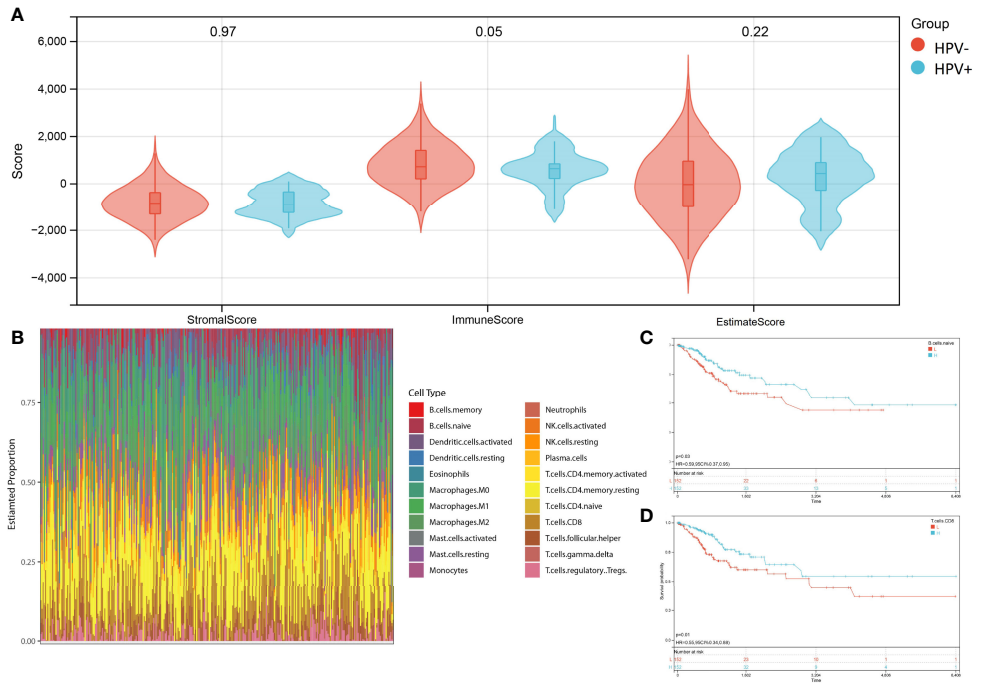


FIGURE 3 | Character of immune infiltration. **(A)** Stromal score, Immune Score and Estimate Score of HPV+ AND HPV- group. **(B)** Bar charts of 22 immune cell proportions in CESC TCGA RNA-seq. **(C)** KM curves of different expression Naive B cell. **(D)** KM curves of different expression CD8+ T cell.

The survival analysis of IKZF3 showed that IKZF3 is favorable in BLCA (**Figure 8B**) and HNSC (**Figure 8C**). No influence of IKZF3 on the survival probability was observed in COAD (**Figure 8D**) and PRAD (**Figure 8E**).

Differential expressions of FOXP3 showed no significant impact on BLCA (**Figure 8F**), PRAD (**Figure 8G**), and COAD (**Figure 8H**), while high expression of FOXP3 was associated with a higher percentage of survival in HNSC (**Figure 8I**).

HNSC patients with high expression of JAK3 tend to have more prolonged survival (**Figure 8J**), and there is no significant impact of JAK3 expressions on COAD (**Figure 8K**), PRAD (**Figure 8L**), and BLCA (**Figure 8M**).

In the scRNA analysis of HPV+ and HPV- HNSCC, the hub genes show a similar tendency as they do in HPV+ and HPV- CESC (**Figures 8N, O**). An intuitive difference could be overserved *via* the quantification of expression profiling by high throughput sequencing (**Figure 8P**).

DISCUSSION

Although it has been widely confirmed that HPV-associated lesions pose a higher risk to become malignant (4), there are few studies comparing immune cell infiltration, gene expression, and tumor heterogeneity between HPV+ and HPV- tumors. The current research shows that single-cell transcriptomics are a powerful tool to explore heterogeneity of HPV+ and HPV- tumors, which facilitates assessing the impact of HPV infection on cancer biology by identifying gene markers for diagnosis, prognosis, and therapy.

We assume that HPV affects the host from transcriptional state to immune infiltration. Therefore, we analyzed the transcriptional differences between HPV+ and HPV- samples by scRNA-seq as well as bulk RNA sequencing. Based on the differences in gene expression, we found that HPV+ samples showed CD8+ T cells and B cells were down-regulated while T reg cells, CD4+ T cells and epithelial cells were up-regulated in HPV+ CESC patients. The analysis of scRNA-seq is consistent with a previous study about immunologic treatments for CESC (17), HPV clearance in basal epithelial cells requires the activation of adaptive immunity and the formation of helper T cells that enable the development of CD8+ cytotoxic T cells against viral early proteins. In addition, T helper cells also support optimal activation of B cells, which can protect against subsequent infections at mucosal and systemic levels.

After learning that there was an immune infiltration difference between HPV+ and HPV- samples, we performed tumor immune infiltration of bulk RNA sequencing samples with survival information by CIBERSORT and found significantly longer survival for samples infiltrated with CD8+ cells and B cells. Therefore, WGCNA analysis was used to screen for differential genes (including low immune cell specificity genes) with the highest correlation to CD8+ cells and B cells and used for subsequent construction of survival and relapse models. Finally, we identified JAK3, FOXP3, and IKZF3, three genes with reduced expression in the HPV+ group, as protective

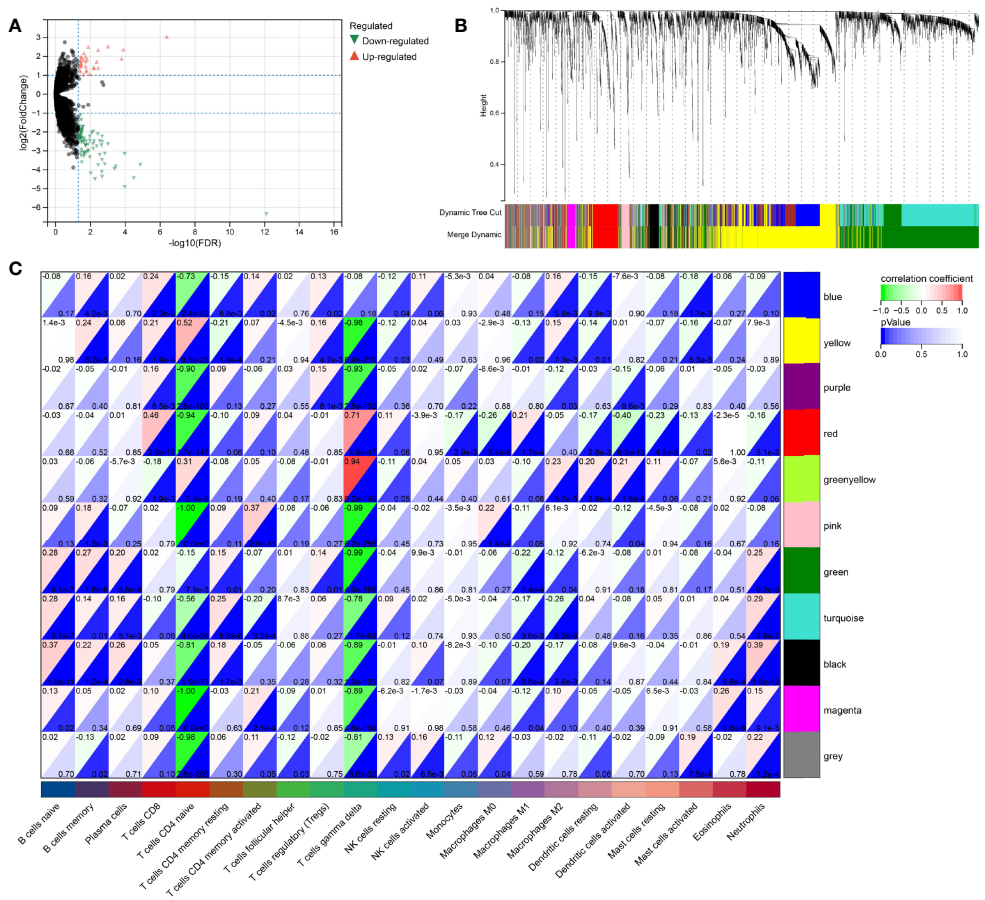


FIGURE 4 | WGCNA analysis for DeRNA. **(A)** Volcano plot of DeRNA. **(B)** Clustering results of minded modules in DeRNA dataset. **(C)** The correlation between different modules and the proportions of 22 immune cells.

factors for survival and relapse. The lower expression of these three, the higher the RiskScore in the model, which means a higher risk of death and recurrence.

The higher expression of three hub genes shows a higher percentage of survival in HNSC, which is consistent with our analyzed difference between HPV+ and HPV- HNSC samples. However, this result could not be observed in other potential HPV-associated cancers, only IKZF3 was found to be favorable in BLCA. As Jørgensen KR and Jensen JB found out, most studies fail to prove clear-cut relevance of HPV in BLCA irrespectively of histological subtype (18). No hub genes could associate expression level with survival state in COAD and PRAD. As KHOURY et al. mentioned (19), no HPV transcripts were detected in prostate and colon adenocarcinomas *via* RNA-Seq data. For this result, we concluded that hub genes are affected by HPV+ and that high expression of hub genes in non-HPV-infected tumors is not protective.

The functions of FOXP3, JAK3, and IKZF3 are widely researched in the field of tumor immunology. As the most specific and reliable biomarker of T reg cells, the studies of FOXP3 are conflicted. The infiltration of tumors with FOXP3+ Tregs was considered unfavorable for patient survival in many types of cancer. However, more recent work has described Helios as a new marker of Tregs. Tregs only have an immunosuppressive function when both FOXP3 and Helios are expressed (20). In the study of HPV+ tonsillar squamous cell carcinoma (20, 21), FOXP3 is a favorable prognostic factor. In addition, The Foxp3 gene was recognized as an immunological regulator, suppressing oncogenes while activating tumor suppressor genes (22). Decreased FOXP3 expression would impair FOXP3-mediated oncogene repression and tumor suppressor activation (23, 24). JAK3 is a tyrosine kinase that belongs to the Janus family of kinases, most commonly expressed in T cells and NK cells (25). Laffort et al. found that patients with HPV disease had severe combined immune deficiency associated with JAK3 deficiency. In addition, JAK3 mutations were identified in HPV+ Squamous Cell Carcinomas of the Oropharynx (OPSCC) (26) and Cervical Precancers (27). The production of IKZF3 is a transcription factor that is important in regulating B lymphocyte proliferation and differentiation and has been described as a target of HPV integration (28). In the study of OPSCC, IKZF3 RNA was detected in HPV+ cell lines, and regardless of tumor cell expression pattern, the immune cell infiltration was significantly positive for IKZF3. In this study,

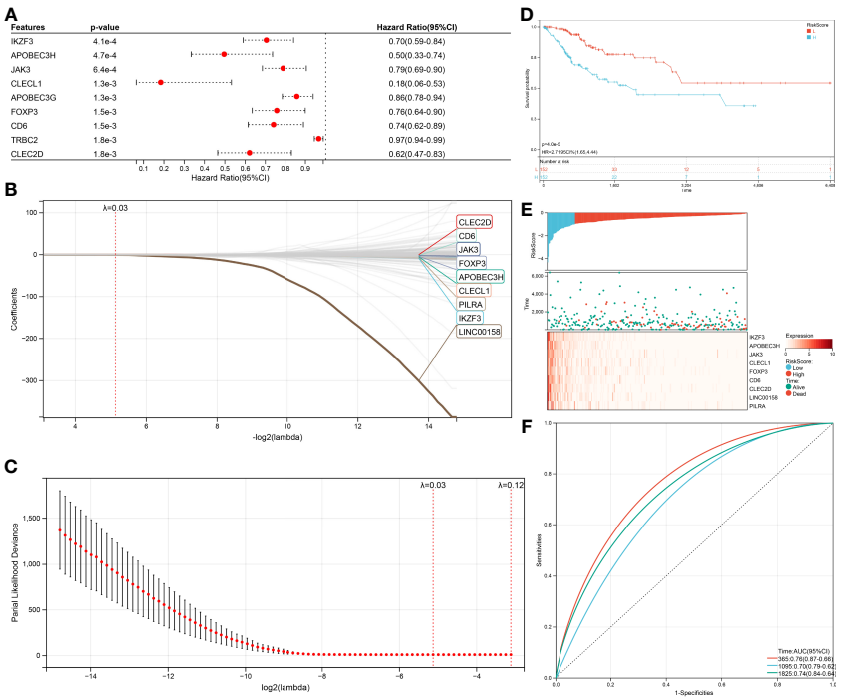


FIGURE 5 | Construction of the Cox and LASSO Cox model. **(A)** Top nine survival-related genes in Cox model. **(B)** The trajectory of each independent variable in the survival-related model: the horizontal axis represents the log2 value of the independent variable lambda, and the vertical axis represents the coefficient of the independent variable. **(C)** The confidence interval under each lambda in the survival-related model. **(D)** Top9 relapse-related genes in Cox model. **(E)** The trajectory of each independent variable in the relapse-related model: the horizontal axis represents the log2 value of the independent variable lambda, and the vertical axis represents the coefficient of the independent variable. **(F)** The confidence interval under each lambda in the relapse-related model.

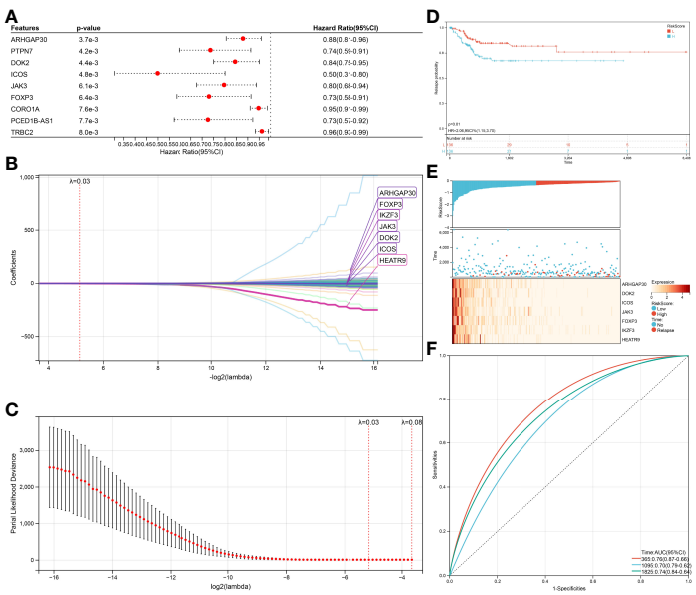


FIGURE 6 | Verification of the prognostic risk models. **(A)** KM curves of different RiskScore in the survival-related model. **(B)** RiskScore and survival time with survival status profile and expression levels of the nine gene signatures. **(C)** ROC curve validation for survival-related model. **(D)** KM curves of different RiskScore in the relapse-related model. **(E)** RiskScore and relapse time with relapse status profile and expression levels of the seven gene signatures. **(F)** ROC curve validation for relapse-related model.

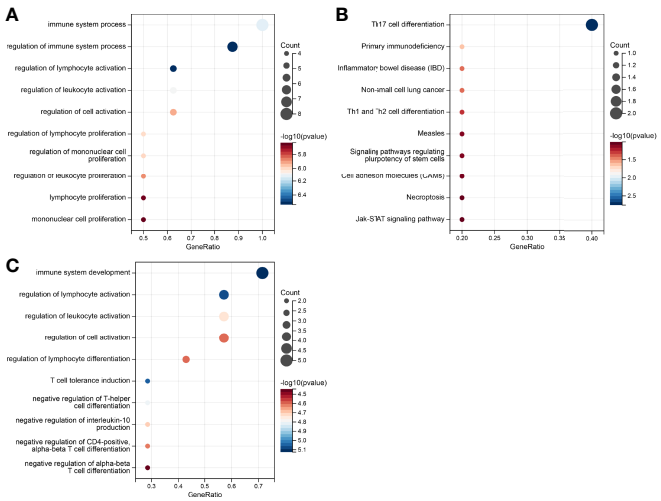


FIGURE 7 | Gene set enrichment analysis of the genes in the prognostic risk models. **(A)** GO enrichment in the survival-related model. **(B)** KEGG pathways in survival-related model. **(C)** GO enrichment in the relapse-related model.

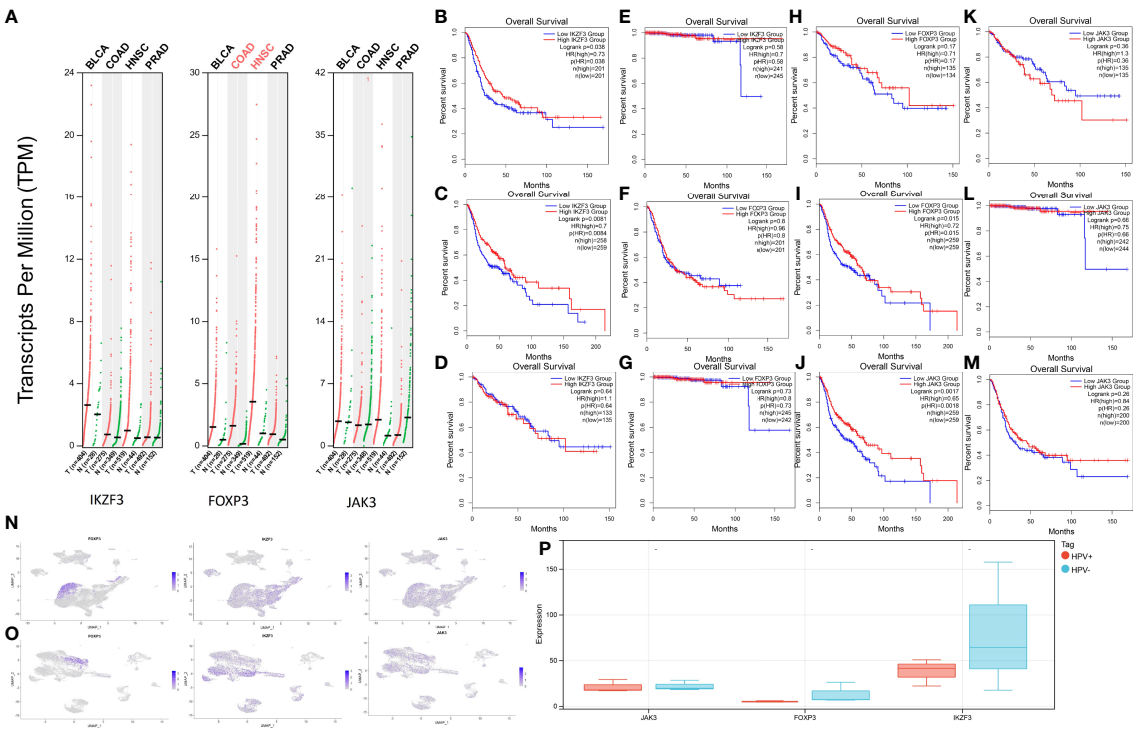


FIGURE 8 | Expression levels and survival analysis in HPV-associated cancers. **(A)** IKZF3, FOXP3, and JAK3 expression levels in BLCA, HNSC, PRAD, and COAD. **(B)** Survival analysis between high-IKZF3 and low-IKZF3 groups in BLCA. **(C)** Survival analysis between high-IKZF3 and low-IKZF3 groups in HNSC. **(D)** Survival analysis between high-IKZF3 and low-IKZF3 groups in COAD. **(E)** Survival analysis between high-IKZF3 and low-IKZF3 groups in PRAD. **(F)** Survival analysis between high-FOXP3 and low-FOXP3 groups in BLCA. **(G)** Survival analysis between high-FOXP3 and low-FOXP3 groups in PRAD. **(H)** Survival analysis between high-FOXP3 and low-FOXP3 groups in COAD. **(I)** Survival analysis between high-FOXP3 and low-FOXP3 groups in HNSC. **(J)** Survival analysis between high-JAK3 and low-JAK3 groups in HNSC. **(K)** Survival analysis between high-JAK3 and low-JAK3 groups in COAD. **(L)** Survival analysis between high-JAK3 and low-JAK3 groups in PRAD. **(M)** Survival analysis between high-JAK3 and low-JAK3 groups in BLCA. **(N)** Expressions of FOXP3, IKZF3, JAK3 in scRNA-seq HPV- HNSC. **(O)** Expressions of FOXP3, IKZF3, JAK3 expression in scRNA-seq HPV+ HNSC. **(P)** Quantification of FOXP3, IKZF3, JAK3 in bulk RNA-seq HPV+ and HPV- HNSC.

IKZF3 had a HR of 0.38, which indicated IKZF3 is protective (29). For the first time, we proposed two signatures based on the heterogeneity of CESC, which may be applied for survival and relapse, and provided potential immunotherapy targets. However, we did not explore the mechanism of genes in two signatures. Future efforts should focus on using many samples to verify the model's accuracy and explore the molecular mechanism of the signature genes, providing experimental evidence for application to risk prediction and treatment in HPV- associated Cancers.

In conclusion, analysis of scRNA-seq and bulk RNA-seq of HPV+ and HPV- CESC samples revealed heterogeneity from transcriptional state to immune infiltration. Based on the difference, we found prognosis-related genes where expression was affected by HPV+. The LASSO Cox regression analysis of these genes constructed survival and recurrence models. IKZF3, FOXP3, and JAK3 represented in both risk models had the similar distribution and protective effects in HPV-associated HNSC, which means the expression of the hub genes are affected by HPV+.

DATA AVAILABILITY STATEMENT

Publicly available datasets were analyzed in this study. This data can be found here: https://www.ncbi.nlm.nih.gov/geo/query/acc.cgi?acc=GSE171894, PRJNA721342, https://www.ncbi.nlm.nih.gov/geo/query/acc.cgi?acc=GSE139324, https://www.ncbi.nlm.nih.gov/geo/query/acc.cgi?acc=GSE142583, https://www.ncbi.nlm.nih.gov/geo/query/acc.cgi?acc=GSE6791, https://www.ncbi.nlm.nih.gov/geo/query/acc.cgi?acc=GSE181805, https://www.ncbi.nlm.nih.gov/geo/query/acc.cgi?acc=GSE190224. In addtion, GSE139324, GSE 6791, GSE190224.

AUTHOR CONTRIBUTIONS

BC-E and MR conceived and designed the study. EW, AR, and JL analyzed the data and drafted the manuscript. EW and LF prepared the figures. All authors contributed to the article and approved the submitted version.

ACKNOWLEDGMENTS

We would like to thank TCGA and GEO databases for the availability of the data.

SUPPLEMENTARY MATERIAL

The Supplementary Material for this article can be found online at: https://www.frontiersin.org/articles/10.3389/fonc.2022.860900/full#supplementary-material

REFERENCES

1. Banuelos-Villegas EG, Perez-yPerez MF, Alvarez-Salas LM. Cervical Cancer, Papillomavirus, and miRNA Dysfunction. *Front Mol Biosci* (2021) 8:758337. doi: 10.3389/fmolb.2021.758337
2. Wardak S. Human Papillomavirus (HPV) and Cervical Cancer. *Medycyna doswiadczalna i mikrobiologia* (2016) 68:73–84.
3. Ljubojevic S, Skerlev M. HPV-Associated Diseases. *Clin Dermatol* (2014) 32:227–34. doi: 10.1016/j.clindermatol.2013.08.007
4. Does H, Does H. *Genital HPV Infection–CDC Fact Sheet*. Available at: https://www.cdc.gov/std/hpv/hpv-Fs-July-2017.pdf.
5. Potter SS. Single-Cell RNA Sequencing for the Study of Development, Physiology and Disease. *Nat Rev Nephrol* (2018) 14:479–92. doi: 10.1038/s41581-018-0021-7
6. Li C, Guo L, Li S, Hua K. Single-Cell Transcriptomics Reveals the Landscape of Intra-Tumoral Heterogeneity and Transcriptional Activities of ECs in CC. *Mol Ther Nucleic Acids* (2021) 24:682–94. doi: 10.1016/j.omtn.2021.03.017
7. Bezzecchi E, Bernardini A, Ronzio M, Miccolo C, Chiocca S, Dolfini D, et al. NF-Y Subunits Overexpression in HNSCC. *Cancers (Basel)* (2021) 13:3019. doi: 10.3390/cancers13123019
8. Hao Y, Hao S, Andersen-Nissen E, Mauck WM3rd, Zheng S, Butler A, et al. Integrated Analysis of Multimodal Single-Cell Data. *Cell* (2021) 184:3573–3587.e29. doi: 10.1016/j.cell.2021.04.048
9. Cao J, Spielmann M, Qiu X, Huang X, Ibrahim DM, Hill AJ, et al. The Single-Cell Transcriptional Landscape of Mammalian Organogenesis. *Nature* (2019) 566:496–502. doi: 10.1038/s41586-019-0969-x
10. Yoshihara K, Shahmoradgoli M, Martínez E, Vegesna R, Kim H, Torres-Garcia W, et al. Inferring Tumour Purity and Stromal and Immune Cell Admixture From Expression Data. *Nat Commun* (2013) 4:1–11. doi: 10.1038/ncomms3612
11. Newman AM, Liu CL, Green MR, Gentles AJ, Feng W, Xu Y, et al. Robust Enumeration of Cell Subsets From Tissue Expression Profiles. *Nat Methods* (2015) 12:453–7. doi: 10.1038/nmeth.3337
12. Ritchie ME, Phipson B, Wu D, Hu Y, Law CW, Shi W, et al. Limma Powers Differential Expression Analyses for RNA-Sequencing and Microarray Studies. *Nucleic Acids Res* (2015) 43:e47. doi: 10.1093/nar/gkv007
13. Zhang B, Horvath S. A General Framework for Weighted Gene Co-Expression Network Analysis. *Stat Appl Genet Mol Biol* (2005) 4. doi: 10.2202/1544-6115.1128
14. Therneau TM. *Extending the Cox Model, Proceedings of the First Seattle Symposium in Biostatistics*. New York: Springer (1997) p. 51–84.
15. Tibshirani R. The Lasso Method for Variable Selection in the Cox Model. *Stat Med* (1997) 16:385–95. doi: 10.1002/(SICI)1097-0258(19970228)16:4<385::AID-SIM380>3.0.CO;2-3
16. Li C, Tang Z, Zhang W, Ye Z, Liu F. GEPIA2021: Integrating Multiple Deconvolution-Based Analysis Into GEPIA. *Nucleic Acids Res* (2021) 49:W242–6. doi: 10.1093/nar/gkab418
17. Vici P, Mariani L, Pizzuti L, Sergi D, Di Lauro L, Vizza E, et al. Immunologic Treatments for Precancerous Lesions and Uterine Cervical Cancer. *J Exp Clin Cancer Res* (2014) 33:29. doi: 10.1186/1756-9966-33-29
18. Jorgensen KR, Jensen JB. Human Papillomavirus and Urinary Bladder Cancer Revisited. *APMIS* (2020) 128:72–9. doi: 10.1111/apm.13016
19. Khoury JD, Tannir NM, Williams MD, Chen Y, Yao H, Zhang J, et al. Landscape of DNA Virus Associations Across Human Malignant Cancers: Analysis of 3,775 Cases Using RNA-Seq. *J Virol* (2013) 87:8916–26. doi: 10.1128/JVI.00340-13
20. Park K, Cho KJ, Lee M, Yoon DH, Kim SB. Importance of FOXP3 in Prognosis and its Relationship With P16 in Tonsillar Squamous Cell Carcinoma. *Anticancer Res* (2013) 33:5667–73.
21. Molling JW, de Gruijl TD, Glim J, Moreno M, Rozendaal L, Meijer CJ, et al. CD4(+)CD25hi Regulatory T-Cell Frequency Correlates With Persistence of Human Papillomavirus Type 16 and T Helper Cell Responses in Patients With Cervical Intraepithelial Neoplasia. *Int J Cancer* (2007) 121:1749–55. doi: 10.1002/ijc.22894
22. Zuo T, Wang L, Morrison C, Chang X, Zhang H, Li W, et al. FOXP3 is an X-Linked Breast Cancer Suppressor Gene and an Important Repressor of the HER-2/ErbB2 Oncogene. *Cell* (2007) 129:1275–86. doi: 10.1016/j.cell.2007.04.034
23. Li W, Wang L, Katoh H, Liu R, Zheng P, Liu Y. Identification of a Tumor Suppressor Relay Between the FOXP3 and the Hippo Pathways in Breast and

Prostate Cancers. *Cancer Res* (2011) 71:2162–71. doi: 10.1158/0008-5472.CAN-10-3268
24. Cezar-Dos-Santos F, Ferreira RS, Okuyama NCM, Trugilo KP, Sena MM, Pereira ER, et al. FOXP3 Immunoregulatory Gene Variants Are Independent Predictors of Human Papillomavirus Infection and Cervical Cancer Precursor Lesions. *J Cancer Res Clin Oncol* (2019) 145:2013–25. doi: 10.1007/s00432-019-02951-x
25. Leonard WJ, O'Shea JJ. Jaks and STATs: Biological Implications. *Annu Rev Immunol* (1998) 16:293–322. doi: 10.1146/annurev.immunol.16.1.293
26. Dogan S, Xu B, Middha S, Vanderbilt CM, Bowman AS, Migliacci J, et al. Identification of Prognostic Molecular Biomarkers in 157 HPV-Positive and HPV-Negative Squamous Cell Carcinomas of the Oropharynx. *Int J Cancer* (2019) 145:3152–62. doi: 10.1002/ijc.32412
27. Regauer S, Reich O, Kashofer K. Cervical Precancers Originate From Infected Proliferating Reserve Cells: A Comparative Histologic and Genetic Study of Thin and Thick High-Grade Squamous Intraepithelial Lesions. *Am J Surg Pathol* (2021) 46(4):519–27. doi: 10.1097/PAS.0000000000001818
28. Rusan M, Li YY, Hammerman PS. Genomic Landscape of Human Papillomavirus–Associated Cancers. *Clin Cancer Res* (2015) 21:2009–19. doi: 10.1158/1078-0432.CCR-14-1101
29. Gleber-Netto FO, Rao X, Guo T, Xi Y, Gao M, Shen L, et al. Variations in HPV Function Are Associated With Survival in Squamous Cell Carcinoma. *JCI Insight* (2019) 4. doi: 10.1172/jci.insight.124762

Conflict of Interest: The authors declare that the research was conducted in the absence of any commercial or financial relationships that could be construed as a potential conflict of interest.

Publisher's Note: All claims expressed in this article are solely those of the authors and do not necessarily represent those of their affiliated organizations, or those of the publisher, the editors and the reviewers. Any product that may be evaluated in this article, or claim that may be made by its manufacturer, is not guaranteed or endorsed by the publisher.

Copyright © 2022 Wei, Reisinger, Li, French, Clanner-Engelshofen and Reinholz. This is an open-access article distributed under the terms of the Creative Commons Attribution License (CC BY). The use, distribution or reproduction in other forums is permitted, provided the original author(s) and the copyright owner(s) are credited and that the original publication in this journal is cited, in accordance with accepted academic practice. No use, distribution or reproduction is permitted which does not comply with these terms.

frontiers | Frontiers in Oncology

ORIGINAL RESEARCH
published: 03 June 2022
doi: 10.3389/fonc.2022.804242

Differences in the Impact of Heart Rate Variability on the Surgical Approach in Patients With Early Cervical Cancer: Laparoscopic versus Open Surgery

Jian Liu[1†], Jingfeng Wang[2,3†], Zhaoya Deng[1], Shiqi Liu[2], Guangqiao Li[2,3], Yilin Sun[1], Longfei Gao[1], Chenghui Li[2] and Bo Shi[2,3*]*

[1] Department of Gynecologic Oncology, First Affiliated Hospital, Bengbu Medical College, Bengbu, China, [2] School of Medical Imaging, Bengbu Medical College, Bengbu, China, [3] Anhui Key Laboratory of Computational Medicine and Intelligent Health, Bengbu Medical College, Bengbu, China

OPEN ACCESS

Edited by:
Polat Dursun,
Consultant, Ankara, Turkey

Reviewed by:
Luigi Turco,
Mater Olbia Hospital, Italy
Nicole Buote,
Cornell University, United States

***Correspondence:**
Bo Shi
shibo@bbmc.edu.cn
Jian Liu
elitelj@126.com

[†]These authors have contributed equally to this work

Specialty section:
This article was submitted to Gynecological Oncology, a section of the journal Frontiers in Oncology

Received: 29 October 2021
Accepted: 06 May 2022
Published: 03 June 2022

Citation:
Liu J, Wang J, Deng Z, Liu S, Li G, Sun Y, Gao L, Li C and Shi B (2022) Differences in the Impact of Heart Rate Variability on the Surgical Approach in Patients With Early Cervical Cancer: Laparoscopic versus Open Surgery. Front. Oncol. 12:804242. doi: 10.3389/fonc.2022.804242

Background: Evidence suggests that the risk of recurrence and death in patients with early cervical cancer (ECC) undergoing minimally invasive surgery is significantly higher than that in patients undergoing open surgery. However, the mechanisms underlying such a difference remain unclear. Heart rate variability (HRV) represents autonomic nerve activity, which is related to tumorgenesis and can be used as a prognostic indicator for various cancers. The main purpose of this study was to explore the difference in the effects of laparoscopic and open surgery on HRV in ECC patients.

Methods: A total of 68 ECC (FIGO IA1 with lymphovascular space invasion -IIA2) patients undergoing radical hysterectomy for the first time (84% open group vs. 16% laparoscopic group) were included. A single-lead micro-ECG recorder was used to collect 5 min electrocardiograms 1 day before the operation and 3 days after the operation, and then HRV time domain and frequency domain indices were analyzed, including mean heart rate (MeanHR), maximum heart rate (MaxHR), minimum heart rate (MinHR), the standard deviation of all normal-to-normal intervals (SDNN), the root mean square of successive interval differences (RMSSD), very low-frequency power (VLF), low-frequency power (LF), high-frequency power (HF), total power (TP), and the ratio of LF to HF (LF/HF).

Results: Heart rate (i.e., MeanHR, MaxHR, and MinHR) were significantly higher, and HRV (i.e., SDNN, RMSSD, LF, HF, and TP) were significantly lower after the operation than before the operation in both the laparoscopic and open groups ($P < 0.05$). The postoperative reduction in RMSSD and HF was significantly higher in the laparoscopic group than in the open group ($P < 0.05$).

Conclusions: These data suggest that radical hysterectomy can lead to increased heart rate and decreased HRV in patients with ECC, which can negatively affect cardiac autonomic regulation. Compared with open surgery, laparoscopic surgery has a greater negative impact on the HRV of ECC patients.

Keywords: early cervical cancer, autonomic nerve, heart rate variability, laparoscopic surgery, open surgery

INTRODUCTION

Cervical cancer (CC) is one of the most common malignant tumors in gynecology, and its morbidity and mortality rank fourth in females worldwide (1). According to the guidelines of the National Comprehensive Cancer Network and the European Society of Gynecological Oncology, radical hysterectomy (laparoscopic surgery or open surgery) is the standard treatment for early cervical cancer (ECC) patients (International Federation of Gynecology and Obstetrics (FIGO) IA-IIA) (2). After surgical treatment, the primary tumor of most ECC patients is removed, which can minimize the tumor load, achieve a better curative effect, and prolong the survival time (3, 4).

Some retrospective studies have shown that no significant differences in the recurrence rate and survival rate have been observed between minimally invasive surgery and open surgery in patients with ECC and locally advanced stage (5–8). In addition, compared with open surgery, laparoscopic surgery has certain advantages, such as less intraoperative blood loss, a lower wound infection rate, a shorter hospital stay and fewer postoperative complications (9–11). Nevertheless, the findings reported in these studies have been questioned due to small sample sizes, short follow-up durations, and a lack of adjustment for potential confounding factors (12). A recent multicenter prospective randomized controlled trial on laparoscopic treatment of ECC demonstrated that compared with open surgery, laparoscopic surgery for ECC patients has a lower disease-free survival rate and overall survival rate and a higher local recurrence rate and mortality rate (13). Additionally, Melamed et al. used the US national database (the National Cancer Database and the Surveillance, Epidemiology, and End Results (SEER) 18-registry database) to compare the survival differences of CC patients undergoing different surgeries. The results showed that during the median follow-up period of 45 months, the 4-year mortality was 9.1% among patients who underwent laparoscopic surgery and 5.3% among those who underwent open surgery (14). Since then, experts have agreed that laparoscopic surgery should no longer be advocated (15). However, the relevant mechanisms leading to this difference remain unknown.

The systemic stress response caused by surgical trauma can affect the autonomic nervous system (ANS) (16). Autonomic disorders not only increase the incidence of postoperative cardiovascular complications but also promote the growth and spread of tumor cells (17–19). Other studies also observed that certain associations between ANS function and disease recurrence and prognosis. In a large epidemiological study, patients with gastric ulcers who underwent vagotomy showed an increased incidence of colonic polyps during long-term follow-up (20). Erin et al. found that inhibition of vagus nerve can increase tumor metastasis in mice with breast cancer (BC) (21). Barron et al. indicated tha BC patients taking β-blockers (propranolol) had a lower specific mortality than patients not taking β-blockers (hazard ratio, 0.19; 95% CI, 0.06 to 0.60) (22). Heart rate variability (HRV), a noninvasive biomarker reflecting the ANS, has been widely used for the evaluation of prognosis in patients with a variety of cancers (23, 24). For example, De Couck et al. showed that compared with healthy people, cancer patients were often accompanied by damage to autonomic nerves, resulting in decreased HRV (25). Arab et al. found that the more advanced the tumor stage of BC patients, the more significant the decrease of HRV time domain parameters (26). Hu et al. demonstrated that the decrease of HRV in patients with gastric cancer predicts an increase in the severity of the tumor. The authors confirmed that HRV was associated with clinical stage, tumor size, tumor invasion, lymph node metastasis and distant organ involvement (27). Furthermore, a recent systematic review of HRV and cancer prognosis indicated that low HRV was associated with shorter survival, higher tumor burden, and worse prognosis (28). As a result, using HRV to detect the autonomic changes that may occur in ECC patients undergoing laparoscopic and open surgery may be able to better explain the differences in survival observed between the two methods. The main purpose of this paper is to test two hypotheses by comparing the effects of two surgical procedures (open surgery/laparoscopic surgery) on HRV in patients with ECC. Hypothesis 1: The HRV of ECC patients decreases significantly after the operation; that is, the operation has a negative effect on the prognosis of ECC patients. Hypothesis 2: Compared with open surgery, laparoscopic surgery has a greater negative impact on the HRV of ECC patients.

METHODS

Subjects

This study was prospective clinical controlled trials. The study participants included 72 patients with CC treated in the Department of Gynecology and Oncology, the First Affiliated Hospital of Bengbu Medical College, from November 2020 to May 2021. These patients underwent radical hysterectomy as a primary therapy. Surgical approach (laparoscopic surgery or open surgery) was determined on an individual basis with each patient after discussion of the risks and benefits of both options. All procedures were performed in accordance with the ethical standards outlined in the 1964 Declaration of Helsinki and its

later amendments. All patients were informed of the experimental details and signed informed consent forms. The study was approved by the Medical Ethics Committee of the First Affiliated Hospital of Bengbu Medical College (Bengbu, Anhui, China) (registration number: 2021KY010).

Inclusion and Exclusion Criteria

The inclusion criteria were as follows: (1) ECC diagnosed by pathological examination; (2) pathological types: squamous cell carcinoma, adenocarcinoma and adenosquamous carcinoma; (3) new patients without surgery, radiotherapy or chemotherapy; (4) met the indications for CC radical surgery and treated with radical hysterectomy; (5) tumor stages IA1 with lymphovascular space invasion -IIA2, based on the guidelines of FIGO 2018; and (6) operative methods: laparoscopic radical hysterectomy + pelvic lymph node dissection (laparoscopic group) or open radical hysterectomy + pelvic lymph node dissection (open group). The exclusion criteria were as follows: (1) pregnancy; (2) patients with primary diseases of the heart, liver, kidney; (3) patients with other tumors; and (4) patients with unqualified clinical stages.

Data Collection

A single-lead electrocardiogram (ECG) recorder (version 2.8.0, Healink-R211B, Healink Ltd., Bengbu, China) was used to collect 5 min supine ECG data from ECC patients at 1 day before the operation and 3 days after the operation. The sampling rate of the ECG recorder was set to 400 Hz, and the signal bandwidth was set to 0.6–40 Hz. All patients were requested to breathe as smoothly as possible in a quiet environment during the measurement. The V6 lead was used, and the measuring electrodes were Ag/AgCl disposable electrodes (JunKang Ltd., Shanghai, China). The environment was kept quiet, and the room temperature was maintained at 23 ± 1°C.

Heart Rate Variability Analysis

The QRS complex in the ECG signal was detected using the Pan-Tompkins algorithm, from which an R-R interval time (RRI) series was obtained (29). The time-varying threshold algorithm was used to automatically correct the artifacts caused by extraction technology, interference and ectopic heartbeat (30). Then, the HRV data were analyzed by time domain and frequency domain methods The main parameters included mean heart rate (MeanHR), maximum heart rate (MaxHR), minimum heart rate (MinHR), standard deviation of all normal-to-normal intervals (SDNN), root mean square of successive interval differences (RMSSD), very low-frequency (VLF: 0–0.04 Hz) power, low-frequency (LF: 0.04–0.15 Hz) power, high-frequency (HF: 0.15–0.40 Hz) power, total power (TP: 0–0.4 Hz) power and the ratio of LF power to HF power (LF/HF). Prior to frequency analysis, the RRI time series was resampled at 4 Hz using cubic spline interpolation (31).

Among these parameters, SDNN and TP reflect overall variability. HF is related to RMSSD, and both are adopted as markers of vagal modulation, whereas LF is considered representative of the modulation of both sympathetic and parasympathetic nerves (23, 32, 33). LF/HF is an indicator of the balance between sympathetic and vagal nerves (23, 32).

HRV analysis was performed using Kubios HRV Premium software (version 3.1.0, https://www.Kubios.Com, Kubios Oy, Kuopio, Finland) (34).

Statistical Analysis

Data were first tested for normality using the Shapiro-Wilk normality test. If the data showed a normal distribution, paired *t*-tests were used to examine the difference in HRV parameters before and after the operation; otherwise, nonparametric Wilcoxon signed-rank tests were used. Cohen's *d* was used to evaluate the effect sizes. The differences in HRV parameters before and after the operation between the two groups were compared by independent sample *t*-tests. All statistical analyses were performed using SPSS, version 23.0 (IBM Corp., Chicago, Illinois, United States of America). $P < 0.05$ was taken as statistically significant.

RESULTS

A total of 72 ECC patients were enrolled in this study. We further excluded several cases due to poor ECG quality ($N = 1$), ectopic heartbeats > 10% of all beats ($N = 1$) or due to abnormal data extremes ($N = 2$). Therefore, data from 68 cases were analyzed in the current study. Open radical hysterectomy was performed in 57 cases (84%) and laparoscopic radical hysterectomy in 11 cases (16%). **Table 1** shows the basic data of the studied ECC patients. There were no significant differences in patient characteristics such as age, body mass index (BMI), diabetes, menopausal status, FIGO stage, lymph node metastasis, pathological type, tumor size and invasion depth between the laparoscopic and open groups (all $P > 0.05$).

The HR and HRV results of the laparoscopic group and open group after radical hysterectomy compared with before are summarized in **Figure 1**. The postoperative HR (i.e., MeanHR, MaxHR, and MinHR) was significantly higher than the preoperative HR in both the laparoscopic and open groups ($P < 0.05$). The postoperative HRV (i.e., SDNN, RMSSD, LF, HF, and TP) was significantly lower than the preoperative HRV in the two groups ($P < 0.05$). A significant increase in LF/HF and a significant decrease in VLF were observed in the open group, while LF/HF and VLF showed no statistically significant difference in the laparoscopic group. The effect sizes of all HR and HRV indices in the laparoscopic group and open group before and after radical hysterectomy are shown in **Figure 2**. In addition, the differences in HR and HRV, indicated by the postoperative value minus the preoperative value, were compared in the laparoscopic group and open group (**Figure 3**). The reduction in RMSSD (laparoscopic group = -18.7 versus open group= -7.8) and HF (laparoscopic group = -365 versus open group = -53) after the operation was significantly higher in the laparoscopic group than in the open group ($P = 0.002$, $P = 0.010$ respectively).

TABLE 1 | Basic data of the CC patients studied.

	Open group (*N* = 57)	Laparoscopic group (*N* = 11)	*p* value
Age (years)	52.4 ± 9.3	46.8 ± 11.6	0.082
BMI (kg/m^2)	24.4 ± 3.0	24.7 ± 3.8	0.741
Diabetes, N (%)	1 (1.8)	1 (9.1)	0.299[c]
yes	56 (98.2)	10 (90.9)	
no			
Menopausal status, N (%)	36 (63.2)	5 (45.5)	0.446[b]
yes	21 (36.8)	6 (54.5)	
no			
FIGO stage, N (%)	42 (73.7)	9 (81.8)	0.849[b]
IA1-IB3	15 (26.3)	2 (18.2)	
IIA1-IIA2			
Lymph node metastasis, N (%)	8 (14.0)	1 (9.1)	1.000[b]
yes	49 (86.0)	10 (90.9)	
no			
Histological type, N (%)	48 (84.2)	9 (81.8)	1.000[b]
SCC	9 (15.8)	2 (18.2)	
AC			
Tumor size, N (%)	38 (66.7)	9 (81.8)	0.523[b]
<4 cm	19 (33.3)	2 (18.2)	
≥4 cm			
Depth of invasion, N (%)	27 (47.4)	8 (72.7)	0.123[a]
<1/2 mm	30 (52.6)	3 (27.3)	
≥1/2 mm			

[a]*Stands for the Pearson's chi squared test.*
[b]*Stands for the chi square test for continuity correction.*
[c]*Stands for the Fisher exact test.*
N, number of individuals; BMI, body mass index; SSC, squamous cell carcinoma; AC, adenomatous carcinoma. FIGO, International Federation of Gynecology and Obstetrics.

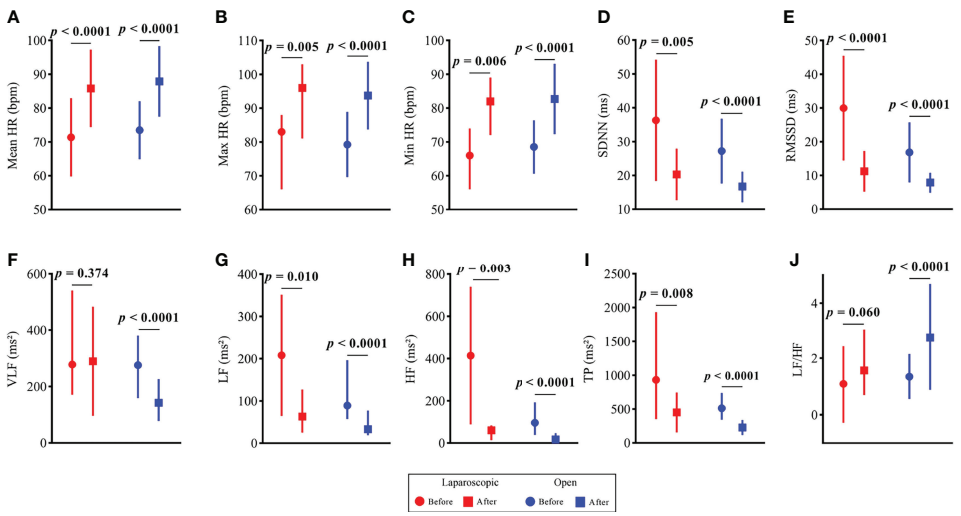


FIGURE 1 | HR and HRV results of the open group and laparoscopic group before vs. after radical hysterectomy. **(A)** Mean HR; **(B)** Max HR; **(C)** Min HR; **(D)** SDNN; **(E)** RMSSD; **(F)** VLF; **(G)** LF; **(H)** HF; **(I)** TP and **(J)** LF/HF.

DISCUSSION

A preliminary study of 68 patients with ECC who underwent radical hysterectomy revealed that HR was significantly higher and the HRV parameters (SDNN, RMSSD, LF, HF, and TP) were significantly lower after the operation than before the operation in both the laparoscopic and open groups. Furthermore, the difference in RMSSD and HF before and after the operation in the laparoscopy group was significantly higher than that in the open group. Thus, this study directly suggested that radical hysterectomy can lead to increased HR and decreased HRV in patients with ECC. Compared with open surgery, laparoscopic surgery has a greater negative impact on the HRV of ECC patients.

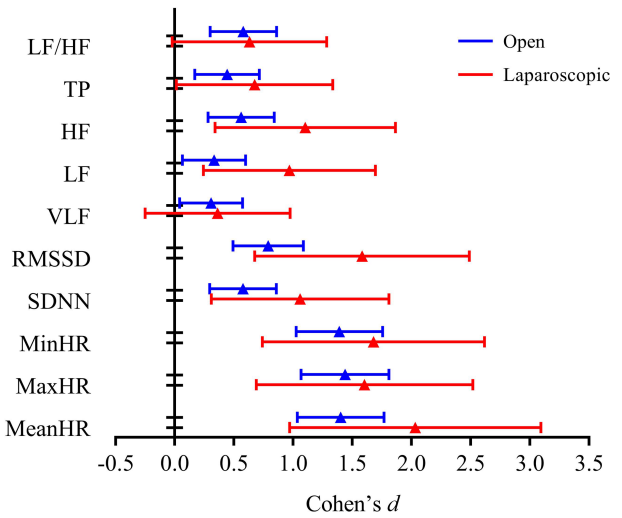


FIGURE 2 | Effect size of all HR and HRV indices in the open group and laparoscopic group before vs. after radical hysterectomy.

Radical hysterectomy is the mainstay of treatment for ECC, but surgery will inevitably cause certain psychological and physical damage to patients. Previous studies showed that HRV could be used to quantify surgical stress response and predict postoperative complications and prognosis. For example, Gogenur et al. confirmed that the HRV and the ANS in surgical patients would develop circadian disturbance, resulting in an increase in short-term and long-term morbidity and mortality of cardiovascular disease (16). Ushiyama et al. found that HRV decreased significantly on postoperative day 1 and day 7 after digestive surgery and HRV indices correlated significantly to operation time, blood loss and operative complications (35). Several studies have also investigated the impact of surgical treatment on HRV in cancer patients. For instance, Amar et al. showed that HRV significantly decreased in cancer patients within the first week after major abdominal or chest surgery (36). Hansen et al. found that BC patients still had alterations in autonomic tone and decreased HRV and experienced the loss of circadian rhythm 14 days after tumor resection (37). Our research was consistent with these results. Surgery results in autonomic nerve injury and a significant decrease in HRV parameters.

The complex interaction between the ANS, endocrine system and immune system is enhanced by surgical trauma. First, surgical trauma as a source of stress will stimulate the sympathetic nerve and hypothalamus-pituitary-adrenal cortex axis, trigger the body's stress response, and lead to sympathetic excitement and cortisol release (38). It was found that the level of cortisol was positively correlated with the severity of the stress response (39). Cortisol can also further enhance the sympathetic-mediated cardiovascular response to stress, ultimately resulting in an increase in HR (40). Second, surgical trauma can cause a series of inflammatory reactions, which affect immune function (41, 42). Some studies have shown that the levels of C-reactive protein (CRP) and interleukin-6 (IL-6) increase within 14 days after abdominal surgery (43). The vagus nerve can inhibit inflammation through the cholinergic anti-inflammatory pathway and regulate the function of immune cells (44, 45). Consequently, the decrease of vagus nerve activity after surgery may be related to the increase of inflammatory factors and the decrease of immune function. The present study found that regardless of open or laparoscopic surgery, the HR of ECC patients 3 days after the operation was higher than that at 1 day before the operation, and most of the HRV indices 3 days after the operation were lower than those at 1 day before the operation, which was basically consistent with the above mechanism. This result suggests that both open and laparoscopic surgery can cause damage to autonomic function in patients with ECC. Further studies are needed to clarify the correlation between postoperative HRV and inflammatory factors and immune function indicators.

However, it is worth noting that the impact of open and laparoscopic surgery on the HRV of ECC patients was slightly

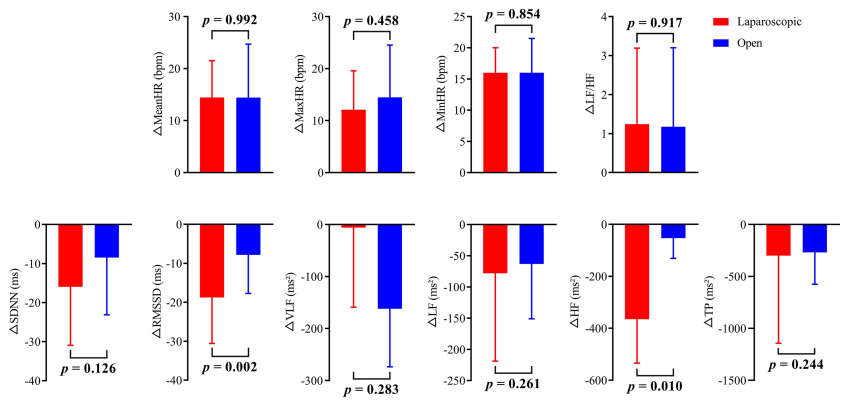


FIGURE 3 | The change in HR and HRV is indicated by the value after radical hysterectomy minus the value before radical hysterectomy for both the open group and laparoscopic group.

different. The postoperative LF/HF of the patients undergoing open surgery was significantly higher and the postoperative VLF was significantly lower after the operation than before the operation, while the postoperative LF/HF and VLF of patients undergoing laparoscopic surgery were not significantly different. A recent report argued that postoperative pain stimulation could cause a significant increase in LF/HF (46). Compared with open surgery, laparoscopic surgery uses artificial ports for intra-abdominal operation, which reduces the trauma and pain stimulation of traditional laparotomy on abdominal wall structure of patients. At the same time, compared with traditional surgery, laparoscopic surgery causes minimal blood loss and leads to lower wound infection rate, decreasing the level of sympathetic stimulation and the effects on LF/HF. Currently, the physiological mechanism of VLF is poorly defined, but it has been proven in recent years that VLF has the characteristics of slow recovery after abnormal stimulation (47). No statistically significant difference was detected between the preoperative and postoperative VLF of patients undergoing laparoscopic surgery, which might be because patients who underwent laparoscopic surgery recovered from surgical stimulation faster than patients who underwent open surgery.

Moreover, we found that the reduction in RMSSD and HF after the operation was significantly higher in the laparoscopic group than in the open group, which means that laparoscopic surgery has a greater negative impact on the HRV of ECC patients. One possible reason is the effect of CO2 pneumoperitoneum. During laparoscopic surgery, CO2-induced positive pressure pneumoperitoneum has adverse effects on cardiac hemodynamics, including the decrease of venous return and cardiac output, and the increase of systemic vascular resistance, pulmonary artery pressure and central venous pressure (48–50). These hemodynamic effects can cause a reflex increase in baroreceptor activity, combined with the direct mechanical effect of CO2 intraperitoneal inflation through diaphragmatic and phrenic nerve stretching and the negative cardiac effect of hypercapnia, which together lead to the increase of sympathetic nerve activity and the decrease of vagus nerve activity (51–54). This may have a relevant impact on patient HRV. RMSSD and HF indicate the vagal nerve tone. The vagal nerve has been proposed to be involved in the regulation of tumor progression. The active vagus nerve has an inhibitory effect on inflammation, oxidative stress and excessive sympathetic activity (55–57). Cancer patients often experience vagus damage, which manifests as a decrease in HRV, and the lower the HRV is, the worse the prognosis (58). Giese-Davis et al. demonstrated that in patients with recurrent or metastatic BC, a higher HF was closely related to longer overall survival (59). Bijoor et al. found that compared with healthy controls, the RMSSD of early and advanced cancer patients decreased significantly. Compared with patients with early cancer (TNM I and II), those with advanced cancer (TNM III and IV) had significantly lower RMSSD (60). These results showed that the lower vagus activity indicated by HRV significantly predicted a worse prognosis. Therefore, the difference in prognosis between laparoscopic and open surgery may be attributed to the difference in vagus nerve activity. This research seems to provide a theoretical basis for the conclusion that the risk of recurrence and death after laparoscopic surgery in ECC patients is significantly higher than that after open surgery. However, The mechanism of laparoscopic and open surgery leading to differences in vagus nerve activity still needs further investigation.

The limitation of this study was that it did not consider the impact of HR changes on HRV. This was because separating the influence of HR on HRV from the influence of surgical methods on HRV would require a large number of subjects, and the number of laparoscopic surgery cases in our study was relatively small. In addition, several possible confounders such as operation time, intraoperative blood loss and intraoperative and postoperative complications were not adjusted, which might affect the difference in HR and HRV before and after operation. Furthermore, more background variables, such as physical activity, stress levels, use of medications, and other relevant medical variables, could not be included. Thus, further studies with larger sample sizes, more detailed background variables and adjustment for relevant confounders should be performed to validate the results of the present study.

In summary, radical hysterectomy, whether performed *via* open or laparoscopic surgery, will cause the decrease of HRV and the damage of autonomic function in patients with ECC. Compared with open surgery, laparoscopic surgery has a greater negative impact on the HRV of ECC patients.

DATA AVAILABILITY STATEMENT

The raw data supporting the conclusions of this article will be made available by the authors, without undue reservation.

ETHICS STATEMENT

The studies involving human participants were reviewed and approved by the Medical Ethics Committee of the First Affiliated Hospital of Bengbu Medical College (Bengbu, Anhui, China). The patients/participants provided their written informed consent to participate in this study.

AUTHOR CONTRIBUTIONS

Conceptualization, BS and JL; methodology, JW and GL; formal analysis, GL and JW; resources, BS and JL; data curation, JL, YS, and LG; writing—original draft preparation, BS, SL, and CL; writing—review and editing, BS, JW, and ZD; supervision, JL; project administration, BS; funding acquisition, BS. All authors have read and agreed to the published version of the manuscript.

FUNDING

This research was funded by the "512" Outstanding Talents Fostering Project of Bengbu Medical College (grant number BY51201312) and the Science Research Project of Bengbu Medical College (grant number 2021byzd057).

REFERENCES

1. Bray F, Ferlay J, Soerjomataram I, Siegel RL, Torre LA, Jemal A, et al. Global Cancer Statistics 2018: GLOBOCAN Estimates of Incidence and Mortality Worldwide for 36 Cancers in 185 Countries. *CA Cancer J Clin* (2018) 68 (6):394–424. doi: 10.3322/caac.21492
2. Cibula D, Pötter R, Planchamp F. The European Society of Gynaecological Oncology/European Society for Radiotherapy and Oncology/European Society of Pathology Guidelines for the Management of Patients With Cervical Cancer. *Virchows Arch* (2018) 472(6):919–36. doi: 10.1007/s00428-018-2362-9
3. Averette HE, Nguyen HN, Donato DM, Penalver MA, Sevin BU, Estape R, et al. Radical Hysterectomy for Invasive Cervical Cancer. A 25-Year Prospective Experience With the Miami Technique. *Cancer* (1993) 71(4 Suppl):1422–37. doi: 10.1002/cncr.2820710407
4. Landoni F, Maneo A, Colombo A, Placa F, Milani R, Perego P, et al. Randomised Study of Radical Surgery Versus Radiotherapy for Stage Ib-IIa Cervical Cancer. *Lancet* (1997) 350(9077):535–40. doi: 10.1016/S0140-6736(97)02250-2
5. Nam JH, Park JY, Kim DY, Kim JH, Kim YM, Kim YT. Laparoscopic Versus Open Radical Hysterectomy in Early-Stage Cervical Cancer: Long-Term Survival Outcomes in a Matched Cohort Study. *Ann Oncol* (2012) 23 (4):903–11. doi: 10.1093/annonc/mdr360
6. Lee EJ, Kang H, Kim DH. A Comparative Study of Laparoscopic Radical Hysterectomy With Radical Abdominal Hysterectomy for Early-Stage Cervical Cancer: A Long-Term Follow-Up Study. *Eur J Obstet Gynecol Reprod Biol* (2011) 156(1):83–6. doi: 10.1016/j.ejogrb.2010.12.016
7. Alfonzo E, Wallin E, Ekdahl L, Staf C, Rådestad AF, Reynisson P, et al. No Survival Difference Between Robotic and Open Radical Hysterectomy for Women With Early-Stage Cervical Cancer: Results From a Nationwide Population-Based Cohort Study. *Eur J Cancer* (2019) 116:169–77. doi: 10.1016/j.ejca.2019.05.016
8. Frumovitz M, dos Reis R, Sun CC, Milam MR, Bevers MW, Brown J, et al. Comparison of Total Laparoscopic and Abdominal Radical Hysterectomy for Patients With Early-Stage Cervical Cancer. *Obstet Gynecol* (2007) 110(1):96–102. doi: 10.1097/01.AOG.0000268798.75353.04
9. Ferrandina G, Gallotta V, Federico A, Fanfani F, Ercoli A, Chiantera V, et al. Minimally Invasive Approaches in Locally Advanced Cervical Cancer Patients Undergoing Radical Surgery After Chemoradiotherapy: A Propensity Score Analysis. *Ann Surg Oncol* (2021) 28(7):3616–26. doi: 10.1245/s10434-020-09302-y
10. Wang YZ, Deng L, Xu HC, Zhang Y, Liang ZQ. Laparoscopy Versus Laparotomy for the Management of Early Stage Cervical Cancer. *BMC Cancer* (2015) 15:928. doi: 10.1186/s12885-015-1818-4
11. Cao T, Feng Y, Huang Q, Wan T, Liu J. Prognostic and Safety Roles in Laparoscopic Versus Abdominal Radical Hysterectomy in Cervical Cancer: A Meta-Analysis. *J Laparoendosc Adv Surg Tech A* (2015) 25(12):990–8. doi: 10.1089/lap.2015.0390
12. Nitecki R, Ramirez PT, Frumovitz M, Krause KJ, Tergas AI, Wright JD, et al. Survival After Minimally Invasive vs Open Radical Hysterectomy for Early-Stage Cervical Cancer: A Systematic Review and Meta-Analysis. *JAMA Oncol* (2020) 6(7):1019–27. doi: 10.1001/jamaoncol.2020.1694
13. Ramirez PT, Frumovitz M, Pareja R, Lopez A, Vieira M, Ribeiro R, et al. Minimally Invasive Versus Abdominal Radical Hysterectomy for Cervical Cancer. *N Engl J Med* (2018) 379(20):1895–904. doi: 10.1056/NEJMoa1806395
14. Melamed A, Margul DJ, Chen L, et al. Survival After Minimally Invasive Radical Hysterectomy for Early-Stage Cervical Cancer. *N Engl J Med* (2018) 379(20):1905–14. doi: 10.1056/NEJMoa1804923
15. Koh WJ, Abu-Rustum NR, Bean S. Cervical Cancer, Version 3.2019, NCCN Clinical Practice Guidelines in Oncology. *J Natl Compr Canc Netw* (2019) 17 (1):64–84. doi: 10.6004/jnccn.2019.0001
16. Gögenur I. Postoperative Circadian Disturbances. *Dan Med Bull* (2010) 57 (12):B4205.
17. Thayer JF, Yamamoto SS, Brosschot JF. The Relationship of Autonomic Imbalance, Heart Rate Variability and Cardiovascular Disease Risk Factors. *Int J Cardiol* (2010) 141(2):122–31. doi: 10.1016/j.ijcard.2009.09.543
18. Ondicova K, Mravec B. Role of Nervous System in Cancer Aetiopathogenesis. *Lancet Oncol* (2010) 11(6):596–601. doi: 10.1016/S1470-2045(09)70337-7
19. Gidron Y, Perry H, Glennie M. Does the Vagus Nerve Inform the Brain About Preclinical Tumours and Modulate Them? *Lancet Oncol* (2005) 6(4):245–8. doi: 10.1016/S1470-2045(05)70096-6
20. Tsibouris P, Kalantzis C, Apostolopoulos P, Mavrogianni P, Alexandrakis G, Kalantzis N. Patients With Selective Vagotomy are at High Risk to Develop a Significant Polyp of the Colon. *J Clin Gastroenterol* (2009) 43(6):599–600. doi: 10.1097/MCG.0b013e31818be196
21. Erin N, Akdas Barkan G, Harms JF, Clawson GA. Vagotomy Enhances Experimental Metastases of 4thmpc Breast Cancer Cells and Alters Substance P Level. *Regul Pept* (2008) 151(1-3):35–42. doi: 10.1016/j.regpep.2008.03.012
22. Barron TI, Connolly RM, Sharp L, Bennett K, Visvanathan K. Beta Blockers and Breast Cancer Mortality: A Population- Based Study. *J Clin Oncol* (2011) 29(19):2635–44. doi: 10.1200/JCO.2010.33.5422
23. Task Force of the European Society of Cardiology and the North American Society of Pacing and ElectrophysiologyHeart Rate Variability: Standards of Measurement, Physiological Interpretation and Clinical Use. Task Force of the European Society of Cardiology and the North American Society of Pacing and Electrophysiology. *Circulation* (1996) 93(5):1043–65. doi: 10.1161/01.cir.93.5.1043
24. Kloter E, Barrueto K, Klein SD, Scholkmann F, Wolf U. Heart Rate Variability as a Prognostic Factor for Cancer Survival - A Systematic Review. *Front Physiol* (2018) 9:623. doi: 10.3389/fphys.2018.00623
25. De Couck M, Gidron Y. Norms of Vagal Nerve Activity, Indexed by Heart Rate Variability, in Cancer Patients. *Cancer Epidemiol* (2013) 37(5):737–41. doi: 10.1016/j.canep.2013.04.016
26. Arab C, Vanderlei LCM, da Silva Paiva L, Fulghum KL, Fristachi CE, Nazario ACP, et al. Cardiac Autonomic Modulation Impairments in Advanced Breast Cancer Patients. *Clin Res Cardiol* (2018) 107(10):924–36. doi: 10.1007/s00392-018-1264-9
27. Hu S, Lou J, Zhang Y, Chen P. Low Heart Rate Variability Relates to the Progression of Gastric Cancer. *World J Surg Oncol* (2018) 16(1):49. doi: 10.1186/s12957-018-1348-z
28. Zhou X, Ma Z, Zhang L, Zhou S, Wang J, Wang B, et al. Heart Rate Variability in the Prediction of Survival in Patients With Cancer: A Systematic Review and Meta-Analysis. *J Psychosom Res* (2016) 89:20–5. doi: 10.1016/j.jpsychores.2016.08.004
29. Pan J, Tompkins WJ. A Real-Time QRS Detection Algorithm. *IEEE Trans BioMed Eng* (1985) 32(3):230–6. doi: 10.1109/TBME.1985.325532
30. Lipponen JA, Tarvainen MP. A Robust Algorithm for Heart Rate Variability Time Series Artefact Correction Using Novel Beat Classification. *J Med Eng Technol* (2019) 43(3):173–81. doi: 10.1080/03091902.2019.1640306
31. Singh D, Vinod K, Saxena SC. Sampling Frequency of the RR Interval Time Series for Spectral Analysis of Heart Rate Variability. *J Med Eng Technol* (2004) 28(6):263–72. doi: 10.1080/03091900410001662350
32. Shaffer F, Ginsberg JP. An Overview of Heart Rate Variability Metrics and Norms. *Front Public Health* (2017) 5:258. doi: 10.3389/fpubh.2017.00258
33. Goldstein DS, Bentho O, Park MY, Sharabi Y. Low-Frequency Power of Heart Rate Variability is Not a Measure of Cardiac Sympathetic Tone But may be a Measure of Modulation of Cardiac Autonomic Outflows by Baroreflexes. *Exp Physiol* (2011) 96(12):1255–61. doi: 10.1113/expphysiol.2010.056259
34. Tarvainen MP, Niskanen JP, Lipponen JA, Ranta-Aho PO, Karjalainen PA. Kubios HRV–heart Rate Variability Analysis Software. *Comput Methods Programs Biomed* (2014) 113(1):210–20. doi: 10.1016/j.cmpb.2013.07.024
35. Ushiyama T, Mizushige K, Wakabayashi H, Nakatsu T, Ishimura K, Tsuboi Y, et al. Analysis of Heart Rate Variability as an Index of Noncardiac Surgical Stress. *Heart Vessels* (2008) 23(1):53–9. doi: 10.1007/s00380-007-0997-6
36. Amar D, Fleisher M, Pantuck CB, Shamoon H, Zhang H, Roistacher N, et al. Persistent Alterations of the Autonomic Nervous System After Noncardiac Surgery. *Anesthesiology* (1998) 89(1):30–42. doi: 10.1097/00000542-199807000-00008
37. Hansen MV, Rosenberg J, Gögenur I. Lack of Circadian Variation and Reduction of Heart Rate Variability in Women With Breast Cancer Undergoing Lumpectomy: A Descriptive Study. *Breast Cancer Res Treat* (2013) 140(2):317–22. doi: 10.1007/s10549-013-2631-x

38. Desborough JP. The Stress Response to Trauma and Surgery. *Br J Anaesth* (2000) 85(1):109–17. doi: 10.1093/bja/85.1.109
39. Widmer IE, Puder JJ, König C, Pargger H, Zerkowski HR, Girard J, et al. Cortisol Response in Relation to the Severity of Stress and Illness. *J Clin Endocrinol Metab* (2005) 90(8):4579–86. doi: 10.1210/jc.2005-0354
40. Sapolsky RM, Romero LM, Munck AU. How do Glucocorticoids Influence Stress Responses? Integrating Permissive, Suppressive, Stimulatory, and Preparative Actions. *Endocr Rev* (2000) 21(1):55–89. doi: 10.1210/edrv.21.1.0389
41. Kohl BA, Deutschman CS. The Inflammatory Response to Surgery and Trauma. *Curr Opin Crit Care* (2006) 12(4):325–32. doi: 10.1097/01.ccx.0000235210.85073.fc
42. Lennard TW, Shenton BK, Borzotta A, Donnelly PK, White M, Gerrie LM, et al. The Influence of Surgical Operations on Components of the Human Immune System. *Br J Surg* (1985) 72(10):771–6. doi: 10.1002/bjs.1800721002
43. Watt DG, Horgan PG, McMillan DC. Routine Clinical Markers of the Magnitude of the Systemic Inflammatory Response After Elective Operation: A Systematic Review. *Surgery* (2015) 157(2):362–80. doi: 10.1016/j.surg.2014.09.009
44. Reijmen E, Vannucci L, De Couck M, De Grève J, Gidron Y. Therapeutic Potential of the Vagus Nerve in Cancer. *Immunol Lett* (2018) 202:38–43. doi: 10.1016/j.imlet.2018.07.006
45. Tracey KJ. Physiology and Immunology of the Cholinergic Antiinflammatory Pathway. *J Clin Invest* (2007) 117(2):289–96. doi: 10.1172/JCI30555
46. Chang LH, Ma TC, Tsay SL, Jong GP. Relationships Between Pain Intensity and Heart Rate Variability in Patients After Abdominal Surgery: A Pilot Study. *Chin Med J (Engl)* (2012) 125(11):1964–9. doi: 10.3760/cma.j.issn.0366-6999.2012.11.023
47. Usui H, Nishida Y. The Very Low-Frequency Band of Heart Rate Variability Represents the Slow Recovery Component After a Mental Stress Task. *PloS One* (2017) 12(8):e0182611. doi: 10.1371/journal.pone.0182611
48. Hirvonen EA, Poikolainen EO, Pääkkönen ME, Nuutinen LS. The Adverse Hemodynamic Effects of Anesthesia, Head-Up Tilt, and Carbon Dioxide Pneumoperitoneum During Laparoscopic Cholecystectomy. *Surg Endosc* (2000) 14(3):272–7. doi: 10.1007/s004640000038
49. Horvath KD, Whelan RL, Lier B, Viscomi S, Barry L, Buck K, et al. The Effects of Elevated Intraabdominal Pressure, Hypercarbia, and Positioning on the Hemodynamic Responses to Laparoscopic Colectomy in Pigs. *Surg Endosc* (1998) 12(2):107–14. doi: 10.1007/s004649900608
50. Galizia G, Prizio G, Lieto E, Castellano P, Pelosio L, Imperatore V, et al. Hemodynamic and Pulmonary Changes During Open, Carbon Dioxide Pneumoperitoneum and Abdominal Wall-Lifting Cholecystectomy. *A prospective randomized study Surg Endosc* (2001) 15(5):477–83. doi: 10.1007/s004640000343
51. Safran DB, Orlando R. Physiologic Effects of Pneumoperitoneum. *Am J Surg* (1994) 167(2):281–6. doi: 10.1016/0002-9610(94)90094-9
52. Bickel A, Yahalom M, Roguin N, Frankel R, Breslava J, Ivry S, et al. Power Spectral Analysis of Heart Rate Variability During Positive Pressure Pneumoperitoneum: The Significance of Increased Cardiac Sympathetic Expression. *Surg Endosc* (2002) 16(9):1341–4. doi: 10.1007/s00464-001-9211-6
53. Sato N, Kawamoto M, Yuge O, Suyama H, Sanuki M, Matsumoto C, et al. Effects of Pneumoperitoneum on Cardiac Autonomic Nervous Activity Evaluated by Heart Rate Variability Analysis During Sevoflurane, Isoflurane, or Propofol Anesthesia. *Surg Endosc* (2000) 14(4):362–6. doi: 10.1007/s004640000155
54. Bickel A, Kukuev E, Popov O, Ivry S, Roguin N, Yahalom M, et al. Power Spectral Analysis of Heart Rate Variability During Helium Pneumoperitoneum: The Mechanism of Increased Cardiac Sympathetic Activity and its Clinical Significance. *Surg Endosc* (2005) 19(1):71–6. doi: 10.1007/s00464-003-9304-5
55. Maki A, Kono H, Gupta M, Asakawa M, Suzuki T, Matsuda M, et al. Predictive Power of Biomarkers of Oxidative Stress and Inflammation in Patients With Hepatitis C Virus-Associated Hepatocellular Carcinoma. *Ann Surg Oncol* (2007) 14(3):1182–90. doi: 10.1245/s10434-006-9049-1
56. Tsutsumi T, Ide T, Yamato M, Kudou W, Andou M, Hirooka Y, et al. Modulation of the Myocardial Redox State by Vagal Nerve Stimulation After Experimental Myocardial Infarction. *Cardiovasc Res* (2008) 77(4):713–21. doi: 10.1093/cvr/cvm092
57. De Couck M, Mravec B, Gidron Y. You may Need the Vagus Nerve to Understand Pathophysiology and to Treat Diseases. *Clin Sci (Lond)* (2012) 122(7):323–8. doi: 10.1042/CS20110299
58. De Couck M, Caers R, Spiegel D, Gidron Y. The Role of the Vagus Nerve in Cancer Prognosis: A Systematic and a Comprehensive Review. *J Oncol* (2018) 2018:1236787. doi: 10.1155/2018/1236787
59. Giese-Davis J, Wilhelm FH, Tamagawa R, Palesh O, Neri E, Taylor CB, et al. Higher Vagal Activity as Related to Survival in Patients With Advanced Breast Cancer: An Analysis of Autonomic Dysregulation. *Psychosom Med* (2015) 77(4):346–55. doi: 10.1097/PSY.0000000000000167
60. Bijoor SN, Subbalakshmi NK, Banerjee S. Influence of Cancer and its Severity on Vagal Nerve Activity Assessed by Time Domain Measures of Heart Rate Variability. *Res J Pharmacol Biol Chem Sci* (2016) 7:1215–20.

Conflict of Interest: A direct family member of BS owns stock in HeaLink Ltd., Bengbu, China.

The remaining authors declare that the research was conducted in the absence of any commercial or financial relationships that could be construed as a potential conflict of interest.

Publisher's Note: All claims expressed in this article are solely those of the authors and do not necessarily represent those of their affiliated organizations, or those of the publisher, the editors and the reviewers. Any product that may be evaluated in this article, or claim that may be made by its manufacturer, is not guaranteed or endorsed by the publisher.

Copyright © 2022 Liu, Wang, Deng, Liu, Li, Sun, Gao, Li and Shi. This is an open-access article distributed under the terms of the Creative Commons Attribution License (CC BY). The use, distribution or reproduction in other forums is permitted, provided the original author(s) and the copyright owner(s) are credited and that the original publication in this journal is cited, in accordance with accepted academic practice. No use, distribution or reproduction is permitted which does not comply with these terms.

frontiers | Frontiers in Oncology

ORIGINAL RESEARCH
published: 07 June 2022
doi: 10.3389/fonc.2022.816982

Nomograms of Combining MRI Multisequences Radiomics and Clinical Factors for Differentiating High-Grade From Low-Grade Serous Ovarian Carcinoma

Cuiping Li[1,2], Hongfei Wang[3], Yulan Chen[2], Chao Zhu[1], Yankun Gao[1], Xia Wang[1], Jiangning Dong[2] and Xingwang Wu[1*]*

[1] Department of Radiology, The First Affiliated Hospital of Anhui Medical University, Hefei, China, [2] Department of Radiology, The First Affiliated Hospital of the University of Science and Technology of China, Anhui Provincial Cancer Hospital, Hefei, China, [3] Department of Radiotherapy, The First Affiliated Hospital, University of Science and Technology of China, Anhui Provincial Cancer Hospital, Hefei, China

OPEN ACCESS

Edited by:
Maria Barbolina, University of Illinois at Chicago, United States

Reviewed by:
Riccardo Faletti, University of Turin, Italy
Chao Fang, Central South University, China

****Correspondence:***
Jiangning Dong
dongjn@163.com
Xingwang Wu
duobi2004@126.com

Specialty section:
This article was submitted to Gynecological Oncology, a section of the journal Frontiers in Oncology

Received: *17 November 2021*
Accepted: *05 May 2022*
Published: *07 June 2022*

Citation:
Li C, Wang H, Chen Y, Zhu C, Gao Y, Wang X, Dong J and Wu X (2022) Nomograms of Combining MRI Multisequences Radiomics and Clinical Factors for Differentiating High-Grade From Low-Grade Serous Ovarian Carcinoma. Front. Oncol. 12:816982. doi: 10.3389/fonc.2022.816982

Objective: To compare the performance of clinical factors, FS-T2WI, DWI, T1WI+C based radiomics and a combined clinic-radiomics model in predicting the type of serous ovarian carcinomas (SOCs).

Methods: In this retrospective analysis, 138 SOC patients were confirmed by histology. Significant clinical factors ($P < 0.05$, and with the area under the curve (AUC) > 0.7) was retained to establish a clinical model. The radiomics model included FS-T2WI, DWI, and T1WI+C, and also, a multisequence model was established. A total of 1,316 radiomics features of each sequence were extracted; the univariate and multivariate logistic regressions, cross-validations were performed to reduce valueless features and then radiomics signatures were developed. Nomogram models using clinical factors, combined with radiomics features, were developed in the training cohort. The predictive performance was validated by receiver operating characteristic curve (ROC) analysis and decision curve analysis (DCA). A stratified analysis was conducted to compare the differences between the combined radiomics model and the clinical model in identifying low- and high-grade SOC.

Results: The AUC of the clinical model and multisequence radiomics model in the training and validation cohorts was 0.90 and 0.89, 0.91 and 0.86, respectively. By incorporating clinical factors and multi-radiomics signature, the AUC of the radiomic-clinical nomogram in the training and validation cohorts was 0.98 and 0.95. The model comparison results show that the AUC of the combined model is higher than that of the uncombined models (P= 0.05, 0.002).

Conclusion: The nomogram models of clinical factors combined with MRI multisequence radiomics signatures can help identifying low- and high-grade SOCs and a provide a more comprehensive, effective method to evaluate preoperative risk stratification for SOCs.

Keywords: serous ovarian carcinoma, radiomics, nomogram, magnetic resonance imaging, subtype

INTRODUCTION

Ovarian cancer (OC) is the deadliest type of gynecological malignancy worldwide (1), and SOC is the most common histological type, accounting for approximately 70% of cases (2). High-grade serous ovarian carcinomas (HGSOCs) are the largest category of OC, comprising 90% of the total, and have high recurrence and mortality rates (3, 4). In contrast, LGSOCs are much less common, accounting for less than 10% of the remaining cancers and have a strong association with borderline tumors (2). Some previous studies have shown that apparent diffusion coefficient (ADC) histogram parameters based on whole solid tumor volume could be helpful for differentiating between HGSOC and LGSOC (2), single or multisequence MRI-based texture features of the whole tumor also might assist in characterizing the differences between borderline tumors and LGSOCs (5), and based on whole solid-tumor histogram analysis, could effectively differentiate benign OCs from malignant OCs (6). HGSOCs and LGSOCs are two separate tumors with distinct genetic risk factors, epidemiological differences, biological behaviors, different spreading patterns, response to chemotherapy, and prognosis (3, 7). Moreover, accurate preoperative diagnosis of subtypes will be helpful for achieving a more effective subtype specific treatment. However, no combination of radiomics and clinical models has been used to distinguish HGSOCs from LGSOCs. Based on the current study progress and the necessity of solving clinical problems, the purpose of the present study was to compare the performance of clinical factors, fat-suppressed T2-wighted imaging (FS-T2WI), diffusion-weighted imaging (DWI), contrast-enhanced FS T1WI (T1WI+C) radiomics, and a combined multiple features model in predicting the subtype of SOCs.

MATERIALS AND METHODS

Patients

The present retrospective study was approved by the institutional review board and the need for an informed patient consent was waived. Between December 2014 and August 2019, a total of 226 patients diagnosed clinically with OCs were identified. In order to eliminate the effects of the MRI parameters and OC subtype on the results, the investigators only included patients with LG- and HGSOCs scanned on the same MRI platform with a unified imaging protocol (n=185). Then, investigators excluded the following patients: (1) MRI contraindications or MRI quality that cannot meet the diagnostic requirements, (2) patients treated with neoadjuvant chemotherapy, and (3) a tumor with few solid components. Finally, 138 patients with ovarian cancers (104 HGSOCs and 34 LGSOCs) confirmed by surgery and histology were included. The mean age was 54.83 ± 11.04 years. The tumors were staged according to the 2014 International Federation of Gynecology and Obstetrics (FIGO) staging system. The process of patient selection is illustrated in **Figure S1**.

MRI Protocol

MRI examination was performed using a unit system (GE Signa HDXT 3.0T MRI scanner, GE Healthcare, USA) equipped with an 8-channel phased-array abdominal coil. Excluding contraindications, all patients received an intramuscular injection of 15 mg hyoscine butylbromide at 30 minutes before the MRI scan to prevent gastrointestinal motility. The bladder was kept approximately half-filled, in order to improve lesion visibility without changing the anatomy. Patients were placed in the supine position and were breathing freely during the acquisition.

The routine pelvic MRI protocol consisted of the following sequences: axial T1-weighted imaging (T1WI), axial/sagittal T2-weighted imaging (T2WI), axial FS T2WI, DWI (b value = 0, 1,000 s/mm^2), and multiple phases of contrast-enhanced (LAVA-FLEX) MRI. When scanning the axial images, the transverse plane was perpendicular to the long axis of the uterine body and for the sagittal images, the longitudinal plane was parallel to the main body of the uterus. T1WI+C sequence was acquired at the arterial, venous, and delayed phases of contrast medium enhancement in axial planes, which were acquired at 25, 60, and 120 s after the intravenous injection of 0.1 mmol/kg gadodiamide (Omniscan, GE Healthcare) using an Ulrich power injector. The scanning sequences and parameters are shown in **Table S1**.

MRI Images Analysis

Two radiologists with more than 10 years of experience in gynecological imaging analyzed the images without knowing the pathological results of these patients and reached a consensus (**Figure 1**). Using the GE ADW 4.6 post-processing workstation, the DWI images of the tumor layer with b = 1000 s/mm^2 were analyzed and the ADC values were calculated. The measurement was repeated three times and the average value was obtained. When sketching for the region of interest (ROI), the T2WI and T1WI+C images were referenced to determine the tumor boundary and the mucus, necrosis, cystic change, and bleeding areas were avoided.

MRI Image Segmentation and Radiomics Feature Extraction

Manual segmentation was performed based on FS-T2WI, DWI, and T1WI+C sequences by using the ITK-SNAP software (version 3.8.0, www.itksnap.org). The region of interest (ROI) of each ovarian tumor was manually contoured along the boundary of the tumor and the VOI was constructed by ROI interpolation for each slice. The interobserver reproducibility was initially analyzed using 30 randomly chosen images for the VOI by the 2 radiologists mentioned above. Intraclass correlation coefficients (ICCs) were used to evaluate the interobserver agreement in the measurement of radiomics features (ICC>0.75 was indicative of almost perfect agreement).

To reduce the discrepancies between imaging parameters, several preprocessing steps of the MR images were applied before the process of radiomics feature extraction. All images were

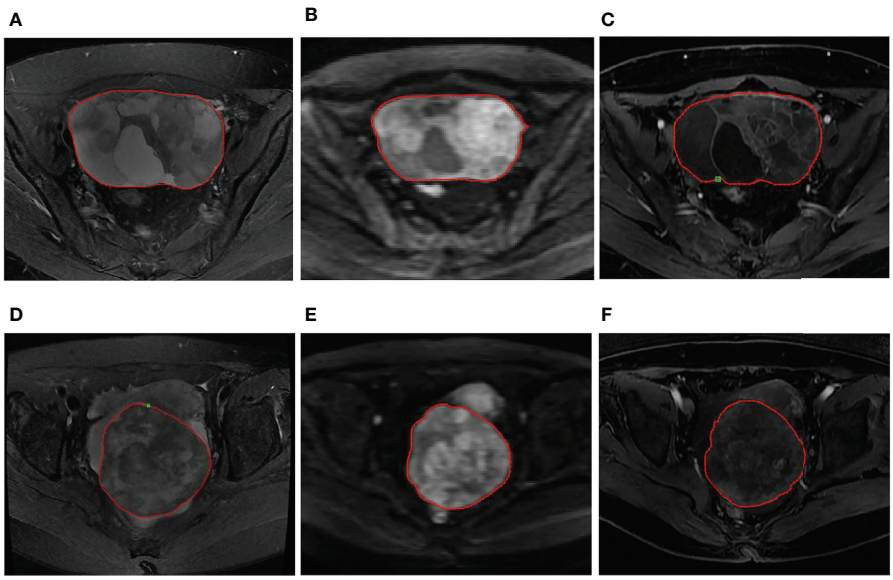


FIGURE 1 | **(A–C)** A 56-year-old woman with LGSOC in the right ovary. **(A)** Axial FS-T2WI shows a mixed cystic-solid mass. **(B)** Axial DWI (b=1000 s/mm^2) shows high signal of the solid component, indicating limited diffusion. **(C)** Axial T1WI+C image shows a mild enhancement in the solid component and septation. The red ROI was manually drawn along the margin of the whole tumor. **(D–F)** A 63-year-old woman with HGSOC in the right ovary. **(D)** Axial FS-T2WI shows a mass with mixed signals dominated by solid components. **(E)** Axial DWI (b=1000 s/mm^2) shows high signal of the tumor, indicating limited diffusion. **(F)** Axial T1WI+C image shows a heterogeneous mild enhancement in the tumor. The red ROI was manually drawn along the margin of the whole tumor.

resampled to a voxel size of 1×1×1 mm^3 using B-Spline interpolation. Each MRI scan was normalized in order to get a standard normal distribution of image intensities. Radiomics features were extracted from 3 types of multisequence MR images (FS-T2WI, DWI, and T1WI+C) for each lesion using PyRadiomics software http://pyradiomics.readthedocs.io/en/latest/index.html, which could automatically obtain the histogram parameters for whole solid tumor VOI. Seven classes of 1,316 radiomics features were extracted: shape features (2D, 3D), first-order features, gray-level cooccurrence matrix (GLCM) features, gray-level run length matrix (GLRLM) features, gray-level size zone matrix (GLSZM) features, neighborhood gray-tone difference matrix (NGTDM) features, and gray-level dependence matrix (GLDM) features (**Table S2**). The detailed description of the radiomics images preprocessing is shown in **Figure 2**.

Data Preprocessing

The dataset was randomly assigned in a 7:3 ratio to either the training cohort or validation cohort. All cases in the training cohort were used to train the predictive model, while cases in the validation cohorts were used to independently evaluate the model's performance.

Before analyses, variables with zero variance were excluded from analyses. Then, the missing values and outlier values were replaced by the median. Finally, the data were standardized by the standardization.

Feature Selection and Classifier Modeling

Firstly, features with ICCs >0.75 were retained. Secondly, feature selection was performed by using univariate logistic analysis (Correlation_xx), multivariate logistic analysis, and gradient boosting decision tree (GBDT) with stepwise selection method. The rad-score value was calculated by the sum of (radiomics signature × coefficient) + intercept. Finally, logistic-based rad-score model and nomogram was built based on the established optimal feature subsets of the training cohort (**Figure 3**).

Receiver operating characteristic (ROC) curve was performed to determine the performance of the machine learning model; accuracy, sensitivity, specificity and area under curve (AUC) was calculated. The differences for radiomics models were compared using the DeLong method (**Figure 4**).

Statistical Analysis

A commercial software (SPSS 22.0, IBM Corporation, Armonk NY, USA) was used for the statistical analysis. We tested whether the numerical variables were normally distributed by using a one-sample Kolmogorov-Smirnov test. The data that had a normal distribution were expressed as mean ± standard deviation (SD), while nonnormally distributed data were expressed in median (interquartile range (IQR), 25th and 75th percentile). Independent sample *t*-test was used to conform to the normal distribution, while Mann-Whitney *U*-test in the nonparametric rank sum test was used to conform to the nonnormal distribution. The Chi-square test was used for

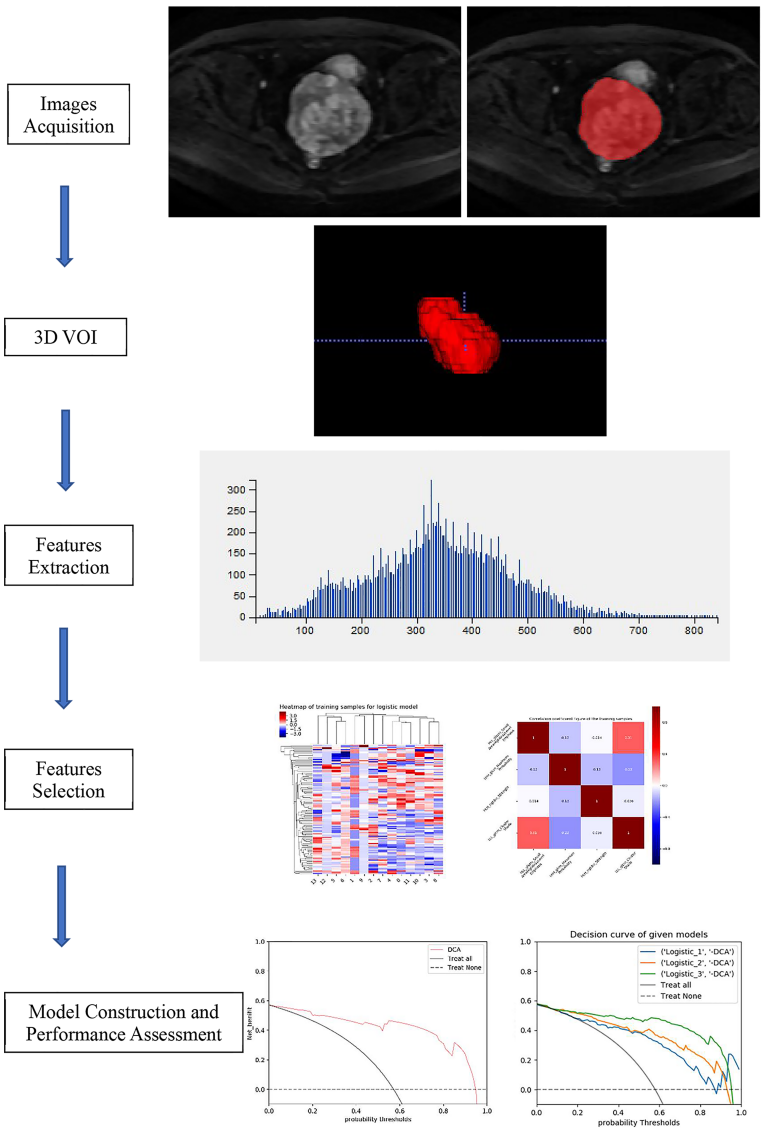


FIGURE 2 | The detailed description of the radiomics images preprocessing.

unordered categorical variables. $P<0.05$ was considered as a statistically significant.

RESULTS

Clinical Factors Analysis

Table 1 reports the comparisons of clinical factors between HGSOCs and LGSOCs. The preoperative carbohydrate antigen 125 (CA125) and human epididymis protein 4 (HE4) indicators in HGSOCs are significantly higher than that of LGSOCs (801.900 (381.100, 2066.750) VS 161.600 (80.622, 422.550) $P<0.001$, 429.550 (213.875, 922.850) VS 109.800 (70.795, 185.825) $P<0.001$, respectively). The ADC value in HGSOCs is 0.865 (0.743, 9.955), which is significantly lower than that of LGSOCs (0.980 (0.817, 1.110), $P<0.001$). No significant difference is found between HGSOCs and LGSOCs in age, peritoneal metastasis (PM), lymph node metastasis (LNM), and location. Based on the variables mentioned above, a clinical model was established, the AUC was 0.89 (95% confidence interval [CI] 0.78–0.96).

Radiomics Models and Model Comparisons

In total, 1,316 radiomics features were extracted from each VOI of the three sequences. The ICC values range from 0.771 to 0.988

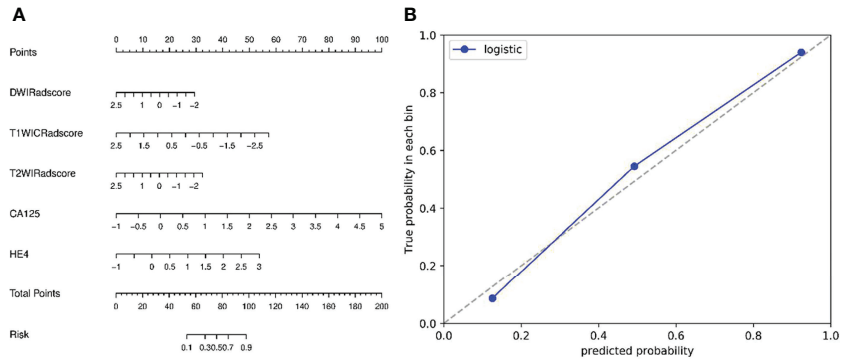


FIGURE 3 | **(A)** Nomogram based on radiomics signatures and clinical factors. In the nomogram, a vertical line was made according to each parameter to determine the corresponding value of points. The total points were the sum of the three points above. Then, a vertical line was made according to the value of the total points to determine the probability type of SOCs. **(B)** Calibration curves of the nomogram model (clinical factors + multisequence radiomics signatures) in validation cohort. The 45° dotted line represents the ideal prediction, while the blue line represents the prediction performance of the nomogram. The closer the blue line is to the dotted line, the better the performance of the nomogram.

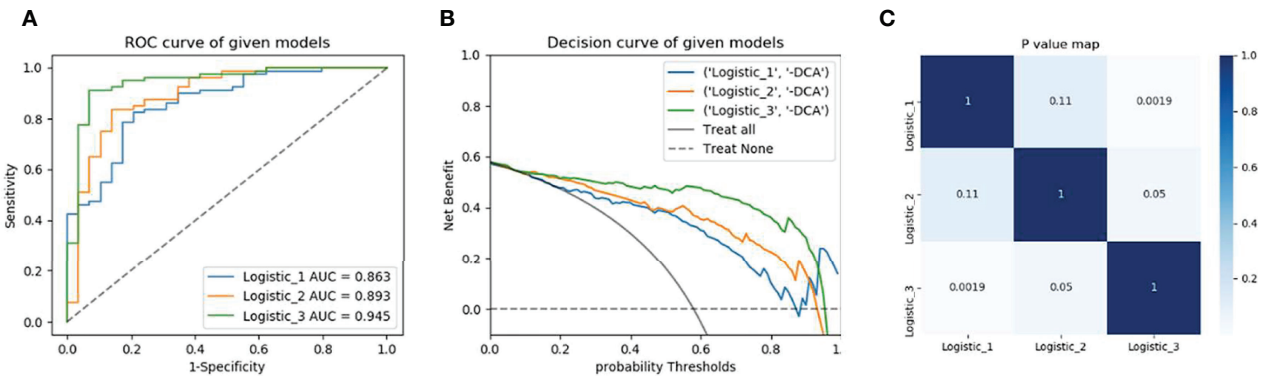


FIGURE 4 | Model's performance assessment and comparison. **(A)** Receiver operating characteristic curve analysis in the validation cohorts. **(B)** Decision curve analysis of radiomics signature, clinical model, and nomogram respectively. **(C)** Delong test for the given models. Model 1is based on MRI multisequence radiomics Model 2 is based on clinical factors and Model 3 is a combination of clinical and multi-radiomics.

and show great interobserver agreement. Four, eight, and six features were extracted from DWI, T1WI+C, and FS-T2WI sequences, respectively (**Table S3**). Based on the above features, the radiomics models of single sequence and multisequence combinations are established, respectively. The AUC of the combined radiomics model was 0.86 (95% CI 0.81–0.97), ACC 0.79. The combination of signatures from the multisequence resulted in a better predictive model than that from a single sequence (**Table 2**).

Then, the Rad-score was calculated for the radiomics features of individual sequences, then new combination model and Nomogram were established with combining clinical factors. The diagnostic efficacy of the combined model was higher than that of the clinical model or radiomics model (AUC = 0.95 (95% CI 0.90-0.98), ACC 0.87. Finally, the DeLong test results of model comparison show that the performance of the combined model is better than that of the uncombined models (P= 0.002, 0.05).

DISCUSSION

Tumor heterogeneity is one of the most important characteristics of malignant tumors (8, 9). It refers to the changes in molecular biology or genes of its daughter cells after multiple division and proliferation in the growth process of the tumor, resulting in differences in tumor growth rate, aggressive behaviors, response to treatment, and other aspects. In general, HGSOCs generally exhibit more aggressive behavior than LGSOCs (3). As a result, patients with HGSOCs have a poor prognosis, with a five-year survival rate of less than 40% (10). The optimal treatments for patients with HGSOCs include comprehensive staging surgery, cytoreductive surgery, and platinum-based chemotherapy (11). Most HGSOC patients, in contrast to LGSOCs, show an initially higher chemosensitivity (3, 12). LGSOCs typically occur in younger women with slow-growing behaviors (3). The treatment strategy of LGSOCs mainly rely on optimal surgical cytoreduction for best long-term survival (2). For patients in

TABLE 1 | Demographic and clinicopathologic characteristics of patients with serous ovarian carcinomas.

Variables	LGSOC (n=34)	HGSOC (n=104)	*P* value
Ages, median (IQR)	52 (45, 62)	55 (50, 64)	0.298[1]
Overall FIGO stage, N (%)			
IA	0 (0)	2 (1.9%)	
IB	1 (2.9%)	2 (1.9%)	
IC	6 (17.6%)	10 (9.6%)	
IIA	1 (2.9%)	0 (0)	
IIB	2 (5.9%)	5 (4.8%)	
IIIA	3 (8.8%)	6 (5.8%)	
IIIB	2 (5.9%)	6 (5.8%)	
IIIC	9 (26.5%)	52 (50.0%)	
IVA	4 (11.8%)	6 (5.8%)	
IVB	6 (17.6%)	15 (14.4%)	
ADC value, median (IQR)	0.980 (0.817, 1.110)	0.865 (0.743, 9.955)	<0.001[1]
CA125, median (IQR)	161.600 (80.622, 422.550)	801.900 (381.100, 2066.750)	<0.001[1]
HE4, median (IQR)	109.800 (70.795, 185.825)	429.550 (213.875, 922.850)	<0.001[1]
Location, N (%)			
Bilateral	20 (58.8%)	46 (44.2%)	0.139[2]
Unilateral	14 (41.2%)	58 (55.8%)	
LNM, N (%)			
–	19 (55.9%)	39 (37.5%)	0.059[2]
+	15 (44.1%)	65 (62.5%)	
PM, N (%)			
–	14 (41.2%)	25 (24.0%)	0.054[2]
+	20 (58.8%)	79 (76.0%)	

LGSOC, low-grade serous ovarian carcinoma; HGSOC, high-grade serous ovarian carcinoma; IQR, interquartile range; FIGO, international federation of gynecology and obstetrics; ADC, apparent diffusion coefficient; CA125, carbohydrate antigen 125; HE4, human epididymis protein 4; LNM, lymph node metastasis; PM, peritoneal metastasis. [1]Mann-Whitney U test, [2]Chi-square test.

advanced stage, the formulation of surgical plan is also very important, not only to maximize the removal of tumor tissue, but also to take into account the postoperative quality of life of patients. Thus, accurate preoperative subtype diagnosis will be necessary for achieving a more effective subtype-specific treatment.

Conventional magnetic resonance imaging (cMRI) plays a significant role in the diagnosis of pelvic diseases due to its high soft-tissue resolution (13, 14). It can clearly reveal the lesion characteristics (cystic, bleeding, edema, fibrosis, and so on), the relationship between the tumor and surrounding tissues, and the status of lymph node disease (metastasis or inflammation). Some previous studies have shown that the qualitative diagnosis of EOCs by MRI is obviously superior to other imaging methods (10), but HGSOC and LGSOC images have many overlapping signs on cMRI (T1WI, T2WI, T1WI+C) sequences, and as a result, it is difficult for experienced radiologists to make a definite diagnosis. In addition, cMRI relies on the experience of radiologists and to some extent lacks objectivity (3). Here, especially the novel technique of DWI, has been widely used to investigate the heterogeneity of tumors in many clinical studies (1, 15–17). DWI can reflect the microbiological state of tissues noninvasively, according to the Brownian motion of water molecule, and indirectly reflect the biological changes in tissues (17–19). Radiomics analysis is a postprocessing method for extracting information by quantifying the spatial distribution of pixels or voxels with different gray intensities and counting the variables, that is, calculating and extracting texture features based on the texture matrix of images (10, 20, 21). However, some previous studies only analyzed simple parameter values, used different ROIs, including round, single-slice, and whole solid tumor volume, for OC analysis (3, 16, 17, 21, 22). This approach inevitably leads to a loss of important heterogeneous information. Considering the large size and complexity of ovarian masses, histogram analysis based on whole solid tumor VOI could more accurately reflect the heterogeneity of OCs by quantifying complex parameter distributions and provide a more accurate information for clinical practice (3, 17).

Our present study developed a series of predictive models based on clinical factors combined with radiomics analysis based on FS-T2WI, DWI, and T1WI+C sequences to provide a practical clinical tool for risk stratification and individualized treatment of SOCs. In the present study, patients with HGSOCs have higher levels of serum CA125 (801.900 (381.100, 2066.750) VS 161.600 (80.622, 422.550), $P<0.001$) and HE4 (429.550 (213.875, 922.850) VS 109.800 (70.795, 185.825), $P<0.001$), these results are consistent with the findings reported in previous studies (1, 12, 23). Indicating that the faster and more aggressive the tumor, the higher the levels of CA125 and HE4 secreted by the body. In other studies, CA125 has been shown to contribute to the early detection of asymptomatic OCs patients, leading to early diagnosis and treatment and eventually improve the prognosis of patients (4, 24). Other studies have pointed that CA125 has an advantage in distinguishing OCs from healthy individuals, but HE4 is more sensitive in distinguishing OCs from benign pelvic masses. And

TABLE 2 | Performance evaluation of the models.

	Training cohort						Validation cohort					
	AUC	ACC	SEN	SPE	PPV	NPV	AUC	ACC	SEN	SPE	PPV	NPV
Clinical model	0.90 (0.84, 0.95)	0.83	0.78	0.90	0.91	0.75	0.89 (0.78, 0.96)	0.85	0.91	0.77	0.84	0.87
DWI Radiomics	0.84 (0.73, 0.92)	0.78	0.71	0.85	0.83	0.75	0.83 (0.76, 0.89)	0.75	0.70	0.79	0.77	0.73
DCE Radiomics	0.89 (0.81, 0.95)	0.80	0.64	0.96	0.95	0.73	0.86 (0.80, 0.91)	0.78	0.65	0.92	0.89	0.72
FS-T2WI Radiomics	0.87 (0.81, 0.93)	0.83	0.89	0.77	0.79	0.88	0.83 (0.73, 0.92)	0.74	0.72	0.72	0.87	0.67
Multi- Radiomics	0.91 (0.83, 0.97)	0.87	0.73	0.87	0.87	0.72	0.86 (0.81, 0.97)	0.78	0.83	0.72	0.80	0.76
Nomogram	0.98 (0.93, 0.99)	0.90	0.91	0.90	0.92	0.88	0.95 (0.90, 0.98)	0.87	0.91	0.83	0.90	0.77

AUC, area under the curve; ACC, accuracy; SEN, sensitivity; SPE, specificity; PPV, positive predictive value; NPV, negative predictive value.

CA125 levels were strongly correlated with clinical evolution during chemotherapy. Not all OCs express CA125 abnormally and HE4 may be a useful addition to the test (23, 25). In addition, the ADC values of HGSOC patients are lower than that of LGSOC patients (0.865 (0.743, 9.955) VS 0.980 (0.817, 1.110), $P<0.001$, AUC<0.7), indicating that HGSOCs have higher tumor cell density and vigorous growth, which is also related to the high invasiveness and high recurrence rate of HGSOCs (1, 2, 12). Too many studies have found similar results, which is why DWI is widely used in clinical practice. However, there was no significant difference in age between the two groups in our study, HGSOC patients are slightly older than LGSOC patients (55 (50, 64) VS 52 (45, 62), $P=0.298$), which is different from the known views (3, 17, 26). The possible reason is that the clinical onset of SOCs is insidious, LGSOCs are less invasive, have a longer course of disease, and the symptoms are severe when hospitalized (16). In the future, we should focus on 'high alert' symptoms: pelvic or abdominal pain, increase abdominal size or bloating and difficulty eating/feeling full (27).

Eighty percent of SOC patients already have metastatic disease at diagnosis, with poor prognosis despite surgery and chemotherapy (28). In the present study, there were no significant differences in tumor location, peritoneal, and lymph node metastasis between the two groups. The present study showed that HGSOC patients were more likely to be unilateral (58/104, 55.8%), while LGSOC patients were slightly more likely to be bilateral (20/34, 58.8%). Our findings are consistent with previous studies that show HGSOC arises from the epithelium of the fallopian tube, whereas LGSOC usually arises from the ovary and is often bilateral (2, 24). Both HGSOC and LGSOC patients are prone to peritoneal metastasis, and HGSOC is more likely to occur (79/104, 76.0% VS 20/34, 58.8%). This may be related to the fact that the two subtypes are often found and treated in an advanced stage (29, 30). Lymph node metastasis was more common in HGSOC patients (65/104, 62.5%) than in LGSOC patients (15/34, 44.1%). The reason may be related to the late stage of patients enrolled in the present study, the high invasiveness of HGSOCs, and the small number of patients in the LGSOCs group. If patients with SOCs can achieve early detection and carry out relevant research at the early stage of the disease, the prognosis should be better. The clinical model based on the above clinical factors were built in the training cohorts to predict the type of SOCs, and validated to have good accuracy, sensitivity, and specificity in the validation cohorts.

In the other part of our study, 4 DWI features, 8 T1WI+C features, and 6 FS-T2WI features were screened out from radiomics analysis, after dimensionality reduction by the univariate, and multivariate logistic regression method, respectively. These radiomics represent the heterogeneity of SOC tumors and reflect the size and spatial distribution of gray level. HGSOCs are more heterogeneous than LGSOCs, which associate with vigorous mass growth, high aggressiveness, and high recurrence. Previous studies have found similar findings, and a convincing explanation is the HGSOCs possess more tortuous vascular structure and heterogeneous cellular morphology, which contribute to intratumoral parenchyma heterogeneity (1, 12, 31). Single sequence and multiple sequences models were established by using the selected radiomics features. After model comparison and DeLong's test, the results show that the multisequence combination model has better performance, higher accuracy and sensitivity (0.86 (0.81, 0.97), 0.78, 0.83), the model based on T1WI+C signatures has the highest specificity (0.92), and all P values were less than 0.05. It has been proved that features based on image texture high-throughput extraction can more objectively and effectively predict the diagnosis, pathological grade, histological classification, lymph node metastasis, and prognosis of different diseases (20, 22, 32, 33). Combined with clinical factors and radiomics features, the nomogram was further established. The results show that the combined model had higher accuracy and sensitivity (0.95 (0.90, 0.98), 0.87, 0.91), but was less specific than the T1WI+C model (0.83 VS 0.92), and the difference was statistically significant (P = 0.002, 0.05, DeLong's test). The results of this study indicate that the nomogram of multisequence features combined with clinical factors has a high diagnostic performance in distinguishing HGSOCs from LGSOCs. Due to the silencing of OCs growth, the tumor was large when it was discovered, accompanied by obvious cystic degeneration, necrosis, hemorrhage, and other manifestations. The tumors performed with obvious heterogeneity and it was difficult to distinguish subtypes only by clinical factors and the differentiation of subtypes was closely related to clinical treatment strategies. Previous studies have mostly used conventional plain scanning of single T2WI sequence, which may lead to the loss of some important features. The combination of non-contrast-enhanced sequences, T1WI+C, and DWI of functional sequences can better delineate the entire tumor profile and perform more detailed imaging analysis of the entire tumor, thus obtaining higher diagnostic value.

There are several limitations in the present study. First of all, this study is a retrospective single-center study and the results may be influenced by sample selection. Therefore, prospective randomized trials with a larger sample, especially external validation, are warranted to validate the generalization capabilities of the prediction model. Secondly, the number of LGSOCs patients is relatively small, which is mainly related to the low morbidity. Finally, manual sketching of VOI was adopted in this study and errors were unavoidable. Further studies are needed to expand the sample size, gradually combine with automatic sketching technology instead of manual sketching VOI, and improve the robustness of the study.

CONCLUSION

In summary, we developed and validated a nomogram model combined with MRI-based multisequence radiomics signatures and clinical factors for the individualized prediction of type in SOCs and showed a favorable prediction performance. The nomogram models provided us a more comprehensive, effective method to evaluate risk stratification for SOCs, and

could further help clinicians to specify personalized treatment strategies to improve patients' prognosis.

DATA AVAILABILITY STATEMENT

The raw data supporting the conclusions of this article will be made available by the authors, without undue reservation.

ETHICS STATEMENT

The studies involving human participants were reviewed and approved by Anhui Provincial Hospital Ethics Committee. Written informed consent for participation was not required for this study in accordance with the national legislation and the institutional requirements.

AUTHOR CONTRIBUTIONS

XwW, JD, CL, XW, CZ, and YG: conception and design. CL, YC, CZ, YG, and HW: collection and arrangement of data. CL, CZ, YG, XwW, and JD: data analysis and manuscript writing. All authors contributed to the article and approved the submitted version.

FUNDING

This work was supported by 2020 SKY Image Research Fund (NO. Z-2014-07-2003-11).

ACKNOWLEDGMENTS

The authors thank all staff members involved in the acquisition of data. They are grateful to the technical assistance provided by GE Healthcare and Huiying Medical Technology (Beijing).

SUPPLEMENTARY MATERIAL

The Supplementary Material for this article can be found online at: https://www.frontiersin.org/articles/10.3389/fonc.2022.816982/full#supplementary-material

REFERENCES

1. Qian L, Ren J, Liu A, Gao Y, Hao F, Zhao L, et al. MR Imaging of Epithelial Ovarian Cancer: A Combined Model to Predict Histologic Subtypes. *Eur Radiol* (2020) 30:5815–25. doi: 10.1007/s00330-020-06993-5
2. Kawaguchi M, Kato H, Hatano Y, Tomita H, Hara A, Suzui N, et al. MR Imaging Findings of Low-Grade Serous Carcinoma of the Ovary: Comparison With Serous Borderline Tumor. *Jpn J Radiol* (2020) 38:782–9. doi: 10.1007/s11604-020-00960-2
3. Li HM, Zhang R, Gu WY, Zhao SH, Lu N, Zhang GF, et al. Whole Solid Tumour Volume Histogram Analysis of the Apparent Diffusion Coefficient for Differentiating High-Grade From Low-Grade Serous Ovarian Carcinoma: Correlation With Ki-67 Proliferation Status. *Clin Radiol* (2019) 74:918–25. doi: 10.1016/j.crad.2019.07.019
4. Sopik V, Iqbal J, Rosen B, Narod SA. Why Have Ovarian Cancer Mortality Rates Declined? Part I. *Incidence Gynecol Oncol* (2015) 138:741–9. doi: 10.1016/j.ygyno.2015.06.017
5. Kurokawa R, Nakai Y, Gonoi W, Mori H, Tsuruga T, Makise N, et al. Differentiation Between Ovarian Metastasis From Colorectal Carcinoma and Primary Ovarian Carcinoma: Evaluation of Tumour Markers and "Mille-Feuille Sign" on Computed Tomography/Magnetic Resonance Imaging. *Eur J Radiol* (2020) 124:108823. doi: 10.1016/j.ejrad.2020.108823
6. Turkoglu S, Kayan M. Differentiation Between Benign and Malignant Ovarian Masses Using Multiparametric MRI. *Diagn Interv Imaging* (2020) 101:147–55. doi: 10.1016/j.diii.2020.01.006
7. Delgado Bolton RC, Aide N, Colletti PM, Ferrero A, Paez D, Skanjeti A, et al. EANM Guideline on the Role of 2-[18F]FDG PET/CT in Diagnosis, Staging, Prognostic Value, Therapy Assessment and Restaging of Ovarian Cancer, Endorsed by the American College of Nuclear Medicine (ACNM), the Society of Nuclear Medicine and Molecular Imaging (SNMMI) and the International Atomic Energy Agency (IAEA). *Eur J Nucl Med Mol Imaging* (2021) 48:3286–302. doi: 10.1007/s00259-021-05450-9
8. Song XL, Ren JL, Zhao D, Wang L, Ren H, Niu J. Radiomics Derived From Dynamic Contrast-Enhanced MRI Pharmacokinetic Protocol Features: The Value of Precision Diagnosis Ovarian Neoplasms. *Eur Radiol* (2021) 31:368–78. doi: 10.1007/s00330-020-07112-0
9. Torre LA, Trabert B, Desantis CE, Miller KD, Samimi G, Runowicz CD, et al. Ovarian Cancer Statistics, 2018. *CA Cancer J Clin* (2018) 68:284–96. doi: 10.3322/caac.21456
10. Li H, Zhang R, Li R, Xia W, Chen X, Zhang J, et al. Noninvasive Prediction of Residual Disease for Advanced High-Grade Serous Ovarian Carcinoma by MRI-Based Radiomic-Clinical Nomogram. *Eur Radiol* (2021) 31:7855–64. doi: 10.1007/s00330-021-07902-0
11. Mulligan KM, Glennon K, Donohoe F, O'brien Y, Donnell BC, Bartels HC, et al. Multidisciplinary Surgical Approach to Increase Complete Cytoreduction Rates for Advanced Ovarian Cancer in a Tertiary Gynecologic Oncology Center. *Ann Surg Oncol* (2021) 28:4553–60. doi: 10.1245/s10434-020-09494-3
12. Wang F, Wang Y, Zhou Y, Liu C, Xie L, Zhou Z, et al. Comparison Between Types I and II Epithelial Ovarian Cancer Using Histogram Analysis of Monoexponential, Biexponential, and Stretched-Exponential Diffusion Models. *J Magn Reson Imaging* (2017) 46:1797–809. doi: 10.1002/jmri.25722
13. Rizzo S, Del Grande M, Manganaro L, Papadia A, Del Grande F. Imaging Before Cytoreductive Surgery in Advanced Ovarian Cancer Patients. *Int J Gynecol Cancer* (2020) 30:133–8. doi: 10.1136/ijgc-2019-000819
14. Wei M, Bo F, Cao H, Zhou W, Shan W, Bai G. Diagnostic Performance of Dynamic Contrast-Enhanced Magnetic Resonance Imaging for Malignant Ovarian Tumors: A Systematic Review and Meta-Analysis. *Acta Radiol* (2021) 62:966–78. doi: 10.1177/0284185120944916
15. Li Y, Jian J, Pickhardt PJ, Ma F, Xia W, Li H, et al. MRI-Based Machine Learning for Differentiating Borderline From Malignant Epithelial Ovarian Tumors: A Multicenter Study. *J Magn Reson Imaging* (2020) 52:897–904. doi: 10.1002/jmri.27084
16. Song XL, Ren JL, Yao TY, Zhao D, Niu J. Radiomics Based on Multisequence Magnetic Resonance Imaging for the Preoperative Prediction of Peritoneal Metastasis in Ovarian Cancer. *Eur Radiol* (2021) 11:8438–46. doi: 10.1007/s00330-021-08004-7
17. Li HM, Tang W, Feng F, Zhao SH, Gu WY, Zhang GF, et al. Whole Solid Tumor Volume Histogram Parameters for Predicting the Recurrence in Patients With Epithelial Ovarian Carcinoma: A Feasibility Study on Quantitative DCE-MRI. *Acta Radiol* (2020) 61:1266–76. doi: 10.1177/0284185119898654

18. Winfield JM, Wakefield JC, Dolling D, Hall M, Freeman S, Brenton JD, et al. Diffusion-Weighted MRI in Advanced Epithelial Ovarian Cancer: Apparent Diffusion Coefficient as a Response Marker. *Radiology* (2019) 293:374–83. doi: 10.1148/radiol.2019190545
19. Ye Z. Editorial for "Histogram Analysis Comparison of Monoexponential, Advanced Diffusion- Weighted Imaging, and Dynamic Contrast-Enhanced MRI for Differentiating Borderline From Malignant Epithelial Ovarian Tumors". *J Magn Reson Imaging* (2020) 52:269–70. doi: 10.1002/jmri.27120
20. Li C, Zheng M, Zheng X, Fang X, Dong J, Wang C, et al. Predictive Ki-67 Proliferation Index of Cervical Squamous Cell Carcinoma Based on IVIM-DWI Combined With Texture Features. *Contrast Media Mol Imaging* (2021) 2021:8873065. doi: 10.1155/2021/8873065
21. Ye R, Weng S, Li Y, Yan C, Chen J, Zhu Y, et al. Texture Analysis of Three-Dimensional MRI Images May Differentiate Borderline and Malignant Epithelial Ovarian Tumors. *Korean J Radiol* (2021) 22:106–17. doi: 10.3348/kjr.2020.0121
22. Nougaret S, Mccague C, Tibermacine H, Vargas HA, Rizzo S, Sala E. Radiomics and Radiogenomics in Ovarian Cancer: A Literature Review. *Abdom Radiol (NY)* (2021) 46:2308–22. doi: 10.1007/s00261-020-02820-z
23. Yang WL, Lu Z, Guo J, Fellman BM, Ning J, Lu KH, et al. Human Epididymis Protein 4 Antigen-Autoantibody Complexes Complement Cancer Antigen 125 for Detecting Early-Stage Ovarian Cancer. *Cancer* (2020) 126:725–36. doi: 10.1002/cncr.32582
24. Forstner R. Early Detection of Ovarian Cancer. *Eur Radiol* (2020) 30:5370–3. doi: 10.1007/s00330-020-06937-z
25. Chandra A, Pius C, Nabeel M, Nair M, Vishwanatha JK, Ahmad S, et al. Ovarian Cancer: Current Status and Strategies for Improving Therapeutic Outcomes. *Cancer Med* (2019) 8:7018–31. doi: 10.1002/cam4.2560
26. Chicago Consensus Working G. The Chicago Consensus on Peritoneal Surface Malignancies: Management of Ovarian Neoplasms. *Cancer* (2020) 126:2553–60. doi: 10.1002/cncr.32867
27. Dilley J, Burnell M, Gentry-Maharaj A, Ryan A, Neophytou C, Apostolidou S, et al. Ovarian Cancer Symptoms, Routes to Diagnosis and Survival - Population Cohort Study in the 'No Screen' Arm of the UK Collaborative Trial of Ovarian Cancer Screening (UKCTOCS). *Gynecol Oncol* (2020) 158:316–22. doi: 10.1016/j.ygyno.2020.05.002
28. Perales-Puchalt A, Wojtak K, Duperret EK, Yang X, Slager AM, Yan J, et al. Engineered DNA Vaccination Against Follicle-Stimulating Hormone Receptor Delays Ovarian Cancer Progression in Animal Models. *Mol Ther* (2019) 27:314–25. doi: 10.1016/j.ymthe.2018.11.014
29. Garcia Prado J, Gonzalez Hernando C, Varillas Delgado D, Saiz Martinez R, Bhosale P, Blazquez Sanchez J, et al. Diffusion-Weighted Magnetic Resonance Imaging in Peritoneal Carcinomatosis From Suspected Ovarian Cancer: Diagnostic Performance in Correlation With Surgical Findings. *Eur J Radiol* (2019) 121:108696. doi: 10.1016/j.ejrad.2019.108696
30. Jonsdottir B, Ripoll MA, Bergman A, Silins I, Poromaa IS, Ahlstrom H, et al. Validation of (18)F-FDG PET/MRI and Diffusion-Weighted MRI for Estimating the Extent of Peritoneal Carcinomatosis in Ovarian and Endometrial Cancer -a Pilot Study. *Cancer Imaging* (2021) 21:34. doi: 10.1186/s40644-021-00399-2
31. Wang R, Cai Y, Lee IK, Hu R, Purkayastha S, Pan I, et al. Evaluation of a Convolutional Neural Network for Ovarian Tumor Differentiation Based on Magnetic Resonance Imaging. *Eur Radiol* (2021) 31:4960–71. doi: 10.1007/s00330-020-07266-x
32. Rizzo S, De Piano F, Buscarino V, Pagan E, Bagnardi V, Zanagnolo V, et al. Pre-Operative Evaluation of Epithelial Ovarian Cancer Patients: Role of Whole Body Diffusion Weighted Imaging MR and CT Scans in the Selection of Patients Suitable for Primary Debulking Surgery. A Single-Centre Study. *Eur J Radiol* (2020) 123:108786. doi: 10.1016/j.ejrad.2019.108786
33. Zhang K, Zhang Y, Fang X, Fang M, Shi B, Dong J, et al. Nomograms of Combining Apparent Diffusion Coefficient Value and Radiomics for Preoperative Risk Evaluation in Endometrial Carcinoma. *Front Oncol* (2021) 11:705456. doi: 10.3389/fonc.2021.705456

Conflict of Interest: The authors declare that the research was conducted in the absence of any commercial or financial relationships that could be construed as a potential conflict of interest.

Publisher's Note: All claims expressed in this article are solely those of the authors and do not necessarily represent those of their affiliated organizations, or those of the publisher, the editors and the reviewers. Any product that may be evaluated in this article, or claim that may be made by its manufacturer, is not guaranteed or endorsed by the publisher.

Copyright © 2022 Li, Wang, Chen, Zhu, Gao, Wang, Dong and Wu. This is an open-access article distributed under the terms of the Creative Commons Attribution License (CC BY). The use, distribution or reproduction in other forums is permitted, provided the original author(s) and the copyright owner(s) are credited and that the original publication in this journal is cited, in accordance with accepted academic practice. No use, distribution or reproduction is permitted which does not comply with these terms.

frontiers | Frontiers in Oncology

ORIGINAL RESEARCH
published: 30 June 2022
doi: 10.3389/fonc.2022.807748

BRCA Variants Do Not Increase the Risk of Adverse Reactions in Patients With Ovarian Cancer: A Single-Center Real-World Study

Kemin Li[1,2], *Jing Zeng*[1,2], *Mengpei Zhang*[1,2], *Rutie Yin*[1,2*†] and *Zhengyu Li*[1,2*†]

[1] The Department of Obstetrics and Gynecology, West China Second University Hospital of Sichuan University, Chengdu, China, [2] Key Laboratory of Birth Defects and Related Diseases of Women and Children (Sichuan University), Ministry of Education, Chengdu, China

OPEN ACCESS

Edited by:
Sophia George,
University of Miami, United States

Reviewed by:
Athina Christopoulou,
General University Hospital of Patras, Greece
Steven Narod,
University of Toronto, Canada
Christine Garcia,
Kaiser Permanente San Francisco Medical Center, United States

***Correspondence:**
Rutie Yin
yrtt2013@163.com
Zhengyu Li
zhengyuli01@126.com

[†]These authors have contributed equally to this work

Specialty section:
This article was submitted to Gynecological Oncology, a section of the journal Frontiers in Oncology

Received: 02 November 2021
Accepted: 02 June 2022
Published: 30 June 2022

Citation:
Li K, Zeng J, Zhang M, Yin R and Li Z (2022) BRCA Variants Do Not Increase the Risk of Adverse Reactions in Patients With Ovarian Cancer: A Single-Center Real-World Study. Front. Oncol. 12:807748. doi: 10.3389/fonc.2022.807748

Objective: To study the correlation between *BRCA* mutation status and the risk of adverse reactions in patients with ovarian cancer.

Method: A real-world study was conducted at the largest gynecological oncology center in western China, the West China Second University Hospital of Sichuan University. The research subjects were patients diagnosed with ovarian cancer who were initially treated in our hospital from January 2016 to January 2020 and had their *BRCA* gene status evaluated. Multivariate Cox analysis was conducted to investigate the correlation between the *BRCA* mutation status and adverse reactions in ovarian cancer patients during initial treatment.

Results: A total of 349 ovarian cancer patients were enrolled, including 79 patients with pathogenic *BRCA* variants, resulting in a pathogenic mutation rate of 22.6%. Among these 79 patients, 57 had *BRCA1* variants and 22 had *BRCA2* variants, yielding a pathogenic mutation rate of 16.3% and 6.3%, respectively. Multivariate COX analysis revealed that pathogenic *BRCA* variants were not related to the risk of adverse reactions, such as myelosuppression and allergies to chemotherapy drugs ($P>0.05$), during the initial treatment of ovarian cancer.

Conclusion: *BRCA* variants did not increase the risk of adverse reactions, such as myelosuppression and allergies to chemotherapy drugs, in ovarian cancer patients during initial treatment.

Keywords: ovarian cancer, BRCA, myelosuppression, allergies to chemotherapy drugs, real-world study

Abbreviations: BRCA, breast cancer susceptibility gene; PTX, paclitaxel; HRR, Homologous recombination repair; DSB, DNA double-strand break; OS, overall survival; HGSOC, high-grade serous ovarian cancers; FIGO, the International Federation of Gynecology and Obstetrics; G-CSF, granulocyte colony-stimulating factor; VUS, variants of unknown significance; CTCAE, Common Terminology Criteria for Adverse Events; AE, Adverse Events; PARP, poly ADP-ribose polymerase.

INTRODUCTION

Ovarian cancer is the fifth leading cause of cancer deaths in women, ranking first among deaths related to gynecological cancer (1). In China, there are approximately 52,100 new cases of ovarian cancer and 22,500 deaths every year (2). Platinum-based chemotherapy remains the first-line treatment for ovarian cancer following satisfactory surgical cytoreduction. Chemotherapy drugs cause various types and degrees of adverse reactions (3). For example, myelosuppression is one of the most common adverse reactions to chemotherapy for ovarian cancer. Studies have shown that among the newly diagnosed advanced ovarian cancer patients treated with paclitaxel (PTX) and carboplatin plus bevacizumab, roughly 12% suffer from Grade 3-4 anemia, and as high as 21% of the patients had neutropenia (4).

Homologous recombination repair (HRR) involves DNA double-strand break (DSB) repair and maintenance of genetic stability, deficiencies in which may lead to malignancies. Studies have shown that up to 50% of high-grade serous ovarian cancers (HGSOC) are related to HRR deficiency and express *BRCA1* or *BRCA2* variants (5). Germline and somatic HRR mutations are highly predictive of primary platinum sensitivity and improvement in overall survival (OS). As reported, the median OS of carriers of germline mutations involved in HRR is 66 months, that of carriers of somatic mutations is 59 months, and that of those without HRR-related mutations is 41 months (6). It has rarely been described whether the *BRCA* mutation status affects the risk of adverse reactions caused by chemotherapy in ovarian cancer patients, and the conclusions are inconsistent. Kotsopoulos et al. (7) reported that *BRCA* variants do not increase the risk of hematological adverse reactions caused by chemotherapy in patients with ovarian cancer; Rolfe et al. (8) reported that *BRCA* variants do not increase the risk of allergic reactions to carboplatin; whereas, Giannone et al. (9) found that the allergic reactions to carboplatin in patients with *BRCA* mutations are significantly increased during chemotherapy.

In the present study, using real-world data, we performed a multi-factor analysis of the correlation between the BRCA mutation status of patients with ovarian cancer and the risk of adverse reactions during initial treatment, providing a basis for the standardized management of adverse reactions in these patients.

MATERIALS AND METHODS

The West China Second University Hospital of Sichuan University (WCSUH) is the largest gynecological oncology diagnostic and treatment center in western China. The patients diagnosed with ovarian cancer who had their initial treatment at our hospital from January 2016 to January 2020 were the research subjects, all of whom were tested for *BRCA* mutation status. There were no restrictions on the age of the research subjects or the pathological type of ovarian cancer. No patients had received radiotherapy, chemotherapy, or other anti-tumor therapy, nor did they have any cancer history of other systems. Real-world clinical parameters of the research subjects who met the enrollment criteria were collected, including age, pathological type, neoadjuvant chemotherapy, *BRCA* mutation, FIGO (the International Federation of Gynecology and Obstetrics) staging, adverse reactions during initial treatment, family history of cancer, and granulocyte colony-stimulating factor (G-CSF) application during treatment.

Genetic testing was performed by the well-known international genetics company BGI Group. The germline mutation status of *BRCA1* and *BRCA1* was tested using patient's blood samples. Target capture combined with second-generation high-through put sequencing technology was used to analyze the variations (including point mutations, deletions, and insertions within 20 bp) in the related gene exons and the adjacent ± 10 bp introns, yielding pathogenic *BRCA* variants, *BRCA* variants of unknown significance (VUS), likely benign *BRCA* variants and benign *BRCA* variants. The pathogenic *BRCA* variants are noted as *BRCA* (+), while *BRCA* VUS and likely benign and benign *BRCA* variants are grouped into *BRCA* (–).

All patients received standard treatment following the FIGO treatment guidelines for ovarian cancer at the time of treatment. After the initial treatment, maintenance therapy, clinical observation, or clinical trials were provided according to the patient's preference, and all patients had lifetime follow-up.

Patient adverse reactions were defined according to the Common Terminology Criteria for Adverse Events (CTCAE), including low white blood cell count (leukopenia), low neutrophil count (neutropenia), low platelet count (thrombocytopenia), anemia, thromboembolism, and allergies to chemotherapy drugs (platinum or PTX).

Data are expressed as the mean ± standard deviation. The multivariate COX model was employed to analyze the correlation between pathogenic *BRCA* variants and various adverse reactions in patients with ovarian cancer during initial treatment. The factors include age, stage, regimens, cycles, neoadjuvant chemotherapy, surgical outcome (R0/R1/R2), thrombosis, family history of cancer, pathological type, adverse reactions (leukopenia, neutropenia, thrombocytopenia, anemia, thromboembolism, and allergies to chemotherapy drugs) and BRCA. $P<0.05$ was considered statistically significant.

RESULTS

Basic Characteristics of Research Subjects

The basic characteristics of the study subjects are shown in **Table 1**. A total of 349 patients with ovarian cancer who met the criteria were included. All patients received paclitaxel + cisplatin/carboplatin. The mean age was 50.0 ± 13.1 years old and 333 cases (95.4%) were ovarian epithelial cancer. According to FIGO staging, there were 68 cases (19.5%) of Stage IA-IIA and 281 cases (80.5%) of Stage ≥IIB. A total of 79 patients carried pathogenic *BRCA* variants, which is a pathogenic mutation

TABLE 1 | Basic characteristics of research subjects.

		BRCA+					
		BRCA1+	BRCA2+	total	BRCA-	total	P
n		57	22	79	270	349	
Years		49.6±13.5	50.6±13.2	50.1±13.3	49.8±12.9	50.0±13.1	0.75
Neoadjuvant chemotherapy		17	10	27	58	85	0.02
Family history		43	14	57	118	175	<0.0001
Pathological type	Epithelial	52	21	73	260	333	0.15
	carcinosarcoma	3	1	4	3	7	0.04
	others	2	0	2	7	9	0.98
FIGO stage	IA-IIA	5	0	5	63	68	0.002
	≥IIB	52	22	74	207	281	0.002
Chemotherapy cycles (mean)	NC	0.8	1.7	1.0	1.0	1.0	0.89
	AC	7.4	7.0	7.4	7.4	7.4	0.79
	total	8.2	8.7	8.8	8.4	8.4	0.86
Regimens	T+P	12	4	16	49	65	0.67
	T+C	10	4	14	45	59	0.83
	T+P/C	35	14	49	176	225	0.61
White blood cell	≥1 grade	57	22	79	263	342	0.3
	≥3 grade	15	6	21	92	113	0.21
neutrophils	≥1 grade	57	22	79	265	344	0.42
	≥3 grade	14	9	23	118	141	0.02
Anemia	≥1 grade	53	21	74	247	321	0.53
	≥3 grade	0	0	0	2	2	0.8
platelets	≥1 grade	31	6	37	106	143	0.23
	≥3 grade	6	1	7	28	35	0.69
thromboembolism		11	2	12	39	52	0.87
allergy	platinum	10	1	11	15	26	0.02
	Taxol	2	1	3	8	11	0.71
G-CSF		37	11	48	161	209	0.86

G-CSF, granulocyte colony stimulating factor; BRCA, Breast Cancer susceptibility gene; NC, neoadjuvant chemotherapy; AC, adjuvant chemotherapy; T, paclitaxel; P, cisplatin; C, carboplatin.

rate of 22.6%. Among these, 57 patients carried *BRCA1* variants and 22 carried *BRCA2* variants, yielding a pathogenic mutation rate of 16.3% and 6.3%, respectively. There were 175 patients with a family history of cancer.

Occurrences of *BRCA* Variants and Adverse Reactions

The occurrences of *BRCA* variants and adverse reactions are shown in **Table 1**. Among the *BRCA* (+) patients, 21 (26.6%), 0 (0%), and 7 (8.9%) patients with CTCAE ≥ Grade 3 experienced leukopenia, anemia, and thrombocytopenia, respectively, which is clearly less than *BRCA* (–) patients whose corresponding values were 113 (41.9%), 2 (0.2%), and 35 (13.0%). Nevertheless, the differences were not statistically significant(P>0.05).

Among the *BRCA* (+) patients, 23 (29.1%) suffered from CTCAE ≥ Grade 3 neutropenia, which is less than 118 (43.7%) of the BRCA (–) patients. The difference was statistically significant (P <0.05). A total of 12 (15.2%) *BRCA* (+) patients suffered from thromboembolism, which is less than 52 (19.3%) of the *BRCA* (–) patients; however, the difference was not statistically significant (P>0.05). Moreover, a total of 48 (60.8%) *BRCA* (+) patients were administered G-CSF due to myelosuppression, which is much less than 209 (77.4%) of the *BRCA* (–) patients; however, the difference was not statistically significant (P>0.05).

Platinum-based chemotherapeutic allergy occurred in 11 (13.9%) *BRCA* (+) patients, which is significantly more than 15 (5.6%) of the *BRCA* (–) patients. This difference was statistically significant (P<0.05). Among the *BRCA* (+) patients, 3 (3.8%) developed an allergy to PTX, while 8 (3.0%) of the *BRCA* (–) patients developed a PTX allergy; however, the difference was not statistically significant (P>0.05).

Correlation Between Pathogenic *BRCA* Variants and Adverse Reactions

The correlation between pathogenic *BRCA* variants and adverse reactions is shown in **Table 2**. According to the multivariate COX model, after considering other factors (age, stage, regimens, cycles, neoadjuvant chemotherapy, surgical outcome (R0/R1/R2), thrombosis, family history of cancer, pathological type), pathogenic *BRCA* variants (including *BRCA1* and *BRCA2*) were not correlated with the occurrence of adverse reactions during the initial treatment of ovarian cancer (P>0.05). The adverse reactions included leukopenia, neutropenia, thrombocytopenia, anemia, thromboembolism, and allergies to chemotherapy drugs (platinum or PTX).

DISCUSSION

PARP is a key enzyme responsible for repairing DNA single-strand breaks (SSB), inhibition of which leads to persistent SSB that transform into severe double-strand breaks (DSB) during DNA replication. During the process of cell division, DSB in normal cells can be effectively repaired by homologous

TABLE 2 | Correlation between pathogenic *BRCA* variants and adverse reactions.

Adverse reactions	genes	Standard error	Wald	P VALUE	95%CI
Allergic reaction	BRCA1	177.6	0.006	0.9382	(0.887-1.228)
	BRCA2	110.9	0.0664	0.7967	(0.793-1.156
Abnormal liver function	BRCA1	0.4873	0.3328	0.564	(0.540-1.226)
	BRCA2	0.7201	0.5238	0.4692	(0.472-2.367)
leukopenia	BRCA1	0.4717	0.3209	0.5711	(0.558-2.154)
	BRCA2	0.8832	2.462	0.1166	(0.332-3.441)
neutropenia	BRCA1	0.4602	0.1066	0.744	(0.792-1.164)
	BRCA2	1.0135	1.8695	0.1715	(0.223-3.471)
anemia	BRCA1	0.4993	0.1056	0.7452	(0.669-1.132)
	BRCA2	0.8745	0.089	0.7654	(0.693-1.201)
thrombocytopenia	BRCA1	0.5124	1.695	0.1929	(0.341-2.998)
	BRCA2	0.9958	0.0635	0.8011	(0.889-1.219)
thromboembolism	BRCA1	0.7396	0.0029	0.9571	(0.993-1.077)
	BRCA2	77.5065	0.0012	0.9725	(0.989-1.041)

BRCA, Breast Cancer susceptibility gene.

recombination repair (HRR). Tumors displaying HRR deficiency, such as ovarian cancer in patients with *BRCA1*/2 variants, cannot accurately repair DNA damage, and accumulation of such damage may lead to cell death. In the same manner, tumor patients carrying germline *BRCA1*/2 variants cannot accurately repair DNA damage following the administration of chemotherapy drugs and similar anti-tumor treatments, and as a result, may also have increased risk or elevated severity of adverse reactions. Should the occurrence of adverse reactions, especially ≥ Grade 3 adverse reactions, significantly increase during chemotherapy in patients with pathogenic *BRCA* variants, then treating pathogenic *BRCA* variant carriers as high-risk patients and improving the standard treatment management would reduce the impact of adverse reactions on patients and improve their quality of life.

Hematological toxicity, such as myelosuppression, is one of the most common adverse reactions to chemotherapy. Whether *BRCA* variants increase the occurrence of myelosuppression in patients undergoing chemotherapy remains controversial. In their study on the toxicity of PTX-based chemotherapy in pathogenic *BRCA* variant carriers with breast cancer, Bayraktar et al. (10) analyzed the hematological toxicity during PTX chemotherapy in a total of 790 patients of various *BRCA* mutation statuses and found that the occurrence of anemia and leukopenia in *BRCA* (–) patients was significantly higher than that in pathogenic *BRCA* variant carriers. Moreover, pathogenic *BRCA2* variants were a predictor of hematological adverse reactions in breast cancer patients during PTX chemotherapy. However, Kotsopoulos *et al.* (7) revealed that pathogenic *BRCA* variants are not related to the hematological toxicity caused by platinum-based combination chemotherapy in ovarian cancer patients. A total of 432 ovarian cancer patients were enrolled, including 130 *BRCA* (+) and 302 *BRCA* (–). The results demonstrated that the risk of neutropenia, anemia, and thrombocytopenia in patients with pathogenic *BRCA* variants did not differ from that in the *BRCA* (–) patients. Using real-world data, the present study shows that the occurrence of myelosuppression (including leukopenia, neutropenia, thrombocytopenia, and anemia) during initial treatment in ovarian cancer patients with pathogenic *BRCA* variants was substantially lower than that in BRCA (–) patients; nevertheless, the multivariate analysis showed no significant correlation between pathogenic *BRCA* variants and the occurrence of myelosuppression.

Infusion reactions and even severe allergic reactions may occur during or after chemotherapy. Whether *BRCA* variants increase the occurrence of allergic reactions to chemotherapy drugs remains in conclusive. Rolfe et al. (8) studied the relationship between *BRCA* mutation status and the risk of carboplatin-related allergic reactions and found that pathogenic *BRCA* variants did not increase the risk of carboplatin allergy in patients with ovarian cancer. However, Giannone (9) et al. systematically evaluated the relationship between pathogenic *BRCA* variants and the risk of carboplatin-related allergic reactions, reviewing a total of 5 studies including 432 patients with ovarian cancer, and found that pathogenic *BRCA* variants significantly increased carboplatin allergy risk in patients with ovarian cancer. The results of our study demonstrate that the occurrence of carboplatin allergic reactions during chemotherapy in ovarian cancer patients with pathogenic *BRCA* variants was substantially increased; however, the multivariate COX analysis did not show statistical significance.

The present study also analyzed whether pathogenic *BRCA* variants increase the risk of thromboembolism and G-CSF application in patients with ovarian cancer during the initial treatment, and reached a negative conclusion. At present, there are few relevant studies and the ratio of patients with allergic reactions in the present study was low; therefore, the reliability of the conclusions needs to be tested further.

Our study was a single-center study with a small sample size, and the low occurrence of some adverse reactions, such as carboplatin and PTX allergies, may affect the reliability of the conclusions. However, so far, the present study is the largest study of real-world data, and considered many confounding factors, such as neoadjuvant chemotherapy, family history of cancer, and pathological tumor type, and adopted multi-factor

analysis to avoid the influence of other factors. Moreover, the adopted real-world data truly represents actual clinical practice and has great value for clinical guidance.

CONCLUSION

BRCA variants did not increase the risk of adverse reactions, such as myelosuppression and allergies to chemotherapy drugs, in ovarian cancer patients during initial treatment.

DATA AVAILABILITY STATEMENT

The original contributions presented in the study are included in the article/supplementary materials. Further inquiries can be directed to the corresponding authors.

ETHICS STATEMENT

The studies involving human participants were reviewed and approved by Approvalled Medical Ethics Committee of West China Second University Hospital, Sichuan University. Ethical Lot Number:20200076. Written informed consent for participation was not required for this study in accordance with the national legislation and the institutional requirements.

AUTHOR CONTRIBUTIONS

Conception: KL, RY. Design: all authors. Data collection: KL, MZ. Data analysis: KL, JZ. Manuscript writing: KL, MZ. All authors contributed to the article and approved the submitted version.

REFERENCES

1. Chen W, Zheng R, Baade PD, Zhang S, Zeng H, Bray F, et al. Cancer Statistics in China, 2015. *CA Cancer J Clin* (2016) 66(2):115–32. doi: 10.3322/caac.21338
2. Siegel RL, Miller KD, Jemal A. Cancer Statistics, 2018. *CA Cancer J Clin* (2018) 68(1):7–30. doi: 10.3322/caac.21442
3. NCCN Clinical Practice Guidelines in Oncology (NCCN Guidelines). *Hematopoietic Growth Factors. Version 1* (2021). Available at: WWW.NCCN.org.
4. Moore KN, Bookman M, Sehouli J, Miller A, Anderson C, Scambia G, et al. Atezolizumab, Bevacizumab, and Chemotherapy for Newly Diagnosed Stage III or IV Ovarian Cancer: Placebo-Controlled Randomized Phase III Trial (IMagyn050/GOG 3015/ENGOT-Ov39). *J Clin Oncol* (2021) 39(17):1842–55. doi: 10.1200/JCO.21.00306
5. Cancer Genome Atlas Research Network. Integrated Genomic Analyses of Ovarian Carcinoma. *Nature* (2011) 474(7353):609 –15. doi: 10.1038/nature10166
6. Pennington KP, Walsh T, Harrell MI, Lee MK, Pennil CC, Rendi MH, et al. Germline and Somatic Mutations in Homologous Recombination Genes Predict Platinum Response and Survival in Ovarian, Fallopian Tube, and Peritoneal Carcinomas. *Clin Cancer Res* (2014) 20:764–75. doi: 10.1158/1078-0432.CCR-13-2287
7. Kotsopoulos J, Willows K, Trat S, Kim RH, Volenik A, Sun P, et al. BRCA Mutation Status is Not Associated With Increased Hematologic Toxicity Among Patients Undergoing Platinum-Based Chemotherapy for Ovarian Cancer. *Int J Gynecol Cancer* (2018) 28(1):69–76. doi: 10.1097/IGC.0000000000001144
8. Rolfe M, Gegeckas C, Turner S, Jr JWO. Predictive Factors for Carboplatin Hypersensitivity Reactions in Gynecologic Cancers: Effect of BRCA Status. *J Oncol Pharm Pract* (2020) 27(7):1704–9. doi: 10.1177/1078155220967988
9. Giannone G, Scotto G, Katsaros D, Giorgi UD, Farolfi A, Borella F, et al. Hypersensitivity to Platinum Salts According to BRCA Status in Ovarian Cancer: A Retrospective Analysis of Clinical Outcomes and Systematic Review of Literature. *Gynecol Oncol* (2021) 162(1):80–7. doi: 10.1016/j.ygyno.2021.04.018
10. Bayraktar S, Zhou JZ, Bassett R, Barrera AMG, Layman RM, Valero V, . Clinical Outcome and Toxicity From Taxanes in Breast Cancer Patients With BRCA1 and BRCA2 Pathogenic Germline Mutations. *Breast J* (2020) 26 (8):1572–82. doi: 10.1111/tbj.13922

Conflict of Interest: The authors declare that the research was conducted in the absence of any commercial or financial relationships that could be construed as a potential conflict of interest.

Publisher's Note: All claims expressed in this article are solely those of the authors and do not necessarily represent those of their affiliated organizations, or those of the publisher, the editors and the reviewers. Any product that may be evaluated in this article, or claim that may be made by its manufacturer, is not guaranteed or endorsed by the publisher.

Copyright © 2022 Li, Zeng, Zhang, Yin and Li. This is an open-access article distributed under the terms of the Creative Commons Attribution License (CC BY). The use, distribution or reproduction in other forums is permitted, provided the original author(s) and the copyright owner(s) are credited and that the original publication in this journal is cited, in accordance with accepted academic practice. No use, distribution or reproduction is permitted which does not comply with these terms.

frontiers | Frontiers in Oncology

SYSTEMATIC REVIEW
published: 06 July 2022
doi: 10.3389/fonc.2022.817772

Exploring the Pharmacological Mechanism of the Effective Chinese Medicines Against Gynecological Cancer Based on Meta-Analysis Combined With Network Pharmacology Analysis

Ning Ren[1†], Lulin Yu[2†], Lihui Qian[2†], Gewei Ye[2], Zhenzheng Zhu[2], Jieru Yu[3], Leitao Sun[4*] and Leyin Zhang[5*]*

[1] Hangzhou TCM Hospital of Zhejiang Chinese Medical University (Hangzhou Hospital of Traditional Chinese Medicine), Hangzhou, China, [2] The First School of Clinical Medicine, Zhejiang Chinese Medical University, Hangzhou, China, [3] School of Basic Medical Sciences, Zhejiang Chinese Medical University, Hangzhou, China, [4] Department of Medical Oncology, The First Affiliated Hospital of Zhejiang Chinese Medical University (Zhejiang Provincial Hospital of Traditional Chinese Medicine), Hangzhou, China, [5] Department of Oncology, Hangzhou TCM Hospital of Zhejiang Chinese Medical University (Hangzhou Hospital of Traditional Chinese Medicine), Hangzhou, China

This meta-analysis plus network pharmacology aimed to investigate whether traditional Chinese medicine (TCM) combined with chemotherapy is associated with more beneficial efficacy data in the treatment of gynecological cancer (GC). A total of 11 randomized controlled trials (RCTs) consisting of 863 GC patients were included. Results showed a better ORR (RR: 1.42, 95% CI: 1.18–1.71; I^2 = 21.4%; p = 0.282), DCR (RR: 1.13, 95% CI: 1.03–1.25; I^2 = 0.0%; p = 0.492), PD (RR: 0.27, 95% CI: 0.11–0.65, p = 0.003; I^2 = 0.0%, p = 0.930), and QOL (SMD: 0.85, 95% CI: 0.38–1.33, p = 0.005) and higher proportions of $CD3^+$ T (WMD: 5.65, 95% CI: 4.23–7.08, p = 0.000; I^2 = 68.3%, p = 0.004), $CD4^+$ T (WMD: 6.97, 95% CI: 5.35–8.59, p = 0.000; I^2 = 83.4%, p = 0.000), and the $CD4^+/CD8^+$ T ratio (WMD: 0.32, 95% CI: 0.23–0.42, p = 0.000; I^2 = 78.0%, p = 0.000). The number of adverse events (AEs) was significantly lower in the TCM + chemotherapy group. The active components and targets of 19 high-frequency Chinese medicines obtained from the meta-analysis were screened and explored in network pharmacology analysis. Also, a regulatory network of active components and targets, a core network and key genes, a diagram of protein interaction, network topology analysis, and gene body GO function and KEGG pathway enrichment analysis were performed. A total of 120 active components were identified. NPM1 and HSPA8 are the most critical target proteins in the core network of protein interaction. HSP90AA1 is the most important target protein in the TCM group. KEGG enrichment analysis showed that it was highly significant in the lipid and atherosclerotic pathways. Therefore, moderate evidence revealed that TCM plus

OPEN ACCESS

Edited by:
Elena Ioana Braicu, Charité Universitätsmedizin Berlin, Germany

Reviewed by:
Pierluigi Giampaolino, University of Naples Federico II, Italy
Shujie Liao, Huazhong University of Science and Technology, China

***Correspondence:**
Leyin Zhang
leyin.zhang@zcmu.edu.cn
Leitao Sun
sunnylt@zcmu.edu.cn
Jieru Yu
jieruyu@zcmu.edu.cn

†These authors have contributed equally to this work and share first authorship

Specialty section:
This article was submitted to Gynecological Oncology, a section of the journal Frontiers in Oncology

Received: *18 November 2021*
Accepted: *01 June 2022*
Published: *06 July 2022*

Citation:
Ren N, Yu L, Qian L, Ye G, Zhu Z, Yu J, Sun L and Zhang L (2022) Exploring the Pharmacological Mechanism of the Effective Chinese Medicines Against Gynecological Cancer Based on Meta-Analysis Combined With Network Pharmacology Analysis. Front. Oncol. 12:817772. doi: 10.3389/fonc.2022.817772

chemotherapy has obvious advantages over chemotherapy alone in terms of tumor responses, QOL, peripheral blood lymphocyte levels, and fewer AEs in the treatment of GC. The potential important targets and core genes were displayed.

Systematic Review Registration: www.crd.york.ac.uk/PROSPERO/, identifier CRD42021252500.

Keywords: gynecological cancer, chemotherapy, traditional Chinese medicine, meta-analysis, network pharmacology

1 INTRODUCTION

More than 8.6 million global women are diagnosed with cancer per year, with approximately 1.3 million cases of gynecological cancer (GC) (1, 2). Despite the progressive enhancement in diagnosis and therapy strategies that has been increasing in the past decades, the prognosis of GC remains not to everyone's satisfaction (3, 4).

The main treatment methods for gynecological tumors include surgery, chemotherapy, radiotherapy, or a combination of them. Chemotherapy is an important part of the treatment of gynecological tumors, but it will inevitably induce adverse effects such as deterioration, myelosuppression, and reduction. Take ovarian cancer (OC), for example. OC is the most common malignant tumor in gynecology, and the current standard treatment plan of which is postcytoreductive surgery combined with "paclitaxel + carboplatin" therapy. Also, emerging treatments such as poly(ADP-ribose) polymerase (PARP) inhibitor (5) and neoadjuvant chemotherapy (NACT) (6) are also popularly chosen to be applied in OC therapy, but how to optimize the clinical treatment plan, reduce the adverse effects of various treatments, and improve the quality of life of patients remains to be further explored.

In China, traditional Chinese medicine (TCM) has gained more and more attention for malignant tumors because of its beneficial effects, such as low toxicity and enhanced efficiency (7, 8). Furthermore, data have shown that TCM can significantly enhance the sensitivity to chemotherapeutic drugs and tumor-suppressing effects and relieve cancer-related adverse events (AEs) (9, 10). However, its clinical characteristics were still not well investigated. It remains uncertain whether TCM plus chemotherapy is more effective than chemotherapy alone for GC, which has not been systematically assessed.

Therefore, we aimed to drive this meta-analysis to investigate the efficacy and safety of combination therapy by using TCM plus chemotherapy compared with chemotherapy alone, in which way we can spot suitable prescriptions to improve patients' survival rates. High-frequency Chinese herbs will be extracted from those beneficial prescriptions. Whereas, there are still large gaps in our understanding of TCM, such as what are the essential effective components in TCM, what are the key potential targets, and whether interplays exist between these herbal components. As a result, we performed network pharmacology analysis to explore the potential pharmacological mechanisms and targets of TCM in the treatment of GC.

Abbreviations: TCM, traditional Chinese medicine; GC, gynecological cancer; CBM, Chinese biological medicine; CNKI, China National Knowledge Infrastructure databases; ORR, objective response rate; DCR, disease control rate; PD, progressive disease; QOL, quality of life; AEs, adverse events; RR, risk ratio; SMD, standardized mean difference; WMD, weighted mean difference; CIs, credible intervals; OC, ovarian cancer; PRISMA, Preferred Reporting Items for Systematic Reviews and Meta-Analysis; CR, complete response; PR, partial response; SD, stable disease; PD, progressive disease; VN, neoplasms; VC, vaginal cancer; UCC, uterine cervix cancer; EC, endometrial carcinoma; FTC, fallopian tube carcinoma; TCMSP, Traditional Chinese Medicine Systems Pharmacology Database and Analysis Platform; GO, gene ontology; KEGG, Kyoto Encyclopedia of Genes and Genomes; OB, oral bioavailability; DL, drug like, BC, betweenness centrality; BP, biological process; CC, cell composition; MF, molecular function; OS, overall survival; PFS, progression-free survival.

2 METHODS

2.1 Protocol and Guidance

This study adhered to the Preferred Reporting Items for Systematic Reviews and Meta-Analysis (PRISMA) guidelines. The protocol for this review was registered with PROSPERO (CRD42021252500).

2.2 Search Strategy

Three investigators independently searched several databases: PubMed, EMBASE, Cochrane, Chinese biological medicine (CBM), China Wanfang database, China National Knowledge Infrastructure databases (CNKI), Chinese Clinical Trial Registry (ChiCTR), ClinicalTrials.gov, and the World Health Organization International Clinical Trials Registry Platform from inception to September 26, 2021. Moreover, we also obtained the data sources from the abstracts and presentations recorded at some annual meetings, symposiums, or congresses such as ASCO, ESMO, ESGO, and so on, to ensure the relevant minutes were not overlooked. The complete search strategy was introduced in the **Supplementary Material**.

2.3 Selection Criteria

2.3.1 Inclusion Criteria

Studies were included if they met the following criteria: if the people enrolled were GC patients (diagnosed based on histological or cytological results); if the subjects included had no contraindication to chemotherapy and no other systemic disease and were expected to live longer than 3 months; if TCM was in combination with chemotherapy for GC in the intervention group; if patients were treated with no TCM, or placebo, or conventional chemotherapy alone in the control group; if tumor response rate, QOL, AEs, serum tumor marker, and peripheral blood lymphocyte levels were reported

(at least one of these outcomes); and if they were randomized controlled trials (RCTs).

2.3.2 Exclusion Criteria

We excluded studies if they had not met our baseline requirements; if they employed the methods of acupuncture, massage, and other TCM treatment; if they did not offer the outcomes we needed; and if they were case reports, case series, observational studies, or other types of articles.

2.4 Study Selection and Data Extraction

Three independent investigators finished this part following the requirements of PRISMA according to the above inclusion and exclusion criteria. All disagreements about selection were discussed and resolved by all investigators. The data extraction included the author, year, country, research type, number of cases, age of patients, and the indicators for demonstrating outcomes. Tumor response was the primary outcome, including complete response (CR), partial response (PR), stable disease (SD), and progressive disease (PD). The CR rates combined with PR rates were equal to the ORR; the CR, PR, and SD rates were equal to the DCR. Quality of life (QOL) and the incidence of AEs were also the main outcomes. Immune function (peripheral blood lymphocyte levels), KPS score, and serum tumor marker were the secondary outcomes. Peripheral blood lymphocytes were evaluated by the levels of $CD3^+$ T, $CD4^+$ T, $CD8^+$ T, and $CD4^+/CD8^+$ T ratio. Serum tumor markers were evaluated by CEA, AFP, and other common tumor markers.

2.5 Risk of Methodological Bias Assessment

Three researchers independently carry out the literature quality evaluation by applying the Cochrane evaluation handbook of RCTs (5.1.0), which includes the following characteristics covering randomization sequence generation (selection bias), allocation concealment (selection bias), blinding of participants and personal (performance bias), blinding of outcome assessment (detection bias), incomplete outcome data (attrition bias), selective reporting (reporting bias), and other bias. We used the Review Manager 5.3 software risk assessment tool to finish this part, and we decided through discussion or consultation with a third party when opinions were inconsistent.

2.6 Statistical Analysis

RevMan (version 5.3.3; The Cochrane Collaboration) and STATA (version 15; Stata Corporation, College Station, Texas, USA) were utilized to perform statistical analyses including pooling the data and producing the forest plots.

The combination of relative ratio (RR) and mean difference (MD) with a 95% confidence interval (CI) was used to assess outcomes and considered a p-value less than 0.05 to be statistically significant. The I^2 test was also used to assess the between-study heterogeneity. If the heterogeneity test is $p \geq 0.1$ and $I^2 \leq 50\%$, it indicates that studies are homogenous between studies, and the fixed-effects model is used for combined analysis. Otherwise, we used a random-effects model to pool effect size. I^2 regarded an estimated value applied to three fixed knots at 25%, 50%, and 75% as an indicator of mild, moderate, and high heterogeneity. Sensitivity analysis was also performed for examining the robustness of included trials to different aspects from methodological bias. In addition to this, publication bias was also estimated by an inverted funnel plot.

2.7 Acquisition of GC Disease Targets

In the NCBI (https://www.ncbi.nlm.nih.gov/), we selected the database GEO datasets. GMS mainly includes vulvar neoplasms (VN), vaginal cancer (VC), uterine cervix cancer (UCC), endometrial carcinoma (EC), OC, and fallopian tube carcinoma (FTC).VC and FTC were too few to have reliable disease samples in the GEOncbi database. Targets of VN, EC, and OC were mainly obtained, while the reliable disease samples of VC and FTC were too few to acquire. We searched for "vulvar neoplasm," "uterine neoplasms," and "ovarian neoplasms," respectively. On the left, only series and expression profiling by an array of human tags are retained to narrow the screening range and obtain the corresponding samples of three tumor diseases (11–13). The platform file GPL571-17391 was selected, and the matrix file GSE63678 was standardized with Perl. The probe matrix was transformed into ID, and the whole gene matrix of VN was obtained. Platform files GPL10558-50081 and GPL887-20438 were then selected, respectively, and the matrix files GSE122697 and GSE12470 were standardized above. Finally, the whole gene matrices of EC and OC were acquired, followed by the differences in the GEO database analyzed for the three groups of gene data. The AveExpr of each gene in all samples was calculated using the R language, and the p-value was numerically corrected. Accordingly, the limma function package was used to construct a comparison matrix based on the ratio of the mean of the experimental group and the normal group, which was compared with the experimental design matrix. The eBayes function was used to make statistical inferences and analyze the difference. Finally, the corresponding gene of $|\log FC|>1$, adj.p-val<0.05 was screened out.

2.8 Acquisition of Target in the Chinese Materia Medica Group

Traditional Chinese Medicine Systems Pharmacology Database and Analysis Platform (TCMSP) was used for obtaining the effective components of each TCM. The medicinal DL ≥0.18 condition played an important role in screening the effective components of TCM. Related targets were entered, and the corresponding targets of the selected active ingredients were derived. Perl has been used as an important tool for gene standardization, converting full names to genetic symbols.

2.9 Construction of a Regulatory Network of TCM

A variety of active ingredients and corresponding targets of TCM were retrieved from the TCMSP database. Perl was used to form the "component-target" database of the active ingredients and GC disease targets in **Section 2.7**. The intersection of the two was taken, and a Venn diagram was drawn.

2.10 Construction and Analysis of Protein (PPI) Interaction Network

The intersected genes were imported into the STRING database (https://string-db.org/), the species was limited to humans, and a score of >0.9 was set to construct the protein interaction network diagram of the TCM group-GC. The data were then saved as TSV files, and the information of Node1, Node2, and combined score are imported into Cytoscape V3.7.2. Finally, the proximity centrality and intermediary centrality of each node are calculated by using the CytoNCA function package and a reference degree value. Finally, the core gene targets with the highest significance in topology analysis were selected.

2.11 Gene Body Function and KEGG Pathway Enrichment Analysis

To clarify the role of target protein in gene function, gene ontology (GO) and Kyoto Encyclopedia of Genes and Genomes (KEGG) enrichment analysis should be performed for the intersection genes of TCM group-GC using the R language. First, the culsterProfiler package is imported, and the enrichGO function is used to import the human gene database through org.Hs.eg. and db function packages according to the intersection gene ID obtained previously. Under the conditions of "pvalueCutoff=0.05" and "qvalueCutoff=0.05," the ID is converted into gene names and output to BP, CC, and MF groups for the GO enrichment analysis. Finally, the enrichPLOT and GGploT2 function packages are used to draw visual diagrams. Secondly, the KEGG enrichment analysis is carried out using the enrichKEGG function, and then the pathway—gene files and node files obtained by Perl are imported into CytoscapeV3.7.2 to build a KEGG network. Based on the above enrichment analysis results, we can predict the action mechanism of GC treated by various TCM.

3 RESULTS

3.1 Identification and Selection

As shown in **Figure 1**, 976 articles from online databases and other manual sources were initially obtained in the literature search, of which 90 publications were excluded for duplications. Also, after browsing titles and abstracts, 845 irrelevant articles were excluded. We continued to review the remaining 41 potentially eligible articles by full text based on the inclusion and exclusion criteria; 11 RCTs (14–24) met the inclusion criteria and were left for further analysis at last.

3.2 Characteristics of Included Studies and Patients

The main characteristics of the 11 included studies are shown in **Table 1**. All trials were RCTs and conducted in China. The publication years ranged from 2001 to 2020, and there were a total of 863 women enrolled for the analysis, with a total of 465 in the intervention group and 398 in the control group. All the intervention groups used TCM plus chemotherapy, while all the control groups used chemotherapy. Four trials reported tumor

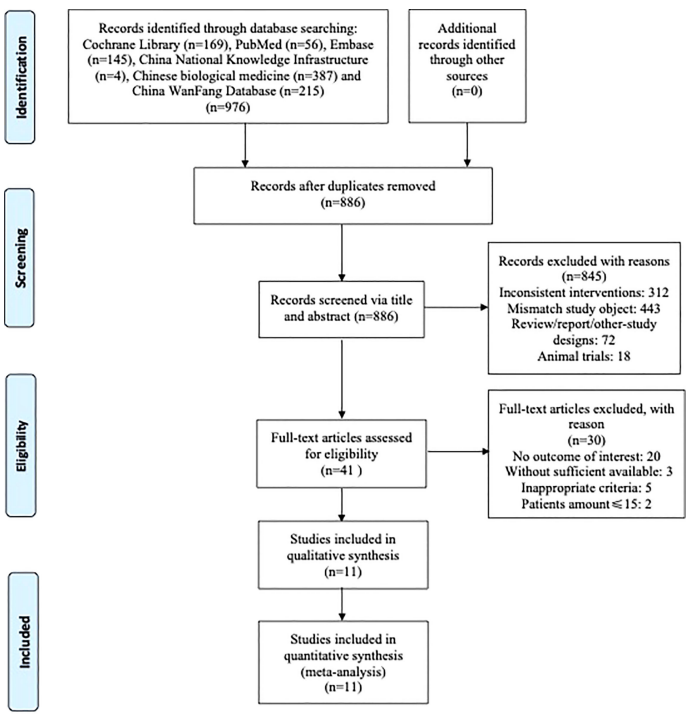


FIGURE 1 | Flow diagram indicating the process of selecting articles for meta-analysis and the steps of network pharmacology analysis.

TABLE 1 | Characteristics of studies included in this meta-analysis.

Author (year)	Research type	Number of cases		Age		Intervention measurement	
		Combination therapy	Chemotherapy	Combination therapy	Chemotherapy	Combination therapy	Chemotherapy
Liu (2001) (19)	OC	90	30	15–77	17–22	Chemotherapy + Yiliu Fang	DDP, 5-FU, CTX, ADM,VP-16, PTX
Gong (2018)(18)	UCC	32	32	47.9 ± 2.4	48.2 ± 2.5	Chemotherapy + Fuzheng drink I	PTX, DDP
Zhang (2019)(23)	OC	45	45	53.5 ± 6.8	52.7 ± 8.2	Chemotherapy + Yiqi anticancer prescription	PTX, DDP
Nan (2015) (20)	UCC	30	30	48.8 ± 6.1	48.7 ± 6.3	Chemotherapy + Bazhen decoction	Irinotecan, DDP
Song (2020)(21)	OC	68	68	66. 79 ± 4. 15	65.46 ± 4.21	Chemotherapy + Fuzheng Jiedu decoction	PTX, DDP
Zhong (2010)(24)	GC	26	22	48.57 ± 6.83		Chemotherapy + Jianpi Bushen decoction	5-FU, PTX, DDP
Gao (2020) (16)	UCC	46	46	42.15 ± 2.91	42.47 ± 2.99	Chemotherapy + Shugan Huayu Jiedu	Docetaxel, oxaliplatin
Yu (2018) (22)	GC	30	30	65.00 ± 10.84	64.03 ± 10.14	Chemotherapy + modified Qi-tonifying and blood-activating prescription	Conventional chemotherapy
Zhang (2006)(14)	GC	25	25	51.24 ± 8.97	50.64 ± 1028	Chemotherapy + TCM	5-FU, PTX, DDP
Huang (2017)(18)	OC	42	42	39.9 ± 16.0	39.7 ± 15.4	Chemotherapy + Guizhi Fuling pill	PTX, CBP
Chan (2011)(15)	OC	31	28	52.9	51.5	Chemotherapy + TCM	Conventional chemotherapy

OC, ovarian cancer; DDP, cisplatin; 5-FU, 5-fluorouracil; CTX, cyclophosphamide; ADM, adriamycin; VP-16, etoposide; PTX, paclitaxel; UCC, uterine cervix cancer, GC, gynecological cancer; TCM, traditional Chinese medicine; CBP, carboplatin.

responses, and four trials reported QOL data. Seven trials reported the peripheral blood lymphocyte levels, and 3 trials mentioned the results of AEs. No trials reported the results of tumor markers, and 2 trials mentioned incomplete KPS results that could not be extracted for meta-analysis.

3.3 Assessment of Methodological Bias

All of the 11 studies referred to randomization. Only 2 trials (15, 21) used a random number table that generated a random sequence, while the other did not mention the method. Only Chan (15) performed the allocation concealment by block randomization, while other studies did not report this method. Also, only one study (15) mentioned double-blinding, while the rest of the studies failed to report the blinding of the investigators, patients, and outcome assessors. Incomplete outcomes existed in Liu (19). In addition, all trials were supposed to have a low risk of other bias and did not have selective reporting. The quality assessment of the included studies is summarized in **Figure 2**.

3.4 Efficacy

3.4.1 Tumor Response

Four trials reported the ORR following WHO or RECIST guidelines. The pooled results show that the ORR of the combination therapy group was significantly higher than that of the chemotherapy-alone group (RR: 1.42; 95% CI: 1.18–1.71; $I^2 = 21.4\%$; $p = 0.000$) (**Figure 3**). Moreover, three trials reported the result of SD and PD. The pooled results show that DCR of combination therapy group was also higher than control group (RR: 1.13; 95% CI: 1.03–1.25; $p = 0.110$; $I^2 = 0.0\%$, $p = 0.492$) (**Figure 4**). While the pooled results show that PD of combination therapy group was significantly lower than that in chemotherapy-alone group (RR: 0.27, 95% CI: 0.11–0.65, $p = 0.003$; $I^2 = 0.0\%$, $p = 0.930$") (**Figure 5**).

3.4.2 Quality of Life

We explored the quality of life of patients who suffered from integrated traditional Chinese medicine plus chemotherapy and chemotherapy alone. The result of the heterogeneity test is: $I^2 = 92.2\%$, $p = 0.000$ (**Figure 6A**). Since the sensitivity analysis showed that Yu's research had a great influence on the results, we eliminated the literature and then summarized the results again. After excluding the study, the heterogeneity had been significantly reduced ($I^2 = 66.9\%$, $p = 0.049$), and a meta-analysis was conducted through a random-effects model. The pooled results show that the quality of life of the combination therapy group is significantly better than that of the chemotherapy alone group (SMD: 0.85, 95% CI: 0.38–1.33, $p = 0.005$) (**Figure 6B**).

3.4.3 Peripheral Blood Lymphocyte Levels

Additionally, we analyzed the levels of $CD3^+$ T, $CD4^+$ T, $CD8^+$ T, and $CD4^+/CD8^+$ T ratio of patients suffering from integrated traditional Chinese medicine plus chemotherapy and chemotherapy alone. The pooled results show that the levels of $CD3^+$ T (WMD: 5.65, 95% CI: 4.23–7.08, $p = 0.000$; $I^2 = 68.3\%$, $p = 0.004$), $CD4^+$ T (WMD: 6.97, 95% CI: 5.35–8.59, $p = 0.000$; $I^2 = 83.4\%$, $p = 0.000$), and $CD4^+/CD8^+$ T ratio (WMD: 0.32, 95% CI: 0.23–0.42, $p = 0.000$; $I^2 = 78.0\%$, $p = 0.000$) of the combination therapy group were significantly higher than

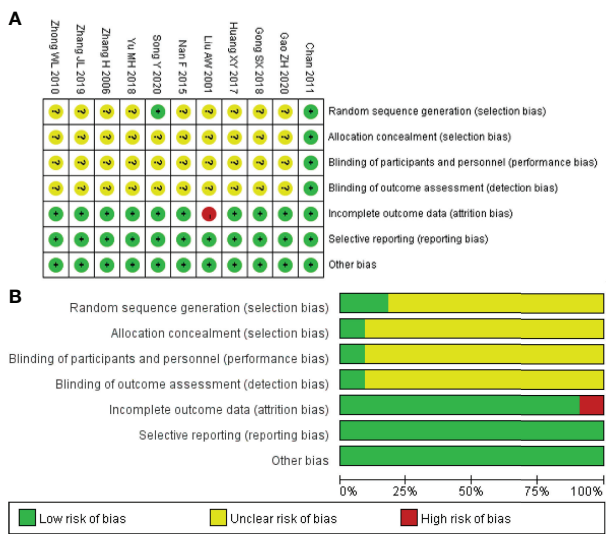


FIGURE 2 | Risk of bias summary **(A)** and diagram **(B)**.

those in the chemotherapy-alone group. While the level of $CD8^+$ T cells of the combination therapy group didn't show an obvious increase (WMD: -3.34, 95% CI: -4.81~ -1.87, p = 0.000; I^2 = 90.0%, p = 0.000) (**Figure 7**).

3.4.4 Safety

Lastly, we pooled the incidence of AEs including gastrointestinal reactions, hepatic and renal dysfunction, fatigue, alopecia, stomatitis, and myelosuppression. However, we could only compare these two treatments by the number of AEs because the data did not provide a classification of them. A meta-analysis was conducted through a fixed-effects model, and the pooled results showed that the incidence of AEs in the combination therapy group was significantly lower than that in the chemotherapy-alone group (RR: 0.47, 95% CI: 0.29–0.75, p = 0.002) (**Figure 8**).

3.4.5 Sensitivity Analysis

Sensitivity analysis eliminates each included study one by one and performs a summary analysis on the remaining studies to assess whether a single included study has an excessive impact on the results of the entire meta-analysis. The result of the sensitivity analysis is shown in **Supplementary Figures S1–S9**. The results showed that almost no studies had an excessive impact on the results of the meta-analysis, indicating that the results of the remaining studies are stable and reliable.

3.4.6 Publication Bias

The funnel plot is shown in **Figure 9**. It can be seen that the funnel plot is not symmetrical, indicating that there may be publication bias in this study.

3.4.7 Effective Herbs Extraction

To discern the commonality of the TCM formulae for combined chemotherapy in the included studies, we analyzed the occurrence frequency and compatibility of the compounds in those Chinese herbal prescriptions.

We analyzed the characteristics of the 10 different TCM prescriptions mentioned in the included trials. Ordered according to their frequency of use, the TCM whose counts were more than three are listed in **Figure 10** and **Table 2**, namely Fuling, Gancao, Baizhu, Danggui, Shengdi, Huangqi, Baishao, Mudanpi, Dangshen, Chuanxiong, Renshen, Shudi, Chenpi, Taoren, Chishao, Banzhilian, Guizhi, Gouqiz, and Shanzhuyu.

In addition, 4 of these studies (40%) used a combination of Dangshen/Renshen, Gancao, Baizhu, and Fuling, which is the most representative prescription for nourishing qi and is known as Sijunzi decoction. Based on these findings, it can be inferred that in the treatment of GC by TCM + chemotherapy, using basic qi tonic TCM to invigorate qi and strengthen the spleen can be an effective method, which was also found in some experiments.

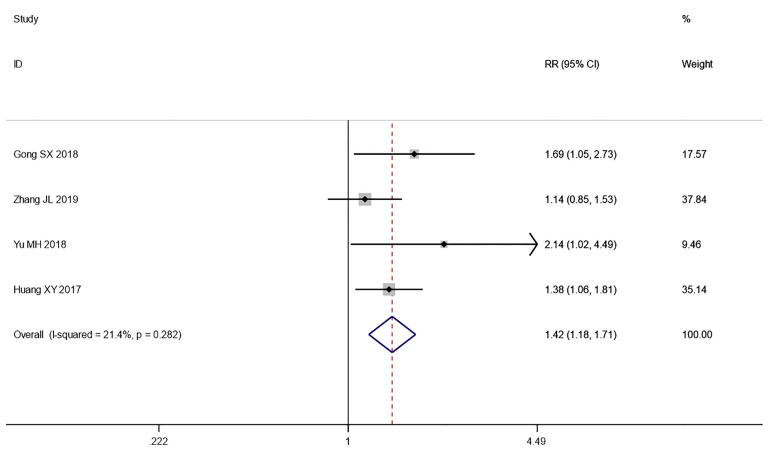


FIGURE 3 | Forest plot of the meta-analysis of the objective response rate (ORR) between the intervention group and the control group.

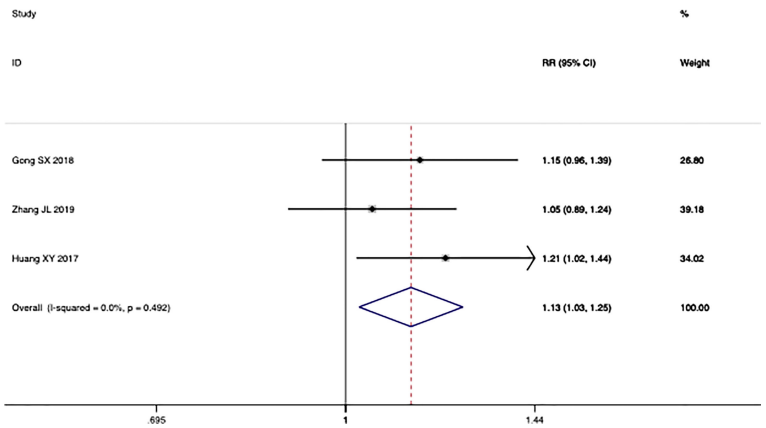


FIGURE 4 | Forest plot of the meta-analysis of the disease control rate (DCR) between the intervention group and the control group.

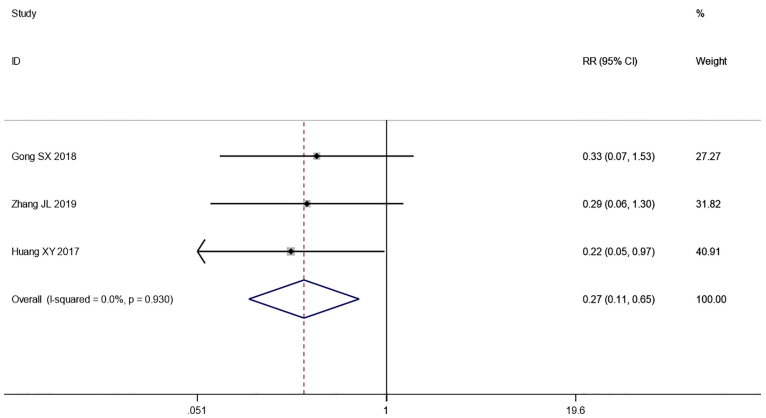


FIGURE 5 | Forest plot of the meta-analysis of progressive disease (PD) between the intervention group and the control group.

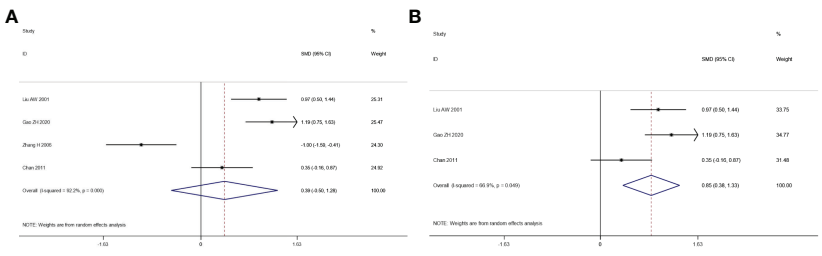


FIGURE 6 | Forest plot of the meta-analysis of quality of life (QOL) before sensitivity analysis **(A)** and after sensitivity analysis **(B)** between the intervention group and the control group.

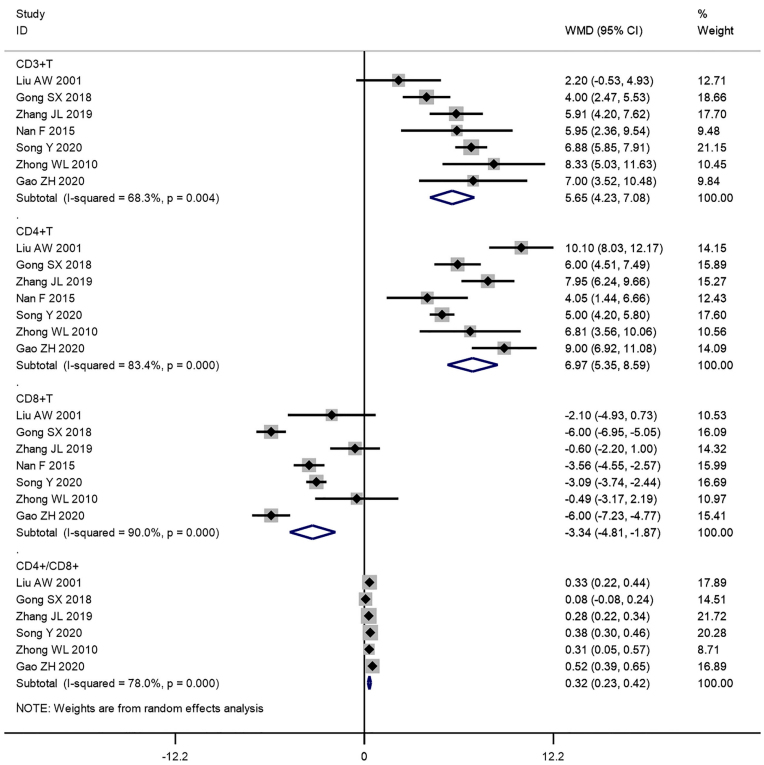


FIGURE 7 | Forest plot of the meta-analysis of immune function indicators including $CD3^+$ T, $CD4^+$ T, $CD8^+$ T, and $CD4^+/CD8^+$ T cells between the intervention group and the control group.

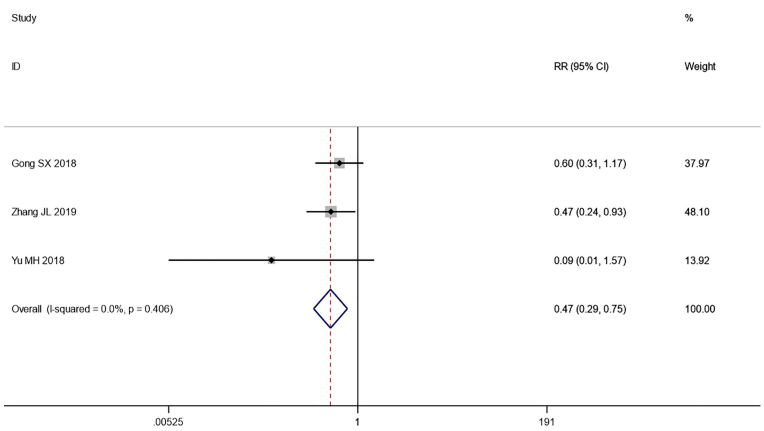


FIGURE 8 | Forest plot of the meta-analysis of AEs between the intervention group and the control group.

A new effective prescription was composed of these 19 herbs for subsequent network pharmacology analysis.

3.4.8 Screening of Effective Components in TCM Group

Through the above meta-analysis, 19 kinds of TCM (Fuling, Gancao, Baizhu, Danggui, Shengdi, Huangqi, Baishao, Mudanpi, Dangshen, Chuanxiong, Renshen, Shudi, Chenpi, Taoren, Chishao, Banzhilian, Guizhi, Gouqiz, Shanzhuyu) have good effects on GC treatment. Due to the large number of Chinese medicines, we took Counts4 as the screening standard, and took the first 9 Chinese medicines as the TCM group.

Using the TCMSP database, the TCM group was entered into the database, and the obtained ingredients were screened according to

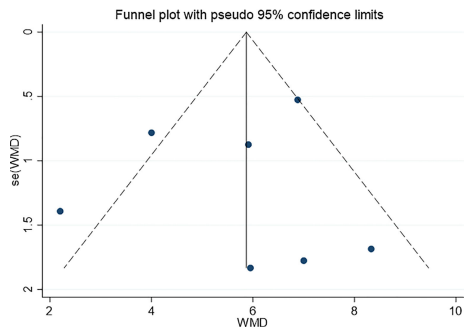


FIGURE 9 | Funnel plot for evaluating the publication bias of this meta-analysis.

oral bioavailability (OB) of ≥30% and drug like (DL) of ≥0.18. Through searching the TCMSP database, there is no effective ingredient in Shengdi that meets ADME standards. Therefore, the remaining 8 TCM in the TCM group are used to screen the effective ingredients. Finally, there were 6 active components in Fuling, 88 active components in Gancao, 4 active components in Baizhu, 2 active components in Danggui, 16 active components in Huangqi, 8 active components in Baishao, 3 active components in Mudanpi, and 12 active components in Dangshen. After weight removal, there were 120 active components in the TCM group.

3.4.9 Screening of Highly Correlated Targets for GC Disease

The GEO database difference analysis was performed on the whole gene matrix of VN, EC, and OC obtained in **Section 2.7**. The genes with a high correlation with GC in |log FC|>1 adj.*p*-val<0.05 were screened by the method in **Section 2.7**. **A** total of 626 high correlation targets in VN, 3,884 high correlation targets in EC, and 5,665 high correlation targets in OC were obtained. As there were few highly correlated targets in VN, we expanded the screening conditions and screened |log FC|>0.5 *p*-val<0.05 as a highly correlated gene of VN. A total of 2,144 highly correlated targets in VN were obtained. After deleting the overlapping targets in the three groups of data, 8,949 high correlation targets of GC disease were obtained.

3.4.10 Construction of a Regulatory Network for the TCM Group

In total, 120 active components were retrieved from the TCMSP database, and 225 directly corresponding targets were obtained after weight removal. A total of 8,949 highly correlated targets of GC disease were retrieved from the GEO and GeneCards databases, including 139 drug-disease common targets. After standardizing the gene, the full name of the gene is transformed into the gene symbol. Finally, Cytospace3.7.2 software was used to construct the regulation network of the TCM group (**Figure 11**).

3.4.11 Construction and Analysis of PPI Network of GC Disease Target in TCM Group

The intersection genes obtained in **Section 3.4.10** were imported into the STRING database, and the species was defined as human. A score of >0.9 was set to hide the disconnected nodes, and the interaction network between the TCM group and GC disease target proteins was constructed, which is illustrated in **Figure 12**.

Topology analysis of the protein–protein interaction (PPI) network was then required. The data in **Figure 13** were saved as a

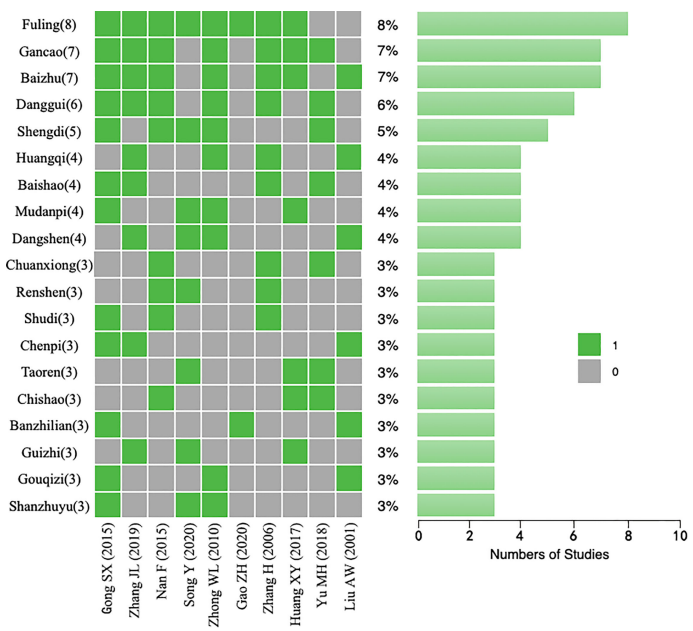


FIGURE 10 | Traditional Chinese medicine (TCM) herbs that appeared in each study.

TABLE 2 | The high-frequency Chinese herbs in each study.

Chinese name	Pharmaceutical name	Counts	Frequency 1 (counts/total herb counts)	Frequency 2 (counts/study numbers)
Fuling	Poria cocos	8	7.27%	80.00%
Gancao	Liquorice	7	6.36%	70.00%
Baizhu	Macrocephala	7	6.36%	70.00%
Danggui	Angelica sinensis	6	5.45%	60.00%
Shengdi	Radix Rehmannia	5	4.55%	50.00%
Huangqi	Astragalus	4	3.64%	40.00%
Baishao	Radix paeoniae alba	4	3.64%	40.00%
Mudanpi	Cortex moutan	4	3.64%	40.00%
Dangshen	Codonopsis pilosula	4	3.64%	40.00%
Chuanxiong	Ligusticum chuanxiong	3	2.73%	30.00%
Renshen	Ginseng	3	2.73%	30.00%
Shudi	Radix rehmannia praeparata	3	2.73%	30.00%
Chenpi	Pericappium citrus reticulata	3	2.73%	30.00%
Taoren	Semen persicae	3	2.73%	30.00%
Chishao	Radix paeoniae rubra	3	2.73%	30.00%
Banzhilian	Scutellaria barbata	3	2.73%	30.00%
Guizhi	Ranmulus cinnamomi	3	2.73%	30.00%
Gouqizi	Fructus lycii	3	2.73%	30.00%
Shanzhuyu	Cornus officinalis	3	2.73%	30.00%

TSV file, and the information for Node1, Node2, and the combined score in the file was imported into the Cytoscape V3.7.2 software. Finally, BisoGenet and CytoNCA in Cytoscape software were used. Referring to the degree value, the "betweenness centrality (BC)" and "closeness centrality" of all nodes were calculated. The top genes of DC and BC were sequentially screened, and the protein interaction core of the TCM group was finally determined (**Figure 13**). The topology parameter analysis is shown in **Table 3**.

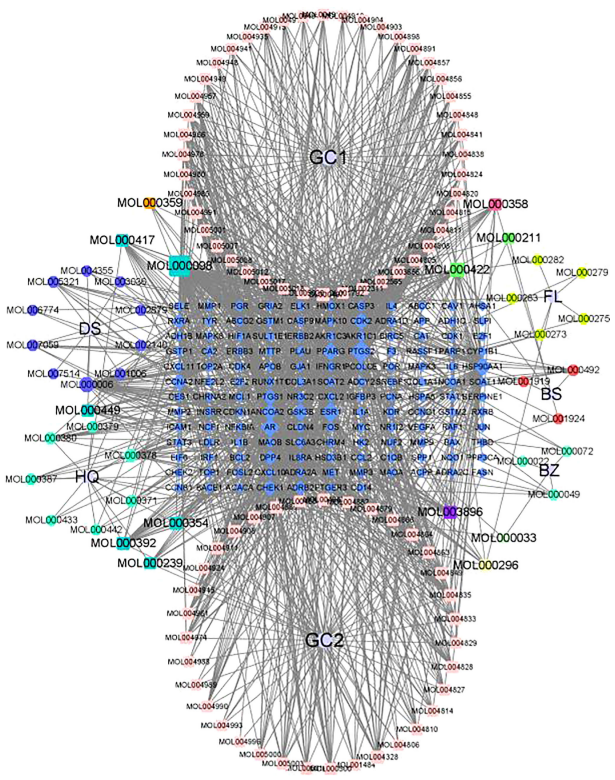


FIGURE 11 | TCM group regulatory network.

According to the results of topological parameter analysis, genes NPM1 and HSPA8 were the most critical genes in GC. Through the PPI core network, HSP90AA1, HSPA5, CDK2, and ESR1 were found to be the core genes directly associated with the effective components of the TCM group, among which HSP90AA1 ranked the highest.

3.4.12 Functional Enrichment Analysis of Gene Body (GO)

An enrichment analysis was carried out for 139 intersection genes of the screened TCM group and GC disease targets, and the analysis results of biological process (BP), cell composition (CC), and molecular function (MF) involved in this core target could be obtained in **Supplementary Figures S10–S12**.

From the analysis of **Supplementary Figure S10**, the core target of metal ions in BP responses to the significance of the highest, followed by oxidation reaction, cell response to chemical stress, steroids, drug reactions, radiation reactions. Besides, the reaction of lipopolysaccharide and active oxygen reaction control have positive influence on nutrient levels and oxidative stress reaction. In terms of CC, the above core targets were most significant in membrane raft, plasma membrane microregion, and membrane region, followed by transcriptional regulatory complex, endoplasmic management cavity, RNA polymerase II transcriptional regulatory complex, organelle outer membrane, and other parts. In terms of MF, DNA-binding transcription factor binding was the most significant, followed by RNA polymerase II-specific DNA-binding transcription factor binding, amide binding, polypeptide binding, and cytokine receptor binding. Therefore, the TCM group may focus on the above biological functions to participate in the treatment of GC diseases.

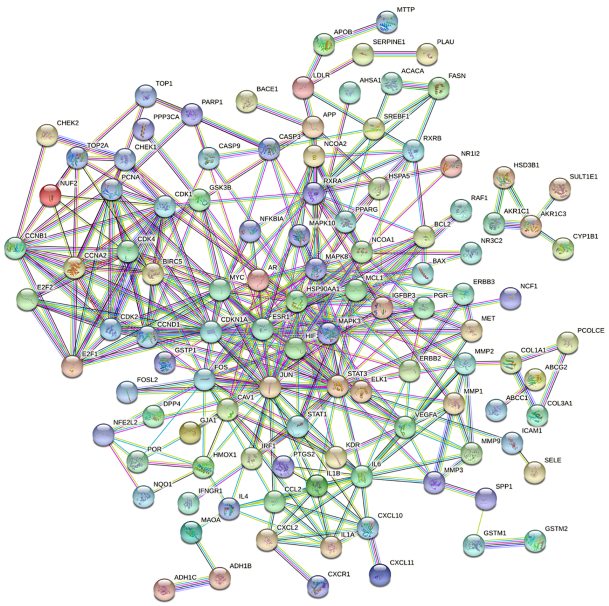


FIGURE 12 | Protein interaction network.

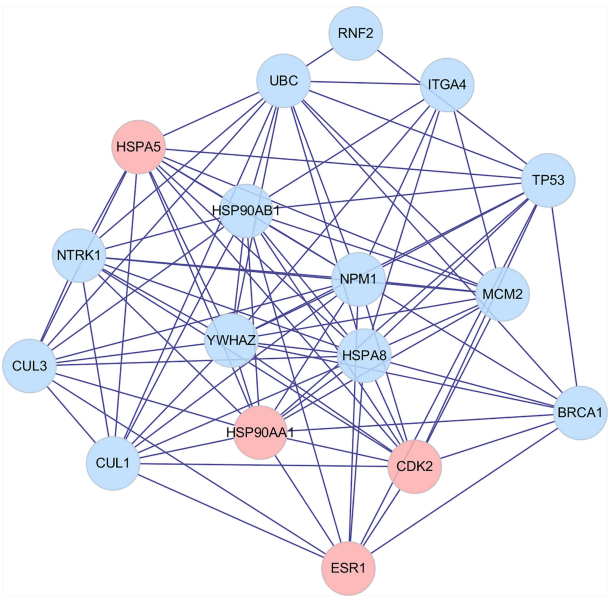


FIGURE 13 | PPI core network.

3.4.13 Enrichment Analysis of KEGG Pathway

Whether the Chinese traditional medicine group—the intersection of GC disease gene KEGG enrichment analysis, gets the core targets in lipid and atherosclerosis, Kaposi's sarcoma-associated herpesvirus infections, hepatitis B, diabetes complications of AGE-RAGE signaling pathways, fluid shear stress and atherosclerosis, and the human cytomegalovirus pathway is salient. It indicates that the components in the TCM group may achieve the purpose of curing diseases by acting on the above signal pathways (**Figure 14**).

Accordingly, the KEGG network is constructed, with the outer circle as the related pathway and the inner circle as the core gene, whose graph size is proportional to the number of associated pathways (**Figure 15**).

4 DISCUSSION

Based on previous studies, it was demonstrated that TCM plays an important role in the treatment of GC, so we conducted a systematic review and meta-analysis integrated with network pharmacology analysis to compare the efficacy of TCM plus chemotherapy with chemotherapy alone, and to identify the potential pharmacological mechanisms and targets of TCM.

As far as our knowledge is concerned, this is the first article that integrated meta-analysis and network pharmacology to evaluate the efficacy and potential pharmacological mechanisms of TCM in patients with GC. Previously, Ge et al. (10) provided a comprehensive meta-analysis for people with OC, but they only investigated the efficacy of TCM concerning survival, QOL, and immune function without assessing its safety. Coincidentally, network pharmacology conducted by Sun et al. (25) also paid attention to the potential targets of TCM for OC patients. However, in our study, which included 11 RCTs consisting of 863 GC patients, it was shown that TCM plus chemotherapy can provide more durable disease control and improve GC patients' QOL without substantially increasing AEs compared with chemotherapy alone, and the major ingredients and major targets involved in the effective treatments were also illustrated.

Based on the guidelines standardized by NCCN, ESMO, and ASCO, the treatment options for patients encompass surgery, chemotherapy, radiotherapy, biological therapy, targeted therapy, immunotherapy, or an integration of these options. Among them, chemotherapy has been successfully and commonly utilized in the treatment of GC. Platinum derivatives, paclitaxel, and antimetabolites, all alkylating drugs, are the most commonly used antitumor agents, whose mechanisms are based on the damage of genomic synthesis and repair mechanisms in cancer cells (26). It will cause extensive DNA damage that exceeds the cellular DNA repair capacity and ultimately leads to apoptotic cancer cell death. These drugs are usually nonselective to cancer cells, and consequently, they induce concurrent damage to healthy tissues and organs. Following chemotherapy, women will be at an increased risk of experiencing AEs, and the next course of treatment is likely to be delayed or terminated due to a high degree of drug toxicity and poor results from the evaluation of its efficacy. Recent studies have also found it is difficult to improve its therapeutic effects, and the response of patients is being reduced in the wake of each subsequent line of therapy (27, 28).

TCM occupies a very important position in the treatment of cancers in China. It has been reported to enhance cytotoxic effects and reduce side effects of chemotherapeutic agents. A bulk

TABLE 3 | Analysis of topology parameters.

Number	Gene	Degree	BC	CC
1	NPM1	14	9.15	0.89
2	HSPA8	14	9.15	0.89
3	YWHAZ	14	7.18	0.89
4	HSP90AB1	14	6.97	0.89
5	UBC	13	21.78	0.84
6	HSP90AA1	13	4.79	0.84
7	CDK2	12	3.73	0.80
8	HSPA5	12	2.19	0.80
9	TP53	11	13.81	0.76
10	NTRK1	11	1.22	0.76

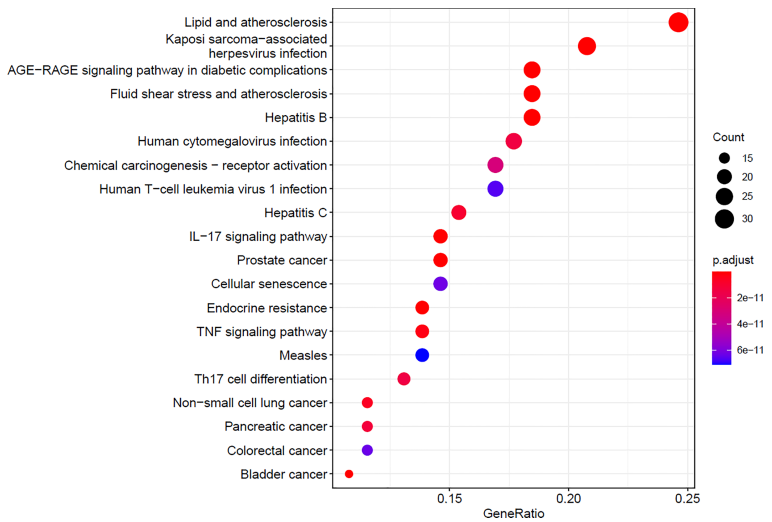


FIGURE 14 | KEGG enrichment analysis.

of studies have proved that TCM has a unique advantage in the treatment of GC. Research by Supoken et al. has shown that TCM can enhance the ability of the body's immunity and resistance to tumors and can relieve chemotherapy-induced immunosuppression. Wu et al. (7) found that TCM could prolong the chemotherapy interval and decrease the incidence of AEs. It was also reported that TCM could effectively alleviate the AEs of chemotherapy and improve QOL (29). The results of our study were also consistent with them, but a few aspects still need to be considered when interpreting our findings.

Firstly, moderate to high heterogeneity was observed across all included trials, which may result from the types of TCM, tumor type, pathogenic type, cancer histotype, and line of treatment. We used sensitivity analysis to detect the article that affected the result and obtained a meaningful result by removing it. As for the newly achieved drug composition from those 11 RCTs, whether it could achieve certain therapeutics in the clinic still needs to be investigated. In our study, none of the included trials completely reported the overall survival (OS) or progression-free survival (PFS); they only illustrated the curative effects of factors including tumor responses, QOL, peripheral blood lymphocyte levels, and AEs in treating GC. Thus, more newly offered evidence needs to be stated to confirm whether TCM plus chemotherapy could prolong the long-term survival rates of GC patients. Among those trials, lacking the data on the applications of injection-based, pill, and external administration of TCM, the included formulas were all oral administration. Also, almost all TCM were used after the chemotherapy cycle ended. The utilization of TCM before or during the chemotherapy cycle still needs more data to support. More studies to determine the best dosage form and use time of TCM are needed in the future.

Myelosuppression, hepatic and renal dysfunction, and gastrointestinal reactions were common chemotherapy-related side effects (30, 31), which could reflect patients' tolerance to chemotherapy. Dose modification and symptomatic treatment are usually involved to relieve this symptom, and in our study, it was found that patients who had taken TCM had a lower incidence of AEs. However, as for the serious AEs of high grades, we were not able to analyze them because of the lack of data on different degrees and types of side effects, for which we only analyzed the difference in the number of AEs.

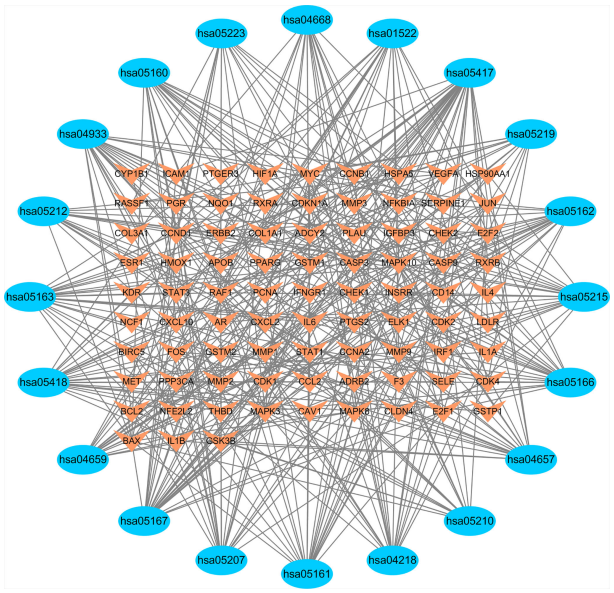


FIGURE 15 | KEGG regulatory network.

We also perform network pharmacology to explore the specific effect of the TCM group on the GC treatment process. According to the results of the PPI and KEGG parts, the TCM group plus three core genes mentioned above and the relevant signaling pathway obtained by GO and KEGG enrichment analysis have more to do with the occurrence and development of malignant tumors. Current studies demonstrate that the level of NPM1 is associated with the promotion of endometrial cancer by circWHSC1 (32). In addition to being involved in inhibiting OC proliferation and apoptosis (33), HSP90AA1 has been shown to inhibit UCC cell invasion and the EMT phenotype (34). Furthermore, HSPA8 is considered to be another candidate biomarker for early diagnosis and treatment of EC in stage I (35), while the levels of plasma intima-media thickness plus serum high-density lipoprotein levels are considered to be a new marker of uterine fibroids (36). Frontier studies have been discussing the relationship between cardiovascular disease and cancer, and the results of our study could also provide new ideas for the development of this field.

NPM1 is a protein widely expressed in the nucleoli, which can travel between the nucleus and cytoplasm, participate in the assembly and transportation of ribosomal proteins, regulate centrosome replication, and regulate the expression of tumor suppressor ARF. Mutations in NPM1 push the protein to transfer from the nucleus to the cytoplasm, causing acute myeloid leukemia. However, Fan et al. (37) showed that in normal fallopian tubes, NPM1 protein was mainly distributed in the nucleus. The expression of NPM1 protein in HGSC was abnormal in the cytoplasm and significantly higher than that in normal oviduct tissue. Furthermore, APE1/Ref-1 interacts with NPM1 to control the DNA damage repair system (38). NPM1 also promotes UCC lymph node metastasis by participating in reprogramming fatty acid metabolism (39). Another study (40) demonstrated that inhibition of nuclear phosphine (NPM1/B23) restores the expression of estrogen receptor (ESR1/ERa) in endometrial cancer cells. This fully demonstrates the importance of this gene to GC.

Moreover, HSPA8 is a component of the HSP70 family expressing homologous proteins and is crucial to many cellular processes. In particular, its regulatory role in autophagy is decisive (41). Functionally, it binds to nascent peptides to promote correct folding. It also acts as an ATPase to break down cypermethrin-coated vesicles during the transport of membrane components through cells. According to a relevant study (42), HSPA8 can be used as a special diagnostic protein marker model for UCC. It was found that Hsp70 and Hsc70 are expressed in a unique and predominantly overlapping pattern in the cervix and endometrium as well (43). In both tissues, the highest levels of these two proteins were found in differentiated, nonproliferating epithelial cells. This means that the HSPA8 gene may also have a common expression in GC, but there is still a lack of relevant studies in this respect.

Furthermore, the HSP90AA1 gene is a core gene directly associated with GC. Functioning as a homologous dimer, the protein it encodes is an inducible molecular chaperone. The encoded proteins contribute to the correct folding of specific target proteins through the cochaperone-regulated ATPase activity. There is evidence (44) that HSP90A plays a key role in the crossroads between the Nanog-TCL1A axis and the multiple attack properties of immunoediting tumor cells. It stabilizes and enhances AKT activation through TCL1A, thereby contributing to the multi-invasive properties of NANOGhigh tumor cells. Importantly, HSP90 inhibition sensitized immune-refractory tumors to adoptive T-cell metastasis and PD-1 blockade and reactivated the immune cycle of tumor-responsive T cells. These results indicate that the HSP9OA-TCL1A-Akt pathway ignited by NANOG is a central molecular axis and potential target of immune-refractory tumors and has a high reference value for GC treatment.

The strengths of our study include our wide-ranging online searches of literature in both English and Chinese databases. We applied broad criteria for pooling studies. We conducted a meta-regression analysis to determine if specific preparation yielded differing effects over the broad group, and in several cases they did.

Some limitations may affect the drawn conclusion. First, there was a lack of large, multicenter, standardized RCTs, and the sample sizes of our included studies were mostly small or of moderate size. More RCTs with larger sample sizes are required to confirm these outcomes. Second, TCM's individualized treatment and self-formulated prescription for inconsistent treatment with Chinese medicine may have led to heterogeneity in the meta-analysis, and none of them were able to provide definitive options for clinical treatment. Moreover, randomization methods, allocation concealment, and blinding are not clearly described in those included trials, which may result in inherent bias and exaggeration of the efficacy of the treatment group. In addition,

our study induced a certain degree of heterogeneity due to the different classifications of tumors, pathologic stage of the tumor, the application of adjuvant therapy, and duration of treatment among included trials. Furthermore, almost all studies were conducted in China, which may lead to unavoidable regional bias. All these limitations may have resulted in insufficient evaluations of the outcome indicators. There are also some shortcomings in network pharmacology analysis. Due to the incomplete research on drug components and targets, the relevant data in the disease database are incomplete, leading to certain limitations and defects in the statistical results of network pharmacology in this paper. Also, the method of screening components of TCM by DL and OB values did not take the active ingredients into full consideration, which may affect the results. Furthermore, network pharmacology studies ignored the influence of component content of TCM on experimental results, and subsequent studies should focus on the relationship between content and curative effect. Moreover, network pharmacology is based on computer simulation analysis and molecular network data, whose statistical and predictive results need to be confirmed by specific experiments *in vivo* and *in vitro*. So we still need to take these compelling results with caution and this study should be carefully disseminated for clinical application. Our findings need to be further confirmed *via* more RCTs conducted in a rigorous manner.

All in all, we hope the findings of this analysis will provide a shred of helpful evidence for clinicians to formulate the best treatment strategy for patients with GC and also provide scientific clues for researchers in this field. Moreover, the methodological ideas of this paper are shown in **Supplementary Figure S13**.

5 CONCLUSION

In summary, our study indicates that TCM plus chemotherapy is highly effective and safe in the treatment of people with GC. TCM plus chemotherapy has the characteristics of multiple pathways, multiple components, and multiple targets in the treatment of GC and diseases. Our study will provide valuable evidence for further evaluation of TCM. Moreover, some limitations increased the risk of bias, which, to some extent, affects the credibility of the satisfactory result. Thus, to confirm these finding, more rigorous randomized controlled trials are needed.

DATA AVAILABILITY STATEMENT

The original contributions presented in the study are included in the article/**Supplementary Material**. Further inquiries can be directed to the corresponding author.

AUTHOR CONTRIBUTIONS

LZ, LS and JY contributed to the design and conception of the study. JY and NR carried out the collection and processing of data. LQ and GY finished the figure diagramming. ZZ and LY performed the data analysis and interpretation. NR and LY wrote the manuscript. LZ, LS and JY revised the manuscript, then LZ gave the final approval of manuscript.

FUNDING

This study was financially subsidized by the Project funded by Plan Project of Zhejiang Province Medical and Health Science and Technology (LS, No. 2022RC215); China Postdoctoral Science Foundation (LS, No. 2021M702928); Young Elite Scientists Sponsorship Program by CAST (LS, No. 2021-QNRC2-B13); Research Project of Zhejiang Chinese Medical University (JY, No. 2021RCZXZK10); The Construction Fund of Medical Key Disciplines of Hangzhou (OO20200385); Research Project of Zhejiang Chinese Medical University (LZ, No.2022JKJNTZ40).

SUPPLEMENTARY MATERIAL

The Supplementary Material for this article can be found online at: https://www.frontiersin.org/articles/10.3389/fonc.2022.817772/full#supplementary-material

REFERENCES

1. Bray F, Ferlay J, Soerjomataram I, Siegel RL, Torre LA, Jemal A. Global Cancer Statistics 2018: GLOBOCAN Estimates of Incidence and Mortality Worldwide for 36 Cancers in 185 Countries. *CA Cancer J Clin* (2018) 68:394–424. doi: 10.3322/caac.21492
2. Ferlay J, Colombet M, Soerjomataram I, Mathers C, Parkin DM, Piñeros M, et al. Estimating the Global Cancer Incidence and Mortality in 2018: GLOBOCAN Sources and Methods. *Int J Cancer* (2019) 144:1941–53. doi: 10.1002/ijc.31937
3. Orr B, Edwards RP. Diagnosis and Treatment of Ovarian Cancer. *Hematol Oncol Clin North Am* (2018) 32:943–64. doi: 10.1016/j.hoc.2018.07.010
4. Cohen PA, Jhingran A, Oaknin A, Denny L. Cervical Cancer. *Lancet* (2019) 393:169–82. doi: 10.1016/s0140-6736(18)32470-x
5. Della Corte L, Foreste V, Di Filippo C, Giampaolino P, Bifulco G. Poly (ADP-Ribose) Polymerase (PARP) as Target for the Treatment of Epithelial Ovarian Cancer: What to Know. *Expert Opin Investig Drugs* (2021) 30:543–54. doi: 10.1080/13543784.2021.1901882
6. Lheureux S, Braunstein M, Oza AM. Epithelial Ovarian Cancer: Evolution of Management in the Era of Precision Medicine. *CA Cancer J Clin* (2019) 69:280–304. doi: 10.3322/caac.21559
7. Wu YH, Chen HY, Lai CH, Yeh CS, Pang JS, Qiu JT, et al. Use of Chinese Herbal Medicine Improves Chemotherapy-Induced Thrombocytopenia Among Gynecological Cancer Patients: An Observational Study. *Evid Based Complement Alternat Med* (2018) 2018:4201325. doi: 10.1155/2018/4201325
8. Wang Y, Zhang Q, Chen Y, Liang CL, Liu H, Qiu F, et al. Antitumor Effects of Immunity-Enhancing Traditional Chinese Medicine. *BioMed Pharmacother* (2020) 121:109570. doi: 10.1016/j.biopha.2019.109570

9. Zhu K, Fukasawa I, Furuno M, Inaba F, Yamazaki T, Kamemori T, et al. Inhibitory Effects of Herbal Drugs on the Growth of Human Ovarian Cancer Cell Lines Through the Induction of Apoptosis. *Gynecol Oncol* (2005) 97:405–9. doi: 10.1016/j.ygyno.2004.12.063
10. Ge S, Xing Q, Zhang A, Wang Y. Effect of Traditional Chinese Medicine (TCM) on Survival, Quality of Life, and Immune Function in Patients With Ovarian Carcinoma: A Protocol for Systematic Review and Meta Analysis. *Med (Baltimore)* (2021) 100:e23904. doi: 10.1097/md.0000000000023904
11. Yoshihara K, Tajima A, Komata D, Yamamoto T, Kodama S, Fujiwara H, et al. Gene Expression Profiling of Advanced-Stage Serous Ovarian Cancers Distinguishes Novel Subclasses and Implicates ZEB2 in Tumor Progression and Prognosis. *Cancer Sci* (2009) 100:1421–8. doi: 10.1111/j.1349-7006.2009.01204.x
12. Roychowdhury A, Samadder S, Das P, Mazumder DI, Chatterjee A, Addya S, et al. Deregulation of H19 is Associated With Cervical Carcinoma. *Genomics* (2020) 112:961–70. doi: 10.1016/j.ygeno.2019.06.012
13. Pappa KI, Polyzos A, Jacob-Hirsch J, Amariglio N, Vlachos GD, Loutradis D, et al. Profiling of Discrete Gynecological Cancers Reveals Novel Transcriptional Modules and Common Features Shared by Other Cancer Types and Embryonic Stem Cells. *PloS One* (2015) 10:e0142229. doi: 10.1371/journal.pone.0142229
14. Zhang H, Han K, Tan Y. Clinical Study on the Effects of TCM Intervention on TCM Symptoms and Quality of Life in Patients With Gynecological Malignant Tumor During Chemotherapy and Rehabilitation. *J New Chin Med* (2006) 38:40–1. doi: 10.13457/j.cnki.jncm.2006.12.021
15. Chan KK, Yao TJ, Jones B, Zhao JF, Ma FK, Leung CY, et al. The Use of Chinese Herbal Medicine to Improve Quality of Life in Women Undergoing Chemotherapy for Ovarian Cancer: A Double-Blind Placebo-Controlled Randomized Trial With Immunological Monitoring. *Ann Oncol* (2011) 22:2241–9. doi: 10.1093/annonc/mdq749
16. Gao ZH, Wang QQ. Therapeutic Effect of Shugan Huayu Jiedu Decoction on Postoperative Chemotherapy of Cervical Cancer and Its Effect on Th1 /Th2 in Serum. *Chin Arch Tradi Chin Med* (2020) 38:240–3. doi: 10.13193/j.issn.1673-7717.2020.06.058
17. Gong SX, You JL, Ren CX. Clinical Effect of Fuzheng Yin I Combined With TP Chemotherapy in the Treatment of Cervical Cancer. *Acta Chin Med Pharm* (2018) 46:98–100. doi: 10. 19664/j. cnki. 1002 - 2392.180024
18. Huang XY. Guizhi Fuling Pill Combined With Western Medicine on Advanced Ovarian Cancer. *Shaanxi J Tradit Chin Med* (2017) 38:643–5. doi: 10.3969/j.issn.1000-7369.2017.05.045
19. Liu AW, Qi C, Hu ZY. Estimation on the Treatment Effect of 90 Patients With Ovarian Cancer by Traditional Chinese Medicine and Chemotherapy. *Liaoning J Tradit Chin Med* (2001) 28:618–20. doi: 10.13192/j.ljtcm.2001.10.43.liuaw.030
20. Nan F, Chen CH. Study on the Clinical Efficacy on 30 Cases of Cervical Cancer Treated With Integrated Chinese and Western Medicine. *World J Integr Tradit West Med* (2015) 10:1586–8. doi: 10.13935/j.cnki.sjzx.151132
21. Song XJ. Effects of Fuzheng Gushen Decoction on Peripheral Blood T Lymphocyte Subsets and Tumor Markers in Elderly Patients With Ovarian Cancer After Operation. *Chin J Gerontol* (2020) 40:2078–81.10. 3969 / j. issn. 1005-9202. 2020. 10. 020
22. Yu MH, Yao YX, Zhang T. Clinical Effect of Modified Qi-Tonifying and Blood-Activating Prescription in Improving Hypercoagulability in Patients With Gynecological Malignancies. *J Anhui Univ Chin Med* (2018) 37:164–5. doi: 10.3969/j. issn. 2095-7246. 2018. 04.005
23. Zhang JL, Cui W. Efficacy of Yiqi Anticancer Prescription Combined With TP Regimen in Treatment of Epithelial Ovarian Cancer and its Influence on the Levels of Immune Checkpoints. *ChinJ Cancer Prev Treat* (2019) 26:876–80. doi: 10.16073/j.cnki.cjcpt.2019.12.011
24. Zhong WL, Yang LH. Clinical Observation on 26 Cases of Gynecological Malignant Tumor With Kidney-Yang Deficiency Treated by Invigorating Spleen and Tonifying Kidney. *J New Chin Med* (2010) 42:38–9. doi: 10.13457/j.cnki.jncm.2010.05.026
25. Sun J, Liu J, Liu D, Wu X. Network Pharmacology-Based and Clinically Relevant Prediction of the Potential Targets of Chinese Herbs in Ovarian Cancer Patients. *BioMed Res Int* (2020) 2020:8965459. doi: 10.1155/2020/8965459
26. Bedoschi G, Navarro PA, Oktay K. Chemotherapy-Induced Damage to Ovary: Mechanisms and Clinical Impact. *Future Oncol* (2016) 12:2333–44. doi: 10.2217/fon-2016-0176
27. Weingart SN, Zhang L, Sweeney M, Hassett M. Chemotherapy Medication Errors. *Lancet Oncol* (2018) 19:e191–9. doi: 10.1016/s1470-2045(18)30094-9
28. Carvalho HA, Villar RC. Radiotherapy and Immune Response: The Systemic Effects of a Local Treatment. *Clinics (Sao Paulo)* (2018) 73:e557s. doi: 10.6061/clinics/2018/e557s
29. You X, Xu Y, Huang J, Zhi Y, Wu F, Ding F, et al. A Data Mining-Based Analysis of Medication Rules in Treating Bone Marrow Suppression by Kidney-Tonifying Method. *Evid Based Complement Alternat Med* (2019) 2019:1907848. doi: 10.1155/2019/1907848
30. Deshpande R, Raina P, Shinde K, Mansara P, Karandikar M, Kaul-Ghanekar R. Flax Seed Oil Reduced Tumor Growth, Modulated Immune Responses and Decreased HPV E6 and E7 Oncoprotein Expression in a Murine Model of Ectopic Cervical Cancer. *Prostaglandins Other Lipid Mediat* (2019) 143:106332. doi: 10.1016/j.prostaglandins.2019.04.002
31. De Nola R, Menga A, Castegna A, Loizzi V, Ranieri G, Cicinelli E, et al. The Crowded Crosstalk Between Cancer Cells and Stromal Microenvironment in Gynecological Malignancies: Biological Pathways and Therapeutic Implication. *Int J Mol Sci* (2019) 20:2401–30. doi: 10.3390/ijms20102401
32. Liu Y, Chen S, Zong ZH, Guan X, Zhao Y. CircRNA WHSC1 Targets the miR-646/NPM1 Pathway to Promote the Development of Endometrial Cancer. *J Cell Mol Med* (2020) 24:6898–907. doi: 10.1111/jcmm.15346
33. Chu SH, Liu YW, Zhang L, Liu B, Li L, Shi JZ, et al. Regulation of Survival and Chemoresistance by HSP90AA1 in Ovarian Cancer SKOV3 Cells. *Mol Biol Rep* (2013) 40:1–6. doi: 10.1007/s11033-012-1930-3
34. Xu D, Dong P, Xiong Y, Yue J, Konno Y, Ihira K, et al. MicroRNA-361-Mediated Inhibition of HSP90 Expression and EMT in Cervical Cancer Is Counteracted by Oncogenic lncRNA Neat1. *Cells* (2020) 9:632–52. doi: 10.3390/cells9030632
35. Shan N, Zhou W, Zhang S, Zhang Y. Identification of HSPA8 as a Candidate Biomarker for Endometrial Carcinoma by Using iTRAQ-Based Proteomic Analysis. *Onco Targets Ther* (2016) 9:2169–79. doi: 10.2147/ott.S97983
36. Aksoy Y, Sivri N, Karaoz B, Sayin C, Yetkin E. Carotid Intima-Media Thickness: A New Marker of Patients With Uterine Leiomyoma. *Eur J Obstet Gynecol Reprod Biol* (2014) 175:54–7. doi: 10.1016/j.ejogrb.2014.01.005
37. Fan X, Wen L, Li Y, Lou L, Liu W, Zhang J. The Expression Profile and Prognostic Value of APE/Ref-1 and NPM1 in High-Grade Serous Ovarian Adenocarcinoma. *Apmis* (2017) 125:857–62. doi: 10.1111/apm.12733
38. Londero AP, Orsaria M, Tell G, Marzinotto S, Capodicasa V, Poletto M, et al. Expression and Prognostic Significance of APE1/Ref-1 and NPM1 Proteins in High-Grade Ovarian Serous Cancer. *Am J Clin Pathol* (2014) 141:404–14. doi: 10.1309/ajcpidkdlsge26cx
39. Shang C, Wang W, Liao Y, Chen Y, Liu T, Du Q, et al. LNMICC Promotes Nodal Metastasis of Cervical Cancer by Reprogramming Fatty Acid Metabolism. *Cancer Res* (2018) 78:877–90. doi: 10.1158/0008-5472.Can-17-2356
40. Lin CY, Chao A, Wang TH, Lee LY, Yang LY, Tsai CL, et al. Nucleophosmin/B23 is a Negative Regulator of Estrogen Receptor α Expression *via* AP2γ in Endometrial Cancer Cells. *Oncotarget* (2016) 7:60038–52. doi: 10.18632/oncotarget.11048
41. Stricher F, Macri C, Ruff M, Muller S. HSPA8/HSC70 Chaperone Protein: Structure, Function, and Chemical Targeting. *Autophagy* (2013) 9:1937–54. doi: 10.4161/auto.26448
42. Lomnytska MI, Becker S, Hellman K, Hellström AC, Souchelnytskyi S, Mints M, et al. Diagnostic Protein Marker Patterns in Squamous Cervical Cancer. *Proteomics Clin Appl* (2010) 4:17–31. doi: 10.1002/prca.200900086
43. Mangurten AB, Brader KR, Loos BM, Lee E, Quiroga AI, Bathori J, et al. Hsp70 and Hsc70 are Preferentially Expressed in Differentiated Epithelial Cells in Normal Human Endometrium and Ectocervix. *Cell Stress Chaperones* (1997) 2:168–74. doi: 10.1379/1466-1268(1997)002<0168:hahape>2.3.co;2
44. Song KH, Oh SJ, Kim S, Cho H, Lee HJ, Song JS, et al. HSP90A Inhibition Promotes Anti-Tumor Immunity by Reversing Multi-Modal Resistance and

Stem-Like Property of Immune-Refractory Tumors. *Nat Commun* (2020) 11:562. doi: 10.1038/s41467-019-14259-y

Conflict of Interest: The authors declare that the research was conducted in the absence of any commercial or financial relationships that could be construed as a potential conflict of interest.

Publisher's Note: All claims expressed in this article are solely those of the authors and do not necessarily represent those of their affiliated organizations, or those of the publisher, the editors and the reviewers. Any product that may be evaluated in this article, or claim that may be made by its manufacturer, is not guaranteed or endorsed by the publisher.

Copyright © 2022 Ren, Yu, Qian, Ye, Zhu, Yu, Sun and Zhang. This is an open-access article distributed under the terms of the Creative Commons Attribution License (CC BY). The use, distribution or reproduction in other forums is permitted, provided the original author(s) and the copyright owner(s) are credited and that the original publication in this journal is cited, in accordance with accepted academic practice. No use, distribution or reproduction is permitted which does not comply with these terms.

frontiers | Frontiers in Oncology

TYPE Clinical Trial
PUBLISHED 25 August 2022
DOI 10.3389/fonc.2022.841547

Check for updates

OPEN ACCESS

EDITED BY
Debabrata Barmon,
Bhubaneswar Borooah Cancer Institute, India

REVIEWED BY
Timothy Abiola Olusesan Oluwasola, University of Ibadan, Nigeria
Megha Nandwani,
Chittaranjan National Cancer Institute, India

*CORRESPONDENCE
Zhen Xiao
seriousdoc@163.com
Xiaoguang Xu
drxgxu@163.com

†These authors have contributed equally to this work and share first authorship

SPECIALTY SECTION
This article was submitted to Gynecological Oncology, a section of the journal Frontiers in Oncology

RECEIVED 22 December 2021
ACCEPTED 13 July 2022
PUBLISHED 25 August 2022

CITATION
Wang Q, He Y, Long F, Li C, Shen Z, Guo D, Zhaxi D, Bumu L, Hua Z, Sun Z, Jiang N, Han X, Li J, Yan K, Bai S, Tao M, Xu X and Xiao Z (2022) Cervical cancer screening in high-altitude areas in China: A large cross-section study of 25,173 women in northern Tibet. *Front. Oncol.* 12:841547. doi: 10.3389/fonc.2022.841547

COPYRIGHT
© 2022 Wang, He, Long, Li, Shen, Guo, Zhaxi, Bumu, Hua, Sun, Jiang, Han, Li, Yan, Bai, Tao, Xu and Xiao. This is an open-access article distributed under the terms of the Creative Commons Attribution License (CC BY). The use, distribution or reproduction in other forums is permitted, provided the original author(s) and the copyright owner(s) are credited and that the original publication in this journal is cited, in accordance with accepted academic practice. No use, distribution or reproduction is permitted which does not comply with these terms.

Cervical cancer screening in high-altitude areas in China: A large cross-section study of 25,173 women in northern Tibet

Qimin Wang[1,2†], Yingying He[1,3†], Fang Long[1,4,5†], Chaoran Li[4,6†], Zhuowei Shen[1,4†], Dongxing Guo[1,4,5†], Duoji Zhaxi[1], Lamu Bumu[5], Zhengyu Hua[7], Zhigang Sun[7], Nan Jiang[7], Xu Han[4], Jing Li[4], Keqing Yan[2], Siqi Bai[4], Muhan Tao[4], Xiaoguang Xu[1,8*] and Zhen Xiao[1,4,5*]

[1]Institute of High Altitude Medicine, People's Hospital of Nagqu affiliated to Dalian Medical University, Nagqu, China, [2]Department of Pathology, Second Affiliated Hospital of Dalian Medical University, Dalian, China, [3]Department of Pathology, Dalian Maternal and Child Medical Group, Dalian, China, [4]Department of Obstetrics and Gynecology, First Affiliated Hospital of Dalian Medical University, Dalian, China, [5]Department of Obstetrics and Gynecology, People's Hospital of Nagqu affiliated to Dalian Medical University, Nagqu, China, [6]Performance and Quality Management Department, First Affiliated Hospital of Dalian Medical University, Dalian, China, [7]Department of Pathology, First Affiliated Hospital of Dalian Medical University, Dalian, China, [8]Department of Neurosurgery, Second Affiliated Hospital of Dalian Medical University, Dalian, China

Background: Cervical cancer has become a worldwide concern owing to its high incidence and mortality rates. To date, high-altitude areas of Tibet have not benefited from any large-scale cervical cancer screening programs. Therefore, we initiated a screening program to investigate the prevalence of human papilloma virus (HPV) and HPV genotype distribution to reveal cervical cancer and its precursor which lead to morbidity among women in the city of Nagqu in northern Tib3et.

Methods: A total of 25,173 women were recruited to undergo HPV genotype tests between June and December 2019. Women infected with HPV 16 and/or 18 underwent colposcopy and histological examination. Women with other high-risk HPV type (hr-HPV) underwent cytological tests to determine whether to conduct further colposcopy and histological examination for diagnosis. HPV prevalence was calculated in the total population and further stratified according to various parameters, such as age group, area location (altitude level), and single or mixed infection status. The HPV genotype distribution was also investigated accordingly. Cervical lesions revealed by further colposcopic findings were also analyzed; high-grade and malignant lesion morbidities were calculated in total and in each county. Most data were collected and analyzed using descriptive and consistency check statistical methods, and a risk factor investigation for HPV infection was performed using logistic regression models.

Results: The total HPV infection rate among women in Nagqu was 13.42%. Of the 25,173 women in the study, 999 (3.97%) were HPV 16/18 positive, 2,379

(9.45%) were other hr-HPV-positive, and 21,795 (86.58%) were HPV-negative. The five most common HPV genotypes, accounting for more than 60% of all HPV infections in Nagqu people, were HPV 16, 58, 31, 18, and 52. Tibetan women younger than 20 years and older than 60 years were the two age groups with the highest rates of HPV infection, 26.7% and 19.8%, respectively. Among the HPV-positive women, 2,656 (78.33%) were infected with a single strain and 732 (21.67%) were infected with multiple strains (more than two genotypes). HPV prevalence increased in high-altitude areas (positive rate highest in Nyima with an altitude of 5,000 m, 23.9%) and decreased in relatively low-altitude areas (positive rate lowest in Lhari with an altitude of 4,000 m, 6.6%). Multiple analyses showed that age, parity, age at first delivery, and altitude of residence were independent factors facilitating HPV infection in Tibetan women. High-grade and malignant cervical lesions revealed by histological findings were different among living locations, with the highest rates in Xainza, Baingoin, and Nyainrong, these being 2.019%, 1.820%, and 1.116%, respectively, among women in these areas.

Conclusion: Our survey provides an overall perspective on HPV genotype infection and cervical lesions in women in northern Tibet. The data not only provide useful information for the treatment of cervical lesions but also has great value in terms of the primary and secondary prevention measures that can be taken for women living in these regions.

Clinical Trial Registration: www.chictr.org.cn, indentifier ChiCTR2000035061.

KEYWORDS

cervical cancer, HPV, cervical cancer screening, genotype, disease distribution

1 Introduction

Cervical cancer is the third most common cancer worldwide and the fourth most common cancer among Chinese women. Reportedly, there are 34,000 and 275,000 cervical cancer-related deaths in China and globally, respectively (1). Human papillomavirus (HPV) has been confirmed as a pathogenic cause of cervical invasive cancer and its precancerous lesions, and cervical cancer is now regarded as a preventable disease (2).

Several cervical screening programs have been developed and applied to populations in various countries to identify precursors of cervical cancer. Multiple strategies are available for cervical cancer screening. The cheapest and simplest method of visual inspection with acetic acid has a high false-positive rate, requires a large number of trained clinicians, and is time-consuming, all of which make it difficult to access in Tibet despite its relative simplicity and low cost. The pap smear or cytology test has been used for several decades (3, 4) ; however, it has low sensitivity and specificity. Primary cytology with HPV triage has been widely used in women older than 30 years (testing HPV together with cytology), and it has high sensitivity and specificity (5–7). However, these tests are expensive and require abundant medical resources. Recently, another screening method solely for HPV testing (as the primary screening test) has been developed following cytology triage (8, 9). This method is extensively used in European countries, and it has an enhanced negative predictive value (10, 11). This screening method allows cervical cancer screening safety intervals to be extended from 3 to 5 years (12).

In most parts of China, for cervical cancer screening, we adopt the principle of "Opportunistic screening." That is, when a woman comes to the hospital for various reasons, doctors suggest additional cervical cancer screening. Usually, combined cytology and HPV tests are used in most Chinese medical affiliations, and patients can afford the expense by themselves (13, 14). However, this strategy has not yet been widely used in Tibet. This is because Tibet has a relatively small population, large territory, and limited medical resources (15). Moreover, the majority of women in Tibet rarely visit hospitals voluntarily, except in emergencies, and they are uninclined to pay for, even affordable, screening programs. Therefore, government-financed HPV primary screening programs for all

the population at right ages (16) may be the best choice for women in Tibet.

This is the first large-scale cervical cancer screening program conducted in the city of Nagqu, northern Tibet. This study aimed to investigate the prevalence and distribution of HPV genotypes and cervical lesions in Nagqu women. This is the first regional epidemiological study to elucidate the incidence of cervical cancer and its precursor which leads to morbidity in Nagqu.

2 Materials and methods

2.1 Study population and screening strategy

A total of 25,173 married women aged 18–65 years in Nagqu City, Tibet Autonomous Region of China, who were available at home and who consented to undergo screening between June and December 2019 were recruited in this study. HPV genotype testing was the first step for all these participants. Women with positive results were divided into two groups. The first group included those with HPV 16 and/or HPV 18 infections, and the second group included high-risk HPV (hr-HPV) infections with genotypes other than 16 and 18. Women with HPV 16 and/or 18 infection in the first group underwent colposcopy and histological examination at the People's Hospital of Nagqu. Women in the second group with other types of hr-HPV infection underwent cytology testing initially. If cytology results showed ASCUS (atypical squamous cells, undetermined significance) or more in these women, they were requested to undergo further colposcopy and histological examination for diagnosis. The flow diagram (Figure 1) summarizes this process.

2.2 HPV and cytology testing

All HPV samplings were performed by trained general practitioners at every primary hospital in all parts of Nagqu City. HPV samples were analyzed using a BGI 16-type HPV genotyping sequencing assay (BGI, Shenzhen, China). HPV testing was performed using an HPV genotyping sequencing system. This assay could detect 16 hr-HPV genotypes (16, 18, 31, 33, 35, 39, 45, 51, 52, 53, 56, 58, 59, 66, 68, and 73), as described here in detail (17, 18). Briefly, this assay aimed to target and amplify DNA of the HPV L1 gene. MiSeq or personal genome machine (PGM) sequencing strategies were used for testing. HPV16/18-positive samples were subjected to histological examination while cytology tests were also maintained for these participants for study purposes; hr-HPVs other than 16/18 infected women were referred for cytology analysis with liquid-based cytology (LBC) (Thin Prep, Hologic, Boxborough, Massachusetts, USA).

2.3 Colposcopy examination

Women who required colposcopy examinations were referred to a single expert gynecologist at the People's Hospital of Nagqu, Tibet. All examinations were conducted according to routine procedures described previously (19). Hematoxylin and eosin (H&E) staining was performed for histological diagnosis.

2.4 Statistical analysis

SPSS 21.0 (version 21.0; SPSS, Inc. Chicago, IL, USA) was used for statistical analysis. All participants were divided by age group and county to calculate the prevalence of the overall HPV genotype, HPV 16/18, and other hr-HPV genotypes. Additionally, a stratifying strategy was used to analyze the cytology and histology results. To compare differences in HPV infection prevalence and cervical lesion rates among various locations and age groups, the chi-square test was used accordingly. Also, a logistic regression model was used to investigate factors influencing HPV infection. The p value was considered significant when $p < 0.05$.

3 Results

3.1 Overview of HPV infection in the women of Nagqu, north of Tibet

3.1.1 Distribution of HPV genotypes in the women of Nagqu

The total HPV infection rate among women in Nagqu was 13.42%. Of the 25,173 women in the study, 999 (3.97%) were HPV 16/18 positive, 2,379 (9.45%) were other hr-HPV HPV positive, and 21,795 (86.58%) were HPV negative (Figure 2A and Table 1).

3.1.2 Distribution of multiple and simple HPV infection in the women of Nagqu

For the HPV-positive patients, the genotyping results showed that 2,646 (78.33%) were singly infected, 575 (17.02%) were doubly infected, 130 (3.85%) were triple infected, 24 (0.71%) were quadruply infected, and only three patients (0.01%) were quintuply infected (Figure 2B and Table 1).

3.1.3 Overall prevalence distribution of each HPV genotype

The overall prevalence of each HPV genotype in the HPV-positive patients is shown in Figure 2C; Table 1. The most frequently detected HPV genotype was HPV 16, which was detected in 577 women (13.6%). The relatively less common

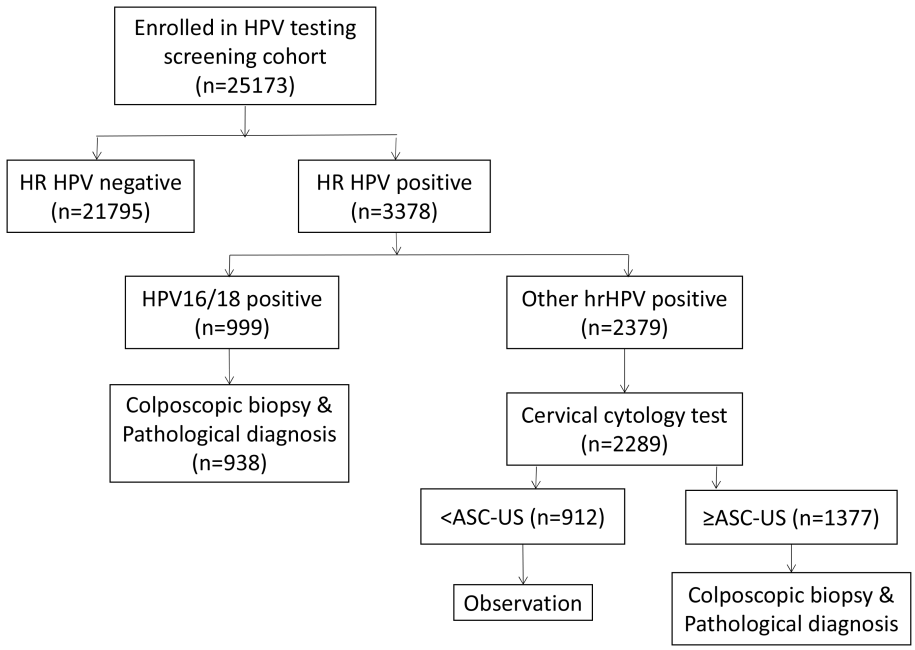


FIGURE 1
Flow of participants in the screening cohort.

genotypes were HPV 58 (557, 13.1%), HPV 31 (512, 12%), HPV 18 (450, 10.6%), HPV 52 (410, 9,6%), HPV 51 (378, 8.9%), HPV 68 (280, 6.6%), HPV 39 (237, 5.6%), HPV 59 (219, 5.1%), HPV 66 (200, 4.7%), HPV 56 (98, 2.3%), HPV 6 (98, 2.3%), HPV 35 (64, 1.5%), HPV 45 (63, 1.5%), HPV 11 (62, 1.5%), and HPV 33 (52, 1.2%). In patients with single and multiple HPV infections, the HPV prevalence was slightly different from the total prevalence, as summarized in Table 1. For example, in

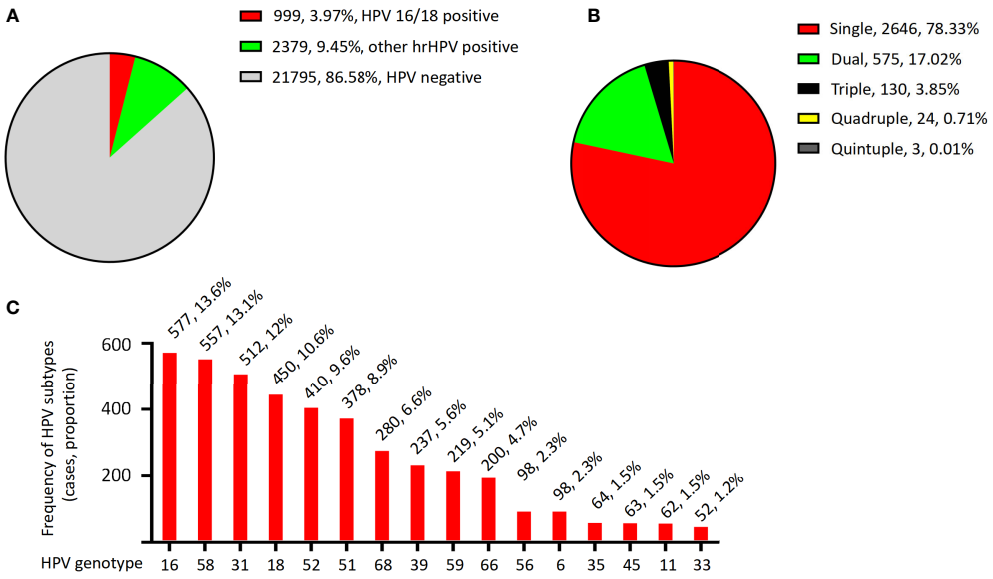


FIGURE 2
The HPV infection distribution. **(A)** Distribution of HPV genotypes in the women of Nagqu. **(B)** Distribution of multiple and simple HPV infection in the women of Nagqu. **(C)** Overall prevalence distribution of each HPV genotype.

TABLE 1 Prevalence of HPV genotypes in all patients and prevalence of HPV genotypes in simple- and multiple-HPV-infection patients.

Overall infection			Simple infection			Dual infection			Triple infection			Quadruple infection			Quintuple infection		
HPV genotype	Frequency	Proportion (%)	HPV genotype	Frequency	Proportion (%)	HPV genotype	Frequency	Proportion (%)	HPV genotype	Frequency	Proportion (%)	HPV genotype	Frequency	Proportion (%)	HPV genotype	Frequency	Proportion (%)
HPV16	577	13.6	**HPV16**	392	14.8	**HPV31**	151	13.4	**HPV31**	48	12.1	**HPV16**	11	15.5	**HPV18**	2	13.3
HPV58	557	13.1	**HPV58**	364	13.8	**HPV58**	142	12.6	**HPV58**	44	11.1	**HPV18**	11	15.5	**HPV51**	2	13.3
HPV31	512	12	**HPV31**	302	11.4	**HPV16**	140	12.4	**HPV52**	42	10.6	**HPV31**	10	14.1	**HPV59**	2	13.3
HPV18	450	10.6	**HPV18**	271	10.2	**HPV18**	128	11.3	**HPV51**	41	10.3	**HPV51**	9	12.7	**HPV52**	2	13.3
HPV52	410	9.6	**HPV52**	245	9.3	**HPV52**	114	10.1	**HPV18**	38	9.5	**HPV52**	7	9.9	**HPV66**	2	13.3
HPV51	378	8.9	**HPV51**	231	8.7	**HPV51**	95	8.4	**HPV59**	35	8.8	**HPV39**	6	8.5	**HPV16**	1	6.6
HPV68	280	6.6	**HPV68**	181	6.8	**HPV68**	71	6.3	**HPV16**	33	8.3	**HPV58**	6	8.5	**HPV68**	1	6.6
HPV39	237	5.6	**HPV39**	149	5.6	**HPV59**	66	5.9	**HPV68**	27	6.8	**HPV35**	3	4.2	**HPV31**	1	6.6
HPV59	219	5.1	**HPV66**	127	4.8	**HPV39**	58	5.1	**HPV39**	24	6	**HPV59**	3	4.2	**HPV35**	1	6.6
HPV66	200	4.7	**HPV59**	113	4.3	**HPV66**	52	4.6	**HPV66**	19	4.8	**HPV45**	2	2.8	**HPV58**	1	6.6
HPV56	98	2.3	**HPV56**	62	2.3	**HPV6**	28	2.5	**HPV11**	13	3.3	**HPV56**	2	2.8			
HPV6	98	2.3	**HPV6**	62	2.3	**HPV56**	25	2.2	**HPV56**	9	2.3	**HPV11**	1	1.4			
HPV35	64	1.5	**HPV33**	39	1.5	**HPV35**	18	1.6	**HPV6**	8	2						
HPV45	63	1.5	**HPV11**	36	1.4	**HPV45**	18	1.6	**HPV35**	7	1.8						
HPV11	62	1.5	**HPV45**	36	1.4	**HPV11**	12	1.1	**HPV45**	7	1.8						
HPV33	52	1.2	**HPV35**	35	1.3	**HPV33**	10	0.9	**HPV33**	3	0.8S						

10.3389/fonc.2022.841547

10.3389/fonc.2022.841547

single- and dual-infection groups, the four most common genotypes were HPV 16, 58, 31, and 18; however, in patients infected with three HPV genotypes, the four most common infection genotypes were HPV 31, 58, 52, and 51.

3.1.4 Distribution of HPV infection in different age groups in the Nagqu area

Based on the age groups, as shown in Table 2, women with a younger age (less than 30 years) and older age (>50 years) had higher total HPV infection rates of 15.9% and 18.4%, respectively, $p < 0.01$. Women with a median age of (31–50 years) had a lower positive rate (12.6%), and the difference was statistically significant.

3.15 Area-specific distribution of HPV infections in Nagqu

As the city of Nagqu has an area of 370,000 km^2, and its 11 counties have different altitudes and different modes of production and life, we calculated the HPV infection rate in women according to each of the 11 areas. Generally, women living in eastern areas with lower altitudes had lower HPV infection rates than those living in western areas with higher altitudes (Figure 3A and Table 3). HPV infection rates in women were lowest in Lhari, Bagen, and Biru counties at 6.6%, 7%, and 9.2%, respectively. The highest infection rate was noted in the ultra-high-altitude areas of Amdo (18.6%), Nyima (23.9%), and Shuanghu (20.3%). When we combined the 11 counties into three regions according to altitude level (region A, altitude level <4,000 m; region B, altitude level within 4,000–5,000 m, region C altitude level >5000 m), we found that regions with lower altitudes had the lowest HPV-positive rate of 9.8%, while the rates in regions B and C were 13.2% and 20.9%, respectively ($p = 0.001$). Correlation analysis also indicated a significant correlation between altitude and HPV infection rates, $p = 0.001$, gamma = -0.251 (Figure 3B).

3.1.6 Independent factors influencing HPV infection in Nagqu, Tibet

According to the above findings, it can be mentioned that HPV infection was associated with factors such as women's age, living locations, and altitude. Our analysis also showed that women with HPV infection had less children and younger age in first delivery. Therefore, we introduced logistic regression to perform multiple-factor analysis to identify the independent factors facilitating HPV infection in Nagqu women. Statistics indicated that age group, living location altitude, and parity were the independent factors influencing HPV infection (Table 4). The P-value was 0.031 for those aged between 31 and 35 years and 0.001 for those aged over 50 years. The P-values for altitude and yield were 0.001.

TABLE 2 Prevalence of HPV genotypes in women of different ages.

Age group(y)	Total No.	HPV16/18 infection		Other HPV infection		Mixed HPV infection		Four most frequently infected genotypes				Total	
		Positive No.	Positive, %	Positive No.	Positive, %	Positive No.	Positive, %	Top1 genotype (No., %)	Top2 genotype (No., %)	Top3 genotype (No., %)	Top4 genotype (No., %)	Positive No.	Positive, %
≤30	572	28	4.9%	56	9.8%	18	3.1%	HPV16 (22,24.2)	HPV31 (17,18.7)	HPV58 (11,12.1)	HPV52 (10,10.9)	84	14.7%
31-50	18503	694	3.8%	1635	8.8%	427	2.3%	HPV16 (403,17.3)	HPV58 (370,15.9)	HPV52 (328,14.1)	HPV18 (309,13.3)	2329	12.6%
≥51	5171	274	5.3%	679	13.1%	284	5.5%	HPV31 (163,17.1)	HPV58 (162,16.9)	HPV16 (150,15.7)	HPV18 (133,13.9)	953	18.4%

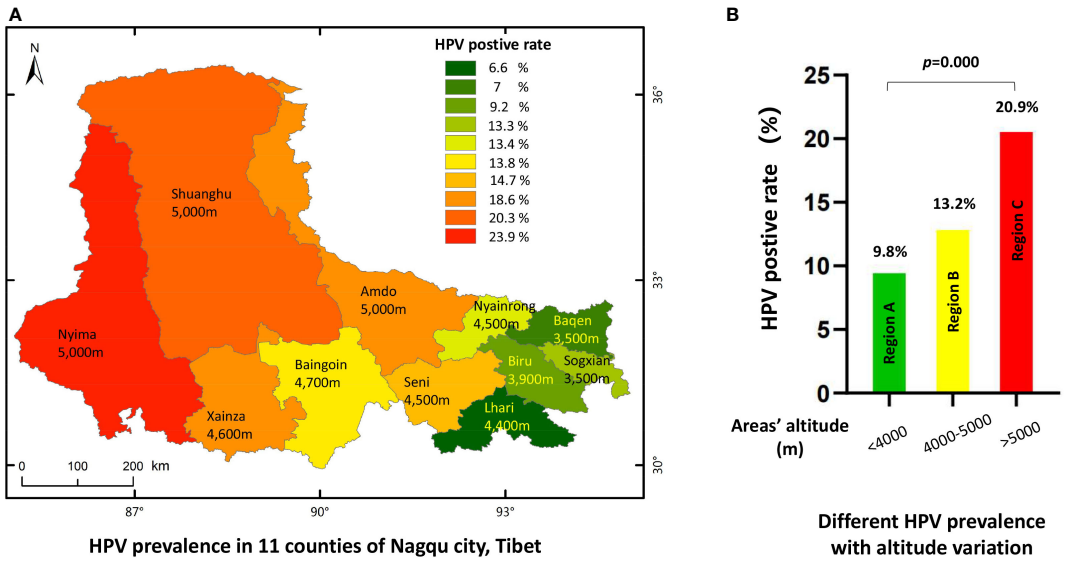


FIGURE 3
The HPV prevalence in 11 countries of Nagqu. **(A)** HPV prevalence in 11 counties of Nagqu City, Tibet. **(B)** Different HPV prevalence with altitude variation.

3.2 Cytology

The most common finding was low-grade squamous intraepithelial lesion (LSIL), and 739 women (78.8%) were diagnosed with HPV 16/18. Meanwhile, among other hr-HPV-positive women, only 53.5% (1206 individuals) were diagnosed with LSIL. Additionally, in cytology tests of HPV 16/18 and other hr-HPV-positive patients, the diagnosis of atypical squamous cells of unknown significance (ASCUS), atypical squamous cells cannot exclude HSIL (ASCH), high-grade squamous intraepithelial lesion (HSIL), and cancer was very rare. The most dominant difference was the proportion of Negative for Intra-epithelial Lesions or malignancies (NILM). In the 16/18-positive patients, only 3.1% (29 women) were diagnosed with NILM, whereas in other hr-HPV-positive patients, nearly 40% were diagnosed with NILM. The results are summarized in Table 5.

3.3 Histology

A total of 2,315 women underwent histological examinations, as shown in Table 5. As shown in Table 5, of HPV 16/18-positive patients, 70.2%, 18.5%, 8.9%, and 2.3% of patients had LSIL, NILM, HSIL, and invasive cancers, respectively. In other hr-HPV-positive patients, the diagnosis of NILM was slightly higher (31.6%), LSIL patients were slightly less than HPV 16/18 patients, with a proportion of 58.2%, HSIL was diagnosed in 9.6% of HPV-positive patients, and cervical cancer was found in only 0.6% of HPV-positive women. The histological differences between the two HPV groups were statistically significant ($p = 0.001$).

As there were different HPV infection rates in different counties, we next investigated the distribution of HSIL and cervical cancer lesions in each of the 1 different counties. The analysis indicated that, consistent with the HPV infection profiles, patients with HSIL and cancer lesions seemed to have a similar distribution (Figure 4A and Table 6). For HPV-positive women, lesions of HSIL and invasive cancer were most prevalent in some high-altitude areas such as Xainza (2.019%), Baingoin (1.820%), and Nyainrong (1.116%), while the incidence was lower in lower-altitude areas such as Sogxian (0.744%) and Baqen (0.826%). After stratifying the lesion rates by the three altitude levels, the HSIL or cancer incidence also presented a significant positive correlation with altitude, as shown in Figure 4B, $p = 0.001$.

4 Discussion

To the best of our knowledge, this is the first large-scale population-based survey in Tibet to investigate the prevalence of HPV infection and related cervical lesions in women. This study revealed that the overall HPV infection rate in the women of Nagqu was 13.42%, consistent with recent studies in other high-altitude areas such as Nyingchi, Tibet, 12.81% (20), and Xining, Qinghai, 16.72% (21), while it was slightly higher compared with the investigation conducted about 10 years ago, in which the HPV positivity rate was 9.82% (22). In previous studies, HPV prevalence varied greatly among areas in China and worldwide. Within China, different districts have different HPV infection rates, such as Shanxi (14.8%), Shenzhen (11.3%), Shenyang (17%), Zhejiang (13.3%), and Shandong (18.1% (23–27). According to reports on global levels,

TABLE 3 Prevalence of HPV genotypes in women from 11 counties of Nagqu city, Tibet.

District	Average Altitude (m)	Total No.	HPV16/18 infection		Other hrHPV infection		Mixed hrHPV infection		Four most frequent infected subtypes				Total	
			Positive No.	Positive, %	Positive No.	Positive, %	Positive No.	Positive, %	Top1	Top2	Top3	Top4	Positive No.	Positive, %
Sogxian	3,500	2284	111	4.9	193	8.5	60	19.1	HPV16 (69,22.7%)	HPV18 (42,13.8%)	HPV58 (35,11.5%)	HPV31 (32,10.5%)	304	13.3
Biru	3,900	4306	107	2.5	289	6.7	71	17.9	HPV16 (71,17.9%)	HPV58 (47,11.9%)	HPV52 (44,11.1%)	HPV51 (42,10.6%)	396	9.2
Lhari	4,400	2981	45	1.5	152	5.1	37	18.8	HPV16 (29,14.7%)	HPV58 (26,13.2%)	HPV31 (22,11.2%)	HPV52 (21,10.67%)	197	6.6
Baqen	4,500	1783	38	2.1	87	4.9	21	16.8	HPV16 (44,18.2%)	HPV58 (33,13.6%)	HPV31 (32,13.2%)	HPV18 (24,9.9%)	125	7
Seni	4,500	4004	165	4.1	422	10.5	114	19.4	HPV16 (102,17.4%)	HPV58 (79,13.5%)	HPV52 (62,10.6%)	HPV18 (62,10.6%)	587	14.7
Xainza	4,600	2377	134	5.6	308	13	91	20.6	HPV16 (69,15.6%)	HPV18 (65,14.7%)	HPV31 (65,14.7%)	HPV51 (45,10.2%)	442	18.6
Baingoin	4,700	1758	68	3.9	174	9.9	54	22.3	HPV16 (24,19.1%)	HPV18 (14,11.2%)	HPV31 (12,9.6%)	HPV58 (11,8.8%)	242	13.8
Nyainrong	4,700	1344	43	3.2	137	10.2	45	25	HPV58 (39,21.7%)	HPV16 (28,15.6%)	HPV31 (17,9.4%)	HPV18 (15,8.3%)	180	13.4
Amdo	5,000	2178	116	5.3	298	13.3	103	25.4	HPV16 (70,17.3%)	HPV31 (68,16.8%)	HPV18 (43,10.6%)	HPV58 (40,9.9%)	405	18.6
Nyima	5,100	1727	153	8.9	260	15.1	112	27.1	HPV18 (91,22%)	HPV16 (62,15%)	HPV31 (62,15%)	HPV58 (44,10.7%)	413	23.9
Shuanghu	5,200	428	19	4.4	68	15.9	24	27.6	HPV31 (21,24.1%)	HPV52 (11,12.6%)	HPV18 (10,11.5%)	HPV16 (9,10.3%)	87	20.3

10.3389/fonc.2022.841547

TABLE 4 Independent factors influencing HPV infection in women of Nagqu.

Factors		OR value	95% CI	*p* value
Age	≤30 years			
	31-50 years	1.315	1.025-1.688	0.031
	>50 years	1.422	1.304-1.551	0.001
Altitude of location	<4,000m			
	4,000-5,000m	2.274	2.044-2.531	0.001
	>5,000m	1.709	1.56-1.872	0.001
Parity	>3			
	≤3	1.212	1.117-1.314	0.001

HPV-positive rates range from 5% to 10% (28–31). Our data also showed that cervical lesion rates fluctuated significantly among women in different counties of Nagqu Tibet, ranging from 0.605% to 2.019% (Table 6).

Intriguingly, there seemed to be a positive correlation between HPV prevalence rate/cervical high-grade lesion incidence and altitude. The higher the altitude, the higher the prevalence of HPV in women. We searched for related studies performed in high-altitude areas all over the world and found that HPV prevalence was high (38.2%) in high-altitude areas of Ecuador, a Latin American country with a largely high altitude, although it was a hospital-based rather than a community-based investigation (32). As mentioned earlier, in China, HPV infection rates at different altitudes in Shanxi were 14.8%, 11.3%, 17%, 13.3%, and 18.1%, respectively. Shanxi, Shenyang, and Shandong are in northern China, whereas Shenzhen, Zhejiang, and Tibet are in the south.

Therefore, we assumed that possible reasons may be attributed to the following two elements: hypoxia from high altitude and cold weather because of extreme climate, both of which facilitate HPV transmission.

Although a few studies have suggested a higher risk of HPV prevalence and cervical cancer in women living in high-altitude areas, there is solid evidence that many types of cancer are more common in high-altitude-living people, such as gastric cancer and breast cancer. The mechanism, which has been comprehensively reviewed (33), is complex and controversial.

Researchers have also revealed an association between cold weather and a high risk of many cancers, such as breast, prostate, and colon cancer. The reasons may be related to evolutionary adaption, high concentrations of certain air pollutants, and low levels of serum vitamin D, although any single factor cannot explain this epidemiological phenomenon (34).

Another possible reason we suspected, although with no scientific data, may be attributed to the social and living styles of Tibetan women, especially in pastoral areas. From our examinations and the subsequent interviews, women in pastoral areas in northern Tibet had very poor sanitation, and many of them did not clean their anogenital areas with tissue or other materials after defecation. In addition, in many places, polyandry and premature sex are common in society. Compared with Han women, Tibetan women have a lower probability of using prenatal care or receiving maternal and child healthcare (35), and Tibetan women have lower knowledge and acceptance of cervical cancer screening (2). All of these behaviors are believed to facilitate HPV transmission.

In our study, we found that the main form of HPV infection was a single infection, while multiple HPV infections were less common, and the results were consistent with those of previous studies. The five most common HPV genotypes in Nagqu people were HPV 16, 58, 31, 18, and 52, accounting for approximately

TABLE 5 Cytology and histology results in HPV positives women in Nagqu.

HPV subtypes		HPV16/18		Other hrHPV		
		cases (N)	percentage (%)		cases (N)	percentage (%)
Cytology results	**NILM**	29	3.1	**NILM**	912	39.8
	ASCUS	63	6.7	**ASCUS**	84	3.2
	ASCH	67	7.2	**ASCH**	59	2.3
	LSIL	739	78.8	**LSIL**	1206	53.5
	HSIL	36	3.8	**HSIL**	23	1
	CANCER	4	0.4	**CANCER**	5	0.2
	Total	938	100	**Total**	2289	100
Histology results	**NILM**	174	18.5	**NILM**	435	31.6
	LSIL	658	70.2	**LSIL**	801	58.2
	HSIL	85	8.9	**HSIL**	132	9.6
	CANCER	21	2.3	**CANCER**	9	0.6
	Total	938	100	**Total**	1377	100

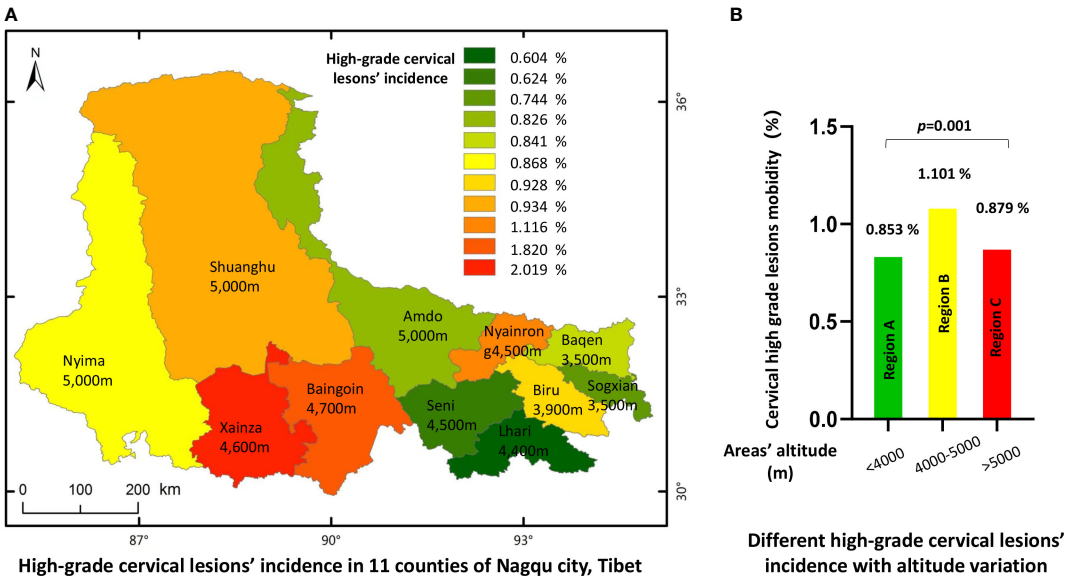


FIGURE 4
Incidence of high grade cervical lesions in 11 countries of Nagqu. **(A)** High-grade cervical lesions' incidence in 11 counties of Nagqu city, Tibet. **(B)** Different high-grade cervical lesions' incidence with altitude variation.

60% of all infections. This result differed slightly from those of previous studies on the top five HPV genotypes in China (36). Fortunately, all five genotypes were within the nine-valent HPV vaccine spectrum. Thus, there should be an HPV vaccine program initiated in northern Tibet, and our data will provide great value in this effort. The manner of infection in Tibet was approximately the same as that encountered in previous studies in other areas of China (37).

As indicated in other studies, our survey also demonstrated that the age-stratified HPV genotype prevalence has a U-shaped pattern. That is, the infection rate was highest in both the youngest and oldest groups and lowest in the median group (38). This was consistent with previous studies in China that showed a bimodal distribution with age (39). Moreover, the prevalence of HPV genotypes differed according to age group. In the group of women younger than 30 years, the top four HPV genotypes were HPV 16, 31, 58, and 52; in those aged 31–50 years, the top four HPV genotypes were HPV 16, 58, 52, and 18. In women aged >50 years, the top four frequently infected HPV genotypes were HPV 31, 58, 16, and 18. Even when we stratified the women into simple and mixed infection groups, this pattern remained consistent. HPV infection is closely related to women's age, and women who are sexually active and postmenopausal women have a higher probability of infection with HPV (37, 40, 41), which is also applicable in the Nagqu area. This may be related to factors such as age at first sexual encounter, number of sexual partners, frequency of sexual intercourse, and sexual hygiene for sexually active women (42). The immune capacity of women decreases with age, especially in pre- and postmenopausal women, and the ability to eliminate past and new infections weakens (43). Furthermore, education, economic status, and awareness of cervical cancer and cervical cancer screening are perhaps also the influencing factors (42), although we did not explore this in detail in this research. Therefore, it is necessary to strengthen health knowledge education, improve women's awareness of self-health care, and conduct regular HPV screening to prevent cervical cancer. Our research may thus be helpful for the prevention of cervical cancer in women in Nagqu.

Although the incidence of HSIL and cervical cancer was nearly the same between the HPV 16/18 infection group and the other hr-HPV infection group, the LSIL frequencies were

TABLE 6 Incidence of HSIL or severe lesion among Tibetan women in different areas.

Counties	Number of cases (n)	Percentage (%)
Amdo	18	0.826
Baqen	15	0.841
Baingoin	32	1.82
Biru	40	0.928
Lhari	18	0.605
Nyima	15	0.868
Nyainrong	15	1.116
Seni	25	0.624
Xainza	48	2.019
Shuanghu	4	0.934
Sogxian	17	0.744

significantly different (44). In the HPV 16/18 group, LSIL was detected in approximately 70.2% of patients, whereas in the other hr-HPV infection group, LSIL only accounted for 58.2% of women. This phenomenon was also observed in other similar research (45–48). According to our data, HPV16/18 positivity results in different LSIL rates in Tibet compared to non-16/18, which may suggest different management strategies for the two types of infection. Previous studies have shown that persistent HPV infections, such as HPV 16, 18, and 31, are closely related to the occurrence of cervical cancer (49). The occurrence of low-risk HPV is closely related to the occurrence of skin venereal diseases such as condyloma acuminatum (50), suggesting that close attention should be paid to hr-HPV infection in the prevention and treatment of cervical cancer.

As mentioned above, the HPV infection rate correlated with altitude; a similar phenomenon was also observed in the histological results (Figure 4 and Table 6). Some studies have indicated that severe lesions might be attributed to the high prevalence of HPV 16/18 infections instead of the overall HPV infection rate (51), which was also verified in our survey. The top three counties with a high incidence of cervical lesions were Xainza (2.019%), Baingoin (1.820%), and Nyainrong (1.116%), and HPV 16/18 infection rates were also higher in 11 counties (5.6%, 3.8%, and 3.1%, respectively).

The strength of this study is highlighted by the fact that it showed a higher prevalence of HPV infection in women residing at higher altitudes in Tibet. Further analysis indicated that HPV infection and cervical lesion incidence might have a certain correlation with location altitude and it might also vary in different age groups. This information not only provides useful information for the treatment of cervical lesions but also has great value in primary and secondary cervical cancer prevention measures for women residing in high-altitude areas.

The weakness of our survey included missing some important information of the women participating in the study such as the number of sex partner, smoking or alcohol drinking habits, and economic status, so that statistical analyses could not be performed to investigate more risk factors facilitating HPV infection and cervical precancer pathogenesis. Further studies are needed not only for more rigorous and comprehensive investigations but also for long-term surveillance of HPV-positive Tibetan women.

Data availability statement

The original contributions presented in the study are included in the article/Supplementary Material. Further inquiries can be directed to the corresponding authors.

Ethics statement

The studies involving human participants were reviewed and approved by Ethics Committee of Nagqu people's Hospital. The patients/participants provided their written informed consent to participate in this study.

Author contributions

QW, YH, FL, CL, ZS, and DG contributed equally to this work and shared first authorship. DZ, LB, ZH, ZS, NJ, XH, JL, KY, SB, and MT helped in writing this article together. ZX and XX are the authors of this article. All authors have made significant contributions to this article. All authors agree to be responsible for the content of this article and have submitted the manuscript.

Funding

National Natural Science Foundation of Liaoning, China, 2019-BS-073 and Public health scientific research project of Futian District, Shenzhen hospital of Guangzhou University of Chinese Medicine, NO. FTWS2019104. Interregion collaborative innovation science and technology program, QYXTZX-NQ2022-03.

Acknowledgments

Science Foundation of Liaoning Provincial Department of Education LZ2019044.

Conflict of interest

The authors declare that the research was conducted in the absence of any commercial or financial relationships that could be construed as a potential conflict of interest.

Publisher's note

All claims expressed in this article are solely those of the authors and do not necessarily represent those of their affiliated organizations, or those of the publisher, the editors and the reviewers. Any product that may be evaluated in this article, or claim that may be made by its manufacturer, is not guaranteed or endorsed by the publisher.

Supplementary material

The Supplementary Material for this article can be found online at: https://www.frontiersin.org/articles/10.3389/fonc.2022.841547/full#supplementary-material

References

1. Youlin ZYQ. Epidemiological status and prevention of cervical cancer. *Chin J Matern Child Clin Med (Electron Ed)* (2015) 11:02.1–6. doi: 10.3877/cma.j.issn.1673-5250.2015.02.001

2. Wu E, Tiggelaar SM, Jiang T, Zhao H, Wu R, Wu R, et al. Cervical cancer prevention-related knowledge and attitudes among female undergraduate students from different ethnic groups within china, a survey-based study. *Women Health* (2018) 58:661–84. doi: 10.1080/03630242.2017.1333076

3. Nayar R, Wilbur DC. The Bethesda system for reporting cervical cytology: A historical perspective. *Acta Cytol* (2017) 61:359–72. doi: 10.1159/000477556

4. Solomon D, Davey D, Kurman R, Moriarty A, O'Connor D, Prey M, et al. The 2001 bethesda system: Terminology for reporting results of cervical cytology. *JAMA* (2002) 287:2114–9. doi: 10.1001/jama.287.16.2114

5. Mariani L, Igidbashian S, Sandri MT, Vici P, Landoni F. The clinical implementation of primary hpv screening. *Int J Gynaecol Obstet* (2017) 136:266–71. doi: 10.1002/ijgo.12065

6. Ogilvie GS, van Niekerk D, Krajden M, Smith LW, Cook D, Gondara L, et al. Effect of screening with primary cervical HPV testing vs cytology testing on high-grade cervical intraepithelial neoplasia at 48 months: The HPV FOCAL randomized clinical trial. *JAMA* (2018) 320:1.43–52. doi: 10.1001/jama.2018.7464

7. Machalek DA, Roberts JM, Garland SM, Thurloe J, Richards A, Chambers I, et al. Routine cervical screening by primary hpv testing: Early findings in the renewed national cervical screening program. *Med J Aust* (2019) 211:113–9. doi: 10.5694/mja2.50223

8. Goodman A. Hpv testing as a screen for cervical cancer. *BMJ* (2015) 350: h2372. doi: 10.1136/bmj.h2372

9. Agorastos T, Chatzistamatiou K, Katsamagkas T, Koliopoulos G, Daponte A, Constantinidis T, et al. Primary screening for cervical cancer based on high-risk human papillomavirus (hpv) detection and hpv 16 and hpv 18 genotyping, in comparison to cytology. *PloS One* (2015) 10:e0119755. doi: 10.1371/journal.pone.0119755

10. Sahlgren H, Elfström KM, Lamin H, Carlsten-Thor A, Eklund C, Dillner J, et al. Colposcopic and histopathologic evaluation of women with hpv persistence exiting an organized screening program. *Am J Obstet Gynecol. Carlsten-Thor Eklund* (2020) 222:253.e1–8. doi: 10.1016/j.ajog.2019.09.039

11. Bergengren L, Lillsunde-Larsson G, Helenius G, Karlsson MG. Hpv-based screening for cervical cancer among women 55-59 years of age. *PloS One* (2019) 14: e0217108. doi: 10.1371/journal.pone.0217108

12. Silver MI, Rositch AF, Phelan-Emrick DF, Gravitt PE. Uptake of hpv testing and extended cervical cancer screening intervals following cytology alone and pap/hpv cotesting in women aged 30–65 years. *Cancer Causes Control* (2018) 29:43–50. doi: 10.1007/s10552-017-0976-x

13. Wang X, Wu S, Li Y. Risks for cervical abnormalities in women with non-16/18 high-risk human papillomavirus infections in south shanghai, China. *J Med Virol* (2021) 93 93:6355–61. doi: 10.1002/jmv.27185

14. Dehui ZJW. Application of liquid-based thin layer cytometry (lct) in cervical cancer screening at high altitude. *Matern Child Health Care China* (2008) 23:3628–9. doi: 10.01-4411(2008)25-3628-02

15. Foggin PM, Dorje D, Xuri W, Marc Foggin J, Torrance J. Assessment of the health status and risk factors of kham tibetan pastoralists in the alpine grasslands of the tibetan plateau. *Soc Sci Med* (2006) 63:2512–32. doi: 10.1016/j.socscimed.2006.06.018

16. Zhong S, Ou Y, Zhang F, Lin Z, Huang R, Nong A, et al. Prevalence trends and risk factors associated with HIV, syphilis, and hepatitis c virus among pregnant women in southwest China, 2009-2018. *AIDS Res Ther* (2022) 19:31. doi: 10.1186/s12981-022-00450-7

17. Gao G, Wang J, Kasperbauer JL, Tombers NM, Teng F, Gou H, et al. Whole genome sequencing reveals complexity in both hpv sequences present and hpv integrations in hpv-positive oropharyngeal squamous cell carcinomas. *BMC Cancer* (2019) 19:352. doi: 10.1186/s12885-019-5536-1

18. Yi JZX, Xu J, Liu T, Liu T. Development and validation of a new genotyping assay based on next-generation sequencing. *Am J Clin Pathol* (2014) 141:796–804. doi: 10.1309/AJCP9P2KJSXEKCJB

19. B L J O K D L M J I M M. *Williams gynecology*. McGraw-Hill Education Press (2018).

20. Jianqi LXL, Zhen L, Jundong W, De Jicuomu YQ. Qu xiwangmu analysis of cervical high-risk human papillomavirus infection status and subtypes of women in rural areas of linzhi city, tibet. *J Pract Med* (2022) 38:4.502–506. doi: 10.3969/j.issn.1006-5725.2022.04.021

21. Cairen Zhuoma ZJ. Wei human papillomavirus infection in 26,622 women in qinghai. *Chin J Fam Plan* (2013) 21:12.812–816. doi: 10.3969/j.issn.1004-8189.2013.12

22. Qiong SKJ, Hui L, Rong ZX, Fang HH, Jinhua L. Investigation and related factors of cervical human papillomavirus infection in women in tibet autonomous region. *Chin Women J Obstet* (2009) 12:898–902. doi: 10.3760/cmaJ.issn.0529-567x2009.12005

23. Bergengren L, Lillsunde-Larsson G, Helenius G, Karlsson MG. HPV-based screening for cervical cancer among women 55-59 years of age. *PloS One* (2019) 14: e0217108. doi: 10.1371/journal.pone.0217108

24. Tang Y, Zheng L, Yang S, Li B, Su H, Zhang LP. Epidemiology and genotype distribution of human papillomavirus (hpv) in southwest china: A cross-sectional five years study in non-vaccinated women. *Virol J* (2017) 14:84. doi: 10.1186/s12985-017-0751-3

25. Yang L, He Z, Huang XY, Liu HN, Tao JY. Prevalence of human papillomavirus and the correlation of HPV infection with cervical disease in weihai, China. *Eur J Gynaecol Oncol* (2015) 36:73–7. doi: 10.12892/ejgo2581.2015

26. Mai Q, Yang X, Cheng H, Wu G, Wu Z. Prevalence and genotype distribution of human papillomavirus among women with cervical lesions in shenzhen city, China. *Hum Vaccin Immunother* (2021) 17:965–71. doi: 10.1080/21645515.2020.1805993

27. Luo LP, He P, Liu QT, Jiang YH, Zhang YN, Li QZ, et al. Prevalence and genotype distribution of hpv infection among 214,715 women from southern china, 2012-2018: Baseline measures prior to mass hpv vaccination. *BMC Infect Dis* (2021) 21:328. doi: 10.1186/s12879-021-06019-5

28. Mutombo AB, Benoy I, Tozin R, Bogers J, Van Geertruyden JP, Jacquemyn Y. Prevalence and distribution of human papillomavirus genotypes among women in Kinshasa. *J Glob Oncol* (2019) 5:1–9. doi: 10.1200/JGO.19.00110

29. Yang J, Wang W, Wang Z, Wang Z, Wang Y, Wang J, et al. Prevalence, genotype distribution and risk factors of cervical hpv infection in yangqu, china: A population-based survey of 10086 women. *Hum Vaccin Immunother* (2020) 16:1645–52. doi: 10.1080/21645515.2019.1689743

30. Sankaranarayanan R, Nene BM, Shastri SS, Jayant K, Muwonge R, Budukh AM, et al. HPV screening for cervical cancer in rural India. *N Engl J Med* (2009) 360:1385–94. doi: 10.1056/NEJMoa0808516

31. Comerlato J, Kops NL, Bessel M, Horvath JD, Fernandes BV, Villa LL, et al. Sex differences in the prevalence and determinants of hpv-related external genital lesions in young adults: A national cross-sectional survey in brazil. *BMC Infect Dis* (2020) 20:683. doi: 10.1186/s12879-020-05376-x

32. Vega Crespo B, Neira VA, Ortíz Segarra J, Rengel RM, López D, Orellana MP, et al. Role of self-sampling for cervical cancer screening: Diagnostic test properties of three tests for the diagnosis of hpv in rural communities of cuenca, Ecuador. *Int J Environ Res Pub Health* (2022) 19:4619. doi: 10.3390/ijerph19084619

33. Calderón-Gerstein WS, Torres-Samaniego G. High altitude and cancer: An old controversy. *Respir Physiol Neurobiol* (2021) 289:103655. doi: 10.1016/j.resp.2021.103655

34. Voskarides K. The "Cancer-cold" hypothesis and possible extensions for the Nordic populations. *Scand J Pub Health* (2019) 47(5):477–481. doi: 10.1177/1403494819831905

35. Huang Y, Shallcross D, Pi L, Tian F, Pan J, Ronsmans C. Ethnicity and maternal and child health outcomes and service coverage in western china: A systematic review and meta-analysis. *Lancet Glob Health* (2018) 6:e39–56. doi: 10.1016/S2214-109X(17)30445-X

36. Zhu B, Liu Y, Zuo T, Cui X, Li M, Zhang J, et al. The prevalence, trends, and geographical distribution of human papillomavirus infection in china: The pooled analysis of 1.7 million women. *Cancer Med* (2019) 8:5373–85. doi: 10.1002/cam4.2017

37. Feng D, Wei S, Chen J, Yu Z, Lhamo Y, Wang H, et al. Human papillomavirus prevalence and genotype distribution landscapes in shannan city, Tibet Tibetan autonomous region, China. *Virol J* (2022) 19:46. doi: 10.1186/s12985-022-01775-5

38. Evans AC, Adamson CS, Papillo JL, St John TL, Leiman G, Cooper K. Distribution of human papillomavirus types in ThinPrep papanicolaou tests classified according to the Bethesda 2001 terminology and correlations with patient age and biopsy outcomes. *Cancer* (2006) 106:1054–64. doi: 10.1002/cncr.21664

39. Yuqian HSZFZ, Wen C, Youlin Q. Multicenter cross-sectional study on cervical human papillomavirus infection and type distribution in Chinese women. *Chin J Epidemiol* (2015) 36:12.1351–1356. doi: 10.3760/cma.j.issn.0254-6450.2015.12.006

40. Guo C, Du H, Qu X, Duan X, Li J, Li R, et al. Prevalence of human papillomavirus among chinese han and mongols minority women in inner mongolia, china: Reflected by self-collected samples in chimust. *Front Public Health* (2022) 10:840879. doi: 10.3389/fpubh.2022.840879

41. Wei L, Ma L, Qin L, Huang Z. The prevalence and genotype distribution of human papillomavirus among women in guangxi, southern China. *Infect Agent Cancer* (2022) 17:19. doi: 10.1186/s13027-022-00431-5

42. Zhixiang LFC, Shujuan W. Analysis of current situation and high risk factors of cervical hpv infection in 680 women. *Ningxia Med J* (2022) 42:6.545–547. doi: 10.13621/j.1001-5949.2020.060.545

43. Carozzi FM, Ocello C, Burroni E, Faust H, Zappa M, Paci E, et al. Effectiveness of HPV vaccination in women reaching screening age in Italy. *J Clin Virol* (2016) 84:74–81. doi: 10.1016/j.jcv.2016.09.011

44. Wei H, Wang N, Zhang Y, Zhang J, Wang S, Zhang S. Distribution of various types of low-risk human papillomavirus according to cervical cytology and histology in northern Chinese women. *Int J Gynaecol Obstet* (2014) 126:28–32. doi: 10.1016/j.ijgo.2014.01.020

45. Lufang DHD, Aimin X, Chun W, Xia H, Meifang Z. Study on the relationship between type specific hr-hpv subtype viral load reflected by ct value detected by cobas 4800 hpv and cervical lesions. *Chin J Obstet Gynecol* (2019) 07:458–63. doi: 10.3760/cma.j.issn.0529-567x.2019.07.005

46. Gallegos-Bolaños J, Rivera-Domínguez JA, Presno-Bernal JM, Cervantes-Villagrana RD. High prevalence of co-infection between human papillomavirus (hpv) 51 and 52 in Mexican population. *BMC Cancer* (2017) 17:531. doi: 10.1186/s12885-017-3519-7

47. Tao X, Zhang H, Zhang H, Xiao J, Li J, Zhou X, et al. Follow-up with histopathology and HPV testing on LSIL cytology in china's largest academic woman's hospital. *Cancer Cytopathol* (2019) 127:258–66. doi: 10.1002/cncy.22119

48. Wu J, Li X, Liu X, Gao Z. Human papillomavirus genotype prevalence in the women of shanghai, china and its association with the severity of cervical neoplasia. *Int J Clin Exp Pathol* (2018) 11:4614–21.

49. Dunne EF, Markowitz LE. Genital human papillomavirus infection. *Clin Infect Dis* (2006) 43:624–9. doi: 10.1086/505982

50. Seong SH, Jeong SM, Jung JH, Kwon DI, Jang JY, Kim JH, et al. Ms. human papillomavirus genotype distribution of genital keratotic lesions. *Australas J Dermatol* (2022). doi: 10.1111/ajd.13867

51. Sjoeborg KD, Tropé A, Lie AK, Jonassen CM, Steinbakk M, Hansen M, et al. HPV genotype distribution according to severity of cervical neoplasia. *Gynecol Oncol* (2010) 118:29–34. doi: 10.1016/j.ygyno.2010.03.007

Frontiers in Oncology

Advances knowledge of carcinogenesis and tumor progression for better treatment and management

The third most-cited oncology journal, which highlights research in carcinogenesis and tumor progression, bridging the gap between basic research and applications to imrpove diagnosis, therapeutics and management strategies.

Discover the latest Research Topics

See more →



Frontiers

Avenue du Tribunal-Fédéral 34
1005 Lausanne, Switzerland
frontiersin.org

Contact us

+41 (0)21 510 17 00
frontiersin.org/about/contact